

# REINFORCED CONCRETE DESIGN OF TALL BUILDINGS



ASCE/SEI 7-05  
2006/2009 IBC  
ASCE/SEI 41-06  
ACI 318-05/08

BUNGALE S. TARANATH, PH.D., P.E., S.E.

**CRSI**



CRC Press  
Taylor & Francis Group

REINFORCED  
CONCRETE  
DESIGN OF  
TALL BUILDINGS





# REINFORCED CONCRETE DESIGN OF TALL BUILDINGS

BUNGALE S. TARANATH, PH.D., P.E., S.E.



**CRC Press**

Taylor & Francis Group  
Boca Raton London New York

CRC Press is an imprint of the  
Taylor & Francis Group, an **informa** business



CRC Press  
Taylor & Francis Group  
6000 Broken Sound Parkway NW, Suite 300  
Boca Raton, FL 33487-2742

© 2010 by Taylor and Francis Group, LLC  
CRC Press is an imprint of Taylor & Francis Group, an Informa business

No claim to original U.S. Government works

Printed in the United States of America on acid-free paper  
10 9 8 7 6 5 4 3 2 1

International Standard Book Number: 978-1-4398-0480-3 (Hardback)

This book contains information obtained from authentic and highly regarded sources. Reasonable efforts have been made to publish reliable data and information, but the author and publisher cannot assume responsibility for the validity of all materials or the consequences of their use. The authors and publishers have attempted to trace the copyright holders of all material reproduced in this publication and apologize to copyright holders if permission to publish in this form has not been obtained. If any copyright material has not been acknowledged please write and let us know so we may rectify in any future reprint.

Except as permitted under U.S. Copyright Law, no part of this book may be reprinted, reproduced, transmitted, or utilized in any form by any electronic, mechanical, or other means, now known or hereafter invented, including photocopying, microfilming, and recording, or in any information storage or retrieval system, without written permission from the publishers.

For permission to photocopy or use material electronically from this work, please access [www.copyright.com](http://www.copyright.com) (<http://www.copyright.com/>) or contact the Copyright Clearance Center, Inc. (CCC), 222 Rosewood Drive, Danvers, MA 01923, 978-750-8400. CCC is a not-for-profit organization that provides licenses and registration for a variety of users. For organizations that have been granted a photocopy license by the CCC, a separate system of payment has been arranged.

**Trademark Notice:** Product or corporate names may be trademarks or registered trademarks, and are used only for identification and explanation without intent to infringe.

---

**Library of Congress Cataloging-in-Publication Data**

---

Taranath, Bungale S.

Reinforced concrete design of tall buildings / by Bungale S. Taranath.

p. cm.

Includes bibliographical references and index.

ISBN 978-1-4398-0480-3 (alk. paper)

1. Reinforced concrete construction. 2. Tall buildings--Design and construction. 3. Tall buildings--Design and construction--Case studies. I. Title.

TH1501.T37 2010

691'.3--dc22

2009024350

---

Visit the Taylor & Francis Web site at  
<http://www.taylorandfrancis.com>

and the CRC Press Web site at  
<http://www.crcpress.com>



*This book is dedicated to my wife*

**SAROJA**

*Without whose patience and devotion, this book would not be.*



---

# Contents

List of Figures .....	xxi
List of Tables .....	xlvi
Foreword .....	li
ICC Foreword.....	lv
Preface.....	lvii
Acknowledgments.....	lxi
A Special Acknowledgment.....	lxiii
Author .....	lxv

<b>Chapter 1</b>	<b>Design Concept .....</b>	<b>1</b>
1.1	Characteristics of Reinforced Concrete.....	1
1.1.1	Confined Concrete.....	1
1.1.2	Ductility.....	4
1.1.3	Hysteresis .....	5
1.1.4	Redundancy.....	6
1.1.5	Detailing.....	6
1.2	Behavior of Reinforced Concrete Elements .....	7
1.2.1	Tension .....	7
1.2.2	Compression .....	7
1.2.3	Bending .....	8
1.2.3.1	Thumb Rules for Beam Design .....	8
1.2.4	Shear.....	14
1.2.5	Sliding Shear (Shear Friction) .....	18
1.2.6	Punching Shear .....	21
1.2.7	Torsion .....	22
1.2.7.1	Elemental Torsion .....	22
1.2.7.2	Overall Building Torsion .....	25
1.3	External Loads .....	26
1.3.1	Earthquakes Loads.....	26
1.3.2	Wind Loads .....	27
1.3.2.1	Extreme Wind Conditions .....	29
1.3.3	Explosion Effects.....	31
1.3.4	Floods.....	32
1.3.5	Vehicle Impact Loads.....	32
1.4	Lateral Load-Resisting Systems .....	32
1.4.1	Shear Walls.....	33
1.4.2	Coupled Shear Walls .....	36
1.4.3	Moment-Resistant Frames.....	37
1.4.4	Dual Systems.....	38
1.4.5	Diaphragm.....	38
1.4.6	Strength and Serviceability .....	39
1.4.7	Self-Straining Forces.....	40
1.4.8	Abnormal Loads.....	40



1.5	Collapse Patterns .....	40
1.5.1	Earthquake Collapse Patterns .....	41
1.5.1.1	Unintended Addition of Stiffness .....	41
1.5.1.2	Inadequate Beam–Column Joint Strength.....	42
1.5.1.3	Tension/Compression Failures.....	42
1.5.1.4	Wall-to-Roof Interconnection Failure .....	43
1.5.1.5	Local Column Failure.....	43
1.5.1.6	Heavy Floor Collapse .....	44
1.5.1.7	Torsion Effects .....	44
1.5.1.8	Soft First-Story Collapse .....	45
1.5.1.9	Midstory Collapse.....	45
1.5.1.10	Pounding.....	45
1.5.1.11	P- $\Delta$ Effect.....	45
1.5.2	Collapse due to Wind Storms.....	47
1.5.3	Explosion Effects.....	47
1.5.4	Progressive Collapse .....	47
1.5.4.1	Design Alternatives for Reducing Progressive Collapse .....	49
1.5.4.2	Guidelines for Achieving Structural Integrity.....	49
1.5.5	Blast Protection of Buildings: The New SEI Standard .....	50
1.6	Buckling of a Tall Building under Its Own Weight.....	50
1.6.1	Circular Building.....	51
1.6.1.1	Building Characteristics .....	52
1.6.2	Rectangular Building .....	53
1.6.2.1	Building Characteristics .....	53
1.6.3	Comments on Stability Analysis .....	53
<b>Chapter 2</b>	<b>Gravity Systems .....</b>	<b>55</b>
2.1	Formwork Considerations .....	55
2.1.1	Design Repetition .....	58
2.1.2	Dimensional Standards .....	58
2.1.3	Dimensional Consistency .....	59
2.1.4	Horizontal Design Techniques .....	60
2.1.5	Vertical Design Strategy .....	63
2.2	Floor Systems .....	65
2.2.1	Flat Plates .....	65
2.2.2	Flat Slabs .....	65
2.2.2.1	Column Capitals and Drop Panels.....	66
2.2.2.2	Comments on Two-Way Slab Systems .....	67
2.2.3	Waffle Systems.....	67
2.2.4	One-Way Concrete Ribbed Slabs .....	67
2.2.5	Skip Joist System.....	67
2.2.6	Band Beam System .....	68
2.2.7	Haunch Girder and Joist System .....	70
2.2.8	Beam and Slab System.....	73
2.3	Design Methods.....	73
2.3.1	One-Way and Two-Way Slab Subassemblies .....	73
2.3.2	Direct Design Method for Two-Way Systems .....	74
2.3.3	Equivalent Frame Method.....	75

2.3.4	Yield-Line Method .....	77
2.3.4.1	Design Example: One-Way Simply Supported Slab.....	78
2.3.4.2	Yield-Line Analysis of a Simply Supported Square Slab .....	81
2.3.4.3	Skewed Yield Lines .....	82
2.3.4.4	Limitations of Yield-Line Method.....	83
2.3.5	Deep Beams .....	83
2.3.6	Strut-and-Tie Method .....	85
2.4	One-Way Slab, T-Beams, and Two-Way Slabs: Hand Calculations .....	92
2.4.1	One-Way Slab; Analysis by ACI 318-05 Provisions .....	92
2.4.2	T-Beam Design.....	97
2.4.2.1	Design for Flexure .....	97
2.4.2.2	Design for Shear .....	100
2.4.3	Two-Way Slabs .....	103
2.4.3.1	Two-Way Slab Design Example.....	106
2.5	Prestressed Concrete Systems .....	108
2.5.1	Prestressing Methods .....	111
2.5.2	Materials.....	111
2.5.2.1	Posttensioning Steel.....	111
2.5.2.2	Concrete.....	112
2.5.3	PT Design.....	113
2.5.3.1	Gravity Systems.....	113
2.5.3.2	Design Thumb Rules .....	115
2.5.3.3	Building Examples .....	118
2.5.4	Cracking Problems in Posttensioned Floors .....	120
2.5.5	Cutting of Prestressed Tendons.....	121
2.5.6	Concept of Secondary Moments .....	123
2.5.6.1	Secondary Moment Design Examples.....	124
2.5.7	Strength Design for Flexure .....	133
2.5.7.1	Strength Design Examples.....	134
2.5.8	Economics of Posttensioning .....	142
2.5.9	Posttensioned Floor Systems in High-Rise Buildings .....	143
2.5.9.1	Transfer Girder Example .....	144
2.5.10	Preliminary Design of PT Floor Systems; Hand Calculations .....	146
2.5.10.1	Preview .....	146
2.5.10.2	Simple Span Beam.....	149
2.5.10.3	Continuous Spans .....	152
2.5.11	Typical Posttensioning Details.....	172
2.6	Foundations .....	172
2.6.1	Pile Foundations.....	178
2.6.2	Mat Foundations.....	179
2.6.2.1	General Considerations.....	179
2.6.2.2	Analysis .....	182
2.6.2.3	Mat for a 25-Story Building .....	183
2.6.2.4	Mat for an 85-Story Building .....	185
2.7	Guidelines for Thinking on Your Feet .....	187
2.8	Unit Quantities.....	187
2.8.1	Unit Quantity of Reinforcement in Columns .....	188
2.8.2	Unit Quantity of Reinforcement and Concrete in Floor Framing Systems .....	197

<b>Chapter 3</b>	<b>Lateral Load-Resisting Systems.....</b>	<b>199</b>
3.1	Flat Slab-Frame System .....	201
3.2	Flat Slab-Frame with Shear Walls.....	203
3.3	Coupled Shear Walls .....	204
3.4	Rigid Frame .....	205
3.4.1	Deflection Characteristics .....	207
3.4.1.1	Cantilever Bending Component.....	207
3.4.1.2	Shear Racking Component .....	207
3.5	Tube System with Widely Spaced Columns.....	210
3.6	Rigid Frame with Haunch Girders .....	210
3.7	Core-Supported Structures.....	212
3.8	Shear Wall–Frame Interaction .....	212
3.8.1	Behavior .....	217
3.8.2	Building Examples .....	218
3.9	Frame Tube System .....	224
3.9.1	Behavior .....	225
3.9.2	Shear Lag.....	225
3.9.3	Irregular Tube.....	229
3.10	Exterior Diagonal Tube .....	230
3.10.1	Example of Exterior Diagonal Tube: Onterie Center, Chicago.....	231
3.11	Bundled Tube.....	232
3.11.1	Example of Bundled Tube: One Magnificent Mile, Chicago.....	232
3.12	Spinal Wall Systems .....	234
3.13	Outrigger and Belt Wall System.....	234
3.13.1	Deflection Calculations .....	238
3.13.1.1	Case 1: Outrigger Wall at the Top .....	238
3.13.1.2	Case 2: Outrigger Wall at Quarter Height from the Top .....	239
3.13.1.3	Case 3: Outrigger Wall at Midheight.....	241
3.13.1.4	Case 4: Outrigger Wall at Quarter Height from the Bottom .....	241
3.13.2	Optimum Location of a Single Outrigger Wall.....	242
3.13.3	Optimum Locations of Two Outrigger Walls.....	247
3.13.4	Recommendations for Optimum Locations .....	250
3.14	Miscellaneous Systems.....	251
<b>Chapter 4</b>	<b>Wind Loads .....</b>	<b>253</b>
4.1	Design Considerations.....	253
4.2	Natural Wind .....	255
4.2.1	Types of Wind .....	256
4.3	Characteristics of Wind.....	256
4.3.1	Variation of Wind Velocity with Height (Velocity Profile).....	257
4.3.2	Wind Turbulence .....	258
4.3.3	Probabilistic Approach.....	260
4.3.4	Vortex Shedding.....	261
4.3.5	Dynamic Nature of Wind.....	264
4.3.6	Pressures and Suctions on Exterior Surfaces .....	264
4.3.6.1	Scaling .....	264
4.3.6.2	Internal Pressures and Differential Pressures .....	265
4.3.6.3	Distribution of Pressures and Suctions .....	265
4.3.6.4	Local Cladding Loads and Overall Design Loads .....	266



4.4	ASCE 7-05: Wind Load Provisions.....	267
4.4.1	Analytical Procedure—Method 2, Overview .....	273
4.4.2	Method 2: Step-by-Step Procedure .....	274
4.4.2.1	Wind Speedup over Hills and Escarpments: $K_{zt}$ Factor.....	280
4.4.2.2	Gust Effect Factor .....	281
4.4.2.3	Determination of Design Wind Pressures Using Graphs.....	289
4.4.2.4	Along-Wind Response .....	292
4.4.2.5	Worksheet for Calculation of Gust Effect Factor, $G_f$ , Along-Wind Displacement and Acceleration .....	296
4.4.2.6	Comparison of Gust Effect Factor and Along-Wind Response .....	299
4.4.2.7	One More Example: Design Wind Pressures for Enclosed Building, Method 2.....	301
4.5	National Building Code of Canada (NBCC 2005): Wind Load Provisions ....	304
4.5.1	Static Procedure .....	304
4.5.1.1	Specified Wind Load .....	304
4.5.1.2	Exposure Factor, $C_e$ .....	305
4.5.1.3	Gust Factors, $C_g$ and $C_{gi}$ .....	305
4.5.1.4	Pressure Coefficient, $C_p$ .....	306
4.5.2	Dynamic Procedure.....	306
4.5.2.1	Gust Effect Factor, $C_g$ (Dynamic Procedure) .....	307
4.5.2.2	Design Example: Calculations for Gust Effect Factor, $C_g$ .....	309
4.5.2.3	Wind-Induced Building Motion .....	311
4.5.2.4	Design Example.....	312
4.5.2.5	Comparison of Along-Wind and Across-Wind Accelerations .....	314
4.5.3	Wind Load Comparison among International Codes and Standards .....	315
4.6	Wind-Tunnels.....	315
4.6.1	Types of Wind-Tunnel Tests .....	320
4.6.1.1	Rigid Pressure Model .....	321
4.6.1.2	High-Frequency Base Balance and High-Frequency Force Balance (HFBB/HFFB Model) Model.....	322
4.6.1.3	Aeroelastic Model .....	324
4.6.1.4	Multidegree-of-Freedom Aeroelastic Model .....	330
4.6.1.5	Option for Wind-Tunnel Testing.....	331
4.6.1.6	Lower Limit on Wind-Tunnel Test Results.....	331
4.6.2	Prediction of Acceleration and Human Comfort .....	331
4.6.3	Load Combination Factors .....	332
4.6.4	Pedestrian Wind Studies .....	332
4.6.5	Motion Perception: Human Response to Building Motions .....	335
4.6.6	Structural Properties Required for Wind-Tunnel Data Analysis .....	335
4.6.6.1	Natural Frequencies.....	336
4.6.6.2	Mode Shapes.....	336
4.6.6.3	Mass Distribution .....	337
4.6.6.4	Damping Ratio.....	337
4.6.6.5	Miscellaneous Information.....	338
4.6.6.6	Example .....	338
4.6.7	Period Determination and Damping Values for Wind Design.....	341

<b>Chapter 5</b>	<b>Seismic Design</b>	347
5.1	Building Behavior	349
5.1.1	Influence of Soil	349
5.1.2	Damping	350
5.1.3	Building Motions and Deflections	352
5.1.4	Building Drift and Separation	352
5.2	Seismic Design Concept	353
5.2.1	Structural Response	353
5.2.2	Load Path	353
5.2.3	Response of Elements Attached to Buildings	354
5.2.4	Adjacent Buildings	354
5.2.5	Irregular Buildings	355
5.2.6	Lateral Force–Resisting Systems	356
5.2.7	Diaphragms	357
5.2.8	Ductility	358
5.2.9	Damage Control Features	360
5.2.10	Continuous Load Path	361
5.2.11	Redundancy	361
5.2.12	Configuration	362
5.2.13	Dynamic Analysis	364
5.2.13.1	Response-Spectrum Method	367
5.2.13.2	Response-Spectrum Concept	371
5.2.13.3	Deformation Response Spectrum	372
5.2.13.4	Pseudo-Velocity Response Spectrum	373
5.2.13.5	Pseudo-Acceleration Response Spectrum	374
5.2.13.6	Tripartite Response Spectrum: Combined Displacement–Velocity–Acceleration ( <i>DVA</i> ) Spectrum	374
5.2.13.7	Characteristics of Response Spectrum	379
5.3	An Overview of 2006 IBC	381
5.3.1	Occupancy Category	381
5.3.2	Overturning, Uplifting, and Sliding	383
5.3.3	Seismic Detailing	383
5.3.4	Live-Load Reduction in Garages	384
5.3.5	Torsional Forces	384
5.3.6	Partition Loads	384
5.4	ASCE 7-05 Seismic Provisions: An Overview	384
5.5	An Overview of Chapter 11 of ASCE 7-05, Seismic Design Criteria	386
5.5.1	Seismic Ground-Motion Values	386
5.5.1.1	Site Coefficients, $F_a$ and $F_v$	388
5.5.1.2	Site Class	389
5.5.1.3	Design Response Spectrum	389
5.5.2	Equivalent Lateral Force Procedure	390
5.5.2.1	Parameters $S_s$ and $S_e$	396
5.5.2.2	Site-Specific Ground Motion Analysis	397
5.5.3	Importance Factor and Occupancy Category	398
5.5.3.1	Importance Factor, $I_E$	398
5.5.3.2	Occupancy Categories	399
5.5.4	Seismic Design Category	400
5.5.5	Design Requirements for SDC A Buildings	401
5.5.6	Geologic Hazards and Geotechnical Investigation	404

5.5.7	Base Shear for Preliminary Design.....	405
5.5.8	Design Response Spectrum for Selected Cities in the U.S.A. ....	414
5.6	An Overview of Chapter 12 of ASCE 7-05, Seismic Design Requirements for Building Structures.....	427
5.6.1	Seismic Design Basis .....	427
5.6.2	Structural System Selection .....	427
5.6.3	Diaphragms .....	429
5.6.3.1	Irregularities .....	430
5.6.4	Seismic Load Effects and Combinations .....	430
5.6.5	Direction of Loading .....	431
5.6.6	Analysis Procedure .....	432
5.6.7	Modeling Criteria .....	432
5.6.8	Modal Analysis .....	433
5.6.9	Diaphragms, Chords, and Collectors .....	433
5.6.10	Structural Walls and Their Anchorage .....	434
5.6.11	Drift and Deformation.....	435
5.6.12	Foundation Design .....	436
5.6.12.1	Foundation Requirements for Structures Assigned to Seismic Design Category C.....	437
5.6.12.2	Foundation Requirements for Structures Assigned to Seismic Design Categories D, E, or F.....	437
5.7	ASCE 7-05, Seismic Design: An In-Depth Discussion.....	438
5.7.1	Seismic Design Basis .....	439
5.7.2	Structural System Selection .....	440
5.7.2.1	Bearing Wall System .....	440
5.7.2.2	Building Frame System .....	441
5.7.2.3	Moment Frame System.....	441
5.7.2.4	Dual System.....	441
5.7.3	Special Reinforced Concrete Shear Wall .....	442
5.7.4	Detailing Requirements .....	442
5.7.5	Building Irregularities.....	443
5.7.5.1	Plan or Horizontal Irregularity.....	446
5.7.5.2	Vertical Irregularity.....	448
5.7.6	Redundancy.....	448
5.7.7	Seismic Load Combinations.....	449
5.7.7.1	Seismic Load Effect.....	450
5.7.7.2	Seismic Load Effect with Overstrength .....	451
5.7.7.3	Elements Supporting Discontinuous Walls or Frames.....	451
5.7.8	Direction of Loading.....	451
5.7.9	Analysis Procedures .....	452
5.7.9.1	Equivalent Lateral-Force Procedure.....	455
5.7.9.2	Modal Response Spectrum Analysis.....	463
5.7.10	Diaphragms, Chords, and Collectors .....	464
5.7.10.1	Diaphragms for SDC A .....	465
5.7.10.2	Diaphragms for SDCs B through F .....	465
5.7.10.3	General Procedure for Diaphragm Design.....	465
5.7.11	Catalog of Seismic Design Requirements.....	473
5.7.11.1	Buildings in SDC A.....	473
5.7.11.2	Buildings in SDC B .....	474



5.7.11.3	Buildings in SDC C .....	475
5.7.11.4	Buildings in SDC D .....	476
5.7.11.5	Buildings in SDC E .....	478
5.7.11.6	Buildings in SDC F.....	478
5.8	Seismic Design Example: Dynamic Analysis Procedure (Response Spectrum Analysis) Using Hand Calculations .....	478
5.9	Anatomy of Computer Response Spectrum Analyses (In Other Words, What Goes on in the Black Box) .....	487
5.10	Dynamic Response Concept.....	497
5.10.1	Difference between Static and Dynamic Analyses.....	500
5.10.2	Dynamic Effects due to Wind Loads .....	503
5.10.3	Seismic Periods .....	504
5.11	Dynamic Analysis Theory .....	505
5.11.1	Single-Degree-of-Freedom Systems .....	505
5.11.2	Multi-Degree-of-Freedom Systems.....	508
5.11.3	Modal Superposition Method.....	511
5.11.4	Normal Coordinates .....	511
5.11.5	Orthogonality .....	512
5.12	Summary .....	518
<b>Chapter 6</b>	<b>Seismic Design Examples and Details.....</b>	<b>523</b>
6.1	Seismic Design Recap .....	523
6.2	Design Techniques to Promote Ductile Behavior .....	526
6.3	Integrity Reinforcement .....	529
6.4	Review of Strength Design.....	530
6.4.1	Load Combinations .....	532
6.4.2	Earthquake Load $E$ .....	532
6.4.2.1	Load Combination for Verifying Building Drift.....	534
6.4.3	Capacity Reduction Factors, $\phi$ .....	534
6.5	Intermediate Moment-Resisting Frames .....	535
6.5.1	General Requirements: Frame Beams .....	535
6.5.2	Flexural and Transverse Reinforcement: Frame Beams .....	535
6.5.3	Transverse Reinforcement: Frame Columns.....	537
6.5.4	Detailing Requirements for Two-Way Slab Systems without Beams.....	538
6.6	Special Moment-Resisting Frames.....	539
6.6.1	General Requirements: Frame Beams .....	539
6.6.2	Flexural Reinforcement: Frame Beams .....	540
6.6.3	Transverse Reinforcement: Frame Beams .....	541
6.6.4	General Requirements: Frame Columns .....	541
6.6.5	Flexural Reinforcement: Frame Columns.....	541
6.6.6	Transverse Reinforcement: Frame Columns.....	544
6.6.7	Transverse Reinforcement: Joints .....	546
6.6.8	Shear Strength of Joint .....	546
6.6.9	Development of Bars in Tension .....	548
6.7	Shear Walls.....	548
6.7.1	Minimum Web Reinforcement: Design for Shear .....	548
6.7.2	Boundary Elements .....	549
6.7.3	Coupling Beams .....	550
6.8	Frame Members Not Designed to Resist Earthquake Forces.....	551

6.9	Diaphragms .....	552
6.9.1	Minimum Thickness and Reinforcement.....	552
6.9.2	Shear Strength .....	552
6.9.3	Boundary Elements .....	553
6.10	Foundations .....	553
6.10.1	Footings, Mats, and Piles .....	553
6.10.2	Grade Beams and Slabs-on-Grade .....	554
6.10.3	Piles, Piers, and Caissons .....	554
6.11	Design Examples .....	554
6.11.1	Frame Beam Example: Ordinary Reinforced Concrete Moment Frame .....	555
6.11.2	Frame Column Example: Ordinary Reinforced Concrete Moment Frame .....	557
6.11.3	Frame Beam Example: Intermediate Reinforced Concrete Moment Frame .....	559
6.11.4	Frame Column Example: Intermediate Reinforced Concrete Moment Frame .....	561
6.11.5	Shear Wall Example: Seismic Design Category A, B, or C.....	563
6.11.6	Frame Beam Example: Special Reinforced Concrete Moment Frame .....	565
6.11.7	Frame Column Example: Special Reinforced Concrete Moment Frame .....	570
6.11.8	Beam–Column Joint Example: Special Reinforced Concrete Frame .....	574
6.11.9	Special Reinforced Concrete Shear Wall.....	577
6.11.9.1	Preliminary Size Determination.....	579
6.11.9.2	Shear Design.....	579
6.11.9.3	Shear Friction (Sliding Shear) .....	580
6.11.9.4	Longitudinal Reinforcement.....	581
6.11.9.5	Web Reinforcement .....	581
6.11.9.6	Boundary Elements .....	583
6.11.10	Special Reinforced Concrete Coupled Shear Walls.....	587
6.11.10.1	Coupling Beams .....	588
6.11.10.2	Wall Piers .....	593
6.12	Typical Details.....	599
6.13	ACI 318-08 Update.....	600
6.13.1	Outline of Major Changes .....	600
6.13.2	Summary of Chapter 21, ACI 318-08.....	605
6.13.3	Analysis and Proportioning of Structural Members .....	605
6.13.4	Reinforcement in Special Moment Frames and Special Structural Walls.....	605
6.13.5	Mechanical Splices in Special Moment Frames and Special Structural Walls.....	606
6.13.6	Welded Splices in Special Moment Frames and Special Structural Walls.....	606
6.13.7	Ordinary Moment Frames, SDC B .....	606
6.13.8	Intermediate Moment Frames .....	606
6.13.9	Two-Way Slabs without Beams .....	607
6.13.10	Flexural Members (Beams) of Special Moment Frames .....	607
6.13.11	Transverse Reinforcement.....	608
6.13.12	Shear Strength Requirements.....	609

6.13.13	Special Moment Frame Members Subjected to Bending and Axial Loads .....	609
6.13.14	Shear Strength Requirements for Columns.....	611
6.13.15	Joints of Special Moment Frames .....	611
6.13.16	Special Structural Walls and Coupling Beams .....	611
6.13.17	Shear Wall Design for Flexure and Axial Loads .....	612
6.13.18	Boundary Elements of Special Structural Walls.....	613
6.13.19	Coupling Beams .....	613
<b>Chapter 7</b>	<b>Seismic Rehabilitation of Existing Buildings .....</b>	<b>617</b>
7.1	Code-Sponsored Design .....	619
7.2	Alternate Design Philosophy .....	619
7.3	Code Provisions for Seismic Upgrade.....	621
7.4	Building Deformations .....	622
7.5	Common Deficiencies and Upgrade Methods.....	623
7.5.1	Diaphragms .....	624
7.5.1.1	Cast-in-Place Concrete Diaphragms.....	624
7.5.1.2	Precast Concrete Diaphragms .....	627
7.5.2	Shear Walls.....	627
7.5.2.1	Increasing Wall Thickness .....	627
7.5.2.2	Increasing Shear Strength of Wall.....	628
7.5.2.3	Infilling between Columns .....	628
7.5.2.4	Addition of Boundary Elements .....	628
7.5.2.5	Addition of Confinement Jackets.....	629
7.5.2.6	Repair of Cracked Coupling Beams .....	629
7.5.2.7	Adding New Walls.....	629
7.5.2.8	Precast Concrete Shear Walls.....	629
7.5.3	Infilling of Moment Frames .....	629
7.5.4	Reinforced Concrete Moment Frames .....	630
7.5.5	Open Storefront .....	631
7.5.6	Clerestory .....	631
7.5.7	Shallow Foundations .....	632
7.5.8	Rehabilitation Measures for Deep Foundations .....	632
7.5.9	Nonstructural Elements.....	633
7.5.9.1	Nonload-Bearing Walls .....	633
7.5.9.2	Precast Concrete Cladding .....	633
7.5.9.3	Stone or Masonry Veneers.....	634
7.5.9.4	Building Ornamentation .....	634
7.5.9.5	Acoustical Ceiling .....	634
7.6	Seismic Rehabilitation of Existing Buildings, ASCE/SEI 41-06 .....	634
7.6.1	Overview of Performance Levels.....	641
7.6.2	Permitted Design Methods.....	642
7.6.3	Systematic Rehabilitation.....	643
7.6.3.1	Determination of Seismic Ground Motions .....	644
7.6.3.2	Determination of As-Built Conditions .....	644
7.6.3.3	Primary and Secondary Components.....	645
7.6.3.4	Setting Up Analytical Model and Determination of Design Forces .....	645
7.6.3.5	Ultimate Load Combinations: Combined Gravity and Seismic Demand .....	647

7.6.3.6	Component Capacity Calculations, $Q_{CE}$ and $Q_{CL}$ .....	648
7.6.3.7	Capacity versus Demand Comparisons .....	649
7.6.3.8	Development of Seismic Strengthening Strategies .....	651
7.6.4	ASCE/SEI 41-06: Design Example .....	661
7.6.4.1	Dual System: Moment Frames and Shear Walls .....	661
7.6.5	Summary of ASCE/SEI 41-06 .....	666
7.7	Fiber-Reinforced Polymer Systems for Strengthening of Concrete Buildings .....	667
7.7.1	Mechanical Properties and Behavior .....	667
7.7.2	Design Philosophy .....	668
7.7.3	Flexural Design .....	668
7.8	Seismic Strengthening Details .....	668
7.8.1	Common Strategies for Seismic Strengthening .....	669
<b>Chapter 8</b>	<b>Tall Buildings .....</b>	<b>685</b>
8.1	Historical Background .....	688
8.2	Review of High-Rise Architecture .....	692
8.3	Functional Requirements .....	694
8.4	Definition of Tall Buildings .....	695
8.5	Lateral Load Design Philosophy .....	695
8.6	Concept of Premium for Height .....	696
8.7	Relative Structural Cost .....	697
8.8	Factors for Reduction in the Weight of Structural Frame .....	697
8.9	Development of High-Rise Architecture .....	699
8.9.1	Architect–Engineer Collaboration .....	704
8.9.2	Sky Scraper Pluralism .....	704
8.9.3	Structural Size .....	705
8.10	Structural Scheme Options .....	705
8.10.1	Space Efficiency of High-Rise Building Columns .....	716
8.10.2	Structural Cost and Plan Density Comparison .....	717
8.11	Summary of Building Technology .....	718
8.12	Structural Concepts .....	719
8.13	Bending and Shear Rigidity Index .....	720
8.14	Case Studies .....	724
8.14.1	Empire State Building, New York, City, New York .....	724
8.14.2	South Walker Tower, Chicago, Illinois .....	724
8.14.3	Miglin-Beitler Tower, Chicago, Illinois .....	726
8.14.4	Trump Tower, Chicago, Illinois .....	730
8.14.4.1	Vital Statistics .....	731
8.14.5	Jin Mao Tower, Shanghai, China .....	731
8.14.6	Petronas Towers, Malaysia .....	734
8.14.7	Central Plaza, Hong Kong .....	736
8.14.8	Singapore Treasury Building .....	739
8.14.9	City Spire, New York City .....	740
8.14.10	NCNB Tower, North Carolina .....	740
8.14.11	Museum Tower, Los Angeles, California .....	743
8.14.12	MGM City Center, Vdara Tower, Las Vegas, Nevada .....	744
8.14.13	Citybank Plaza, Hong Kong .....	746
8.14.14	Trump Tower, New York .....	746

8.14.15	Two Prudential Plaza, Chicago, Illinois.....	747
8.14.16	Cent Trust Tower, Miami, Florida.....	749
8.14.17	Metropolitan Tower, New York City .....	751
8.14.18	Carnegie Hall Tower, New York City .....	752
8.14.19	Hopewell Center, Hong Kong .....	753
8.14.20	Cobalt Condominiums, Minneapolis, Minnesota.....	754
8.14.21	The Cosmopolitan Resort & Casino, Las Vegas, Nevada.....	757
8.14.22	Elysian Hotel and Private Residences, Chicago, Illinois .....	759
8.14.22.1	Foundations .....	759
8.14.22.2	Floor Systems.....	760
8.14.22.3	Gravity System.....	761
8.14.22.4	Lateral System .....	761
8.14.22.5	Tuned Liquid Damper.....	761
8.14.23	Shangri-La New York (610 Lexington Avenue), New York.....	762
8.14.24	Millennium Tower, 301 Mission Street, San Francisco, California.....	768
8.14.25	Al Bateen Towers, Dubai, UAE .....	773
8.14.25.1	Wind Loads .....	777
8.14.25.2	Seismic Loads .....	778
8.14.26	SRZ Tower, Dubai, UAE.....	778
8.14.26.1	Wind Loads .....	779
8.14.26.2	Seismic Loads .....	782
8.14.26.3	Computer Model .....	782
8.14.26.4	Building Behavior .....	783
8.14.26.5	Wind.....	783
8.14.27	The Four Seasons Hotel and Tower, Miami, Florida .....	783
8.14.28	Burj Dubai.....	786
8.15	Future of Tall Buildings .....	791

## **Chapter 9** Special Topics..... 793

9.1	Damping Devices for Reducing Motion Perception .....	793
9.1.1	Passive Viscoelastic Dampers.....	793
9.1.2	Tuned Mass Damper.....	795
9.1.2.1	Citicorp Tower, New York .....	796
9.1.2.2	John Hancock Tower, Boston, Massachusetts .....	798
9.1.2.3	Design Considerations for TMD .....	799
9.1.3	Sloshing Water Damper.....	799
9.1.4	Tuned Liquid Column Damper.....	799
9.1.4.1	Wall Center, Vancouver, British Columbia.....	800
9.1.4.2	Highcliff Apartment Building, Hong Kong.....	800
9.1.5	Simple Pendulum Damper.....	800
9.1.5.1	Taipei Financial Center.....	802
9.1.6	Nested Pendulum Damper.....	803
9.2	Seismic Isolation .....	804
9.2.1	Salient Features .....	806
9.2.2	Mechanical Properties of Seismic Isolation Systems.....	808
9.2.3	Elastomeric Isolators .....	808
9.2.4	Sliding Isolators.....	810
9.2.5	Seismically Isolated Structures: ASCE 7-05 Design Provisions .....	810

9.2.5.1	Equivalent Lateral Force Procedure .....	813
9.2.5.2	Lateral Displacements .....	813
9.2.5.3	Minimum Lateral Forces for the Design of Isolation System and Structural Elements at or below Isolation System.....	816
9.2.5.4	Minimum Lateral Forces for the Design of Structural Elements above Isolation System .....	816
9.2.5.5	Drift Limits.....	817
9.2.5.6	Illustrative Example: Static Procedure .....	817
9.3	Passive Energy Dissipation .....	829
9.4	Preliminary Analysis Techniques .....	830
9.4.1	Portal Method .....	833
9.4.2	Cantilever Method .....	834
9.4.3	Lateral Stiffness of Frames.....	837
9.4.4	Framed Tube Structures.....	845
9.5	Torsion.....	846
9.5.1	Preview.....	846
9.5.2	Concept of Warping Behavior .....	857
9.5.3	Sectorial Coordinate $\omega'$ .....	861
9.5.4	Shear Center.....	863
9.5.4.1	Evaluation of Product Integrals .....	865
9.5.5	Principal Sectorial Coordinate $\omega_s$ Diagram.....	865
9.5.5.1	Sectorial Moment of Inertia $I_\omega$ .....	865
9.5.6	Torsion Constant $J$ .....	865
9.5.7	Calculation of Sectorial Properties: Worked Example .....	866
9.5.8	General Theory of Warping Torsion.....	867
9.5.8.1	Warping Torsion Equations for Shear Wall Structures .....	870
9.5.9	Torsion Analysis of Shear Wall Building: Worked Example.....	871
9.5.10	Warping Torsion Constants for Open Sections.....	881
9.5.11	Stiffness Method Using Warping-Column Model.....	883
9.6	Performance-Based Design .....	885
9.6.1	Design Ideology .....	885
9.6.2	Performance-Based Engineering .....	886
9.6.3	Linear Response History Procedure .....	887
9.6.4	Nonlinear Response History Procedure .....	887
9.6.5	Member Strength .....	888
9.6.6	Design Review .....	888
9.6.7	New Building Forms.....	889
9.7	Wind Deflections .....	890
9.8	2009 International Building Code (2009 IBC) Updates.....	892
9.8.1	An Overview of Structural Revisions .....	892
9.8.1.1	Earthquake Loads .....	892
9.8.1.2	Wind Loads.....	892
9.8.1.3	Structural Integrity .....	893
9.8.1.4	Other Updates in Chapter 16.....	893
9.8.1.5	Chapter 18: Soils and Foundations.....	893
9.8.1.6	Chapter 19: Concrete.....	893
9.8.2	Detail Discussion of Structural Revisions .....	893
9.8.2.1	Section 1604.8.2: Walls .....	893
9.8.2.2	Section 1604.8.3: Decks.....	894
9.8.2.3	Section 1605.1.1: Stability .....	894

9.8.2.4	Sections 1607.3 and 1607.4: Uniformly Distributed Live Loads and Concentrated Live Loads .....	894
9.8.2.5	Section 1607.7.3: Vehicle Barrier Systems .....	894
9.8.2.6	Section 1607.9.1.1: One-Way Slabs .....	894
9.8.2.7	Section 1609.1.1.2: Wind Tunnel Test Limitations.....	894
9.8.2.8	Section 1613.7: ASCE 7-05, Section 11.7.5: Anchorage of Walls.....	897
9.8.2.9	Section 1607.11.2.2: Special Purpose Roofs .....	897
9.8.2.10	Section 1613: Earthquake Loads .....	897
9.8.2.11	Minimum Distance for Building Separation.....	898
9.8.2.12	Section 1613.6.7: Minimum Distance for Building Separation .....	899
9.8.2.13	Section 1614: Structural Integrity .....	899
9.8.3	Chapter 17: Structural Tests and Special Inspections.....	900
9.8.3.1	Section 1704.1: General .....	900
9.8.3.2	Section 1704.4: Concrete Construction.....	900
9.8.3.3	Section 1704.10: Helical Pile Foundations .....	900
9.8.3.4	Section 1706: Special Inspections for Wind Requirements .....	900
9.8.4	Chapter 18: Soils and Foundations.....	900
9.8.4.1	Section 1803: Geotechnical Investigations .....	900
9.8.4.2	Section 1807.2.3: Safety Factor.....	900
9.8.4.3	Section 1808.3.1: Seismic Overturning .....	901
9.8.4.4	Sections 1810.3.1.5 and 1810.3.5.3.3: Helical Piles.....	901
9.8.5	Chapter 19: Concrete .....	901
9.8.5.1	Section 1908.1: General.....	901
9.8.5.2	Section 1908.1.9: ACI 318, Section D.3.3 .....	901
9.8.5.3	Sections 1909.6.1 and 1909.6.3: Basement Walls and Openings in Walls .....	901
9.8.6	Anticipated Revisions in 2012 IBC .....	901
<b>References .....</b>		<b>903</b>
<b>Index .....</b>		<b>907</b>

# List of Figures

<b>FIGURE 1.1</b>	Confinement of column concrete by transverse reinforcement: (a) confinement by spiral or circular hoops, (b) confinement by a rectangular hoop, and (c) confinement by hoops and cross ties. ....	2
<b>FIGURE 1.2</b>	Confinement of circular column: (a) column with circular ties, (b) radial forces, and (c) free-body of upper portion of tie. ....	2
<b>FIGURE 1.3</b>	Column ties and seismic hooks: (a) overlapping 90° hooks at corners cannot confine a concrete core after concrete cover spalls, (b) 135° hooks, required in high seismic areas, provide the necessary confinement for the core while simultaneously resisting buckling of column vertical bars, and (c) seismic hook. ...	3
<b>FIGURE 1.4</b>	Frame-beam subjected to cyclic loads: (a) cracks due to $-M_u$ and (b) cracks due to $+M_u$ . ....	4
<b>FIGURE 1.5</b>	Ductility model. The ability of the structure to provide resistance in the inelastic domain of response is termed “ductility”. $\Delta_u$ is the limit to ductility corresponding to a specified limit of strength degradation. ....	5
<b>FIGURE 1.6</b>	Hysteresis loops. (a) Idealized elastoplastic loop. (b) Well-detailed beam plastic hinge loop. ....	6
<b>FIGURE 1.7</b>	Tension member in a transfer truss. <i>Note:</i> Column C not required for truss action but recommended. ....	8
<b>FIGURE 1.8</b>	Transfer girder: schematic elevation with concrete column. ....	9
<b>FIGURE 1.9</b>	Transfer girder: schematic elevation with encased composite column. ....	10
<b>FIGURE 1.10</b>	Transfer girder: schematic elevation with filled steel column. ....	11
<b>FIGURE 1.11</b>	Tension member in a strut-and-tie model. <i>Note:</i> Capacity reduction factor, $\phi = 0.75$ . ....	12
<b>FIGURE 1.12</b>	Development of cracks in a flexural member. Vertical cracks may develop near midspan, stable, hairline cracks are normal, but widening cracks indicate impending failure. ....	12
<b>FIGURE 1.13</b>	Two-way slab systems: (a) flat plate, (b) flat plate with column capitols, (c) flat plate with drop panels, (d) band beams, (e) one-way beam and slab, (f) skip joist system, (g) waffle slab, and (h) standard joist system. ....	14
<b>FIGURE 1.14</b>	Unit shearing stresses acting at right angles to each other. ....	14
<b>FIGURE 1.15</b>	Shear stress distribution in a rectangular beam. ....	15
<b>FIGURE 1.16</b>	Complimentary shear stresses. (a) Rectangular beam subject to vertical shear force $V_u$ , (b) beam element between two parallel sections, and (c) shear stresses on perpendicular faces of a beam element. ....	16
<b>FIGURE 1.17</b>	Diagonal tension. ....	17
<b>FIGURE 1.18</b>	Shear-resisting forces along a diagonal crack: $V_{ext} = V_{cy} + V_{iy} + V_d + V_s$ . ....	17



<b>FIGURE 1.19</b>	Frictional resistance generated by shear-friction reinforcement. (a) Applied shear, (b) enlarged crack surface, and (c) free body diagram of concrete above crack. ....	19
<b>FIGURE 1.20</b>	Potential locations of sliding shear. (a–c) Squat wall, (d) tall wall, and (e) plastic hinge region in a frame beam. ....	20
<b>FIGURE 1.21</b>	Punching shear failure in a two-way slab system. It is the tendency of the slab to drop as a unit around the column. ....	21
<b>FIGURE 1.22</b>	Transfer of slab load into columns. ....	22
<b>FIGURE 1.23</b>	Strut-and-tie model for punching shear. ....	22
<b>FIGURE 1.24</b>	Torsion in spandrel beams. ....	23
<b>FIGURE 1.25</b>	Equilibrium torsion. ....	23
<b>FIGURE 1.26</b>	Compatibility torsion. ....	24
<b>FIGURE 1.27</b>	Earthquake loading: Dynamic action of earthquakes can be simplified as a group of horizontal forces that are applied to the structure in proportion to its mass, and to the height of the mass above the ground. ....	27
<b>FIGURE 1.28</b>	Circulation of world's winds. ....	28
<b>FIGURE 1.29</b>	Wind load distribution: positive pressure on windward wall, and negative pressure (suction) on leeward wall and roof. For a hermetically sealed building, internal pressures cancel out, hence no effect on overall building loads. ....	29
<b>FIGURE 1.30</b>	Shear deformations in a shear wall. ....	33
<b>FIGURE 1.31</b>	Diaphragm concept. <i>Note:</i> Seismic elements in the E–W direction not shown for clarity. ....	34
<b>FIGURE 1.32</b>	Floor plan: building with shear walls and perimeter frame. ....	35
<b>FIGURE 1.33</b>	Building with perimeter shear walls. ....	35
<b>FIGURE 1.34</b>	Shear walls with openings. ....	36
<b>FIGURE 1.35</b>	Lateral load-resistance of single and coupled shear walls. ....	36
<b>FIGURE 1.36</b>	Coupling beam resistance. ....	37
<b>FIGURE 1.37</b>	Moment-resisting frame: The lateral resistance is provided by keeping the frame from changing into a parallelogram. The interconnection of columns and beams is rigid. ....	37
<b>FIGURE 1.38</b>	Shear wall–frame interaction. ....	38
<b>FIGURE 1.39</b>	Diaphragms with openings. ....	39
<b>FIGURE 1.40</b>	Distress in columns due to unintended stiffness addition. ....	42
<b>FIGURE 1.41</b>	Column joint failure. Concrete in columns is not well enough confined by rebar ties, resulting in failure as concrete splits off and rebar buckles. ....	42
<b>FIGURE 1.42</b>	Collapse patterns. (a) Inadequate shear strength. (b) Inadequate beam/column strength. (c) Tension/compression failure due to overturning. ....	43
<b>FIGURE 1.43</b>	More collapse patterns. ....	43

<b>FIGURE 1.44</b>	Heavy floor collapse: Major force is in inertia of floors and is concentrated at each level. If columns crack and fail, heavy floors collapse. ....	44
<b>FIGURE 1.45</b>	Torsion effect: property-line walls placed on one side of a frame structure, create eccentric condition which can lead to collapse. ....	44
<b>FIGURE 1.46</b>	Soft story collapse: Lower story that is weakened by too many openings becomes racked (rectangles become parallelograms). This may result in failure of first story columns due to mismatch of demand versus strength. ....	45
<b>FIGURE 1.47</b>	P- $\Delta$ effect; simple cantilever model. $M_u = V_u H + W_g \Delta$ . ....	46
<b>FIGURE 1.48</b>	P- $\Delta$ effect: Shear wall-frame system. ....	46
<b>FIGURE 1.49</b>	Collapse due to P- $\Delta$ effect. ....	47
<b>FIGURE 1.50</b>	Exterior explosion. ....	48
<b>FIGURE 1.51</b>	Damage due to exterior explosion. (a) Exterior windows, columns, and walls. (b) Roof and floor slabs. (c) Building sway due to ground shock. ....	48
<b>FIGURE 1.52</b>	Interior explosion: when explosions occur within structures, pressures can build up within confined spaces, causing lightly attached wall, floor, and roof surfaces to be blown away. ....	49
<b>FIGURE 1.53</b>	Buckling of tall building under its own weight: (a) equivalent cantilever, (b) circular building, (c) rectangular building, and (d) equivalent channels to account for shear lag effects. ....	51
<b>FIGURE 2.1</b>	Common types of floor systems: (a) Two-way flat plate, (b) Two-way waffle, (c) Two-way flat slab with drops, (d) One-way beam and slab, (e) Skip joist wide module, (f) Two-way beam and slab, (g) One-way joist slab, and (h) One-way flat slab. ....	56
<b>FIGURE 2.2</b>	Relative form cost, live load = 125 psf. ....	57
<b>FIGURE 2.3</b>	Relative form cost, live load = 60 psf. ....	57
<b>FIGURE 2.4</b>	Influence of lumber dimension on site-cast concrete. Designing for nominal lumber dimensions results in economy. ....	58
<b>FIGURE 2.5</b>	Pilasters and wall columns. ....	59
<b>FIGURE 2.6</b>	Pour strip as a simple span supported by cantilevers. ....	60
<b>FIGURE 2.7</b>	Drop panel dimensions: (a) plan view and (b) section view. Dimensions $d$ , $x$ , and $y$ should remain constant throughout for maximum economy. ....	61
<b>FIGURE 2.8</b>	Soffit at the same horizontal level. ....	61
<b>FIGURE 2.9</b>	Band and narrow beams: Band beam, Section A, is more economical than narrow deep beam, Section B. ....	61
<b>FIGURE 2.10</b>	Suggested formwork dimensions for deep beams. ....	62
<b>FIGURE 2.11</b>	Beam haunches: (a) plan and (b) section. ....	62
<b>FIGURE 2.12</b>	Formwork for spandrel beams. Narrow and deep spandrels framing into columns result in more expensive formwork. ....	63
<b>FIGURE 2.13</b>	Suggestions for economical framing: (a) use locally available modulus, (b) maintain soffit at same elevation, and (c) step down wall thickness as shown in the figure. ....	64

<b>FIGURE 2.14</b>	Flat plate system. ....	66
<b>FIGURE 2.15</b>	Flat slab system. ....	66
<b>FIGURE 2.16</b>	Waffle system. ....	67
<b>FIGURE 2.17</b>	One-way joist system: (a) building plan and (b) Section A. ....	68
<b>FIGURE 2.18</b>	Skip joist system: (a) building plan and (b) Section A. ....	69
<b>FIGURE 2.19</b>	Skip joist system, another example: (a) plan view, (b) Section A, and (c) Section B. ....	69
<b>FIGURE 2.20</b>	Band beam system: (a) floor plan and (b) section. ....	70
<b>FIGURE 2.21</b>	Haunch girder-framing system. ....	71
<b>FIGURE 2.22</b>	Tapered haunch girder. ....	71
<b>FIGURE 2.23</b>	Hammerhead haunch girder. ....	71
<b>FIGURE 2.24</b>	10 m × 20 m (32.81 ft × 65.62 ft) gird; haunch girder with transverse beams: Plan. ....	72
<b>FIGURE 2.25</b>	Section AA: haunch girder elevation. ....	73
<b>FIGURE 2.26</b>	Typical frame design strip. ....	75
<b>FIGURE 2.27</b>	Equivalent frame concept, N–S direction. ....	75
<b>FIGURE 2.28</b>	Moment transfer through torsion. ....	76
<b>FIGURE 2.29</b>	Formation of yield lines. Yielding starts in regions of high moment and spreads to areas that are still elastic. ....	77
<b>FIGURE 2.30</b>	Yield-line design example. (a) Yield-line at center span. (b) Yield-line rotations. ....	78
<b>FIGURE 2.31</b>	Yield-line design example. (a) Yield line at a varter span. (b) Yield-line rotations. ....	79
<b>FIGURE 2.32</b>	Yield-line patterns. (a) Simply supported slab with uniformly distributed load. (b) Same as (a) but with built-in edges. (c) Equilateral, triangular simply supported slab with uniformly distributed load. (d) same as (b) but with built-in edges. ....	81
<b>FIGURE 2.33</b>	Yield-line analysis of simply supported square slab: (a) yield lines and (b) yield-line rotations. ....	81
<b>FIGURE 2.34</b>	Stress distribution in deep beams: (a) $l/h = 4$ , (b) $l/h = 2$ , (c) $l/h = 1$ , and (d) $l/h < 1.0$ . ....	84
<b>FIGURE 2.35</b>	Example of Saint-Venant's principle: pinched region is similar to the discontinuity, D, region (ACI 318-08, Appendix A). Regions away from D are bending, B, regions. ....	86
<b>FIGURE 2.36</b>	Strut-and-tie terminology: (a) strut-and-tie model (b) C-C-C node resisting three compressive forces (c) and (d) C-C-T nodes resisting two compressive, and one tensile force. ....	86
<b>FIGURE 2.37</b>	Strut-and-tie model: Node and element identification. ....	88

<b>FIGURE 2.38</b>	Strut-and-tie model: (a) C-C-C node and (b) C-C-T node. ....	88
<b>FIGURE 2.39</b>	Member stress limits and effective widths. ....	89
<b>FIGURE 2.40</b>	Factored forces and design strengths. ....	89
<b>FIGURE 2.41</b>	Stress ratios. ....	89
<b>FIGURE 2.42</b>	Design Summary. <i>Note:</i> Struts E4, E5, and E6 are transfer column and supporting columns. Nodes N4, N5, and N6 are at the face of transfer column and supporting columns. ....	90
<b>FIGURE 2.43</b>	Transfer girder-schematic reinforcement. ....	91
<b>FIGURE 2.44</b>	One-way slab example: (a) typical 1 ft strip; (b) slab modeled as a continuous beam; and (c) design moments. ....	92
<b>FIGURE 2.45</b>	ACI coefficients for positive moments: (a) interior span, (b) exterior span, discontinuous end integral with supports, and (c) exterior span, discontinuous end unrestrained. ....	93
<b>FIGURE 2.46</b>	ACI coefficients for negative moments: (a) at interior supports; (b) at exterior face of first interior support, more than two spans; and (c) at exterior face of first interior support, two spans. ....	94
<b>FIGURE 2.47</b>	Design example, one-way slab: (a) partial floor plan and (b) section. See Figure 2.44 for dimensions and loading. ....	95
<b>FIGURE 2.48</b>	T-beam design example. ....	98
<b>FIGURE 2.49</b>	Shear reinforcement. ....	102
<b>FIGURE 2.50</b>	Interior span moments. ....	104
<b>FIGURE 2.51</b>	Exterior span moments. ....	105
<b>FIGURE 2.52</b>	Design example: Two-way slab. ....	106
<b>FIGURE 2.53</b>	Two-way posttensioned flat plate system. ....	119
<b>FIGURE 2.54</b>	Band-beam system. ....	119
<b>FIGURE 2.55</b>	Cracking in PT slab caused by restraint of perimeter walls. ....	120
<b>FIGURE 2.56</b>	Recommended distance between pour strips. 1. 150 ft $\pm$ typical. 2. 200 ft $\pm$ if restraint is minimal. 3. 300 ft $\pm$ maximum length PT slab irrespective of the number of pour strips. ....	121
<b>FIGURE 2.57</b>	Method of minimizing restraining forces: (a) temporary sliding joint, (b) sleeves around rebar dowels, (i) section and (ii) plan, and (c) temporary pour strips: (i) at perimeter of building; (ii) at interior of slab. ....	121
<b>FIGURE 2.58</b>	Concept of secondary moments: (a) two-span continuous beam, (b) vertical upward displacement due to PT, (c) primary moment, (d) reactions due to PT, (e) secondary moment, and (f) final moments. ....	124
<b>FIGURE 2.59</b>	Secondary moment example 2A: (a) Two-span continuous prestressed beam, (b) equivalent loads due to prestress, consisting of upward load, horizontal compression due to prestress $W_p$ and downward loads at A, B, and C, (c) shear force diagram, statically indeterminate beam, (d) moment diagram, statically indeterminate beam, (e) primary shear force diagram, (f) primary moment diagram, and (h) secondary moments. ....	126

<b>FIGURE 2.60</b>	Secondary moment: Compatibility method: Example 2B. (a) two-span continuous beam, (b) equivalent loads, (c) upward deflection $\Delta_1$ due to $W_p$ , (d) downward deflection $\Delta_2$ due to a load of 66.15 kip at center span, (e) load $P_s$ corresponding to $\Delta_1$ – $\Delta_2$ , and (f) secondary moments. ....	129
<b>FIGURE 2.61</b>	Secondary moment: Example 2C: (a) two-span continuous beam, (b) equivalent moment $M = Pe$ at center of span, (c) equivalent loads and moments, (d) upward deflection $\Delta_1$ due to $W_p$ , (e) downward deflection $\Delta_2$ due to a load of 66.15 at center of span, (f) downward deflection $\Delta_3$ due to moments $M = Pe$ at center of span, (g) load $P_s$ corresponding to $\Delta_1$ – $\Delta_2$ – $\Delta_3$ , and (h) secondary moments. ....	131
<b>FIGURE 2.62</b>	Idealized stress–strain curve (Adapted from <i>Posttensioning Concrete Institute Design Handbook</i> , 5th Edn.) Typical stress-strain curve with seven-wire low-relaxation prestressing strand. These curves can be approximated by the following equations:	
	<div style="display: flex; justify-content: space-around;"> <div style="text-align: center;"> <p>250 ksi</p> <math display="block">\epsilon_{ps} \leq 0.0076: f_{ps} = 28,500 \epsilon_{ps} \text{ (ksi)}</math> <math display="block">\epsilon_{ps} &gt; 0.0076: f_{ps} = 250 - \frac{0.04}{\epsilon_{ps} - 0.0064} \text{ (ksi)}</math> </div> <div style="text-align: center;"> <p>270 ksi</p> <math display="block">\epsilon_{ps} \leq 0.0086: f_{ps} = 28,500 \epsilon_{ps} \text{ (ksi)}</math> <math display="block">\epsilon_{ps} &gt; 0.0086: f_{ps} = 270 - \frac{0.04}{\epsilon_{ps} - 0.007} \text{ (ksi)}</math> </div> </div>	134
<b>FIGURE 2.63</b>	Strength design example 1: beam section. ....	135
<b>FIGURE 2.64</b>	Example 1: strain diagram, first trial. ....	135
<b>FIGURE 2.65</b>	Example 1: strain diagram, second trial. ....	136
<b>FIGURE 2.66</b>	Example 1: force diagram. ....	137
<b>FIGURE 2.67</b>	Example 2: strain diagram, first trial. ....	138
<b>FIGURE 2.68</b>	Example 2: strain diagram, second trial. ....	139
<b>FIGURE 2.69</b>	Example 3: prestressed T-beams. ....	140
<b>FIGURE 2.70</b>	Example 3: strain diagram, first trial. ....	141
<b>FIGURE 2.71</b>	Example 3: strain diagram, second trial. ....	141
<b>FIGURE 2.72</b>	Posttensioned transfer girder: (a) elevation and (b) section. ....	145
<b>FIGURE 2.73</b>	Load balancing concept; (a) beam with parabolic tendon; and (b) free-body diagram. ....	148
<b>FIGURE 2.74</b>	Equivalent loads and moments due to sloped tendon: (a) upward uniform load due to parabolic tendon; (b) constant moment due to straight tendon; (c) upward uniform load and end moments due to parabolic tendon not passing through the centroid at the ends; and (d) vertical point load due to sloped tendon. ....	148
<b>FIGURE 2.75</b>	Preliminary design: simple span beam. ....	150
<b>FIGURE 2.76</b>	Tendon profile in continuous beam: (a) simple parabolic profile and (b) reverse curvature in tendon profile. ....	152
<b>FIGURE 2.77</b>	Tendon profile: (a) typical exterior span and (b) typical interior span. ....	153

<b>FIGURE 2.78</b>	Equivalent loads due to prestress. ....	154
<b>FIGURE 2.79</b>	Example 1: one-way posttensioned slab. ....	154
<b>FIGURE 2.80</b>	Example 1: one-way moment diagram. ....	155
<b>FIGURE 2.81</b>	Example 1: one-way tendon profile; interior bay. ....	155
<b>FIGURE 2.82</b>	Characteristics of tendon profile. ....	156
<b>FIGURE 2.83</b>	Example 2: posttensioned continuous beam dimensions and loading. ....	161
<b>FIGURE 2.84</b>	Example 2: posttensioned continuous beam: service load moments. ....	162
<b>FIGURE 2.85</b>	Example 3: flat plate design: (a) span and loading and (b) elastic moments due to dead load. ....	164
<b>FIGURE 2.86</b>	End bay tendon profiles. ....	165
<b>FIGURE 2.87</b>	Anchorage of added tendons. ....	168
<b>FIGURE 2.88</b>	Example problem 3: flat plate, tendon profiles: (a) interior span; (b) exterior span, reverse curvature at right support; and (c) exterior span, reverse curvature at both supports. ....	169
<b>FIGURE 2.89</b>	Anchor device at distributed tendons: (a) dead end and (b) stressing end. ....	173
<b>FIGURE 2.90</b>	Anchor device at banded tendons; (a) dead end and (b) stressing end. ....	174
<b>FIGURE 2.91</b>	Construction joint with intermediate stressing. ....	174
<b>FIGURE 2.92</b>	Typical reinforcement of tendon band at slab edge or at intermediate stressing. ....	175
<b>FIGURE 2.93</b>	Placement of added tendon. ....	175
<b>FIGURE 2.94</b>	Flaring of banded tendons at slab edge. ....	176
<b>FIGURE 2.95</b>	Typical column-slab section. ....	176
<b>FIGURE 2.96</b>	Typical interior column. ....	177
<b>FIGURE 2.97</b>	Typical column section. ....	177
<b>FIGURE 2.98</b>	Typical drop panel section. ....	178
<b>FIGURE 2.99</b>	Foundation system for a corner column of an exterior X-braced tube building: (a) plan and (b) schematic section. ....	180
<b>FIGURE 2.100</b>	Foundation mat for a 25-story building: finite element idealization and column ultimate loads. ....	184
<b>FIGURE 2.101</b>	Vertical deflection of mat along section $x-x$ . ....	185
<b>FIGURE 2.102</b>	Bending moment variation along section $x-x$ . ....	185
<b>FIGURE 2.103</b>	Foundation mat for a proposed 85-story office building: (a) finite element idealization and (b) cross section $x-x$ . ....	186
<b>FIGURE 2.104</b>	Contact pressure contour, ksf: (a) dead plus live loads (b) dead plus live plus wind. <i>Note:</i> $K = 100 \text{ lb/in.}^3$ . ....	186
<b>FIGURE 2.105</b>	Flat slab with drop panels. ....	187
<b>FIGURE 2.106</b>	Beam and slab system 26 ft $\times$ 26 ft bays. ....	188

<b>FIGURE 2.107</b>	Beam and slab system 30 ft × 40 ft bays. ....	189
<b>FIGURE 2.108</b>	One-way joist (par joist) system 30 ft × 30 ft bays. ....	189
<b>FIGURE 2.109</b>	One-way joist system 30 ft × 40 ft bays. ....	190
<b>FIGURE 2.110</b>	One-way joist with constant depth girders 30 ft × 40 ft bays. ....	190
<b>FIGURE 2.111</b>	One-way skip joist with haunch girders 30 ft × 40 ft bays. ....	191
<b>FIGURE 2.112</b>	Waffle slab (two-way joist) system 30 ft × 30 ft bays. ....	191
<b>FIGURE 2.113</b>	Waffle slab (two-way joist) system 30 ft × 40 ft bays. ....	192
<b>FIGURE 2.114</b>	Posttensioned system for parking structure 20 ft × 60 ft bays. ....	192
<b>FIGURE 2.115</b>	Posttensioned flat plato 26 ft × 26 ft bays. ....	193
<b>FIGURE 2.116</b>	One-way solid slabs, unit quantities: (a) reinforcement and (b) concrete. ....	193
<b>FIGURE 2.117</b>	One-way pan joists, unit quantities: (a) reinforcement and (b) concrete. ....	194
<b>FIGURE 2.118</b>	Two-way slabs, unit quantities: (a) reinforcement and (b) concrete. ....	194
<b>FIGURE 2.119</b>	Waffle slabs, unit quantities: (a) reinforcement and (b) concrete. ....	195
<b>FIGURE 2.120</b>	Flat plates, unit quantities: (a) reinforcement and (b) concrete. ....	195
<b>FIGURE 2.121</b>	Flat slabs, unit quantities: (a) reinforcement and (b) concrete. ....	196
<b>FIGURE 2.122</b>	Unit quantity of reinforcement in columns. ....	197
<b>FIGURE 2.123</b>	Preliminary design and material quantities for floor systems. ....	198
<b>FIGURE 3.1</b>	Structural systems categories. ....	200
<b>FIGURE 3.2</b>	Response of flat slab-frames to lateral loads: Displacement compatibility between slab and walls. ....	202
<b>FIGURE 3.3</b>	Typical floor systems for flat slab-frames: (a) flat plate; (b) flat slab with drop panels; (c) two-way waffle system. ....	202
<b>FIGURE 3.4</b>	Flat slab-frame with shear walls. ....	204
<b>FIGURE 3.5</b>	Coupled shear walls. ....	204
<b>FIGURE 3.6</b>	Representation of coupled shear wall by continuum model: (a) Wall with openings. (b) Analytical model for close-form solution. ....	205
<b>FIGURE 3.7</b>	Rigid frame: Forces and deformations. ....	206
<b>FIGURE 3.8</b>	Shear wall–frame interaction. ....	206
<b>FIGURE 3.9</b>	Bending deformation of rigid frame: (a) Moment resisted by axial loads in columns. (b) Cantilever bending of shear wall. ....	207
<b>FIGURE 3.10</b>	Shear deflection analogy: The lateral deflections of a story-high rigid frame due to beam and column rotations may be considered analogous to the shear deflections of a story-high segment of a shear wall. ....	208
<b>FIGURE 3.11</b>	Story mechanism: Strong-column-weak beam requirement aims at preventing story mechanism. ....	209
<b>FIGURE 3.12</b>	Tube building with widely spaced perimeter columns. ....	210
<b>FIGURE 3.13</b>	Typical floor framing plan: Haunch girder scheme. ....	211
<b>FIGURE 3.14</b>	Haunch girder elevation and reinforcement. ....	211

<b>FIGURE 3.15</b>	Haunch girder section. ....	212
<b>FIGURE 3.16</b>	The Huntington. (Architects, Talbot Wilson & Associates; structural engineers, Walter P. Moore and Associates; contractor, W. S. Bellows Construction Corp.). ....	212
<b>FIGURE 3.17</b>	A 28-story haunch girder building, Houston, Texas. (a) Typical floor plan and (b) photograph. (Structural engineers, Walter P. Moore and Associates.) ...	213
<b>FIGURE 3.18</b>	Examples of core-supported buildings. (a) cast-in-place shear walls with precast surround; (b) shear walls with posttensioned flat plate, and (c) shear walls with one-way joist system. ....	214
<b>FIGURE 3.19</b>	Concrete core with steel surround. ....	214
<b>FIGURE 3.20</b>	Shear walls with perimeter frames. ....	215
<b>FIGURE 3.21</b>	Shear walls with interior frames. ....	216
<b>FIGURE 3.22</b>	Shear walls with outrigger girders. ....	216
<b>FIGURE 3.23</b>	Full depth interior shear walls acting as gaint K-brace. (a) Plan and (b) schematic section. ....	216
<b>FIGURE 3.24</b>	Example of shear wall–frame interaction: Typical floor plan. ....	218
<b>FIGURE 3.25</b>	Simplified analytical model of bygone era. With the availability of computer software, simplified methods are no longer in use. ....	219
<b>FIGURE 3.26</b>	Shear force distribution. ....	220
<b>FIGURE 3.27</b>	Example of shear wall–frame interaction: 50-Plus-story haunch girder—shear wall building. ....	220
<b>FIGURE 3.28</b>	Framing plans. (a) Levels 2 through 14 floor plan, (b) levels 15 through 26 floor plan, (c) levels 27 through 39 floor plan, (d) levels 40 through 47 floor plan, (e) levels 48 and 49 floor plan, and (f) levels 50 and 51 floor plan. ....	221
<b>FIGURE 3.29</b>	Distribution of shear forces. ....	224
<b>FIGURE 3.30</b>	Frame tube building. (a) Schematic plan and (b) isometric view. ....	225
<b>FIGURE 3.31</b>	Shear lag effects in a hollow tube structure: (a) cantilever tube subjected to lateral loads, (b) shear stress distribution, and (c) distortion of flange element caused by shear stresses. ....	226
<b>FIGURE 3.32</b>	Axial stress distribution in a square hollow tube with and without shear lag. ....	226
<b>FIGURE 3.33</b>	Free-form tubular configurations. ....	227
<b>FIGURE 3.34</b>	Shear lag in framed tube. ....	227
<b>FIGURE 3.35</b>	Cantilever box beam with two end channels. ....	228
<b>FIGURE 3.36</b>	Shear lag effects in T-beams flanges: (a) Cross-section of T beam. (b) Horizontal shear stresses between beam web and flange. (c) Nonuniform distribution of compressive stresses in flange. ....	229
<b>FIGURE 3.37</b>	Secondary frame action in an irregular tube; schematic axial forces in perimeter columns. ....	230



<b>FIGURE 3.38</b>	Exterior diagonal braces in a tall steel building. ....	231
<b>FIGURE 3.39</b>	Example of exterior diagonal tube: Onterie Center, Chicago, IL. ....	232
<b>FIGURE 3.40</b>	Bundled tube: schematic plan. ....	232
<b>FIGURE 3.41</b>	Schematics of bundled tubes. ....	233
<b>FIGURE 3.42</b>	One Magnificent Mile, Chicago, IL; structural system. ....	233
<b>FIGURE 3.43</b>	Burj Dubai, schematic plan. ....	234
<b>FIGURE 3.44</b>	Outrigger and belt wall system with centrally located core. ....	235
<b>FIGURE 3.45</b>	Outrigger and belt wall system with an offset core. ....	235
<b>FIGURE 3.46</b>	Vierendeel frames acting as outrigger and belt wall system. ....	236
<b>FIGURE 3.47</b>	Haunch girders as outriggers. ....	236
<b>FIGURE 3.48</b>	Cap wall system: (a) Plan. (b) Schematic section. ....	237
<b>FIGURE 3.49</b>	Outrigger located at top, $z = L$ . ....	238
<b>FIGURE 3.50</b>	Outrigger at quarter-height from top, $z = 0.75L$ . ....	240
<b>FIGURE 3.51</b>	Outrigger at midheight, $z = 0.5L$ . ....	241
<b>FIGURE 3.52</b>	Outrigger at quarter-height from bottom, $z = 0.25L$ . ....	242
<b>FIGURE 3.53</b>	Outrigger at distance $x$ from top. ....	243
<b>FIGURE 3.54</b>	Schematic plan of a steel building with outriggers and belt trusses at a single level. ....	245
<b>FIGURE 3.55</b>	Schematic plan of a concrete building with outriggers and belt walls at a single level. ....	246
<b>FIGURE 3.56</b>	Schematic section showing outriggers and belt walls at a single level. ....	246
<b>FIGURE 3.57</b>	Deflection index verses outrigger and belt wall location. <i>Note:</i> DI = Deflection without outrigger/Deflection with outrigger. ....	247
<b>FIGURE 3.58</b>	Structural schematics; building with outrigger and belt walls at two locations. ....	248
<b>FIGURE 3.59</b>	Analytical model of a building with outriggers and belt walls at two locations. ....	248
<b>FIGURE 3.60</b>	Method of analysis for two outrigger system: (a) Two-outrigger structure, (b) external moment diagram, (c) $M_1$ diagram, (d) $M_2$ diagram, and (e) core resultant moment diagram. ....	249
<b>FIGURE 3.61</b>	Deflection index verses belt wall and outrigger locations. ....	250
<b>FIGURE 3.62</b>	Optimum location of outriggers, (a) single outrigger, (b) two outriggers, (c) three outriggers, and (d) four outriggers. ....	251
<b>FIGURE 3.63</b>	Cellular tube with interior vierendeel frames. ....	251
<b>FIGURE 3.64</b>	Structural concept for supertall buildings. ....	252
<b>FIGURE 4.1</b>	Wind flow around buildings. ....	254
<b>FIGURE 4.2</b>	Wind velocity profiles as defined in the ASCE 7-05. Velocity profiles are determined by fitting curves to observed wind speeds. ....	257

<b>FIGURE 4.3</b>	Schematic record of wind speed measured by an anemometer. ....	258
<b>FIGURE 4.4</b>	Critical components of wind in aeronautical engineering. ....	261
<b>FIGURE 4.5</b>	Simplified wind flow consisting of along-wind and across-wind. ....	262
<b>FIGURE 4.6</b>	Vortex shedding: periodic shedding of vortices generates building vibrations in the transverse direction. ....	262
<b>FIGURE 4.7</b>	High pressures and suctions around building corners. ....	266
<b>FIGURE 4.8</b>	Pressure contours as measured in a wind tunnel test: (a) building elevation showing suction (negative pressures); (b) building elevation showing positive pressures. ....	268
<b>FIGURE 4.9</b>	Wind pressure diagram for cladding design: (a) block diagram relating measured pressures, psf, to building grid system; (b) pressures measured in wind tunnel, psf. ....	269
<b>FIGURE 4.10</b>	Wind speed map for United States and Alaska. (a) Map of the United States, (b) western Gulf of Mexico hurricane coastline (enlarged), (c) eastern Gulf of Mexico and southeastern United States hurricane coastline (enlarged), (d) mid- and north-Atlantic hurricane coastline (enlarged). (Adapted from ASCE 7-05). ....	271
<b>FIGURE 4.11</b>	Topographic factor $K_{zt}$ (From ASCE 7-05 Figure 6.4). ....	275
<b>FIGURE 4.12</b>	Topographic factor $K_{zt}$ based on equations. ....	276
<b>FIGURE 4.13</b>	External pressure coefficient $C_p$ with respect to plan aspect ratio $L/B$ : (a) $0 \leq L/B \leq 1$ ; (b) $L/B = 2$ ; (c) $L/B > 4$ . Linear variation permitted for leeward suction (see Figure 4.15). ....	277
<b>FIGURE 4.14</b>	Building elevation showing variation of $C_p$ : (a) $0 \leq L/B \leq 1$ , (b) $L/B = 2$ , and (c) $L/B > 4$ . ....	277
<b>FIGURE 4.15</b>	Leeward suction $C_p$ versus plan aspect ratio, $W/D$ . ....	278
<b>FIGURE 4.16</b>	Combined velocity pressure and exposure coefficients, $K_h$ and $K_z$ . ....	278
<b>FIGURE 4.17</b>	$K_z$ values for buildings up to 1500 ft tall. ....	279
<b>FIGURE 4.18</b>	Variation of positive velocity pressure, $q_z$ , versus wind speed and exposure categories. <i>Note:</i> Gust factor, $G_f$ , varies from 1.05 to 1.25. ....	281
<b>FIGURE 4.19</b>	Variation of velocity pressure, $q_z$ , versus wind speed. ....	282
<b>FIGURE 4.20</b>	Comparison of topographic effects, Exposure C, wind on narrow face. ....	283
<b>FIGURE 4.21</b>	Comparison of topographic effect, Exposure C, wind on broad face. ....	283
<b>FIGURE 4.22</b>	Variation of gust factor, $G_f$ . ....	289
<b>FIGURE 4.23</b>	Building period versus height. ....	302
<b>FIGURE 4.24</b>	Design wind pressure perpendicular to 200 ft wall. <i>Note:</i> $G_f = 1.24$ , $I_w = 1.15$ . ....	303
<b>FIGURE 4.25</b>	Design wind pressure perpendicular to 120 ft wall. <i>Note:</i> $G_f = 1.24$ , $I_w = 1.15$ . ....	304
<b>FIGURE 4.26</b>	External wind pressure coefficient $C_p$ . (Adapted from NBCC 2005.) ....	306

<b>FIGURE 4.27</b>	Exposure factor $C_{eH}$ . (From NBCC 2005.)	308
<b>FIGURE 4.28</b>	Background turbulence factor, $B$ , as a function of height and width of building. (From NBCC 2005.)	308
<b>FIGURE 4.29</b>	Size reduction factor, $s$ , as a function of width, height, and reduced frequency of the building. (From NBCC 2005.)	309
<b>FIGURE 4.30</b>	Gust energy ratio, $F$ , as a function of wave number. (From NBCC 2005.)	309
<b>FIGURE 4.31</b>	Peak factor, $g_p$ , as a function of average fluctuation rate. (From NBCC 2005.)	311
<b>FIGURE 4.32</b>	Wind induced peak accelerations; NBCC 2005 procedure: (a) 30-story building, wind on narrow face; (b) 30-story building, wind on broad face; (c) 60-story building with equal plan dimensions.	314
<b>FIGURE 4.33</b>	Schematics of 33 m-long wind tunnel; overall size 33 m $\times$ 2.4 m $\times$ 2.15 m.	315
<b>FIGURE 4.34</b>	Schematics of 64 m-long wind tunnel; over all size 64 m $\times$ 15 m $\times$ 6 m.	316
<b>FIGURE 4.35</b>	Schematics of two additional wind tunnels.	316
<b>FIGURE 4.36</b>	Photographs of rigid model in wind tunnel. Chifley Plaza, Sydney. (Courtesy of CPP Wind Engineering & Air Quality Consultants.)	316
<b>FIGURE 4.37</b>	Model in wind tunnel: DIFC Dubai. (Courtesy of CPP Wind Engineering & Air Quality Consultants.)	317
<b>FIGURE 4.38</b>	Close-up of model in wind tunnel: Pentominium, Dubai. (Courtesy of CPP Wind Engineering & Air Quality Consultants.)	317
<b>FIGURE 4.39</b>	Mode in wind tunnel: Shams, Dubai.	318
<b>FIGURE 4.40</b>	(a) Rigid model in wind tunnel. (b) Close-up of a rigid model. (Photos courtesy of Rowan, Williams, Davis, and Irwin, RWDI.)	318
<b>FIGURE 4.41</b>	Simple stick aeroelastic model.	323
<b>FIGURE 4.42</b>	Aeroelastic model.	323
<b>FIGURE 4.43</b>	Rigid aeroelastic model mounted as a flexible steel bar.	324
<b>FIGURE 4.44</b>	High-frequency force balance model.	324
<b>FIGURE 4.45</b>	Detail view of high-frequency force balance model: (a,b) Close-up view of instrumentation and (c) model.	325
<b>FIGURE 4.46</b>	Schematic of five-component force balance model.	325
<b>FIGURE 4.47</b>	Aeroelastic model: cutaway view.	326
<b>FIGURE 4.48</b>	Aeroelastic model with provisions for simulating torsion.	326
<b>FIGURE 4.49</b>	Aeroelastic model with rotation simulators.	327
<b>FIGURE 4.50</b>	Aeroelastic model; schematic section.	327
<b>FIGURE 4.51</b>	Aeroelastic model: (a) A proposed tower in Chicago and (b) close-up view of instrumentation.	328
<b>FIGURE 4.52</b>	Simple stick aeroelastic model.	328
<b>FIGURE 4.53</b>	Aeroelastic model.	329
<b>FIGURE 4.54</b>	Pedestrian reactions (a–d).	333

<b>FIGURE 4.55</b>	Measured peak accelerations for the Allied Bank Tower during hurricane Alicia. ....	336
<b>FIGURE 4.56</b>	Mode shapes using different units. (a) Mode dominated by translation, (b) mode dominated by twist. ....	337
<b>FIGURE 4.57</b>	Building typical floor plan. ....	338
<b>FIGURE 4.58</b>	Tabulation of building properties. ....	339
<b>FIGURE 4.59</b>	Modes shapes: (a) Modes 1, 2, and 3, (b) modes 4, 5, and 6. ....	341
<b>FIGURE 4.60</b>	Tabulation of dynamic properties. ....	343
<b>FIGURE 5.1</b>	Building behavior during earthquakes. ....	348
<b>FIGURE 5.2</b>	Schematic representation of seismic forces. ....	349
<b>FIGURE 5.3</b>	Concept of 100%g (1g). ....	351
<b>FIGURE 5.4</b>	Linear viscous damper. ....	351
<b>FIGURE 5.5</b>	Bilinear force–displacement hysteresis loop. ....	352
<b>FIGURE 5.6</b>	Plan irregularities: (a) geometric irregularities, (b) irregularity due to mass-resistance eccentricity, and (c) irregularity due to discontinuity in diaphragm stiffness. ....	356
<b>FIGURE 5.7</b>	Elevation irregularities: (a) abrupt change in geometry, (b) large difference in floor masses, and (c) large difference in story stiffnesses. ....	357
<b>FIGURE 5.8</b>	Diaphragm drag and chord reinforcement for north–south seismic loads. ....	358
<b>FIGURE 5.9</b>	Diaphragm web failure due to large opening. ....	359
<b>FIGURE 5.10</b>	Hysteric behavior: (a) curve representing large energy dissipation and (b) curve representing limited energy dissipation. ....	360
<b>FIGURE 5.11</b>	Examples of nonuniform ductility in structural systems due to vertical discontinuities. (Adapted from SEAOC Blue Book, 1999 Edition.). ....	361
<b>FIGURE 5.12</b>	Reentrant corners in L-, T-, and H-shaped buildings. (As a solution, add collector elements and/or stiffen end walls.) ....	364
<b>FIGURE 5.13</b>	Idealized SDOF system. ....	365
<b>FIGURE 5.14</b>	Undamped free vibrations of SDOF system. ....	365
<b>FIGURE 5.15</b>	Damped free vibration of SDOF system. ....	365
<b>FIGURE 5.16</b>	Representation of a multi-mass system by a single-mass system: (a) fundamental mode of a multi-mass system and (b) equivalent single-mass system. ....	366
<b>FIGURE 5.17</b>	Graphical description of response spectrum. ....	367
<b>FIGURE 5.18</b>	Concept of response spectrum (a, b) buildings of varying heights and (c, d) pendulums of varying lengths. ....	368
<b>FIGURE 5.19</b>	Acceleration spectrum: El Centro earthquake. ....	369
<b>FIGURE 5.20</b>	Examples of SDOF systems: (a) elevated water tank. (b) Restaurant atop tall concrete core. Note from Figure 5.19, the acceleration = 26.25 ft/s <sup>2</sup> for $T = 0.5$ s and $\beta = 0.05$ (water tank), and the acceleration = 11.25 ft/s <sup>2</sup> for $T = 1.00$ s and $\beta = 0.10$ (restaurant). ....	369

<b>FIGURE 5.21</b>	Recorded ground acceleration: El Centro earthquake. ....	370
<b>FIGURE 5.22</b>	(a) Ground acceleration; (b) deformation response of three SDOF systems with $\beta = 2\%$ and $T_n = 0.5, 1, \text{ and } 2 \text{ s}$ ; and (c) deformation response spectrum for $\beta = 2\%$ . ....	372
<b>FIGURE 5.23</b>	Response spectra ( $\beta = 2\%$ ) for El Centro ground motion: (a) deformation response spectrum, (b) pseudo-velocity response spectrum, and (c) pseudo-acceleration response spectrum. ....	373
<b>FIGURE 5.24</b>	Pseudo-acceleration response of SDOF systems to El Centro ground motion. ....	375
<b>FIGURE 5.25</b>	Combined DVA response for El Centro ground motion; $\beta = 2\%$ . ....	376
<b>FIGURE 5.26</b>	Tripartite site-specific response spectra: (a) earthquake A, (b) earthquake B, (c) earthquake C, and (d) earthquake D. ....	377
<b>FIGURE 5.27</b>	Velocity, displacement, and acceleration readout from response spectra. ....	379
<b>FIGURE 5.28</b>	Idealized response spectrum for El Centro ground motion. ....	380
<b>FIGURE 5.29</b>	Schematic response of rigid and flexible systems. (a) Rigid system, acceleration at top is nearly equal to the ground acceleration; (b) flexible system, structural response is most directly related to ground displacement. ....	380
<b>FIGURE 5.30</b>	MCE ground motion for the United States, 0.2 s. Spectral response acceleration, $S_s$ , as a percent of gravity, site class B with 5% critical damping. ....	387
<b>FIGURE 5.31</b>	MCE ground motion for the United States, 1.0 s. Spectral response acceleration, $S_1$ , as a percent of gravity, site class B with 5% critical damping. ....	387
<b>FIGURE 5.32</b>	Design response spectrum. ....	389
<b>FIGURE 5.33</b>	Locations of cities cited in Tables 5.20, 5.21 and Figure 5.34. ....	414
<b>FIGURE 5.34</b>	Design response spectrum for selected cities in the United States. ....	415
<b>FIGURE 5.35</b>	Different systems used along two orthogonal axes; use appropriate value of $R$ for each system. ....	428
<b>FIGURE 5.36</b>	Different systems used over the height of a structure. The response modification coefficient, $R$ , for any story above, shall not exceed the lowest value, in the direction under consideration. ....	428
<b>FIGURE 5.37</b>	(a) Highly redundant structure and (b) not-so-redundant structure. ....	447
<b>FIGURE 5.38</b>	Permitted analysis procedures for seismic design. (Developed from ASCE 7-05, Table 12.6-1.) ....	453
<b>FIGURE 5.39</b>	Tributary weights for seismic dead-load calculation. ....	456
<b>FIGURE 5.40</b>	Column deformation for use in compatibility considerations. Deformation of column = building deflection $\Delta_b$ + diaphragm deflection $\Delta_p$ . (Adapted from SEAOC Blue Book, 1999 edition.) ....	462

<b>FIGURE 5.41</b>	Deformation compatibility consideration of foundation flexibility. (Adapted from SEAOC Blue Book, 1999 edition.)	463
<b>FIGURE 5.42</b>	Eccentric collector: $F_c$ is the axial force concentric to wall and $F_e$ is the axial force eccentric to wall.	466
<b>FIGURE 5.43</b>	Diaphragm design example: (a) floor plan, (b) equivalent loads due to primary diaphragm action, (c) equivalent loads due to torsional effects, (d) final equivalent loads (= (b) + (c)), (e) shear diagram, and (f) bending moment diagram.	469
<b>FIGURE 5.44</b>	Summary of unit shears.	472
<b>FIGURE 5.45</b>	Two-story example: dynamic analysis hand calculations.	479
<b>FIGURE 5.46</b>	Vibration modes, two-story example: (a) first mode and (b) second mode.	482
<b>FIGURE 5.47</b>	Distribution of modal shears: (a) first mode and (b) second mode.	487
<b>FIGURE 5.48</b>	Three-story building example: dynamic analysis.	488
<b>FIGURE 5.49</b>	Three-story building: response spectrum.	489
<b>FIGURE 5.50</b>	Three-story building: modal analysis to determine base shears.	490
<b>FIGURE 5.51</b>	Three-story building: modal analysis to determine story forces, accelerations, and displacements.	491
<b>FIGURE 5.52</b>	Three-story building: comparison of modal story shears and the SRSS story shears.	491
<b>FIGURE 5.53</b>	Seven-story building example: dynamic analysis.	492
<b>FIGURE 5.54</b>	Response spectrum for seven-story building example: (a) acceleration spectrum, (b) tripartite diagram, and (c) response spectra numerical representation.	493
<b>FIGURE 5.55</b>	Seven-story building: modal analysis to determine base shears.	494
<b>FIGURE 5.56</b>	Seven-story building: first-mode forces and displacements.	495
<b>FIGURE 5.57</b>	Seven-story building: second-mode forces and displacements.	496
<b>FIGURE 5.58</b>	Seven-story building: third-mode forces and displacements.	497
<b>FIGURE 5.59</b>	Seven-story building, modal analysis summary: (a) modal story forces, kip; (b) modal story shears, kip; (c) modal story overturning moments, kip-ft; (d) modal story accelerations, $g$ ; and (e) modal lateral displacement, inches.	498
<b>FIGURE 5.60</b>	Time-load functions. (a) Rectangular pulse (b) triangular pulse and (c) constant force with finite rise time. <i>Note:</i> $F_t$ = Load function, $t_d$ = time function.	499
<b>FIGURE 5.61</b>	Dynamic response of a cantilever. <i>Note:</i> Dynamic Load Factor, DLF, is equal to 2.0 for a load applied instantaneously.	499
<b>FIGURE 5.62</b>	Dynamic load factor, DLF, for common time-load functions. $t_d$ = time duration of pulse, $T$ = fundamental period of the system to which load is applied.	500
<b>FIGURE 5.63</b>	Cantiveler column with weight at top.	501

<b>FIGURE 5.64</b>	Acceleration response spectrum. ....	502
<b>FIGURE 5.65</b>	Single-bay single-story portal frame. ....	505
<b>FIGURE 5.66</b>	Analytical models for SDOF system: (a) model in horizontal position and (b) model in vertical position. ....	506
<b>FIGURE 5.67</b>	Damped oscillator: (a) analytical model and (b) forces in equilibrium. ....	506
<b>FIGURE 5.68</b>	MDOF: (a) multistory analytical model with lumped masses. ....	509
<b>FIGURE 5.69</b>	Generalized displacement of a simply supported beam: (a) loading, (b) full-sine curve, (c) half-sine curve, (d) one-third-sine curve, and (e) one-fourth-sine curve. ....	512
<b>FIGURE 5.70</b>	Two-story lumped-mass system illustrating Betti's reciprocal theorem: (a) lumped model, (b) forces during first mode of vibration, and (c) forces acting during second mode of vibration. ....	512
<b>FIGURE 5.71</b>	Two-story shear building, free vibrations: (a) building with masses, (b) mathematical model, and (c) free-body diagram with masses. ....	514
<b>FIGURE 5.72</b>	Major earthquake faults in California. ....	520
<b>FIGURE 6.1</b>	Shear strength of joints. ....	527
<b>FIGURE 6.2</b>	Structural integrity reinforcement in flat slabs without beams. ....	530
<b>FIGURE 6.3</b>	Structural integrity reinforcement in joists. ....	530
<b>FIGURE 6.4</b>	Integrity reinforcement in perimeter beams: (a) perimeter beam elevation and (b) Section 1. ....	531
<b>FIGURE 6.5</b>	Integrity reinforcement in beams other than perimeter beams. ....	531
<b>FIGURE 6.6</b>	IMRF: flexural reinforcement requirements for frame beams. ....	536
<b>FIGURE 6.7</b>	IMRF: transverse reinforcement requirements for frame beams. ....	536
<b>FIGURE 6.8</b>	IMRF: transverse reinforcement requirements for frame columns. ....	537
<b>FIGURE 6.9</b>	Seismic detailing requirements for two-way slabs in areas of moderate seismic risk; flat slab-beams not permitted in UBC zones 3 and 4, or for buildings assigned to SDC C, D, E, or F. ....	538
<b>FIGURE 6.10</b>	Seismic detailing requirements for two-way slabs in areas of moderate seismic risk: column strip. ....	539
<b>FIGURE 6.11</b>	Seismic detailing requirements for two-way slabs in areas of moderate seismic risk: middle strip. ....	539
<b>FIGURE 6.12</b>	Frame beam: general requirements, special moment frame. ....	540
<b>FIGURE 6.13</b>	Frame beam: transverse reinforcement requirements, special moment frame. ....	542
<b>FIGURE 6.14</b>	Arrangement of hoops and crossties: frame beams; special moment frame. ....	543
<b>FIGURE 6.15</b>	Frame column: detailing requirements, special moment frame. ....	544
<b>FIGURE 6.16</b>	Examples of minimum transverse reinforcement in frame columns of SMRF. <i>Note:</i> $f'_c = 5$ ksi, $f_y = 60$ ksi. Vertical spacing of ties = 4 in. Ties #5 for 24 in. $\times$ 24 in. and 30 in. $\times$ 30 in. columns. #4 for 38 in. $\times$ 38 in. and 44 in. $\times$ 44 in. columns. ....	545

<b>FIGURE 6.17</b>	Ductile frame, SMRF: schematic reinforcement detail. ....	547
<b>FIGURE 6.18</b>	Frame beam and column example; OMF: (a) plan and (b) elevation. ....	555
<b>FIGURE 6.19</b>	Design example, frame beam; OMF. For this example problem, although by calculations no shear reinforcement is required in the midsection of the beam, it is good practice to provide #3 four-legged stirrups at 15 in. spacing. ....	557
<b>FIGURE 6.20</b>	Design example, frame column; OMF. ....	559
<b>FIGURE 6.21</b>	Frame beam and column example; IMF. ....	559
<b>FIGURE 6.22</b>	Design example, frame beam; IMF. ....	561
<b>FIGURE 6.23</b>	Design example, frame column; OMF. <i>Note:</i> $\ell_o$ is the same as for columns of SMRF. There is no requirement to splice column bars at mid-height. ....	563
<b>FIGURE 6.24</b>	Shear wall: low-to-moderate seismic zones (SDC A, B, or C). <i>Note:</i> Vertical reinforcement of #7 @ 9 in. at each end is enclosed by lateral ties, since the reinforcement area of eight #7 vertical bars equal to $8 \times 0.6 = 4.8 \text{ in.}^2$ is greater than 0.01 times the area of concrete = $12 \times 30 = 360 \text{ in.}^2$ (see ACI 318-05 Section 14.3.6). ....	564
<b>FIGURE 6.25</b>	Design example, frame beam; special moment frame. ....	570
<b>FIGURE 6.26</b>	Design example, frame column; special moment frame. ....	571
<b>FIGURE 6.27</b>	Column panel shear forces. ....	575
<b>FIGURE 6.28</b>	Beam–column joint analysis: (a) forces and moments, case 1; (b) forces and moments, case 2; (c) resolved forces, case 1; and (d) resolved forces, case 2. ....	576
<b>FIGURE 6.29</b>	Beam–column joint; special moment frame. Transverse reinforcing in the joint is the same as for the frame column. A 50% reduction is allowed if the joint is confined on all the four faces. Maximum spacing of transverse reinforcement is equal to 6 in. ....	577
<b>FIGURE 6.30</b>	Design example; partial shear wall elevation and plan. ....	578
<b>FIGURE 6.31</b>	(a) Shear wall load/moment interaction diagram and (b) cross section of wall. ....	582
<b>FIGURE 6.32</b>	Shear wall example; schematic reinforcement. ....	585
<b>FIGURE 6.33</b>	Wall elevation showing schematic placement of reinforcement. ....	587
<b>FIGURE 6.34</b>	Coupled shear walls: (a) partial elevation and (b) plan. ....	588
<b>FIGURE 6.35</b>	Geometry for calculating $\alpha$ , the angle between the diagonal reinforcement and the longitudinal axis of the coupling beam. <i>Note:</i> $\tan \alpha = h/2 - x/\cos \alpha/\ell_n/2$ (solve for $\alpha$ by trial and error). ....	590
<b>FIGURE 6.36</b>	Parameters for calculating diagonal beam reinforcement. ....	592
<b>FIGURE 6.37</b>	Coupling beam with diagonal reinforcement. Each diagonal reinforcement must consist of at least four bars with closely spaced ties. Use wider closed ties or crossties at central intersection. Use crossties to confine development length $\ell_d$ . ....	593



<b>FIGURE 6.38</b>	Section 1.1. Schematic section through coupling beam. The purpose of this sketch is to ensure that the wall is thick enough for the proper placement of wall and diagonal beam reinforcement and concrete. ....	594
<b>FIGURE 6.39</b>	(a) Wall pier W1, load/moment interaction diagram and (b) cross section of wall pier W1. ....	596
<b>FIGURE 6.40</b>	Schematic reinforcement layout for the wall pier, example 2. ....	599
<b>FIGURE 6.41</b>	Exterior joint detailing; schematics: (a) plan and (b) section. ....	599
<b>FIGURE 6.42</b>	Interior joint detailing; schematics: (a) plan and (b) section. ....	600
<b>FIGURE 6.43</b>	Beam bar placement. ....	601
<b>FIGURE 6.44</b>	SDC D, E, or F: Frame columns. ....	602
<b>FIGURE 6.45</b>	SDC D, E, or F: Gravity columns in which induced moments and shears due to deformation compatibility, combined with factored gravity moments and shears do not exceed design moments and shears. ....	602
<b>FIGURE 6.46</b>	Typical caisson detail. ....	603
<b>FIGURE 6.47</b>	SDC C: Frame columns and, SDC D, E, or F: Gravity columns, that is, columns not designed as part of a lateral system in which: (1) Induced moment or shear due to deformation compatibility exceeds design moment or shear. (2) Induced moments and shears to deformation compatibility are not calculated. ....	604
<b>FIGURE 6.48</b>	Design shears for IMFs: (a) moment frame, (b) loads on frame beams, (c) beam shear, (d) loads on frame columns, and (e) column shear. ....	607
<b>FIGURE 6.49</b>	Two-way slabs: Effective width concept placement for reinforcement: (a) corner column and (b) interior column. ....	608
<b>FIGURE 6.50</b>	Reinforcement placement in two-way slabs without beams. (Applies to both top and bottom reinforcement.) <i>Note:</i> $h$ = slab thickness. ....	608
<b>FIGURE 6.51</b>	Two-way slabs: Arrangement of reinforcement in (a) column and (b) middle strips. ....	609
<b>FIGURE 6.52</b>	Definition of effective width of wide beams for placement of transverse reinforcement: (a) plan and (b) Section A-A. ....	610
<b>FIGURE 6.53</b>	Design shears for special moment frames: (a) moment frame, (b) loads on frame beams (same as for IMFs), (c) beam shear, (d) loads on frame columns, and (e) column shear. ....	612
<b>FIGURE 6.54</b>	Diagonal reinforcement in coupling beams. Detail 1: ACI 318-05 required confinement of individual diagonals. Detail 2: As an option, ACI 318-08 allows full-depth confinement of diagonals. ....	614
<b>FIGURE 6.55</b>	Coupling beam diagonal reinforcement. Detail 1: Confinement of individual diagonals: (a) elevation and (b) section. ....	615
<b>FIGURE 6.56</b>	Coupling beam diagonal reinforcement. Detail 2: Full-depth confinement of diagonals: (a) elevation and (b) section. ....	616
<b>FIGURE 7.1</b>	Idealized earthquake force–displacement relationships. ....	620
<b>FIGURE 7.2</b>	Superimposed diaphragm slab at an existing concrete wall. ....	625

<b>FIGURE 7.3</b>	Diaphragm chord for existing concrete slab. ....	625
<b>FIGURE 7.4</b>	Strengthening of openings in a superimposed diaphragm; (a) Section, (b) Plan. ....	626
<b>FIGURE 7.5</b>	New chords at reentrant corners. ....	626
<b>FIGURE 7.6</b>	Common methods for upgrading buildings with open storefronts. ....	631
<b>FIGURE 7.7</b>	(N) openings in an (E) 3-story concrete shear wall building. The seismic upgrade consisted of providing concrete overlay to restore shear capacity of walls and adding boundary elements around (N) openings: (a) wall elevation, (b) concrete overlay with (N) beam below (E) slab; (c) concrete overlay with (N) beam above (E) slab, (d) plan detail at (N) boundary element. <i>Note:</i> (E), existing, (N), new. ....	670
<b>FIGURE 7.8</b>	Seismic upgrade of a concrete hospital building with an external concrete moment frame. Modifications were restricted to the periphery of the building to keep the building operational. (a) Plan showing (N) foundations, (N) concrete overlay in the transverse direction, and (N) moment frames in the longitudinal direction. (b) Enlarged plan at (N) coupling beam and shear wall overlay. (c) Section through longitudinal frame. (d) Section through transverse wall. (e) Connection between (N) and (E) frame. ....	672
<b>FIGURE 7.9</b>	Fiber wrap of a transfer girder: (a) elevation and (b) section. ....	675
<b>FIGURE 7.10</b>	Strengthening of existing connecting beams in reinforced concrete walls. ....	676
<b>FIGURE 7.11</b>	Upgrading of an existing pile foundation. Add additional piles or piers, remove, replace, or enlarge existing pile caps. <i>Note:</i> Existing framing to be temporarily shored to permit removal of existing pile cap and column base plate. Drive new piles; weld new base plate and moment connection to column; pour new pile cap; and drypack under base plate. ....	677
<b>FIGURE 7.12</b>	Strengthening of an existing concrete frame building by adding (N) a reinforced concrete shear wall: (a) section a–a; (b) section b–b, and (c) elevation. ....	678
<b>FIGURE 7.13</b>	New concrete shear wall at existing slab. ....	679
<b>FIGURE 7.14</b>	Strengthening of existing reinforced concrete wall or piers. ....	679
<b>FIGURE 7.15</b>	Strengthening of existing reinforced concrete walls by filling in openings. ....	680
<b>FIGURE 7.16</b>	Jacketing of circular column. ....	680
<b>FIGURE 7.17</b>	Braced structural steel buttresses to strengthen an existing reinforced concrete building. ....	681
<b>FIGURE 7.18</b>	(a) Building plan showing locations of (N) steel props. (b) Section A; elevation of (N) steel prop. ....	682
<b>FIGURE 7.19</b>	Upgrading an existing building with external frames. ....	683
<b>FIGURE 8.1</b>	Empire State Building, New York City. ....	686
<b>FIGURE 8.2</b>	World Trade Center Twin Towers, New York City. ....	686
<b>FIGURE 8.3</b>	Petronas Towers, Kuala Lumpur. ....	687

<b>FIGURE 8.4</b>	Burj Dubai. ....	687
<b>FIGURE 8.5</b>	Monadock Building, Chicago. ....	689
<b>FIGURE 8.6</b>	Woolworth Building, New York City. ....	690
<b>FIGURE 8.7</b>	Chrysler Building, New York City. ....	690
<b>FIGURE 8.8</b>	Sears Tower, Chicago. ....	691
<b>FIGURE 8.9</b>	Rockefeller Center, New York City. ....	693
<b>FIGURE 8.10</b>	John Hancock Center, Chicago. ....	694
<b>FIGURE 8.11</b>	Chicago skyline. ....	695
<b>FIGURE 8.12</b>	Concept of premium for height. ....	697
<b>FIGURE 8.13</b>	Tubular system: Closely spaced exterior columns interconnected with deep spandrels. ....	701
<b>FIGURE 8.14</b>	(a) Transamerica Tower, San Francisco, California. (b) Transamerica Tower, schematic. ....	702
<b>FIGURE 8.15</b>	City Corp Building, New York City. ....	703
<b>FIGURE 8.16</b>	Structural system study: 62-story building. (a) Plan and (b) elevation. ....	706
<b>FIGURE 8.17</b>	Exterior braced tube: plan. ....	706
<b>FIGURE 8.18</b>	Isometric of exterior braced tube. ....	707
<b>FIGURE 8.19</b>	Isometric view of four-story high braced tube. ....	707
<b>FIGURE 8.20</b>	Interior cross bracing system: plan. ....	708
<b>FIGURE 8.21</b>	Isometric of interior cross bracing system. ....	708
<b>FIGURE 8.22</b>	Interacting framed tube and braced frame. ....	709
<b>FIGURE 8.23</b>	Isometric of framed tube and brace frame. ....	709
<b>FIGURE 8.24</b>	Framed tube with 10 and 15 ft column spacing. ....	710
<b>FIGURE 8.25</b>	Framed tube with 10 ft column spacing. ....	710
<b>FIGURE 8.26</b>	Twin-tube system with 10 ft column spacing. ....	711
<b>FIGURE 8.27</b>	Framed tube with 15 ft column spacing. ....	711
<b>FIGURE 8.28</b>	Twin-tube system with 15 ft column spacing. ....	712
<b>FIGURE 8.29</b>	Framed tube with 20 ft column spacing. ....	712
<b>FIGURE 8.30</b>	Twin-tube system with 20 ft column spacing. ....	712
<b>FIGURE 8.31</b>	Shear wall frame interacting system. ....	713
<b>FIGURE 8.32</b>	Moment frame and braced core system. ....	713
<b>FIGURE 8.33</b>	Outrigger and belt truss system: schematic plan. ....	714
<b>FIGURE 8.34</b>	Jumbo column scheme. ....	715
<b>FIGURE 8.35</b>	Structural concept of tall building. ....	719
<b>FIGURE 8.36</b>	Building shear resistance: (a) building must not break and (b) building must not have excessive shear deflection. ....	719

<b>FIGURE 8.37</b>	Bending resistance of building: (a) building must not overturn, (b) columns must not fail in tension or compression, and (c) bending deflection must not be excessive. ....	720
<b>FIGURE 8.38</b>	Building plan forms: (a) uniform distribution of columns and (b) columns concentrated at the edges. ....	721
<b>FIGURE 8.39</b>	Column layout and BRI: (a) square building with corner columns, BRI = 100; (b) traditional building of the 1930s, (c) modern tube building, BRI = 33; (d) Sears Towers, BRI = 33; (e) City Corp Tower, BRI = 31; (f) building with corner and core columns, BRI = 56; and (g) Bank of Southwest Tower, BRI = 63. ....	722
<b>FIGURE 8.40</b>	Tall building shear systems (a) shear wall system; (b) diagonal web system; (c) web system with diagonals and horizontals; (d–g) rigid frames. ....	723
<b>FIGURE 8.41</b>	Empire State Building, New York City. ....	725
<b>FIGURE 8.42</b>	South Walker Tower, Chicago, Illinois. ....	725
<b>FIGURE 8.43</b>	Miglin-Beitler Tower, Chicago: (a) elevation and (b) plan; (c) typical floor framing plan, and (d) lateral loads; (i) building elevation (ii) effective static wind pressure (iii) shear force and (iv) overturning moment. ....	726
<b>FIGURE 8.44</b>	Trump Tower, Chicago: (a) architectural rendering, (b) photograph, (c) 20th floor framing plan, (d) schematic elevation, (e) schematic section, (f) schematic 3-D. ....	728
<b>FIGURE 8.45</b>	Jin Mao Tower, Shanghai, China: (a) typical office floor framing plan; (b) structural system elevation. ....	732
<b>FIGURE 8.46</b>	Petronas Towers, Malaysia. (a) Elevation and (b) structural system plan. (c) Height comparison: (1) Petronas Towers and (2) Sears Tower, Chicago. ....	735
<b>FIGURE 8.47</b>	Central Plaza, Hong Kong: (a) elevation; (b, c) floor plans. ....	737
<b>FIGURE 8.48</b>	Singapore Treasury Building, Singapore: (a) schematic section and (b) typical floor framing plan. ....	739
<b>FIGURE 8.49</b>	City Spire, New York City. ....	741
<b>FIGURE 8.50</b>	NCNB Tower, North Carolina. ....	742
<b>FIGURE 8.51</b>	Museum Tower, Los Angeles: (a) building elevation; (b) lateral bracing system; (c) typical floor framing plan. ....	743
<b>FIGURE 8.52</b>	Vdara tower; MGM Block B, Las Vegas, Nevada: (a) floor plan and (b–d) construction photos. ....	745
<b>FIGURE 8.53</b>	City Bank Plaza, Hong Kong. ....	746
<b>FIGURE 8.54</b>	Trump Tower, New York City. ....	748
<b>FIGURE 8.55</b>	Two Prudential Plaza, Chicago. ....	749
<b>FIGURE 8.56</b>	Cent Trust Tower, Miami, Florida. (a) Schematic plan, (b) shear wall layout, and (c) column transfer. ....	750
<b>FIGURE 8.57</b>	Metropolitan Tower, New York City. (a, b) Framing plans. ....	752

<b>FIGURE 8.58</b>	Carnegie Hall Tower, New York City. (a, b) Framing plans. ....	753
<b>FIGURE 8.59</b>	Hopewell Center, Hong Kong. Schematic Plan. ....	754
<b>FIGURE 8.60</b>	Cobalt Condominiums, Minneapolis, Minnesota: (a) photograph of completed building, (b) erection of prestressed precast truss, (c) eighth floor framing plan, (d) interior truss, and (e) truss reinforcement details. ....	755
<b>FIGURE 8.61</b>	The Cosmopolitan Resort & Casino, Las Vegas, Nevada. (a) East tower, (b) West tower, (c–f) project photographs. ....	757
<b>FIGURE 8.62</b>	Elysian Hotel and Private Residences, Chicago. (a) Schematic foundation plan, (b) foundation bracing system, (c) mat foundation, (d) levels 5–10 post-tensioning plan, and (e) levels 30–34 post-tensioning plan. ....	762
<b>FIGURE 8.63</b>	Shangri La New York City (610 Lexington Avenue), New York City. (a) Schematic elevation, (b) structural system consists of (1) 10 in. thick conventionally reinforced concrete slab, (2) posttensioned shear walls, (3) concrete belt and hat walls, (c) typical floor framing plan, (d) core framing details, (e) high-rise tower connection to 10-story podium (f) schematics of folded pendulum tuned mass damper, TMD; two 375 t TMDs will be located on either side of the core, below the roof parapet. ....	765
<b>FIGURE 8.64</b>	Millennium Tower, 310 Mission Street, San Francisco, California: (a) Architectural rendering, (b) building plan, (c) isometric of shear walls and outriggers, (d) construction photograph, (e) outrigger reinforcement, (f) building section, (g) sloping columns, (h) test specimens (i) conventional hoops and ties, (j) welded reinforcement grid, (k) photograph of link beams, and (l) details of outrigger reinforcement. ....	769
<b>FIGURE 8.65</b>	Al Bateen Towers, Dubai, UAE: (a) upper residential and hotel tower framing plans, (b) mid-residential and hotel room framing plans, (c) lower-residential and hotel room framing plans, (d) garage section. (e) residential deflected shape (wind on broad face), (f) residential tower effective applied wind pressure versus height, (g) hotel tower effective applied wind pressure versus height, and (h) residential tower, 10-year inter-story drift. ....	774
<b>FIGURE 8.66</b>	SRZ Tower, Dubai, UAE: (a) 1st to 30th floor plan, (b) E-line elevation, (c) maximum stress in reinforced concrete core, (d) maximum stress in outrigger columns, (e) story shear (transverse direction), (f) overturning moment (transverse direction), (g) story shear (longitudinal direction), and (h) overturning moment (longitudinal direction). ....	779
<b>FIGURE 8.67</b>	The Four Seasons hotel and tower, Miami, Florida: (a) lower level framing plan; (b) Upper level framing plan, and (c) photograph. ....	784
<b>FIGURE 8.68</b>	Burj Dubai: (a) Boundary-layer wind-tunnel facility, (b) wind tunnel high frequency force balance model, (c) wind tunnel aeroelastic model, (d) wind tunnel cladding model, (e) pedestrian level wind study, (f) photograph, (g), schematic floor plan showing six major wind directions, and (h) view from top of Burj Dubai. ....	786
<b>FIGURE 8.69</b>	Comparative heights of several of the world's tallest buildings. ....	792
<b>FIGURE 9.1</b>	Schematics of viscoelastic damper. ....	794

<b>FIGURE 9.2</b>	Viscoelastic dampers in World Trade Center Towers. ....	794
<b>FIGURE 9.3</b>	Viscoelastic dampers, schematics. ....	795
<b>FIGURE 9.4</b>	Tuned mass damper (TMD) for City Corp, New York: (a) building elevation, (b) first-mode response, (c) TMD atop the building, and (d) plan. ....	797
<b>FIGURE 9.5</b>	Schematics of TMD, City Corp Center, New York. ....	797
<b>FIGURE 9.6</b>	Dual TMD: John Hancock Tower, Boston, MA. ....	798
<b>FIGURE 9.7</b>	Sloshing water damper, schematics. ....	798
<b>FIGURE 9.8</b>	Tuned liquid column dampers, TLCD, Wall Center, Vancouver, BC. ....	800
<b>FIGURE 9.9</b>	TLCD, Wall Center, Vancouver, BC. ....	801
<b>FIGURE 9.10</b>	Highcliff apartments, Hong Kong. ....	801
<b>FIGURE 9.11</b>	(a) Simple pendulum damper. (b) Hydraulic dampers attached to mass block. ....	802
<b>FIGURE 9.12</b>	Spherical tuned mass pendulum damper, TMPD, Taipei Financial Center. ....	802
<b>FIGURE 9.13</b>	Taipei 101, tuned mass pendulum damper: (a) TMPD, (b) TMPD principle, and (c) schematics. ....	803
<b>FIGURE 9.14</b>	(a) Simple pendulum damper. (b) Nested pendulum damper. ....	804
<b>FIGURE 9.15</b>	Design concept for base-isolated buildings. ....	805
<b>FIGURE 9.16</b>	Comparison of response of fixed-base and base-isolated building: (a) fixed-base and (b) base-isolated. ....	806
<b>FIGURE 9.17</b>	Moat around base-isolated building. ....	807
<b>FIGURE 9.18</b>	Moat detail at ground level. ....	808
<b>FIGURE 9.19</b>	Elastomeric isolators: (a) high-damping rubber bearing made by bonding rubber sheets to steel plates and (b) high-damping rubber bearing. ....	809
<b>FIGURE 9.20</b>	(a) Lead-rubber bearing under interior columns. (b) Lead-rubber bearing for an interior column for a five-story steel frame building: approximate dimensions. (c) Natural rubber bearing with press-fit lead core. ....	809
<b>FIGURE 9.21</b>	Single stage friction pendulum. ....	811
<b>FIGURE 9.22</b>	Sliding bearing: friction pendulum system base-isolation. ....	811
<b>FIGURE 9.23</b>	Friction pendulum system, details. ....	811
<b>FIGURE 9.24</b>	Installation details, FPS under existing interior columns. ....	812
<b>FIGURE 9.25</b>	Base isolator operating in concert with viscous damper. ....	812
<b>FIGURE 9.26</b>	(a) Base isolation: ASCE 7-05 nomenclature. (b) Isolator displacements: ASCE 7-05 definitions. ....	814
<b>FIGURE 9.27</b>	Isolator displacement terminology. ....	814
<b>FIGURE 9.28</b>	Idealized force–displacement relationship for base-isolation systems: (a) hysteretic system and (b) viscous system. ....	821

<b>FIGURE 9.29</b>	Fluid viscous damper consisting of a piston in a damping housing filled with a compound of silicone or similar type of fluid. ....	830
<b>FIGURE 9.30</b>	Example frame; dimensions and properties. ....	834
<b>FIGURE 9.31</b>	Portal method. (a) Moments and forces at roof level. (b) Moments and forces at level 15. (c) Moments and forces at level 2. ....	835
<b>FIGURE 9.32</b>	Cantilever method: (a) moments and forces at roof level, (b) moments and forces at level 29, (c) moments and forces at level 15, and (d) Moments and forces at level 2. ....	836
<b>FIGURE 9.33</b>	Moments and forces at (a) roof level, (b) level 29, (c) level 15, and (d) level 2. ....	838
<b>FIGURE 9.34</b>	Portal frame shear deflections: (a) Frame subjected to lateral loads and (b) typical story segment. ....	839
<b>FIGURE 9.35</b>	Lateral deflection due to bending of columns. ....	839
<b>FIGURE 9.36</b>	(a) Lateral deflection due to girder rotations and (b) deflection comparison (30-story frame). ....	840
<b>FIGURE 9.37</b>	Example portal frame for deflection calculations. ....	842
<b>FIGURE 9.38</b>	Equivalent cantilever. ....	843
<b>FIGURE 9.39</b>	Shear deformation of a cantilever of unit height $h$ . ....	843
<b>FIGURE 9.40</b>	Deflection comparison. ....	844
<b>FIGURE 9.41</b>	Infinitely rigid panel zones. ....	845
<b>FIGURE 9.42</b>	Framed tube: (a) axial stress distribution with shear lag and (b) axial stresses distribution in equivalent channels without shear lag. ....	846
<b>FIGURE 9.43</b>	Axial forces in tube columns assuming two equivalent curvilinear channels. ....	847
<b>FIGURE 9.44</b>	Axial forces in tube columns from three dimensional analysis of framed tube. ....	847
<b>FIGURE 9.45</b>	(a) Singly symmetrical shear wall. (b) Shear center $S$ as it relates to centroid $C$ . (c) Shear forces in flanges. (d) Shear center in a T-section shear wall. (e) Shear center concept; shear walls bending about a common neutral axis. ....	848
<b>FIGURE 9.46</b>	(a,b) Twisting of circular shaft. (c) Torsion failure of a brittle material by tension cracking along a $45^\circ$ helical surface. ....	852
<b>FIGURE 9.47</b>	Variation of torsional shear stresses in circular shaft. ....	852
<b>FIGURE 9.48</b>	Shear flow in a rectangular section. ....	852
<b>FIGURE 9.49</b>	Shear flow in thin-walled sections: load at shear center. ....	853
<b>FIGURE 9.50</b>	Shear center in C-section. ....	853
<b>FIGURE 9.51</b>	Shear stresses in hollow section: load at shear center. ....	854
<b>FIGURE 9.52</b>	Shear stresses in hollow rectangular section. ....	855

<b>FIGURE 9.53</b>	Shear flow in cellular sections: (a) load at shear center, (b) section rendered open with two cuts, (c) shear flows required for compatibility, and (d) final shear flow = (b) + (c). .....	855
<b>FIGURE 9.54</b>	(a) Warping of solid beams. (b) Thin rectangular beam: bending moment due to warping restraint. ....	856
<b>FIGURE 9.55</b>	Bimoment in wide flange column. ....	857
<b>FIGURE 9.56</b>	I-section core. ....	857
<b>FIGURE 9.57</b>	Core properties. ....	858
<b>FIGURE 9.58</b>	(a) Bending of flanges due to torque. (b) Shear forces due to warping torsion. ....	859
<b>FIGURE 9.59</b>	(a) Section profile, (b) sectorial coordinate $\omega_s$ diagram, (c) singly symmetric curve, (d) $\omega_s$ diagram, (e) $y$ -coordinate diagram, (f) principal sectional coordinates, and (g) sectorial coordinates for common profiles. ....	862
<b>FIGURE 9.60</b>	Calculation of sectorial properties: (a) cross section, (b) $\omega_p$ diagram, (c) $x$ -coordinate diagram, and (d) principal sectorial coordinate $\omega_s$ diagram. ....	866
<b>FIGURE 9.61</b>	Cantilever column of solid section: (a) vertical load at corner, (b) symmetrical axial loading, (c) bending about $x$ -axis, (d) bending about $y$ -axis, and (e) self-equilibrating loading producing bimoment. ....	868
<b>FIGURE 9.62</b>	I-shaped cantilever beam: (a) vertical load at a corner, (b) symmetrical axial loading, (c) bending about $x$ -axis, (d) bending about $y$ -axis, and (e) self-equilibrating loading producing bimoment. ....	869
<b>FIGURE 9.63</b>	Plan section of I-shaped column: (a) displacement of flanges due to bimoment load and (b) rotation due to geometric compatibility between flanges and web. ....	869
<b>FIGURE 9.64</b>	(a) Twin-core example. (b) Core properties. (c) $\omega_s$ diagram (sectorial coordinates). (d) Comparison of stresses: (i) bending stress $\sigma_b$ and (ii) warping stress $\sigma_\omega$ . ....	871
<b>FIGURE 9.65</b>	Torsion example; randomly distributed shear walls. (a) Plan, (b) Warping coordinates. (c) Axial stresses due to torsion. (d) Rotation comparison. ....	876
<b>FIGURE 9.66</b>	(a) $12 \times 12$ stiffness matrix for prismatic three-dimensional element, (b) coordinate axes, and (c) positive sign convention. ....	884
<b>FIGURE 9.67</b>	(a) $14 \times 14$ stiffness matrix for thin walled open section, (b) coordinate axes, and (c) positive sign convention. ....	885





# List of Tables

<b>TABLE 1.1</b>	Comparison of Flexural Reinforcement .....	13
<b>TABLE 2.1</b>	Minimum Thickness of Beams or One-Way Slabs Unless Deflections Are Computed .....	95
<b>TABLE 2.2</b>	Percentage of Positive Moment to Column Strip, Interior Span .....	104
<b>TABLE 2.3</b>	Percentage of Negative Moment to Column Strip at an Interior Support.....	104
<b>TABLE 2.4</b>	Percentage of Negative Moment to Column Strip at an Exterior Support.....	105
<b>TABLE 2.5</b>	Minimum Thickness of Slabs Without Interior Beams .....	107
<b>TABLE 2.6</b>	Approximate Span Depth Ratios for Posttensioned Systems.....	107
<b>TABLE 2.7</b>	Sample Unit Quantities for Hotels .....	114
<b>TABLE 2.8</b>	Unit Quantity of Reinforcement in Mat Foundations .....	196
<b>TABLE 2.9</b>	Unit Quantity of Reinforcement in Columns .....	197
<b>TABLE 4.1</b>	Probability of Exceeding Design Wind Speed during Design Life of Building....	261
<b>TABLE 4.2</b>	Terrain Exposure Constants.....	280
<b>TABLE 4.3</b>	Design Wind Pressures, Graphical Procedure Using ASCE 7-05 .....	291
<b>TABLE 4.4</b>	Buildings' Characteristics and Wind Environment .....	299
<b>TABLE 4.5</b>	Design Parameters for Example Buildings .....	300
<b>TABLE 4.6</b>	Comparison of Dynamic Response of Example Buildings.....	300
<b>TABLE 5.1</b>	Horizontal Structural Irregularities.....	362
<b>TABLE 5.2</b>	Vertical Structural Irregularities.....	363
<b>TABLE 5.3</b>	Occupancy Category of Buildings and Importance Factors .....	382
<b>TABLE 5.4</b>	Site Coefficient, $F_a$ .....	388
<b>TABLE 5.5</b>	Site Coefficient, $F_v$ .....	388
<b>TABLE 5.6</b>	Importance Factors.....	391
<b>TABLE 5.7</b>	Values of Approximate Period Parameters $C_t$ and $x$ .....	393
<b>TABLE 5.8</b>	Coefficient for Upper Limit on Calculated Period .....	393
<b>TABLE 5.9</b>	Design Coefficients and Factors for Seismic Force-Resisting Systems: ASCE 7-05.....	394
<b>TABLE 5.10</b>	Ordinary Reinforced Concrete Moment Frames: Seismic Factors .....	395
<b>TABLE 5.11</b>	Intermediate Reinforced Concrete Moment Frames: Seismic Factors.....	395
<b>TABLE 5.12</b>	Special Reinforced Concrete Moment Frames: Seismic Factors .....	395
<b>TABLE 5.13</b>	Ordinary Reinforced Concrete Shear Walls: Seismic Factors .....	396

<b>TABLE 5.14</b>	Special Reinforced Concrete Shear Walls: Seismic Factors .....	396
<b>TABLE 5.15</b>	Permitted Building Systems for Different SDC .....	397
<b>TABLE 5.16</b>	SDC Based on Short-Period Response Acceleration Parameter .....	399
<b>TABLE 5.17</b>	SDC Based on 1 s-Period Response Acceleration Parameter .....	399
<b>TABLE 5.18</b>	SDC Based on $S_{DI}$ and $S_1$ .....	401
<b>TABLE 5.19</b>	SDC Based on $S_{DS}$ and $S_1$ .....	402
<b>TABLE 5.20</b>	Approximate Base Shear as a Percent of Building Weight: Site Class D.....	406
<b>TABLE 5.21</b>	Approximate Base Shear as a Percent of Building Weight: Site Class C .....	410
<b>TABLE 5.22</b>	Allowable Story Drift, $\Delta_a^{a,b}$ .....	435
<b>TABLE 5.23</b>	Horizontal Irregularities .....	444
<b>TABLE 5.24</b>	Vertical Irregularities.....	445
<b>TABLE 5.25</b>	Requirements for Each Story Resisting More Than 35% of the Base Shear .....	450
<b>TABLE 5.26</b>	Permitted Analytical Procedures .....	452
<b>TABLE 6.1</b>	Design Criteria Comparison, ACI 318-05, Moment Frames.....	525
<b>TABLE 6.2</b>	Design Criteria Comparison, ACI 318-05, Shear Walls .....	526
<b>TABLE 6.3</b>	Design Bending Moments and Shear Forces for Frame Beam B3: OMF.....	556
<b>TABLE 6.4</b>	Design Axial Forces, Bending Moments, and Shear Forces for Frame Column C3: OMF.....	557
<b>TABLE 6.5</b>	Design Bending Moments and Shear Forces for B2: Special Moment Frame .....	558
<b>TABLE 7.1</b>	Rehabilitation Objectives.....	637
<b>TABLE 7.2</b>	Structural Performance Levels and Damage <sup>a,b,c</sup> —Vertical Elements.....	639
<b>TABLE 7.3</b>	Structural Performance Levels and Damage <sup>a,b</sup> —Horizontal Elements .....	640
<b>TABLE 7.4</b>	Effective Stiffness Values <sup>a</sup> .....	644
<b>TABLE 7.5</b>	Default Lower-Bound Tensile and Yield Properties of Reinforcing for Various ASTM Specifications and Periods <sup>a</sup> .....	650
<b>TABLE 7.6</b>	Default Lower-Bound Compressive Strength of Structural Concrete (psi) .....	651
<b>TABLE 7.7</b>	Factors to Translate Lower-Bound Material Properties to Expected Strength Material Properties .....	651
<b>TABLE 7.8</b>	Numerical Acceptance Criteria for Linear Procedures—Reinforced Concrete Beams.....	652
<b>TABLE 7.9</b>	Numerical Acceptance Criteria for Linear Procedures—Reinforced Concrete Columns .....	653
<b>TABLE 7.10</b>	Numerical Acceptance Criteria for Linear Procedures—Reinforced Concrete Beam—Column Joints .....	654
<b>TABLE 7.11</b>	Numerical Acceptance Criteria for Linear Procedures—Two-Way Slabs and Slab—Column Connections .....	655

<b>TABLE 7.12</b>	Numerical Acceptance Criteria for Linear Procedures—Reinforced Concrete Shear Walls and Associated Components Controlled by Flexure .....	656
<b>TABLE 7.13</b>	Numerical Acceptance Criteria for Linear Procedures—Reinforced Concrete Shear Walls and Associated Components Controlled by Shear .....	657
<b>TABLE 7.14</b>	Numerical Acceptance Criteria for Linear Procedures—Reinforced Concrete Infilled Frames .....	658
<b>TABLE 8.1</b>	Structural Cost and Column Density Comparison .....	717
<b>TABLE 9.1</b>	Lower-Bound Limits on Dynamic Procedures Specified in Relation to ELF Procedure Requirements .....	818
<b>TABLE 9.2</b>	Lateral Loads for 30-Story Building Shown in Figure 9.30.....	835
<b>TABLE 9.3</b>	Torsion Terminology.....	851
<b>TABLE 9.4</b>	Analogy between Bending and Warping Torsion.....	851
<b>TABLE 9.5</b>	Product Integral Tables .....	864
<b>TABLE 9.6</b>	Calculations for Integral $\omega_p dA$ .....	867
<b>TABLE 9.7</b>	Calculations for Sectorial Moment of Inertia .....	868
<b>TABLE 9.8</b>	Torsion Constants for Open Sections.....	881



---

# Foreword

In 1980, an ACI convention was convened in San Francisco. During the presentations, the qualities of concrete with respect to strength and durability were discussed, among other properties. It was clear from the reaction of the local audience that certain sections of the structural engineering profession believed and expressed their beliefs that concrete was not a viable product for seismic areas and loads.

However, during this convention, it became apparent that many representatives from other parts of the world were in fact determined to present this material as modern and capable of being a strong, durable, and flexible building product. The facts for such a large demonstration for concrete came from the Caribbean, South Africa, the Middle East, and most of Africa—all areas where structural steel cannot be easily procured.

Since then, we have witnessed the science of enhanced concrete properties. We have developed high-strength concrete from 10 to 14 ksi. We have learned that improved aggregates can create a variable modulus of elasticity. Tests have also shown that steel ratios are important in improving durability.

Having said this, we owe a great debt of gratitude to Dr. Taranath. He has created a state-of-the-art book on modern concrete systems, and environmental responses.

His introduction is worth the price of this book. He doesn't confine his expertise to concrete buildings; he expresses his concern about the state of the industry concerning our loss of judgment, and our sixth sense as engineers. His description of being able to smell a reasonable solution is really the same as what the great engineer Pier Luigi Nervi meant when he said there is no substitute for intuition. Intuition, that is, smell, is not an emotional response but rather that wonderful ability we have to accumulate experiences, and to bring them together at the proper time to create a solution.

I think one of the charming attributes of this book is that it reflects the writer in an easy, humorous way. Dr. Taranath expresses his concern for technology versus judgment and is undoubtedly a teacher with natural ability. This book reads like a novel. It first tackles simple issues and then works its way up to some esoteric topics. It covers performance-based designs as well as the most advanced science of seismic engineering and retrofitting.

The chapters in this book are rationally organized. Each chapter builds on the other. The beginning of each chapter discusses in detail the phenomenon the chapter deals with, for example, seismic systems, etc., and then it applies this phenomenon to concrete and concludes with several diagrams and details.

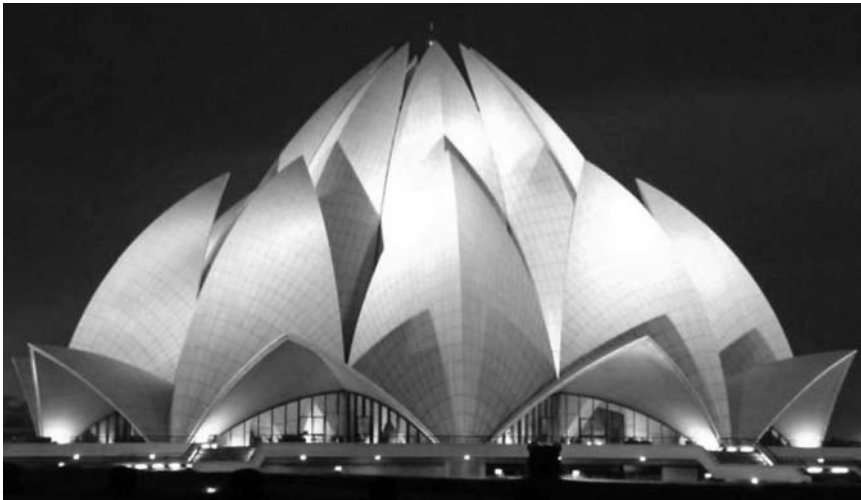
Dr. Taranath has turned concrete into a modern building material with modern systems. This book is complete and spectacular. There is no doubt that reinforced concrete is the most widely used building material in the world. Concrete can be as simple as local stone and cement, or as complex as aggregate, silica fume, and cement and admixtures. Concrete is used for block masonry in emerging nations and for super-high-rise buildings such as the wonderful Burj Dubai, which towers at 2,684 ft.

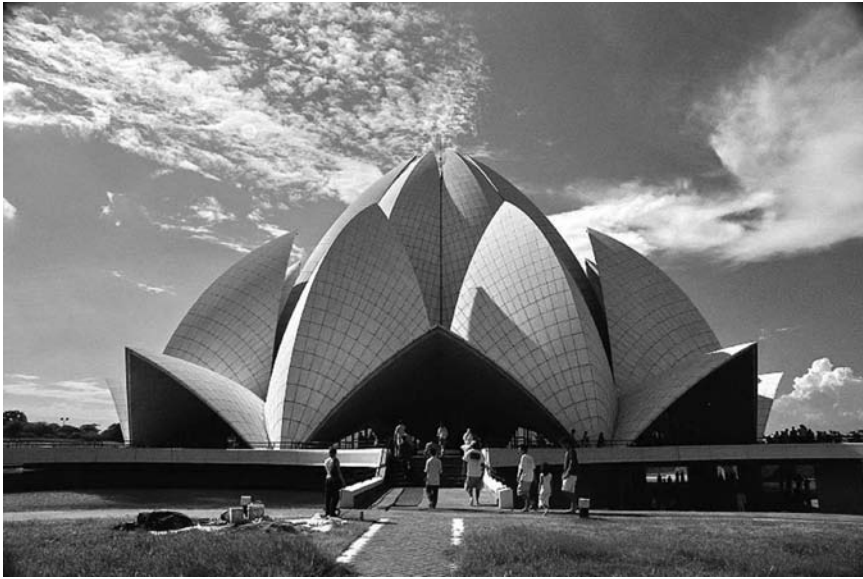
As a building product, it can be molded into any form that is required. Its production is safe, and there is no danger of molten fluids. Concrete, in the words of I.M. Pei, is a material with a soul. People are often puzzled by this statement. How can concrete have a soul? Concrete can be formed and shaped; it can have its color varied and its surface textured; it can be delivered by placement or pumping; and of all the modern building materials, it comes the closest to being able to replicate the Hagia Sophia or the Cathedral at Chartres. Thus, it has a soul.

One of the greatest concrete buildings is the Baha'i House of Worship in New Delhi, India. This temple was cast on wooden forms. The concrete was placed on the forms to resemble a giant lotus blossom—the icon for the sect. The Baha'i temple is approximately 131 ft high and comprises of 26 acres of land including surrounding gardens. The structure is absolutely amazing. The complexity of the building belies the nature of its construction; thousands of workers worked tirelessly taking filled concrete pans atop steep scaffoldings. It is easy to see how concrete can have a soul when you see this building.

Concrete is a common denominator throughout the world. It is found everywhere. When I designed the Jianguo Hotel in Beijing in 1978, we did not even have an ambassador to that country. The preferred material was reinforced concrete. There was no steel construction close enough to cater to this first American/Communist Chinese hotel in China. These were early times in the development of our nations, yet concrete was the vernacular that I and the number one construction company in Peking chose.

The Jianguo went up as a simple reinforced concrete-bearing wall structure. The forms were wood, the concrete locally produced, and the workforce from the surrounding city; thus a safe seismic-resistant egg crate was developed.





Lotus Temple—Bahá'í House of Worship, New Delhi, India. Built in 1986 using reinforced concrete, the Bahá'í House of Worship comprises of 27 freestanding concrete forms that cluster together to resemble a lotus flower. Architect: Fariborz Sahba. Structural Engineer: Flint & Neil Partnership.

The Northrup Avations Peace Hawk V program in Saudi Arabia demonstrated the versatility of concrete. The F-5 fighter program was supported by ground avionics. The facilities consisted of hangars, offices, aviation departments, and warehouses. The material and product used were concrete. This concrete, however, was made into concrete blocks with the use of a very primitive U.S. aid machine, which literally stamped the shape of an ASTM C-90 Block. These blocks were placed up to 20 ft high, reinforced in their cells, and grouted. I made a discovery at that time. Due to the variable nature of the ingredients in cements then (1976), we experienced unusual amounts of drying shrinkage. In order to avoid demolishing and removing these pavements and jet plane runways, it was decided to put a 6 in. sand dike around the concrete area and flood the area with water. The concrete was submerged for six days under water, resulting in a dense and translucent concrete that looked like marble. All the cracks were autogenously healed. The water was reintroduced into the hydration cycle of the concrete, mixed with unhydrated cement, and quickly refilled until the cracks could no longer be located other than thin marble-like veins, which, as in the human body, can be self-healing. Just as a human skeleton is strongest at a previous fracture, so too is concrete.

Because concrete is easily formed and shaped, its compression strength makes it the ideal material for shells of any nature. The work of Felix Candela in developing plates and shells wherein he spans 100 m with a 5 cm concrete shell truly opens the possibility for the free form Catia-driven shapes of Gehry Buildings in concrete.

Concrete is perfect for membrane stresses. The potential was realized in my design of the 120 ft diameter roof of the Lebanon Senior High School. This roof was flat and was spanned using a 20 in. thick hollow slab. This span and thickness of concrete were made possible by the fact that as a circular shell deflects, it creates compression in membrane stresses, thus minimizing the deflection. Dr. Timoshenko, the father of concrete plates and shells, shows that the span of a circular slab is represented by the radius of the circle rather than its diameter.

The grand dome of the Meridian Hotel in Chennai, India, was constructed using concrete. This dome was created by hundreds of workers who climbed scaffoldings with pans full of concrete on their heads. The dome was constructed in concentric rings. There were no doubt cold joints in the concrete, but the dome was in compression and the issue was minimized.



A dome was simultaneously being built in the Bahamas at Paradise Island's Atlantis Resort. This dome was built with two men instead of hundreds using balloon technology. A balloon was inflated with a 140 ft diameter and the balloon took on the form of the dome. This is an example of the same material being used with two totally different technologies, which clearly shows the versatility and ability of concrete to be adjusted to different levels of technology. No other building material has this quality.

There is no doubt that concrete has life and form, and will probably be the material of the future. Advances in exotic reinforcing and chemical admixtures can now produce concrete batches with up to 24ksi strength in the laboratory.

This book is the key to understanding not only the technology of concrete structures but also the organic nature of this basic material, which is used in every corner of the world.

**Vincent J. DeSimone**

*DeSimone Consulting Engineers*

*Miami, Florida*

---

# ICC Foreword

The field of structural engineering and concrete design of buildings has gone through enormous changes since the time I was in college in the mid-1970s. At that time, one of the best books on the subject of concrete was *Reinforced Concrete Fundamentals* by Phil M. Ferguson. Computerized design of concrete buildings was in its infancy, and I took my stack of 100 “punch cards” for even the simplest design of a reinforced concrete column to a computer center to be processed by a room-sized central campus computer.

Advances in technology, state-of-the-art research, globalization in the immediate transfer of information, and many other trends have transformed design by leaps and bounds. While the basics of flexure member design, compression, torsion, and related concepts have remained fundamentally the same, today’s structural engineering students and practicing engineers have access to multiple computer design programs through the most powerful computers on their laptops. Hence, it is much more difficult to assist today’s engineers in identifying the best and most appropriate resources among hundreds of textbooks, articles, research papers, and online information. Tall and super-tall concrete buildings are very common now, not just in developed countries, but in most parts of the world, including highly populated countries such as China and India.

*Reinforced Concrete Design of Tall Buildings* by Dr. Taranath leads readers through an exploration of the intricacies of today’s concrete design in a skillful manner keeping real-life issues in mind. The most complicated issues of design are presented in an easy-to-understand language, supplemented by numerous illustrations to further enhance the understanding of the subject. This book is packed with design examples, with Chapter 6 dedicated entirely to seismic design examples.

The most recent findings of building damage or failures caused by seismic or high-wind events have resulted in extensive changes in the areas of seismic and wind designs and detailing. Advances in research and technology necessitate that the International Building Code (IBC) and ACI 318 be published every three years to keep up with innovations and new technologies and research. Both seismic and wind designs based on today’s building codes seem to be more complicated than ever before. Accordingly, Dr. Taranath has included updates to ACI 318–08 and the recently released 2009 IBC, as well as the new wind-design provisions of the National Building Code of Canada. To facilitate easy application and use, complete chapters have been dedicated to seismic and wind designs.

Failure patterns, considerations for explosions, progressive collapse, and alternative designs for the reduction of the potential for progressive collapse are other important and current design issues that are covered in this book. Finally, the seismic rehabilitation of existing buildings, which is seldom found in a reinforced concrete design book, is extensively addressed in the last chapter.

In addition to overseeing most of the technical support publications of the International Code Council (ICC), many of which are in the field of structural engineering, I also review an extensive number of books for the ICC’s joint efforts and partnerships on a regular basis. This book is truly one of the most interesting and well-laid-out publications that I have reviewed, which is why it was an easy decision for the ICC to be a partner in its co-branding. Structural engineers comprise the most important core of building safety and sustainability professionals by developing responsible, efficient, effective, safe, and economical designs. This book is a significant contribution to that effort.

**Hamid A. Naderi**  
*International Code Council*



---

# Preface

As I reflect on my career as a practicing engineer, I am struck by the profound conceptual and methodological changes that computer-enhanced design has brought to our field. Today, and especially in the last decade or so of computer use and software engineering, we can develop numerical solutions to an astonishing number of decimals with a degree of precision that was previously unfathomable. On account of liability issues, engineering innovations these days must also be analytically proven and strenuously tested to an extent unknown in the past. In spite of these concerns, the art of being able to smell or feel a reasonable solution must necessarily continue to exist. Without such intuition and creativity, we might tend to rely on computer applications as engineering itself, instead of as a necessary tool.

As structural engineers, our primary task is to take someone else's vision of a project, convert it into analytical and numerical models, and then produce a set of buildable documents. However, the current trend in engineering education seems to focus more on the behavior of computer-based mathematical models while seldom acknowledging their fallibilities. Given this scenario, one may wonder if the era of engineers who endorsed structural attitudes based on their qualitative knowledge of the behavior of the structures is gone.

There is no doubt that navigating complicated software is certainly a critical and necessary part of a designer's vocabulary. My sense, however, is that such skills would be more powerful, accurate, and useful if built upon a solid foundation of engineering principles and conceptual knowledge. I am not alone in voicing these ideas; a plethora of recently published journal articles, opinion pieces, and conference presentations address this ever-increasing gap between the conceptual approach and the scientific illusion created by computer solutions.

These thoughts occur to me in my day-to-day engineering and more specifically as I was preparing this manuscript. Therefore, the challenge I set for myself in this book was to bridge these two approaches: one that was based on intuitive skill and experience, and the other that relied on computer skills. Imagine then the design possibilities when experiential intuition marries unfathomable precision and numerical accuracy.

Engineers are generally characterized as imaginative in their design approach as supported by historical evidence, which includes the creation of ancient structures, medieval cathedrals, and the skyscrapers of today. None of these structures, except for those built in the last decade, were developed using intense calculations as we know them today, but were more products of inventive imagery.

Even with the availability of immense analytical backup, imaginative thinking can and must be effectively used to apply basic concepts to complex problems. Therefore, the stimulus for writing this book was to develop imaginative approaches by examples, and, where appropriate, relate these specific examples to building codes that are essential and mandatory tools of the trade.

The motivation that propelled me into writing this book addresses the question frequently proposed to the designer by the architects: "Can we do this?" And, in the flash-track world that we live in, the time frame allowed for coming up with an answer is measured in days, and, sometimes, even in hours. Such a time constraint does not allow for extensive research or for time-consuming analytical procedures. What is needed is the proverbial back-of-the-envelope analysis that serves as a quick means of evaluating the efficacy of a concept that would then also serve as a check of computer solutions.

Typically, when we prepare a back-of-the-envelope design, the purpose is to make sure we get into the ballpark; once you are in, it is easy enough to find the right row in the analysis phase, and, eventually, to find the right seat.

Finding the ballpark is thus an essential part of the conceptual design. As a designer you will soon learn that once a building program is set it cannot be changed, and the only real option is to mitigate mistakes in concept. On the other hand, if the first step is in the right direction with allowances for potential contingencies, the design will flow smoothly so long as the design has some breathing room.

Chapter 1 discusses selected fundamental concepts. The objective is to develop a “feeling” for overall structural behavior and to provide the designer with the basic insight necessary to the effective development of a design. The subsequent chapters provide detailed discussions of the basic concepts.

Chapter 2 deals with the behavior of gravity components. In addition to common types of framings such as one-way and two-way slabs, novel systems, such as haunch girder systems, are also discussed. An in-depth discussion of prestressed concrete design is presented along with approximate methods to assist engineers in “doing schematics in a meeting.”

The focus of Chapter 3 is the design of lateral load-resisting systems. The objective is to control the building behavior through a bracing program that is effective from both the perspectives of cost and behavior. The design concept must be less expensive and better than its alternative if it is to be accepted or adapted. Thus, it is incumbent on the designer to create a cost-effective design in order for it to be realized. This chapter discusses flat slab-frames, coupled shear walls, core-supported structures, tube buildings, and spine-wall structures.

Chapter 4 deals with the determination of design wind loads using the provisions of ASCE 7–05. Wind-tunnel procedures using rigid, high-frequency base and aeroelastic models are discussed, including analytical methods for determining wind response and motion perception. Guidelines are presented for evaluating the acceptability of wind-induced motions of tall buildings.

Chapter 5 covers seismic designs. It develops a design methodology for each component and shows how seismically induced demands may force members to deform well beyond their elastic limits. Detailing considerations for such nonelastic excursions are discussed, and, where appropriate, codification concepts are reduced to a level of analytical simplicity appropriate for the design. The goals are to reduce component design to as simple a process as possible and to highlight design objectives often concealed in the codification procedure. Also discussed in this chapter is the design approach prior to IBC 2002, in which the magnitude of seismic force and level of detailing were strictly a function of the structure’s location. This is compared with relatively recent provisions, in which these are not only a function of the structure’s location but also of its use and occupancy, and of the type of soil it rests upon. This comparison will be particularly useful for engineers practicing in seismically low- and moderate-risk areas of the United States, who previously did not have to deal with aspects of seismic design. This chapter concludes with an in-depth review of structural dynamic theory.

Chapter 6 provides examples of seismic designs and detailing requirements of concrete buildings. Detailing provisions prescribed in ACI 318–05/08 (Chapters 1 through 20 for buildings assigned to SDC A or B, and in Chapter 21 for those in SDC C and higher) are discussed. Also presented are the designs of special moment frames, shear walls, floor diaphragm-chords, and collectors. Recent revisions to ACI 318 are discussed in the final section.

Chapter 7 is devoted to the structural rehabilitation of seismically vulnerable buildings. Design differences between a code-sponsored approach and the concept of ductility trade-off for strength are discussed, including seismic deficiencies and common upgrade methods.

Chapter 8 is dedicated to the design of tall buildings. It begins with a discussion on the evolution of their structural forms. Case studies of structural systems that range from run-of-the-mill bracing techniques to unique systems—including megaframes and spine-wall structures—are examined.

Finally, Chapter 9 covers a wide range of topics. It begins with a discussion on damping devices that are used to reduce the perception of building motions, including passive viscoelastic dampers, tuned mass dampers, slashing water dampers, tuned liquid column dampers, and simple and nested pendulum dampers. It then deals with seismic isolation and energy dissipation techniques. This is

followed by a discussion on preliminary analysis techniques such as portal and cantilever methods and an in-depth discourse on torsion analysis of open section shear walls with a particular emphasis on their warping behavior. The final section of this chapter covers performance-based designs (PBDs) for the structural design of new buildings. This approach, used for the seismic design of very tall buildings constructed in the western United States within the last few years, has set in motion new ways of doing things. A discussion on the more challenging design issues that may defy codified doctrines, such as height limits, the selection of response modification factors, and peer-review requirements, is presented to introduce engineers to this emerging technology.

Before concluding the preface, it is worth remembering that reinforced concrete as a building material provides a medium that inspires architectural freedom. The design is not peculiar to the material and must satisfy the same basic fundamental laws of equilibrium, compatibility, and compliance with the appropriate stress–strain relationship. The choice of concrete does not pose constraints on the architectural expressionism of structure nor on the free form of today’s architectural styles.

This book is a modest attempt to explore the world of concrete as it applies to the construction of buildings while simultaneously striving to seek answers to the challenges I set for myself. It is directed toward consulting engineers, and, within the academy, the book may be helpful to educators and students alike, particularly as a teaching tool in courses for students who have completed an introductory course in structural engineering and seek a deeper understanding of structural design principles and practices. It is my hope that this book serves as a comprehensive reference for the structural design of reinforced concrete buildings, particularly those that are tall.

**Bungale S. Taranath**

*DeSimone Consulting Engineers*

*Las Vegas, Nevada*



---

# Acknowledgments

I wish to express my sincere appreciation and thanks to Vincent J. DeSimone, chairman, DeSimone Consulting Engineers, for his support and encouragement during the preparation of this book and for setting a positive tone for the entire book by writing an eloquent foreword.

My sincere gratitude to Farro Tofighi, managing principal, DeSimone Consulting Engineers, Las Vegas, Nevada, for reviewing the entire manuscript and offering valuable suggestions. I am indebted to him for his confidence in me and will always remain true to his friendship.

I would like to acknowledge the following individuals for their help in the preparation of this book: Samantha Roy, Nichole Hern, Ken Martin, Daniel Schepp, Dr. Ali Shirazi, Alan Dyck, Carol McCullough, David Sze, Elie Elriachi, Felix Madrigal, Filbert Apanay, Frank Reppi, Heinz Kuo, Hui Li, Jason Crabtree, Rani Alhelou, Robert Fortney, Roozbeh Tabatabaai, Sandy Peltyn, Tarek Bannoura, Vijayarajan Krishnaswamy, William Schaffer, and Kyle Fisher, with special thanks to Michael Stavropoulos for organizing tables and graphs in the book.

We are also grateful to Brian Breukelman, consultant, CPP Wind Engineering & Air Quality Consultants, Fort Collins, Colorado, for reviewing the wind chapter and offering constructive suggestions.

My sincere appreciation and thanks to Mark A. Johnson, senior vice president of business and product development, International Code Council (ICC), and Mike C. Mota, manager, Atlantic Region, Concrete Reinforcing Steel Institute (CRSI), for their help in co-branding this book.

Thanks are also due to Jennifer Ahringer, production coordinator, editorial product development, and Joseph Clements, acquisitions editor, CRC press, Taylor & Francis, for their patience and cooperation in the production of this book.

Thanks in no small measure are due to my friend of many years, M.V. Ravindra, president and CEO, LeMessurier Consultants, Cambridge, Massachusetts, for valuable advice during the preparation of this book.

Everlasting thanks to my daughter, Dr. Anupama Taranath; son-in-law, Dr. Rajesh Rao; son, Abhi Taranath; daughter-in-law, Kristin Taranath; grandsons, Vijay and Kavi; and granddaughters, Anika and Maya, for their love throughout the writing of this book that stole valuable time from my family life.





---

# A Special Acknowledgment

This book, like my other ones, would not have been written had it not been for my wife Saroja Taranath. Her wisdom, generosity, and power of reassurance are awe-inspiring. I can only wonder at my good fortune at having met her in this life, and say from the bottom of my heart, thank you for all you have given me.

My source of inspiration, she helped shepherd the manuscript through its many stages with good humor and grace. Her patience and unyielding support, unconditional love, and congenial manner, always present over the many years of my book-writing career, have often left me astounded. Without her absolute commitment, this modest contribution to structural engineering would not have been possible.



---

# Author



**Dr. Bungale S. Taranath, PhD, SE**, is a corporate consultant to DeSimone Consulting Engineers, a consulting firm, with offices in New York, Miami, San Francisco, New Haven, Las Vegas, Hong Kong, and Abu Dhabi. He has extensive experience in the design of concrete, steel, and composite tall buildings and has served as principal-in-charge for many notable high-rise buildings. He has held positions as a senior project engineer in Chicago, Illinois, and as vice president and principal-in-charge with two consulting firms in Houston, Texas; he has also served as a senior project manager with a consulting firm in Los Angeles, California. Dr.

Taranath is a member of the American Society of Civil Engineers and the American Concrete Institute, and a registered structural and professional engineer in several states. He has conducted research into the behavior of tall buildings and shear wall structures and is the author of a number of published papers on torsion analysis and multistory construction projects. He has previously published three books: *Structural Analysis and Design of Tall Buildings*; *Steel, Concrete, and Composite Design of Tall Buildings*; and *Wind and Earthquake Resistant Buildings, Structural Analysis and Design*. Two of his books were translated into Chinese and Korean and were widely accepted in Asia. Dr. Taranath has conducted seminars on tall-building design in the United States, China, Hong Kong, Singapore, Mexico, India, and England. He was awarded a bronze medal in recognition of a paper presented in London, when he was a fellow of the Institution of Structural Engineers, London, England. Taranath's passion for tall buildings has never slackened. Today his greatest joy is sharing that enthusiasm with owners, architects, and fellow structural engineers to develop imaginative solutions for seemingly impossible structures.



---

# 1 Design Concept

Design concept is an impressive term that we use to describe the intrinsic essentials of design. The concept encompasses reasons for our choice of design loads, analytical techniques, design procedures, preference for particular structural systems, and of course, our desire for economic optimization of the structure. To assist engineers in tackling the design challenge, this introductory chapter is devoted to developing a “feeling” for behavior of structural systems.

It is this “feeling” for the nature of loads and their effect on structural systems that paves the way for our understanding of structural behavior and allows the designer to match structural systems to specific types of loading. For example, designers of tall buildings, recognizing the cost premium for carrying lateral loads by frame action alone, select a more appropriate system such as a belt and outrigger wall or a tubular system instead. And engineers designing for intense earthquakes knowing that building structures must sustain gravity loads at large deformations, select moment frames and/or shear walls with ductile connections to provide for the deformation capacity.

As with other materials, the strength and deformation characteristics of reinforced concrete members are important in the design of buildings. In particular, buildings designed to resist seismic forces must have well-detailed members and joints such that the building can sustain large lateral deformations without losing its vertical load-carrying capacity.

In reinforced concrete structures, the reinforcing bars and concrete are almost always subject to axial stress in tension or compression resulting from various load applications. However, they are usually stressed in a manner quite different from that in a simple axial compression or tensile test.

## 1.1 CHARACTERISTICS OF REINFORCED CONCRETE

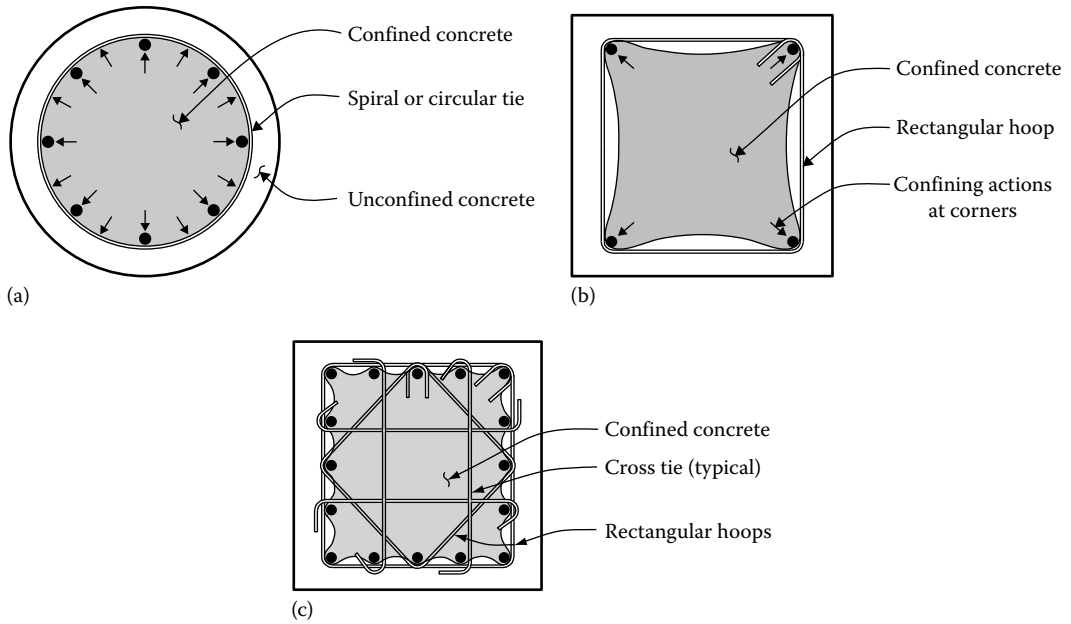
### 1.1.1 CONFINED CONCRETE

The term “confined concrete” generally applies to a condition in which concrete is confined in all directions. A reinforced concrete member with closely spaced spiral reinforcement or hoops is one such example. The confining reinforcement restrains the lateral strain in the concrete by increasing both its strength and ductility, as compared to unconfined concrete.

Examples of confined concrete elements are circular columns provided with transverse reinforcement in the form of continuous helical reinforcement, often referred to as spiral reinforcement or circular hoops. Rectangular columns enclosed by rectangular hoops, more common in building construction, are another example. Note that the transverse reinforcement is not stressed until an axial load is reached at which point the unconfined concrete tends to develop appreciable lateral strains. This generally occurs at about 85% of the unconfined strength. Beyond this point, the concrete tends to push against the transverse reinforcement, thereby creating a confining reaction as indicated schematically in Figure 1.1.

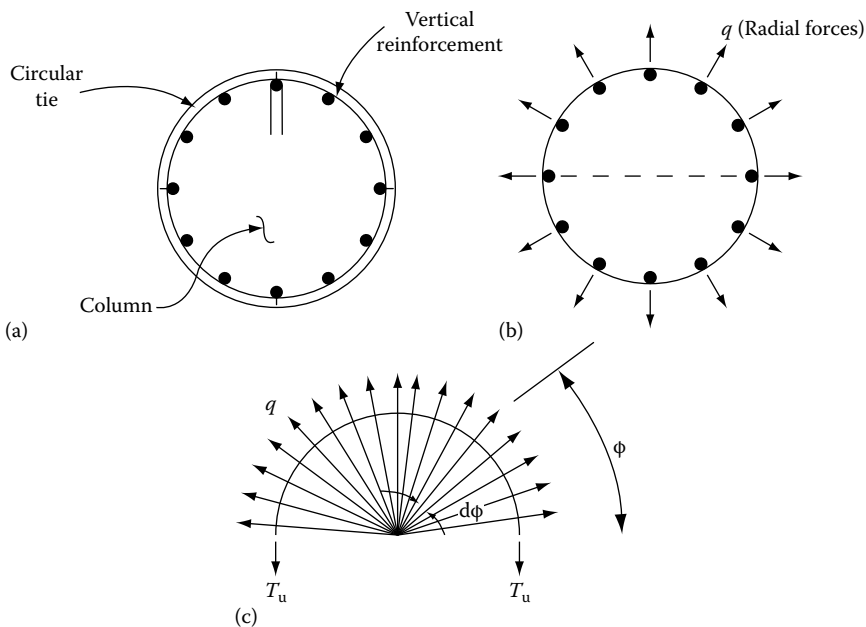
The shape of stress–strain curve for reinforced concrete member, among other variables, is a function of spacing and diameter of the transverse reinforcement.

Transverse reinforcement in a rectangular column acts merely as ties between the vertical bars and bow outward rather than effectively confining the concrete between the vertical bars. The larger the diameter of the tie, greater is its bending stiffness, resulting in better confinement. In the case of circular tie, this bending stiffness has no significance. This is because given its shape, the spiral will be in axial tension and will apply a uniform radial pressure to the concrete.



**FIGURE 1.1** Confinement of column concrete by transverse reinforcement: (a) confinement by spiral or circular hoops, (b) confinement by a rectangular hoop, and (c) confinement by hoops and cross ties.

The bursting force in a circular column due to lateral expansion of concrete may be considered equivalent to a system of uniformly distributed radial forces acting along the circumference of the transverse tie. The radial forces produce a uniform enlargement of the tie resulting in a tensile force  $T_u$ . To determine  $T_u$ , let us imagine that the tie is cut at the horizontal diametral section (Figure 1.2) and consider the upper portion of the tie as a free body. If  $q$  denotes the uniform radial load per unit



**FIGURE 1.2** Confinement of circular column: (a) column with circular ties, (b) radial forces, and (c) free-body of upper portion of tie.

length of the ring, and  $r_c$  is the radius of the ring, the force acting on an element of the ring cut by two radial cross sections will be  $q_c d\phi$ , where  $d\phi$  is the angle corresponding to the element. Taking the sum of the vertical components of all the forces acting on half the ring, the following equation of equilibrium will be obtained

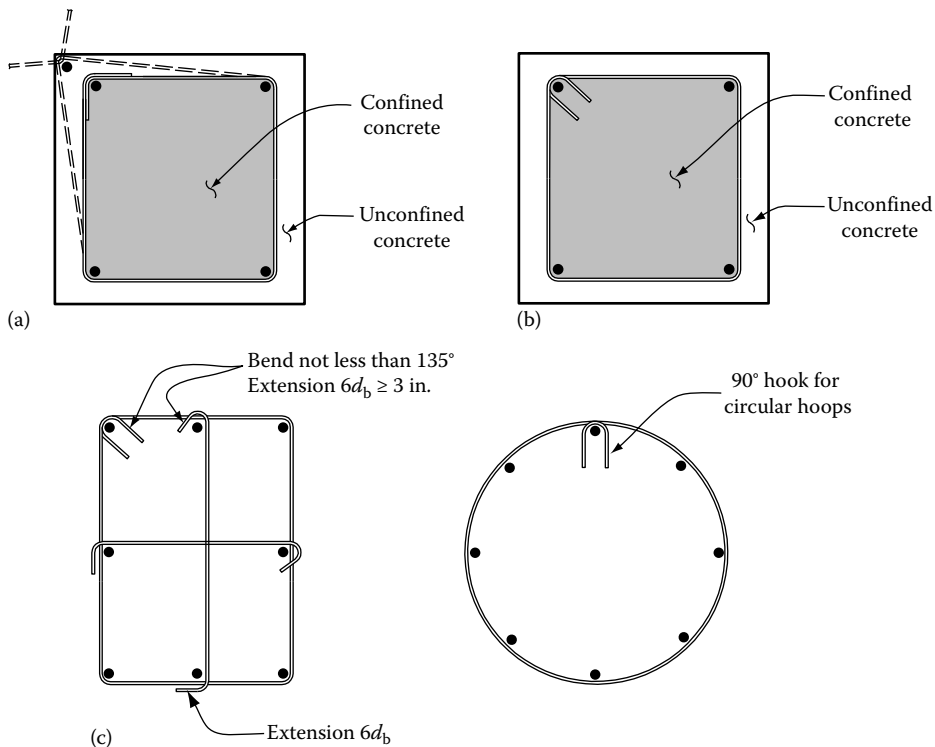
$$2T_u = 2 \int_0^{\pi/2} q r_c \sin \phi d\phi$$

from which

$$T_u = q r_c$$

This tension,  $T_u$ , is often referred to as hoop tension.

In a spiral column, the lateral expansion of the concrete inside the spiral stresses the spiral in tension and this, in turn, causes a confining pressure on the core concrete, leading to an increase in the strength and ductility of the core. This is the reason why the ACI 318 in the seismic design Chapter 21, requires that beams, columns, and ends of shear walls have hoops in regions where the reinforcement is expected to yield in compression. Hoops are closely spaced closed ties or continuously wound ties or spirals, the ends of which have 135° hooks commonly referred to as seismic hooks, with 6 bar diameter (but no less than 3 in.) extensions (see Figure 1.3). The hoops must enclose



**FIGURE 1.3** Column ties and seismic hooks: (a) overlapping 90° hooks at corners cannot confine a concrete core after concrete cover spalls, (b) 135° hooks, required in high seismic areas, provide the necessary confinement for the core while simultaneously resisting buckling of column vertical bars, and (c) seismic hook.



the longitudinal reinforcement and give lateral support to those bars in the manner required for column ties. Although hoops can be circular, they most often are rectangular since most beams and columns have rectangular cross sections. In addition to confining the core concrete, the hoops restrain the buckling of the longitudinal bars and act as shear reinforcement as well. Reinforced concrete frames with confining hoops that are in compliance with the ductile detailing requirements of the ACI 318-05/08 Chapter 21 can achieve deflection ductilities in excess of 5 and shear walls about 4, compared to 1 to 2 for conventionally reinforced nonductile concrete frames.

### 1.1.2 DUCTILITY

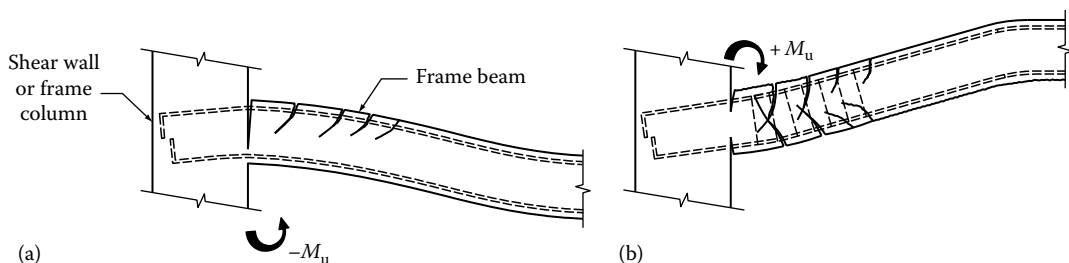
An excellent example for discussing “ductility” of reinforced concrete members is a frame-beam shown in Figure 1.4. The term “frame-beam” applies to a beam that is designed as part of a lateral system. Otherwise it is simply referred to as a gravity beam.

When subjected to seismic ground motions, the frame sways back and forth resulting in flexural and shear cracks in the beam. These cracks close and open alternately due to load reversal and following several cycles of loading, the beam will resemble Figure 1.4. As a result of the back and forth lateral deflections, the two ends of the beam are divided into a series of blocks of concrete held together by the reinforced cage.

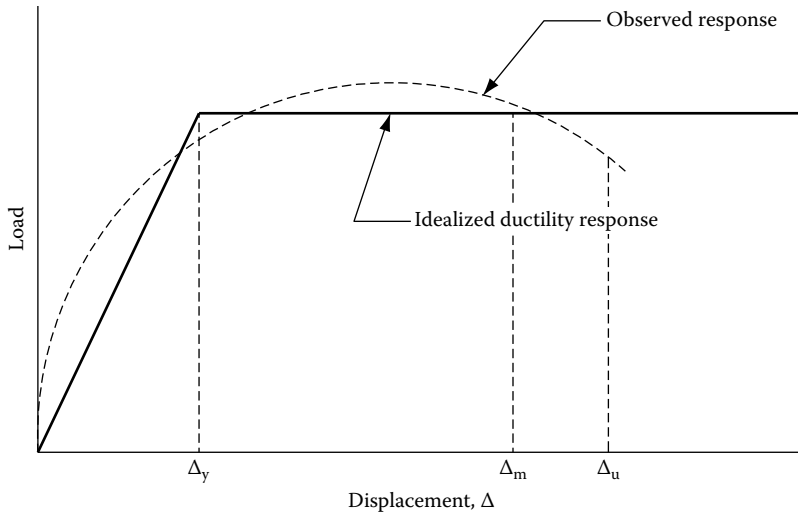
If the beam cracks through, shear is transferred across the crack by the dowel action of the longitudinal reinforcement and shear friction along the crack. After the concrete outside the reinforcement crushes, the longitudinal bar will buckle unless restrained by closely spaced stirrups or hoops. The hoop also provides confinement of the core concrete increasing its ductility.

Ductility is the general term that describes the ability of the structure or its components to provide resistance in the inelastic domain of response. It includes the ability to sustain large deformations and a capacity to absorb energy by hysteretic behavior, the characteristics that are vital to a building’s survival during and after a large earthquake. This capability of sustaining a high proportion of their strength that ensures survival of buildings when a major earthquake imposes large deformation is the single most important property sought by the designer of buildings located in regions of significant seismicity.

The limit to ductility, such as the displacement of  $\Delta_u$ , typically corresponds to a specified limit to strength degradation. Even after attaining this limit, sometimes termed “failure,” significant additional inelastic deformations may still be possible without structural collapse. Brittle failure, on the other hand, implies near-complete loss of resistance, often complete disintegration without adequate warning. For these reasons, brittle failure, which is the overwhelming cause for collapse of buildings in earthquakes, and the consequent loss of lives, must be avoided.



**FIGURE 1.4** Frame-beam subjected to cyclic loads: (a) cracks due to  $-M_u$  and (b) cracks due to  $+M_u$ .



**FIGURE 1.5** Ductility model. The ability of the structure to provide resistance in the inelastic domain of response is termed “ductility.”  $\Delta_u$  is the limit to ductility corresponding to a specified limit of strength degradation.

Ductility is defined by the ratio of the total imposed displacements  $\Delta$  at any instant to that at the onset of yield  $\Delta_y$ . From Figure 1.5, we have

$$\mu = \Delta / \Delta_y > 1 \quad (1.1)$$

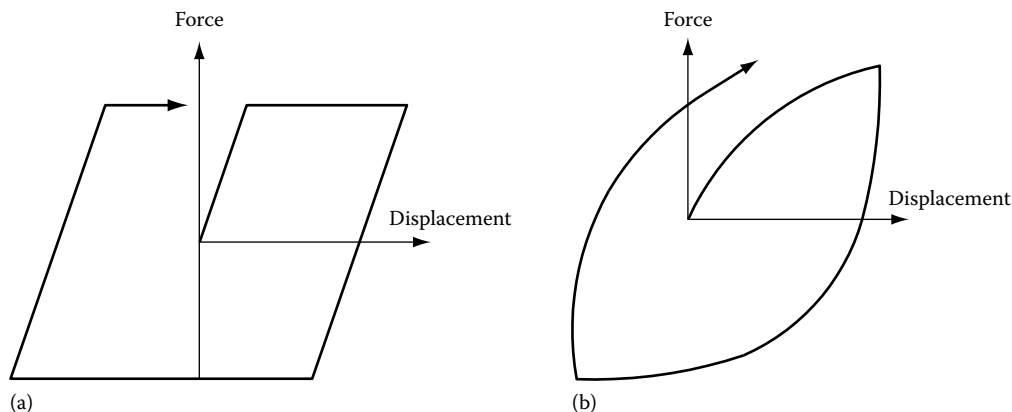
Ductility may also be defined in terms of strain, curvature, rotation, or deflection. An important consideration in the determination of the required seismic resistance will be that the estimated maximum ductility demand during shaking,  $\mu_m = \Delta_m / \Delta_y$  does not exceed the ductility potential  $\mu_u$ .

In structural engineering, the roles of both stiffness and strength of members, as well as their quantification is well understood. However, quantification and utilization of the concept of ductility as a design tool are generally less well understood. For this reason, many aspects of ductile structural response and its application in seismic design are examined in considerable detail in subsequent chapters of this book.

Ductility in structural members can be developed only if the constituent material itself is ductile. Concrete is an inherently brittle material. Although its tensile strength cannot be relied upon as a primary source of resistance, it is eminently suited to carry compression stresses. However, the maximum strains developed in compression are rather limited to about 0.003, unless special precautions are taken. Therefore, the primary aim of seismic detailing of concrete structures is to combine mild steel reinforcement and concrete in such way as to produce ductile members that are capable of meeting the inelastic deformation demands imposed by severe earthquakes.

### 1.1.3 HYSTERESIS

When the structure is able to respond inelastically without significant strength degradation to a design-level earthquake, typically defined as an event with a recurrence interval of once in 2500 years, it is said to possess ductility. Observe that ductility must be provided for the full duration of the earthquake, possibly implying many inelastic excursions in each direction.



**FIGURE 1.6** Hysteresis loops. (a) Idealized elastoplastic loop. (b) Well-detailed beam plastic hinge loop.

Perfect ductility is defined by the ideal elastic/perfectly plastic (often also called elastoplastic) model shown in Figure 1.6, which describes typical response in terms of force versus displacement at the center of mass. Diagrams of this form are termed “hysteresis loops.”

The structural response indicated in Figure 1.6a is a structural ideal, seldom if ever achieved in the real world. Hysteresis loops more typical of reinforced concrete are shown in Figure 1.6b. In reinforced concrete frames, it is desirable to concentrate the inelastic deformation in plastic hinges occurring in the beams, adjacent to column faces. Under ideal conditions, hysteresis loops of the form shown in Figure 1.6b typically provide energy absorption of perhaps 70%–80% of the absorption of an equivalent elastoplastic loop. When energy is dissipated in plastic hinges located in columns, the loops diverge further from the ideal elastoplastic shape indicating less energy absorption.

Properly detailed reinforced concrete structural elements exhibit dependable ductile behavior although with hysteresis loops different from the elastoplastic loops. However, all the loops represent essentially ductile behavior, in that they do not indicate excessive strength degradation with increasing displacement or with successive cycling to the same deflection. It should be noted that the area inside the loop is a measure of the energy that can be dissipated by the plastic hinge.

The fullness of a hysteresis loop has always been considered as a positive attribute. How full must it be to have the desired control over building response? At this time (2009), explicit answers are nonexistent, but it is believed that considerable improvement in building response will result, provided that reasonable levels of both strength and energy dissipation are provided.

#### 1.1.4 REDUNDANCY

Especially for buildings in seismic design category (SDC) C and above, it is important for the lateral load system to possess some degree of redundancy.

The SDCs discussed at length in Chapter 5, establish among other requirements, the energy-absorbing capacity of various structural systems. Six SDCs (A through F) are assigned to buildings in ASCE 7-05, A being the least and F the most severe.

Redundancy in a structure means that there is more than one path of resistance for lateral forces. As an example, redundancy can be achieved by having a moment-resistant frame with many columns and beams, all with ductile connections or by having a dual system, such as shear walls plus a moment-resistant frame.

#### 1.1.5 DETAILING

Detailing incorporates a design process by which the designer ensures that each part of the structure can perform safely under service load conditions and also when specially selected critical regions

are to accommodate large inelastic deformations. Thus detailing based on an understanding of a feeling for structural behavior, with due regard to the limitations of construction practices, is what makes structural design both a science and an art.

## 1.2 BEHAVIOR OF REINFORCED CONCRETE ELEMENTS

In the previous section, we discussed certain aspects of seismic design such as confinement, ductility, and hysteresis behavior. However, it should be remembered that a great majority of buildings built in the United States are assigned to lower SDC, that is, A or B, that do not require as much detailing for ductility. The design provisions given in Chapters 1 through 20 and 22 of ACI 318-05/08 are deemed adequate for the design of such buildings. With this in mind, we will review in general terms, the basic behavior of reinforced concrete elements subjected to external loadings such as seismic load.

- Tension (discussed in Section 1.2.1)
- Compression (discussed in Section 1.2.2)
- Bending (discussed in Section 1.2.3)
- Shear (discussed in Section 1.2.4)
- Sliding shear (shear friction) (discussed in Section 1.2.5)
- Punching shear (discussed in Section 1.2.6)
- Torsion (discussed in Section 1.2.7)

### 1.2.1 TENSION

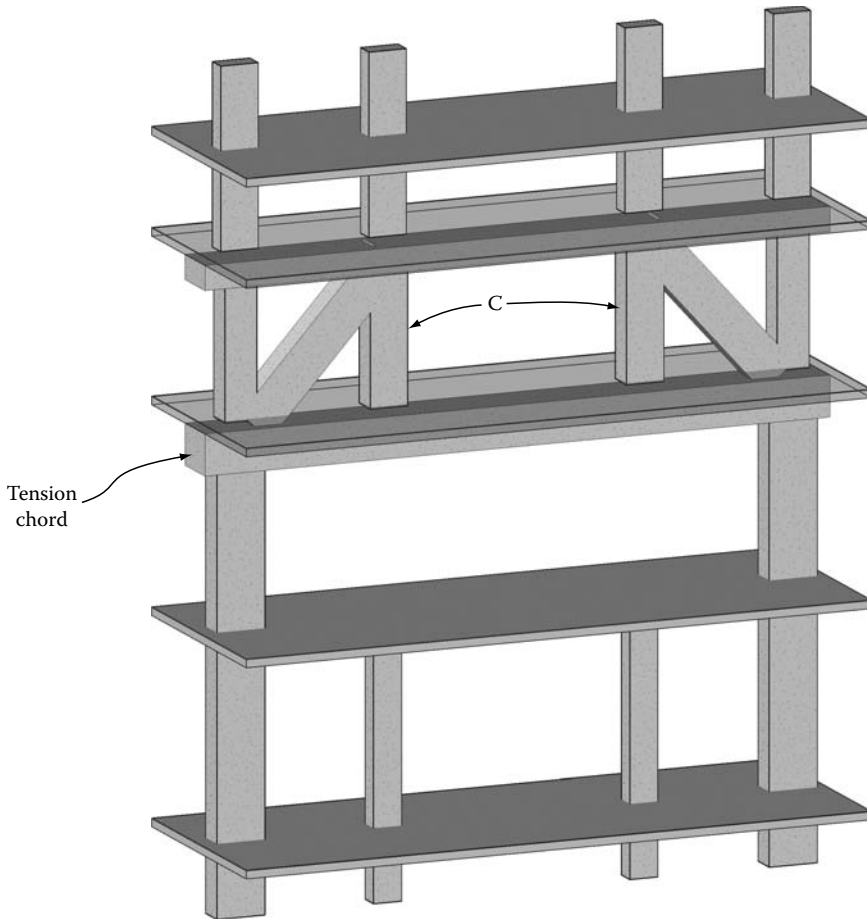
Tension forces stretch members. Concrete has no reliable tension strength. It is essentially cast rock that is strong in compression but weak in tension and shear. Mild steel reinforcement cast into concrete provides for the longitudinal tension while the enclosing ties and stirrups provide for confinement and shear resistance. Sufficient reinforcement can be added to provide adequate toughness for seismic resistance, enabling reinforced concrete to exhibit ductile properties.

Direct tension in reinforced concrete members is not as rare as one may think. Consider, for example, the transfer system shown in Figure 1.7 proposed for a high density resort and casino development in Las Vegas, Nevada. The system is intended for transferring gravity loads from typical interior columns of a multistory residential tower. The tower uses a typical posttensioned flat plate construction with columns spaced at 30 ft centers in the longitudinal direction. Extending the tower interior columns all the way to the foundation would have disrupted a considerable amount of convention, meeting, retail, and casino space in the podium. The solution was to create a reinforced concrete transfer truss as shown in Figures 1.8 through 1.10 with three options for columns below the transfer girder.

Another example of reinforced concrete members subjected to direct tension is a deep beam analyzed using the strut-and-tie model (see Figure 1.11). Note that the mild steel reinforcement for the tie is calculated using a strength reduction factor  $\phi = 0.75$ , as opposed to  $\phi = 0.9$  typically used for tension-controlled design.

### 1.2.2 COMPRESSION

Compression forces push on members and can lead to crushing of materials when the members are short and relatively fat. At bearing surfaces between concrete beams and columns, crushing can also occur. The crushing failures tend to give warning in form of local splitting of concrete and other visible changes. When long, slender members are loaded in compression, they can fail suddenly by buckling or bowing. This type of sudden failure is to be avoided.



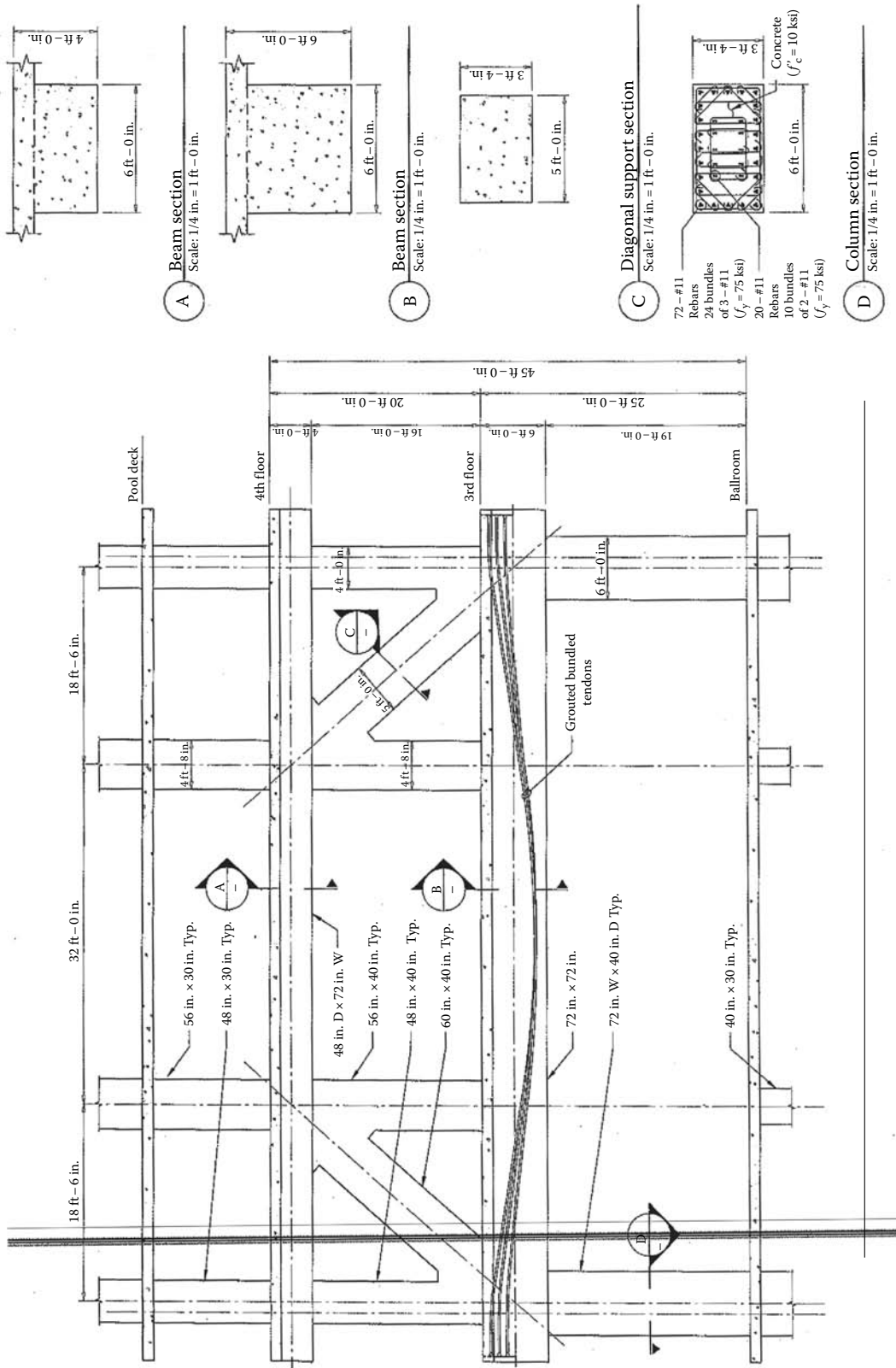
**FIGURE 1.7** Tension member in a transfer truss. *Note:* Column C not required for truss action but recommended.

### 1.2.3 BENDING

Bending forces occur mostly as a result of vertical loads applied to floor slabs and beams. Bending causes the bottoms of simple beams to become stretched in tension and the tops of beams to be pushed together in compression. Continuous beams and cantilever beams have tension forces at the top and a compression at the bottom near their supports. At midspan, the forces are in the same locations as for simple beams and slabs. Vertical cracks develop near the midspan of concrete, since the tension force causes the concrete to crack (see Figure 1.12). The reinforcing steel provided in the tension zones is assumed to resist the entire tension force. This tension cracking can be observed in damaged structures and may be used to monitor and determine the potential for collapse. Stable, hairline cracks are normal, but widening cracks indicate impending failure. As stated previously, beams in reinforced concrete moment-resistant frames may experience tension and compression stresses alternately due to stress reversals during earthquakes.

#### 1.2.3.1 Thumb Rules for Beam Design

Thumb rules have been in existence ever since humans started building structures. With passage of time, the rules have been refined based on construction experience. One thumb rule used quite extensively by engineers at present for determining beam depths in concrete buildings is the following: For every foot of beam span, use  $\frac{3}{4}$  in. as the depth. Thus, a 30 ft span beam would have a depth of  $0.75 \times 30 = 22.5$ , say 22 in., and a 40 ft span, a depth of  $0.75 \times 40 = 30.0$  in.



**FIGURE 1.8** Transfer girder: schematic elevation with concrete column.

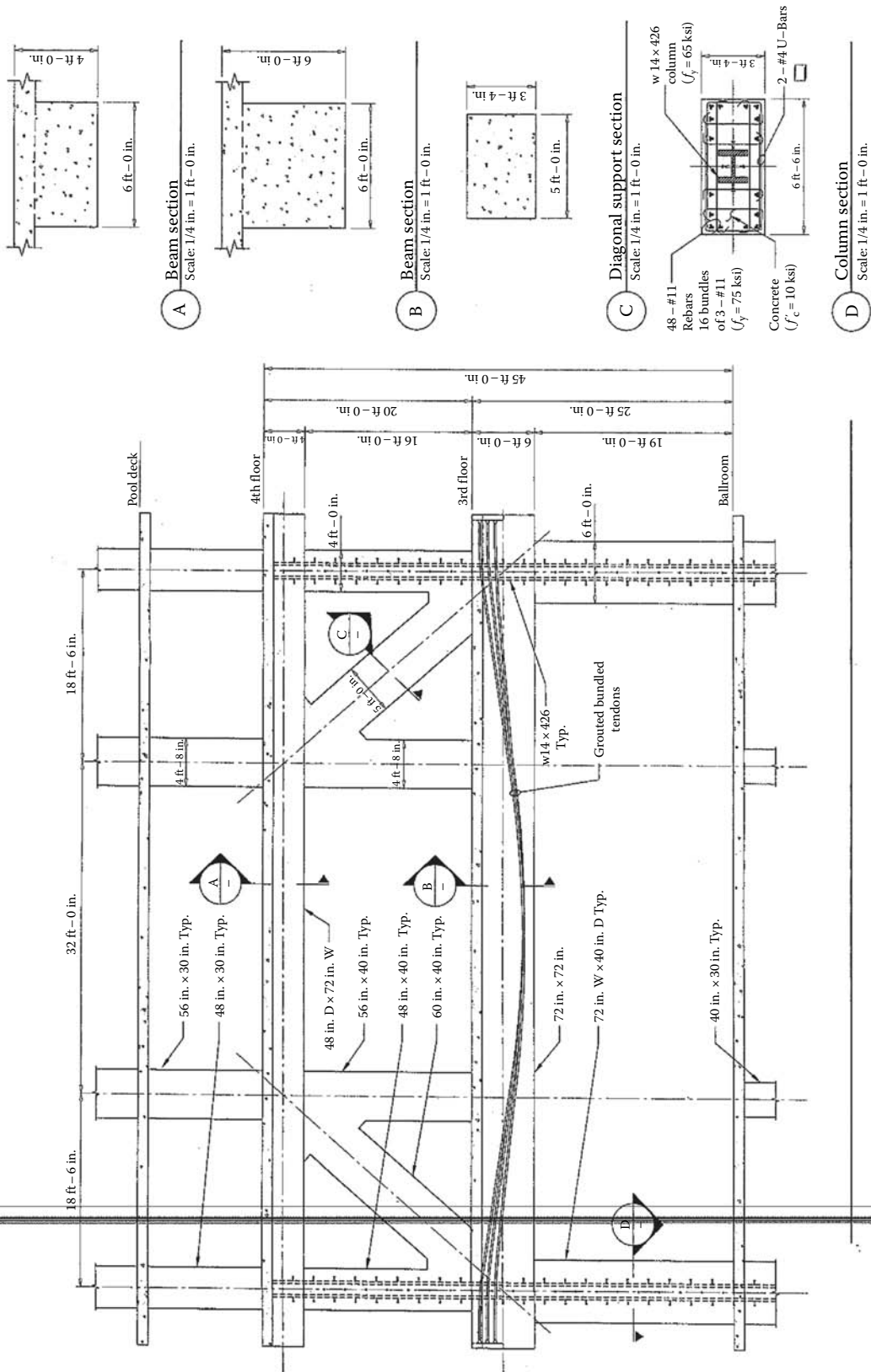
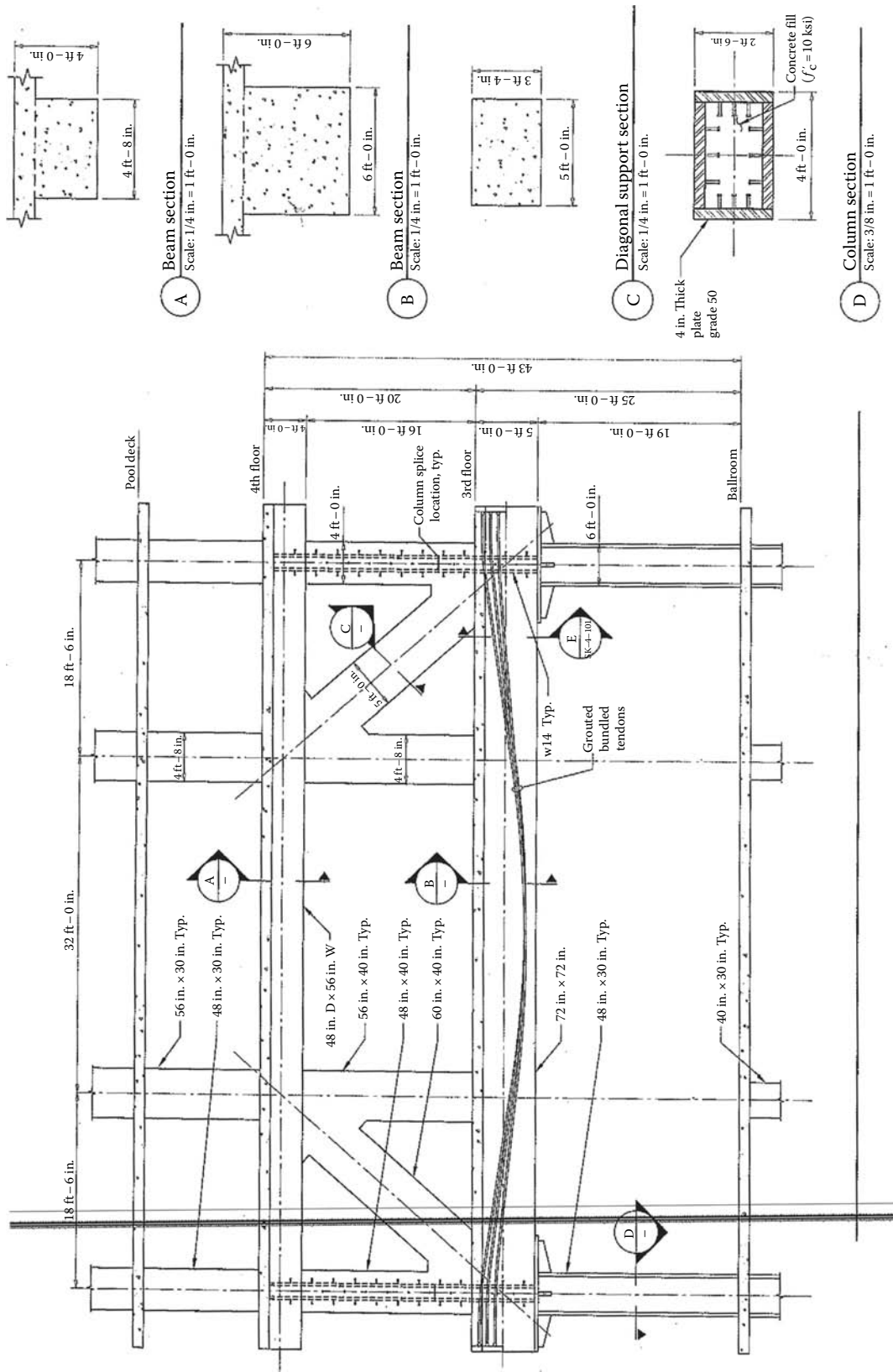
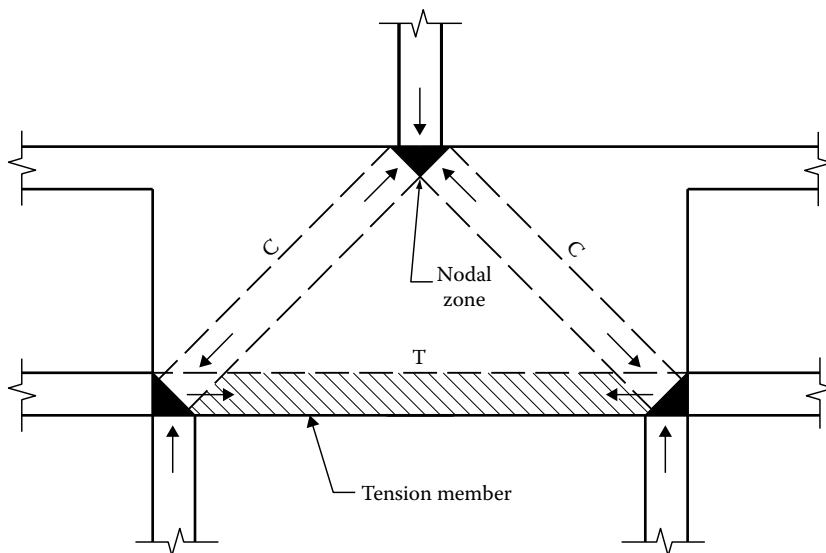


FIGURE 1.9 Transfer girder: schematic elevation with encased composite column.

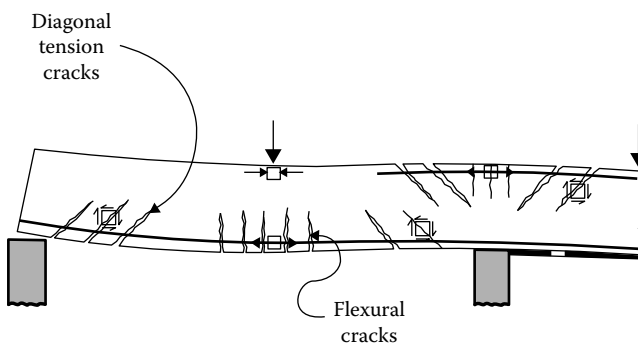


**FIGURE 1.10** Transfer girder: schematic elevation with filled steel column.





**FIGURE 1.11** Tension member in a strut-and-tie model. *Note:* Capacity reduction factor,  $\phi = 0.75$ .



**FIGURE 1.12** Development of cracks in a flexural member. Vertical cracks may develop near midspan, stable, hairline cracks are normal, but widening cracks indicate impending failure.

There also exists another easy to remember rule for determining the area of flexural reinforcement in beams:

$$A_s = \frac{M_u}{4d} \quad (1.2)$$

where

$M_u$  is the ultimate design moment (kip-ft)

$A_s$  is the area of flexural reinforcement (in.<sup>2</sup>)

$d$  is the effective depth of flexural reinforcement from the compression face (in.)

This thumb rule works quite well for members with reinforcement ratios of 1%–1.5%. Noting that minimum flexural reinforcement is about ¼% with a maximum at around 2%–2.5%, beam designs using the thumb rule given in Equation 1.2 generally turn out to be quite economical.

Example 1.1

Given

Span = 36 ft  
 $M_u = 500$  kip-ft

Required

Area of flexural reinforcement

Solution

Beam depth =  $0.75 \times 36 = 27$  in.  
Depth,  $d = 27 - 2.5 = 24.5$  in.

$$A_s = \frac{500}{4 \times 24.5} = 5.1 \text{ in.}^2$$

To demonstrate the accuracy of this quick method, a comparison is shown in Table 1.1. It is seen that the approximate method is applicable for a wide range of  $M_u$  values.

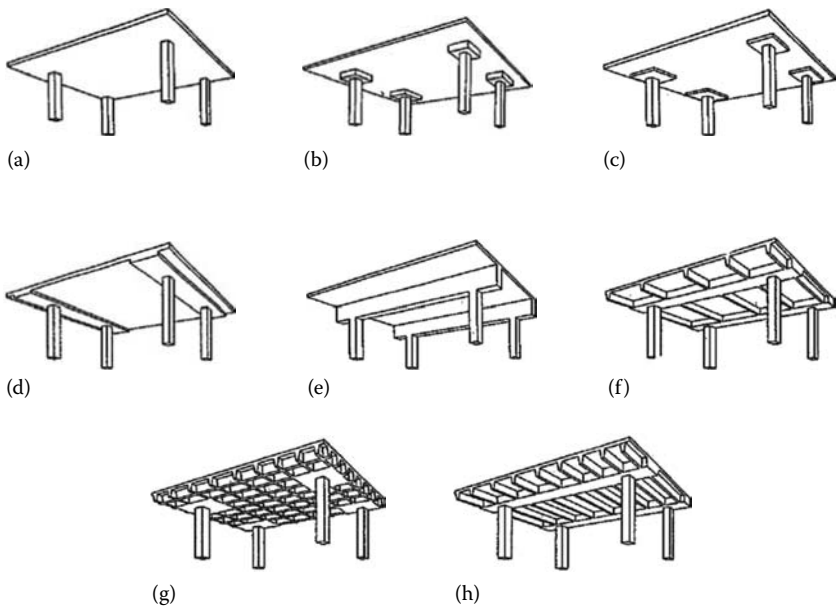
For purposes of resisting gravity loads, horizontal concrete systems such as beams and slabs can also be reinforced by adding high-strength cables or tendons that are pretensioned prior to their being loaded by the structure’s weight and superimposed loads. One type commonly referred as precast, prestressed systems may be manufactured in a factory using cables that are stretched in a form, and then bonded to the concrete when it is cast. Another method is to place cables that are enclosed in plastic sleeves in the forms at a job site, cast the concrete, and then stretch and anchor the cables after the concrete has cured and achieved sufficient strength. Using this method, two types of construction are possible. In the first type, the cables are left unbonded to the concrete, but only anchored at the edges of the structures. In the second type, the entire length of tendons is bonded to the concrete. These two methods are commonly referred to unbonded and bonded systems, respectively.

Concrete shrinks, cracks, and creeps under normal circumstances, and this behavior needs to be differentiated from the cracking and spalling that indicates failure. As stated previously, properly reinforced concrete can provide seismically resistant construction if the reinforcing is proportioned such that the configuring ties, hoops, and stirrups are sufficient to resist the shear that can be generated by the overall structural configuration.

As compared to flexural design of beams, rational analysis of two-way slab has always lagged behind design and construction practices. In fact, more than 100 flat slab buildings had already been built when the first rational analysis was published in 1914.

TABLE 1.1  
Comparison of Flexural Reinforcement

$M_u$ (kip-ft)	Effective Depth, $d$ (in.)	$A_s$ (in. <sup>2</sup> )	
		Quick Method	Computer Method
500	25.5	4.9	5.08
650	28.5	5.7	5.53
800	30.5	6.56	6.35
1000	35	7.14	7.0
1200	39.5	7.59	7.62
2000	46	10.87	10.16



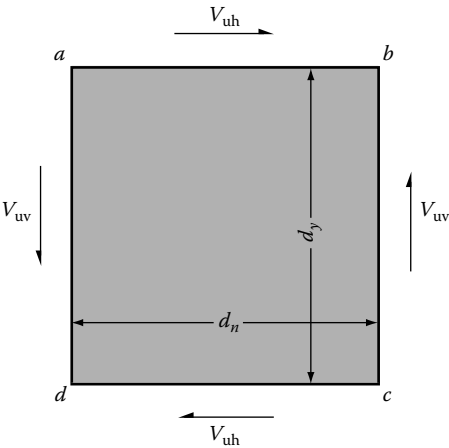
**FIGURE 1.13** Two-way slab systems: (a) flat plate, (b) flat plate with column capitols, (c) flat plate with drop panels, (d) band beams, (e) one-way beam and slab, (f) skip joist system, (g) waffle slab, and (h) standard joist system.

The major types of two-way slabs are shown in Figure 1.13. The choice of slab type depends largely on the ease of formwork, superimposed loads, and span. The flat plate system is suitable for lighter loads and moderate spans, the characteristics that make it a popular system for residential constructions such as apartments and hotels. Slabs with beams or drop panels are more suitable for office and institutional buildings with heavier loads.

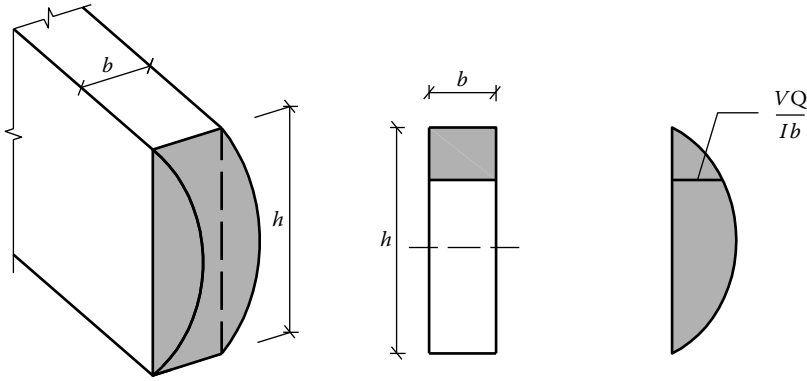
1.2.4 SHEAR

We begin with a discussion of horizontal shear stresses that occur in a beam as a result of vertical shear stresses.

To explain this concept, let *abcd* (Figure 1.14) represent an infinitely small prismatical element of unit thickness cut out of a beam subjected to shear stress. If there is a shear stress,  $V_{uv}$ , acting on



**FIGURE 1.14** Unit shearing stresses acting at right angles to each other.



**FIGURE 1.15** Shear stress distribution in a rectangular beam.

the right-hand face, the shear force acting on this face is  $V_{uv} \times d_y \times 1$  and there must be an equal and opposite force on the left-hand face in order that the sum of the  $y$ -component be zero for equilibrium. These two forces, however, constitute a couple and to prevent rotation, there must be another couple made up of horizontal shear forces  $V_{uh} \times d_x \times 1$  acting on the top and bottom faces. These two couples must be numerically equal and must act in opposite directions. The moment arm of the first couple is  $d_x$  and that of the second couple is  $d_y$ . Thus,  $V_{uv} \times d_y \times d_x = V_{uh} \times d_x \times d_y$  and accordingly

$$V_{uv} = V_{uh}$$

Thus, the unit shearing stresses acting at a point and lying in planes that are at right angles to each other are numerically equal.

Let us consider the simplest case, with a beam of rectangular cross section having width  $b$  and height  $h$  (Figures 1.14 through 1.16). We can reasonably assume that (1) the shear stress  $V_u$  acts parallel to vertical sides of the cross section and (2) the distribution of shear is uniform across the width of the beam. These two assumptions will enable us to determine completely the distribution of shear stresses acting on the cross section.

Consider a small element of the beam cut out between two planes that are parallel to the neutral surface, as shown in Figure 1.15. Considering the foregoing assumptions, the vertical shear stresses  $V_u$  are uniformly distributed on the vertical faces of the element. Recall that shear stresses acting one side of an element are accompanied by shear stresses of equal magnitude acting on perpendicular faces of the element (Figure 1.16).

Thus there will be horizontal shear stresses between horizontal layers of the beam as well as transverse shear stresses on the vertical cross sections. At any point within the beam, the vertical and the complementary horizontal shear stresses are equal in magnitude.

The foregoing discussion leads to the well-known shear stress formula,

$$V_u = v_u Q / Ib \quad (1.3)$$

where

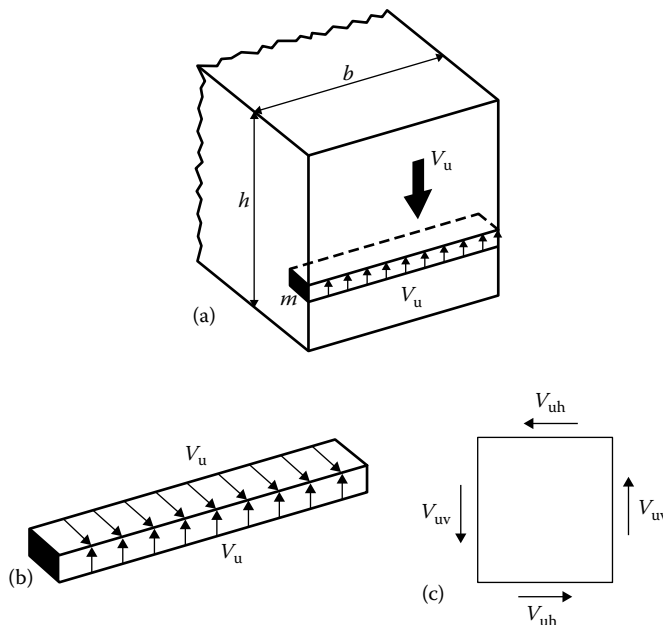
$V_u$  is the total ultimate shear at a given section

$v_u$  is the shear stress at the cross section

$Q$  is the statical moment about neutral axis of that portion of cross section lying between a line through point in question parallel to neutral axis and nearest face (upper and lower) of beam

$I$  is the moment of inertia of cross section about the neutral axis

$b$  is the width of beam at given point



**FIGURE 1.16** Complimentary shear stresses. (a) Rectangular beam subject to vertical shear force  $V_u$ , (b) beam element between two parallel sections, and (c) shear stresses on perpendicular faces of a beam element.

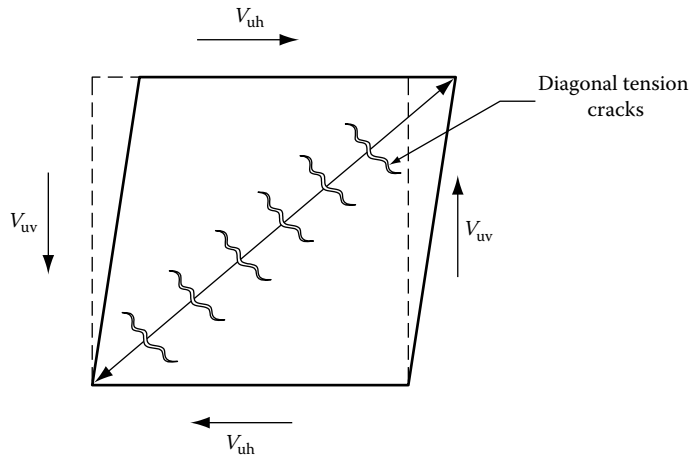
The intensity of shear along a vertical cross section in a rectangular beam varies as the ordinates of a parabola, the intensity being zero at the outer fibers of the beam and maximum at the neutral axis. The maximum is  $3/2V/bd$ , since at the neutral axis,  $Q = bd^2/8$  and  $I = bd^3/12$  (see Figures 1.14 through 1.16).

Shear forces occurring in beams are greatest adjacent to supports in gravity beams. Shear stress can be described as the tendency to tear apart the vertical surfaces of the beams. In concrete beams, these shear stresses do not produce significant vertical cracks, but develop diagonal tension cracks, since concrete is weak in tension.

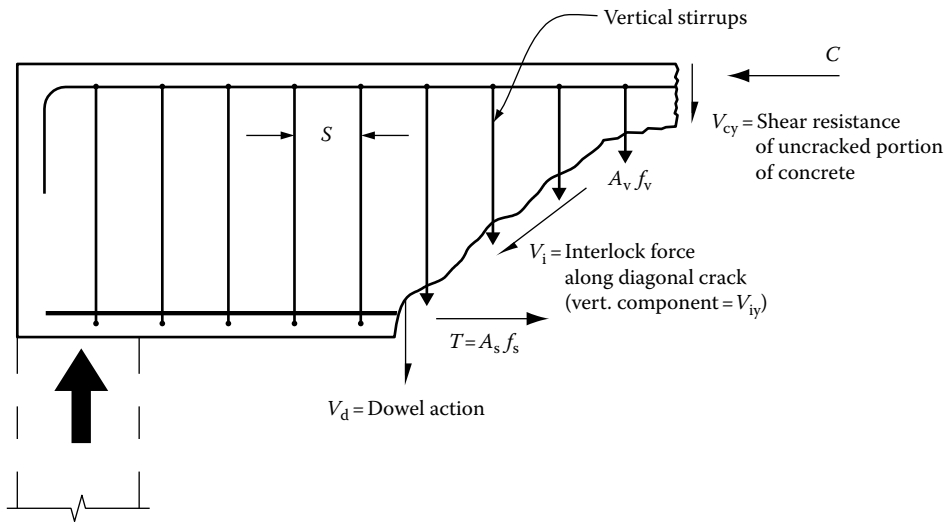
The behavior of reinforced concrete members subjected to an external shear force is difficult to predict. This is because the shear stress formula (Equation 1.3) is applicable for homogeneous beams working in the elastic range. Reinforced concrete is neither homogeneous nor its behavior elastic. Therefore, it is important to realize that shear analysis and reinforcement design of reinforced concrete members is not really concerned with the determination of shear stresses as such. The real concern is with diagonal tension stress, resulting from the combination of shear stress and longitudinal bending stresses. Since the tension capacity of concrete is low, it is necessary to carefully consider the tension stress resulting from diagonal tension.

The action of vertical and horizontal shear stresses, combined with the flexural stresses, gives rise to a pair of inclined compressive stresses and a pair of inclined tension stresses, which are at right angles to each other. These stresses are known as principal stresses. Of particular concern in reinforced concrete design are the tension stresses that occur as a result of the principal stresses (see Figure 1.17). These stresses commonly referred to as diagonal tension stresses must be carefully considered in design by providing shear reinforcement, most frequently consisting of vertical stirrups. It is important, particularly in seismic design, to ensure that flexural failure would occur prior to shear failure should the member be overloaded.

Shown in Figure 1.18 are the resisting forces at diagonal crack in a beam that has been reinforced with vertical stirrups. Consider the part of the beam to the left of the diagonal crack subjected to an external shear force  $V_u$ . No tension force perpendicular to the crack can be transmitted across it



**FIGURE 1.17** Diagonal tension.



**FIGURE 1.18** Shear-resisting forces along a diagonal crack:  $V_{ext} = V_{cy} + V_{iy} + V_d + V_s$ .

once the crack is formed. However, a sizable force, denoted as  $V_i$  in Figure 1.18, can still be transmitted along the crack through interlocking of the surface roughness. The vertical component of this force  $V_i$ , denoted as  $V_{iy}$  may be considered to provide part of resistance to external shear force  $V_u$ . Two other components of vertical resistance also manifest in resisting the shear force. These are the shear force in the uncracked portion of the concrete denoted by  $V_{cy}$  and the dowel action of the bottom reinforcement,  $V_d$ . The fourth and the final component of the internal resistance is the force  $V_s = A_v f_v$  exerted by the stirrup traversing the crack.

Equilibrium of external shear force  $V_u$  and the internal resistance gives

$$V_u = V_{cy} + V_d + V_{iy} + V_s \quad (1.4)$$

Of the four components of internal shear resistance shown above, only the shear resistance provided by the stirrups is known with any certainty. The other three do not lend themselves for analytical

quantification. However, for design convenience, the contribution of the three resistances  $V_{cy}$ ,  $V_d$ , and  $V_{iy}$  are conservatively lumped into a single term,  $V_c$ , somewhat loosely referred to as the shear strength contribution of the concrete to the total shear resistance.

Thus

$$V_c = V_{cy} + V_d + V_{iy} \quad (1.5)$$

The ACI 318-05/08 gives several equations for calculating the shear strength  $V_c$ , the most simple one being

$$V_c = 2\sqrt{f'_c} bd \quad (1.6)$$

### 1.2.5 SLIDING SHEAR (SHEAR FRICTION)

The preceding section dealt with shear in the context of flexural loading of beams in which shear is used merely as a convenient measure of diagonal tension. In contrast, there are circumstances such that direct shear may cause failure of reinforced concrete members. Potential failure planes can be postulated for such cases along which direct shear stresses are high, and failure to provide adequate reinforcement across such planes may produce unwelcome results.

The necessary reinforcement may be determined on the basis of the shear-friction method of design. The basic approach is to assume that slip occurs along a predetermined plane of weakness. Reinforcement must be provided crossing the potential plane to prevent direct shear failure.

The shear-friction theory is very simple. A shear resistance  $V_n$  acts parallel to the crack, and the resulting tendency for the upper block to slip relative to the lower is resisted largely by friction along the concrete interface at the crack. Since the crack surface is typically rough and irregular, the effective coefficient of friction is quite high. In addition, the irregular surface will cause the two blocks of concrete to separate slightly, as shown in Figure 1.19.

If reinforcement is present perpendicular to the crack, then slippage and subsequent separation of the concrete will stress the steel in tension. The resulting tensile force sets up an equal and opposite clamping pressure between the concrete faces on either side of the crack. The maximum value of this interface pressure is  $A_{vf}f_y$ , where  $A_{vf}$  is the total area of steel crossing the crack, and  $f_y$  is its yield strength, limited to 60,000 psi.

The relative movement of the concrete on opposite sides of the crack also subjects the individual reinforcing bars to shearing action, and the dowel resistance of the bars to this shearing action contributes to shear resistance. However, it is customary to neglect the dowel effect for simplicity in design, and to compensate for this by using a relatively high value of the friction coefficient.

The required area of shear reinforcement is computed using

$$A_{vf} = V_u / \phi f_y \mu \quad (1.7)$$

where

$A_{vf}$  is the area of shear-friction reinforcement (in.<sup>2</sup>)

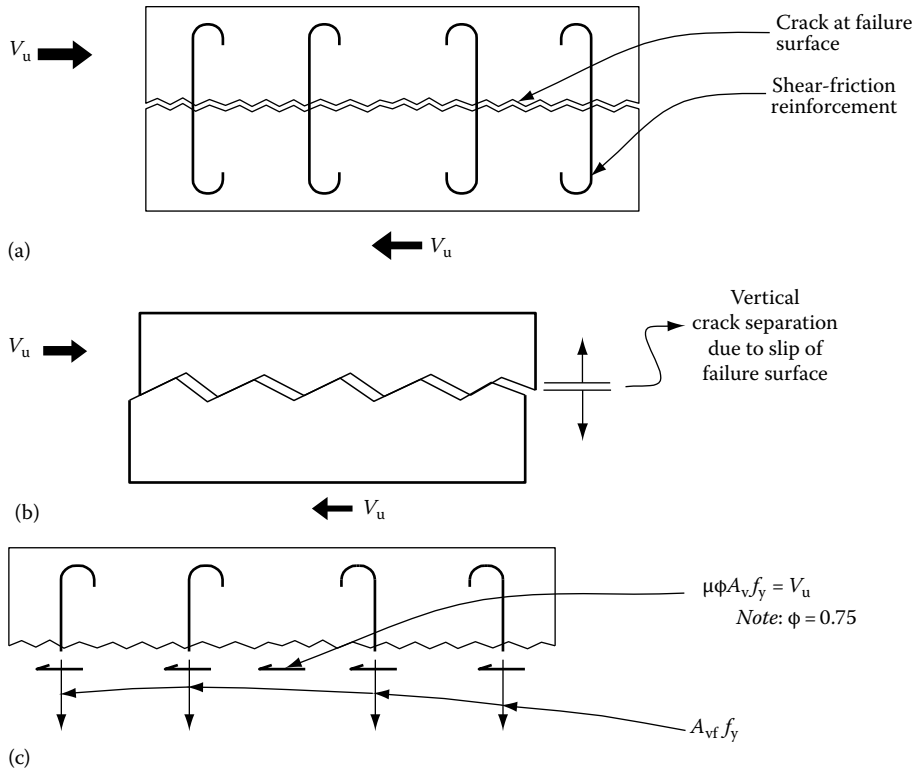
$V_u$  is the factored shear force (lbs)

$\phi$  is the strength reduction factor equal to 0.75

$f_y$  is the yield strength of reinforcement (psi)

$\mu$  is the coefficient of friction, equal to 0.6 for normal weight concrete placed against existing concrete not intentionally roughened

The nominal shear strength  $V_n = V_u / \phi$  for normal weight monolithic concrete or concrete placed against intentionally roughened surface shall not exceed the smallest of



**FIGURE 1.19** Frictional resistance generated by shear-friction reinforcement. (a) Applied shear, (b) enlarged crack surface, and (c) free body diagram of concrete above crack.

$$V_n = V_u / \phi \leq 0.2 f'_c A_c \quad (1.8)$$

$$\leq (480 \pm 0.88 f'_c) A_c \quad (1.9)$$

$$\leq 1800 A_c \quad (1.10)$$

For all other cases,

$$V_n = V_u / \phi \leq f'_c A_c \quad (1.11)$$

$$\leq 800 A_c \quad (1.12)$$

The effect of shear-friction reinforcement,  $A_{vf}$ , may be considered in a conceptual sense, similar to a gravity load that increases the sliding resistance along the shear plane. For example, a #9 bar of  $A_{vf} = 1 \text{ in.}^2$ , fully developed on either side of an unroughened sliding plane is conceptually equivalent to vertical load of 60 kip, resulting in a horizontal resistance of 27 kip (with a coefficient of friction equal to 0.45). If the surface is intentionally roughened of the #9 rebar increases to 45 kip, a pretty impressive resistance indeed in either of the two cases.

The yield strength of the reinforcement is not to exceed 60,000 psi. Direct tension across the shear plane, if present, is to be provided for by additional reinforcement, and permanent net compression



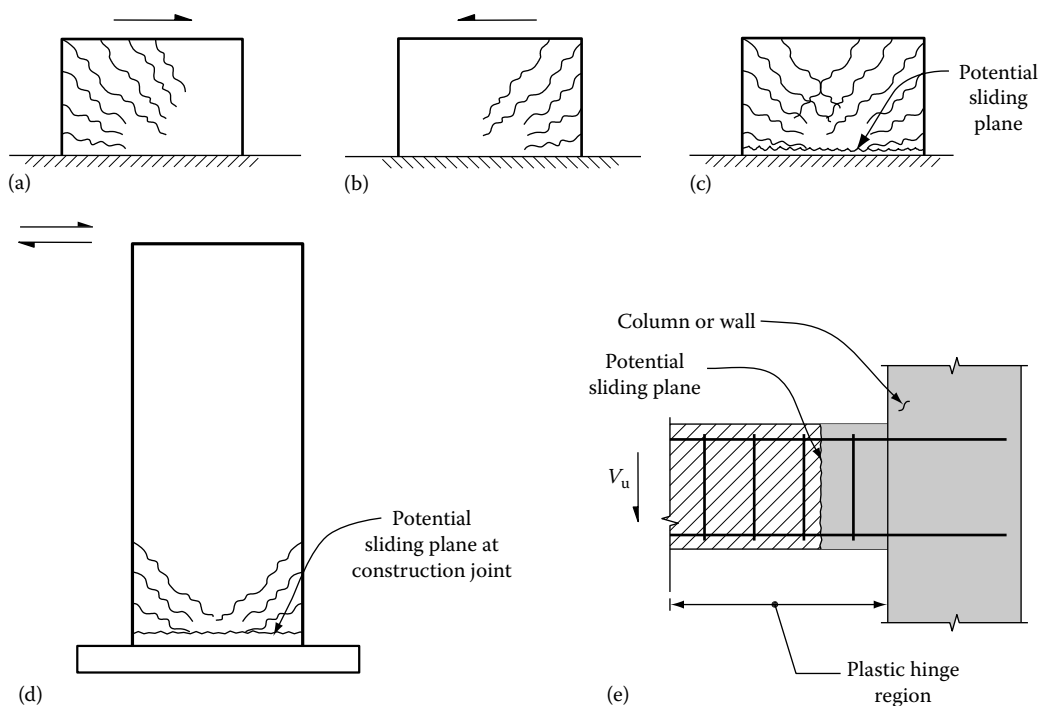
across the shear plane may be taken as additive to the force in the shear-friction reinforcement  $A_{vf}f_y$  when calculating the required  $A_{vf}$ .

When shear is transferred between newly placed concrete against existing hardened concrete, the surface roughness is an important variable. For purposes of design, an intentionally roughened surface is defined as one having a full amplitude of approximately  $\frac{1}{4}$  in.

Certain precautions should be observed in applying the shear-friction method of design. Reinforcement, of whatever type, should be well anchored to develop the yield strength of the steel, by the full development length or by hooks or bends, or by proper heads and welding.

The failure by sliding shear is a possibility in structures subjected to earthquakes. Construction joints across members, particularly when poorly prepared, present special hazards. Flexural cracks, interconnected during reversed cyclic loading, may also become potential sliding planes. Such possible locations shown in Figure 1.20 include

1. *Sliding shear in walls and diaphragms:* Shear transfer across potential sliding planes across walls and diaphragms, where construction joints occur or where wide flexural cracks originating from each of the two edges.
2. *Sliding shear in beams:* Sliding displacements along interconnected flexural and diagonal cracks in regions of plastic hinges can significantly reduce energy dissipation in beams. With reversed cyclic high-intensity shear load, eventually a sliding shear failure may develop.
3. *Sliding shear in columns:* For purposes of verifying sliding shear, particularly in potential plastic hinge regions, it is advisable to consider columns as beams. However, when the vertical reinforcement is evenly distributed around the periphery of the column section as is typical, more reliance may be placed on the dowel resistance against sliding of the vertical



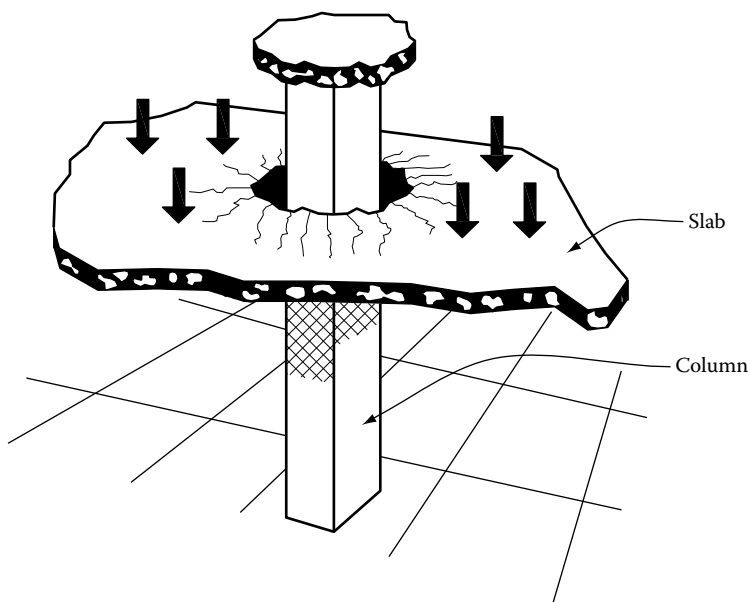
**FIGURE 1.20** Potential locations of sliding shear. (a–c) Squat wall, (d) tall wall, and (e) plastic hinge region in a frame beam.

bars. Any axial compression on the column that may be present will greatly increase resistance against sliding shear. Therefore, no consideration need be given to sliding shear in columns constructed with a relatively even distribution of vertical reinforcement.

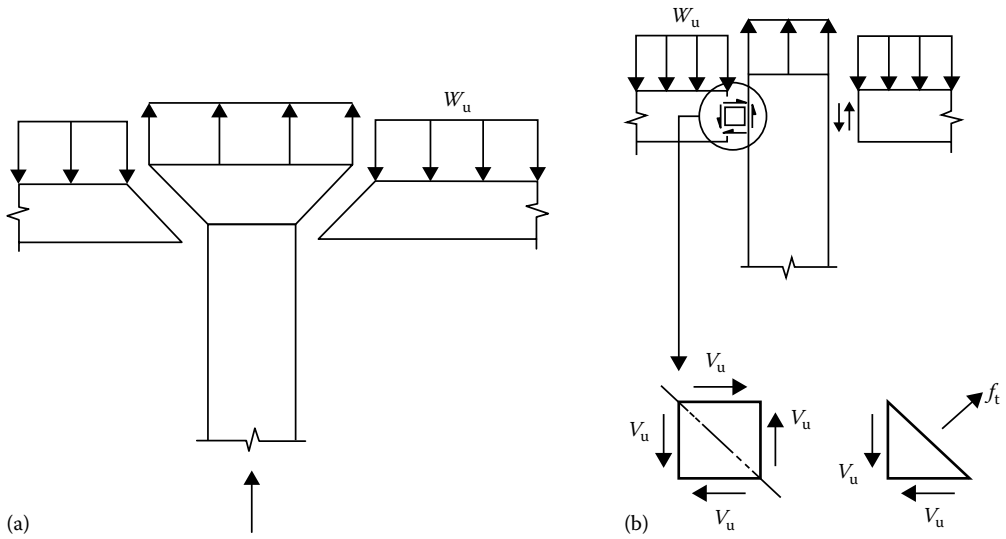
### 1.2.6 PUNCHING SHEAR

Punching shear occurs where a two-way concrete flat slab or plate is connected to a column without beams. It is the tendency of the slab to drop as a unit around the column, as shown schematically in Figure 1.21. The column appears to “punch” through the slab, hence the term “punching shear.” The cracking due to the overstress, which may lead to this type of collapse, is most visible on the top surface of the slab.

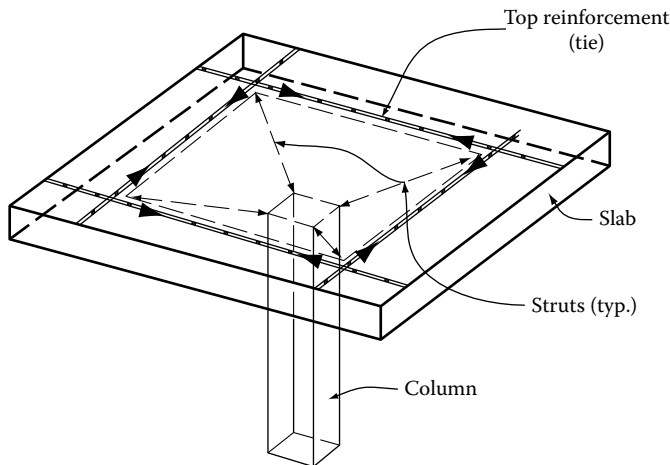
For expediency in design, the ACI 318 allows the punching shear check through a hypothetical stress distribution such as shown in Figure 1.22. In this design the column is visualized to punch through an assumed critical section. A set of hypothetical stresses over the critical section is computed to be in equilibrium with the associated applied moment and shear. The design procedure aims to keep the computed hypothetical stresses below stipulated, allowable values. These values are  $6\sqrt{f'_c}$  and  $4\sqrt{f'_c}$  for slabs with and without shear reinforcement, respectively. The computed values are not meant to represent true stresses, such as would be obtained from an elastic analysis. In reality, the cracking of concrete and the role of reinforcement over the support dictate a different load path, similar to the simplified strut-and-tie model illustrated in Figure 1.23, in which the top reinforcement becomes central for the load-carrying ability of the joint. The safety of the joint is tied with the tension capacity of reinforcement over the columns. The dearth of reports on punching shear failure for structures built over the last several decades suggests that the minimum top reinforcement requirement over the columns included in the design for flexure in the ACI 318 05/08 is adequate to supplement the punching shear demand. Therefore, although not codified at this time (2009), it appears that wherever an irregularity at a column/slab joint prevents direct application of the hypothetical stress computation formula, the solution to a safe design is best sought by providing an adequate strut-and-tie model. Refined elastic formulations aimed at revealing maximum stresses in the irregular geometry may not be warranted.



**FIGURE 1.21** Punching shear failure in a two-way slab system. It is the tendency of the slab to drop as a unit around the column.



**FIGURE 1.22** Transfer of slab load into columns.



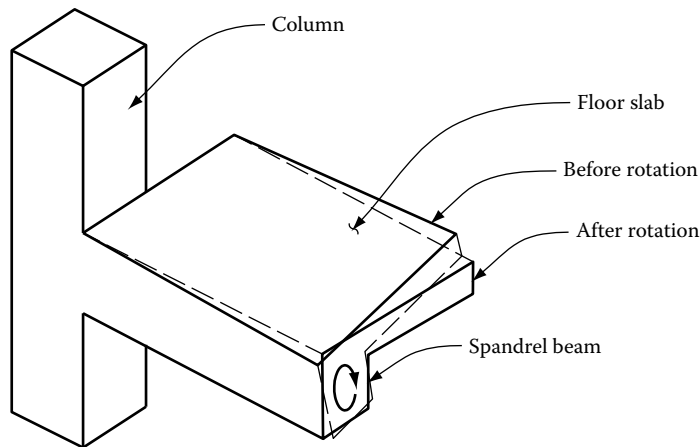
**FIGURE 1.23** Strut-and-tie model for punching shear.

## 1.2.7 TORSION

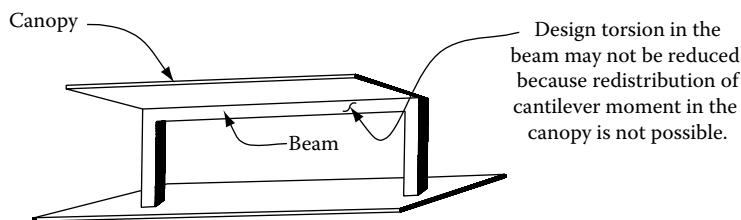
### 1.2.7.1 Elemental Torsion

The distribution of gravity loads produces bending and shear forces in just about all the resisting elements. The load path travels from the slab—to floor beams—to girders and finally to the vertical support system. Because of the monolithic nature of reinforced concrete construction, rotational forces including torsion are also transmitted along the load path. Shown in Figure 1.24 is an example of a perimeter spandrel beam subject to torsion.

In designing reinforced concrete members for torsion, the loadings can be separated in two categories.



**FIGURE 1.24** Torsion in spandrel beams.



**FIGURE 1.25** Equilibrium torsion.

1. Equilibrium torsion
2. Compatibility torsion

When design is for the equilibrium torsion, the entire calculated torsion needs to be accounted for in the analysis.

However, where the torsional moment results from the compatibility of deformations between members meeting at a joint, the designer is permitted to reduce the calculated torsion. This is based on the well-known concept of redistribution of moments in reinforced concrete members (see Figures 1.25 and 1.26).

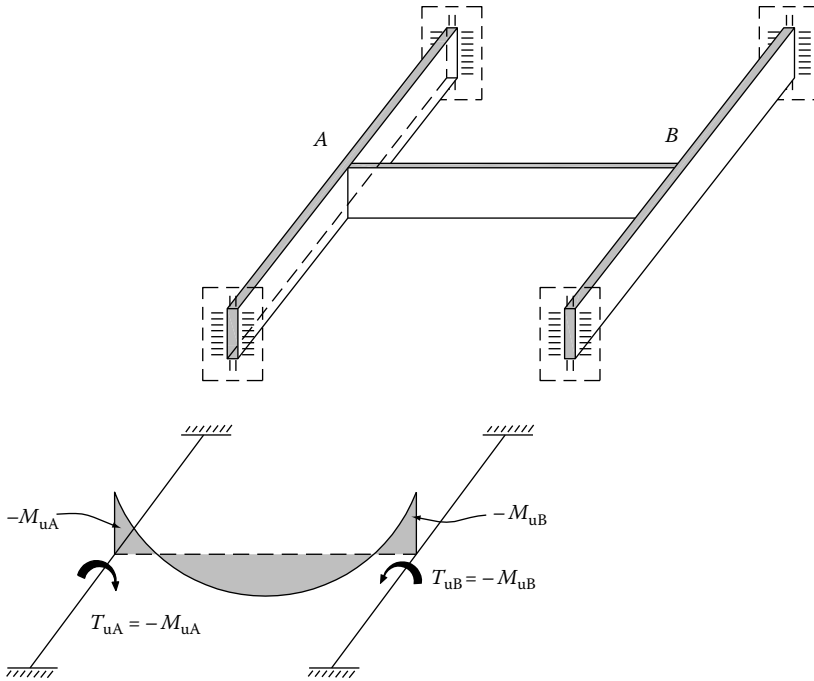
#### 1.2.7.1.1 ACI Design Method for Torsion

The design procedure for combined moment, shear, and torsion involves designing for the moment first, ignoring torsion and shear, and then calculating the stirrups and longitudinal reinforcement to provide the required resistance to the calculated vertical and torsional shear. Conceptual design steps are as follows:

1. For a given set of  $+M_u$ ,  $-M_u$ , and  $V_u$ , determine the flexural reinforcement  $+A_s$  and  $-A_s$  and the shear reinforcement,  $A_v$ .
2. Determine if torsion should be considered in the analysis by comparing the calculated torsion,  $T_u$  to the threshold torsion value, given by

$$T_o = \phi 4\lambda \sqrt{f'_c} (A_{cp}^2 / P_{cp}) \quad (1.13)$$

If  $T_u > T_o$ , torsion cannot be ignored.



**FIGURE 1.26** Compatibility torsion.

- From an inspection of the given problem, determine if the design torsion,  $T_u$ , is due to equilibrium torsion or due to compatibility torsion. If it is due to equilibrium, design of member for the entire calculated torsion. If  $T_u$  is due to compatibility requirements, as in statically indeterminate structures, it is permissible to reduce  $T_u$  to a maximum value,  $T_o$  given by

$$T_u(\text{max}) = \phi 4 \sqrt{f'_c} (A_{cp}^2 / P_{cp}) = T_o \quad (1.14)$$

- Determine the area of stirrups,  $A_t$ , required for resisting torsion  $T_u$  by the equation:

$$A_t = \frac{T_n S}{2 A_o f_y \cot \theta} \quad (1.15)$$

where

$A_t$  is the area of one leg of a close stirrup resisting torsion within a spacing of  $S$  in.<sup>2</sup>

$A_o$  is the area enclosed by centerline of the outermost closed transverse torsional reinforcement, in.<sup>2</sup>

$\theta$  is the  $45^\circ$  for nonprestressed beams

$f_y$  is the specified yield strength of reinforcement, psi

$T_n$  nominal torsion moment strength, in.-lb

- Add the stirrup requirements for torsion and shear using the equation:

$$\text{Total} \left( \frac{A_{v+t}}{S} \right) = \frac{A_v}{S} + \frac{2A_t}{S} \quad (1.16)$$

Note that even when the shear stirrup,  $A_v$ , has multiple legs, only the stirrups adjacent to the beam sides are permitted to be included in the summation. This is because inner legs would be ineffective in resisting torsional moments.

6. Check minimum stirrups:

$$(A_v + 2A_t) = 0.75\sqrt{f'_c} \left( \frac{b_w S}{f_{yt}} \right) \quad \text{and} \quad \frac{50b_w S}{f_{yt}} \quad (1.17)$$

7. Determine the additional area of longitudinal reinforcement to resist torsion,  $A_t$ . Use ACI 318-05, Equation 11.24.

Refer to ACI 318-05/08, Chapter 11 for a complete description of various terms used in the equations above.

### 1.2.7.2 Overall Building Torsion

To avoid excessive lateral displacements torsional effects should be minimized by reducing the distance between the center of mass (CM), where horizontal seismic floor forces are applied, and the center of rigidity (CR) of the vertical elements resisting the lateral loads. A conceptual explanation of CM and CR follows.

#### 1.2.7.2.1 Center of Mass

During earthquakes, acceleration-induced inertia forces will be generated at each floor level, where the mass of an entire story may be assumed to be concentrated. Hence the location of seismic force at a particular level will be determined by the center of the accelerated mass at that level. In regular buildings, the positions of the centers of floor masses will differ very little from level to level. However, irregular mass distribution over the height of a building may result in variations in centers of masses, which will need to be evaluated.

#### 1.2.7.2.2 Center of Rigidity

This point, defined as the center of rigidity or center of stiffness, locates the position of a story shear force  $V_j$ , which will cause only relative floor translations and no torsion. Displacements due to story twist, when combined with those resulting from floor translations, can result in total interstory displacements that may be difficult to accommodate. For this reason, the distance between the CR and the CM should be minimized, but may not be possible due to building geometry. Invariably, effects of torsion are present in all buildings although analysis may show that in some buildings torsional effects are negligible. This is because torsion occurs as a result of variations in material properties, section geometry, and also due to the effects of torsional component of ground motion. Thus, torsion arises also in theoretically perfectly symmetrical buildings. Hence the seismic requirement that allowance be made in all buildings for so-called accidental torsion. For nonflexible diaphragm buildings, the ASCE 7-05/08 requires that in addition to the calculated torsion, an accidental torsion caused by an assumed displacement of center of mass by a distance equal to 5% of the dimension of the building perpendicular to the direction of force be included. However, the specified accidental torsion need not be applied simultaneously in two directions.

Regarding the simultaneous application of loads in two mutually perpendicular directions, it is worth noting that for buildings in SDC B, the earthquake loads are assumed to act independently along the two orthogonal axes of the buildings. For SDC C buildings having nonparallel lateral load-resisting systems, and for all buildings in SDC D and higher, 100% of the forces for one direction are added to 30% of the forces in the perpendicular direction, the directions chosen to give the worst effect for the member being designed.

If a building is subject to twist, as all are, the torsional stiffness of the core, in a “core-only” structure can be a significant part of the total torsional resistance of the building. The torsional behavior of cores is a topic that is relatively unfamiliar to many engineers. The proportions of the height, length, and thickness of the core walls of a typical building obligate us to analytically treat the core as a thin-walled beam. Consequently, when the core twists originally plane sections of the core warp. Because the core is restrained from warping by the foundation, and to a smaller extent

by the floor slabs, warping stresses somewhat similar to axial stresses are induced throughout the height of core walls. In buildings that are predominantly dependent on a core for torsional and lateral resistance, it is imperative that consideration be given to warping effects. Further explanation of this phenomenon is given in Chapter 9.

### 1.3 EXTERNAL LOADS

In this section, we will review loads typically considered in building design. These are

- Earthquake loads (Section 1.3.1)
- Wind loads (Section 1.3.2)
- Explosion effects (Section 1.3.3)
- Floods (Section 1.3.4)
- Vehicle impact loads (Section 1.3.5)

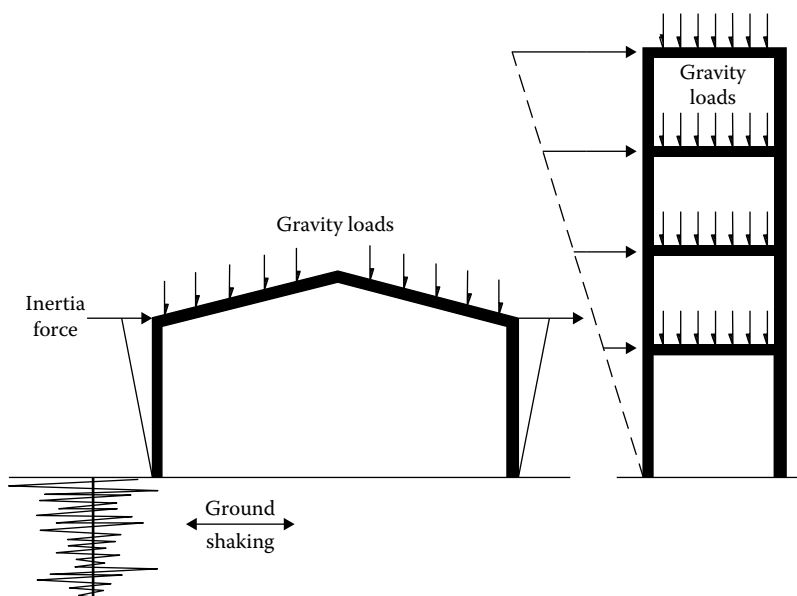
#### 1.3.1 EARTHQUAKES LOADS

Earthquakes are catastrophic events that occur mostly at the boundaries of portions of the earth's crust called tectonic plates. When movement occurs in these regions, along faults, waves are generated at the earth's surface that can produce very destructive effects.

Aftershocks are smaller quakes that occur after all large earthquakes. They are usually most intense in size and number within the first week of the original quake. They can cause very significant re-shaking of damaged structures, which makes earthquake-induced disasters more hazardous. A number of moderate quakes (6+ magnitude on the Richter scale) have had aftershocks that were very similar in size to the original quake. Aftershocks diminish in intensity and number with time. They generally follow a pattern of being at least 1 large (within magnitude 1 on the Richter scale) aftershock, at least 10 lesser (within magnitude 2 on the Richter scale) aftershocks, 100 within magnitude 3 on the Richter scale, and so on. The Loma Prieta earthquake had many aftershocks, but the largest was only magnitude 5.0, with the original quake being magnitude 7.1.

Some of the most destructive effects caused by shaking as a result of the earthquake are those that produce lateral loads in a structure. The input shaking causes the foundation of a building to oscillate back and forth in a more or less horizontal plane. The building mass has inertia and wants to remain where it is and therefore, lateral forces are exerted on the mass in order to bring it along with the foundation. For analysis purposes, this dynamic action is simplified as a group of horizontal forces that are applied to the structure in proportion to its mass and to the height of the mass above the ground. In multistory buildings with floors of equal weight, the loading is further simplified as a group of loads, each being applied at a floor line, and each being greater than the one below in a triangular distribution (see Figure 1.27). Seismically resistant structures are designed to resist these lateral forces through inelastic action and must, therefore, be detailed accordingly. These loads are often expressed in terms of a percent of gravity weight of the building and can vary from a few percent to near 50% of gravity weight. There are also vertical loads generated in a structure by earthquake shaking, but these forces rarely overload the vertical load-resisting system. However, earthquake-induced vertical forces have caused damage to structures with high dead load compared to design live load. These vertical forces also increase the chance of collapse due to either increased or decreased compression forces in the columns. Increased compression may exceed the axial compressive capacity of columns while decreased compression may reduce the bending strength of columns.

In earthquake engineering, we deal with random variables and therefore the design must be treated differently from the orthodox design. The orthodox viewpoint maintains that the objective of design is to prevent failure; it idealizes variables as deterministic. This simple approach is still valid and applied to design under only mild uncertainty. But when confronted with the effects of earthquakes, this orthodox viewpoint seems so overtrustful as to be worthless. In dealing with



**FIGURE 1.27** Earthquake loading: Dynamic action of earthquakes can be simplified as a group of horizontal forces that are applied to the structure in proportion to its mass, and to the height of the mass above the ground.

earthquakes, we must contend with appreciable probabilities that failure will occur in the near future. Otherwise, all the wealth of this world would prove insufficient to fill our needs: the most modest structures would be fortresses. We must also face uncertainty on a large scale while designing engineering systems—whose pertinent properties are still debated to resist future earthquakes—about whose characteristics we know even less.

Although over the years, experience and research have diminished our uncertainties and concerns regarding the characteristics of earthquake motions and manifestations, it is unlikely, though, that there will be such a change in the nature of knowledge to relieve us of the necessity of dealing openly with random variables. In a way, earthquake engineering is a parody of other branches of engineering. Earthquake effects on structures systematically bring out the mistakes made in design and construction, even the minutest mistakes. Add to this the undeniable dynamic nature of disturbances, the importance of soil structure interaction, and the extremely random nature of it all; it could be said that earthquake engineering is to the rest of the engineering disciplines what psychiatry is to other branches of medicine. This aspect of earthquake engineering makes it challenging and fascinating, and gives it an educational value beyond its immediate objectives. If structural engineers are to acquire fruitful experience in a brief span of time, expose them to the concepts of earthquake engineering, even if their interest in earthquake-resistant design is indirect. Sooner or later, they will learn that the difficulties encountered in seismic design are technically intriguing and begin to exercise that nebulous trait called engineering judgment to make allowance for these unknown factors.

### 1.3.2 WIND LOADS

Wind is a term used to describe horizontal motion of air. Motion in a vertical direction is called a current. Winds are produced by differences in atmospheric pressure that are primarily attributable to differences in temperature. These differences are caused largely by unequal distribution of heat from the sun, and the difference in thermal properties of land and ocean surfaces. When temperatures of adjacent regions become unequal, the warmer, lighter air rises and flows over the colder, heavier air. Winds initiated in this way are modified by rotation of the earth.



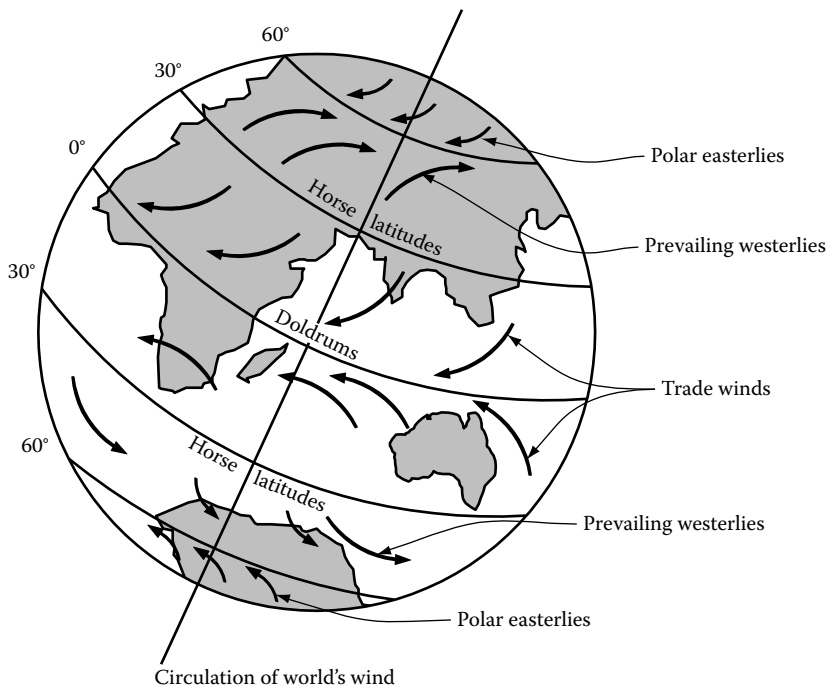
In describing global circulation of wind, modern meteorology relies on wind phrases used by early long-distance sailors. For example, terms like trade winds and westerlies were used by sailors who recognized the occurrence of steady winds blowing for long periods of time in the same direction.

Near the equator, the lower atmosphere is warmed by the sun's heat. The warm air rises, depositing much precipitation and creating a uniform low-pressure area. Into this low-pressure area, air is drawn from the relatively cold high-pressure regions from northern and southern hemispheres, giving rise to trade winds between the latitudes of  $30^\circ$  from the equator. The air going aloft flows counter to the trade winds to descend into these latitudes, creating a region of high pressure. Flowing northward and southward from these latitudes in the northern and southern hemispheres, respectively, are the prevailing westerlies, which meet the cold dense air flowing away from the poles in a low-pressure region characterized by stormy variable winds. It is this interface between cold, dense air and warm, moist air which is of main interest to the television meteorologists of northern Europe and North America.

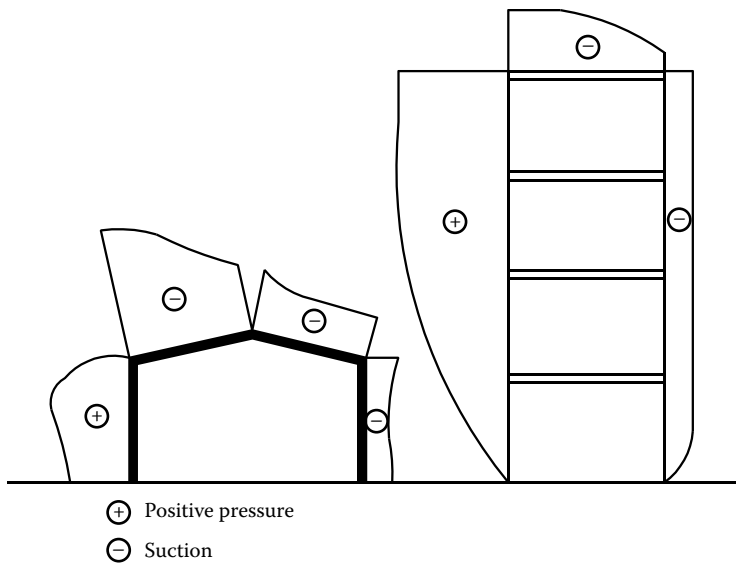
As the air above hot earth expands and rises, air from cooler areas such as the oceans floats in to take its place. The process produces two types of wind circulation:

1. General global circulation extending around the earth
2. Smaller secondary circulations producing local wind conditions

Figure 1.28 shows a model of circulation of prevailing winds that result from the general movement of air around the earth. Observe that there are no prevailing winds within the equatorial belt, which lies roughly between latitudes  $10^\circ$  S and  $10^\circ$  N. Therefore, near the equator and up to about 700 miles (1127 km) on either side of it, there exists a region of relative calm called the doldrums. In both hemispheres, some of the air that has risen at the equator returns to the earth's surface at about  $30^\circ$  latitude, producing little or no wind. These high-pressure areas are called horse latitudes, possibly



**FIGURE 1.28** Circulation of world's winds.



**FIGURE 1.29** Wind load distribution: positive pressure on windward wall, and negative pressure (suction) on leeward wall and roof. For a hermetically sealed building, internal pressures cancel out, hence no effect on overall building loads.

because many horses died on the sailing ships that got stalled because of lack of wind. The winds that blow between the horse latitudes and the doldrums are called trade winds because sailors relied on them for sailing ships. The direction of trade winds is greatly modified by the rotation of the earth as they blow from east to west. Two other kinds of winds that result from the general circulation of the atmosphere are called the prevailing winds and the polar easterlies. The prevailing winds blow into the belts bounded by the horse latitudes and  $60^\circ$  north and south of the equator. Thus the moving surface air produces six belts of winds around the earth as shown in Figure 1.28.

Forces due to wind are generated on the exterior of the building based on its height, local ground surface roughness (hills, trees, and other buildings) and the square of the wind velocity. The weight of the building, unlike in earthquake design, has little effect on wind forces, but is helpful in resisting uplift forces. Unless the structure has large openings, all the wind forces are applied to the exterior surfaces of the building. This is in contrast to earthquake forces where both exterior and interior walls are loaded proportionally to their weight. Wind pressures act inward on the windward side of a building and outward on most other sides and most roof surfaces (see Figure 1.29). Special concentrations of outward force, due to aerodynamic lift, occur at building corners and roof edges, particularly so at overhangs. The overall structure is designed for the sum of all lateral and uplift pressures and the individual parts to resist the outward and inward pressure concentrations. They must be connected to supporting members to form a continuous load path. Forces are also generated on structures by airborne missiles such as those caused by dislodging of roofing gravel from neighboring buildings.

### 1.3.2.1 Extreme Wind Conditions

Extreme winds, such as thunderstorms, hurricanes, tornadoes, and typhoons, impose loads on structures that are many times more than those assumed in their design. Some standards, such as those published by the American National Standards Institute, provide for hurricane wind speeds for a specified probability of occurrence but do not consider directly the effect of other types of extreme wind conditions. A brief description of the characteristics of extreme winds and their effect on structures follows.

### 1.3.2.1.1 *Thunderstorms*

Thunderstorms are one of the most familiar features of temperate summer weather, characterized by long hot spells punctuated by release of torrential rain. The essential conditions for the development of thunderstorms are warm, moist air in the lower atmosphere and cold, dense air at higher altitudes. Under these conditions, warm air at ground level rises, and once it has started rising, it continues to rise faster and faster, building storm clouds in the upper atmosphere. Thunder and lightning accompany downpours, creating gusty winds that sometimes blow violently at great speeds. Wind speeds of 20–70 mph (9–31 m/s) are typically reached in a thunderstorm and are often accompanied with swirling wind action exerting high suction forces on roofing and cladding elements.

### 1.3.2.1.2 *Hurricanes*

Hurricanes are severe atmospheric disturbances that originate in the tropical regions of the Atlantic Ocean or Caribbean Sea. They travel north, northwest, or northeast from their point of origin and usually cause heavy rains. They originate in the doldrums and consist of high-velocity winds blowing circularly around a low-pressure center known as the eye of the storm. The low-pressure center develops when the warm saturated air prevalent in the doldrums interacts with the cooler air. From the edge of the storm toward its center, the atmospheric pressure drops sharply and the wind velocity rises. In a fully developed hurricane, winds reach speeds up to 70–80 mph (31–36 m/s), and in severe hurricanes, it can attain velocities as high as 200 mph (90 m/s). Within the eye of the storm, the winds cease abruptly, the storm clouds lift, and the seas become exceptionally violent.

The maximum basic wind velocity (3 s gust) for any area of the United States specified in ASCE 7-05 is 150 mph (67 m/s), which is less than the highest wind speeds in hurricanes. Except in rare instances, such as defense installations, a structure is not normally designed for full hurricane wind speeds.

Hurricanes are one of the most spectacular forms of terrestrial disturbances and produce the heaviest rains known on earth. They have two basic components, warmth and moisture, and consequently they develop only in the tropics. Almost invariably they move in a westerly direction at first and then swing away from the equator, either striking land with devastating results or moving out over the oceans until they encounter cool surface water and die out naturally. The region of greatest storm frequency is the northwestern Pacific, where the storms are called typhoons, a name of Chinese origin meaning “wind which strikes.” The storms that occur in the Bay of Bengal and the seas of north Australia are called cyclones. Although there are some general characteristics common to all hurricanes, no two are exactly alike. However, a typical hurricane can be considered to have a 375 mile (600 km) diameter, with its circulating winds spiraling in toward the center at speeds up to 112 mph (50 m/s). The size of the eye can vary in diameter from as little as 3.7–25 miles (6–40 km). However, the typhoon that roared past the island of Guam in 1979 had a very large diameter of 1400 miles (2252 km) with the highest wind reaching 190 mph (85 m/s). Storms of such violence have been known to drive a plank of wood right through the trunk of a tree and blow straws end-on through a metal deck. Fortunately, storms of such magnitude are not common.

### 1.3.2.1.3 *Tornadoes*

Tornadoes develop within severe thunderstorms and occasionally in hurricanes. They consist of a rotating column of air usually accompanied by a funnel-shaped downward extension of a dense cloud having a vortex of several hundred feet, typically 200–800 ft (61–244 m) in diameter whirling destructively at speeds up to 300 mph (134 m/s). A tornado contains the most destructive of all wind forces, usually destroying everything along its path of approximately 10 miles (16 km) long and directed predominately toward the northeast. Tornadoes form when a cold storm front runs over warm, moist surface air. The warm air rises through the overlaying cold storm clouds and is intercepted by the high-altitude winds, which are even colder and are rapidly moving above the clouds. Warm air collides with the cooler air and begins to whirl. The pressure at the center of the spinning column of air is reduced because of the centrifugal force. This reduction in pressure causes more warm air to be sucked into it, creating a violent outlet for the warm air trapped under the storm.

As the velocity increases, more warm air is drawn in to the low-pressure area created in the center of the vortex. As the vortex gains strength, the funnel begins to extend toward the ground, eventually touching it. Funnels usually form close to the leading edge of the storm. Larger tornadoes may have several vortices within a single funnel. If the bottom of the funnel can be seen, it usually means that the tornado has touched down and begun to pick up visible debris from the ground. A typical tornado travels 20–30 mph (9–14 m/s), touches ground for 5–6 miles (8–10 km), and has a funnel 300–500 ft (92–152 m) wide. Distance from the ground to the cloud averages about 2000 ft (610 m). Although it is impractical to design buildings to sustain a direct hit from a tornado, it behooves the engineer to pay extra attention to anchorage of roof decks and curtain walls for buildings in areas of high tornado frequency. Rolling plains and flat country make a natural home for tornadoes. Statistically, flat plains get more tornadoes than other parts of the country. In North America, communities in Kansas, Nebraska, and Texas experience many tornadoes and are classified as “tornado belt” areas. No accurate measurement of the inner speed of a tornado has been made because tornadoes destroy standard measuring instruments. However, photographs of tornadoes suggest the wind speeds are of the order of 167–224 mph (75–100 m/s). Although there definitely are tornado seasons, tornadoes can occur at any time. Like a hurricane, the tornado consists of a mass of unstable air rotating furiously and rising rapidly around the center of an area with low atmospheric pressure. The similarity ends here, because whereas the hurricane is generally of the order of 300–400 miles (483–644 km) in diameter, a large tornado is unlikely to be more than 1500 feet (458 m) across. However, in terms of destructive violence, no other atmospheric disturbance comes even close to that caused by tornadoes.

Although the probability of any one particular building being hit by a tornado is very small (less than 10 per year), tornadoes account for the greatest incidence of death and serious injury of building occupants due to structural failure and cause considerable economic loss. With some exceptions, such as nuclear power plants, it is generally not economical to design buildings for tornadoes. It is, however, important to provide key construction details for the safety of building occupants. Investigations of tornado-damaged areas have shown that the buildings in which well over 90% of the occupants were killed or seriously injured by tornadoes did not satisfy the following two key details of building construction:

- The anchorage of house floors into the foundation or ground (the floor takes off with the occupant in it)
- The anchorage of roofs to concrete block walls (the roof takes off and the unsupported block wall collapses onto the occupants)

Deficiency of the second construction detail is especially serious for open assembly occupancies because there is nothing inside, such as stored goods, to protect the occupants from wall collapse. For such buildings in tornado-prone areas, it is recommended that the block walls contain vertical reinforcing linking the roof to the foundation.

For tornado protection, key details such as those indicated above should be designed on the basis of a factored uplift wind suction of 50 psf on the roof, a factored lateral wind pressure of 25 psf on the windward wall, and suction of 50 psf on the leeward wall, as recommended by the National Building Code of Canada, NBC 2005.

### 1.3.3 EXPLOSION EFFECTS

Explosions occur when a solid or concentrated gas is transformed into a large volume of hot gases in a fraction of a second. In the case of high explosives, detonation conversion of energy occurs at a very high rate (as high as 4 miles/s), while low explosives such as gunpowder undergo rapid burning at the rate of about 900 ft/s. The resulting rapid release of energy consists of sound (bang), heat and light (fireball), and a shock wave that propagates radically outward from the source at subsonic

speeds for most low explosives and supersonic speeds for high explosives. It is the shock wave consisting of highly compressed particles of air that causes most of the damage to structures. When natural gas explosions occur within structures, gas pressures can build up within confined spaces, causing extensive damage. In all explosions, large, weak, and/or lightly attached wall, floor and roof surfaces may be blown away. The columns and beams may survive a blast, but their stability may be compromised by the removal of their bracing elements such as floor diaphragms. In large explosions, concrete slabs, walls, and even columns may be blown away, leading to conditions that will produce progressive collapse. In 1967, a progressive collapse started when a natural gas explosion caused the collapse of an exterior wall on the 18th floor of a 22-story building. The force of falling debris from floors 19 to the roof then caused the remaining floors to collapse in that section of the building. In the case of an exterior explosion such as from a bomb, the shock wave is initially reflected and amplified by the building face and then penetrates through openings, subjecting floor and wall surfaces to great pressure. Diffraction occurs as the shock propagates around corners, creating areas of amplification and reduction in pressure. Finally the entire building is engulfed by the shock wave, subjecting all building surfaces to the overpressure. A secondary effect of an air blast is a very high velocity wind that propels the debris, which becomes deadly missiles. In very large explosions at close proximity to building surfaces, the effect can be so severe that the structure is locally disintegrated and separated away from the main structure.

### **1.3.4 FLOODS**

Forces are generated on buildings due to hydrostatic lateral and lifting pressure, hydrodynamic forces, and debris impacts. Hydrostatic pressures can overload foundation and basement walls and lift up structures, when water level is not equalized between exterior and interior spaces. River and ocean currents may load frontal and side walls that are submerged and ocean waves can produce pressures as high as 1000 psf. Debris varying in sizes from floating wood pieces to floating structures can impact a building, causing anything from broken windows to a total collapse.

### **1.3.5 VEHICLE IMPACT LOADS**

Structures have been severely damaged and set on fire by vehicle impacts. The most hazardous configurations include soft (high, open) first stories and open-front buildings typical of retail one and two-story structures.

## **1.4 LATERAL LOAD-RESISTING SYSTEMS**

It can be said that there are as many types of lateral systems as there are engineers. However, most of the systems can be grouped into three basic types: (1) shear wall system, (2) frame system, and (3) combination of the two, the shear wall–frame system (dual system). Perhaps the most common of the three for design of buildings taller than, say 40 stories, is the dual system. However, in recent years (2009), there is a trend to push the height limits of the “core-only” type of shear wall systems without moment frames even for buildings assigned to high SDCs. These aspects are discussed in more detail in Chapter 9.

The selection of a structural system for buildings is influenced primarily by the intended function, architectural considerations, internal traffic flow, height, and aspect ratio, and to a lesser extent, the intensity of loading. The selection of a building’s configuration often dictated by architectural considerations is perhaps one of the most important aspects of the overall design. It may impose severe limitations on the structure in its role to provide seismic protection. Some structural forms of construction such as a flat slab system supported by columns are considered unsuitable on its own to provide satisfactory performance under seismic actions although its use is quite prevalent in areas of low seismicity. The seismic issue arises because of excessive lateral displacements and the difficulty of providing for adequate and dependable shear transfer between columns and slabs.

Structural systems considered in this section are as follows:

- Shear walls (Section 1.4.1)
- Coupled shear walls (Section 1.4.2)
- Moment-resistant frames (Section 1.4.3)
- Dual systems (Section 1.4.4)

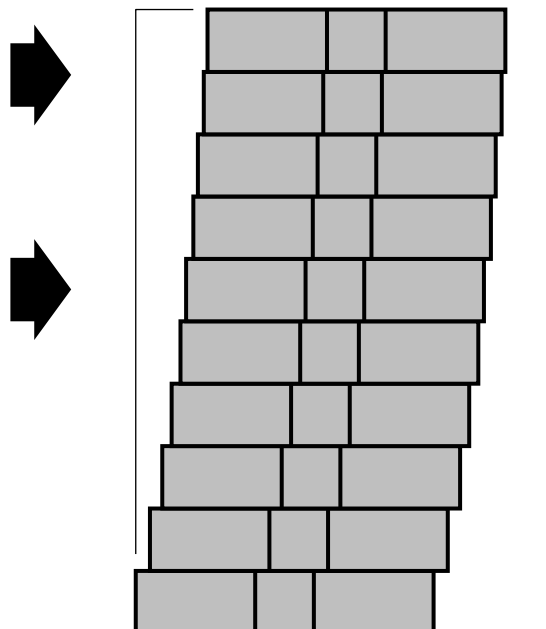
### 1.4.1 SHEAR WALLS

Buildings engineered with structural walls are almost always stiffer than framed structures, reducing the possibility of excessive deformations and hence damage. The necessary strength to avoid structural damage under earthquakes can be achieved by providing a properly detailed longitudinal and transverse reinforcement. By adopting special detailing measures, dependable ductile response can be achieved under major earthquakes.

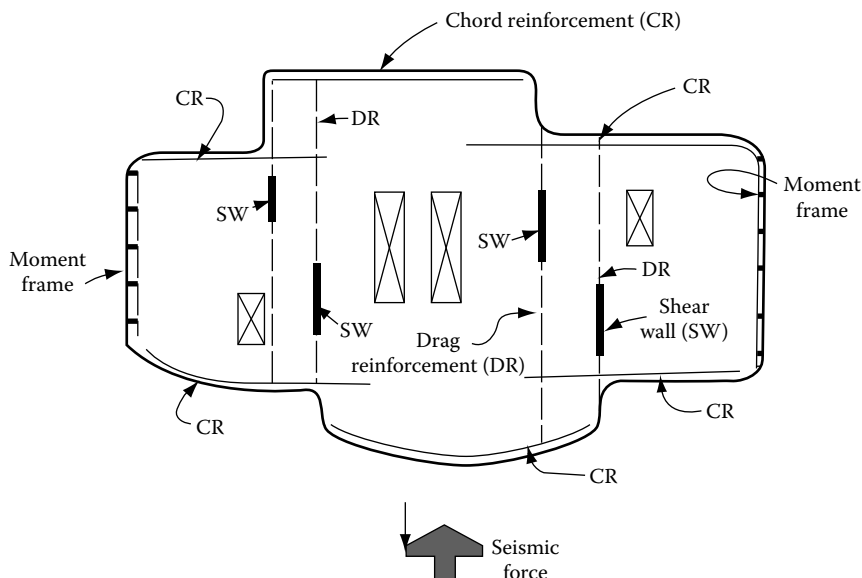
Lateral forces, that is, the forces applied horizontally to a structure derived from winds or earthquakes cause shear and overturning moments in walls. The shear forces tend to tear the wall just as if you had a piece of paper attached to a frame and changed the frame's shape from a rectangle to a parallelogram (see Figure 1.30). The changing of shape from a rectangle to a parallelogram is generally referred to as racking. At the ends of shear walls, there is a tendency for the wall to be lifted up at the end where the lateral force is applied, and a tendency for the wall to be pushed down at the end away from the force. This action provides resistance to overturning moments.

Because of a large fraction of, if not the entire, lateral shear force is often assigned to structural walls, they are usually referred to as shear walls. The name is in appropriate, for it presupposes that shear controls their behavior. This need not be so. And in earthquakes design, this must not be so: every attempt should therefore be made to inhibit inelastic shear modes of deformations. This is achieved readily in practice because shear walls provide nearly optimum means of providing stiffness, strengths, and ductility.

To receive gravity loads from the floors and roof, while simultaneously providing resistance to wind and seismic loads, the walls are typically connected by floor and roof planes often referred to as diaphragms. These planes act like giant beams as stresses in tension and compression are



**FIGURE 1.30** Shear deformations in a shear wall.



**FIGURE 1.31** Diaphragm concept. *Note:* Seismic elements in the E–W direction not shown for clarity.

generated at the edges while shear stresses are distributed throughout the plane. The diaphragm spans horizontally between vertical elements resisting lateral loads as illustrated in Figure 1.31.

The first task of the designers will be to select a structural system most conducive to satisfactory wind and seismic performance within the constraints dictated by architectural requirements. They should discuss alternative structural configurations at the earliest stage of concept development to ensure that undesirable geometry is not locked-in to the system before structural design begins. Irregularities, often unavoidable, contribute to the complexity of structural behavior. When not recognized, they may result in unexpected damage and even collapse. Drastic changes in geometry, interruptions in load paths, discontinuities in both strength and stiffness, disruptions in critical regions by openings, unusual proportions of members, reentrant corners, lack of redundancy, and interference with structural deformations are only a few of the possible structural irregularities. The recognition of many of these irregularities and of conceptions for remedial measures for the avoidance or mitigation of their undesired effects relies on sound understanding of structural behavior. Awareness to search for undesired structural features and design experience in mitigating their adverse effects are invaluable attributes.

When functional requirements permit it, resistance to lateral forces may be assigned entirely to structural walls. Usually, there are also other elements within such a building, which are assigned to carry only gravity loads. Their contribution to lateral force resistance, if any, is often neglected. However, for buildings assigned to SDC D or higher, deformation compatibility of these elements must be verified using magnified elastic displacement. This aspect is discussed in Chapter 4 in more detail.

For buildings up to 20 stories, the use of structural walls is often a matter of choice. For buildings over 30 stories, structural walls may become imperative from the point of view of economy and control of lateral deflection.

Individual walls may be subjected to axial, translational, and torsional displacements. The extent to which a wall will contribute to the resistance of overturning moments, story shear forces, and story torsion depends on its geometric configuration, orientation, and location within the building. While it is relatively easy to accommodate any kind of wall arrangements to resist wind forces, it is much more difficult to ensure satisfactory overall building response to large earthquakes when wall locations deviate considerably. This is because, in the case of wind, a fully elastic response is expected, while during large earthquake demands, inelastic deformations will arise.

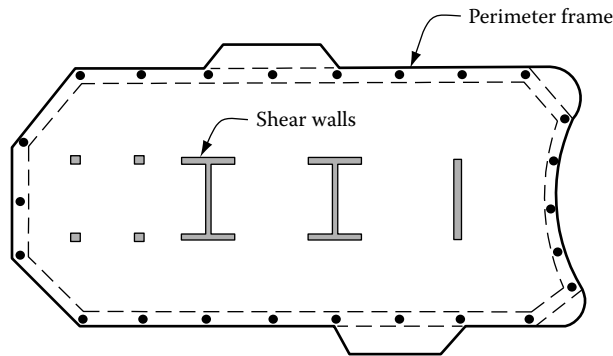
The major structural considerations for individual structural walls will be aspects of symmetry in stiffness torsional stability, and available overturning capacity of the foundations. The key in the

strategy of planning for structural walls is the desire that the inelastic deformations be distributed reasonably uniformly over the whole plan of the building rather than being allowed to concentrate in only a few walls. The latter case leads to the underutilization of some walls, while others might be subjected to excessive ductility demands.

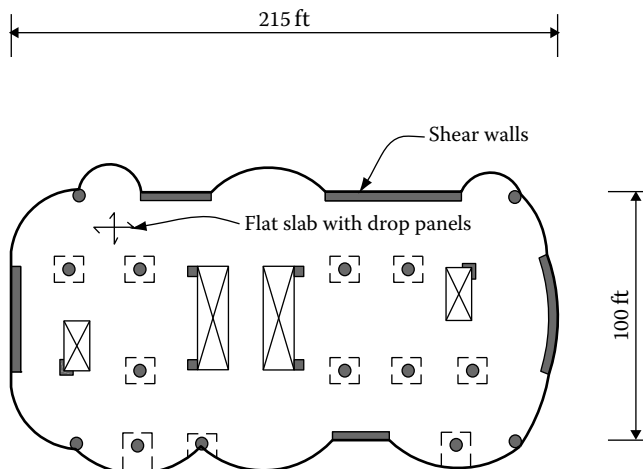
Elevator shafts and stairwells lend themselves to the formation of reinforced concrete core. Traditionally, these have been used to provide the major component of lateral force resistance in multistory office and residential buildings. Additional resistance may be derived, if necessary, from perimeter frames shown in Figure 1.32. Such a centrally positioned large core may also provide sufficient torsional resistance without requiring additional perimeter framing.

In choosing suitable locations for structural walls, the following additional aspects should be considered:

1. For the best torsional resistance, locate as many of the walls as possible at the periphery of the building. Such an example is shown in Figure 1.33. The walls on each side may be single or they may be coupled to each other.
2. Route as much gravity load to the foundations as possible via a structural wall. This will lower the demand for flexural reinforcement in that wall. And more importantly uplift forces will be reduced in the foundations.



**FIGURE 1.32** Floor plan: building with shear walls and perimeter frame.



**FIGURE 1.33** Building with perimeter shear walls.



1.4.2 COUPLED SHEAR WALLS

In many shear wall buildings, a regular pattern of openings will be required to accommodate windows or doors or both. Highly efficient structural systems, particularly suited for ductile response with good energy dissipation characteristics, can be conceived when openings are arranged in a regular pattern. Examples are shown in Figure 1.34 where a number of walls are interconnected or coupled to each other by beams. These walls are generally referred to as coupled shear walls.

The load-resisting mechanisms in a coupled shear wall are shown qualitatively in Figure 1.35b and c. It is seen that the total overturning moment,  $M$ , in the wall without openings shown in Figure 1.35a, is resisted at the base entirely by flexural stresses. On the other hand, in the coupled walls shown in Figure 1.35b and c, axial forces as well as moments occur at the base to resist the overturning moment,  $M$ , resulting in the following equilibrium statement:

$$M = M_1 + M_2 + Td \tag{1.18}$$

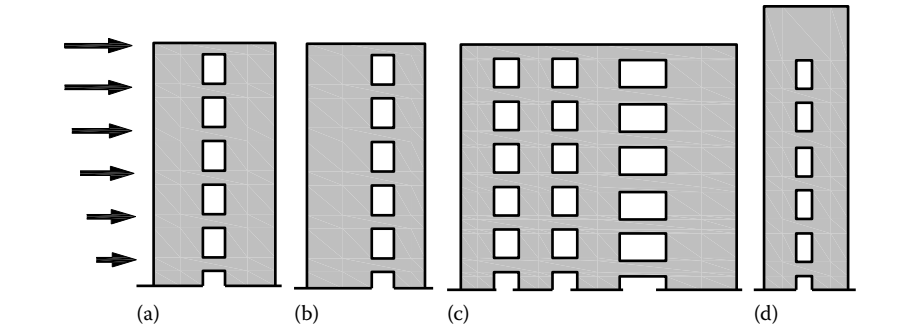


FIGURE 1.34 Shear walls with openings.

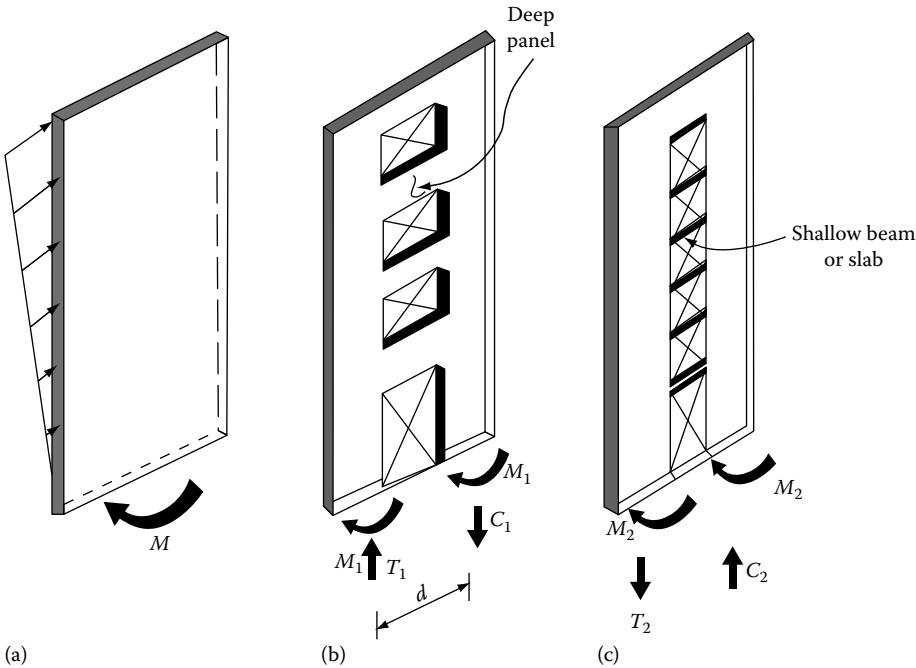
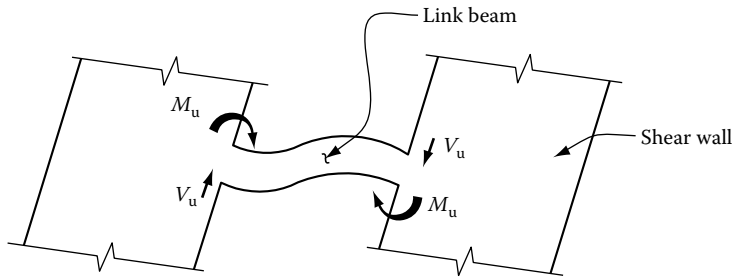


FIGURE 1.35 Lateral load-resistance of single and coupled shear walls.



**FIGURE 1.36** Coupling beam resistance.

The magnitude of the axial force,  $T = C$ , is given by the sum of the shear forces occurring in the coupling beams above the level under consideration.

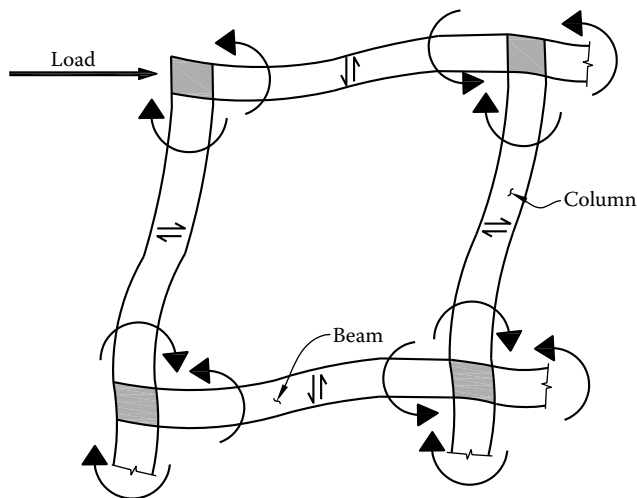
When the coupling is relatively weak, as is often the case in apartment buildings because of limited beam depth, the major portion of moment resistance is due to moment components. On the other hand, if coupling beams are stiff, major moment resistance is by the couple generated by the equal and opposite axial forces in the wall piers.

The resistance of a coupling beam, also referred to as link beam, is shown schematically in Figure 1.36.

Unless adequately designed for flexural ductility and shear force expected under strong ground shaking, flexural or shear failures may develop in structural walls. Additionally, link beams that couple structural walls may be subjected to high ductility demands and high shear forces as a consequence of their short length. To prevent excessive strength degradation in such elements, special detailing measures are adopted using diagonal reinforcement. Further discussion of the detailing requirements is presented in Chapters 5 and 6.

### 1.4.3 MOMENT-RESISTANT FRAMES

In this system, the lateral load resistance is provided by the interaction of girders and the columns as shown schematically in Figure 1.37. The resulting “frame” consisting of the beams and columns



**FIGURE 1.37** Moment-resisting frame: The lateral resistance is provided by keeping the frame from changing into a parallelogram. The interconnection of columns and beams is rigid.

is designed to keep from changing into a parallelogram by making the connections rigid. Structural toughness, which is the ability to repeatedly sustain reversible stresses in the inelastic range without significant degradation, is essential for a moment-resistant frame designed to resist seismic forces. Tall buildings with moment frames may generate significant tension and compression forces in the columns. High tensions can be very detrimental, since severe cracking can result in catastrophic failures when the loading is reversed and the member is also required to resist bending. For this reason, the ACI 318-05/08 requires that the flexural strengths of columns be at least 20% more than the sum of the corresponding strength of the connecting beams at any story. This is to assure that when inelastic action occurs, it will form plastic hinges in the beams, not the columns. Moment-resistant frames can be used in combination with concrete shear walls to provide dual system.

#### 1.4.4 DUAL SYSTEMS

In these systems, reinforced concrete frames interacting with shear walls together provide the necessary resistance to lateral forces, while each system carries its appropriate share of the gravity load. Because the deflected shape of a laterally loaded wall is quite different from that of a frame, the wall responds as a propped cantilever as shown in Figure 1.38.

#### 1.4.5 DIAPHRAGM

A prerequisite for a desirable response of a building is to interconnect all lateral-force-resisting components with a relatively rigid surface. This is achieved with the use of floor and roof systems, which generally possess large in-plane stiffness. Vertical elements such as walls and frames will thus contribute to the total lateral force resistance, in proportion to their own stiffness.

The function of a floor or roof, acting as a diaphragm, is to transmit inertia forces generated by earthquake accelerations of the floor mass at a given level to all horizontal-force-resisting elements. At certain levels, as a response to architectural requirements, particularly in lower stories, significant horizontal forces from one element, such as a frame or shear wall, may need to be transferred to another, usually stiffer element, such as a wall. These actions generate significant shear forces and bending moments within a diaphragm, particularly in long or articulated floor plans. Reentrant

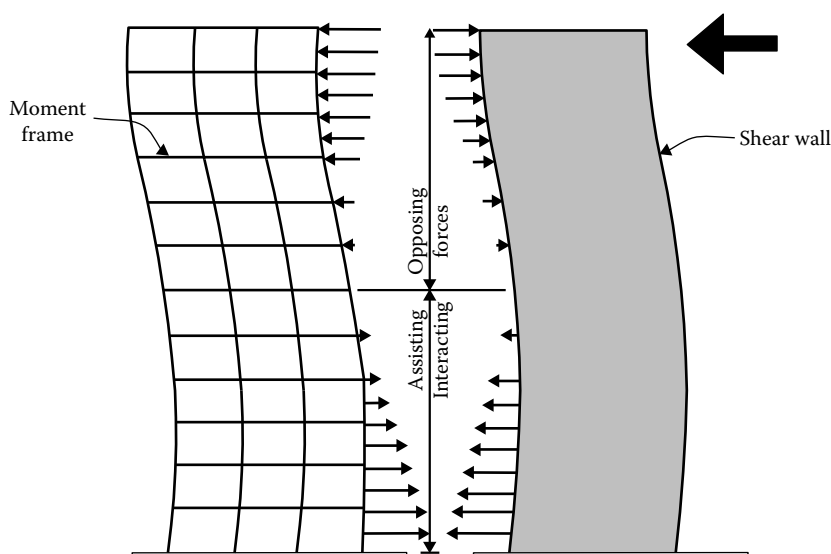
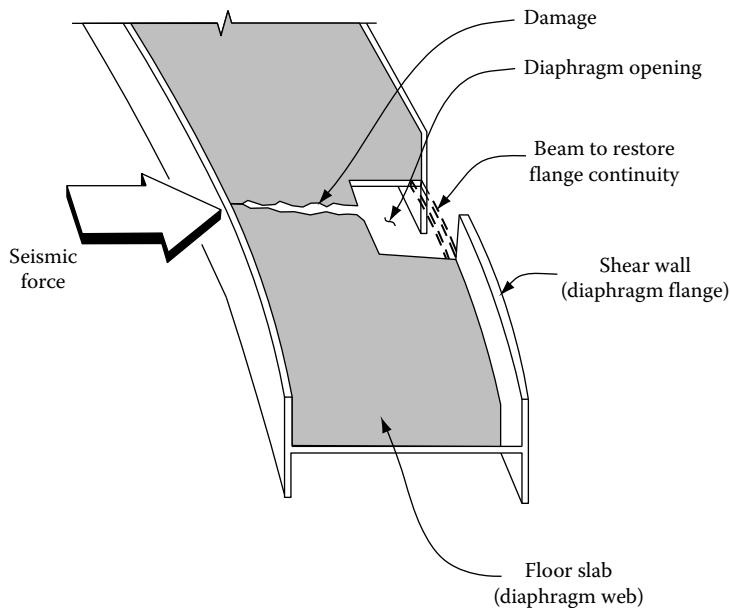


FIGURE 1.38 Shear wall–frame interaction.



**FIGURE 1.39** Diaphragms with openings.

corners, inviting stress concentrations, may result in premature damage. When such configurations are necessary, it is preferable to provide structural separations. This may lead to a number of simple, compact, and independent plans. Gaps separating adjacent structures must be large enough to ensure that even during a major seismic event, no hammering of adjacent structures will occur due to out-of-phase relative motions of the independent substructures. Inelastic deflections, resulting from ductile dynamic response, must be allowed for. It should be noted that diaphragm action may be jeopardized if openings significantly reduce the ability of the diaphragm to resist in-plane flexure and shear. An example is shown in Figure 1.39.

In their role as diaphragms, the floor and roof surfaces act as horizontal beams spanning between lateral support points and may effectively engage beam elements at the perimeter as top and bottom “chords” or “flanges.” In this case, the bending moment is resolved into a tension and compression couple and considered resisted by beam elements with shear resisted by the diaphragm surface. In the absence of such flange elements to resist the moment couple, the diaphragm must act as a deep plate resisting both bending and shear forces. Either type of the diaphragm behavior requires effective transfer of bending and shear forces, necessitating careful detailing of connections between the diaphragm and the lateral support systems.

#### 1.4.6 STRENGTH AND SERVICEABILITY

Buildings must satisfy “strength” limit states in which members are proportioned to carry the design loads safely to resist buckling, yielding, fracture, and so forth. In addition to strength limit states, buildings must also satisfy “serviceability” limit states that define functional performance and behavior under load and include such items as deflection and vibration. Strength limit states have traditionally been specified in building codes because they control the safety of the structure. Serviceability limit states, on the other hand, are usually noncatastrophic and involve the perceptions and expectations of the owner or user and are a contractual matter between the owner or user and the designer and builder. It is for these reasons, and because the benefits are often subjective and difficult to define or quantify, that serviceability limit states for the most part are not included within the model United States Building Codes.

### 1.4.7 SELF-STRAINING FORCES

Constrained structures that experience dimensional changes develop self-straining forces. Examples include moments in rigid frames that undergo differential foundation settlements and shears in bearing walls that support concrete slabs that shrink. Unless provisions are made for self-straining forces, stresses in structural elements, either alone or in combination with stresses from external loads, they can be high enough to cause structural distress.

Generally, the magnitude of self-straining forces can be anticipated by analyses of expected shrinkage, temperature fluctuations, foundation movement, and so forth. However, it is not always practical to calculate the magnitude of self-straining forces. Therefore, it is better to provide for self-straining forces by specifying relief joints, suitable framing systems, or other details to minimize the effects of self-straining forces.

### 1.4.8 ABNORMAL LOADS

Through accident, misuse, or sabotage, properly designed structures may be subjected to conditions that could lead to either general or local collapse. It is usually impractical for a structure to be designed to resist general collapse caused by gross misuse of a large part of the system or severe abnormal loads acting directly on a large portion of it. However, precautions can be taken in the designs of structures to limit the effects of local collapse, and to prevent or minimize progressive collapse. Progressive collapse is defined as the spread of an initial local failure from element to element, eventually resulting in the collapse of an entire structure or a disproportionately large part of it.

Because accidents, misuse, and sabotage are normally unforeseeable events, they cannot be defined precisely. Likewise, general structural integrity is a quality that cannot be stated in simple terms.

In addition to unintentional or willful misuse, some of the incidents that may cause local collapse are explosions due to ignition of gas or industrial liquids; boiler failures; vehicle impact; impact of falling objects; effects of adjacent excavations; gross construction errors; very high winds such as tornadoes; and sabotage. Generally, such abnormal events would not be a part of normal design considerations.

## 1.5 COLLAPSE PATTERNS

In this section, the following collapse patterns are discussed:

- Earthquake collapse patterns (Section 1.5.1)
- Collapse due to unintended addition of stiffness (Section 1.5.1.1)
- Inadequate beam–column joint strength (Section 1.5.1.2)
- Tension/compression failures (Section 1.5.1.3)
- Wall-to-roof interconnection failures (Section 1.5.1.4)
- Local column failure (Section 1.5.1.5)
- Heavy floor collapse (Section 1.5.1.6)
- Torsional effects (Section 1.5.1.7)
- Soft first-story collapse (Section 1.5.1.8)
- Midstory collapse (Section 1.5.1.9)
- Pounding (Section 1.5.1.10)
- $P-\Delta$  effect (1.5.1.11)
- Collapse due to wind storms (Section 1.5.2)
- Explosion effects (Section 1.5.3)
- Progressive collapse (Section 1.5.4)
- Design alternatives for reducing progressive collapse (Section 1.5.4.1)
- Guidelines for achieving structural integrity (Section 1.5.4.2)

### 1.5.1 EARTHQUAKE COLLAPSE PATTERNS

We typically accept higher risks of damage under seismic design forces than under other comparable extreme loads, such as maximum live load or wind forces. The corresponding seismic design forces are generally too high to be resisted within the elastic range of material response, and it is common to design for strengths, which are a fraction of that corresponding to elastic response, and to expect the structures to survive large earthquakes by inelastic deformations and energy dissipation corresponding to material distress.

Earthquake shaking causes damage to structure but it is the gravity that causes collapse. Redundancy and ductile behavior can prevent or reduce extent of collapse. On the other hand brittle behavior enhances possibility and increases extent of collapse.

With increased awareness that excessive strength is not essential or even necessarily desirable, the emphasis in seismic design has shifted from the resistance of large seismic forces to the “evasion” of these forces. Inelastic structural response has become an essential reality in the assessment of structural design for earthquake forces. Deformations that provide ductility are considered the essential attribute of maintaining strength while the structure is subjected to reversals of inelastic deformations under seismic response.

Seismic design should encourage structural forms that are more likely to possess ductility than those that do not. Thus for concrete structures, the shear strength provided must exceed the actual flexural strength to ensure that inelastic shear deformations, associated with large deterioration of stiffness and strength, which could lead to failure, cannot occur.

One of the most common causes of failure in earthquakes is the “soft story mechanism.” Where one level, typically the lowest, is weaker than upper levels, a column sway mechanism can develop with high local ductility demand. This condition results from a functional desire to open the lower levels to the maximum extent possible. Under ductile response to earthquakes, high compression strains should be expected from the combined effects of axial force and bending moment. Unless adequate, closely spaced, well-detailed transverse reinforcement is placed in the potential plastic hinge region, spalling of concrete followed by instability of the compression reinforcement will follow. It must be recognized that even with a weak beam/strong column design philosophy, which seeks to dissipate seismic energy primarily in well-confined beam plastic hinges, a column plastic hinge may still form at the base of the column.

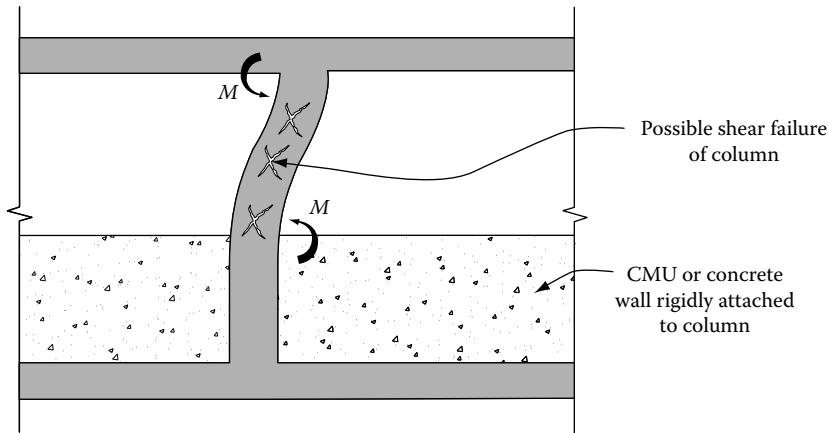
While there is something new to be learned from each earthquake, it may be said that the majority of structural lessons have been learned. However, there is still widespread lack of appreciation of the unpredictable and unquantifiable effects of earthquakes on buildings.

Well-established techniques, used for design of structures for various static loads, including wind forces, cannot simply be extended and applied to conditions that arise during earthquakes. In earthquake design, it is imperative that we consider forces corresponding to the largest seismic displacement.

#### 1.5.1.1 Unintended Addition of Stiffness

A source of major damage, particularly in columns and repeatedly observed in earthquakes, is the interference with the deformations of members by rigid nonstructural elements, such as infill walls. As Figure 1.40 shows, the top edge of a brick wall will reduce the effective length of one of the columns, thereby increasing its stiffness in terms of lateral forces. Since seismic forces are attracted in proportion to element stiffness, the column may thus attract larger horizontal shear forces than it would be capable of resisting. The unexpected failure of such major gravity-load-carrying elements may lead to the collapse of the entire building. Therefore, it is very important to ensure that intended deformations, including those of primary lateral-force-resisting components in the inelastic range of seismic response, can take place without interference.

Most building collapses occur due to loss of stability; that is, the basic shape is significantly changed when subjected to a combination of forces. The new, changed shape is much less capable of carrying



**FIGURE 1.40** Distress in columns due to unintended stiffness addition.

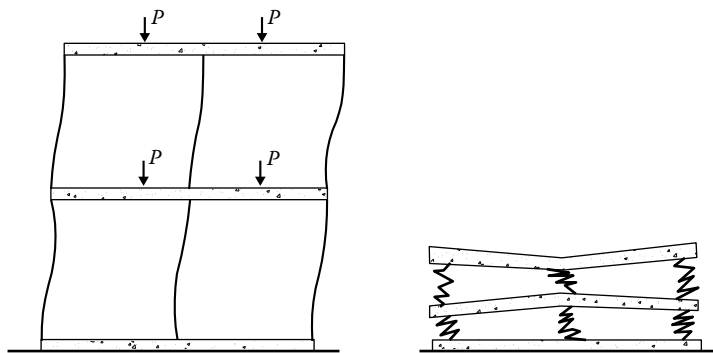
the forces and, therefore, the structure will rapidly continue to change its deformation shape until it finds a new shape that is stable. A typical example of lost stability is that of the slender columns that “gets out of the way of the load by buckling,” as the load comes to rest on the ground/foundation.

#### 1.5.1.2 Inadequate Beam–Column Joint Strength

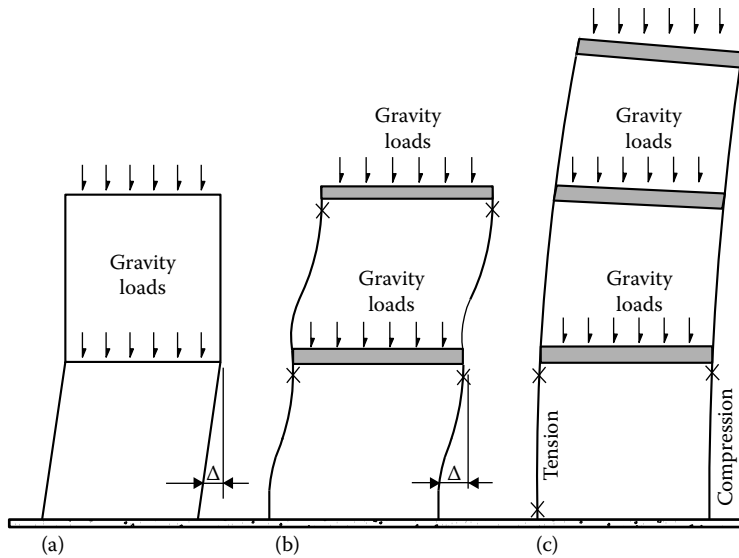
Failures are caused by earthquake shaking of buildings that have joints with poorly confined concrete. The cycling of the structure when excited by the earthquake causes moment-resistant joints to unravel as concrete chunks are stripped away from the reinforcing steel cage. The gravity load can no longer be supported by these columns, and it drives the structure earthward until it stops on the ground or lower floors that have sufficient strength to stop the falling mass as shown schematically in Figure 1.41. The result of this type of collapse may be a pancaked group of slabs held apart by broken columns and buildings contents, or a condition where columns are left standing, punched through the slabs.

#### 1.5.1.3 Tension/Compression Failures

These types of failures usually occur in taller structures (see Figure 1.42). The tension that is concentrated at the edges of a concrete frame or shear wall can produce very rapid loss of stability. In walls, if the reinforcing steel is inadequately proportioned or poorly embedded, it can fail in tension and result in rapid collapse of the wall by overturning. A more common condition occurs, when the



**FIGURE 1.41** Column joint failure. Concrete in columns is not well enough confined by rebar ties, resulting in failure as concrete splits off and rebar buckles.



**FIGURE 1.42** Collapse patterns. (a) Inadequate shear strength. (b) Inadequate beam/column strength. (c) Tension/compression failure due to overturning.

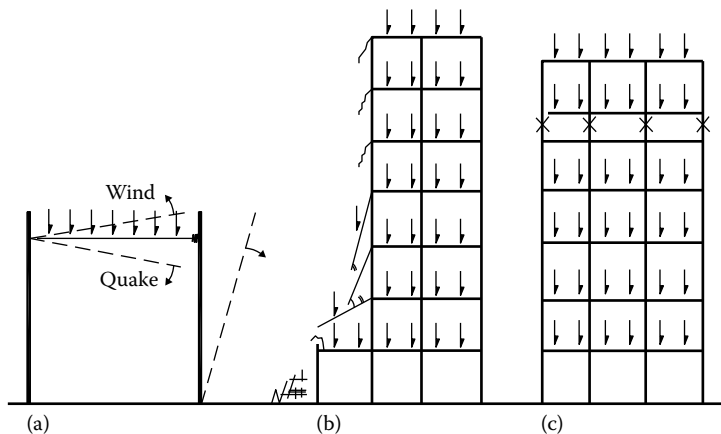
tension causes the joints in a concrete moment frame to lose bending and shear strength. A rapid degradation of the structure can result in partial or complete pancaking as in beam/column failure.

#### 1.5.1.4 Wall-to-Roof Interconnection Failure

Stability is lost in this case since the vertical support of the roof is lost, as well as the horizontal out-of-plane support of the wall (see Figure 1.43).

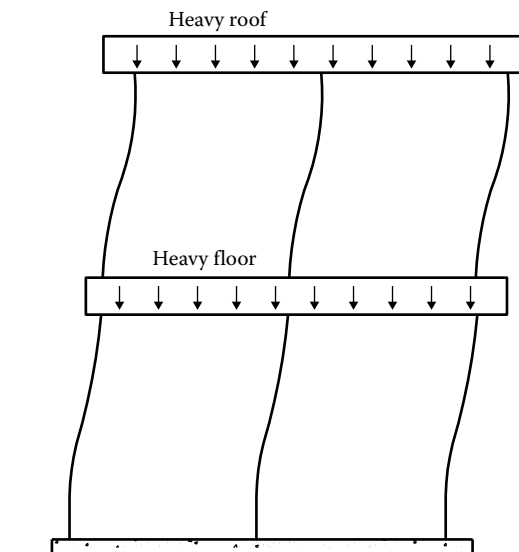
#### 1.5.1.5 Local Column Failure

Local column failure can lead to loss of stability and/or progressive collapse in part of a structure as shown schematically in Figure 1.43. It is observed that in most collapses, the driving force is the gravity load acting on a structure that has become unstable due to horizontal offset or insufficient vertical capacity. In addition, subsequent lateral loads from wind or aftershocks can increase the offset, exaggerating the instability. The structure is often disorderly as it collapses. Some parts may remain supported by uncollapsed adjacent bays.



**FIGURE 1.43** More collapse patterns.





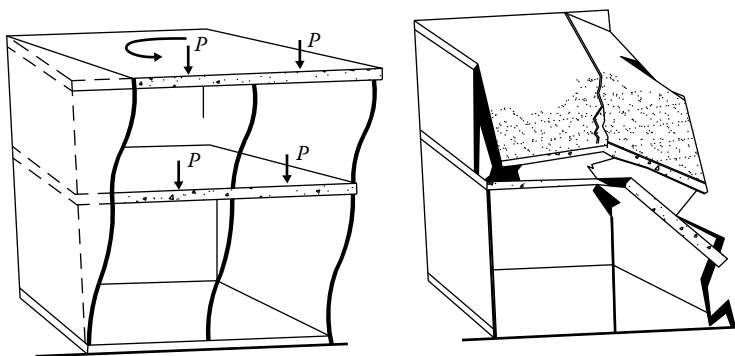
**FIGURE 1.44** Heavy floor collapse: Major force is in inertia of floors and is concentrated at each level. If columns crack and fail, heavy floors collapse.

#### 1.5.1.6 Heavy Floor Collapse

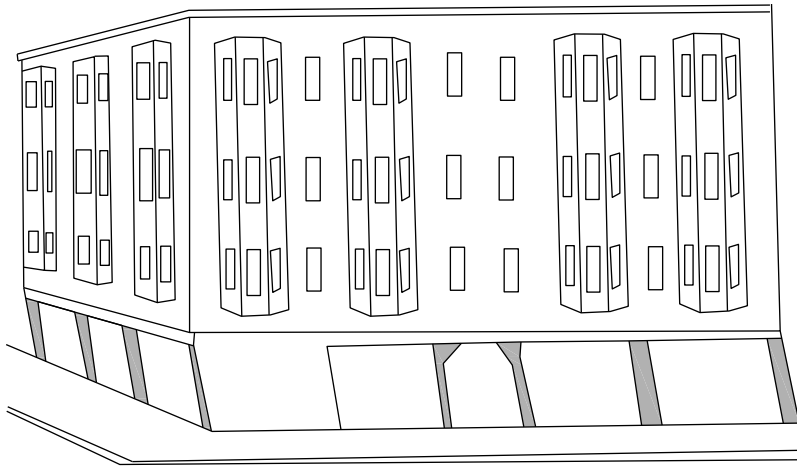
Heavy floor collapse is schematically shown in Figure 1.44, which can be partial to complete. It is usually caused when columns or walls, weakened by quake motion, are unable to support the heavy floors. Tall, moment frame structures, where tension to compression reversal causes an almost explosive failure of exterior columns, may overturn, but more often they will collapse within their plan boundaries due to high gravity forces. Many partially collapsed concrete frame structures will contain parts of slabs and/or walls that are hanging off an uncollapsed area. This has been observed in corner buildings when only the street-front bays collapse due to torsion effects, and in long buildings or those with several wings, where some bays do not collapse.

#### 1.5.1.7 Torsion Effects

Torsion effects may occur in frame structures when an infill wall is placed in between columns. These walls become stiffer than all other parts of the building and cause a temporary, eccentric condition, which can lead to a collapse (see Figure 1.45).



**FIGURE 1.45** Torsion effect: property-line walls placed on one side of a frame structure, create eccentric condition which can lead to collapse.



**FIGURE 1.46** Soft story collapse: Lower story that is weakened by too many openings becomes racked (rectangles become parallelograms). This may result in failure of first story columns due to mismatch of demand versus strength.

#### 1.5.1.8 Soft First-Story Collapse

This occurs in buildings that are configured such that they have significantly less stiffness because much fewer or no walls are provided in the first story than in the stories above (see Figure 1.46). The collapse is often limited to the one story only, as the building becomes one story shorter.

#### 1.5.1.9 Midstory Collapse

This can occur when a midstory is configured with much different stiffness than the stories above and below. Examples are when a story has no walls and the ones above and below have significant walls, or when a story has stiff, short columns and the ones above and below have longer, more limber columns.

#### 1.5.1.10 Pounding

Pounding collapse normally occurs when two adjacent buildings have floors that are at different elevations. The very stiff/strong edge of a floor in one building may cause damage to or even collapse of the adjacent building's column when they collide.

#### 1.5.1.11 P-Δ Effect

When flexible structures are subjected to lateral forces, the resulting horizontal displacements lead to additional overturning moments because the gravity load is also displaced. Thus in the simple cantilever model of Figures 1.47 through 1.49, the total base moment is

$$M_{ub} = V_u H + P_u \Delta \quad (1.19)$$

Therefore, in addition to the overturning moments produced by lateral force,  $V_u$ , the secondary moment  $P_u \Delta$  must also be resisted. This moment increment in turn will produce additional lateral displacement, and hence  $\Delta$  will increase further. In very flexible structures, instability, resulting in collapse, may occur.

It is necessary to recognize when assessing seismic design forces that the importance of P-Δ effects will generally be more significant for structures in regions of low-to-moderate seismicity than for structures in regions of high seismicity, where design lateral forces will be correspondingly higher. Therefore, in most situations, particularly in regions where large seismic design forces need to be considered, P-Δ phenomena will not control the design of frames.

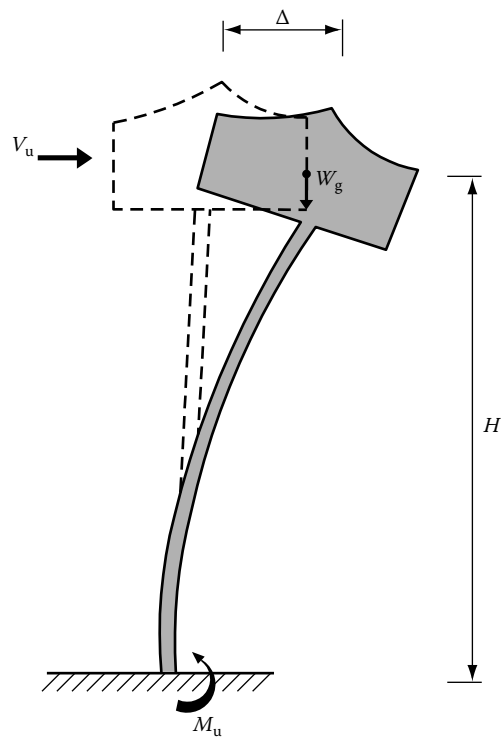


FIGURE 1.47 P-Δ effect; simple cantilever model.  $M_u = V_u H + W_g \Delta$ .

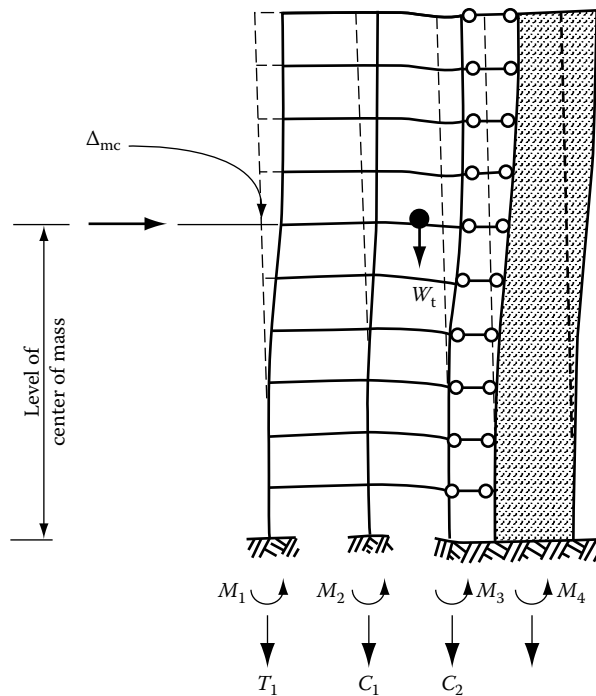
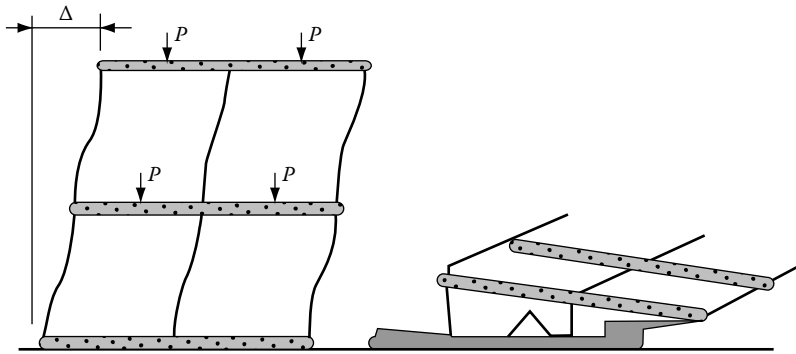


FIGURE 1.48 P-Δ effect: Shear wall-frame system.



**FIGURE 1.49** Collapse due to P-Δ effect.

As expected, P-Δ phenomena will increase drift, but analyses of typical building frames have indicated that effects are small when maximum interstory drift is less than 1%. However, for greater interstory drifts, P-Δ effects may lead to rapidly increasing augmentation of these drifts.

It should be recognized that in so far as the inelastic behavior is concerned that increasing strength of a frame is more effective in controlling drift than increasing stiffness. This is because the more vigorously a frame responds in the inelastic range, the less is the significance of stiffness.

### 1.5.2 COLLAPSE DUE TO WIND STORMS

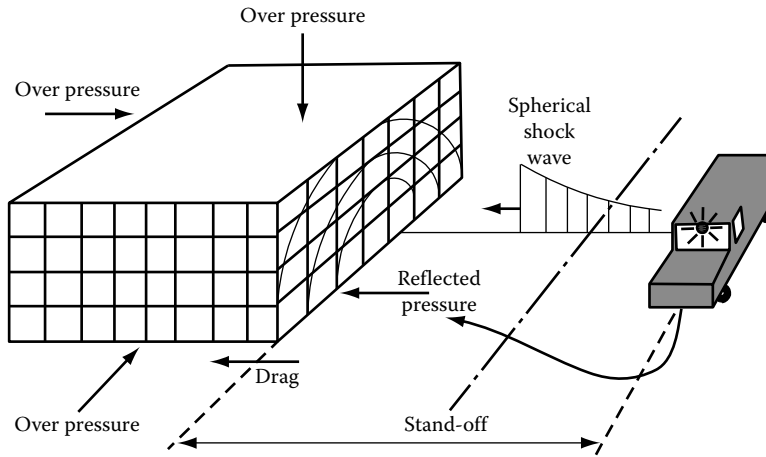
Well-engineered structures are designed to resist wind forces by elastic action (as contrasted to the inelastic response that is assumed in earthquake design) and, therefore, it is unusual to have buildings sustain significant wind damage. Water surge especially that associated with coastal windstorms can produce damage and even the collapse, but those that are usually affected are lighter structures.

### 1.5.3 EXPLOSION EFFECTS

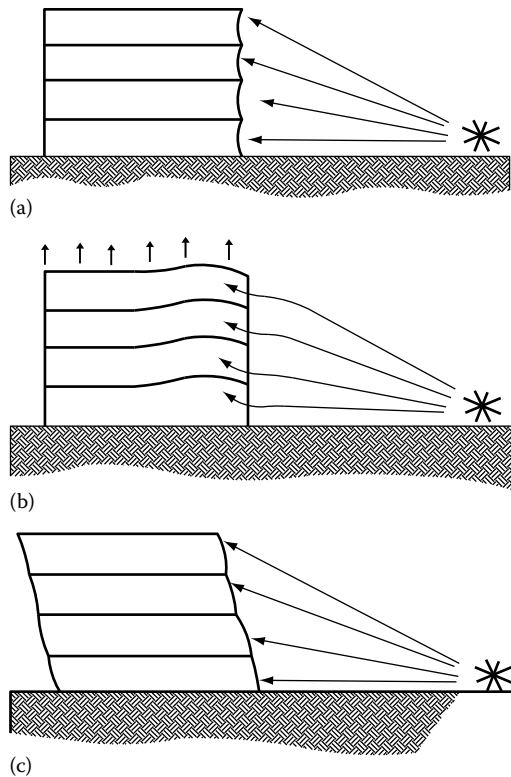
The pressures exerted on buildings by explosions may be many orders of magnitude higher, 5000 psi-plus, than normal design pressures, but their duration is in milliseconds. The resulting pressures are inversely proportional to the cube of the distance from the center of the source. Damage to structures may be severe, but it is only a fraction of what a proportional static pressure would cause. When large surfaces are engaged by blast pressures, they will be moved as the shock wave passes, but the direction of the net force (initial uplift—overpressure) will be determined by the complexities of the wave path and time. Heavy columns tend to survive, but may have problems if some of the floors that laterally brace them are removed. The wall and floor planes in building have large surfaces that will receive most of the blast pressure. They likely will be ripped away from their connections, leading to collapse of at least part of the structure (see Figures 1.50 through 1.52).

### 1.5.4 PROGRESSIVE COLLAPSE

A prominent case of local collapse that progressed to a disproportionate part of the whole building was the Ronan Point disaster, which brought the attention of the profession to the matter of general structural integrity in buildings. This 22-story apartment building was built using precast-concrete, load-bearing panels in Canning Town, England. In March 1968, a gas explosion in an 18-story apartment blew out a living room wall. The loss of the wall led to the collapse of the whole corner of the building. The apartments above the 18th story, suddenly losing support from below and being insufficiently tied and reinforced, collapsed one after the other. The falling debris ruptured successive floors and walls below the 18th story, and the failure progressed to the ground. Better continuity and ductility might have reduced the amount of damage.

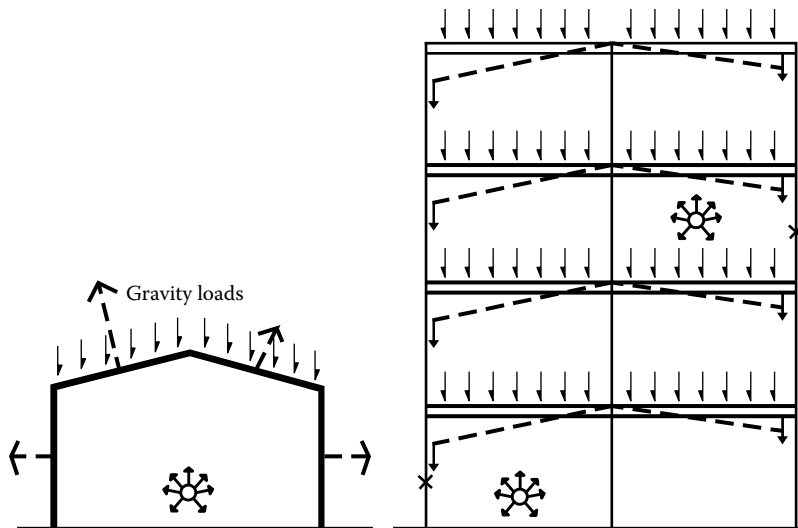


**FIGURE 1.50** Exterior explosion.



**FIGURE 1.51** Damage due to exterior explosion. (a) Exterior windows, columns, and walls. (b) Roof and floor slabs. (c) Building sway due to ground shock.

Another example of progressive collapse is the Alfred P. Murrah Federal Building, Oklahoma. On April 19, 1995 a truck containing approximately 4000lb of fertilizer-based explosive was parked near the sidewalk next to the nine-story reinforced concrete office building. The side facing the blast had corner columns and four other perimeter columns. The blast shock wave disintegrated one of the  $20 \times 36$  in. perimeter column and caused brittle failures of two others. The transfer girder at the third level above these columns failed, and the upper-story floors collapsed



**FIGURE 1.52** Interior explosion: when explosions occur within structures, pressures can build up within confined spaces, causing lightly attached wall, floor, and roof surfaces to be blown away.

in a progressive fashion. Approximately 70% of the building experienced dramatic collapse. One hundred sixty-eight people died, many of them as a direct result of progressive collapse. Damage might have been less had this structure not relied on transfer girders for support of upper floors, if there had been better detailing for ductility and greater redundancy, and if there had been resistance for uplift loads on floor slabs.

#### 1.5.4.1 Design Alternatives for Reducing Progressive Collapse

There are a number of ways to obtain resistance to progressive collapse and the important among them are the following:

1. During the design process, consider resistance to progressive collapse through the provision of minimum levels of strength, continuity, and ductility.
2. Provide alternate load paths so that the damage is absorbed and major collapse is averted.
3. Provide sufficient strength to resist failure from accidents or misuse.
4. Provide specific local resistance in regions of high risk to have sufficient strength to resist abnormal loads in order for the structure as a whole to develop alternate paths.

#### 1.5.4.2 Guidelines for Achieving Structural Integrity

1. Generally, connections between structural components should be ductile and have a capacity for relatively large deformations and energy absorption under the effect of abnormal conditions.
2. *Good plan layout.* An important factor in achieving integrity is the proper plan layout of walls and columns. In bearing-wall structures, there should be an arrangement of interior longitudinal walls to support and reduce the span of long sections of crosswall, thus enhancing the stability of individual walls and of the structures as a whole. In the case of local failure, this will also decrease the length of wall likely to be affected.
3. Provide an integrated system of ties among the principal elements of the structural system. These ties may be designed specifically as components of secondary load-carrying systems, which often must sustain very large deformations during catastrophic events.
4. *Returns on walls.* Returns on interior and exterior walls will make them more stable.

5. *Changing directions of span of floor slab.* Where a one-way floor slab is reinforced to span in the main direction, provide spanning capability in its secondary direction also, perhaps using a lower safety factor. With this approach, the collapse of the slab will be prevented and the debris loading of other parts of the structure will be minimized. Often, shrinkage and temperature steel may be enough to enable the slab to span in the secondary direction.
6. *Load-bearing interior partitions.* The interior walls must be capable of carrying enough load to achieve the change of span direction in the floor slabs.
7. *Catenary action of floor slab.* Where the slab cannot change span direction, the span will increase if an intermediate supporting wall is removed. In this case, if there is enough reinforcement throughout the slab and enough continuity and restraint, and slab may be capable of carrying the loads by catenary action, though very large deflections will result.
8. *Beam action of walls.* Walls may be assumed to be capable of spanning an opening if sufficient tying steel at the top and bottom of the walls allows them to act as the web of a beam with the slabs above and below acting as flanges.
9. *Redundant structural systems.* Provide a secondary load path (e.g., an upper-level transfer girder system that allows the lower floors of a multistory building to hang from the upper floors in an emergency) that allows framing to survive removal of key support elements.
10. *Ductile detailing.* Avoid low-ductility detailing in elements that might be subject to dynamic loads or very large distortions during localized failures. Consider the implications of shear failures in beams or supported slabs under the influence of building weights falling from above.
11. Provide additional reinforcement to resist blast and load reversal when blast loads are considered in design.
12. Consider the use of compartmentalized construction in combination with special moment-resisting frames in the design of new buildings when considering blast protection.

While not directly adding to structural integrity for the prevention of progressive collapse, the use of special, nonfrangible glass for fenestration can greatly reduce risk to occupants during exterior blasts. To the extent that nonfrangible glass isolates a building's interior from blast shock waves, it can also reduce the likelihood of slab failure.

### 1.5.5 BLAST PROTECTION OF BUILDINGS: THE NEW SEI STANDARD

Until now, in the wake of September 11, 2001, structural engineers concerned about the potential effects of accidental or malicious explosions on their projects had little guidance on what to do to protect these facilities. However, this is expected to change shortly. In the future, sometime in 2009, the Structural Engineering Institute (SEI) will provide a document, *Standard for Blast Protection of Buildings*, detailing recommendations for assessing the blast resistance of buildings.

The events of September 11, 2001, had a profound impact on the building design community. Although the weapons employed that day were fueled commercial aircraft, the industry turned considerable attention to the most common tactic historically employed in terrorist attacks around the world: the improvised explosive device (IED). While information for addressing this threat existed, it was largely confined to military and other government publications that were neither readily available nor directly applicable to facilities constructed by private sectors. The new SEI standard is expected to remedy this situation.

## 1.6 BUCKLING OF A TALL BUILDING UNDER ITS OWN WEIGHT

Let us consider the tantalizing possibility of a prismatic tall building buckling under its own weight. Can this phenomenon ever occur in a practical, superslim, supertall building? Let us examine this probability by considering a tall building as an equivalent cantilever with its lower

end vertically built-in, and the upper end free. We can, for analytical purposes, assume the building weight is uniformly distributed along the height of the equivalent vertical cantilever (see Figure 1.53a). The cantilever shown in the figure has a tendency to buckle under its own weight as shown by the dotted line. This problem involving solution of a differential equation of the deflected curve was discussed first by Leonard Euler (1707–1783), and then eventually solved by mathematician A.G. Greenhill (1793–1841). He established that the lowest buckling load,  $q_{cr}$ , per unit height of the cantilever is given by

$$q_{cr} = 7.837 EI / \ell^3$$

where

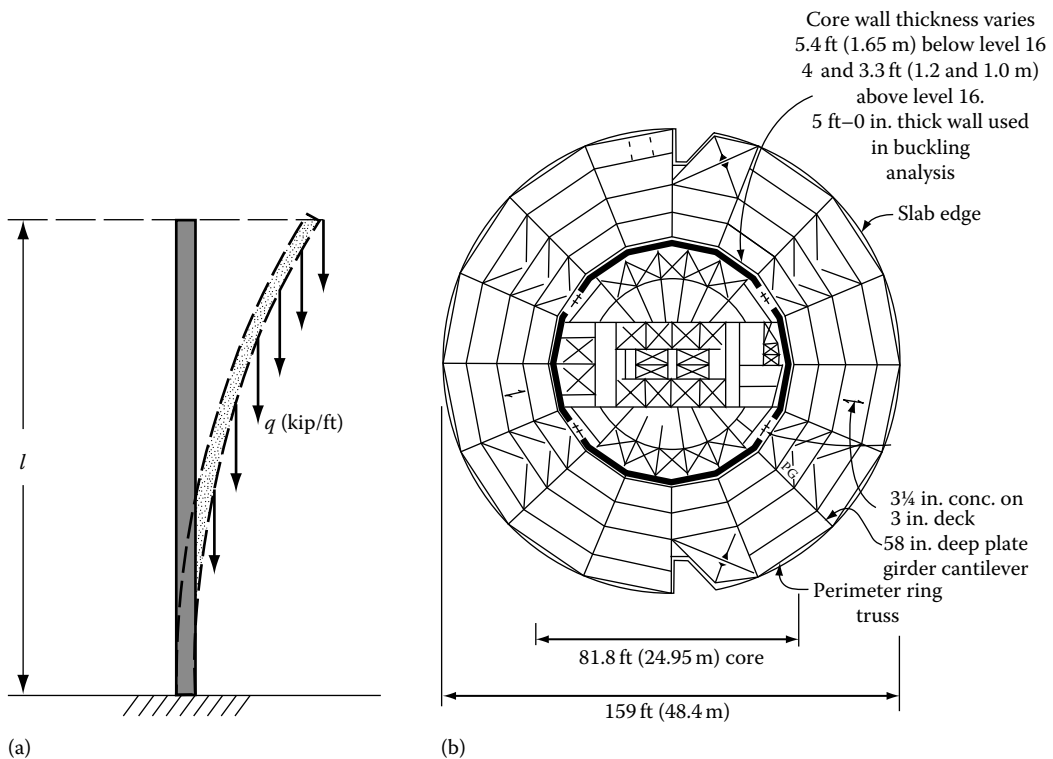
$E$  is the modulus of elasticity of the construction material of the building

$I$  is the moment of inertia of the building in the direction of bending

$\ell$  is the height of the building

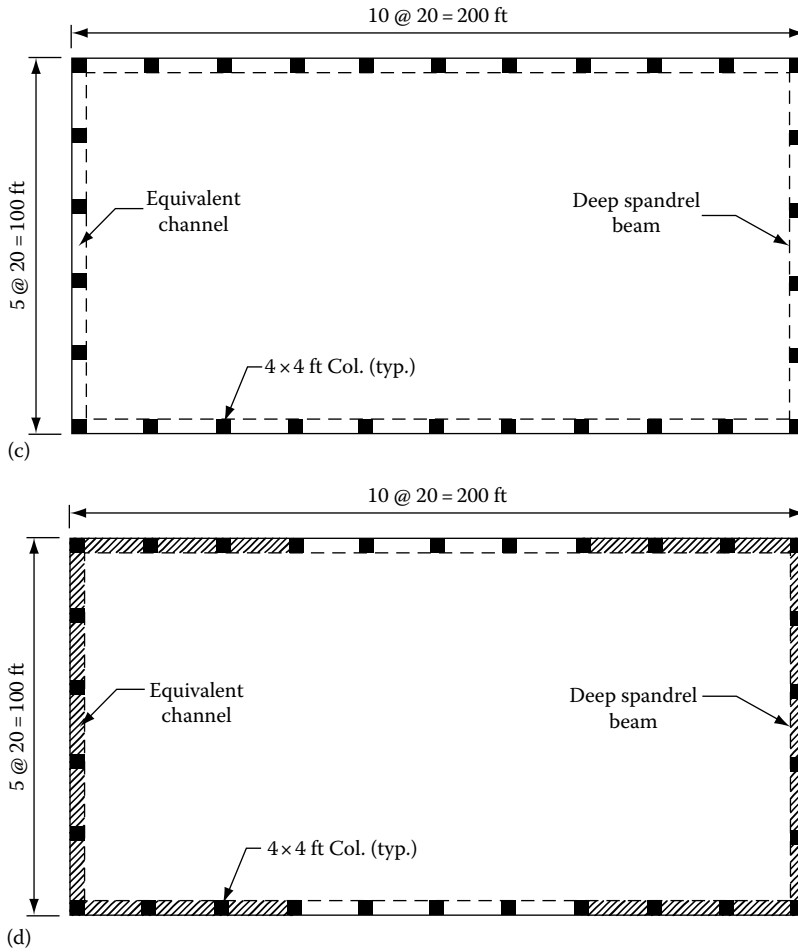
### 1.6.1 CIRCULAR BUILDING

To get a feel for what this equation means for a contemporary tall concrete building, let us consider a 50-story building shown in Figure 1.53b. The lateral resistance is provided entirely by the interior core walls, assumed here for analytical purposes to be 5 ft-thick. For purposes of analysis, we assume uncracked properties.



**FIGURE 1.53** Buckling of tall building under its own weight: (a) equivalent cantilever, (b) circular building, *(continued)*





**FIGURE 1.53 (continued)** (c) rectangular building, and (d) equivalent channels to account for shear lag effects.

### 1.6.1.1 Building Characteristics

#### Example 1.2

1. Building plan area =  $\pi \times 159^2/4 = 19,855 \text{ ft}^2$ .
2. Building height at 12 ft floor-to-floor =  $12 \times 50 = 600 \text{ ft}$ .
3. Unit dead load including self-weight of structural and nonstructural elements, curtain walls, interior partitions, finishes, and allowance for sustained live load = 225 psf of floor area. Therefore, the self-weight,  $q = 225 \times 19,855/12 = 372.3 \text{ kip/ft}$ .
4. Moment of inertia ( $I$ ) about the axis through the center =  $0.049087 (81.8^4 - 71.8^4) = 893,196 \text{ ft}^4$ .
5. Modulus of elasticity ( $E$ ) for concrete shear walls = 4415 ksi = 635,760 ksf.
6. The lowest buckling load,  $q_{cr}$ , is given by

$$\begin{aligned}
 q_{cr} &= 7.837 EI / \ell^3 \\
 &= 7.837 \times 635,760 \times 893,196 / 600^3 = 20,603 \text{ kip/ft}.
 \end{aligned}$$

Comparing this to the estimated self-weight of 372.3 kip/ft, we notice we have a quite a comfortable margin of safety against buckling =  $20,603/372.3 = 55.34$ . Even with an overly pessimistic assumption of fully cracked walls, that is,  $I_{\text{cracked}} = I_{\text{gross}}/2$ , our margin of safety is still quite healthy =  $55.34/2 = 27.67$ , which is pretty large indeed.

## 1.6.2 RECTANGULAR BUILDING

### 1.6.2.1 Building Characteristics

#### Example 1.3

1. Building height 40 stories at 13.5 ft floor-to-floor =  $40 \times 13.5 = 540$  ft.
2. Typical floor area =  $100 \times 200$  ft = 20,000 ft<sup>2</sup>.
3. Floor weight at 225 psf =  $20,000 \times 225/1000 = 4500$  kip.
4. Unit weight,  $q = 4500/13.5 = 333.3$  kip/ft.
5.  $E = 635,760$  ksf.
6.  $I = 704,512$  ft<sup>4</sup> (assuming two equivalent channels as shown in Figure 1.46d and uncracked properties).
7. Critical buckling load,  $q_{cr} = 7.837 EI / \ell^3$   

$$= 7.837 \times 635,760 \times 704,512 / 540^3$$

$$= 22,292 \text{ kip/ft.}$$

Comparing this to the estimated weight  $q = 333.3$  kip/ft it is seen that we have a lavish factor of safety equal to  $22,292/333.3 = 66.9$ , against buckling of the building under its own weight.

Based on these two examples (Examples 1.2 and 1.3), it is reasonable to conclude that an adequate factor of safety exists even for ultra tall buildings in the 2500 ft plus range.

### 1.6.3 COMMENTS ON STABILITY ANALYSIS

The examples given above are based on certain implicit assumptions. Chief among them are

1. The building is perfectly straight without any initial curvature.
2. There is no initial eccentricity in the application of vertical loads.
3. Only the buckling of the building as a whole is considered ignoring the possibility of local buckling.
4. The shear mode of deformation characteristic of low- and mid-rise buildings has no effect on the stability of the building.
5. The simultaneous action of axial and lateral loads is ignored.

In a practical building, these assumptions are breached to various degrees. For example, the construction tolerance permitted in the verticality of the building and the inevitable eccentric distribution of mass over the height invariably result in an initial bending curvature increasing the P-Δ effects. Additionally, the buildings are subject to lateral loads, including wind and seismic loads, resulting in the simultaneous application of vertical and lateral loads.

All these consequences have the effect of diminishing the critical load determined earlier for a particular case of inelastic stability. However, no attempt is made here to go beyond the basic hypothesis.



---

# 2 Gravity Systems

Safety, functionality, economy, and nowadays, satisfying “legality of design” are the principal design objectives. Safety is established by demonstrating that the designed system can withstand the code-stipulated loads without collapse and serves as a guarantee of a defined level of performance within the range of loading specified in the applicable code. To establish “safety,” it is sufficient to demonstrate that under the code-stipulated loading conditions, the structure can develop an uninterrupted load path—from the point of load application to the foundation—capable of sustaining the applied load and all corresponding actions generated in the structure. Toward this effort the common design procedure for safety aims to ensure two criteria—that an envisaged load path is adequate, and that on demand it would be mobilized.

The adequacy of a load path is implemented by ensuring that, at any point along its path, it can withstand the actions occurring at that point. In design practice, adequacy is determined for only one engineer-selected load path, generally referred to as the “structural system.” The engineer-selected load path is a “designated path,” meaning that the natural load path of the loads may be different from the path selected by the engineer. The designated load path design provides an acceptable design, as long as the engineer can demonstrate that it is adequate.

A structure’s natural load path is generally more economical than other load paths, because the load always tries to follow a path of least resistance. However, other considerations, such as selection of construction technique, may favor alternative load paths. Therefore, while the natural load path is a value in the development of sound engineering judgment, it is not required for a successful structural design.

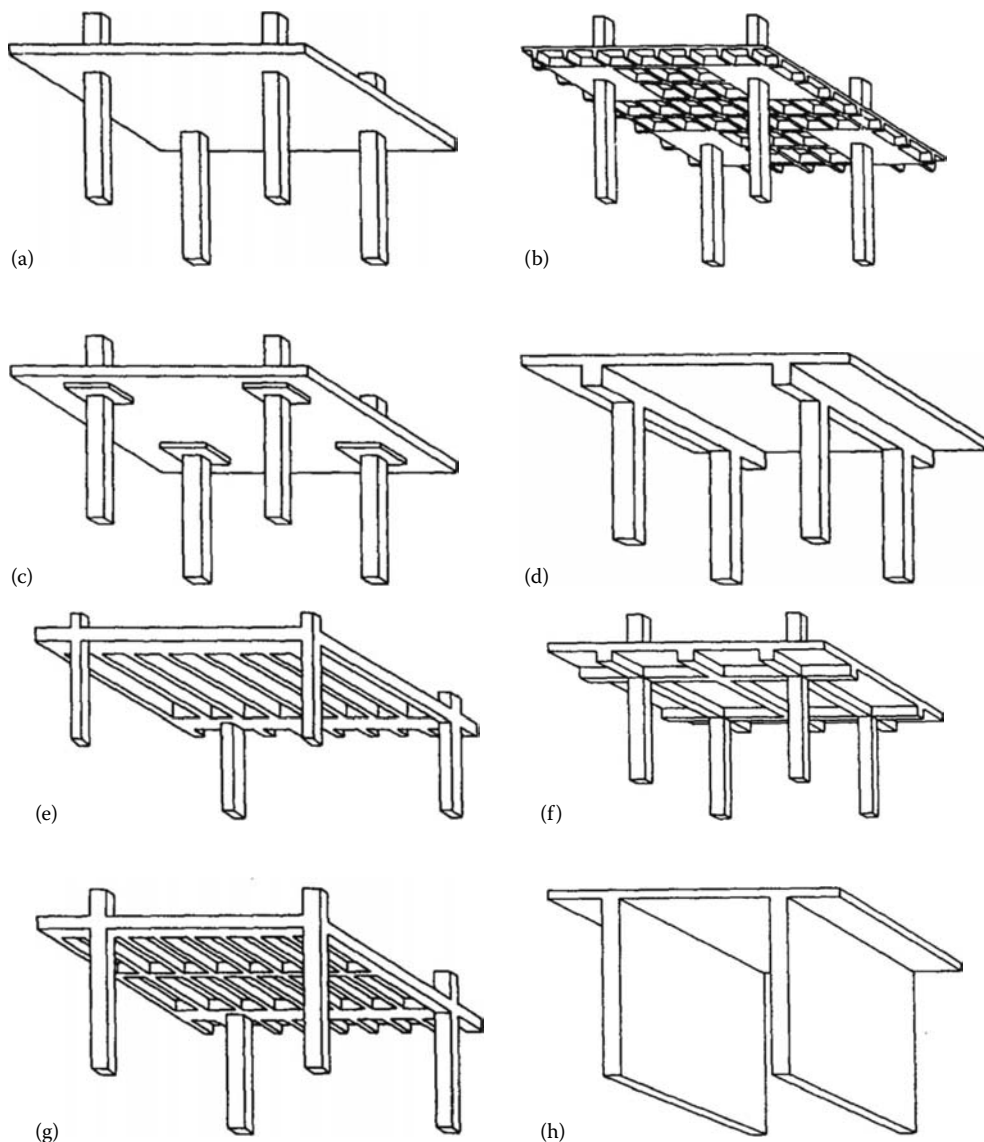
In designating a load path, the engineers must ensure that the structure has reliable strength and adequate ductility. In concrete design, ductility is achieved by controlling the reinforcement in a member. Excessive reinforcement inhibits ductility, since it may not yield prior to concrete failure of the section.

In this chapter, we discuss the common practice for the design of concrete floor systems and vertical elements consisting of columns and walls. The presentation begins with a review of the impact of formwork on the total cost of the structural frame. Then a description of various floor framing techniques is given followed by a description of plate behavior and analysis techniques central to the design of concrete floor systems. The emphasis is to explore the assumptions, procedures, and the considerations involved in the use of these analytical methods, as opposed to detailed computations. The scope of the material included here is limited to the specific requirements of gravity design only; no other loading situations are considered. The structural participation and design of floor systems, columns, and walls to resist wind and seismic forces is covered in subsequent chapters.

## 2.1 FORMWORK CONSIDERATIONS

The following explanation of formwork design, not commonly found in structural engineering textbooks, neither asks the building designer to assume the role of a formwork planner, nor does it make the structural design a subservient to formwork considerations. Its basic premise is merely that practical awareness of formwork costs may help the designer take advantage of less expensive structural solutions that are equally appropriate in terms of the aesthetics, quality, and function of the building. To use this pragmatic approach, the designer need only visualize the forms, the field labor required to form various structural members, and be aware of the direct proportion between complexity and cost.

The more common concrete floor systems currently in use are shown schematically in Figure 2.1a through h. The figures list the features of each system including typical dimensions, loading, material



**FIGURE 2.1** Common types of floor systems: (a) Two-way flat plate, (b) Two-way waffle, (c) Two-way flat slab with drops, (d) One-way beam and slab, (e) Skip joist wide module, (f) Two-way beam and slab, (g) One-way joist slab, and (h) One-way flat slab.

quantities, and the principal limitation of application. As can be seen there are seemingly endless ways to design a floor system for a site-cast concrete building. However, it behooves to keep in mind that of all structure costs, the framework is usually the largest component with the majority of cost usually attributable to formwork associated with the horizontal elements. Consequently, the first priority in designing for economy is selecting the structural system that offers lowest overall cost while meeting load requirements.

For the typical floor systems shown in Figure 2.1, the relative total cost intensity of these systems is a function of bay size and load condition. The graphs shown in Figures 2.2 and 2.3 depict this shifting cost relationship.

During the value engineering process for concrete frames, the common approach—both in theory and in practice—is to search for ways to cut back on materials. In the pursuit of economy, each structural

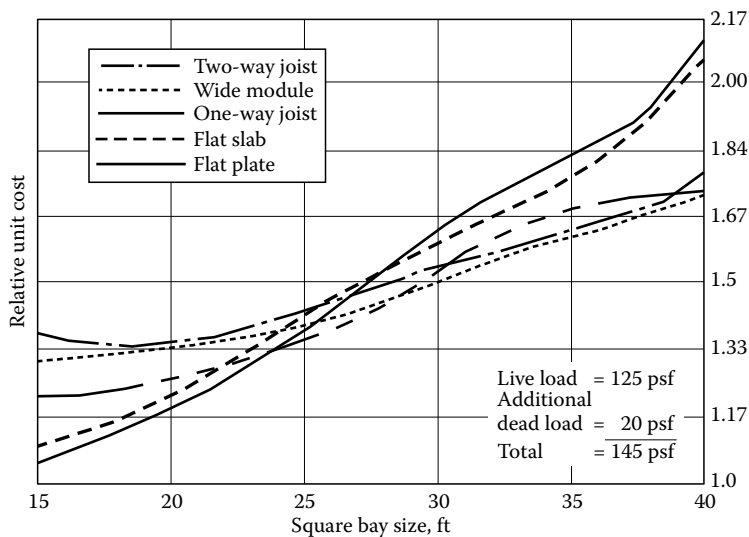


FIGURE 2.2 Relative form cost, live load = 125 psf.

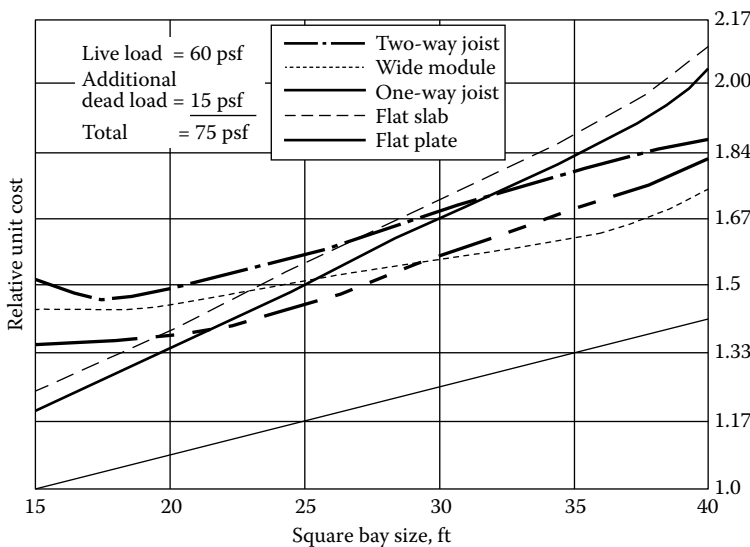


FIGURE 2.3 Relative form cost, live load = 60 psf.

element is carefully examined to make sure that it is no heavier, wider, or deeper than required for the load. To concentrate solely on permanent material reduction is to overlook the most important influence on concrete structural frame cost—formwork which can account for up to 50% of the cost of a site-cast concrete frame. It follows then, that any realistic effort to economize must integrate the construction process in its entirety: materials, plus time, labor, and equipment.

Concrete frame economy begins in the design development stage. Often, two or more structural solutions will meet the design objective equally well. One may be significantly less expensive to build. To arrive at that optimal solution at the initial design stage, not later, requires a basic sense of formwork logic.

Site-cast concrete is “monolithic.” Structurally this means that there is continuity among elements, allowing the loads to “flow” through the structure. This is accomplished because the walls, floors, and columns all work together as a one-piece unit to transfer loads. Since concrete structures

are usually designed with continuous elements, the designer typically has greater flexibility in meeting a wide range of load and span requirements.

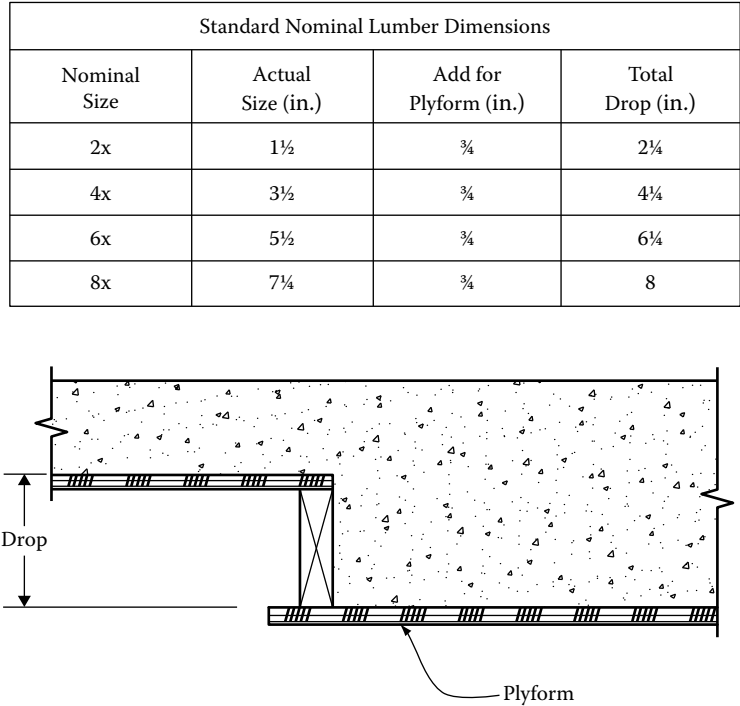
As stated previously, formwork is the single largest cost component of a concrete building’s structural frame. Fortunately, it is also the component that yields most readily to cost reduction strategy. Priority on formwork design can reduce total frame costs substantially, anywhere from 20%–50%. Constructability, meaning building a structural frame faster, simpler, and less costly to build (yet meeting all quality standards) can be a design objective. Therefore, constructability is a cost-justified objective as well. Further, starting the design with constructability as an objective is more productive than modifying a design later to reduce costs. The designer can integrate constructability into a project by allowing three basic tenants of formwork logic to govern the work.

2.1.1 DESIGN REPETITION

Repeating the same layout from bay to bay of each floor, and from floor to floor to roof, permits a production line work flow and optimum labor productivity. The same equipment can be recycled quickly from one finished area to begin another floor. Conversely, constant changes in layout result in delays while plans are interpreted, equipment is modified, measurements are verified; all of which reduce jobsite labor productivity and increase total structure cost.

2.1.2 DIMENSIONAL STANDARDS

The construction industry in North America has standardized member sizes. Correspondingly, standard size forms are commonly available from suppliers. Basing the design on readily available standard form sizes is far less costly than specifying custom-built forms for the project. Standard nominal lumber dimensions are also important to cost control. The dimensions of site-cast structural members reflect the dimensions of material used to form it, as in Figure 2.4. Designs that



**FIGURE 2.4** Influence of lumber dimension on site-cast concrete. Designing for nominal lumber dimensions results in economy.

deviate from standard lumber dimensions require costly carpentry: sawing, piecing together, waste, and time. Any drop below the soffit elevation of a framing system, whether for a deep beam or a drop panel in a flat slab, is a discontinuity of the basic formwork. It interrupts production as crews stop one basic formwork framing system at that point, and piece and fit to start and finish another.

The special forming required for pilasters sometimes can be eliminated by merging their function with that of the wall. By adding reinforcement, pilaster column loads can be transferred into the wall, to create a wall-column or transfer beam action, as in Figure 2.5. However, if pilasters are unavoidable, standardizing their dimensions and spacing them uniformly facilitates production-line forming. Further, a rake-sided pilaster configuration accelerates form removal.

Where pour strips are used (time-delayed pours allow for shrinkage in long posttensioned structures) the backshoring condition may be avoided by designing the slabs adjacent to the pour strips as cantilevers. The pour strip is designed as simple span, as in Figure 2.6.

### 2.1.3 DIMENSIONAL CONSISTENCY

As it applies to formwork costs, this concept has a much more practical meaning. Consistency and simplicity yield savings, complexity increases costs.

Specific examples of opportunities to simplify framework include maintaining

- Constant depth of horizontal construction
- Constant spacing of beams and joists

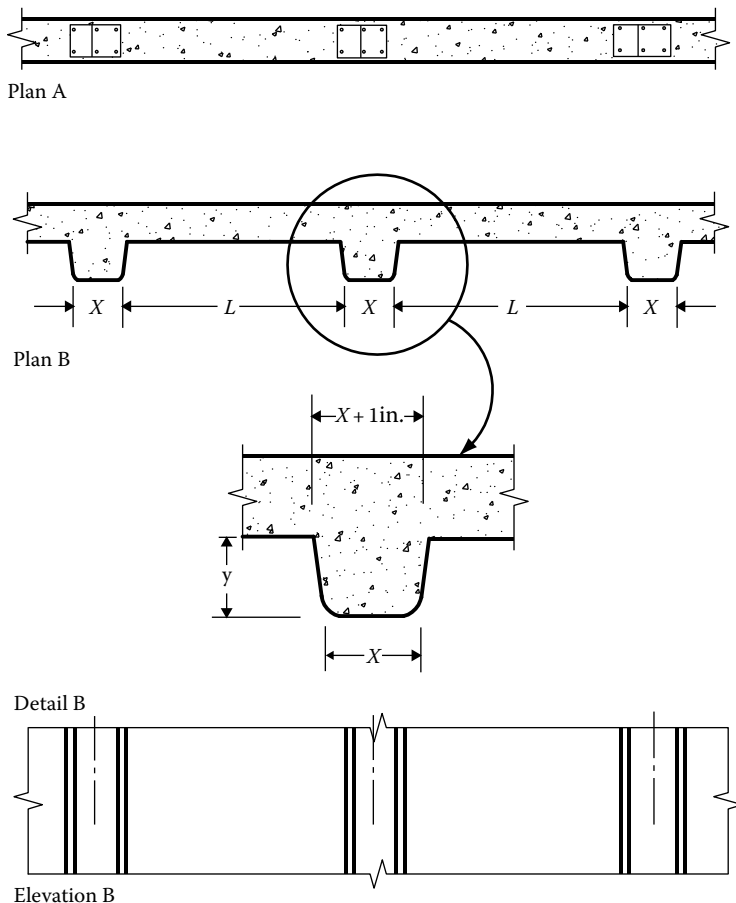


FIGURE 2.5 Pilasters and wall columns.



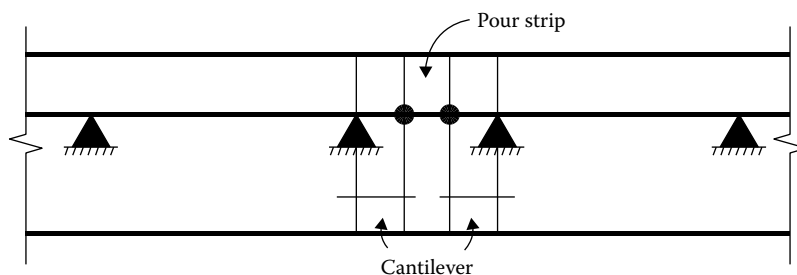


FIGURE 2.6 Pour strip as a simple span supported by cantilevers.

- Constant column dimensions from floor to floor
- Constant story heights

Economies of scale may cost-justify some variations, but usually not. When work interruptions are taken into account, a trade-off may occur. The added cost of stop-and-start field work—slowdowns to interpret plans, to make and verify new measurements, to cut and piece lumber and other materials to form complex shapes—may more than offset any expected permanent material savings. In general, simplicity and design consistency will bring the project in at lower cost.

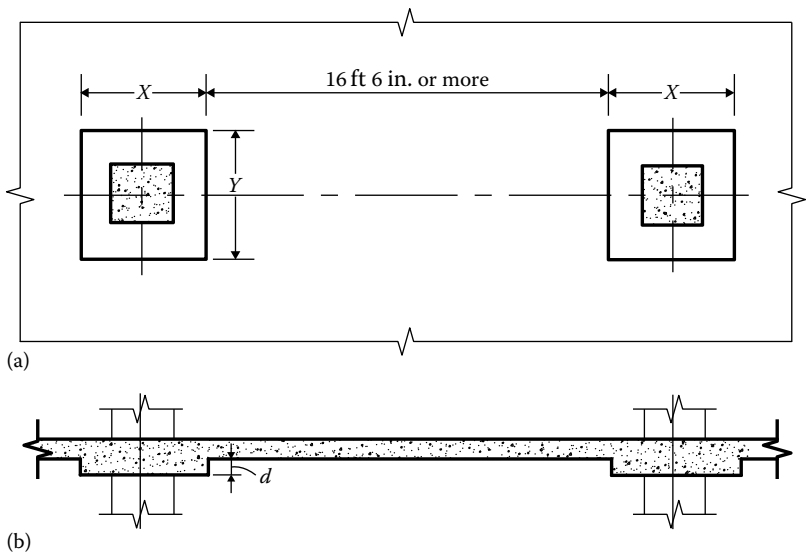
Repetitive depth of horizontal construction is a major cost consideration. By standardizing joist size and varying the width, not depth, of beams, most requirements can be met at lower cost because forms can be reused for all floors, including roofs. Going one step further, it is more cost efficient to increase concrete strength or the amount of reinforcing material (to accommodate differing loads and spans) than to vary the size of the structural member.

Changing joist depths, or beam and columns sizes might achieve minor savings in materials, but it is likely that these will be more than offset by higher labor costs. Specifying a uniform depth will achieve major savings in forming costs, and hence, total building costs.

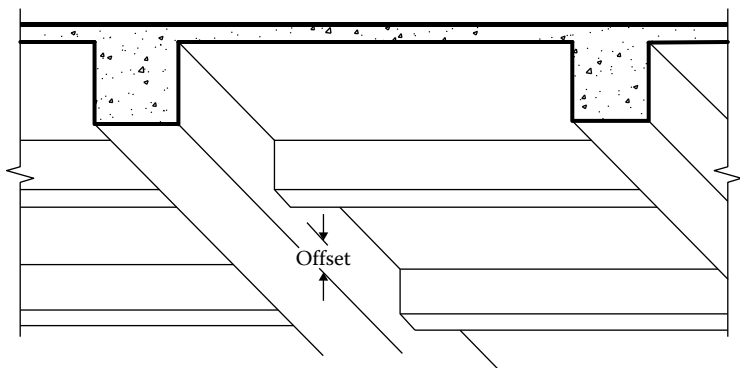
### 2.1.4 HORIZONTAL DESIGN TECHNIQUES

Once the most economical floor structural system has been selected, there are specific design techniques which help minimize overall costs. Some of these are

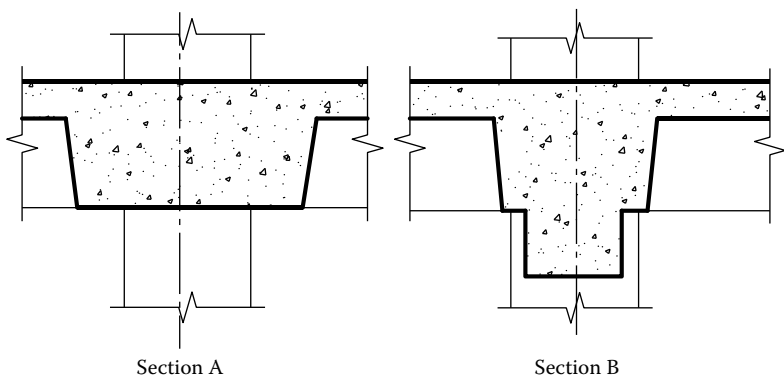
- **Flat systems:** In general, any soffit offset or irregularity may cause a stop-and-start disruption of labor, requiring additional cutting and waste of materials. When drop panels at columns are used, consideration should be given for a minimum spacing between drop panels that will allow the use of standard lumber lengths without cutting. Dimensional consistency of drop panels in both plan and section reduces complexity and cost. Drop dimensions should consider nominal lumber dimensions as well. See Figure 2.7.
- **Joist systems:** For maximum economy, spacing between joists should be consistent and based on standard form dimensions. A consistent soffit elevation, with the depth of beam equal to the depth of the joist, is extremely cost effective, because the bottom of the entire floor is on one horizontal plane (Figure 2.8). Added benefits of uniform soffit elevation are reduced installation cost for HVAC, plumbing, electrical, interior partitioning, and ceiling work.
- **Beam and slab systems:** Standardization and repetition are of particular importance when using this relatively expensive system. Consistency in depth is the first priority; wide, flat beams are more economical to form than narrow deep beams. Figure 2.9, Section A, shows a system that may meet the same design objective as deep beams, Section B, but at lower cost. If deep beams are necessary (Figure 2.10), they should be designed to nominal lumber



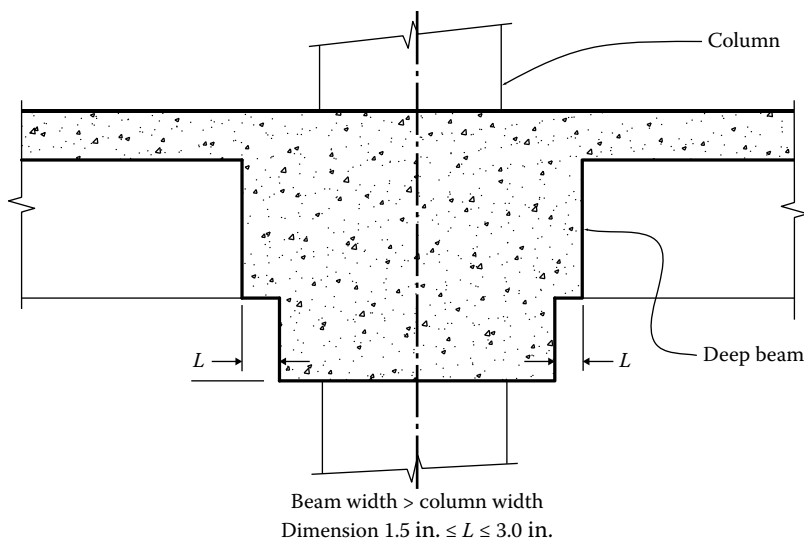
**FIGURE 2.7** Drop panel dimensions: (a) plan view and (b) section view. Dimensions  $d$ ,  $x$ , and  $y$  should remain constant throughout for maximum economy.



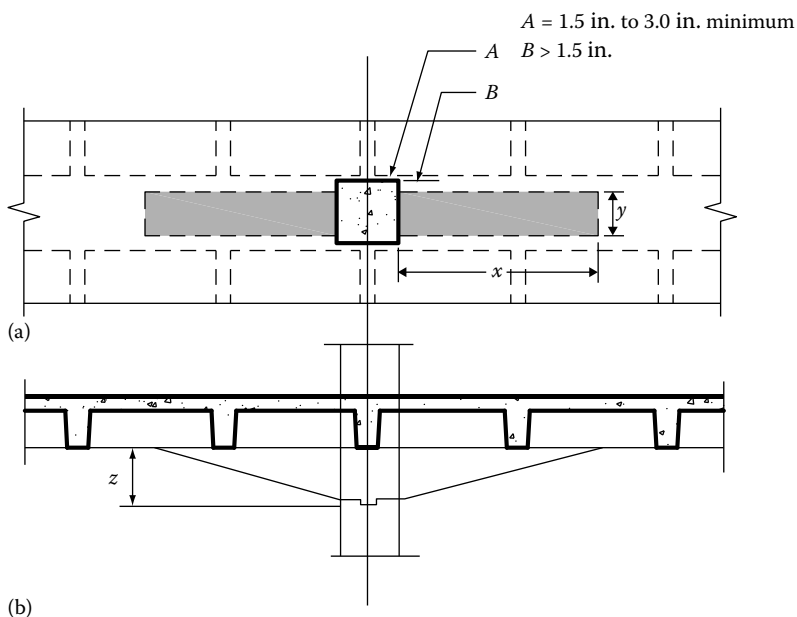
**FIGURE 2.8** Soffit at the same horizontal level.



**FIGURE 2.9** Band and narrow beams: Band beam, Section A, is more economical than narrow deep beam, Section B.



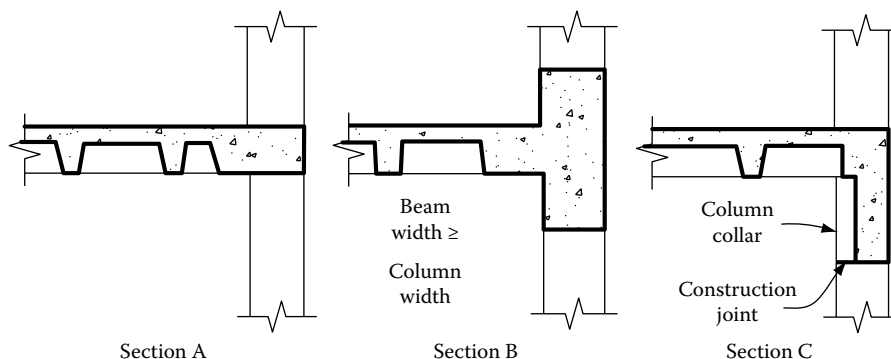
**FIGURE 2.10** Suggested formwork dimensions for deep beams.



**FIGURE 2.11** Beam haunches: (a) plan and (b) section.

dimensions. Consistency in width ranks next to depth consistency in cost impact. The skip joist/wide module systems are an example of standardization and repetition for beam and slab construction. Rake-sided beams accelerate the process of stripping forms significantly.

- **Beam haunches:** When beam haunches are required, dimensional standardization is important. As shown in Figure 2.11, standardizing dimensions “x”, “y”, and “z” allows changes in column width (if necessary) without requiring new forms to be built.
- **Spandrel beams:** Flat beams (same depth as floor construction) are less costly than deep beams. The deeper and narrower, the more costly to build. In addition, deep spandrel beams may limit the use of flying form systems. Forming a column supporting a deep, narrow spandrel (Figure 2.12, Section C) is quite expensive. Figure 2.12, Section A, shows a far more



**FIGURE 2.12** Formwork for spandrel beams. Narrow and deep spandrels framing into columns result in more expensive formwork.

economical solution. If deep beams are required for tube or moment frame design, beam width equal to columns width eliminates very costly beams/column intersections. Secondly, making the beam upturn (or partially so) reduces cost. Similarly parapet walls designed as beams are less costly to form than deep beams below the slab. See Figure 2.13, Section B. Additional suggestions for economical floor and wall framing are shown in Figure 2.13.

### 2.1.5 VERTICAL DESIGN STRATEGY

Forming cost for vertical structural elements such as walls, columns, and elevator and stair cores is typically less than for horizontal elements. Only in the tallest high-rises does the vertical component for gravity and lateral forces exceed the cost of the floor framing system.

Walls present an excellent opportunity for combining multiple structural functions into a single element. For example, a fire enclosure for stairs or elevator shafts, columns for vertical support, and horizontal bracing for lateral loads can all be incorporated into the same wall.

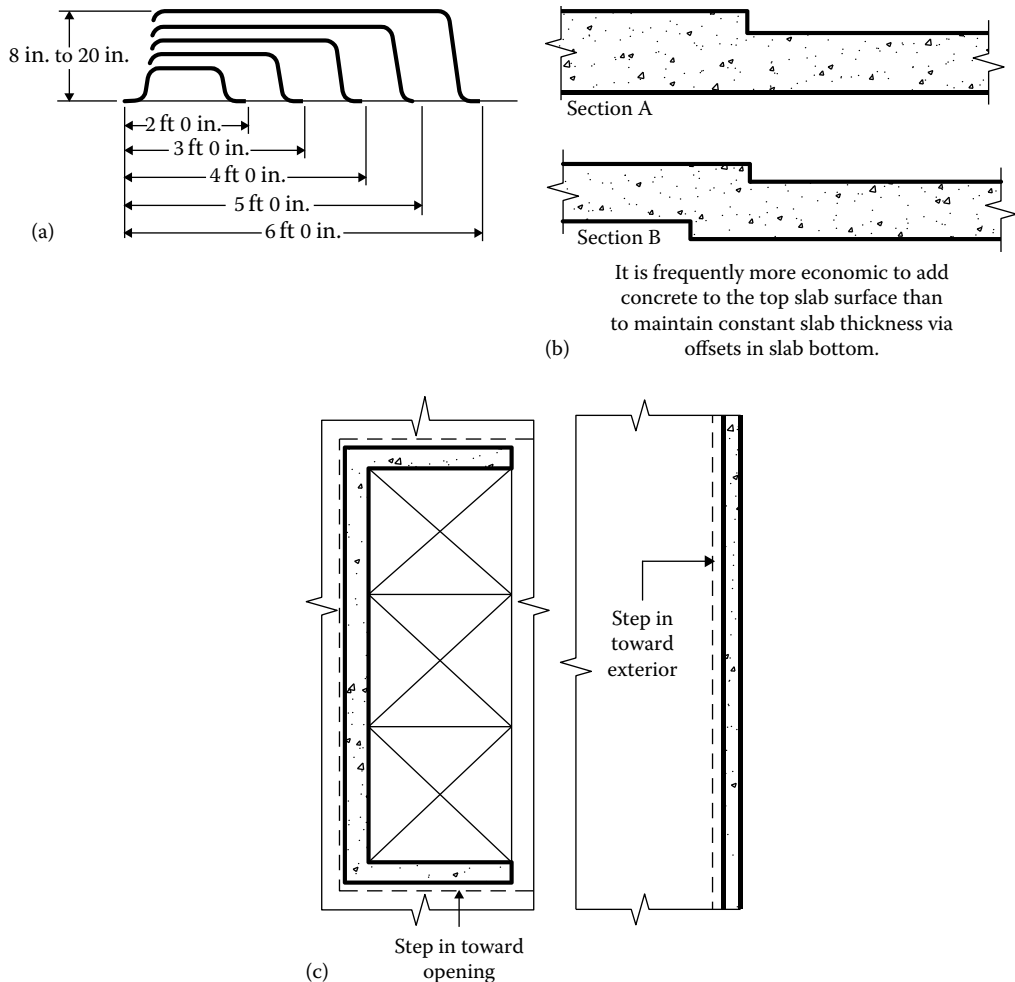
Core areas for elevators and stairs are notoriously cost-intensive if formwork economies are neglected. In extreme cases, the core alone may require more labor than the rest of the floor, on a per-foot basis. Formwork economy here is achieved through a simplification strategy: eliminate as much complexity from the core configuration as possible.

The core will cost less to build, if the design follows the principles listed below:

- The shape is symmetrical, rectilinear, without acute angles.
- The number of floor openings is minimized.
- Floor and wall openings are constant in size and location within the core.
- The core framing pattern for walls and floors is repeated on as many floors as possible.

The option to use highly productive floor forming systems, such as flying forms or panelization, may be ruled out by certain column designs. Thus, column strategy has a serious impact not only on column cost, but on all formwork efficiency and cost. Four aspects of column design are particularly important to high productivity:

1. Column sizes—The fewer changes in column size, the lower the column formwork cost. To accommodate an increase in load, increasing concrete strength and/or reinforcement is preferable to increasing columns size. If column size change is mandatory, increasing one dimension at a time is most efficient for handset systems. For a gang system, changing both dimensions is most cost effective.
2. Column orientation—Columns that depart from the established orientation cause major formwork disruptions at their intersections with the horizontal framing.



**FIGURE 2.13** Suggestions for economical framing: (a) use locally available modulus, (b) maintain soffit at same elevation, and (c) step down wall thickness as shown in the figure.

3. Column layout—A uniform, symmetrical column pattern facilitates the use of high-productivity systems such as gang or flying forms for the floor structural system. Scattered and irregular positioning of columns may eliminate the possibility of using these cost-effective systems. Even with conventional handset forming systems, a uniform column layout accelerates construction measurably.
4. Column/slab intersections—Column capitals especially if tapered, require additional labor and materials. The best approach is to avoid them altogether by providing shear reinforcement or stud rails within the floor slab. If this is not feasible, rectangular drop panels with drop equivalent to lumber dimensions located above columns serve the same structural purpose as capitals, but at far lower total costs.

**Wall Thickness:** Trade-offs must be evaluated when designing wall thickness. Reasons to maintain constant wall thickness include repetitive use of standard forms, tie lengths, and hardware. However, in tall buildings there are reasons to change wall thickness including accumulation of gravity load. So when wall thicknesses are changed, incremental steps of 2 in. or 4 in. are most efficient. Further, steps should be designed only on the wall face of the elevator and stair cores.

## 2.2 FLOOR SYSTEMS

Concrete floor systems are cast on temporary formwork or centering of lumber, plywood, or metal panels that are removed when the concrete has reached sufficient strength to support its own weight and construction loads. This procedure dictates that formwork be simple to erect and remove and be repetitive to achieve maximum economy. Although in general, floor systems for high-rise buildings are the same as for their lower brethren, there are several characteristics which are unique to high-rise buildings. Floor systems in high-rise buildings are duplicated many times over, necessitating optimum solutions in their design because

1. Savings that might otherwise be insignificant for a single floor may add up to a considerable sum because of large number of floors.
2. Dead load of floor system has a major impact on the design of vertical-load-bearing elements such as walls and columns.

The desire to minimize dead loads is not unique to concrete floor systems but is of greater significance because the weight of concrete floor system tends to be heavier than steel floors and therefore has a greater impact on the design of vertical elements and foundation system. Another consideration is the impact of floor depth on the floor-to-floor height. Thus it is important to design a floor system that is relatively lightweight without being too deep.

One of the necessary features of cast-in-place concrete construction is the large demand for job-site labor. Formwork, reinforcing steel, and the placing of concrete are the three aspects that demand most labor. Repetition of formwork is a necessity for economical construction of cast-in-place high-rise buildings. Forms which can be used repetitively are “ganged” together and carried forward, or up the building, in large units, often combining column, beam, and slab elements in a large piece of formwork. Where the layout of the building frame is maintained constant for several stories, these result in economy of handling and placing costs. “Flying” form for flat work is another type that is used to place concrete for large floor areas. In a conventional construction method sometimes called the stick method, plywood sheets are nailed to a formed solid decking built on adjustable shores. When concrete has attained sufficient strength, the shores are removed and the plywood sheets are stripped, and if undamaged, they are stored for reuse for the next floor. This method of forming is labor-intensive and also time consuming. If the floor-to-floor cycle is delayed 1 day because of formwork, the construction time of a tall building can be lengthened significantly. The flying form system typically shortens the construction time. In this system, floor forms are attached to a unit consisting of deck surface, adjustable jack, and supporting frame work. For stripping, the form is lowered, slipped out of the slab, and shifted to the next floor as one rigid structure, resulting in economy of handling and placing.

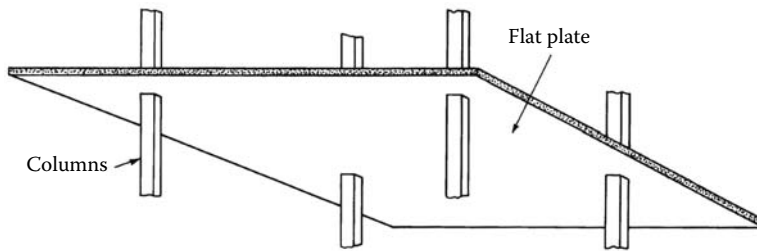
### 2.2.1 FLAT PLATES

Concrete slabs are often used to carry vertical loads directly to walls and columns without the use of beams and girders. Such a system called a flat plate (Figure 2.14) is used where spans are not large and loads are not heavy as in apartment and hotel buildings.

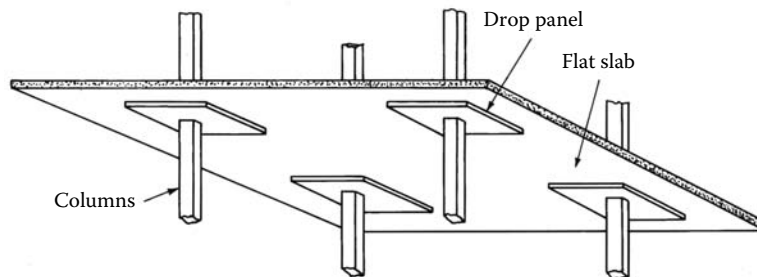
Flat plate is the term used for a slab system without any column flares or drop panels. Although column patterns are usually on a rectangular grid, flat plates can be used with irregularly spaced column layouts. They have been successfully built using columns on triangular grids and other variations.

### 2.2.2 FLAT SLABS

Flat slab (Figure 2.15) is also a two-way system of beamless construction but incorporates a thickened slab in the region of columns and walls. In addition to the thickened slab, the system can have



**FIGURE 2.14** Flat plate system.



**FIGURE 2.15** Flat slab system.

flared columns. The thickened slab and column flares, referred to as drop panels and column capitals, reduce shear and negative bending stresses around the columns.

A flat plate system with a beamless ceiling has minimum structural depth, and allows for maximum flexibility in the arrangement of air-conditioning ducts and light fixtures. For apartments and hotels, the slab can serve as a finished ceiling for the floor below and therefore is more economical. Since there are no beams, the slab itself replaces the action of the beams by bending in two orthogonal directions. Therefore, the slab is designed to transmit the full load in each direction, carrying the entire load in shear and in bending.

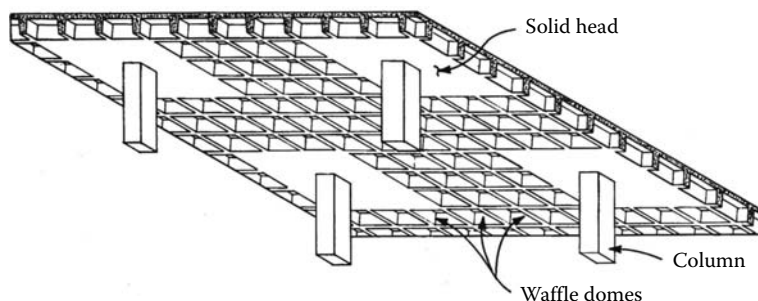
The limitations of span are dependent upon the use of column capitals or drop panels. The criterion for thickness of the slab is usually the punching shear around columns and long-term deflection of the slab. In high-rise buildings, the slabs are generally 5–10 in. (127–254 mm) thick with spans of 15–25 ft (4.56–7.6 m).

### 2.2.2.1 Column Capitals and Drop Panels

Where added strength over a support is required, thickened slabs around columns are used to increase the local shear capacity. A drop cap, also referred to as a column capital, is defined by the ACI 318–05/08 as a thickening, which does not extend into the span beyond one-sixth of the span length. A drop panel, on the other hand, extends into the span one-sixth of the span length or beyond. It is permitted by the ACI to increase the negative moment capacity of the slab by using the increased thickness of the slab in drop panel regions.

Traditionally, drop caps and panels around columns are used for two principal reasons:

1. Column capitals, or drop caps, are used to improve the punching shear capacity of the column/slab joint only.
2. Drop panels are used to increase the bending moment capacity of the joint, reduce deflection, and increase the punching shear capacity.



**FIGURE 2.16** Waffle system.

### 2.2.2.2 Comments on Two-Way Slab Systems

The two-way slab design is a heavy-duty design, compared to the flat plate. For heavier loads and longer span combinations, the flat slab with adjustable drop panel depth will require less concrete and reinforcement and can utilize smaller columns than the flat plate for the slight added cost of forming drop panels. The two-way flat plate or flat slab designs are most efficient for square or nearly square panels. For parking, storage, or industrial structures, the drop panel soffit is usually an acceptable ceiling. For longer spans, the waffle system discussed presently in this section will provide increased stiffness with less self-weight for the overall economy. The choice of a two-way system, however, usually depends on particular job conditions.

### 2.2.3 WAFFLE SYSTEMS

This system also called a two-way joist system (Figure 2.16) is closely related to the flat slab system. To reduce the dead load of a solid slab construction, metal or fiberglass domes are used in the formwork in a rectilinear pattern, as shown in Figure 2.16. Domes are omitted near columns resulting in solid slabs to resist the high bending and shear stresses in these critical areas.

In contrast to a joist which carries loads in a one-way action, a waffle system carries the loads simultaneously in two directions. The system is therefore more suitable for square bays than rectangular bays. The overall behavior of the system is similar to a flat slab. However, the waffle is more efficient for spans in the 30–40 ft (9.1–12.2 m) range because it has greater overall depth than a flat slab without the penalty of added dead weight.

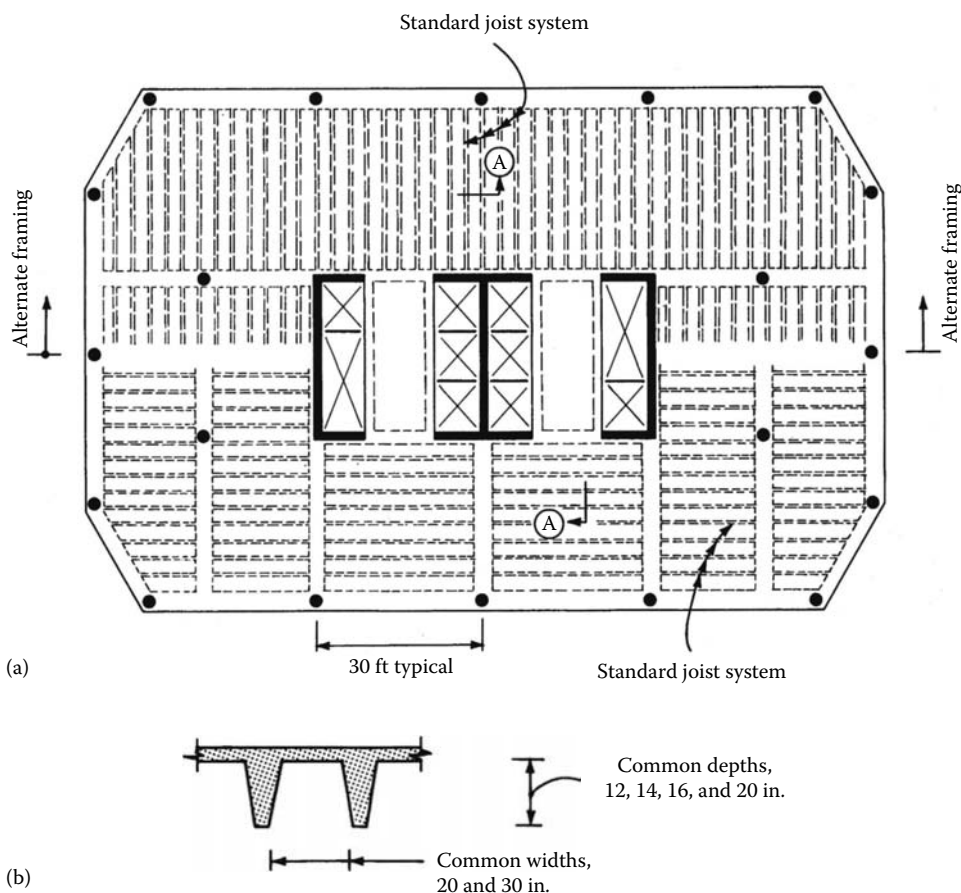
### 2.2.4 ONE-WAY CONCRETE RIBBED SLABS

This system also referred to as a one-way joist system is one of the most popular systems for high-rise office building construction in North America. The system is based on the well-founded premise that concrete in a solid slab below the neutral axis is well in excess of that required for shear and much of it can be eliminated by forming voids. The resulting system shown in Figure 2.17 has voids between the joists made with removable forms of steel, wood, plastic, or other material. The joists are designed as one-way T-beams for the full-moment tributary to its width. However, in calculating the shear capacity, ACI 318–05/08 allows for a 10% increase in the allowable shear stress of concrete. It is a standard practice to use distribution ribs at approximately 10 ft (3.0 m) centers for spans greater than 20 ft (6 m). For maximum economy of formwork, the depth of beams and girders should be made the same as for joists.

### 2.2.5 SKIP JOIST SYSTEM

In this system instead of a standard 3 ft (0.91 m) spacing, joists are spaced at 5 ft or 6 ft 6 in. (1.52 and 1.98 m) spacings using 53 and 66 in. (1346 and 1676 mm) wide pans. The joists are designed as beams without using 10% increase in the shear capacity allowed for standard joist. Also the system





**FIGURE 2.17** One-way joist system: (a) building plan and (b) Section A.

is designed without distribution ribs thus requiring even less concrete. The spacing of temporary vertical shores can be larger than for standard pan construction. Consequently the formwork is more economical. Figures 2.18 and 2.19 show typical layouts.

The fire rating requirements for floor systems is normally specified in the governing building codes. The most usual method of obtaining the rating is to provide a slab that will meet the code requirement without the use of sprayed-on fireproofing. In the United States, normally the slab thickness required for 2h fire rating is 4 in. (101.6 mm) for lightweight concrete and 4½–5 in. (114.3–127 mm) for normal-weight concrete, depending upon the type of aggregate. Therefore, the thickness of the slab required for fire rating may be much in excess of that required by structural design. Therefore, use of special pan forms with joists at 8–10 ft centers (2.43–3.04 m) should be investigated for large projects.

### 2.2.6 BAND BEAM SYSTEM

When the support arrangement of a uniform floor slab is such that the spans in one direction are substantially longer than in the perpendicular direction, the length of the longer spans typically governs the slab thickness. The unfavorable effects of longer spans can be reduced if a band beam, also called slab band, is used in the long span direction. Slab bands are thickenings below slab. The dimensions of the slab band are selected so as to avoid significant increase in the stiffness of the slab and retain the two-way action of the floor system. The recommended dimensions for a 30×30 ft bay

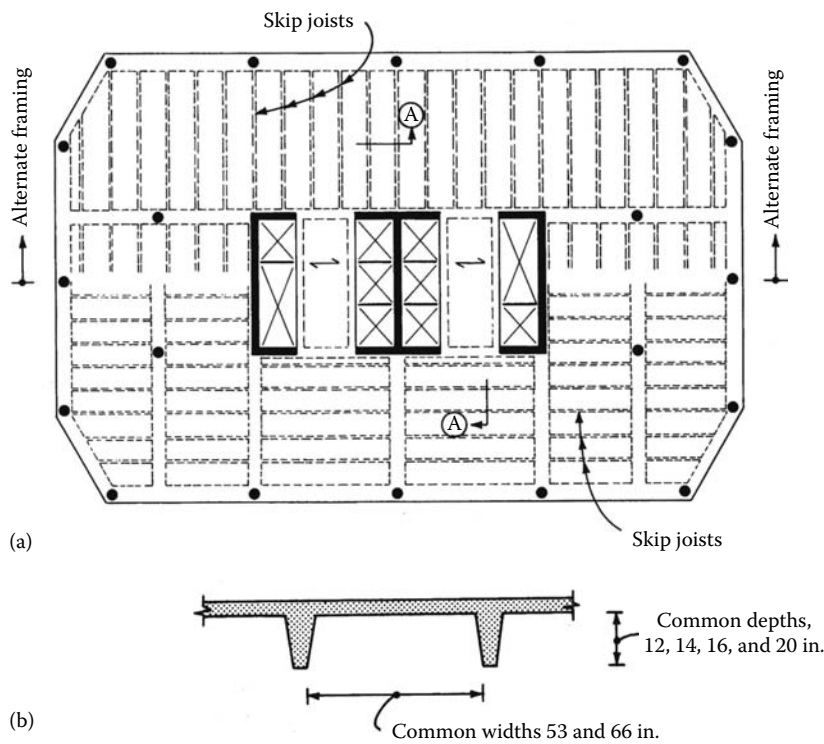


FIGURE 2.18 Skip joist system: (a) building plan and (b) Section A.

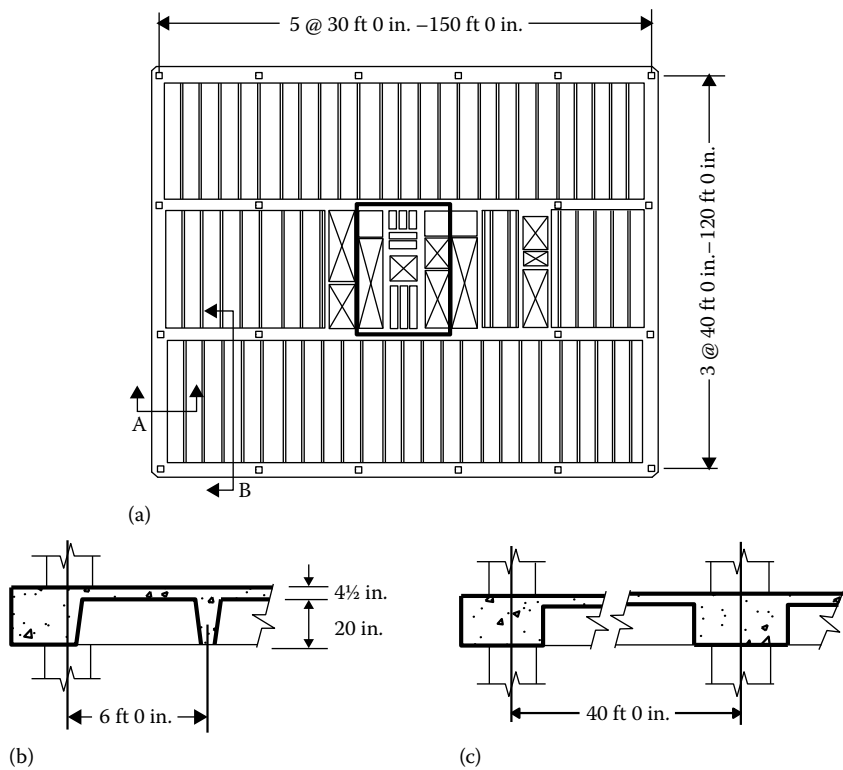
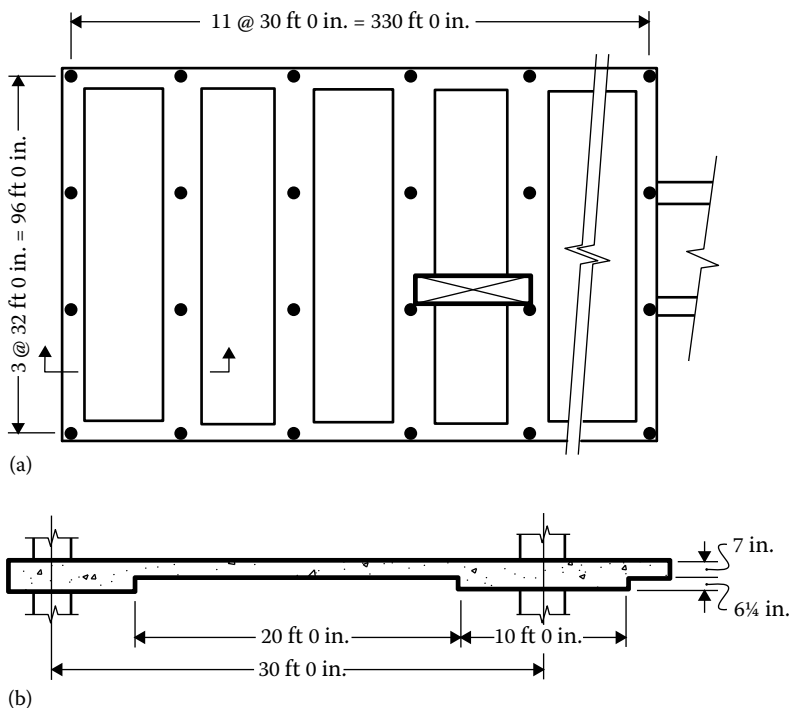


FIGURE 2.19 Skip joist system, another example: (a) plan view, (b) Section A, and (c) Section B.



**FIGURE 2.20** Band beam system: (a) floor plan and (b) section.

are shown in Figure 2.20. When using slab bands in the longer direction, the thickness of the slab is determined by applying the applicable span-to-depth ratios to the span in the shorter direction. The span length used is the column centerline-to-centerline dimension in the short direction. A shallow slab band with dimensions limited to a maximum of twice the thickness of slab does not provide adequate stiffness for the slab in the short direction to be considered as spanning the clear distance between the faces of the slab band. For design purposes, the reduction of the computed moments to the face-of-support must be applied to the face of the column, and not the face of the slab band.

Use of wide shallow beams should be investigated for buildings in which the floor-to-floor height is critical. Note if the building has perimeter beams, it is not necessary to line up the band beams with the exterior columns.

The slab in between the band beams may also be designed as a bending member with varying moment of inertia by taking into account the increased thickness of slab for the width of band beams. A variation of the scheme uses standard or skip joists between band beams.

### 2.2.7 HAUNCH GIRDER AND JOIST SYSTEM

A floor-framing system with girders of constant depth crisscrossing the interior space between the core and the exterior often presents nonstructural problems because it limits the space available for the passage of air-conditioning ducts. The haunch girder system widely accepted in certain parts of North America, achieves more headroom without making undue compromises in the structure. The basic system shown in Figure 2.21 consists of a girder of variable depth. The shallow depth at the center facilitates the passage of mechanical ducts and reduces the need to raise the floor-to-floor height. Two types of haunch girders are in vogue. One uses a tapered haunch (Figure 2.22) and the other a square haunch (Figure 2.23).

Shown in Figures 2.24 and 2.25 is a haunch girder scheme for a  $10\text{ m} \times 20\text{ m}$  ( $32.83\text{ ft} \times 65.2\text{ ft}$ ) bay.

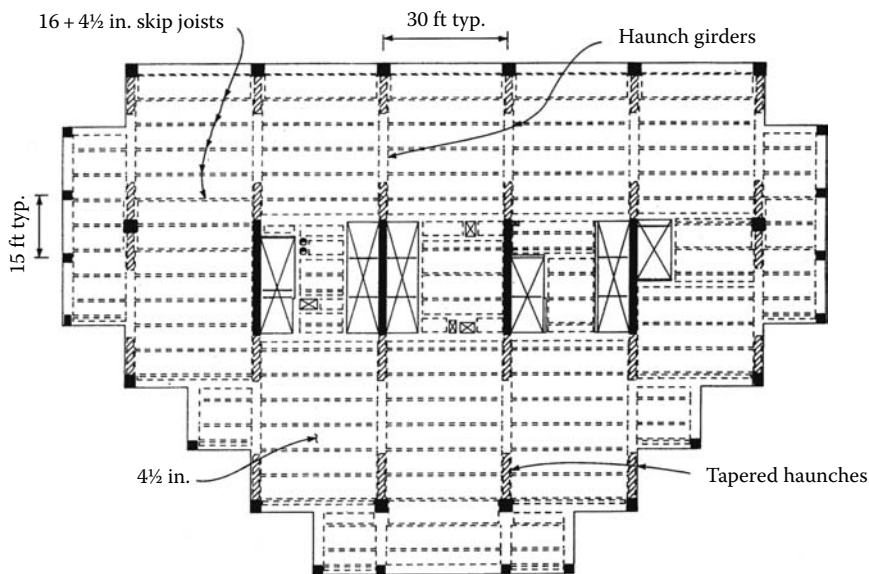


FIGURE 2.21 Haunch girder-framing system.

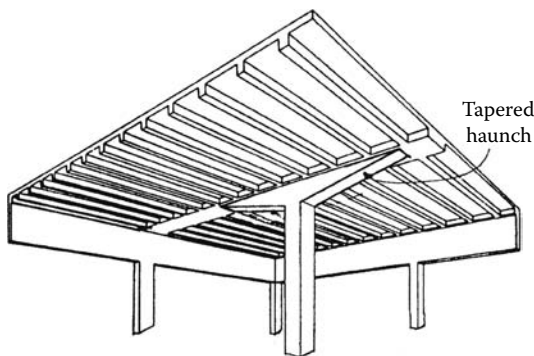


FIGURE 2.22 Tapered haunch girder.

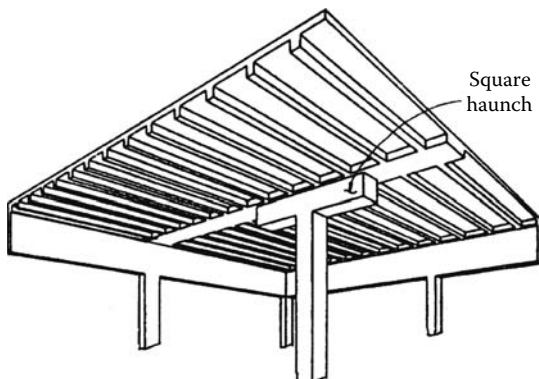
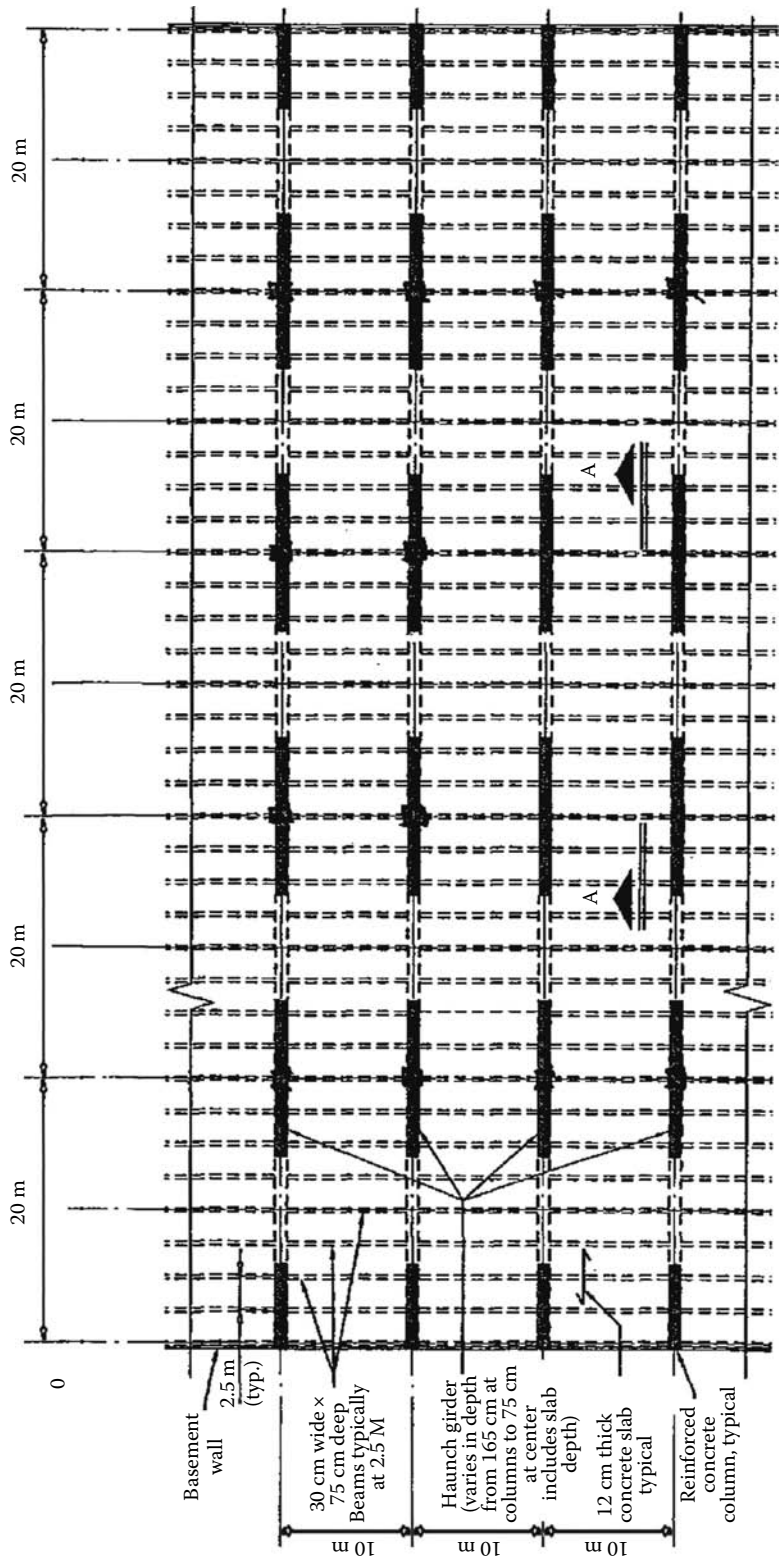
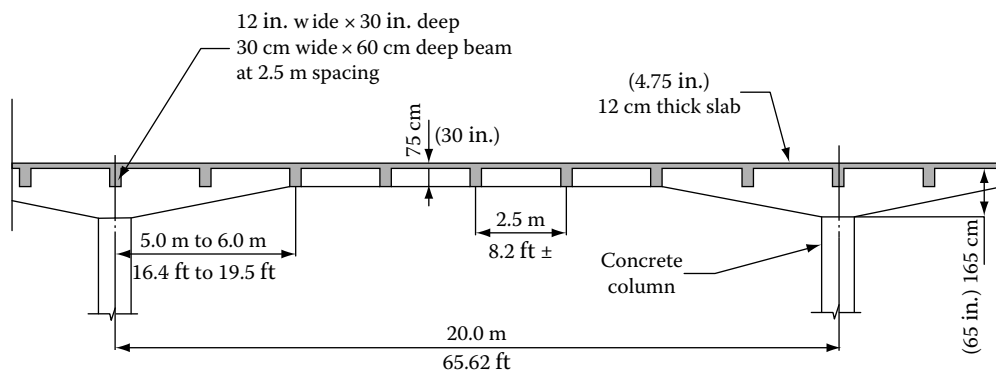


FIGURE 2.23 Hammerhead haunch girder.



**FIGURE 2.24** 10 m × 20 m (32.81 ft × 65.62 ft) girder haunch girder with transverse beams: Plan.



**FIGURE 2.25** Section AA: haunch girder elevation.

### 2.2.8 BEAM AND SLAB SYSTEM

This system consists of a continuous slab supported by beams generally spaced at 10–20 ft (3.04–6.08 m) on center. The thickness of the slab is selected from structural considerations and is invariably much in excess of that required for fire rating. The system has broad application and is generally limited by the depth available in the ceiling space for the beam stem. This system considered a “heavy-duty” system is often used for framing nontypical floors such as ground floor and plaza levels, which are typically subjected to heavier superimposed loads due to landscape and other architectural features.

## 2.3 DESIGN METHODS

In today’s business environment, computer-assisted finite element solutions are common for analysis and design of floor systems. However, to gain an insight into their behavior, we will examine some of the simple procedures that were used in the not too distant past.

### 2.3.1 ONE-WAY AND TWO-WAY SLAB SUBASSEMBLIES

The traditional design of concrete floors, using the equivalent frame or similar procedure, requires the floor to be designed as either one-way or two-way structural system. The essential difference between the two is that in a one-way system the constituents of the load path are visualized as parallel rows of skeletal members with the capability to transfer loading along their length only, like planks spanning between walls or beams. On the other hand, in a two-way system, the floor may be considered as consisting of rows of intersecting members which allows the applied loads to be resisted by one member or shared by the intersecting members. The one-and two-way designations were originally introduced due to limitations in the commonly used design methods. Now the designations are consolidated in to a single procedure with a somewhat different design criterion for each.

Finite element technology, however, can model and analyze the entire floor system as one unit, using slab and beam components which as an assembly possess an inherent biaxial load-carrying capability. Hence, the question of whether a floor should be categorized as a one-way or two-way system, prior to the design, does not arise. Also, by modeling the entire floor system and its components as one assembly, it is no longer necessary to preassign a load path, as is the case in most other modeling techniques. The participatory contribution of a floor region or a component such as

a beam, in carrying the applied load in one or more directions is determined automatically from the geometry, material properties, and loading of the entire floor as part of the solution.

The outcome of a finite element analysis consists of values for displacements and actions at all points through the slab. In order to complete the design, it is only necessary to supplement the analysis by designing for reinforcement, to meet the strength demand stipulated in the codes.

### 2.3.2 DIRECT DESIGN METHOD FOR TWO-WAY SYSTEMS

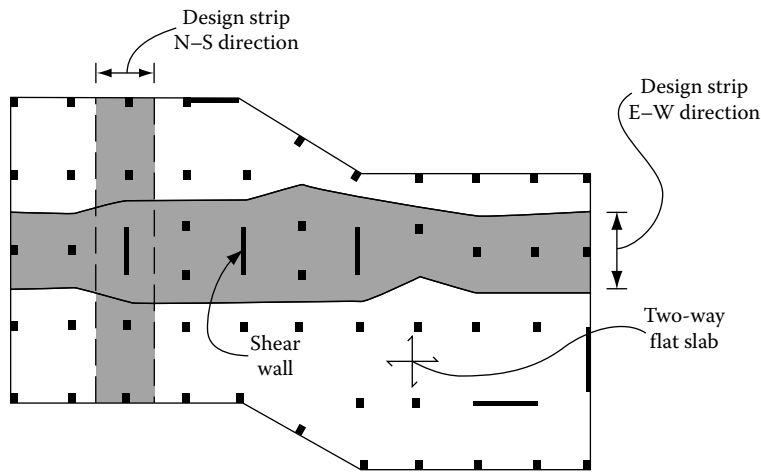
The direct design method includes a set of rules for the proportioning of non-prestressed slab and beam sections to resist code-specified loading. It does not apply to prestressed slabs. The rules have been developed to satisfy all applicable safety and serviceability requirements simultaneously. Application of this method is limited to highly regular slabs supported by an orthogonal array of columns. The slab is of a uniform thickness with no significant thickening around columns. Drop caps provided to resist punching shear do not disqualify the floor system as a flat slab. However, when the slab is designed by the direct design method, any flexural contributions due to drop caps are ignored.

The primary objective of the method is to provide the engineer with an effective tool for the design of flat slab configurations, without necessitating the application of rigorous plate analysis techniques and the specialized knowledge they require. The direct design method is quick and easy to learn and implement, but it does have certain restrictions. The restrictions are

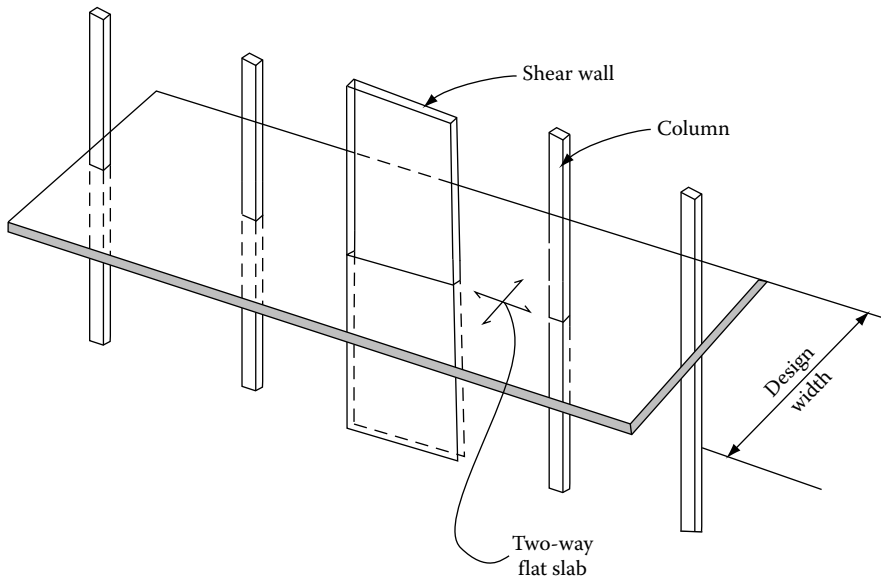
1. There shall be a minimum of three continuous spans in each direction.
2. Panels shall be rectangular with a ratio of the longer to the shorter span (support centerline-to-centerline) not greater than 2.
3. Successive spans (support centerline-to-centerline) in each direction shall not differ by more than one-third the longer span.
4. Columns may be offset a maximum of 10% of the span length from the axis drawn between the centerline of successive columns.
5. All loads shall be due to gravity only, uniformly distributed over an entire panel. Live loading shall not exceed three times the dead loading.

In this method, the structure is assumed to consist of a series of frames along the column support lines in each of the orthogonal directions. Figure 2.26 shows a typical frame in one direction with its associated tributary. Each frame, consisting of the slab tributary and the columns immediately below and above is analyzed in isolation and designed for gravity loading (see Figure 2.27). The general procedure follows four fundamental steps:

1. Determine the factored static moment or design moment,  $M_0$ . The design moment,  $M_0$ , is simply the total factored static moment caused by loading on the entire tributary of each span in the frame.
2. Distribute the total factored static moment,  $M_0$ , to positive and negative components in the middle and at the face-of-support. The distribution is achieved using code-stipulated factors.
3. Distribute negative and positive factored moments in the transverse direction. In this step, a larger portion of the moment is assigned to the region next to the column—the “column strip”—and a smaller portion is assigned to the region away from the column—the “middle strip.”
4. Determine reinforcement required at each critical section based on the calculated moment for that section.



**FIGURE 2.26** Typical frame design strip.



**FIGURE 2.27** Equivalent frame concept, N-S direction.

### 2.3.3 EQUIVALENT FRAME METHOD

The equivalent frame method is currently the most common method of analysis in designing concrete floor systems, including posttensioned floors. It is flexible and efficient, equally suited for both regular and irregular floor systems. This method involves modeling of the three-dimensional slab system as a series of two-dimensional frames which are independently analyzed for loads assumed to act in the plane of each frame. Although similar to the direct design method, this method uses approximations that more accurately capture the actual behavior of the slab.

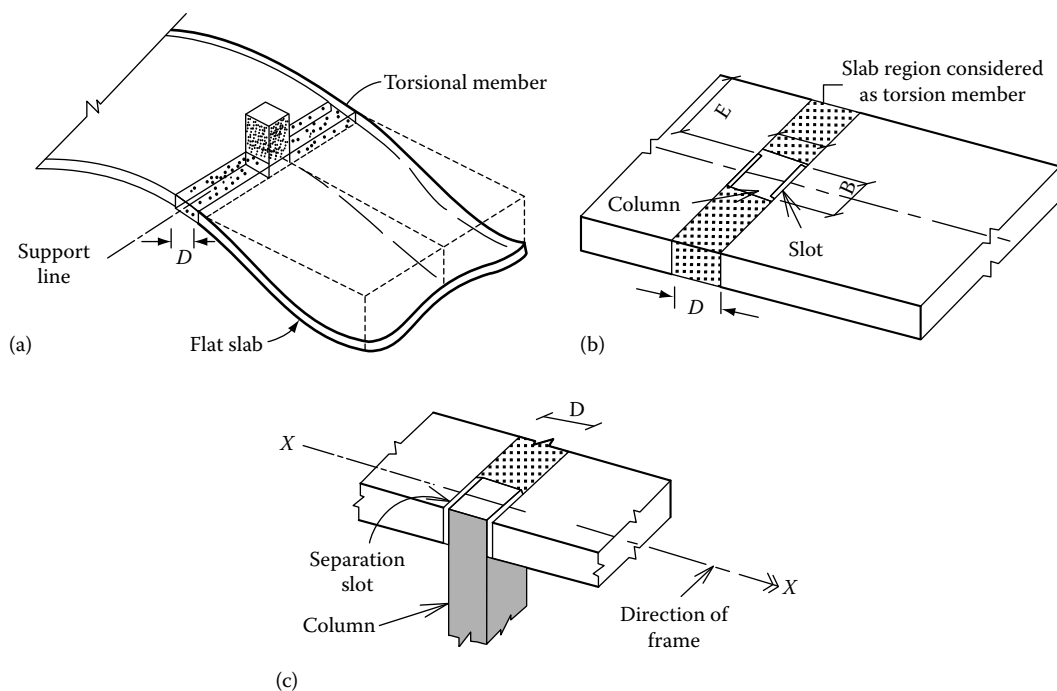
The procedure rests on a strategy whereby the two-dimensional model of each frame is modified to approximate the effect of torsional rotations.



The approximation of torsional rotations is achieved through the introduction of torsional elements in the two-dimensional frame. Moment transfer between the slab and column is then modeled to take place through these torsional elements, as described below.

1. The structure is divided into a series of equivalent frames along support lines (columns and walls) taken longitudinally and transversely through the structure. Each frame consists of a row of columns or supports and the corresponding slab-beam strip, bounded laterally by the centerline of the slab panel on each side of the support centerline.
2. To account for torsion in the slab, and its corresponding impact on column moments, the supports are assumed to be attached to the slab strips by torsional members, which are perpendicular to the direction of the span and extending to the slab panel centerlines on each side of the column.
3. Figure 2.28 illustrates the torsional elements within the slab strip included to represent slab torsioned stiffness. The moment transfer between the slab and column is assumed to take place through the torsional members only. There is no moment transfer through the slab-column connection at the face-of-support.
4. The torsional effects of the slab are included in the analysis by substituting each column and its attached torsional members with an equivalent column. The stiffness of the equivalent column is simply the combined stiffness of the column and its torsional members. The equivalent column stiffnesses are then used when calculating the design actions in the slab. Note that the equivalent stiffness of column is less than the actual stiffness of the column.

The physical significance of this model is that the resulting column moments are lower than those associated with a simple frame analysis, resulting in reduced reinforcement requirements and a more efficient design in the negative moment regions of the slab.



**FIGURE 2.28** Moment transfer through torsion.

One other advantage of the equivalent frame is that both the slab and the columns are modeled as nonprismatic members, which allows for variations in slab thickness and tributaries as well as drop panels, caps, and openings.

### 2.3.4 YIELD-LINE METHOD

Is the yield-line method of analysis sanctioned by the ACI 318-05/08 provisions? Yes, and it is an emphatic yes. Note in Section 13.5.1, ACI 318 for many years has stated

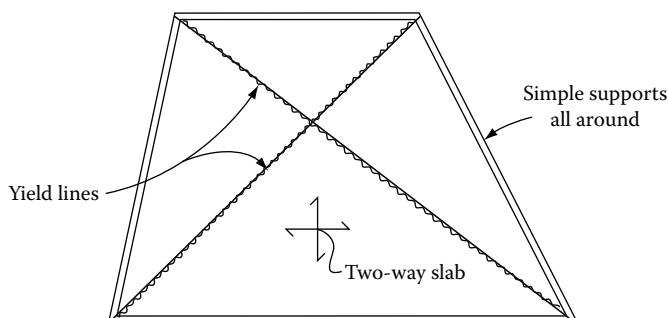
A slab system shall be designed by any procedure satisfying conditions of equilibrium and geometric compatibility, if shown that the design strength at every section is at least equal to the required strength set forth in 9.2 and 9.3, and that all serviceability conditions, including limits on deflections, are met.

Additionally the second sentence of the Commentary Section R13.5.1 affirms that

The design of the slab may be achieved through the combined use of classic solutions based on a linearly elastic continuum, numerical solutions based on discrete elements, or yield-line analyses, including, in all cases, evaluation of the stress conditions around the supports in relation to shear and torsion as well as flexure. The designer should consider that the design of a slab system involves more than its analysis, and justify any deviations in physical dimensions of the slab from common practice on the basis of knowledge of the expected loads and the reliability of the calculated stresses and deformations of the structure.

This method is an excellent tool to justify moment capacity of existing slab systems that are functioning satisfactorily for serviceability requirements but may not pencil out for the flexural reinforcement requirements. Although not much of a description of the method is given in the ACI 318, its use by design procedures given in related textbooks is explicitly allowed for in the design of two-way slabs.

The method is based on the principle that in a slab failing in flexure under overload conditions, the reinforcement will yield first in a region of highest moment. When this occurs, the slab in this region hinges along a line commonly referred to as a yield line. The slab is able to resist loads corresponding to its “hinging moment,” but no more. When the load is increased further, the hinging region rotates as a plastic hinge and moments due to additional loads are redistributed to adjacent sections, causing them to yield in turn, as shown in Figure 2.29. Eventually, enough yield lines form until a failure mechanism manifests by itself leading to plastic deformation of the slab without an



**FIGURE 2.29** Formation of yield lines. Yielding starts in regions of high moment and spreads to areas that are still elastic.

increase in the applied loading. Thus plastic theory may be used to compute the failure load corresponding to a given plastic moment resistance along assumed yield lines. It should be noted that yield-line analysis does not give any information about deflections. However, a distinct advantage of this method is that simple and quick solutions are possible for any plate geometry.

Two procedures are available for the yield-line analyses, both based on classic methods: (1) the equilibrium method and (2) the method of virtual work. In the first method, equilibrium equations are written for each plate segment taking particular care to assign correct sign convention for the twisting moments along the yield lines. It should be noted, because of the possibility of errors, some building codes require that yield-line calculations be done by the virtual work method.

It should be emphasized that the method of virtual work is an upper bound method, in the sense the slab resistance predicted may be higher than the true resistance, unless the yield-line pattern chosen happens to be the correct one.

The design method given in Chapter 13 of ACI 318 is applicable to flat slabs, flat plates, two-way slabs, and waffle systems. Also included are two-way wideband systems. Much of the design rules are based not on rigorous theory, but on the results of extensive tests and the well-established performance record of various slab systems.

It should be noted that one-way slabs designed to resist flexural stresses in only one direction are excluded from the general procedures given in ACI 318-08, Chapter 13. Whether this exclusion applies to the yield-line analysis is not immediately apparent in the ACI provisions, although standard textbooks on reinforced concrete design include one-way slabs in their discussions of the method. In view of this, we will introduce the fundamentals of yield-line theory and its application by discussing the one-way simply supported slab.

### 2.3.4.1 Design Example: One-Way Simply Supported Slab

**Given:** The one-way simply supported slab shown in Figure 2.30, has a reinforcement of #5 @ 12 in. at bottom in the east–west direction and is subjected to a uniformly distributed ultimate load of  $W_u$  per unit area. Temperature and shrinkage reinforcement are not shown for clarity. Effective depth,  $d = 8$  in.

**Required:** Determine the ultimate load,  $W_u$ , using virtual work method.

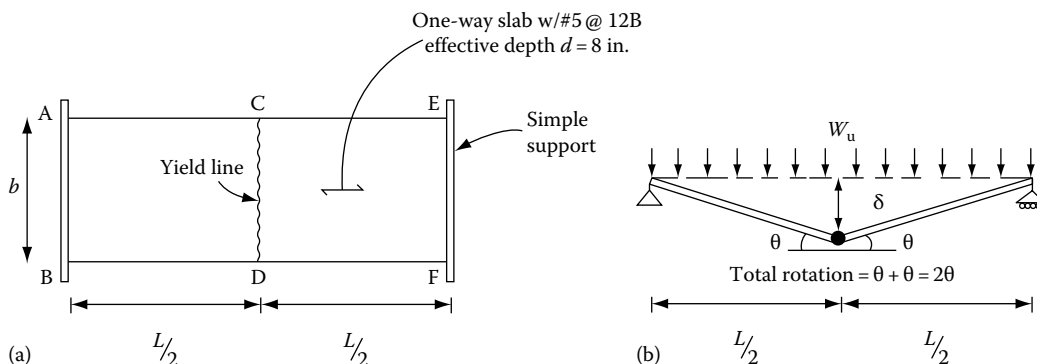
**Solution:**

1. Locate yield lines

The slab is simply supported and is subjected to a uniform load. By inspection, we determine that the yield line will form along the center of span.

2. Give the slab a virtual displacement

Displace the slab downward by an amount  $\delta$ , along line CD (see Figure 2.30b).



**FIGURE 2.30** Yield-line design example. (a) Yield-line at center span. (b) Yield-line rotations.

3. Compute the external work done by the load  $W_u$

The displacement of the load on one-half of the slab area,  $(L/2 \times b)$ , is  $\Delta_c = \delta/2$ .

Therefore, external work done on the area ABCD is

$$\frac{W_u L b \delta}{4}$$

The total external work on the entire slab area ABEF is

$$\frac{2W_u L b \delta}{4} = \frac{W_u L b \delta}{2}$$

4. Compute the internal work

The positive moment yield line at the center span, line CD, rotates through an angle  $\theta + \theta = 2\theta$ , where  $\theta = \delta/L/2$ . The internal work done by the yield line at CD in rotating through this

angle of  $2\theta$  is  $\left(\frac{2M_u b \delta}{L}\right)^2$

5. Equate the external work and internal work

$$\frac{W_u L b \delta}{2} = \frac{4M_u b \delta}{L}$$

This simplifies to  $M_u = W_u L^2/8$  or  $W_u = 8M_u/L^2$

6. Determine  $W_u$

For the given reinforcement of #5 @ 12 bottom, and an effective depth  $d = 8$  in, the approximate ultimate moment per foot width is

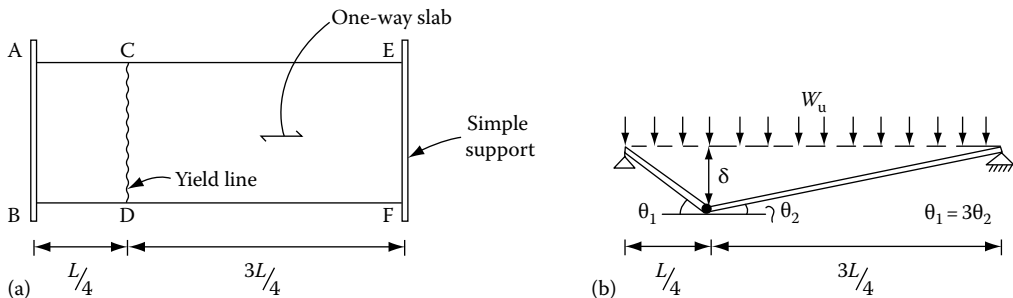
$$M_u = A_s \times 4 \times d = 0.31 \times 4 \times 8 = 9.92 \text{ kip-ft/ft}$$

$$W_u = 8 \times 9.92/16^2 = 0.310 \text{ kip/ft}^2$$

Note:  $W_u = 1.2D + 1.6L$

**Consequence of Choosing Incorrect Yield Lines.** We will rework the same problem, deliberately opting for a yield line at an incorrect location, as for example, at  $L/4$  from AB. See Figure 2.31.

1. Locate the yield line CD now at a distance of  $L/4$  from AB.
2. Give the slab a virtual displacement of  $\delta$  along CD.
3. The average displacement of the external load,  $W_u$ , on the slab segment to the left of CD is  $\delta/2$ .



**FIGURE 2.31** Yield-line design example. (a) Yield line at a quarter span. (b) Yield-line rotations.

Therefore, external work =  $\frac{W_u L b \delta}{\delta}$  (for area ABCD). Similarly the external work of load on the slab segment to the right of CD is

$$\frac{3W_u L b \delta}{\delta}$$

The total external work as before is

$$\frac{W_u L b \delta}{2}$$

Note external work is the same as before. It is independent of the yield mechanism.

4. Compute the internal work.

Line CD rotates through an angle  $\theta_1 + \theta_2$ , where

$$\theta_1 = \frac{4\delta}{L} \text{ and } \theta_2 = \frac{4\delta}{3L}, \text{ giving } \theta_1 = 3\theta_2$$

Therefore,  $\theta_1 + \theta_2 = 4\theta_2$

Internal work =  $M_u \times 4\theta_2 \times b$

$$= \frac{16M_u \delta b}{3L}$$

Equating internal work to external work, we get

$$M_u \times \delta \times 16 \times b = W_u \times L \times \delta \times b/2$$

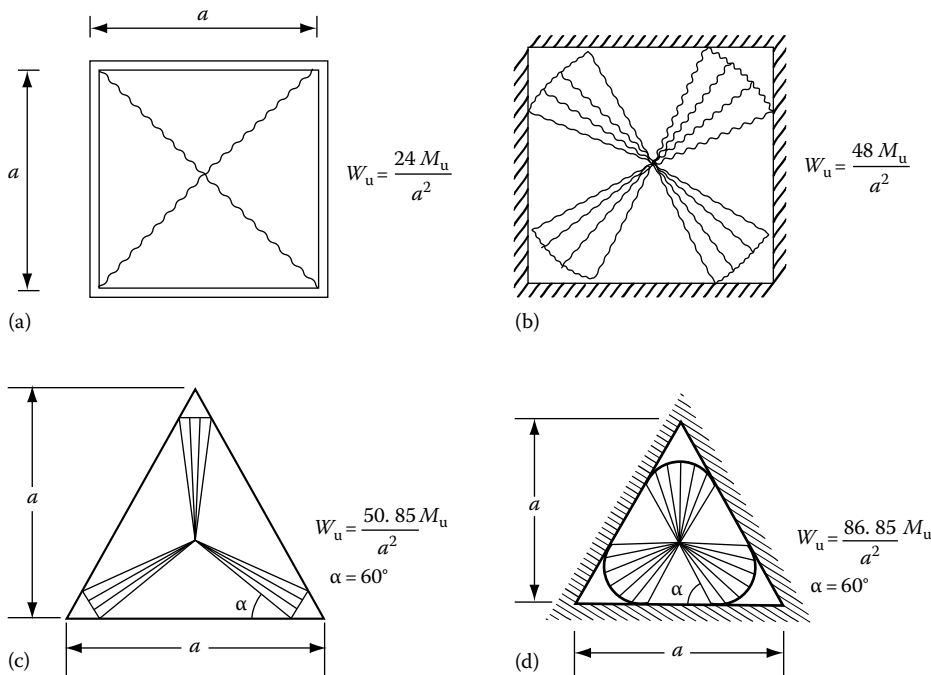
Simplifying

$$W_u = \frac{32M_u}{3L^2} = \frac{32 \times 9.92}{3 \times 16^2} = 0.413 \text{ kip/ft}^2$$

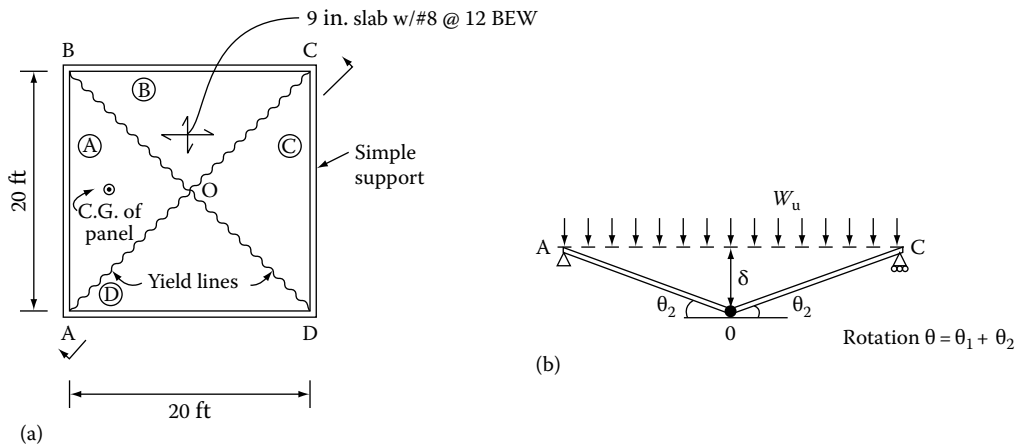
Note this value of 0.413 kip/ft<sup>2</sup> is quite significantly higher than the correct value of 0.310 kip/ft<sup>2</sup> predicted by the previous analysis. This example clearly demonstrates the upper bound characteristics of the yield-line method of analysis.

A major drawback, as demonstrated by the previous example, is virtual work method that provides an upper bound leading to potentially unconservative solution because for a given slab, any number of failure mechanisms may be assumed. However, only one of these represents the actual failure mechanism. For each assumed failure mechanism, there exists a loading which causes the slab to fail in the assumed mechanism. This loading is the load capacity associated with the particular mechanism. The slab's actual failure occurs by the failure mechanism associated with the lowest capacity—that is to say the lowest value of applied loading. Since the other assumed mechanisms produce equal or larger capacities, they may overestimate the capacity of the slab. Therefore, a yield-line analysis solution may overestimate the actual capacity of the slab unless the failure mechanism selected is the true one. For this reason, the solution is referred to as an upper bound solution. Once the significance of its upper bound solution is understood, the method can be used as an effective design tool. It should be noted, however, for most practical problems the actual yield-line patterns are already known, as shown in Figure 2.32. Therefore, gross overestimation of loads is unlikely. For unusual geometries or loadings, several yield-line patterns with small variations may occur. The one which results in the lowest capacity should be selected for design.

A distinct advantage of this method is that solutions are possible for any shape of a slab whereas most other approaches, other than the finite element method, are applicable only to well-defined regular shapes. The engineers can with ease find the moment capacity for any conceivable shape



**FIGURE 2.32** Yield-line patterns. (a) Simply supported slab with uniformly distributed load. (b) Same as (a) but with built-in edges. (c) Equilateral, triangular simply supported slab with uniformly distributed load. (d) same as (b) but with built-in edges.



**FIGURE 2.33** Yield-line analysis of simply supported square slab: (a) yield lines and (b) yield-line rotations.

such as a triangular-, rectangular-, trapezoidal-, and circular-shaped slabs. The only requirement is that the yield-line mechanism be known or predictable. As stated previously, since most failure patterns are identifiable, solutions can be readily obtained.

### 2.3.4.2 Yield-Line Analysis of a Simply Supported Square Slab

**Given:** A 9 in. thick two-way, simply supported square slab spanning 20 ft. See Figure 2.33. The slab is reinforced with #8 @ 12 each way at the bottom. Using the method of virtual work, determine the ultimate uniform load capacity  $W_u$  of the slab. Assume an effective depth  $d = 7.75$  in.,  $f_y = 60,000$  psi, and  $f'_c = 5,000$  psi.

**Solution:** The location and orientation of the positive yield lines are evident for the slab. There are no negative yield lines adjacent to supports because the slab is simply supported. The terms positive yield line and negative yield line are used to distinguish between those associated with tension at the bottom and tension at the top of the slab, respectively.

### External Work

A unit vertical deflection is given to the center of slab at O. From Figure 2.33, the displacement at the centroid of the typical panel A is equal to  $1/3$  units. The external work done by the load on panel A (and for that matter also on panels B, C, and D) is

$$W_u \times \frac{1}{2} \times 20 \times 10 \times \frac{1}{3} = 33.33 W_u$$

$$\text{Total for panels A, B, C, and D} = 4 \times 33.3 W_u = 133.33 W_u$$

### Internal Work

Consider the diagonal yield line AO. Its length is  $\ell = L/2 \cos \theta$ , where  $L = 20$  ft.

In our example,  $\theta = 45^\circ$ . Therefore  $\ell = L/2 \cos 45 = 14.14$  ft.

As is shown in Figure 2.33, the rotation of yield line AO is

$$\theta = \theta_1 + \theta_2. \text{ Since } \theta_1 = \theta_2, \theta = 2\theta_1$$

$$\text{The rotation } \theta_1 = \frac{\delta \times \sqrt{2}}{L} = \theta_2$$

$$\theta = \frac{2\sqrt{2} \times \delta}{L}$$

which for the example problem for a unit displacement (i.e.,  $\delta = 1$ ) is

$$\theta = \frac{2\sqrt{2}}{20} = 0.141 \text{ rad}$$

### Calculate the Ultimate Moment Capacity, $M_u$

Using the formula

$$M_u = A_s \times 4 \times d = 0.79 \times 4 \times 7.75 = 24.49 \text{ kip-ft/ft}$$

$$\text{Internal work} = M_u \theta = 24.49 \times 0.141 = 3.453$$

$$M_u \text{ for yield line AO} = 3.453 \times 14.14 = 48.827 \text{ kip-ft}$$

$$M_u \text{ for the entire slab} = 4 \times 48.827 = 195.3 \text{ kip-ft}$$

### Equate External Work to Internal Work

$$133.33 W_u = 195.3$$

$$W_u = 195.3/133.33 = 1.465 \text{ kip/ft}^2$$

#### 2.3.4.3 Skewed Yield Lines

Oftentimes yield lines will form at an angle to the direction established by the reinforcement. For yield-line analysis, it is necessary to calculate the resisting moment, per unit length along such skewed yield lines. This requires calculation of contribution to resistance from each of the two sets of reinforcement, typically normal to each other. It can be shown, the resisting moment per unit length of a yield line, skewed at an angle  $\alpha$ , is equal to

$$M_\alpha = M_x \cos^2 \alpha + M_y \sin^2 \alpha$$

where

- $M_\alpha$  is the yield moment along the  $\alpha$ -axis
- $M_x$  is the yield moment along the  $x$ -axis
- $M_y$  is the yield moment along the  $y$ -axis

Observe that for the special case of a slab with the same reinforcement in each direction

$$M_\alpha = M_y = M$$

resulting in

$$M_\alpha = M (\cos^2 \alpha + \sin^2 \alpha) = M$$

This in fact, was the case in the previous example.

#### 2.3.4.4 Limitations of Yield-Line Method

In using this method, it must be borne in mind that the analysis is predicted on the assumption that adequate rotation capacity exists at the yield lines. If this is not the case, it is likely that the required rotation will exceed the available rotation capacity leading to premature failure. However, in general, building slabs are lightly reinforced and will have adequate rotation capacity to attain loads predicted by yield-line analysis. It should also be kept in mind that the yield-line analysis is based only on the moment capacity of the slab. It is presumed that earlier failures will not occur due to bond, shear, or other causes. Although yield-line analysis gives no indication on deflections, stresses, or severity of cracking under service loads, it is an excellent tool for justifying moment capacity of existing slabs that are otherwise satisfactory under service load conditions.

#### 2.3.5 DEEP BEAMS

Deep beams are members loaded on one face and supported on the opposite face so that compression struts can develop between the loads and line supports, and have either of the following:

1. The clear span,  $\ell_n$ , is less than or equal to four times the overall depth of beam
2. Concentrated loads occur very near the supports (within twice the member depth from the face of the support)

There are two choices for designing deep beams: (1) by taking into account nonlinear distribution of strain or (2) by using the strut-and-tie models as given in ACI 318.08 Appendix A.

Some of the design requirements are

1. The nominal shear strength,  $V_n$ , shall not exceed  $10\sqrt{f'_c} b_w d$ .
2. The area of shear reinforcement,  $A_v$ , shall not be less than  $0.0025 b_w s$ . The spacing,  $s$ , shall not exceed  $d/5$  or 12 in.
3. The area of shear reinforcement,  $A_{vh}$ , parallel to the flexural tension reinforcement shall not be less than  $0.0015 b_w s_2$ . The spacing  $s_2$  shall not exceed  $d/5$  or 12 in.

In lieu of the aforementioned minimum shear reinforcement, we are permitted to provide reinforcement that satisfies the requirement of strut-and-tie models.

4. The minimum area of flexural tension reinforcement,  $A_{s,min}$  shall not be less than

$$A_{s,min} = 3 \sqrt{\frac{f'_c}{f_y}} b_w d \quad \text{or} \quad 200 \frac{b_w d}{f_y}$$

5. Where the overall depth,  $h$ , exceeds 36 in., longitudinal skin reinforcement is required to control cracking in the web near the tension zone.

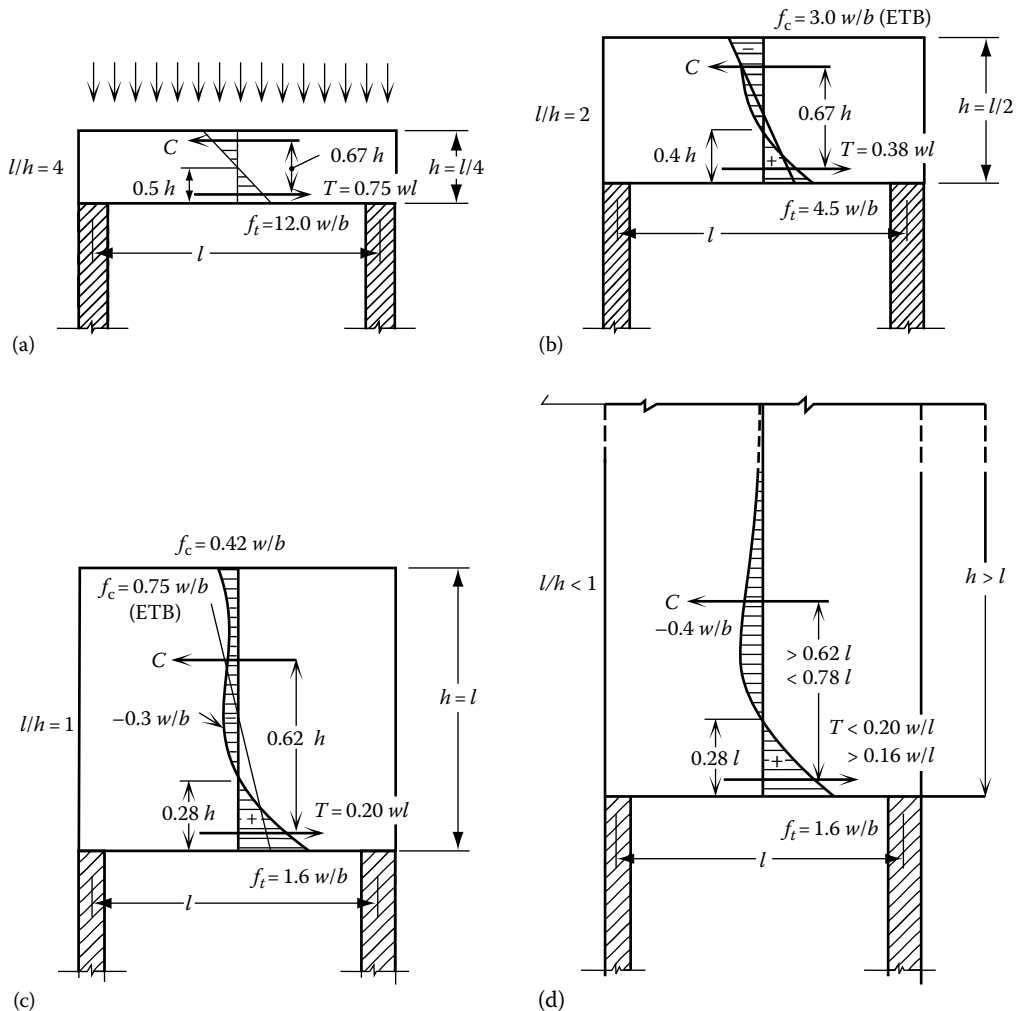


The ACI 318-08 like its predecessors does not contain detailed requirements for designing deep beams for flexure except that nonlinearity of strain distribution and lateral buckling is to be considered.

As mentioned previously, when the span-to-depth ratio of a beam is less than or equal to four, it is customary to define these beams as deep. The traditional principles of stress analysis using the engineers bending theory, ETB are neither suitable nor adequate.

The stresses in homogeneous deep beams before cracking can be determined using sophisticated analysis such as a finite element solution. These analyses indicate that the smaller the span/depth ratio, the more pronounced the deviation of the stress from the ETB. As an example, Figure 2.34 shows the distribution of bending stresses at midspan of simply supported beams having different span-depth ( $l/h$ ) ratios, when carrying a uniformly distributed load. It is noted from Figure 2.34 that for  $l/h = 1$ , the tensile stresses are more than twice the intensity obtained from the simple building theory.

Considering again the square beam ( $l/h = 1.0$ ), two observations may be made from Figure 2.34. First, the tension zone at the bottom of the beam is relatively small, approximately equal to  $0.25 \ell$ , suggesting that the tension reinforcement should be placed in this area. Second, the tensile force, and hence the reinforcement that is of primary interest, could be computed by using the internal



**FIGURE 2.34** Stress distribution in deep beams: (a)  $l/h = 4$ , (b)  $l/h = 2$ , (c)  $l/h = 1$ , and (d)  $l/h < 1.0$ .

lever arm,  $jd = 0.62h$ . It is interesting that this is approximately the same for all beams; that is, it is not affected greatly by the span/depth ratio,  $l/h$ .

### 2.3.6 STRUT-AND-TIE METHOD

The strut-and-tie method is a simple and intuitive method based on static equilibrium.

The method is typically applied to structural elements in which the assumption of simple bending theory do not strictly apply. One such assumption is that in a flexural member such as a beam, plane sections before bending remain plane after bending. This assumption is valid at all cross sections of the beam except at the immediate proximity to applied loads and reactions. An example of a member in which plane sections do not remain plain is a beam with clear span,  $l_n$ , equal to or less than four times the over all member depth. Therefore, instead of using the simple bending theory, we use a more appropriate approach such as a truss analogy to define a load path. The analysis begins by assuming an internal load path, consisting of appropriate struts and ties within the member being designed, and then designing the elements for the resulting forces.

Structural elements in a typical load path consist of a truss model that has

1. Inclined and vertical compressive struts
2. Longitudinal tension members also called ties
3. Node regions at all joints of chords, struts, and ties

The sizes of the members and joint regions in the truss model are chosen so that the computed demand forces in the struts, ties, and the nodes due to factored loads will not exceed respective design capacity. It should be kept in mind that for the mobilization of the tensile reinforcement, the tension ties shall be effectively anchored to transfer the required tension to the truss node regions.

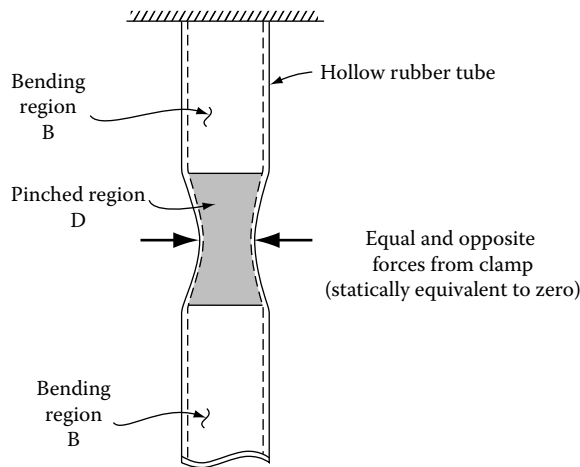
The paramount requirement for the safety of a design using the strut-and ties method is that the member must have adequate ductility to enable redistribution of actions to the designated load path.

It is worth noting that for any given condition, more than one truss configuration can be selected to resist the applied loading. While one truss configuration may be more efficient than another from the design standpoint, it is sufficient to demonstrate that the chosen truss can sustain the load, and has adequate ductility to mobilize it.

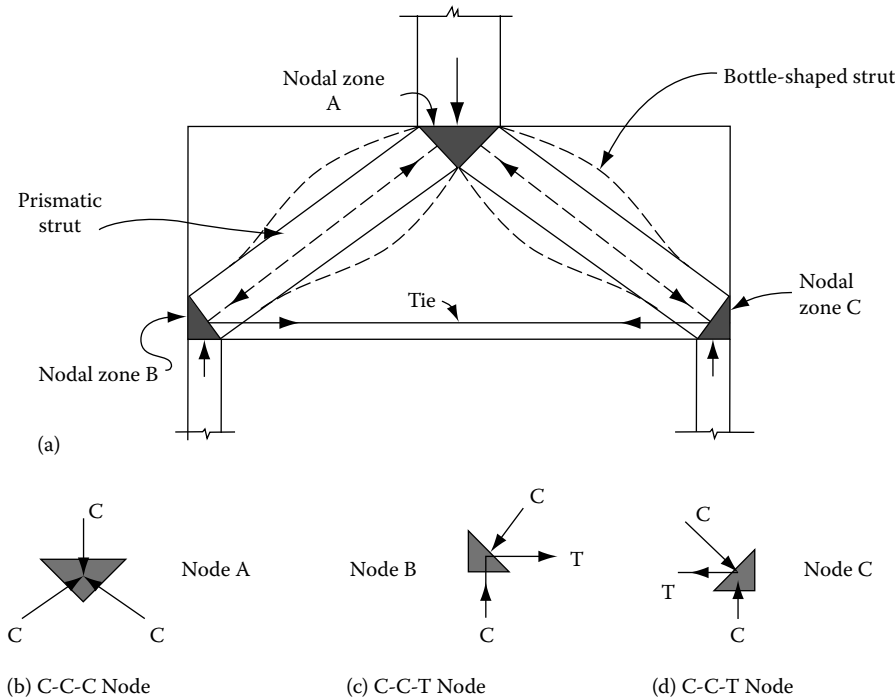
Before further discussing the truss-and-tie model, it is perhaps instructive to briefly dwell on the so-called-*Saint-Venant's Principle* on which the analysis is based. In discussing the elementary theory of simple bending, commonly referred to as engineers theory of building, ETB, French elastician Saint-Venant (1797–1886) formulates the principle which now carries his name. He states that the stress distribution given by the elementary bending theory is correct only when the external forces are applied to the member in the same manner as the bending stresses are distributed over intermediate cross sections. He further states the solutions obtained from the ETB will be accurate enough in most cross sections except at the immediate vicinity of the applied forces and reactions.

To get an insight into this principle, consider Figure 2.35 that shows one of Saint-Venant's examples. The two equal and opposite forces exerted by the clamp produce only a local deformation. Hence stresses are produced only in the vicinity of clip, and at a distance sufficiently far away from the clip, the tube is practically unaffected. The critical distance over which the local effects occur is typically taken equal to one to two times the characteristic dimension of the member.

The strut-and-tie method of analysis for the design of deep beams given in ACI 318-08, Appendix A is based on the Saint-Venant's principle described above. The *pinched* region of tube shown in Figure 2.35 is similar to the *Discontinuity region* described in the ACI 318. This region is assumed to extend no more than one-member depth from the point of application of loads and reactions. *The Bending regions, B* referenced in the ACI on the other hand are those that are sufficiently far away from the regions of discontinuity where the ETB may be applied without significant errors.



**FIGURE 2.35** Example of Saint-Venant’s principle: pinched region is similar to the discontinuity, D, region (ACI 318-08, Appendix A). Regions away from D are bending, B, regions.



**FIGURE 2.36** Strut-and-tie terminology: (a) strut-and-tie model, (b) C-C-C node resisting three compressive forces, (c) and (d) C-C-T nodes resisting two compressive, and one tensile force.

Certain terms unique to strut-an-tie models are defined in the ACI 318. The first term *nodal zone*, shown in Figure 2.36, describes the volume of concrete around a node that is assumed to transfer the strut-and-tie axial forces through the nodes. The second term *strut* is a compression member while the third term *tie* refers to a member carrying tension.

The design methodology is quite similar to what we typically use in the ultimate design of concrete members: we compare the calculated internal forces,  $F_u$ , in the struts, ties, and nodal zones to the usable capacity  $\phi F_u$ , and declare the design to be satisfactory if

$$\phi F_u \geq F_u$$

The design of deep beams using strut-and-tie models is essentially by a trial-and-error method. Hence it is well suited for an interactive spread sheet application.

The design steps are

1. Assume the center of gravity of the lower tension chord AC is located at a certain distance above the bottom of beam. A good value to use is  $0.05D$  where  $D$  is the beam depth.
2. Similarly assume the center of gravity of the top node B at a distance of  $0.05D$  below the top of the beam.
3. The above assumptions permit us to define the geometry and hence the flow of forces, tension in the bottom chord AC, and compression in the struts AB and BC. The resulting forces denoted by  $F_u$  are the factored forces in the strut, tie, or on the face of node.
4. Compute the nominal strength,  $F_n$ , of the strut, tie, or nodal zone using the following equations:

$$\text{Struts: } f_{ce} = 0.85\beta_s f'_c$$

where

$\beta_s = 1.0$  for prismatic struts

$\beta_s = 0.75$  for bottle-shaped struts with reinforcements

$\beta_s = 0.60\lambda$  for bottle-shaped struts without reinforcement.  $\lambda$  is the reduction factor for lightweight concrete (See ACI Section 8.6.1)

$$\text{Ties: } F_{nt} = A_{ts} F_y \text{ (for non-prestressed ties)}$$

Note that tension reinforcement shall be anchored by straight bar development, standard hooks, or mechanical devices.

$$\text{Nodal zones: } F_{nn} = f_{ce} A_{nz}$$

where

$F_{nn}$  is the nominal compression of a nodal zone

$A_{nz}$  is the area of the nodal face on which  $F_u$  acts

$f_{ce}$  is the effective compressive stress on a face of a modal zone  $= 0.85 \beta_n f'_c$

where

$\beta_n = 1.0$  for a C-C-C node

$= 0.8$  for a C-C-T node

$= 0.60$  for C-C-T node

### Design Example

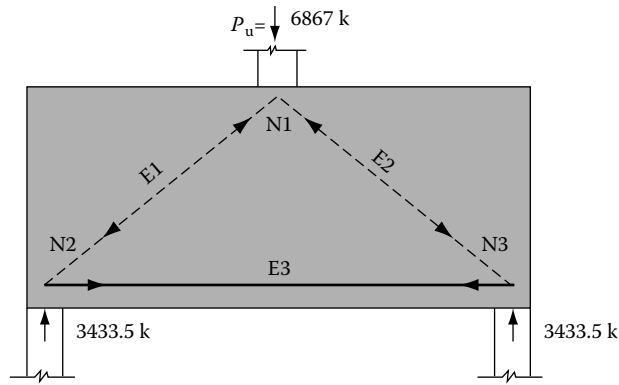
**Given:** A single span deep beam, 31 ft 10 in. long and 15 ft deep with a carried column at the center of span. The ultimate load including the weight of beam is 6867 kip. See Figure 2.37.

**Required:** Design of transfer beam using strut-and-tie method.

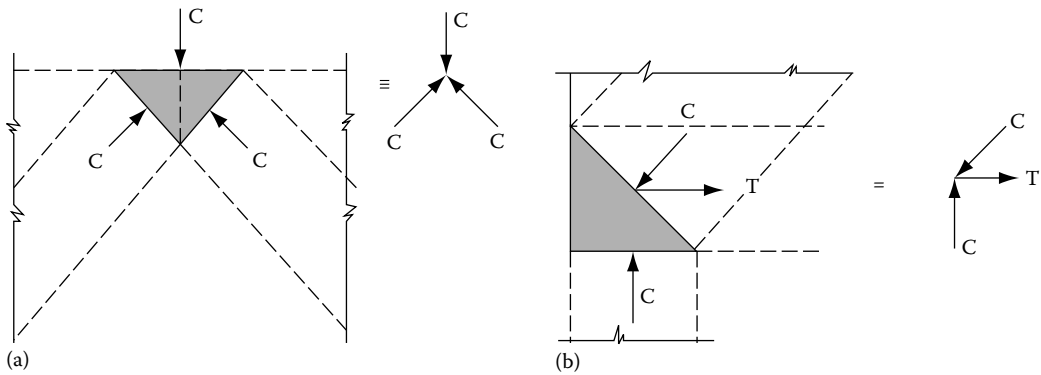
**Solution:**

- Step 1 Select a strut-and-tie model consisting of two struts, one tie, and three nodal zones. Compute the reactions at A and B after adding the ultimate dead load of the beam to the column load. In our case, total load  $P_u = 6867$  kips as given in the statement of the problem. Therefore,

$$R_A = R_B = \frac{6867}{2} = 3433.5 \text{ kip}$$



**FIGURE 2.37** Strut-and-tie model: Node and element identification.



**FIGURE 2.38** Strut-and-tie model: (a) C-C-C node and (b) C-C-T node.

Step 2 For the first trial, assume the height  $h_b$  of the bottom nodes A and B, and the height  $h_t$  of the top node C, to be the same, at  $0.05D = 0.05 \times 15 \text{ ft} = 0.75 \text{ ft} = 9 \text{ in.}$

Step 3 Effective compression strength,  $\phi f_{cu}$ , for the nodal zones.

Using the ACI 318 nomenclature, nodes B and C are classified as C-C-T nodes meaning that the nodes resist two compressive forces, and one tensile force. The node at the top, below the carried column, is referred to as a C-C-C node meaning all forces resisted by this node are compressive. (see Figure 2.38).

For the C-C-T nodes A and C, the effective compressive stress,  $f_{ce}$ , from ACI Section A.5.2 is

$$f_{ce} = 0.85\beta_n f'_c$$

In this equation,  $\beta_n$  is a penalty factor that measures how well the tension member (if any) is anchored at a node. If the node is a C-C-C node (meaning no ties), there is no penalty. Hence  $\beta_n = 1.0$ . On the other extreme, if the node is a C-T-T node,  $\beta_n = 0.6$  and if it is a C-C-T node,  $\beta_n$  is the average of the two  $= 1.0 + 0.6/2 = 0.8$ .

Referring to nodes A and C,

$$f_{ce} = 0.85 \times 0.8 \times f'_c = 0.68 f'_c = 0.68 \times 10,000 \text{ psi} = 6.8 \text{ ksi}$$

$$\text{For node B } f_{ce} = 0.85 \times 1.0 \times f'_c = 8500 \text{ psi} = 8.5 \text{ ksi}$$

Step 4 Compute effective compression strengths for struts AB and BC.

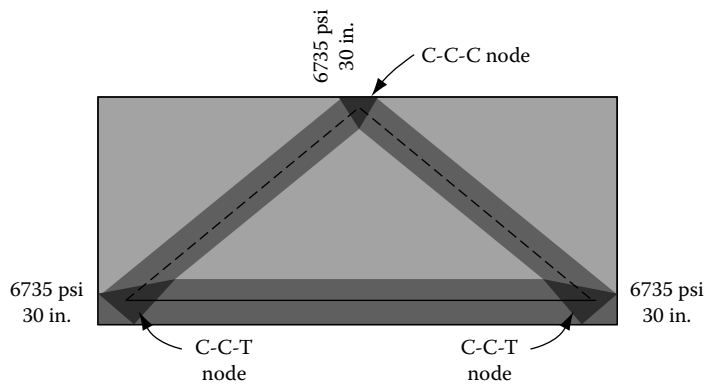
From ACI 318-08 Section A.3.2:

$$f_{ce} = 0.85\beta_s f'_c$$

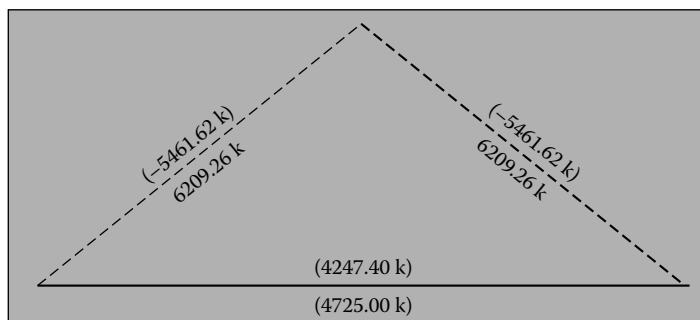
For a strut of uniform section,  $\beta = 1.0$ .

Therefore,  $f_{ce} = 0.85 \times 1.0 \times 10,000 = 8500 \text{ psi} = 8.5 \text{ ksi}$

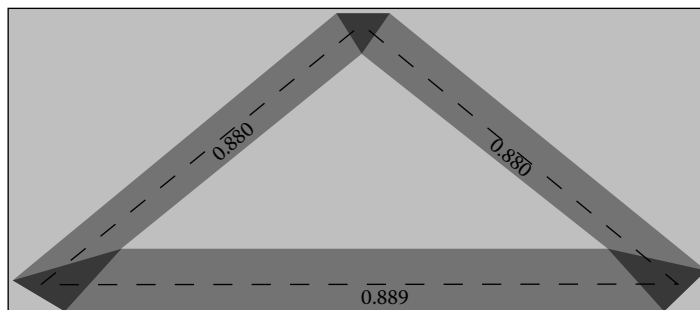
Schematic results obtained from a spreadsheet for the transfer beam shown in Figure 2.37 are summarized in Figures 2.39 through 2.42. A practical reinforcement layout for the transfer girder and adjacent beams is shown in Figure 2.43.



**FIGURE 2.39** Member stress limits and effective widths.



**FIGURE 2.40** Factored forces and design strengths.



**FIGURE 2.41** Stress ratios.

Struts						
Strut ID	Demand $F_u$ (k)	$\beta_s$	$\phi$	$\phi f'_c = \phi(0.85)\beta_s f'_c$ (psi)	Effective Width (in.)	Effective Thickness Scale Factor (in.)
E1	-5461.62	0.750	0.750	4781.	27.06	1.000
E2	-5461.62	0.750	0.750	4781.	27.06	1.000
E4	-6867.00	1.000	0.750	6375.	30.00	1.000
E5	-3433.50	1.000	0.750	6375.	30.00	1.000
E6	-3433.50	1.000	0.750	6375.	30.00	1.000
Ties						
Tie ID	$F_u$ (k)	Required $A_s$ (in. <sup>2</sup> )	Provided $A_s$ (in. <sup>2</sup> )	$\phi$	$\phi F_{ts}$ (k)	
E3	4247.40	75.51	84.00	0.750	4725.00	
Nodes						
Node ID	Node Face	Demand $F_u$ (k)	$\beta_n$	$\phi$	$\phi f_c = \phi(0.85)\beta_n f_c$ (psi)	Effective Width (in.)
N1	E1	-5461.62	1.000	0.750	6375.	27.06
N1	E2	-5461.62	1.000	0.750	6375.	27.06
N1	E4	-6867.00	1.000	0.750	6375.	30.00
N2	E1	-5461.62	0.800	0.750	5100.	27.06
N2	E3	4247.40	0.800	0.750	5100.	36.00
N2	E5	-3433.50	0.800	0.750	5100.	30.00
N3	E2	-5461.62	0.800	0.750	5100.	27.06
N3	E3	4247.40	0.800	0.750	5100.	36.00
N3	E6	-3433.50	0.800	0.750	5100.	30.00
N4	E4	-6867.00	1.000	0.750	6375.	30.00
N5	E5	-3433.50	0.800	0.750	5100.	30.00
N6	E6	-3433.50	0.800	0.750	5100.	30.00
						Capacity $\phi F_{nn}$ (k)
						8279.01
						8279.01
						9180.00
						6623.21
						8812.80
						7344.00
						6623.21
						8812.80
						7344.00
						9180.00
						7344.00
						7344.00

**FIGURE 2.42** Design Summary. *Note:* Struts E4, E5, and E6 are transfer column and supporting columns. Nodes N4, N5, and N6 are at the face of transfer column and supporting columns.

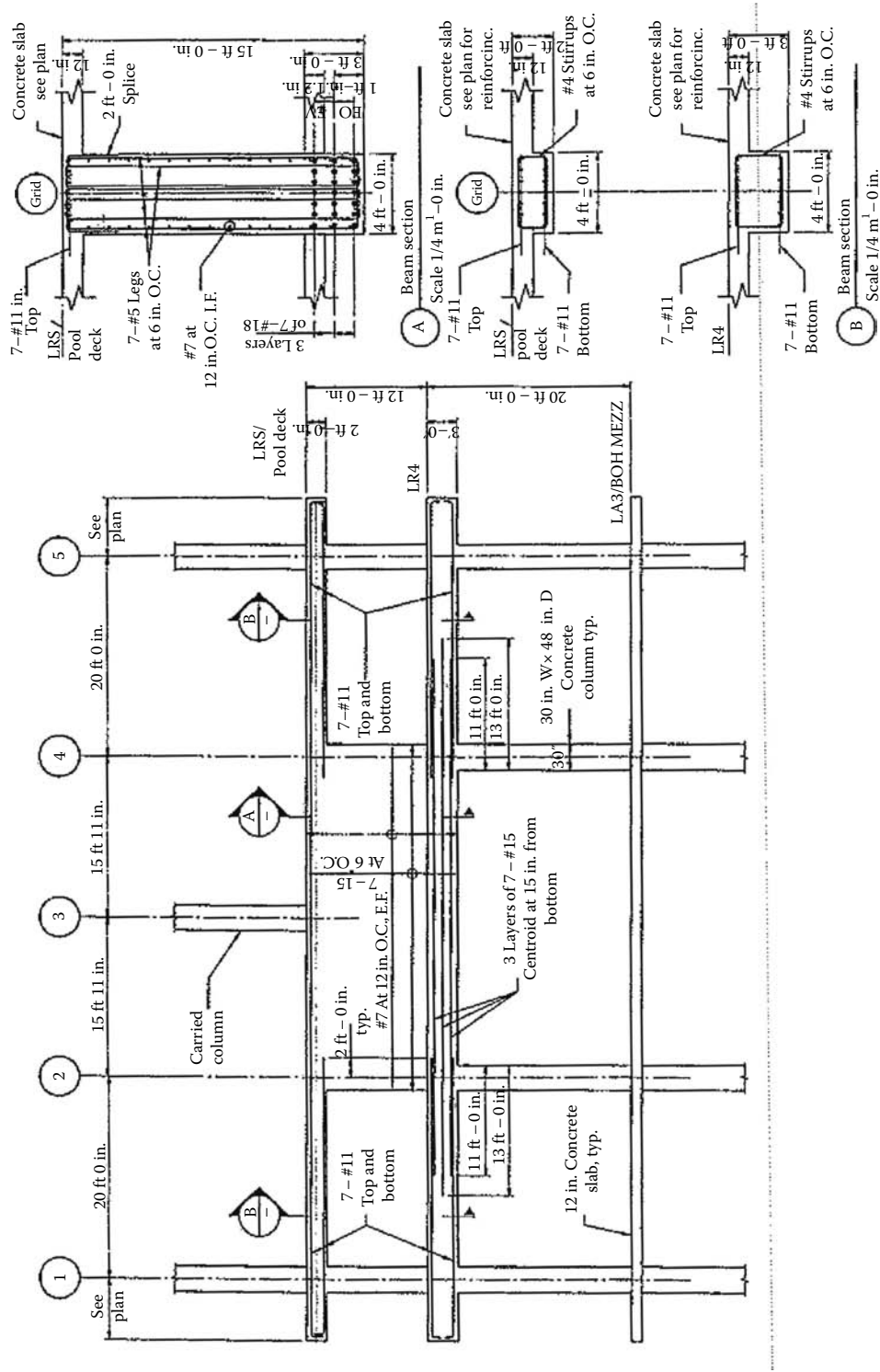


FIGURE 2.43 Transfer girder-schematic reinforcement.



## 2.4 ONE-WAY SLAB, T-BEAMS, AND TWO-WAY SLABS: HAND CALCULATIONS

As stated previously, nowadays it is hard to come by a structural engineering office that uses hand calculations for design of floor systems. However, in fulfilling the stated objective of this work, namely to promote understanding of basic behavior of structural systems, we will indulge in some hand calculations. These will include

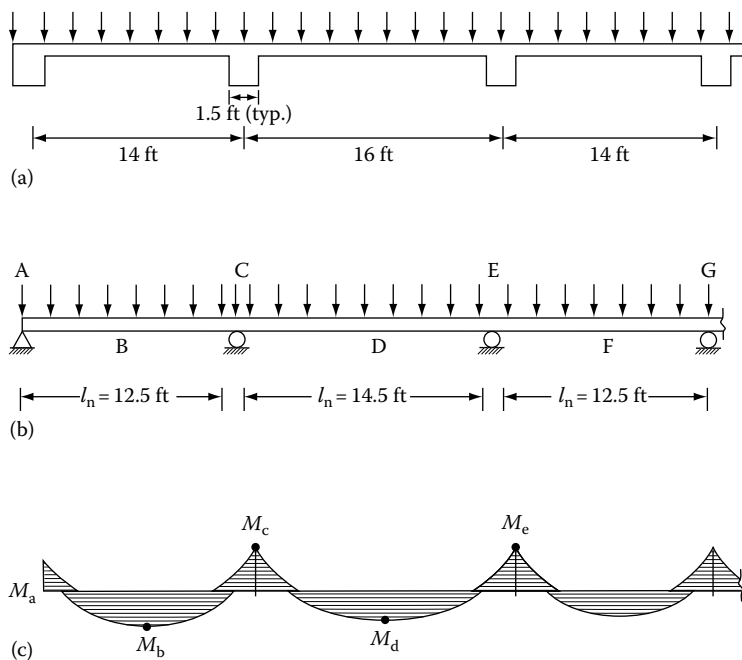
1. One-way slabs
2. T-beams
3. Two-way slabs

### 2.4.1 ONE-WAY SLAB; ANALYSIS BY ACI 318-05 PROVISIONS

One-way slabs are discussed here to illustrate the simplifications commonly made in a design office to analyze these systems.

Figure 2.44 shows a uniformly loaded floor slab with intermediate beams that divide the slab into a series of one-way slabs. If a typical 1 ft width of slab is cut out as a free body in the longitudinal direction, it is evident that the slab will bend with a positive curvature between the supporting beams, and a negative curvature at the supporting beams. The deflected shape is similar to that of a continuous beam spanning across transverse girders, which act as simple supports. The assumption of simple support neglects the torsional stiffness of the beams supporting the slab. If the distance between the beams is the same, and if the slabs carry approximately the same load, the torsional stiffness of the beams has little influence on the moments in the slab.

However, the slab twists the exterior beams, which are loaded from one side only. The resistance to the end rotation of the slab offered by the exterior beam is dependent on the torsional stiffness of

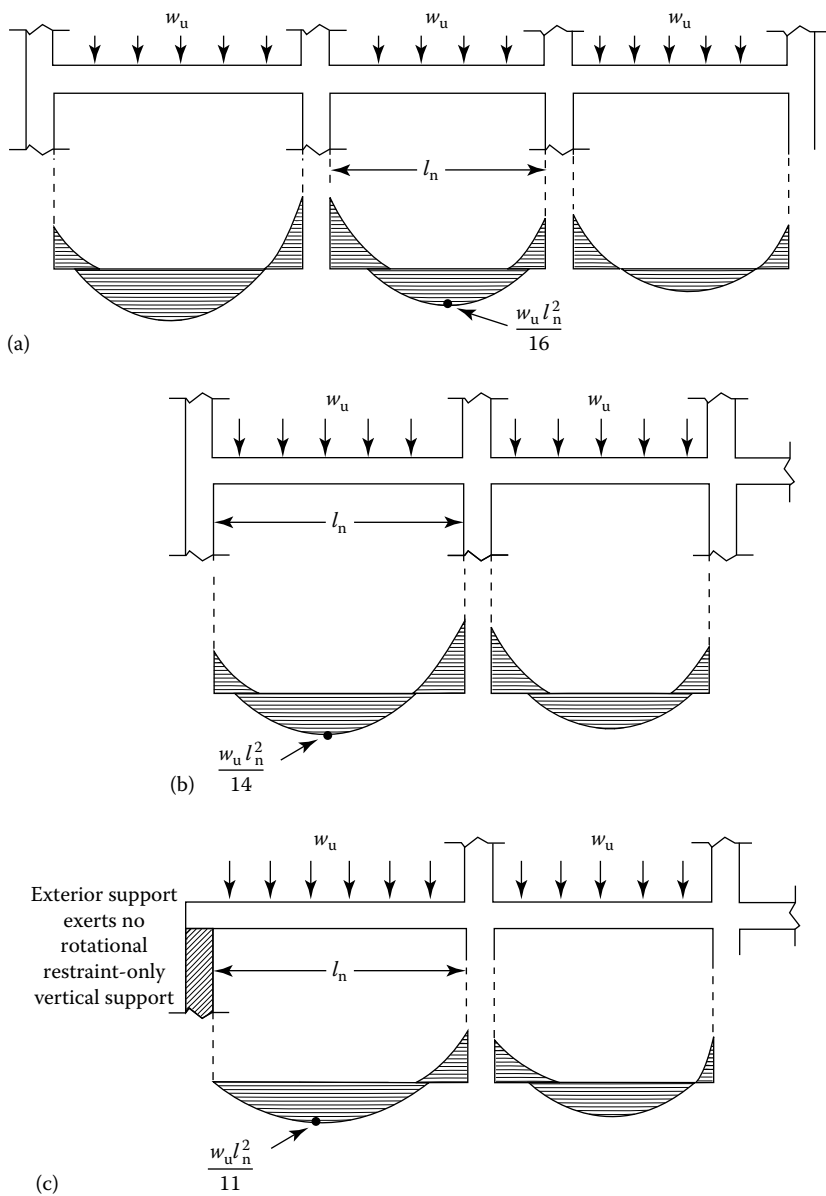


**FIGURE 2.44** One-way slab example: (a) typical 1 ft strip; (b) slab modeled as a continuous beam; and (c) design moments.

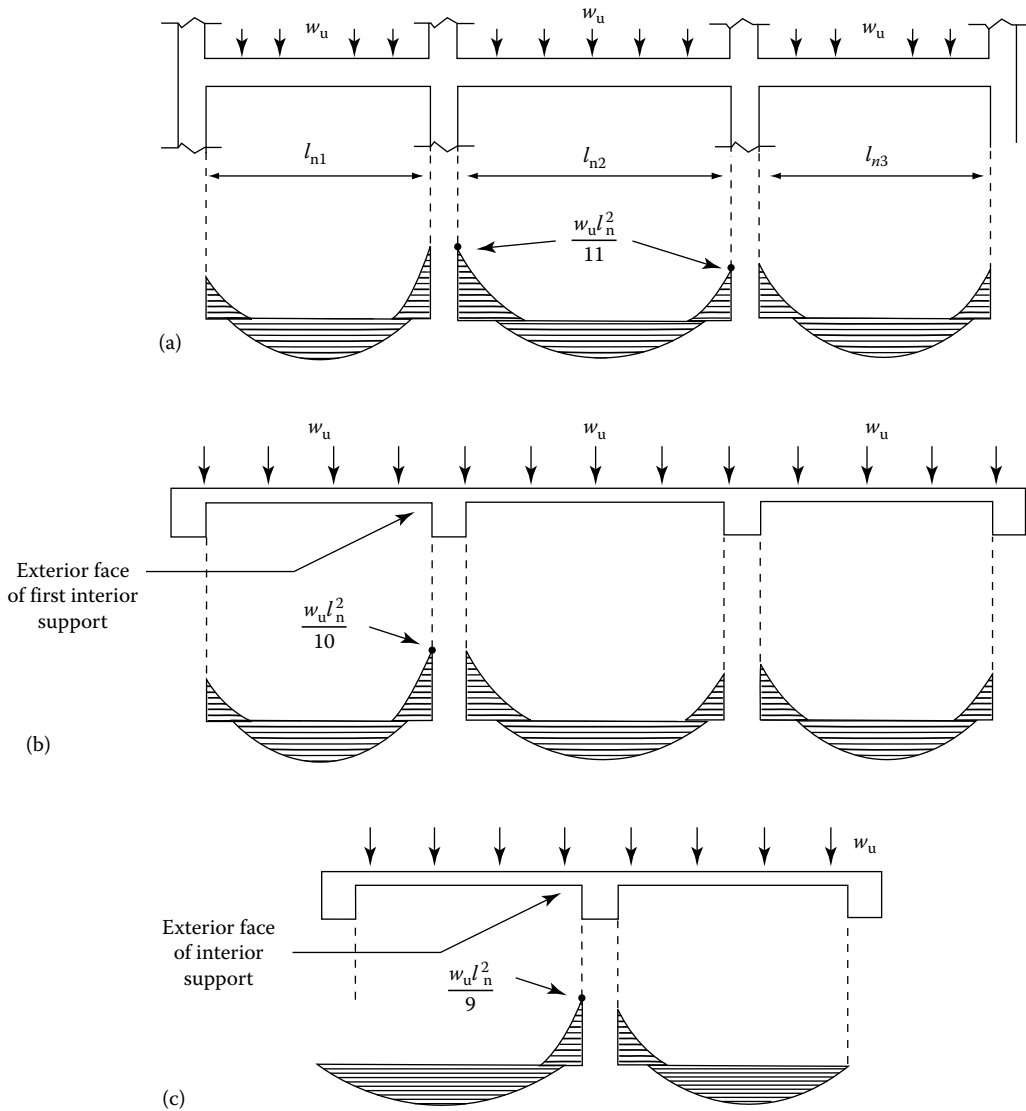
the beam. If the beam is small and its torsional stiffness low, a pin support may be assumed at the exterior edge of slab. On the other hand, if the exterior beam is large with a high torsional rigidity, it will apply a significant restraining moment to the slab. The beam, in turn, will be subjected to a torsional moment that must be considered in design.

Analysis by the ACI 318 method is limited to structures in which (1) the span lengths are approximately the same (with the maximum span difference between adjacent spans no more than 20%); (2) the loads are uniformly distributed; and (3) the live load does not exceed three times the dead load.

Before we procede with the design of one-way slab, it is useful to catalog the ACI design coefficients for positive and negative design moments as illustrated in Figures 2.45 and 2.46.



**FIGURE 2.45** ACI coefficients for positive moments: (a) interior span, (b) exterior span, discontinuous end integral with supports, and (c) exterior span, discontinuous end unrestrained.



**FIGURE 2.46** ACI coefficients for negative moments: (a) at interior supports; (b) at exterior face of first interior support, more than two spans; and (c) at exterior face of first interior support, two spans.

Observe that  $l_n$  equals the clear span for positive moment and shear, and the average of adjacent clear spans for negative moment.

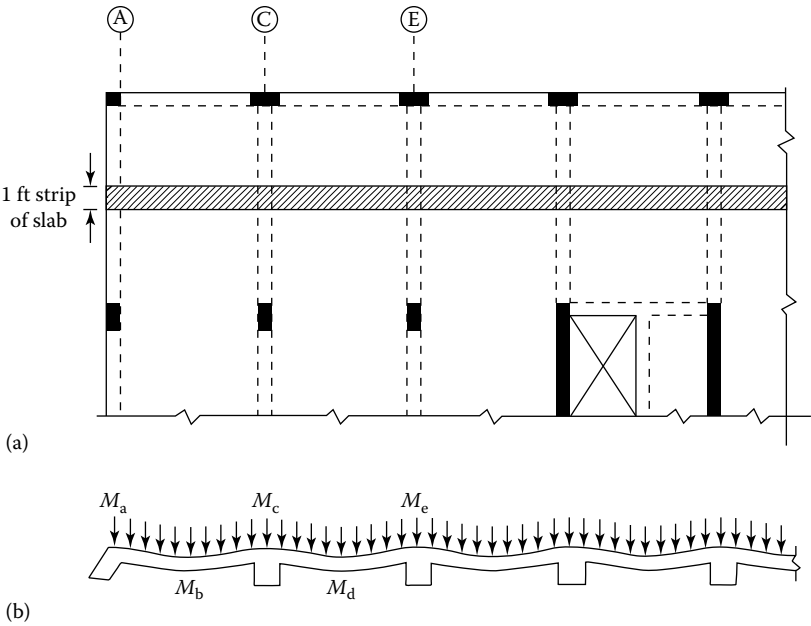
**Example:** One-way mild steel reinforced slab.

**Given:** A one-way continuous slab as shown in Figures 2.44 and 2.47.

$$f'_c = 4 \text{ ksi}, \quad f_y = 60 \text{ ksi}$$

Ultimate load = 0.32 kip/ft

**Required:** Flexural reinforcement design for interior span between grids C and E.



**FIGURE 2.47** Design example, one-way slab: (a) partial floor plan and (b) section. See Figure 2.44 for dimensions and loading.

**TABLE 2.1**  
**Minimum Thickness of Beams or One-Way Slabs Unless Deflections Are Computed**

	Minimum Thickness $h$			
	Simply Supported	One End Continuous	Both Ends Continuous	Cantilever
Solid one-way slabs	$l/20$	$l/24$	$l/28$	$l/10$
Beams or ribbed one-way slabs	$l/16$	$l/18.5$	$l/21$	$l/8$

*Source:* From ACI 318-08 Table 9.5a.

*Note:* Members not supporting or attached to partitions or other construction are likely to be damaged by large deflections. Span length  $l$  in inches. Values in the table apply to normal-weight concrete reinforced with steel of  $f_y = 60,000 \text{ lb/in.}^2$ . For lightweight concrete with a unit weight between 90 and 120  $\text{lb/ft}^3$ , multiply the table values by 1.65–0.005 $w$ , respectively, but by not less than 1.09; the unit weight  $w$  is in  $\text{lb/ft}^3$ . For reinforcement having a yield point other than 60,000  $\text{lb/in.}^2$ , multiply the table values by 0.4 +  $f_y/100,000$  with  $f_y$  in  $\text{lb/in.}^2$ .

**Solution:** Use Table 2.1 to determine the minimum slab thickness required to satisfy deflection limitations. Using  $l$  = center-to-center span = 16 ft,

$$h_{\min} = \frac{l}{28} = \frac{12 \times 16}{28} = 6.86 \text{ in.} \quad \text{Use } 6\frac{1}{2} \text{ in. (165 mm).}$$

Analyze a 1 ft width of slab as a continuous beam using ACI coefficients to establish design moments for positive and negative steel. Using a clear span  $l_n = 12.5 \text{ ft}$  for the first bay

$$M_a = \frac{w_u l_n^2}{24} = \frac{0.32 \times 12.5^2}{24} = 2.08 \text{ kip-ft (-ve)}$$

$$M_b = \frac{w_u l_n^2}{11} = \frac{0.32 \times 12.5^2}{11} = 4.55 \text{ kip-ft (+ve)}$$

$$M_c = \frac{w_u l_n^2}{10} = \frac{0.32 \times 13.5^2}{10} = 5.83 \text{ kip-ft (-ve)}$$

$$M_d = \frac{w_u l_n^2}{16} = \frac{0.32 \times 14.5^2}{16} = 4.21 \text{ kip-ft (+ve)}$$

$$M_e = \frac{w_u l_n^2}{11} = \frac{0.32 \times 14.5^2}{11} = 6.12 \text{ kip-ft (-ve)}$$

Compute reinforcement  $A_s$  per foot width of slab at critical sections. For example, at the second interior support, top steel must carry  $M_e = 6.12$  kip-ft. Note that ACI code requires a minimum of  $\frac{3}{4}$  in. cover for slab steel not exposed to weather or in contact with the ground.

We will use the trial method of determining the area of steel. In this method, the moment of the internal force couple is estimated. Next, the tension force  $T$  is evaluated by equating the applied moment to the internal force couple, that is,

$$M_u = \phi T \times \text{arm}$$

$$T = \frac{M_u}{\phi \times \text{arm}}$$

where

$\phi = 0.9$  for flexure

$M_u$  is the factored moment

To start the procedure, the moment arm is estimated as  $d - a/2$  by assuming a value of  $a = 0.15d$ , where  $d$  is the effective depth. The appropriate area of steel  $A_s$  is computed by dividing  $T$  by  $f_y$ .

To get a more accurate value of  $A_s$ , the components of the internal couple are equated to find a close estimate of the area  $A_c$  of the stress block. The compressive force  $C$  in the stress block is equated to the tension force  $T$ .

$$C = T$$

$$0.85 f'_c A_c = T$$

$$A_c = \frac{T}{0.85 f'_c}$$

Once  $A_c$  has been evaluated, locate the position of  $C$ , which is the centroid of  $A_c$ , and recompute the arm between  $C$  and  $T$ . Using the improved value, find the second estimates of  $T$  and  $A_s$ . Regardless of the initial assumption for the arm, two cycles should be adequate for determining the required steel area.

For the example problem, the effective depth  $d$  for the slab is given by

$$d = h - \left( 0.75 + \frac{d_b}{2} \right) = 6.5 - (0.75 + 0.25) = 5.5 \text{ in.}$$

$$M_u = \phi T (d - a/2)$$

As a first trial, assume  $a = 0.15d = 0.15 \times 5.5 = 0.83$  in.

$$6.12 \times 12 = 0.9T \left( 5.5 - \frac{0.83}{2} \right) = 4.58T$$

$$T = 16.03 \text{ kip}$$

$$A_s = \frac{T}{f_y} = \frac{16.03}{60} = 0.27 \text{ in.}^2/\text{ft}$$

Repeat the procedure using an arm based on an improved value of  $a$ . Equate  $T = C$ :

$$16.03 = 0.85 f'_c A_c = 0.85 \times 4 \times a \times 12$$

$$a = 0.39 \text{ in.}$$

$$\text{Arm} = d - \frac{a}{2} = 5.5 - \frac{0.39}{2} = 5.31 \text{ in.}$$

$$T = \frac{M_u}{\phi \left( d - \frac{a}{2} \right)} = \frac{6.12 \times 12}{0.9 \times 5.31} = 15.37 \text{ kip}$$

$$A_s = \frac{15.37}{60} = 0.26 \text{ in.}^2$$

Check for temperature steel  $= 0.0018 A_g$

$$= 0.0018 \times 6.5 \times 12 = 0.14 \text{ in.}^2/\text{ft} < 0.26 \text{ in.}^2/\text{ft}$$

Determine spacing of slab reinforcement to supply  $0.26 \text{ in.}^2/\text{ft}$ .

$$\text{Using \#4 rebars, } s = \frac{0.20}{0.26} \times 12 \text{ in.} \quad \text{Say, 9 in.}$$

$$\text{Using \#5 rebars, } s = \frac{0.31}{0.26} \times 12 = 14.31 \text{ in.} \quad \text{Say, 14 in.}$$

Use #4 @ 9 top at support  $e$ . Also by ACI code, the maximum spacing of flexural reinforcement should not exceed 18 in. or three times the slab thickness.

9 in.  $< 3$  (6.5 in.) = 19.5 in. 9 in. spacing is OK.

## 2.4.2 T-BEAM DESIGN

### 2.4.2.1 Design for Flexure

**Given:**  $f'_c = 4 \text{ ksi}$ ,  $f_y = 60 \text{ ksi}$

$DL = 2.0 \text{ k/ft}$  (includes the self-weight of beam)

$LL = 1.62 \text{ k/ft}$

$$U = 1.2 \times 2.0 + 1.6 \times 1.62 = 5 \text{ kip-ft}$$

See Figure 2.48 for loads and bending moments. The minimum depth of beam to control deflections from Table 2.1 is

$$h_{\min} = \frac{l}{16} = \frac{30 \times 12}{16} = 22.5 \text{ in.} \quad \text{Use 22.5 in.}$$

Try  $b_w = 18$  in. The width must be adequate to carry shear and allow for proper spacing between reinforcing bars.

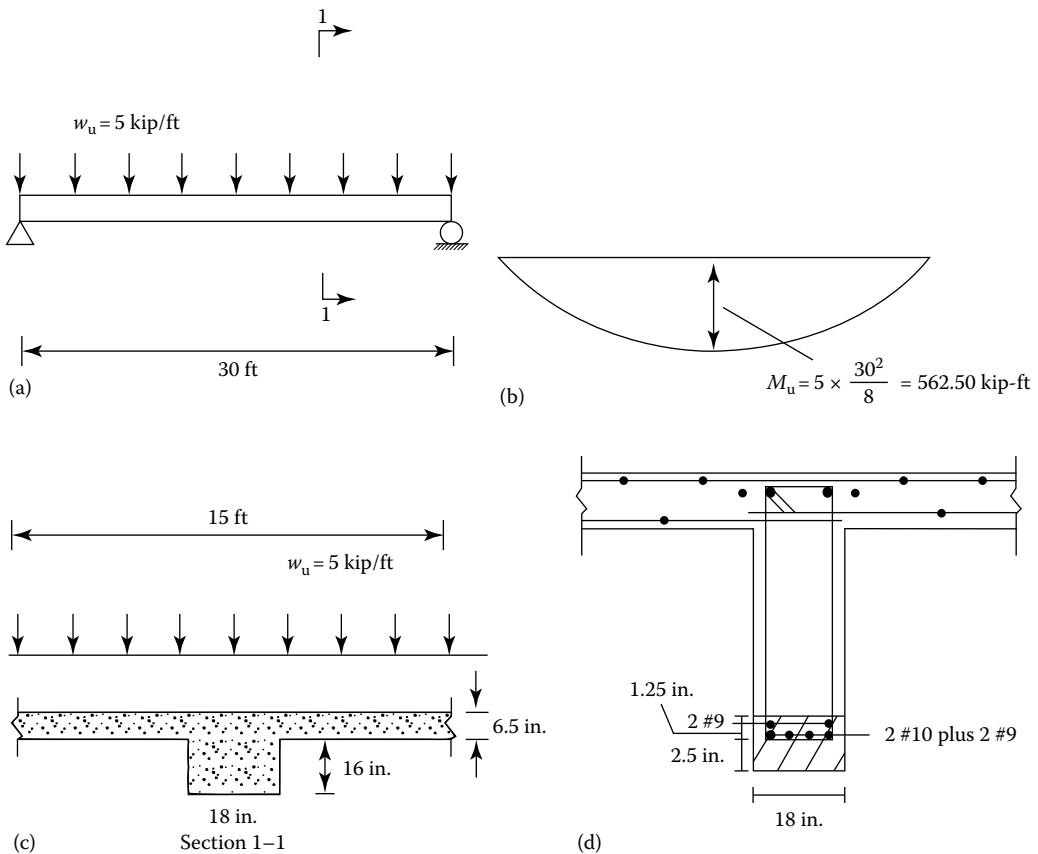
The effective width of the  $T$  beam  $b_{\text{eff}}$  is the smallest of

1. One-fourth the beam span:

$$\frac{30}{4} = 7.5 \text{ ft} = 90 \text{ in.} \quad (\text{controls})$$

2. Eight times the slab thickness on each side of the stem plus the stem thickness:

$$8 \times 6.5 \times 2 + 18 = 122 \text{ in.}$$



**FIGURE 2.48** T-beam design example.

3. Center-to-center spacing of the panel:

$$\frac{(16+14)}{2} \times 12 = 180 \text{ in.}$$

Select the flexural steel  $A_s$  for  $M_n = 562.50 \text{ kip-ft}$  using the trial method.

The effective depth  $d = h - 2.6 = 22.5 - 2.6 = 19.9 \text{ in.}$

$$M_u = \phi T \left( d - \frac{a}{2} \right) \text{ Assume depth of compression block, } a = 0.8 \text{ in.}$$

$$562.50 \times 12 = 0.9T \left( 19.9 - \frac{0.8}{2} \right) = 17.55T$$

$$T = 384.62$$

$$A_s = \frac{T}{f_y} = \frac{384.62}{60} = 6.41 \text{ in.}^2$$

Check value of  $a$ .

$$\begin{aligned} 384.62 = T = C &= ab_{\text{eff}}(0.85f_c) \\ &= a(90)(0.85)4 \\ a &= 1.26 \end{aligned}$$

Repeat the procedure using a moment arm based on the improved value of  $a$ .

$$M_u = 562.50 \times 12 = 0.9T \left( 19.9 - \frac{1.26}{2} \right) = 17.34T$$

$$T = \frac{562.50 \times 12}{17.34} = 389.2 \text{ kip}$$

Check value of  $a$ .

$$389.2 = T = C = a \times 90 \times 0.85 \times 4$$

$a = 1.27 \text{ in.}$  Very nearly the same as before. No further iteration is necessary.

$$A_s = \frac{T}{f_y} = \frac{389.2}{60} = 6.49 \text{ in.}^2$$

$$A_{s,\min} = \frac{200b_w d}{f_y} = \frac{200 \times 18 \times 19.9}{60,000} = 1.19 \text{ in.}^2 < 6.49 \text{ in.}^2$$

Since  $6.49 \text{ in.}^2$  controls, use two #10 and four #9 bars.

$$A_{s,\text{provided}} = 6.54 \text{ in.}^2$$



The spacing  $s$  of reinforcement closest to a tension surface must not exceed

$$s = 15 \left( \frac{40,000}{f_s} \right) - 2.5 C_c \quad [\text{ACI 318-05, Equation 10.4}]$$

and may not be greater than  $12 (40,000/f_s)$

where  $C_c$  is the least distance from surface of reinforcement or prestressing steel to the tension face, in inches.

For the example problem, using  $f_s = 36$  ksi and  $C_c = 2.0$  in., the minimum spacing is given by

$$s = \frac{15 \times 40,000}{36,000} - 2.5 \times 2 = 11.67 \text{ in.} \leftarrow \text{controls}$$

$$s \leq 12 \times \frac{40,000}{36,000} = 13.33 \text{ in.}$$

For the example beam, the spacing provided is equal to

$$s = \frac{1}{3} \left[ 18 - 2 \left( 2.0 + 0.5 + \frac{1.128}{2} \right) \right] \cong 5 \text{ in.} < 11.67 \text{ in.} \quad \text{OK}$$

#### 2.4.2.2 Design for Shear

The ACI procedure for shear design is an empirical method based on the assumption that a shear failure occurs on a vertical plane when shear force at that section due to factored service loads exceeds the concrete's fictitious vertical shear strength. The shear stress equation by strength of materials is given by

$$v = \frac{VQ}{Ib}$$

where

$v$  is the shear stress at a cross section under consideration

$V$  is the shear force on the member

$I$  is the moment of inertia of the cross section about centroidal axis

$b$  is the thickness of member at which  $v$  is computed

$Q$  is the moment about centroidal axis of area between section at which  $v$  is computed and outside face of member

This expression is not directly applicable to reinforced concrete beams. The ACI 318-08, therefore, uses a simple equation to calculate the average stress on the cross section,

$$v_c = \frac{V}{b_w d}$$

where

$v_c$  is the nominal shear stress

$V$  is the shear force

$b_w$  is the width of beam web

$d$  is the distance between centroid of tension steel and compression surface

For nonseismic design, ACI 318-05/08 assumes that concrete can carry some shear regardless of the magnitude of the external shearing force and that shear reinforcement must carry the remainder. Thus,

$$V_u \leq \phi V_n = \phi (V_c + V_s)$$

where

$V_u$  is the factored or ultimate shear force

$V_n$  is the nominal shear strength provided by concrete and reinforcement

$V_c$  is the nominal shear strength provided by concrete

$V_s$  is the nominal reinforcement provided by shear reinforcement

$\phi$  is the strength reduction factor = for shear and torsion

$$= 0.75$$

Continuing with the T-beam example:

$$V_u = \phi (V_c + V_s)$$

For the example problem

$$V_u = 70 \text{ kip}$$

$$V_c = 2\sqrt{f'_c}b_wd$$

$$= 2\sqrt{4000}(18 \times 19.9)$$

$$= 45 \text{ kip}$$

$$\phi \frac{V_c}{2} = 0.85 \times \frac{45}{2} = 19.1 \text{ kip}$$

Since  $V_u = 75 \text{ kip}$  exceeds  $\phi V_c/2$ , stirrups are required.

$$V_s = \frac{V_u}{\phi} - V_c$$

$$= \frac{75}{0.85} - 45 = 43.24 \text{ kip}$$

Spacing for two-legged #4 stirrups

$$s = \frac{A_v f_y d}{V_s}$$

$$= \frac{2 \times 0.2 \times 60 \times 19.9}{43.24}$$

$$= 11.04 \text{ in.}$$

Since  $V_s$  is less than  $4\sqrt{f'_c}b_wd = 90 \text{ kip}$ ,

$$s = \frac{d}{2} = \frac{19.9}{2} = 9.9, \text{ say, } 9 \text{ in.}$$

If  $V_s \geq 4\sqrt{f'_c}b_wd$ , the maximum spacing would have been  $d/4$  but not to exceed 12 in.

$$\begin{aligned} A_{v,\min} &= \frac{50b_ws}{f_y} \\ &= \frac{50 \times 18 \times 9}{60,000} \\ &= 0.135 \text{ in.}^2 \end{aligned}$$

$$A_{v,\text{provided}} = 0.4 \text{ in.}^2 > 0.135 \text{ in.}^2$$

Use #4 two-legged stirrups at 9 in. near the supports. See Figure 2.49 for placement of shear reinforcement.

Stirrups are not required in beam regions where  $V_u \leq \frac{\phi V_c}{2} = 0.75 \times \frac{45}{2} = 16.87 \text{ kip}$ . This occurs at a distance  $x$  from the center line of beam at each side. Distance  $x$  is given by

$$\begin{aligned} \frac{66.7}{13.34} &= \frac{16.67}{x} \\ x &= 3.33 \text{ ft} \end{aligned}$$

Therefore, no shear reinforcement is required within the middle  $(3.33 \times 2 = 6.66 \text{ ft})$ . However, it is a good practice to provide at least some shear reinforcement, even when not required by calculations.

For the example problem, we use conservatively #4 at  $(d/2) = (19.9/2) \cong 9 \text{ in.}$  for the entire span.

Observe that for perimeter beams, ACI 318-05 Section 7.13.2 requires the stirrups to have 135° hooks around continuous bars. As an alternate, one-piece closed stirrups may be used.

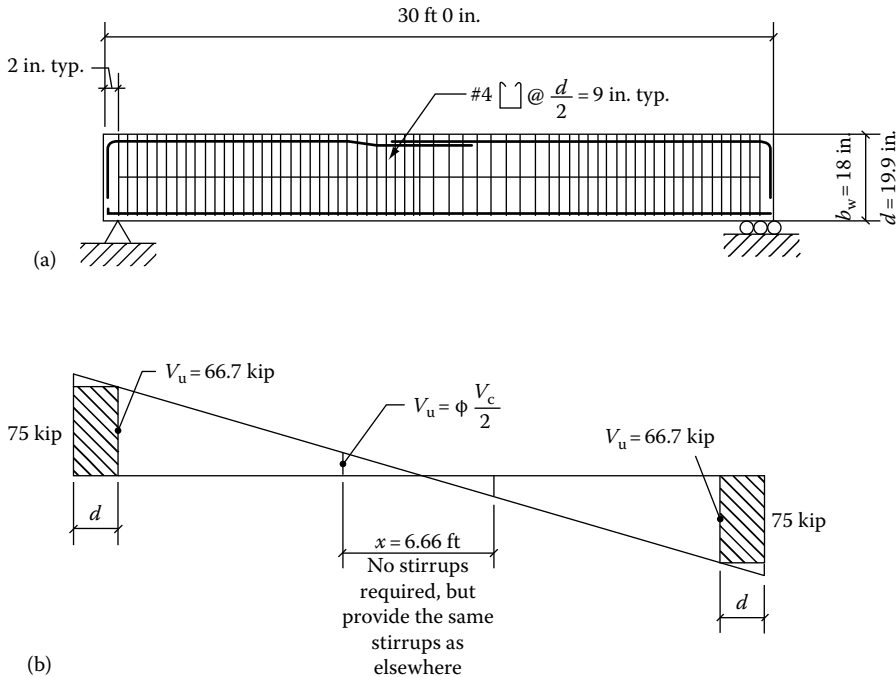


FIGURE 2.49 Shear reinforcement.

#### 2.4.2.2.1 Summary of Shear Design Provision; ACI 318-05

Using the most common loads—dead ( $D$ ), live ( $L$ ), wind ( $W$ ), and earthquake ( $E$ )—the simplified ultimate load combinations are

$$\begin{aligned}
 & \left. \begin{aligned} U &= 1.4D \\ U &= 1.2D + 1.6L \end{aligned} \right\} && \text{Dead and live loads} \\
 & \left. \begin{aligned} U &= 1.2D + 1.6L + 0.8W \\ U &= 1.2D + 1.0L + 1.6W \\ U &= 0.9D + 1.6W \end{aligned} \right\} && \text{Dead, live, and wind loads} \\
 & \left. \begin{aligned} U &= 1.2D + 1.0L + 1.0E \\ U &= 0.9D + 1.0E \end{aligned} \right\} && \text{Dead, live, and earthquake loads}
 \end{aligned}$$

- Strength reduction factor for shear and torsion  $\phi = 0.75$ .
- If  $V_u - \phi V_c > \phi 8\sqrt{f'_c} b_w d$ , increase  $f'_c$ ,  $b_w$ , or  $d$ , as required.
- If  $V_u \leq \phi V_c/2$ , no stirrups are required, but provide nominal stirrups.
- If  $\phi V_c \geq V_u > \phi V_c/2$ , the required area of stirrups  $A_v$  is given by

$$A_v = 0.75\sqrt{f'_c} \frac{b_w s}{f_y} \geq \frac{50b_w s}{f_y}$$

$$\text{Stirrup spacing required } s = \frac{A_v f_y}{0.75\sqrt{f'_c} b_w} \leq \frac{A_v f_y}{50b_w} \leq \frac{d}{2} \leq 24 \text{ in.}$$

- If  $V_u > \phi V_c$ , the required area of stirrups  $A_v$  is given by

$$A_v = \frac{(V_u - \phi V_c)s}{\phi f_y d}$$

$$\text{Stirrup spacing required } s = \frac{\phi A_v f_y d}{V_u - \phi V_c}$$

- Maximum spacing  $\left\{ \begin{aligned} s &= \frac{d}{2} \leq 24 \text{ in. for } (V_u - \phi V_c) \leq \phi 4\sqrt{f'_c} b_w d \\ s &= \frac{d}{4} \leq 12 \text{ in. for } (V_u - \phi V_c) > \phi 4\sqrt{f'_c} b_w d \end{aligned} \right.$

### 2.4.3 TWO-WAY SLABS

Although two-way slabs may be designed by any method that satisfies the strength and serviceability requirements of the ACI code, most usually they are designed by the “equivalent frame method” using computers. In this section, however, only the direct design method is discussed.

In this method, the simple beam moment in each span of a two-way system is distributed as positive and negative moments at midspan and at supports. Since stiffness considerations, except at the exterior supports, are not required, computations are simple and can be carried out rapidly.

Three steps are required for the determination of positive and negative design moments.

1. Determine simple beam moment:

$$M_0 = \frac{W_u l_2 l_n^2}{8}$$

where

- $M_0$  is a simple beam moment
- $W_u$  is the ultimate uniform load
- $l_2$  is the slab width between columns transverse to the span under consideration
- $l_n$  is the clear span between face of columns or capitals

2. For interior spans, divide  $M_0$  into  $M_c$  and  $M_s$  midspan and support moments, as shown in Figure 2.50; for exterior spans, use Figure 2.51 to divide  $M_0$  into moments  $M_1$ ,  $M_2$ , and  $M_3$ .

Observe in Figure 2.50 for an interior span, the positive moment  $M_c$  at midspan equals  $0.35 M_0$ , and the negative moment  $M_s$  at each support equals  $0.65 M_0$ , values that are approximately the same as for a uniformly loaded fixed-end beam. These values are based on the assumption that an interior joint undergoes no significant rotation, a condition that is assured by the ACI restrictions that limit (1) the difference between adjacent span lengths to one-third of the longer span; and (2) the maximum ratio of live load to dead load to 3.

3. The final step is to distribute the positive and negative moments in the transverse direction between column strip and middle strips. The distribution factors are tabulated (Tables 2.2 and 2.3) for three values (0.5, 1, and 2) of panel dimensions  $l_2/l_1$ , and two values (0 and 1) of  $\alpha_1$  ( $l_1/l_2$ ). For intermediate values, linear interpolation may be used. Table 2.3 is for interior spans while Table 2.4 is for exterior spans. For exterior spans, the distribution of moment is influenced by the torsional stiffness of the spandrel

TABLE 2.2  
Percentage of Positive Moment to Column Strip, Interior Span

$\alpha_1 \frac{l_2}{l_1}$	$\frac{l_2}{l_1}$		
	0.5	1.0	2.0
0	60	60	60
$\geq 1$	90	75	45

TABLE 2.3  
Percentage of Negative Moment to Column Strip at an Interior Support

$\alpha_1 \frac{l_2}{l_1}$	$\frac{l_2}{l_1}$		
	0.5	1.0	2.0
0	75	75	75
$\geq 1$	90	75	45

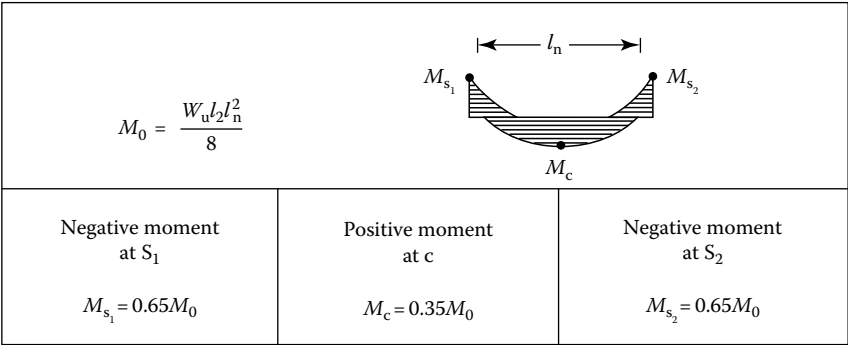


FIGURE 2.50 Interior span moments.

beam. Therefore, an additional parameter  $\beta$ , the ratio of the torsional stiffness of the spandrel beam to flexural stiffness of the slab is given in Table 2.4.

For exterior spans, the distribution of total negative and positive moments between columns strips and middle strips is given in terms of the ratio  $l_2/l_1$ , the relative stiffness of the beam and slab, and the degree of torsional restraint provided by the edge beam. The parameter  $\alpha = (E_{cb}I_b)/(E_{cs}I_s)$  is used to define the relative stiffness of the beam and slab spanning in either direction. The terms  $E_{cb}$  and  $E_{cs}$  are the moduli of elasticity of the beam and slab, respectively, and  $I_b$  and  $I_s$  are the moments of inertia, respectively. Subscripted parameters  $\alpha_1$  and  $\alpha_2$  are used to identify  $\alpha$  for the directions of  $l_1$  and  $l_2$ , respectively.

The parameter  $\beta$  in Table 2.4 defines the torsional restraint of edge beam. If there is no edge beam, that is,  $\beta = 0$ , all of the exterior moment at (Figure 2.51) is apportioned to the column

TABLE 2.4  
Percentage of Negative  
Moment to Column Strip  
at an Exterior Support

$\alpha_1 \frac{l_2}{l_1}$	$\frac{l_2}{l_1}$			
	$\beta_1$	0.5	1.0	2.0
0	0	100	100	100
0	$\geq 2.5$	75	75	75
$\geq 1$	0	100	100	100
$\geq 1$	$\geq 2.5$	90	75	45

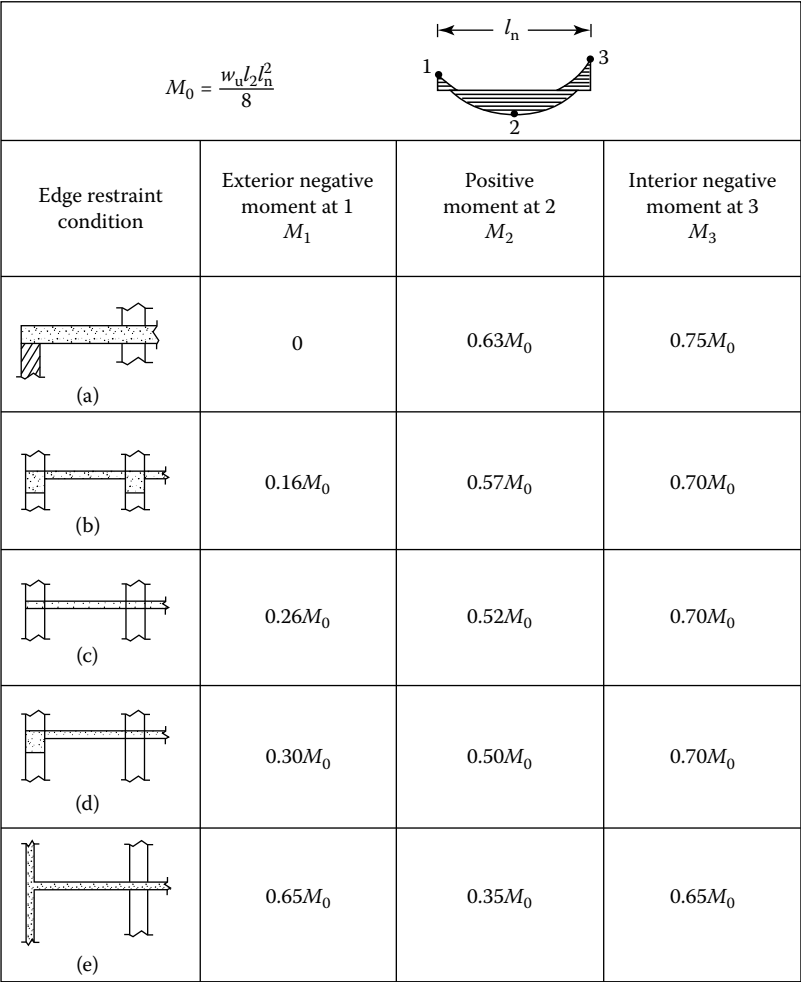


FIGURE 2.51 Exterior span moments.

strip. For  $\beta \geq 2.5$ , that is, for very stiff-edge beams, 75% of the moment at is assigned to the column strip. For values of  $\beta$  between 0 and 2.5, linear interpolation is permitted. In most practical designs, distributing 100% of the moment to the column strip while using minimum slab reinforcement in the middle strip yields acceptable results.

### 2.4.3.1 Two-Way Slab Design Example

**Given:** A two-way slab system is shown in Figure 2.52.

$$w_d = 155 \text{ psf}, \quad w_l = 100 \text{ psf}$$

Determine the slab depth and design moments by the direct design method at all critical sections in the exterior and interior span along column line B.

**Solution:** From Tables 2.5 and 2.6, for  $f_y = 60$  ksi, and for slabs without drop panels, the minimum thickness of the slab is determined to be  $l_n/33$  for the interior panels. The same thickness is used for the exterior panels since the system has beams between the columns along the exterior edges.

For the example, the clear span in the long direction,  $l_n = 24 - 2 = 22$  ft. The minimum thickness  $h = (22 \times 12)/33 = 8$  in.

#### Interior Span

$$w_u = 1.2(0.155) + 1.6(0.10) = 0.346 \text{ ksf}$$

$$\begin{aligned} M_0 &= \frac{w_u l_2 l_u^2}{8} \\ &= \frac{0.346 \times 20 \times 22^2}{8} \\ &= 418.7 \text{ kip-ft} \end{aligned}$$

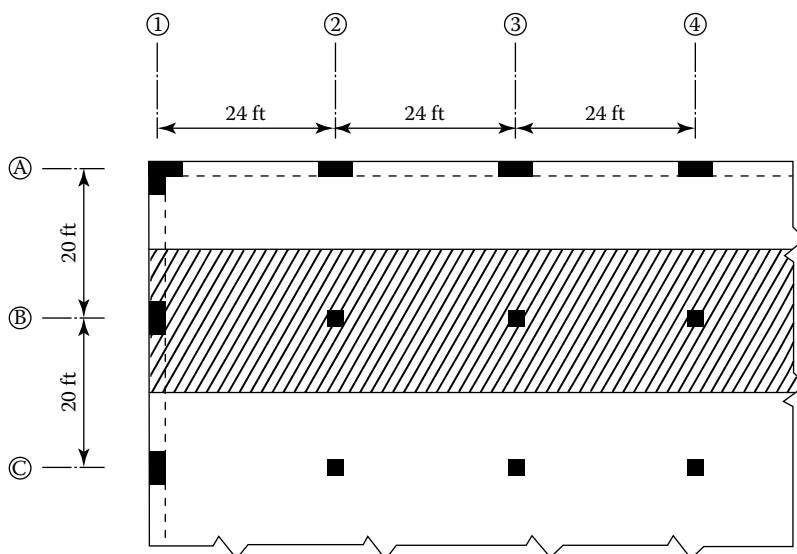


FIGURE 2.52 Design example: Two-way slab.

**TABLE 2.5**  
**Minimum Thickness of Slabs Without Interior Beams**

Yield Strength, $f_y$ , psi <sup>b</sup>	Without Drop Panels <sup>a</sup>			With Drop Panels <sup>a</sup>		
	Exterior Panels		Interior Panels	Exterior Panels		Interior Panels
	Without Edge Beams	With Edge Beams <sup>c</sup>		Without Edge Beams	With Edge Beams <sup>c</sup>	
40,000	$\frac{l_n}{33}$	$\frac{l_n}{36}$	$\frac{l_n}{36}$	$\frac{l_n}{36}$	$\frac{l_n}{40}$	$\frac{l_n}{40}$
60,000	$\frac{l_n}{30}$	$\frac{l_n}{33}$	$\frac{l_n}{33}$	$\frac{l_n}{33}$	$\frac{l_n}{36}$	$\frac{l_n}{36}$
75,000	$\frac{l_n}{28}$	$\frac{l_n}{31}$	$\frac{l_n}{31}$	$\frac{l_n}{31}$	$\frac{l_n}{34}$	$\frac{l_n}{34}$

Source: ACI 318-08, Table 9.5c.

<sup>a</sup> Drop panel is defined in 13.3.7.1 and 13.3.7.2.

<sup>b</sup> For values of reinforcement yield strength between the values given in the table, minimum thickness shall be determined by linear interpolation.

<sup>c</sup> Slabs with beams between columns along exterior edges. The value of  $\alpha$  for the edge beam shall not be less than 0.8.

**TABLE 2.6**  
**Approximate Span Depth Ratios for Posttensioned Systems**

Floor System	Simple Spans	Continuous Spans	Cantilever Spans
One-way solid slabs	48–48	42–50	14–16
Two-way flat slabs	36–45	40–48	13–15
Wide band beams	26–30	30–35	10–12
One-way joists	20–28	24–30	8–10
Beams	18–22	20–25	7–8
Girders	14–20	16–24	5–8

*Note:* The values are intended as a preliminary guide for the design of building floors subjected to a uniformly distributed superimposed live load of 50–100 psf (2394–4788 Pa). For the final design, it is necessary to investigate for possible effects of camber, deflections, vibrations, and damping. The designer should verify that adequate clearance exists for proper placement of posttensioning anchors.

Divide  $M_0$  between sections of positive and negative moments.

At midspan:

$$\begin{aligned}
 M_c &= 0.35M_0 \\
 &= 0.35 \times 418.7 = 146.5 \text{ kip-ft}
 \end{aligned}$$

At supports:

$$\begin{aligned}
 M_s &= 0.65M_0 \\
 &= 0.65 \times 418.7 = 272.2 \text{ kip-ft}
 \end{aligned}$$



For the distribution of the midspan moment  $M_c$  between column and middle strips, use Table 2.4. The value for  $\alpha_1$ , the ratio of beam stiffness to slab stiffness for the example problem is zero since there are no beams in the span direction under consideration. The ratio  $l_2/l_1 = 20/24 = 0.833$ . From Table 2.2 the column strip moment is 60% of the total moment.

$$\text{Moment to column strip} = 0.60 \times 146.5 = 87.9 \text{ kip-ft}$$

$$\text{Moment to middle strip} = 0.40 \times 146.5 = 58.6 \text{ kip-ft}$$

For the distribution of support moment  $M_s$  between column and middle strips, use Table 2.4. Since  $\alpha_1 = 0$ , and  $l_2/l_1 = 0.833$ , from Table 2.3 the column strip moment is 75% of the total moment.

$$\text{Moment in column strip} = 0.75 \times 272.2 = 204 \text{ kip-ft}$$

$$\text{Moment in middle strip} = 0.25 \times 272.2 = 68 \text{ kip-ft}$$

**Exterior Span:** The magnitude of the moments at critical sections in the exterior span is a function of both  $M_0$ , the simple beam moment, and  $\alpha_{ec}$ , the ratio of stiffness of exterior equivalent column to the sum of the stiffness of the slab and beam framing into the exterior joint. Instead of computing  $\alpha_{ec}$ , we use edge condition (d) given in Figure 2.51 to evaluate the design moments at critical sections.

At the exterior column face:

$$M_1 = 0.30 \times M_0 = 0.30 \times 418.7 = 125.6 \text{ kip-ft}$$

At midspan:

$$M_2 = 0.50 \times M_0 = 0.50 \times 418.7 = 209.4 \text{ kip-ft}$$

At the interior column face:

$$M_3 = 0.7 \times M_0 = 0.7 \times 418.7 = 293 \text{ kip-ft}$$

At the exterior edge of the slab, the transverse distribution of the design moment and the column strip is given in Table 2.4. Instead of calculating the value of  $\beta$ , we conservatively assign 100% of the exterior moment to the column strip.

The moment to the column strip =  $1 \times 125.6 \text{ kip-ft}$ . The middle strip is assumed to be controlled by the minimum steel requirements, an assumption which is satisfactory for almost all practical designs.

## 2.5 PRESTRESSED CONCRETE SYSTEMS

The first use of posttensioned concrete was on the Walnut Lane Bridge in Philadelphia in 1949. The bridge had precast girders posttensioned with the European Magnel system. The first posttensioning in U.S. building construction was in the mid- to late-1950s in buildings using the lift-slab construction method.

Originally, the concrete floor slabs were reinforced with mild steel in lift-slab buildings. The slabs were precast on the ground in a stack and then lifted individually into position using hydraulic jacks at the top of the columns. While this was an inherently efficient process, there were two problems. First, the slabs tended to stick together as they were lifted, their weight causing them to crack as they were pulled apart. Second, since spans of 28–30 ft were common and the slabs were 10–12 in. thick,

deflection was a serious problem. Midspan deflections of 2–3 in. and partition cracking were common in early lift-slab construction. Once the lifting companies started posttensioning their slabs, the deflection problems virtually disappeared.

Lift-slab construction in the earlier days used a so-called button-headed tendon system. A button-headed tendon had parallel, ¼ in. diameter cold-wires, each with about a 7 kip (7000-pound) effective force, generally six or seven wires per tendon. To secure the wires at each end, they were passed through round holes in a rectangular steel-bearing plate and a circular stressing washer, usually externally threaded. Then a “button” was formed on each end of the wire by dynamic impact—basically hammering the steel end of the tendon. The buttons, too big to pass through the holes, were then anchored against the stressing washer. A mastic coating was applied to the wires for corrosion protection, and they were wrapped in heavy waxed paper to prevent bond with the concrete. All of this was done in the shop, and then these tendon assemblies were transported to the job. Tendon assemblies were installed into the forms, and the concrete was placed. When the concrete reached a minimum strength, the tendons were stressed to the required tension and elongation with a hydraulic jack attached to the threaded stressing washer. A steel shim exactly as long as the calculated elongation was then inserted between the bearing plate and the stressing washer to hold the elongation and stress in the wires. There was no room for error; the length of the wires and shims had to be exactly predetermined.

There were actually two major problems with the button-headed tendons. First, of course, was the problem with the exact length. Any deviation between the tendon length and the length between edge forms required either a new tendon or moving the edge forms before pouring the concrete. Second, because the shims and the stressing washer ended up on the outside edges of the constructed slab, they had to be covered with a second concrete pour. This was done by either recessing the anchor inside the finished slab edge in a “stressing pocket” that was filled with the concrete later, or by casting continuous pour strip at the slab edge to cover the anchors.

In addition to solving deflection problems, posttensioning helps in reducing slab thickness. Since posttensioning makes much more efficient use of a concrete cross section, 8 or 9 in. slabs could be used instead of the 12 in. thick floor slabs required for nonprestressed slabs. Thinner slabs means savings in material, time, and labor for the contractor.

In the early 1960s, the button-headed tendon system was replaced by tendons using seven-wire prestressing strand and wedge anchors. The strand system was much more economical than the button-headed tendon system and eliminated all of its major construction drawbacks, such as exact length and stressing pockets. After 5 or 6 years of fierce competition with the button-headed tendon system, the seven-wire strand system won the battle of the marketplace. By the late 1960s, the button-headed tendon was extinct, and virtually all posttensioned tendons for building construction were strand tendons.

Prior to 1963, analysis techniques for indeterminate prestressed members were tedious, highly mathematical, and nonintuitive. T.Y. Lin solved this problem for the design engineer. In 1963, in the *ACI Journal*, Lin published a revolutionary paper on the analysis of indeterminate prestressed concrete members using a method he called “load balancing.” He demonstrated how during design the tendons could be thought of as being replaced by the loads they exert on the concrete member. Once this was done, the structure could be designed like any other nonprestressed structure. Using load balancing, posttensioned structures could be analyzed fully and accurately using any standard structural engineering technique, such as a moment distribution. The introduction of the load-balancing method made the design of indeterminate posttensioned concrete members about as easy for the practicing engineer as the design of nonprestressed members.

Posttensioned concrete construction grew exponentially as a result of this new simplified tool for design. The simplified structural engineering method for design of posttensioned concrete buildings was the major reason for the explosive growth of posttensioning in the late 1960s and 1970s. It is interesting to note that ACI 318-71 virtually ignored posttensioning design, mainly addressing determinate pretensioned members. ACI 318-77 was much improved, recognizing banded tendon

distribution for two-way slabs. Since then there have been quite a few advances in construction methods particularly in two-way slab construction. In the old days, tendons in two-way slab systems were laid out with some in the “column strips” and some in the “middle strips,” similar to rebar in nonprestressed two-way slabs. Since the tendons in the two perpendicular directions were draped in a curved profile—high at the column lines, low at midspans—and since the tendons were continuous from one end of the slab to the other, the tendons had to be woven just like a basket, starting with the single tendon that was below all other tendons and proceeding to the single tendon that was above all other tendons—what was called the “basket weave” system. Detailers would figure out the tendon sequence, and if a mistake was made, the tendon had to be pulled out and rethreaded through the in-place tendons. This was a tedious and labor-intensive procedure.

The basket weave system of placing tendons was replaced by the banded tendon distribution. The banded tendon distribution was first used in the late 1960s in the notoriously famous Watergate apartments in Washington D.C. In this system, all of the tendons running in one direction are grouped together in a narrow “band” 3–4 ft wide over the columns, and the tendons in the perpendicular direction are spaced uniformly. In this way, all banded tendons are placed first, and all uniform tendons are placed next. There are only two sequence numbers. This is a blessing for the ironworker, as banding eliminated sequencing and weaving.

Design engineers also benefit from the banded tendon distribution. In two-way slabs with irregular and complex column layouts, it makes the visualization of load paths much easier, helping to ensure that all slab loads are transferred to columns. Laboratory tests and hundreds of millions of square feet of successful slab installations have verified the structural functionality of the banded tendon distribution.

There are two problems in posttension construction that need special consideration: restraint to shortening and tendon corrosion. It should be noted that the mechanics of slab shortening are different in posttensioned slabs than in rebar slabs. Engineers had to learn how to design posttensioned slabs with levels of cracking no greater than those normally found and accepted in rebar slabs. This is accomplished largely by means of joining details between the posttensioned members and the attached walls and columns. But tendon corrosion has been the biggest problem faced by the industry. When the earliest posttensioned buildings were about 15 years old, corrosion problems started to surface. It was realized that some tendon sheathings and coatings could not adequately resist corrosion in the most aggressive environments, such as where deicing salts are applied to slab surfaces. Tendon material specifications developed by PTI, starting in the mid-1970s, have largely solved the corrosion problems with improvements in sheathing, coatings, and, in the most aggressive environments, complete encapsulation of the tendons.

Posttensioning system has great potential in strengthening existing buildings. The use of externally applied posttensioned tendons is an effective way of increasing the load-carrying capacity of buildings with all types of framing and materials, even wood.

Tall buildings, say 20 stories or higher, where historically most framing has been structural steel, concrete offers substantial cost and performance benefits. Posttensioned concrete also offers significant performance benefits in tall buildings, particularly in the areas of fire resistance, sound transmission, and floor stiffness. Posttensioning the floors of tall concrete buildings minimizes their weight, and combined with the use of high-strength concrete, has made the construction of tall concrete buildings more and more feasible.

Prestressing boosts the span range of conventionally reinforced floor systems by about 30%–40%. This is the primary reason for the increase in the use of prestressed concrete. Some of the other reasons are

1. Prestressed concrete is generally crack-free and is therefore more durable.
2. Prestressing applies forces to members that oppose the service loads. Consequently, there is less net force to cause deflections.
3. Prestressed concrete is resilient. Cracks due to overloading completely close and deformations are recovered soon after removal of the overload.

4. Fatigue strength (though not a design consideration in building design) is considerably more than that of conventionally reinforced concrete because tendons are subjected to smaller variations in stress due to repeated loadings.
5. Prestressed concrete members are generally crack-free, and are therefore stiffer than conventional concrete members of the same dimensions.
6. The structural members are self-tested for materials and workmanship during stressing operations, thereby safeguarding against unexpected poor performance in service.
7. Prestress design is more controllable than mild steel design because a predetermined force is introduced in the system; the magnitude, location, and technique of introduction of such an additional force are left to the designer, who can tailor the design according to project requirements.

There are some disadvantages to the use of prestressed concrete, such as fire, the explosion resistance of unbonded systems, and difficulty in making penetrations due to the fear of cutting tendons.

A major motivation for the use of prestressed concrete comes from the reduced structural depth, which translates into lower floor-to-floor height and a reduction in the area of curtain wall and building volume with a consequent reduction in heating and cooling loads.

In prestressed systems, the savings in mild steel reinforcement resulting from prestress are just about offset by the higher unit cost of prestressing steel. The cost savings come from the reduction in the quantity of concrete combined with indirect nonstructural savings resulting from reduced floor-to-floor height. Although from an initial cost consideration prestressed concrete may be the least expensive, other costs associated with future tenant improvements such as providing for large openings in floor slabs must be considered before selecting the final scheme.

## 2.5.1 PRESTRESSING METHODS

Current methods of prestressing can be studied under two groups, pretensioning and posttensioning. In pretensioning, the tendons are stretched and anchored against external bulkheads. Then concrete is placed around the tendons. After the concrete hardens, the anchors are released, which imparts compression forces in the concrete as the tendon attempts to return to its original length.

In posttensioning, the tendons are tensioned and anchored against the concrete after it has hardened. The tendons are stressed using hydraulic jacks after the concrete has reached a minimum of about 75% of the design strength. Tendon elongations are measured and compared against the calculated values; if satisfactory, the tendons projecting beyond the concrete are cut off. Formwork is removed after posttensioning. However, the floor is back-shored to support construction loads from the floors above.

Posttensioning is accomplished using high-strength strands, wires, or bars as tendons. In North America, the use of strands by far leads the other two types. The strands are either bonded or unbonded depending upon the project requirements. In bonded construction, the tendons are installed in ducts that are filled with a mortar grout after stressing the tendons.

In building applications, unbonded construction is the preferred choice because it eliminates the need for grouting. Posttensioned floor systems in buildings consist of slabs, joists, beams, and girders, with a large number of small tendons. Grouting each of the multitude of tendons is a time-consuming and expensive operation. Therefore, unbonded construction is more popular.

## 2.5.2 MATERIALS

### 2.5.2.1 Posttensioning Steel

The basic requirements for posttensioning steel is that the loss of tension in the steel due to shrinkage and creep of concrete and the effects of stress relaxation of the tendon should be a relatively small portion of the total prestress. In practice, the loss of prestress generally varies from a low of

15 ksi (103.4 MPa) to a high of 50 ksi (344.7 MPa). If mild steel having a yield of 60 ksi (413.7 MPa) were employed with an initial prestress of, say, 40 ksi, it is very likely that most of the prestress, if not the entire prestress, would be lost because of shrinkage and creep losses. To limit the prestress losses to a small percentage of, say, 20% of the applied prestress, the initial stress in the steel must be in excess of 200 ksi (1379 MPa). Therefore, high-strength steel is invariably used in prestressed concrete construction.

High-strength steel in North America is available in three basic forms: (1) uncoated stress-relieved wires; (2) uncoated stress-relieved strands; and (3) uncoated high-strength steel bars. Stress-relieved wires and high-strength steel bars are not generally used for posttensioning. The most common high-strength strands are fabricated by helically twisting a group of six wires around a slightly larger center wire by a mechanical process called stranding. The resulting seven-wire strands are stress-relieved by a continuous heat-treatment process to produce the required mechanical properties.

ASTM specification A416 specifies two grades of steel, 250 and 270 ksi (1724 and 1862 MPa), the higher strength being more common in the building industry. A modulus of elasticity of 27,500 ksi (189,610 MPa) is used for calculating the elongation of strands. To prevent the use of brittle steel, which would result in a failure pattern similar to that of an over-reinforced beam, ASTM A-416 specifies a minimum elongation of 3.5% at rupture.

A special type of strand called low-relaxation strand is increasingly used because it has a very low loss due to relaxation, usually about 20%–25% of that for stress-relieved strand. With this strand, less posttensioning steel is required, but the cost is greater because of the special process used in its manufacture.

Corrosion of unbonded strand is possible, but can be prevented by using galvanized strands. This is not, however, popular in North America because (1) various anchorage devices in use for posttensioned systems are not suitable for use with galvanized strand because of low coefficient of friction; (2) damage can result to the strand because the heavy bite of the anchoring system can ruin the galvanizing; and (3) galvanized strands are more expensive.

A little understood and of infrequent occurrence of great concern in engineering is the so-called stress corrosion that occurs in highly stressed strands. The reason for the phenomenon is little known, but chemicals such as chlorides, sulfides, and nitrates are known to start this type of corrosion under certain conditions. It is also known that high-strength steels exposed to hydrogen ions are susceptible to failure because of loss in ductility and tensile strength. The phenomenon is called hydrogen embrittlement and is best counteracted by confining the strands in an environment having a pH value greater than 8. Incidentally, the pH value of concrete is  $\pm 12.5$ . Therefore, it produces a good pH environment.

### 2.5.2.2 Concrete

Concrete with compressive strengths of 5000–6000 psi (34 to 41 MN) is commonly employed in the prestress industry. This relatively high strength is desirable for the following reasons. First, high-strength concrete is required to resist the high stresses transferred to the concrete at post-tensioning anchors. Second, it is needed to develop rapid strength gain for productivity. Third, high-strength concrete has higher resistance in tension, shear, bond and bearing, and is desirable for prestressed structures that are typically under higher stresses than those with ordinary reinforced concrete. Fourth, its higher modulus of elasticity and smaller creep result in smaller loss of prestress.

Posttensioned concrete is considered a self-testing system because if the concrete is not crushed under the application of prestress, it should withstand subsequent loadings in view of the strength gain that comes with age. In practice, it is not the 28 day strength that dictates the mix design, but rather the strength of concrete at the transfer of prestress.

Although high-early strength (type III) Portland cement is well suited for posttension work because of its ability to gain the required strength for stressing relatively early, it is not generally used because of higher cost. Invariably, type I cement conforming to ASTM C-150 is employed in buildings.

The use of admixtures and fly ash is considered a good practice. However, use of calcium chlorides or other chlorides is prohibited because the chloride ion may result in stress corrosion of prestressing tendons. Fly ash reduces the rate of strength gain, and therefore increases the time until stresses can be transferred, leading to loss of productivity.

A slump of 3–6 in. (76–127 mm) gives good results. The aggregate used in the normal production of concrete is usually satisfactory in prestressed concrete, including lightweight aggregates. However, care must be exercised in estimating volumetric changes so that a reasonable prestress loss can be calculated. Lightweight aggregates manufactured using expanded clay or shale have been used in posttensioned buildings. Lightweight aggregates that are not crushed after burning maintain their coating and therefore absorb less water. Such aggregates have drying and shrinkage characteristics similar to the normal-weight aggregates, although the available test reports are somewhat conflicting. The size of aggregate, whether lightweight or normal weight, has a more profound effect on shrinkage. Larger aggregates offer more resistance to shrinkage and also require less water to achieve the same consistency, resulting in as much as 40% reduction in shrinkage when the aggregate size is increased from, say,  $\frac{3}{4}$ –1½ in. (19–38 mm). It is generally agreed that both shrinkage and creep are more functions of cement paste than of the type of aggregate. Since 1955, lightweight aggregate has been gaining acceptance in prestressed construction and has a good track record.

### 2.5.3 PT DESIGN

The design involves the following steps:

1. Determination of the size of concrete member
2. Establishment of the tendon profile
3. Calculation of the prestressing force
4. Verification of the section for ultimate bending and shear capacity
5. Verification of the serviceability characteristics, primarily in terms of stresses and long-term deflections

Deflections of prestressed members tend to be small because under service loads they are usually uncracked and are much stiffer than non-prestressed members of the same cross section. Also, the prestressing force induces deflections in an opposite direction to those produced by external loads. The final deflection, therefore, is a function of tendon profile and magnitude of prestress. Appreciating this fact, the ACI code does not specify minimum depth requirements for prestressed members. However, as a rough guide, the suggested span-to-depth ratios given in Table 2.7 can be used to establish the depth of continuous flexural members. Another way of looking at the suggested span-to-depth ratios is to consider, in effect, that prestressing increases the span range by about 30%–40% over and above the values normally used in non-prestressed concrete construction.

#### 2.5.3.1 Gravity Systems

The tendon profile is established based on the type and distribution of load with due regard to clear cover required for fire resistance and corrosion protection. Clear spacing between tendons must be sufficient to permit easy placing of concrete. For maximum economy, the tendon should be located eccentric to the center of gravity of the concrete section to produce maximum counteracting effect to the external loads. For members subjected to uniformly distributed loads, a simple parabolic profile is ideal, but in continuous structures parabolic segments forming a smooth reversed curve at the support are more practical. The effect is to shift the point of contraflexure away from the supports. This reverse curvature modifies the load imposed by posttensioning from those assumed using a parabolic profile between tendon high points.

The posttension force in the tendon immediately after releasing the hydraulic jack is less than the jacking force because of (1) slippage of anchors, (2) frictional losses along tendon profile, and

TABLE 2.7  
Sample Unit Quantities for Hotels

TABLE 2.7 Sample Unit Quantities for Hotels																		
Hotel Location	No. of Floors	Wind Controls	Seismic Controls	Concrete Quantity Equiv. inches/S.F. of Superstructure				Reinforcing Quantity PSF of Tower Area						Lineal Ft. of Shear Wall per 15,000sq ft of Typ. Floor Plate	Equivalent Rebar per cubic Yd.	w/o P.T.		
				Slab	Cols.	Walls	Shear	Total	P.T. + 4	Rebar	Total	Cols.	Walls				Shear	Total PSF
Miami, FL	9	Yes		7.00	0.75	0.60	8.35	—	—	2.75	2.75	0.70	0.50	3.95	144	153 lb	No PT	
Miami, FL	14	Yes		7.00	0.68	0.53	8.21	—	—	4.08	4.08	1.01	0.84	5.93	161	234 lb	No PT	
Miami, FL	30	Yes		7.50	0.81	4.67	12.98	—	—	3.40	3.40	1.10	6.82	11.32	516	282 lb	No PT	
Nashville, TN	18	Yes		6.50	0.60	2.50	9.60	2.60	2.60	1.45	4.05	0.90	1.35	6.30	398	212 lb	125	
Houston, TX	25	Yes		7.00	0.80	3.40	11.20	2.80	2.80	2.37	5.17	1.25	2.93	9.35	314	270 lb	189	
El Paso, TX	6		Yes	6.50	0.40	1.00	7.90	2.60	2.60	1.40	4.00	1.40	0.70	6.10	184	250 lb	144	
Irvine, CA	16		Yes	6.50	1.08	4.25	11.83	2.60	2.60	2.10	4.70	0.58	4.30	9.58	423	262 lb	191	
Albuquerque, NM	16		Yes	7.80	1.00	3.50	12.30	2.84	2.84	2.80	5.64	1.00	2.40	9.04	310	238 lb	163	
Atlantic City, NJ	20	Yes		NA	NA	NA	NA	NA	NA	NA	NA	NA	NA	NA	229	NA	NA	
San Jose, CA	10		Yes	7.50	0.34	2.37	10.21	2.72	2.72	1.86	4.58	0.31	1.44	6.33	367	201 lb	115	
Santa Clare, CA	13		Yes	6.50	0.70	2.09	9.29	2.60	2.60	2.35	4.95	1.37	2.91	9.23	293	321 lb	231	
Note: NA, Not available.																		

Note: NA, Not available.

(3) elastic shortening of concrete. The force is reduced further over a period of months or even years due to change in the length of concrete member resulting from shrinkage and creep of concrete and relaxation of the highly stressed steel. The effective prestress is the force in the tendon after all the losses have taken place. For routine designs, empirical expressions for estimating prestress losses yield sufficiently accurate results, but in cases with unusual member geometry, tendon profile, and construction methods, it may be necessary to make refined calculations.

Prestressing may be considered as a method of balancing a certain portion of the applied loads. This method, first developed by T.Y. Lin, is applicable to statically indeterminate systems just as easily as to statically determinate structures. Also, the procedure gives a simple method of calculating deflections by considering only that portion of the applied load not balanced by the prestress. If the effective prestress completely balances the applied load, the posttensioned member will undergo no deflection and will remain horizontal, irrespective of the modulus of rigidity or flexural creep of concrete.

A question that usually arises in prestress design is how much of the applied load is to be balanced. The answer, however, is not simple. Balancing all the dead load often results in too much prestressing, leading to uneconomical design. On the other hand, there are situations in which the live load is significantly heavier than the dead load, making it more economical to prestress not only for full dead loads, but also for a significant portion of the live load. However, in the design of typical floor framing systems, the prestressing force is normally selected to balance about 70%–90% of the dead load and, occasionally, a small portion of the live load. This leads to an ideal condition with the structure having little or no deflection under dead loads.

Limiting the maximum tensile and compressive stresses permitted in concrete does not in itself assure that the prestressed member has an adequate factor of safety against flexural failure. Therefore, its nominal bending strength is computed in a procedure similar to that of a reinforced concrete beam. Under-reinforced beams are assumed to have reached the failure load when the concrete strain reaches a value of 0.003. Since the yield point of prestressing steel is not well defined, empirical relations based on tests are used in evaluating the strain and hence the stress in tendons.

The shear reinforcement in posttensioned members is designed in a manner almost identical to that of non-prestressed concrete members, with due consideration for the longitudinal stresses induced by the posttensioned tendons. Another feature unique to the design of posttensioned members is the high stresses in the vicinity of anchors. Prestressing force is transferred to concrete at the tendon anchorages. Large stresses are developed in the concrete at the anchorages, which requires provision of well-positioned reinforcement in the region of high stresses. At a cross section of a beam sufficiently far away (usually two to three times the larger cross-sectional dimensions of the beam) from the anchor zone, the axial and bending stresses in the beam due to an eccentric prestressing force are given by the usual  $P/A$  and  $MC/I$  relations. But in the vicinity of stress application, the stresses are distributed in a complex manner. Of importance are the transverse tensile forces generated at the end blocks for which reinforcement is to be provided. The tensile stress has a maximum value at  $90^\circ$  to the axis of the prestressing force. Its distribution depends on the location of bearing area and its relative proportion with respect to the areas of the end face.

Because of the indeterminate nature and intensity of the stresses, the design of reinforcement for the end block is primarily based on empirical expressions. It usually consists of closely spaced stirrups tied together with longitudinal bars.

### 2.5.3.2 Design Thumb Rules

Certain rules of thumb such as span-to-depth ratios and the average value of posttensioning stresses are useful in conceptual design. The span-to-depth for slabs usually works between  $L/40$  and  $L/50$ , whereas the joists it is between  $L/25$  and  $L/35$ . Beams can be much shallower than joists, with a depth in the range of  $L/20$  and  $L/30$ . Band beams, defined as those with a width-to-depth ratio in excess of 4, offer perhaps the least depth without using as much concrete as flat slab construction. Although a span-to-depth ratio approaching 35 is adequate for band beams from strength and serviceability considerations, clearance requirements for proper detailing of anchorages and for



accessing stressing equipment may dictate a deeper section. As a rule of thumb, a minimum compression of 125–150 psi (862–1034 kPa) is a practical and economical range for slabs. For beams, the range is 250–300 psi (1724–2068 kPa). Compression stresses as high as 500 psi (3447 kPa) have been used in band-beam systems. Even higher stresses may be required for transfer girders.

#### 2.5.3.2.1 General Considerations

For a given member geometry, support conditions, and loading, the design of a posttensioned member depends on three parameters that need to be established by the design engineer:

1. The average precompression
2. Percentage of load to balance (uplift due to tendon drape)
3. Tendon profile (shape and drape)

From the many possible design solutions for a posttensioned member, the one that meets the ACI 318 requirements for serviceability and strength generally is the least expensive to build and thus the preferred solution. Typically, for a given slab dimension, loading, and construction method, less material means more economical design. As stated previously, there is a unique value for the design moment,  $M_u$ , for the conventionally reinforced beam that leads to a unique value for the required area of steel,  $A_s$ . For a posttensioned alternative, the design moment includes secondary (hyperstatic) effects and thus the design moment is a function of the posttensioning force itself.

#### 2.5.3.2.2 PT Systems: North American Practice

In the United States and Canada, posttensioned buildings and parking garages are typically constructed with seven-wire, 0.5 in. diameter (12.7 mm), unbonded single-strand (monostrand) tendons. These tendons, with a typical strength of 270 ksi (1860 MPa), are also greased and sheathed. One reason for the widespread use of the 0.5 in.-diameter strand is the ACI 318 requirement that the tendon spacing should not be greater than eight times the slab thickness. The use of 0.5 in.-diameter, 270 ksi (1860 MPa) strands permits 4½–5 in. thick (110–125 mm) slabs to meet both minimum 125 psi (0.85 MPa) average precompression and the maximum tendon spacing requirements. In addition, the tendons and stressing equipment are light enough for workers to handle them efficiently on site. Larger diameter (0.6 in. [15.3 mm]) strands are primarily used in pretensioning and bridge construction. Higher strength steels and smaller diameter strands are also available but are not commonly used for new construction.

#### 2.5.3.2.3 Analysis Considerations

In both one- and two-way systems, specifying the structural model includes defining the design strips, irrespective of analysis is used. Column-supported floors generally qualify as two-way systems; beam- and wall-supported slabs and beams generally qualify as one-way systems.

The fixity of the connections must also be specified. In some instances, such as corner columns in flat slabs, the assumption of full fixity does not yield a satisfactory design. Such connections may be assumed as hinged connections but must be detailed to allow rotation. The integrity of the joint must be retained by limiting crack width and allowing for transfer of axial and shear forces through the joint. Another instance where a hinge connection may be beneficial is for short gravity columns at split levels in parking structures, which have a ramp on one side and a level floor on the other side.

#### 2.5.3.2.4 Design Considerations

There is a major difference between the design of a posttensioned member and the design of a conventionally reinforced concrete member. Once the geometry, loading, support conditions, and material properties of a conventionally reinforced member are established, the required area of reinforcement,  $A_s$ , is given by a well-defined formula. Thus, there is a unique design to a given problem. For a posttensioned member, however, there are a number of acceptable designs because there are several additional parameters that must be determined.

#### 2.5.3.2.5 *Average Prestress*

The average precompression is the total posttensioning force divided by the gross cross-sectional area normal to the force. ACI 318 05/08 requires a minimum of 125 psi (0.85 MPa) effective precompression after all prestress losses. In general, 125 psi (0.85 MPa) should be used for the initial average precompression. For roofs and parking structures, use 150–200 psi (1.0–1.4 MPa) if watertightness or cracking is a concern. However, an increase in precompression does not guarantee watertightness and may not completely eliminate cracking. To avoid leakage, the increased posttensioning must be supplemented by other measures, such as a membrane overlay. In stemmed structures, such as one-way slab and beam construction, the entire cross-sectional area of the member should be used when computing the average precompression. In one-way slab and beam construction, the member for calculating average prestress is defined as the beam and its tributary slab area. For reasons of economy, maximum precompression should be limited; 275 psi (2.0 MPa) for slabs and 350 psi (2.50 MPa) for beams, values less than the code's limit of maximum compressive stress. However, values much higher than these are typically required for the design of transfer girders. It is not unusual to have as much as 800 psi of prestress in large transfer girders.

#### 2.5.3.2.6 *Percent of Load Balance*

Posttensioning is typically thought of as a system of loads that counteracts the dead load of structure. This is expressed as the ratio (percentage) of the dead load that is balanced. For slabs, it is customary to balance between 60% and 80% of the dead load. For beams, this is usually increased to between 80% and 110%. One reason for higher balanced loading for the beams is that beam deflection is more critical to service performance of a floor system. To determine the required posttensioning force, we start with the critical span (generally, this is the longest span). Using the maximum permissible tendon drape in this span as a one limiting criterion, and the minimum precompression as the other, we then determine a posttensioning force to balance the desired percentage of the dead load.

#### 2.5.3.2.7 *Tendon Profile*

In practice, tendon profiles are reversed parabolas. Tendons thus exert both upward and downward forces in the same span. For beam tendons and slab tendons in the distributed direction, a reversed parabolic profile with inflection points at one-tenth of the span length is typically used. For the banded direction, a partial parabola with a straight length of approximately 4 ft (1.2 m) over the supports is more practical.

The low points of the tendon profile are typically set at midspan for both interior and exterior spans. In terms of posttensioning force efficiency, however, it is preferable if the low point in the exterior spans is closer to the exterior of the building (approximately 40% of the span length).

The high point of the tendon profile should be as close to the top surface of the member as practical, allowing for clearance and reinforcement in the orthogonal direction. At the low point of the profile, it is best to place the tendons as close to the soffit of the member as allowable, to take full advantage of the uplift forces in the tendons and their contribution to ultimate strength. This arrangement is possible for the critical spans in a continuous member but may need to be adjusted for the other spans.

If using the maximum drape results in excessive uplift in a span other than the critical span, the first choice should be to reduce the prestressing force. If this is not practical, raise the tendon at midspan to reduce the drape. When selecting tendon heights, use intervals of 0.25 in. (5 mm) for construction purposes. Keeping the tendon high point fixed conforms with the placement of non-prestressed reinforcement at the maximum height over the supports.

Tendons along and over interior walls should be laid out flat (without profile) at their high point. Continuous wall support eliminates the necessity of profiling a tendon for uplift. Placing the tendon at high point is best suited to resist negative moments typical over wall supports.

Likewise, tendons along exterior walls should be placed flat and anchored at the centroid of the slab in the first span. Tendons should be anchored at the centroid of the slab even if there is a transverse beam or drop cap/panel at the slab edge. Tendons anchored eccentric with respect to the

centroid of a member result in a moment in addition to precompression. The option of eccentric anchoring should be used only if the impact of the added moment is recognized in design.

Similarly, banded tendons along an interior wall may all be placed flat and at their high point, either over or adjacent to the wall. Distributed tendons parallel to an interior wall should be placed flat at their high point over a fraction of their tributary. The remainder of the distributed tendons can be transitioned by gradual modification of their low point to follow the profile of adjacent design strips.

Tendons along continuous exterior walls are generally selected to provide a nominal precompression over the tributary of the exterior wall equal to that used for the rest of the slab. The function of posttensioning in this case is to provide a precompression compatible with the rest of the floor system to improve the in-service performance of the floor system. The preferred tendon layout for two-way slabs is to concentrate the tendons over the supports in one direction (the banded tendons) and distribute them uniformly in the other direction (the distributed tendons). Typically, banded tendons should be placed in the long direction of the slab. This minimizes the number of wedge-shaped regions between the bands where additional reinforcement will be necessary due to insufficient precompression. If the supports in the short direction do not line up, however, place the banded tendons in the orthogonal direction, parallel to one another, making sure that a minimum of two tendons pass over each support as required by ACI 318.

#### 2.5.3.2.8 *Tendon Stressing*

Most engineers in North America design with final effective forces—the posttensioning forces after all prestress losses. The posttensioning supplier determines the number of tendons required to provide the force shown on the structural drawings, based on the effective force of a tendon. The effective force of a tendon is a function of a number of parameters, including the tendon profile, certain properties of the concrete, and the environment. For typical designs, however, a constant force of 27 kip (120 kN) may be assumed for 0.5 in. (12.7 mm) unbonded tendons, provided the following stressing conditions are met:

1. Tendon length (length between anchorages) is less than 240 ft (72 m)
2. Tendons less than 120 ft (36 m) long are stressed at one end
3. Tendons longer than 120 ft but less than 240 ft are stressed at both ends

Tendons that do not meet these conditions may be used, as long as the assumed effective force is lowered to account for the higher friction losses.

#### 2.5.3.2.9 *Cover for Fire Resistance*

When determining fire ratings, designers typically consider the end spans in column-supported structures unrestrained. To achieve fire resistance equal to that of interior spans, provide a larger cover for tendons at the low point of exterior spans unless the end support is a wall or transverse edge beam. Only the first and last spans of tendons along a slab edge are considered as “edge spans.”

### 2.5.3.3 **Building Examples**

The first example shows a two-way posttensioned flat plate system for a residential tower (Figure 2.53). The tendons are ½ in. diameter (12.7 mm) strands that are banded in the north–south direction. Uniformly distributed tendons run from left to right across the building width. Additional tendons are used in the end panels to resist increased moments due to lack of continuity at one end.

As a second example, Figure 2.54 shows the framing plan for a posttensioned band beam–slab system. Shallow beams only 16 in. (0.40 m) deep span across two exterior bays of 40 ft (12.19 m) and an interior bay of 21 ft (6.38 m). Posttensioned slabs 8 in. (203 mm) deep span between the band beams, typically spaced at 30 ft (9.14 m) on center. In the design of the slab, additional beam depth is considered as a haunch at each end. Primary tendons for the slab run across the building width, while the tendons that control the temperature and shrinkage are placed in the north–south direction between the band beams.

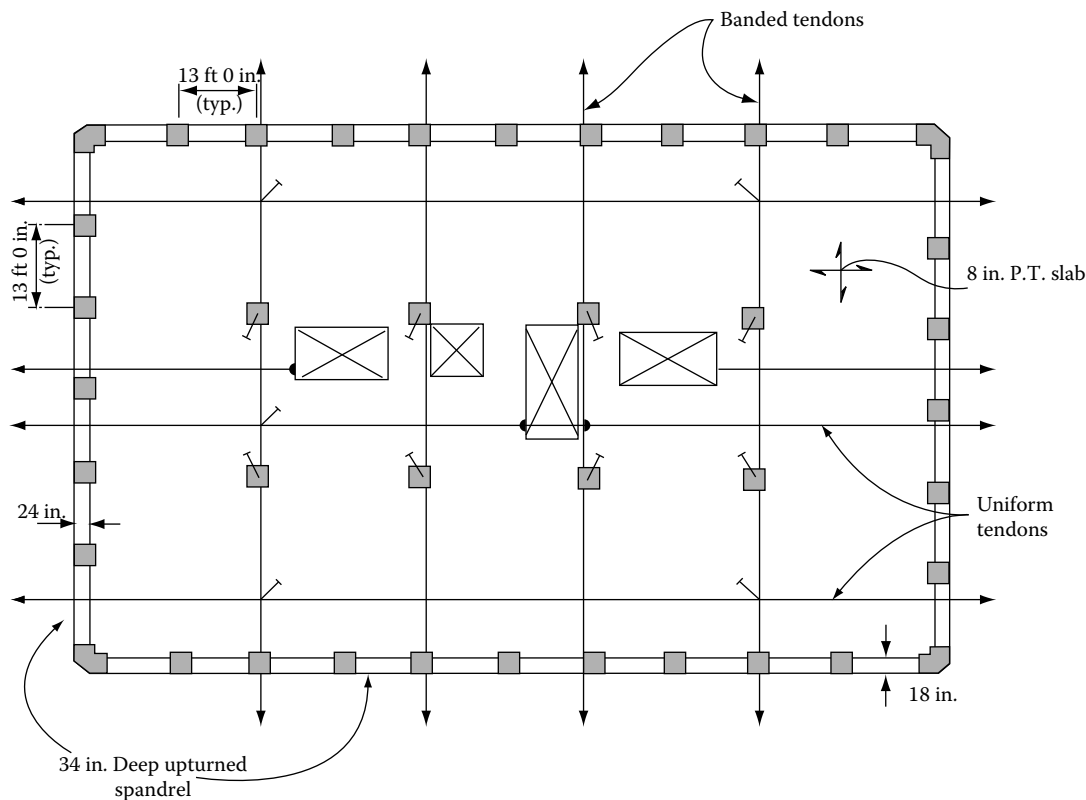


FIGURE 2.53 Two-way posttensioned flat plate system.

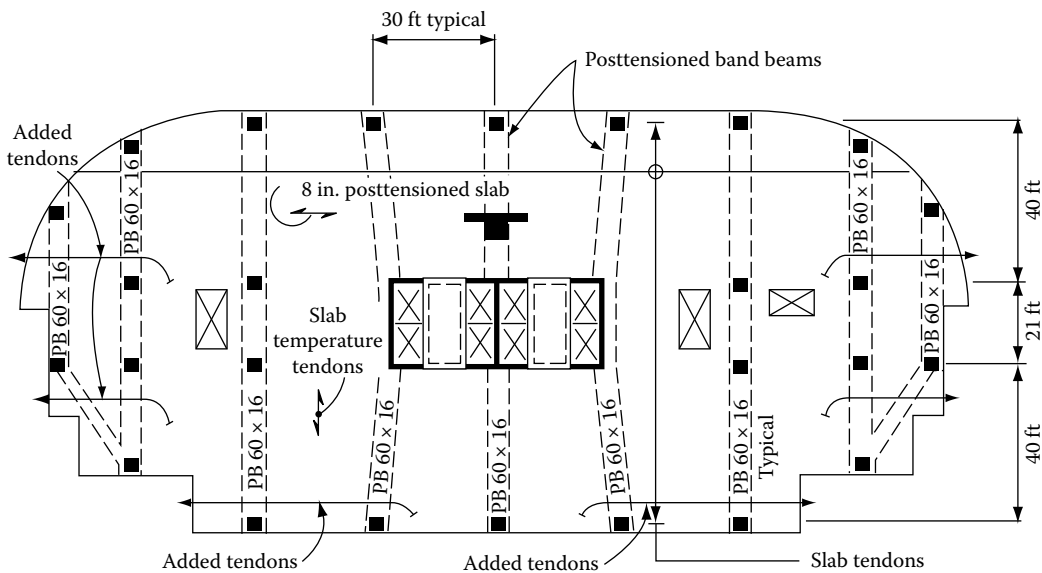


FIGURE 2.54 Band-beam system.

### 2.5.4 CRACKING PROBLEMS IN POSTTENSIONED FLOORS

Cracking caused by restraint to shortening is one of the biggest problems associated with post-tensioned floor systems. The reason is that shortening of a floor state is a time-dependent complex phenomenon. Only subjective empirical solutions exist to predict the behavior.

Shrinkage of concrete is the biggest contributor to shortening in both prestressed and non-prestressed concrete. In prestressed concrete, out of the total shortening, only about 15% is due to elastic shortening and creep. Therefore the problem is not in the magnitude of shortening itself, but in the manner in which it occurs.

When a non-prestressed concrete slab tries to shorten, its movement is resisted internally by the bonded mild steel reinforcement. The reinforcement is put into compression while the concrete is in tension. As the concrete tension builds up, the slab cracks at fairly regular intervals allowing the ends of the slab to remain in the same position they were in while they were cast. In a manner of speaking, the concrete has shortened by about the same magnitude as a posttensioned system, but not in overall dimensions. Instead of the total shortening occurring at the ends, the combined widths of many cracks which occur across the slab make up for the total shortening. The reinforcement distributes the shortening throughout the length of the slab in the form of numerous cracks. Thus reinforced concrete tends to take care of its own shortening problems internally by the formation of numerous small cracks, each small enough to be considered acceptable. Restraints provided by stiff vertical elements such as walls and columns tend to be a minor significance, since provision for total movement had been provided by the cracks in concrete.

This is not the case with posttensioned systems in which shrinkage cracks, which would have formed otherwise, are closed by the posttensioning force. Much less mild steel is present and consequently the restraint to shortening is less. The slab tends to shorten at each end generating large restraining forces in the walls and columns particularly at the ends where the movement is greatest (Figure 2.55). These restraining forces can produce severe cracking in the slab, walls, or columns at the slab extremities, causing problems to engineers and building owners alike. The most serious consequence is perhaps water leakage through the cracks.

The solution to the problem lies in eliminating the restraint by separating the slab from the restraining vertical elements. If a permanent separation is not feasible, cracking can be minimized by using temporary separations to allow enough shortening to occur prior to making the connection.

Cracking in a posttensioned slab also tends to be proportional to initial pour size. Some general guidelines that have evolved over the years are as follows: (1) the maximum length between temporary pour strips (Figure 2.56) is 150 ft (200 ft is restraint due to vertical elements is minimal); and

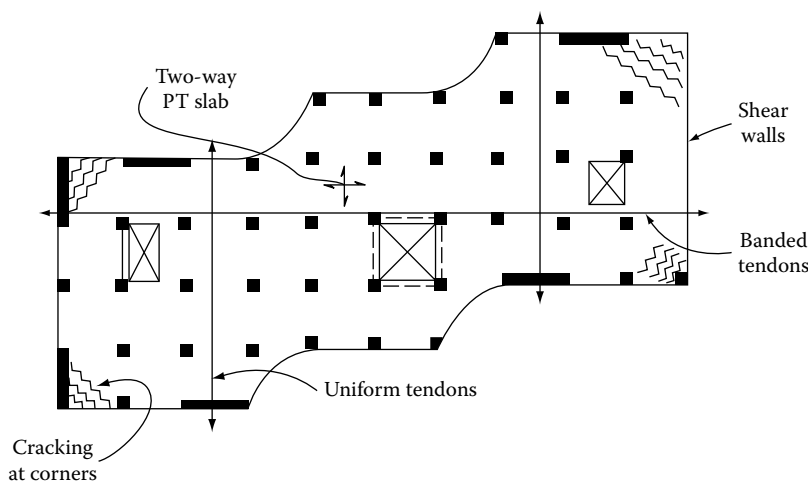
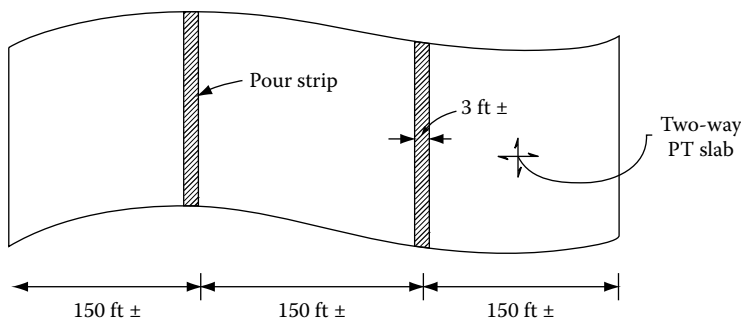


FIGURE 2.55 Cracking in PT slab caused by restraint of perimeter walls.



**FIGURE 2.56** Recommended distance between pour strips. 1. 150 ft  $\pm$  typical. 2. 200 ft  $\pm$  if restraint is minimal. 3. 300 ft  $\pm$  maximum length PT slab irrespective of the number of pour strips.

(2) the maximum length of posttensioned slab irrespective of the number of pour strips provided is 300 ft. The length of time for leaving the pour strips open is critical and can range anywhere from 30 to 60 days. A 30 day period is considered adequate for average restraint conditions with relatively centered, modest length walls, while a 60 day period is more the norm for severe shortening conditions with large pour sizes and stiff walls at the ends.

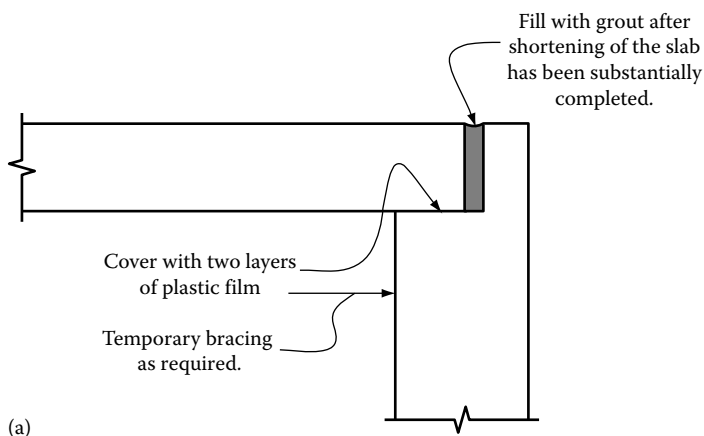
To minimize cracking caused by restraint to shortening, it is a good idea to provide a continuous mat of reinforcing steel in both directions of the slab. As a minimum, one layer of #4 bars placed at mid-depth of slab, at 36 in. on center both ways is recommended for typical conditions. For slab pours in excess of 150 ft in length with relatively stiff walls at the ends, the minimum reinforcement should be increased to #4 bars at 24 in. on centers both ways.

Methods of minimizing adverse effects of slab shortening are shown schematically in Figure 2.57.

### 2.5.5 CUTTING OF PRESTRESSED TENDONS

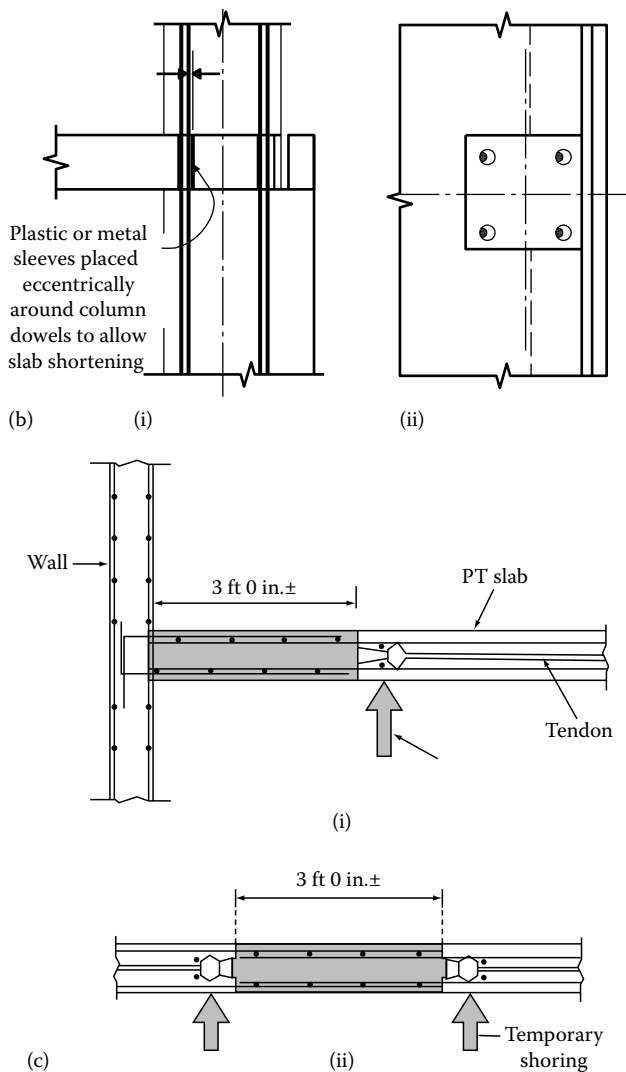
One of the main drawbacks of posttensioned systems is the difficulty of dealing with stressed stands and tendons during structure modifications or demolition. Although modifications are more difficult, some procedures have been developed to make this process easier.

Small penetrations required to meet changes to plumbing or similar requirements are the most common of all modifications that are made to the floor system. The size of these penetrations is typically from 5 to 10 in. (125 to 250 mm) in diameter. As a posttensioned floor relies on the posttensioned tendons for its strength, it is preferable to avoid cutting the tendons when drilling through the floor for the new penetration. Finding the tendons in a floor to permit the location of penetrations without damaging any



**FIGURE 2.57** Method of minimizing restraining forces: (a) temporary sliding joint,

(continued)



**FIGURE 2.57 (continued)** (b) sleeves around rebar dowels, (i) section and (ii) plan, and (c) temporary pour strips: (i) at perimeter of building; (ii) at interior of slab.

tendons is very simple procedure that is carried out with the aid of an electronic tendon locator. Tendons are accurately located using this system without any need to remove floor coverings or ceilings.

In a typical posttensioned floor it is possible to locate penetrations of up to 3 in.  $\times$  9 in. (1000 mm  $\times$  3000 mm) between posttensioned tendons and to require no other modification to the floor. Penetrations that require cutting of the posttensioned tendons will need to be checked and designed as would any large penetration in any floor system. The procedure commonly adopted in a floor using bonded tendons is as follows:

1. Design the modified floor structure in the vicinity of the penetration, assuming that the cut posttensioned tendons are dead-ended at the penetration.
2. Install any strengthening required.
3. Locate tendons and inspect grouting.
4. If there is no doubt as to the quality of the grouting, proceed to step 5. Otherwise strip off ducting, clean out grout, and epoxy grout the strands over a length of 20 in. (500 mm) immediately adjacent to the penetration.

5. Install shoring.
6. Core drill the corners of the penetration to eliminate the need for overcutting, and then cut the perimeter using a diamond saw.
7. Cut up the slab and remove.
8. Paint an epoxy-protective coating over the ends of the strands to prevent corrosion.
9. Remove shoring.

If a large penetration through a floor cannot be located within the slab area but must intersect a primary support beam, then substantial strengthening of adjacent beams will usually be necessary.

When cutting openings into floors built using unbonded posttensioned tendons the procedures used for bonded posttensioned tendons cannot be applied. The preferred procedure that has been developed to permit controlled cutting of unbonded strands is to use a special detensioning jack. The jack grips the strand, which is to be cut, with the force in the strands being released slowly. New anchorages are then installed at each side of the new opening and the strands are restressed.

Extensive experience has been gained in demolition procedures for posttensioned floors, and some general comments can be made. In bonded systems the procedure for demolition are the same as for reinforced concrete. The individual strands will not dislodge at stressing anchorages. In unbonded systems the strand capacity is lost over its entire length when cut; therefore the floor will require back shoring during demolition. The individual cut strands will dislodge at stressing anchorages, but will move generally less than 450 mm (18 in). However, precautions should always be taken in case the strands move more than this.

### 2.5.6 CONCEPT OF SECONDARY MOMENTS

In a prestressed statically determinate beam, such as a single-span simply supported beam, the moment  $M_p$  due to prestress is given by the eccentricity  $e$  of prestress multiplied by the prestress  $P$ . In prestressed design, the moment  $M_p = Pe$  is commonly referred to as the primary moment. In a simple beam or any other statically determinate beam, no support reactions can be induced by prestressing. No matter how much the beam is prestressed, only the internal stresses will be affected by the prestressing. The external reactions, being determined by statics, will depend on the dead and live loads, but are not affected by the prestress. Thus there are no secondary moments in a statically determinate beam. The total moment in the beam due to prestress is simply equal to the primary moment  $M_0 = Pe$ .

The magnitude and nature of secondary moments may be illustrated by considering a two-span, continuous, prismatic beam that is not restrained by its supports but remains in contact with them. Consider the beam is prestressed with a straight tendon with force  $P$  and eccentricity  $e$  (see Figure 2.58).

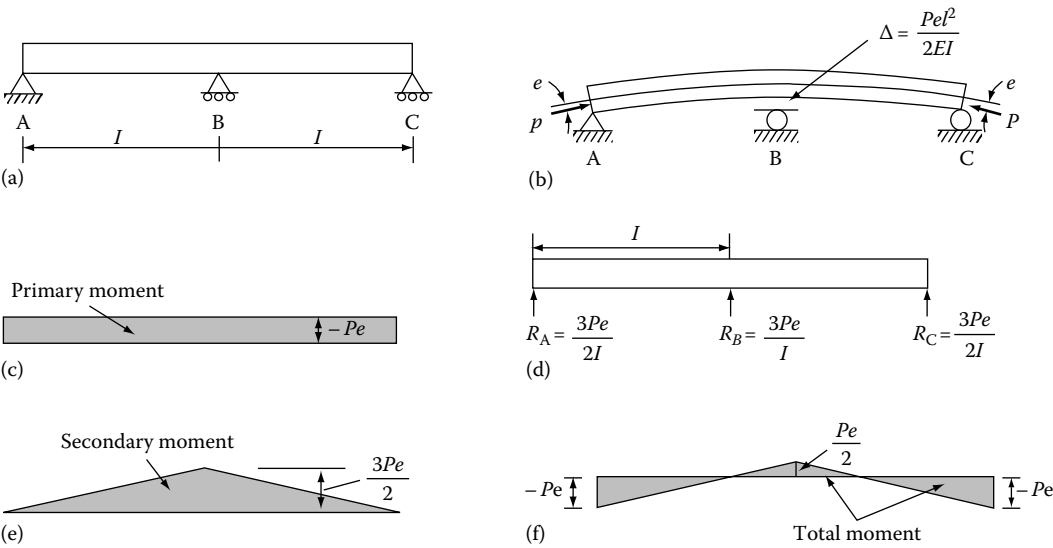
When the beam is prestressed, it bends and deflects upwards. The bending of the beam can be such that the beam will tend to deflect itself away from B. Because the beam is restrained from deflection at B, a vertical reaction must be exerted to the beam to hold it there. The induced reaction produces secondary moments in the beam. These are called secondary because they are by-products of prestressing and do not exist in a statically determinate beam. However, the term secondary is misleading because the moments are secondary in nature, but not necessarily in magnitude.

One of the principal reasons for determining the magnitude of secondary moments is because they are required in the computations of ultimate flexural strength. An elastic analysis of a prestressed beam offers no control over the failure mode or the factor of safety. To assure that prestressed members will be designed with an adequate factor of safety against failure, ACI 318-08 like its predecessors, requires that  $M_u$ , the moment due to factored service loads including secondary moments, must not exceed  $\phi M_n$ , the flexural design strength of the member. The ultimate factored moment  $M_u$  is calculated by the following load combinations:

$$M_u = 1.2M_D + 1.6M_L + 1.0M_{sec}$$

Since the factored load combination must include the effects due to secondary moments, its determination is necessary in prestress designs.





**FIGURE 2.58** Concept of secondary moments: (a) two-span continuous beam, (b) vertical upward displacement due to PT, (c) primary moment, (d) reactions due to PT, (e) secondary moment, and (f) final moments.

To further enhance our understanding of secondary moments, three numerical examples are given here:

1. A two-span continuous beam with a prestressed tendon at a constant eccentricity  $e$ .
2. The same beam as in the preceding example except the tendon is parabolic between the supports. There is no eccentricity of the tendon at the supports.
3. The same as in example 2, but the tendon has an eccentricity at the center support.

**2.5.6.1 Secondary Moment Design Examples**

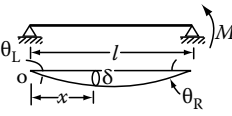
**Example 1**

**Given:** A two-span prestressed beam with a tendon placed at a constant eccentricity  $e$  from the C.G. of the beam. The prestress in the tendon is equal to  $P$  (see Figure 2.58).

**Required:** Secondary moments in the beam due to prestress  $P$ .

**Solution:** The beam is statically indeterminate to the first degree because it is continuous at the center support B. It is rendered determinate by removing the support at B. Due to the moments  $M_0 = Pe$  at the ends, the beam bends and deflects upward. The magnitude of vertical deflection  $\delta_B$  due to moment  $M_0$  is calculated using standard beam formulas such as the one that follows.

**Beam Deflection Formula:**

Type of Load	Slope as Shown	Maximum Deflection	Deflection Equation
Simply supported beam		Bending moment applied at one end	
	$\theta_L = \frac{Ml}{6EI}$	$\delta = \frac{Ml^2}{9\sqrt{3}EI}$	$\delta = \frac{Mlx}{6EI} \left( 1 - \frac{x^2}{l^2} \right)$
	$\theta_R = \frac{Ml}{3EI}$	at $x = l/\sqrt{3}$	

In our case, moment  $M$  is applied at both ends. Therefore

$$\begin{aligned}\delta &= \frac{Mlx}{3EI} \left( 1 - \frac{x^2}{l^2} \right) \\ \delta_{in} &= \frac{Ml \times l}{3EI \times 2} \left( 1 - \frac{l^2}{4l^2} \right) \\ &= \frac{Ml^2}{8EI}\end{aligned}$$

Consider the example problem,  $l = 2L$ .

$$\begin{aligned}\text{Therefore, deflection } \delta_B \text{ at support B} &= \delta_L = \frac{M \times (2L)^2}{8EI} \\ &= \frac{ML^2}{2EI}\end{aligned}$$

Since the beam is restrained from deflecting upward at B, a downward reaction  $R_{B,sec}$  must be exerted to the beam to hold it there. The reaction  $R_{B,sec}$  is given by

$$\begin{aligned}\delta_B &= \frac{R_{B,sec}(2L)^3}{48EI} \\ R_{B,sec} &= \frac{48EI}{(2L)^3} \delta_B \\ &= \frac{48EI}{(2L)^3} \times \frac{M_0 L^2}{2EI} \\ &= \frac{3M_0}{L}\end{aligned}$$

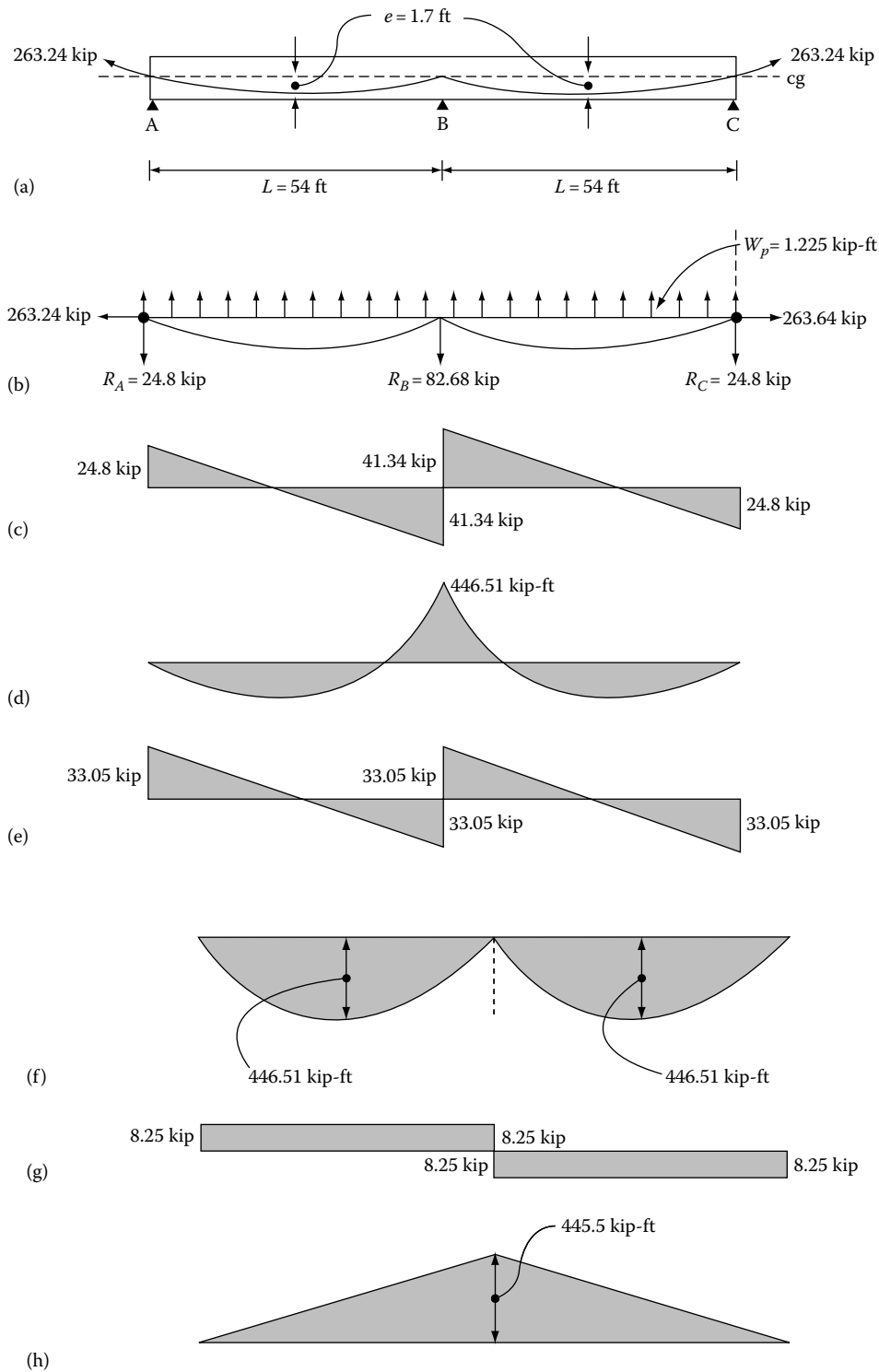
The secondary moment induced due to the reaction  $R_{B,sec}$  at the support B is given by

$$\begin{aligned}M_{B,sec} &= R_{B,sec} \times \frac{2L}{4} \\ &= \frac{3M_0}{L} \times \frac{2L}{4} \\ &= \frac{3}{2} M_0\end{aligned}$$

Observe that in this example, the secondary moment at B = 150% of the primary moment due to prestress. The secondary moment is thus secondary in nature, but not in magnitude.

### Example 2A

**Given:** The two-span prestressed concrete beam shown in Figure 2.59 has a parabolic tendon in each span with zero eccentricity at the A and C ends, and at the center support B. Eccentricity of the tendon at the center of each span = 1.7 ft. The prestress force  $P = 263.24$  kip.



**FIGURE 2.59** Secondary moment example 2A: (a) Two-span continuous prestressed beam, (b) equivalent loads due to prestress, consisting of upward load, horizontal compression due to prestress  $W_p$  and downward loads at A, B, and C, (c) shear force diagram, statically indeterminate beam, (d) moment diagram, statically indeterminate beam, (e) primary shear force diagram, (f) primary moment diagram, and (h) secondary moments.

**Required:** Secondary reactions and moments.

**Solution:** The approach here is similar to that typically used in commercially available computer programs. However, in the computer programs, statically indeterminate structures such as the example problem are typically analyzed using a stiffness matrix approach. Here we take the easy street: We use beam formulas to analyze the two-span continuous beam. It should be noted that the analysis could be performed using other classical methods such as the moment distribution method or slope-deflection method.

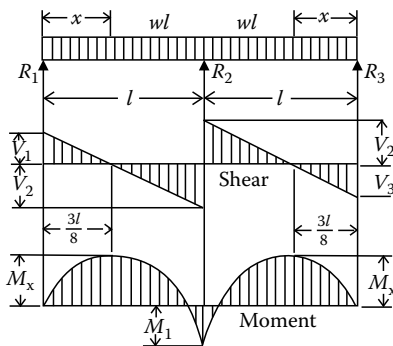
First, we determine the equivalent load due to prestress  $P = 263.24$  kip acting at eccentricity  $e = 1.7$  ft at the center of the two spans. The equivalent load consists of (1) an upward uniformly distributed load  $W_p$  due to drape in the tendon; (2) a horizontal compression  $P$  equal to 263.24 kip at the ends; (3) downward loads at A, B, and C to equilibrate the upward load  $W_p$ ; and (4) additional reactions at A, B, and C due to the restraining effect of support at B. The last set of loads need not be considered for this example, because the loads are implicitly included in the formulas for the statically indeterminate beam.

Of the equivalent loads shown in Figure 2.59b only the uniformly distributed load  $W_p$  corresponding to  $P$  acting at eccentricity  $e$  induces bending action in the beam.  $W_p$  is determined by the relation

$$\begin{aligned}
 Pe &= \frac{W_p L^2}{8} \\
 W_p &= \frac{Pe \times 8}{L^2} \\
 &= \frac{263.24 \times 1.7 \times 8}{54^2} \\
 &= 1.227 \text{ kip-ft}
 \end{aligned}$$

Having determined the equivalent loads, we can proceed to determine the bending moments in our statically indeterminate beam, as for any continuous beam. As mentioned earlier, we use the formulas for continuous beams given in standard textbooks. One such formula follows.

#### Continuous beam with two equal spans and uniform load on both spans



$$R_1 = V_1 = R_3 = V_3 = \frac{3}{8} wl$$

$$R_2 = 2V_2 = \frac{10}{8} wl$$

$$V_2 = \frac{5}{8} wl$$

$$M_x = R_1 X - \frac{wX^2}{2}$$

$$M_x \left( \text{at } X = \frac{3l}{8} \right) = \frac{9}{128} wl^2$$

$$M_1 \text{ (at support } R_2) = -\frac{wl^2}{8}$$

$$\Delta_{\text{Max.}} (0.4215l \text{ from } R_1 \text{ or } R_3) = wl^2/185EI$$

$$\Delta_x = \frac{wX}{48EI} (l^3 - 3l^2 + 2X^3)$$

In our case,  $w = W_p = 1.225$  kip-ft,  $l = L = 54$  ft. Therefore

$$\begin{aligned}
 V_1 &= \frac{3}{8} W_p L \\
 &= \frac{3}{8} \times 1.225 \times 54 \\
 &= 24.8 \text{ kip} \\
 V_2 &= \frac{5}{8} W_p L \\
 &= \frac{5}{8} \times 1.225 \times 54 \\
 &= 41.34 \text{ kip} \\
 M_1 = M_B &= \frac{W_p L^2}{8} = \frac{1.225 \times 54^2}{8} = 446.50 \text{ kip-ft}
 \end{aligned}$$

The shear force and bending moment diagrams are shown in Figure 2.59c and d.

Since the formulas account for the beam continuity, the resulting shear force and bending moments shown in Figure 2.59c and d include the effect of secondary moments. The resulting moment due to prestress, then, is the algebraic sum of the primary and secondary moments. Once the resulting moments are determined, the secondary moments can be calculated by the relation

$$M_{\text{bal}} = M_p + M_{\text{sec}}$$

where

$M_{\text{bal}}$  is the resulting moment, also referred to as the total moment in the redundant beam due to equivalent loads

$M_p$  is the primary moment that would exist if the beam were a statically determinate beam ( $M_p$  is given by the eccentricity of the prestress multiplied by the prestress.)

$M_{\text{sec}}$  is the secondary moment due to redundant secondary reactions

With the known primary moment acting on the continuous beam, the secondary moment caused by induced reactions can be computed from the relation

$$M_{\text{sec}} = M_{\text{bal}} - M_p$$

A similar equation is used to calculate the shear forces.

The resulting secondary shear forces and bending moments are shown in Figure 2.59g and h, while the primary shear forces and bending moments are shown in Figure 2.59e and f.

### Example 2B

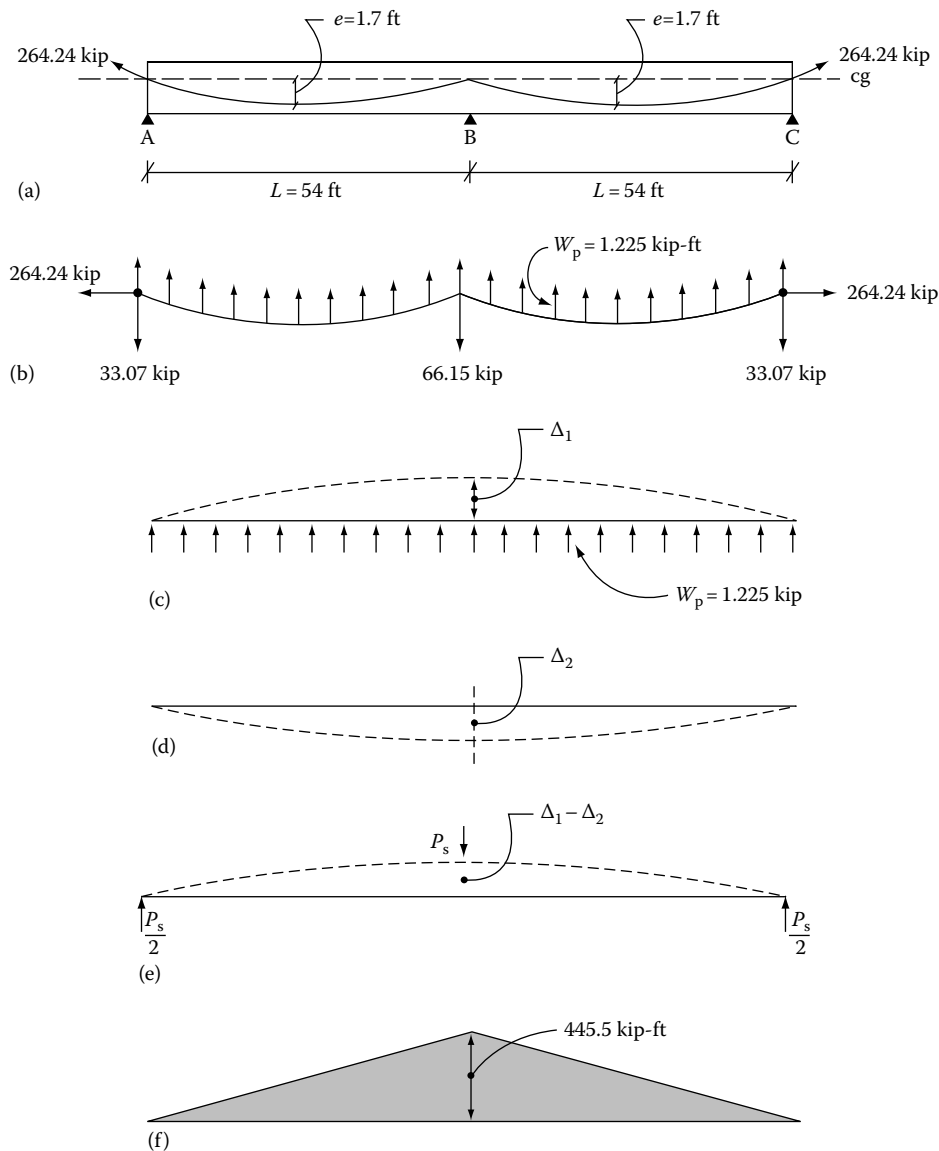
**Compatibility Method:** To firm up our concept of secondary reactions and moments, perhaps it is instructive to redo the previous example using a compatibility approach. In this method the beam is rendered statically determinate by removing the redundant reaction at B. The net vertical deflection (which happens to be upward in our case) is calculated at B due to  $W_p = 1.225$  kip-ft acting upward and a vertical downward load  $= 1.225 \times 54 = 66.15$  kip acting downward at B. Observe that the reaction at B, along with those at A and C, equilibrates the vertical load of 1.225 kip-ft action on the tendon in its precise profile but does not necessarily guarantee compatibility at B.

**Given:** A two-span continuous beam analyzed previously, shown again for convenience in Figure 2.60.

**Required:** Secondary moments and shear forces using a compatibility approach.

**Solution:** The equivalent loads required to balance the effect of prestressed, draped tendons are shown in Figure 2.60b. As before,  $W_p = 1.225$  kip-ft. However, the reactions at A, B, and C do not include those due to secondary effects. The reactions are in equilibrium with load  $W_p$  and do not necessarily assure continuity of the beam at support B. (If continuity were established, their magnitudes would have been the same as calculated in the previous example.)

In determining the equivalent loads, we have not considered the effect of continuity at support B. Therefore, the beam has a tendency to move away from the support due to the upward-acting equivalent



**FIGURE 2.60** Secondary moment: Compatibility method: Example 2B. (a) two-span continuous beam, (b) equivalent loads, (c) upward deflection  $\Delta_1$  due to  $W_p$ , (d) downward deflection  $\Delta_2$  due to a load of  $66.15$  kip at center span, (e) load  $P_s$  corresponding to  $\Delta_1 - \Delta_2$ , and (f) secondary moments.

loads. Because the beam, by compatibility requirements, stays attached to support B, another set of reactions is needed to keep the beam in contact with support B. These are the secondary reactions, and the resulting moments are the secondary moments. Of the loads shown in Figure 2.58 only the upward load  $W_p = 1.225$  kip-ft and the downward reaction  $R_B = 66.15$  kip influence the vertical deflection at B. The upward deflection of the beam at B due to  $W_p$  is given by the standard formula

$$\Delta_{up} = \frac{5wl^4}{385EI} \quad (\text{see Figure 2.60c})$$

In our case,  $w = W_p = 1.225$  kip-ft,  $l = 2 \times 54 = 108$  ft. Therefore

$$\begin{aligned} \Delta_{up} &= \frac{5 \times 1.225 \times 108^4}{385EI} \\ &= \frac{2,170,050}{EI} \quad \uparrow \text{ upward} \end{aligned}$$

The downward deflection at B due to reaction  $R_B$  is given by

$$\Delta_{down} = \frac{R_B L^3}{48EI}$$

In our case  $R_B = 66.15$  kip,  $L = 108$  ft

$$\begin{aligned} \Delta_{down} &= \frac{66.15 \times 108^3}{48EI} \\ &= \frac{1,736,040}{EI} \quad \downarrow \text{ downward} \quad (\text{see Figure 2.60d}) \end{aligned}$$

The net deflection at B

$$\Delta_B = \frac{2,170,050 - 1,736,040}{EI} = \frac{434,010}{EI} \quad \uparrow \text{ upward} \quad (\text{see Figure 2.60e})$$

Because the beam is attached to support B, for compatibility the vertical deflection at B should be zero. This condition is satisfied by imposing a vertically downward secondary reaction  $R_{B,sec}$  at B given by the relation

$$\begin{aligned} \frac{R_{B,sec} \times 108^3}{48EI} &= \frac{434,010}{EI} \\ R_{B,sec} &= 16.54 \text{ kip} \end{aligned}$$

The resulting secondary reactions and moments shown in Figure 2.60f are exactly the same as calculated previously.

### Example 2C

**Given:** Same data as in Example 2B. The only difference is that the tendon at the center support B has an eccentricity of 0.638 ft.

**Required:** Secondary moments using a compatibility analysis.

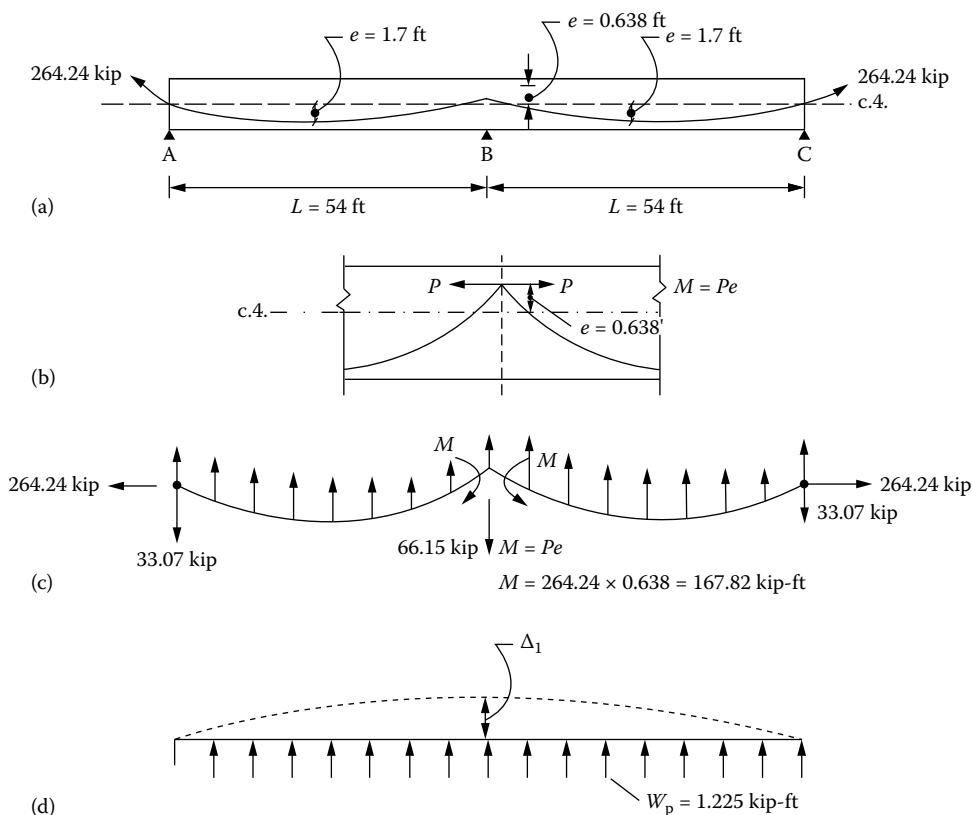
**Solution:** The equivalent loads balancing the effects of prestressed, draped tendons with eccentricities at the centers of spans and at the interior support B are shown in Figure 2.61.

Notice the two equal and opposite moments equal to the prestress of 264.24 kip times the eccentricity of 0.638 ft at the center support (see Figure 2.61b and c). The solution follows the same procedure as used in the previous example, except that we include the effect of moments at B in deflection calculations.

As before,  $W_p = 1.23$  kip-ft. Upward deflection at B due to  $W_p$  is given by

$$\begin{aligned}\Delta_{up} &= \frac{5}{384} \frac{W_p (2L)^4}{EI} \\ &= \frac{5 \times 1.23 \times (2 \times 54)^4}{384 \times EI} \\ &= \frac{2,170,050}{EI} \uparrow \text{ upward (see Figure 2.61d)}\end{aligned}$$

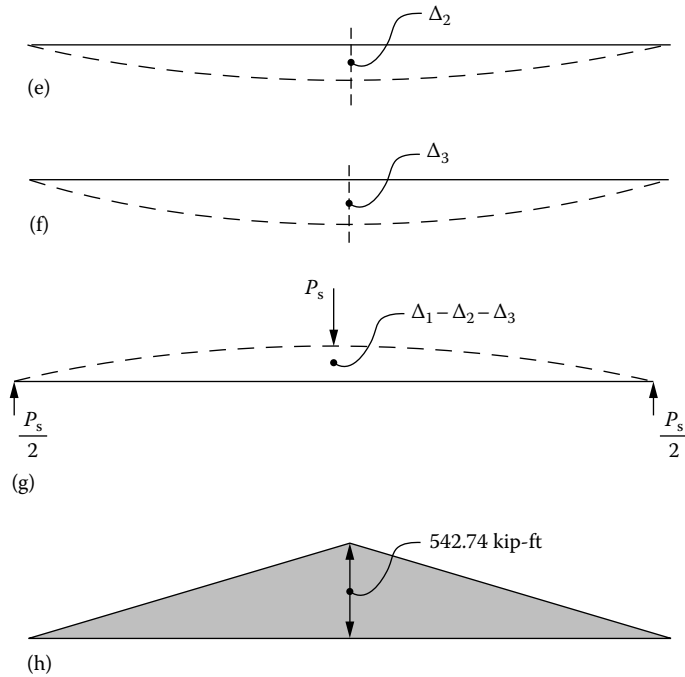
The vertical reaction  $R_B$  at B to maintain vertical equilibrium is equal to  $1.23 \times 54 = 66.42$  kip. The downward deflection at B due to this load is



**FIGURE 2.61** Secondary moment: Example 2C: (a) two-span continuous beam, (b) equivalent moment  $M = Pe$  at center of span, (c) equivalent loads and moments, (d) upward deflection  $\Delta_1$  due to  $W_p$ ,

(continued)





**FIGURE 2.61 (continued)** (e) downward deflection  $\Delta_2$  due to a load of 66.15 at center of span, (f) downward deflection  $\Delta_3$  due to moments  $M = Pe$  at center of span, (g) load  $P_s$  corresponding to  $\Delta_1 - \Delta_2 - \Delta_3$ , and (h) secondary moments.

$$\begin{aligned}
 \Delta_{\text{down}, R_B} &= \frac{R_B \times (54 \times 2)^3}{48EI} \\
 &= \frac{66.42 \times (108)^3}{48EI} \\
 &= \frac{1,743,126}{EI} \quad \downarrow \text{downward} \quad (\text{see Figure 2.61e})
 \end{aligned}$$

In addition to the upward and downward deflections at B, there is a third component to the vertical deflection due to the moment at B =  $263.24 \times 0.638 = 167.95$  kip-ft.

For purposes of deflection calculations, moment  $M_B$  at B may be replaced by an equivalent point load equal to  $\frac{2M_B}{L}$ .

The downward deflection at B due to  $M_B$ , then, is

$$\begin{aligned}
 \Delta_{\text{down}, M_B} &= \frac{2M_B \times (2L)^3}{L48EI} \\
 &= \frac{M_B L^2}{3EI} \quad (\text{see Figure 2.61f})
 \end{aligned}$$

For the example,  $M_B = 167.95$  kip-ft,  $L = 54$  ft

$$\begin{aligned}\Delta_{\text{down}, M_B} &= \frac{167.95 \times 54^2}{3EI} \\ &= \frac{163,150}{EI} \quad \downarrow \text{ downward}\end{aligned}$$

The net upward deflection due to  $W_p$ ,  $R_B$ , and  $M_B$  is

$$\frac{1}{EI}(2,170,050 - 1,43,126 - 163,150) = \frac{263,774}{EI} \quad \uparrow \text{ upward} \quad (\text{see Figure 2.61g})$$

The secondary reaction to establish vertical compatibility at B is given by

$$\begin{aligned}\frac{R_{B,\text{sec}} \times (2L)^3}{48EI} &= \frac{263,774}{EI} \\ R_{B,\text{sec}} &= \frac{48 \times 263,774}{(2 \times 54)^3} = 10.05 \text{ kip}\end{aligned}$$

The secondary moments due to this redundant reaction are shown in Figure 2.61h.

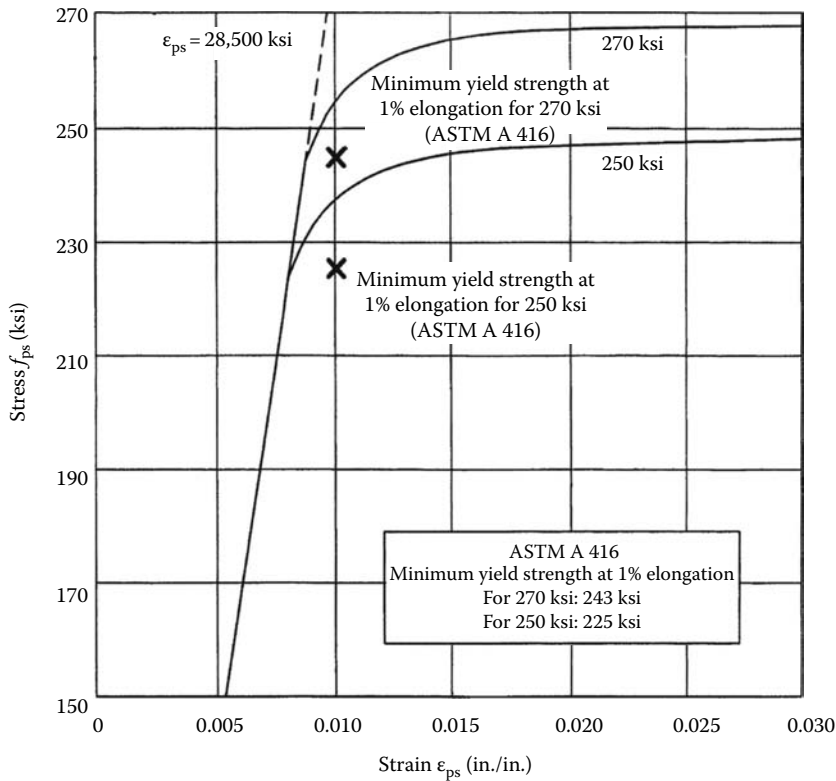
### 2.5.7 STRENGTH DESIGN FOR FLEXURE

In the design of prestress members it is not enough to limit the maximum values of tensile and compressive stresses within the permitted values at various loading stages. This is because although such a design may limit deflections, control cracking, and prevent crushing of concrete, an elastic analysis offers no control over the ultimate behavior or the factor-of-safety of a prestressed member. To ensure that prestressed members will be designed with an adequate factor-of-safety against failure, ACI 318-08, similar to its predecessors, requires that  $M_u$ , the moment due to factored service loads, not exceed  $\phi M_n$ , the flexural design strength of the member.

The nominal bending strength of a prestressed beam with bonded tendons is computed in nearly the same manner as that of a reinforced concrete beam. The only difference is in the method of stress calculation in the tendon at failure. This is because the stress-strain curves of high-yield-point steels used as tendons do not develop a horizontal yield range once the yield strength is reached. It continues upward at a reduced slope. Therefore, the final stress in the tendon at failure  $f_{ps}$  must be predicted by an empirical relationship.

The method of computing the bending strength of a prestressed beam given in the following section applies only to beams with bonded tendons. The analysis is performed using strain compatibility. Because by definition there is no strain compatibility between the tendon and concrete in an unbonded prestressed beam, this method cannot be used for prestressed beams with unbonded tendons; the empirical approach given in ACI 318-05/08, Section 18.7 is the recommended method.

The procedure for bonded tendons consists of assuming the location of the neutral axis, computing the strains in the prestressed and non-prestressed reinforcement, and establishing the compression stress block. Knowing the stress-strain relationship for the reinforcement and assuming that the maximum strain in concrete is 0.003, the forces in the prestressed and non-prestressed reinforcement are determined and the sum of compression and tension forces are computed. If necessary, the neutral axis location is adjusted on a trial-and-error basis until the sum of the forces is zero. The moment of these forces is then computed to obtain the nominal strength of the section. To compute the stress in the prestressing strand, the idealized curve shown in Figure 2.62 is used.



**FIGURE 2.62** Idealized stress–strain curve. (Adapted from *Posttensioning Concrete Institute Design Handbook*, 5th Edn.) Typical stress–strain curve with seven-wire low-relaxation prestressing strand. These curves can be approximated by the following equations:

<p>250 ksi</p> $\epsilon_{ps} \leq 0.0076: f_{ps} = 28,500 \epsilon_{ps} \text{ (ksi)}$ $\epsilon_{ps} > 0.0076: f_{ps} = 250 - \frac{0.04}{\epsilon_{ps} - 0.0064} \text{ (ksi)}$	<p>270 ksi</p> $\epsilon_{ps} \leq 0.0086: f_{ps} = 28,500 \epsilon_{ps} \text{ (ksi)}$ $\epsilon_{ps} > 0.0086: f_{ps} = 270 - \frac{0.04}{\epsilon_{ps} - 0.007} \text{ (ksi)}$
--	---

The analysis presented here follows a slightly different procedure than explained above. Instead of assuming the location of the neutral axis, we assume a force in the prestressing strand, and compare it to the derived value. The analysis is continued until the desired convergence is reached.

### 2.5.7.1 Strength Design Examples

#### 2.5.7.1.1 Example 1

**Given:** A rectangular prestressed concrete beam, as shown in Figure 2.63.

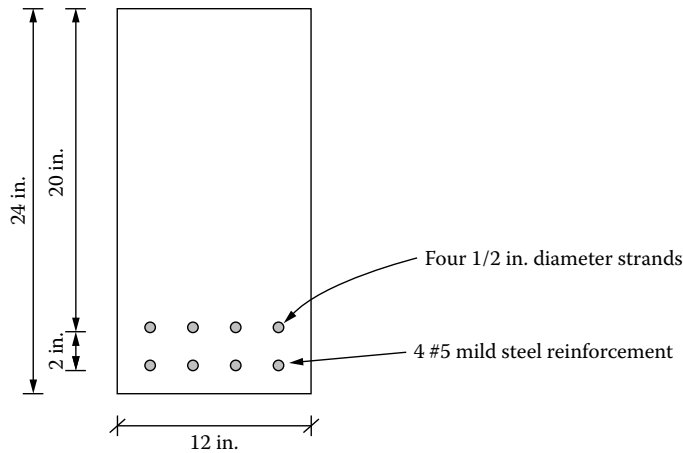
$$f'_c = 5000 \text{ psi}$$

Mild steel reinforcement = 4 #5 bars at bottom,  $f_y = 60 \text{ ksi}$

Prestressed strands = Four ½ in.  $\phi$ ,  $f_{ps} = 270 \text{ ksi}$

**Required:** Ultimate flexural moment capacity of the beam

**Solution:** A trial-and-error procedure is used.



**FIGURE 2.63** Strength design example 1: beam section.

### First Trial

For the first trial, assume the stress in the prestressed strands = 250 ksi and the yield stress in the mild steel is 60 ksi.

The total tension  $T$  at the tension zone of the beam consists of  $T_1$ , the tension due to prestressed strands, plus  $T_2$ , the tension due to mild steel reinforcement.

$$\text{Thus } T = T_1 + T_2$$

$$T_1 = \text{area of stands} \times \text{assumed stress in prestressing steel}$$

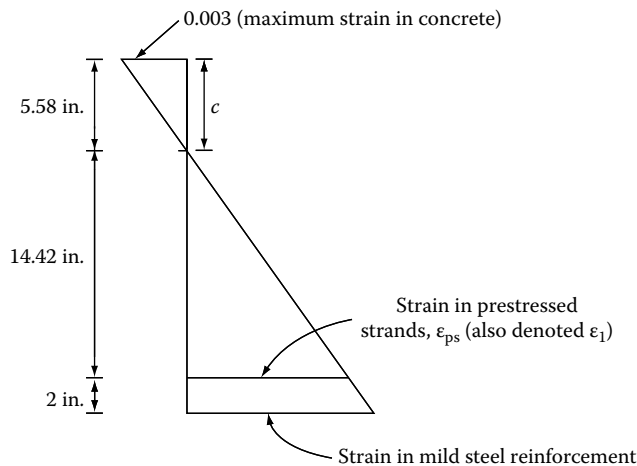
$$= 4 \times 0.153 \times 250 = 153 \text{ kip}$$

$$T_2 = \text{area of mild steel reinforcement} \times \text{yield stress}$$

$$= 4 \times 0.31 \times 60 = 74.40 \text{ kip}$$

$$T = 153 + 74.40 = 227.4 \text{ kip}$$

Draw a strain diagram for the beam at the nominal moment strength defined by a compressive strain of 0.003 at the extreme compression fiber. Using the strain diagram, find the compressive force  $C = 0.85 f'_c ab$ . See Figure 2.64.



**FIGURE 2.64** Example 1: strain diagram, first trial.

$$C = T = 227.4 \text{ kip}$$

$$a = \frac{227.4}{0.85 f'_c b}$$

$$= \frac{227.4}{0.85 \times f'_c \times 12} = 4.46 \text{ in.}$$

$$c = \frac{a}{\beta_1} \quad \beta_1 = 0.8 \quad \text{for } f'_c = 5 \text{ ksi}$$

$$= \frac{4.46}{0.8} = 5.58 \text{ in.}$$

Compute the strain in the prestressing steel and the corresponding stress.

$$\frac{0.003}{5.58} = \frac{\epsilon_1}{14.42}$$

$$\epsilon_1 = 0.00775$$

Since the strain = 0.00775, the corresponding stress is in the elastic region of the stress–strain curve. See Figure 2.62. The stress in the prestressed strand is given by

$$f_{ps} = 28500 \times \epsilon_1$$

$$= 28500 \times 0.00775 = 221 \text{ ksi}$$

$$T_1 = 4 \times 0.153 \times 221 = 135.4 \text{ kip}$$

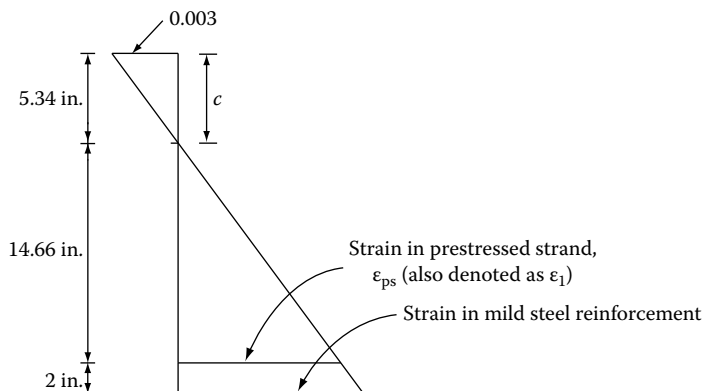
$$T_2 = 74.40 \text{ kip as before}$$

$$T = T_1 + T_2 = 135.4 + 74.40 = 209.8 \text{ kip}$$

Comparing this to  $T = 227.4 \text{ kip}$ , by inspection we estimate that an improved value of  $T = C =$  average of the two values.

$$= (227.4 + 209.8)/2 = 218.6 \text{ kip, say, 218 kip}$$

Use this value for the second trial. See Figure 2.65.



**FIGURE 2.65** Example 1: strain diagram, second trial.

**Second Trial**

$$C = T = 218 \text{ kip}$$

$$a = \frac{218}{0.85f'_c b} = \frac{218}{0.85 \times 5 \times 12} = 4.27 \text{ in.}$$

$$c = \frac{a}{\beta_1} = \frac{4.27}{0.8} = 5.34 \text{ in.}$$

$$\frac{0.003}{5.34} = \frac{\epsilon_1}{14.66}$$

$$\epsilon_1 = 0.0082 < 0.0086$$

Therefore

$$f_{ps} = 28500 \times 0.00824 \quad (\text{see Figure 2.62})$$

$$= 234.7 \text{ kip}$$

$$T_1 = 4 \times 0.153 \times 234.7 = 143.7$$

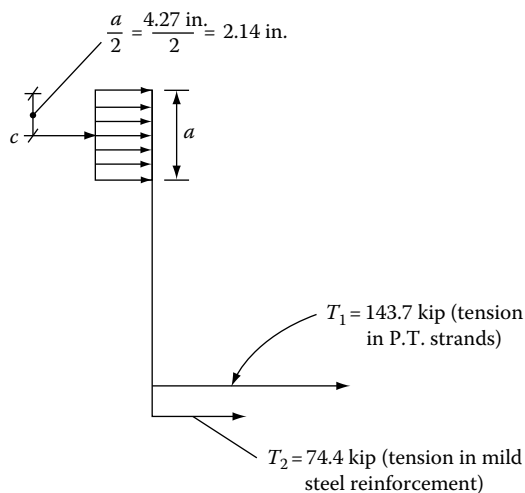
$$T = 143.7 + 74.4 = 218.1 \text{ kip}$$

This is practically the same as the value we assumed in the second trial. Therefore  $T = 218 \text{ kip}$  may be used to compute the flexural strength of the beam.

**Flexural Strength:** The nominal moment strength is obtained by summing the moments of  $T_1$  and  $T_2$  about the C.G. of compressive force  $C$  (see Figure 2.66).

$$M_n = 74.4 \times (22 - 2.14) + 143.7(20 - 2.14)$$

$$= 4044 \text{ kip-in} = 337 \text{ kip-ft}$$



**FIGURE 2.66** Example 1: force diagram.

$$\begin{aligned}
 \text{Usable capacity of the beam} &= \phi M_n \\
 &= 0.9 \times 337 \text{ kip-ft} \\
 &= 303.3 \text{ kip-ft}
 \end{aligned}$$

### 2.5.7.1.2 Example 2

**Given:** Same data as for example 1, except three  $\frac{1}{2}$  in.  $\phi$  strands are used instead of four  $\frac{1}{2}$  in.  $\phi$  strands. This example illustrates the calculation of stress in the strand in the nonelastic range of the stress-strain curve shown in Figure 2.62.

**Required:** Ultimate flexural capacity of the beam.

**Solution:** As before, we use a trial-and-error procedure.

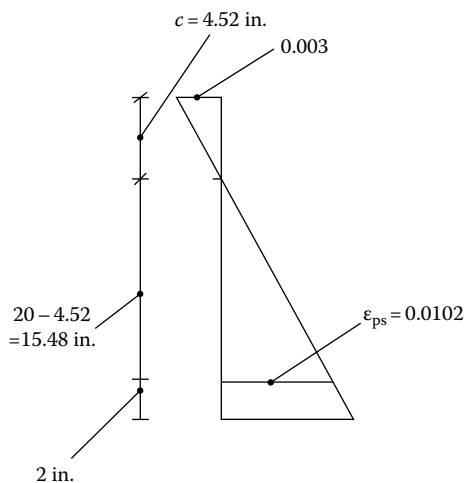
**First Trial:** Assume stress in the strands = 240 ksi.

$$\begin{aligned}
 \text{Total tension } T &= T_1 + T_2 \\
 &= 3 \times 0.0153 \times 240 + 4 \times 0.31 \times 60 \\
 &= 110.16 + 74.4 = 184.56 \text{ kip}
 \end{aligned}$$

$$T = C = 0.85 \times 12 \times 5 \times a = 184.56 \text{ kip}$$

$$a = \frac{184.56}{0.85 \times 12 \times 5} = 3.62 \text{ in.}$$

$$c = \frac{3.62}{0.80} = 4.52 \text{ in. (see Figure 2.67).}$$



**FIGURE 2.67** Example 2: strain diagram, first trial.

$$\frac{0.003}{4.52} = \frac{\epsilon_{ps}}{15.48}$$

$$\epsilon_{ps} = 0.0102$$

$$f_{ps} = 270 - \frac{0.04}{0.0102 - 0.007} \quad (\text{see Figure 2.62})$$

$$= 270 - 12.22 = 257.8 \text{ ksi}$$

$$T = T_1 + T_2$$

$$= 3 \times 0.0153 \times 257.8 + 74.4$$

$$= 192.7 \text{ kip compared to } 184.56 \text{ kip}$$

Use an average value  $T = \frac{192.7 + 184.56}{2} = 188.6$ , say, 189 kip for the second trial.

### Second Trial

$$C = T = 189 \text{ kip}$$

$$a = \frac{189}{0.85 \times 12 \times 5} = 3.71 \text{ in.}$$

$$c = \frac{3.71}{0.8} = 4.63 \text{ in.} \quad (\text{see Figure 2.68}).$$

$$\frac{0.003}{4.63} = \frac{\epsilon_{ps}}{15.37}$$

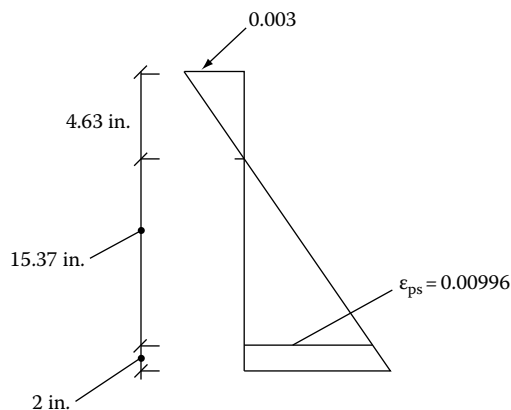
$$\epsilon_{ps} = 0.00996$$

$$f_s = 270 - \frac{0.04}{0.00996 - 0.007}$$

$$= 270 - 13.5 = 256.5 \text{ kip}$$

$$T_1 = 0.459 \times 256.5 + 74.4$$

$$= 117.72 + 74.4 = 192 \text{ kip}$$



**FIGURE 2.68** Example 2: strain diagram, second trial.



Compared to 189 kip used at the beginning of the second trial, this is considered sufficiently accurate for all practical purposes.

Calculate the nominal moment  $M_n$  by taking moments of  $T_1$  and  $T_2$  about the C.G. of compression block.

$$\begin{aligned} M_u &= 117.72(20 - 2.14) + 74.4(22 - 24) \\ &= 2102.5 + 1477.6 = 3580 \text{ kip-in.} \\ &= 298.4 \\ \phi M_u &= 0.9 \times 298.4 = 268.5 \text{ kip-ft} \end{aligned}$$

### 2.5.7.1.3 Example 3: Prestressed T-beam

**Given:** See Figure 2.69 for the beam geometry. The area of prestressed strands  $= 2.4 \text{ in.}^2$   $f'_c = 5 \text{ ksi}$ .

**Required:** Ultimate flexural capacity of the T-beam.

#### First Trial

Assume  $f_{ps} = 250 \text{ ksi}$

$$T = T_1 \quad T_2 = 0, \text{ since there is no mild steel reinforcement}$$

$$= 2.4 \times 250 = 600 \text{ kip}$$

$$C = T = 600 \text{ kip}$$

$$a = \frac{600}{0.85 \times 48 \times 5} = 2.94 \text{ in.}$$

$$c = \frac{a}{\beta_1} = \frac{2.94}{0.8} = 3.68 \text{ in.}$$

$$\frac{0.003}{3.68} = \frac{\epsilon_1}{20.32} \quad (\text{see Figure 2.70})$$

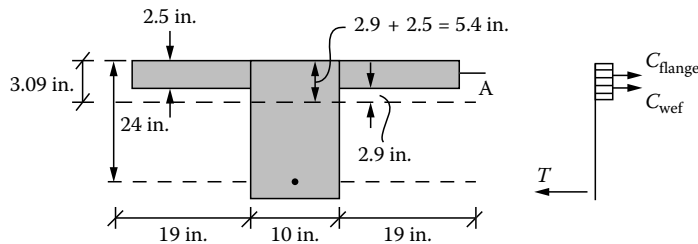
$$\epsilon_1 = 0.01657$$

$$f_{ps} = 270 - \frac{0.04}{0.01657 - 0.007} \quad (\text{see Figure 2.62})$$

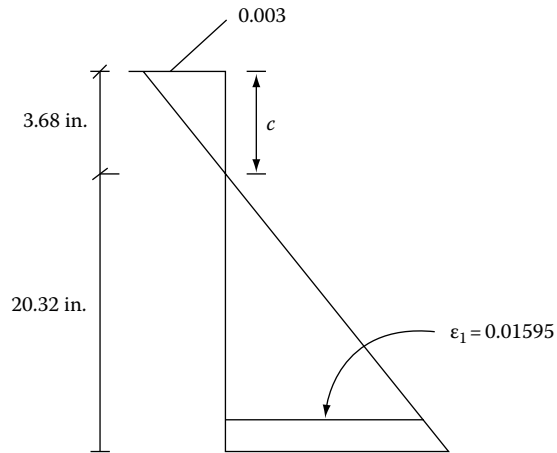
$$= 270 - 4.18 \approx 265.8 \text{ ksi}$$

$$T = 265.8 \times 2.4 = 638 \text{ kip} \quad (\text{compared to the starting value of 600 kip})$$

Use an average of the two,  $\frac{638 + 600}{2} = 619 \text{ kip}$ , for the second trial.



**FIGURE 2.69** Example 3: prestressed T-beams.



**FIGURE 2.70** Example 3: strain diagram, first trial.

### Second Trial

$$T = 619 \text{ kip}$$

$$c = \frac{3.68}{600} \times 619 = 3.80 \text{ in.}$$

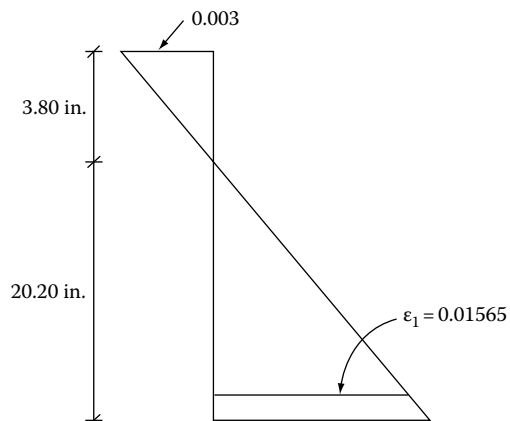
$$\frac{0.003}{3.80} = \frac{\epsilon_1}{20.20} \quad (\text{see Figure 2.71})$$

$$\epsilon_1 = 0.01595$$

$$f_{ps} = 270 - \frac{0.04}{0.01595 - 0.07} = 265.5 \text{ ksi} \quad (\text{see Figure 2.62})$$

$$T = 265.5 \times 2.4 = 636 \text{ kip.}$$

Use  $T = \frac{619 + 636}{2} = 627.5$ , say, 630 kip for the third trial.



**FIGURE 2.71** Example 3: strain diagram, second trial.

**Third Trial**

$$T = 630 \text{ kip}$$

$$c = \frac{3.68}{600} \times 630 = 3.86 \text{ in.}$$

$$a = 0.8 \times 3.86 \\ = 3.09 \text{ in.}$$

$$\frac{0.003}{3.86} = \frac{\epsilon_1}{20.14}$$

$$\epsilon_1 = 0.01565$$

$$f_{ps} = 270 - \frac{0.04}{0.01565 - 0.007} = 265.37 \text{ ksi} \quad T = 265.37 \times 2.4 = 637 \text{ kip}$$

This value is nearly the same as the value of 630 kip used at the beginning of the third iteration. However, use average value equal to  $(630 + 637)/2 = 633.5$  kip for calculating  $M_n$ .

**Flexural Strength**

$$633.5 = A_c(0.85 f'_c)$$

$$A_c = \frac{633.5}{0.85 \times 5} = 149 \text{ in.}^2$$

Since the area of flange  $= 2.5 \times 48 = 120 \text{ in.}^2$  is less than  $149 \text{ in.}^2$ , the stress block extends into the web:  $149 - 120 = \frac{29}{10} = 2.9 \text{ in.}$  (see Figure 2.69). Compute  $M_n$  by separating the compression zone into two areas and summing moments of forces about the tendon force  $T$ .

$$\begin{aligned} M_u &= C_{\text{flg}} \left( 24 - \frac{2.5}{2} \right) + C_{\text{web}} \left( 24 - \frac{5.4}{2} \right) \\ &= 38 \times 2.5 \times 0.85 \times 5 \times 22.75 + 5.4 \times 10 \times 0.85 \times 5 \times 21.30 \\ &= 9185.3 + 4888 = 14073 \text{ kip-in.} \\ &= 1172.8 \text{ kip-ft} \end{aligned}$$

$$\text{Usable flexural capacity of beam} = \phi M_u$$

$$= 0.9 \times 1172.8$$

$$= 1055.5 \text{ kip-ft}$$

**2.5.8 ECONOMICS OF POSTTENSIONING**

Posttensioned concrete floors will usually result in economics in the total construction cost because of the following:

- Less concrete used because of shallower floor structures
- Less load on columns and footings
- Shallower structural depth, resulting in reduced story height

The last item can be very significant as any height reduction translates directly into savings in all vertical structural, architectural, and building service elements.

The construction will proceed with the same speed as a normal reinforced concrete floor, with 4 day floor-to-floor construction cycles being achieved regularly on high-rise office buildings with posttensioned floors. Three-day cycles can also be achieved using an additional set of forms and higher strength concretes to shorten posttensioning time.

A major cost variable in posttensioned floors is the length of the tendons. Short tendons are relatively expensive compared to long tendons. Nevertheless, even though most tendons in a high-rise office building floors will be only around 35–50 ft (10–15 m), the system is economical because of savings in floor depth. It is desirable because of control of deflections. The optimum economical size has been found to be the four- to five-strand tendon in a flat duct because the anchorages are compact and readily accommodated within normal size of building members and because stressing is carried out with a light jack easily handled by one person.

Comparing the cost of bonded and unbonded tendons will generally show the unbonded system as being more economical. This is because unbonded posttensioning usually requires less strand due to lower friction and greater available drape. Unbonded strand also does not need grouting with its cost of time and labor. As a floor using unbonded strand will require more reinforcement than a bonded system due to lower ultimate flexural strength and code requirements, the combined cost of the strand and untensioned reinforcement will be almost the same as that for bonded systems.

The cost of a posttensioned system is further affected by the building floor geometry and irregularities. For example

- The higher the perimeter-to-area ratio, the higher the normal reinforcement content since reinforcement in the perimeter can be a significant percentage of the total.
- Angled perimeters increase reinforcement and make anchorage pockets larger and more difficult to form.
- Internal stressing from the floor surface increases costs due to the provision of the wedge-shaped stressing pockets and increased amounts of reinforcement.
- Slab steps and penetrations will increase posttensioning costs if they decrease the length of tendons.

### 2.5.9 POSTTENSIONED FLOOR SYSTEMS IN HIGH-RISE BUILDINGS

High-rise office buildings usually have long-span floors some 40–45 ft to achieve the desirable column-free space and the spans are usually noncontinuous between the core and the façade. To achieve long spans and still maintain acceptable deflections requires a deep floor system. However, by using posttensioned concrete systems it is possible to achieve a shallow floor depth and still maintain acceptable deflections without the need for precambering.

High-rise residential buildings usually do not require long spans because column-free space is not a selling point; the tenant or buyer sees the space already subdivided by walls, which effectively hide the columns. Hence continuous spans can be achieved. Unlike office buildings, residential buildings do not as a rule have suspended ceilings—the ceiling may be just a sprayed high-build coating on the slab soffit or a plasterboard ceiling on battens fixed to the slab soffit. Flat plate floors are therefore required and deflection control is an important design consideration. Where the columns form a reasonably regular grid, prestressing can be very effective in minimizing the slab thickness while at the same time controlling deflections.

Posttensioned floor systems use either 0.5 or 0.6 in. (12.7 or 15.2 mm) high-strength steel strand formed into tendons. The tendons can be either “unbonded,” where individual strands are greased and sheathed in plastic, or “bonded” where groups of four or five strands are placed inside flat metal ducts that are filled with cement grout after stressing. In the United States, typically for building construction unbonded system is preferred because of economic reasons. However, on a world-wide basis, bonded systems are preferred in high-rise buildings because they have demonstrated better long-term durability than unbonded systems. Although unbonded systems used today have improved corrosion resistance compared to earlier systems, there are still a large number of older buildings that exhibit corrosion problems in their unbonded tendons. Another reason that bonded posttensioned systems are preferred is that cutting tendons for renovations or demolition is both simpler and safer when the tendons are bonded to the concrete.

The most common posttensioned systems are

- Posttensioned flat slabs and flat plates
- Posttensioned beams supporting posttensioned slabs
- Posttensioned beams supporting reinforced concrete slabs

Untensioned steel is then added to satisfy the ultimate limit state. Deflections and shear capacity must also be checked.

The span-to-depth ratio of a single-span noncontinuous floor beam will be about 25; for a continuous beam it will be about 28, and for a flat plate about 45 for an internal span and 40 for an end span. However, in practice it is common to use constant depth of slab and to use added tendons at end spans.

In high-rise buildings it is preferable to avoid running floor beams into heavily reinforced perimeter columns for two reasons:

1. There are difficulties in accommodating tendon anchorages, which compete for space with the column reinforcement.
2. Frame action development between beams and columns causes the design bending moment between floors to vary as the frames resist lateral load, thereby diminishing the number of identical floors that can be designed, detailed, and constructed. However, use of PT beams and columns as a lateral load resisting frame is not that common in U.S. practice.

Therefore, instead of being directly supported by columns, the floor beams should be supported by the spandrel beams.

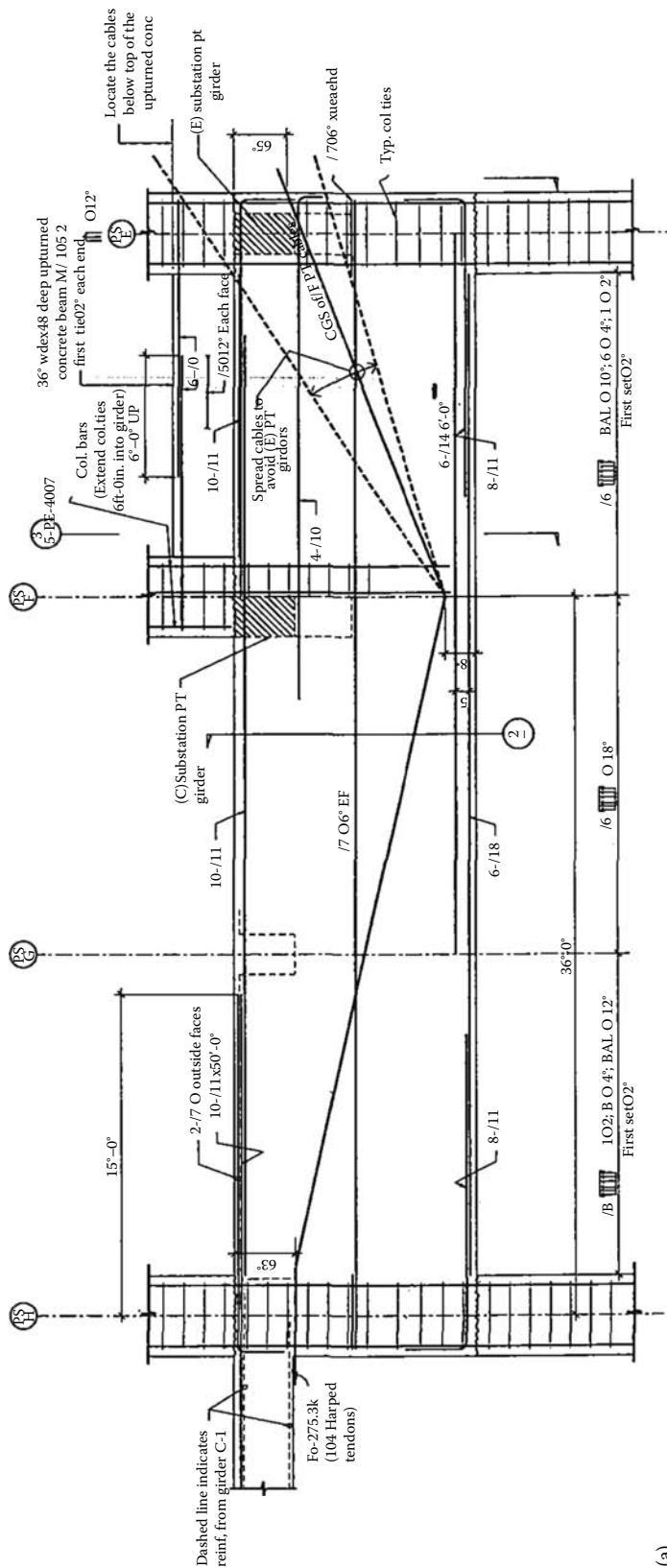
Prestressing anchorage can be on the outside of the building (requiring external access) or in a pocket at the top of the floor. Top-of-floor pockets have the disadvantage that they usually cause local variations in the flatness of the floor and rough patches, which may need to be ground flush.

Because posttensioning causes axial shortening of the prestressed member, it is necessary to consider the effects of axial restraint, that is, the effects of stiff columns and walls. Such restraint has two potential effects: it can overstress the columns or walls in bending and shear, and it can reduce the amount of prestress in the floor.

The stiff core of a high-rise building is usually fairly central so that the axial shortening of the floor can be generally in a direction toward the core. This means that the perimeter columns move inward, but because they move by the same amount from story to story, no significant permanent bending stresses occur except in the first story above a non-prestressed floor, which is often the ground floor. As this story is usually higher than a typical story, the flexibility of the columns is greater and the induced bending moments may be easily accommodated. However, the loss of prestress in the floor may necessitate some additional untensioned reinforcement.

### 2.5.9.1 Transfer Girder Example

See Figure 2.72 for an example of a posttensioned transfer girder in high-rise application.



**FIGURE 2.72** Posttensioned transfer girder: (a) elevation and

(continued)

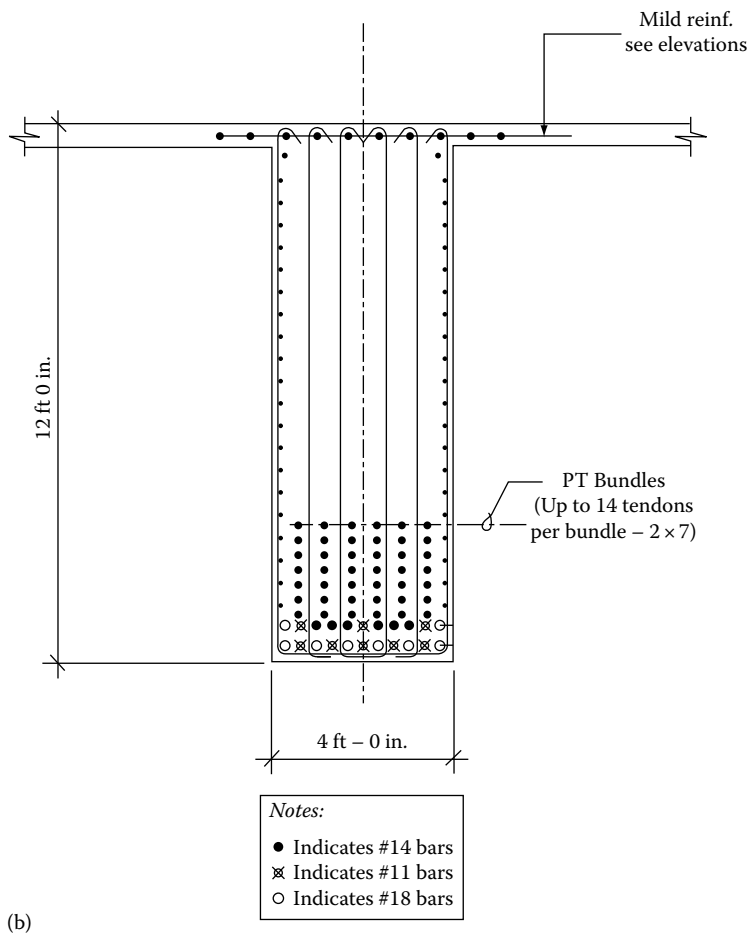


FIGURE 2.72 (continued) (b) section.

2.5.10 PRELIMINARY DESIGN OF PT FLOOR SYSTEMS; HAND CALCULATIONS

2.5.10.1 Preview

In this section, procedures are presented for an accurate and rapid means of determining prestress forces for preliminary designs. It combines the well-known load balancing technique with allowable stress requirements. The method provides a valuable tool for verifying computer results.

The method is based on load balancing technique and relies on the simple fact that a tendon profile can be established to produce loads that “mirror” the distribution of imposed loads. Thus a uniform load logically dictates a parabolically draped tendon because this profile will produce an upward uniform load. Similarly, point loads require harped tendons while imposed end moments require straight tendons. A combination of load types can be resisted by superposing appropriate tendon profiles. Here, we will confine our discussion to structures supporting uniform loads.

It is rarely necessary to provide a prestress force to fully balance the imposed loads and usually only a portion of the entire load is balanced. Regardless of the proportion balanced, the moments due to equivalent loads will be linearly related to the moments from imposed loads. This relationship allows the designer to sidestep the usual requirements of determining primary and secondary moments by calculating the total moments directly.

Once the tendon force and profile have been established, the stresses produced from the combination of imposed loads and prestress force are investigated. Subtracting the moments caused by

equivalent loads from those due to imposed loads gives the net unbalanced moments that produce the flexural stresses. To the flexural stresses, the axial compression from prestressing is added giving the final stress distribution.

After the final stress distribution is obtained, the maximum compressive and tensile stresses are compared to the allowable values given in Chapter 18 of the ACI 318–08. If the comparisons are favorable, an acceptable combination of prestress force and tendon profile has been found. If not, we revise either the tendon profile and force or the cross-sectional shape of the structure to arrive at an acceptable solution.

While the iteration procedure may appear to be long and tedious, the checking process is greatly simplified by recognizing that for most conditions, the design is dictated by a few discrete points in the structure. Since the final design is realized by satisfying certain allowable stress criteria, the points governing the design are those where the combination of moment and section properties have created the greatest stresses. For prismatic structures, these points are the maximum negative and positive moment locations. For non-prismatic structures, other locations may be critical.

The presentation given in Sections 2.5.10.2 and 2.5.10.3 is arranged in two parts. In the first part, hand calculations for the design of simple span beams are presented (Section 2.5.10.2). The second part is concerned with the iterative design of continuous spans (Section 2.5.10.3).

Included are worked examples for

- One-way PT slab (2.5.10.3.1)
- Continuous PT beam (2.5.10.3.2)
- PT flat plate (2.5.10.3.3)

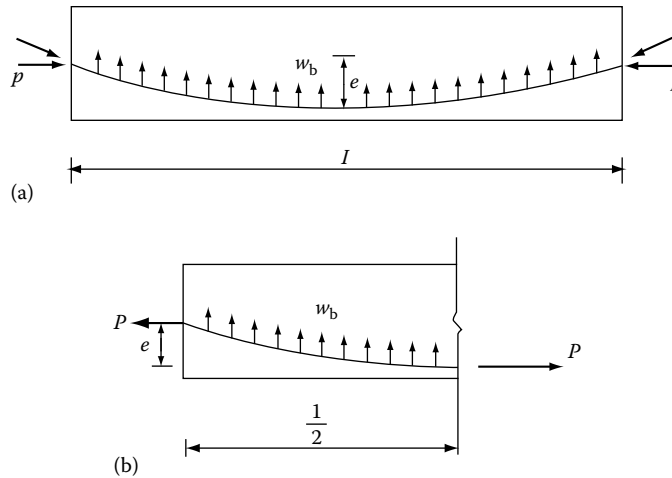
The aim of posttension design is to determine the required prestressing force and hence the number, size, and profile of tendons for satisfactory behavior at service loads. The ultimate capacity must then be checked at critical sections to assure that prestressed members have an adequate factor of safety against failure.

The design method presented in this section uses the technique of load balancing in which the effect of prestressing is considered as an equivalent load. Take, for example, a prismatic simply supported beam with a tendon of parabolic profile, shown in Figure 2.73. The tendon exerts a horizontal force equal to  $P \cos \phi = P$  (for small values of  $\phi$ ) at the ends along with vertical components equal to  $P \sin \phi$ . The vertical component is neglected in design because it occurs directly over the supports. In addition to these loads, the parabolic tendon exerts a continuous upward force on the beam along its entire length. By neglecting friction between the tendon and concrete, we can assume that (1) the upward pressure exerted is normal to the plane of contact and (2) tension in the tendon is constant. The upward pressure is exerted by the tendon profile. Due to the shallow nature of posttensioned structures, the vertical component of the tendon force may be assumed constant. Considering one-half of the beam as a free body (Figure 2.73b), the vertical load exerted by the tendon may be derived by summing moments about the left support. Thus the equivalent, load  $W_p = 8Pe/L^2$ . Equivalent loads and moments produced by other types of tendon profile are shown in Figure 2.74.

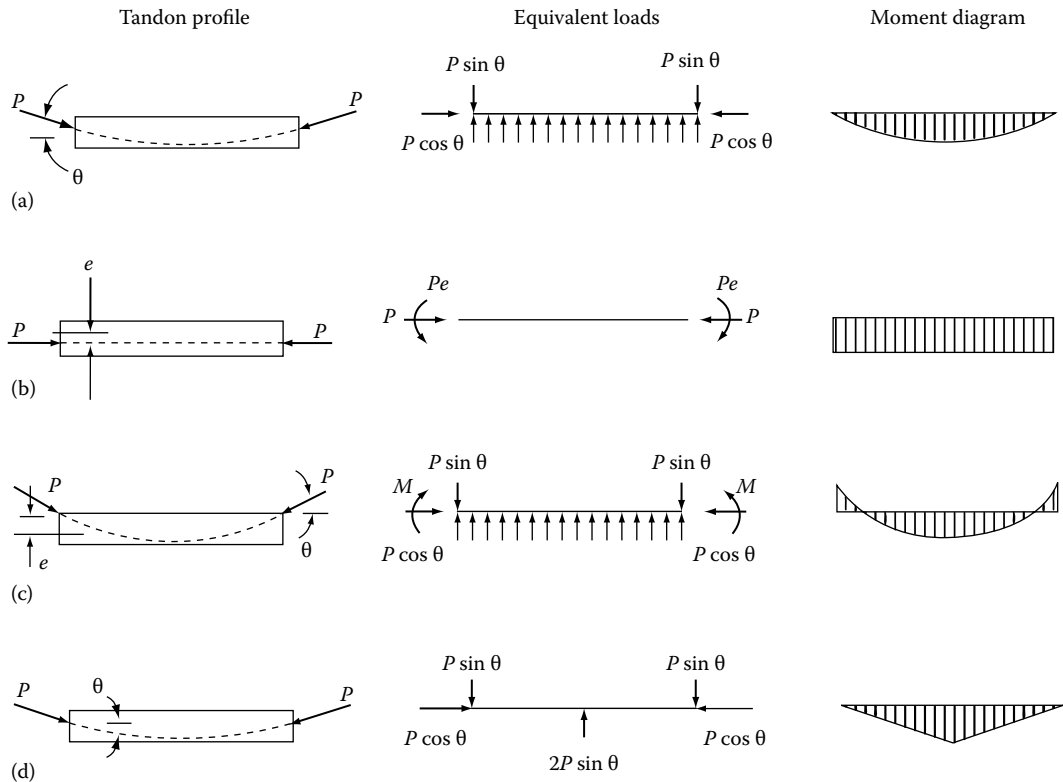
The step-by-step procedure is as follows:

1. Determine preliminary size of prestressed concrete members using the values given in Table 2.7 as a guide.
2. Determine section properties of the members: area  $A$ , moment of inertia  $I$ , and section moduli  $S_1$  and  $S_b$ .
3. Determine tendon profile with due regard to cover and location of mild steel reinforcement.
4. Determine effective span  $L_e$ , by assuming  $L_1 = 1/16$ – $1/19$  of the span length for slabs, and  $L = 1/10$ – $1/12$  of the span length for beams.  $L_1$  is the distance between the center line of support and the inflection point. The concept of effective length will be explained shortly.





**FIGURE 2.73** Load balancing concept; (a) beam with parabolic tendon; and (b) free-body diagram.



**FIGURE 2.74** Equivalent loads and moments due to sloped tendon: (a) upward uniform load due to parabolic tendon; (b) constant moment due to straight tendon; (c) upward uniform load and end moments due to parabolic tendon not passing through the centroid at the ends; and (d) vertical point load due to sloped tendon.

5. Start with an assumed value for balanced load  $W_p$  equal to, say, 0.7–0.9 times the total dead load.
6. Determine the elastic moments for the total dead plus live loads (working loads). For continuous beams and slabs use a computer plane-frame analysis program, moment distribution method, or ACI coefficients, if applicable, in decreasing order of preference.

7. Reduce negative moments to the face of supports.
8. By proportioning the unbalanced load to the total load, determine the unbalanced moments  $M_{ub}$  at critical sections such as at the supports and at the center of spans.
9. Calculate the bending stresses  $f_b$  and  $f_t$  at the bottom and top of the cross section due to  $M_{ub}$  at critical sections. Typically at supports, the stresses  $f_t$  and  $f_b$  are in tension and compression, respectively. At the center of spans, the stresses are typically compression and tension at the top and bottom, respectively.
10. Calculate the minimum required posttension stress  $f_p$  by using the following equations.  
For negative zones of one-way slabs and beams

$$f_p = f_t - 6\sqrt{f'_c}$$

For positive moments in two-way slabs

$$f_p = f_t - 2\sqrt{f'_c}$$

11. Find the posttension force  $P$  by the relation  $P = f_p \times A$  where  $A$  is the area of the cross section of the beam.
12. Calculate the balanced load  $W_p$  due to  $P$  by the relation

$$W_p = 8 \times Pe / L_e^2$$

where

$e$  is the drupe of the tendon

$L_e$  is the effective length of tendon between inflection points

13. Compare the calculated value of  $W_p$  from step 12 with the value assumed in step 5. If they are about the same, the selection of posttension force for the given loads and tendon profile is complete. If not, repeat steps 9–13 with a revised value of  $W_p = 0.75W_{p1} + 0.25W_{p2}$ .  $W_{p1}$  is the value of  $W_p$  assumed at the beginning of step 5, and  $W_{p2}$  is the derived value of  $W_p$  at the end of step 12. Convergence is fast requiring no more than three cycles in most cases.

### 2.5.10.2 Simple Span Beam

The concept of preliminary design discussed in this section is illustrated in Figure 2.75, where a parabolic profile with an eccentricity of 12 in. is selected to counteract part of the applied load consisting of a uniformly distributed dead load of 1.5 kip-ft and a live load of 0.5 kip-ft.

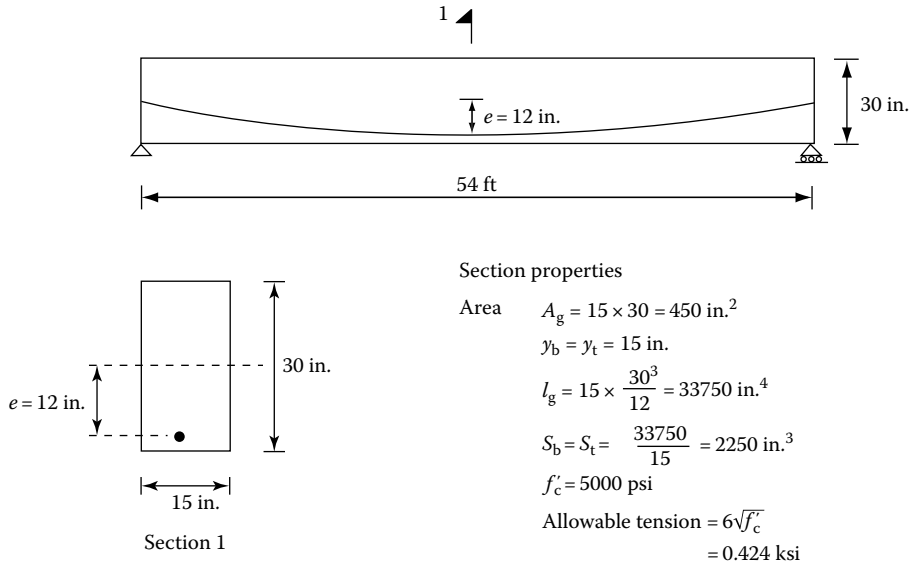
In practice, it is rarely necessary to provide a prestress force to fully balance the imposed loads. A value of prestress, often used for building system, is 75%–95% of the dead load. For the illustrative problem, we begin with an assumed 80% of the dead load as the unbalanced load.

**First Cycle:** The load being balanced is equal to  $0.80 \times 1.5 = 1.20$  kip-ft. The total service dead plus live load  $= 1.5 + 0.5 = 2.0$  kip-ft, of which 1.20 kip-ft is assumed in the first cycle to be balanced by the prestressing force in the tendon. The remainder of the load equal to  $2.0 - 1.20 = 0.80$  kip-ft acts vertically downward, producing a maximum unbalanced moment  $M_{ub}$  at center span given by

$$\begin{aligned} M_{ub} &= 0.80 \times 54^2 / 8 \\ &= 291.6 \text{ kip-ft} \end{aligned}$$

The tension and compression in the section due to  $M_{ub}$  is given by

$$f_c = f_b = 291.6 \times 12 / 2250$$



**FIGURE 2.75** Preliminary design: simple span beam.

The minimum prestress required to limit the tensile stress to  $6\sqrt{f'_c} = 0.424$  is given by

$$f_p = 1.55 - 0.424 = 1.13 \text{ ksi}$$

Therefore, the required minimum prestressing force  $P = \text{area of beam} \times 1.13 = 450 \times 1.13 = 509 \text{ kip}$ . The load balanced by this force is given by

$$W_p \times 54^2/8 = Pe = 509 \times 1$$

and so  $W_p = 1.396 \text{ kip-ft}$  compared to the value of 1.20 used in the first cycle. Since the two values are not close to each other, we repeat the above calculations starting with a more precise value for  $W_p$  in the second cycle.

### Second Cycle

We start with a new value of  $W_p$  by assuming a new value equal to 75% of the initial value + 25% of the derived value. The new value of

$$W_p = 0.75 \times 1.20 + 0.25 \times 1.396 = 1.25 \text{ kip-ft}$$

$$M_{ub} = (2 - 1.25) \times 54^2/8 = 273.3 \text{ kip-ft}$$

$$f_b = f_t = 273.3 \times 12/2250 = 1.458 \text{ ksi}$$

The minimum stress required to limit the tensile stress to  $6\sqrt{f'_c} = \sqrt{5000} = 0.424 \text{ ksi}$  is given by

$$f_p = 1.458 - 0.424 = 1.03 \text{ ksi}$$

Minimum prestressing force  $P = 1.03 \times 450 = 465 \text{ kip}$ . The balanced load corresponding to the prestress value of 465 is given by

$$W_p = 8Pe/L^2 = 8 \times 465 \times 1/54^2 = 1.27 \text{ kip-ft}$$

Therefore,  $W_p = 1.27$  kip-ft, nearly equal to the value assumed in the second cycle. Thus the minimum prestress required to limit the tensile stress in concrete to  $6\sqrt{f'_c}$  is 465 kip.

To demonstrate how rapidly the method converges to the desired answer, we will rework the problem by assuming an initial value of  $W_p = 1.0$  kip-ft in the first cycle.

### First Cycle

$$W_p = 1.0 \text{ kip-ft}$$

$$M_{ub} = (2-1) \times 54^2/8 = 364.5 \text{ kip-ft}$$

$$f_b = f_t = 364.5 \times 12/2250 = 1.944 \text{ ksi}$$

$$f_p = 1.944 - 0.454 = 1.49 \text{ ksi}$$

$$P = 1.49 \times 450 = 670.5 \text{ kip}$$

$$W_p \times 54^2/8 = 670.5 \times 1$$

$$W_p = 1.84 \text{ kip-ft}$$

compared to 1.0 kip-ft used at the beginning of the first cycle.

### Second Cycle

$$W_p = 0.75 \times 1 + 0.25 \times 1.84 = 1.21 \text{ kip-ft}$$

$$M_{ub} = (2-1.21) \times 54^2/8 = 288 \text{ kip-ft}$$

$$f_b = f_c = 388 \times 12/2250 = 1.536 \text{ ksi}$$

$$f_p = 1.536 - 0.454 = 1.082 \text{ ksi}$$

$$P = 1.082 \times 450 = 486.8 \text{ kip}$$

$$W_p = 486.8 \times 1 \times 8/54^2 = 1.336 \text{ kip-ft}$$

compared to the value of 1.21 used at the beginning of second cycle.

### Third Cycle

$$W_p = 0.75 \times 1.21 - 1.21 \times 0.25 \times 1.336 = 1.24 \text{ kip-ft}$$

$$M_{ub} = (2 - 1.24) \times 54^2/8 = 276.67 \text{ kip-ft}$$

$$f_b = f_c = 276.47 \times 12/2250 = 1.475 \text{ ksi}$$

$$f_p = 1.475 - 0.454 = 1.021 \text{ ksi}$$

$$P = 1.021 \times 450 = 459.3 \text{ kip}$$

$$W_p = 459.3 \times 1 \times 8/54^2 = 1.26 \text{ kip-ft}$$

Compared to 1.24 assumed at the beginning of third cycle. The value of 1.26 kip-ft is considered close enough for design purposes.

### 2.5.10.3 Continuous Spans

The above example illustrates the salient features of load balancing. Generally, the prestressing force is selected to counteract or balance a portion of dead load, and under this loading condition the net stress in the tension fibers is limited to a value  $= 6\sqrt{f'_c}$ . If it is desired to design the member for zero stress at the bottom fiber at center span (or any other value less than the code allowed maximum value of  $6\sqrt{f'_c}$ , it is only necessary to adjust the amount of posttensioning provided in the member.

There are some qualifications to the foregoing procedure that should be kept in mind when applying the technique to continuous beams. The chief among them is the fact that it is not usually practical to install tendons with sharp break in curvature over supports, as shown in Figure 2.76a. The stiffness of tendons requires a reverse curvature (Figure 2.76b) in the tendon profile with a point of contraflexure some distance from the supports. Although this reverse curvature modifies the equivalent loads imposed by posttensioning from those assumed for a pure parabolic profile between the supports, a simple revision to the effective length of tendon, as will be seen shortly, yields results sufficiently accurate for preliminary designs.

Consider the tendon profiles shown in Figure 2.77a and b for a typical exterior and an interior span. Observe three important features.

1. The effective span  $L_e$ , the distance between the inflection points which is considerably shorter than the actual span.
2. The sag or drape of the tendon is numerically equal to average height of inflection points, less the height on the tendon midway between the inflection points.
3. The point midway between the inflection points is not necessarily the lowest point on the profile.

The upward equivalent uniform load produced by the tendon is given by

$$W_p = 8Pe/L_e^2$$

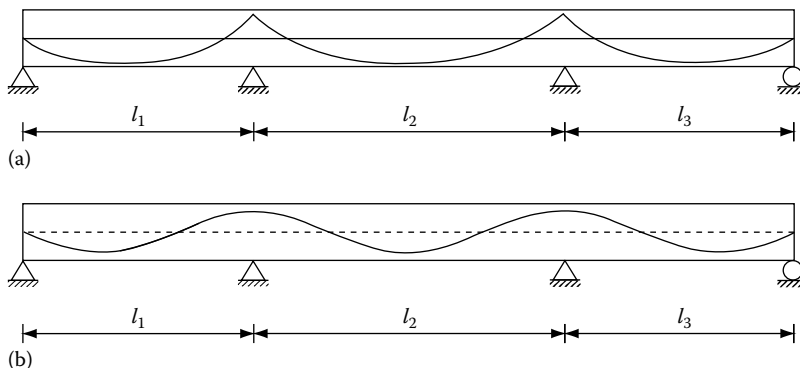
where

$W_p$  is the equivalent upward uniform load due to prestress

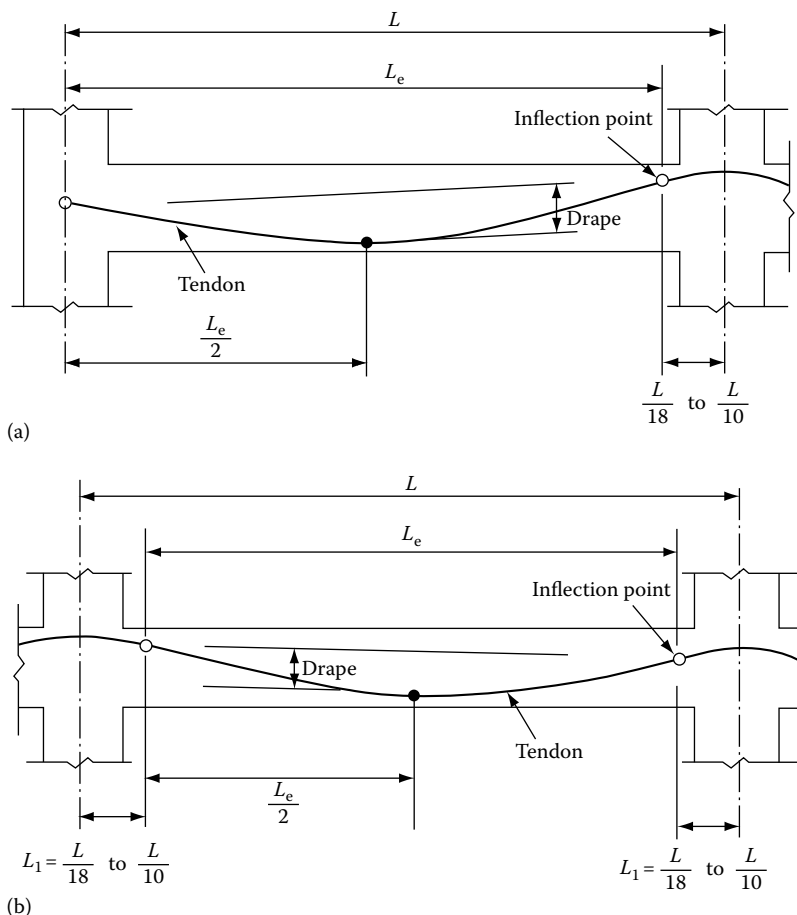
$P$  is the prestress force

$e$  is the cable drape between inflection points

$L_e$  is the effective length between inflection points



**FIGURE 2.76** Tendon profile in continuous beam: (a) simple parabolic profile and (b) reverse curvature in tendon profile.



**FIGURE 2.77** Tendon profile: (a) typical exterior span and (b) typical interior span.

Note that relatively high loads acting downward over the supports result from the sharply curved tendon profiles located within these regions (Figure 2.78).

Since the large downward loads are confined to a small region, typically 1/10–1/8 of the span, their effect is secondary as compared to the upward loads. Slight differences occur in the negative moment regions between the applied load moments and the moment due to prestressing force. The differences are of minor significance and can be neglected in the design without losing meaningful accuracy.

As in simple spans the moments caused by the equivalent loads are subtracted from those due to applied loads, to obtain the net unbalanced moment that produces the flexural stresses. To the flexural stresses, the axial compressive stresses from the prestress are added to obtain the final stress distribution in the members. The maximum compressive and tensile stresses are compared to the allowable values. If the comparisons are favorable, an acceptable design has been found. If not, either the tendon profile or the force (and very rarely the cross-sectional shape of the structure) is revised to arrive at an acceptable solution.

In this method, since the moments due to equivalent loads are linearly related to the moments due to applied loads, the designer can bypass the usual requirement of determining the primary and secondary moments.

#### 2.5.10.3.1 Example 1: One-Way PT Slab

Given a 30ft 0in. column grid layout, design a one-way slab spanning between the beams shown in Figure 2.79.

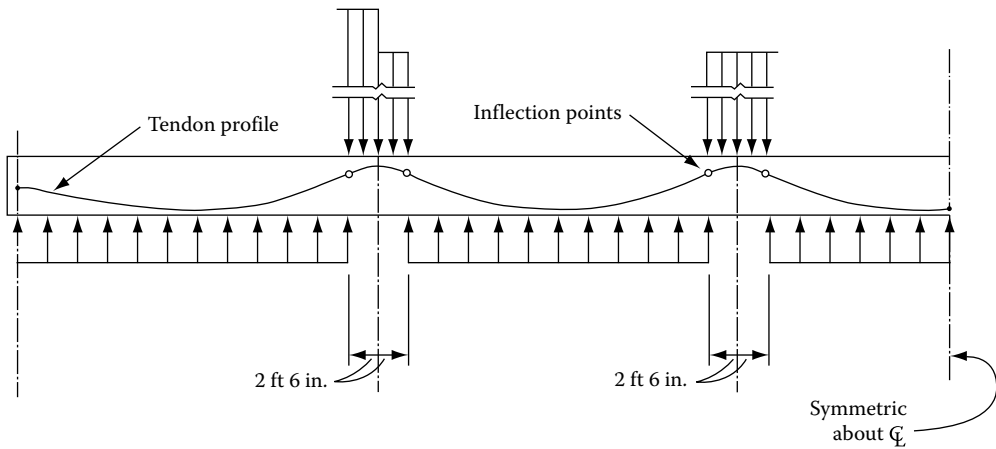


FIGURE 2.78 Equivalent loads due to prestress.

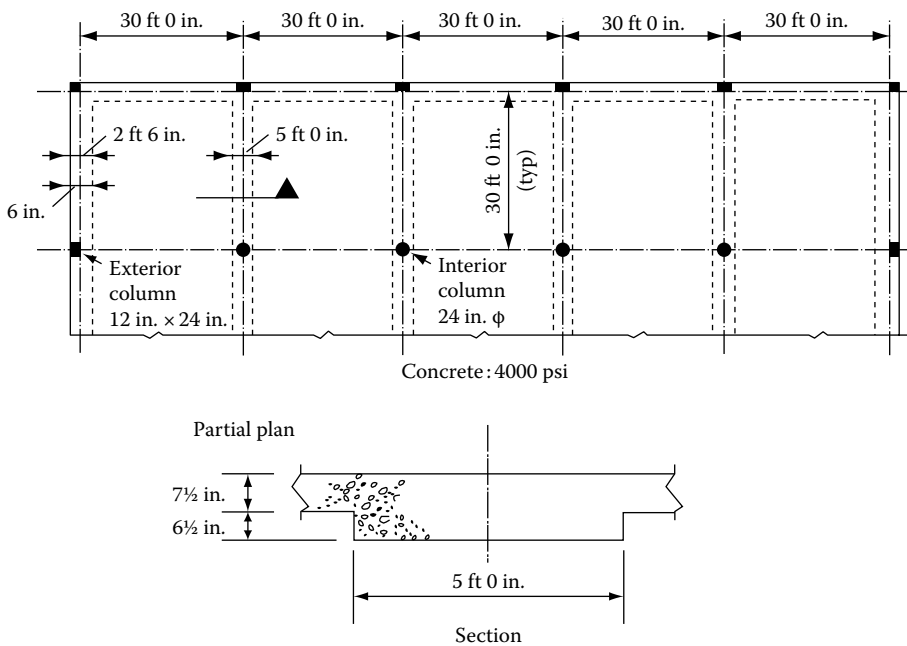


FIGURE 2.79 Example 1: one-way posttensioned slab.

Slab and beam depths:

Clear span of slab =  $30 - 5 = 25$  ft

Recommended slab depth =  $\text{span}/40 = 25 \times 12/40 = 7.5$  in.

Clear span for beams = 30 ft center-to-center span, less 2 ft 0 in. for column width =  $30 - 2 = 28$  ft.

Recommended beam depth =  $\text{span}/25 = 28 \times 12/25 = 13.44$  in. Use 14 in.

Loading:

Dead load: 7.5 in. slab = 94 psf

Mech. and lights = 6 psf

Ceiling = 6 psf

Partitions = 20 psf

Total dead load = 126 psf

Live load: Office load = 100 psf  
Code minimum 50 psf  
Use 100 psf per owner's request  
Total  $D + L = 226$  psf

Slab design: Slab properties for 1 ft–0 in. wide strip:

$$I = bd^3/12 = 12 \times 7.5^3/12 = 422 \text{ in.}^4$$
$$S_{\text{top}} = S_{\text{bot}} = 422/3.75 = 112.5 \text{ in.}^3$$
$$\text{Area} = 12 \times 7.5 = 90 \text{ in.}^2$$

A 1 ft width of slab is analyzed as a continuous beam. The effect of column stiffness is ignored.

The moment diagram for a service load of 226 psf is shown in Figure 2.80.

Moments at the face of supports have been used in the design instead of center line moments. Negative center line moments are reduced by a  $Va/3$  factor ( $V$  = shear at that support,  $a$  = total support width), and positive moments are reduced by  $Va/6$  using average adjacent values for shear and support widths. A frame analysis may be used to obtain more accurate results.

The design of continuous strands will be based on the negative moment of 10.6 kip-ft.

The additional prestressing required for the negative moment of 16.8 kip-ft will be provided by additional tendons in the end bays only.

**Determination of Tendon Profile:** Maximum tendon efficiency is obtained when the cable drape is as large as the structure will allow. Typically, the high points of the tendon over the supports and the low point within the span are dictated by concrete cover requirements and the placement of mild steel.

The high and low points of tendon in the interior bay of the example problem are shown in Figure 2.81. Next, the location of inflection points are determined. For slabs, the inflection points

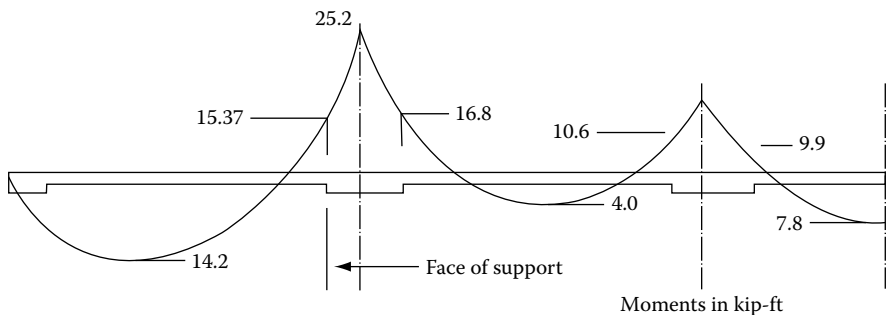


FIGURE 2.80 Example 1: one-way moment diagram.

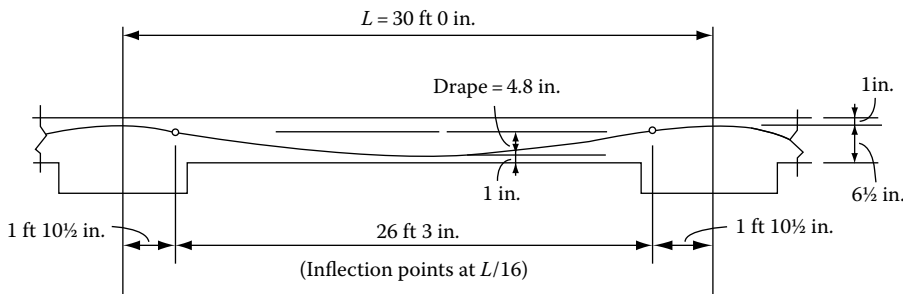
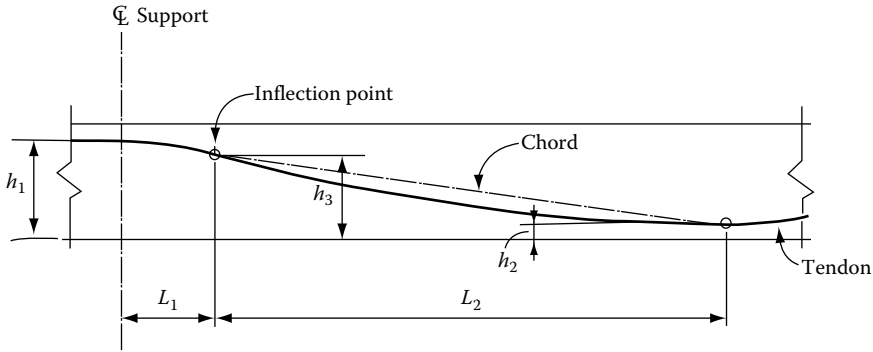


FIGURE 2.81 Example 1: one-way tendon profile; interior bay.





**FIGURE 2.82** Characteristics of tendon profile.

usually range within 1/16–1/19 of the span. The fraction of span length used is a matter of judgment, and is based on the type of structure. For this example, we choose 1/16 of span which works out to 1 ft 10½ in.

An interesting property useful in determining the tendon profile shown in Figure 2.82 is that, if a straight line (chord) is drawn connecting the tendon high point over the support and the low point midway between, it intersects the tendon at the inflection point. Thus, the height of the tendon can be found by proportion. From the height, the bottom cover is subtracted to find the drape.

Referring to Figure 2.82,

$$\text{Slope of the chord line} = h_1 - h_2/(L_1 + L_2)$$

$$h_s = h_2 + L_2 \times (\text{slope})$$

$$= h_2 + L_2(h_1 - h_2)/(L_1 + L_2)$$

This simplifies to  $h_3 = (h_1L_2 + h_2L_1)/(L_1 + L_2)$

The drape  $h_d$  is obtained by subtracting  $h_2$  from the foregoing equation. Note that notion  $e$  is also used in these examples to denote drape  $h_d$ .

In this case, the height of the inflection point is exact for symmetrical layout of the tendon about the center span. If the tendon is not symmetrical, the value is approximate but sufficiently accurate for preliminary design.

Returning to our example problem we have  $h_1 = 6.5$  in.  $h_2 = 1$  in.  $L_1 = 1.875$  ft and  $L_2 = 13.125$  ft.

Height of tendon at the inflection point:

$$h_3 = (h_1L_2 + h_2L_1)/(L_1 + L_2)$$

$$= 6.5 \times 13.125 + 1 \times 1.875 / (1.875 + 13.125) = 5.812 \text{ in.}$$

Drape  $h_d = e = 5.813 - 1 = 4.813$  in. Use 4.8 in.

Allowable stresses from ACI 318-99 are as follows:

$$f_t = \text{tensile stress } 6\sqrt{f'_c}$$

$$f_c = \text{compressive stress} = 0.45f'_c$$

For

$$f'_c = 4000 \text{ psi concrete}$$

$$f_t = 6\sqrt{4000} = 380 \text{ psi}$$

$$f_c = 0.45 \times 4000 = 1800 \text{ psi}$$

**Design of Through Strands:** The design procedure is started by making an initial assumption of the equivalent load produced by the prestress. A first value of 65% of the total dead load is used.

### First Cycle

Assume

$$W_p = 0.65W_d$$

where

$W_p$  is the equivalent upward load due to posttensioning, also denoted as  $W_{pt}$

$W_d$  is the total dead load

Therefore,  $W_p = 0.65 \times 126 = 82 \text{ plf}$

The balancing moment caused by the equivalent load is calculated from

$$M_{pt} = M_s W_{pt}/W_s$$

where

$M_{pt}$  is the balancing moment due to equivalent load  
(also indicated by notation  $M_b$ )

$M_s$  is the moment due to service load,  $D + L$

$W_s$  is the total applied load,  $D + L$

In our example,  $M_s = 10.6 \text{ kip-ft}$  for the interior span

$$M_{pt} = 10.6 \times 82/226 = 3.85 \text{ kip-ft}$$

Next,  $M_{pt}$  is subtracted from  $M_s$  to give the unbalanced moment  $M_{ub}$ . The flexural stresses are then obtained by dividing  $M_{ub}$  by the section moduli of the structure's cross section at the point where  $M_s$  is determined. Thus

$$f_t = M_{ub}/S_t$$

$$f_b = M_{ub}/S_b$$

In our case,  $M_{ub} = 10.6 - 3.85 = 6.75 \text{ kip-ft}$ . The flexural stress at the top of the section is found by

$$f_t = M_{ub}/S_t = 6.75 \times 12/112.5 = 0.72 \text{ ksi}$$

The minimum required compressive prestress is found by subtracting the maximum allowable tensile stress  $f_a$  given below, from the tensile stresses calculated above. The smallest required compressive stress is

$$f_p = f_{ts} - f_a$$

where

$f_{ts}$  is the computed tensile stress

$f_a = 6\sqrt{f'_c}$  for one-way slabs or beams from the negative zones

$f_a = 2\sqrt{f'_c}$  for positive moments in two-way slabs

In our case

$$f_p = 0.720 - 0.380 = 0.34 \text{ ksi}$$

and

$$P = 0.34 \times 7.5 \times 12 = 30.60 \text{ kip-ft}$$

Use the following equation to find the equivalent load due to prestress:

$$\begin{aligned} W_p &= 8Pe/L_e^2 \\ &= 8 \times 30.6 \times 4.81/12 \times (26.25)^2 = 0.142 \text{ klf} = 142 \text{ plf} \end{aligned}$$

This is more than 82 plf. N.G.

Since the derived value of  $W_p$  is not equal to the initial assumed value, the procedure is repeated until convergence is achieved. Convergence is rapid by using a new initial value for the subsequent cycle, equal to 75% of the previous initial value of  $W_{p1}$  plus 25% of the derived value  $W_{p2}$ , for that cycle.

### Second Cycle

Use the above criteria to find the new value of  $W_p$  for the second cycle.

$$\begin{aligned} W_p &= 0.75W_{p1} + 0.25W_{p2} = 0.75 \times 82 + 0.25 \times 142 = 97 \text{ plf} \\ M_b &= 97/226 \times 10.6 = 4.55 \text{ kip-ft} \\ M_{ub} &= 10.6 - 4.55 = 6.05 \text{ kip-ft} \\ f_t &= f_b = 6.05 \times 12/112.5 = 0.645 \text{ ksi} \\ f_p &= 0.645 - 0.380 = 0.265 \text{ ksi} \\ P &= 0.265 \times 90 = 23.89 \text{ kip} \\ W_p &= 8 \times 23.89 \times 4.81/12 \times (26.25)^2 = 0.111 \text{ klf} = 111 \text{ plf} \end{aligned}$$

This is more than 97 psf. N.G.

### Third Cycle

$$\begin{aligned} W_p &= 0.75 \times 97 + 0.25 \times 111 = 100.5 \text{ plf} \\ M_b &= 100.5/226 \times 10.6 = 4.71 \text{ kip-ft} \\ M_{ub} &= 10.6 - 4.71 = 5.89 \text{ kip-ft} \\ f_t &= f_b = 5.89 \times 12/112.5 = 0.629 \text{ ksi} \\ f_p &= 0.629 - 0.380 = 0.248 \text{ ksi} \\ P &= 0.248 \times 90 = 22.3 \text{ kip} \\ W_p &= 8 \times 22.3 \times 4.81/12 \times (26.25)^2 = 0.104 \text{ klf} = 104 \text{ plf} \end{aligned}$$

This is nearly equal to 100.5 plf. Therefore, it is satisfactory.

Check compressive stress at the section.

Bottom flexural stress = 0.629 ksi

Direct axial stress due to prestress =  $22.3/90 = 0.46$  ksi

Total compressive stress =  $0.629 + 0.246 = 0.876$  ksi is less than  $0.45f'_c = 1.8$  ksi

Therefore, it is satisfactory.

**End Bay Design:** Design end bay prestressing using the same procedure for a negative moment of 15.37 kip-ft.

Assume that at the left support, the tendon is anchored at the center of gravity of the slab with a reversed curvature. Assume further that the center of gravity of the tendon is at a distance 1.75 in. from the bottom of the slab. With these assumptions we have  $h_1 = 3.75$  in.,  $h_2 = 1.75$  in.,  $L_1 = 1.875$  ft, and  $L_2 = 13.125$  ft.

The height of the tendon inflection point at left end

$$h_3 = 3.75 \times 13.125 + 1.75 \times 1.875/15 = 3.25 \text{ in.}$$

The height of the right end

$$h_3 = 6.5 \times 13.125 + 1.75 \times 1.875/15 = 5.906 \text{ in.}$$

Average height of tendon =  $3.25 + 5.906/2 = 4.578$  in. Use 4.6 in.

$$\text{Drape } h_d = e = 4.6 - 1.75 = 2.85 \text{ in.}$$

### First Cycle

We start with the first cycle, as for the interior span, by assuming  $W_{pt} = 82$  plf.

$$M_{pt} = 15.37 \times 82/226 = 5.58 \text{ kip-ft}$$

$$M_{ub} = 15.37 - 5.58 = 9.79 \text{ kip-ft}$$

$$f_t = f_b = 9.79 \times 12/112.5 = 1.04 \text{ ksi}$$

$$f_p = 1.04 - 0.380 = 0.664 \text{ ksi}$$

$$P = 0.664 \times 90 = 59.7 \text{ kip}$$

$$W_p = 8 \times 59.7 \times 2.85/12 \times (26.25)^2 = 0.165 \text{ klf} = 165 \text{ plf}$$

This is more than 82 plf. N.G.

### Second Cycle

$$W_p = 0.75 \times 82 + 0.25 \times 165 = 103 \text{ plf}$$

$$M_{pt} = 15.37 \times 103/226 = 7.0 \text{ kip-ft}$$

$$M_{ub} = 15.37 - 7.0 = 8.37 \text{ kip-ft}$$

$$f_t = f_b = 8.37 \times 12/112.5 = 0.893 \text{ ksi}$$

$$f_p = 0.893 - 0.380 = 0.513 \text{ ksi}$$

$$P = 0.513 \times 90 = 46.1 \text{ kip}$$

$$W_p = 8 \times 46.1 \times 2.85/12 \times (26.25)^2 = 0.127 \text{ klf} = 127 \text{ plf}$$

This is more than 103 plf. N.G.

**Third Cycle**

$$W_p = 0.75 \times 103 + 0.25 \times 127 = 109 \text{ plf}$$

$$M_{pt} = 15.37 \times 109 / 226 = 7.41 \text{ kip-ft}$$

$$M_{ub} = 15.37 - 7.41 = 7.96 \text{ kip-ft}$$

$$f_t = f_b = 7.96 \times 12 / 112.5 = 0.849 \text{ ksi}$$

$$f_p = 0.849 - 0.380 = 0.469 \text{ ksi}$$

$$P = 0.469 \times 90 = 42.21 \text{ kip}$$

$$W_p = 8 \times 42.21 \times 2.85 / 12 \times (26.25)^2 = 0.116 \text{ klf} = 116 \text{ plf}$$

This is nearly equal to 109 plf used at the start of third cycle. Therefore, it is satisfactory.

Check compressive stress at the section:

$$f_b = 0.849 \text{ ksi}$$

Axial stress due to prestress =  $42.21 / 90 = 0.469 \text{ ksi}$

Total compressive stress =  $0.849 + 0.469 = 1.38 \text{ ksi}$

This is less than 1.8 ksi. Therefore, the design is OK.

Check the design against positive moment of 14.33 kip-ft:

$$W_p = 116 \text{ plf}$$

$$M_b = 14.33 \times 116 / 226 = 7.36 \text{ kip-ft}$$

$$M_{ub} = 14.33 - 7.36 = 6.97 \text{ kip-ft}$$

Bottom flexural stress =  $6.97 \times 12 / 122.5 = 0.744 \text{ ksi}$  (tension)

Axial compression due to prestress =  $42.21 / 12 \times 7.5 = 0.469 \text{ ksi}$

Tensile stress at bottom =  $0.744 - 0.469 = 0.275 \text{ ksi}$

This is less than 0.380 ksi. Therefore, the end bay design is OK.

#### 2.5.10.3.2 Example 2: Continuous PT Beam

Refer to Figure 2.83 for dimensions and loading. Determine flange width of beam using the criteria given in ACI 318-08.

The flange width  $b_f$  is the least of

1. Span/4
2. Web width +  $16 \times$  (flange thickness)
3. Web width +  $\frac{1}{2}$  clear distance to next web

Therefore

$$b_f = 30 / 4 = 7.5 \text{ ft (controls)}$$

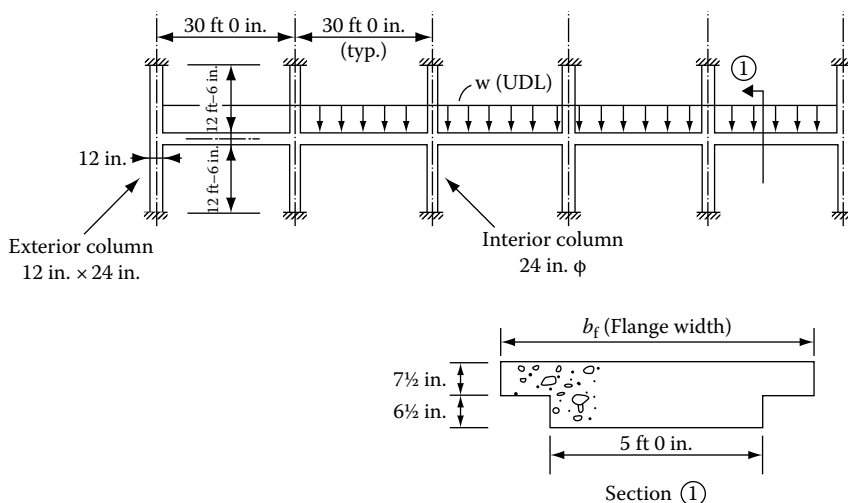
$$= 5 + 16 \times 7.5 / 12 = 15 \text{ ft}$$

$$= 5 + 25 / 2 = 17.5 \text{ ft}$$

Section properties:

$$I = 16,650 \text{ in.}^4$$

$$Y = 7.69 \text{ in.}$$



**FIGURE 2.83** Example 2: posttensioned continuous beam dimensions and loading.

$$St = 2637 \text{ in.}^8$$

$$Sb = 2166 \text{ in.}^3$$

$$A = 1065 \text{ in.}^2$$

Loading:

Dead load of 7½ in slab = 94 psf

Mechanical and electrical = 6 psf

Ceiling = 6 psf

Partitions = 20 psf

Additional dead load due to beam self-weight =  $615 \times 60 \times 150/144 \times 30 = 13.5 = 14 \text{ psf}$

Total dead load = 140 psf

Live load at owner's request = 80 psf

$$D + L = 220 \text{ psf}$$

Uniform load per feet of beam =  $0.220 \times 30 = 6.6 \text{ klf}$ . The resulting service load moments are shown in Figure 2.84. As before we design for the moments at the face of supports.

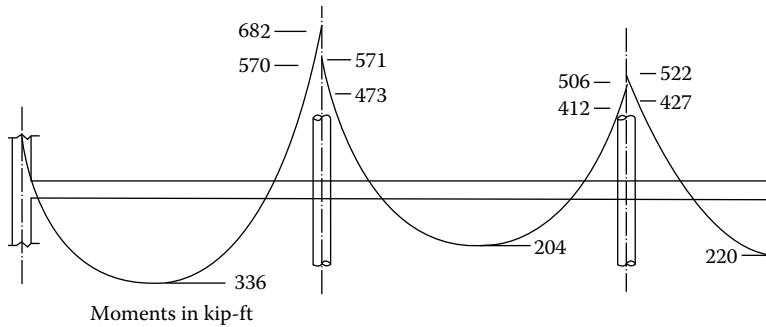
**Interior Span:** Calculate through tendons by using interior span moment of 427 kip-ft at the inside face of third column (Figure 2.84).

Assume  $h_1 = 11.5 \text{ in.}$ ,  $h_2 = 2.5 \text{ in.}$ ,  $L_1 = 2.5 \text{ ft}$ , and  $L_2 = 12.5 \text{ ft}$ .

The height of inflection point

$$h_3 = 11.5 \times 12.5 + 2.5 \times 2.5/15 = 10 \text{ in.}$$

$$h_d = e = 10 - 2.5 = 7.5 \text{ in.}$$



**FIGURE 2.84** Example 2: posttensioned continuous beam: service load moments.

### First Cycle

Assume  $W_p = 3.5$  klf

$$M_p = 3.5/6.6 \times 427 = 226 \text{ kip-ft}$$

$$M_{ub} = 427 - 226 = 201 \text{ kip-ft}$$

$$f_t = 201 \times 12/2637 = 0.915 \text{ ksi}$$

$$f_p = 0.915 - 0.380 = 0.535 \text{ ksi}$$

$$P = 0.535 \times 106.5 = 570 \text{ kip}$$

$$W_p = 8 \times 570 \times 7.5/12 \times (26.25)^2 = 3.77 \text{ klf}$$

which is greater than 3.5 klf. N.G.

### Second Cycle

New value of

$$W_p = 0.75 \times 3.5 + 0.25 \times 3.77 = 3.57 \text{ klf}$$

$$M_p = 3.57/6.6 \times 427 = 231 \text{ kip-ft}$$

$$M_{ub} = 427 - 231 = 196 \text{ kip-ft}$$

$$f_t = 196 \times 12/2637 = 0.892 \text{ ksi}$$

$$f_p = 0.892 - 0.380 = 0.512 \text{ ksi}$$

$$P = 0.512 \times 1065 = 545 \text{ kip}$$

$$W_p = 8 \times 545 \times 7.5/12 \times (26.25)^2 = 3.60 \text{ klf}$$

which is nearly equal to 3.57 klf. Therefore, the design is satisfactory.

Check design against positive moment of 220 kip-ft

$$M_p = 3.6 \times 220/6.6 = 120 \text{ kip-ft}$$

$$M_{ub} = 220 - 120 = 100 \text{ kip-ft}$$

$$F_{bot} = 100 \times 12/2166 = 0.554 \text{ ksi (tension)}$$

Axial compression stress =  $545/1065 = 0.512$  ksi (comp)

$$F_{total} = 0.554 - 0.512 = 0.045 \text{ ksi (tension)}$$

This is less than the allowable tensile stress of 0.380 ksi. Therefore, the design is satisfactory.

**End Span:** Determine end bay prestressing for a negative moment of 570 kip-ft at the face of first interior column (Figure 2.84).

### First Cycle

As before, assume

$$W_p = 3.5 \text{ klf}$$

$$M_p = 3.5/6.6 \times 570 = 302 \text{ kip-ft}$$

$$M_{ub} = 570 - 302 = 268 \text{ kip-ft}$$

$$f_t = 268 \times 12/2637 = 1.22 \text{ ksi}$$

$$f_p = 1.22 - 0.380 = 0.84 \text{ ksi}$$

$$P = 0.84 \times 1065 = 894 \text{ kip}$$

$$W_p = 8 \times 894 \times 7.5/12 \times (26.25)^2 = 5.912 \text{ klf}$$

which is greater than 3.5 klf. N.G.

### Second Cycle

New value of

$$W_p = 0.74 \times 3.5 + 0.25 \times 5.912 = 4.1 \text{ klf}$$

$$M_p = 4.1/6.6 \times 570 = 354 \text{ kip-ft}$$

$$M_{ub} = 570 - 354 = 216 \text{ kip-ft}$$

$$f_t = 216 \times 12/2637 = 0.983 \text{ ksi}$$

$$f_p = 0.983 - 0.380 = 0.603 \text{ ksi}$$

$$P = 0.603 \times 1065 = 642 \text{ kip}$$

$$W_p = 8 \times 642 \times 7.5/12 \times (26.25)^2 = 4.24 \text{ klf}$$

This is nearly equal to 4.1 klf. However, a more accurate value is calculated as follows:

$$W_p = 0.75 \times 4.1 + 0.25 \times 4.24 = 4.13 \text{ klf}$$

Check the design against positive moment of 336 kip-ft:

$$M_p = 4.13/6.6 \times 336 = 210 \text{ kip-ft}$$

$$M_{ub} = 336 - 210 = 126 \text{ kip-ft}$$

Bottom flexural stress =  $126 \times 12/2166 = 0.698 \text{ ksi}$  (tension)

Axial compressive stress due to posttension =  $642/1065 = 0.603 \text{ ksi}$  (comp)

$$F_{total} = 0.698 - 0.603 = 0.095 \text{ ksi}$$

This is less than the allowable tensile stress of 0.380 ksi. Therefore, the design is OK.



### 2.5.10.3.3 Example 3: PT Flat Plate

Figure 2.85 shows a schematic section of a two-way flat plate system. Design of posttension slab for an office-type loading is required.

#### Given:

Specified compressive strength of concrete  $f'_c = 4000$  psi

Modulus of elasticity of concrete:  $E_c = 3834$  ksi

Allowable tensile stress is precompressed tensile zone  $= 6\sqrt{f'_c} = 380$  psi

Allowable fiber stress in compression  $= 0.45 f'_c = 0.45 \times 4000 = 1800$  psi

Tendon cover: Interior spans      Top 0.75 in.  
    Bottom 0.75 in.

Exterior spans      Top 0.75 in  
                                  Bottom 1.50 in

Tendon diameter  $= \frac{1}{2}$  in.

Minimum area of bonded reinforcement:

In negative moment areas at column supports:

$$A_s = 0.00075 A_{cf}$$

where

$A_{cf}$  is the larger gross cross-sectional area of the slab beam strips of two orthogonal equivalent frames intersecting at a column of a two-way slab, in in.<sup>2</sup>

In positive moment areas where computed concrete stress in tension exceeds  $\sqrt{f'_c}$ :

$$A_x = N_c / 0.5 f_y$$

where

$N_c$  is the tensile force in concrete due to unfactored dead load plus live load ( $D + L$ ), in lb

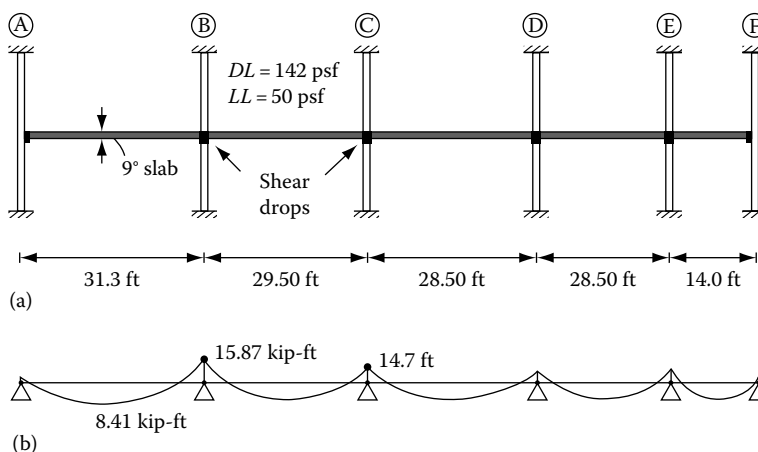
Rebar yield stress = 60 ksi. Max bar size = #4.

Rebar cover 1.63 in. at top and bottom

Posttension requirements:

Minimum posttensioned stress = 125 psi (See ACI 318-02, Section 18.12.4)

Minimum balanced load = 65% of total dead load



**FIGURE 2.85** Example 3; flat plate design: (a) span and loading and (b) elastic moments due to dead load.

**Design:** The flat plate is sized using the span:depth ratios given in Table 2.7. The maximum span is 31 ft 4 in. between grids A and B. Using a span:depth ratio of 40, the slab thickness is  $31.33 \times 12/40 = 9.4$  in., rounded to 9 in.

The flat plate has “shear drops” intended to increase only the shear strength and flexural support width. The shear heads are smaller than a regular drop panel as defined in the ACI code. Therefore shear heads cannot be included in calculating the bending resistance.

Loading:	Dead load of 9 in. slab	112 psf
	Partitions	20 psf
	Ceiling and mechanical	10 psf
	Reduced live load	50 psf

Total service load =  $112 + 20 + 10 + 50 = 192$  psf

Ultimate load =  $1.4 \times 142 + 1.7 \times 50 = 285$  psf

Slab properties (for a 1 ft wide strip):

$$I = bh^3/12 = 12 \times 9^3/12 = 729 \text{ in.}^4$$

$$S_{\text{top}} = S_{\text{bot}} = 729/4.5 = 162 \text{ in.}^3$$

$$\text{Area} = 12 \times 9 = 108 \text{ in.}^2$$

The moment diagram for a 1 ft wide strip of slab subjected to a service load of 192 psf is shown in Figure 2.86.

The design of continuous strands will be based on a negative moment of 14.7 kip-ft at the second interior span. The end bay prestressing will be based on a negative moment of 15.87 kip-ft.

**Interior Span:** Calculate the drape of tendon using the procedure given for the previous problem. See Figure 2.82.

$$h_3 = h_1 L_2 + h_2 L_1 / L_1 + L_2$$

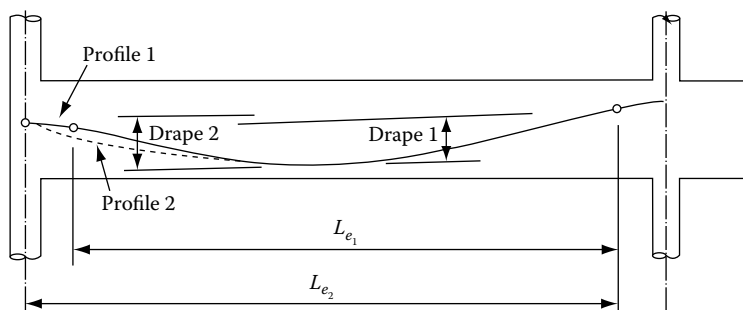
$$L_1 = 1.84 \text{ ft} \quad h_1 = 8 \text{ in.}$$

$$L_2 = 12.90 \text{ ft} \quad h_2 = 1.25 \text{ in.}$$

$$L_e = 12.9 \times 2 = 25.8 \text{ ft}$$

$$h_3 = 8 \times 12.90 + 1.25 \times 1.84/14.75 = 7.153 \text{ in.}$$

$$\text{Tendon drape} = 7.153 - 1.25 = 5.90 \text{ in.}$$



**FIGURE 2.86** End bay tendon profiles.

**First Cycle**

$$\begin{aligned}\text{Minimum balanced load} &= 0.65 \times (\text{total DL}) \\ &= 0.65(112 + 10 + 20) = 92 \text{ psf}\end{aligned}$$

$$\begin{aligned}\text{Moment due to balanced load} &= \frac{92}{192} \times 14.7 \\ &= 7.04 \text{ kip-ft}\end{aligned}$$

This is subtracted from the total service load moment of 14.7 kip-ft to obtain the unbalanced moment  $M_{ub}$ .

$$M_{ub} = 14.7 - 7.04 = 7.66 \text{ kip-ft}$$

The flexural stresses at the top and bottom are obtained by dividing  $M_{ub}$  by the section moduli of the structure's cross section.

$$f_t = \frac{7.66 \times 12}{162} = 0.567 \text{ ksi}$$

$$f_b = \frac{7.66 \times 12}{162} = 0.567 \text{ ksi}$$

the minimum required compressive prestress  $f_p$  is found by subtracting the maximum allowable tensile stress  $f_a = 6\sqrt{f_c}$  from the calculated tensile stress. Thus, the smallest required compressive stress is

$$\begin{aligned}f_p &= f_t - f_a \\ &= 0.567 - 380 = 0.187 \text{ ksi}\end{aligned}$$

The prestress force is calculated by multiplying  $f_p$  by the cross-sectional area:

$$P = 0.187 \times 9 \times 12 = 20.20 \text{ kip-ft}$$

Determine the equivalent load due to prestress force  $P$  by the relation

$$W_p = \frac{8Pe}{L_e^2}$$

For the example problem,

$$P = 20.20 \text{ kip-ft}, \quad e = 5.90 \text{ in.}$$

$$L_e = 2 \times 12.90 = 25.8 \text{ ft}$$

$$\text{Therefore } W_p = \frac{8 \times 20.20 \times 5.90}{25.8^2 \times 12} = 0.120 \text{ klf} = 120 \text{ plf}$$

Comparing this with the value of 93 plf assumed at the beginning of first cycle, we find the two values are not equal. Therefore, we assume a new value and repeat the procedure until convergence is obtained.

### Second Cycle

$$W_p = 0.75 \times 92 + 0.25(120) = 99 \text{ plf}$$

$$M_b = \frac{99}{192} \times 14.7 = 7.58 \text{ kip-ft}$$

$$M_{ub} = 14.7 - 7.58 = 7.12 \text{ kip-ft}$$

$$f_t = f_b = \frac{7.12 \times 12}{162} = 0.527 \text{ ksi}$$

$$f_p = 0.527 - 0.380 = 0.147 \text{ ksi}$$

$$P = 0.147 \times 9 \times 12 = 15.92 \text{ kip-ft}$$

$$W_p = \frac{8 \times 15.92 \times 5.90}{25.8^2 \times 12} = 0.094 \text{ klf} = 94 \text{ plf}$$

This is less than 99 plf assumed at the beginning of second cycle. Therefore, we assume a new value and repeat the procedure.

### Third Cycle

$$W_p = 0.75 \times 99 + 0.25(94) = 97.7 \text{ plf}$$

$$M_b = \frac{97.7 \times 14.7}{192} = 7.48 \text{ kip-ft}$$

$$M_{ub} = 14.7 - 7.48 = 7.22 \text{ kip-ft}$$

$$f_t = f_b = \frac{7.22 \times 12}{162} = 0.535 \text{ ksi}$$

$$f_p = 0.535 - 0.380 = 0.155 \text{ ksi}$$

$$P = 0.155 \times 9 \times 12 = 16.74 \text{ kip-ft}$$

$$W_p = \frac{8 \times 16.74 \times 5.90}{25.8^2 \times 12} = 0.99 \text{ klf} = 99 \text{ plf}$$

This is nearly equal to 97.7 plf assumed at the beginning of the third cycle. Therefore, it is OK.

Check compressive stress at the support:

$$M_p = \frac{99 \times 14.7}{192} = 7.58 \text{ ksi-ft}$$

$$M_{ub} = 14.7 - 7.58 = 7.12 \text{ kip-ft}$$

$$f_b = \frac{7.12 \times 12}{162} = 0.527 \text{ ksi} = 527 \text{ ksi}$$

$$\text{Axial compressive stress due to posttension} = \frac{16.74 \times 1000}{9 \times 12} = 155 \text{ psi}$$

$$\text{Total compressive stress} = 527 + 155 = 682 \text{ psi}$$

This is less than the allowable compressive stress of 1800 psi; therefore, the design is satisfactory.

**End Bay Design:** The placement of tendons within the end bay presents a few problems. The first problem is in determining the location of the tendon over the exterior support. Placing the tendon above the neutral axis of the member results in an increase in the total tendon drape, allowing the designer to use less prestress than would otherwise be required. Raising the tendon, however, introduces an extra moment that effectively cancels out some of the benefits from the increased drape. For this reason, the tendon is usually placed at a neutral axis at exterior supports.

The second problem is in making a choice in the tendon profile: whether to use a profile with a reverse curvature over each support (see Figure 2.86, profile 1), or over the first interior support only (see Figure 2.86, profile 2). A profile with the reversed curvature over the first interior support only gives a greater cable drape than the first profile, suggesting a larger equivalent load with the same amount of prestress. On the other hand, the effective length  $L_e$  between inflection points of profile 1 is less than that of profile 2 which suggests the opposite. To determine which profile is in fact more efficient, it is necessary to evaluate the amount of prestress for both profiles. More usually, a tendon profile with reverse curvature over both supports is 5%–10% more efficient since the equivalent load produced is a function of the square of the effective length.

The last item addresses the extra end bay prestressing required in most situations. The exterior span in an equal span structure has the greatest moments due to support rotations. Because of this, extra prestressing is commonly added to end bays to allow efficient design to end spans. For design purposes, the extra end bay prestressing is considered to act within the end bay only. These tendons actually extend well into the adjacent span for anchorage, as shown in Figure 2.87. Advantage can be taken of this condition by designing the through tendons using the largest moment found within the interior spans, including the moment at the interior face of the first support. The end bay interior spans, including the moment at the interior face of the first support. The end bay prestress force is determined using the largest moment within the exterior span. The stress at the inside face of the first support is checked using the equivalent loads produced by the through tendons and the axial compression provided by both the through and added tendons. If the calculated stresses are less than the allowable values, the design is complete. If not, more stress is provided either by through tendons or added tendons or both.

The design of end bay using profiles 1 and 2 follows.

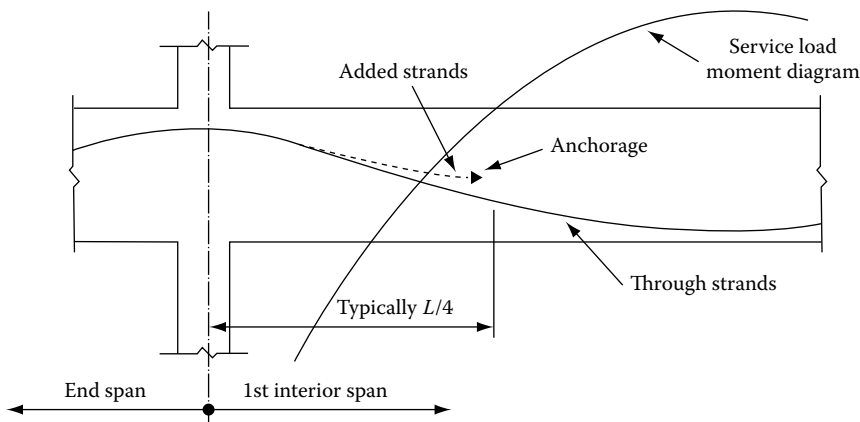


FIGURE 2.87 Anchorage of added tendons.

**Profile 1: Reverse Curvature at Interior Support Only (Figure 2.88b).** Observe that the height of inflection point is exact if the tendon profile is symmetrical about the center span. If it is not, as in span 1 of the example problem, sufficiently accurate value can be obtained by taking the average of the tendon inflection point at each end as follows.

Left end:

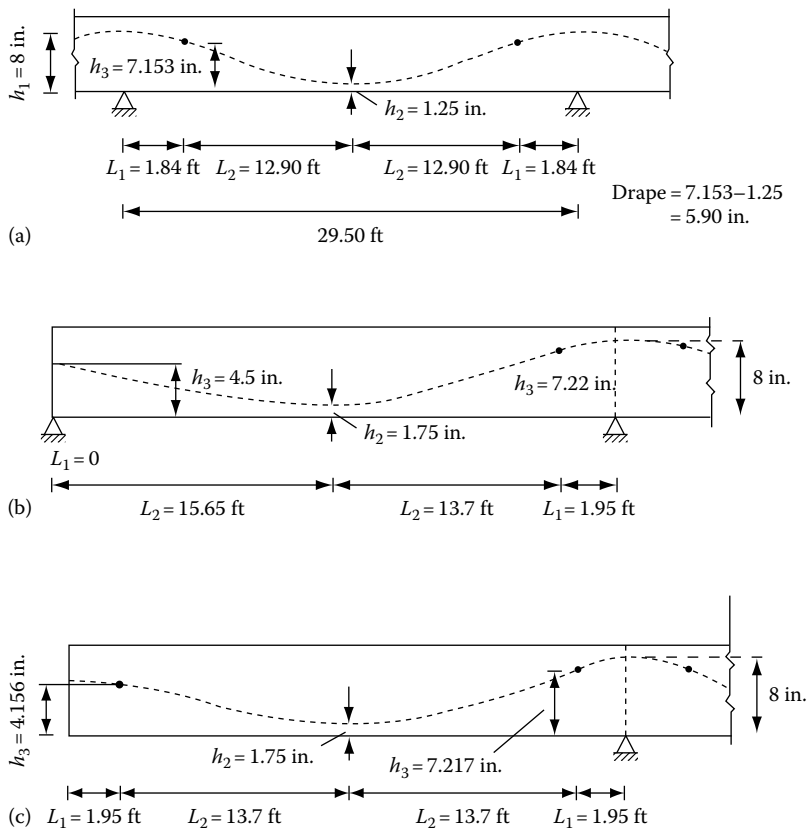
$$h_3 = \frac{4.5 \times 15.6 + 1.75 \times 0}{0 + 15.67} = 4.5 \text{ in.}$$

Right end:

$$h_3 = \frac{8 \times 13.7 + 1.75 \times 1.95}{1.95 + 13.70} = 7.22 \text{ in.}$$

$$\text{Average } h_3 = \frac{4.5 + 7.22}{2} = 5.86 \text{ in.}$$

$$\text{Drape} = 5.86 - 1.75 = 4.11 \text{ in.}$$



**FIGURE 2.88** Example problem 3: flat plate, tendon profiles: (a) interior span; (b) exterior span, reverse curvature at right support; and (c) exterior span, reverse curvature at both supports.

**First Cycle**

To show the quick convergence of the procedure, we start with a rather high value of

$$W_p = 0.75 DL = 0.75 \times 142 = 106 \text{ plf}$$

$$M_b = \frac{106}{192} \times 15.87 = 8.76 \text{ kip-ft}$$

$$M_{ub} = 15.87 - 8.76 = 7.11 \text{ kip-ft}$$

$$f_t = f_b = \frac{7.11 \times 12}{162} = 0.527 \text{ ksi}$$

$$f_p = 0.527 - 0.380 = 0.147 \text{ ksi}$$

$$P = 0.147 \times 9 \times 12 = 15.87 \text{ kip-ft}$$

$$\begin{aligned} W_p &= \frac{8Pe}{L_e^2} \\ &= \frac{8 \times 15.87 \times 4.11}{29.35^2 \times 12} \\ &= 0.050 \text{ klf} = 50.0 \text{ plf} \end{aligned}$$

This is less than 106. N.G.

**Second Cycle**

$$W_p = 0.75(106) + 0.25(50.0) = 92 \text{ plf}$$

$$M_b = \frac{92}{192} \times 15.87 = 7.60 \text{ kip-ft}$$

$$M_{ub} = 15.87 - 7.60 = 8.27 \text{ kip-ft}$$

$$f_t = f_b = \frac{8.27 \times 12}{162} = 0.612 \text{ ksi}$$

$$f_p = 0.612 - 0.380 = 0.233 \text{ ksi}$$

$$P = 0.233 \times 12 \times 9 = 25.16 \text{ kip-ft}$$

$$\begin{aligned} W_p &= \frac{8 \times 25.16 \times 4.11}{29.35^2 \times 12} \\ &= 0.080 \text{ klf} = 80.0 \text{ plf} \end{aligned}$$

This is less than 91.5 psi used at the beginning of second cycle. N.G.

**Third Cycle**

$$W_p = 0.75 \times 92 + 0.25 \times 80 = 89 \text{ plf}$$

$$M_b = \frac{89}{192} \times 15.87 = 7.356 \text{ kip-ft}$$

$$M_{ub} = 15.87 - 7.356 = 8.5 \text{ kip-ft}$$

$$f_t = f_b = \frac{8.5 \times 12}{162} = 0.631 \text{ ksi}$$

$$f_p = 0.631 - 0.380 = 0.251 \text{ ksi}$$

$$P = 0.251 \times 12 \times 9 = 27.10 \text{ kip-ft}$$

$$W_p = \frac{8 \times 27.10 \times 4.11}{29.35^2 \times 12} = 0.086 \text{ klf} = 86 \text{ plf}$$

This is nearly equal to 89 plf used at the beginning of third cycle. Therefore, it is OK.

**Profile 2: Reverse Curvature over Each Support (Figure 2.88c).**

Left end:

$$h_3 = \frac{4.5 \times 13.70 + 1.75 \times 1.95}{(13.70 + 1.95)} = 4.156 \text{ in.}$$

Right end:

$$h_3 = \frac{8 \times 13.70 + 1.75 \times 1.95}{(13.70 + 1.95)} = 7.221 \text{ in.}$$

$$\text{Average } h_3 = \frac{4.156 + 7.221}{2} = 5.689 \text{ in.}$$

$$e = h_d = 5.689 - 1.75 = 3.939 \text{ in.}$$

**First Cycle**

We start with an assumed balanced load of 0.65  $DL = 7.60 \text{ kip-ft}$

$$\text{Balanced moment } M_b = 15.87 \times \frac{92}{192} = 7.60 \text{ kip-ft}$$

$$M_{ub} = 15.87 - 7.6 = 8.27 \text{ kip-ft}$$

$$f_t = f_b = \frac{8.27 \times 12}{162} = 0.613 \text{ ksi}$$

$$f_p = 0.613 - 0.380 = 0.233 \text{ ksi}$$

$$P = 0.233 \times 12 \times 9 = 25.16 \text{ kip}$$

$$W_p = \frac{8 \times 25.12 \times 3.937}{27.38^2 \times 12} = 0.088 \text{ klf} = 88 \text{ plf}$$

This is less than 92 plf. N.G.

**Second Cycle**

$$W_p = 0.75 \times 92 + 0.25 \times 88 = 91 \text{ plf}$$

$$M_b = 15.87 \times \frac{91}{192} = 7.52 \text{ ksi-ft}$$

$$M_{ub} = 15.87 - 7.52 = 8.348 \text{ kip-ft}$$

$$f_t = f_b = \frac{8.348}{162} \times 12 = 0.618 \text{ ksi}$$



$$f_p = 0.618 - 0.380 = 0.238 \text{ ksi}$$

$$P = 0.238 \times 9 \times 12 = 25.75 \text{ kip}$$

$$W_p = \frac{8 \times 25.75 \times 3.937}{(27.38)^2 \times 12} = 0.090 \text{ klf} = 90 \text{ klf}$$

This is nearly equal to the value at the beginning of second cycle. Therefore, it is OK.

Check the design against positive moment of 8.41 kip-ft:

$$W_p = 0.090 \text{ klf}$$

$$M_b = 8.41 \times \frac{0.090}{0.142} = 5.33 \text{ kip-ft}$$

$$M_{ub} = 8.41 - 5.33 = 3.08 \text{ kip-ft}$$

$$\text{Bottom flexural stress} = \frac{3.08 \times 12}{162} = 0.288 \text{ ksi (tension)}$$

$$\text{Axial compression due to posttension} = \frac{25.75}{12 \times 9} = 0.238 \text{ ksi}$$

$$\text{Total stress at bottom} = 0.228 - 0.238 = -0.10 \text{ ksi (Compression)}$$

This is less than allowable tension of 0.380 ksi. Therefore, design OK.

### 2.5.11 TYPICAL POSTTENSIONING DETAILS

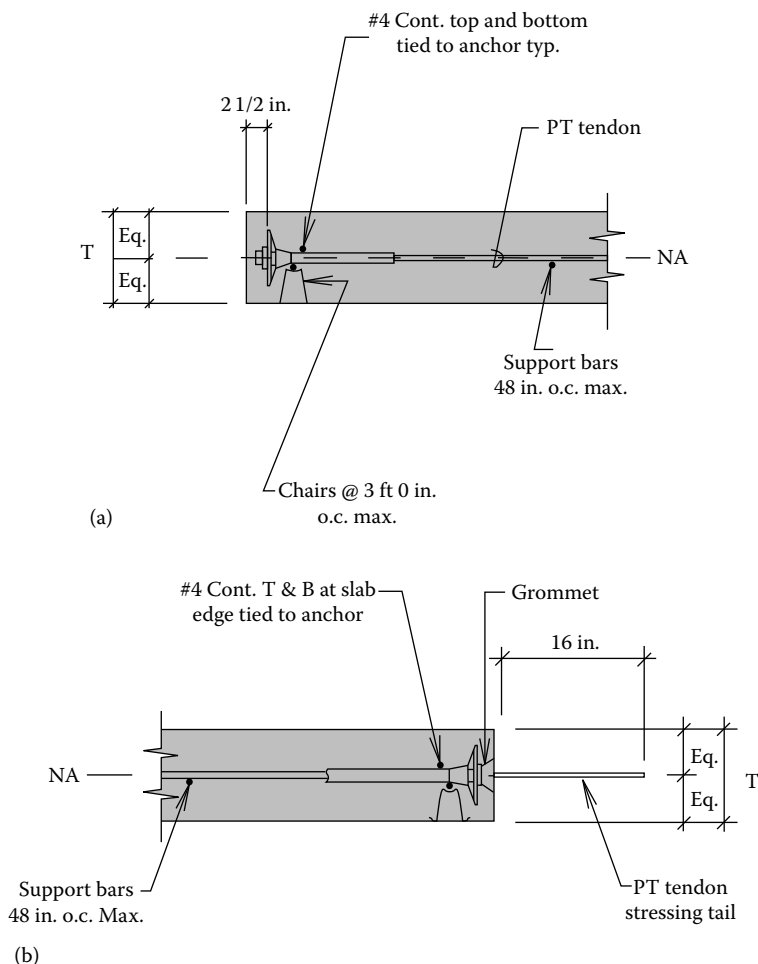
Posttensioning details typically used in North American practice are shown in Figures 2.89 through 2.98.

## 2.6 FOUNDATIONS

The structural design of a skyscraper foundation is primarily determined by loads transmitted by its many floors to the ground on which the building stands. To keep its balance in high windstorms and earthquakes, its foundation requires special consideration because the lateral loads which must be delivered to the soil are rather large. Where load-bearing rock or stable soils such as compact glacial tills are encountered at reasonable depth, as in Dallas with limestone with a bearing pressure of 50 tons per square foot ( $47.88 \times 10^2 \text{ kPa}$ ), Chicago with hard pan at 20 to 40 tons per square foot ( $19.15 \times 10^2$  to  $38.3 \times 10^2 \text{ kPa}$ ), the foundation may be directly carried down to the load-bearing strata. This is accomplished by utilizing deep basements, caissons, or piles to carry the column loads down through poor spoils to compact materials. The primary objective of a foundation system is to provide reasonable flexibility and freedom in architectural layout; it should be able to accommodate large variations in column loadings and spacing without adversely affecting the structural system due to differential settlements.

Many principal cities of the world are fortunate to be underlain by incompressible bedrock at shallow depths, but certain others rest on thick deposits of compressible soil. The soils underlying downtown Houston, for example, are primarily clays that are susceptible to significant volume changes due to changes in applied loads. The loads of such compressible soils must be controlled to keep settlements to acceptable limits.

Usually this is done by excavating a weight of soil equal to a significant portion of the gross weight of the structure. The net allowable pressure that the soil can be subjected to, is dependent upon the physical characteristics of the soil. Where soil conditions are poor, a weight of the soil equal to the weight of the building may have to be excavated to result in what is commonly known as fully compensated foundation. Construction of deep foundations may create a serious menace



**FIGURE 2.89** Anchor device at distributed tendons: (a) dead end and (b) stressing end.

to many older neighboring buildings in many ways. If the water table is high, installation of pumps may be required to reduce the water pressure during the construction of basements and may even require a permanent dewatering system. Depending upon the nature of subsoil conditions, the water table under the adjoining facilities can be lowered, creating an adverse effect on neighboring buildings. Another effect to be kept in mind is the settlement of nearby structures from the weight of the new building.

For buildings in seismic zones, in addition to the stiffness and load distribution, it is important to consider the rigidity of the foundation. During earthquakes, the building displacements are increased by the angular rotation of the foundation due to rocking action. The effect is an increase in the natural period of vibration of the building.

Loads resulting at the foundation level due to wind or earthquake must be delivered ultimately to the soil. The vertical component due to overturning effects is resisted by the soil in a manner similar to the effects of gravity loads. The lateral components is resisted by (1) shear resistance of piles or piers; (2) axial loads in batter piles; (3) shear along the base of the structure; and (4) lateral resistance of soil pressure acting against foundation walls, piers, etc. Depending upon the type of foundation, one or more of the above may play a predominant role in resisting the lateral component.



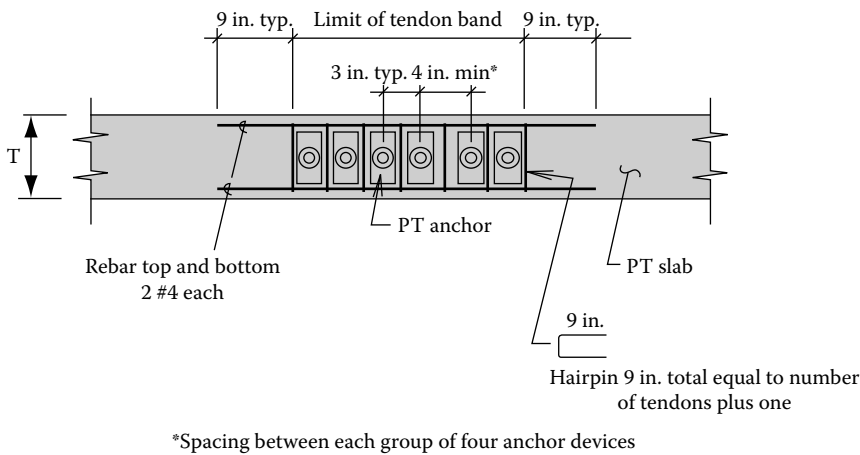


FIGURE 2.92 Typical reinforcement of tendon band at slab edge or at intermediate stressing.

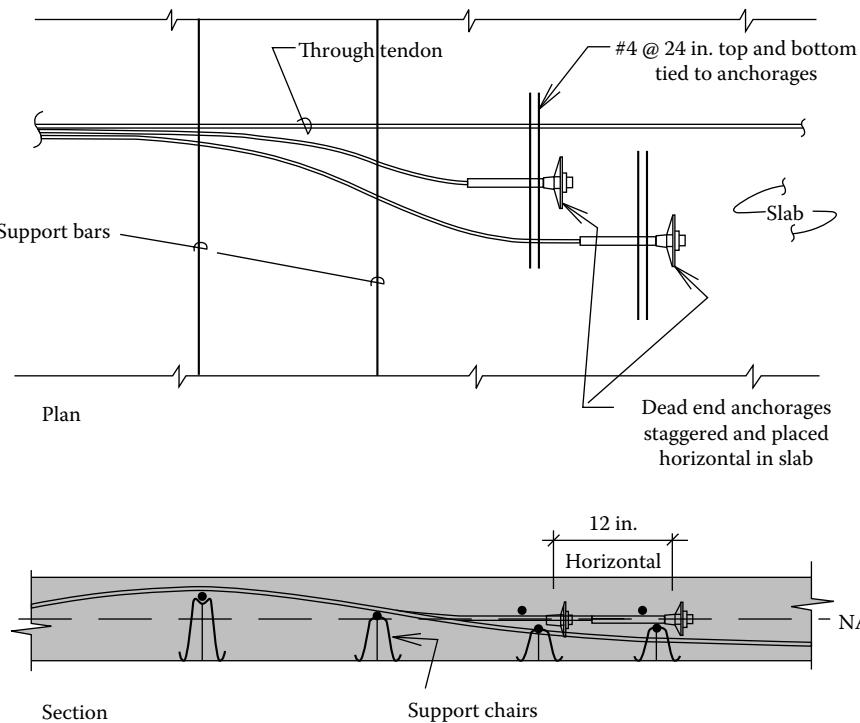


FIGURE 2.93 Placement of added tendon.

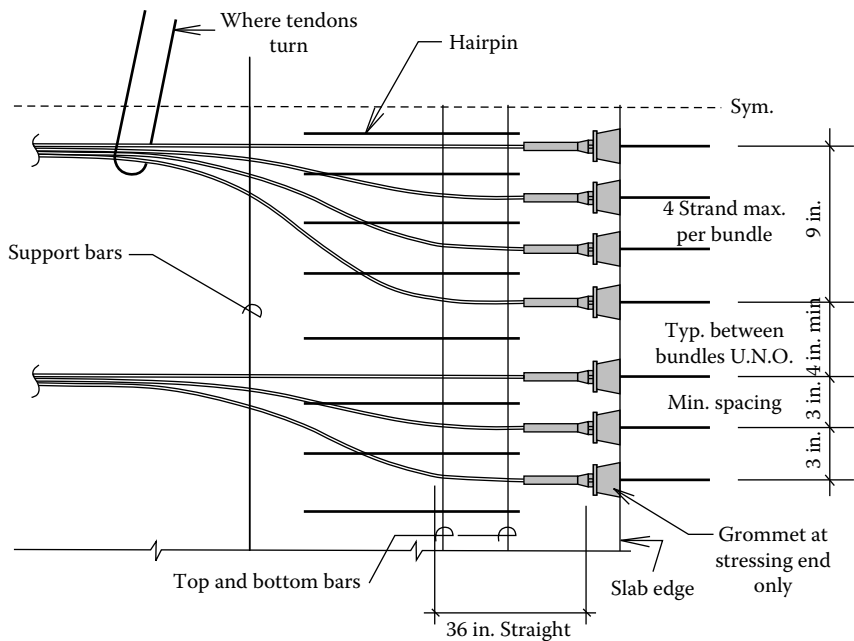


FIGURE 2.94 Flaring of banded tendons at slab edge.

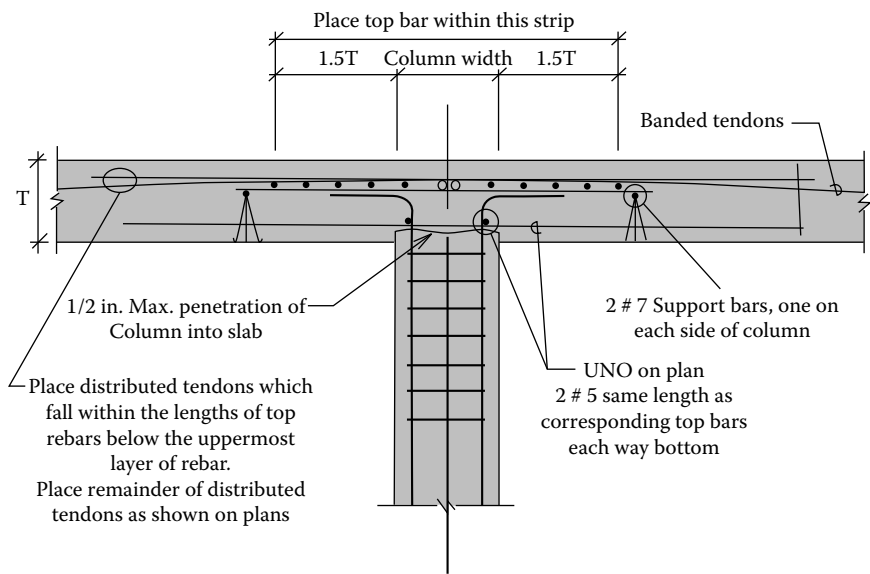


FIGURE 2.95 Typical column-slab section.

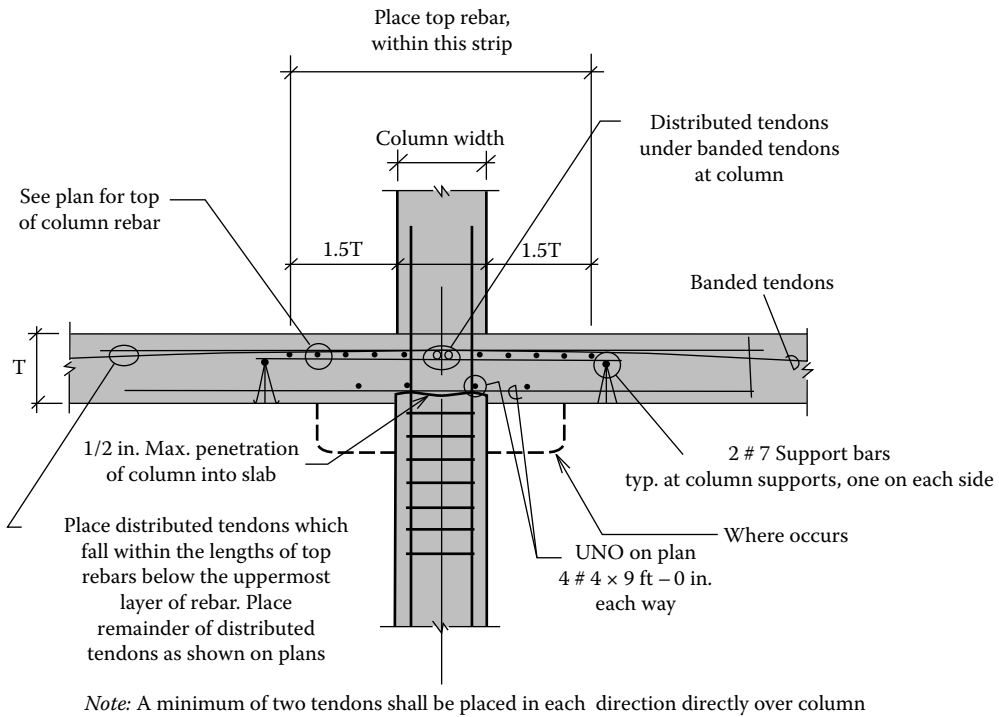


FIGURE 2.96 Typical interior column.

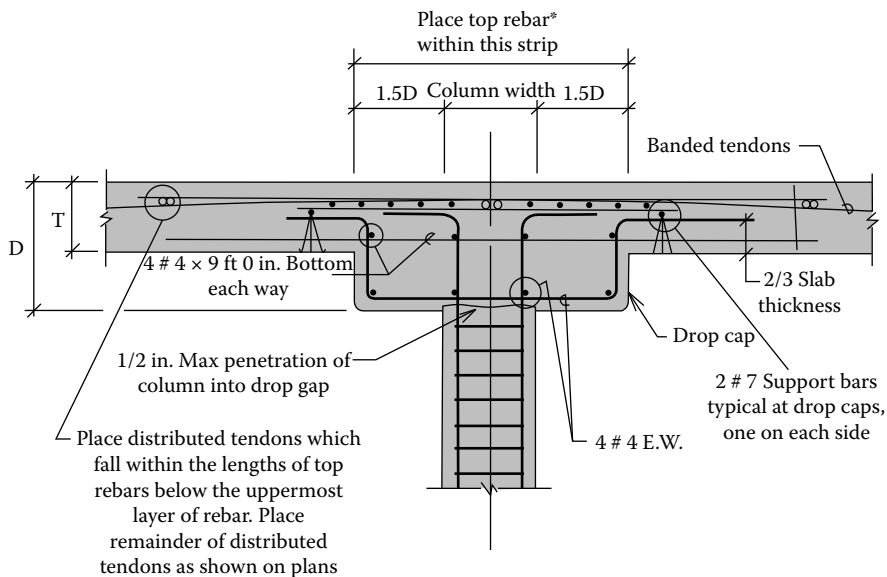
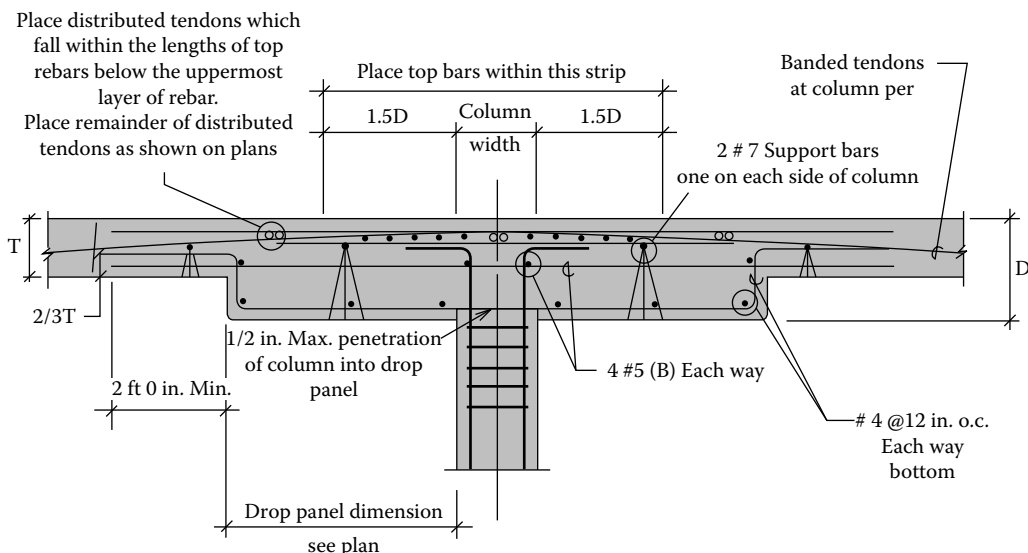


FIGURE 2.97 Typical column section.



*Note:* A minimum of two tendons shall be placed in each direction directly over column

**FIGURE 2.98** Typical drop panel section.

Much engineering judgment is required to reach a sound conclusion on the allowable movements that can be safely tolerated in a tall building. A number of factors need to be taken into account. These are

1. Type of framing employed for the building
2. Magnitude of total as well as differential movement
3. Rate at which the predicted movement takes place
4. Type of movement whether the deformation of the soil causes tilting or vertical displacement of the building

Every city has its own particular characteristics in regard to design and construction of foundations for tall buildings which are characterized by the local geology and groundwater conditions. Their choice for a particular project is primarily influenced by economic and soil conditions, and even under identical conditions can vary in different geographical locations. In this section a brief description of two types, namely, the pile and mat foundations, is given, highlighting their practical aspects.

### 2.6.1 PILE FOUNDATIONS

Pile foundation using either driven piles or drilled piers (also called caissons) are finding more and more application in tall building foundation systems. Driven piles usually consist of prestressed precast piles, or structural steel pipes, box, or steel H sections. Drilled piers may consist of either straight shafts or may have bells or underreams at the bottom. The number of different pile and caisson types in use is continually changing with the development of pile-driving and earth-drilling equipment.

Driven piles can be satisfactorily founded in nearly all types of soil conditions. When soils overlying the foundation stratum are soft, normally no problem is encountered in driving the piles. If variations occur in the level of the bearing stratum, it will be necessary to use different lengths of piles over the site. A bearing type of pile or pier receives its principal vertical support from a soil or rock layer at the bottom of the pier, while a friction-type pier receives its vertical support from skin resistance developed along the shaft. A combination pier, as the name implies, provides resistance from a combination of bearing at the bottom and friction along the shaft. The function

of a foundation is to transfer axial loads, lateral loads, and bending moments to the soil or rock surrounding and supporting it.

The design of a pier consists of two steps: (1) determination of pier size, based on allowable bearing and skin friction if any, of the foundation material; and (2) design of the concrete pier itself as a compression member. Piers that cannot be designed in plain concrete with practical dimensions can be designed in reinforced concrete. When tall buildings are constructed with deep basements, the earth pressure on the basement walls may be sufficient to resist the lateral loads from the superstructure. However, the necessary resistance must be provided by the piers when there is no basement, when the depth of basement walls below the surface is too shallow, or when the lateral movements associated with the mobilization of adequate earth pressure are too large to be tolerated. In such cases it is necessary to design the piers for lateral forces at the top, axial forces from gravity loads and overturning, and concentrated moments at the top. One method of evaluating lateral response of piers is to use the theory of beam on elastic foundation by considering the lateral reaction of the soil as an equivalent lateral elastic spring.

The effect of higher concentration of gravity loading over the plan area of a tall building often necessitates use of piles in large groups. In comparison to the stresses in the soil produced by a single pile, the influence of a group of piles extends to a significantly greater distance both laterally and vertically. The resultant effect on both ultimate resistance to failure and overall settlement are significantly different than the summation of individual pile contributions. Because of group action, the ultimate resistance is less while the overall settlement is more.

Often times the engineers and architects are challenged to create a floating effect for the building. This is usually achieved by not bringing the façade right to the ground in order to create an open lobby. A structural system which uses a heavily braced core and a nominal moment frame on the perimeter presents itself as a solution, the core resisting most of the overturning moment and shear while the perimeter frame provides the torsional resistance. Because of the limited width of the core, strong uplift forces are created in the core columns due to lateral loads. A similar situation develops in the corner columns of exterior-braced tube structures. One of the methods of overcoming the uplift forces is to literally anchor the columns into bedrock. A concrete pier constructed below the foundation is secured to the rock by the posttensioned anchors. Anchor bolts for steel columns cast in the pier transfer the tensile forces from columns to the pier. Another method of securing the columns is to thread the posttensioned anchors directly through the base plate assemblies of the column.

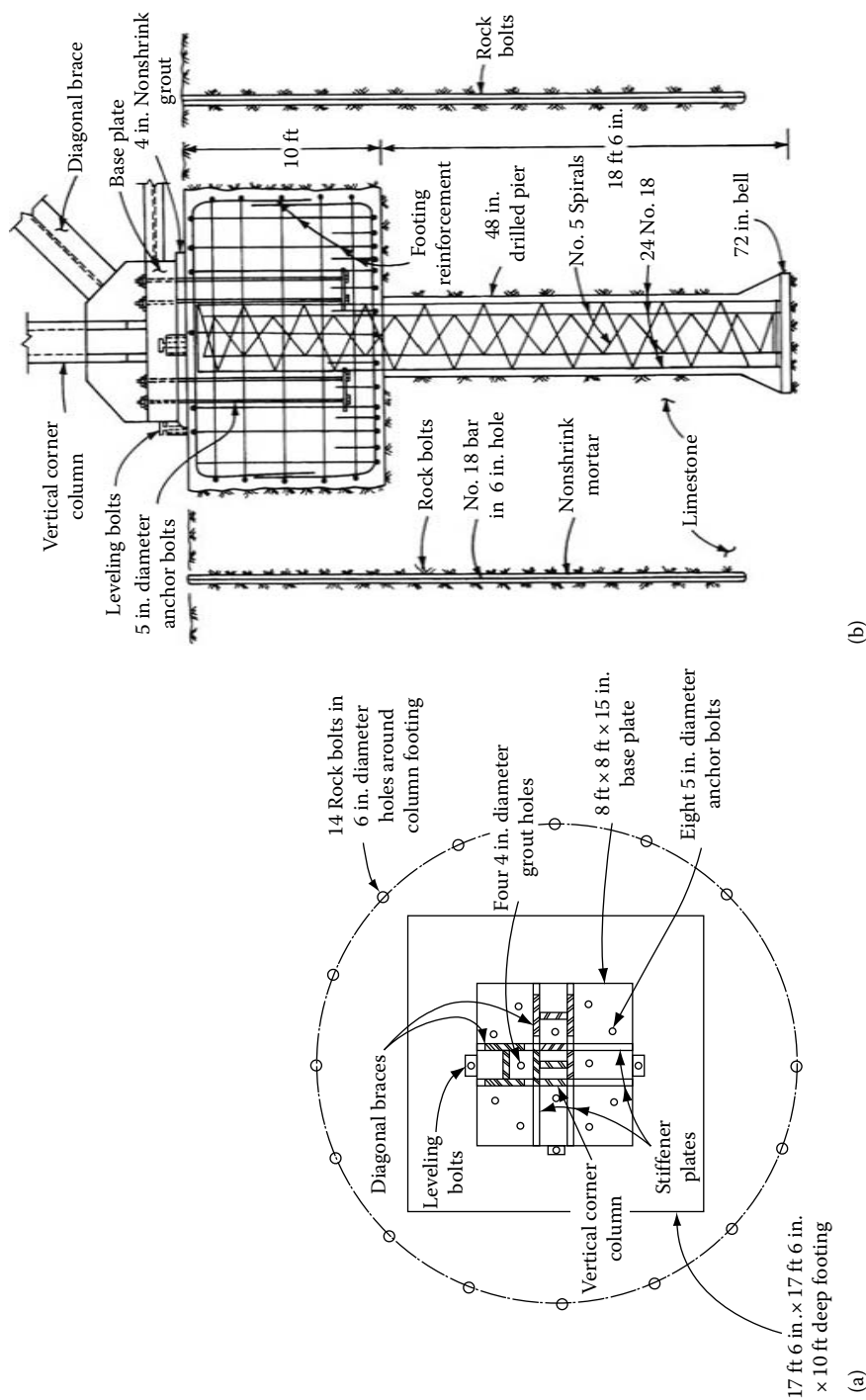
Figure 2.99 shows the plan and cross section of a foundation system for a corner column of an X-braced tube building. The spread footing founded on limestone resists the compressive forces while the belled pier under the spread footing is designed to resist uplift forces. To guard against the failure of rock due to horizontal fissures a series of rock bolts are installed around the perimeter of spread footing.

## **2.6.2 MAT FOUNDATIONS**

### **2.6.2.1 General Considerations**

The absence of high bearing and side friction capacities of stratum at a reasonable depth beneath the footprint of the building precludes the use of piles or deep underreamed footings. In such circumstances, mat foundations are routinely used under tall buildings, particularly when the soil conditions result in conventional footings or piles occupying most of the footprint of the building. Although it may be possible to construct a multitude of individual or combined footings under each vertical load-bearing element, mat foundations are preferred because of the tendency of the mat to equalize the foundation settlements. Because of continuity, mat foundations have the capacity to bridge across local weak spots in substratums. Mat foundations are predominantly used in two instances: (1) whenever the underlying load-bearing stratum consists of soft, compressible material with low bearing capacity and (2) as a giant pile cap to distribute the building load to a cluster of piles placed under the footprint of the building.





**FIGURE 2.99** Foundation system for a corner column of an exterior X-braced tube building: (a) plan and (b) schematic section.

Mat foundations are ideal when the superstructure load is delivered to the foundation through a series of vertical elements resulting in a more or less uniform bearing pressure. It may not be a good solution when high concentrations of loading occur over limited plan area. For example, in a core-supported structure carrying most of the building load, if not the entire load, it is uneconomical to spread the load over the entire footprint of the building because this would involve construction of exceptionally thick and heavily reinforced mat. A more direct solution is to use driven piles or drilled caissons directly under the core.

The plan dimensions of the mat are determined such that the mat contact pressure does not exceed the allowable bearing capacity prescribed by the geotechnical consultant. Typically three types of allowable pressures are to be recognized: (1) net sustained pressure under sustained gravity loads; (2) gross pressure under total design gravity loads; and (3) gross pressure under both gravity and lateral loads.

In arriving at the net sustained pressure, the loads to be considered on the mat area should consist of

1. Gravity load due to the weight of the structural frame
2. Weight of curtain wall, cooling tower, and other mechanical equipment
3. An allowance for actual ceiling construction including air conditioning duct work, light sprinklers, and fireproofing
4. Probable weight of partition based on single and multitenant layouts
5. Probable sustained live load
6. Loads applied to the mat from backfill, slab, pavings, etc.
7. Weight of mat
8. Weight of soil removed from grade to the bottom of the mat

This last item accounts for the reduction in overburden pressure and therefore is subtracted in calculating the net sustained pressure.

In calculating the sustained pressure on mats, typically less than the code prescribed values are used for items 4 and 5, requiring engineering judgment in their estimation. A total of 20 psf (958 Pa) for these items appears to be adequate. A limit on sustained pressure is basically a limit on the settlement of the mat. In practical cases of mat design it is not uncommon to have the calculated sustained pressure under isolated regions of mat somewhat larger than the prescribed limits. This situation should be reviewed with the geotechnical engineer and usually is of no concern as long as the over-stress is limited to a small portion of the mat.

The gross pressure on the mat is equivalent to the loads obtained from items 1 through 7. The weight of the soil removed from grade to the bottom of the mat is not subtracted from the total load because of gross pressure is of concern. Also, in calculating the weight of partition and live loads, the code-specified values are used.

The transitory nature of lateral loads is recognized in mat design by allowing a temporary over-stress on the soil. This concept is similar to the 33% increase in stresses previously allowed in the working stress design for wind and seismic loads. From an academic point of view, the ideal thickness for a mat is the one that is just right from punching shear considerations. At the same time, minimum reinforcement for temperature would be most economical if it worked also for flexure. However, in practice it is more economical to construct pedestals or provide shear reinforcement in the mat rather than to increase thickness for punching shear.

In detailing the flexural reinforcement there appear to be two schools of thought. One school maintains that it is more economical to limit the largest bar size to a #11 bar which can be lap-spliced. However, this limitation may force using as many as four layers of reinforcement both at top and bottom of mat. The other school promotes the use of #14 and #18 bars with mechanical tension splices. This requires fewer bars, resulting in cost savings in the placement of reinforcement. The choice is, of course, project specific.

### 2.6.2.2 Analysis

A vast majority of soil–structure interaction takes place under sustained gravity loads. Although the interaction is complicated by the nonlinear and time-dependent behavior of soils, it is convenient for analytical purposes to represent the soil, as an equivalent elastic spring. This concept was first proposed by Winkler in 1867 and hence the name Winkler spring. He proposed that the force and vertical displacement relationship of the soil be expressed in terms of a constant  $K$  called the modulus of subgrade reaction. It is easy to incorporate the effect of the soil by simply including a spring with a stiffness factor in terms of force per unit length beneath each reaction. However, it should be remembered that the modulus is not a fundamental property of the soil. It depends on many things, including the size of the loaded area and the length of time it is loaded. Consequently, the modulus of subgrade reaction used for calculating the spring constants must be consistent with the type and duration of loading applied to the mat.

Prior to the availability of finite element programs, mat analysis used to be undertaken by using a grid analysis by treating the mat as an assemblage of linear elements. The grid members are assigned equivalent properties of a rectangular mat section tributary to the grid. The magnitude of the Winkler's spring-constant at each grid intersection is calculated on the basis of tributary area of the joint.

The preferred method for analyzing mats under tall buildings is to use a finite element computer program. With the availability of computers, analytical solutions for complex mats are no longer cumbersome; engineers can incorporate the following complexities into the solution with a minimum of effort:

1. Varying subgrade modulus
2. Mats of complex shapes
3. Mats with nonuniform thickness
4. Mats subjected to arbitrary loads due to axial loads and moments
5. Soil–structure interaction in cases where the rigidity of the structure significantly affects the mat behavior

As in other finite element idealizations, the mathematical model for the mat consists of an assemblage of discretized elements interconnected at the nodes. It is usual practice to use rectangular or square elements instead of triangular elements because of the superiority of the former in solving plate-bending problems. The element normally employed is a plate-bending element with 12 degrees of freedom for three generalized displacements at each node. The reaction of the soil is modeled as a series of independent elastic springs located at each node in the compute model. The behavior of the soil tributary to each node is mathematically represented as a Winkler spring at each node. There is no continuity between the springs other than through the mat. Also, the springs because of their very nature can only resist compression loads although computationally it is not possible to impose this restriction in a linear elastic analysis. Therefore, it is necessary to review the spring reactions for any possible tensile support reactions. Should this occur, it is necessary to set the spring constant to zero at these nodes and to perform a new analysis. This iterative procedure is carried out until the analysis shows no tensile forces in springs.

In modeling the mat as an assemblage of finite elements, the following key factors should be considered:

1. Grid lines that delineate the mat into finite elements should encompass the boundaries of the slab, as well as all openings. They should also occur between elements with changes in thickness. Skew boundaries of mat not parallel to the orthogonal grid lines may be approximated by steps that closely resemble the skewed boundary.
2. Grid lines should intersect preferably at the location of all columns. Minor deviations are permissible without loss of meaningful accuracy.

3. A finer grid should be used to define regions subjected to severe displacement gradients. This can be achieved by inserting additional grid lines adjacent to major columns and shear walls.

Although it is possible to construct an analytical model consisting of both mat and superstructure, practical considerations preclude use of such complex analyses in everyday practice. Admittedly the trend, with the availability of computers and general analysis programs, is certainly toward this end. However, the current practice of accounting for superstructure interaction is to simulate the stiffness of superstructure by incorporating artificially stiff elements in mat analysis. Although the procedure is approximate, it has the advantage of being simple and yet capable of capturing the essential stiffness contribution of the superstructure.

The complex soil–structure interaction can be accounted for in the design by the following iterative procedure. Initially the pressure distribution under the mat is calculated on the assumption of a rigid mat. The geotechnical engineer uses this value to obtain the deformation and hence the modulus of subgrade reaction at various points under the footprint of the mat. Under uniform pressure the soil generally shows greater deformations at the center than at the edges of the mat. The modulus of subgrade reaction, which is a function of the displacement of the soil, therefore has higher values at the edges than at the center. The finite element mat analysis is performed using the varying moduli of subgrade reaction at different regions of the mat. A new set of values for contact pressures is obtained and processed by the geotechnical engineer to obtain a new set of values of soil displacement and hence the moduli of subgrade reaction. The process is repeated until the deflections predicted by the mat finite element analysis and the settlement predicted by the soil deflection due to consolidation and recompression of soil stratum converge to a desirable degree.

Two examples are presented in the following section to give the reader a feel for the physical behavior of mats. The first consists of a mat for a 25-story concrete office building and the second example highlights the behavior of an octagonal mat for an 85-story composite building.

### 2.6.2.3 Mat for a 25-Story Building

The floor framing for the building consists of a system of haunch girders running between the interior core walls and columns to the exterior. The haunch girders are spaced at 30 ft (9 m) on centers and run parallel to the narrow face of the building. Skip joists spaced at 6 ft (1.81 m) center-to-center span between the haunch girders. A 4 in. (101.6 mm) thick concrete slab spanning between the skip joist completes the floor framing system. Lightweight concrete is used for floor framing members while normal weight concrete is employed for columns and shear walls.

Shown in Figure 2.100 is a finite element idealization of the mat. The typical element size of  $12 \times 10$  ft ( $3.63 \times 3.03$  m) may appear to be rather coarse, but an analysis that used a finer mesh size of  $3 \times 2.5$  ft ( $0.9 \times 0.76$  m) showed results identical to that obtained for the coarse mesh. The calculated ultimate loads at the top of the mat are shown in Figure 2.100. It may be noted that the finite element idealization is chosen in such a manner that the location of almost all columns, with the exception of four exterior columns on the narrow face, coincide with the intersection of the finite element mesh. The loads at these locations are applied directly at the nodes. The loads on the four exterior columns are however, divided into two equal loads and applied at the two nodes nearest to the column. The resulting discrepancy in the analytical results has very little impact, if any, on the settlement behavior and the selection of reinforcement for the mat.

Assuming a value of  $100 \text{ lb/in}^3$  ( $743 \text{ kg/mm}^3$ ) for the subgrade modulus, the spring constant at a typical interior node may be shown to be equal to  $1728 \text{ kip/in.}$  ( $196 \times 103 \text{ N/m}$ ). Figure 2.101 shows the mat deflection comparison for two values of subgrade reaction, namely 100 and  $25 \text{ lb/in.}^3$  ( $743$  and  $185.75 \text{ kg/mm}^3$ ). As can be expected, the mat experiences a larger deflection when supported on relatively softer springs (Figure 2.101). The variation of curvature, which is a measure of bending moments in the mat, is relatively constant for the two cases. This can be verified further by comparing the bending-moment diagrams shown in Figure 2.102. Also shown in this figure are the bending

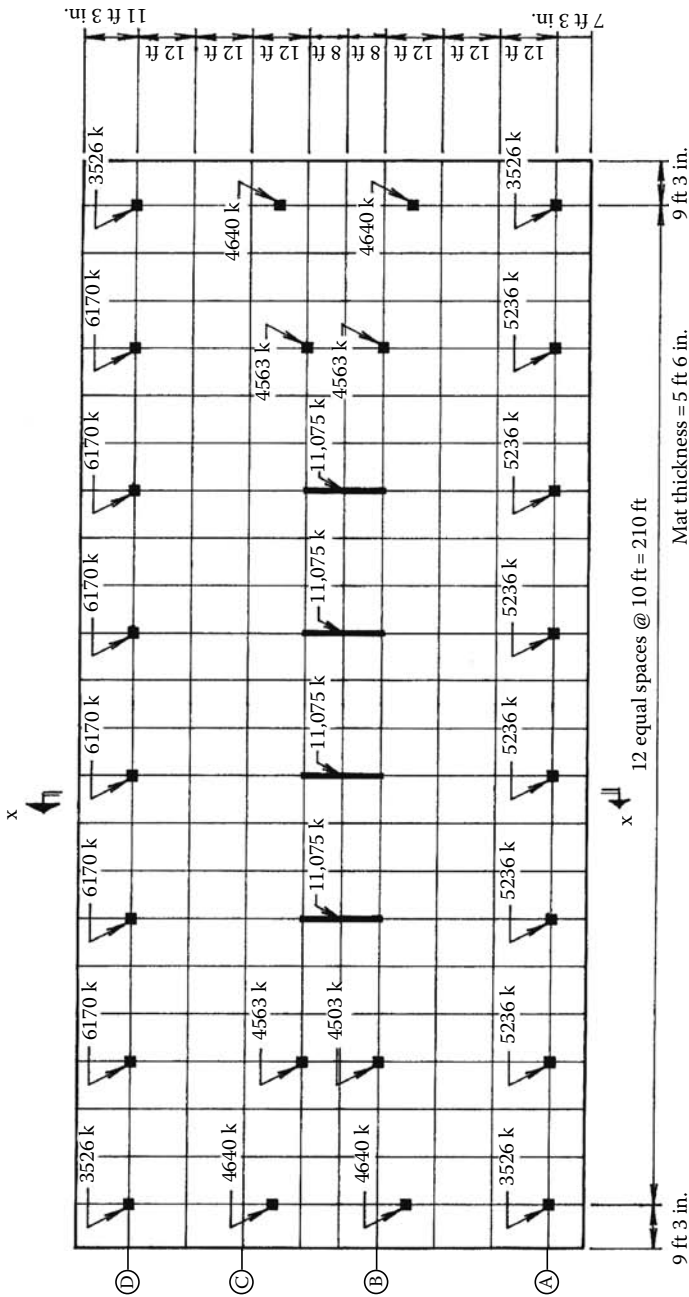


FIGURE 2.100 Foundation mat for a 25-story building: finite element idealization and column ultimate loads.

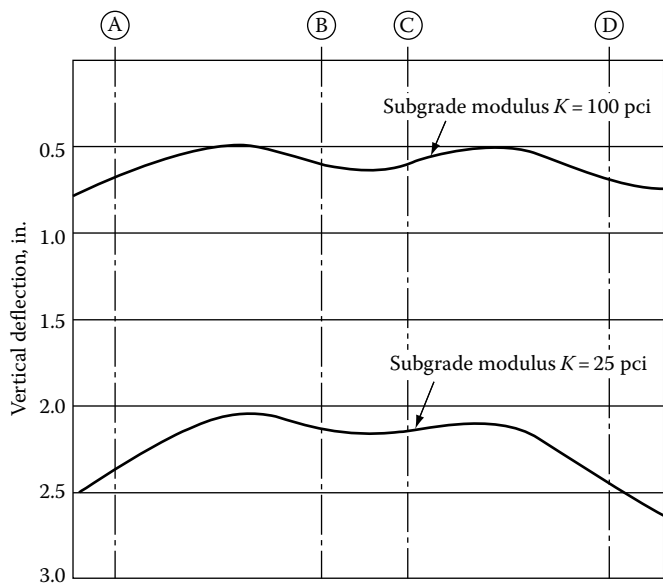


FIGURE 2.101 Vertical deflection of mat along section  $x-x$ .

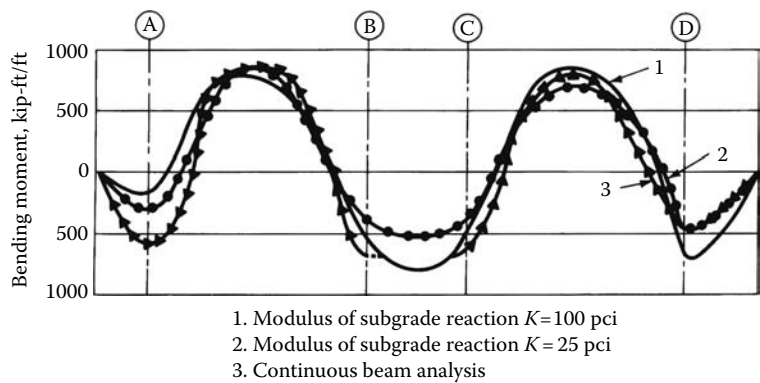
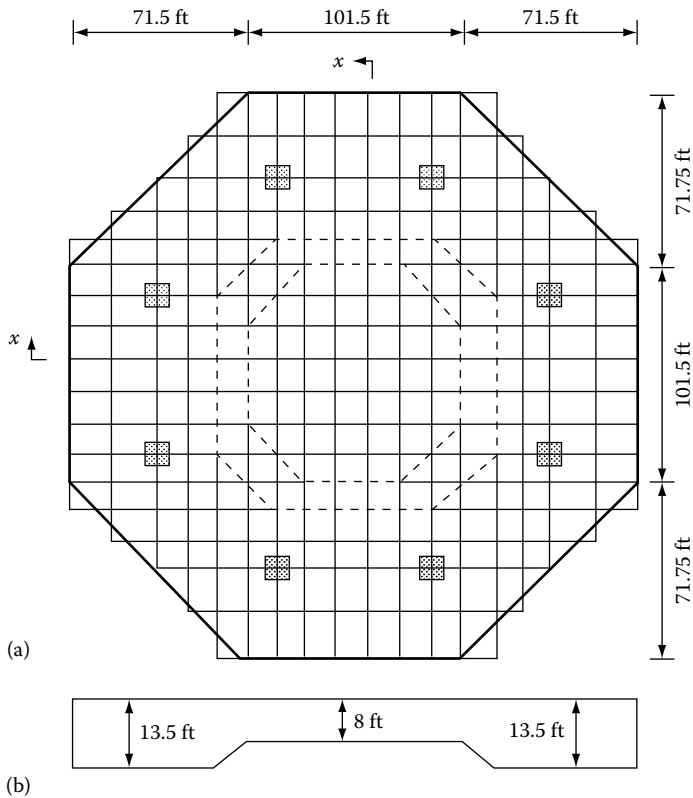


FIGURE 2.102 Bending moment variation along section  $x-x$ .

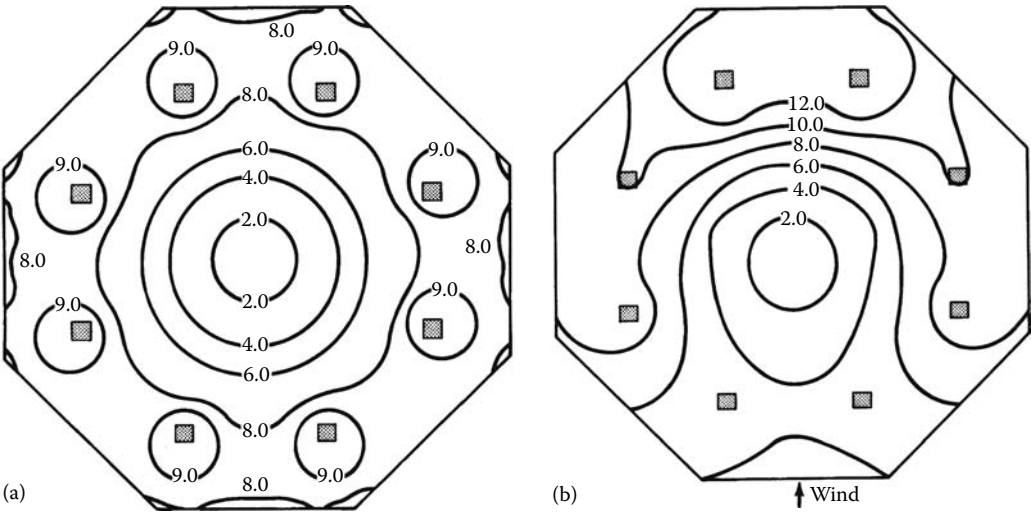
moments obtained by assuming the mat as a continuous beam supported by three rows of supports corresponding to exterior columns and interior shear walls, and subjected to the reaction of the soil acting vertically upward. The results for the example mat appear to indicate that mat reinforcement selected on the basis of any of the three analyses will result in adequate design.

#### 2.6.2.4 Mat for an 85-Story Building

Figure 2.103 shows a finite element idealization of a mat for proposed 85-story composite building, in Houston, Texas. Note that diagonal boundaries of the mat are approximated in a stepwise pattern using rectangular finite elements. To achieve economy, the thickness of the mat was varied; a thicker mat was proposed under the columns where the loads and thus the bending of the mat were expected to be severe. A relatively thin mat section was proposed for the center of the mat. The appropriateness of choosing two mat thickness can be appreciated by studying the pressure contours in Figure 2.104a and b. The pressure contours plotted in these figures were obtained from computer



**FIGURE 2.103** Foundation mat for a proposed 85-story office building: (a) finite element idealization and (b) cross section  $x-x$ .



**FIGURE 2.104** Contact pressure contour, ksf: (a) dead plus live loads and (b) dead plus live plus wind. *Note:*  $K = 100 \text{ lb/in.}^3$ .

analyses for two different loading conditions—gravity alone acting alone and gravity loads combined with wind loads. No uplift due to wind loads was evident.

2.7 GUIDELINES FOR THINKING ON YOUR FEET

Throughout this chapter we have discussed thumb rules for determining approximate member sizes for various gravity systems. In this section more or less, the same information is presented using schematic illustrations. See Figures 2.105 through 2.115. The design information given in these illustrations should prove useful in preliminary estimating, for establishing sizes and clearances, and for comparing different types of construction. It should be noted that the guidelines for selection of member sizes given in here are typical as used in the building industry. They are not mandatory: For example where vibration is not critical and live loads are light such as in parking structures, a slab thickness of 4.5 in. (120 mm) for a 17 ft (7 m) span has been successfully used.

2.8 UNIT QUANTITIES

Unit structural quantities such as cubic feet of concrete, pounds of mild steel reinforcement, and prestressed strands (if applicable) per square foot of building framed area, are required for preliminary cost estimate. These quantities are items of construction to which unit costs are assigned to arrive at total construction cost. These are relatively easy to calculate once the working drawings and specifications have been prepared. Prior to this stage however, the estimator must make a “conceptual estimate” to determine the approximate cost of the project. Conceptual estimates require considerable judgment to modify the so-called average unit cost to reflect complexity of construction operations, expected time required for construction, etc. of the project under consideration.

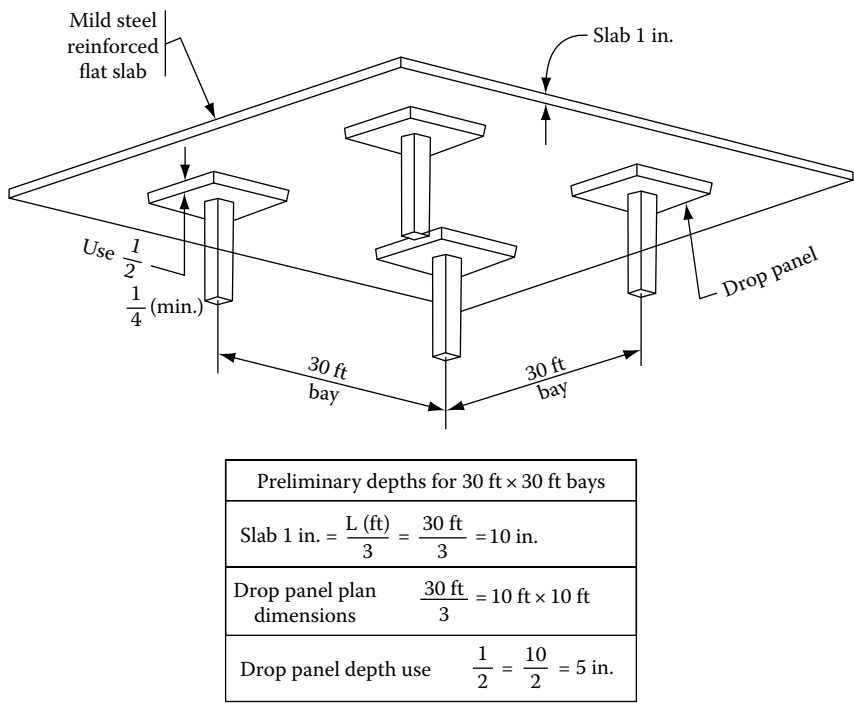
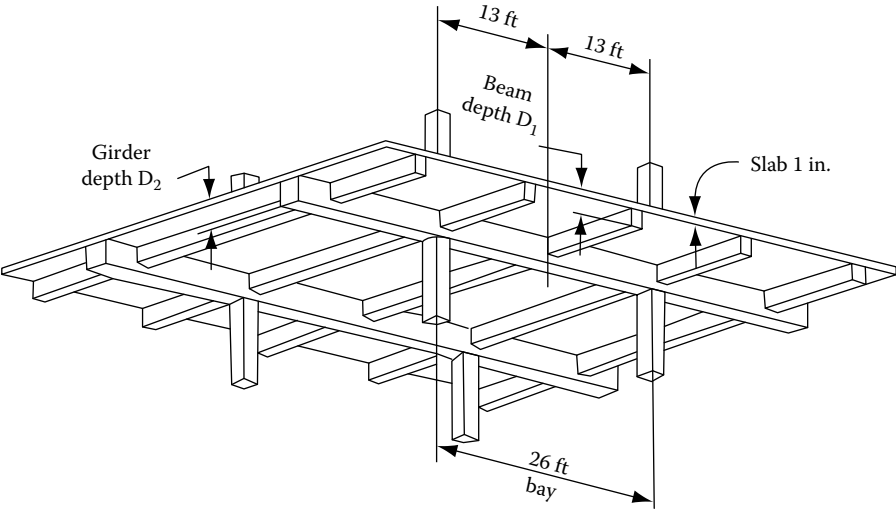


FIGURE 2.105 Flat slab with drop panels.





Preliminary depths for 26 ft × 26 ft bays
Slab t in. = $\frac{\text{Span}}{3} + 1$ $= \frac{13}{3} + 1 = 5.33$ so 5½ in.
Beam $D_1 = \frac{\text{Span}}{1.5} = \frac{26}{1.5} = 17.3$ in. so 18 in.
Girder $D_2 = \frac{\text{Span}}{1.5} + 2 = 19.3$ in. so 20 in.

FIGURE 2.106 Beam and slab system 26 ft × 26 ft bays.

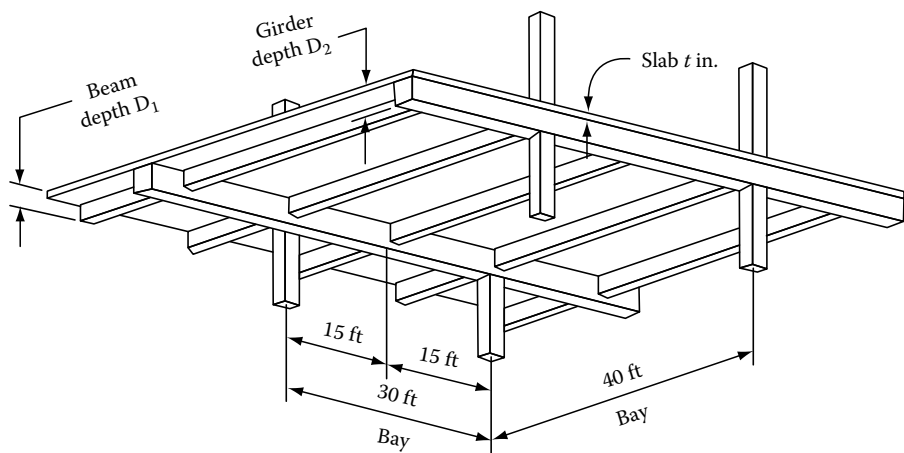
Typically, in the United States, units of structural quantities are dimensional, based on linear feet, square feet, or cubic feet. These result in unit quantities such as pounds per linear foot (plf), pounds per square foot (psf), etc.

Reinforcement and concrete unit quantities for various concrete floor-framing systems are shown in Figures 2.116 through 2.121. Live loads shown are working loads, and range from a typical office live load of 50psf to a maximum of 200psf appropriate for heavily loaded warehouse floors. The rebar quantities shown are for reinforcement required by design and do not include the reinforcement required for crack control, support bars, and additional lengths required for laps, etc. The estimator should make allowances for these in the preliminary estimates by discussing these items with the design engineer.

Table 2.7 gives estimated unit quantities of concrete, rebars, and posttensioning steel for hotels built in various regions of the United States. Also included is the estimated length of shear walls for a given number of stories. Given in Table 2.8 are the unit quantities of reinforcement for mat foundations of several tall buildings constructed in Houston, Texas.

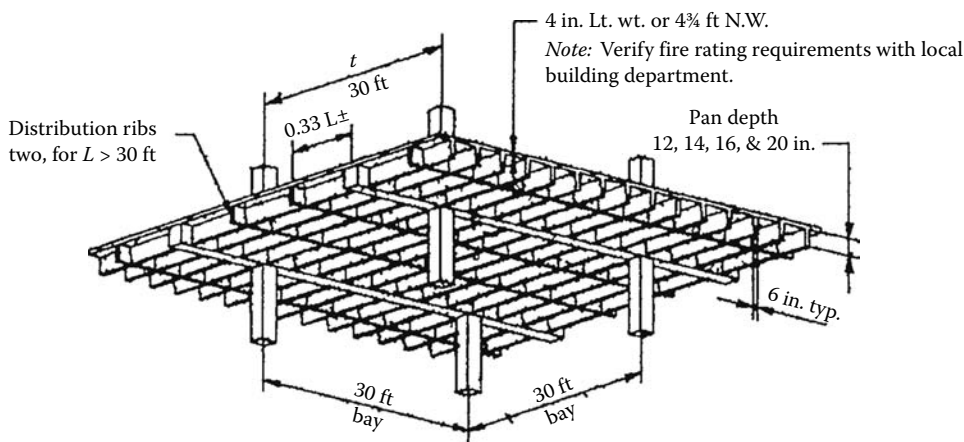
2.8.1 UNIT QUANTITY OF REINFORCEMENT IN COLUMNS

During the preparation of preliminary schemes for purposes of conceptual estimates, engineers are often directed to provide unit quantities of materials for the structural elements proposed for the scheme. One such measure commonly used for vertical elements such as columns, is the weight of



Preliminary depths for 30 ft × 40 ft bays	
$\text{Slab } t \text{ in.} = \frac{\text{Span}}{3} + 1$ $= \frac{15}{3} + 1 = 6 \text{ ft}$	
$\text{Beam } D_1 = \frac{\text{Span}}{1.5} = \frac{40}{15} = 26.6 \text{ in. Use 26 in.}$	
$\text{Girder } D_2 = \frac{\text{Span}}{15} = \frac{30}{15} = 20 \text{ ft Use 26 ft}$ <p style="text-align: center;">to match beam depth</p>	

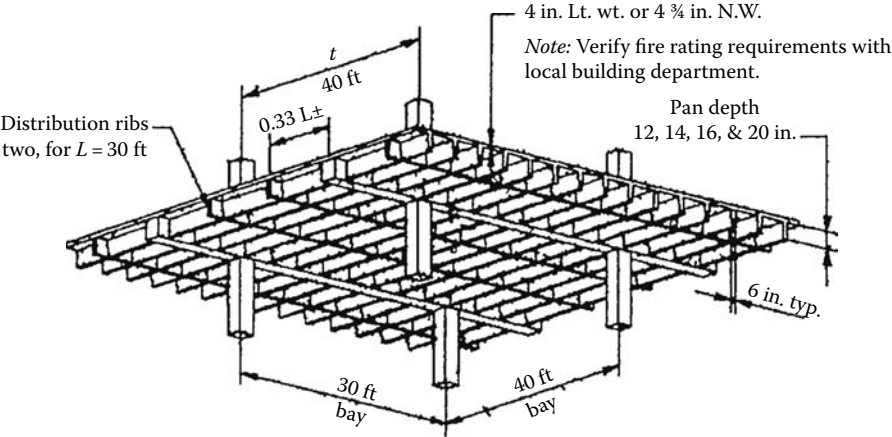
FIGURE 2.107 Beam and slab system 30 ft × 40 ft bays.



Preliminary depths for 30 ft × 30 ft bays
$\text{Joist depth} = \frac{L}{1.5} = \frac{30}{1.5} = 20 \text{ in.}$
$\text{Girder depth} = \frac{L}{1.5} + 2 = 22 \text{ in.}$

Note: Depth includes 4 in. for the thickness of slab.

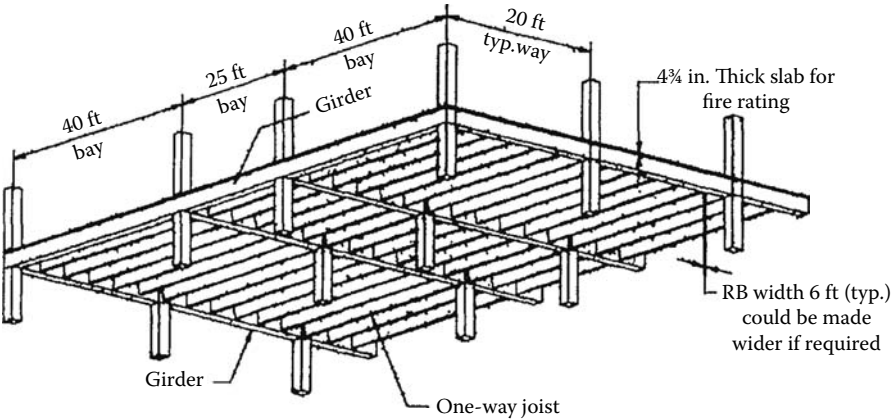
FIGURE 2.108 One-way joist (pan joist) system 30 ft × 30 ft bays.



Preliminary depths for 30 ft × 40 ft bays	
Joist depth = $\frac{L}{1.5} = \frac{40}{1.5} = 26.6$ in.	bay 26 in.
Girder depth = $\frac{L}{1.5} + 2 = \frac{30}{1.5} + 2 = 22$ in.	Use 26 in. to match joist depth

Note: Depth includes 4 in. for the thickness of slab.

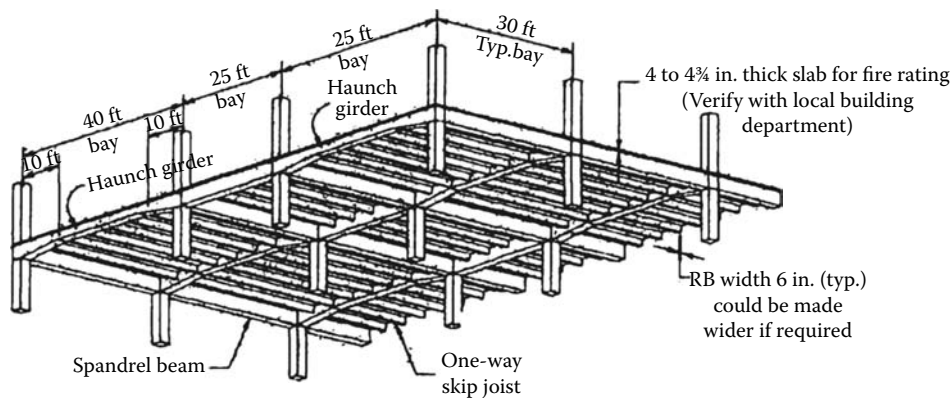
FIGURE 2.109 One-way joist system 30 ft × 40 ft bays.



Preliminary depths for 30 ft × 40 ft bays	
Girder depth = $\frac{t \text{ ft}}{1.5} = \frac{30}{1.5} = 20.0$	joy 24 ft
Joist depth = $\frac{t \text{ ft}}{2} = \frac{40}{2} = 20$	joy 22 ft

Note: Depth includes 4 ft for the thickness of slab.

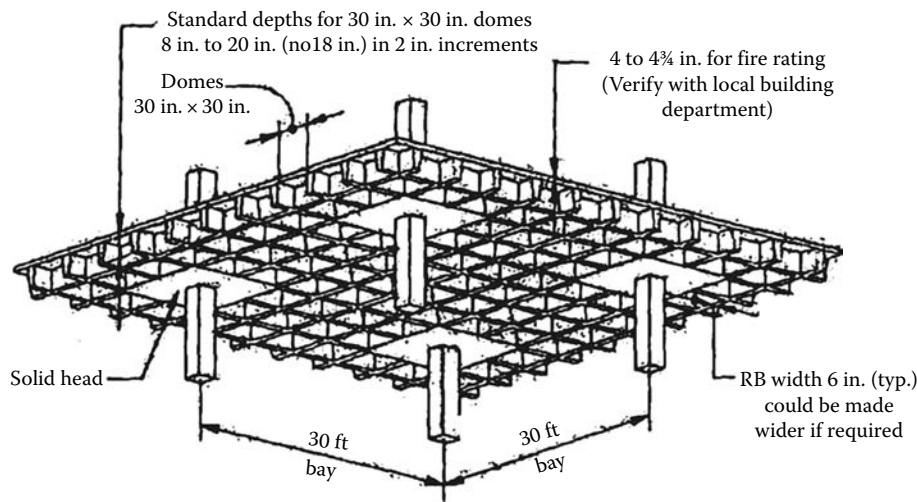
FIGURE 2.110 One-way joist with constant depth girders 30 ft × 40 ft bays.



Preliminary depths for 30 ft × 40 ft bays
Prismatic girder depth = $\frac{40}{15} = 26.6$ in. joy 26 in.
Haunch girder depth at center = 26 in. – 6 in. – 20 in.
Haunch girder depth at haunch = 26 in. + 6 in. – 32 in.
Skip joist depth for 30 ft span = $\frac{L}{1.5} = \frac{30}{1.5} = 20$ in.

Note: Depth includes 4 in. for the thickness of slab.

FIGURE 2.111 One-way skip joist with haunch girders 30 ft × 40 ft bays.



Preliminary depths for 30 ft × 30 ft bays
Waffle depth (in.) = $\frac{L}{2} = \frac{30}{2} = 15$ in. joy 16 in. includes slab depth

FIGURE 2.112 Waffle slab (two-way joist) system 30 ft × 30 ft bays.

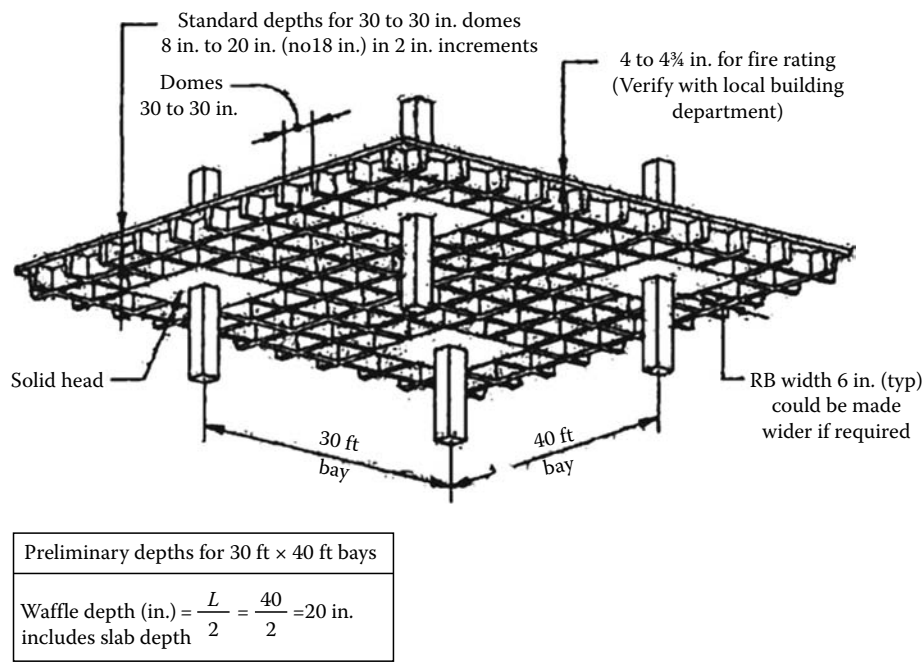


FIGURE 2.113 Waffle slab (two-way joist) system 30 ft  $\times$  40 ft bays.

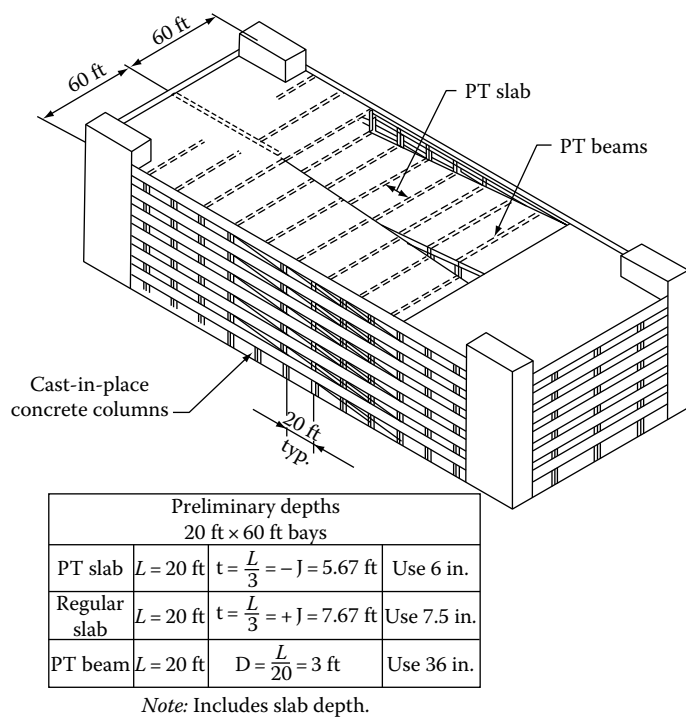
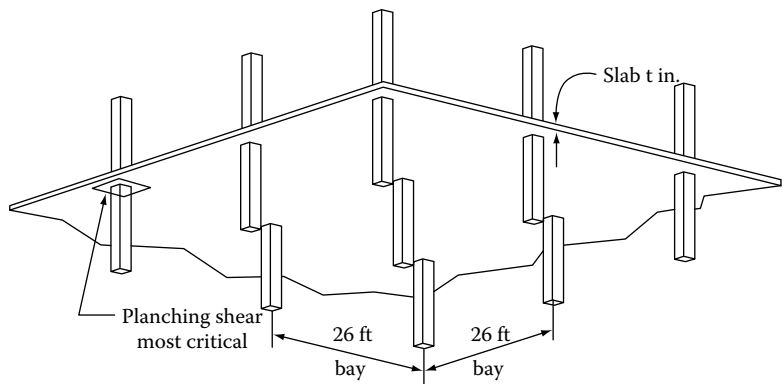


FIGURE 2.114 Posttensioned system for parking structure 20 ft  $\times$  60 ft bays.



Preliminary depth for 26 ft × 26 ft bays		
PT Slab	$t = \frac{L}{3} - 1$	Use 7 or 8 in.
$L = 26 \text{ ft}$	$= \frac{26}{3} - 1 = 7.6 \text{ ft}$	

FIGURE 2.115 Posttensioned flat plato 26 ft × 26 ft bays.

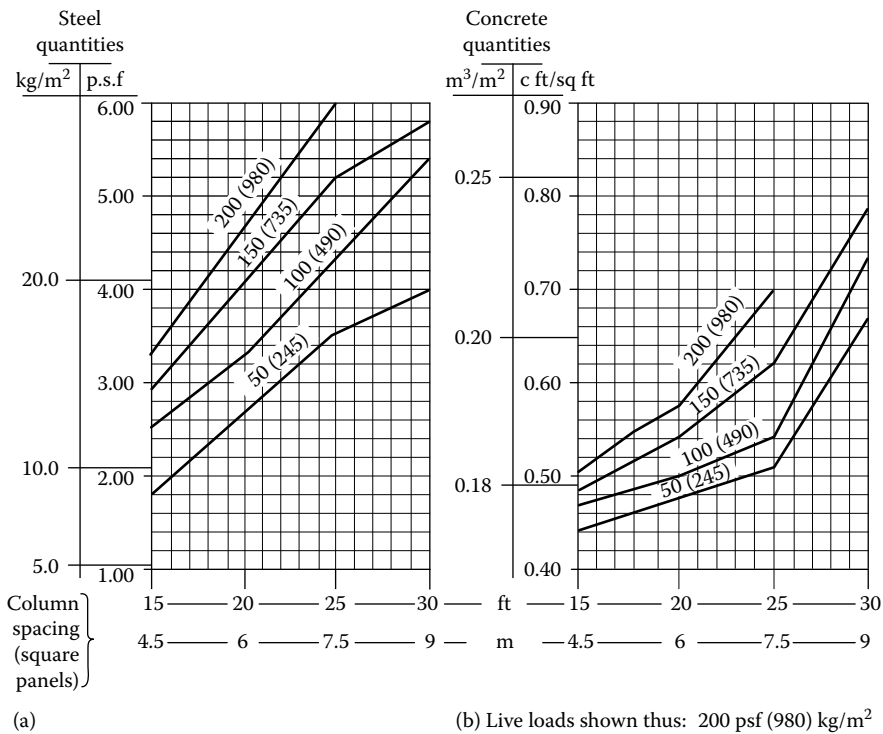


FIGURE 2.116 One-way solid slabs, unit quantities: (a) reinforcement and (b) concrete.

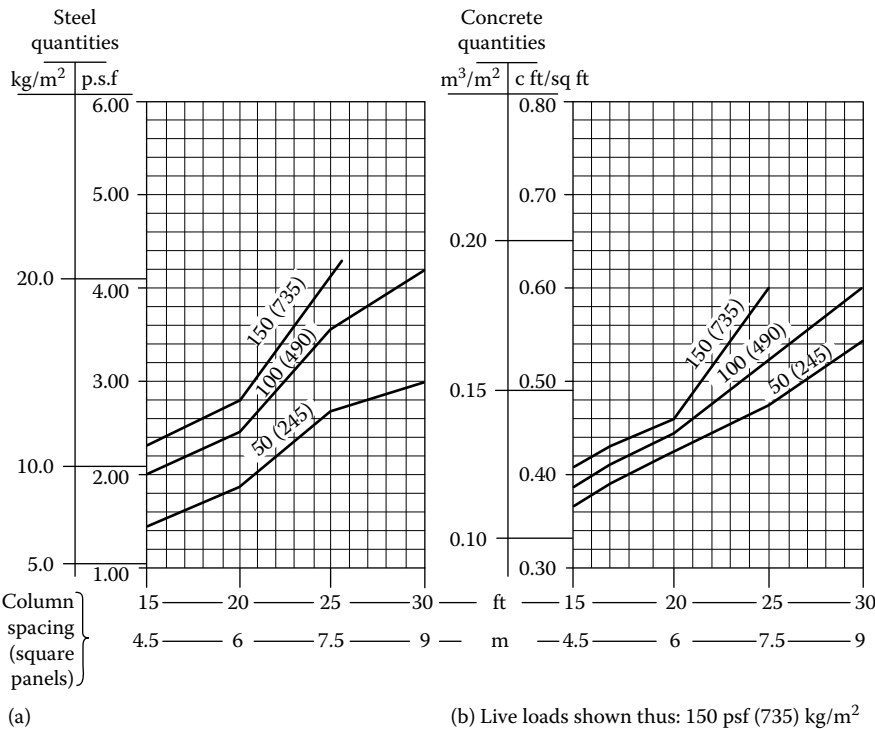


FIGURE 2.117 One-way pan joists, unit quantities: (a) reinforcement and (b) concrete.

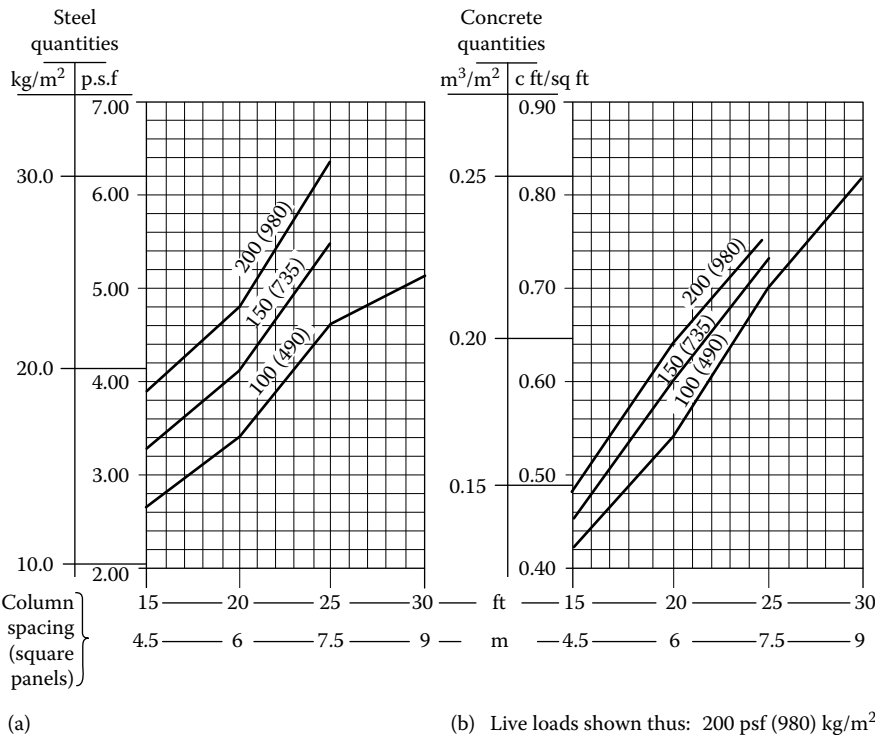


FIGURE 2.118 Two-way slabs, unit quantities: (a) reinforcement and (b) concrete.

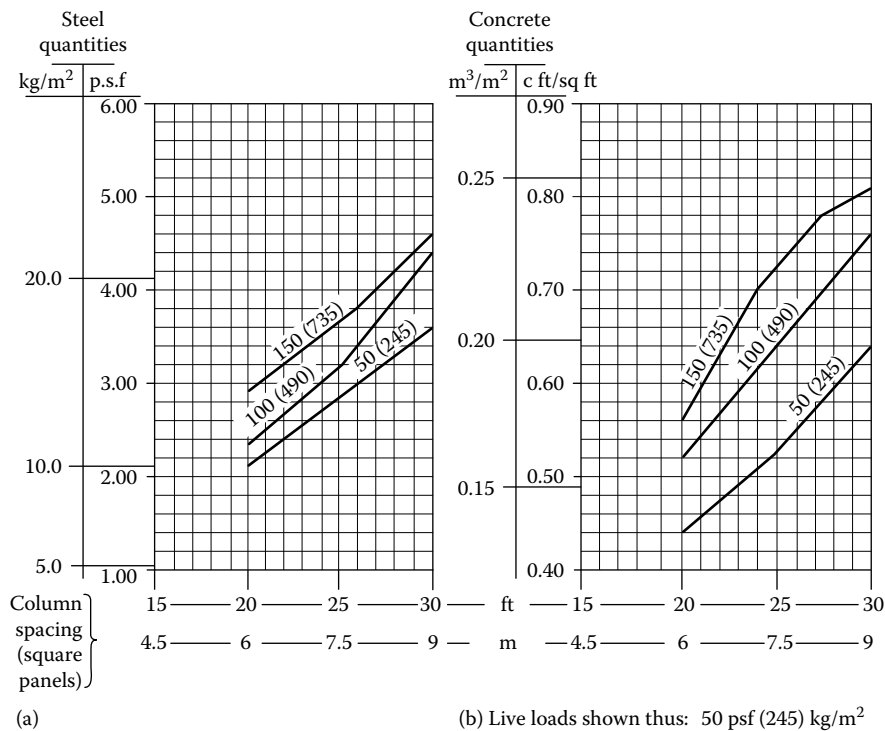


FIGURE 2.119 Waffle slabs, unit quantities: (a) reinforcement and (b) concrete.

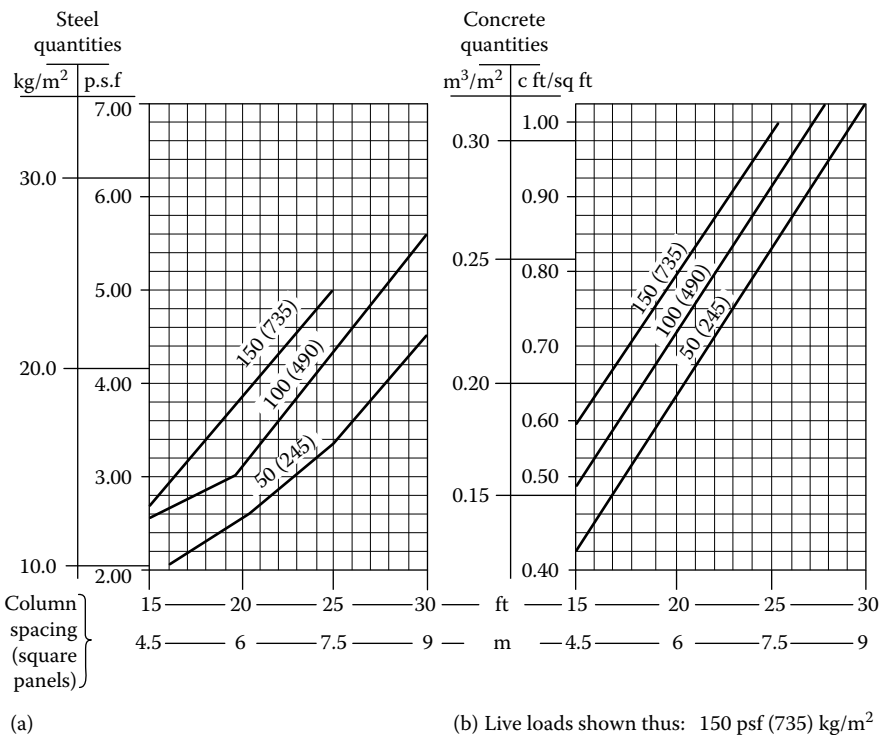


FIGURE 2.120 Flat plates, unit quantities: (a) reinforcement and (b) concrete.



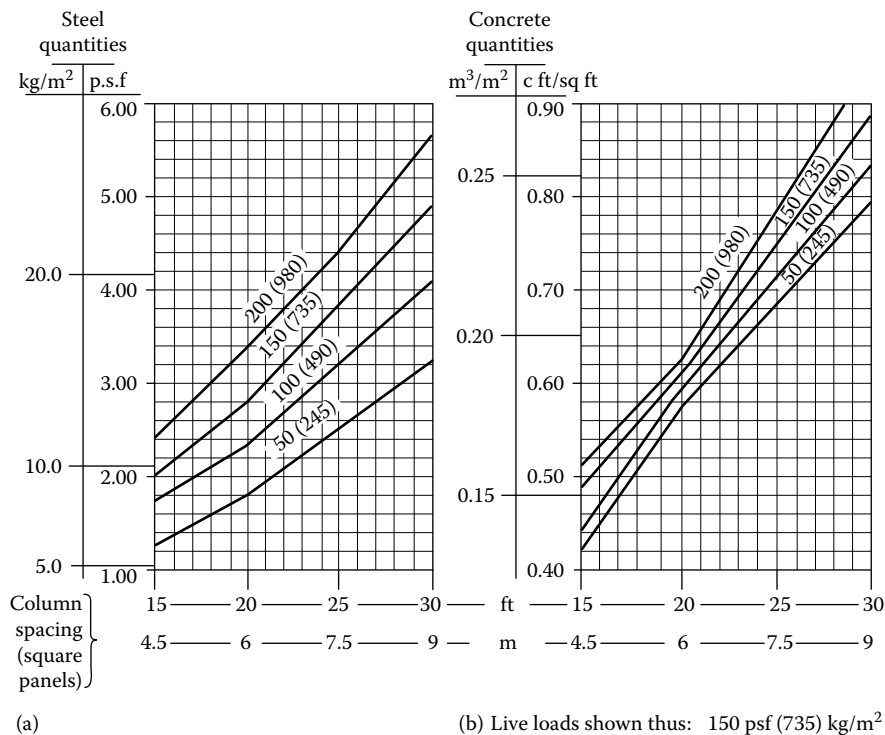


FIGURE 2.121 Flat slabs, unit quantities: (a) reinforcement and (b) concrete.

TABLE 2.8  
Unit Quantity of Reinforcement in Mat Foundations

Building #	No. of Stories	Excavation Depth, ft	Mat Thickness, ft	Mat Area Square Foot	Unit Quantity of Rebar, lbs/CY
1	85 (NB) <sup>a</sup>	67	13.5 and 8	49720	260
2	75	63	9.75	43800	224
3	71	63	9.5	NA <sup>b</sup>	165
4	62	34	8	44370	179
5	56	53	8	33800	170
6	52	33	6.66	37560	148
7	50	30	8 and 6	41000	219
8	49	28	7	43490	153
9	44	35	6	NA <sup>b</sup>	165
10	25	25	6 and 4.5	25890	207

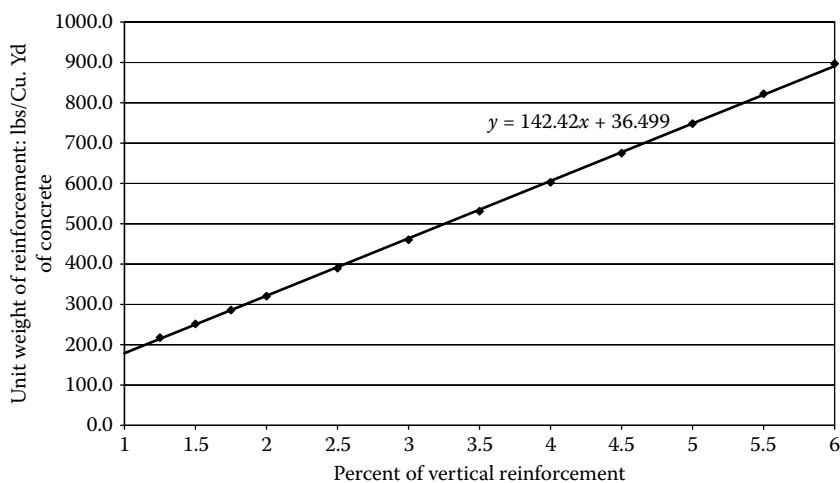
Note: Based on Buildings constructed in Houston, Texas.

<sup>a</sup> NB, Not built.

<sup>b</sup> NA, Not available.

**TABLE 2.9**  
**Unit Quantity of Reinforcement in Columns**

Percent reinforcement (includes allowance for ties)	1	1.25	1.5	1.75	2	2.5	3	3.5	4	4.5	5	5.5	6
Average steel Reinforcement (lbs/Cu. Yd)	183.5	217.5	251.6	285.9	320.4	389.9	460.1	531.0	602.7	675.1	748.3	822.2	897.0

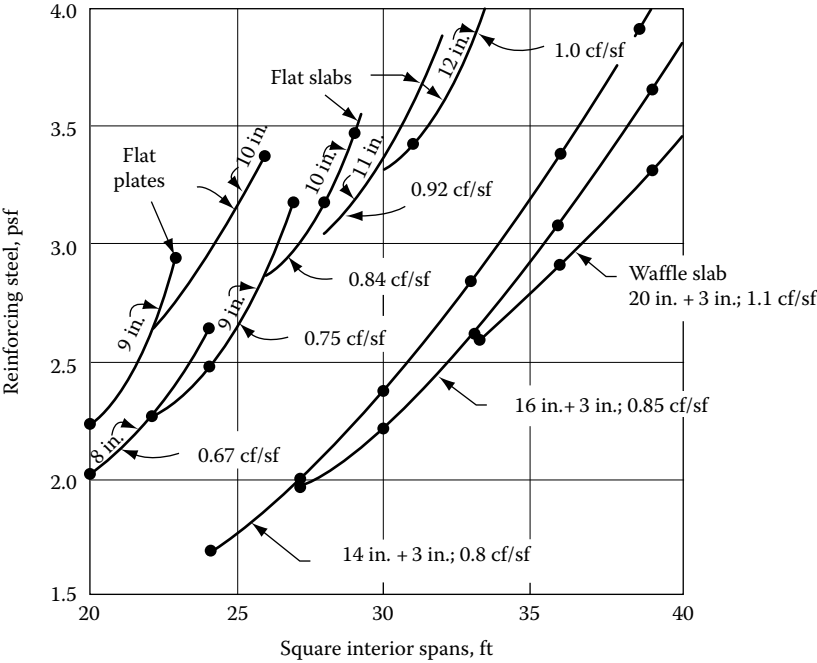


**FIGURE 2.122** Unit quantity of reinforcement in columns.

mild steel reinforcement, typically expressed as “so many pounds of reinforcement per cubic yard of column concrete.” These quantities are relatively easy to calculate once the working drawings are complete. However, prior to this point, when we are still in the conceptual design stage, it is useful to have this information tied to the expected percentage of vertical reinforcement in columns. Table 2.9 and the associated graph, Figure 2.122 provided here serve that purpose. It should be noted that allowance for column ties has been made in the unity quantities shown in the table and in the graph.

**2.8.2 UNIT QUANTITY OF REINFORCEMENT AND CONCRETE IN FLOOR FRAMING SYSTEMS**

For purposes of cost estimation, preliminary designs of floor systems are often compared using tables published by the concrete industry. Such a table published by the Concrete Reinforcing Steel Institute, CRSI, is shown in Figure 2.123 with slight modifications. It should be noted that integrity reinforcement, stirrups, shear reinforcement at columns and welded wire reinforcement in the top slab of joist and waffle systems are not included. Similarly the concrete quantities for distribution joists are also not included. The factored superimposed load,  $w_u$  consists of live load, floor finishes, and allowance for partitions. The weight of structural concrete multiplied by the appropriate load factors is not included.



- Notes:
- Superimposed factor load  $w_u = 200$  psf
  - $f'_c = 4$  ksi,  $f_y = 60$  ksi

FIGURE 2.123 Preliminary design and material quantities for floor systems.

---

# 3 Lateral Load-Resisting Systems

In nature, the structures of organisms differ according to their size. For example, the structure of a large animal such as an elephant is radically different from that of a dog or a mosquito. However, in spite of these obvious differences, until about the middle of the seventeenth century, scientists believed that it was possible to build larger structures simply by duplicating the form and proportion of a smaller one. The prevailing opinion was that if the ratios between structural elements in the larger structure were made identical to the ratios in the smaller structure, the two structures would behave in a similar manner. In 1638, Galileo was the first scientist to refute this principle by citing examples from animate and inanimate structures, thus formulating the idea of an ultimate size for structures. He clearly recognized the effect of self-weight on the efficiency of structures. These principles have since been extended, and engineers have come to recognize that different scales require different types of structures. For example, in the field of bridge engineering, it is well known that for maximum efficiency each type of bridge structure has an upper and lower span limit.

The built-up plate girder scheme for a steel bridge structure, for example, may be economical for continuous spans up to about 800 ft (243.8 m), whereas for spans from 1000 to 1200 ft (305 to 366 m), a truss system may be the best solution. Finally, very large spans in the range of the present maximum of 4200 ft (1281 m) with predictable limits in the range of 10,000 ft (3048 m) would require a totally different system, such as a cable suspension structure, to make the project economically feasible. Similarly, structural engineering of tall buildings requires the use of different systems for different building heights. Each system, therefore, has an economical height range, beyond which a different system is required. The requirements of these systems and their ranges are somewhat imprecise because the demands imposed on the structure significantly influence these systems. However, knowledge of different structural systems, their approximate ranges of application, and the premium that would result in extending their range is indispensable for a successful solution of a tall building project because engineers, like other human beings, are creatures of habit with a strong temptation to repeat concepts that were used successfully on earlier, similar projects. This is understandable because not only are the methods of analysis well established for these systems, but it also makes good business sense. Fortunately, in the design of high-rise structures, the engineer is not subject to this boredom and stagnation of using the same idea over and over again. Thanks to the architects for coming up with an array of new forms and daring concepts and to the ever-increasing building heights. The engineering challenge remains well and alive and promises to intensify in the future.

In today's business world, architects and owners are assisted by a host of experts who look at the bottom line and demand more efficient plans with maximum rentable areas. As was common some two decades ago, no longer can the engineer get away with proposing only one or two structural solutions. Even though the proposed systems may make the most sense from the structural engineering point of view, they may not be so from space planning considerations. Therefore, without getting emotionally attached to a particular scheme, the structural engineer should remember that there are more ways than one to solve a design problem. With an open mind, the engineer should consider it a challenge to look at alternative schemes and to think through a series of conceptual designs by applying existing knowledge to new applications. The merits and demerits of each scheme should be evaluated not only from structural cost but also the overall sense of the project. During the preliminary design, the engineer should not be overly concerned with the details, but should allow for sufficient load paths in the structure to obey the inescapable laws of nature. Analysis is the easy part because today we can analyze almost any structure with computers. Design is the hard part—it is the conceptualization of something that never was.

After having indulged in a philosophical discussion of structural design, we will examine the range of structural systems available for the engineering of low-rise, mid-rise, high-rise, supertall, and ultratall reinforced concrete buildings.

Reinforced concrete, known to humans since the nineteenth century, offers a wide range of structural systems that may be grouped into distinct categories, each with an applicable height range, as shown in Figure 3.1. The height for each group, although logical for normally proportioned buildings, should be verified for a specific application by considering such factors as building geometry, severity of wind exposure, and the Seismic Design Category (SDC) assigned to the buildings. The SDC establishes the allowable height, permitted structural system and irregularities, analysis procedure, and detailing requirements necessary for formulating the energy absorbing capacity. Six SDCs, A, B, C, D, E, and F, are assigned to buildings in the ASCE 7-05, with A being the least and F the most severe. Further discussion of SDCs is presented in Chapter 5.

For buildings assigned to SDC A, the systems shown in Figure 3.1 and any other system that has a recognizable and adequate load path for gravity and lateral loads is permitted under the provisions of ASCE 7-05 without height limits. The same is true for buildings in SDC B, except that cantilevered column systems using special, intermediate, or ordinary moment frames are limited to a maximum height of 35 ft.

Before we begin a description of the systems shown in Figure 3.1, it is of interest to dwell on the evaluation of outrigger and belt wall systems that are being increasingly used in the construction of ultratall buildings.

For a tall building to be successful, at a minimum, the structure should employ systems and materials appropriate to the building’s height and configuration. The system must perform well and lend itself for efficient construction. It must satisfy the desired look expected of the “modern” generation tall buildings. Its organization, appearance, transparency, and solidity must all be related to its architecture, for it is the architecture that drives the building’s shape and form.

What does make an efficient tall building? Given that the primary influence on structural design is due to gravity and lateral loads, our ability to affect gravity design, other than using lightweight materials, is somewhat limited. There is very little revolutionary that can be achieved. However, we

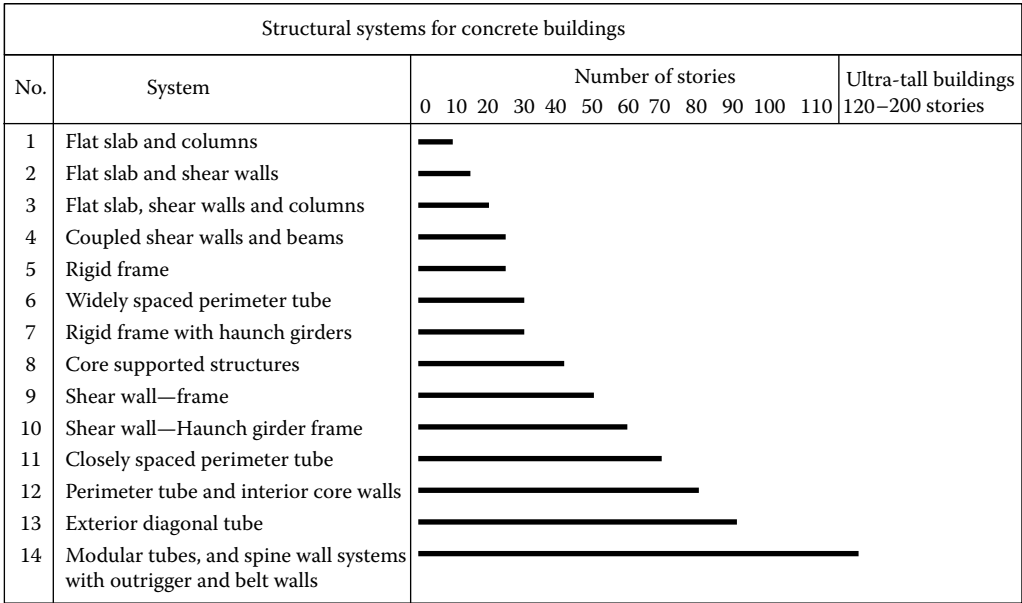


FIGURE 3.1 Structural systems categories.

do have certain options in the area of resisting lateral loads and controlling deformations. It is in this forte that the structural ingenuity has the greatest effect.

The principles of efficient tall building structural design, known for some time, are quite simple:

1. Resist overturning forces due to lateral loads by using vertical elements placed as far apart as possible from the geometric center of the building
2. Channel gravity loads to those vertical elements resisting overturning forces
3. Link these vertical elements together with shear-resisting structural elements that experience a minimum of shear lag effects such that the entire perimeter of the building resists the overturning moments
4. Resist lateral forces with members axially loaded in compression rather than those loaded in tension due to overturning

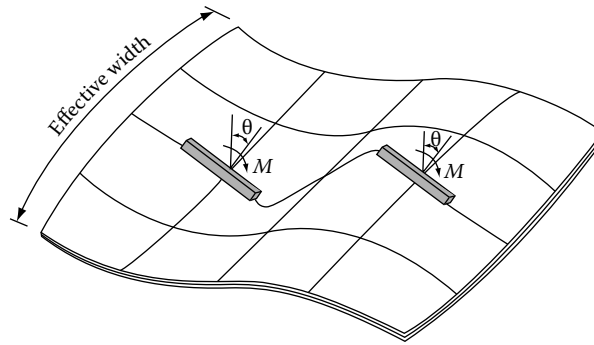
“Tube” structures, as will be discussed presently in this chapter, more or less, follow these principles. They are characterized by closely spaced, wide columns organized in small bays around the perimeter of the building. The columns are connected together with deep spandrel beams. The behavior of the system is not unlike that of a hollow tube formed by the perimeter of the building. This system, introduced by the late Dr. Fazlur Khan of Skidmore, Owings and Merrill, in the 1970s, follows the principles outlined above in that the lateral load-resisting system is placed on the perimeter of the building and thus provides the broadest possible base for the structure. With a proper layout of the interior framing, a large portion of the gravity loads may be channeled to the tube columns. The perimeter spandrels, being relatively rigid, impart a stiffness very nearly equal to that of a solid wall, thus engaging the windward and leeward walls as integral parts of the entire building footprint. Variations on this concept have been in use for some time such as “tube-in-tube” systems (to take advantage of resistance available from an inner structure around the central core), “bundled tube” systems (with additional tube-frames through the interior of the building to link across the building plan), and “braced tubes” (that links opposite faces of a building together).

The structural vocabulary in 2008 is markedly different from the earlier tubular systems, particularly for ultratall buildings. A relatively new concept has become quite popular. Commonly referred to as a belt and outrigger or spine wall system, it is made up of a stiff central spine, usually around a central core, with one-story-high outrigger walls or several-story-high outrigger walls extending from the core to perimeter columns at several levels to help stabilize the slender core structure. Although the structural advantages of this system are several, perhaps the motivation stems from the much desired architectural transparency bestowed at the building facade. The perimeter columns are effectively gravity columns, which can be smaller than frame columns and organized in large bays, creating significantly more transparency.

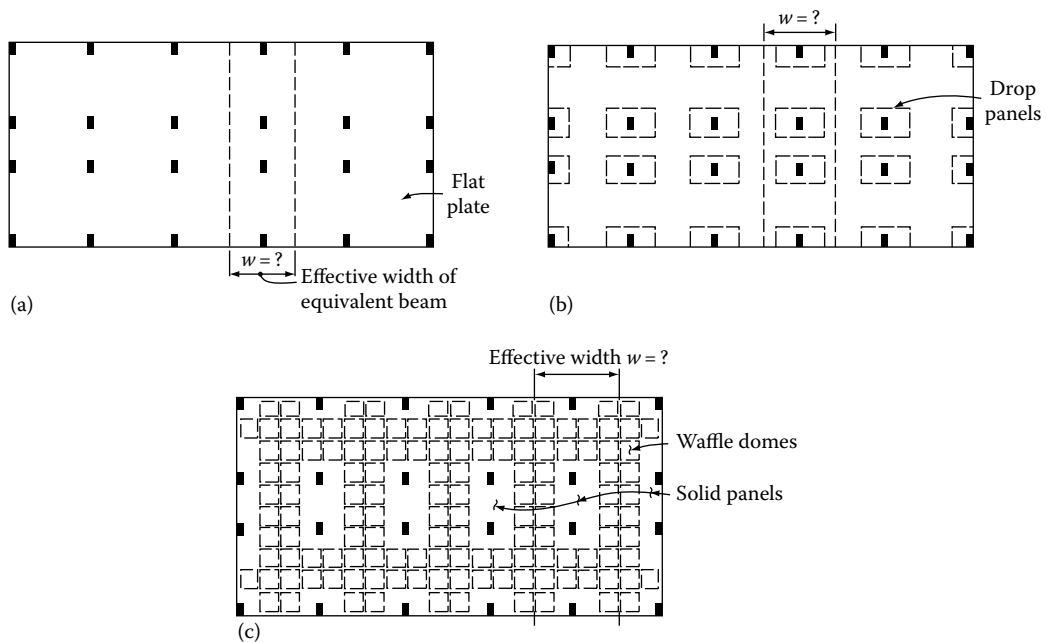
The concept of “optimum location” for belt and outriggers explaining their fundamental behavior was first introduced by the author (see Ref. [45]). A condensed version of this paper is presented later in this chapter.

### 3.1 FLAT SLAB-FRAME SYSTEM

Perhaps one of the simplest framing techniques for a concrete building consists of a two-way floor slab framing directly into columns without beams. This system, referred to as a flat slab-frame, has stringent detailing requirements for buildings assigned to high SDCs, although buildings in SDC A or B may be designed without any limitations on height. However, lateral drift requirements limit their economical height to about 10 stories, as shown in Figure 3.1. The nonductile detailing requirements given in the first 20 chapters of the American Concrete Institute’s ACE 318-05/08 are presumed to be sufficient to provide the necessary strength and nominal ductility for buildings assigned to SDC A or B. However, for higher SDCs, stress concentrations due to compatibility of



**FIGURE 3.2** Response of flat slab-frames to lateral loads: Displacement compatibility between slab and walls.



**FIGURE 3.3** Typical floor systems for flat slab-frames: (a) flat plate, (b) flat slab with drop panels, and (c) two-way waffle system.

displacement shown in Figure 3.2, present detailing problems in the placement of slab reinforcement. Hence they are seldom used in regions of high seismicity.

The term flat slab-frame signifies that the flat slab behaves as a beam, responding to lateral loads by developing bending moments and shear forces. The floor framing typically consists of a two-way system such as a flat plate, flat slab, or waffle slab (Figure 3.3). A flat slab has column capitals, drop panels, or both. The intent of providing these is to increase the shear and moment resistance of the system at the columns where the shears and moment are greatest. A drop panel is considered as part of a slab and its design is part of the slab design, whereas a column capital is deemed part of a column and its design is considered along with the column design.

A waffle slab consists of orthogonal rows of joists commonly formed by using square domes. The domes are omitted around the columns to increase the moment and shear capacity of the slab. Any of the three systems may be used in buildings assigned to SDC A or B as an integral part of a lateral-resisting system.

The slab system has two distinct actions in resisting lateral loads. First, because of its high in-plane stiffness, it distributes the lateral loads to various vertical elements in proportion to their stiffness. Second, because of its significant out-of-plane stiffness, it restrains the vertical displacements and rotations of columns and walls as if they were interconnected by a shallow wide beam.

The concept of effective width can be used to determine the equivalent width of a flat slab-beam. Although physically no beam exists between the columns, for analytical purposes, a certain width of slab may be considered as a beam framing between the columns. The effective width is, however, dependent on various parameters, such as column aspect ratios, distance between the columns, thickness of the slab, etc. Research has shown that values less than, equal to, and greater than full width are all valid depending upon the parameters mentioned above.

The American Concrete Institute Publication ACI 318-08, like its predictions, permits a full width of slab between adjacent panel center lines for both gravity and lateral load analyses with the stipulation that the effect of slab cracking be considered in evaluating the stiffness of frame members. Use of a full width is explicit for gravity analysis, and implicit (because it is not specifically prohibited) for the lateral loads. However, engineers generally agree that the use of a full width is unconservative for lateral analysis. It overestimates the column stiffness, compounding the error in the distribution of moments due to lateral loads.

Of particular concern in the design of a flat slab-frame is the problem of shear stress concentration at the column-slab joint. Shear reinforcement is necessary to improve joint behavior and avoid early stiffness deterioration under lateral cyclic loading. This is one of the primary reasons that two-way slab systems are not permitted by the ACI in regions of high seismic risk (UBC zones 3 and 4), or for buildings assigned to SDC C, D, E, or F. Their use in regions of moderate seismic risk (UBC zones 2 and 2B) or in SDC buildings A or B is permitted, subject to certain requirements, mainly relating to reinforcement placement in the column strip.

In general, for lateral load analysis of flat slab-frames, the analytical model may be based upon any approach that is shown to satisfy equilibrium and geometric compatibility and to be in reasonable agreement with test data. Acceptable approaches include models using finite elements, effective beam widths, and equivalent frames. The stiffness values for frame members used in the analysis must reflect the effects of slab cracking, geometric parameters, and concentration of reinforcement.

The stiffness of slabs is affected not only by cracking, but also by other parameters such as relative span lengths, and on concentration of reinforcement in the slab width. This concentration of reinforcement increases stiffness by preventing premature yielding and softening in the slab near the column supports. Consideration of the stiffness due to these factors is important for lateral load analysis because lateral displacement can significantly affect the moments in the columns, especially in tall buildings.

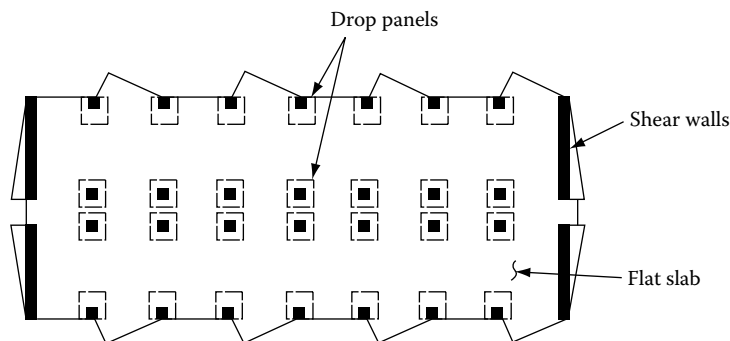
Cracking reduces the stiffness of the slab-beams. The magnitude of the loss of stiffness will depend on the type of slab system and the reinforcement details. For example, prestressed slab systems and slab systems with beams between columns will lose less stiffness than a conventional reinforced flat plate system. Since it is difficult to evaluate the effect of cracking on stiffness, it is usually sufficient to use a lower bound value. Except under very severe conditions, such as underdesign earthquakes, one-fourth of the full width is expected to provide a safe lower bound for stiffness.

## 3.2 FLAT SLAB-FRAME WITH SHEAR WALLS

Frame action provided by a flat slab-beam and column interaction is generally insufficient to provide the required strength and stiffness for buildings taller than about 10 stories. A system consisting of shear walls and flat slab-frames may provide an appropriate lateral bracing system. Figure 3.4 shows an example.

Coupling of walls and columns solely by slabs is a relatively weak source of energy dissipation. When sufficiently large rotations occur in the walls during an earthquake, shear transmission from the slab into wall occurs mainly around the inner edges of the wall. Because of cracking of the





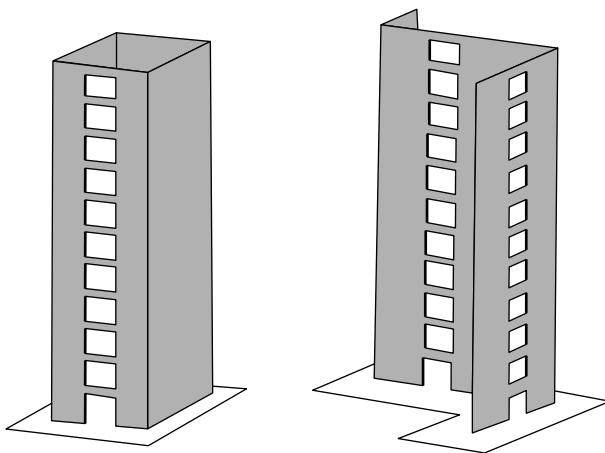
**FIGURE 3.4** Flat slab-frame with shear walls.

slab and shear distortions around the columns, the system's hysteretic response is poor. Therefore, ACI 318-08, like its predecessors, discourages the use of slab-beam frames by limiting the width of the slab that can be considered as an equivalent frame-beam in lateral analysis. For buildings in high seismic zones (UBC zones 3 and 4) or for SDC C, D, E, or F buildings, the width of the equivalent beam is limited to the width of the supporting column plus 1.5 times the thickness of the slab. Only in this limited width are we allowed to place the top and bottom flexural reinforcement of the slab-beam. This requirement invariably precludes the use of flat slab-beams as part of a seismic system in regions of high seismicity or for buildings assigned to high SDC. It should be noted that deformation compatibility requirements impose severe punching stress demands in the flat slabs of buildings assigned to SDC C and above.

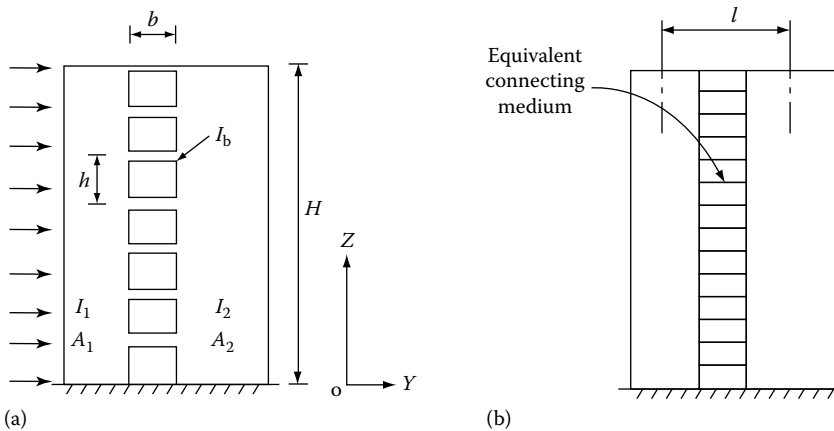
### 3.3 COUPLED SHEAR WALLS

A system of interconnected shear walls such as those shown in Figure 3.5, exhibits a stiffness that far exceeds the summation of the individual wall stiffnesses. This is because the interconnecting slab or beam restrains the cantilever bending of individual walls by forcing the system to work as a composite unit. The walls behave as if they are connected through a continuous shear-resisting medium (see Figure 3.6).

The system is economical for buildings in the 40-story range. Since planar shear walls carry loads only in their plane, walls in two orthogonal directions are generally required to resist lateral



**FIGURE 3.5** Coupled shear walls.



**FIGURE 3.6** Representation of coupled shear wall by continuum model: (a) Wall with openings. (b) Analytical model for close-form solution.

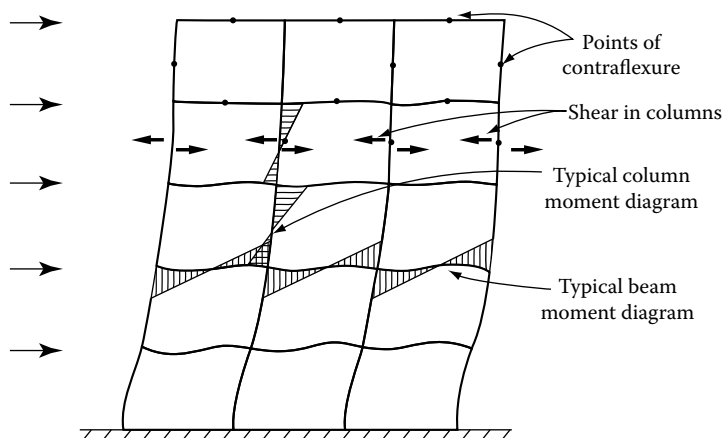
loads in two directions. Placement of walls around elevators, stairs, and utility shafts is common because they do not interfere with interior architectural layout. However, resistance to torsional loads must be considered in determining their location.

### 3.4 RIGID FRAME

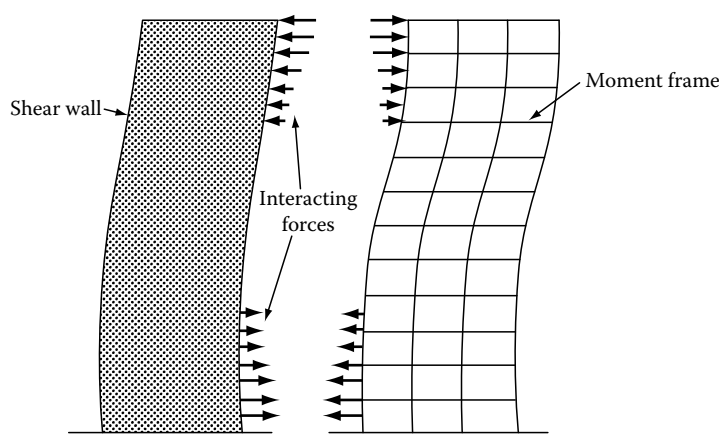
Cast-in-place concrete has an inherent advantage of continuity at joints but the design and detailing of joints at the intersection of beams and columns may be of concern particularly in buildings assigned to SDC C and above. This is because the column height within the depth of the girder, often referred to as a panel zone, is subjected to large shear forces. Horizontal seismic ties at very close spacing may be required to avoid uncontrolled diagonal cracking and disintegration of concrete and to promote ductile behavior. The intent is to have a system that can respond to earthquake loads without loss in gravity-load carrying capacity.

A rigid frame is characterized by flexure of beams and columns and rotation at the joints. Interior rigid frames for office buildings are generally inefficient because (1) the number of columns in any given frame is limited due to leasing considerations and (2) the beam depths are often limited by the floor-to-floor height. However, frames located at the building exterior do not necessarily have these limitations. An efficient frame action can thus be developed by providing closely spaced columns and deep spandrels at the building exterior.

A rigid-frame high-rise structure typically comprises of parallel or orthogonally arranged bents consisting of columns and girders with moment-resistant joints. The continuity of the frame also increases resistance to gravity loading by reducing the positive moments in the girders. The advantages of a rigid frame are the simplicity and convenience of its rectangular form. Its unobstructed arrangement, clear of structural walls, allows freedom internally for the layout and externally for the fenestration. Rigid frames are considered economical for buildings of up to about 25 stories, above which their drift resistance is costly to control. If, however, a rigid frame is combined with shear walls, the resulting structure is very much stiffer so that its height potential may extend up to 50 stories or more. The horizontal stiffness of a rigid frame is governed mainly by the bending resistance of the girders, the columns, and their connections, and in a tall frame, also by the axial rigidity of the columns. The accumulated horizontal shear above any story of a rigid frame is resisted by shear in the columns of that story (Figure 3.7). The shear causes the story-height columns to bend in double curvature with points of contraflexure at approximately midstory-height. The moments applied to a joint from the columns above and below a particular level are resisted by the attached girders, which also bend in double curvature, with points of contraflexure at approximately midspan.



**FIGURE 3.7** Rigid frame: Forces and deformations.

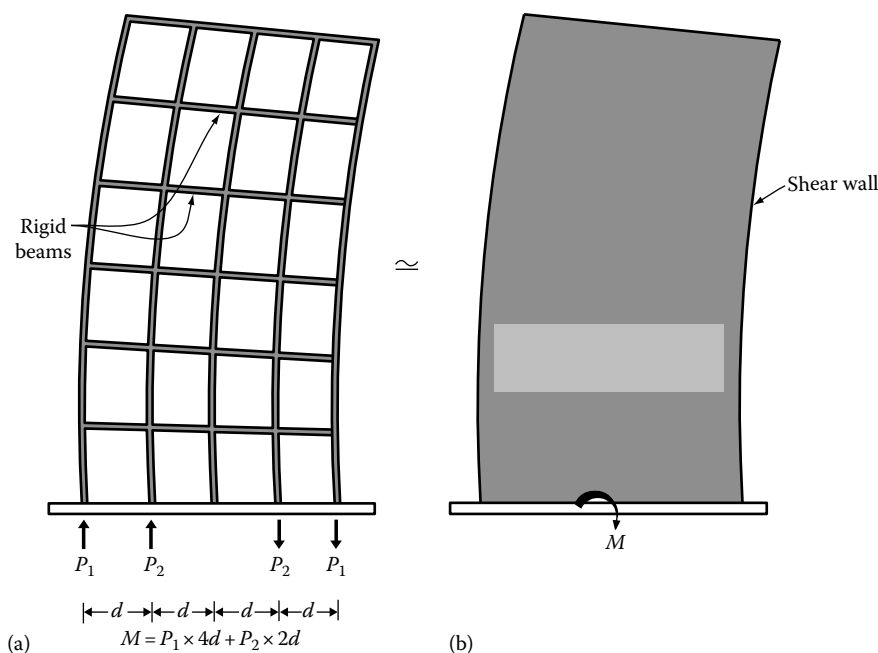


**FIGURE 3.8** Shear wall-frame interaction.

These rotational deformations of the columns and girders result in shear deflection, often referred to as frame racking, greatly contributing to the horizontal deflection. The deflected shape of a rigid frame due to racking has a shear configuration with concavity upwind that has a maximum inclination near the base and a minimum at the top, as shown in Figure 3.8.

The overall external moment is resisted at each level by a couple resulting from the axial tensile and compressive forces in the columns on opposite sides of the structure (Figure 3.9). The extension and shortening of the columns cause overall bending and associated horizontal displacements due to curvature of the structure. Because of the cumulative rotation up the height, the story drift due to overall bending increases with height, while that due to racking tends to decrease. Consequently the contribution to story drift from overall bending may, in the uppermost stories, exceed that from racking. The contribution of overall bending to the total drift, however, will usually be much less, no more than 30% of that of racking.

To limit story drift under lateral loads, the sizes of frame members in tall buildings are often controlled by stiffness rather than strength. The story drift, defined as the lateral displacement of one level relative to the level below, is of concern in verifying the integrity of building cladding under lateral load effects. Drift limits in common usage for wind design are of the order of 1/400 to 1/500 of the story height. These limits are believed to be generally sufficient to minimize damage to cladding and nonstructural walls and partitions.



**FIGURE 3.9** Bending deformation of rigid frame: (a) Moment resisted by axial loads in columns. (b) Cantilever bending of shear wall.

### 3.4.1 DEFLECTION CHARACTERISTICS

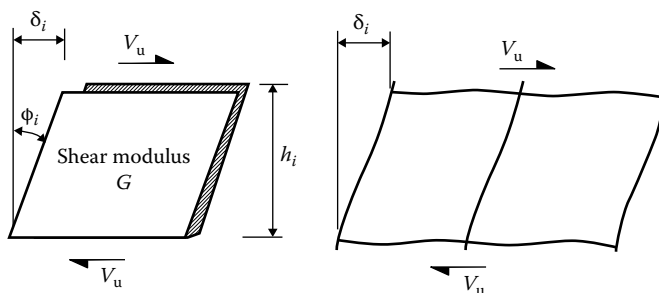
Because of rigidity of beam-to-column connections, a moment frame cannot displace laterally without bending of beams and columns. The lateral stiffness of the entire frame is therefore dependent, to a large extent, on the bending stiffness of the frame members, and to a lesser extent on the axial compression and tension of the columns. To understand lateral deflection characteristics, it is convenient to compare the deflections of a rigid frame to that of a vertical cantilever column. The primary deflection of the cantilever column of a reasonable height is due to bending and the secondary component is due to shear. Unless the column is relatively short, the shear component may even be ignored in its deflection computations. However, in a moment frame, both of these components, which are usually referred to as the cantilever bending and frame racking components, are equally important.

#### 3.4.1.1 Cantilever Bending Component

In resisting overturning moments, a moment frame responds as a vertical cantilever, resulting in axial deformation of the columns. The columns on the windward side lengthen while those on the leeward side shorten. This change in column lengths causes the frame to rotate about a horizontal axis. The resulting lateral deflection is analogous to the bending deflection component of the cantilever column.

#### 3.4.1.2 Shear Racking Component

This type of response in a rigid frame, shown in Figure 3.10, is similar to shear deflection of the cantilever column. As the frame displaces laterally, by virtue of the rigid beam-to-column connections, bending moments and shears are developed in the beams and columns. The external shear above a given level due to lateral loads is resisted by the internal shear in each of the columns of that story. This shear in turn causes the story-height columns to bend in double curvature with points of contraflexure at approximately midheight of the columns. To satisfy equilibrium, the sum



**FIGURE 3.10** Shear deflection analogy: The lateral deflections of a story-high rigid frame due to beam and column rotations may be considered analogous to the shear deflections of a story-high segment of a shear wall.

of column moments above and below a joint must equal the sum of the beam moments on either side of the column. In resisting bending, the beams also bend in a double curvature, with points of contraflexure at approximately midspan. The cumulative bending of the columns and beams results in a shear deflection configuration, often referred to as shear racking component, as shown in Figure 3.10.

The shear mode of deformation accounts for about 70% of the total sway of a moment frame, with the beam flexure contributing about 10%–15%, and the column bending furnishing the remainder. This is because in a rigid frame, typically the column stiffness, as measured by the  $I_c/L_c$  ratio, is substantially greater than the beam stiffness ratio,  $I_b/L_b$ , where  $I_b$ , moment of inertia of the beam;  $I_c$ , moment of inertia of the column;  $L_b$ , length of the beam; and  $L_c$ , length of the column.

Therefore, in general, to reduce lateral deflection, the place to start adding stiffness is in the beams. However, in nontypical frames, such as for those in framed tubes with column spacing approaching floor-to-floor height, it is prudent to study the relative beam and column stiffnesses before making adjustments to the member stiffnesses.

Because of the cumulative effect of rotation up the height, the story drift increases with height, while that due to shear racking tends to stay the same up the height. The contribution to story drift due to cantilever bending in the uppermost stories exceeds that of shear racking. However, the bending effect usually does not exceed 10%–20% of that due to shear racking, except in very tall and slender rigid frames. Therefore, the overall deflected shape of a frame for a moderately tall building usually has a shear deflection configuration. Thus, the total lateral deflection of a rigid frame may be considered a combination of the following:

Cantilever deflection due to axial deformation of columns (15%–20%).

Frame shear racking due to bending of beams (50%–60%).

Frame racking due to bending of columns (15%–20%).

In addition to the preceding factors, the deformations of a beam–column joint also contribute to the total lateral. Its effect, however, is negligible and may be ignored.

As stated previously, the typical proportioning of member sizes in tall rigid frames is such that girder flexure is the major cause of drift, with column flexure a close second. Therefore, the most effective and economical way of correcting excessive drift is usually by increasing the girder bending stiffness.

A relatively simple check on whether the girders or columns should be adjusted is as follows: let us assume we are designing a 40-story building that has rigid frames for lateral resistance. Assume that a computer analysis shows that the building has excessive drift at the 20th floor. Do we increase the size of columns or girders at this level to correct the drift?

To arrive at a solution, we compute for a typical joint across the floor levels above and below the level in question, the value of a parameter  $\psi$ , which is defined as follows:

$$\psi = \frac{I_c}{h} / \sum \frac{I_g}{L}$$

in which  $\sum I_g/L$  refers to the girders connecting into the joint and  $I_c/h$  refers to the columns. If a scan of the resulting values of  $\psi$  indicates that

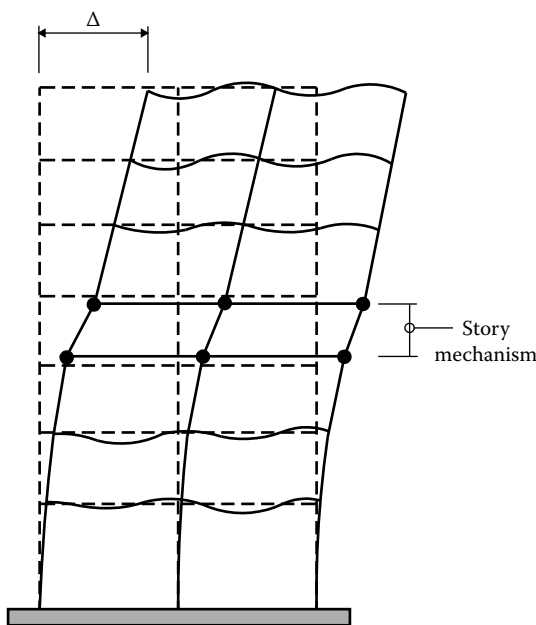
1.  $\psi \gg 0.5$ , adjust the girder sizes
2.  $\psi \ll 0.5$ , adjust the column sizes
3.  $\psi \approx 0.5$ , adjust both column and girder sizes

Design of special moment frames entails an entirely different set of conditions as discussed in the following section.

A special moment frame is designed using a seismic force-reduction factor,  $R = 8$ , (the highest value allowed for any system) that reflects a high degree of inelastic response expected for design-level ground motions. Hence, a special moment frame is expected to have a high degree of ductility capacity and thus be capable of sustaining multiple excursions in the inelastic range. This is ensured by

1. Achieving a strong-column/weak beam design that spreads inelastic response over several stores
2. Avoiding shear failure
3. Providing details that enable ductile response in yielding zones

As shown in Figure 3.11, if a building frame has weak columns, the lateral drift during an earthquake tends to concentrate in a single or a few stories only. On the other hand, the drift is likely to



**FIGURE 3.11** Story mechanism: Strong-column-weak beam requirement aims at preventing story mechanism.

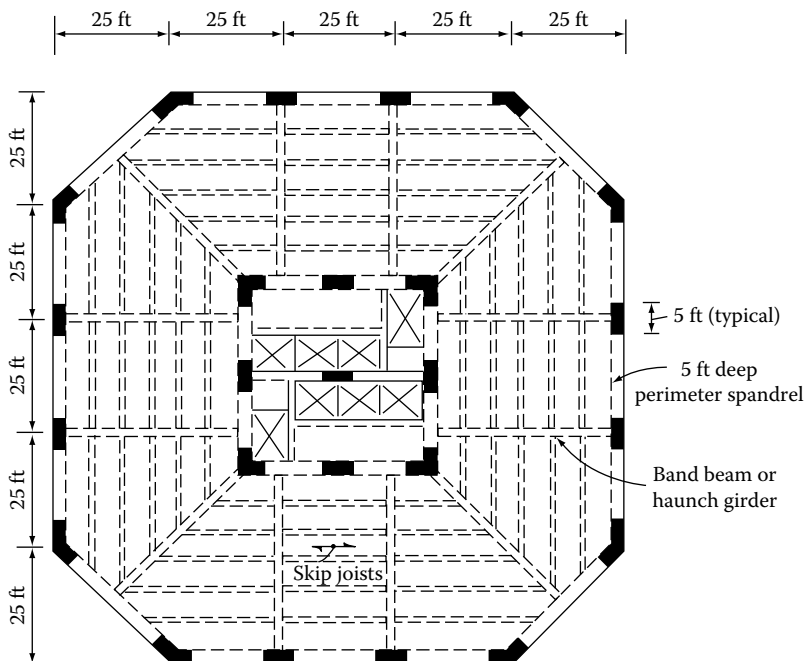
be distributed more evenly over the height if the columns provide a strong and stiff support over the entire building height. Additionally, it is important to keep in mind that columns in a given story support the entire weight of the building above those columns, whereas the beams only support the weight of the floor system tributary to those beams. Therefore, failure of a column is of greater consequence than a beam failure. Thus strong-column-weak beam principle is vital in achieving a safe behavior during strong ground shaking. This is specified in the ACI 318 by requiring that the sum of the column flexural strengths exceed the sum of beam flexural strengths at each beam–column connection by at least 20%.

### 3.5 TUBE SYSTEM WITH WIDELY SPACED COLUMNS

The term tube, in usual building terminology, suggests a system of closely spaced columns say, 8–15 ft on center (2.43–4.57 m), tied together with a relatively deep spandrel. However, for buildings with compact plans, it is possible to achieve tube action with relatively widely spaced columns interconnected with deep spandrels. As an example, the plan of a 28-story building constructed in New Orleans is shown in Figure 3.12. Lateral resistance is provided by a perimeter frame consisting of columns 5 ft (1.5 m) wide, spaced at 25 ft (7.62 m) centers, and tied together with a spandrel 5 ft (1.53 m) deep.

### 3.6 RIGID FRAME WITH HAUNCH GIRDERS

Typical office buildings usually have a lease depth of about 40 ft (12.19 m) from the core to the building exterior without interior columns. To span a distance of 40 ft, a girder depth of about 2 ft 6 in. (0.76 m) is required unless the girder is posttensioned. Because the beam depth has quite an impact on the floor-to-floor height, and is often limited due to additional cost for the increased height of interior partitions, curtain wall, and the added heating and cooling loads due



**FIGURE 3.12** Tube building with widely spaced perimeter columns.

to the increased volume of the building, it is common practice to seek shallow framing systems. A variable-depth haunch girder, as shown in Figures 3.13 through 3.15 is one such solution. Using this system, no increase in floor-to-floor height is expected because the bottom elevation of girder at midsection is flush with the shallow floor system transverse to the haunch girder. Ample beamless space exists for passage of mechanical ducts. Examples of haunch girder buildings are shown in Figures 3.16 and 3.17.

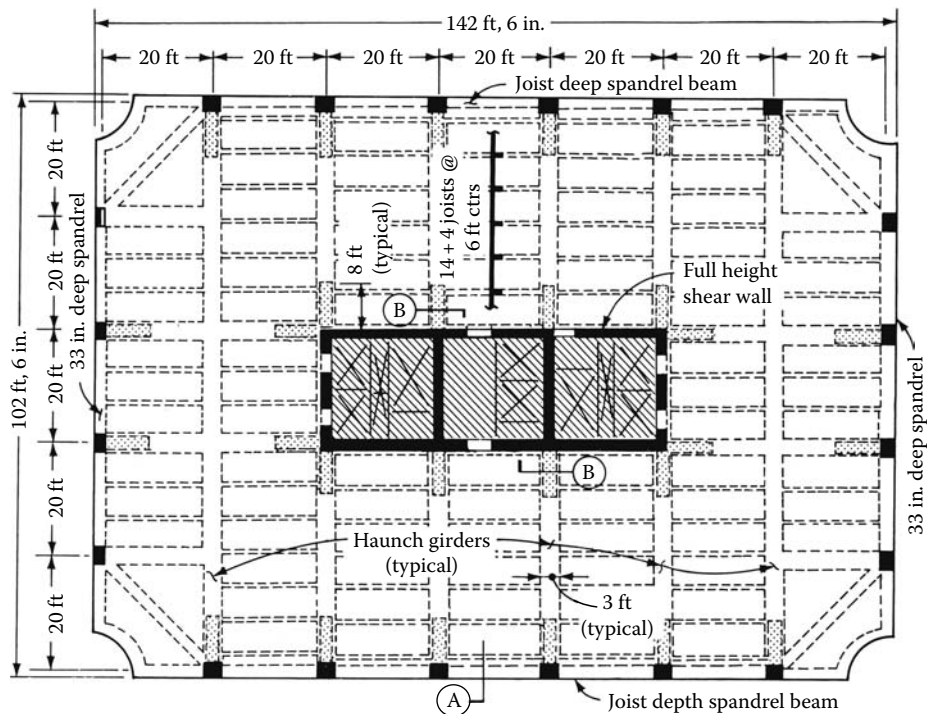


FIGURE 3.13 Typical floor framing plan: Haunch girder scheme.

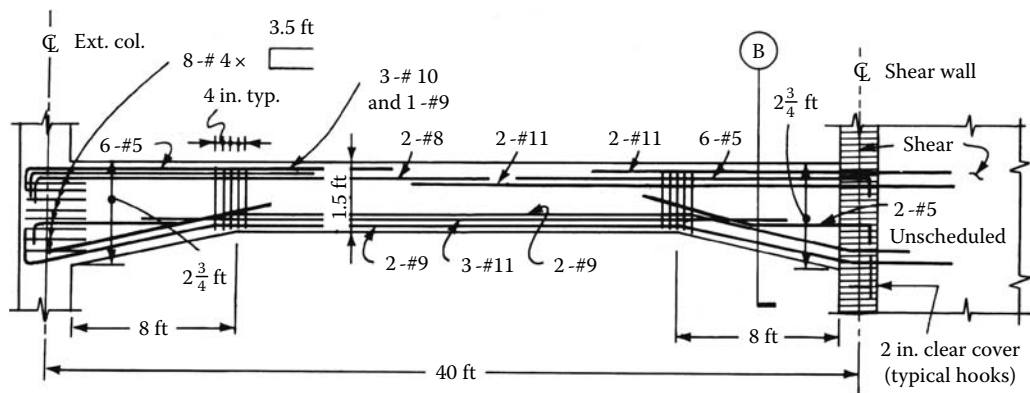


FIGURE 3.14 Haunch girder elevation and reinforcement.



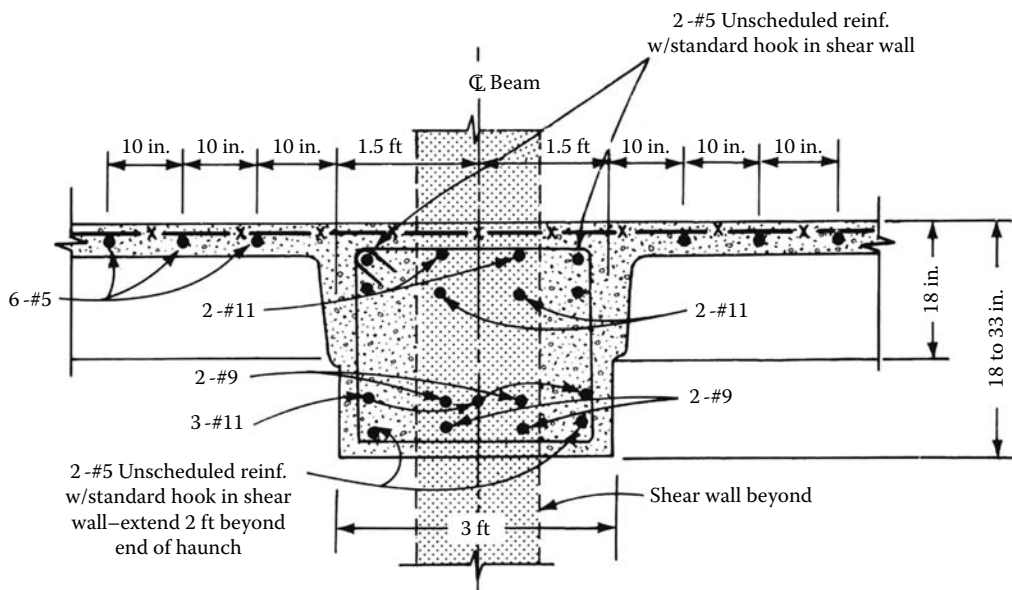


FIGURE 3.15 Haunch girder section.

### 3.7 CORE-SUPPORTED STRUCTURES

Shear walls placed around building services such as elevators and stair cores can be considered as a spatial system capable of transmitting lateral loads in both directions. The advantage is that, being spatial structures, they are able to resist shear forces and bending moments in two directions and also torsion particularly so when link beams are provided between the openings. The shape of the core is typically dictated by the elevator and stair requirements and can vary from a single rectangular core to multiple cores. Floor framing around the core typically consist of systems such as cast-in-place mild steel reinforced or posttensioned concrete. See Figure 3.18 for other examples. Composite structural steel beams with metal deck is also used as floor framing around core supported buildings (see Figure 3.19).

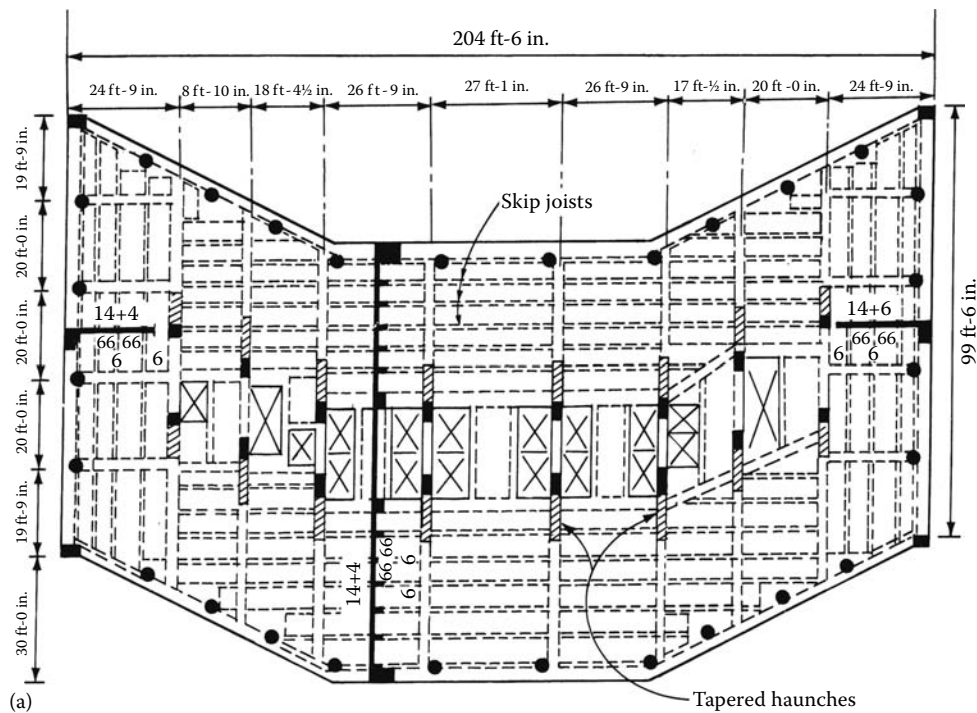
### 3.8 SHEAR WALL-FRAME INTERACTION

In this system, resistance to horizontal loading is provided by a combination of shear walls and rigid frames. The shear walls are often placed around elevator and service cores while the frames with relatively deep spandrels occur at the building perimeter.

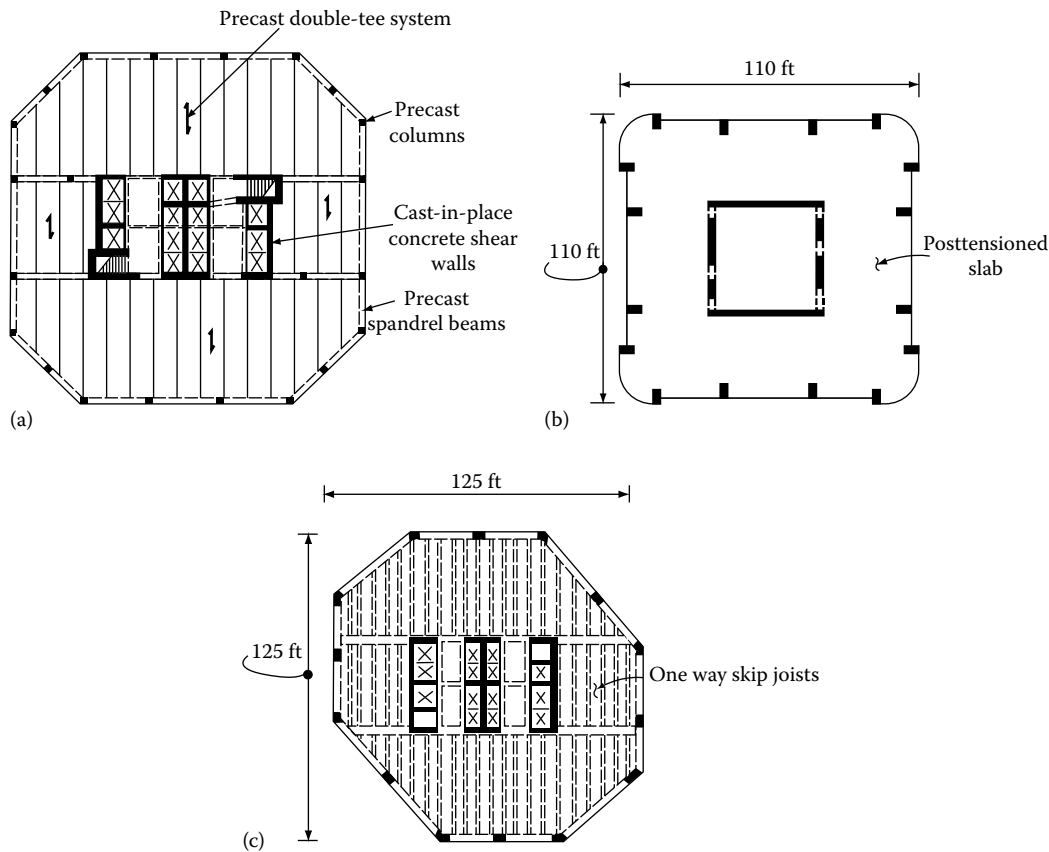
When a wall-frame structure is loaded laterally, the distinctly different deflected forms of the walls and the frames can be quite effective in reducing the lateral deflections to the extent that buildings of up to 50 stories or more are economical. The potential advantages of a wall-frame structure depend on the intensity of horizontal interaction, which is governed by the relative stiffness of the walls and frames, and the height of the structure. The taller the building and the stiffer the frames, the greater the interaction.



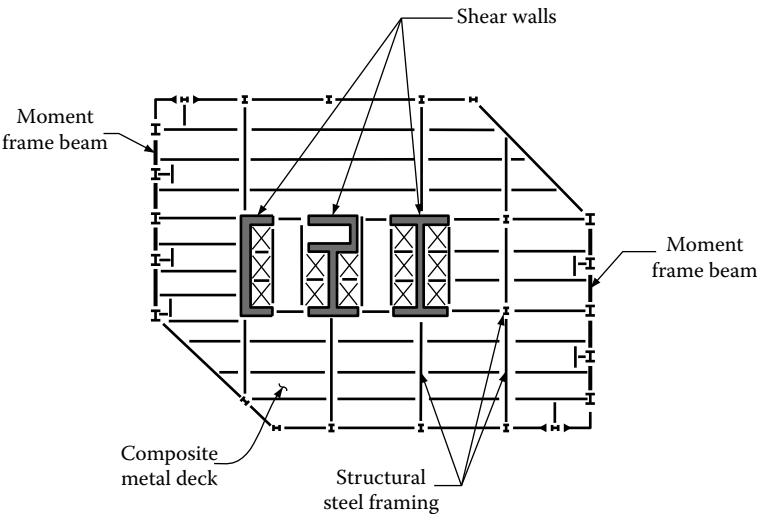
FIGURE 3.16 The Huntington. (Architects, Talbot Wilson & Associates; structural engineers, Walter P. Moore and Associates; contractor, W. S. Bellows Construction Corp.)



**FIGURE 3.17** A 28-story haunch girder building, Houston, Texas. (a) Typical floor plan and (b) photograph. (Structural engineers, Walter P. Moore and Associates.)



**FIGURE 3.18** Examples of core-supported buildings: (a) cast-in-place shear walls with precast surround, (b) shear walls with posttensioned flat plate, and (c) shear walls with one-way joist system.



**FIGURE 3.19** Concrete core with steel surround.

Without a question, this system is one of the most—if not the most—popular system for resisting lateral loads in medium- to high-rise buildings. The system has a broad range of application and has been used for buildings as low as 10 stories to as high as 50 stories or even taller. With the advent of haunch girders, the applicability of the system can be extended to buildings in the 70- to 80-story range.

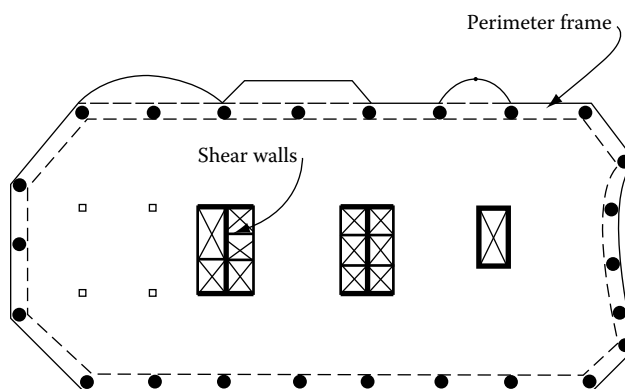
The classical mode of interaction between a prismatic shear wall and a moment frame is shown in Figure 3.8. The frame deflects in a so-called shear mode whereas the shear wall predominantly responds in bending as a cantilever. Compatibility of horizontal deflection generates interaction between the two. The linear sway of the moment frame, combined with the parabolic sway of the shear wall, results in enhanced stiffness of the system because the wall is restrained by the frame at the upper levels while at the lower levels, the shear wall restrains the frame. However, a frame consisting of closely spaced columns and deep beams tends to behave more like a shear wall responding predominantly in a bending mode. And similarly, a shear wall weakened by large openings acts more like a frame by deflecting in a shear mode. The combined structural action, therefore, depends on the relative rigidity of the two and their modes of deformation.

Even for buildings in the 10- to 15-story range, unreasonably thick shear walls may be required if the walls are placed only around the building's service core. For such buildings, using a combination of rigid frames with shear walls might be a better option. Although relatively deep girders are required for a substantial frame action, rigid frames are often architecturally preferred because they are least objectionable from the interior space planning considerations. When used on the building exterior, deep spandrels and closely spaced columns may be even better because columns usually will not interfere with the space planning and the depth of spandrels need not be shallow as for interior beams, for the passage of air conditioning and other utility ducts. A schematic floor plan of a building using this concept is shown in Figure 3.20.

As an alternative to perimeter frames, interior frames can also be used with the core walls, as shown in Figure 3.21. Yet another option is to use haunch girders between interior walls and perimeter columns, as shown in Figure 3.22. In this example, the girders may be considered as outriggers connecting the exterior columns to the interior shear walls.

For slender buildings with height-to-width ratios in excess of say 6, an interacting system of moment frames and shear walls becomes uneconomical if the walls are placed only within the building core. A good structural solution, if architecturally acceptable, is to use shear walls for the full, or a good portion of the width of the building.

Another possibility is to use segmented story-high shear walls for the full-depth at the interior of the building, as shown in Figure 3.23a and b. The walls stretched out for the full depth



**FIGURE 3.20** Shear walls with perimeter frames.

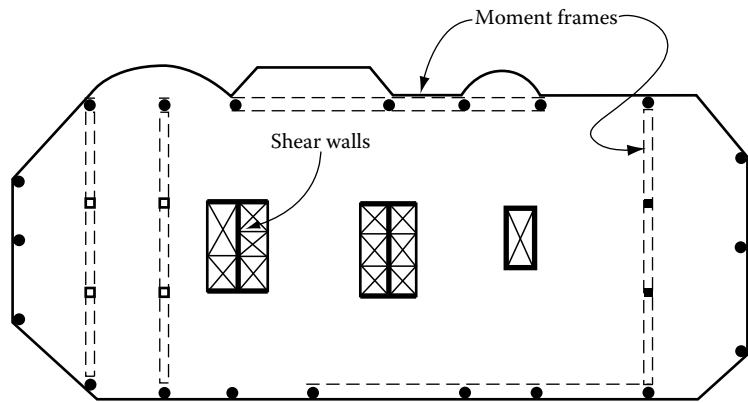


FIGURE 3.21 Shear walls with interior frames.

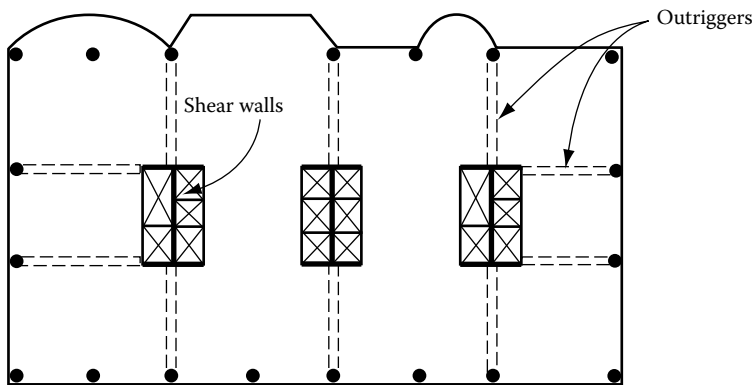


FIGURE 3.22 Shear walls with outrigger girders.

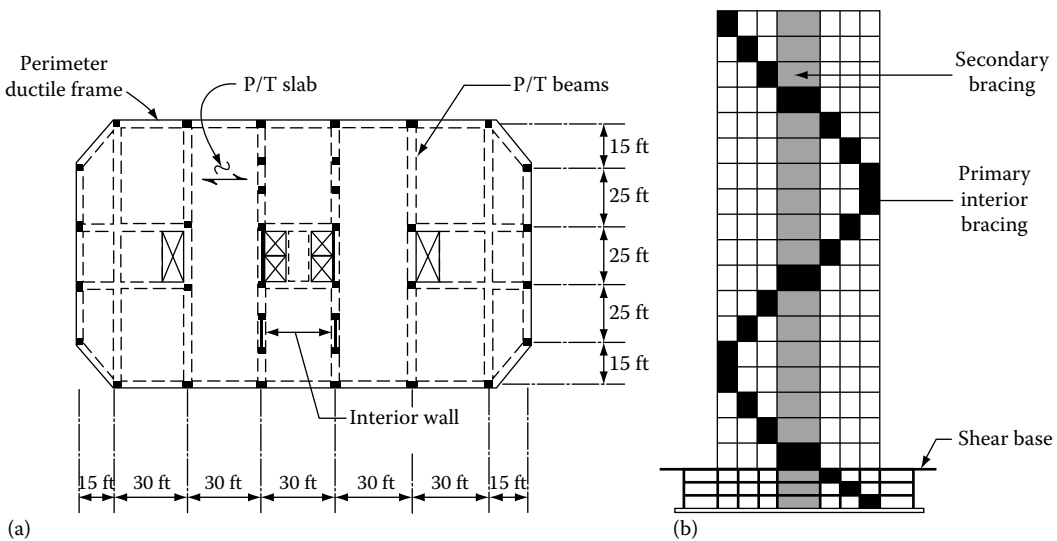


FIGURE 3.23 Full depth interior shear walls acting as gaint K-brace. (a) Plan and (b) schematic section.

of the building act as giant K-braces, resisting overturning and shear forces by developing predominantly axial forces. A transverse cross-section of a building using such a system is shown in Figure 3.23b. In this case, the interior shear walls act as a secondary bracing system to transfer lateral loads to the panel points of the K-braces. The walls running through the interior lease space of the building will have to architecturally acknowledged as a trade-off for structural efficiency.

All of the aforementioned systems or any number of their variations can be used singly or in combination with one another, depending on the layout of the building and architectural requirements.

### 3.8.1 BEHAVIOR

As stated previously, if the deflection modes of shear walls and moment frames were similar, the lateral loads would be distributed between the two systems more or less, according to their relative stiffness. However, in general, the two systems deform with their own characteristic shapes. The interaction between the two, particularly at the upper levels of the buildings, results in quite a different lateral load distribution.

The lateral deflections of a shear wall may be considered as similar to those of a cantilever column. Near the bottom, the shear wall is relatively stiff, and therefore, the floor-to-floor deflections will be less than half the values near the top. At top floors, the deflections increase rather rapidly, mainly from the cumulative effect of wall rotation.

Moment frames, on the other hand, deform predominantly in a shear mode. The relative story deflections depend primarily on the magnitude of shear applied at each story level. Although the deflections are larger near the bottom and smaller near the top as compared to the shear walls, the floor-to-floor deflections can be considered more nearly uniform throughout the height. When the two systems—the shear walls and moment frames—are connected by rigid floor diaphragms, a nonuniform shear force develops between the two. The resulting interaction typically results in a more economical structural system.

Refer back to Figure 3.8 which shows the deformation patterns of a shear wall and moment frame subjected to lateral loads. Also shown therein are the horizontal shear forces between the two, the length of arrows schematically representing the level of interaction. Observe that the shear wall acts as a vertical cantilever column, with a greater slope at the top.

The moment frame, on the other hand, deforms in a shear mode, with the slope greater at the base of the structure where the shear is maximum. Since the lateral deflection characteristics of the two frames are entirely different, the moment frame tends to pull back the shear wall in the upper levels of the building while pushing it forward in the lower levels. As a result, the frame participates more effectively in the upper portions of the building where lateral shears are relatively weaker, while the shear wall carries most of the shear in the lower portion of the building. Because of the distinct difference in the deflection characteristics, the two systems tend to help each other a great deal. The frame tends to reduce the lateral deflection of the shear wall at the top, while the shear wall supports the frame near the base. A typical variation of horizontal shear carried by each system is shown in Figure 3.8, in which the lengths of arrows conceptually indicate the magnitude of interacting shear forces.

Without a question, the shear wall–frame system is one of the most, if not the most, common system for resisting lateral loads. The system has a broad range of application and has been used for buildings as low as 10 stories to as high as 50-story or even taller buildings. With the advent of haunch girders, the applicability of the system is easily extended to buildings in the 70- to 80-story range.

As stated earlier, the linear sway of the moment frame, when combined with the parabolic deformation of the shear wall, results in an enhanced stiffness of the entire system because the wall is restrained by the frame at the upper levels while at lower levels, the shear wall is restrained by the frame. However, it is not always easy to differentiate between the two modes because a frame consisting of closely spaced columns and deep beams tends to behave more like a shear wall responding

predominately in a bending mode. The combined structural action, therefore, depends on the relative rigidity of the two and their modes of deformation. Furthermore, the simple interaction diagram shown in Figure 3.8 is valid only if:

- The shear wall and frame have constant stiffness throughout the height or
- If stiffnesses vary—the relative stiffness of the wall and frame remains unchanged throughout the height

Since architectural and other functional requirements frequently influence the configuration of structural elements, the above conditions are rarely met in a practical building. In a contemporary high-rise building, very rarely can the geometry of walls and frames be the same over the full height. For example, walls around the elevators are routinely stopped at levels corresponding to the elevator drop-offs, columns are made smaller as they go up, and the building geometry is very rarely the same for the full height. Because of abrupt changes in the stiffness of walls and frames combined with the variation in the geometry of the building, the simple interaction shown in Figure 3.8 does not even come close to predicting the actual behavior of the building structures. However, with the availability of computer software, capturing the essential behavior of the shear wall frame system is within the reach of everyday engineering practice.

### 3.8.2 BUILDING EXAMPLES

To understand the qualitative nature of interaction between shear walls and frames, consider the framing plan shown in Figure 3.24. The building shown is rather unusual in that it exhibits almost perfect symmetry in two directions and maintains a reasonably constant stiffness throughout its height.

The building is 25 stories and consists of four levels of basement below grade. The floor framing consists of 6 in. wide  $\times$  20 in. deep (152.4  $\times$  508 mm) skip joist framing between haunch girders which span the distance of 35 ft 6 in. (10.82 m) between the shear walls and the exterior of the building. The girders are 42 in. wide  $\times$  20 in. deep (1.06  $\times$  0.5 m) for the exterior 28 ft. 6 in. (8.67 m) length, with a haunch at the interior tapering from a pan depth of 20–33 in. (0.5–0.84 m). Four shear walls of dimensions 1 ft 6 in.  $\times$  19 ft 6 in. (0.45  $\times$  5.96 m) rise for the full height from a 5 ft (1.52 m) deep mat foundation. The exterior columns vary from 38  $\times$  34 in. (965  $\times$  864 mm) at the bottom to 38  $\times$  42 in.

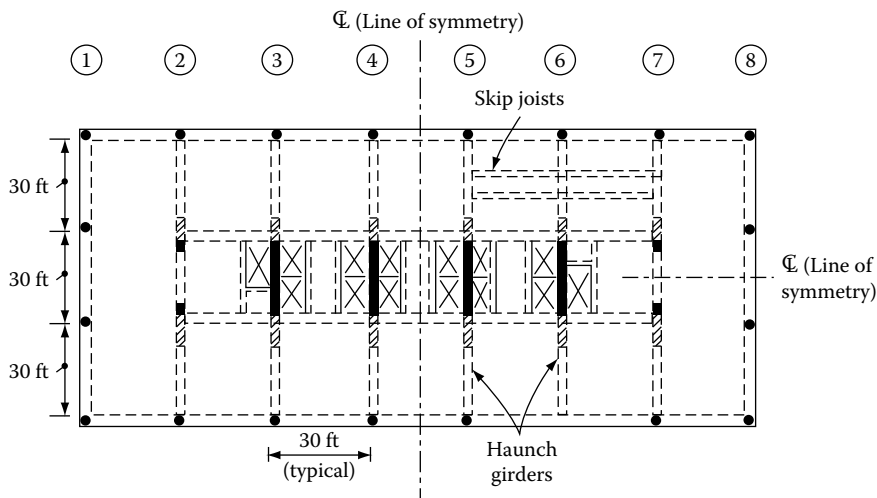


FIGURE 3.24 Example of shear wall–frame interaction: Typical floor plan.

(965 × 610 mm) at the top. Note that the girder is made deliberately wider than the exterior column to simplify removal of flying forms.

The lateral load resistance in the short direction of the building is provided by a combination of three types of frames:

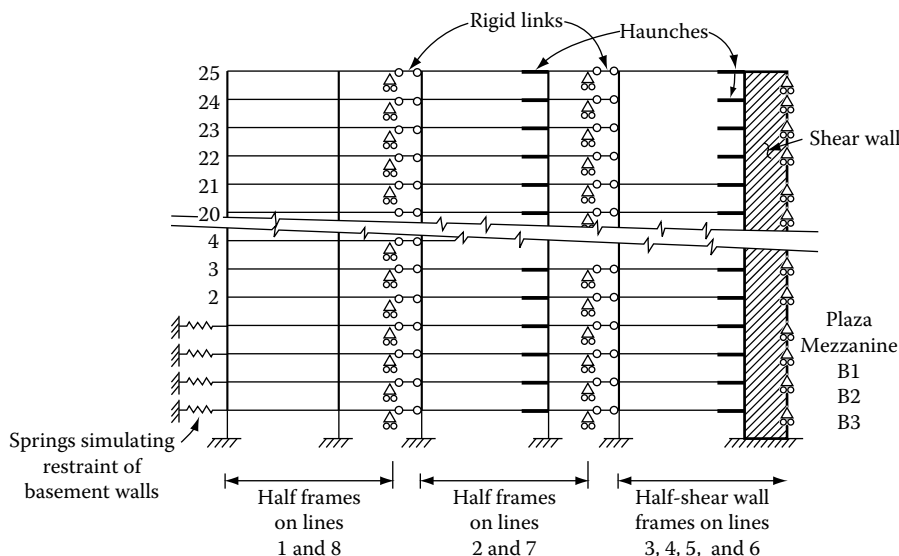
1. Two exterior frames along grids 1 and 8
2. Two haunch girder frames along grids 2 and 7
3. Four shear wall-haunch girder frames along grids 3 through 6

The lateral load resistance in the long direction is provided primarily by frame action of the exterior columns and spandrels along the broad faces.

For purposes of structural analysis, the building is considered symmetrical about the two center-lines. The lateral load analysis can be carried out by lumping together similar frames and using only one-half the building in the computer model. This is shown in Figure 3.25 for a two-dimensional computer model for analysis of wind forces on the broad face. In the model only three equivalent frames are used to represent the lateral load resistance of eight frames, and only one-half of each frame is used to stimulate the structural action of a full frame. The latter simplification is achieved by restraining the vertical displacement at the end of each frame as shown in Figure 3.25. Note the spring restraints at the basement levels B1, B2, B3, and at the plaza are used to stimulate the lateral restraint of the basement walls and soil structure interaction. The rigid links shown in Figure 3.25 between the individual frames simulate the diaphragm action of the floor slab by maintaining the lateral displacements of each frame the same at each level.

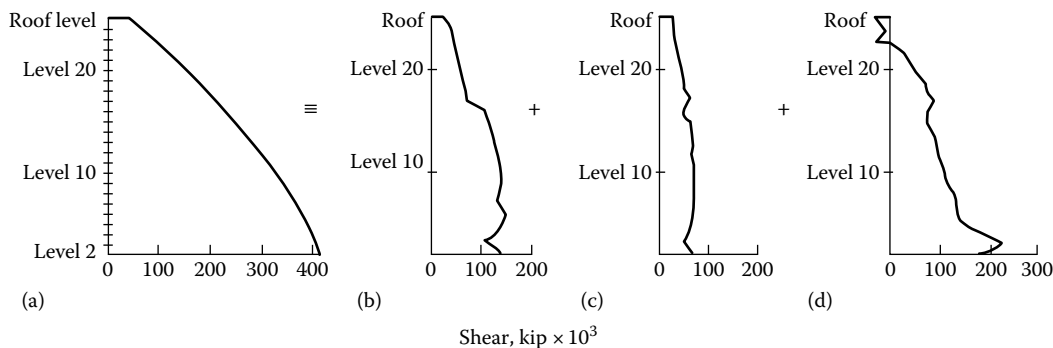
The modeling techniques explained in here belong to an earlier period when computers were not used. With the availability computer software, the modeling simplifications are no longer necessary. The purpose here is to highlight the nature of interaction between shear walls and frames.

Part (a) of Figure 3.26 shows the cumulative shear forces along the broad face of the building. The distribution of the shear forces among the three types of frames is indicated in parts (b) through (d). Note the reversal in the direction of the shear force at top, which causes the shear wall to behave as a propped cantilever, not unlike the behavior observed in the simplified shear wall–frame interaction



**FIGURE 3.25** Simplified analytical model of bygone era. With the availability of computer software, simplified methods are no longer in use.





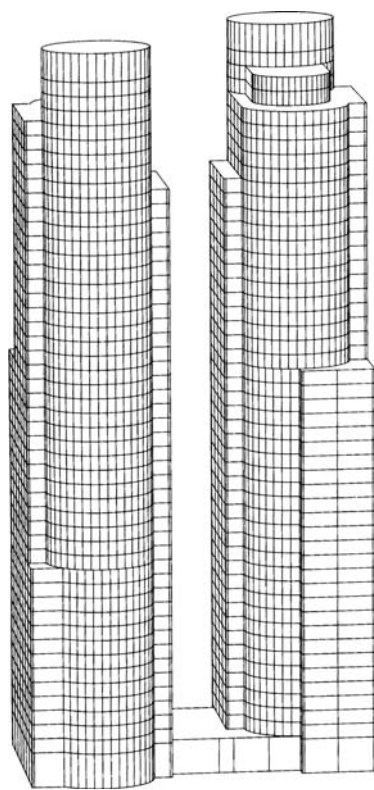
**FIGURE 3.26** Shear force distribution.

studied earlier. This is not surprising because although the example consists of a combination of three different types of frames, in essence the structural system responds as a single shear wall acting in combination with a single frame. This is due to the uniformity of stiffness of the walls and frames along the building height.

Although the example shown is taken from an actual project, it is somewhat unusual because it is symmetrical and has no significant structural discontinuity over its height. More usually, there is asymmetry either due to shear wall drop-offs or change in the building's shape.

As a second example, let us consider a building that has asymmetrical floor plans and abrupt variation in stiffness (see Figure 3.27). The office building, proposed for construction in Dallas, Texas, is 655 ft tall (200 m) and consists of 50 stories above grade. A variety of floor plans occur between the second and the roof levels, resulting in a number of setbacks, and a major transfer of columns at level 40 (Figure 3.28a through f). The floor plan, essentially rectangular at the second floor, progressively transforms into a circular shape at the upper levels. The resistance to lateral load is provided by a system of I- and C-shaped shear walls interacting with haunch girder frames. The floor framing consists of a 4 in. thick lightweight concrete slab spanning between 6 in. (152.4 mm) wide  $\times$  16 in. deep skip joists spaced at 6 ft 6 in. (1.98 m) centers. The 20 in. (508 mm) depth of haunch girders at midspan matches the depth of pan joist construction. Tapered haunches are used at both ends of girders that vary from a depth of 20 in. (508 mm) at midbay to a depth of 2 ft 9 in. (0.84 m) at the face of columns and shear walls. High-strength normal-weight concrete of up to 10 ksi (68.95 mPa) is used in the design of columns and shear walls. The shear walls around the low, mid, mid-low, mid-high, and high-rise elevators are terminated at various levels corresponding to the elevator drop-offs.

Figure 3.29 shows the distribution of horizontal shear forces among various lateral-load-resisting elements for wind forces acting on the broad face of the building. The lateral loads in the shear wall frames are shown by the curves designated as 12, 13, 14, and 15, which correspond to their locations on the grid lines shown in Figure 3.29a through f. The shear forces in the frames are shown by



**FIGURE 3.27** Example of shear wall-frame interaction: 50-Plus-story haunch girder—shear wall building.

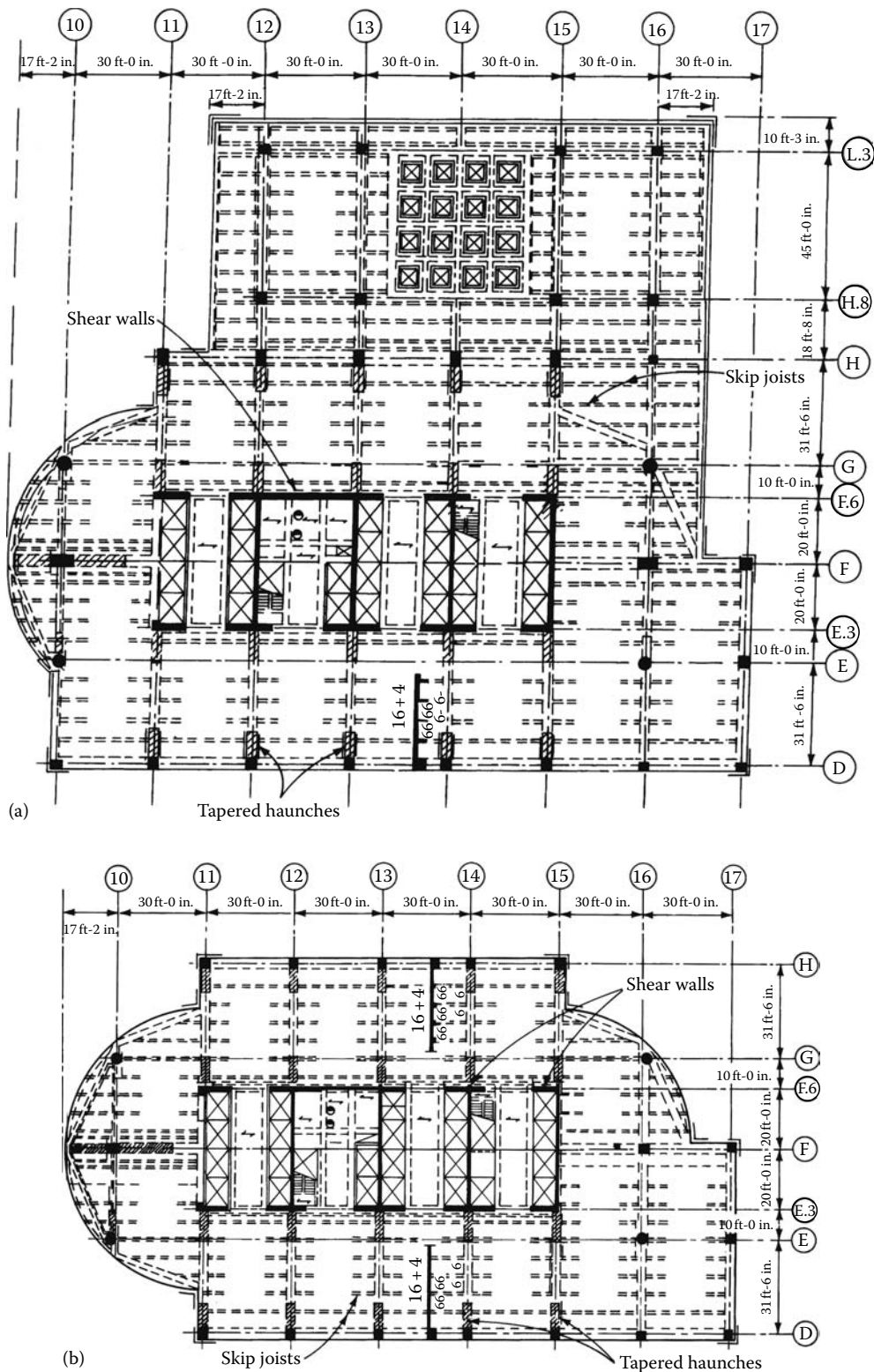


FIGURE 3.28 Framing plans. (a) Levels 2 through 14 floor plan, (b) levels 15 through 26 floor plan, (continued)

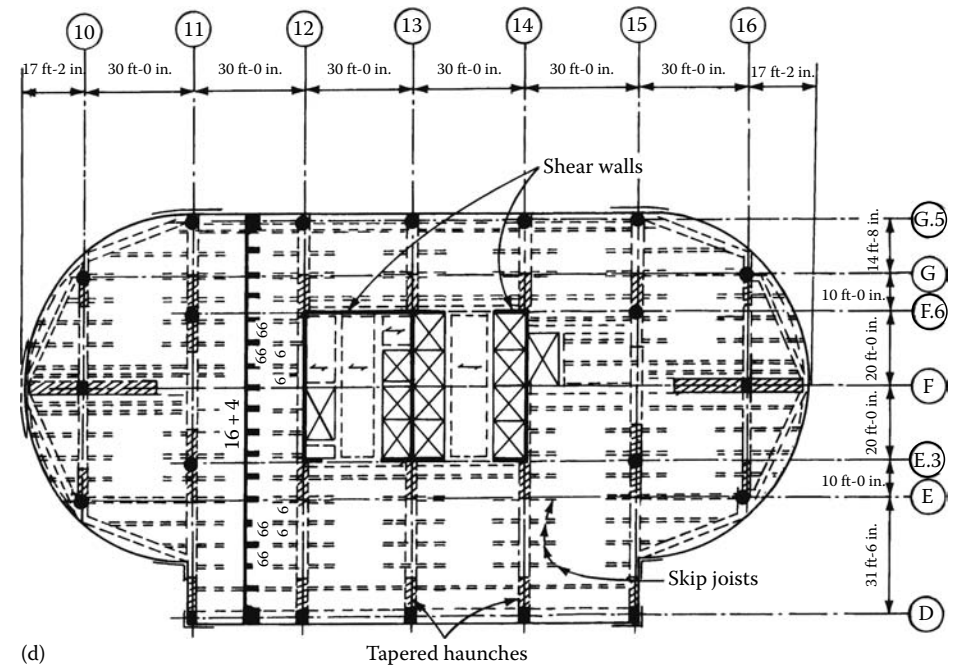
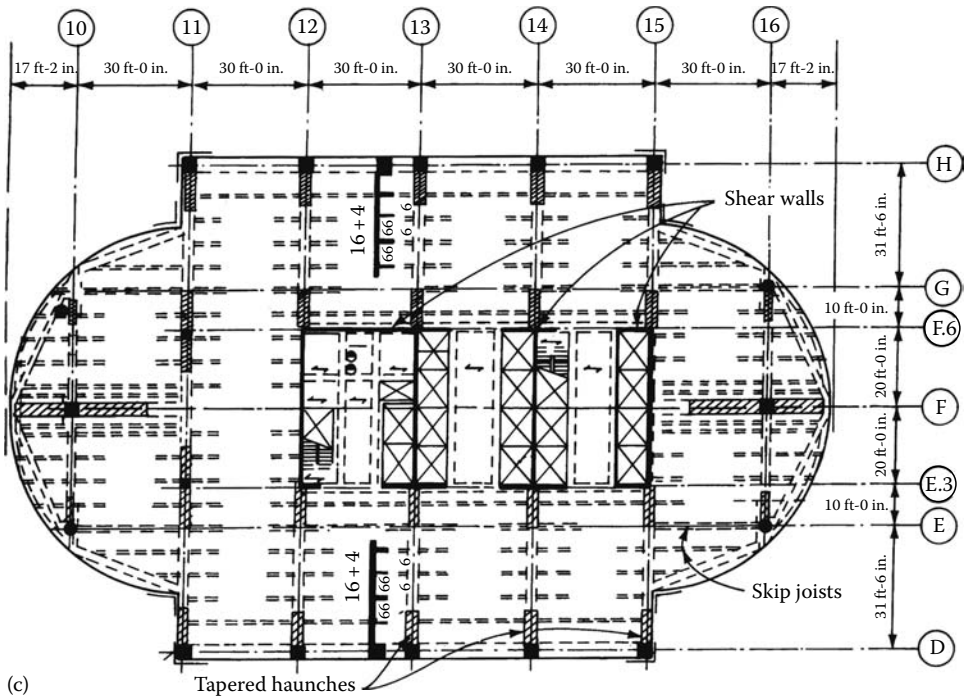


FIGURE 3.28 (continued) (c) levels 27 through 39 floor plan, (d) levels 40 through 47 floor plan,

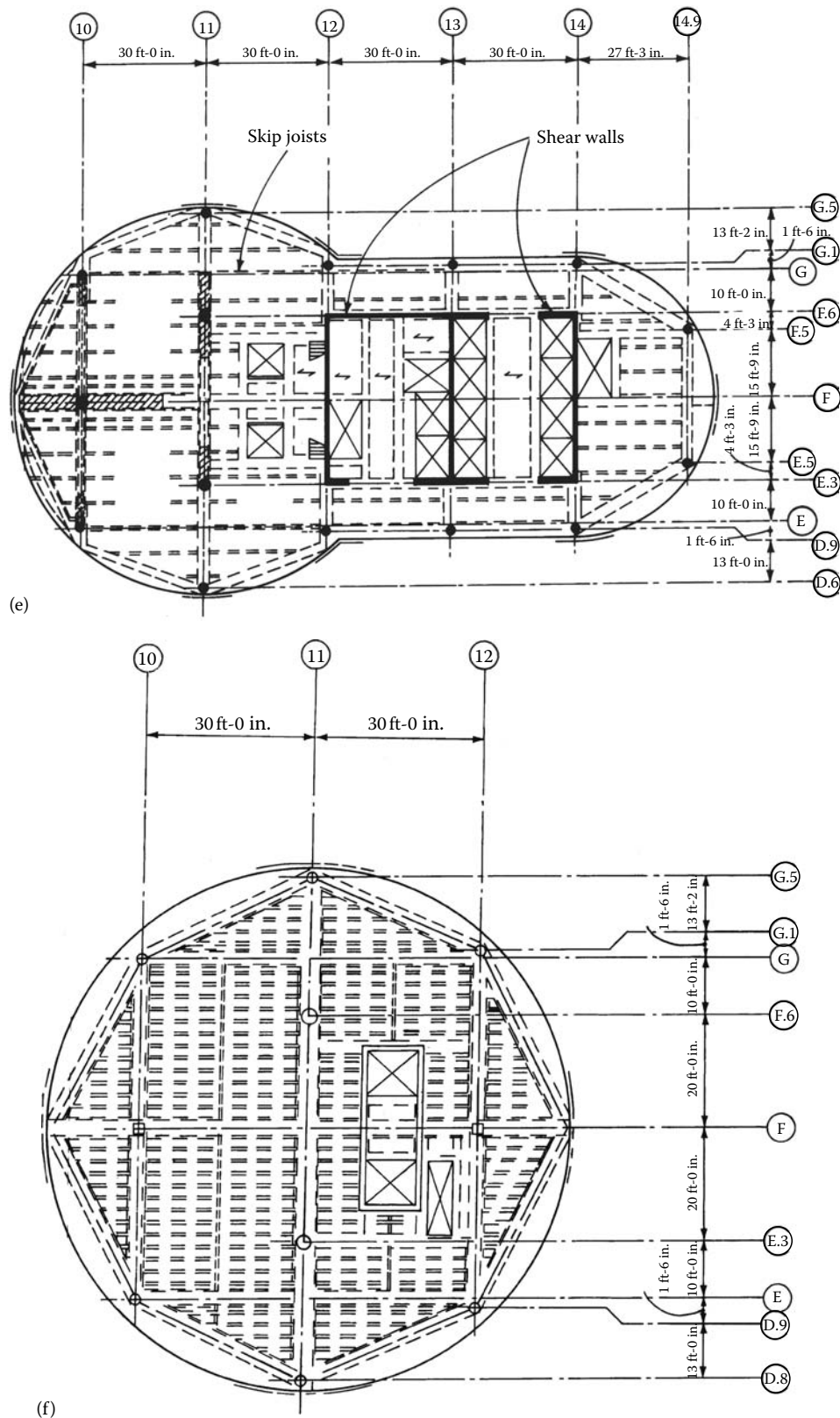
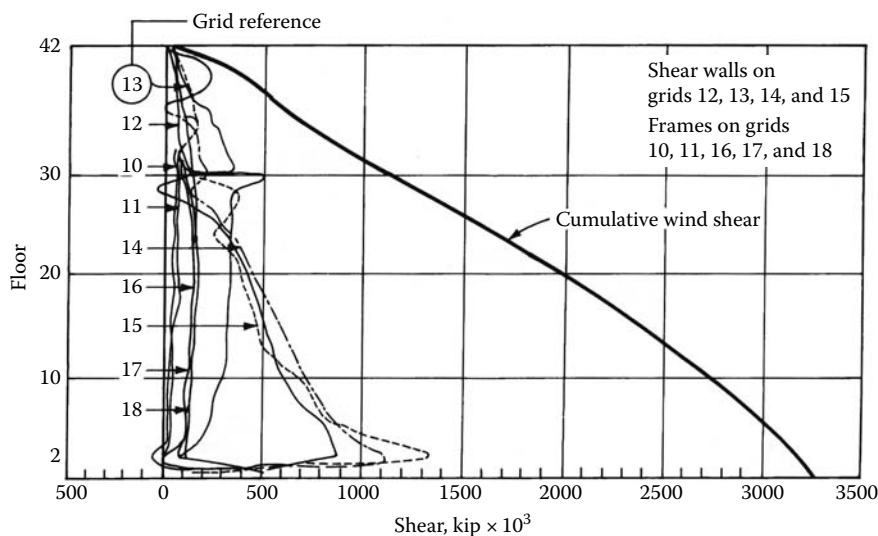


FIGURE 3.28 (continued) (e) levels 48 and 49 floor plan, and (f) levels 50 and 51 floor plan.



**FIGURE 3.29** Distribution of shear forces.

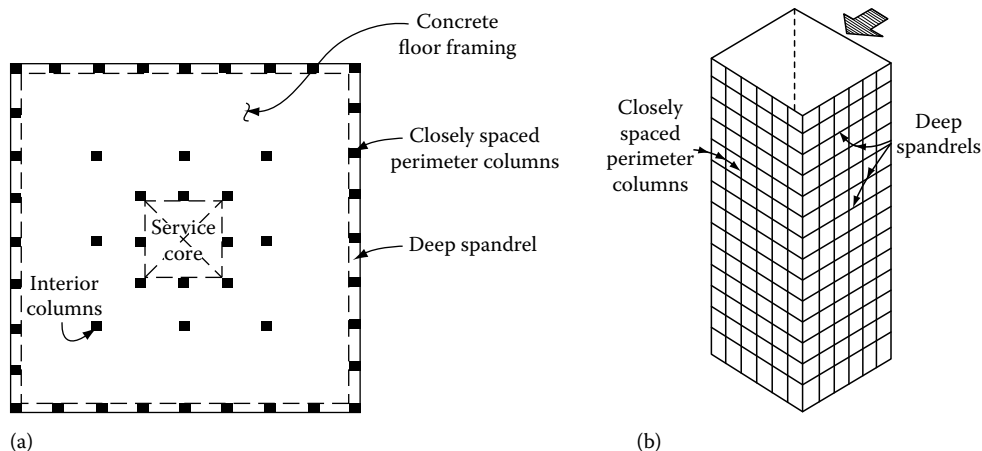
curves designated as 10, 11, 16, 17, and 18. The results shown are from an earlier version of the tower, which consisted of 42 floors with slight modifications to the floor plans shown in Figure 3.28.

The purpose here is to show how the distribution of transverse shear is considerably different than in a structure with regular full-height shear walls and frames of uniform stiffness. The large difference in the transverse shear distribution among various frames and walls occurs for two reasons. First, the structure is complex, with stiffness varying significantly over the height. Second, the assumption of rigid diaphragm commonly used in modeling of the floor slab results in sharp shear transfers at levels where the stiffness of the walls change abruptly. However, it is possible and indeed necessary, particularly when the floor diaphragm has large openings, to smooth out the abrupt distribution and sudden reversals of transverse shear by modeling floor slabs as flexible diaphragms.

### 3.9 FRAME TUBE SYSTEM

In this system, the perimeter of the building consists of closely spaced columns connected by deep spandrels. The system works quite efficiently as a hollow vertical cantilever. However, lateral drift due to the axial displacement of the columns—commonly referred to as chord drift—and web drift, caused by shear and bending deformations of the spandrels and columns, may be quite large depending upon the tube geometry. For example, if the plan aspect ratio is large, say, much in excess of 1:2.5, it is likely that supplemental lateral bracing may be necessary to satisfy drift limitations. The economy of the tube system therefore depends on factors such as spacing and size of columns, depth of perimeter spandrels, and the plan aspect ratio of the building. This system should, however, be given serious consideration for buildings taller than about 40 stories.

In its simplest terms, a framed tube can be defined as a three-dimensional system that engages the entire building perimeter to resist lateral loads. A necessary requirement to create a wall-like three-dimensional structure is to place columns on the building exterior relatively close to each other, joined by deep spandrel girders. In practice, columns are placed 10 ft (4 m) to as much as 20 ft (6.1 m) apart, with spandrel depths varying from about 3 to 5 ft (0.90 to 1.52 m). A somewhat different type of tube, often referred to as a braced tube, permits greater spacing of columns. As the name implies, the tube has diagonal bracing at the building exterior. Yet another variation of tube called bundled tube uses two or more tubes tied together to form a single, multicell tube.



**FIGURE 3.30** Frame tube building. (a) Schematic plan and (b) isometric view.

### 3.9.1 BEHAVIOR

To understand the behavior of a framed tube, consider a building shown in Figure 3.30 in which the entire lateral resistance is provided by closely spaced exterior columns and deep spandrel beams. The floor system, typically considered rigid in its own plane, distributes the lateral load to various elements according to their stiffness. Its contribution to lateral resistance in terms of out-of-plane stiffness is considered negligible. The lateral load-resisting system thus comprises four orthogonally oriented, rigidly jointed frame panels forming a tube in plan, as shown in Figure 3.30.

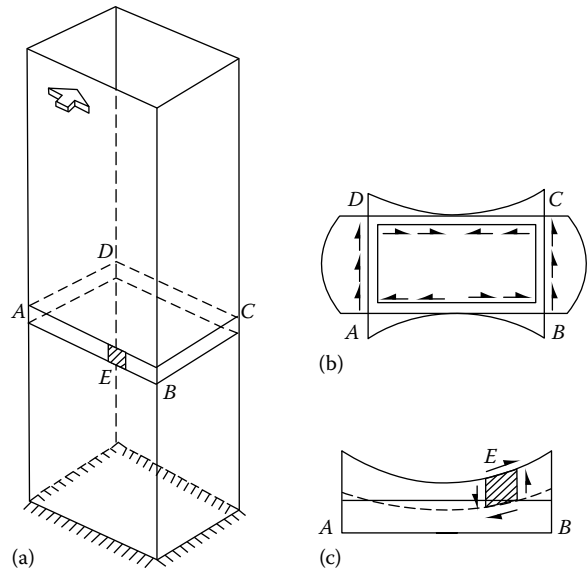
The “strong” bending direction of the columns is typically aligned along the face of the building, in contrast to a typical transverse rigid frame where it is aligned perpendicular to the face. The frames parallel to the lateral load act as webs of the perforated tube, while the frames normal to the load act as the flanges. When subjected to bending, the columns on opposite sides of the neutral axis of the tube are subjected to tensile and compressive forces. In addition, the frames parallel to the direction of the lateral load are subjected to the in-plane bending and the shearing forces associated with an independent rigid frame action. The discrete columns and spandrels distributed around the building periphery may be considered, in a conceptual sense, equivalent to a hollow tube cantilevering from the ground, as shown in Figure 3.31.

Although the structure has a tube-like form, its behavior is much more complex than that of a solid tube. Unlike a solid tube, it is subjected to the effects of shear lag, which has a tendency to modify the axial distribution in the columns. The influence of shear lag, considered presently in the following section, is to increase the axial stresses in the corner columns while simultaneously reducing the same in the inner columns of the flange and the web panels, as shown in Figure 3.32.

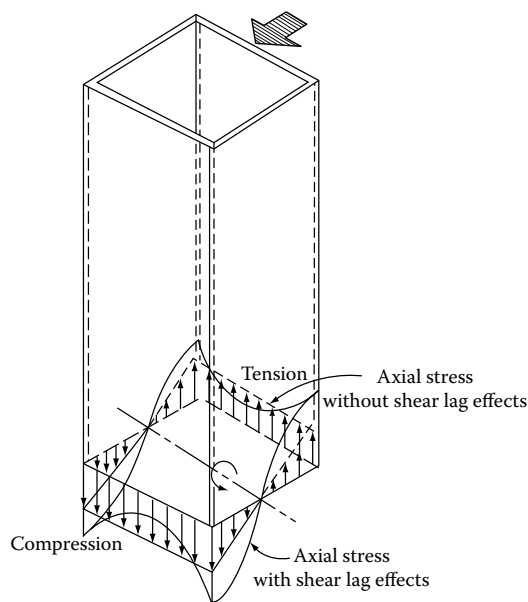
The fundamental behavior explained with reference to the tube in Figures 3.31 and 3.32 is also applicable, in a broad sense, to free-form tubular configurations. Some examples are shown in Figure 3.33. Although in simplistic terms, the tube is similar to a hollow cantilever, in reality its response to lateral loads is in a combined bending and shear mode. The bending mode is due to axial shortening and elongation tube of the columns, whereas the shear mode is due to bending of individual columns and spandrels. The underlying principle for an efficient design is to eliminate or minimize shear deformation.

### 3.9.2 SHEAR LAG

Consider Figure 3.34, in which columns of a tubular building are noted as T and C. T denotes a column in tension while C denotes a column in compression. The primary resistance to lateral



**FIGURE 3.31** Shear lag effects in a hollow tube structure: (a) cantilever tube subjected to lateral loads, (b) shear stress distribution, and (c) distortion of flange element caused by shear stresses.



**FIGURE 3.32** Axial stress distribution in a square hollow tube with and without shear lag.

loads comes from the web frames with the T columns in tension and the C columns in compression (Figure 3.34). The web frames are subjected to the usual in-plane bending and racking action associated with an independent rigid frame. The primary action is modified by the flexibility of the spandrel beams, which causes the axial stresses in the corner columns to increase and those in the interior columns to decrease.

The principal interaction between the web and flange frames occurs through the axial displacements of the corner columns. When column C, for example, is under compression, it will tend to

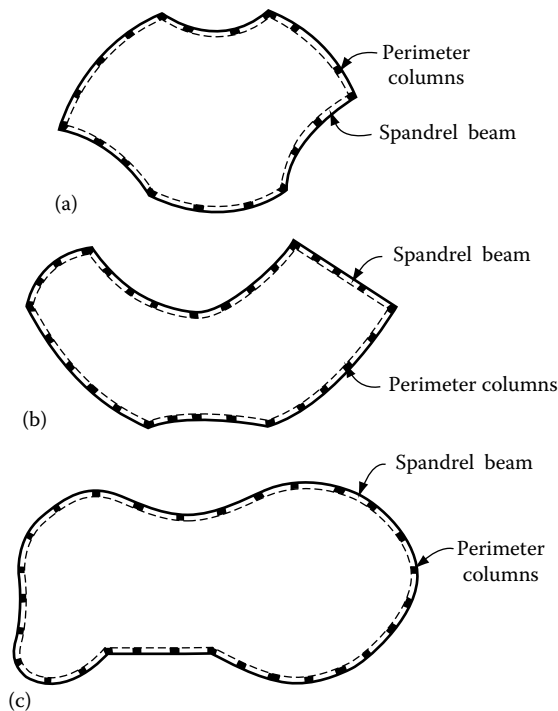


FIGURE 3.33 Free-form tubular configurations.

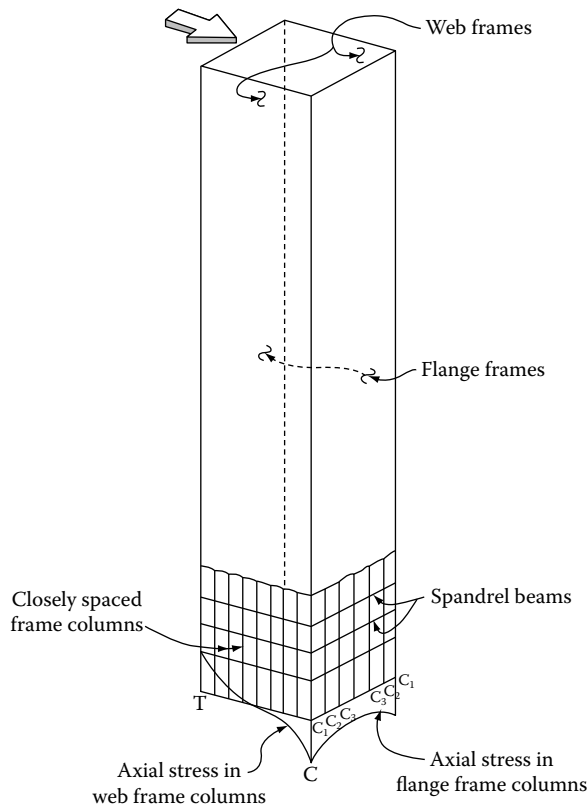


FIGURE 3.34 Shear lag in framed tube.



compress the adjacent column  $C_1$  (Figure 3.34) because the two are connected by the spandrel beams. The compressive deformations of  $C_1$  will not be identical to that of corner column  $C$  since the connecting spandrel beam will bend. The axial deformation of  $C_1$  will be less, by an amount depending on the stiffness of the connecting beam. The deformation of column  $C_1$  will, in turn, induce compressive deformations of the next inner column  $C_2$ , but the deformation will again be less. Thus, each successive interior column will experience a smaller deformation and hence a lower stress than the outer ones. The stresses in the corner column will be greater than those from a pure tubular action, and those in the inner columns will be less. The stresses in the inner columns lag behind those in the corner columns, hence the term shear lag.

The difference between stress distribution as predicted by ordinary beam theory, which assumes that plane sections remain in plane, and the actual distribution due to shear lag is illustrated in Figure 3.34. Because the column stresses are distributed less effectively than in an ideal tube, the moment resistance and the flexural rigidity of a tubular building are much less. Thus, although a framed tube is highly efficient, it does not fully utilize the potential stiffness and strength of the structure because of the effects of shear lag.

To firm up our understanding of shear lag phenomenon, let us consider two examples. The first is a cantilevered box beam (Figure 3.35), formed from two steel channels to which are attached two thin steel sheets by welding along the edges. If the beam is loaded by two forces  $P$  at the free end, the elementary bending theory will give a tensile bending stress in the top sheet uniformly distributed across any section. Similarly, a uniform compressive stress occurs at the bottom sheet. Both the tensile and compressive stresses are communicated to the sheets by the channels.

The distribution of stresses, tensile at the top and compressive at the bottom sheet, will not be uniform, but, will be higher at the edges than at the middle. Note, for clarity, only the stress distribution in the top sheet is shown. This departure from the uniformity-assumed distribution given by the elementary theory is known as “shear lag,” since it is due to shear deformations in the sheets. The axial stresses in the interior of the sheets “lag” behind those at the edges because of shear deformation. Hence the expression shear lag.

As a second example, take the case of a T beam shown in Figure 3.36. Assuming that the beam is simply supported at the ends and loaded vertically, we observe that there are shearing stresses acting between the flanges and the beam rib along the surfaces  $mn$ , horizontal and directed as shown in Figure 3.36b. It is seen that these stresses tend to reduce the deflection of the rib, that is, to

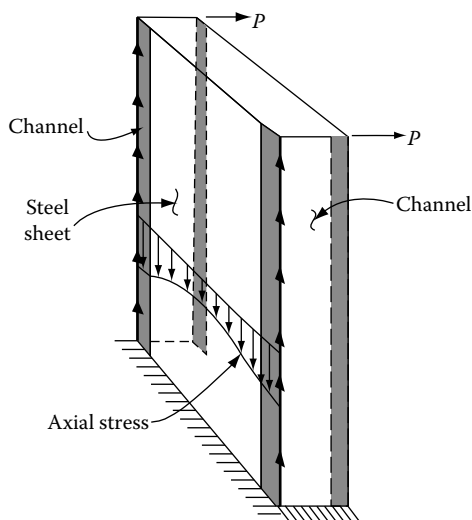
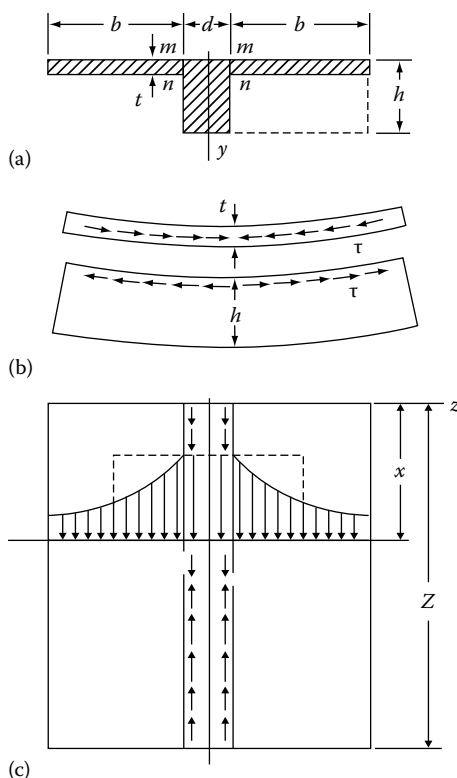


FIGURE 3.35 Cantilever box beam with two end channels.



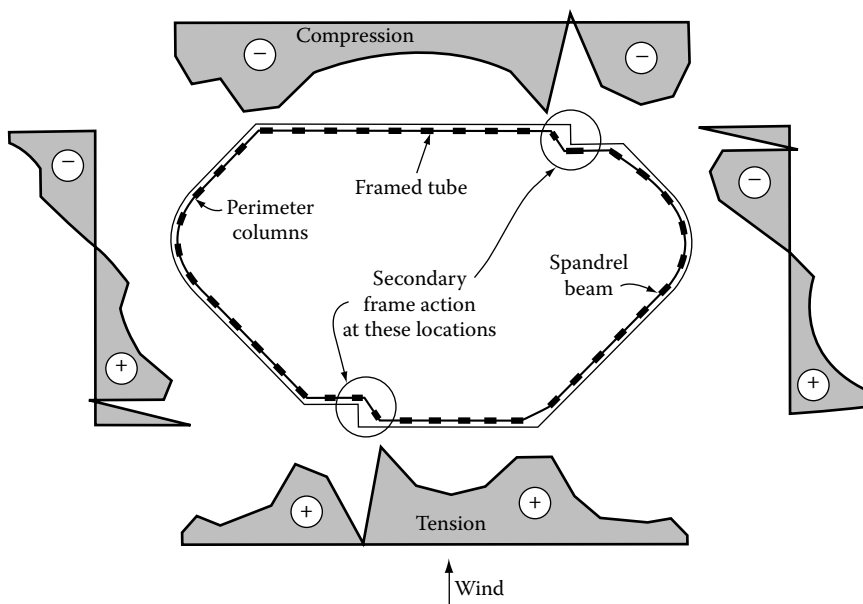
**FIGURE 3.36** Shear lag effects in T-beams flanges: (a) Cross-section of T beam. (b) Horizontal shear stresses between beam web and flange. (c) Nonuniform distribution of compressive stresses in flange.

make it stiffer. At the same time, they produce compression of the flanges. Considering a flange at one side of the rib as a rectangular plate subjected to the action of shearing forces along one edge, we see that the compressive stresses will not be uniformly distributed along the width of the flange. A rigorous analysis shows that the distribution will be as indicated in Figure 3.36c, by the maximum stress in the flange being the same as in the upper fibers of the rib. This nonuniformity of stress distribution once again demonstrates the effect of shear lag.

### 3.9.3 IRREGULAR TUBE

As stated previously the framed tube concept can be executed with any reasonable arrangement of column and spandrels around the building parameter (see Figure 3.33). However, noncompact plans and plans with reentrant corners considerably reduce the efficiency of the system. For framed tubes, a compact plan may be defined as one with an aspect ratio not greater than 1.5 or so. Elongated plans with larger aspect ratios impose considerable premium on the system because of the following reasons:

1. In wind-controlled design, the elongated building elevation acts like a sail collecting large wind loads.
2. The resulting shear forces most usually require closer spacing and/or larger columns and spandrels parallel to the wind.
3. Shear lag effects are more pronounced, especially for columns oriented perpendicular to the direction of wind.



**FIGURE 3.37** Secondary frame action in an irregular tube; schematic axial forces in perimeter columns.

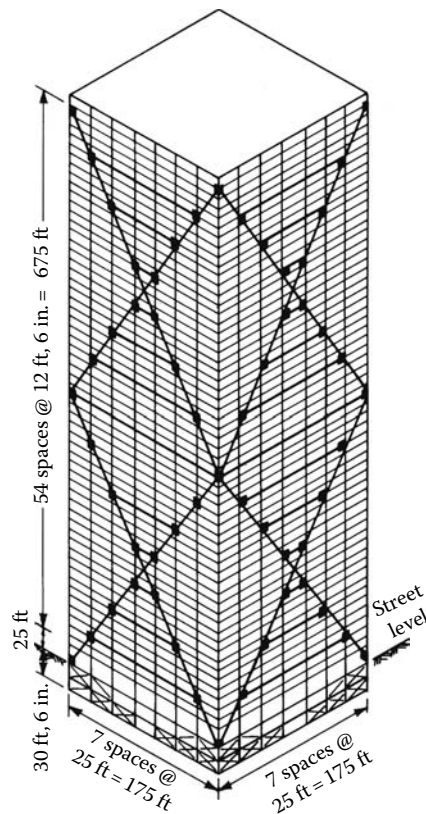
In a similar manner, a sharp change in the tubular form results in a less efficient system because the shear flow must pass around the corners solely through axial shortening of the columns. Also, a secondary frame action at these locations alters the load distribution in the framed tube columns (see Figure 3.37).

### 3.10 EXTERIOR DIAGONAL TUBE

A trussed tube system improves the efficiency of the framed tube by increasing its potential for use in taller buildings and allowing greater spacing between the columns. This is achieved by adding diagonal bracing at the faces of the tube to virtually eliminate the shear lag in both the flange and web frames.

The framed tube, as discussed previously, even with its close spacing of columns is somewhat flexible because the high axial stresses in the columns cannot be transferred effectively around the corners. For maximum efficiency, the tube should respond to lateral loads with the purity of a cantilever, with compression and tension forces spread uniformly across the windward and leeward faces. The framed tube, however, behaves more like a thin-walled tube with openings. The axial forces tend to diminish as they travel around the corners, with the result that the columns in the middle of the windward and leeward faces may not sustain their fair share of compressive and tensile forces. This effect, referred to previously as the shear lag, limits the framed tube application to 50- or 60-story buildings unless the column spacing is very close, as was the case in the now nonexisting 109-story World Trade Center Towers, New York, which had columns at 3.28 ft (1.0 m).

In a tall steel building, addition of diagonal braces, as shown in Figure 3.38, is by far the most usual method of increasing the efficiency of a framed tube. The fascia diagonals interact with the trusses on the perpendicular faces to achieve a three-dimensional behavior, virtually eliminating the effects of shear lag in both the flange and web frames. Consequently, the spacing of the columns can be greater and the size of the columns and spandrels less, thereby allowing larger windows than in a conventional tube structure. The bracing also contributes to the improved performance of the tube in carrying gravity loading. Differences between gravity load stresses in the



**FIGURE 3.38** Exterior diagonal braces in a tall steel building.

columns are evened out by the braces, which transfer axial loading from the more highly to the less stressed columns.

By applying structural principles similar to those of a trussed steel tube, it is possible to visualize a concrete system consisting of closely spaced exterior columns with blocked-out windows at each floor to create a diagonal pattern on the building facade. The diagonals carry lateral shear forces in axial compression and tension, thus eliminating bending in the columns and girders. Currently, two buildings have been built using this approach. The first is a 50-story office building in New York, and the second is a mixed-use building in Chicago described in the following Section 3.10.1. The structural system for the building in New York consists of a combination of a framed and a trussed tube interacting with a system of interior core walls. The building is 570 ft (173.73 m) tall with a height-to-width ratio of 8:1. Additional description of this building is given in Chapter 8.

### 3.10.1 EXAMPLE OF EXTERIOR DIAGONAL TUBE: ONTERIE CENTER, CHICAGO

Onterie Center, a 58-story complex located on Lake Michigan shore line, near downtown, Chicago, is an example of diagonal tube system. It comprises of a main tower with a tapering auxiliary low-rise building (see Figure 3.39). The entire lateral loads are resisted by closely spaced columns and spandrels, as is common in framed tubes. However, to achieve additional lateral stiffness, window space at selected locations is infilled with reinforced concrete to form two exterior diagonal channels, one at each end of the tower. Interior columns are designed to carry gravity loads only, thus allowing flexibility in interior space planning. The architectural and structural design is by Skidmore, Owings and Merrill, Chicago.

### 3.11 BUNDLED TUBE

The underlying principle to achieve a bundled tube response is to connect two or more individual tubes into a single bundle. The main purpose is to decrease shear lag effects.

A bundled tube as shown in Figure 3.40 typically consists of a number of individual tubes interconnected to form a multicell tube, in which the frames in the lateral load direction resist the shears, while the flange frames carry most of the overturning moments. The cells can be stopped at selected heights without diminishing structural integrity. The torsional loads are readily resisted by the closed form of the modules. The greater spacing of the columns and shallower spandrels permitted by the more efficient bundled tube provide for larger window openings than are possible in a single-tube structure.

The shear lag effect present in conventional framed tubes may be greatly reduced by the addition of interior framed web panels across the entire width of the building. When subjected to bending, the high in-plane rigidity of the floor slab forces the interior web frames to deflect along with the exterior web frames. Thus, the shear carried by web frames is proportional to their lateral stiffness. Since the end columns of the interior webs are activated directly by the webs, they are more highly stressed than in a single tube where they are activated indirectly by the flange frames. Consequently, the presence of the interior webs reduces the nonuniformity of column forces caused by shear lag. The vertical stresses are more nearly uniform, and the structural behavior is much closer to that of a braced tube than a framed tube.

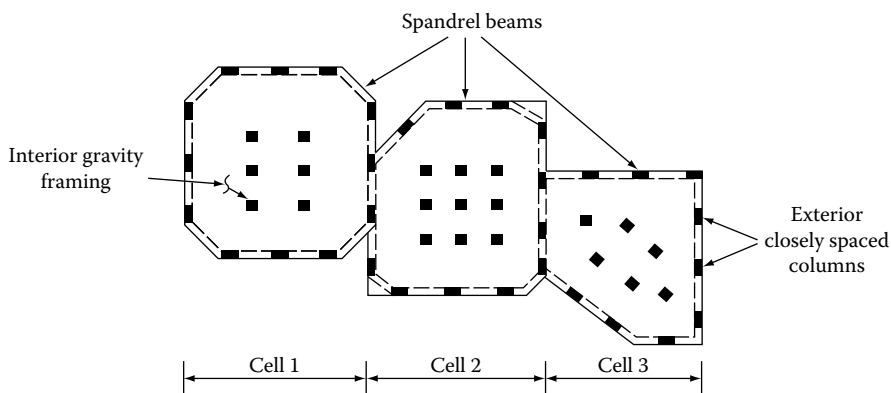
Because a bundled tube is configured from a layout of individual tubes, it is possible to achieve a variety of floor configurations by simply terminating a given tube at any desired level (see Figure 3.41).



**FIGURE 3.39** Example of exterior diagonal tube: Onyiah Center, Chicago, IL.

#### 3.11.1 EXAMPLE OF BUNDLED TUBE: ONE MAGNIFICENT MILE, CHICAGO

The 57-story, “One Magnificent Mile” project in Chicago is an example of the use of bundled tube for achieving both structural efficiency and vertical mixed use occupancies: Commercial and office occupancies occur at the lower floors and apartments at the more desirable upper floors. The



**FIGURE 3.40** Bundled tube: schematic plan.

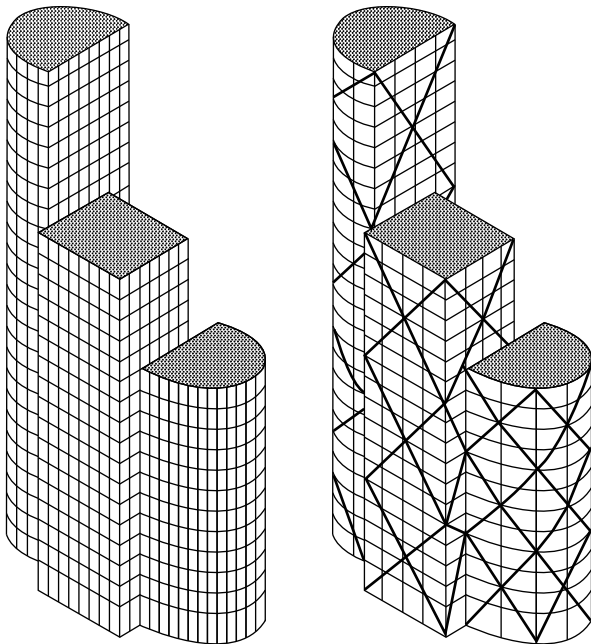


FIGURE 3.41 Schematics of bundled tubes.

building consists of three near-hexagonal reinforced concrete framed tubes with highest tube rising to 57 stories and the others to 49 and 22 stories (see Figure 3.42). The arrangement of tubes was dictated by the desire to maximize view of Lake Michigan. The architectural and structural design is by the Chicago office of Skidmore, Owings and Merrill.

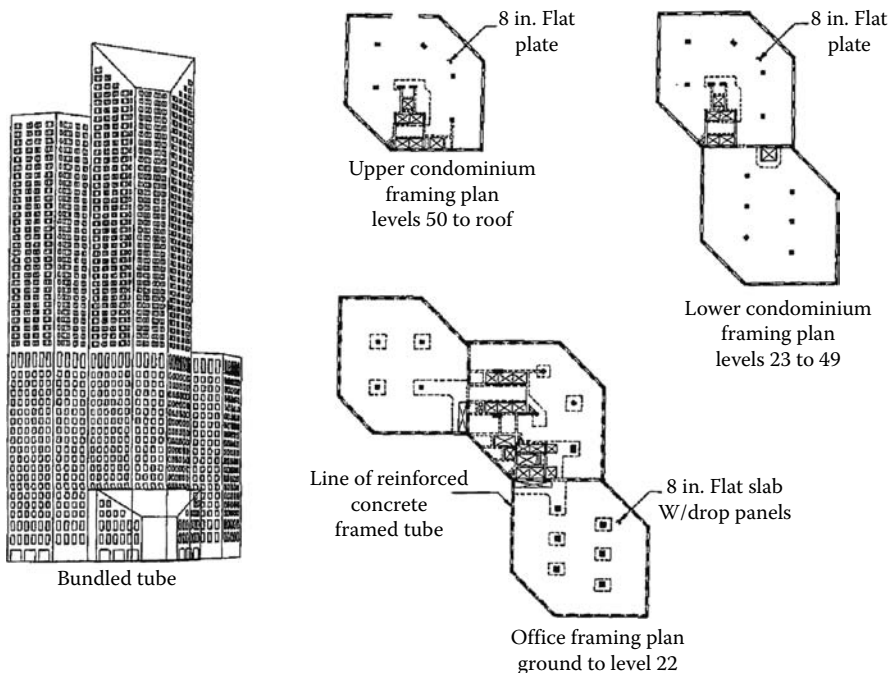
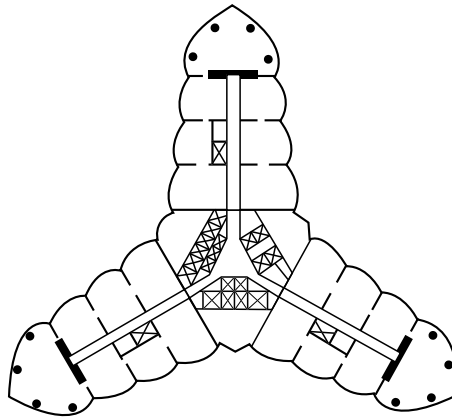


FIGURE 3.42 One Magnificent Mile, Chicago, IL; structural system.



**FIGURE 3.43** Burj Dubai, schematic plan.

### 3.12 SPINAL WALL SYSTEMS

In this relatively new system, well suited for ultra tall residential towers, shear walls are placed along both sides of corridors. These walls, often referred to as “spine” walls, run through the length of the floors to resist lateral loads acting parallel to the corridors. To resist loads in a perpendicular direction, cross walls are placed in an orthogonal direction to the spine walls. Interaction between the cross walls occurs through the interconnecting floor system and/or link beams. To improve the torsional resistance, additional shear walls are placed around the elevator and stair cores.

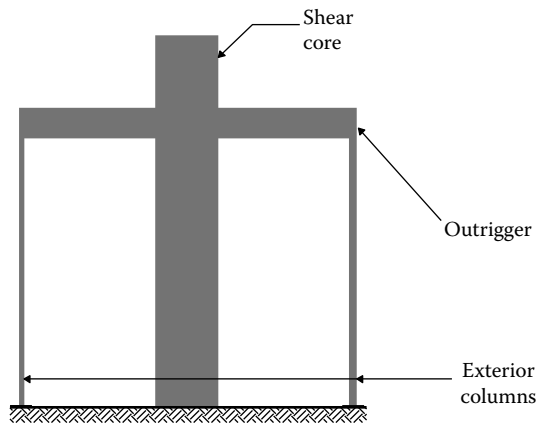
An outstanding example is the Burj Dubai, the “world’s tallest” building in Dubai, UAE (Figure 3.43). The building is “Y”-shaped in plan. Each wing, with its own core and perimeter columns, buttresses the others via a six-sided core or hub. Each tier of the building steps back in a spiral pattern. Further discussion of this building is presented in Chapter 8. The architectural and structural design is by the Chicago office of Skidmore Owings and Merrill.

### 3.13 OUTRIGGER AND BELT WALL SYSTEM

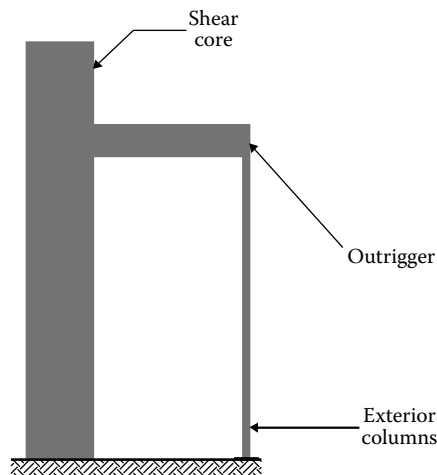
The structural arrangement for this system consists of a main concrete core connected to exterior columns by relatively stiff horizontal members such as a one or two-story deep walls commonly referred to as outriggers. The core may be centrally located with outriggers extending on both sides (Figure 3.44), or it may be located on one side of the building with outriggers extending to the building columns on one side (Figure 3.45).

The basic structural response of the system is quite simple. When subjected to lateral loads, the column-restrained outriggers resist the rotation of the core, causing the lateral deflections and moments in the core to be smaller than if the freestanding core alone resisted the loading. The external moment is now resisted not by bending of the core alone, but also by the axial tension and compression of the exterior columns connected to the outriggers. As a result, the effective depth of the structure for resisting bending is increased when the core flexes as a vertical cantilever, by the development of tension in the windward columns, and by compression in the leeward columns.

In addition to those columns located at the ends of the outriggers, it is usual to also mobilize other peripheral columns to assist in restraining the rotation of outriggers. This is achieved by tying the exterior columns with a one- or two-story deep wall commonly referred to as a “belt wall,” around the building.



**FIGURE 3.44** Outrigger and belt wall system with centrally located core.



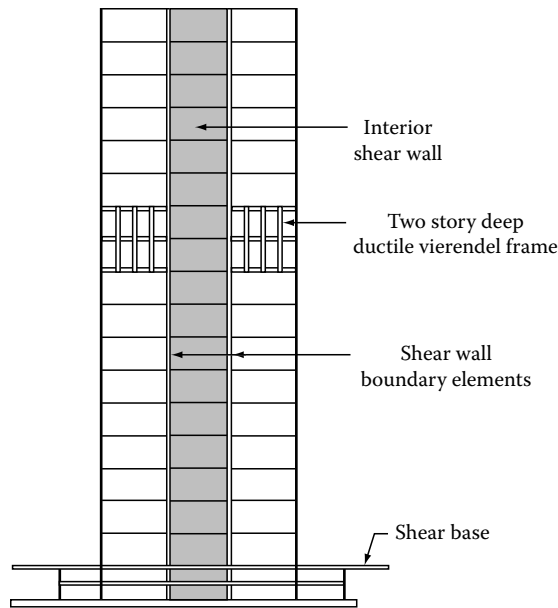
**FIGURE 3.45** Outrigger and belt wall system with an offset core.

To achieve efficiency, the outriggers and belt walls are made one—and often two—stories deep with door-size openings in the outriggers for circulation. It is also possible to use vierendeel frames extending through several floors to act as outriggers, as shown in Figure 3.46. Yet another option is to use girders, such as haunch girders, at each floor (see Figure 3.47). It should be noted that whereas the outrigger is effective in increasing the structure's flexural stiffness, it does not increase resistance to shear, which must be carried only by the core.

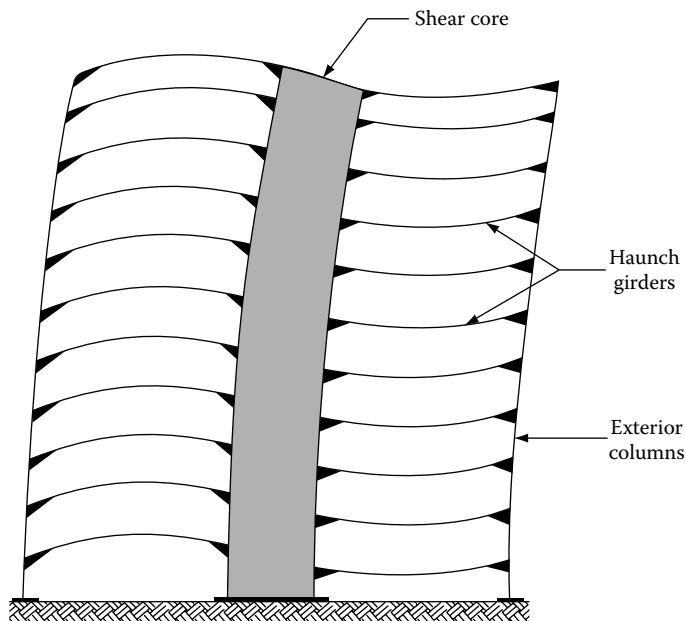
To understand the behavior of an outrigger system, consider a building stiffened by a story-high outrigger wall at top, as shown in Figure 3.48. Because the outrigger is at the top, the system is often referred to as a cap or hat wall system. The tie-down action of the cap wall generates a restoring couple at the building top, resulting in the occurrence of a point of contraflexure some distance from the top. The resulting reversal in curvature reduces the bending moment in the core and hence the building drift.

Although belt walls function as a horizontal fascia stiffener mobilizing other exterior columns, for simplicity in explaining the structural behavior, we will assume that the cumulative effect of the exterior columns may be represented by two equivalent columns, one at each end





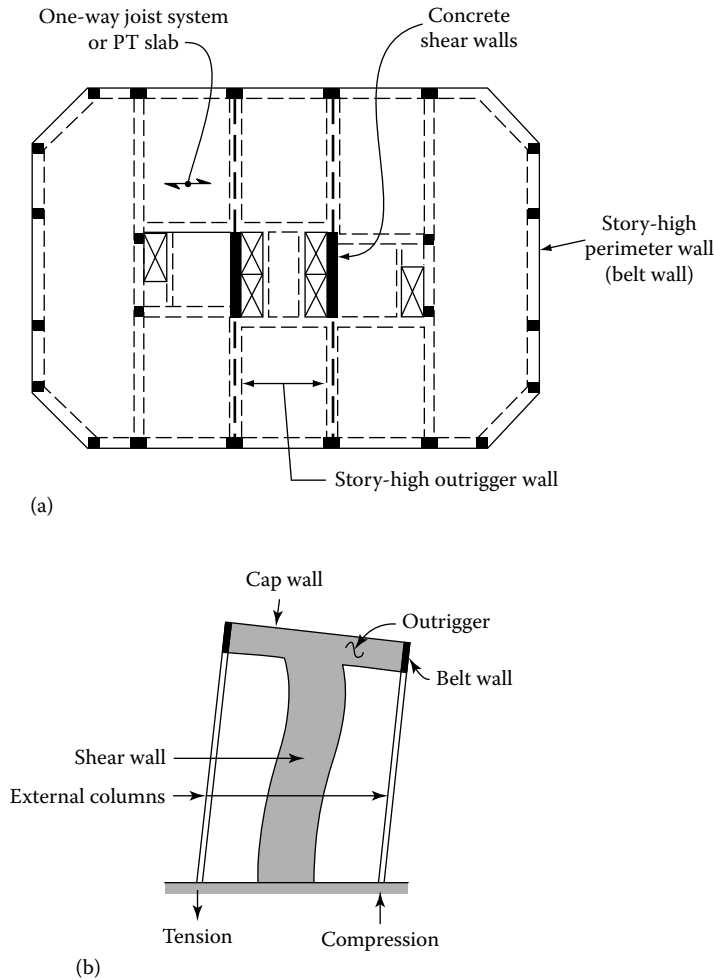
**FIGURE 3.46** Vierendeel frames acting as outrigger and belt wall system.



**FIGURE 3.47** Haunch girders as outriggers.

of the outrigger wall. This idealization is not necessary in developing the theory, but keeps the explanation simple.

The core may be considered as a single-redundant cantilever with the rotation restrained at the top by the stretching and shortening of windward and leeward columns. The resultant of these forces is equivalent to a restoring couple opposing the rotation of the core. Therefore, the cap wall may be conceptualized as a restraining spring located at the top of the shear core. Its rotational stiffness may be defined as the restoring couple due to a unit rotation of the core at the top.



**FIGURE 3.48** Cap wall system: (a) Plan and (b) Schematic section.

Assuming bending rigidity of the cap truss as infinitely rigid, the axial elongation and shortening of columns is simply equal to the rotation of the core multiplied by their respective distances from the center of the core. If the distance of the equivalent columns is  $d/2$  from the center of the core, the axial deformation of the columns is then equal to  $\theta d/2$ , where  $\theta$  is the rotation of the core. Since the equivalent spring stiffness is calculated for unit rotation of the core (i.e.,  $\theta = 1$ ), the axial deformation of the equivalent columns is equal to  $1 \times d/2 = d/2$  units.

The corresponding axial load is given by

$$P = AEd/2L$$

where

$P$  is the axial load in the column

$A$  is the area of column

$E$  is the modulus of elasticity

$d$  is the distance between the exterior columns ( $d/2$  from the center of core to exterior columns)

$L$  is the height of the building

The restoring couple, that is, the rotational stiffness of the cap truss, is given by the axial load in the equivalent columns multiplied by their distance from the center of the core. Using the notion  $K$  for the rotational stiffness, and noting that there are two equivalent columns, each located at a distance  $d/2$  from the core, we get

$$\begin{aligned} K &= P \times d/2 \times 2 \\ &= Pd \end{aligned}$$

Substituting

$$P = \frac{AEd}{2L} \quad \text{we get}$$

$$K = \frac{AE}{L} \frac{d^2}{2}$$

The reduction in the building drift due to the presence of outrigger and belt walls depends on the equivalent stiffness  $K$  of the system and the magnitude of rotation  $\theta$  at the top.

Before proceeding with the calculations for drift reduction, let us ask ourself certain engaging questions related to the interaction of the core with the outriggers located not at the top, but somewhere up the height. How does the location of outriggers influence the building drift and moment in the core? Is the top location the best for achieving maximum efficiency? What if the outrigger is moved toward the bottom, say, to the midheight of the building? Is there an optimum location that reduces the drift to a minimum?

Before answering these rather intriguing questions, it is perhaps instructive to study the behavior of the system with an outrigger located at specific heights of the building, say, at the top, three-quarters height, midheight, and one-quarter height.

### 3.13.1 DEFLECTION CALCULATIONS

#### 3.13.1.1 Case 1: Outrigger Wall at the Top

The rotation compatibility condition at  $z = L$  (see Figure 3.49) can be written as

$$\theta_w - \theta_s = \theta_L \quad (3.a)$$

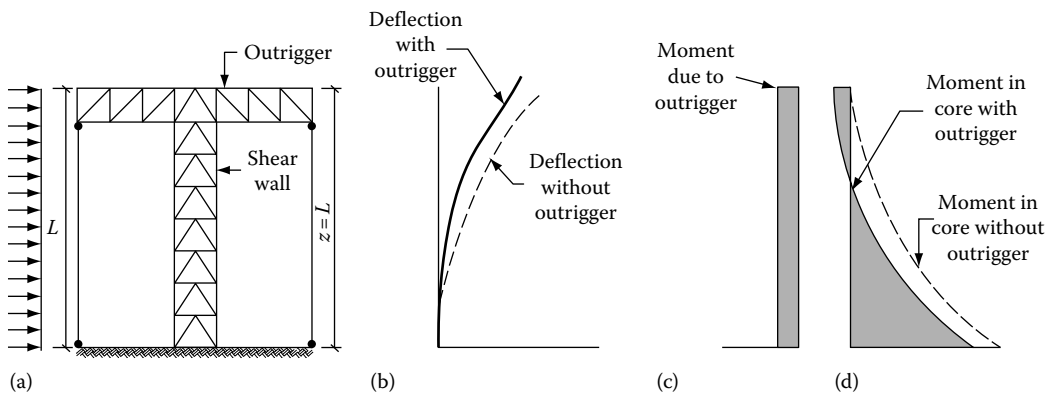


FIGURE 3.49 Outrigger located at top,  $z = L$ .

where

$\theta_w$  is the rotation of the cantilever at  $z = L$  due to a uniform lateral load  $W$  (rad)

$\theta_s$  is the rotation due to spring restraint located at  $z = L$  (rad). The negative sign for  $\theta_s$  in Equation 3.a indicates that the rotation of the cantilever due to the spring stiffness is in a direction opposite to the rotation due to the external load

$\theta_L$  is the final rotation of the cantilever at  $z = L$  (rad)

For a cantilever with uniform moment of inertia  $I$  and modulus of elasticity  $E$  subjected to uniform horizontal load  $W$

$$\theta_w = \frac{WL^3}{6EI}$$

If  $M_1$  and  $K_1$  represent the moment and stiffness of the spring located at  $z = L$ , Equation 3.a can be rewritten as

$$\frac{WL^3}{6EI} - \frac{M_1 L}{EI} = \frac{M_1}{K_1}$$

and

$$M_1 = \frac{WL^3/6EI}{MK_1 + L/EI} \quad (3.b)$$

The resulting deflection  $\Delta_1$  at the building top can be obtained by superposing the deflection of the cantilever due to the external uniform load  $W$ , and the deflection due to the moment induced by the spring, thus

$$\begin{aligned} \Delta_1 &= \Delta_{\text{load}} - \Delta L_{\text{spring}} \\ &= \frac{WL^4}{8EI} - \frac{M_1 L^2}{2EI} \\ &= \frac{L^2}{2EI} \left( \frac{WL^2}{4} - M_1 \right) \end{aligned} \quad (3.1)$$

### 3.13.1.2 Case 2: Outrigger Wall at Quarter-Height from the Top

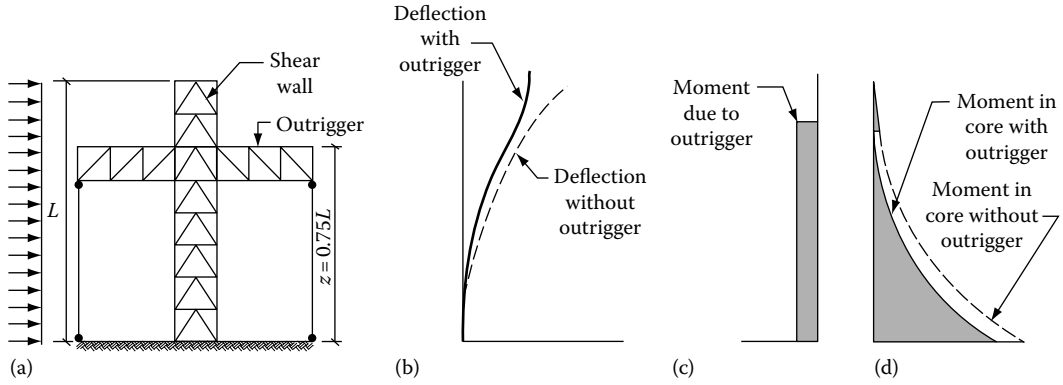
The general expression for lateral deflection  $y$ , at distance  $x$  measured from the top for a cantilever subjected to a uniform lateral load (see Figure 3.50) is given by

$$y = \frac{W}{24EI} (x^4 - 4L^3x + 3L^4)$$

Note that  $x$  is measured from the top and is equal to  $(L - z)$ .

Differentiating the Equation above, with respect to  $x$ , the general expression for the slope of the cantilever is given by

$$\frac{dy}{dx} = \frac{W}{6EI} (x^3 - L^3)$$



**FIGURE 3.50** Outrigger at quarter-height from top,  $z = 0.75L$ .

The slope at the spring location is given by substituting  $z = 3L/4$ , that is,  $x = L/4$  in Equation 3.8. Thus

$$\begin{aligned} \frac{dy}{dx} \left( \text{at } z = \frac{3L}{4} \right) &= \frac{W}{6EI} \left( \frac{L^3}{64} - L^3 \right) \\ &= \frac{WL^3}{6EI} \times \frac{63}{64} \end{aligned}$$

Using the notation  $M_2$  and  $K_2$  to represent the moment and the stiffness of spring at  $z = 3L/4$ , the compatibility equation at location 2 can be written as

$$\frac{WL^3}{6EI} \left( \frac{63}{64} \right) - \frac{M_2}{EI} \left( \frac{3L}{4} \right) = \frac{M_2}{K_2}$$

Noting that  $K_2 = 4K_1/3$ , the expression for  $M_2$  can be written as

$$M_2 = \left( \frac{WL^3/6EI}{1/K_1 + L/EI} \right) \frac{63/64}{3/4} = \left( \frac{WL^3/6EI}{1/K_1 + L/EI} \right) 1.31$$

Noting that the terms in the parentheses represent  $M_1$ , Equation 3.11 can be expressed in terms of  $M_1$ :

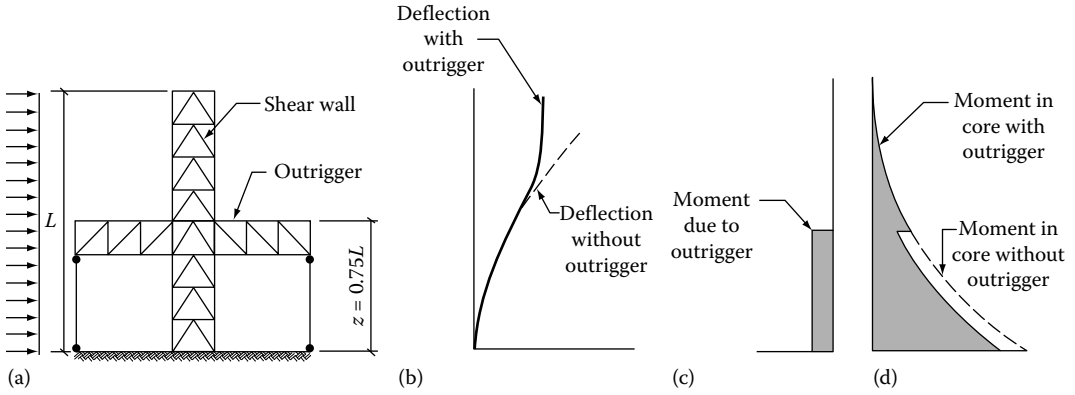
$$M_2 = 1.31M_1$$

The drift is given by the relation

$$\Delta_2 = \frac{WL^4}{8EI} - \frac{M_2 3L}{4EI} \left( L - \frac{3L}{8} \right)$$

or

$$\Delta_2 = \frac{L^2}{2EI} \left( \frac{WL^2}{4} - 1.23M_1 \right) \quad (3.2)$$



**FIGURE 3.51** Outrigger at midheight,  $z = 0.5L$ .

### 3.13.1.3 Case 3: Outrigger Wall at Midheight

The rotation at  $z = L/2$  due to external load  $W$  (see Figure 3.51) can be shown to be equal to  $7WL^3/48EI$ , resulting in the rotation compatibility equation

$$\frac{7WL^3}{48EI} - \frac{M_3L}{2EI} = \frac{M_3}{K_3}$$

where  $M_3$  and  $K_3$  represent the moment and stiffness of the spring at  $z = L/2$ . Noting that  $K_3 = 2K_1$ , the equation for  $M_3$  works out as

$$M_3 = \left( \frac{WL^3/6EI}{1/K_1 + L/EI} \right) \times \frac{7}{4}$$

Since the equation in the parentheses is equal to  $M_1$ ,  $M_3$  can be expressed in terms of  $M_1$ :

$$M_3 = 1.75M_1$$

The drift is given by the equation

$$\Delta_3 = \frac{WL^4}{8EI} - \frac{M_3L}{2EI} \left( L - \frac{L}{4} \right)$$

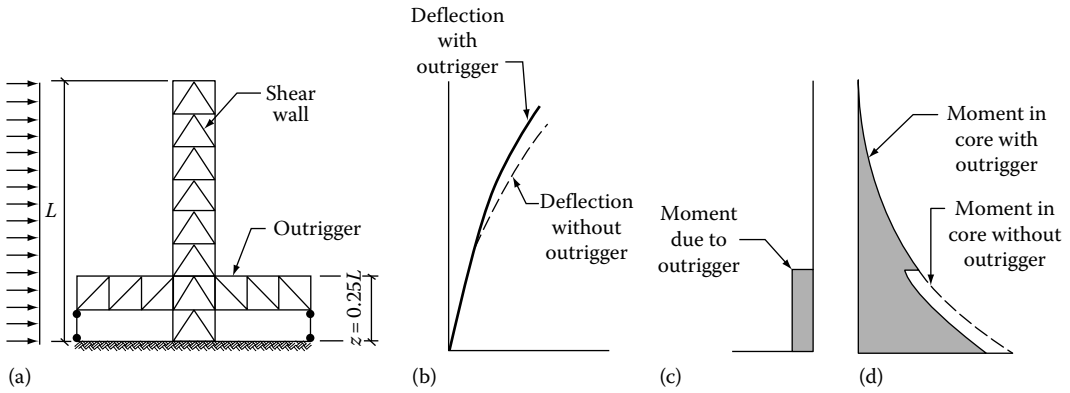
or

$$\Delta_3 = \frac{L^2}{2EI} \left( \frac{WL^2}{4} - 1.31M_1 \right) \quad (3.3)$$

### 3.13.1.4 Case 4: Outrigger Wall at Quarter-Height from the Bottom

The rotation at  $z = L/4$  due to the uniform lateral load (see Figure 3.52) can be shown to be equal to  $WL^3/6EI[(37/64)]$ , giving the rotation compatibility equation

$$\frac{WL^3}{6EI} \left( \frac{37}{64} \right) - \frac{M_4L}{4EI} = \frac{M_4}{K_4}$$



**FIGURE 3.52** Outrigger at quarter-height from bottom,  $z = 0.25L$ .

where  $M_4$  and  $K_4$  represent the moment and the stiffness of the spring at  $z = L/4$ . Noting that  $K_4 = 4K_1$ ,  $M_4$  in Equation 3.19 can be expressed in terms of  $M_1$ :

$$M_4 = 2.3M_1$$

The drift for this case is given by the expression

$$\Delta_4 = \frac{WL^4}{8EI} - \frac{M_4L}{4EI} \left( L - \frac{L}{8} \right)$$

or

$$\Delta_4 = \frac{L^2}{2EI} \left( \frac{WL^2}{4} - M_1 \right) \quad (3.4)$$

Equations 3.1 through 3.4 give the building drift for the four selected locations of the belt and outrigger walls. All these equations are in terms of  $M_1$  (see Equation 3.b).

Thus, given the following parameters:

1. Building height  $L$ , and distance  $d$  between the perimeter columns
2. Magnitude of uniformly distribute lateral load  $W$
3.  $A$ ,  $E$ , and  $I$  of the equivalent perimeter columns

we can determine the reduced lateral deflection for the four selected locations of belt and outrigger system.

### 3.13.2 OPTIMUM LOCATION OF A SINGLE OUTRIGGER WALL

The preceding analysis has indicated that the beneficial action of outrigger is a function of two distinct characteristics: (1) the stiffness of the equivalent spring; and (2) the magnitude of the rotation of the cantilever at the spring location due to lateral loads. The spring stiffness, which is a function of column length below the outrigger location, varies inversely as the distance of the outrigger from the base. For example, the stiffness is at a minimum when the outrigger is located at the top and a maximum when at the bottom. On the other hand, the rotation,  $\theta$ , of the free cantilever subjected to a uniformly distributed horizontal load varies parabolically with a maximum value at the top

to zero at the bottom. Therefore, from the point of view of spring stiffness, it is desirable to locate the outrigger at the bottom, whereas from consideration of its rotation, the converse is true. It must therefore be obvious that the optimum location is somewhere in between.

To search for the optimum location of a single outrigger, we start with the following assumptions:

1. The building is prismatic and vertically is uniform; that is, the perimeter columns have a constant area and the core has a constant moment of inertia for the full height.
2. The outrigger and the belt walls are flexurally rigid.
3. The lateral resistance is provided only by the bending resistance of the core and the tie-down action of the exterior columns.
4. The core is rigidly fixed at the base.
5. The rotation of the core due to its shear deformation is negligible.
6. The lateral load is constant for the full height.
7. The exterior columns are pin-connected at the base.

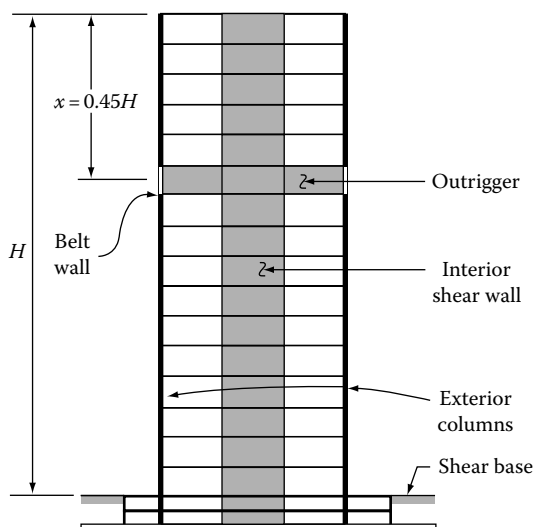
Consider Figure 3.53, which shows schematics of a single outrigger located at a distance  $x$  from the building top. To evaluate the optimum location, first the restoring moment  $M_x$  of the outrigger located at  $x$  is evaluated. Next, an algebraic equation for the deflection of the core at the top due to  $M_x$  is derived. Differentiating this equation and equating a zero results in a third-degree polynomial, the solution of which yields the outrigger optimum location corresponding to the minimum deflection of the building at top due to external load. The details are as follows.

The rotation  $\theta$  of the cantilever at a distance  $x$  from the top, due to uniformly distributed load  $w$ , is given by the relation

$$\theta = \frac{W}{EI}(x^3 - L^3)$$

The rotation at the top due to the restoring couple  $M_x$  is given by the relation

$$\theta = \frac{M_x}{EI}(L - x)$$



**FIGURE 3.53** Outrigger at distance  $x$  from top.



The rotation compatibility relation at  $x$  is given by

$$\frac{W}{6EI}(x^3 - L^3) - \frac{M_x}{EI}(L - x) = \frac{M_x}{K_x}$$

where

$W$  is the intensity of lateral load per unit height of the building

$M_x$  is the resorting moment due to outrigger restraint

$K_x$  is the spring stiffness at  $x$  equal to  $AE(L - x) \times (d^2/2)$

$E$  is the modulus of elasticity of the core

$I$  is the moment of inertia of the core

$A$  is the area of the perimeter columns

$L$  is the height of the building

$x$  is the location of truss measured from the top

$d$  is the distance out-to-out of perimeter columns

Next, obtain the deflection at the top due to  $M_x$ :

$$Y_M = \frac{M_x(L - x)(L + x)}{2EI}$$

From our definition, the optimum location of the outrigger is that location for which the deflection  $Y_M$  is a maximum. This is obtained by substituting for  $M_x$  into the equation above and differentiating with respect to  $x$  and equating to zero. Thus,  $dy/dx$  of

$$\left[ \frac{W(x^3 - L^3)(L + x)}{12(EI)^2 (1/AE + 1/EI)} \right] = 0$$

Simplifying this equation, we get a cubic equation in  $x$ :

$$4x^3 + 3x^2L - L^3 = 0$$

This cubic equation has a single positive root,  $x = 0.445L$ . The solution is by trial-and-error.

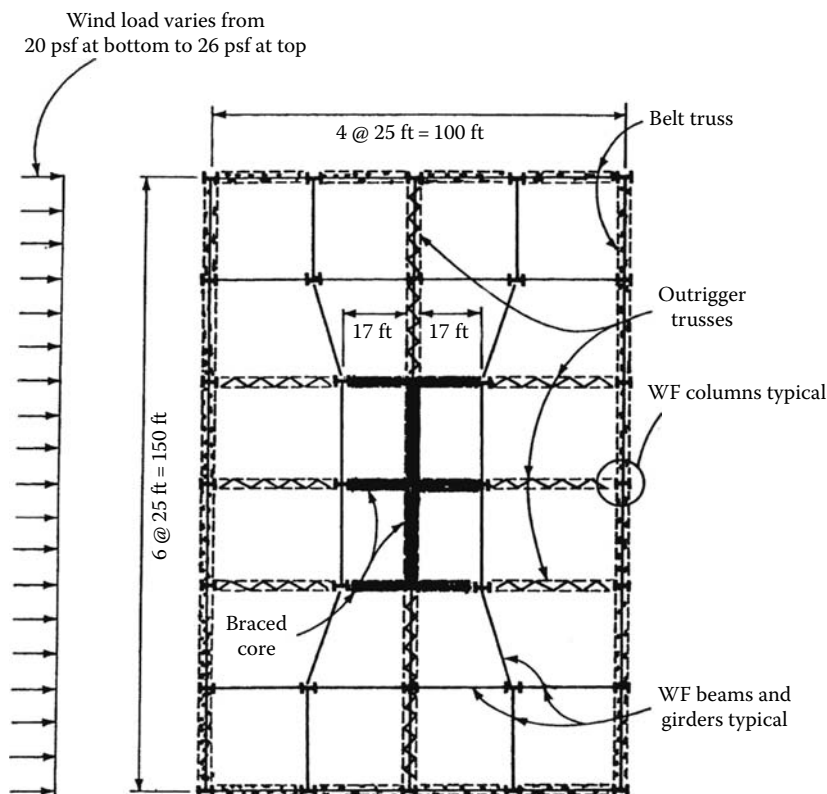
Therefore, to minimize drift, the outrigger must be located at a distance  $x = 0.455L$  from the top or, say, approximately at midheight of the building.

In the preceding discussion, several assumptions were necessary to simplify the problem for hand calculations. However, in a practical building, many of these assumptions are rarely satisfied.

For example:

- The lateral load does not remain constant up the building height. It varies in a trapezoidal or triangular manner, the former representative of wind loads and the latter, seismic loads.
- The cross-sectional areas of both the exterior columns and interior shear walls typically reduce up the building height. A linear variation is perhaps more representative of a practical building column, particularly so for a tall building of say, 40-plus stories.
- As the areas of core columns decrease up the height, so does the moment of inertia of the core. Therefore, a linear variation of the moment of inertia of the core, up the height is more appropriate.

Incorporating the aforementioned modifications aligns the analytical model closer to a practical structure, but renders the hand calculations all but impossible. Therefore, a computer-assisted



**FIGURE 3.54** Schematic plan of a steel building with outriggers and belt trusses at a single level.

analysis has been performed on a representative 46-story steel building using the modified assumptions previously mentioned. A schematic plan of the building, its concrete version, and an elevation of the idealized structural system, subject to lateral loading are shown in Figures 3.54 through 3.56. The lateral deflections at the building top are shown in a graphical format in Figure 3.57 for various outrigger locations.

The deflections shown in a nondimensional format in Figure 3.57 are relative to that of the core without the outrigger. Thus, the vertical ordinate with a value of unity at the extreme right of Figure 3.57 is the deflection of the building without the restraining effects of the outrigger. The deflections including the effect of the outriggers are shown in curve designed "S." This curve is obtained by successively varying the outrigger location starting at the very top and progressively lowering its location in single-story increments, down through the building height.

It is seen that lowering the outrigger down from its top location decreases the building drift progressively until the outrigger reaches level 26. Moving it either above or below this "optimum location" only reduces its efficiency. Observe that this level is at distance  $(46 - 26/46)L = 0.435L$  from the top, very close to the optimum location of  $x = 0.455L$  for the building with uniform characteristics. Furthermore, it can be seen from Figure 3.57 that the efficiency of the outrigger placed at midheight; that is, at level 23, is very close to that when it is at the optimum location. Therefore, as a rule of thumb, the optimum location for a single outrigger may be considered at midheight.

Observe that when the outrigger is at the top, the building drift is reduced to nearly half the deflection of the unrestrained core. Thus, for example, if the drift of the unrestrained core is, say, 20 in. at the top, the corresponding deflection with an outrigger at level 46 is reduced to  $0.48 \times 20 = 9.6$  in. A rather impressive reduction indeed, but what is more important is that the deflection continues to reduce as the outrigger is lowered from level 46 downward. The deflection reaches a

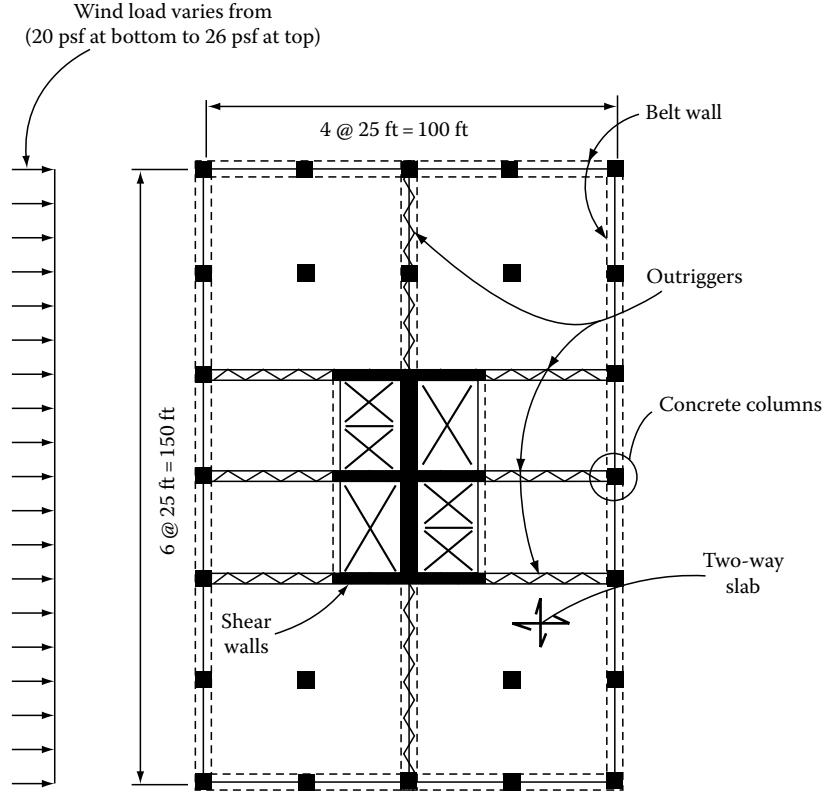


FIGURE 3.55 Schematic plan of a concrete building with outriggers and belt walls at a single level.

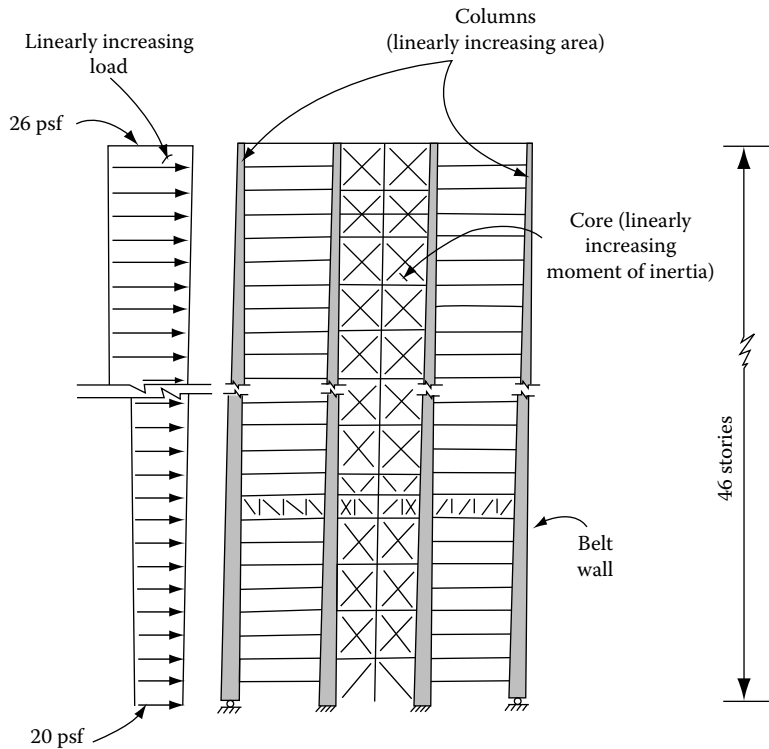
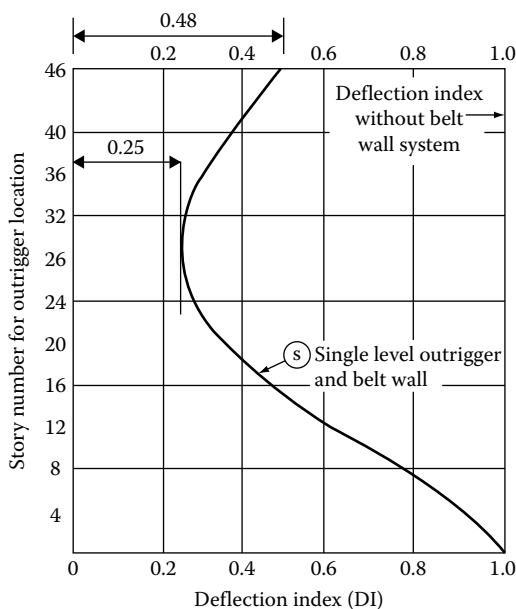


FIGURE 3.56 Schematic section showing outriggers and belt walls at a single level.



**FIGURE 3.57** Deflection index versus outrigger and belt wall location.

Note:  $DI = \frac{\text{Deflection without outrigger}}{\text{Deflection with outrigger}}$ .

minimum value of  $0.25 \times 20 = 5$  in. as shown in Figure 3.57 when the outrigger is placed at the optimum location, level 26. Further lowering of the outrigger will not reduce the drift, but increases it. Its beneficial effect vanishes to nearly nothing when placed very close to the bottom of the building, say, at level 2 of the example problem.

Using the results of the example problem, the following conclusions can be drawn:

- Given a choice, the best location for a single outrigger is at about midheight of the building.
- An outrigger placed at top, acting as a cap or hat wall, is about 50% less efficient than that placed at midheight. However, in many practical situations, it may be more permissible to locate the outrigger at the building top. Therefore, although not as efficient as when at midheight, the benefits of a cap truss are nevertheless quite impressive, resulting in up to a 50% reduction in building drift.

### 3.13.3 OPTIMUM LOCATIONS OF TWO OUTRIGGER WALLS

In the preceding conceptual analyses, only one compatibility equation was necessary because the one-outrigger structure is once-redundant. On the other hand, a two-outrigger structure is twice-redundant, requiring a solution of two compatibility equations. To seek a solution to the problem, we proceed as before assuming the sectional areas of the exterior columns and the moment of inertia of the core decrease linearly up the height. A trapezoidal distribution is assumed, as before, for the lateral load. Schematics of conceptual analytical model and behavior of the structural system are shown in Figures 3.58 through 3.61.

The method of analysis for calculating the deflections at the top is similar to that used for the single outrigger. The moments at the outrigger locations are chosen as the unknown arbitrary constants  $M_1$  and  $M_2$ , see Figure 3.60. The structure is then rendered statically determinate by removing the rotational restraints at the outrigger locations. Next, the compatibility equations for the rotations at the truss locations are set up and solved simultaneously to obtain the values to  $M_1$  and  $M_2$ . The final deflection at the top is obtained by a superposition of the deflection due

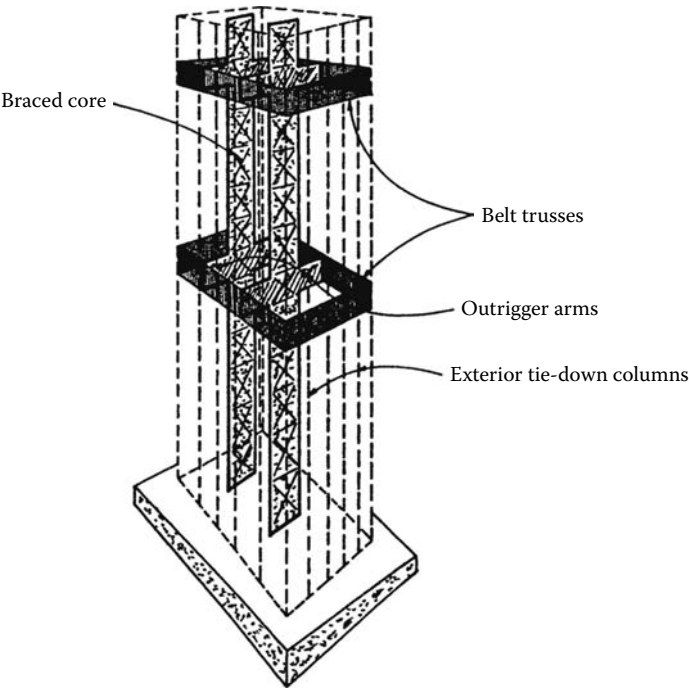


FIGURE 3.58 Structural schematics; building with outrigger and belt walls at two locations.

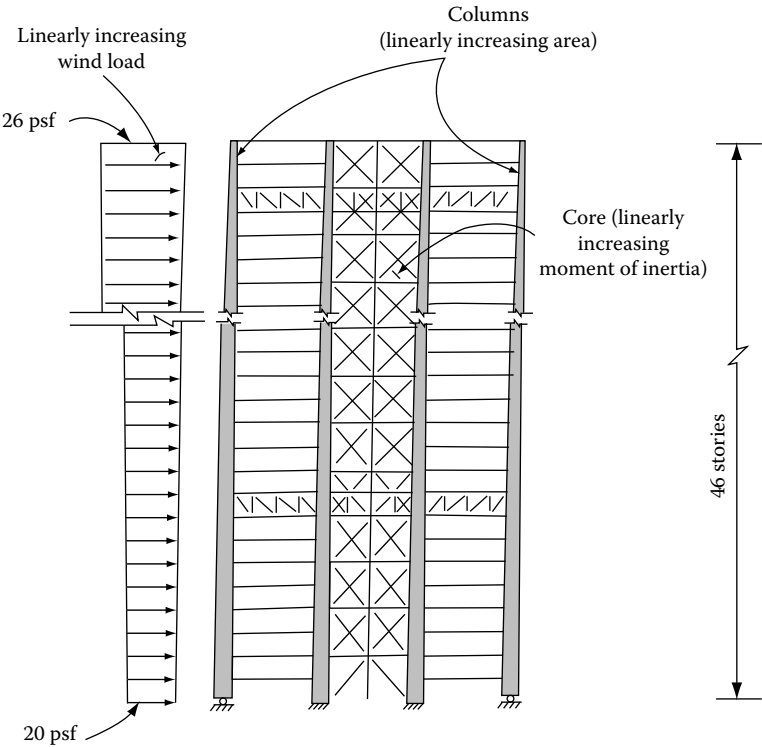
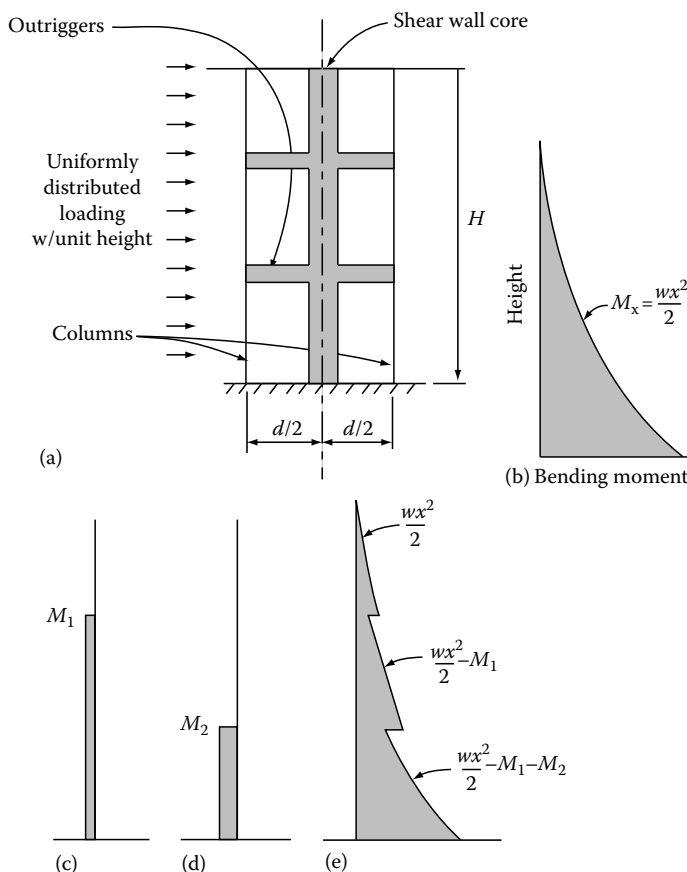


FIGURE 3.59 Analytical model of a building with outriggers and belt walls at two locations.



**FIGURE 3.60** Method of analysis for two outrigger system: (a) Two-outrigger structure, (b) external moment diagram, (c)  $M_1$  diagram, (d)  $M_2$  diagram, and (e) core resultant moment diagram.

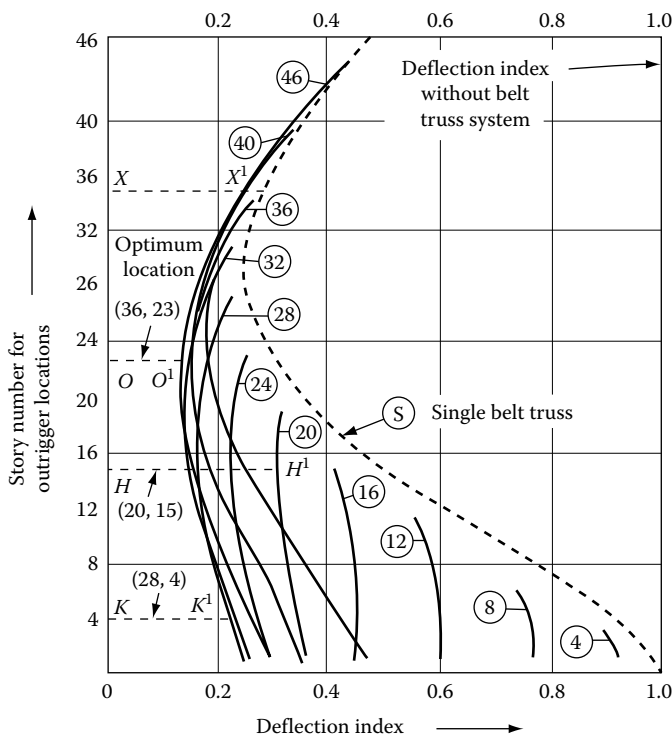
to the external load and a counteracting deflection due to the moments  $M_1$  and  $M_2$ . The resulting deflections are summarized in Figure 3.61.

The building deflection at top for a given location of the two outriggers is presented for three conditions by assuming that the lateral loads are resisted by (1) core alone; (2) core acting together with a single outrigger; and (3) core acting in conjunction with two outriggers.

As before, the vertical ordinate shown with a value of unity at the extreme right of Figure 3.61 is the deflection index at the top derived by neglecting the restraining effect of the outriggers. The resistance is provided by the cantilever action of the braced core alone. Curve S represents the top deflection of the core restrained by a single outrigger located anywhere up the height of the structure.

The curves designated as 4, 8, ..., 46 represent the deflections at the top for two outriggers located anywhere up the height of the structure. To plot each curve, the location of the upper outrigger was considered fixed in relation to the building height, while the location of the lower outrigger was moved in single-story increments, starting from the floor immediately below the top outrigger.

The number designations of the curves represent the floor number at which the upper outrigger is located. The second outrigger location is shown by story levels on the vertical axis. The horizontal distance between the curves and the vertical axis is the relative building drift for the particular combination of outrigger locations given by the curve designation and the story level. For example, let us assume that the relative deflection at the top is desired for a combination (20, 15), the numbers 20 and 15 representing the floors at which the upper and lower outriggers are located. To find the deflection index for this particular combination, the procedure is to select the curve with the



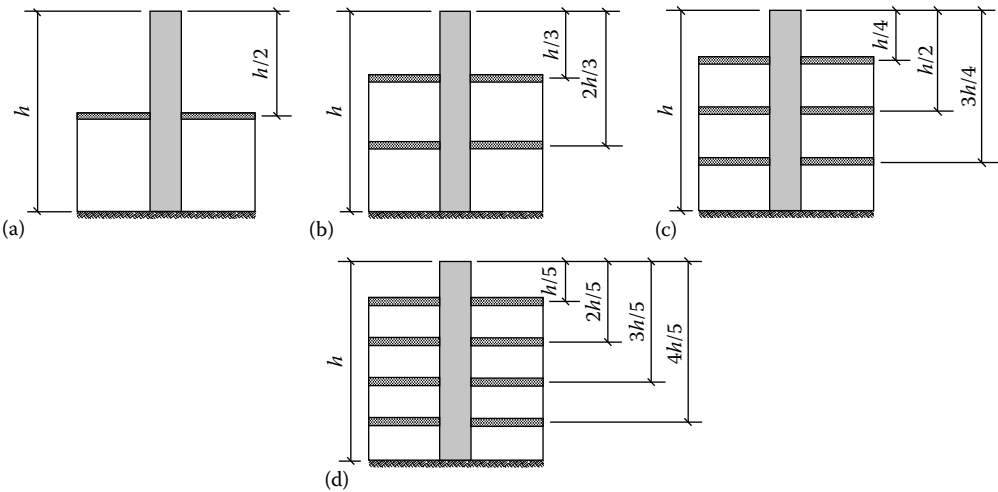
**FIGURE 3.61** Deflection index versus belt wall and outrigger locations.

designation 20, go down the vertical axis to level 15, and draw a horizontal line from this level to curve 20. The required relative top deflection is the horizontal distance between level 15 and curve 20 (distance  $HH^1$  in Figure 3.60). Similarly, the length  $KK^1$  gives the relative deflection at the top for the combination (28, 4). It is seen from Figure 3.60 that the relative location of the outriggers has a significant effect on controlling the drift. Furthermore, it is evident that a deflection very nearly equal to the minimum can be achieved by placing the trusses at levels other than at their optimum locations. For the example building, a relative deflection of 0.15, which differs negligibly from the optimum value of 0.13, is achieved by placing the outriggers at (40, 23), (32, 33), etc.

### 3.13.4 RECOMMENDATIONS FOR OPTIMUM LOCATIONS

Based on conceptual study presented thus far, the following recommendations are made for optimum locations for outriggers. As stated previously the primary purpose to minimize the lateral drift.

- The optimum location for a single outrigger is, perhaps unexpectedly, not at the top. The reduction in the drift with the outriggers located at top is about 50%, as compared to a maximum of 75% achievable by placing it at approximately midheight. However, since other architectural requirements take precedence in a structural layout, the benefits of placing a truss at the top are still worth pursuing.
- A two-outrigger structure appears to offer more options in the placements of outriggers. Reductions in building deflections close to the optimum results may be achieved with outriggers placed at levels entirely different from the optimum locations. Thus, the engineer and architect have some leeway in choosing the outrigger locations. However, as a rule of thumb, the optimum location for a two-outrigger structure is at one-third and two-third heights. And for a three-rigger system, they should be at the one-quarter, one-half, and three-quarter heights, and so on. Therefore, for the optimum performance on an outrigger



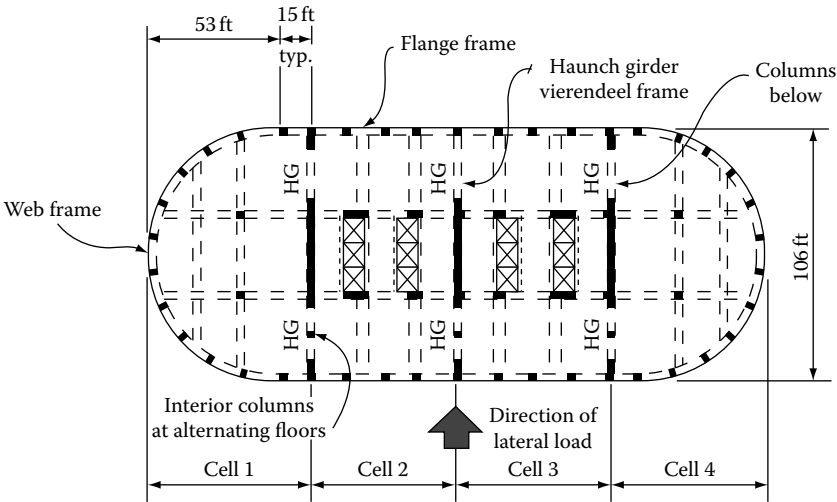
**FIGURE 3.62** Optimum location of outriggers, (a) single outrigger, (b) two outriggers, (c) three outriggers, and (d) four outriggers.

structure, the outriggers should be placed at  $(1/n + 1)$ ,  $(2/n + 1)$ ,  $(3/n + 1)$ ,  $(4/n + 1)$ , ...,  $(n/n + 1)$  height locations. For example, in an 80-story building with four outriggers (i.e.,  $n = 4$ ), the optimum locations are at the 16th, 32nd, 48th, and 64th levels. A summary of the recommendations is shown in Figure 3.62.

Although the analysis presented thus far is for a steel building, the author believes that the conclusions are applicable equally to reinforced concrete buildings.

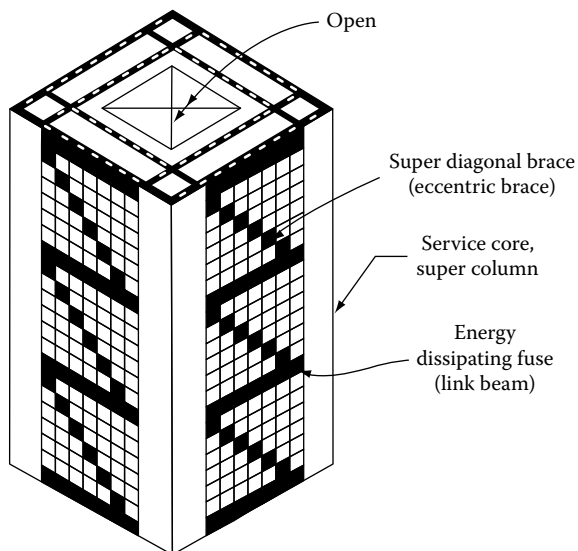
**3.14 MISCELLANEOUS SYSTEMS**

Figure 3.62 shows a building with a high plan aspect ratio. Buildings of this type tend to be inefficient in resisting lateral loads because of shear lag effects. However, by introducing a limited number of interior columns (three at every other floor in the example building shown in Figure 3.63),



**FIGURE 3.63** Cellular tube with interior vierendeel frames.





**FIGURE 3.64** Structural concept for supertall buildings.

it is possible to reduce the effect of shear lag, and thus increase efficiency for resisting lateral loads. Using a two-story tall haunch girder vierendeel frame at every other floor is one such method. The vierendeel frame effectively ties the building exterior to the interior shear walls, thus mobilizing the entire building exterior in resisting the overturning moments.

Shown in Figure 3.64 is a system suitable for supertall buildings—taller than, say, 80 stories. It consists of a service core located at each corner of the building interconnected by a super diagonal in-fill walls. The service core at each corner acts as a giant column carrying a majority of the gravity load and overturning moments. The eccentricity between the super diagonals and exterior columns is a deliberate design strategy to enhance the ductility of the lateral bracing system for buildings assigned to high SDC. The ductile response of the links is anticipated to help in dissipating seismic energy, thus assuring the gravity-carrying capacity of the building during and after a large earthquake.

---

# 4 Wind Loads

Wind pressure on a building surface depends primarily on its velocity, the shape and surface structure of the building, the protection from wind offered by surrounding natural terrain or man-made structures, and to a smaller degree, the density of air which decreases with altitude and temperature. All other factors remaining the same, the pressure due to wind is proportionate to the square of the velocity:

$$p = 0.00256V^2 \quad (4.1)$$

where

$p$  is the pressure, in psf

$V$  is the velocity of wind, in miles per second

During storms, velocities for a 3 s gust wind may reach values up to or greater than 150 mph, which corresponds to dynamic pressure of about 90 psf at a height of 500 ft (153 m). Pressure as high as this is exceptional, and, in general, values of 40–50 psf are common.

In an engineered structure, wind loads have long been a factor in the design of lateral force resisting system, with added significance as the height of the building increased. For many decades, the cladding systems of high-rise buildings, particularly around corners of buildings, have been scrutinized for the effects of wind on building enclosure. Glass and curtain wall systems are regularly developed and tested to resist cladding pressures and suctions induced by the postulated wind event.

As wind hits the structure and flows around it, several effects are possible, as illustrated in Figure 4.1. Pressure on the windward face and suction on the leeward face creates *drag forces*. Analogous to flow around an airplane wing, unsymmetrical flow around the structure can create *lift forces*. Air turbulence around the leeward corners and edges can create *vortices*, which are high-velocity air currents that create circular updrafts and suction streams adjacent to the building. Periodic shedding of vortices causes the building to oscillate in a direction transverse to the direction of the wind and may result in unacceptable accelerations at the upper floors of tall buildings. The effects of downdrafts must also be considered: Downdrafts have been known to completely strip trees in plaza areas and to buffet pedestrians dangerously. Some tall buildings that extend into high wind velocity regions have been known to sway excessively in strong winds. High suction forces have blown off improperly anchored lightweight roofs.

## 4.1 DESIGN CONSIDERATIONS

In designing for wind, a building cannot be considered independent of its surroundings because configuration of nearby buildings and natural terrain has substantial influence on the design loads, and hence on the sway response of the building. Sway is defined as the horizontal displacement at the top of a building. The sway at the top of a tall building caused by wind may not be seen by a passerby, but may be of concern to those experiencing wind-motion problems at the top floors. There is scant evidence that winds, except those due to a tornado or hurricane, have caused major structural damage to buildings. Nevertheless, it is prudent to investigate wind-related behavior of modern

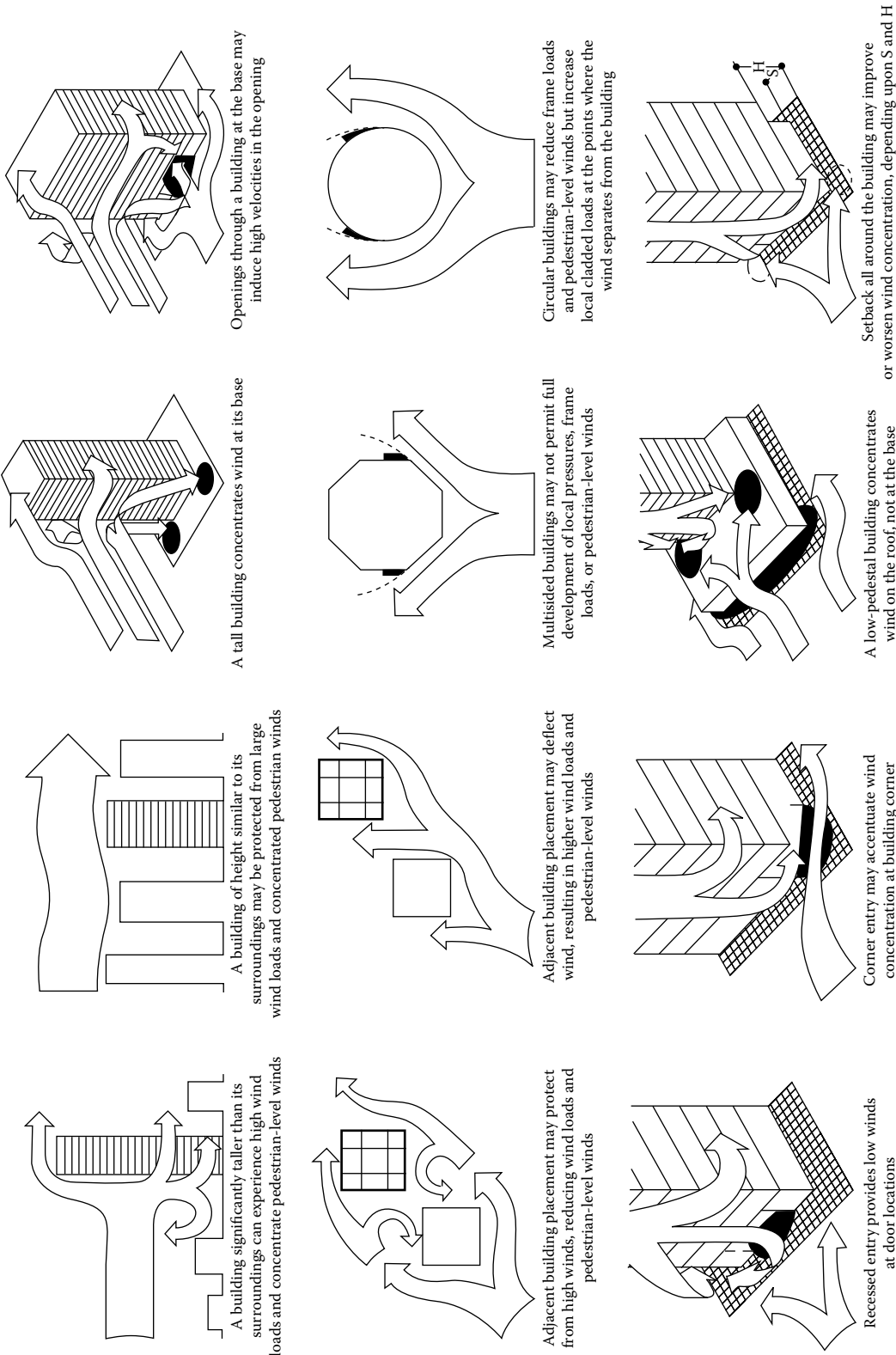


FIGURE 4.1 Wind flow around buildings.

skyscrapers, typically built using lightweight curtain walls, dry partitions, and high-strength materials, because they are more prone to wind-motion problems than the early skyscrapers, which had the weight advantage of heavy masonry partitions, stone facades, and massive structural members.

To be sure, all buildings sway during windstorms, but the motion in old tall buildings with heavy full-height partitions has usually been imperceptible and, therefore, has not been a cause for concern. Structural innovations coupled with lightweight construction have reduced the stiffness, mass, and damping characteristics of modern buildings. In these buildings, objects may vibrate, doors and chandeliers may swing, pictures may lean, and books may fall off shelves. Additionally if the building has a twisting action, its occupants may get an illusory sense that the world outside is moving, creating symptoms of vertigo and disorientation. In more violent storms, windows may break, creating safety problems for pedestrians below. Sometimes, strange and frightening noises may be heard by occupants as the wind shakes elevators, strains floors and walls, and whistles around the building sides.

It is generally agreed that acceleration response that includes the effects of torsion at the top floors of a tall building, is the best standard for evaluation of motion perception. A commonly used criterion is to limit accelerations of the building's upper floors to no more than 2% of gravity (20 milli-g) for a 10 year wind. Other commonly applied guidelines include those published by the Council on Tall Buildings and Urban Habitat (CTBUH), and the International Organization for Standardization (ISO 6899-1984).

## 4.2 NATURAL WIND

Wind is not constant either with height or time, is not uniform over the windward side of the building, and does not always cause positive pressure. In fact, wind is a complicated phenomenon; it is air in turbulent flow, which means that motion of individual particles is so erratic that in studying wind, one ought to be concerned with statistical distributions of speeds and directions rather than with simple averages.

*Wind* is the term used for air in motion and is usually applied to the natural horizontal motion of the atmosphere. Motion in a vertical or nearly vertical direction is called a *current*. Movement of air near the surface of the earth is three-dimensional, with horizontal motion much greater than the vertical motion. Vertical air motion is of importance in meteorology but is of less importance near the ground surface. On the other hand, the horizontal motion of air, particularly the gradual retardation of wind speed and high turbulence that occur near the ground surface, are of importance in building engineering. In urban areas, this zone of wind turbulence often referred to as *surface boundary layer*, extends to a height of approximately one-quarter of a mile aboveground. Above this layer, the horizontal airflow is no longer influenced by the retarding effect of the ground surface. The wind speed at this height is called *gradient wind speed*, and it is precisely within this boundary layer where human construction activity occurs. Therefore, how wind effects are felt within this zone is of concern in building design.

Although one cannot see wind, we know by experience, its flow is quite random and turbulent. Imagine taking a walk on a windy day. You will no doubt experience a constant flow of wind, but intermittently you may also experience sudden gusts of rushing wind. This sudden variation in wind speed, called gustiness or *turbulence*, is an important factor in determining dynamic response of tall buildings.

Air flowing over the earth's surface is slowed down and made turbulent by the roughness of the surface. As the distance from the surface increases, these friction effects are felt less and less until a height is reached where the influence of the surface roughness is negligible. This height, as mentioned earlier, is referred to as the *gradient height*, and the layer of air below this, where the wind is turbulent and its speed increases with height, is referred to as the *boundary layer*. The gradient height or depth of the earth's boundary layer is determined largely by the terrain roughness and

typically varies from 900 ft (270 m) over open country to about 1660 ft (500 m) over built-up urban areas.

The wind-tunnel testing provides information regarding the response of buildings subject to differing wind speed and direction. In order to make the most rational use of this aerodynamic information, it is necessary to synthesize test results with the actual wind climate characteristics at the site.

#### 4.2.1 TYPES OF WIND

Winds that are of interest in the design of buildings can be classified into three major types: prevailing winds, seasonal winds, and local winds.

1. *Prevailing winds*: Surface air moving toward the low-pressure equatorial belt is called prevailing wind or trade wind. In the northern hemisphere, the northerly wind blowing toward the equator is deflected by the rotation of the earth to a northeasterly direction, and hence commonly known as the northeast trade wind. The corresponding wind in the southern hemisphere is the southeast trade wind.
2. *Seasonal winds*: Air over the land is warmer in summer and colder in winter than the air adjacent to oceans during the same seasons. During summer, the continents become seats of low pressure, with wind blowing in from the colder oceans. In winter, the continents experience high pressure with winds directed toward the warmer oceans. These movements of air caused by variations in pressure difference are called seasonal winds. The monsoons of the China Sea and the Indian Ocean are examples of these movements of air.
3. *Local winds*: These are associated with the regional weather patterns and include whirlwinds and thunderstorms. They are caused by daily changes in temperature and pressure, generating local effects in winds. The daily variations in temperature and pressure may occur over irregular terrain, causing valley and mountain breezes.

All three types of wind are of importance in building design. However, for the purpose of determining wind loads, the characteristics of prevailing and seasonal winds are grouped together, whereas those of local winds are studied separately. This grouping is to distinguish between the widely differing scales of fluctuations of the winds; prevailing and seasonal winds fluctuate over a period of several months, whereas local winds may vary every few seconds. The variations in the mean velocity of prevailing and seasonal winds are referred to as *fluctuations* whereas the variations in local winds occurring over a very short period of time are referred to as *gusts*.

Flow of wind unlike that of other fluids, is not steady and fluctuates in a random fashion. Because of this, wind loads for building design are studied statistically.

#### 4.3 CHARACTERISTICS OF WIND

Wind flow is complex because numerous flow situations arise from the interaction of wind with structures. However, in wind engineering, simplifications are made to arrive at the design wind loads by distinguishing the following characteristics:

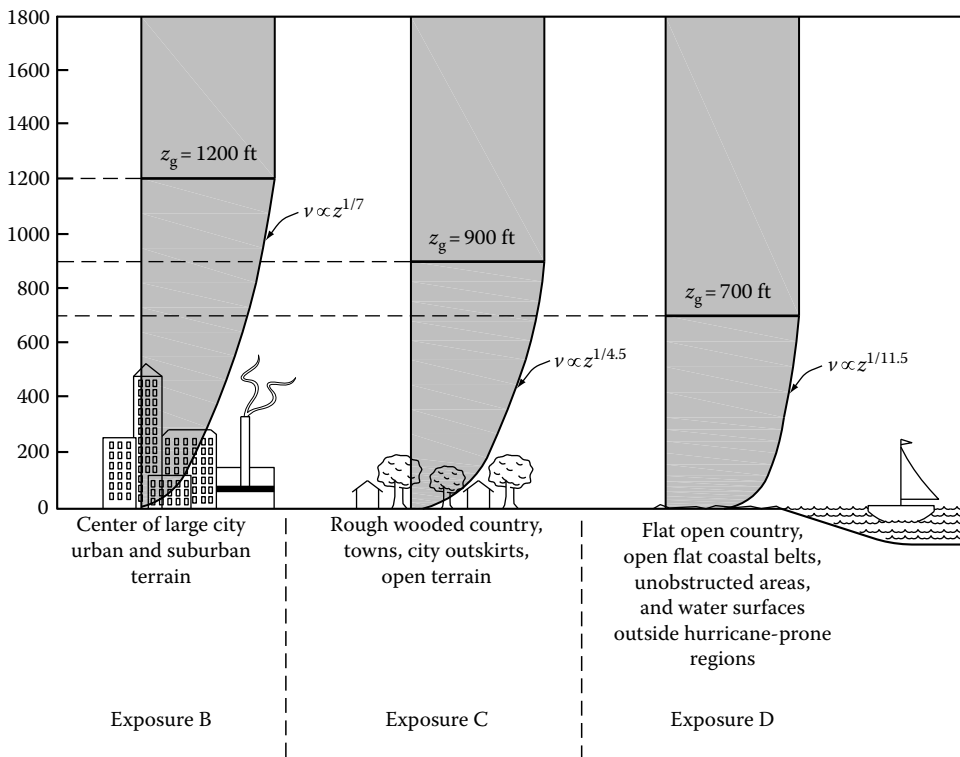
- Variation of wind velocity with height (velocity profile)
- Wind turbulence
- Statistical probability
- Vortex shedding
- Dynamic nature of wind–structure interaction

### 4.3.1 VARIATION OF WIND VELOCITY WITH HEIGHT (VELOCITY PROFILE)

The roughness of the earth's surface which causes drag, converts some of the wind's energy into mechanical turbulence. Since turbulence is generated at the surface, surface wind speed is much less than wind speed at high levels. Turbulence includes vertical as well as horizontal air movement and hence the effect of surface frictional drag is propagated upward. The effect of frictional drag gradually decreases with height, and at gradient level (around 1000–2000 ft) frictional drag effect is negligible. At and above this level wind blows almost parallel to isobars (lines on a map having equal barometric pressure). For strong winds, the shape of wind speed profile depends mainly on the degree of surface roughness, caused by the overall drag effect of buildings, trees, and other projections that impede flow of wind at the earth's surface. This is illustrated in the three typical wind velocity profiles shown in Figure 4.2.

The viscosity of air reduces its velocity adjacent to the earth's surface to almost zero. The maximum retarding effect occurs in wind layers nearest to the ground. These layers in turn successively slow the higher layers. Thus the effect of slowdown reduces at each layer as the height increases, and eventually becomes negligible. The height at which the slowdown effect ceases to exist is called *gradient height*, and the corresponding velocity, *gradient velocity*. This characteristic increase of wind velocity with height is a well-understood phenomenon, as evidenced by higher design pressures specified at higher elevations in most building standards.

At heights of approximately 1200 ft (366 m) aboveground, the wind speed is virtually unaffected by surface friction. Its movement at and above this level, is solely a function of seasonal and local wind effects. The ensuing height in which the wind speed is affected by topography is called the *atmospheric boundary layer*.



**FIGURE 4.2** Wind velocity profiles as defined in the ASCE 7-05. Velocity profiles are determined by fitting curves to observed wind speeds.

The wind speed profile within the atmospheric boundary layer is given by

$$V_z = V_g(z/z_g)^{1/\alpha} \quad (4.1a)$$

where

$V_z$  is the mean wind speed at height  $z$  aboveground

$V_g$  is the gradient wind speed assumed constant above the boundary layer

$z$  is the height aboveground

$z_g$  is the height of boundary layer, which depends on the exposure (values for  $z$  are given in Figure 4.2)

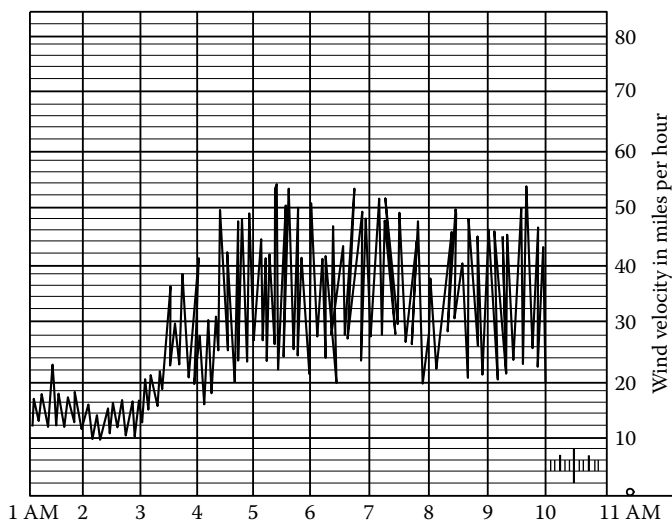
$\alpha$  is the power law coefficient

With known values of mean wind speed at gradient height and exponent  $\alpha$ , wind speeds at height  $z$  are calculated by using Equation 4.1a. The exponent  $1/\alpha$  and the depth of boundary layer  $z_g$  vary with terrain roughness and the averaging time used in calculating wind speed. The coefficient  $\alpha$  signifies that wind speed reaches its maximum over a greater height in an urban terrain than in the open country.

### 4.3.2 WIND TURBULENCE

Motion of wind is turbulent. A concise mathematical definition of turbulence is difficult to give, except to state that it occurs in wind flow because air has a very low viscosity—about one-sixteenth that of water. Any movement of air at speeds greater than 2–3 mph (0.9–1.3 m/s) is turbulent, causing particles of air to move randomly in all directions. This is in contrast to the laminar flow of particles of heavy fluids, which move predominantly parallel to the direction of flow.

The velocity profiles, shown in Figure 4.2, describe only one aspect of wind at lower levels. Superimposed on mean speed are gusts and lulls, which are deviations above and below the mean values. These gusts and lulls have a random distribution over a wide range of frequencies and amplitudes in both time and space, as shown in Figure 4.3, which is a schematic record of the unsteady nature of wind speed measured by an anemometer. Gusts are frequently the result of the introduction of fast moving parcels of air from higher levels into slower moving air strata. This mixing produces turbulence due to surface roughness and thermal instability. When this occurs, turbulence



**FIGURE 4.3** Schematic record of wind speed measured by an anemometer.

may result with eddies separating first from one side and then forming again. Turbulence generated by obstacles may persist downwind from projections as much as 100 times their height. Large-scale topographical features are not included in the above-mentioned surface roughness. They can influence the flow, so they are given special consideration in design by using a topographic factor,  $K_z$ . For instance, wind is usually much stronger over the brow of a hill or ridge. This is because, to pass the same quantity of air over the obstructing feature, a higher speed is required. Large valleys often have a strong funneling effect that increases wind speed along the axis of the valley.

Every structure has a natural frequency of vibration. Should dynamic loading occur at or near its natural frequency, structural damage, out of all proportion to size of load, may result. It is well known, for example, bridges capable of carrying far greater loads than the weight of a company of soldiers may oscillate dangerously and may even break down under dynamic loading of soldiers marching over them in step. Similarly, certain periodic gust within the wide spectrum of gustiness in wind may find resonance with the natural vibration frequency of a building, and although the total force caused by that particular gust frequency would be much less than the static design load for the building, dangerous oscillations may be set up. This applies not only to the structure as a whole, but also to components such as curtain wall panels and sheets of glass. A second dynamic effect is caused by instability of flow around certain structures. Long narrow structures such as smoke stacks, light standards, and suspension bridges are particularly susceptible to this sort of loading, causing an alternating pattern of eddies to form in its wake. A side thrust is thus exerted on the object similar to the lift on an aerofoil, and since this thrust alternates in direction, a vibration may result. Side-to-side wobbling effect of a straight stick pulled through water is an example of this phenomenon.

For structural engineering purposes, the atmospheric motion of air may be separated into two distinct categories:

1. Turbulent speed, with locally stationary statistical properties
2. Quasi-steady mean speeds associated with slowly varying climatological time scales

For wind-tunnel situations, the first category is modeled by the wind-tunnel flow itself, which reproduces the turbulence characteristics of the natural wind. The second category is taken into account by the wind climate model developed for the site, based on historical climatological records.

In regions where less frequent storms contribute significantly to the wind climate, available wind records may not be sufficient for design purposes. Such regions would include, for example, those frequented by tornadoes or by tropical cyclones. The severest of the latter are commonly termed hurricanes. Along the U.S. Gulf Coast and Florida Peninsula in the United States, severe tropical cyclones dominate the climate of strong winds. Along the New England Coast such storms contribute to the wind climate but to a lesser extent than along the Gulf Coast. Because of the rarity of these storms and their relatively small size, a typical 20 year record is not sufficient to obtain a reliable statistical estimate. Furthermore, there is the difficulty that instruments often fail in hurricane force winds. Similar comments can be made regarding the contribution to the wind climate by tornado-generating thunderstorms in the Midwestern U.S. region.

A different approach, based on computer simulations of events such as tropical cyclones, can lead to more reliable statistical predictions of building response. Such an approach is typically used by the Boundary Layer Wind Tunnel (BLWT) Laboratory.

The reliability of the wind model can also be affected by severe topography in two ways. Large hills or mountains can severely distort surface wind measurements, and can essentially increase the height at which gradient conditions are first approximated. Furthermore, severe winds can originate in regions near mountain ranges due to thermal instabilities in the atmosphere. These downslope winds are referred to by several names such as Santa Ana and Chinooks and are particularly prevalent in West Coast areas and areas just east of the Rocky Mountains. Their detailed structure is not well understood, particularly in regions close to the mountains where significant vertical flows can



occur, leading to severe spatial inhomogeneities near the ground. Away from the close proximity of the mountains, the flow appears to take on the characteristics of “normal” storm winds, although little information exists on the boundary-layer structure away from the surface. In areas affected by such winds, conservative modeling of the approaching flows is the current state of the art.

### 4.3.3 PROBABILISTIC APPROACH

In many engineering sciences, the intensity of certain events is considered to be a function of the duration recurrence interval (return period). For example, in hydrology the intensity of rainfall expected in a region is considered in terms of a return period because the rainfall expected once in 10 years is less than the one expected once every 50 years. Similarly, in wind engineering the speed of wind is considered to vary with return periods. For example, the fastest mile wind 33 ft (10 m) aboveground in Dallas, Texas, corresponding to a 50 year return period, is 67 mph (30 m/s), compared to the value of 71 mph (31.7 m/s) for a 100 year recurrence interval.

A 50 year return-period wind of 67 mph (30 m/s) means that on the average, Dallas will experience a wind faster than 67 mph within a period of 50 years. A return period of 50 years corresponds to a probability of occurrence of  $1/50 = 0.02 = 2\%$ . Thus the chance that a wind exceeding 67 mph (30 m/s) will occur in Dallas within a given year is 2%. Suppose a building is designed for a 100 year lifetime using a design wind speed of 67 mph. What is the probability that this wind will exceed the design speed within the lifetime of the structure? The probability that this wind speed will not be exceeded in any year is  $49/50$ . The probability that this speed will not be exceeded 100 years in a row is  $(49/50)^{100}$ . Therefore, the probability that this wind speed will be exceeded at least once in 100 years is

$$1 - (49/50)^{100} = 0.87 = 87\% \quad (4.2)$$

This signifies that although a wind with low annual probability of occurrence (such as a 50 year wind) is used to design structures, there still exists a high probability of the wind being exceeded within the lifetime of the structure. However, in structural engineering practice it is believed that the actual probability of overstressing a structure is much less because of the factors of safety and the generally conservative values of wind speeds used in design.

It is important to understand the notion of probability of occurrence of design wind speeds during the service life of buildings. The general expression for probability  $P$  that a design wind speed will be exceeded at least once during the exposed period of  $n$  years is given by

$$P = 1 - (1 - P_a)^n \quad (4.3)$$

where

$P_a$  is the annual probability of being exceeded (reciprocal of the mean recurrence interval)

$n$  is the exposure period in years

Consider again the building in Dallas designed for a 50 year service life instead of 100 years. The probability of exceeding the design wind speed at least once during the 50 year lifetime of the building is

$$P = 1 - (1 - 0.02)^{50} = 1 - 0.36 = 0.64 = 64\%$$

Thus the probability that wind speeds of a given magnitude will be exceeded increases with a longer exposure period of the building and the mean recurrence interval used in the design. Values of  $P$  for a given mean recurrence interval and a given exposure period are shown in Table 4.1.

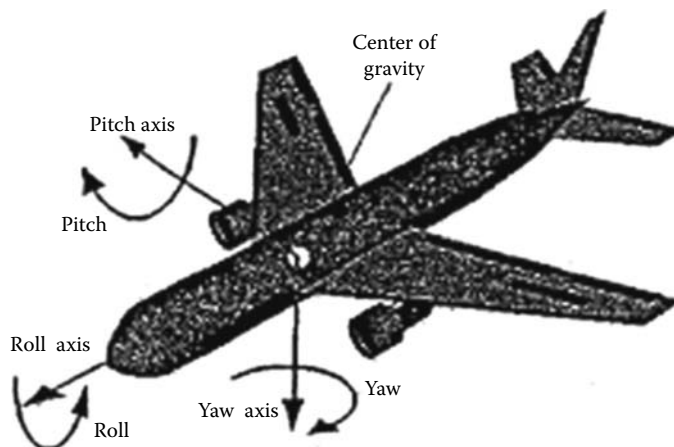
**TABLE 4.1**  
**Probability of Exceeding Design Wind Speed during Design**  
**Life of Building**

Annual Probability $P_a$	Mean Recurrence Interval ( $1/P_a$ ) Years	Exposure Period (Design Life), $n$ (Years)					
		1	5	10	25	50	100
0.1	10	0.1	0.41	0.15	0.93	0.994	0.999
0.04	25	0.04	0.18	0.34	0.64	0.87	0.98
0.034	30	0.034	0.15	0.29	0.58	0.82	0.97
0.02	50	0.02	0.10	0.18	0.40	0.64	0.87
0.013	75	0.013	0.06	0.12	0.28	0.49	0.73
0.01	100	0.01	0.05	0.10	0.22	0.40	0.64
0.0067	150	0.0067	0.03	0.06	0.15	0.28	0.49
0.005	200	0.005	0.02	0.05	0.10	0.22	0.39

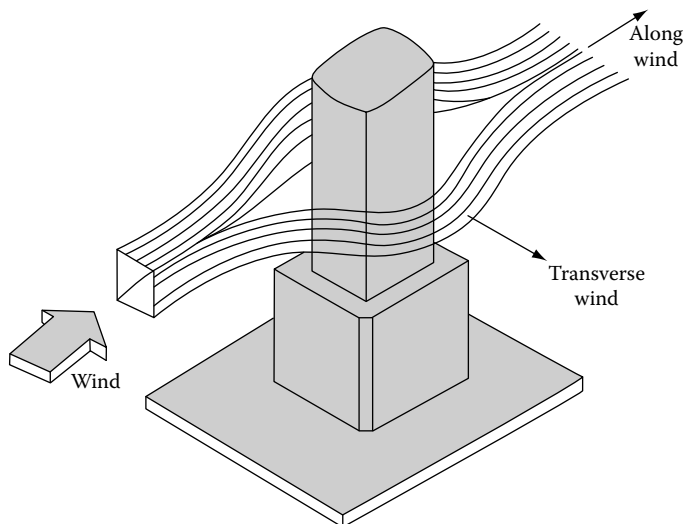
Wind velocities (measured with anemometers usually installed at airports across the country) are averages of the fluctuating velocities measured during an infinite interval of time. The benchmark velocity usually reported in the United States, until the publication of the American Society of Civil Engineers' ASCE 7-95 Standard, was the average of the velocities recorded during the time it takes a horizontal column of air, 1 mile long, to pass a fixed point. This is commonly referred to as the *fastest mile wind*. For example, if a 1 mile column of air is moving at an average velocity of 60 mph, it passes an anemometer in 60 s, the reported velocity being the average of the velocities recorded in 60 s. The fastest mile used in design is the highest velocity recorded in 1 day. The annual extreme mile is the largest of the daily maximums. Furthermore, since the annual extreme mile varies from year to year, wind pressures used in design are based on a wind velocity having a specific mean recurrence interval. Mean recurrence intervals of 20 and 50 years are generally used in building design, the former for determining comfort of occupants, and the latter for designing lateral resisting elements.

#### 4.3.4 VORTEX SHEDDING

In general, wind buffeting against a bluff body is diverted in three mutually perpendicular directions, giving rise to these sets of forces and moments, as shown in Figure 4.4. In aeronautical engineering, all six components, as shown in Figure 4.4, are significant. However, in civil and structural



**FIGURE 4.4** Critical components of wind in aeronautical engineering.



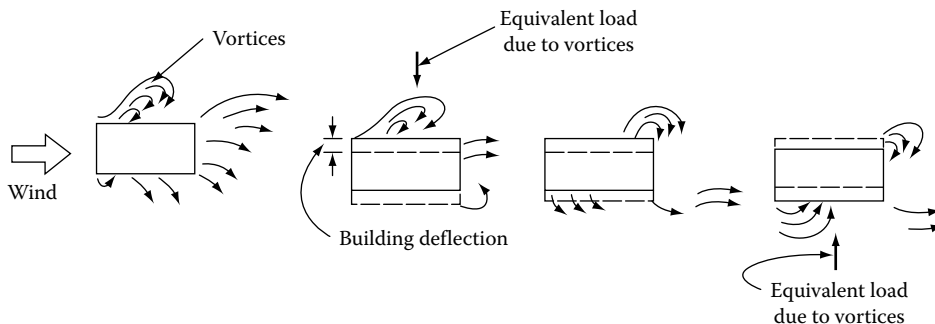
**FIGURE 4.5** Simplified wind flow consisting of along-wind and across-wind.

engineering the force and moment corresponding to the vertical axis (lift and yawing moment) are of little significance. Therefore, aside from the effects of uplift forces on large roof areas, flow of wind is considered two-dimensional, as shown in Figure 4.5, consisting of *along wind* and *transverse wind*.

The term *along wind*—or simply *wind*—is used to refer to drag forces while *transverse wind* is the term used to describe crosswind. Generally, in tall building design, the crosswind motion perpendicular to the direction of wind is often more critical than along-wind motion.

Consider a prismatic building subjected to a smooth wind flow. The originally parallel upwind streamlines are displaced on either side of the building, as illustrated in Figure 4.6. This results in spiral vortices being shed periodically from the sides into the downstream flow of wind. At relatively low wind speeds of, say, 50–60 mph (22.3–26.8 m/s), the vortices are shed symmetrically in pairs, one from each side. When the vortices are shed, that is, break away from the surface of the building, an impulse is applied in the transverse direction.

At low wind speeds, since the shedding occurs at the same instant on either side of the building, there is no tendency for the building to vibrate in the transverse direction. Therefore the building experiences only along-wind oscillations parallel to wind direction. However, at higher speeds, vortices are shed alternately, first from one side and then from the other side. When this occurs, there is an impulse in the along-wind direction as before, but in addition, there is an impulse in the



**FIGURE 4.6** Vortex shedding: periodic shedding of vortices generates building vibrations in the transverse direction.

transverse direction. However, the transverse impulse occurs alternately on opposite sides of the building with a frequency that is precisely half that of the along-wind impulse. This impulse due to transverse shedding gives rise to vibrations in the transverse direction. The phenomenon is called *vortex shedding* or *Karman vortex street*, terms well known in the field of fluid mechanics.

There is a simple formula to calculate the frequency of the transverse pulsating forces caused by vortex shedding:

$$f = \left\{ \frac{V \times S}{D} \right\} \quad (4.4)$$

where

$f$  is the frequency of vortex shedding in hertz

$V$  is the mean wind speed at the top of the building

$S$  is a dimensionless parameter called the Strouhal number for the given shape

$D$  is the diameter of the building

In Equation 4.4, the parameters  $V$  and  $D$  are expressed in consistent units such as ft/s and ft, respectively.

The Strouhal number is not a constant but varies irregularly with wind velocity. At low air velocities,  $S$  is low and increases with velocity up to a limit of 0.21 for a smooth cylinder. This limit is reached for a velocity of about 50 mph (22.4 m/s) and remains almost a constant at 0.20 for wind velocities between 50 and 115 mph (22.4 and 51 m/s).

Consider for illustration purposes, a circular prismatic-shaped high-rise building having a diameter equal to 110 ft (33.5 m) and a height-to-width ratio of 6 with a natural frequency of vibration equal to 0.16 Hz. Assuming a wind velocity of 60 mph (27 m/s), the vortex-shedding frequency is given by

$$f = \frac{V \times 0.2}{110} = 0.16 \text{ Hz}$$

where  $V$  is in ft/s.

If the wind velocity increases from 0 to 60 mph (27.0 m/s), the frequency of vortex excitation will rise from 0 to a maximum of 0.16 Hz. Since this frequency happens to be very close to the natural frequency of the building, and assuming very little damping, the structure would vibrate as if its stiffness were zero at a wind speed somewhere around 60 mph (27 m/s). Note the similarity of this phenomenon to the ringing of church bells or the shaking of a tall lamppost whereby a small impulse added to the moving mass at each end of the cycle greatly increases the kinetic energy of the system. Similarly, during vortex shedding an increase in deflection occurs at the end of each swing. If the damping characteristics are small, the vortex shedding can cause building displacements far beyond those predicted on the basis of static analysis.

When the wind speed is such that the shedding frequency becomes approximately the same as the natural frequency of the building, a resonance condition is created. After the structure starts resonating, further increase in wind speed by a few percent will not change the shedding frequency, because the shedding is now controlled by the natural frequency of the structure. The vortex-shedding frequency has, so to speak, locked in with the buildings natural frequency. When the wind speed increases significantly above that causing the lock-in phenomenon, the frequency of shedding is again controlled by the speed of the wind. The structure vibrates with the resonant frequency only in the lock-in range. For wind speeds either below or above this range, the vortex shedding will not be critical.

Vortex shedding occurs for many building shapes. The value of  $S$  for different shapes is determined in wind-tunnel tests by measuring the frequency of shedding for a range of wind velocities. One does not have to know the value of  $S$  very precisely because the lock-in phenomenon occurs within a range of about 10% of the exact frequency of the structure.

#### 4.3.5 DYNAMIC NATURE OF WIND

Unlike steady flow of wind, which for design purposes is considered static, turbulent wind associated with gustiness cannot be treated in the same manner. This is because gusty wind velocities change rapidly and even abruptly, creating effects much larger than if the same loads were static. Wind loads, therefore, need to be studied as if they were dynamic, somewhat similar to seismic loads. The intensity of dynamic load depends on how fast the velocity varies and also on the response of the structure itself. Therefore, whether pressures on a building due to wind gust, is dynamic or static entirely depends on the gustiness of wind and the dynamic properties of the building to which it is applied.

Consider, for example, the lateral movement of an 800 ft tall building designed for a drift index of  $H/400$ , subjected to a wind gust. Under wind loads, the building bends slightly as its top moves. It first moves in the direction of wind, with a magnitude of, say, 2 ft (0.61 m), and then starts oscillating back and forth. After moving in the direction of wind, the top goes through its neutral position, then moves approximately 2 ft (0.61 m) in the opposite direction, and continues oscillating back and forth progressively with smaller drifts, until it eventually stops. The time it takes a building to cycle through a complete oscillation is known as the *period* of the building. The period of oscillation for a tall steel building in the height range of 700–1400 ft (214–427 m) normally is in the range of 10–15 s, whereas for a 10-story concrete or masonry building it may be in the range of 0.5–1 s. The dynamic action of a wind gust depends not only on how long it takes for the gust to reach its maximum intensity and decrease again, but on the period of the subject building itself. If the wind gust reaches its maximum value and vanishes in a time much shorter than the period of the building, its effects are dynamic. On the other hand, the gusts can be considered as static loads if the wind load increases and vanishes in a time much longer than the period of the building. For example, a wind gust that develops to its strongest intensity and decreases to zero in 2 s is a dynamic load for a tall building with a period of considerably larger than 2 s, but the same 2 s gust is a static load for a low-rise with a period of less than 2 s. See Section 5.10.2 for further discussion of dynamic effects of wind.

#### 4.3.6 PRESSURES AND SUCTIONS ON EXTERIOR SURFACES

Detailed measurements of pressures and suctions on exterior surfaces of buildings are made in wind tunnel tests using a rigid models. The model contains numerous (typically 300–800) ports or “taps” which are connected via tubing to pressure transducers. The transducers convert the pressure at the point where the tap is located to an electrical signal which is then measured simultaneously for a particular wind direction. Measurements are usually made at 10° intervals for the full 360° azimuth range.

These aerodynamic measurements made in the wind tunnel are subsequently combined with the statistics of the full-scale wind climate at the site to provide predictions of pressures and suctions for various return periods. This information is used in the design of cladding.

##### 4.3.6.1 Scaling

The aerodynamic pressure coefficients measured in wind tunnel tests are converted to full-scale pressure values based on consistent length, time, and velocity scaling between full scale and model scale. This applies very well for sharp-edged structures. For structures with curved surfaces, additional care has to be taken to ensure that the flow regime is consistent in model and full scale.

For typical building tests, length scale is in the order of 1:300–1:500. Velocity scale is approximately 1:3–1:5. Time scale is in the order of 1:100. For example, 36 s in model scale represents about an hour in full scale.

#### 4.3.6.2 Internal Pressures and Differential Pressures

The net load on cladding is the difference between the external and internal pressures. The internal pressures are subtracted from the appropriate external pressure coefficients to obtain differential pressure coefficients, and then combined with the statistics of the full-scale wind climate at the site, to provide predictions of differential pressures and suctions for various return periods.

In the case of large opening due to operable windows or breach of the building envelope, large internal pressures may develop. Typically, the external pressure at the opening will be transmitted into the building interior volume. Building envelope at other locations within the building volume will experience both the external pressures at those external locations as well as the large internal pressure transmitted from the opening.

For freestanding elements with both sides exposed to air, such as parapets and canopies, the net differential pressures are the instantaneous difference in pressures on the opposite sides.

Estimates of internal pressures are needed in determining net wind loads for the design of the cladding and glazing of buildings. These may be obtained from building code specifications, or from wind-tunnel studies.

Although the importance of determining internal pressures is clear, it is not a quantity which can be determined exactly. In fact, internal pressures are influenced by many factors, which are uncertain in themselves, such as the character of the leakage paths and windows or other exterior openings being left open or being broken during windstorms. The complex distribution of exterior pressures and their influence on the internal pressures must also be taken into account.

In spite of these difficulties, reasonable estimates of the internal pressure can be made by expressing the uncertainties in statistical terms.

Internal pressures are those induced by wind and neither include stack effects nor any effects of interior partitions and other restriction of interior flows, which could lead to considerably higher load in special cases.

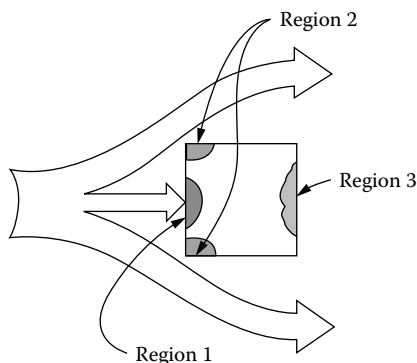
Although failure of exterior cladding resulting in broken glass may be of less consequence than collapse of a building, the expense of replacement and hazards posed to pedestrians is of major concern. Cladding breakage in a windstorm is an erratic occurrence, as witnessed in hurricane Alicia, which hit Galveston and downtown Houston, Texas on August 18, 1983, causing breakage of glass in several buildings. It is now known that glass breakage is also influenced by other factors, such as solar radiation, mullion and sealant details, tempering of the glass, double- or single-glazing, and fatigue of glass. It is also known with certainty that glass failure starts at nicks and scratches that may have occurred during manufacture and handling operations.

There appears to be no analytical approach available for rational design of curtain walls that come in all shapes and sizes. Although most codes identify regions of high wind loads such as building corners, the modern architectural trend with nonprismatic and curvilinear shapes combined with unique topography of each site, has made wind-tunnel determination of design loads a common and necessary practice.

In the past two decades, curtain wall has developed into an ornamental item and has emerged as a significant architectural statement. Sizes of window panes have increased considerably, requiring glass panes to be designed for various combinations of forces due to wind, shadow effects, and temperature movement. Glass in curtain walls must not only resist large wind forces, particularly in tall buildings, but must also be designed to accommodate various distortions of the total building structure.

#### 4.3.6.3 Distribution of Pressures and Suctions

Winds flowing around edges of a building result in higher pressures and suctions at corners than those at the center of elevation. This has been evidenced by damage caused to corner windows,



**FIGURE 4.7** High pressures and suctions around building corners.

eave and ridge tiles, etc., in windstorms. Wind-tunnel studies on scale models of buildings have confirmed that three distinct high pressure and suction areas develop around buildings, as shown schematically in Figure 4.7:

1. Positive pressure zone on the upstream face (Region 1).
2. Negative pressure zones at the upstream corners (Regions 2).
3. Negative pressure zone on the downstream face (Region 3).

The highest negative pressures are generated in the upstream corners designated as Regions 2 in Figure 4.7. Wind pressures on a building's surface are not constant, but fluctuate continuously. The positive pressure on the upstream or the windward face fluctuates more than the negative pressure on the downstream or the leeward face. The negative-pressure region remains relatively steady compared to the positive-pressure zone. The fluctuation of pressure is random and varies from point to point on the building surface. Therefore, the design of the cladding is strongly influenced by local pressures. As mentioned earlier, the design pressure can be thought of as a combination of the mean and the fluctuating velocity. As in the design of buildings, whether or not the pressure component arising from the fluctuating velocity of wind is treated as a dynamic or as a pseudostatic load is a function of the period of the cladding. The period of cladding on a building is usually on the order of 0.2–0.02 s, which is much shorter than the period it takes for the wind to fluctuate from a gust velocity to a mean velocity. Therefore, it is sufficiently accurate to consider both the static and the gust components of winds as equivalent static loads in the design of cladding.

The strength of glass, and indeed of any other cladding material, is not known with the same certainty as the strength of other construction materials such as steel or concrete. For example, it is not possible to buy glass based on yield strength criteria as with steel. Therefore, the selection, testing, and acceptance criteria for glass are based on statistical probabilities rather than on absolute strength. The glass industry has addressed this problem, and commonly uses 8 failures per 1000 lights (panes) of glass as an acceptable probability of failure.

#### 4.3.6.4 Local Cladding Loads and Overall Design Loads

The design wind loads that we use in lateral analysis is an overall combination of positive and negative pressures occurring simultaneously around the building. The local wind loads that act on specific areas of the building are not required for overall building design, but are vital for design of exterior cladding elements and their connections to building. The methodology of determining the the design loads for: (1) overall building design load and (2) loads for design of cladding are quite different. Important differences are

1. Local winds are more influenced by the configuration of the building than the overall loading.
2. Local load is the maximum load that may occur at any location at any instant of time on any wall surface, whereas the overall load is the summation of positive and negative pressures occurring simultaneously over the entire building surface.
3. Intensity and character of local loading for any given wind direction and velocity differ substantially on various parts of the building surface, whereas the overall load is considered to have a specific intensity and direction.
4. Local loading is sensitive to the momentary nature of wind, but in determining critical overall loading, only gusts of about 2 s or more are significant.
5. Generally, maximum local negative pressures, also referred to as suctions, are of greater intensity than overall load.
6. Internal pressures caused by leakage of air through cladding systems have a significant effect on local cladding loads but are of no consequence in determining overall load on typical fully enclosed buildings.

The relative importance of designing for these two types of wind loading is quite obvious. Although proper assessment of overall wind load is important, very few buildings, if any, have been toppled by winds. There are no classic examples of building failures comparable to the Tacoma bridge disaster. On the other hand, local failures of roofs, windows, and wall cladding are not uncommon.

The analytical determination of wind pressure or suction at a specific surface of a building under varying wind direction and velocity is a complex problem. Contributing to the complexity are the vagaries of wind action as influenced both by adjacent surroundings and the configuration of the wall surface itself. Much research is needed on the micro effects of common architectural features such as projecting mullions, column covers, and deep window reveals. In the meantime, model testing of buildings in wind tunnels is perhaps the only recourse.

Probably the most important fact established by tests is that the negative or outward-acting wind loads on wall surfaces are greater and more critical than had formerly been assumed. They may be as much as twice the magnitude of positive loading. In most instances of local cladding failures, glass panels have blown off the building, not into it, and the majority of such failures have occurred in areas near building corners. Therefore it is important to give careful attention to the design of both anchorage and glazing details to resist outward-acting forces, particularly near the corners.

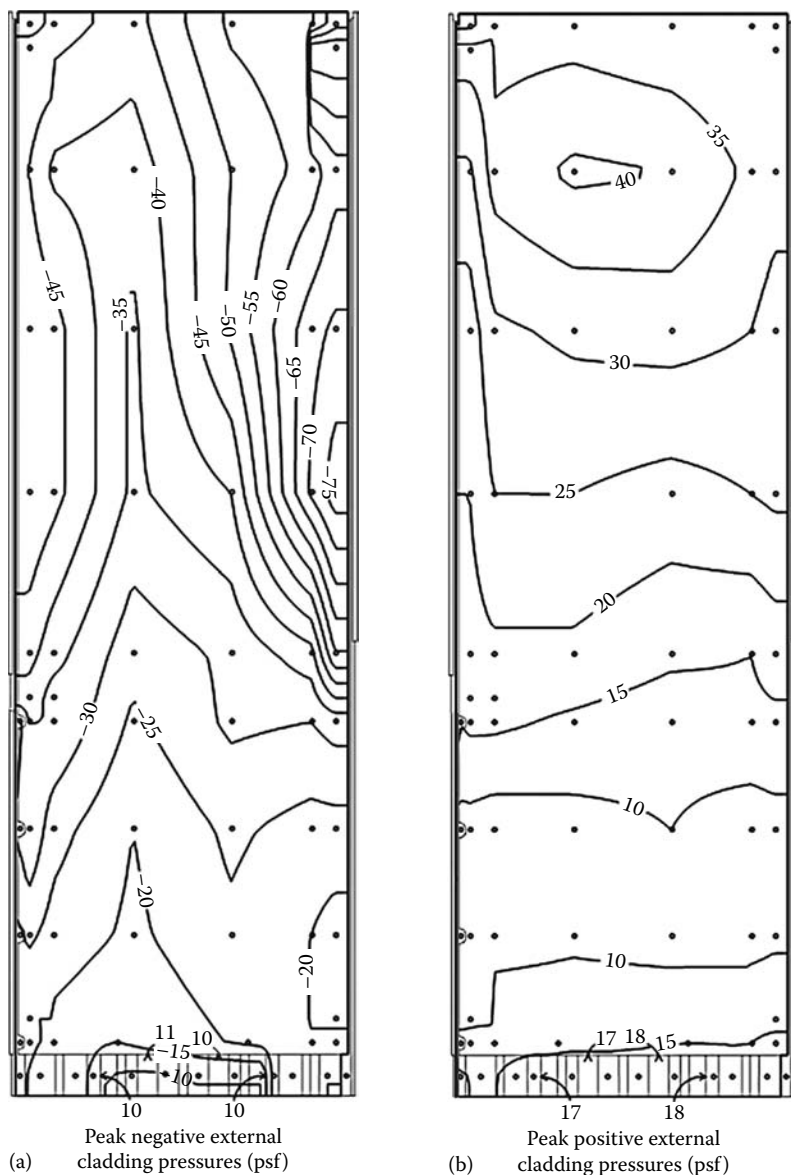
Another feature that has come to light from model testing is that wind loads, both positive and negative, do not vary in proportion to height aboveground. Typically, the positive-pressure contours follow a concentric pattern as illustrated in Figure 4.8, with the highest pressure near the lower center of the facade, and pressures at the very top somewhat less than those a few stories below the roof. Figure 4.8 shows a pressure diagram for the design of cladding of a high-rise building measured in wind-tunnel tests. Shown in Figure 4.9 are measured pressure contours for another tall building. The results are given in a block diagram format relating measured test results to the building grid system.

#### 4.4 ASCE 7-05: WIND LOAD PROVISIONS

It has been nearly 50 years since the ASCE published a novel article entitled *Wind Forces on Structures* in its proceedings. This article was incorporated into the wind provisions of the then American National Standards Institute, ANSI, A58.1, 1972. In 1985, ASCE took over the duties of maintaining that document, which has now been revised eight times, including the 2005 edition. The next edition is expected in 2010 and will be referenced in the 2012 IBC.

The full title of this standard is American Society of Civil Engineers *Minimum Design Loads for Buildings and Other Structures*. In one of its 23 chapters, Chapter 6, ASCE 7-05 gives three procedures for calculating wind loads for the design of buildings, main wind-force-resisting systems (MWFRS), and components and cladding.



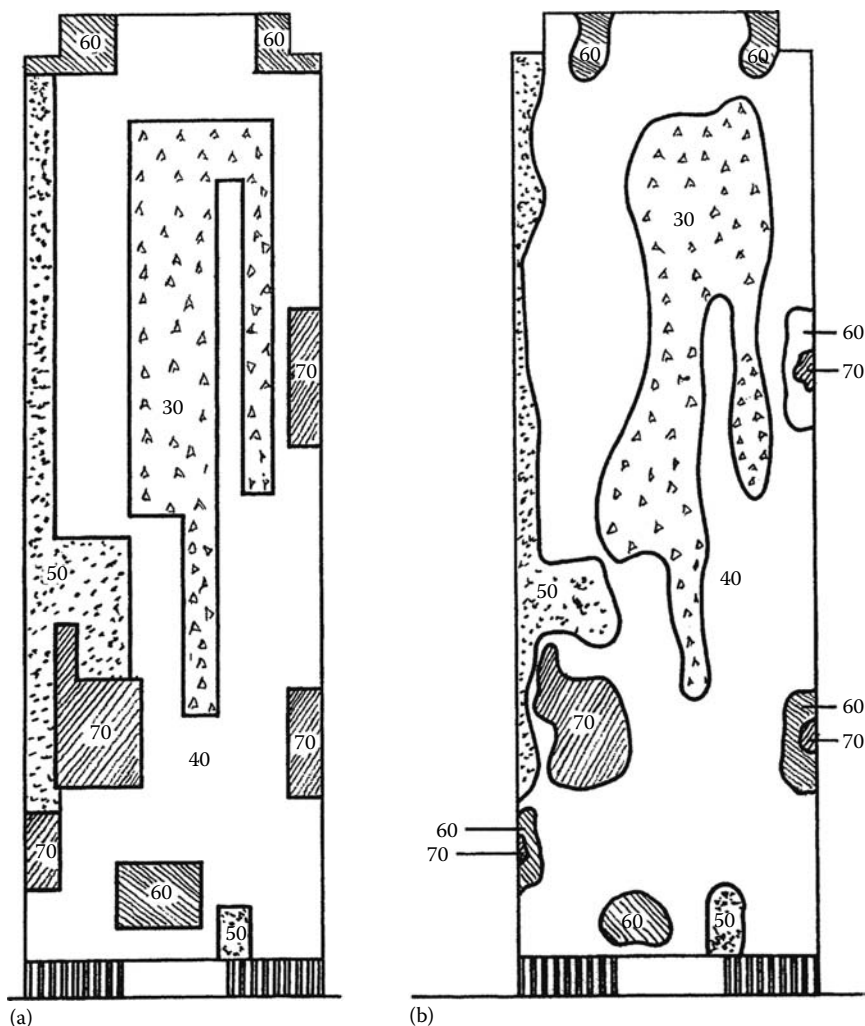


**FIGURE 4.8** Pressure contours as measured in a wind tunnel test: (a) building elevation showing suction (negative pressures); (b) building elevation showing positive pressures.

The methods are

1. Method 1, Simplified Method
2. Method 2, Analytical Procedure
3. Method 3, Wind-Tunnel Procedure

(See Chapter 9, Section 9.8.2.7.5 for Alternate All-Heights Method, 2009 IBC) Method 1 was first published in the 2000 IBC. Its coefficients were developed from research done for Metal Building Manufacturers Association, MBMA, in the 1980s using wind-tunnel tests. Method 1 is restricted to regular-shaped “simple diaphragm buildings,” has many constraints, and is restricted to a maximum height of 60 ft.

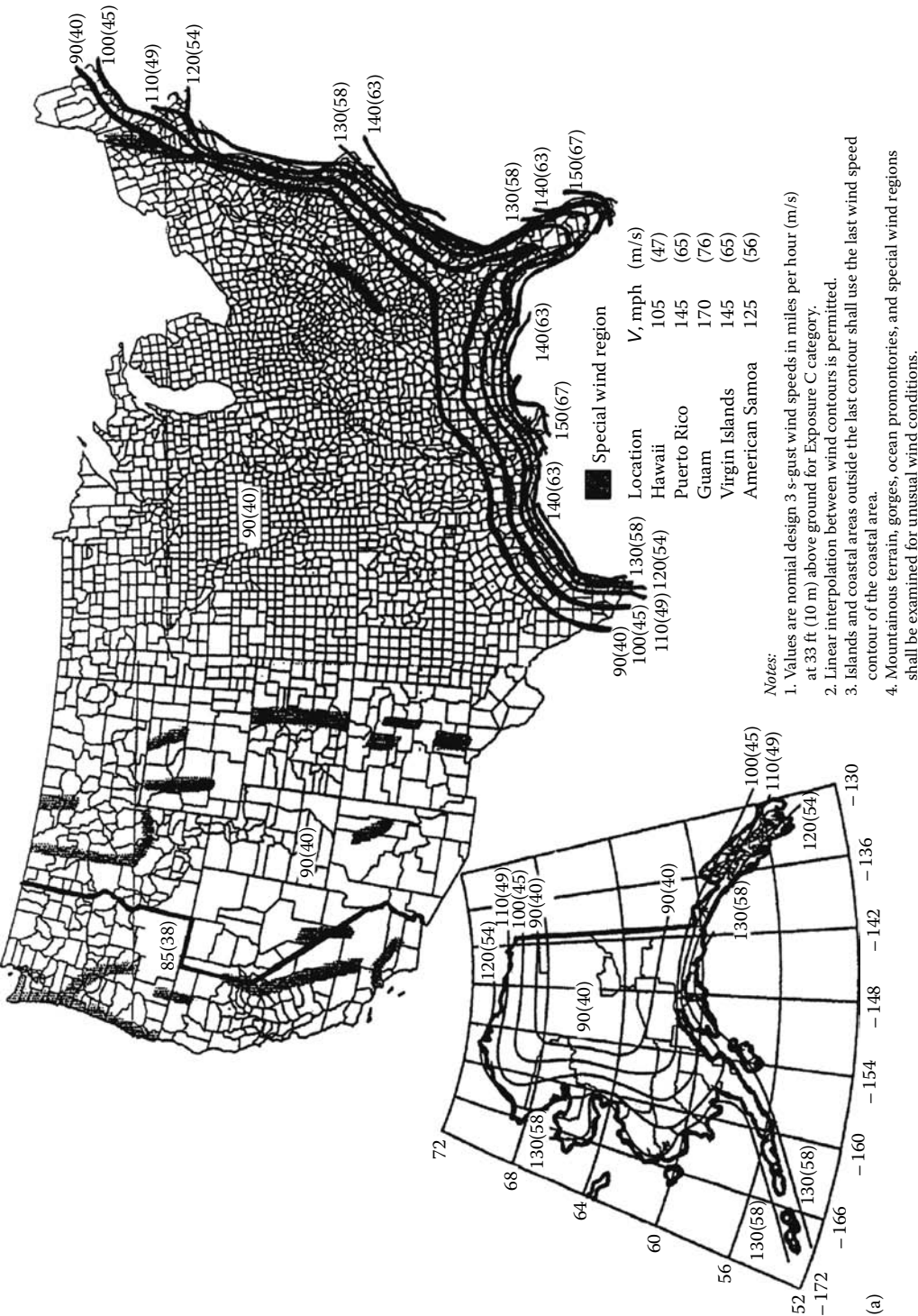


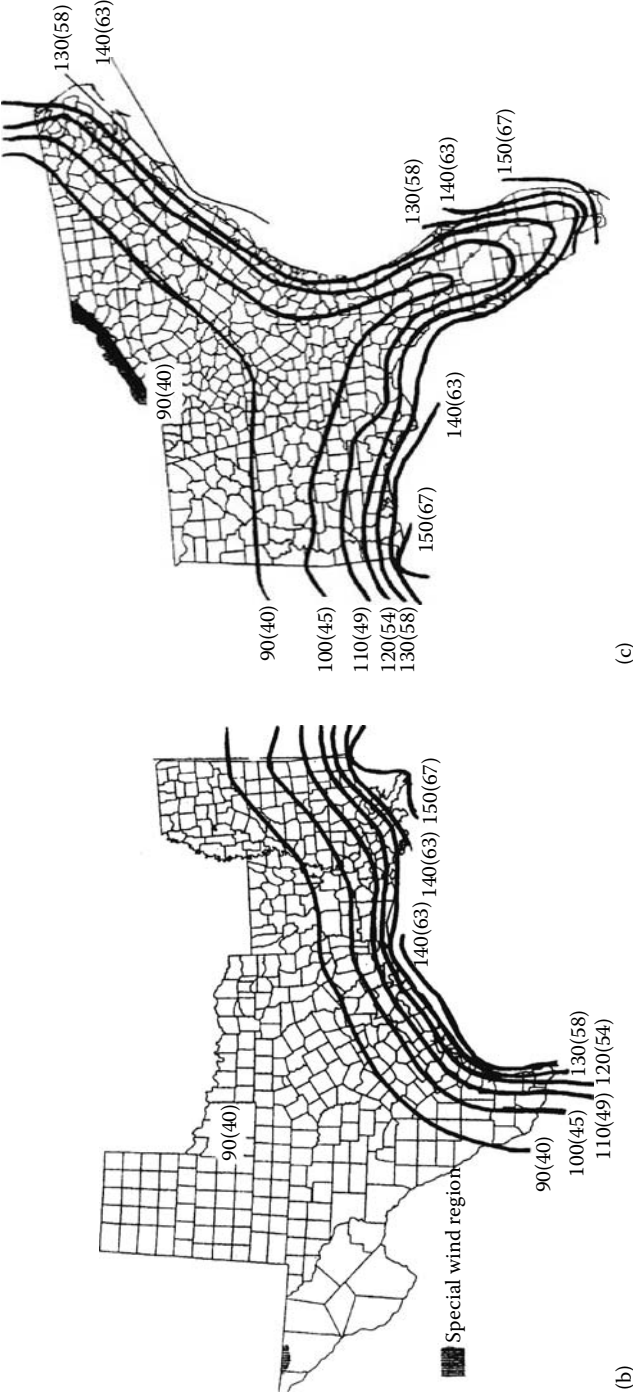
**FIGURE 4.9** Wind pressure diagram for cladding design: (a) block diagram relating measured pressures, psf, to building grid system; (b) pressures measured in wind tunnel, psf.

The designer can use Method 1, the simplified procedure, to select wind pressures directly without calculations when the building is less than 60 ft in height and meets all requirements given in the ASCE Sections 6.4.1.1 and 6.4.1.2. Method 2, the analytical procedure, may be used for buildings of any height that are regular in shape, provided they are not sensitive to across-wind loading, vortex shedding, or instability due to galloping or flutter; or do not have a site for which channeling effects warrant special consideration. Method 3 is wind-tunnel procedure that may be used in lieu of Methods 1 and 2 for any building. Method 3 is recommended for buildings that exhibit the following characteristics:

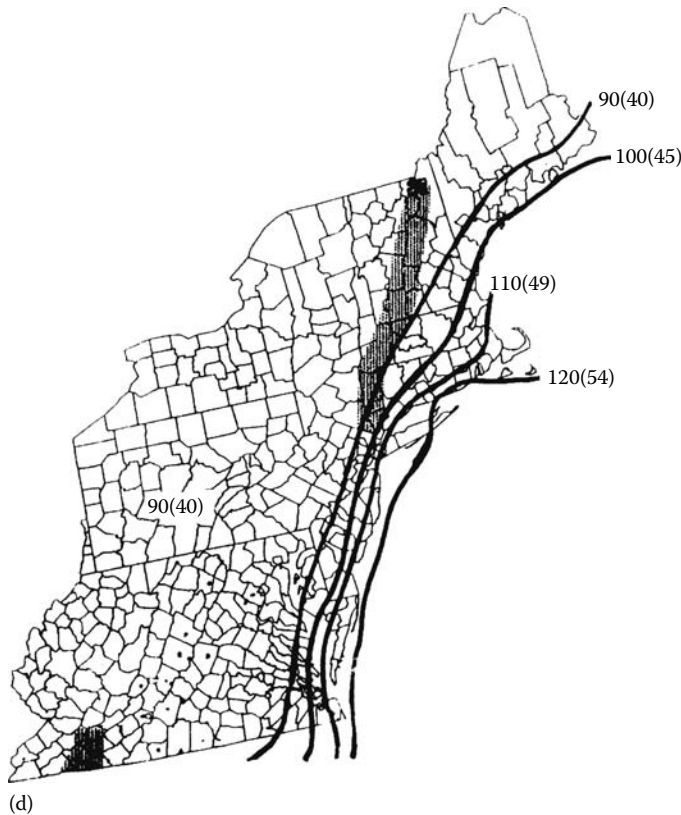
- Nonuniform shapes
- Flexible with natural frequencies less than 1 Hz
- Subject to significant buffeting by the wake of upwind buildings or other structures
- Subject to accelerated flow of wind by channeling or local topographic features

Basic wind speeds for any location in the continental United States and Alaska are shown on a map having isotachs (lines of equal pressure) representing a 3 s gust speed at 33 ft (10 m) above the ground (see Figure 4.10). For Hawaii and Puerto Rico, basic wind speeds are given in a table as 105 and





**FIGURE 4.10** Wind speed map for United States and Alaska. (a) Map of the United States, (b) western Gulf of Mexico hurricane coastline (enlarged), (c) eastern Gulf of Mexico and southeastern United States hurricane coastline (enlarged), (continued)



**FIGURE 4.10 (continued)** (d) mid- and north-Atlantic hurricane coastline (enlarged). (Adapted from ASCE 7-05.)

145 mph (47 and 65 m/s), respectively. The map is standardized for a 50 year recurrence interval for exposure C topography (flat, open, country and grasslands with open terrain and scattered obstructions generally less than 30 ft (9 m) in height). The minimum wind speed provided in the standard is 85 mph (38 m/s). Increasing the minimum wind speed for special topographies such as mountain terrain, gorges, and ocean fronts is recommended.

The abandonment of the fastest mile speed in favor of a 3 s-gust speed first took place in the ASCE 7-1995 edition. The reasons are as follows: (1) modern weather stations no longer measure wind speeds using the fastest-mile method; (2) the 3 s gust speed is closer to the sensational wind speeds often quoted by news media; and (3) it matches closely the wind speeds experienced by small buildings and components of all buildings.

Method 1, the simplified procedure, is not discussed here. The emphasis is on Method 2.

This method, also called, the analytical procedure, applies to a majority of buildings. It takes into account

1. Basic wind speed
2. Mean recurrence interval of the wind speed considered appropriate for the design
3. Characteristics of the terrain surrounding the building
4. Height at which the wind load is being determined
5. Directional properties of the wind climate
6. Size, geometry, and aerodynamics of the building
7. Positions of the area acted on by the wind flow
8. Magnitude of the area of interest

9. Porosity of the building envelope
10. Structural properties that may make the building susceptible to dynamic effects
11. Speed-up effect of topographic features such as hills and escarpments

#### 4.4.1 ANALYTICAL PROCEDURE—METHOD 2, OVERVIEW

The more robust design procedure is Method 2, which applies for most “rigid” structures of all heights and shapes. It can even design “flexible” structures with some limitations. Most practicing engineers use this method.

A significant benefit of this method is its applicability to a large variety of structures. It provides pressure coefficients for myriad shapes and heights of any type of regular-shaped buildings and structures. In this method, internal pressure coefficients related to enclosure classification are determined and then combined algebraically with external coefficients, both of which can be positive or negative relative to the exterior and interior building surfaces. In determining design wind loads for enclosed buildings, any internal pressure can be ignored because the pressure pushes or pulls equally on all walls and therefore, can be canceled out. However, roofs will be directly affected by internal pressure and it must be accounted for. And all partially enclosed buildings always need to account for internal pressures on all surfaces.

ASCE 7-05, Method 2 is built around two fundamental equations, the velocity pressure,  $q_z$  equation, and the design wind pressure,  $p$ , equation:

$$q_z = 0.00256 K_z K_{zt} K_d V^2 I \quad (4.5)$$

$$p = qGC_p - q_i(GC_{pi}) \quad (4.6)$$

These two equations, when combined, represent the well known Bernoulli equation of fluid dynamics for determining for wind forces. They convert the chaotic nature of wind forces on a building to a reasonable elastic basis.

The velocity pressure  $q_z$ , at elevation  $z$  is given by

$$q_z = 0.00256 K_z K_{zt} K_d V^2 I \quad (q_z \text{ in psf, } V \text{ in mph}) \quad (4.7)$$

where

$q_z$  is the velocity pressure at height  $z$  above ground level

$K_z$  is the velocity exposure coefficient

$K_{zt}$  is the topographic factor

$K_d$  is the directionality factor

$V$  is the wind speed at an elevation 33 ft (10 m) above ground in flat open country (Exposure C), as given in Figure 4.10

$I$  is the wind importance factor commonly denoted as  $I_w$

The wind directionality factor,  $K_d$ , accounts for the directionality of wind. Directionality refers to the fact that wind rarely, if ever, strikes along the most critical direction of a building. Wind direction changes from one instant to the next. And can be instantaneous along the most critical direction because at the very next instant, it will not be from the same direction. This fact used to be taken into account through a relatively low load factor of 1.3 on the effect of wind in strength design load combinations. But then ASCE 7 received comments that engineers using allowable stress design (ASD) could not take advantage of the directionality of wind. The ASCE 7 decision to include  $K_d = 0.85$  for buildings in the definition of the wind pressure was in response to these comments. In order not to design using lower-factored wind forces in strength design, the 1.3 load factor on wind was

adjusted up. A load factor of  $1.3/0.85 = 1.53$  would have maintained status quo exactly. However, it was rounded up to 1.6, which resulted in an effective 5% increase in the wind load factor.

The basic wind speed  $V$ , given in Figure 4.10, corresponds to a 50 year mean recurrence interval. It represents the speed from any direction at an elevation 33 ft (10 m) aboveground in a flat open country (Exposure C).

The velocity pressure exposure coefficient  $K_z$  adjusts the basic wind speed  $V$  to a height  $z$  and, terrain roughness (i.e., exposure category). Three exposure categories—B, C, and D—are defined. Exposure A, meant for heavily built-up city centers, was deleted in the 2002 edition of ASCE 7.

Exposure B corresponds to surface roughness typical of urban and suburban areas, while exposure C represents surface roughness in a flat open country. Exposure D is representative of a flat unobstructed area and water surface outside hurricane-prone regions. Exposure C, the default category applies to all cases where exposures B and D do not. Interpolation between exposure categories permitted for the first time in the ASCE 7-02 is still valid.

The wind importance factor  $I$ , commonly denoted as  $I_w$ , is a factor that accounts for the degree of hazard to human life and damage to property. For Category II buildings, representative of typical occupancy,  $I_w = 1.0$ . For Category I buildings representing low hazard in the event of failure (e.g., agriculture facilities),  $I_w = 0.87$  or  $0.77$ , depending upon whether the building site is located in hurricane-prone regions. For buildings in Category III posing a substantial hazard to human life in the event of failure (e.g., buildings where more than 300 people congregate in one area, and essential facilities such as fire stations),  $I_w = 1.15$ . For Category IV buildings deemed as essential facilities,  $I_w = 1.15$ , the same as for Category III. See ASCE 7-05, Table 6.1 for wind importance factors.

The topographic factor  $K_{zt}$  is given by

$$K_{zt} = (1 + K_1 K_2 K_3)^2 \quad (4.8)$$

It reflects the speedup effect over hills and escarpments. The multipliers  $K_1$ ,  $K_2$ , and  $K_3$  are given in Figure 6.4 of the Standard (Figures 4.11 and 4.12 of this text).

Wind directionality is explicitly accounted for by a new factor  $K_d$  introduced in the ASCE 7-02. Prior to introduction of  $K_d$ , the load factor for wind was 1.3. Now it is 1.6. However, it should be noted that the factored wind load is the same as before.

For enclosed buildings internal pressures and suctions do not affect wind load calculations for the MWFRS. Therefore, pressures and suctions may be calculated using the following simplified equations:

$$p_z = q_z G_f C_p \text{ (windward positive pressures)} \quad (4.9)$$

$$p_z = q_h G_f C_p \text{ (leeward negative pressures)} \quad (4.10)$$

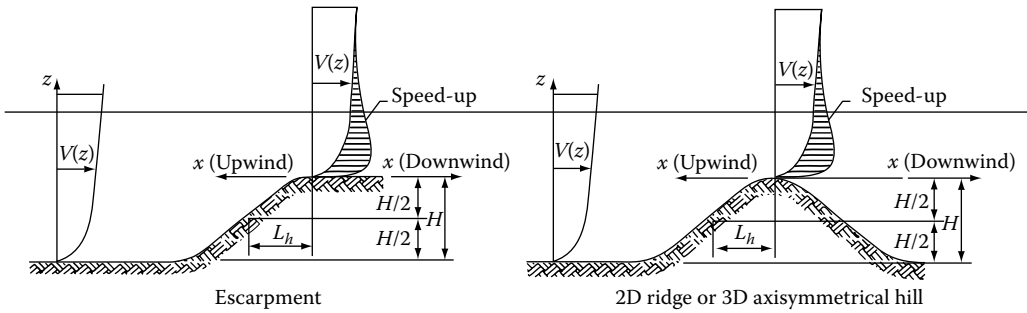
The overall wind load is the summation of positive and negative pressures on the windward and leeward walls, respectively. Using the permitted value of  $G_f = 0.85$ , and  $C_p = 0.8$  and  $0.5$  for the windward and leeward walls, the overall wind pressure at  $z$  for a typical squarish building is given by

$$p_z = 0.85(0.8q_z + 0.5q_h)$$

#### 4.4.2 METHOD 2: STEP-BY-STEP PROCEDURE

Design wind pressure or suction on a building surface is given by the equation:

$$p_z = q_z \times G_f \times C_p \quad (4.11)$$



Topographic multipliers for exposure C										
$H/L_h$	$K_1$ Multiplier			$x/L_h$	$K_2$ Multiplier		$z/L_h$	$K_3$ Multiplier		
	2D Ridge	2D Escarp.	3D Axisym. hill		2D Escarp.	All other cases		2D Ridge	2D Escarp.	3D Axisym. hill
0.20	0.29	0.17	0.21	0.00	1.00	1.00	0.00	1.00	1.00	1.00
0.25	0.36	0.21	0.26	0.50	0.88	0.67	0.10	0.74	0.78	0.67
0.30	0.43	0.26	0.32	1.00	0.75	0.33	0.20	0.55	0.61	0.45
0.35	0.51	0.30	0.37	1.50	0.63	0.00	0.30	0.41	0.47	0.30
0.40	0.58	0.34	0.42	2.00	0.50	0.00	0.40	0.30	0.37	0.20
0.35	0.65	0.38	0.47	2.50	0.38	0.00	0.50	0.22	0.29	0.14
0.50	0.72	0.43	0.53	3.00	0.25	0.00	0.60	0.17	0.22	0.09
				3.50	0.13	0.00	0.70	0.12	0.17	0.06
				4.00	0.00	0.00	0.80	0.09	0.14	0.04
							0.90	0.07	0.11	0.03
							1.00	0.05	0.08	0.02
							1.50	0.01	0.02	0.00
							2.00	0.00	0.00	0.00

- Notes:
- 1. For values of  $H/L_h$ ,  $x/L_h$ , and  $z/L_h$  other than those shown, linear interpolation is permitted.
  - 2. For  $H/L_h > 0.5$ , assume  $H/L_h = 0.5$  for evaluating  $K_1$  and substitute  $2H$  for  $L_h$  for evaluating  $K_2$  and  $K_3$ .
  - 3. Multipliers are based on the assumption that wind approaches the hill or escarpment along the direction of maximum slope.
  - 4. Notation:
    - $H$ : Height of hill or escarpment relative to the upwind terrain, in ft (m).
    - $L_h$ : Distance upwind of crest to where the difference in ground elevation is half the height of hill or escarpment, in ft (m).
    - $K_1$ : Factor to account for shape of topographic feature and maximum speed-up effect.
    - $K_2$ : Factor to account for reduction in speed-up with distance upwind or downwind of crest.
    - $K_3$ : Factor to account for reduction in speed-up with height above local terrain.
    - $x$ : Distance (upwind or downwind) from the crest to the building site, in ft (m).
    - $z$ : Height above local ground level, in ft (m).
    - $\mu$ : Horizontal attenuation factor.
    - $\gamma$ : Height attenuation factor.

FIGURE 4.11 Topographic factor  $K_{zt}$  (From ASCE 7-05 Figure 6.4).

where

$p_z$  is the design wind pressure or suction, in psf, at height  $z$ , above ground level

$q_z$  is the velocity pressure, in psf, determined at height  $z$  above ground for positive pressure, and at roof height  $h$  for suction

$G_f$  is the gust effect factor, dimensionless, denoted as  $G$  for rigid buildings, and  $G_f$  for flexible buildings

$C_p$  is the external pressure coefficient, which varies with building height acting as pressure (positive load) on windward face, and as suction (negative load) on the leeward face and roof



Parameters for Speed-Up Over Hills and Escarpments						
Hill Shape	$K_1/(H/L_h)$			$\gamma$	$\mu$	
	Exposure				Upwind of Crest	Downwind of Crest
	B	C	D			
Two-dimensional ridges (or valleys with negative $H$ in $K_1/(H/L_h)$ )	1.30	1.45	1.55	3	1.5	1.5
Two-dimensional escarpments	0.75	0.85	0.95	2.5	1.5	4
Three-dimensional axisym, hill	0.95	1.05	1.15	4	1.5	1.5

$$K_{zt} = (1 + K_1 K_2 K_3)^2$$

$K_1$  determined from table

$$K_2 = \left( 1 - \frac{|x|}{\mu L_h} \right)$$

$$K_3 = e^{-\gamma z/L_h}$$

(From Figure 6.4 in ASCE 7-05)

**FIGURE 4.12** Topographic factor  $K_{zt}$  based on equations.

The values of  $C_p$ , are shown in Figures 4.13 through 4.15 for various ratios of building width to depth.

The velocity pressure and suction  $q_z$  and  $q_h$  are given by

$$q_z = 0.00256 K_z K_{zt} K_d V^2 I \text{ (positive pressure on windward face)}$$

$$q_h = 0.00256 K_h K_{zt} K_d V^2 I \text{ (negative pressure or suction on nonwind ward face and roof)}$$

where

$K_h$  and  $K_z$  are the combined velocity pressure exposure coefficients (dimensionless), which take into account changes in wind speed aboveground and the nature of the terrain (Exposure category B, C, or D) (see Figures 4.16 and 4.17)

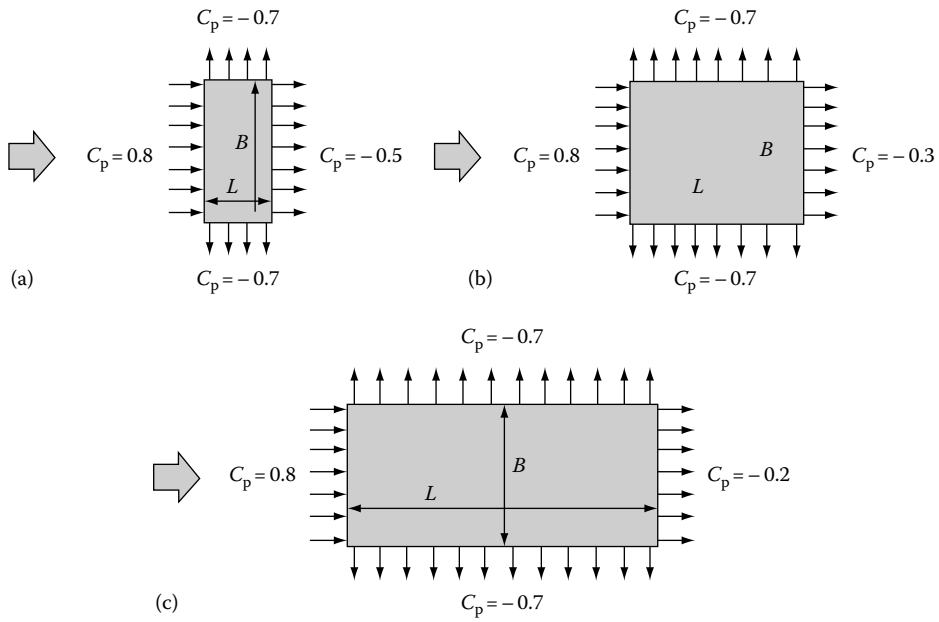
$K_{zt}$  is the topographic factor

$I$  is the importance factor, a dimensionless parameter that accounts for the degree of hazard to human life and damage to property

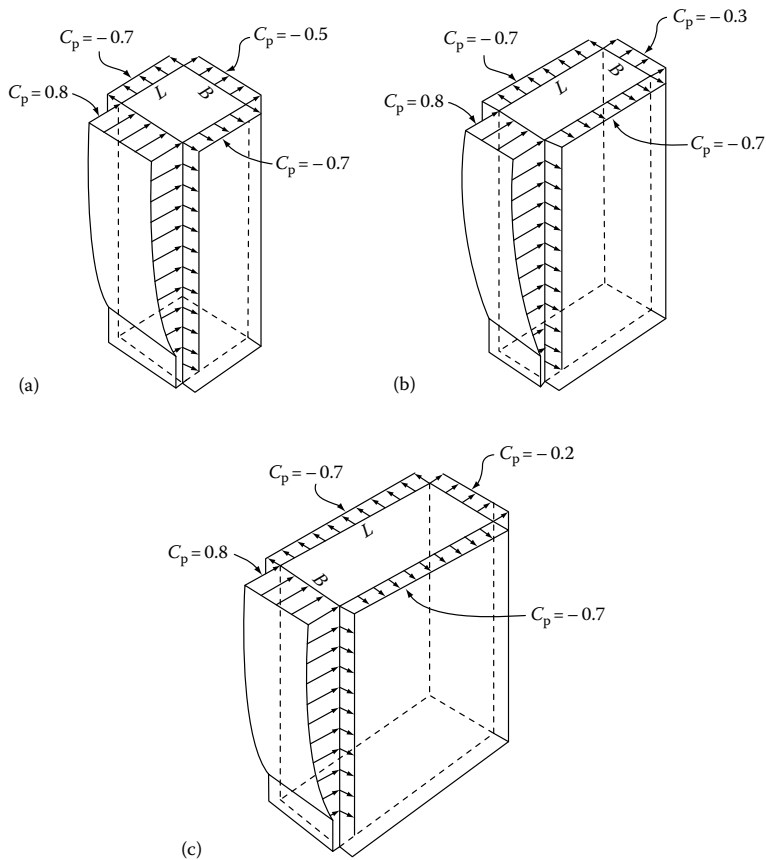
$V$  is the basic wind speed in miles per hour that corresponds to a 3 s gust speed at 33 ft (10 m) aboveground, Exposure category C, for a 50 year mean recurrence interval (see Figure 4.10)

$K_d$  is the wind directionality factor that varies from 0.85 to 0.95 depending on the structure type (ASCE 7-05 Table 6.4)

It should be noted that AISC 7-05 gives only a general formula, Equation 4.7 above, for the velocity pressure  $q_z$ , at any height  $z$ , above ground. However, there are many situations where a specific value of  $z$  is referenced. An example is height, or mean height of roof used in the calculation of suction on leeward side of buildings. Therefore, whenever the subscript  $h$  is called for, it is understood that  $z$  becomes  $h$  in the appropriate equations.



**FIGURE 4.13** External pressure coefficient  $C_p$  with respect to plan aspect ratio  $L/B$ : (a)  $0 \leq L/B \leq 1$ ; (b)  $L/B = 2$ ; (c)  $L/B > 4$ . Linear variation permitted for leeward suction (see Figure 4.15).



**FIGURE 4.14** Building elevation showing variation of  $C_p$ : (a)  $0 \leq L/B \leq 1$ , (b)  $L/B = 2$ , and (c)  $L/B > 4$ .

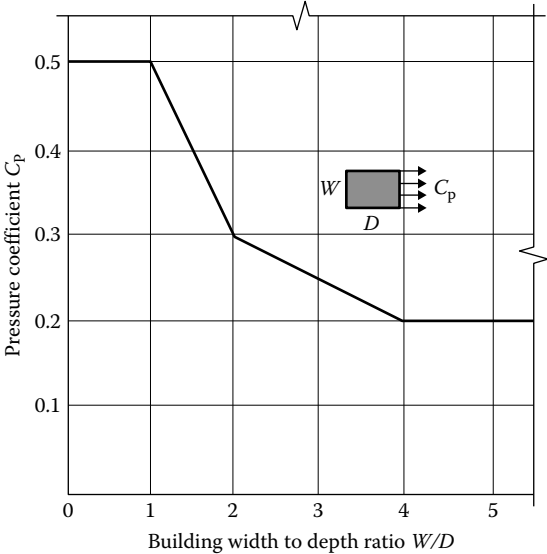


FIGURE 4.15 Leeward suction  $C_p$  versus plan aspect ratio,  $W/D$ .

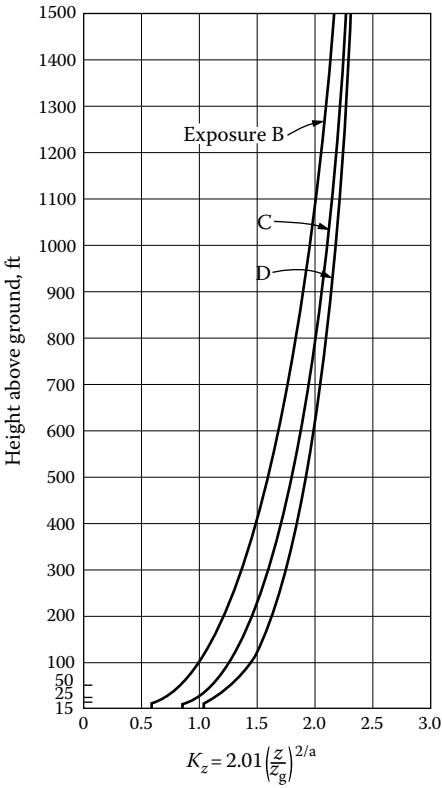


FIGURE 4.16 Combined velocity pressure and exposure coefficients,  $K_h$  and  $K_z$ .

Velocity Pressure Exposure Coefficients, $K_z^{a,b}$				
Height above Ground Level, $z$		Exposure Category		
ft	(m)	B	C	D
0–15	(0–4.6)	0.57	0.85	1.03
20	(6.1)	0.62	0.90	1.08
25	(7.6)	0.66	0.94	1.12
30	(9.1)	0.70	0.98	1.16
40	(12.2)	0.76	1.04	1.22
50	(15.2)	0.81	1.09	1.27
60	(18)	0.85	1.13	1.31
70	(21.3)	0.89	1.17	1.34
80	(24.4)	0.93	1.21	1.38
90	(27.4)	0.96	1.24	1.40
100	(30.5)	0.99	1.26	1.43
120	(36.6)	1.04	1.31	1.48
140	(42.7)	1.09	1.36	1.52
160	(48.8)	1.13	1.39	1.55
180	(54.9)	1.17	1.43	1.58
200	(61.0)	1.20	1.46	1.61
250	(76.2)	1.28	1.53	1.68
300	(91.4)	1.35	1.59	1.73
350	(106.7)	1.41	1.64	1.78
400	(121.9)	1.47	1.69	1.82
450	(137.2)	1.52	1.73	1.86
500	(152.4)	1.56	1.77	1.89
550	(167.6)	1.61	1.81	1.93
600	(182.9)	1.65	1.85	1.96
650	(191.1)	1.69	1.88	1.98
700	(213.3)	1.72	1.91	2.01
750	(228.6)	1.76	1.93	2.03
800	(243.8)	1.79	1.96	2.06
850	(259.1)	1.82	1.99	2.08
900	(274.3)	1.85	2.01	2.10
950	(289.5)	1.88	2.03	2.12
1000	(304.8)	1.91	2.06	2.14
1050	(320)	1.93	2.08	2.16
1100	(335.3)	1.96	2.10	2.17
1150	(350.5)	1.99	2.12	2.19
1200	(365.7)	2.01	2.14	2.21
1250	(381)	2.03	2.15	2.22
1300	(396.2)	2.06	2.17	2.24
1350	(411.5)	2.08	2.19	2.26
1400	(426.7)	2.10	2.21	2.27
1450	(441.9)	2.12	2.22	2.28
1500	(457.2)	2.14	2.24	2.29

(Adapted from Table 6.3 of ASCE 7-05.)

<sup>a</sup> The velocity pressure exposure coefficient  $K_z$  may be determined from the following formula:  
For  $15\text{ ft} \leq z \leq z_g$ ,  $K_z = 2.01 (z/z_g)^{2/\alpha}$ .  
For  $z < 15\text{ ft}$ ,  $K_z = 2.01 (15/z_g)^{2/\alpha}$ .

<sup>b</sup> All main wind force resisting systems in buildings and in other structures except those in low-rise buildings.

FIGURE 4.17  $K_z$  values for buildings up to 1500 ft tall.

The wind directionality factor,  $K_d$ , accounts for two effects:

- The reduced probability of maximum winds blowing from any given direction
- The reduced probability of the maximum pressure coefficient occurring for any given direction

As mentioned previously, wind velocity within the boundary layer increases with the height above ground level. The factor  $K_z$  accounts for this and for exposure category. It is used as a multiplier to increase the basic wind speed  $V$ , to the design speed at height  $z$  above ground level.

It also varies with the characteristics of ground surface irregularities at the building site that arise as a result of natural topographic variations as well as human-made features.

The power coefficient  $\alpha$  (see ASCE 7-05 Table 6.2, Table 4.2 of this text) is the exponent for velocity increase in height, and has respective values of 7.0, 9.5, and 11.5 for exposure B, C, and D. As stated previously the values of  $K_z$  for the three exposures up to a height of 500 ft (152.6 m) are given in ASCE 7-05. An extended version up to a height of 1500 ft (457 m) is given in Figures 4.16 and 4.17.  $K_z$  is assumed constant for heights less than 15 ft (4.6 m) and for heights greater than the gradient height. A graph showing variation of velocity pressure  $q_z$  for gradient speeds of 85, 90, 110, 130, and 150 mph, for exposure categories B, C, and D is shown in Figures 4.18 and 4.19.

#### 4.4.2.1 Wind Speedup over Hills and Escarpments: $K_{zt}$ Factor

As stated previously, the topographic factor  $K_{zt}$  accounts for the effect of isolated hills or escarpments located in exposures B, C, and D. Buildings sited on upper half of isolated hill or escarpment experience significantly higher wind speeds than buildings situated at local level ground. To account for these higher wind speeds, the velocity pressure exposure coefficient is multiplied by a topographic factor  $K_{zt}$ , determined from the three multipliers  $K_1$ ,  $K_2$ , and  $K_3$  (Figure 4.11).  $K_1$  is related to the shape of the topographic feature and the maximum speedup with distance upwind or downward of the crest.  $K_2$  accounts for the reduction in speedup with distance upwind or downwind of the crest, and  $K_3$  for the reduction in speedup with height above the local ground surface.

The ASCE 7-05 equations for calculating the topographic factor,  $K_{zt}$ , are approximations derived from curve fitting of these equations to the accumulated data from wind-tunnel tests. The equations and curves are complex, and the use of footnotes given in the ASCE 7-05 is somewhat confusing. Even experienced engineers often miscalculate the topographic factor. Much of the confusion in the calculation of  $K_{zt}$  is based on how the equations are manipulated when the height,  $H$ , of the topographic feature exceeds half of  $L_h$ , the half-length of the topographic feature.

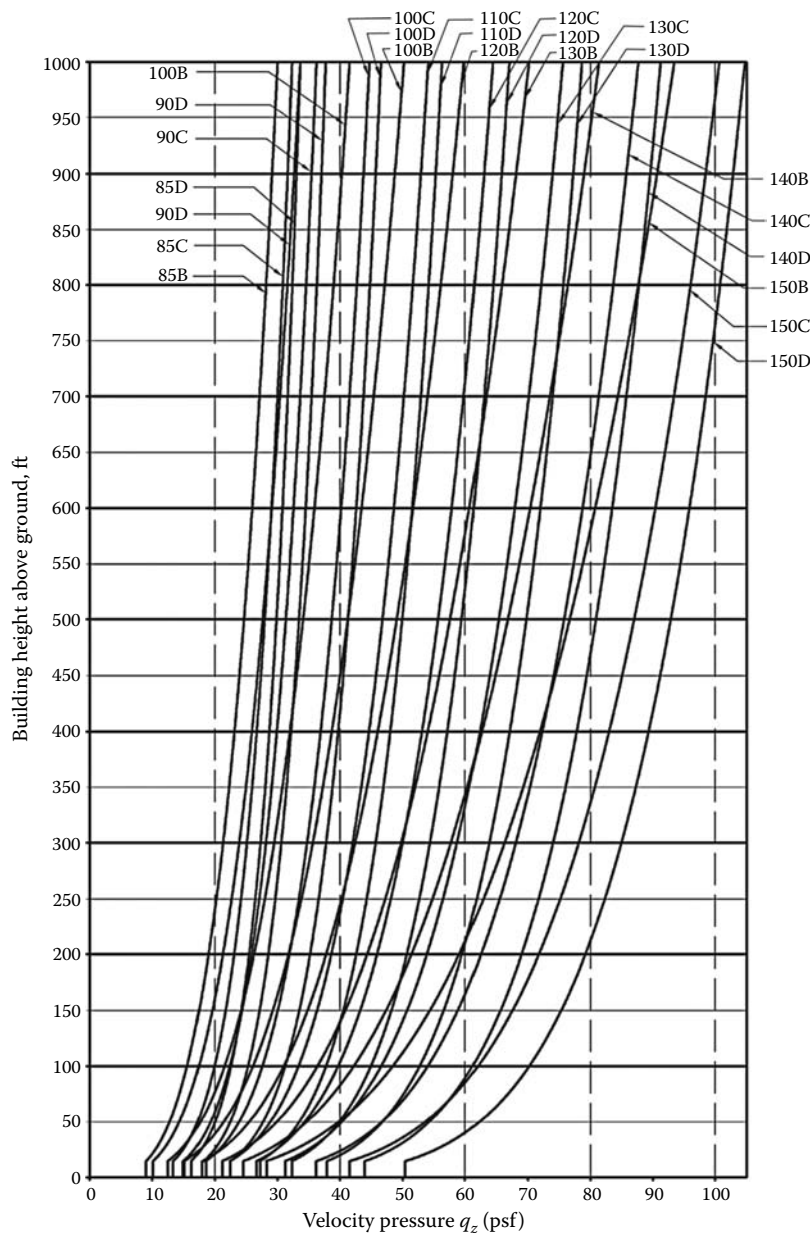
However, to get a feel for the  $K_{zt}$  factor, results of design pressure,  $p$ , are given for a relatively short building in Figures 4.20 and 4.21.

**TABLE 4.2**  
**Terrain Exposure Constants**

Exposure	$\alpha$	$z_g$ (ft)	$\hat{a}$	$\hat{b}$	$\bar{\alpha}$	$\bar{b}$	$c$	$\ell$ (ft)	$\bar{e}$	$z_{\min}$ (ft) <sup>a</sup>
B	7.0	1200	1/7	0.84	1/4.0	0.45	0.30	320	1/3.0	30
C	9.5	900	1/9.5	1.00	1/6.5	0.65	0.20	500	1/5.0	15
D	11.5	700	1/11.5	1.07	1/9.0	0.80	0.15	650	1/8.0	7

(From ASCE 7-05, Table 6.2.)

<sup>a</sup>  $z_{\min}$  = minimum height used to ensure that the equivalent height  $\bar{z}$  is the greater of  $0.6h$  or  $z_{\min}$ . For building with  $h \leq z_{\min}$ ,  $\bar{z}$  shall be taken as  $z_{\min}$ .



**FIGURE 4.18** Variation of positive velocity pressure,  $q_z$ , versus wind speed and exposure categories.  
*Note:* Gust factor,  $G_f$ , varies from 1.05 to 1.25.

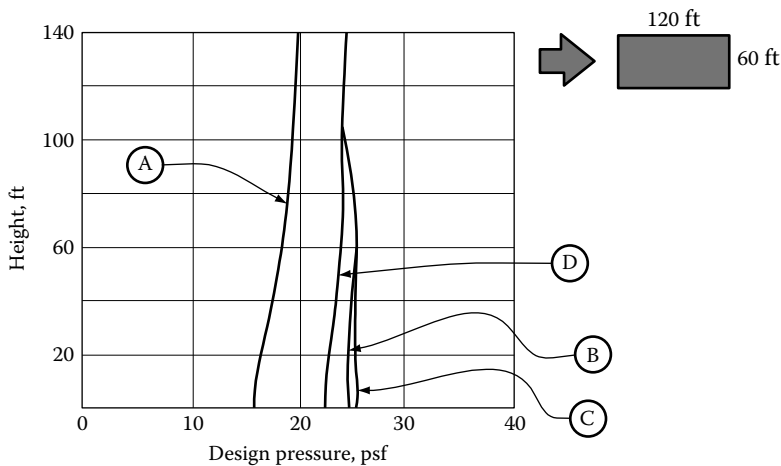
**4.4.2.2 Gust Effect Factor**

This factor accounts for dynamic amplification of loading in the along-wind direction due to wind turbulence and structure interaction. It does not include allowances for across-wind loading effects, vortex shedding, instability due to galloping or flutter, or dynamic torsional effects. Buildings susceptible to these effects should be designed using wind-tunnel test results.

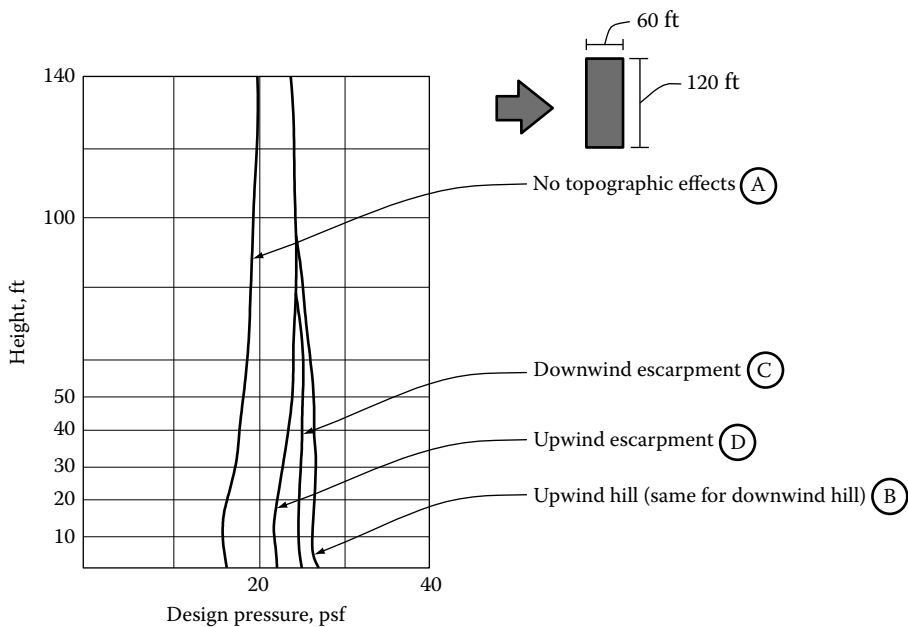
Three methods are permitted for calculating  $G$ . The first two are for rigid structures and the third is for flexible or dynamically sensitive structures.

Building height above ground, ft	Velocity Pressure $q_z$ (psf)																							
	85B	85C	85D	90B	90C	90D	100B	100C	100D	110B	110C	110D	120B	120C	120D	130B	130C	130D	140B	140C	140D	150B	150C	150D
0 to 15	9.04	13.35	16.20	10.13	14.96	18.16	12.51	18.47	22.42	15.13	22.35	27.13	18.01	26.60	32.28	21.13	31.22	37.89	24.51	36.20	43.94	28.14	41.56	50.44
25.0	10.46	14.86	17.70	11.72	16.66	19.85	14.47	20.57	24.50	17.51	24.89	29.65	20.84	29.62	35.28	24.46	34.76	41.41	28.36	40.32	48.02	32.56	46.28	55.13
50.0	12.75	17.20	19.97	14.29	19.28	22.38	17.64	23.80	27.64	21.34	28.80	33.44	25.40	34.27	39.80	29.81	40.22	46.71	34.58	46.65	54.17	39.69	53.55	62.19
100.0	15.54	19.90	22.53	17.42	22.31	25.26	21.50	27.54	31.18	26.02	33.32	37.73	30.97	39.66	44.90	36.34	46.54	52.69	42.15	53.98	61.11	48.38	61.96	70.16
150.0	17.44	21.67	24.17	19.56	24.30	27.10	24.15	20.00	33.46	29.22	36.29	40.48	34.77	43.19	48.18	40.81	50.69	56.54	47.32	58.79	65.58	54.33	67.49	75.28
200.0	18.94	23.02	25.41	21.23	25.81	28.49	26.21	31.87	35.18	31.72	38.58	42.56	37.75	45.89	50.65	44.30	53.85	59.45	51.38	62.46	68.94	58.98	71.70	79.14
250.0	20.19	24.13	26.42	22.63	27.05	29.62	27.94	33.40	36.57	33.81	40.41	44.25	40.23	48.10	52.66	47.22	56.44	61.80	54.76	65.46	71.67	62.86	75.15	82.28
300.0	21.27	25.08	27.27	23.84	28.11	30.57	29.43	34.71	37.74	35.61	41.99	45.67	42.38	49.98	54.35	49.74	58.65	63.79	57.69	68.02	73.98	66.22	78.09	84.93
350.0	22.22	25.90	28.01	24.91	29.04	31.40	30.76	35.85	38.77	37.22	43.38	46.91	44.29	51.63	55.83	51.98	60.59	65.52	60.29	70.27	75.99	69.21	80.66	87.23
400.0	23.09	26.64	28.67	25.88	29.87	32.14	31.95	36.87	39.68	38.67	44.62	48.01	46.01	53.10	57.14	54.00	62.32	67.06	62.63	72.27	77.78	71.90	82.96	89.28
450.0	23.88	27.31	29.26	26.77	30.62	32.81	33.05	37.80	40.50	39.99	45.74	49.01	47.59	54.43	58.32	55.85	63.88	68.45	64.77	74.09	79.39	74.36	85.05	91.13
500.0	24.61	27.92	29.80	27.59	31.30	33.41	34.06	38.65	41.25	41.21	46.76	49.91	49.04	55.65	59.40	57.56	65.31	69.72	66.75	75.75	80.85	76.63	86.96	92.82
550.0	25.29	28.49	30.30	28.35	31.94	33.97	35.00	39.43	41.94	42.35	47.71	50.75	50.40	56.78	60.40	59.15	66.64	70.88	68.60	77.28	82.20	78.75	88.72	94.37
600.0	25.92	29.01	30.76	29.06	32.53	34.49	35.88	40.16	42.58	43.41	48.59	51.62	51.67	57.83	61.32	60.64	67.87	71.96	70.32	78.71	83.46	80.73	90.36	95.81
650.0	26.52	29.51	31.20	29.73	33.08	34.97	36.71	40.84	43.18	44.42	49.42	52.24	52.86	58.81	62.18	62.04	69.02	72.97	71.95	80.05	84.63	82.60	91.89	97.15
700.0	27.09	29.97	31.60	30.37	33.60	35.43	37.50	41.48	43.74	45.37	50.20	52.92	53.99	59.74	62.98	63.37	70.11	73.92	73.49	81.31	85.73	84.36	93.34	98.41
750.0	27.63	30.41	31.98	30.98	34.09	35.86	38.24	42.09	44.27	46.27	50.93	53.56	55.07	60.61	63.74	64.63	71.13	74.81	74.95	82.50	86.76	86.04	94.70	99.60
800.0	28.14	30.83	32.34	31.55	34.56	36.26	38.95	42.67	44.77	47.13	51.63	54.17	56.09	61.44	64.46	65.83	72.11	75.65	76.35	83.63	87.74	87.64	96.00	100.72
850.0	28.64	31.22	32.69	32.10	35.00	36.64	39.63	43.21	45.24	47.96	52.29	54.74	57.07	62.23	65.15	66.98	73.03	76.46	77.68	84.70	88.67	89.18	97.23	101.79
900.0	29.11	31.60	33.01	32.63	35.43	37.01	40.29	43.74	45.69	48.75	52.92	55.29	58.01	62.98	65.80	68.08	73.92	77.22	78.96	85.73	89.56	90.64	98.41	102.81
950.0	29.56	31.96	33.32	33.14	35.83	37.36	40.91	44.24	46.12	49.51	53.53	55.81	58.92	63.70	66.42	69.14	74.76	77.95	80.19	86.71	90.40	92.06	99.54	103.78
1000.0	30.00	32.31	33.62	33.63	36.22	37.69	41.52	44.72	46.54	50.24	54.11	56.31	59.79	64.39	67.01	70.16	75.57	78.65	81.37	87.65	91.21	93.41	100.62	104.71

FIGURE 4.19 Variation of velocity pressure,  $q_z$ , versus wind speed.



**FIGURE 4.20** Comparison of topographic effects, Exposure C, wind on narrow face.



**FIGURE 4.21** Comparison of topographic effect, Exposure C, wind on broad face.

4.4.2.2.1 Gust Effect Factor  $G$  for Rigid Structure: Simplified Method

For rigid structures (defined as those having a natural frequency of vibration greater than 1 Hz), the engineer may use a single value of  $G = 0.85$ , irrespective of exposure category.

4.4.2.2.2 Gust Effect Factor  $G$  for Rigid Structure: Improved Method

As an option to using  $G = 0.85$ , the engineer may calculate a more accurate value by including specific features of the wind environment at the building site.



The gust effect factor,  $G$ , is given by

$$G = 0.925 \left( \frac{1 + 1.7 g_Q I_{\bar{z}} Q}{1 + 1.7 g_v I_{\bar{z}}} \right)$$

$$I_{\bar{z}} = C(33 / \bar{z})^{1/6} \quad (4.12)$$

where  $I_{\bar{z}}$  is the intensity of turbulence at height  $\bar{z}$ , and  $\bar{z}$  is the equivalent height of the structure defined as  $0.6h$  but not less than  $z_{\min}$  for all building heights  $h$ .  $z_{\min}$  and  $c$  are listed for each exposure in Table 4.2 of this text (ASCE 7-05, Table 6.2);  $g_Q$  and  $g_v$  shall be taken as 3.4. The background response,  $Q$ , is given by

$$Q = \sqrt{\frac{1}{1 + 0.63(B + h/L_{\bar{z}})^{0.63}}} \quad (4.13)$$

where  $B$ ,  $h$  are defined in Section 6.3; and  $L_{\bar{z}}$  is the integral length scale of turbulence at the equivalent height given by

$$L_{\bar{z}} = l(\bar{z}/33)^{\bar{\epsilon}}$$

in which  $l$  and  $\bar{\epsilon}$  are constants listed in Table 6.2 of ASCE 7-05 (Table 4.2 of this chapter).

#### Design Example: Gust Effect Factor $G$ : Improved Method

**Given:** A 10-story concrete building with the following characteristics:

- Height,  $h = 12$  ft
- Width perpendicular to wind,  $B = 90$  ft
- Exposure category = C
- Basic wind speed,  $V = 100$  mph
- Topographic factor,  $K_{zt} = 1.0$
- Building depth parallel to wind,  $L = 95$  ft
- Building natural frequency,  $n_1 = 1.1$  Hz

**Required:** Gust effect factor  $G$ , using the improved method.

**Solution:**

ASCE 7-05 Formulas	Commentary
$\bar{z} = 0.6 \times h = 0.6 \times 112 = 67.2$ ft	$h$ = building height = 112 ft, given $c$ from Table 6.4
$I_{\bar{z}} = C \left( \frac{33}{\bar{z}} \right)^{1/6} = 0.2 \left( \frac{33}{67.2} \right)^{1/6} = 0.1776$	$l$ and $\epsilon$ from Table 6.4
$L_{\bar{z}} = l \left( \frac{\bar{z}}{33} \right)^{\epsilon}$	
$= 500 \left( \frac{67.2}{33} \right)^{1/5}$	
$= 576$	

(continued)

ASCE 7-05 Formulas	Commentary
$Q = \sqrt{\frac{1}{1 + 0.63(B + h / L_z)^{0.63}}}$ $= \sqrt{\frac{1}{1 + 0.63(90 + 112 / 576)^{0.63}}}$ $= 0.87$	$Q$ = background response $B$ = building width perpendicular to wind = 112 ft, given
$G = 0.925 \left( \frac{1 + 1.7g_Q I_z Q}{1 + 1.7g_v I_z} \right)$ $= 0.925 \left( \frac{1 + 1.7 \times 3.4 \times 0.1776 \times 0.86}{1 + 1.7 \times 3.4 \times 0.1776} \right)$ $= 0.86$	$G$ = gust effect factor

Observe this is not much different from  $G = 0.85$  permitted for rigid structures, because its natural frequency of 1.1 Hz, is very nearly equal to 1.0 Hz, the cutoff frequency between rigid and flexible structures.

#### 4.4.2.2.3 Gust Effect Factor $G_f$ for Flexible or Dynamically Sensitive Buildings

Gust effect factor,  $G_f$ , depends on

- Basic wind speed  $V$
- Exposure category B, C, or D
- Building natural frequency
- Building damping

ASCE 7-05 defines a rigid building as “A building whose fundamental frequency is greater than or equal to 1 Hz.” The commentary of ASCE 7 goes on to state, “When buildings or other structures have a height exceeding four times the least horizontal dimension or when there is reason to believe that the natural frequency is less than 1 Hz (natural period greater than 1 s), the natural frequency for it should be investigated.” The ASCE 7 commentary explains the difference between the natural frequency calculated by approximate methods for seismic design and appropriate estimates of natural frequency for wind design. Approximate equations of natural frequency developed for seismic design tend to give higher estimates of the natural frequency (lower estimates of the structure’s period), as this gives conservative approximation of the seismic base shear. For wind design, the opposite case exists. That is, these higher estimates of the structure’s natural frequency can incorrectly categorize very slender buildings as rigid, when they are in fact, flexible. Alternate equations for natural frequency of various building types and comparison of results of these equations to values used in other countries, are given in the ASCE 7-05 commentary. When using ASCE 7, an engineer needs to determine whether the structure can be categorized as rigid.

A building is considered flexible if it contains a significant dynamic response. Resonant response depends on the gust structure contained in the approaching wind, on wind loading pressures generated by the wind flow about the building, and on dynamic properties of the building. Gust energy in wind is smaller at frequencies about 1 Hz; therefore resonant response of most buildings and structures with lowest natural frequency above 1 Hz will be sufficiently small that resonant response can often be ignored. When buildings have a height exceeding four times the least horizontal dimension or when there is reason to believe that the natural frequency is less than 1 Hz (natural period greater than 1 s), the natural frequency should be investigated.

The formula for calculating  $G_f$  is as follows:

$$G_f = 0.925 \left( \frac{1 + 1.7I_{\bar{z}} \sqrt{g_Q^2 Q^2 + g_R^2 R^2}}{1 + 1.7g_v I_{\bar{z}}} \right) \quad (4.14)$$

where  $g_Q$  and  $g_v$  shall be taken as 3.4 and  $g_R$  is given by

$$g_R = \sqrt{2 \ln(3600n_1)} + \frac{0.577}{\sqrt{2 \ln(3600n_1)}} \quad (4.15)$$

and where  $R$ , the resonant response factor, is given by

$$R = \sqrt{\frac{1}{\beta} R_n R_h R_B (0.53 + 0.47 R_L)} \quad (4.16)$$

$$R_n = \frac{7.47 N_1}{(1 + 10.3 N_1)^{5/3}} \quad (4.17)$$

$$N_1 = \frac{n_1 L_{\bar{z}}}{\bar{V}_{\bar{z}}} \quad (4.18)$$

$$R_\ell = \frac{1}{\eta} - \frac{1}{2\eta^2} (1 - e^{-2\eta}) \quad \text{for } \eta > 0 \quad (4.19)$$

$$R_\ell = 1 \quad \text{for } \eta = 0 \quad (4.20)$$

where

the subscript  $\ell$  in Equation 4.19 shall be taken as  $h$ ,  $B$ , and  $L$ , respectively

$n_1$  is the building natural frequency

$R_\ell = R_h$  setting  $\eta = 4.6n_1 h / \bar{V}_{\bar{z}}$

$R_\ell = R_B$  setting  $\eta = 6.4n_1 B / \bar{V}_{\bar{z}}$

$R_\ell = R_L$  setting  $\eta = 15.4n_1 L / \bar{V}_{\bar{z}}$

$\beta$  is the damping ratio, percent of critical  $h$ ,  $B$ ,  $L$  are defined in Section 6.3

$\bar{V}_{\bar{z}}$  is the mean hourly wind speed (ft/s) at height  $\bar{z}$  determined from equation:

$$\bar{V}_{\bar{z}} = \bar{b} \left( \frac{\bar{z}}{33} \right)^{\bar{\alpha}} V \left( \frac{88}{60} \right) \quad (4.21)$$

where

$\bar{b}$  and  $\bar{\alpha}$  are constants listed in Table 4.10

$V$  is the basic wind speed in miles per hour

**Design Example: Gust Effect Factor  $G_f$ : Flexible Structure Given****Given:**

- Building height,  $h = 600$  ft
- Building width perpendicular to wind,  $B = 100$  ft
- Building depth parallel to wind,  $L = 100$  ft
- Building natural frequency,  $n_1 = 0.2$  Hz
- Damping ratio = 0.015
- Exposure category = C
- Basic wind speed,  $V = 140$  mph

**Required:** Gust effect factor  $G_f$ **Calculation of Gust Effect Factor,  $G_f$** **ASCE 7-05 Formulas****Commentary** $V$  = wind speed in ft/s $V = 140$  mph, given

$$= V_{\text{mph}} \times 1.467$$

$$= 140 \times 1.467 = 205 \text{ ft/s}$$

 $\bar{z} = 0.6h$ , but not less than  $z_{\min}$  $h$  = building height

$$= 0.6 \times 600 = 360 \text{ ft} > \bar{z}_{\min} = 15 \text{ ft OK}$$

= 600 ft, given

 $\bar{z}_{\min} = 15$  ft, from Table 6.4 $c = 0.20$ , from Table 6.4

$$I_{\bar{z}} = C \left( \frac{33}{\bar{z}} \right)^{1/6} = 0.20 \left( \frac{33}{360} \right)^{1/6} = 0.134$$

$$L_{\bar{z}} = I \left( \frac{\bar{z}}{33} \right)^{\epsilon} = 500 \left( \frac{360}{33} \right)^{1/6} = 806 \text{ ft}$$

 $l = 500$  ft,  $\epsilon = 1/5$ , from Table 6.4

$$Q = \sqrt{\frac{1}{1 + 0.63(B + h/L_{\bar{z}})^{0.63}}}$$

$$= \sqrt{\frac{1}{1 + 0.63(100 + 600/761)^{0.63}}}$$

$$= 0.796, \quad Q^2 = 0.634$$

 $Q$  = background response $B$  = building width perpendicular to wind

= 100 ft, given

$$\bar{V}_{\bar{z}} = \bar{b} \left( \frac{\bar{z}}{33} \right)^{\bar{\alpha}} V = 0.65 \left( \frac{360}{33} \right)^{1/6.5} \times 205 = 192 \text{ ft/s}$$

 $\bar{b} = 0.65$ , $\bar{\alpha} = 1/6.5$ , from Table 6.4

$$\hat{V}_{\bar{z}} = \hat{b} \left( \frac{\bar{z}}{33} \right)^{\hat{\alpha}} V = 1.0 \times \left( \frac{360}{33} \right)^{1/9.5} \times 205 = 264 \text{ ft/s}$$

 $\hat{b} = 1.0$ ,  $\hat{\alpha} = 1.0$ , from Table 6.4

$$N_1 = \frac{n_1 L_{\bar{z}}}{\bar{V}_{\bar{z}}} = \frac{0.2 \times 806}{192} = 0.84$$

 $n_1$  = natural frequency

= 0.2 Hz, given

$$R_n = \frac{7.47 N_1}{(1 + 10.3 N_1)^{5/3}}$$

$$= \frac{7.47 \times 0.84}{(1 + 10.3 \times 0.84)^{5/3}} = 0.143$$

(continued)

### Calculation of Gust Effect Factor, $G_f$ (continued)

#### ASCE 7-05 Formulas

#### Commentary

$$\eta_b = \frac{4.6n_b B}{V_z} = \frac{4.6 \times 0.2 \times 100}{192} = 0.479$$

$$e = 2.71$$

$$\begin{aligned} R_b &= \frac{1}{\eta_b} - \frac{1}{2\eta_b^2} (1 - e^{-2\eta_b}) \\ &= \frac{1}{0.479} - \frac{1}{2 \times 0.479^2} (1 - 2.71^{-2 \times 0.479}) \\ &= 0.739 \end{aligned}$$

$$\eta_h = \frac{4.6n_h h}{V_z} = \frac{4.6 \times 0.2 \times 600}{192} = 2.875$$

$$\begin{aligned} R_h &= \frac{1}{\eta_h} - \frac{1}{2\eta_h^2} (1 - e^{-2\eta_h}) \\ &= \frac{1}{2.875} - \frac{1}{2 \times 2.875^2} (1 - 2.71^{-2 \times 2.875}) \\ &= 0.288 \end{aligned}$$

$$\eta_L = \frac{15.4n_L L}{V_z} = \frac{15.4 \times 0.2 \times 100}{192} = 1.604$$

$L$  = building breadth parallel to wind = 100 ft, given

$$\begin{aligned} R_L &= \frac{1}{\eta_L} - \frac{1}{2\eta_L^2} (1 - 2.71^{-2\eta_L}) \\ &= \frac{1}{1.604} - \frac{1}{2 \times 1.604^2} (1 - 2.71^{-2 \times 1.604}) \\ &= 0.618 \end{aligned}$$

$$\begin{aligned} R^2 &= \frac{1}{\beta} R_b R_h R_L (0.53 + 0.47 R_L) \\ &= \frac{1}{0.015} \times 0.143 \times 0.288 \times 0.739 (0.53 + 0.47 \times 0.618) \\ &= 1.665, \quad R = \sqrt{1.665} = 1.29 \end{aligned}$$

$\beta$  = damping ratio = 0.015, given

$$\begin{aligned} g_R &= \sqrt{2 \ln(3600 \times n_1)} + \frac{0.577}{\sqrt{2 \ln(3600 \times n_1)}} \\ &= \sqrt{2 \ln(3600 \times 0.2)} + \frac{0.577}{\sqrt{2 \ln(3600 \times 0.2)}} \\ &= 3.789 \end{aligned}$$

In means logarithm to base  $e = 2.71$

$$\begin{aligned} G &= 0.925 \left( \frac{1 + 1.7 I_{\bar{x}} \sqrt{g_Q^2 Q^2 + g_R R^2}}{1 + 1.7 g_v I_{\bar{x}}} \right) \\ &= 0.925 \left( \frac{1 + 1.7 \times 0.134 \sqrt{3.4^2 \times 0.634 + 3.789^{-2} \times 1.665}}{1 + 1.7 \times 3.4 \times 0.134} \right) \\ &= 1.185 \end{aligned}$$

$G$  is the gust factor  $g_Q = g_v = 3.4$  (defined in the equation for  $G$ )

Wind Speed, mph	Gust Effect Factor, $G_f$		
	Exposure Category		
	B	C	D
150	1.32	1.28	1.25
140	1.28	1.25	1.22
130	1.24	1.21	1.20
120	1.20	1.18	1.17
110	1.16	1.14	1.13
100	1.11	1.11	1.10
90	1.07	1.07	1.07
85	1.05	1.05	1.05

**FIGURE 4.22** Variation of gust factor,  $G_f$ .

#### 4.4.2.2.4 Sensitivity Study of Gust Effect Factor $G_f$

**Given:** A concrete building of height 1000 ft.

- Building width = 250 ft
- Building length = 150 ft
- Topographic factor  $K_{zt} = 1.0$
- Building frequency = 0.10 Hz (period 10 s)

**Required:** Calculate gust effect factor,  $G_f$ , for basic wind speeds of 85, 90, 100, 110, 120, 130, 140, and 150 mph. Prepare a table showing values of  $G_f$  for exposure categories B, C, and D.

**Solution:** The values of  $G_f$  calculated by using a spread sheet are shown in Figure 4.22.

#### 4.4.2.3 Determination of Design Wind Pressures Using Graphs

Using this procedure the engineer can quickly determine wind pressures for the design of MWFRS. An illustrative example follows.

**Given:**

A concrete building located in a hurricane-prone region with the following characteristics:

- Building height = 450 ft (137.15 m)
- Building plan dimensions =  $185 \times 125$  ft ( $56.396 \times 38.10$  m)
- Exposure category = C
- Basic wind speed = 110 mph (49 m/s)
- The building is sited on the upper half of a 2D ridge and has the following topographic parameters:

$$L_h = 200 \text{ ft}, H = 200 \text{ ft}, x = 50 \text{ ft}$$

(see Figure 4.20 for definitions)

- The building is for typical office occupancy. However, it does have designated areas where more than 300 people congregate in one area
- Damping ratio = 0.02 (2% of critical)

**Required:** Using the graph given in Figure 4.18 determine design wind pressures for the MWFRS of the building for wind parallel to the short side. Also determine wind pressures assuming  $K_{zt} = 1.0$ .

**Solution:**

- The building is for office occupancy with certain areas designated for the congregation of more than 300 people. From Table 1.1 of ASCE 7-05, the classification of the building for wind is category III, and importance factor for wind  $I_w = 1.15$ .
- Exposure category is C and basic wind speed  $V = 110$  mph, as given in the statement of the problem. We select the curve designated as 110C in Figure 4.18 to read the positive and negative pressures up the building height.
- The building's height- to least-horizontal dimension is  $450/125 = 3.6$ , less than 4.
- Therefore, the building may be considered rigid from the first definition given in ASCE 7-05 Commentary Section C6.2. The second definition refers to the fundamental period  $T$  of the building. Using the formula given in Section 12.8.2.1 of the ASCE 7-05, we get

$$T_a = C_t h_n^{3/4} \quad (4.22)$$

where

$T$  is the fundamental period of the building, in seconds

$h_n$  is the height of the building, in feet

$C_t$  is the coefficient equal to 0.030 for concrete moment frame buildings

$T_a = 0.030 \times 450^{3/4} = 2.93$  s (say, 3 s)

The natural frequency,  $n$ , which is the reciprocal of the period, is equal to  $1/T = 1/3 = 0.33$  Hz. This is less than 1 Hz, the limiting frequency that delineates a rigid structure from a flexible structure. Therefore gust effect factor  $G_f$  must be determined using the procedure given in ASCE 7-05 Section 6.5.8.2. However, to emphasize the graphical procedure, for now we will use a value of  $G_f = 0.910$ . This value will be determined in the next section in which calculations for along-wind response of the example building are also shown.

- Because the building is located on a 2D ridge, it may experience higher winds than buildings situated on level ground. Therefore, we consider topographic effects in the determination of design wind pressures.

For the given values of  $L_h$ ,  $H$ , and  $x$ , the multipliers  $K_1$ ,  $K_2$ , and  $K_3$  are obtained from Figure 4.11. Observe that for  $H/L_h > 0.5$ , Note 2 of ASCE Figure 6.4, alerts us to assume  $H/L_h = 0.5$  for evaluating  $K_1$  and to substitute  $2H$  for  $L_h$  for evaluating  $K_2$  and  $K_3$ . Therefore, for  $H/L_h = 200/200 = 1.0$ , which is greater than 0.5. Thus for exposure C, for a 2D ridge,  $K_1 = 0.725$ .

Substituting  $2H$  for  $H$ ,  $x/H = x/2H = 50/400 = 0.125$ , and from ASCE Figure 6.4,  $K_2 = 0.92$ . Instead of the tabulated values, we may also use the formulas given in Figure 6.4, page 46 of ASCE 7-05, to calculate  $K_2$  and  $K_3$ . Thus

$$\begin{aligned} K_2 &= \left( 1 - \frac{|x|}{\mu L_h} \right) \\ &= \left( 1 - \frac{50}{1.5 \times 400} \right) = 0.92 \quad (\text{note that for } H/L_h > 0.5, L_h = 2H, \text{ for calculating } K_2) \end{aligned}$$

The parameter  $K_3$  varies with the ratio  $x/L_h$ . It may be obtained by using either the tabulated values in Figure 4.11 or the formula given in Figure 4.12.

$$K_3 = e^{-\gamma(z/L_h)}$$

Again, substituting  $2H$  for  $L_h$ , and  $\gamma = 3$

$$K_3 = e^{-3(z/400)}$$

We use the preceding formula to calculate  $K_3$  for the selected  $z/L_h$  values shown below. Note that  $\gamma = 3$  for 2D ridges, which is the topography for our building.

$z$ (ft)	450	350	250	150	100	50	30	15
$z/L_h$	2.25	1.75	1.25	0.75	0.50	0.25	0.15	0.08
$K_3$	0.001	0.005	0.023	0.106	0.224	0.473	0.638	0.78

**Wind Parallel to short side of Building:** From the building's plan dimensions,  $L/B = 125/180 = 0.694 < 1.0$ . Therefore, from Figure 4.14,  $C_p$  for the windward face = 0.8, and  $C_p$  for the leeward face =  $-0.5$ . From Figure 4.18, select the curve identified as 110C. C stands for exposure C, and 110 stands for  $V = 110$  mph. Use the graph to read the values of  $q_z$  at various heights. For example, at  $h = 150$  ft,  $q_z = 36.3$  psf.

However, since the  $q_z$  and  $q_h$  values in Figure 4.18 are normalized for  $K_{zt} = 1.0$ ,  $K_d = 0.85$ , and  $I_w = 1.0$ , we multiply these values by the  $K_{zt}$  and  $I_w$  values of the example problem before recording the corresponding values in columns (7) and (8) of Table 4.10. For example,  $q_z = 36.3$  psf at  $z = 150$  ft, obtained from the graph is multiplied by  $K_{zt} = 1.145$  and  $I_w = 1.15$ , to get a value of  $q_z = 47.79$  psf, shown in column (7).

Observe that  $K_{zt}$  varies up the height. Values of  $q_z$  for different heights are recorded in column (7) of Table 4.10 after multiplication by  $K_{zt}$  and  $I_w$ . The suction  $q_h$  in column (8) is the value from the graph at  $z = h = 450$  ft multiplied by  $K_{zt} = 1.002$  and  $I_w = 1.15$ . Observe that the suction  $q_h$  referenced at roof height remains constant for the entire height of leeward wall. Column (9) gives the total design wind pressure. It is the summation of  $0.8q_z$ , the positive pressure on the windward wall, plus  $0.5q_h$ , the suction on the leeward wall, multiplied by the gust effect factor  $G_f = 0.91$ .

For comparative purposes, the last column of Table 4.3 gives the design pressures  $P$  for the building assuming that it is located on a flat terrain, that is,  $K_{zt} = 1.0$ .

**TABLE 4.3**  
**Design Wind Pressures, Graphical Procedure Using ASCE 7-05**

Height (ft)	$K_z$	$K_h$	$K_1$	$K_2$	$K_3$	$K_{zt} =$ $(1 + K_1 K_2 K_3)^2$	$q_z \times I_w \times K_{zt}$	$q_h$ (psf)	Design Pressure $P = (0.8q_z +$ $0.5q_h) \times G_f$	Design Pressure with Topographic Factor $K_u = 1.0$
450	1.74	1.74	0.725	0.92	0.00	1.002	52.68	52.68	63.4	62.2
400	1.69	1.74	0.725	0.92	0.00	1.003	54.48	52.68	62.5	61.3
350	1.65	1.74	0.725	0.92	0.01	1.007	50.24	52.68	61.6	60.2
300	1.59	1.74	0.725	0.92	0.01	1.014	49.01	52.68	60.7	59.1
250	1.53	1.74	0.725	0.92	0.02	1.031	47.94	52.68	59.9	57.7
200	1.46	1.74	0.725	0.92	0.05	1.067	47.33	52.68	59.5	56.2
150	1.38	1.74	0.725	0.92	0.11	1.145	47.79	52.68	59.8	54.3
100	1.26	1.74	0.725	0.92	0.22	1.318	50.53	52.68	61.8	51.8
50	1.09	1.74	0.725	0.92	0.47	1.726	57.18	52.68	66.6	48.0
30	0.98	1.74	0.725	0.92	0.64	2.027	60.29	52.68	68.9	45.6
15	0.85	1.74	0.725	0.92	0.80	2.343	60.22	52.68	68.9	42.6

Notes:  $G_f = 0.91$ ,  $I_w = 1.15$ ,  $K_d = 0.85$ .



#### 4.4.2.4 Along-Wind Response

Typical modern high-rise buildings are more than likely to be lightweight and flexible and therefore, more prone to dynamic motion problems than their earlier counterparts which had heavy cladding and masonry partitions. However, their dynamic excitations during earthquakes, insofar as perception of motion by the occupants is concerned, are irrelevant because occupants are thankful to have survived the trauma and are less prone to complain about motion perception. On the other hand, the sentiment when estimating peak dynamic response of buildings to fluctuating wind forces is quite different. This may be because windstorms occur more frequently and are not as traumatic as earthquakes. Consequently, it has become necessary to evaluate the buildings dynamic behavior related to wind-induced accelerations at top floors to assess occupants comfort.

When considering the response of a tall building to wind gusts, both along-wind and across-wind responses must be considered. These arise from different effects of wind, the former due to buffeting effects caused by turbulence; the latter due to vortex shedding on opposite sides of building. The cross-wind response may be of particular importance with regard to the comfort of occupants because it is likely to exceed along-wind accelerations. This would occur if the building is slender about both axes with a geometric ratio  $\sqrt{WD/H}$  less than one-third, where  $W$  and  $D$  are the across- and along-wind plan dimensions, and  $H$  is the building height.

The most important criterion for verifying comfort of building's occupants is the peak acceleration they are likely to experience. It is thus important to estimate the probable maximum accelerations in both the along-wind and across-wind directions. ASCE 7-05 gives a method for predicting along-wind responses, including peak acceleration, but does not provide a procedure for estimating across-wind response. However, the National Building Code of Canada (NBCC), addressed presently in this chapter, gives such a procedure.

##### 4.4.2.4.1 Along-Wind Displacement

The maximum along-wind displacement  $X_{\max}(z)$  as a function of height above the ground surface is given by

$$X_{\max} = (z) = \frac{\phi(z)\rho\xi h C_{fx} \hat{V}_z^2}{2m_1(2\pi n_1)^2} - KG \quad (4.23)$$

where

$\phi(z)$  is the fundamental model shape  $= (z/h)^\xi$

$\xi$  is the mode exponent

$\rho$  is the air density

$C_{fx}$  is the mean along-wind force coefficient

$m_1 = \text{modal mass} = \int_0^h \mu(z)\phi^2(z)dz$

where  $\mu(z) = \text{mass per unit height}$ .

$$K = (1.65)^{\hat{\alpha}}/(\hat{\alpha} + \xi + 1) \quad (4.24)$$

$\bar{V}_z$  is the 3 s gust speed at height  $z$ . This can be evaluated as  $\hat{V}_z = \hat{b}(z/33)^{\hat{\alpha}}V$ , where  $V$  is the 3 s gust speed in exposure C at the reference height (obtained from Figure 4.10),  $\hat{b}$  and  $\hat{\alpha}$  are given in Table 4.10.

#### 4.4.2.4.2 Along-Wind Acceleration

The rms along-wind acceleration  $\sigma_{\ddot{x}}(z)$  as a function of height above the ground surface is given by

$$\sigma_{\ddot{x}}(z) = \frac{0.85\phi(z)\rho B h C_{fx} \bar{V}_z^2}{m_1} I_z K R \quad (4.25)$$

where  $\bar{V}_z$  is the mean hourly wind speed at height  $\bar{z}$ , ft/s

$$\bar{V}_z = \bar{b} \left( \frac{\bar{z}}{33} \right)^{\bar{\alpha}} V \quad (4.26)$$

where  $\bar{b}$  and  $\bar{\alpha}$  are defined in Table 4.10a.

The maximum along-wind acceleration as a function of height above the ground surface is given by

$$\ddot{X}_{\max}(z) = g_{\ddot{x}} \sigma_{\ddot{x}}(z) \quad (4.27)$$

$$g_{\ddot{x}} = \sqrt{2 \ln(n_1 T)} + \frac{0.5772}{\sqrt{2 \ln(n_1 T)}} \quad (4.28)$$

where  $T$  is the length of time over which the acceleration is computed, usually taken to be 3600 s to represent 1 h.

#### 4.4.2.4.3 Calculations for Gust Effect Factor, $G_f$ , Along-Wind Displacements and Accelerations

As stated previously, to place emphasis on graphical procedure, we assumed  $G_f = 0.91$  in our previous example. We now calculate this value, and also illustrate numerical procedure for evaluating maximum along-wind displacement and acceleration.

**Given:** The building characteristics and wind environment data are the same as the previous example. However, they are repeated here for convenience.

- Building height = 450 ft (137.15 m)
- Plan dimensions = 185 × 125 ft (36.4 × 38.1 m)
- Exposure category = C
- Basic wind speed  $V = 110$  mph (49 m/s)

**Required:** Gust effect factor  $G_f$  and maximum along-wind displacement and acceleration.

---

#### Calculation for Gust Effect Factor $G_f$ and Maximum Along-Wind Displacement and Accelerations

##### ASCE 7-05 Formulas

$V$  = wind speed in ft/s

$$= V_{\text{mph}} \times 1.467$$

$$= 110 \times 1.467 = 161 \text{ ft/s}$$

$\bar{z} = 0.6 \times h$ , but not less than  $z_{\min}$

$$= 0.6 \times 450 = 270 \text{ ft} > \bar{z}_{\min} = 15 \text{ ft OK}$$

##### Commentary

$V = 110$  mph, given

$h$  = building height = 450 ft, given

$\bar{z}_{\min} = 15$  ft, from Table 6.4

---

(continued)

### Calculations for Gust Effect Factor $G_f$ and Maximum Along-Wind Displacement and Accelerations (continued)

#### ASCE 7-05 Formulas

#### Commentary

$$I_z = C \left( \frac{33}{z} \right)^{1/6} = 0.20 \left( \frac{33}{270} \right)^{1/6} = 0.141$$

$C = 0.20$ , from Table 6.4

$$L_z = l \left( \frac{z}{33} \right)^{\epsilon} = 500 \left( \frac{270}{33} \right)^{1/5} = 761.3 \text{ ft}$$

$l = 500 \text{ ft}$ ,  $\epsilon = 1/5$ , from Table 6.4

$$Q = \sqrt{\frac{1}{1 + 0.63(B + h / L_z)^{0.63}}}$$

$$= \sqrt{\frac{1}{1 + 0.63(185 + 450 / 761)^{0.63}}}$$

$$= 0.80, \quad Q^2 = 0.64$$

$Q$  = the background response  
 $B$  = building width perpendicular to wind  
 = 185 ft, given

$$\bar{V}_z = \bar{b} \left( \frac{z}{33} \right)^{\bar{\alpha}} V = 0.65 \left( \frac{270}{33} \right)^{1/6.5} \times 161 = 144.9 \text{ ft/s}$$

$\bar{b} = 0.65$ ,  $\bar{\alpha} = 1/6.5$ , from Table 6.4

$$\hat{V}_z = \hat{b} \left( \frac{z}{33} \right)^{\hat{\alpha}} V = 1.0 \times \left( \frac{270}{33} \right)^{1/9.5} \times 161 = 201 \text{ ft/s}$$

$\hat{b} = 1.0$ ,  $\hat{\alpha} = 1.0$ , from Table 6.4

$$N_1 = \frac{n_1 L_z}{\bar{V}_z} = \frac{0.33 \times 761}{144.9} = 1.751$$

$n_1$  = natural frequency  
 = 0.33 Hz, given

$$R_n = \frac{7.47 N_1}{(1 + 10.3 N_1)^{5/3}}$$

$$= \frac{7.47 \times 1.751}{(1 + 10.3 \times 1.751)^{5/3}}$$

$$= 0.096$$

$$\eta_b = \frac{4.6 n_1 B}{\bar{V}_z} = \frac{4.6 \times 0.33 \times 185}{144.9} = 1.958$$

$e = 2.71$

$$R_B = \frac{1}{\eta_b} - \frac{1}{2\eta_b^2} (1 - e^{-2\eta_b})$$

$$= \frac{1}{1.958} - \frac{1}{2 \times 1.958^2} (1 - 2.71^{-2 \times 1.958})$$

$$= 0.383$$

$$\eta_h = \frac{4.6 n_1 h}{\bar{V}_z} = \frac{4.6 \times 0.33 \times 450}{144.9} = 4.762$$

$$R_h = \frac{1}{\eta_h} - \frac{1}{2\eta_h^2} (1 - e^{-2\eta_h})$$

$$= \frac{1}{4.762} - \frac{1}{2 \times 4.762^2} (1 - 2.71^{-2 \times 4.762})$$

$$= 0.188$$

$$\eta_L = \frac{15.4 n_1 L}{\bar{V}_z} = \frac{15.4 \times 0.33 \times 125}{144.9} = 4.429$$

$L$  = building breadth parallel to wind  
 = 125 ft, given

### Calculation for Gust Effect Factor $G_f$ and Maximum Along-Wind Displacement and Accelerations (continued)

ASCE 7-05 Formulas

Commentary

$$\begin{aligned}
 R_L &= \frac{1}{\eta_L} - \frac{1}{2\eta_L^2}(1 - 2.71^{-2\eta_L}) \\
 &= \frac{1}{4.429} - \frac{1}{2 \times 4.429^2}(1 - 2.71^{-2 \times 4.429}) \\
 &= 0.200
 \end{aligned}$$

$$\begin{aligned}
 R^2 &= \frac{1}{\beta} R_n R_h R_B (0.53 + 0.47 R_L) & \beta = \text{damping ratio} = 0.02, \text{ given} \\
 &= \frac{1}{0.02} \times 0.096 \times 0.188 \times 0.388 (0.53 + 0.47 \times 0.200) \\
 &= 0.216, \quad R = \sqrt{0.216} = 0.465
 \end{aligned}$$

$$\begin{aligned}
 g_R &= \sqrt{2 \ln(3600 \times n_1)} + \frac{0.577}{\sqrt{2 \ln(3600 \times n_1)}} & \ln \text{ means logarithm to base } e = 2.71 \\
 &= \sqrt{2 \ln(3600 \times 0.33)} + \frac{0.577}{\sqrt{2 \ln(3600 \times 0.33)}} \\
 &= 3.919
 \end{aligned}$$

$$\begin{aligned}
 G &= 0.925 \left( \frac{1 + 1.7 I_{\bar{x}} \sqrt{g_Q^2 Q^2 + g_R R^2}}{1 + 1.7 g_v I_{\bar{z}}} \right) & G \text{ is the gust factor} \\
 & & g_Q = g_v = 3.4 \text{ (defined in the} \\
 & & \text{equation for } G) \\
 &= 0.925 \left( \frac{1 + 1.7 \times 0.141 \sqrt{3.4^2 \times 0.64 + 3.919^2 \times 0.216}}{1 + 1.7 \times 3.4 \times 0.141} \right) \\
 &= 0.910
 \end{aligned}$$

For comparative purposes, it may be of interest to calculate the gust factor  $G_j$  for this building using the improved method for rigid structures:

$$G = 0.925 \left( \frac{1 + 1.7 g_Q I_{\bar{x}} Q}{1 + 1.7 g_v I_{\bar{z}}} \right)$$

$$I_z = C \left( \frac{33}{z} \right)^{1/6} = 0.141$$

$$L_z = 761, \quad Q = 0.80$$

$$\begin{aligned}
 G &= 0.925 \left( \frac{1 + 1.7 \times 3.4 \times 0.141 \times 0.80}{1 + 1.7 \times 3.4 \times 0.141} \right) \\
 &= 0.912
 \end{aligned}$$

Observe that this value of 0.912 is not much different from 0.910 calculated using the more complex procedure:

$$K = \frac{1.65^{\hat{\alpha}}}{\hat{\alpha} + \xi + 1} = \frac{1.65^{1/9.5}}{(1/9.5) + 1 + 1} = 0.50 \quad \xi = \text{the first mode exponent taken} = 1.0$$

$$g_{\ddot{x}} = g_R = 3.91$$

### Maximum Along-Wind Displacement:

$$X_{\max(z)} = \frac{\phi_{(z)} \rho B h C_{fx} \hat{V}^2}{3 m_1 (2\pi n_1)^2}$$

$$= \frac{1 \times 0.0024 \times 185 \times 450 \times 1.3 \times 201^2}{2 \times 1,618,200 (2 \times \pi \times 0.3)^2} \quad \rho = \text{air density} = 0.0024 \text{ slugs}$$

$$\times 0.5 \times 0.925$$

$$= 0.4221 \text{ ft}$$

*Note:*  $X_{\max(z)}$  is also commonly referred to as lateral drift,  $\Delta$ . Tall buildings are usually designed for a drift index  $\frac{\Delta}{h} \cong \frac{1}{500}$ . In our case,  $\frac{\Delta}{h} = \frac{0.4221}{450} = \frac{1}{1056}$ , indicating that the example building is quite stiff:

$$\sigma_{\ddot{x}(z)} = \frac{0.85 \phi_{cl} \rho B h C_{fx} \bar{v}^2}{m_1} \times I_z K R$$

$$= \frac{0.85 \times 1 \times 0.0024 \times 185 \times 450 \times 1.3 \times 144.6^2}{1,618,200} \times 0.141 \times 0.5 \times 0.5196$$

$$= 0.104 \text{ ft/s}^2$$

### Maximum Along-Wind Acceleration:

$$\ddot{X}_{\max(z)} = g_{\ddot{x}} \sigma_{\ddot{x}(z)}$$

$$= 3.89 \times 0.1040$$

$$= 0.40 \text{ ft/s}^2$$

$$= 0.40 \times 31.11 = 12.58 \text{ mg}$$

This is well below the normally accepted limit of 20 milli-g, warranting no further investigation.

#### 4.4.2.5 Worksheet for Calculation of Gust Effect Factor, $G_f$ , Along-Wind Displacement and Acceleration

The formulas given in the ASCE 7-05 are not easy to crack because they are in a concise format. Therefore, to make the calculations somewhat less forbidding, they are given in a worksheet format in the following section. Also included are some helpful comments.

## Worksheet for Calculating Gust Effect Factor, Along-Wind Displacement, and Accelerations

### ASCE 7-05 Formulas

### Commentary

$V$  = wind speed in ft/s =  $V_{\text{mph}} \times 1.467$

$V$  from wind map, converted from mph to ft/s

$\bar{z} = 0.6 \times h$ , but not less than  $\bar{z}_{\text{min}}$

$z_{\text{min}}$  from Table 6.4

$h$  = building height, ft

$$I_{\bar{z}} = C \left( \frac{33}{\bar{z}} \right)^{1/6}$$

$C$  from Table 6.4

$$L_{\bar{z}} = l \left( \frac{\bar{z}}{33} \right)^{\epsilon}$$

$l$  and  $\epsilon$  from Table 6.4

$$Q = \sqrt{\frac{1}{1 + 0.63(B + h / L_{\bar{z}})^{0.63}}}$$

$B$  = building width perpendicular to wind

$h$  = building height

$Q$  = background response, a term used in random vibration theory

$$\bar{V}_{\bar{z}} = \bar{b} \left( \frac{\bar{z}}{33} \right)^{\bar{\alpha}} V$$

$\bar{b}$  and  $\bar{\alpha}$  from Table 6.4

$$\hat{V}_{\bar{z}} = \hat{b} \left( \frac{\bar{z}}{33} \right)^{\hat{\alpha}}$$

$\hat{b}$  and  $\hat{\alpha}$  from Table 6.4

$$N_1 = \frac{n_1 L_{\bar{z}}}{\bar{V}_{\bar{z}}}$$

$n_1$  = natural frequency of the building

$$R_n = \frac{7.47 N_1}{(1 + 10.3 N_1)^{5/3}}$$

$R_n$  is a parameter required for calculating  $R^2$

$$\eta_b = \frac{4.6 n_1 B}{\bar{V}_{\bar{z}}}$$

$$R_b = \frac{1}{\eta} - \frac{1}{2\eta_b^2} (1 - e^{-2\eta_b}) \quad \text{for } \eta_b > 0$$

$R_b$  is a parameter required for calculating  $R^2$

$$R_b = 1, \quad \text{for } \eta_b = 0$$

$$\eta_h = \frac{4.6 n_1 h}{\bar{V}_{\bar{z}}}$$

$$R_h = \frac{1}{\eta_h} - \frac{1}{2\eta_h^2} (1 - e^{-2\eta_h}) \quad \text{for } \eta_h > 0$$

$R_h$  is a parameter required for calculating  $R^2$

$$R_h = 1, \quad \text{for } \eta_h = 0$$

$$\eta_L = \frac{15.4 n_1 L}{\bar{V}_{\bar{z}}}$$

$$R_L = \frac{1}{\eta_L} - \frac{1}{2\eta_L^2} (1 - e^{-2\eta_L}) \quad \text{for } \eta_L > 0$$

$R_L$  is a parameter required for calculating  $R^2$

$$R_L = 1 \quad \text{for } \eta_L = 0$$

$$R^2 = \frac{1}{\beta} R_n R_b R_h (0.53 + 0.47 R_L)$$

$\beta$  = damping ratio, percent of critical

(continued)

### Worksheet for Calculating Gust Effect Factor, Along-Wind Displacement, and Accelerations (continued)

#### ASCE 7-05 Formulas

#### Commentary

$$G = 0.925 \left( \frac{1 + 1.7I_z \sqrt{g_Q^2 Q^2 + g_R^2 R^2}}{1 + 1.7g_v I_z} \right)$$

$g_Q$  = peak factor for background response

$g_R$  = peak factor for resonance response

$G$  = gust factor

$g_v$  = peak factor for wind response

$g_Q = g_v$ , always taken = 3.4

$$k = \frac{1.65^{\bar{\alpha}}}{(\bar{\alpha} + \xi + 1)}$$

$\xi$  = mode exponent

$$g_{\ddot{x}} = 2 \ln(n_1 T) + \frac{0.5772}{\sqrt{2 \ln(n_1 T)}}$$

$\ln$  means logarithm to base  $e = 2.71$

$$m_1 = \text{modal mass} = \int_0^h \mu_z Q^2 dz$$

$\mu_z$  = mass per unit height, slugs/ft

$h$  = building height

$$= \mu_z \times \frac{h}{3} \text{ as shown below}$$

For a linear first-mode shape,  $Q = x/h$ , where  $x$  is the displacement of the building at the top. If we assume that  $\mu_z$  is constant for the full height of the building (meaning that the building is uniform with a constant density =  $\mu$  slugs/ft<sup>3</sup>), the modal mass is given by

$$\begin{aligned} m &= \int_0^h \mu_z Q^2 dz \\ &= \mu_z \int_0^h \frac{x^2}{h^2} dz \\ &= \mu_z \left[ \frac{x^3}{3h^2} \right]_0^h \\ &= \mu_z \times \frac{h}{3} \end{aligned}$$

#### Maximum Along-Wind Acceleration:

$$X_{\max(z)} = \frac{\phi(z) \rho B h C_{fA} \hat{V}_z^2}{2m_1 (2\pi n_1)^2} K G$$

At  $z = h$ ,  $X_{\max(h)}$  gives the maximum lateral load deflection at the top

$\rho$  = air density = 0.0024 slugs/ft<sup>3</sup>

$C_{fA}$  = mean along-wind force coefficient, typically equal to 1.3

$$g_{\ddot{x}} = \sqrt{2 \ln(n_1 T)} + \frac{0.5772}{\sqrt{2 \ln(n_1 T)}}$$

$T$  = time in seconds over which acceleration is computed, usually taken to be 1 h = 3600 s

$$\sigma_{\ddot{x}(z)} = \frac{0.85 \phi(z) \rho B h C_{fA} \bar{V}_z^2}{m_1} I_z K R$$

$\sigma_{\ddot{x}(z)}$  = the root-mean-square along-wind acceleration above the ground surface

(continued)

$\ddot{X}_{\max(z)} = g_x \sigma_{\ddot{X}(z)}$	$\ddot{X}_{\max(z)}$ = the maximum along-wind acceleration as a function of height above the ground surface
$\ddot{X}_{\max(h)} = g_x \sigma_{\ddot{X}(h)}$	$\ddot{X}_{\max(h)}$ = the maximum acceleration at the building top—the item of interest. If greater than 20 milli-g, further investigation is recommended

#### 4.4.2.6 Comparison of Gust Effect Factor and Along-Wind Response

As stated previously, ASCE 7-05 permits the use of a gust effect factor equal to 0.85 for rigid buildings whose fundamental frequency is greater than or equal to 1 Hz. As an option, specific features of the building and wind environment may be used to account loading effects due to wind turbulence–structure interaction, and dynamic amplification due to along-wind response.

Along-wind displacements and accelerations are entirely due to the action of the turbulence in the longitudinal direction. A criterion for evaluating comfort of the building's occupants is the peak accelerations they are likely to experience in a windstorm. Human perception of building motion is influenced by many cues, such as the movement of suspended objects; noise due to ruffling between building components; and, if the building twists, apparent movement of objects at a distance viewed by the occupants. Although at present there are no comprehensive comfort criteria, a generally accepted benchmark value in North American practice is to limit the acceleration at the upper floor of a building to 20 milli-g. This limit applies to both human comfort and motion perception.

A windstorm postulated to occur at a frequency of once every 10 years is used to evaluate motion perception. The threshold of acceleration for residential properties is more stringent—about 15 milli-g for a 10 year windstorm. The rationale is that occupants are likely to remain longer in a give location of a residence, than in a typical office setting.

To get a feel for gust effect factor and along-wind response, four example buildings are considered here. Building 1 is located in wind terrain exposure category A, a category that is no longer recognized since the publication of ASCE 7-05. We use this solely for comparison.

Table 4.4 gives the summary of building characteristics and their wind environment. The parameters such as  $z_{\min}$ ,  $E$ , etc., shown in Table 4.5, are obtained from ASCE 7-05 Table 6.2 (Table 4.2 of this text).

Instead of presenting all examples in excruciating detail, only the final values of the derived parameters (as many as 24 for each example) are given in Table 4.6. However, for Building No. 3, the worked example follows the step-by-step procedure using the worksheet.

**TABLE 4.4**  
**Buildings' Characteristics and Wind Environment**

Problem #	Exposure Category	Basic Wind Speed at		Height, $h$ (ft)	Base, $B$ (ft)	Depth, $L$ (ft)	Frequency, Hz (Period, s)	Damping Ratio, $\beta$	Building Density (Slugs/cu ft <sup>a</sup> )
		Exposure C, $V$ (mph)	Speed at $h$ (ft)						
1	A	90	600	100	100	0.2 Hz (5 s)	0.01	0.3727	
2	C	90	600	100	100	0.2 Hz (5 s)	0.01	0.3727	
3	B	120	394	98.5	164	0.222 Hz (4.5 s)	0.01	0.287	
4	C	130	788	164	164	0.125 Hz (8 s)	0.015	0.3346	

<sup>a</sup> 1 slug = 32.171b.



**TABLE 4.5**  
**Design Parameters for Example Buildings**

	Problem #			
	1	2	3	4
$z_{\min}$	60 ft	15 ft	30 ft	15 ft
$\bar{\epsilon}$	0.5	0.2	0.333	0.2
$c$	0.45	0.20	0.30	0.20
$\bar{b}$	0.3	0.65	0.45	0.65
$\bar{\alpha}$	0.33	0.1538	0.25	0.1538
$\bar{b}$	0.64	1.0	0.84	1.0
$\bar{\alpha}$	0.2	0.1053	0.143	0.1053
$\ell$	180	500	320	500
$C_{fx}$	1.3	1.3	1.3	1.3
$\xi$	1	1.0	1.0	1.0

*Note:* Design Parameters from ASCE 7-05, Table 6.2, or Table 4.2 of this text.

**TABLE 4.6**  
**Comparison of Dynamic Response of Example Buildings**

Calculated Values	Example 1	Example 2	Example 3	Example 4
$V$	132 ft/s	132 ft/s	176 ft/s	191 ft/s
$\bar{z}$	360 ft	360 ft	236 ft	473 ft
$I_{\bar{z}}$	0.302	0.1343	0.216	0.128
$L_{\bar{z}}$	594.52 ft	806 ft	616 ft	852 ft
$Q^2$	0.589	0.634	0.64	0.596
$\bar{V}_z$	87.83 ft/s	124 ft/s	130 ft/s	187 ft/s
$\hat{V}_z$	136.24 ft/s	170 ft/s	195 ft/s	253 ft/s
$N_1$	1.354	1.30	1.051	0.5695
$R_n$	0.111	0.114	0.128	0.171
$H$	1.047	0.742	0.773	0.504
$R_B$	0.555	0.646	0.6360	0.74
$\eta$	6.285	4.451	3.095	2.423
$R_h$	0.146	0.1994	0.271	0.328
$H$	3.507	2.484	4.31	1.688
$R_L$	0.245	0.322	0.205	0.423
$R^2$	0.580	1.00	1.381	2.01
$G$	1.055	1.074	1.20	1.204
$K$	0.502	0.50	0.501	0.50
$m_1$	745,400 slugs	745,400 slugs	608,887 slugs	236,4000 slugs
$g_R$	3.787	3.787	3.813	3.66
$X_{\max}$	0.78 ft	1.23 ft	1.16 ft	5.3 ft
$g_{\ddot{x}}$	3.786	3.786	3.814	3.66
$\sigma_{\ddot{x}}$	0.19	0.22	0.363	0.463
$\ddot{X}_{\max}$	0.72 ft/s <sup>2</sup> (22.39 milli-g)	0.834 ft/s <sup>2</sup> (26 milli-g)	1.385 ft/s <sup>2</sup> (43 milli-g)	1.68 ft/s <sup>2</sup> (52.26 milli-g)

**Discussions of Results:** Because the example buildings are chosen randomly, it is impractical to make a comprehensive qualitative comparison. However, it may be appropriate to record the following observations regarding their wind-induced response characteristics.

- Building No. 1 has a rather large height-to-width ratio of  $600/100 = 6$ . Yet, because it is located in exposure category A, the most favorable wind terrain (per ASCE 7-98), and is subjected to a relatively low wind velocity of 90 mph, its lateral response to wind is not sensitive. The calculated acceleration of the top floor is 26 milli-g, as compared to the threshold value of 20 milli-g (2% of g).
- Building No. 2 has the same physical characteristics as Building No. 1, but is sited in exposure category C, the second most severe exposure category. Because the basic wind is the same as for the first its peak acceleration is only slightly higher than for Building 1. Pushing exposure category from A to C does not appear to unduly alter the wind sensitivity of the building.
- Building No. 3 is not that tall. It is only 394 ft, equivalent to a 30-story office building at a floor-to-floor height of 12 ft 6 in. At a fundamental frequency of 4.5 s, its lateral stiffness is quite in line with buildings designed in high seismic zones. But because it is subjected to hurricane winds of 120 mph, its peak acceleration is a head-turning 43 milli-g—more than twice the threshold value of 20 milli-g.
- Building No. 4 is the tallest of the four, equivalent to a 60-plus story building. Its height-to-width ratio is not very large (only 4.8) but it appears to be quite flexible at a fundamental frequency of 8 s and a calculated peak acceleration of 52.26 milli-g. This raises a red flag. It is doubtful that even with the addition of a supplemental damping, such as a tuned mass damper (TMD) or a simple pendulum damper (discussed in Chapter 7), the building oscillations can be tamed. Consultations with an engineering expert specializing in designing damping systems should be recommended before finalizing the structural system.

#### 4.4.2.7 One More Example: Design Wind Pressures for Enclosed Building, Method 2

##### Given:

- A 40-story concrete tube building in a hurricane-prone coastal region, Key West, Florida.
- Basic wind speed  $V = 150$  mph (maximum basic wind speed anywhere in the United States).
- Terrain: open water front.
- Plan dimensions:  $120 \times 200$  ft.
- Building height: 600 ft.
- Building lateral system: perimeter tube with exterior columns typically spaced at 15 ft.
- Building period (as calculated by approximate equation given in ASCE 7-05, Table 12.8.2) = 5.06 s. (ASCE formula may be unconservative for wind design. See discussion in Section 4.6.7.)
- The building is regular, as defined in ASCE 7-05, Section 6.2. It does not have unusual geometric irregularities.
- It does not have response characteristics that would subject the building to across-wind loading, vortex shedding, or instability due to galloping or flutter. The building does not have a site location for which channeling effects or buffeting in the wake of upwind obstructions warrant special consideration.
- Damping factor: 1.5% of critical.
- Topographic factor  $K_{zt} = 1.0$ .
- The building wind importance factor,  $I_w$ , as mandated by the governing authority:  $I_w = 1.15$ .
- The glazing panels are resistant to wind-borne debris impact. Therefore, the building is considered enclosed.

**Required:**

Wind pressures for the design of MWFRS.

**Solution:**

We start the solution with a brief discussion of the fundamental period we should use for our building. As stated in the problem, the approximate formula given in ASCE 7-05, Table 12.8.2 has been used to determine the building period,  $T_a$  as follows:

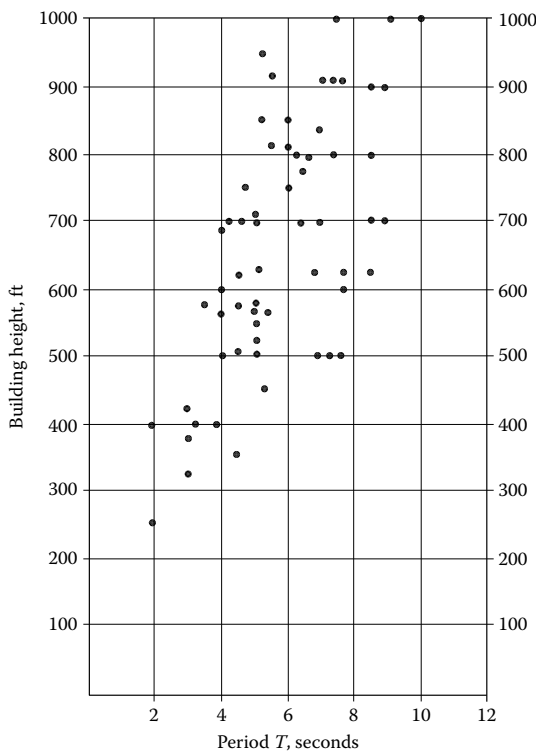
$$T_a = C_t h_n^x \quad (4.29)$$

$$\begin{aligned} T &= 0.016 \times 600^{0.9} \\ &= 5.06 \text{ s} \end{aligned}$$

It should be noted that approximate equations of building periods developed for seismic design tend to give lower estimates of the period, as this gives conservative approximations of the seismic base shear.

For wind design, the opposite is true. Meaning, these lower estimates of fundamental period can incorrectly categorize slender buildings as rigid, when they may be, in fact, flexible. Therefore, when using ASCE seismic equations for wind design, the engineer needs to determine the period by using appropriate methods that do not “low ball” its dynamic behavior.

Shown in Figure 4.23 is a plot of fundamental period  $T$  versus building heights. The plot is based on limited information gathered by the author. Using this, we conservatively determine the period  $T = 8 \text{ s}$  ( $f = 0.25 \text{ Hz}$ ) for the example building.



**FIGURE 4.23** Building period versus height.

With this explanation, we now proceed to calculate design pressure,  $p$ , for the example building.

Velocity pressure $q_z$	$= 0.00256K_zK_dK_{zt}V^2I_w$	ASCE 7-05 Reference
Exposure	$= C$	
Roof height $h$	$= 600\text{ft}$	
Exposure coefficient $K_z$	$=$ Section 6.5.6.6. is obtained from Table 6.3, Case 2 for MWFRS	
Topography factor $K_{zt}$	$= 1.00$ (Given)	6.5.7.2, Figure 6.2
Directionality factor $K_d$	$= 0.85$	Table 6.4
Wind speed $V$	$= 150\text{ mph}$ (Given)	
Importance factor $I_w$	$= 1.15$ (Given)	Table 6.1
$q_z$	$= 56.30K_z\text{ psf}$	
Internal pressure coefficient ( $GC_{pi}$ )	$= \pm 0.18$	Figure 6.5 for enclosed building
Gust effect factor $G_f$	$= 1.24$ (by calculations, not shown here)	6.5.8.1
Pressures for MWFRS $P$	$= qGC_p - q_i (GC_{pi})$	(6–17)
Wall external pressure coefficients		
$C_p$ from ASCE 7-05 Figure 6.6		
Wind normal to 120 ft wall $L/B$	$= 1.67$	
Windward wall $C_p$	$= 0.8$	
Leeward wall $C_p$	$= -0.367$ for $L/B = 1.67$	
Side wall $C_p$	$= -0.7$	
Wind parallel to 120 ft wall $L/B$	$= 0.60$	
Windward wall $C_p$	$= 0.8$	
Leeward wall $C_p$	$= -0.500$ for $L/B = 0.60$	
Side wall $C_p$	$= -0.7$	

The calculated design pressures are shown in Figures 4.24 and 4.25.

### Design Wind Pressures $p$ , Perpendicular to 200 ft Wall

Height $z$ (ft)	$K_z$ (1)	Windward Wall (WW)		Leeward Wall (LW)		Total Design Pressure $p$
		$q_z$ (2)	$p = q_zG_fC_p$ (3)	$q_h$ (4)	$p = q_zG_fC_p$ (5)	WW + LW (6) = (3) + (5)
600	1.85	103.91	103.08	103.91	64.4	167
550	1.81	102.03	101.21	103.91	64.4	166
500	1.78	100.00	99.2	103.91	64.4	163
450	1.74	97.80	97.00	103.91	64.4	161
400	1.69	95.41	94.65	103.91	64.4	159
350	1.65	92.76	92.00	103.91	64.4	156
300	1.59	89.80	89.00	103.91	64.4	153
250	1.53	86.42	85.73	103.91	64.4	150
200	1.46	82.45	81.80	103.91	64.4	146
150	1.38	77.61	77	103.91	64.4	141
100	1.27	71.26	70.68	103.91	64.4	135
80	1.21	68.00	67.45	103.91	64.4	132
60	1.14	64.00	63.48	103.91	64.4	128
40	1.04	58.76	58.29	103.91	64.4	122
20	0.90	50.78	50.38	103.91	64.4	114
15	0.85	47.80	47.41	103.91	64.4	111
0						

**FIGURE 4.24** Design wind pressure perpendicular to 200 ft wall. *Note:*  $G_f = 1.24$ ,  $I_w = 1.15$ .

### Design Wind Pressures $p$ , Perpendicular to 120 ft Wall

Height $z$ (ft)	$K_z$ (1)	Windward Wall (WW)		Leeward Wall (LW)		Total Design Pressure $p$
		$q_z$ (2)	$p = q_z G_r C_p$ (3)	$q_h$ (4)	$p = q_z G_r C_p$ (5)	WW + LW (6) = (3) + (5)
600	1.85	103.91	103.08	103.91	47.28	150
550	1.81	102.03	101.21	103.91	47.28	149
500	1.78	100.00	99.2	103.91	47.28	146
450	1.74	97.80	97.00	103.91	47.28	144
400	1.69	95.41	94.65	103.91	47.28	141
350	1.65	92.76	92.00	103.91	47.28	139
300	1.59	89.80	89.00	103.91	47.28	136
250	1.53	86.42	85.73	103.91	47.28	133
200	1.46	82.45	81.80	103.91	47.28	129
150	1.38	77.61	77	103.91	47.28	124
100	1.27	71.26	70.65	103.91	47.28	118
80	1.21	68.00	67.45	103.91	47.28	114
60	1.14	64.00	63.48	103.91	47.28	110
40	1.04	58.76	58.29	103.91	47.28	105
20	0.90	50.08	50.38	103.91	47.28	9
15	0.85	47.80	47.41	103.91	47.28	94
0						

**FIGURE 4.25** Design wind pressure perpendicular to 120 ft wall. *Note:*  $G_r = 1.24$ ,  $I_w = 1.15$ .

## 4.5 NATIONAL BUILDING CODE OF CANADA (NBCC 2005): WIND LOAD PROVISIONS

*The reason for including this section is quite simply to provide readers with an analytical procedure for estimating across-wind response of tall, flexible buildings. To the best of author's knowledge, NBCC is the only code in North America to provide such a method.*

Three different procedures of determining design wind load on buildings are given in NBCC 2005:

1. Static procedure
2. Dynamic procedure
3. Experimental procedure

The emphasis here is on the dynamic procedure for estimating across-wind response.

### 4.5.1 STATIC PROCEDURE

This procedure is appropriate for most cases, including the design of the structure of most low- and medium-rise buildings as well as the cladding of all buildings. The structure or element to be designed in these cases is relatively rigid. Detailed knowledge of the dynamic properties of these structures or elements is not required and dynamic actions of the wind can be represented by equivalent static loads.

#### 4.5.1.1 Specified Wind Load

The specified external pressure or suction due to wind on a part or all of a surface of a building is calculated using the chain equation:

$$p = I_w q C_e C_g C_p \quad (4.30)$$

where

$p$  is the specified external pressure acting statically and in a direction normal to the surface, either as a pressure directed toward the surface or as a suction directed away from the surface

$I_w$  is the importance factor for wind load based on importance category

$q$  is the reference velocity pressure, based on a probability of being exceeded in any 1 year of 1/50

$C_e$  is the exposure factor

$C_g$  is the gust effect factor

$C_p$  is the external pressure coefficient, averaged over the area of the surface considered

The importance factor,  $I_w = 0.8, 1.0, 1.15$ , and  $1.25$ , respectively, for importance category of low, normal, high, and post-disaster facilities.

The value of  $q$  in kilopascals, KPa, is given by

$$q = 0.00064645V^2 \quad (4.31)$$

where  $V$  is the reference velocity based on the return period of 50 years. These may be obtained from Table C-1 of NBCC 2005.

The net wind load for the building as a whole shall be the algebraic difference of the loads on the windward and leeward surfaces, and in some cases, may be calculated as the sum of the products of the external pressures or suctions and the areas of the surfaces over which they are averaged as provided.

The net specified pressure due to wind on a part or all of a surface of a building shall be the algebraic difference of the external pressure or suction and the specified internal pressure or suction due to wind calculated using the following formula:

$$p_i = I_w q C_e C_g C_p \quad (4.32)$$

where

$p_i$  is the specified external pressure acting statically and in a direction normal to the surface, either as a pressure directed toward the surface or as a suction directed away from the surface

$I_w$  is the importance factor for wind load

$q$  is the reference velocity pressure

$C_e$  is the exposure factor

$C_g$  is the gust effect factor

$C_p$  is the external pressure coefficient

#### 4.5.1.2 Exposure Factor, $C_e$

The values of  $C_e$  are given for smooth and rough terrain with an intermediate value for terrains that change from smooth to rough. The values are

1.  $(h/10)^{0.2}$  but not less than 0.9 for open (smooth) terrain
2.  $0.7 (h/12)^{0.3}$  but not less than 0.7 for rough terrain
3. An intermediate transition value for terrains that change from smooth to rough (refer to NBCC 2005 for applicable formula)

#### 4.5.1.3 Gust Factors $C_g$ and $C_{gi}$

1. For building as a whole and main structural members,  $C_g = 2.0$
2. For external pressures and suctions on small elements including cladding,  $C_g = 2.5$
3. For internal pressures,  $C_{gi} = 2.0$  or a value determined by detailed calculation that takes into account the sizes of the openings in the building envelope, the internal volume, and the flexibility of the building envelope

4.5.1.4 Pressure Coefficient,  $C_p$

$C_p$  is a nondimensional ratio of wind-induced pressure on a building to the velocity pressure of the wind speed at the reference height. It depends on the shape of the building, wind direction, and profile of the wind velocity, and can be determined most reliably from wind-tunnel tests. However, for the static procedure, based on some limited measurements on full-scale buildings supplemented by wind-tunnel tests, NBCC 2005 gives the following values of  $C_p$  for simple building shapes:

Windward surface:	$C_p = 0.8$ for $H/D \geq 1$ $= 0.27 (H/D + 2)$ for $0.25 < H/D < 1$ $= 0.6$ for $H/D < 0.25$
Leeward surface:	$C_p = 0.5$ for $H/D \geq 1$ $= 0.27 (H/D + 0.88)$ for $0.25 < H/D < 1$ $= 0.3$ for $H/D < 0.25$
Side walls:	$C_p = -0.7$ for all values of $H/D$
Roof surface:	$C_p = -1.0$ for $H/D \geq 1$ $C_p = -0.1$ for $H/D < 1$ , for roof width = $H$ $C_p = -0.5$ for $H/D < 1$ , for roof width = $D - H$

These are shown schematically in Figure 4.26 for a flat roofed building. The reader is referred to Figure 1.15 of NBCC 2005 for coefficients  $C_p$ , applicable to high local suction values.

4.5.2 DYNAMIC PROCEDURE

In this method, a series of calculations is performed to determine more accurate values for the gust factor  $C_g$ , the exposure factor,  $C_e$ , and the pressure coefficient  $C_p$ . The end product of the

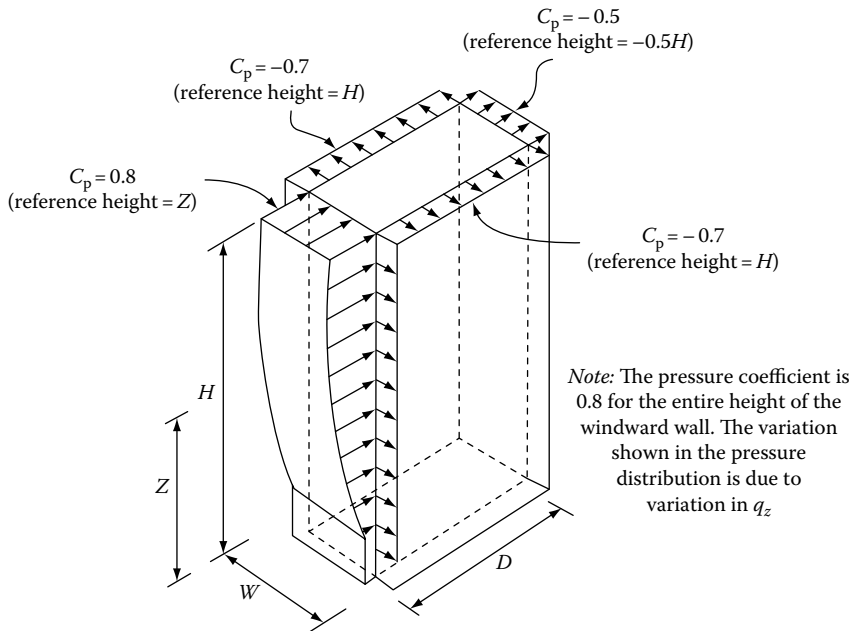


FIGURE 4.26 External wind pressure coefficient  $C_p$ . (Adapted from NBCC 2005.)

calculations yields a static design pressure, which is expected to produce the same peak effect as the actual turbulent wind, with due consideration for building properties such as height, width, natural frequency of vibration, and damping. This approach is primarily for determining the overall wind loading and response of tall slender structures, and is not intended for determining exterior pressure coefficients for cladding design.

In the following section, a method for determining the gust factor,  $C_g$ , for use in dynamic procedure is given. The reader is referred to NBCC 2005 for determining the  $C_e$  and  $C_p$  factors appropriate for dynamic procedure.

#### 4.5.2.1 Gust Effect Factor, $C_g$ (Dynamic Procedure)

A general expression for the maximum or peak load effect, denoted  $W_p$ , is given by

$$W_p = \mu + g_p \sigma \quad (4.33)$$

where

$\mu$  is the mean loading effect

$\sigma$  is the root-mean-square loading effect

$g_p$  is a peak factor for the loading effect

The dynamic gust response factor is defined as the ratio of peak loading to mean loading:

$$C_g = W_p / \mu \quad (4.34)$$

$$= 1 + g_p \left( \frac{\sigma}{\mu} \right) \quad (4.35)$$

The parameter  $\sigma/\mu$  is given by the expression:

$$\frac{\sigma}{\mu} = \sqrt{\frac{K}{C_{eH}} \left( B + \frac{sF}{\beta} \right)} \quad (4.36)$$

where

$K$  is a factor related to the surface roughness coefficient of the terrain and  $K = 0.08$  for exposure A,

$K = 0.10$  for exposure B,  $K = 0.14$  for exposure C

$C_{eH}$  is the exposure factor at the top of the building,  $H$ , evaluated using Figure 4.27

$B$  is a background turbulence factor obtained from Figure 4.28 is a function of building width-to-height ratio  $W/H$

$H$  is the height of the building

$W$  is the width of windward face of the building

$s$  is a size reduction factor obtained from Figure 4.29 as a function of  $W/H$  and reduced frequency  $n_0 H / V_H$

$n_0$  is the natural frequency of vibration, Hz

$V_H$  is the mean wind speed (m/s) at the top of structure,  $H$

$F$  is the gust energy ratio at the natural frequency of the structure obtained from Figure 4.30 as a function of wave number  $n_0 / V_H$

$\beta$  is the critical damping ratio, with commonly used values of 0.01 for steel, 0.015 for composite, and 0.02 for cast-in place concrete buildings



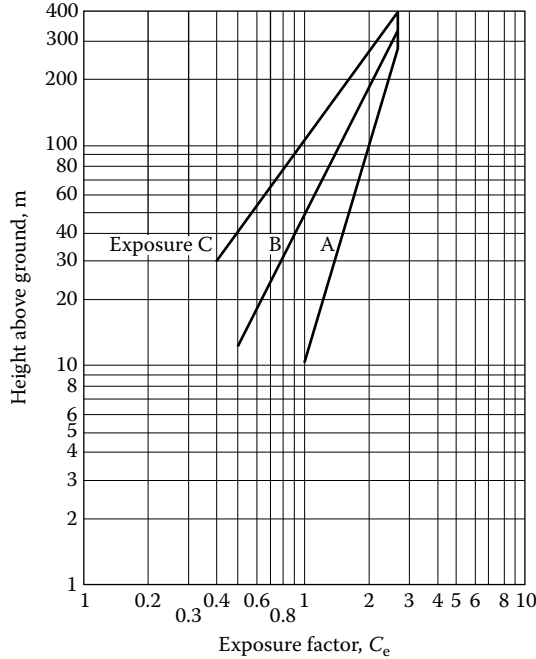


FIGURE 4.27 Exposure factor  $C_{eH}$ . (From NBCC 2005.)

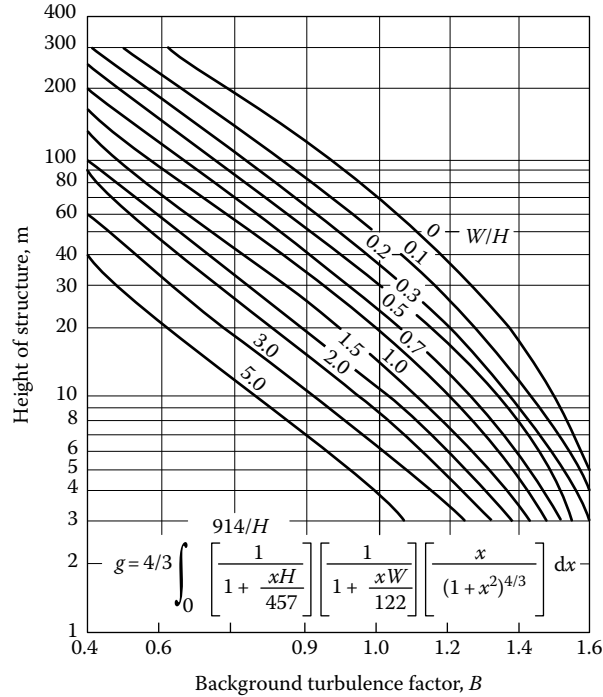
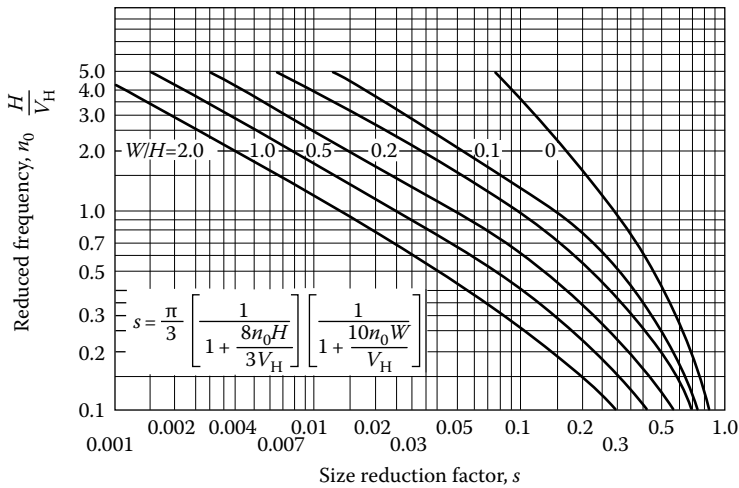
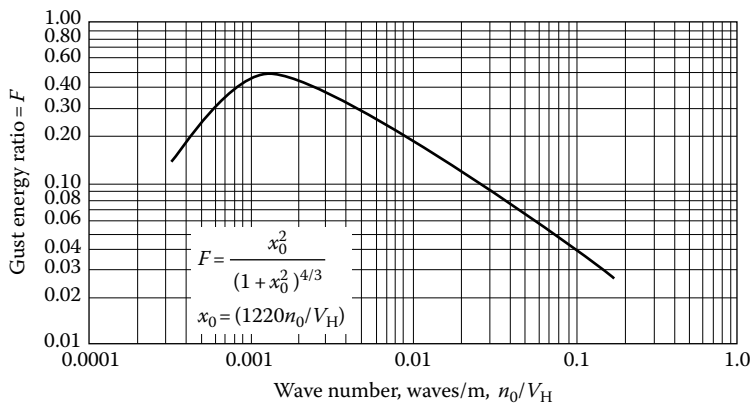


FIGURE 4.28 Background turbulence factor,  $B$ , as a function of height and width of building. (From NBCC 2005.)



**FIGURE 4.29** Size reduction factor,  $s$ , as a function of width, height, and reduced frequency of the building. (From NBCC 2005.)



**FIGURE 4.30** Gust energy ratio,  $F$ , as a function of wave number. (From NBCC 2005.)

#### 4.5.2.2 Design Example: Calculations for Gust Effect Factor, $C_g$

##### Given:

- Height  $H = 240$  m (787.5 ft)
- Width  $W$  (across wind) = 50 m (164 ft)
- Depth  $D$  (along wind) = 50 m (164 ft)
- Fundamental frequency  $n_0 = 0.125$  Hz (period = 8 s)
- Critical damping ratio  $\beta = 0.010$
- Average density of the building =  $195 \text{ kg/m}^3$  (12.2 pcf)
- Terrain for site = exposure B
- Reference wind speed at 10 m, open terrain (exposure A) =  $26.4 \text{ m/s}$  (60 mph)

**Required:** Gust factor  $C_g$

**Solution:** From Figure 4.27 for  $H = 240$  m and exposure category B, exposure factor  $C_{CH} = 2.17$   
Mean wind speed  $V_H$  at the top

$$\begin{aligned} V_H &= \bar{V} \sqrt{C_{CH}} \\ &= 26.4 \sqrt{2.17} \\ &= 38.88 \text{ m/s} \end{aligned}$$

$$\text{Aspect ratio } \frac{W}{H} = \frac{50}{240} = 0.208$$

$$\begin{aligned} \text{Wave number } F &= \frac{n_0}{V_H} \\ &= \frac{0.125}{38.8} = 0.00322 \\ \frac{n_0 H}{V_H} &= \frac{0.125 \times 240}{38.80} = 0.772 \end{aligned}$$

Calculate  $\sigma/\mu$  using the following parameters:

1.  $K = 0.10$  for exposure B
2.  $B = 0.50$  from Figure 4.28 for  $W/H = 0.208$
3.  $s = 0.14$  from Figure 4.29 for  $n_0 H/V_H = 0.772$  and  $W/H = 0.208$
4.  $F = 0.36$  from Figure 4.30 for  $n_0/V_H = 0.0032$
5.  $\beta = 0.010$ , given value of damping:

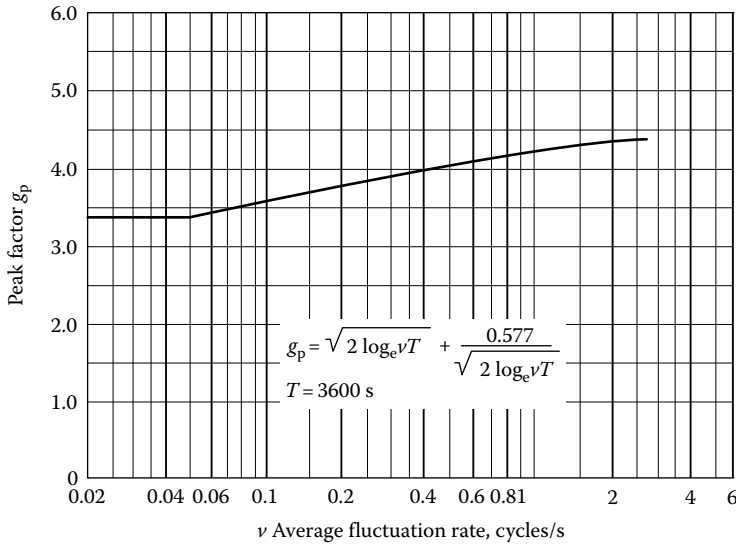
$$\begin{aligned} \frac{\sigma}{\mu} &= \sqrt{\frac{K}{C_{eH}} \left( B + \frac{sF}{\beta} \right)} \\ 6. &= \sqrt{\frac{0.10}{2.17} \left( 0.50 + \frac{0.14 \times 0.36}{0.010} \right)} \\ &= 0.505 \end{aligned}$$

Calculate  $v$  from the equation:

$$\begin{aligned} v &= n_0 \sqrt{\frac{sF}{sF + \beta B}} \\ &= 0.125 \sqrt{\frac{0.14 \times 0.36}{0.14 \times 0.36 + 0.01 \times 0.5}} \\ &= 0.119 \text{ cycles/s} \end{aligned}$$

Using Figure 4.31 read the peak factor  $g_p$  corresponding to  $v = 0.119$ :

$$g_p = 3.6$$



**FIGURE 4.31** Peak factor,  $g_p$ , as a function of average fluctuation rate. (From NBCC 2005.)

Calculate the required gust response factor  $C_g$  from the formula:

$$\begin{aligned}
 C_g &= 1 + g_p \left( \frac{\sigma}{\mu} \right) \\
 &= 1 + 3.6 \times 0.505 \\
 &= 2.82
 \end{aligned}$$

With the known gust effect factor  $C_g$  peak dynamic forces are determined by multiplying mean wind pressures by  $C_g$ .

#### 4.5.2.3 Wind-Induced Building Motion

Although the maximum lateral deflection is generally in a direction parallel to wind (along-wind direction), the maximum acceleration leading to possible human perception of motion or even discomfort may occur in a direction perpendicular to the wind (across-wind direction). Across-wind accelerations are likely to exceed along-wind accelerations if the building is slender about both axes, with the aspect ratio  $\sqrt{WD}/H$  less than one-third, where  $W$  and  $D$  are the across-wind and along-wind plan dimensions and  $H$  is the height of the building.

Based on wind-tunnel studies, NBCC gives two expressions for determining the across- and along-wind accelerations.

The across-wind acceleration  $a_w$  is given by

$$a_w = n_w^2 g_p \sqrt{WD} \left( \frac{a_r}{\rho_B g \sqrt{\beta_w}} \right) \quad (4.37)$$

The along-wind acceleration  $a_D$  is given by

$$a_D = 4\pi^2 n_D^2 g_p \sqrt{\frac{KsF}{C_e \beta_D}} \frac{\Delta}{C_g} \quad (4.38)$$

Observe that  $\Delta$ , the maximum wind-induced lateral displacement in the along-wind direction is typically obtained from a computer analysis. Substitution of this value in Equation 4.38 yields the best estimation of  $a_D$ . However, as a rough guess for: preliminary evaluations,  $\Delta$  can be assumed to be equal to  $H/450$ , the drift index normally used in wind design of tall buildings.

Using a linear modal representation for the building motion, the maximum deflection,  $\Delta$  can be related to the fundamental frequency of the building. The resulting expression is shown in Equation 1.60 for the ratio  $a_D/g$ :

$$\frac{a_D}{g} = g_p \sqrt{\frac{KsF}{C_e \beta_D}} \left( \frac{3.9}{2 + \alpha} \right) \left( \frac{C_e q}{D_g \rho_B} \right) \quad (4.39)$$

where

$a_D$  is the acceleration in the along-wind direction

$g$  is the acceleration due to gravity =  $9.81 \text{ m/s}^2$

$g_p$  is the a statistical peak factor for the loading effect

$K$  is a factor related to surface roughness coefficient of terrain and  $K = 0.08$  for exposure A,

$K = 0.10$  for exposure B,  $K = 0.14$  for exposure C

$s$  is the size reduction factor, from Figure 4.29

$F$  is the gust energy ratio, from Figure 4.30

$C_e$  is the exposure factor

$\beta_D$  is the critical damping ratio, in the along-wind direction

$\alpha$  is the power coefficient related to  $C_e$  and  $\alpha = 0.28$  for exposure A,  $\alpha = 0.50$  for exposure B,

$\alpha = 0.72$  for exposure C

$q$  is the reference wind pressure,  $\text{kPa} = 650 \times 10^{-6} \times \bar{V}^2$ , ( $\bar{V}$  in meters per second)

$D$  is the building depth parallel to wind, m

$\rho_B$  is the mass density of building,  $\text{kg/m}^3$

#### 4.5.2.4 Design Example

A representative calculation for  $a_w$  and  $a_D$  using Equations 4.37 and 4.38 will be made for the sample problem worked earlier to illustrate the calculation of gust factor.

**Given:**

- Building frequency  $n_w = n_D = 0.125 \text{ Hz}$
- Damping coefficient  $\beta_w = \beta_D = 0.01$
- Building density  $\rho_B = 195 \text{ kg/m}^3$  (12.2 pcf)
- All other data as given for the previous illustrative problem

**Required:** Building accelerations in both across-wind, along-wind directions.

**Solution:**

**Step 1.** Calculate  $a_r$

$$\begin{aligned} a_r &= 78.5 \times 10^{-3} \left[ \frac{V_H}{n_w \sqrt{WD}} \right]^{3.3} \\ &= 78.5 \times 10^{-3} \left[ \frac{38.88}{0.125 \times 50} \right]^{3.3} \\ &= 32.7 \text{ m/s}^2 \end{aligned}$$

**Step 2.** Calculate  $a_w$  (across-wind response)

In our case,  $n_0 = n_w = n_D = 0.125$  and  $\beta_w = \beta_D = 0.10$

$$\begin{aligned}
 a_w &= n_w^2 g_p \sqrt{WD} \left( \frac{a_r}{\rho_B g \sqrt{\beta_w}} \right) \\
 &= 0.125^2 \times 3.6 \times \sqrt{50 \times 50} \left( \frac{32.7}{165 \times 9.81 \sqrt{0.01}} \right) \\
 &= 0.482 \text{ m/s}^2 \\
 \frac{a_w}{g} &= \frac{0.482}{9.81} \times 100 = 4.91\% \text{ of gravity}
 \end{aligned}$$

The calculated value of across-wind acceleration  $a_w$  exceeds the acceptable limit of 3% of gravity for office buildings, warranting a detailed boundary-layer wind-tunnel study.

**Step 3.** Calculate  $q$  (reference wind pressure)

$$\begin{aligned}
 q &= C \bar{V}^2 \\
 &= 650 \times 10^{-6} \times 26.4^2 \\
 &= 0.453
 \end{aligned}$$

**Step 4.** Calculate along-wind response  $a_D$ 

$$\begin{aligned}
 a_D &= g_p \sqrt{\frac{KsF}{C_e \beta_D} \left( \frac{3.9}{2 + \alpha} \right) \left( \frac{C_e q}{D \rho_B} \right)} \\
 &= 3.6 \sqrt{\frac{0.10 \times 0.14 \times 0.36}{2.17 \times 0.010} \left( \frac{3.9}{2 + 0.5} \right) \left( \frac{2.17 \times 0.453}{50 \times 195} \right)}
 \end{aligned}$$

For the example problem we have

$g_p = 3.6$	$\beta_D = 0.010$	$q = C \bar{V}^2$
$K = 0.10$	$\alpha = 0.5$	$= 650 \times 10^{-6} \times 26.4^2$
$s = 0.14$	$D = 50 \text{ m}$	$= 0.453 \text{ kPa}$
$F = 0.36$	$g = 9.81 \text{ m/s}^2$	
$C_e = C_H = 2.17$	$\rho_B = 195 \text{ kg/m}^3$	

Substituting the preceding values in Equation 4.39:

$$\begin{aligned}
 \frac{a_D}{g} &= 3.6 \sqrt{\frac{0.10 \times 0.14 \times 0.36}{2.17 \times 0.010} \left( \frac{3.9}{2 + 0.5} \right) \left( \frac{2.17 \times 0.453}{50 \times 0.00981 \times 195} \right)} \\
 &= 0.027 = 2.7\% \text{ of gravity}
 \end{aligned}$$

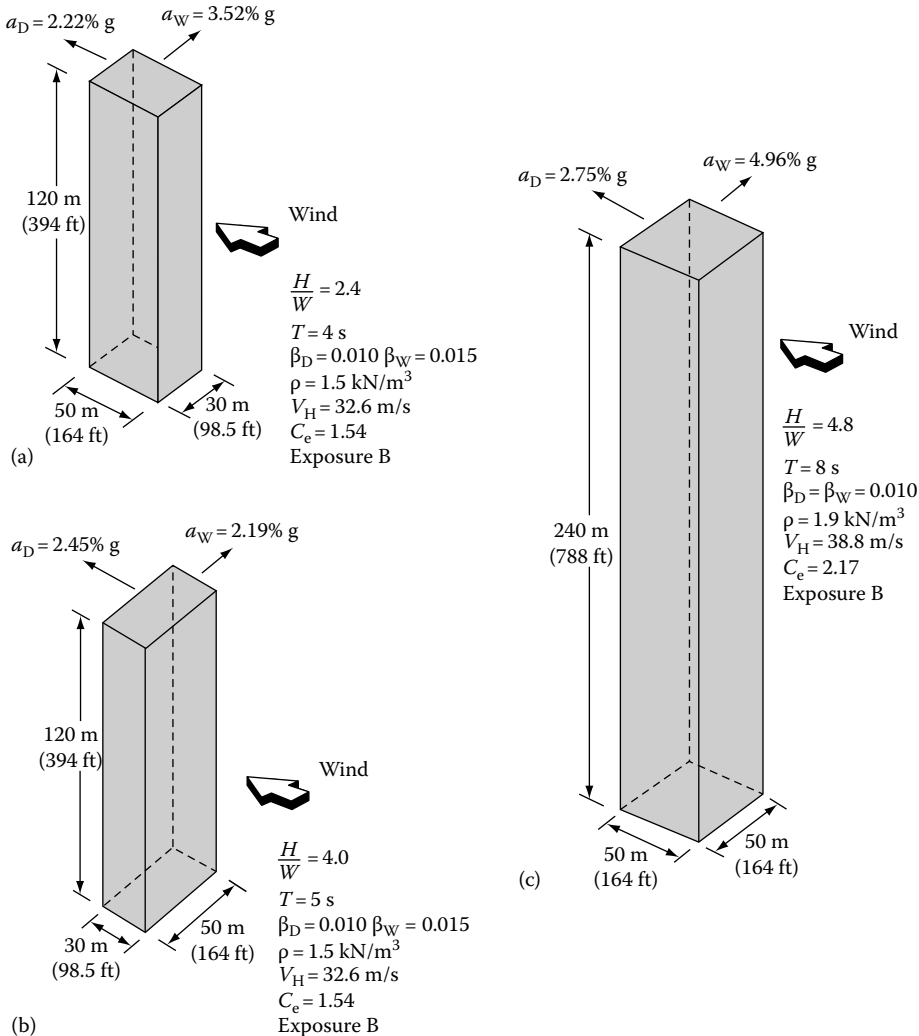
The calculated value is below the 3% limit. Its along-wind response is unlikely to disturb the comfort and equanimity of the building's occupants.

#### 4.5.2.5 Comparison of Along-Wind and Across-Wind Accelerations

To get a feel for the along-wind and across-wind response of tall buildings, the results for two buildings are given in a summary format. One is a 30-story rectangular building, shown in Figure 4.32a and b, and is examined for wind accelerations along both its principal axes. The other, shown in Figure 4.32c is a square building with a height corresponding approximately to a 60-story-plus building. Results for both are given for suburban exposure B.

Response characteristics were also evaluated for the other two types of exposure categories. From the calculations performed but not shown here, it appears that the type of exposure has a significant effect on both along-wind and across-wind response. Accelerations were about 20%–50% greater for an open-terrain exposure A. The reductions for an urban setting, exposure C, were of the same order of magnitude.

Observe that for the 30-story building, the maximum acceleration occurs in a direction perpendicular to the wind (across-wind direction) because the building is considerably more slender in the



**FIGURE 4.32** Wind induced peak accelerations; NBCC 2005 procedure: (a) 30-story building, wind on narrow face; (b) 30-story building, wind on broad face; (c) 60-story building with equal plan dimensions.

across-wind direction than in the along-wind direction. It should be noted that across-wind accelerations control the design for buildings that are slender about both axes, that is, if  $\sqrt{WD/H}$  is less than one-third, where  $W$  and  $D$  are the across-wind plan dimensions and  $H$  is the building height.

Since the along-wind and across-wind accelerations are sensitive to the natural frequency of the building, use of approximate formulas for period calculations are not appropriate. Therefore, results of more rigorous methods such as computer dynamic analyses are recommended for use in these formulas.

In addition to acceleration, many other factors such as visual cues, body position and orientation, and state of mind of occupants during windstorms influence human perception of motion. However, research has shown that when the amplitude of acceleration is in the range of 0.5%–1.5% of acceleration due to gravity, movement of buildings becomes perceptible to most building occupants. Based on this and other information, a tentative acceleration limit of 1%–3% of gravity is recommended. The lower value is considered appropriate for apartment buildings, the higher values for office buildings.

#### 4.5.3 WIND LOAD COMPARISON AMONG INTERNATIONAL CODES AND STANDARDS

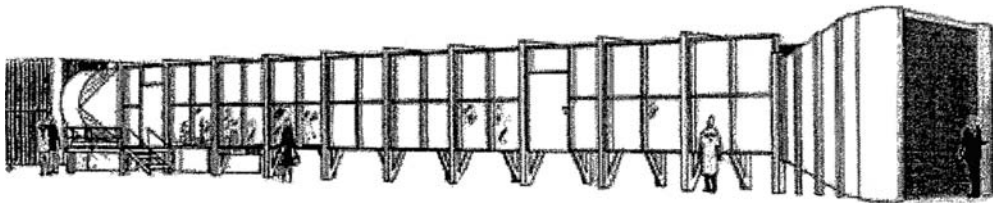
In a paper published in the CTBUH (Council on Tall Buildings and Urban Habitat), Tall Building Conference 2003, authors Kikitsu, Okada, and Okuda present a comparison of external cladding pressures among several international codes and standards. Defining unified air density, return period and averaging time of basic wind velocity, reference height, and vertical profile, they point out that significant discrepancies exist in the adjusted peak pressure values. The degree of discrepancies is approximately as follows:

- 25%–40% for windward wall
- 20%–30% for leeward and side walls
- 20% for flat roof

#### 4.6 WIND-TUNNELS\*

Shown in Figures 4.33 through 4.35 are schematics of typical boundary layer wind tunnels, BLWTs, that range in lengths from 108–210 ft (33–64 m). Photographs of test section interiors with building models mounted on turntables are shown in Figures 4.36 through 4.40.

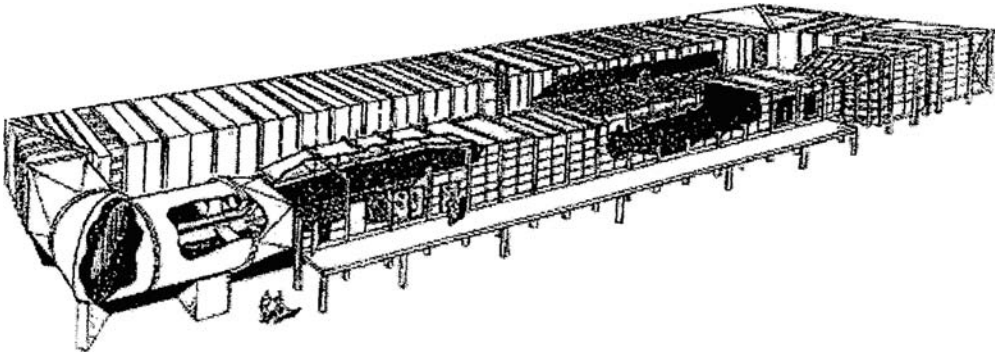
Wind tunnels such as those shown in Figures 4.33 through 4.35 are used, among other things, to provide accurate distributions of wind pressure on buildings as well as investigate aeroelastic behavior of slender and light weight structures.



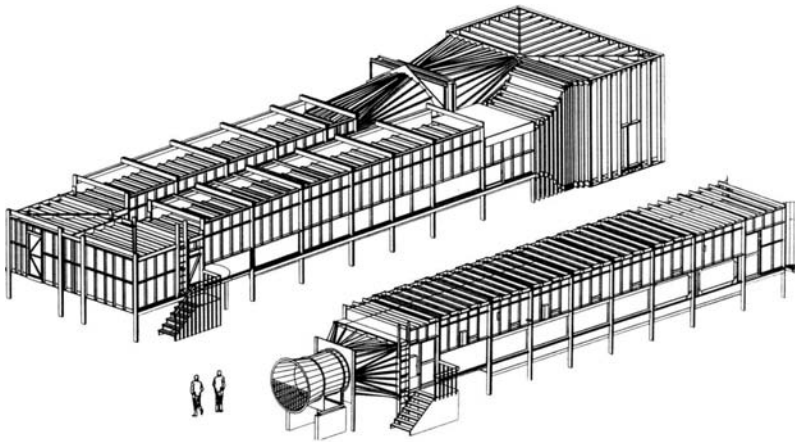
**FIGURE 4.33** Schematics of 33 m-long wind tunnel; overall size 33 m × 2.4 m × 2.15 m.

\* The author wishes to acknowledge his gratitude to Mr. Brian Breukelman, Consultant, CPP Wind Engineering & Air Quality Consultants, Fort Collins, Colorado, for reviewing this section and making valuable suggestions.





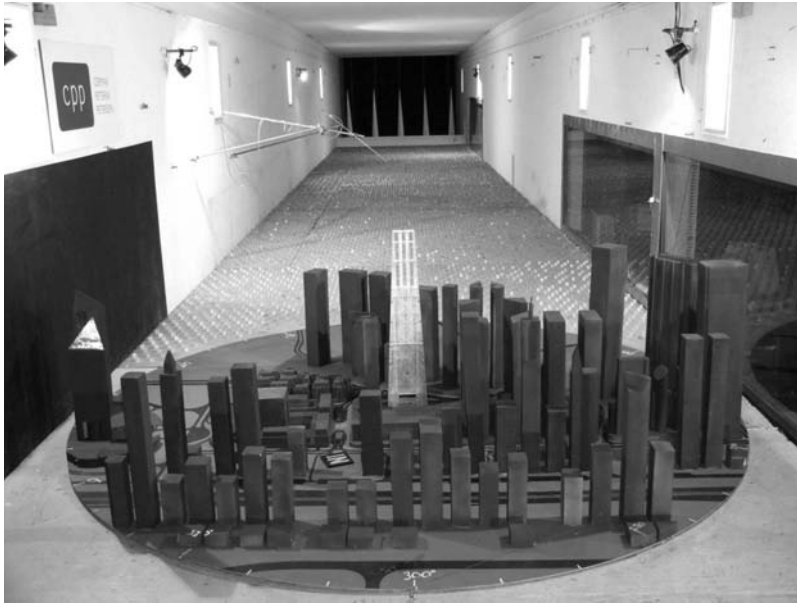
**FIGURE 4.34** Schematics of 64-m-long wind tunnel; overall size  $64\text{ m} \times 15\text{ m} \times 6\text{ m}$ .



**FIGURE 4.35** Schematics of two additional wind tunnels.



**FIGURE 4.36** Photographs of rigid model in wind tunnel. Chifley Plaza, Sydney. (Courtesy of CPP Wind Engineering & Air Quality Consultants.)



**FIGURE 4.37** Model in wind tunnel: DIFC Dubai. (Courtesy of CPP Wind Engineering & Air Quality Consultants.)



**FIGURE 4.38** Close-up of model in wind tunnel: Pentominium, Dubai. (Courtesy of CPP Wind Engineering & Air Quality Consultants.)

Services provided by a wind tunnel consultant typically offer the following benefits:

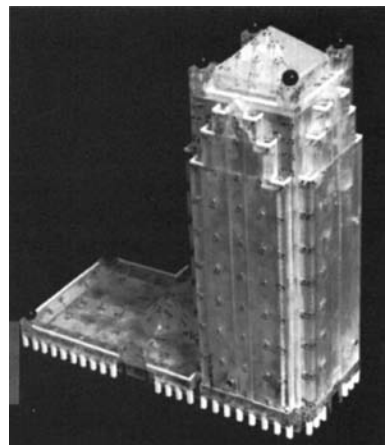
- Provides an accurate distribution of wind loads, especially for structures in a built-up environment by determining directly the impact of surrounding structures.
- Provides predictions of wind-induced building motions (accelerations and torsional velocities) likely to be experienced by occupants of the top floors, and compares the test results to available serviceability criteria. Complaints by building occupants of excessive motion



**FIGURE 4.39** Mode in wind tunnel: Shams, Dubai.



(a)



(b)

**FIGURE 4.40** (a) Rigid model in wind tunnel. (b) Close-up of a rigid model. (Photos courtesy of Rowan, Williams, Davis, and Irwin, RWDI.)

can compromise the value of a development. Information provided by tests enables the design team (structural engineers, architect, and developer) to make timely and appropriate modifications, if required, to architectural and structural design.

- Pretest estimate of cladding pressures and overall loads by a wind engineer, based on a review of similar buildings, with appropriate consideration of the local meteorological data can help the engineer, the architect, and the facade engineer to develop a preliminary foundation design and initial cost estimate for the curtain wall.
- Provides an assessment of expected pedestrian wind comfort along with any conceptual recommendations for improvement to key pedestrian areas (e.g., main entrances, pool decks, etc.).

- Because wind-tunnel studies consider the effect of nearby buildings and directional variations in the local wind climate, the overall design wind loads are generally (but not always) lower than code wind loads resulting in lower cost.

In determining the effects of wind for a particular building, there are two main components to consider. The first comprises the aerodynamic characteristics of the building. These are simply the effects of the wind when it blows from various directions. This information only has limited value, however, without knowing how likely it is that the wind will flow from those directions and how strongly it is likely to blow. This climatological information, in the form of a probability distribution of wind speed and direction, is the second main ingredient needed for determining wind effects for a particular development. The aerodynamic information is characteristic of the particular building and its immediate surroundings, while the wind climate information is characteristic of the geographical location of the development. Both are necessary to determine the wind effects for a particular building and, when combined, provide statistical prediction of the wind effect.

The aerodynamic characteristics of the building are commonly determined through model studies of the building. These studies may include measurement of various types of information of interest, such as cladding loads, structural loads, and pedestrian-level wind speeds. The probability distribution of wind speed and direction, is determined from analyses of historical wind speed and direction records taken from an airport or other meteorological source. Tropical cyclones, such as a hurricane or typhoon winds present a special case and their associated statistical characteristics are handled separately using Monte Carlo prediction techniques.

Wind-tunnel testing of buildings is an offshoot of aeronautical engineering, in which the flow characteristics at high Reynold's Numbers (high speeds) is duplicated. Aeronautical wind tunnels used for testing airplanes are configured to minimize the effects of turbulence, and as such, they do not duplicate atmospheric boundary layer or wind turbulence that occurs within a height of 1200 ft or so above ground. On the other hand, with the exception of super tall buildings protruding well above the boundary layer, the construction activity of typical high rises occurs within this atmospheric boundary layer, characterized by a gradual retardation of wind speed and high turbulence near the surface of the earth. Therefore, for testing of buildings, aeronautical wind tunnels have been modified and entirely new facilities have been built within the last three decades to reproduce turbulence and natural flow of wind within the boundary layer. Tests conducted in these boundary-layer wind tunnels (BLWT), provide information for the design for overall structural loads, cladding, and components, as well as the assessment of human comfort in building motion, pedestrian-level wind environment, and air quality impacts.

Wind-tunnel tests (or similar tests employing fluids other than air) are considered to be properly conducted only if the following conditions are satisfied:

1. The natural atmospheric boundary layer has been modeled to account for the variation of wind speed with height.
2. The length scale of the longitudinal component of atmospheric turbulence is modeled to approximately the same scale as that used to model the building.
3. The modeled building and the surrounding structures and topography are geometrically similar to their full-scale counterparts.
4. The projected area of the modeled building and its surroundings is less than 8% of the test section cross-sectional area unless correction is made for blockage.
5. The longitudinal pressure gradient in the wind-tunnel test section is accounted for.
6. Reynolds number effects on pressures and forces are minimized.
7. Response characteristics of the wind-tunnel instrumentation are consistent with the required measurements.

BLWT capable of developing flows that meet the conditions stipulated above typically have test-section dimensions in the following ranges: width, 6–12 ft (2–4 m); height, 6–10 ft (2–3 m); and length, 50–100 ft (15–30 m). Maximum wind speeds are ordinarily in the range of 25–100 mph (10–45 m/s).

BLWT are designed with a relatively long test section, to permit extended models of upwind terrain to be placed in front of the model of the building under test as well as sufficient distance to develop the appropriate boundary layer characteristics. The modeling is done in more detail close to the site. The wind-tunnel flow then develops characteristics which are similar to the wind over the terrain approaching the actual site.

The modeling is comprised of the following components:

1. A detailed model of the building. Different types of model are used for the various types of tests.
2. A detailed proximity model of the surrounding area and structures, typically constructed using blocks of wood and styrofoam. Depending on the scale and size of the model, this may extend for a radius of approximately 500–600 m.
3. Coarsely modeled upstream terrains, chosen to represent the general roughness upstream of the site for particular wind directions.

For project sites close to hilly terrain or with unusual topography, a topographic study may be carried out to establish the wind characteristics at the site. This may be in the form of topographic model study at a small scale (~1:3000) or computational methods. The resulting target wind characteristics will be modeled in the large scale building tests.

The fundamental concept is that the model of the structure and of the wind should be at approximately the same scale. The natural scaling of the flow in the wind tunnel is in the range 1:400–1:600; however, in some cases, instrumentation or other requirements may demand a larger model. In these cases, additional flow modification devices may be used to approximate large-scale flows.

In all cases, it is the mean wind speed profile and the turbulence characteristics over the structure that are most important to match with those expected in full scale. Data obtained through the scale measurements are used to ensure that the test speeds near the top of the building are properly matched with full-scale wind speeds predicted to occur at the full-scale site.

#### 4.6.1 TYPES OF WIND-TUNNEL TESTS

Three basic types of wind-tunnel modeling techniques are commonly used:

1. Rigid pressure model (PM)
2. Rigid high-frequency base balance model (HFBB/HFFB)
3. Aeroelastic model (AM)

The pressure model provides local peak pressures for design of cladding elements and mean pressures for the determination of overall mean loads. The high-frequency model measures overall fluctuating loads for the determination of dynamic responses. The aeroelastic model is used for direct measurement of responses such as, deflections, and accelerations, and is deemed necessary, when the lateral motions of a building are considered to have a large influence on wind loading, and for measuring effects of higher modes.

The BLWT by virtue of having a long working section with roughened floor and turbulence generators at the upward end, simulates the mean wind profile and turbulence. The model is mounted on a turntable to allow measurement of pressures for any wind direction. Near-field characteristics around the building are duplicated, typically using polystyrene foam models.

#### 4.6.1.1 Rigid Pressure Model

Although the primary purpose of the rigid-model test is for obtaining cladding design pressures, the data acquired from the wind-tunnel tests may be integrated to provide floor-by-floor shear forces for design of the overall MWFRS, provided there is sufficient distribution of pressure taps.

Most commonly, pressure study models are made from methyl methacrylate commonly known as Plexiglas, Lucite, and Perspex. This material has several advantages over wooden or aluminum alloy models because it can be easily and accurately machined and drilled and is transparent, facilitating observation of the instrumentation inside the model. It can also be formed into curved shapes by heating the material to about 200°C. Model panels can either be cemented together or joined, using flush-mount screws. More recently, advances in rapid proto typing have allowed models to be directly produced from plastic resin using 3D printing technologies.

A scale model of the prototype typically in a 1:300–1:500 range is constructed using architectural drawings of the proposed project. Building features of significance to wind flow, such as building profile, protruding mullions, and overhangs are simulated.

The model is typically instrumented with as many as 500–700 pressure taps. It includes detailed topography of nearby surroundings within a radius of 1500 ft (457 m). Flexible, transparent vinyl or polyethylene tubing of about 1/16 in (1.5 mm) internal diameter is used to connect the pressure taps to the solid state pressure transducers. Pressure tap locations are generally more concentrated in regions of high-pressure gradients such as around corners or other changes in building geometry.

The wind-tunnel test is run for a duration of about 60 s which corresponds to approximately 1 h in real time. Typically measurements are taken for wind direction of 10° increments, sufficient numbers of readings are gathered from each port to offset the effects of time-dependent fluctuations. The measured pressures are divided by a reference pressure measured in the wind tunnel. Subsequent analysis of the pressure coefficients produce the largest positive, largest negative, mean and root mean square, RMS values.

The BLWT by virtue of having a long working section with roughened floor and turbulence generators at the upwind end, is believed to correctly simulate the mean wind profile and turbulence. The model mounted on a turntable allows measurement of pressures for any wind direction. Near-field characteristics around the building are duplicated, typically using polystyrene foam models.

The aerodynamic damping which is building-motion dependent, cannot be measured using rigid-pressure model studies. It can be measured however, by using aeroelastic models. Nevertheless, the value of the aerodynamic damping is generally small and positive for typical buildings in the along-wind direction, and positive as well in the across-wind direction up to the velocity where vortex shedding has a major contribution to the response. Because this velocity is usually higher than typical design wind speeds, the aerodynamic damping is usually of little consequence in typical building design.

##### 4.6.1.1.1 Cladding Pressures

From the data acquired, full-scale peak exterior pressures and suctions at each tap location are derived by combining the wind-tunnel data with a statistical model of windstorms expected at the building site. The results are typically given for 25, 50, and 100 year return periods.

In evaluating peak wind loads on the exterior of the prototype, the effects of internal pressures arising from air leakage, mechanical equipment, and stack effect must be included. The possibility of window breakage caused by roof gravel scoured from roofs of adjacent buildings and other flying debris during a windstorm should also be included. As a rough guide, the resulting internal pressure can be considered to be in the range of  $\pm 5$  psf at the base, to as much as  $\pm 20$  psf at the roof of a 50-story building.

In the design of glass, a 1 min loading is commonly used. The duration of measured peak pressure in wind tunnels is quite different from the 1 min interval used in design. Usually it corresponds to 5–10 s. Therefore, it is necessary to reduce the peak loads measured in wind-tunnel tests. Empirical

reduction factors of 0.80, 0.94, and 0.97 are given in glass manufacturers' recommendations for three different types of glass—annealed float glass, heat-strengthened glass, and tempered glass.

#### 4.6.1.1.2 Overall Building Loads

Although rigid-model test results are primarily used to predict wind loads for design of glass and other cladding elements, they can nevertheless be integrated to provide lateral loads for the design of the MWFRS. The procedure entails combining wind load information with the building response characteristics using random vibration theory.

In spite of the fact that rigid-model wind study does not take into account many of the factors typically considered in an aeroelastic study, it is still considered adequate to provide design data for buildings with height-to-width ratios of less than 5.

The development of solid-state pressure scanners, which permit the simultaneous measurement of pressures at many points on the surface of a building, allows the determination of instantaneous overall wind forces from the local pressure measurements. The advantages of this technique are that a single model used in a single testing session can produce both overall structural loads and cladding loads. The testing parameters would be extended to ensure that the local pressure data taken is also sufficient for the analysis of structural loads.

A disadvantage of this technique is that the cladding pressure test model typically includes more instrumentation and can take longer to construct than a force balance test model. Also, like the force balance technique, it does not include any effects of the building's motion through the air, such as aerodynamic damping; however, neglecting these effects is usually slightly conservative. Proper integration of local pressures to obtain overall wind forces requires that all buildings surfaces are adequately represented in the model instrumentation and subsequent calculations. This may not be possible for buildings or structures with complex geometry or where insufficient simultaneous pressure measurements are not possible.

In summary, the determination of total design loads from the simultaneous measurement of external point pressures is as follows: The instantaneous generalized forces are determined from the pressure measurements and are then used in a standard random vibration analysis to provide estimates of the total dynamic loads and responses of the structure. These loads and responses are then combined with the statistics of the full-scale wind climate at the site, to provide predictions of loads and responses for various return periods.

#### 4.6.1.2 High-Frequency Base Balance and High-Frequency Force Balance (HFBB/HFFB) Model

The effect of wind load on a flexible building can be considered as an integrated response resulting from three distinct components. The first is the mean wind load that bends and twists the building. The second is the fluctuating load from the unsteady wind that causes oscillation of the building about a steady deflected shape. The third contribution comes from the inertia forces similar to the lateral forces induced during earthquakes. However, for design purposes, the inertial effects can be considered as an additional equivalent wind load.

A rigid model, as mentioned previously, is convenient for measuring local positive and negative pressures distributed uniquely around a building. These local pressures can be integrated to derive net lateral forces in two perpendicular directions and a torsional moment about a vertical axis, at each level. The cumulative shear, and the overturning and torsional moments at each floor are obtained from simple statics, as are the base shear and overturning moments.

A force-balance model test performs a similar integration as a pressure model, except that the number of pressure points used in the pressure integration is limitless. The cumulative impact of every molecule of air is measured in this test.

This technology has clear advantage over a pressure integration approach, especially for unusually shaped structures or where too few pressure tubes can be routed through the model.

Two basic types of force balance models are utilized. In the first type, the outer shell of the model is connected to a rigid metal cantilever bar. Strain gauges are fitted into the model, and the aerodynamic forces are derived from the strain measurements. In the second type, a simple foam model of the building is mounted on a five-component, high-sensitivity force balance that measures bending moments and shear forces in two orthogonal directions and torsion about a vertical axis. In both models, the resulting overall fluctuating loads are determined, and by performing an analysis using random vibration theory, the information of interest to the structural engineer—floor-by-floor lateral loads—and the expected acceleration at the top floors is determined.

#### 4.6.1.2.1 HFBB Model (Figures 4.41 through 4.45)

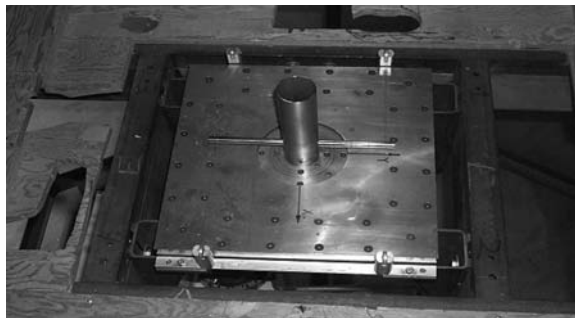
The model consists of a lightweight rigid model mounted on a high-frequency-response base balance. Design lateral loads and expected building motions are computed from the test results. The method is suitable when building motion does not, itself, affect the aerodynamic forces, and when torsional effects are not of prime concern. In practice, this method is applicable to many tall buildings.

The model is typically constructed to a scale on the order of 1:500. The model itself is constructed of a lightweight material such as balsa wood. Strain gauges attached to the base measure the instantaneous overturning and torsional moments at the base.

From the measured bending and twisting moments and known frequency and mass distribution of the prototype, wind forces at each floor and the expected peak acceleration are derived.



**FIGURE 4.41** Simple stick aeroelastic model.



**FIGURE 4.42** Aeroelastic model.





**FIGURE 4.43** Rigid aeroelastic model mounted on a flexible steel bar.

#### 4.6.1.2.2 Five-Component High-Frequency: Force Balance Model, HFFB Model (Figure 4.46)

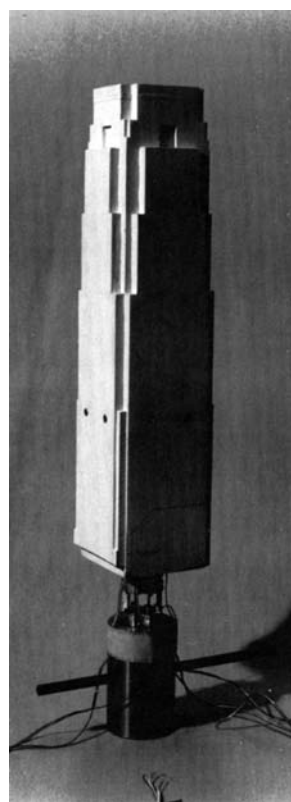
In this model, prototype building is represented as a rigid model. Made of lightweight material such as polystyrene foam, the model is attached to a measuring device consisting of a set of five highly sensitive load cells attached to a three-legged miniature frame and an interconnecting rigid beam. A typical configuration is shown in Figure 4.46, in which the load cells are schematically represented as extension springs. Horizontal forces acting in the  $x$  direction produce extension of the vertical spring at 1, that can be related to the base overturning moment  $M_y$ , with the known extension of the spring and the pivotal distance  $P_x$ . Similarly, the base-overturning moment  $M_y$  can be calculated from a knowledge of extension of the spring at 2 and the pivotal distance  $P_y$ . The horizontal spring at 3, measures the shear force in the  $x$  direction, while those at 4 and 5 measure the shear force in the  $y$  direction. The difference in the measurements of springs at 4 and 5 serves to compute the torsional moment at the base about the  $z$ -axis. It should be noted, however, that the test results for torsion are an approximation of the true response because the model does not account for the relative twist present in the prototype.

#### 4.6.1.3 Aeroelastic Model (Figures 4.47 through 4.53)

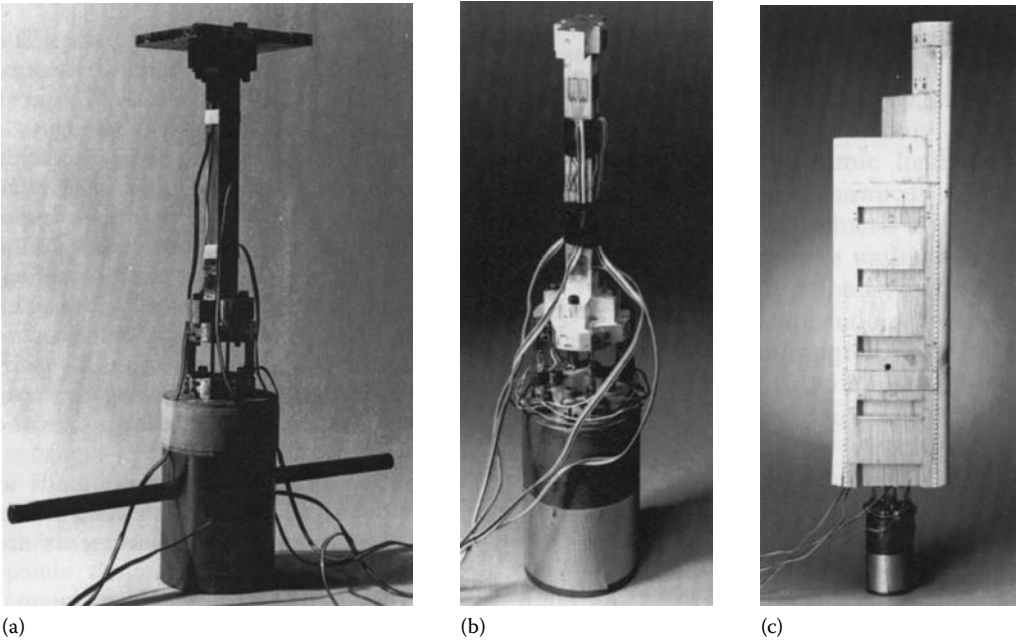
In situations where the dynamic response of a structure may exhibit instabilities (Tacoma Narrow Bridge, c.1940) or to capture the resonant behavior precisely, an aeroelastic model test should be conducted. This technique allows the aerodynamic damping (which can become negative) to be evaluated as well as the determination of other higher order effects.

A variety of models ranging from very simple rigid models mounted on flexible supports to models that mimic multimode vibration characteristics of tall buildings are used for this purpose. The more common types can be broadly classified into two categories: (1) stick models; and (2) multidegree-of-freedom models.

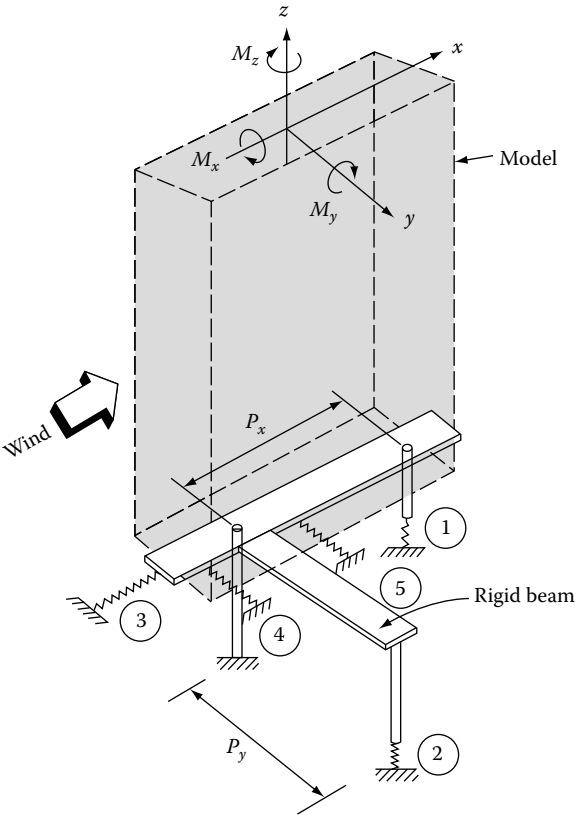
In addition to the similarity of the exterior geometry between the prototype and the model, the aeroelastic study requires similarity in inertia, stiffness, and damping characteristics of the



**FIGURE 4.44** High-frequency force balance model.



**FIGURE 4.45** Detail view of high-frequency force balance model: (a,b) Close-up view of instrumentation and (c) model.



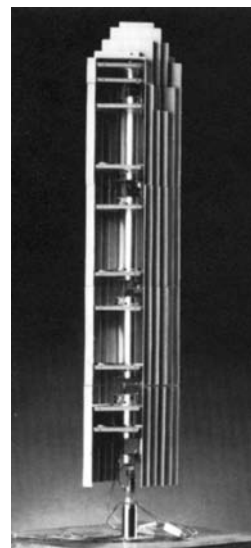
**FIGURE 4.46** Schematic of five-component force balance model.

building. Although a building in reality responds dynamically to wind loads in a multimode configuration sufficient evidence exists to show that the dynamic response occurs primarily in the lower modes of vibration. Therefore, it is possible to study dynamic behavior of buildings by using simple dynamic models.

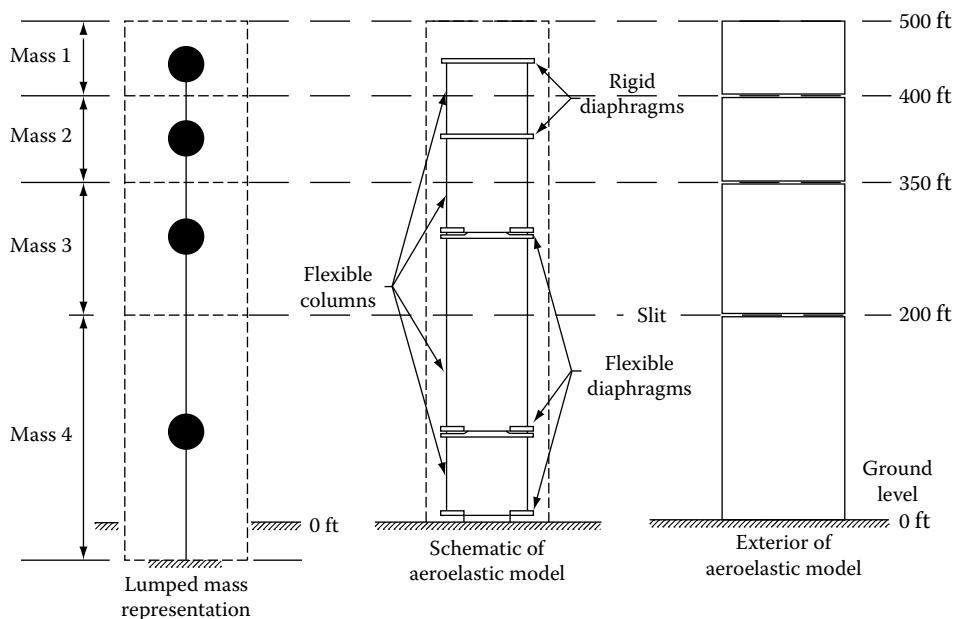
The stick model aeroelastic test requires the dynamic properties (mass, stiffness, and period) of the building in the fundamental sway modes and measuring the response to wind loads directly. The building is modeled as a rigid body, pivoted near the base, with the elasticity provided by appropriately selected springs. Implicit in this technique is the assumption that the sway modes do not include any coupling and can be approximated as linear, and that torsion is unimportant. These prove to be reasonable assumptions for a large range of buildings.

The advantages of this technique are: (1) The measurements will include effects of aerodynamic damping that are not included when using the force balance technique. (2) It is also a simpler, less expensive technique than a multidegree-of-freedom aeroelastic test. The disadvantages of the technique are: (1) It is limited by the assumptions noted above and it is more complicated and expensive than the force balance technique. (2) It is less accommodating of changes to the dynamic properties of the building after the test. (3) Its advantage over the force balance technique, namely, the inclusion of aerodynamic damping effects, rarely proves to be necessary since the aerodynamic damping is usually small.

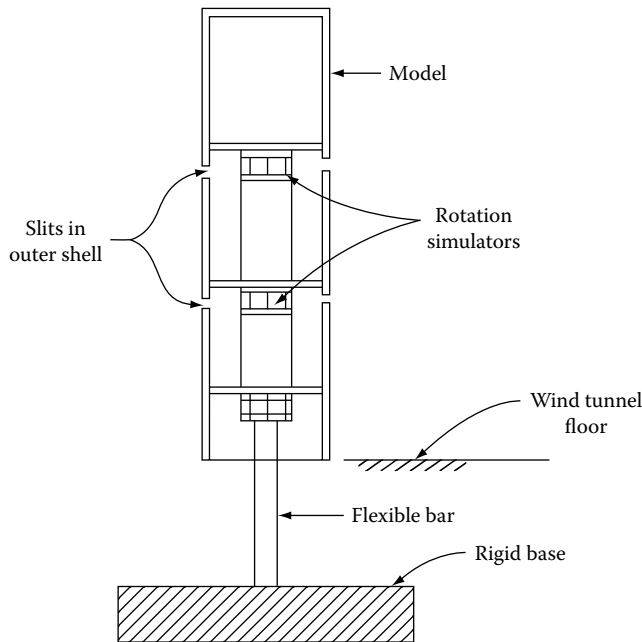
As with other types of tests, once the aerodynamic data has been measured, it is combined with the statistics of the full-scale wind climate at the site, to provide predictions of loads and responses for various return periods. Generally only a few key wind directions are studied in this manner.



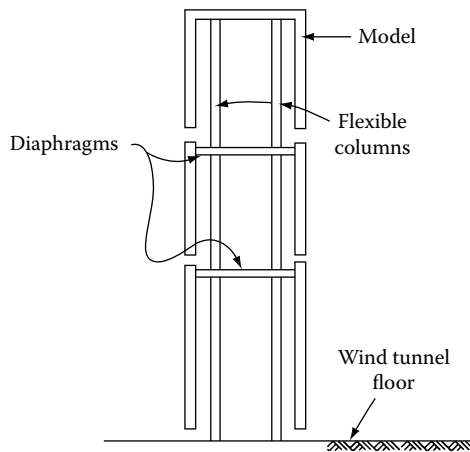
**FIGURE 4.47** Aeroelastic model: cutaway view.



**FIGURE 4.48** Aeroelastic model with provisions for simulating torsion.

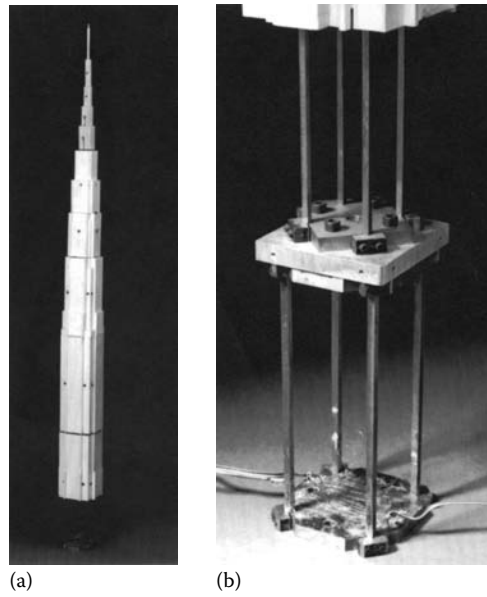


**FIGURE 4.49** Aeroelastic model with rotation simulators.

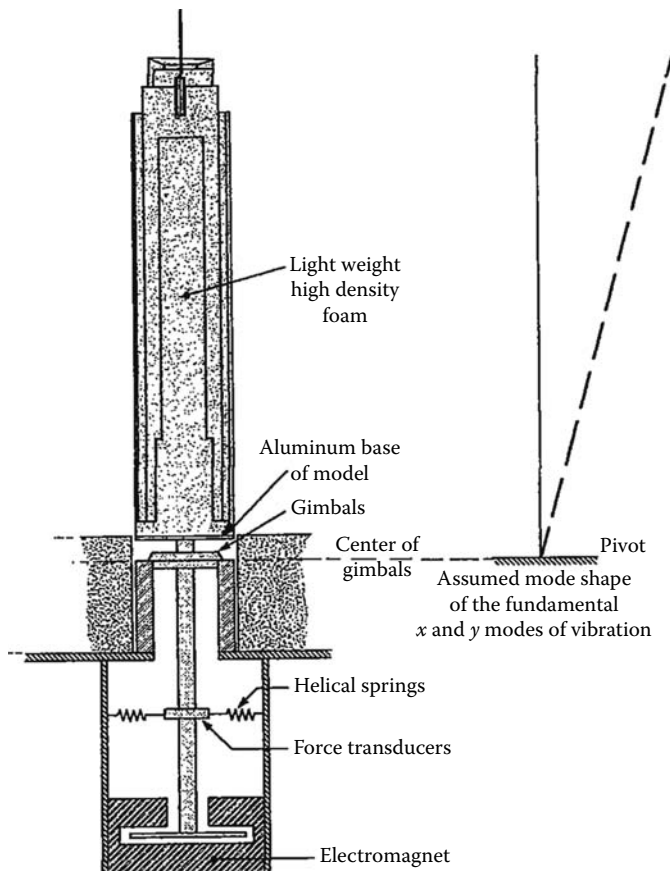


**FIGURE 4.50** Aeroelastic model; schematic section.

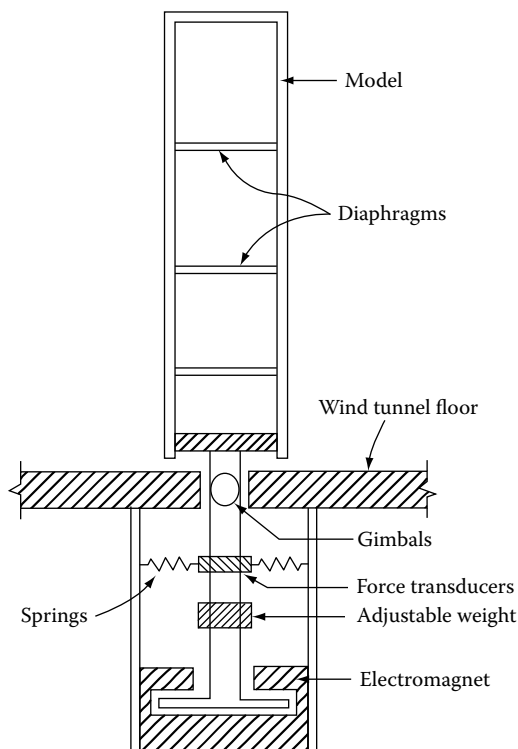
Rigid-model study is based on the assumption that the fundamental displacement mode of a tall building varies linearly along the height. In terms of aerodynamic modeling, it is not necessary to achieve the correct density distribution along the building height as long as the mass moment of inertia (MMI) about a chosen pivot point is the same as that of the correct density distribution. It should be noted that the pivot point is chosen to obtain a mode shape that provides the best agreement with the calculated fundamental mode shapes of the prototype. For example, modal calculations for a tall building with a relatively stiff podium may show that the pivot point is located at the intersection of podium and the tower and not at the ground level. Therefore the pivot point for the model should be at a location corresponding to this intersection point rather than at the base of the building.



**FIGURE 4.51** Aeroelastic model: (a) A proposed tower in Chicago and (b) close-up view of instrumentation.



**FIGURE 4.52** Simple stick aeroelastic model.



**FIGURE 4.53** Aeroelastic model.

Figures 4.52 and 4.53 shows a rigid aeroelastic model mounted on gimbals. The purpose of springs located near the gimbals is to achieve the correct model scale frequency correlation in the two fundamental sway modes. An electromagnet or oil dashpot provides the model with a structural damping corresponding to that of the full-scale building.

Typically, aeroelastic response measurements are carried out at several wind speeds because engineers need information on both relatively common events, such as 10 year wind loads for assessing serviceability and occupant comfort, and relatively rare events, such as 50 and 100 year winds to determine loads for strength design. As mentioned earlier, the modeling of dynamic properties requires simulation of inertial, stiffness, and damping characteristics. It is necessary, however, to simulate these properties for only those modes of vibration which are susceptible to wind excitation.

It is often difficult to determine quantitatively when aeroelastic study is required. The following factors may be used as a guide in making a decision:

1. The building height-to-width ratio is greater than about 5–8; that is, the building is relatively slender.
2. Approximate calculations show that there is a likelihood of significant across-wind response.
3. The structure is light in density on the order of  $8\text{--}10\text{ lb/ft}^3$  ( $1.25\text{--}1.57\text{ kN/m}^3$ ).
4. The structure has very little inherent damping, such as a building with welded steel construction.
5. The structural stiffness is concentrated in the interior of the building, making it torsionally flexible. A building with a central concrete core is one example.
6. The calculated period of oscillation of the building is long, in excess of 5 or 6 s.
7. Existence of nearby buildings that could create unusual channeling of wind, resulting in torsional loads and strong buffeting action.

8. The building is sited such that predominant winds occur from a direction most sensitive to the building oscillations.
9. The building is a high-rise apartment, condominium, or hotel. Occupants in these buildings are more likely to experience discomfort from building oscillations. This is because residents in these buildings are likely to remain longer in a given location than they would in a typical office setting.

#### 4.6.1.4 Multidegree-of-Freedom Aeroelastic Model

For a building that is uniform for the entire height, it is reasonable to assume that sway modes of vibration vary linearly along the height. However, for buildings of complex shapes with step backs or major variations in stiffness, this assumption may not yield satisfactory results because fundamental mode shape may not be linear, and more importantly higher modes could contribute significantly to the dynamic behavior.

In such cases, it is essential to simulate the multimode behavior of the building. This is achieved using a model with several lumped masses interconnected with elastic columns. Schematic of such a model is shown in Figure 4.48, in which the building is divided into four zones, with the mass of each zone located at the center. The masses are concentrated in the diaphragms representing the floor system that are interconnected by flexible columns. A lightweight shell simulating the building shape encloses the assembly of the floor system, masses, and columns. The outer shell is cut at the diaphragm levels to allow for relative movements between the masses. Similarity between elastic properties of the prototype and the model is achieved to varying degrees depending upon the predominant characteristics of the building.

The required structural damping is achieved by adding strips of foam tape that connect the floors. These strips add negligible stiffness while dissipating vibrational energy. The geometric modeling is completed with sections of balsa wood skins, which are attached to each floor so as not to make contact with each other.

This technique requires scaling the dynamic properties (mass, stiffness, periods, and mode shapes) of the building in the fundamental sway modes and the fundamental torsion mode, including any coupling within modes. Some higher modes of vibration are also modeled. The responses to wind loads are then measured directly.

The advantage of this technique is that the measurements will include effects of aerodynamic damping, vortex shedding, coupling within modes, and some higher modes that are not fully dealt with when using the force balance technique. For most buildings, however, it can be argued that the aerodynamic damping effects are likely to be small, higher modes can be neglected, and that the force balance adequately handles coupled modes analytically. Nevertheless, for more complicated structures, the additional reassurance of an aeroelastic test may be justified.

The disadvantages of the technique are that the model is time consuming and expensive to build. The model is also designed for a single set of building dynamic properties and approximations must be made if these change during the course of the design process. The force balance technique on the other hand yields results equally applicable to any set of building dynamic properties.

As with other types of tests, once the aerodynamic data has been measured for a full range of wind directions, it is combined with the statistics of the full-scale wind climate at the site, to provide predictions of loads and responses for various return periods.

The completed model is attached to a strain-gauged balance at its base. The balance measures overall base bending moments and torsion. Additional strain gauges may be placed at key locations on the model to capture the response of higher modes. Three accelerometers are normally located at the top mass to provide measures of the translational and the rotational accelerations at the height. One accelerometer is mounted to measure acceleration in one direction, say the  $x$  direction, while the other two are mounted to measure accelerations in the orthogonal direction. These two

accelerometers are mounted symmetrically about the axis of twist so that their difference yields values of the torsional acceleration.

#### **4.6.1.5 Option for Wind-Tunnel Testing**

As an option to the wind-tunnel procedure, ASCE 7-05 in Section 6.5.2, permits an analytical procedure using recognized literature documenting such wind load effects. These effects principally consist of load magnification caused by gusts in resonance with along-wind vibrations of flexible buildings.

#### **4.6.1.6 Lower Limit on Wind-Tunnel Test Results**

Wind-tunnel test frequently measure wind loads that are significantly lower than required by ASCE 7-05. This feature is principally due to the shape of the building, shielding in excess of that implied by exposure categories, and necessary conservatism in enveloping load coefficients. In some cases, adjacent structures may shield the structure sufficiently that removal of one or two structures could significantly increase wind loads. Additional wind-tunnel testing without specific nearby buildings (or with additional buildings if they might cause increased loads through channeling or buffeting) is an effective method for determining the influence of adjacent buildings. It would be prudent to test any known conditions that change the test results and to discuss the results among the owner, designers, and wind-tunnel laboratory. However it is impossible to anticipate all possible changes to the surrounding environment that could significantly impact pressures for the MWFRS and for cladding. Also, additional testing may not be cost effective. Suggestions provided in the ASCE 7-05 commentary, (expected to be included in the next edition of ASCE 7-10 wind provisions) for placing a lower limit on wind-tunnel results are given in the following text.

##### *4.6.1.6.1 Lower Limit on Pressures for a Main Wind-Force-Resisting System*

Forces and pressure determined by wind-tunnel testing shall be limited to not less than 80% of the design forces and pressures that would be obtained in Section 6.5 for the structures unless specific testing is performed to show that it is the aerodynamic coefficient of the building, rather than shielding from nearby structures, that is responsible for the lower values. The 80% limit may be adjusted with the ratio of the frame load at critical wind directions, as determined from wind-tunnel testing without specific adjacent buildings, but including appropriate upwind roughness, to that determined by Section 6.5.

##### *4.6.1.6.2 Lower Limit on Pressures for Components and Cladding*

The design pressures for components and cladding on walls or roofs shall be selected as the greater of the wind-tunnel test results or 80% of the pressure obtained for Zone 4 for walls and Zone 1 for roofs, as determined in Section 6.5, unless specific testing is performed to show that it is the aerodynamic coefficient of the building, rather than shielding from nearby structures, that is responsible for the lower values. Alternatively, limited tests at a few wind directions without specific adjacent buildings, but in the presence of an appropriate upwind roughness, may be used to demonstrate that the lower pressures are due to the shape of the building and not due to shielding.

### **4.6.2 PREDICTION OF ACCELERATION AND HUMAN COMFORT**

One of the basic reasons for conducting wind tunnel testing is to evaluate the effect of building motions on the comfort of its occupants. It is generally known that quantitative prediction of human discomfort is difficult if not impossible to determine in absolute terms because perception of motion and associated discomfort are subjective by their very nature. However, in practice certain thresholds of comfort have been established by relating acceleration due to building motion at the top floors to the frequency of windstorms. One such criterion is to limit predicted accelerations of top floors to 20 milli-g (2% of acceleration due to gravity) in a 10 year windstorm.



In wind-tunnel tests, accelerations are measured directly by accelerometers. Two accelerometers are typically used to measure components in the  $x$  and  $y$  directions, while a third records the torsional component. Peak acceleration is evaluated from the expression:

$$a = \sqrt{a_x^2 + a_y^2 + a_z^2}$$

where

$a$  is the peak acceleration

$a_x$  and  $a_y$  are the accelerations due to the sway components in the  $x$  and  $y$  directions

$a_z$  is the acceleration due to torsional component

The peak accelerations measured for a series of wind directions and speeds are combined with the meteorological data to predict frequency of occurrence of human discomfort, for various levels of accelerations. A commonly accepted criterion is that for human comfort, the maximum acceleration in upper floors should not exceed 2.0% of gravitational acceleration for a 10 year return-period storm.

Shown in Figure 4.51 is a comparison of predicted peak accelerations from wind-tunnel tests and full-scale measurements for a 70 plus-story steel building. The measurements were taken on August 18, 1983 during Hurricane Alicia.

### 4.6.3 LOAD COMBINATION FACTORS

The determination of the wind loads by BLWT treats the load direction independently. It should be recognized that wind loads in all three principal directions of a building will occur simultaneously although the peak loads in each respective direction will not all occur at the same time. Therefore, load combination factors are used to specify the required simultaneous application of loads in the three principal directions such that the major load effects are reproduced for design purposes. These can be in the form of (1) general load reduction factors applied to all three load directions or (2) a combination of load factors where the full application of the load in the main load direction is accompanied by reduced loads in the other load directions. This information is generally provided to the design engineer by the wind tunnel consultant.

### 4.6.4 PEDESTRIAN WIND STUDIES

A sheet of air moving over the earth's surface is reluctant to rise when it meets an obstacle such as a tall building. If the topography permits, it prefers to flow around the building rather than over it. Some examples are shown in Figure 4.1. There are good physical reasons for this tendency, the predominant one being that wind, if it has to pass an obstacle, will find the path of least resistance, that is, a path that requires minimum expenditure of energy. As a rule, it requires less energy for wind to flow around an obstacle at the same level than for it to rise. Also, if wind has to go up or down, additional energy is required to compress the column of air above or below it. Generally, wind will try to seek a gap at the same level. However, during high winds when the air stream is blocked by the broadside of a tall, flat building, its tendency is to drift in a vertical direction rather than to go around the building at the same level; the circuitous path around the building would require expenditure of more energy. Thus, wind is driven in two directions. Some of it will be deflected upward, but most of it will spiral to the ground, creating a so-called standing vortex or mini tornado at sidewalk level.

Buildings and their smooth walls are not the only victims of wind buffeting. Pedestrians who walk past tall, smooth-skinned skyscrapers may be subjected to what is called the Mary Poppins effect, referring to the tendency of the wind to lift the pedestrian literally off his or her feet. Another effect, known humorously as the Marilyn Monroe effect, refers to the billowing action of women's skirts in the turbulence of wind around and in the vicinity of a building. The point is that during

windy days, even a simple activity such as crossing a plaza or taking an afternoon stroll becomes an extremely unpleasant experience to pedestrians, especially during winter months in cold climates. Walking may become irregular, and the only way to keep walking in the direction of the wind is to bend the upper body windward (see Figure 4.54a through d).

Although one can get some idea of wind flow patterns from the preceding examples, analytically it is impossible to estimate pedestrian-level wind conditions in the outdoor areas of building complexes. This is because there are innumerable variations in building location, orientation, shape, and topography, making it impossible to formulate an analytical solution. Based on actual field experience and results of wind-tunnel studies, it is, however, possible to qualitatively recognize situations that adversely affect pedestrian comfort within a building complex.

Model studies can provide reliable estimates of pedestrian-level wind conditions based on considerations of both safety and comfort. From pedestrian-level wind speed measurements taken at specific locations of the model, acceptance criteria can be established in terms of how often wind speed occurrence is permitted to occur for various levels of activity. The criterion is given for both summer and winter seasons, with the acceptance criteria being more severe during the winter months. For example, the occurrence once a week of a mean speed of 15 mph (6.7 m/s) may be considered acceptable for walking during the summer, whereas only 10 mph (4.47 m/s) would be considered acceptable during winter months.



(a)



(b)



(c)



(d)

**FIGURE 4.54** Pedestrian reactions (a–d).

The pedestrian-level wind speed test is usually performed using the same model that was used for the cladding loads test, and may include some landscaping details. The model is instrumented with omnidirectional wind speed sensors at various locations around the development where measurements of the mean and fluctuating wind speed are made for a full range of wind angles, usually at  $10^\circ$  intervals.

The scaling involved is the same as that of the modeled wind flow. Thus, the ratio of wind speed near the ground to a reference wind speed near the top of the building is assumed to be the same in model and full scale, and to be invariant with both test speed and prototype speed. Since the thermal effects in the full-scale wind are neglected, strictly speaking, the results are only applicable to neutrally stable flows which are usually associated with stronger wind speeds. However, near tall buildings, local acceleration effects due to the local geometry are usually dominant over thermal effects, and are also the most important for design considerations.

The measured aerodynamic data is combined with the statistics of the full-scale wind climate at the site, to provide predictions of wind speeds at the site. Two types of predictions are typically provided:

1. Wind speeds exceeded for various percentages of the time on an annual basis. Wind speeds exceeded 5% of the time can be compared to comfort criteria for various levels of activity. Very roughly, this is equivalent to a storm of several hours duration occurring about once a week.
2. Predictions of wind speeds exceed during events or storms with different frequencies of occurrence. Wind speeds exceeded once per year can be compared to criteria for pedestrian safety.

Other, nonquantitative techniques are also available to determine levels of windiness over a project site. One of these techniques is a scour technique in which a granular material is spread uniformly over the area of interest. The wind speed is then slowly increased in increments. The areas where the granular material is scoured away first are the windiest areas; areas that are scoured later as the wind speed increases represent progressively less windy areas. Photographs of the scour patterns at increasing wind speeds can be superimposed using image processing technology to develop contour diagrams of windiness. This information can be used to determine locations for quantitative measurements, or simply to identify problem area where remedial measures are necessary. Testing several configurations can provide comparative information for use in evaluating the effects of various architectural or landscaping details. The advantage of the scour technique is that it can provide continuous information on windiness over a broad area, as opposed to the quantitative techniques which provide wind speeds as discrete points.

An even more qualitative technique is to introduce smoke to visualize flow paths and accelerations at arbitrary places. This can be a useful exploratory technique to understand the flow mechanisms and how best to alter them.

Pedestrian comfort depends largely on the magnitude of the ground-level wind speed regardless of the local wind direction. As a result, quantitative evaluation of the pedestrian-level wind environment at the wind-tunnel laboratory is normally restricted to measurements of the magnitude of ground-level wind speeds unless information on local wind direction is of special interest. Measurements are made of coefficients of wind speed (pedestrian-level wind speed as a fraction of an upper level reference speed) for a full range of wind directions at various locations near the site, and in some cases, at a location well away from the building to provide a form of calibration with existing experience.

These wind speed coefficients are subsequently combined with the design probability distribution of gradient wind speed and direction for the area to provide predictions of the full-scale pedestrian-level wind environment.

#### 4.6.5 MOTION PERCEPTION: HUMAN RESPONSE TO BUILDING MOTIONS

Every building must satisfy a strength criterion typically requiring each member be sized to carry its design load without buckling, yielding, or fracture. It should also satisfy the intended function (serviceability) without excessive deflection and vibration. While strength requirements are traditionally specified, serviceability limit states are generally not included in building codes. The reasons for not codifying the serviceability requirements are several: Failure to meet serviceability limits is generally not catastrophic; it is a matter of judgment as to the requirements' application, and entails the perceptions and expectations of the user or owner because the benefits themselves are often subjective and difficult to quantify. However, the fact that serviceability limits are not codified should not diminish their importance. A building that is designed for code loads may nonetheless be too flexible for its occupants, due to lack of deflection criteria. Excessive building drifts can cause safety-related frame stability problems because of large  $P\Delta$  effects. It can also cause portions of building cladding to fall, potentially injuring pedestrians below.

Perception of building motion under the action of wind is a serviceability issue. In locations where buildings are close together, the relative motion of an adjacent building may make occupants of the other buildings more sensitive to an otherwise imperceptible motion. Human response to building motions is a complex phenomenon encompassing many physiological and psychological factors. Some people are more sensitive than others to building motions. Although building motion can be described by various physical quantities, including maximum values of velocity, acceleration, and rate of change of acceleration—sometimes called jerk—it is generally agreed that acceleration, especially when associated with torsional rotations, is the best standard for evaluation of motion perception in tall buildings. A commonly used criterion is to limit the acceleration of a building's upper floors to no more than 2.0% of gravity (20 milli-g) for a 10 year return period. The building motions associated with this acceleration are believed to not seriously affect the comfort and equanimity of the building's occupants.

There are few comparisons of full scale measurements of peak accelerations with tunnel results. However, based on available measurements, it appears that the full scale measured peak accelerations are in good agreement with those predicted from wind tunnel test data (see Figure 4.55).

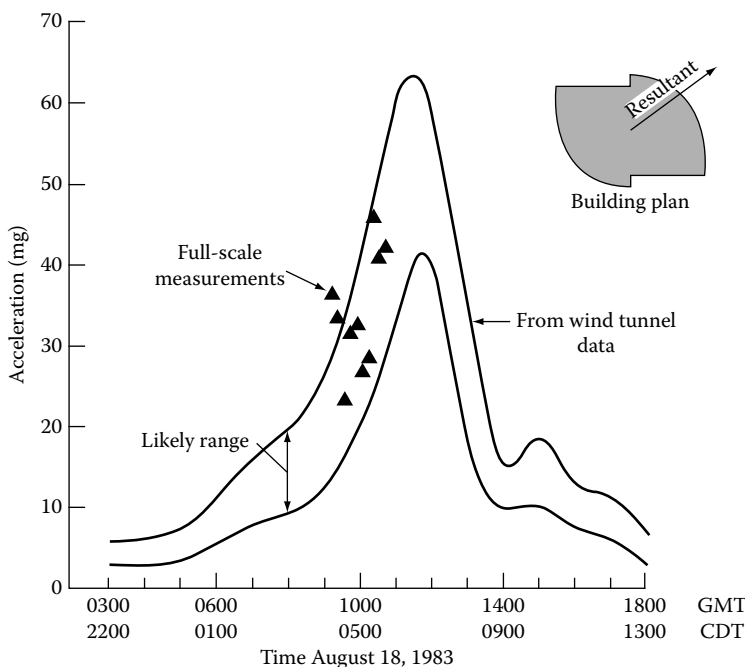
The Council on Tall Buildings and Urban Habitat (CTBUH) recommends 10 year peak resultant accelerations of 10–15 milli-g for residential buildings, 15–20 milli-g for hotels and 20–25 milli-g for office buildings. Generally, more stringent requirements are suggested for residential buildings, which would have continuous occupancy in comparison to office buildings usually occupied only part of the time and whose occupants have the option of leaving the building before a windstorm occurs.

However, on some of the extremely slender towers this proves difficult to achieve structurally even after doing all that it is practically possible in terms of adding stiffness and mass. It seems the only remaining measure that can be taken is to install a supplementary damping system.

#### 4.6.6 STRUCTURAL PROPERTIES REQUIRED FOR WIND-TUNNEL DATA ANALYSIS

For a rigorous interpretation of wind-tunnel test results, certain dynamic properties of a structure are required. These are furnished by the structural engineer and consist of

1. Natural frequencies of the first six modes of vibration
2. Mode shapes for the first six modes of vibration
3. Mass distribution, mass moments of inertia, and centroid location for each floor
4. Damping ratio
5. Miscellaneous information such as origin and orientation of the global coordinate system, floor heights, and reference elevation for “base” overturning moments



**FIGURE 4.55** Measured peak accelerations for the Allied Bank Tower during hurricane Alicia.

#### 4.6.6.1 Natural Frequencies

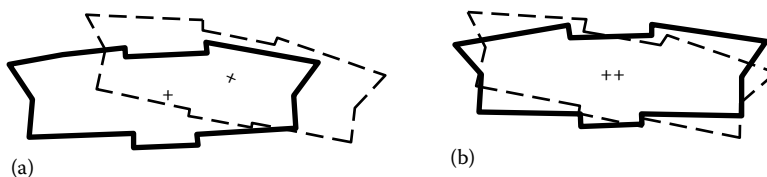
The natural frequencies (or periods) are the fundamental result of a dynamic analysis of the structure. Usually this is performed by a 3D computer program, which has the capability of performing an “eigenvalue” or model analysis. Generally, only the first three modes are used as these will correspond to the fundamental modes in each of the sway ( $x$ ,  $y$ ) and torsional ( $z$ ) directions. It should be noted that if the structure or mass distribution is unsymmetrical, then at least two of these components will be coupled together in some modes. Normally, the higher modes (four through six) are required only to insure that all of the fundamental directions have been included.

#### 4.6.6.2 Mode Shapes

Each mode of vibration is described by both a natural frequency and a shape. The mode shapes consist of tabulated values of the  $x$ ,  $y$ , and  $z$  deformations of each degree of freedom in the structure. For wind-engineering purposes, the floor diaphragm is typically considered rigid, and a single set of  $x$ ,  $y$ , and  $z$  deformations is established for each floor.

Mode shapes have no units. They are of indeterminate magnitude and can be scaled to any desired size. However, it should be remembered that when multidimensional mode shapes include both translational and rotational (twist) components, the same scaling factor must be applied to all components. The significance of this is illustrated in Figure 4.56. The two shapes shown, derived from the same numerical data but with different units, are obviously different: the left depiction can be described as dominated by translation whereas the right is apparently dominated by twist.

Another aspect of mode shapes concerns the reference system used in conveying the mode shapes. Most commercial programs specify the components with respect to the center of mass of each floor. If the shape consists of coupled twist and displacement, then the displacement magnitude is dependent on the location of the reference origin. If the centers of mass do not align on a straight



**FIGURE 4.56** Mode shapes using different units. (a) Mode dominated by translation, (b) mode dominated by twist.

vertical axis—as in setbacks or shear wall drop-offs—then the displacements will contain offsets or “kinks.” It is essential, therefore, that the wind engineer knows the reference system used in the modal data received from the structure engineer.

#### 4.6.6.3 Mass Distribution

The mass and the mass moment of inertia, MMI, are required at each floor, which typically include the structure’s dead weight and some allowance of live load. The MMI is taken about a vertical axis through the centroid (center of mass) of each floor. The location of the centroid is also needed.

All of the mass in the structure should be included since it will affect the natural frequency, which in turn, will influence the loads determined from the wind-tunnel tests. As a crude rule of thumb, an  $x$  percent change in the natural frequency may cause the loads to change by  $0.5x$  to  $2x$  percent.

The mass distribution is needed for two reasons. First, the mass and mode shape are used together with the natural frequency to determine the generalized stiffness of each mode. The stiffness is combined with the generalized load (measured on the wind-tunnel model) to determine the fluctuating displacement response in each mode. This is needed to evaluate the acceleration at the top of the building and to determine inertial wind loads.

Second, the static-equivalent loads from the wind-tunnel analysis consist of mean, background, and resonant contributions. The resonant contributions (which in many cases are the single largest contributor) are applied to the structure as concentrated forces at each concentrated mass, and are in proportion to the mass (and also to the modal displacement of that mass). Thus, the accuracy of the wind-tunnel load distribution (i.e., the floor-by-floor forces) is dependent on the relative mass throughout the structure.

#### 4.6.6.4 Damping Ratio

Currently there is no simple method to compute the damping ratio. Therefore, assumptions are made based on analysis of available field data. The customary practice in many parts of the world is to use a value of 0.01 for a steel frame structure, and 0.02 for a concrete structure for the prediction of 50–100 year loads. For special structures, for example, a mixed or composite frame, or those with extreme aspect ratios, other values may be appropriate. It should be noted that wind design is based on different principles from earthquake design, for which very high values of damping, usually 0.05, are considered. This value comes from those schooled in seismic design, based on ultimate conditions that do not apply to wind design. Therefore, wind engineers strongly encourage structural engineers to consider a lower value. As stated above, a service-level damping ratio of 0.01 or 0.02 is still the most used to determine the service load effects. An extreme damping level (say, 0.03 to 0.05) in combination with wind speeds that have recurrence interval of approximately 500–1000 years could also be used. For the prediction of low return-period accelerations such as a 10 year return period, it may be appropriate to use a lower damping value.

#### 4.6.6.5 Miscellaneous Information

- *Global coordinate system.* The engineer typically creates and uses this system when inputting nodal point locations in the horizontal (usually  $x, y$ ) plane. Computer output will report the center of masses using this same system. A supplemental sketch is required to define both the origin and coordinate directions relative to the structure.
- *Floor heights.* Provide a tabulation of the relative floor heights and some reference to an absolute height (datum).
- *Reference “base” elevation.* In addition to concentrated floor forces and torques to be applied at each floor level, a summary of information will be provided by the wind engineer as “base” overturning moments and torques. These moments are typically evaluated at “ground” level or “foundation” level (top of footing or pile caps, etc.) but they can be reported by the wind engineer at any elevation desired by the structural engineer.

#### 4.6.6.6 Example

The typical floor plan of a high-rise building shown in Figure 4.57 is referenced here to illustrate the typical format used when reporting the computer-generated structural dynamic properties for analyses of wind-tunnel test data. First, the structural engineer provides the wind engineer a floor-by-floor tabulation of the building properties. For each diaphragm, the mass, the center-of-mass's location, the center-of-rotation's location, and the mass-moment of inertia are given. See Figure 4.58.

The mass should account for the weights of structural slabs, beams, columns, and walls; and nonstructural components such as floor topping, roofing, fireproofing material, fixed electrical and mechanical equipment, partitions, and ceilings. When partition locations are subjected to change (as in office buildings), a uniform distributed dead load of at least 10 psf of floor area is used in calculating the mass. Typical miscellaneous items such as ducts, piping, and conduits can be accounted for by using an additional 2–5 psf. In storage areas, 25% of the design live load is included in the calculation of seismic weight. In areas of heavy snow, a load of 30 psf should be used where the snow load is greater than 30 psf. However, it may be reduced to as little as 7.5 psf when approved by building officials.

Recall that mass moment of inertia, MMI, is a structural property of the floor system that, in a manner of speaking, defines the rotational characteristics of the floor about the center of rotation. The larger the MMI, the more prone the building is to torsional rotations.

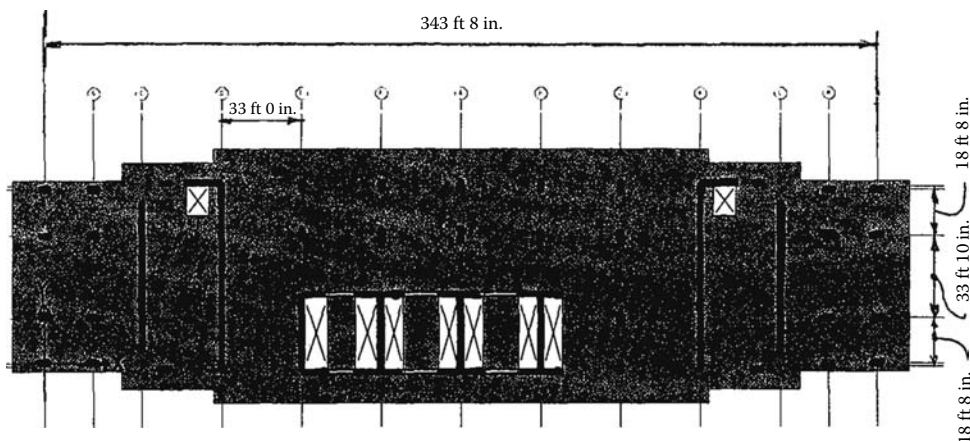


FIGURE 4.57 Building typical floor plan.

Story	Mass X [kip-s <sup>2</sup> /ft]	Mass Y [kip-s <sup>2</sup> /ft]	XCM [ft]	YCM [ft]	XCR [ft]	YCR [ft]	Mass Moment of Inertia [kip-s <sup>2</sup> /ft]
HI RF	193.2	193.2	157.0	-30.3	156.1	-18.4	1.111E+06
46	278.1	278.1	156.8	-30.9	156.4	-18.1	1.537E+06
45	138.0	138.0	156.7	-31.4	156.4	-18.0	7.577E+05
44	138.0	138.0	156.7	-31.4	156.5	-18.0	7.577E+05
43	138.0	138.0	156.7	-31.4	156.6	-18.0	7.577E+05
42	138.6	138.6	156.7	-31.5	156.6	-18.0	7.634E+05
41	153.7	153.7	156.4	-31.9	156.6	-18.0	1.030E+06
40	155.0	155.0	156.2	-32.0	156.6	-18.1	1.055E+06
39	155.0	155.0	156.2	-32.0	156.6	-18.1	1.055E+06
38	158.4	158.4	156.2	-32.1	156.6	-18.1	1.103E+06
37	184.1	184.1	155.9	-32.6	156.6	-18.1	1.531E+06
36	185.4	185.4	155.7	-32.6	156.6	-18.1	1.564E+06
35	185.4	185.4	155.7	-32.6	156.6	-18.2	1.564E+06
34	185.7	185.7	155.7	-32.7	156.6	-18.2	1.564E+06
33	187.9	187.9	155.9	-32.7	156.6	-18.3	1.618E+06
32	187.9	187.9	155.9	-32.7	156.6	-18.3	1.618E+06
31	187.9	187.9	155.9	-32.7	156.6	-18.4	1.618E+06
30	187.9	187.9	155.9	-32.7	156.6	-18.4	1.618E+06
29	187.9	187.9	155.9	-32.7	156.6	-18.5	1.618E+06
28	187.9	187.9	155.9	-32.7	156.5	-18.6	1.618E+06
27	187.9	187.9	155.9	-32.7	156.5	-18.7	1.618E+06
26	193.6	193.6	154.9	-32.2	156.5	-18.8	1.628E+06
25	192.6	192.6	155.0	-32.3	156.4	-18.9	1.628E+06
24	193.7	193.7	155.0	-32.4	156.4	-19.0	1.640E+06
23	194.7	194.7	154.9	-32.5	156.3	-19.2	1.652E+06
22	194.7	194.7	154.9	-32.5	156.3	-19.3	1.652E+06
21	194.7	194.7	154.9	-32.5	156.2	-19.4	1.652E+06
20	194.7	194.7	154.9	-32.5	156.2	-19.6	1.652E+06
19	194.7	194.7	154.9	-32.5	156.1	-19.7	1.652E+06
18	194.7	194.7	154.9	-32.5	156.1	-19.8	1.652E+06
17	194.7	194.7	154.9	-32.5	156.1	-20.0	1.652E+06
16	194.7	194.7	154.9	-32.5	156.0	-20.1	1.652E+06
15	194.7	194.7	154.9	-32.5	156.0	-20.2	1.652E+06
14	195.0	195.0	155.0	-32.5	156.0	-20.3	1.655E+06
13	195.2	195.2	155.0	-32.5	155.9	-20.4	1.659E+06
12	198.0	198.0	152.9	-32.6	155.9	-20.4	1.720E+06

FIGURE 4.58 Tabulation of building properities.

(continued)



Story	Mass X [kip-s <sup>2</sup> /ft]	Mass Y [kip-s <sup>2</sup> /ft]	XCM [ft]	YCM [ft]	XCR [ft]	YCR [ft]	Mass moment of Inertia [kip-s <sup>2</sup> /ft]
11	199.2	199.2	151.7	-32.6	155.8	-20.4	1.766E+06
10	199.8	199.8	151.3	-32.6	155.8	-20.3	1.780E+06
9	199.8	199.8	151.3	-32.6	155.8	-20.2	1.780E+06
8	199.8	199.8	151.3	-32.6	155.7	-19.9	1.780E+06
7	199.8	199.8	151.3	-32.6	155.7	-19.6	1.780E+06
6	199.8	199.8	151.3	-32.6	155.7	-19.1	1.780E+06
5	199.8	199.8	151.3	-32.6	155.6	-18.5	1.780E+06
4	210.6	210.6	153.3	-32.8	155.6	-17.9	1.910E+06
3	210.4	210.4	153.2	-32.8	155.6	-17.2	1.908E+06
2	210.4	210.4	153.2	-32.8	155.5	-16.5	1.908E+06
1	251.1	251.1	160.1	-33.1	155.5	-16.1	2.429E+06
PODIUM 4	291.9	291.9	159.6	-32.1	155.5	-16.0	2.747E+06
PODIUM 3M	329.7	329.7	153.6	-31.1	155.5	-16.1	2.869E+06
PODIUM 3M	348.4	348.4	153.6	-30.8	155.4	-16.2	3.010E+06
PODIUM 2	348.4	348.4	153.6	-30.8	155.4	-16.0	3.010E+06
PODIUM 1	343.6	343.6	153.6	-31.0	155.3	-13.3	2.968E+06

Shown here is a table listing the mass, the center of mass, the center of rigidity and the mass-moment of inertia for a building with a floor plan similar to Figure 4.55; the difference is that the shear wall core is located on the northern half of the floor plan. The origin is located at the plan's northwest corner.

**FIGURE 4.58 (continued)**

Next, we turn our attention to the modal information shown in Figures 4.59 and 4.60 to understand the dynamic deformations likely to be experienced by the building when subjected to ground motions. Take, for example, the numbers shown in row 1 Figure 4.60. The fundamental period of the building, 7.07 s as given in column 2, is the period at which the building “wants” to vibrate when set in motion by some sort of disturbance such as a seismic or wind event. Columns 2 through 13 give the mode shapes, (also shown in Figure 4.59) and the percentage of modal partition in each of the mode shapes.

$U_x$ ,  $U_y$  shown in the table represent the familiar translational displacements.  $U_z$ , refers to axial displacement in the vertical,  $z$ , direction which for dynamic analysis purposes is considered zero.

The value of  $R_z = 2.4$  indicates that the torsional rotation of the building is small in the first mode. The last three columns, sum  $R_x$ , etc., record of summation of modal participation up to and including that level. A study of the modal graphs along with the numerical values of Figure 4.60 will clarify the procedure for interpreting the computer results. The sixth through eighth columns show the percentage of mass participating in the translational  $x$  and  $y$  directions, and the vertical up and down movement in the  $z$  direction. The mass participation in the  $x$  direction is 56% as implied by the number 56 in column 6. Our building wants to oscillate principally in the  $x$  direction, because the percentage of participation in the  $y$  direction is zero as given in column 8. Note the building does not vibrate up and down, hence  $U_z$  is zero for the entire period range.

$R_x$  and  $R_y$  are the building rotational components in the  $x$  and  $y$  directions while  $R_z$  is the rotation about the  $z$ -axis. Observe the  $R_x$  component is large for the first mode because the  $Y$  displacement of the building is dominant in that mode.

4.6.7 PERIOD DETERMINATION AND DAMPING VALUES FOR WIND DESIGN

Many simple formulas have been proposed over the years to estimate a tall building’s fundamental period, for preliminary design purposes, until a rigorous calculation can be made. Sometimes this rough approximation is the only calculation of fundamental period that can be made when the

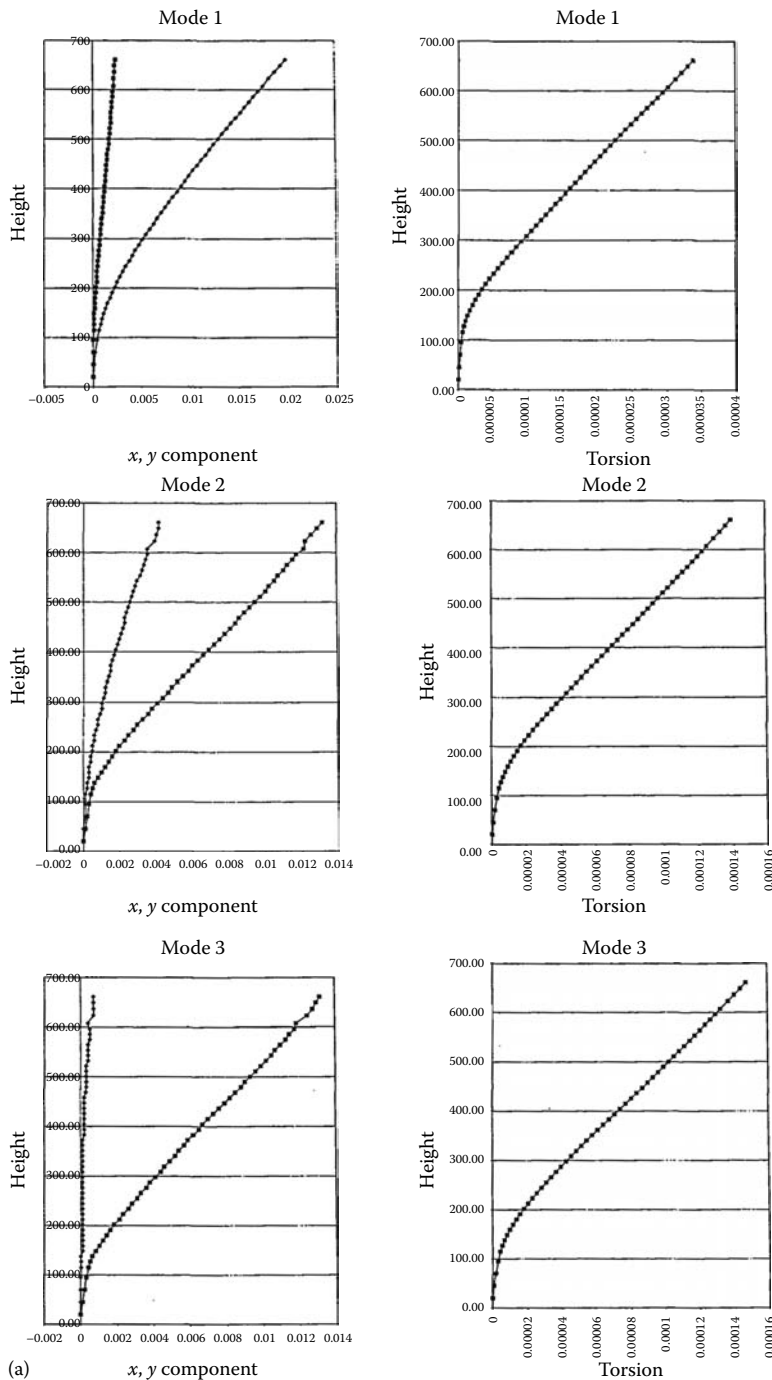


FIGURE 4.59 Modes shapes: (a) Modes 1, 2, and 3.

(continued)

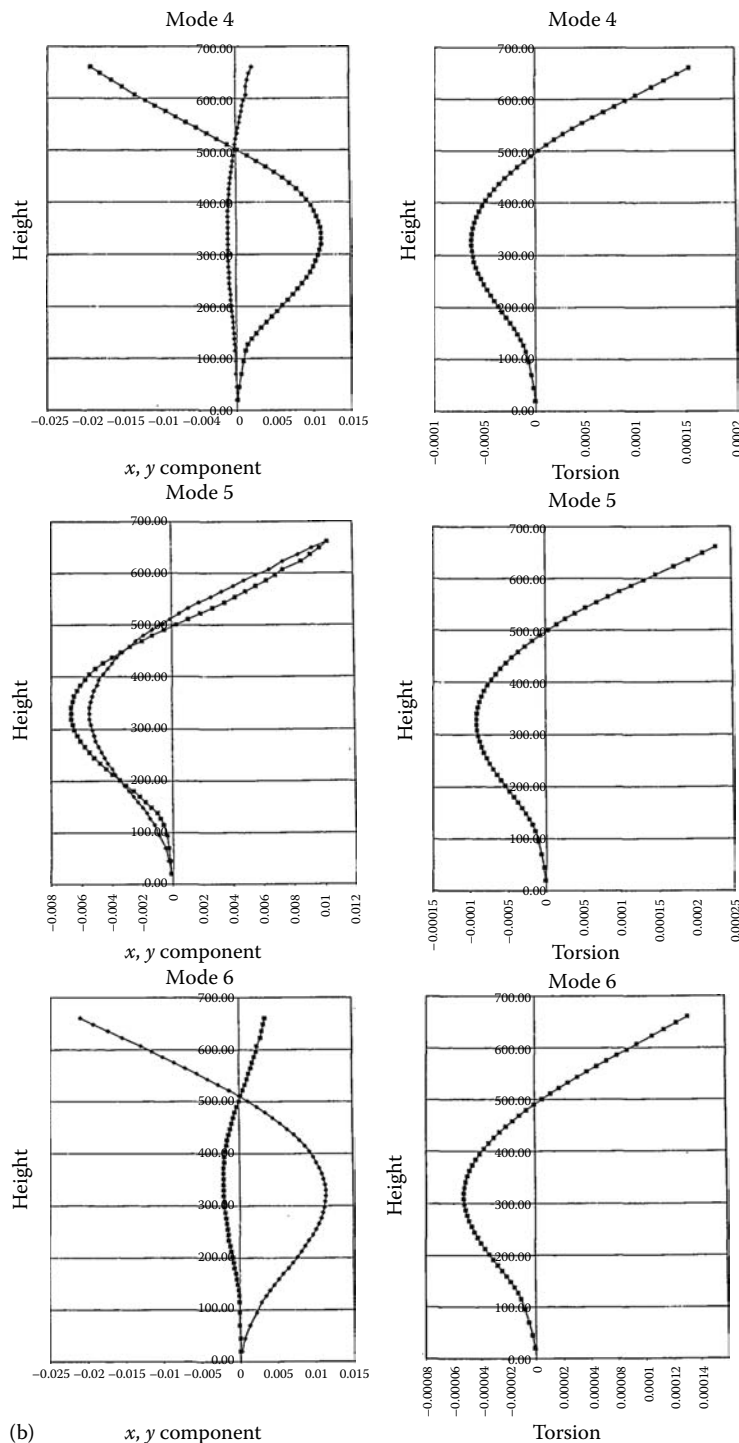


FIGURE 4.59 (continued) (b) modes 4, 5, and 6.

wind-tunnel engineer is asked to perform a “desktop” prediction of the eventual loads. The formula most widely recognized today for wind design is

$$T = \frac{H \text{ (ft)}}{150} \tag{4.40}$$

Mode	Period	UX	UY	UZ	SumUX	SumUY	SumUZ	RX	RY	RZ	SumRX	SumRY	SumRZ
1	7.07	18.01	23.95	0.00	18.01	23.95	0.00	39.34	28.84	16.17	39.34	28.84	16.17
2	6.86	15.70	33.41	0.00	33.71	57.36	0.00	55.04	25.09	8.96	94.38	53.93	25.12
3	5.50	26.53	0.17	0.00	60.24	57.53	0.00	0.28	42.32	31.60	94.66	96.25	56.73
4	1.99	10.07	0.11	0.00	70.31	57.64	0.00	0.03	1.47	3.40	94.69	97.72	60.13
5	1.54	2.95	2.57	0.00	73.25	60.21	0.00	0.58	0.44	9.29	95.27	98.16	69.42
6	1.38	0.15	16.68	0.00	73.41	76.89	0.00	3.51	0.02	2.21	98.78	98.19	71.63
7	0.97	4.87	0.06	0.00	78.28	76.95	0.00	0.01	0.65	1.50	98.79	98.84	73.13
8	0.73	0.95	0.47	0.00	79.23	77.42	0.00	0.05	0.13	6.66	98.84	98.97	79.80
9	0.59	4.20	0.09	0.00	83.42	77.51	0.00	0.01	0.35	0.90	98.85	99.32	80.70
10	0.57	0.13	8.33	0.00	83.56	85.84	0.00	0.79	0.01	0.34	99.64	99.33	81.04
11	0.43	0.01	0.20	0.00	83.56	86.04	0.00	0.01	0.00	6.07	99.65	99.33	87.11
12	0.41	4.81	0.01	0.00	88.37	86.05	0.00	0.00	0.37	0.02	99.65	99.70	87.14
13	0.32	0.02	4.46	0.00	88.39	90.51	0.00	0.22	0.00	0.44	99.87	99.70	87.57
14	0.31	3.20	0.17	0.00	91.59	90.68	0.00	0.01	0.16	0.12	99.88	99.86	87.69
15	0.29	0.52	0.22	0.00	92.11	90.90	0.00	0.01	0.03	3.61	99.89	99.89	91.31
16	0.24	1.96	0.00	0.00	94.07	90.90	0.00	0.00	0.07	0.00	99.89	99.96	91.31
17	0.21	0.06	1.06	0.00	94.13	91.96	0.00	0.03	0.00	1.27	99.92	99.96	92.58
18	0.20	0.02	1.37	0.00	94.15	93.33	0.00	0.04	0.00	0.69	99.96	99.96	93.27
19	0.19	1.08	0.00	0.00	95.23	93.33	0.00	0.00	0.02	0.01	99.96	99.99	93.28
20	0.15	0.07	0.00	0.00	95.30	93.33	0.00	0.00	0.00	0.74	99.96	99.99	94.02
21	0.15	0.53	0.01	0.00	95.83	93.34	0.00	0.00	0.01	0.26	99.96	100.00	94.28
22	0.14	0.00	1.30	0.00	95.83	94.64	0.00	0.02	0.00	0.00	99.98	100.00	94.28
23	0.12	0.35	0.00	0.00	96.18	94.64	0.00	0.00	0.00	0.17	99.98	100.00	94.44
24	0.12	0.12	0.00	0.00	96.30	94.65	0.00	0.00	0.00	0.58	99.98	100.00	95.02

FIGURE 4.60    Tabulation of dynamic properties. (continued)

Mode	Period	UX	UY	UZ	SumUX	SumUY	SumUZ	RX	RY	RZ	SumRX	SumRY	SumRZ
25	0.11	0.00	0.87	0.00	96.30	95.52	0.00	0.01	0.00	0.00	99.99	100.00	95.03
26	0.10	0.41	0.00	0.00	96.71	95.52	0.00	0.00	0.00	0.08	99.99	100.00	95.11
27	0.10	0.04	0.01	0.00	96.74	95.53	0.00	0.00	0.00	0.64	99.99	100.00	95.75
28	0.09	0.58	0.00	0.00	97.32	95.53	0.00	0.00	0.00	0.07	99.99	100.00	95.82
29	0.09	0.00	0.77	0.00	97.32	96.30	0.00	0.00	0.00	0.00	99.99	100.00	95.83
30	0.08	0.09	0.00	0.00	97.41	96.30	0.00	0.00	0.00	0.65	99.99	100.00	96.47
31	0.08	0.51	0.00	0.00	97.93	96.30	0.00	0.00	0.00	0.11	99.99	100.00	96.58
32	0.07	0.01	0.75	0.00	97.94	97.06	0.00	0.00	0.00	0.00	100.00	100.00	96.59
33	0.07	0.33	0.02	0.00	98.27	97.08	0.00	0.00	0.00	0.03	100.00	100.00	96.61
34	0.07	0.06	0.00	0.00	98.33	97.08	0.00	0.00	0.00	0.70	100.00	100.00	97.31
35	0.06	0.20	0.00	0.00	98.54	97.08	0.00	0.00	0.00	0.00	100.00	100.00	97.31
36	0.06	0.00	0.63	0.00	98.54	97.70	0.00	0.00	0.00	0.04	100.00	100.00	97.35
37	0.06	0.04	0.06	0.00	98.58	97.77	0.00	0.00	0.00	0.57	100.00	100.00	97.92
38	0.06	0.12	0.00	0.00	98.70	97.77	0.00	0.00	0.00	0.00	100.00	100.00	97.92
39	0.05	0.02	0.00	0.00	98.72	97.77	0.00	0.00	0.00	0.38	100.00	100.00	98.30
40	0.05	0.00	0.47	0.00	98.72	98.24	0.00	0.00	0.00	0.00	100.00	100.00	98.30
41	0.05	0.12	0.00	0.00	98.83	98.24	0.00	0.00	0.00	0.00	100.00	100.00	98.30
42	0.05	0.00	0.00	0.00	98.84	98.24	0.00	0.00	0.00	0.21	100.00	100.00	98.51
43	0.05	0.07	0.15	0.00	98.90	98.39	0.00	0.00	0.00	0.00	100.00	100.00	98.52
44	0.05	0.07	0.13	0.00	98.97	98.52	0.00	0.00	0.00	0.00	100.00	100.00	98.52
45	0.04	0.17	0.00	0.00	99.15	98.52	0.00	0.00	0.00	0.02	100.00	100.00	98.54
46	0.04	0.01	0.01	0.00	99.15	98.53	0.00	0.00	0.00	0.12	100.00	100.00	98.66
47	0.04	0.00	0.19	0.00	99.15	98.72	0.00	0.00	0.00	0.00	100.00	100.00	98.67
48	0.04	0.16	0.00	0.00	99.32	98.72	0.00	0.00	0.00	0.01	100.00	100.00	98.68
49	0.04	0.00	0.01	0.00	99.32	98.73	0.00	0.00	0.00	0.12	100.00	100.00	98.80
50	0.04	0.12	0.00	0.00	99.44	98.73	0.00	0.00	0.00	0.00	100.00	100.00	98.80

FIGURE 4.60 (continued)

which is apparently in reasonable agreement with many field measurements. However, this value is not in good agreement with the generally accepted eigenvalue analyses.

It is not known if this observed discrepancy is due to

1. Errors in the field measurements
2. Computer modeling inaccuracies and oversimplified modeling assumptions.

Wind-tunnel engineers are typically hesitant to “outguess” the design engineer or substitute their own estimate of the structure’s period. They are most likely to produce loads consistent with the modal properties provided the engineer. So, this is an issue worthy of further research. Until then, it is appropriate for discussion between the wind-tunnel engineer and design engineer.

Another consideration that goes hand-in-hand with the determination of building periods is the value of damping for the structure. Damping for buildings is any effect that reduces its amplitude of vibrations. It results from many conditions ranging from the presence of interior partition walls, to concrete cracking, to deliberately engineered damping devices. While for seismic design, 5% of critical damping is typically assumed for systems without engineered damping devices, the corresponding values for wind design are much lower as buildings subject to wind loads generally respond within the elastic range as opposed to inelastic range for seismic loading. The additional damping for seismic design is assumed to come from severe concrete cracking and plastic hinging.

The ASCE 7-05 Commentary suggests a damping value of 1% for steel buildings and 2% for concrete buildings. These wind damping values are typically associated with determining wind loads for serviceability check. Without recommending specific values, the commentary implicitly suggests that higher values may be appropriate for checking the survivability states.

So, what design values are engineers supposed to use for ultimate level (1.6W) wind loads? Several resources are available as for example, the references cited in the ASCE 7-05 Commentary, but the values vary greatly depending upon which reference, is used. The type of lateral force resisting system influences the damping value that may vary from a low of 0.5% to a high of 10% or more.

Although the level of damping has only a minor effect on the overall base shear for wind design for a large majority of low- and mid-rise buildings, for tall buildings, a more in-depth study of damping criteria is typically warranted.

While the use of the fundamental building period for seismic design calculations is well established, the parameters used for wind design have not been as clear. For wind design, the building period is only relevant for those buildings designated as “flexible” (having a fundamental building period exceeding 1 s). When a building is designated as flexible, the natural frequency (inverse of the building’s fundamental period) is introduced into the gust-effect factor,  $G_F$ .

Prior to ASCE 7-05, designers typically used either the approximate equations within the seismic section or the values provided by a computer eigenvalue analysis. The first can actually be unconservative because the approximate seismic equations are intentionally skewed toward shorter building periods. Thus for wind design, where longer periods equate to higher base shears, their use can provide potentially unconservative results. Also, the results of an eigenvalue analysis can yield building periods much longer than those observed in actual tests, thus providing potentially overly conservative results.

The period determination for wind analysis is therefore, a point at issue worthy of further research.

In summary, the choice of building period and damping for initial design continues to be a subject of discussion for building engineers. This choice is compounded by our increasing complexity of structures, including buildings linked at top. For many of these projects there may be no way around performing an initial Finite Element Analysis, FEA, to obtain a starting point for wind load determination. Ongoing research into damping mechanisms combined with an increase in buildings with monitoring systems will help the design community make more informed decisions regarding the value of damping to use in design.



---

# 5 Seismic Design

Although structural design for seismic loading is primarily concerned with structural safety during major earthquakes, serviceability and the potential for economic loss are also of concern. As such, seismic design requires an understanding of the structural behavior under large inelastic, cyclic deformations. Behavior under this loading is fundamentally different from wind or gravity loading. It requires a more detailed analysis, and the application of a number of stringent detailing requirements to assure acceptable seismic performance beyond the elastic range. Some structural damage can be expected when the building experiences design ground motions because almost all building codes allow inelastic energy dissipation in structural systems.

The seismic analysis and design of buildings has traditionally focused on reducing the risk of the loss of life in the largest expected earthquake. Building codes base their provisions on the historic performance of buildings and their deficiencies and have developed provisions around life-safety concerns by focusing their attention to prevent collapse under the most intense earthquake expected at a site during the life of a structure. These provisions are based on the concept that the successful performance of buildings in areas of high seismicity depends on a combination of strength; ductility manifested in the details of construction; and the presence of a fully interconnected, balanced, and complete lateral force-resisting system. In regions of low seismicity, the need for ductility reduces substantially. And in fact, strength may even substitute for a lack of ductility. Very brittle lateral force-resisting systems can be excellent performers as long as they are never pushed beyond their elastic strength.

Seismic provisions typically specify criteria for the design and construction of new structures subjected to earthquake ground motions with three goals: (1) minimize the hazard to life from all structures, (2) increase the expected performance of structures having a substantial public hazard due to occupancy or use, and (3) improve the capability of essential facilities to function after an earthquake.

Some structural damage can be expected as a result of design ground motion because the codes allow inelastic energy dissipation in the structural system. For ground motions in excess of the design levels, the intent of the codes is for structures to have a low likelihood of collapse.

In most structures that are subjected to moderate-to-strong earthquakes, economical earthquake resistance is achieved by allowing yielding to take place in some structural members. It is generally impractical as well as uneconomical to design a structure to respond in the elastic range to the maximum expected earthquake-induced inertia forces. Therefore, in seismic design, yielding is permitted in predetermined structural members or locations, with the provision that the vertical load-carrying capacity of the structure is maintained even after strong earthquakes. However, for certain types of structures such as nuclear facilities, yielding cannot be tolerated and as such, the design needs to be elastic.

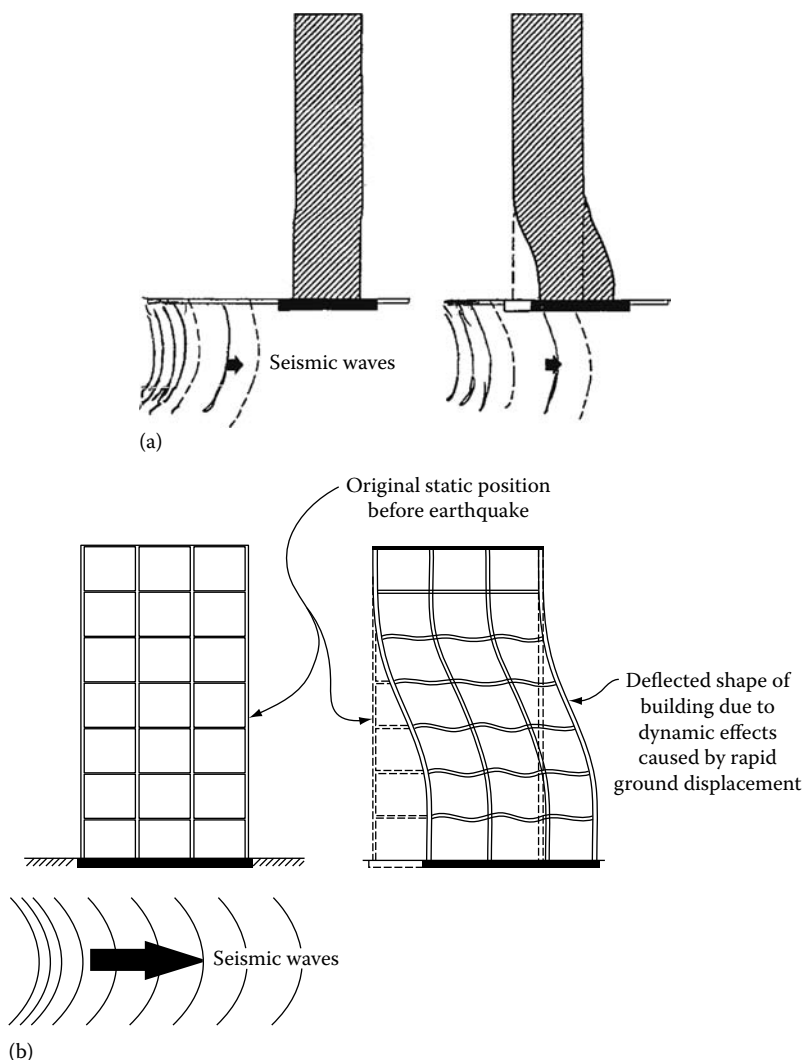
Structures that contain facilities critical to post-earthquake operations—such as hospitals, fire stations, power plants, and communication centers—must not only survive without collapse, but must also remain operational after an earthquake. Therefore, in addition to life safety, damage control is an important design consideration for structures deemed vital to post-earthquake functions.

In general, most earthquake code provisions implicitly require that structures be able to resist

1. Minor earthquakes without any damage.
2. Moderate earthquakes with negligible structural damage and some nonstructural damage.
3. Major earthquakes with some structural and nonstructural damage but without collapse.

The structure is expected to undergo fairly large deformations by yielding in some structural members.





**FIGURE 5.1** Building behavior during earthquakes.

An idea of the behavior of a building during an earthquake may be grasped by considering the simplified response shape shown in Figure 5.1. As the ground on which the building rests is displaced, the base of the building moves with it. However, the building above the base is reluctant to move with it because the inertia of the building mass resists motion and causes the building to distort. This distortion wave travels along the height of the structure, and with continued shaking of the base, causes the building to undergo a complex series of oscillations.

Although both wind and seismic forces are essentially dynamic, there is a fundamental difference in the manner in which they are induced in a structure. Wind loads, applied as external loads, are characteristically proportional to the exposed surface of a structure, while the earthquake forces are principally internal forces resulting from the distortion produced by the inertial resistance of the structure to earthquake motions.

The magnitude of earthquake forces is a function of the mass of the structure rather than its exposed surface. Whereas in wind design, one would feel greater assurance about the safety of a structure made up of heavy sections, in seismic design, this does not necessarily produce a safer design.

## 5.1 BUILDING BEHAVIOR

The behavior of a building during an earthquake is a vibration problem. The seismic motions of the ground do not damage a building by impact, as does a wrecker's ball, or by externally applied pressure such as wind, but by internally generated inertial forces caused by the vibration of the building mass. An increase in mass has two undesirable effects on the earthquake design. First, it results in an increase in the force, and second, it can cause buckling or crushing of columns and walls when the mass pushes down on a member bent or moved out of plumb by the lateral forces. This effect is known as the  $P\Delta$  effect and the greater the vertical forces, the greater the movement due to  $P\Delta$ . It is almost always the vertical load that causes buildings to collapse; in earthquakes, buildings very rarely fall over—they fall down. The distribution of dynamic deformations caused by the ground motions and the duration of motion are of concern in seismic design. Although the duration of strong motion is an important design issue, it is not presently (2009) explicitly accounted for in design.

In general, tall buildings respond to seismic motion differently than low-rise buildings. The magnitude of inertia forces induced in an earthquake depends on the building mass, ground acceleration, the nature of the foundation, and the dynamic characteristics of the structure (Figure 5.2). If a building and its foundation were infinitely rigid, it would have the same acceleration as the ground, resulting in an inertia force  $F = ma$ , for a given ground acceleration,  $a$ . However, because buildings have certain flexibility, the force tends to be less than the product of buildings mass and acceleration. Tall buildings are invariably more flexible than low-rise buildings, and in general, they experience much lower accelerations than low-rise buildings. But a flexible building subjected to ground motions for a prolonged period may experience much larger forces if its natural period is near that of the ground waves. Thus, the magnitude of lateral force is not a function of the acceleration of the ground alone, but is influenced to a great extent by the type of response of the structure itself and its foundation as well. This interrelationship of building behavior and seismic ground motion also depends on the building period as formulated in the so-called response spectrum, explained later in this chapter.

### 5.1.1 INFLUENCE OF SOIL

The intensity of ground motion reduces with the distance from the epicenter of the earthquake. The reduction, called attenuation, occurs at a faster rate for higher frequency (short-period) components

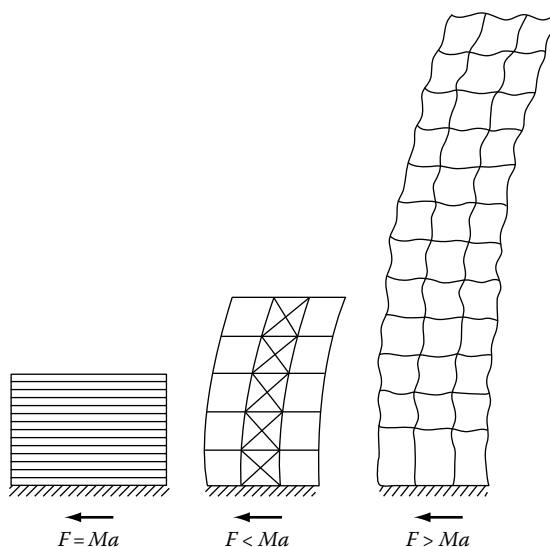


FIGURE 5.2 Schematic representation of seismic forces.

than for lower frequency (long-period) components. The cause of the change in attenuation rate is not understood, but its existence is certain. This is a significant factor in the design of tall buildings, because a tall building, although situated farther from a causative fault than a low-rise building, may experience greater seismic loads because long-period components are not attenuated as fast as the short-period components. Therefore, the area influenced by ground shaking potentially damaging to, say, a 50-story building is much greater than for a 1-story building.

As a building vibrates due to ground motion, its acceleration will be amplified if the fundamental period of the building coincides with the period of vibrations being transmitted through the soil. This amplified response is called resonance. Natural periods of soil are in the range of 0.5–1.0 s. Therefore, it is entirely possible for the building and ground it rests upon to have the same fundamental period. This was the case for many 5- to 10-story buildings in the September 1985 earthquake in Mexico City. An obvious design strategy is to ensure that buildings have a natural period different from that of the expected ground vibration to prevent amplification.

### 5.1.2 DAMPING

Buildings do not resonate with the purity of a tuning fork because they are damped; the extent of damping depends upon the construction materials, the type of connections, and the influence of nonstructural elements on the stiffness characteristics of the building. Damping is measured as a percentage of critical damping.

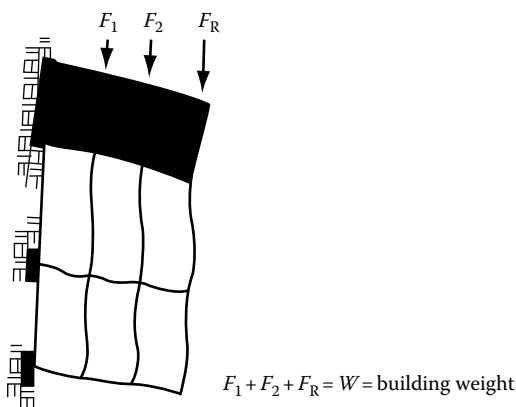
In a dynamic system, critical damping is defined as the minimum amount of damping necessary to prevent oscillation altogether. To visualize critical damping, imagine a tensioned string immersed in water. When the string is plucked, it oscillates about its rest position several times before stopping. If we replace water with a liquid of higher viscosity, the string will oscillate, but certainly not as many times as it did in water. By progressively increasing the viscosity of the liquid, it is easy to visualize that a state can be reached where the string, once plucked, will return to its neutral position without ever crossing it. The minimum viscosity of the liquid that prevents the vibration of the string altogether can be considered equivalent to the critical damping.

The damping of structures is influenced by a number of external and internal sources. Chief among them are

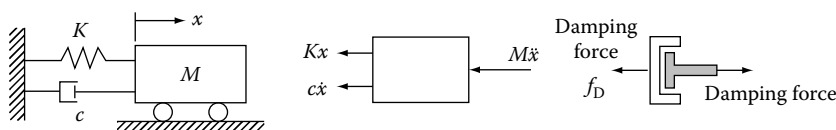
1. External viscous damping caused by air surrounding the building. Since the viscosity of air is low, this effect is negligible in comparison to other types of damping.
2. Internal viscous damping associated with the material viscosity. This is proportional to velocity and increases in proportion to the natural frequency of the structure.
3. Friction damping, also called Coulomb damping, occurring at connections and support points of the structure. It is a constant, irrespective of the velocity or amount of displacement.
4. Hysteretic damping that contributes to a major portion of the energy absorbed in ductile structures.

For analytical purposes, it is a common practice to lump different sources of damping into a single viscous damping. For nonbase-isolated buildings, analyzed for code-prescribed loads, the damping ratios used in practice vary anywhere from 1% to 10% of critical. The low-end values are for wind, while those of the upper end are for seismic design. The damping ratio used in the analysis of seismic base-isolated buildings is rather large compared to values used for nonisolated buildings, and varies from about 0.20 to 0.35 (20% to 35% of critical damping).

Base isolation, discussed in Chapter 8, consists of mounting a building on an isolation system to prevent horizontal seismic ground motions from entering the building. This strategy results in significant reductions in interstory drifts and floor accelerations, thereby protecting the building and its contents from earthquake damage.



**FIGURE 5.3** Concept of 100%g (1g).



**FIGURE 5.4** Linear viscous damper.

A level of ground acceleration on the order of  $0.1g$ , where  $g$  is the acceleration due to gravity, is often sufficient to produce some damage to weak construction. An acceleration of  $1.0g$ , or 100% of gravity, is analytically equivalent, in the static sense, to a building that cantilevers horizontally from a vertical surface (Figure 5.3).

As stated previously, the process by which free vibration steadily diminishes in amplitude is called damping. In damping, the energy of the vibrating system is dissipated by various mechanisms, and often more than one mechanism may be present at the same time. In simple laboratory models, most of the energy dissipation arises from the thermal effect of the repeated elastic straining of the material and from the internal friction. In actual structures, however, many other mechanisms also contribute to the energy dissipation. In a vibrating concrete building, these include the opening and closing of microcracks in concrete, friction between the structure itself and nonstructural elements such as partition walls. Invariably, it is impossible to identify or describe mathematically each of these energy-dissipating mechanisms in an actual building.

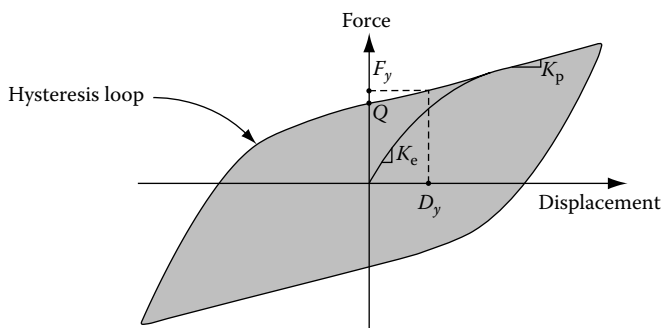
Therefore, the damping in actual structures is usually represented in a highly idealized manner. For many purposes, the actual damping in structures can be idealized satisfactorily by a linear viscous damper or dashpot. The damping coefficient is selected so that the vibrational energy that dissipates is equivalent to the energy dissipated in all the damping mechanisms. This idealization is called equivalent viscous damping.

Figure 5.4 shows a linear viscous damper subjected to a force,  $f_D$ . The damping force,  $f_D$ , is related to the velocity  $\dot{u}$  across the linear viscous damper by

$$f_D = c\dot{u}$$

where the constant  $c$  is the viscous damping coefficient; it has units of force  $\times$  time/length.

Unlike the stiffness of a structure, the damping coefficient cannot be calculated from the dimensions of the structure and the sizes of the structural elements. This is understandable because it is not feasible to identify all the mechanisms that dissipate the vibrational energy of actual structures.



**FIGURE 5.5** Bilinear force–displacement hysteresis loop.

Thus, vibration experiments on actual structures provide the data for evaluating the damping coefficient. These may be free-vibration experiments that lead to measured rate at which motion decays in free vibration. The damping property may also be determined from forced-vibration experiments.

The equivalent viscous damper is intended to model the energy dissipation at deformation amplitudes within the linear elastic limit of the overall structure. Over this range of deformations, the damping coefficient  $c$  determined from experiments may vary with the deformation amplitude. This nonlinearity of the damping property is usually not considered explicitly in dynamic analyses. It may be handled indirectly by selecting a value for the damping coefficient that is appropriate for the expected deformation amplitude, usually taken as the deformation associated with the linearly elastic limit of the structure. Additional energy is dissipated due to the inelastic behavior of the structure at larger deformations. Under cyclic forces or deformations, this behavior implies the formation of a force–displacement hysteresis loop (Figure 5.5). The damping energy dissipated during one deformation cycle between deformation limits  $\pm u_o$  is given by the area within the hysteresis loop  $abcd$  (Figure 5.5). This energy dissipation is usually not modeled by a viscous damper, especially if the excitation is earthquake ground motion. Instead, the most common and direct approach to account for the energy dissipation through inelastic behavior is to recognize the inelastic relationship between resisting force and deformation. Such force–deformation relationships are obtained from experiments on structures or structural components at slow rates of deformation, thus excluding any energy dissipation arising from rate-dependent effects.

### 5.1.3 BUILDING MOTIONS AND DEFLECTIONS

Earthquake-induced motions, even when they are more violent than those induced by wind, evoke a totally different human response—first, because earthquakes occur much less frequently than windstorms, and second, because the duration of motion caused by an earthquake is generally short. People who experience earthquakes are grateful that they have survived the trauma and are less inclined to be critical of the building motion. Earthquake-induced motions are, therefore, a safety rather than a human discomfort issue.

Lateral deflections that occur during earthquakes should be limited to prevent distress in structural members and architectural components. Nonload-bearing in-fills, external wall panels, and window glazing should be designed with sufficient clearance or with flexible supports to accommodate the anticipated movements.

### 5.1.4 BUILDING DRIFT AND SEPARATION

Drift is generally defined as the lateral displacement of one floor relative to the floor below. Drift control is necessary to limit damage to interior partitions, elevator and stair enclosures, glass, and cladding

systems. Stress or strength limitations in ductile materials do not always provide adequate drift control, especially for tall buildings with relatively flexible moment-resisting frames or narrow shear walls.

Total building drift is the absolute displacement of any point relative to the base. Adjoining buildings or adjoining sections of the same building may not have identical modes of response, and therefore may have a tendency to pound against one another. Building separations or joints must be provided to permit adjoining buildings to respond independently to earthquake ground motion.

## 5.2 SEISMIC DESIGN CONCEPT

An effective seismic design generally includes

1. Selecting an overall structural concept including layout of a lateral force-resisting system that is appropriate to the anticipated level of ground shaking. This includes providing a redundant and continuous load path to ensure that a building responds as a unit when subjected to ground motion.
2. Determining code-prescribed forces and deformations generated by the ground motion, and distributing the forces vertically to the lateral force-resisting system. The structural system, configuration, and site characteristics are all considered when determining these forces.
3. Analyzing the building for the combined effects of gravity and seismic loads to verify that adequate vertical and lateral strengths and stiffnesses are achieved to satisfy the structural performance and acceptable deformation levels prescribed in the governing building code.
4. Providing details to assure that the structure has sufficient inelastic deformability to undergo large deformations when subjected to a major earthquake. Appropriately detailed members possess the necessary characteristics to dissipate energy by inelastic deformations.

### 5.2.1 STRUCTURAL RESPONSE

If the base of a structure is suddenly moved, as in a seismic event, the upper part of the structure will not respond instantaneously, but will lag because of the inertial resistance and flexibility of the structure. The resulting stresses and distortions in the building are the same as if the base of the structure were to remain stationary while time-varying horizontal forces are applied to the upper part of the building. These forces, called inertia forces, are equal to the product of the mass of the structure times acceleration, that is,  $F = ma$  (the mass  $m$  is equal to weight divided by the acceleration of gravity, i.e.,  $m = w/g$ ). Because earthquake ground motion is three-dimensional (3D; one vertical and two horizontal), the structure, in general, deforms in a 3D manner. Generally, the inertia forces generated by the horizontal components of ground motion require greater consideration for seismic design since adequate resistance to vertical seismic loads is usually provided by the member capacities required for gravity load design. In the equivalent static procedure, the inertia forces are represented by equivalent static forces.

### 5.2.2 LOAD PATH

Buildings typically consist of vertical and horizontal structural elements. The vertical elements that transfer lateral and gravity loads are the shear walls and columns. The horizontal elements such as floor and roof slabs distribute lateral forces to the vertical elements acting as horizontal diaphragms. In special situations, horizontal bracing may be required in the diaphragms to transfer large shears from discontinuous walls or braces. The inertia forces proportional to the mass and acceleration of the building elements must be transmitted to the lateral force-resisting elements, through the diaphragms and then to the base of the structure and into the ground, via the vertical lateral load-resisting elements.

A complete load path is a basic requirement. There must be a complete gravity and lateral force-resisting system that forms a continuous load path between the foundation and all portions of the building. The general load path is as follows. Seismic forces originating throughout the building are delivered through connections to horizontal diaphragms; the diaphragms distribute these forces to lateral force-resisting elements such as shear walls and frames; the vertical elements transfer the forces into the foundation; and the foundation transfers the forces into the supporting soil.

If there is a discontinuity in the load path, the building is unable to resist seismic forces regardless of the strength of the elements. Interconnecting the elements needed to complete the load path is necessary to achieve the required seismic performance. Examples of gaps in the load path would include a shear wall that does not extend to the foundation, a missing shear transfer connection between a diaphragm and vertical elements, a discontinuous chord at a diaphragm's notch, or a missing collector.

A good way to remember this important design strategy is to ask yourself the question, "How does the inertia load get from here (meaning the point at which it originates) to there (meaning the shear base of the structure, typically the foundations)?"

Seismic loads result directly from the distortions induced in the structure by the motion of the ground on which it rests. Base motion is characterized by displacements, velocities, and accelerations that are erratic in direction, magnitude, duration, and sequence. Earthquake loads are inertia forces related to the mass, stiffness, and energy-absorbing (e.g., damping and ductility) characteristics of the structure. During its life, a building located in a seismically active zone is generally expected to go through many small, some moderate, one or more large, and possibly one very severe earthquakes. As stated previously, in general, it is uneconomical or impractical to design buildings to resist the forces resulting from large or severe earthquakes within the elastic range of stress. In severe earthquakes, most buildings are designed to experience yielding in at least some of their members. The energy-absorption capacity of yielding will limit the damage to properly designed and detailed buildings. These can survive earthquake forces substantially greater than the design forces determined from an elastic analysis.

### **5.2.3 RESPONSE OF ELEMENTS ATTACHED TO BUILDINGS**

Elements attached to the floors of buildings (e.g., mechanical equipment, ornamentation, piping, and nonstructural partitions) respond to floor motion in much the same manner as the building responds to ground motion. However, the floor motion may vary substantially from the ground motion. The high-frequency components of the ground motion tend to be filtered out at the higher levels in the building, whereas the components of ground motion that correspond to the natural periods of vibrations of the building tend to be magnified. If the elements are rigid and are rigidly attached to the structure, the forces on the elements will be in the same proportion to the mass as the forces on the structure. But elements that are flexible and have periods of vibration close to any of the predominant modes of the building vibration will experience forces in proportion substantially greater than the forces on the structure.

### **5.2.4 ADJACENT BUILDINGS**

Buildings are often built right up to property lines in order to make the maximum use of space. Historically, buildings have been built as if the adjacent structures do not exist. As a result, the buildings may pound during an earthquake. Building pounding can alter the dynamic response of both buildings, and impart additional inertial loads to them.

Buildings that are the same height and have matching floors are likely to exhibit similar dynamic behavior. If the buildings pound, floors will impact other floors, so damage usually will be limited to nonstructural components. When floors of adjacent buildings are at different elevations, the floors

of one building will impact the columns of the adjacent building, causing structural damage. When buildings are of different heights, the shorter building may act as a buttress for the taller neighbor. The shorter building receives an unexpected load while the taller building suffers from a major discontinuity that alters its dynamic response. Since neither is designed to weather such conditions, there is potential for extensive damage and possible collapse.

One of the basic goals in seismic design is to distribute yielding throughout the structure. Distributed yielding dissipates more energy and helps prevent the premature failure of any one element or group of elements. For example, in moment frames, it is desirable to have strong columns relative to the beams to help distribute the formation of plastic hinges in the beams throughout the building and prevent a story-collapse mechanism.

### 5.2.5 IRREGULAR BUILDINGS

The seismic design of regular buildings is based on two concepts. First, the linearly varying lateral force distribution is a reasonable and conservative representation of the actual response distribution due to earthquake ground motions. Second, the cyclic inelastic deformation demands are reasonably uniform in all of the seismic force-resisting elements. However, when a structure has irregularities, these concepts may not be valid, requiring corrective factors and procedures to meet the design objectives.

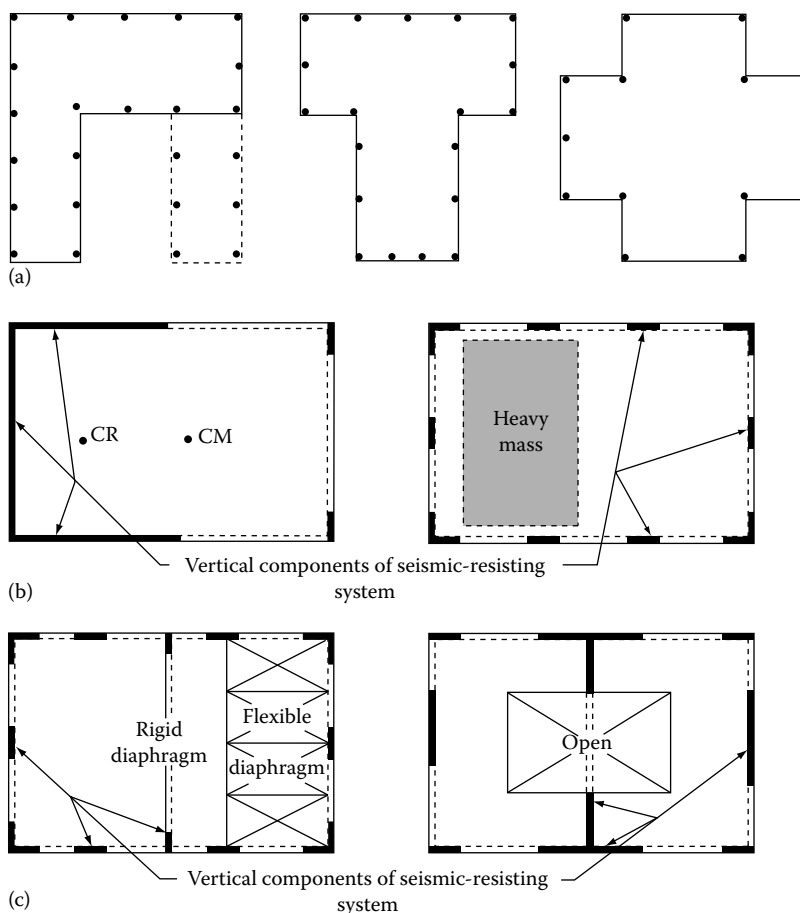
The impact of irregular parameters in estimating seismic force levels, first introduced into the Uniform Building Code (UBC) in 1973, long remained a matter of engineering judgment. Beginning in 1988, however, some configuration parameters have been quantified to establish the condition of irregularity. Additionally, specific analytical treatments and/or corrective measures have been mandated to address these flaws.

Typical building configuration deficiencies include an irregular geometry, a weakness in a story, a concentration of mass, or a discontinuity in the lateral force-resisting system. Vertical irregularities are defined in terms of strength, stiffness, geometry, and mass. Although these are evaluated separately, they are related to one another, and may occur simultaneously. For example, a building that has a tall first story can be irregular because of a soft story, a weak story, or both, depending on the stiffness and strength of this story relative to those above.

Those who have studied the performance of buildings in earthquakes generally agree that the building's form has a major influence on performance. This is because the shapes and proportions of the building have a major effect on the distribution of earthquake forces as they work their way through the building. Geometric configuration, type of structural members, details of connections, and materials of construction, all have a profound effect on the structural-dynamic response of a building. When a building has irregular features, such as asymmetry in plan or vertical discontinuity, the assumptions used in developing seismic criteria for buildings with regular features may not apply. Therefore, it is best to avoid creating buildings with irregular features. For example, omitting exterior walls in the first story of a building to permit an open ground floor leaves the columns at the ground level as the only elements available to resist lateral forces, thus causing an abrupt change in rigidity at that level. This condition may be desirable from space-planning considerations, but it is advisable to carry all shear walls down to the foundation. When irregular features are unavoidable, special design considerations are required to account for the unusual dynamic characteristics and the load transfer and stress concentrations that occur at abrupt changes in structural resistance. Examples of plan and elevation irregularities are illustrated in Figures 5.6 and 5.7. Note that plan irregularities are also referred to as horizontal irregularities.

The ASCE 7-05 quantifies the idea of irregularity by defining geometrically or by using dimensional ratios the points at which a specific irregularity becomes an issue requiring remedial measures. These issues are discussed later in this chapter. It will be seen shortly that no structural premium is required for mitigating many irregularity effects, other than to perform a modal analysis for determining the design seismic forces.





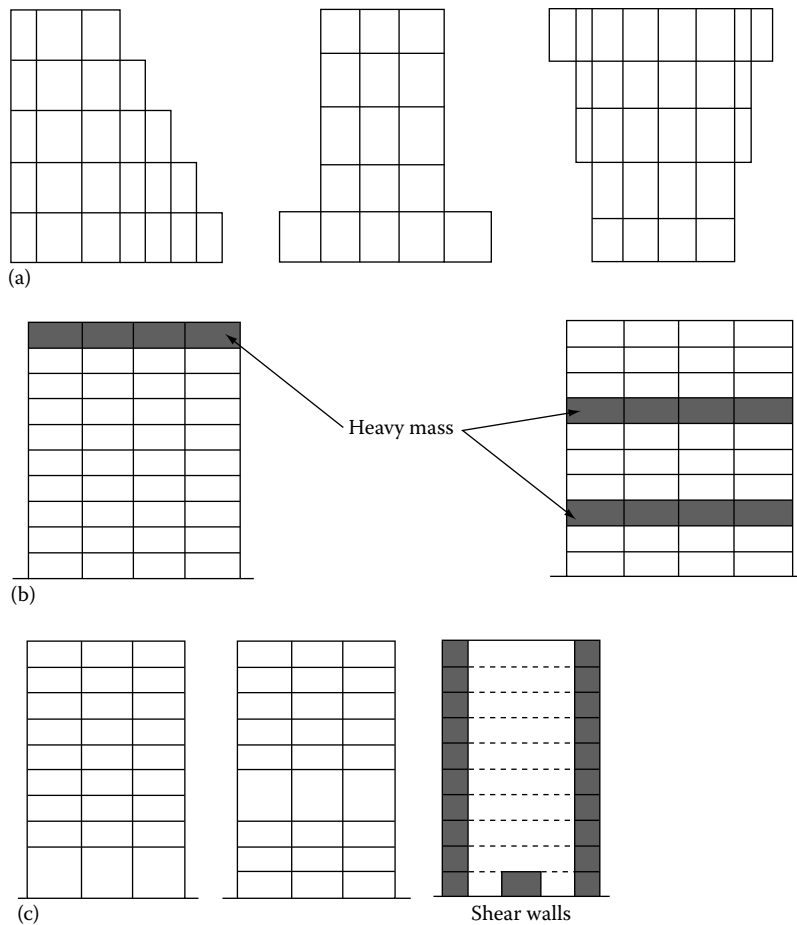
**FIGURE 5.6** Plan irregularities: (a) geometric irregularities, (b) irregularity due to mass-resistance eccentricity, and (c) irregularity due to discontinuity in diaphragm stiffness.

The irregularities are divided into two broad categories: (1) vertical and (2) plan irregularities. Vertical irregularities include soft or weak stories, large changes in mass from floor to floor, and discontinuities in the dimensions or in-plane locations of lateral load-resisting elements. Buildings with plan irregularities include those that undergo substantial torsion when subjected to seismic loads or have reentrant corners, discontinuities in floor diaphragms, discontinuity in the lateral force path, or lateral load-resisting elements that are not parallel to each other or to the principal axes of the building.

### 5.2.6 LATERAL FORCE-RESISTING SYSTEMS

Several systems can be used to effectively provide resistance to seismic forces. Some of the most common systems consist of moment frames and shear walls acting singly or in combination with each other.

Moment frames resist earthquake forces by the bending of columns and beams. During a large earthquake, the story-to-story deflection (story drift) may be accommodated within the structural system by plastic hinging of the beam without causing column failure. However, the drift may be large and cause damage to elements rigidly tied to the structural system. Examples of elements prone to distress are brittle partitions, stairways, plumbing, exterior walls, and other elements that



**FIGURE 5.7** Elevation irregularities: (a) abrupt change in geometry, (b) large difference in floor masses, and (c) large difference in story stiffnesses.

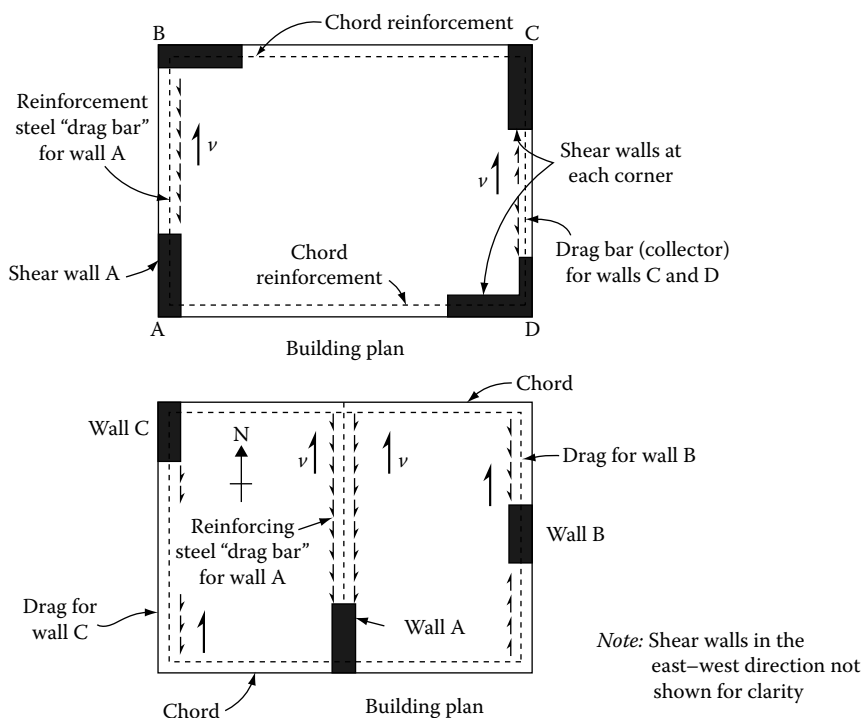
extend between floors. Therefore, a moment-frame building can have substantial interior and exterior nonstructural damage and still be structurally safe. For certain types of buildings, this system may be a poor economic risk unless special damage-control measures are taken.

A shear-wall building is typically more rigid than a framed structure. Deflections due to lateral forces are relatively small unless the height-to-width ratio of the wall becomes large enough to cause overturning problems. This would generally occur when there are excessive openings in the shear walls or when the height-to-width ratio of wall is in excess of five or so. Also, if the soil beneath the wall footings is relatively soft, the entire shear wall may rotate, causing large lateral deflections.

Moment frames and shear walls may be used singly or in combination with each other. When the frames and shear walls interact, the system is called a dual system if the frame alone can resist 25% of the seismic lateral load. Otherwise, it is referred to as a combined system.

## 5.2.7 DIAPHRAGMS

Earthquake loads at any level of a building will be distributed to the lateral load-resisting vertical elements through the floor and roof slabs. For analytical purpose, these are assumed to behave as deep beams. The slab is the web of the beam carrying the shear, and the perimeter spandrel or wall, if any, is the flange of the beam-resisting bending. In the absence of perimeter members, the slab is analyzed as a plate subjected to in-plane bending.



**FIGURE 5.8** Diaphragm drag and chord reinforcement for north-south seismic loads.

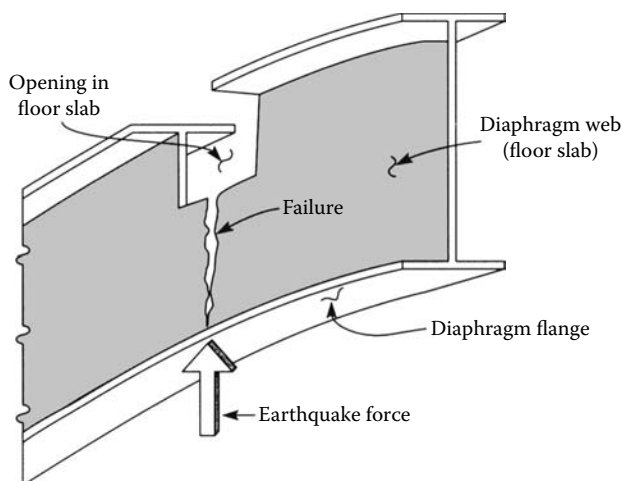
Three factors are important in diaphragm design:

1. The diaphragm must be adequate to resist both the bending and shear stresses and be tied together to act as one unit.
2. The collectors and drag members (see Figure 5.8) must be adequate to transfer loads from the diaphragm into the lateral load-resisting vertical elements.
3. Openings or reentrant corners in the diaphragm must be properly placed and adequately reinforced.

Inappropriate location or large-size openings for stairs or elevator cores, atriums, skylights, etc. create problems similar to those related to cutting the flanges and holes in the web of a steel beam adjacent to the flange. This reduces the ability of the diaphragm to transfer the chord forces and may cause rupture in the web (Figure 5.9).

### 5.2.8 DUCTILITY

It will soon become clear that in seismic design, all structures are designed for forces much smaller than those the design ground motion would produce in a structure with completely linear-elastic response. This reduction is possible for a number of reasons. As the structure begins to yield and deform inelastically, the effective period of the response of the structure tends to lengthen, which for many structures, results in a reduction in strength demand. Furthermore, the inelastic action results in a significant amount of energy dissipation, also known as hysteretic damping. The effect, which is also known as the ductility reduction, explains why a properly designed structure with a fully yielded strength that is significantly lower than the elastic seismic force-demand can be capable of providing satisfactory performance under the design ground-motion excitations.

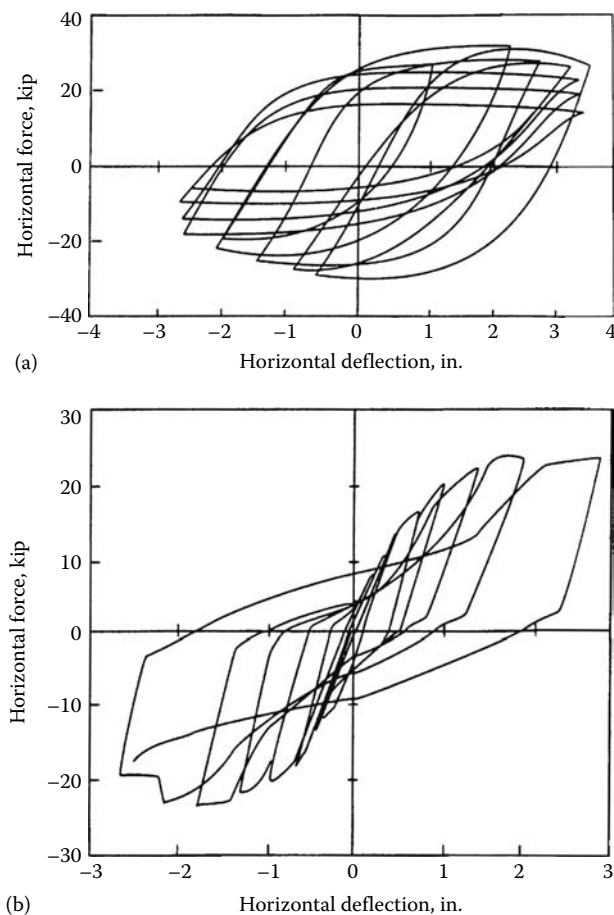


**FIGURE 5.9** Diaphragm web failure due to large opening.

The energy dissipation resulting from hysteretic behavior can be measured as the area enclosed by the force-deformation curve of the structure as it experiences several cycles of excitation. Some structures have far more energy-dissipation capacity than do others. The extent of energy-dissipation capacity available is largely dependent on the amount of stiffness and strength degradation that the structure undergoes as it experiences repeated cycles of inelastic deformation. Figure 5.10 indicates representative load-deformation curves for two simple substructures, such as beam-column assembly in a frame. Hysteretic curve in Figure 5.10a is representative of the behavior of substructures that have been detailed for ductile behavior. The substructure can maintain nearly all of its strength and stiffness over a number of large cycles of inelastic deformation. The resulting force-deformation “loops” are quite wide and open, resulting in a large amount of energy-dissipation capacity. Hysteretic curve in Figure 5.10b represents the behavior of a substructure that has not been detailed for ductile behavior. It rapidly loses stiffness under inelastic deformation and the resulting hysteretic loops are quite pinched. The energy-dissipation capacity of such a substructure is much lower than that for the substructure in Figure 5.10a. Hence structural systems with large energy-dissipation capacity are assigned higher  $R$  values, resulting in design for lower forces, than systems with relatively limited energy-dissipation capacity.

Ductility is the capacity of building materials, systems, or structures to absorb energy by deforming into the inelastic range. The capability of a structure to absorb energy, with acceptable deformations and without failure, is a very desirable characteristic in any earthquake-resistant design. Concrete, a brittle material, must be properly reinforced with steel to provide the ductility necessary to resist seismic forces. In concrete columns, for example, the combined effects of flexure (due to frame action) and compression (due to the action of the overturning moment of the structure as a whole) produce a common mode of failure: buckling of the vertical steel and spalling of the concrete cover near the floor levels. Columns must, therefore, be detailed with proper spiral reinforcing or hoops to have greater reserve strength and ductility.

Ductility may be evaluated by the hysteretic behavior of critical components such as a column-beam assembly of a moment frame. It is obtained by cyclic testing of moment rotation (or force-deflection) behavior of the assembly. Ductility or hysteretic behavior may be considered as an energy-dissipating mechanism due to inelastic behavior of the structure at large deformations. The energy dissipated during cyclic deformations is given by the area of hysteric loop (see Figure 5.10a and b). The areas within the loop may be full and fat, or lean and pinched. Structural assemblies with loops enclosing large areas representing large dissipated energy are regarded as superior systems for resisting seismic loading.



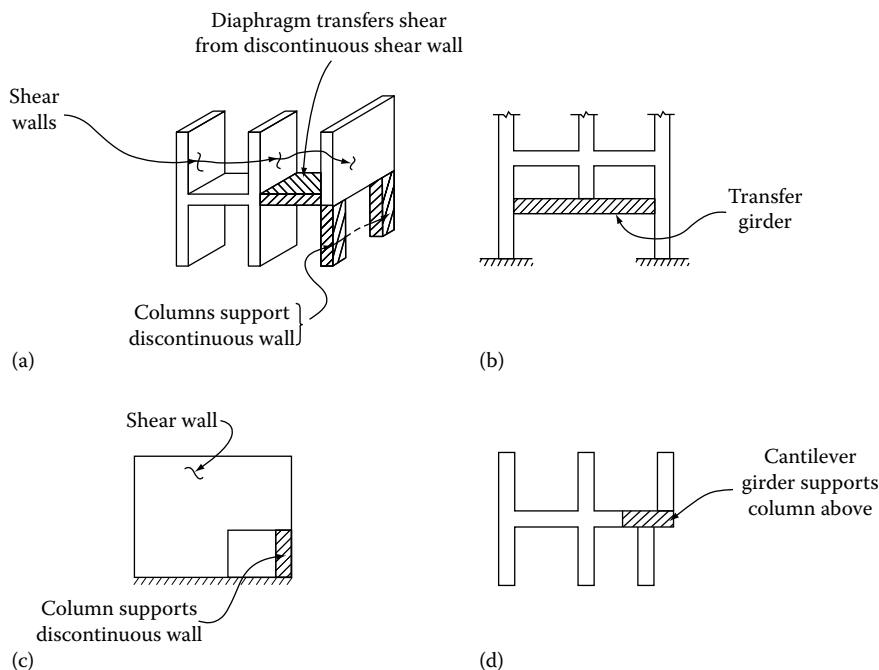
**FIGURE 5.10** Hysteric behavior: (a) curve representing large energy dissipation and (b) curve representing limited energy dissipation.

In providing for ductility, it should be kept in mind that severe penalties are imposed by seismic provisions on structures with nonuniform ductility (see Figure 5.11).

### 5.2.9 DAMAGE CONTROL FEATURES

The design of a structure in accordance with seismic provisions will not fully ensure against earthquake damage. A list of features that can minimize earthquake damage are as follows:

1. Provide details that allow structural movement without damage to nonstructural elements. Damage to such items as piping, glass, plaster, veneer, and partitions may constitute a major financial loss. To minimize this type of damage, special care in detailing, either to isolate these elements or to accommodate the movement, is required.
2. Breakage of glass windows can be minimized by providing adequate clearance at edges to allow for frame distortions.
3. Damage to rigid nonstructural partitions can be largely eliminated by providing a detail at the top and sides, which will permit relative movement between the partitions and the adjacent structural elements.
4. In piping installations, the expansion loops and flexible joints used to accommodate temperature movement are often adaptable to handling the relative seismic deflections between adjacent equipment items attached to floors.



**FIGURE 5.11** Examples of nonuniform ductility in structural systems due to vertical discontinuities. (Adapted from SEAOC Blue Book, 1999 Edition.)

5. Fasten freestanding shelving to walls to prevent toppling.
6. Concrete stairways often suffer seismic damage due to their inhibition of drift between connected floors. This can be avoided by providing a slip joint at the lower end of each stairway to eliminate the bracing effect of the stairway or by tying stairways to stairway shear walls.

### 5.2.10 CONTINUOUS LOAD PATH

A continuous load path, or preferably more than one path, with adequate strength and stiffness should be provided from the origin of the load to the final lateral load-resisting elements. The general path for load transfer is in reverse to the direction in which seismic loads are delivered to the structural elements. Thus, the path for load transfer is as follows: inertia forces generated in an element, such as a segment of exterior curtain wall, are delivered through structural connections to a horizontal diaphragm (i.e., floor slab or roof); the diaphragms distribute these forces to vertical components such as moment frames and shear walls; and finally, the vertical elements transfer the forces into the foundations. While providing a continuous load path is an obvious requirement, examples of common flaws in load paths are a missing collector, or a discontinuous chord because of an opening in the floor diaphragm, or a connection that is inadequate to deliver diaphragm shear to a frame or shear wall.

### 5.2.11 REDUNDANCY

Redundancy is a fundamental characteristic for good performance in earthquakes. It tends to mitigate high demands imposed on the performance of members. It is a good practice to provide a building with a redundant system such that the failure of a single connection or component does not adversely affect the lateral stability of the structure. Otherwise, all components must remain operative for the structure to retain its lateral stability.

### 5.2.12 CONFIGURATION

A building with an irregular configuration may be designed to meet all code requirements, but it will not perform as well as a building with a regular configuration. If the building has an odd shape that is not properly considered in the design, good details and construction are of a secondary value.

Two types of structural irregularities, as stated previously, are typically defined in most seismic standards as vertical irregularities and plan irregularities (see Tables 5.1 and 5.2 for ASCE 7-05 definitions). These irregularities result in building responses significantly different from those assumed

**TABLE 5.1**  
**Horizontal Structural Irregularities**

Irregularity Type and Description	Reference Section of ASCE 7-05	SDC Application
1a. <b>Torsional irregularity</b> is defined to exist where the maximum story drift, computed including accidental torsion, at one end of the structure transverse to an axis is more than 1.2 times the average of the story drifts at the two ends of the structure. Torsional irregularity requirements in the reference sections apply only to structures in which the diaphragms are rigid or semirigid.	12.3.3.4 12.8.4.3 12.7.3 12.12.1 Table 12.6-1 16.2.2	D through F C through F B through F C through F D through F B through F
1b. <b>Extreme torsional irregularity</b> is defined to exist where the maximum story drift, computed including accidental torsion, at one end of the structure transverse to an axis is more than 1.4 times the average of the story drifts at the two ends of the structure. Extreme torsional irregularity requirements in the reference sections apply only to structures in which the diaphragms are rigid or semirigid.	12.3.3.1 12.3.3.4 12.7.3 12.8.4.3 12.12.1 Table 12.6-1 16.2.2	E and F D B through D C and D C and D D B through D
2. <b>Reentrant corner irregularity</b> is defined to exist where both plan projections of the structure beyond a reentrant corner are greater than 15% of the plan dimension of the structure in the given direction.	12.3.3.4 Table 12.6-1	D through F D through F
3. <b>Diaphragm discontinuity irregularity</b> is defined to exist where there are diaphragms with abrupt discontinuities or variations in stiffness, including those having cutout or open areas greater than 50% of the gross enclosed diaphragm area, or changes in effective diaphragm stiffness of more than 50% from one story to the next.	12.3.3.4 Table 12.6-1	D through F D through F
4. <b>Out-of-plane offsets irregularity</b> is defined to exist where there are discontinuities in a lateral force–resistance path, such as out-of-plane offsets of the vertical elements.	12.3.3.4 12.3.3.3 12.7.3 Table 12.6-1 16.2.2	D through F B through F B through F D through F B through F
5. <b>Nonparallel systems irregularity</b> is defined to exist where the vertical lateral force–resisting elements are not parallel to or symmetric about the major orthogonal axes of the seismic force–resisting system.	12.5.3 12.7.3 Table 12.6-1 16.2.2	C through F B through F D through F B through F

Source: ASCE 7-05, Table 12.3-1.

**TABLE 5.2**  
**Vertical Structural Irregularities**

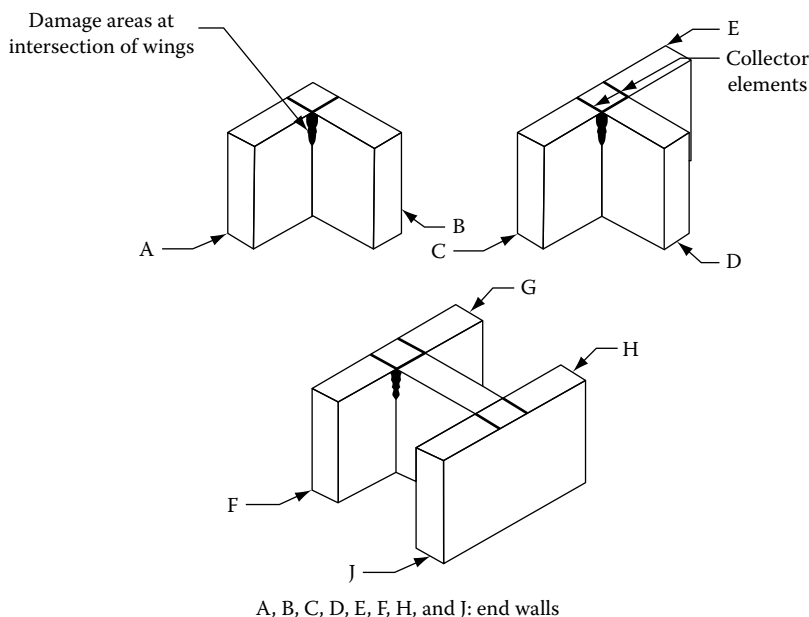
<b>Irregularity Type and Description</b>	<b>Reference Section of ASCE 7-05</b>	<b>SDC Application</b>
1a. <b>Stiffness soft story irregularity</b> is defined to exist where there is a story in which the lateral stiffness is less than 70% of that in the story above or less than 80% of the average stiffness of the three stories above.	Table 12.6-1	D through F
1b. <b>Stiffness extreme soft story irregularity</b> is defined to exist where there is a story in which the lateral stiffness is less than 60% of that in the story above or less than 70% of the average stiffness of the three stories above.	12.3.3.1 Table 12.6-1	E and F D through F
2. <b>Weight (mass) irregularity</b> is defined to exist where the effective mass of any story is more than 150% of the effective mass of an adjacent story. A roof that is lighter than the floor below need not be considered.	Table 12.6-1	D through F
3. <b>Vertical geometric irregularity</b> is defined to exist where the horizontal dimension of the seismic force-resisting system in any story is more than 130% of that in an adjacent story.	Table 12.6-1	D through F
4. <b>In-plane discontinuity in vertical lateral force-resisting element irregularity</b> is defined to exist where an in-plane offset of the lateral force-resisting elements is greater than the length of those elements or there exists a reduction in the stiffness of the resisting element in the story below.	12.3.3.3 12.3.3.4 Table 12.6-1	B through F D through F D through F
5a. <b>Discontinuity in lateral strength-weak story irregularity</b> is defined to exist where the story lateral strength is less than 80% of that in the story above. The story lateral strength is the total lateral strength of all seismic-resisting elements sharing the story shear for the direction under consideration.	12.3.3.1 Table 12.6-1	E and F D through F
5b. <b>Discontinuity in lateral strength-extreme weak story irregularity</b> is defined to exist where the story lateral strength is less than 65% of that in the story above. The story strength is the total strength of all seismic-resisting elements sharing the story shear for the direction under consideration.	12.3.3.1 12.3.3.2 Table 12.6-1	D through F B and C D through F

Source: ASCE 7-05, Table 12.3-2.

in the equivalent static-force procedure, and to a lesser extent from the dynamic-analysis procedure. Although seismic provisions give certain recommendations for assessing the degree of irregularity and corresponding penalties and restrictions, it is important to understand that these recommendations are not an endorsement of their design; rather, the intent is to make the designer aware of the potential detrimental effects of irregularities.

Consider, for example, a reentrant corner, resulting from an irregularity characteristic of a building's plan shape. If the configuration of a building has an inside corner, as shown in Figure 5.12, then it is considered to have a reentrant corner. It is the characteristic of buildings with an L, H, T, X, or variations of these shapes.





**FIGURE 5.12** Reentrant corners in L-, T-, and H-shaped buildings. (As a solution, add collector elements and/or stiffen end walls.)

Two problems related to seismic performance are created by these shapes: (1) differential vibrations between different wings of the building may result in a local stress concentration at the reentrant corner and (2) torsion may result because the center of rigidity and the center of mass for this configuration do not coincide.

There are two alternative solutions to this problem: Tie the building together at lines of stress concentration and locate seismic-resisting elements at the extremity of the wings to reduce torsion, or separate the building into simple shapes. The width of the separation joint must allow for the estimated inelastic deflections of adjacent wings. The purpose of the separation is to allow adjoining portions of buildings to respond to earthquake ground motions independently without pounding on each other. If it is decided to dispense with the separation joints, collectors at the intersection must be added to transfer forces across the intersection areas. Since the free ends of the wings tend to distort most, it is beneficial to place seismic-resisting members at these locations.

### 5.2.13 DYNAMIC ANALYSIS

Symmetrical buildings with uniform mass and stiffness distribution behave in a fairly predictable manner, whereas buildings that are asymmetrical or with areas of discontinuity or irregularity do not. For such buildings, dynamic analysis is used to determine significant response characteristics such as (1) the effects of the structure's dynamic characteristics on the vertical distribution of lateral forces; (2) the increase in dynamic loads due to torsional motions; and (3) the influence of higher modes, resulting in an increase in story shears and deformations.

Static methods specified in building codes are based on single-mode response with simple corrections for including higher mode effects. While appropriate for simple regular structures, the simplified procedures do not take into account the full range of seismic behavior of complex structures. Therefore, dynamic analysis is the preferred method for the design of buildings with unusual or irregular geometry.

Two methods of dynamic analysis are permitted: (1) elastic response-spectrum analysis and (2) elastic or inelastic time-history analysis. The response-spectrum analysis is the preferred method

because it is easier to use. The time-history procedure is used if it is important to represent inelastic response characteristics or to incorporate time-dependent effects when computing the structure’s dynamic response.

Structures that are built into the ground and extended vertically some distance above-ground respond as vertical oscillators when subject to ground motions. A simple oscillator may be idealized by a single lumped mass at the upper end of a vertically cantilevered pole (see Figure 5.13).

The idealized system represents two kinds of structures: (1) a single-column structure with a relatively large mass at its top and (2) a single-story frame with flexible columns and a rigid beam. The mass  $M$  is the weight  $W$  of the system divided by the acceleration of gravity  $g$ , that is,  $M = W/g$ .

The stiffness  $K$  of the system is the force  $F$  divided by the corresponding displacement  $\Delta$ . If the mass is deflected and then suddenly released, it will vibrate at a certain frequency, called its natural or fundamental frequency of vibration. The reciprocal of frequency is the period of vibration. It represents the time for the mass to move through one complete cycle. The period  $T$  is given by the relation

$$T = 2\pi\sqrt{M/K}$$

An ideal system with no damping would vibrate forever (Figure 5.14). However, in a real system, with some damping, the amplitude of motion will gradually decrease for each cycle until the structure comes to a complete stop (Figure 5.15). The system responds in a similar manner if, instead of displacing the mass at the top, a sudden impulse is applied to the base.

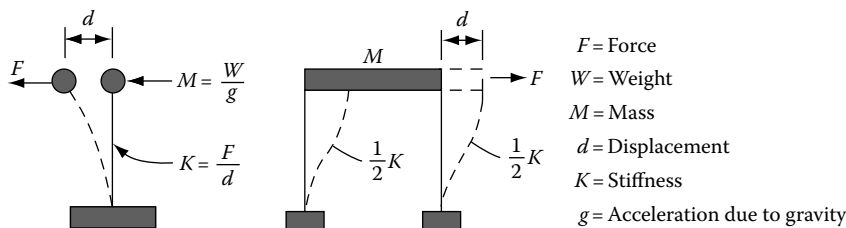


FIGURE 5.13 Idealized SDOF system.

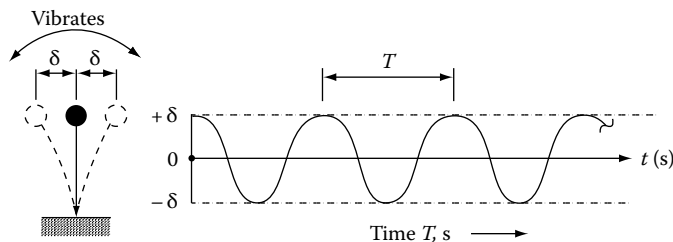


FIGURE 5.14 Undamped free vibrations of SDOF system.

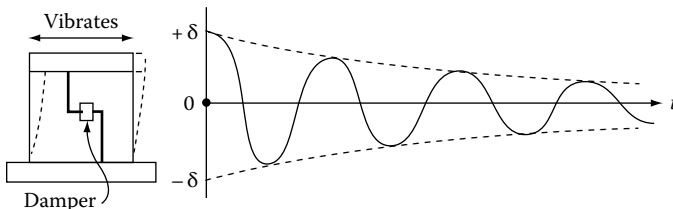
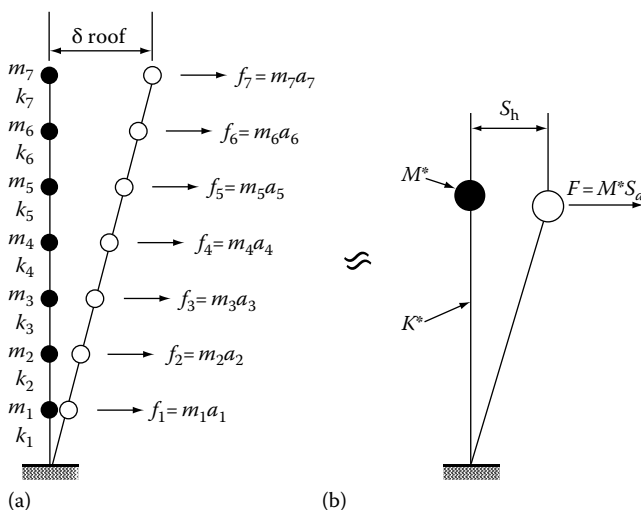


FIGURE 5.15 Damped free vibration of SDOF system.

Buildings are analyzed as multi-degree-of-freedom (MDOF) systems by lumping story-masses at intervals along the length of a vertically cantilevered pole. During vibration, each mass will deflect in one direction or another. For higher modes of vibration, some masses may move in opposite directions. Or all masses may simultaneously deflect in the same direction as in the fundamental mode. An idealized MDOF system has a number of modes equal to the number of masses. Each mode has its own natural period of vibration with a unique mode shape by a line connecting the deflected masses. When ground motion is applied to the base of a multi-mass system, the deflected shape of the system is a combination of all mode shapes, but modes having periods near predominant periods of the base motion will be excited more than the other modes. Each mode of a multi-mass system can be represented by an equivalent single-mass system having generalized values  $M$  and  $K$  for mass and stiffness, respectively. The generalized values represent the equivalent combined effects of story masses  $m_1, m_2, \dots$  and  $k_1, k_2, \dots$ . This concept, shown in Figure 5.16, provides a computational basis for using response spectra based on single-mass systems for analyzing multistoried buildings. Given the period, mode shape, and mass distribution of a multistoried building, we can use the response spectra of a single-degree-of-freedom (SDOF) system for computing the deflected shape, story accelerations, forces, and overturning moments. Each predominant mode is analyzed separately and the results are combined statistically to compute the multimode response.

Buildings with symmetrical shape, stiffness, and mass distribution and with vertical continuity and uniformity behave in a fairly predictable manner, whereas when buildings are eccentric or have areas of discontinuity or irregularity, the behavioral characteristics are very complex. The predominant response of the building may be skewed from the apparent principal axes of the building. The resulting torsional response as well as the coupling or interaction of the two translational directions of response must be considered by using a 3D model for the analysis.

For a building that is regular and essentially symmetrical, a 2D model is generally sufficient. Note that when the floor-plan aspect ratio (length-to-width) of the building is large, torsion response may be predominant, thus requiring a 3D analysis in an otherwise symmetrical and regular building. For most buildings, inelastic response can be expected to occur during a major earthquake, implying that an inelastic analysis is more proper for design. However, in spite of the availability of nonlinear inelastic programs, they are not used in typical design practice because (1) their proper use requires the knowledge of their inner workings and theories, (2) the results produced



**FIGURE 5.16** Representation of a multi-mass system by a single-mass system: (a) fundamental mode of a multi-mass system and (b) equivalent single-mass system.

are difficult to interpret and apply to traditional design criteria, and (3) the necessary computations are expensive. Therefore, analyses in practice typically use linear elastic procedures based on the response-spectrum method.

### 5.2.13.1 Response-Spectrum Method

The word “spectrum” in seismic engineering conveys the idea that the response of buildings having a broad range of periods is summarized in a single graph. For a given earthquake motion and a percentage of critical damping, a typical response spectrum gives a plot of earthquake-related responses such as acceleration, velocity, and deflection for a complete range, or spectrum, of building periods. An understanding of the concept of response spectrum is pivotal to performing seismic design.

Thus, a response spectrum (Figures 5.17 and 5.18a and c) may be visualized as a graphical representation of the dynamic response of a series of progressively longer cantilever pendulums with increasing natural periods subjected to a common lateral seismic motion of the base. Imagine that the fixed base of the cantilevers shown in Figure 5.18d, is moved rapidly back and forth in the horizontal direction, its motion corresponding to that occurring in a given earthquake. A plot of maximum dynamic response, such as accelerations versus the periods of the pendulums, gives us an acceleration response spectrum as shown in Figure 5.18c for the given earthquake motion. In this figure, the absolute value of the peak acceleration occurring during the excitation for each pendulum is represented by a point on the acceleration spectrum curve. Similarly in a conceptual sense, we may consider the response of a series of progressively taller buildings analogous to that postulated for the cantilevers, see Figures 5.18a and b. An example, an acceleration response spectrum for the 1940 El Centro earthquake is illustrated in Figure 5.19. Using ground acceleration as an input, a family of response-spectrum curves can be generated for various levels of damping, where higher values of damping result in lower spectral response.

To establish the concept of how a response spectrum is used to evaluate seismic lateral forces, consider two SDOF structures: (1) an elevated water tank supported on columns and (2) a revolving restaurant supported at the top of a tall concrete core (see Figure 5.20). We will neglect the mass of the columns supporting the tank, and consider only the mass  $m_1$  of the tank in the dynamic analysis. Similarly, the mass  $m_2$  assigned to the restaurant is the only mass considered in the second structure. Given the simplified models, let us examine how we can calculate the lateral loads for both these structures resulting from an earthquake, for example, one that has the same ground-motion characteristics as the 1940 El Centro earthquake shown in Figure 5.21. To evaluate the seismic lateral loads, we shall use the recorded ground acceleration for the first 30 s. Observe that the maximum acceleration recorded is 0.33g. This occurred about 2 s after the recording starts.

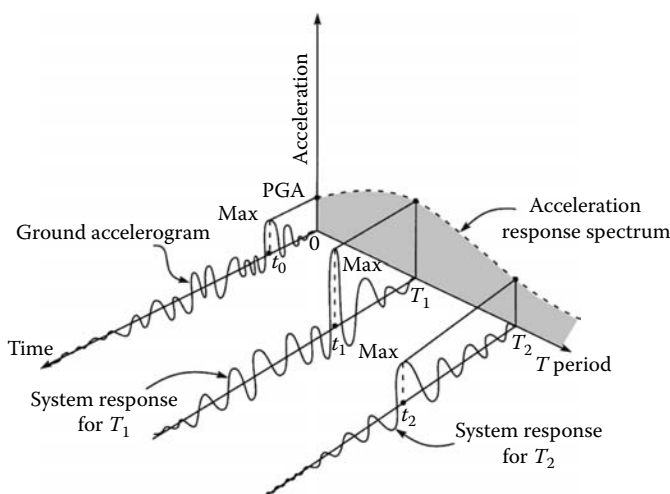
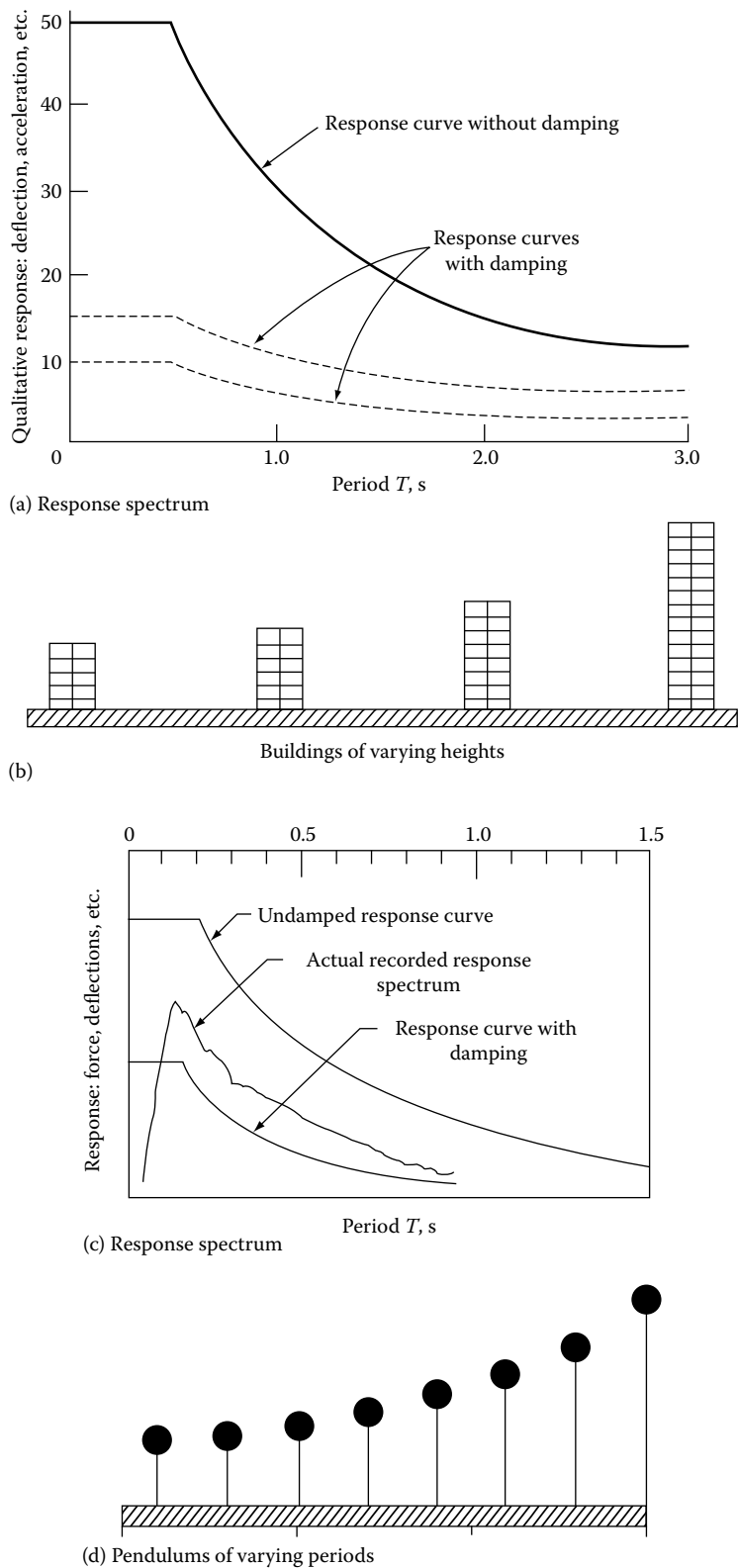
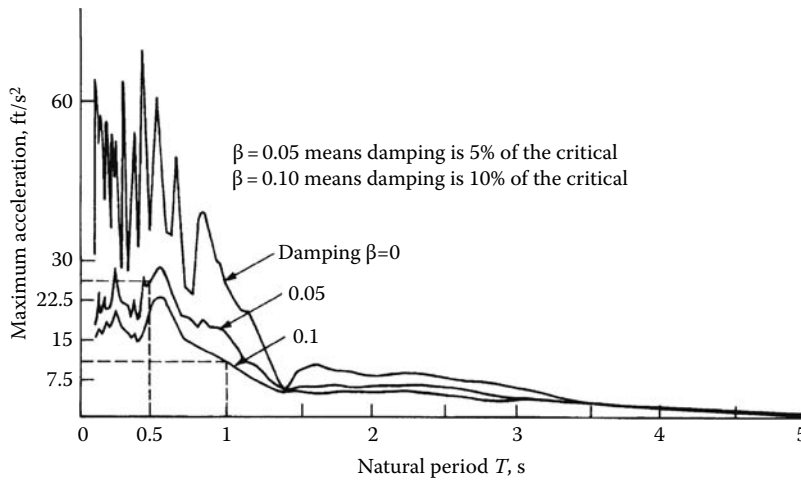


FIGURE 5.17 Graphical description of response spectrum.



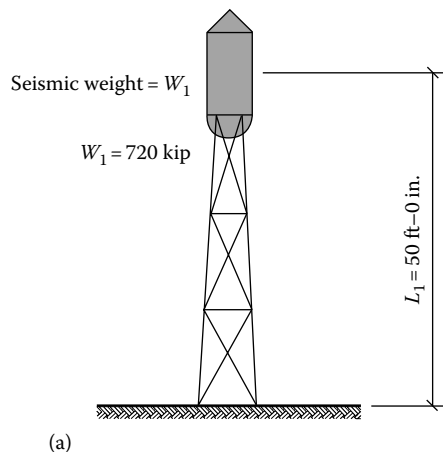
**FIGURE 5.18** Concept of response spectrum (a,b) buildings of varying heights and (c,d) pendulums of varying lengths.



**FIGURE 5.19** Acceleration spectrum: El Centro earthquake.

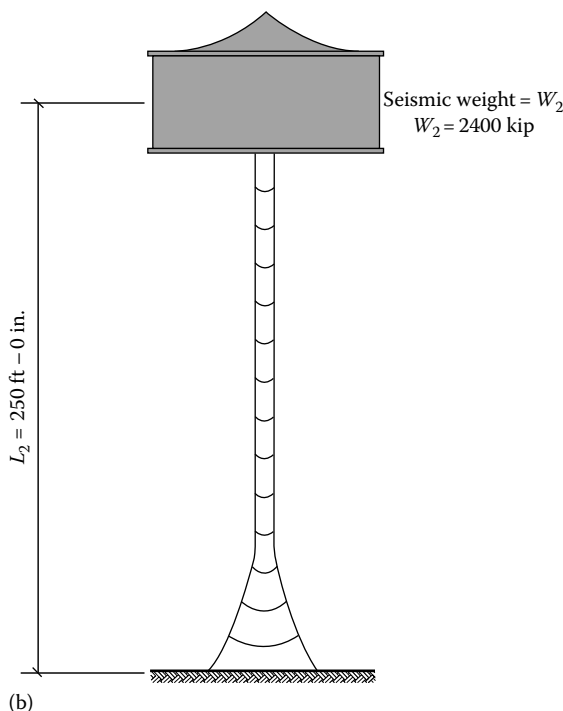
As a first step, the base of the two structures is analytically subjected to the same acceleration as the El Centro-recorded acceleration. The purpose is to calculate the maximum dynamic response experienced by the two masses during the first 30 s of the earthquake. The maximum response such as displacement, velocity, and acceleration for the two examples may be obtained by considering the earthquake effects as a series of impulsive loads, and then integrating the effect of individual impulses over the duration of the earthquake. This procedure, the Duhamel integration method, requires considerable analytical effort. However, in seismic design, fortunately for us, it is generally not necessary to carry out the integration because the maximum response for many previously recorded and synthetic earthquakes are already established or may be derived by using procedures given in seismic standards such as ASCE 7-05. The spectral acceleration response for the north–south component of the El Centro earthquake, shown in Figure 5.19, is one such example.

To determine the seismic lateral loads, assume the tank and restaurant structures weigh 720 (3,202 kN) and 2,400 kip (10,675 kN), with corresponding periods of vibration of 0.5 and 1 s, respectively. Since the response of a structure is strongly influenced by damping, it is necessary to estimate the damping factors for the two structures. Let us assume that the percentages of critical damping  $\beta$

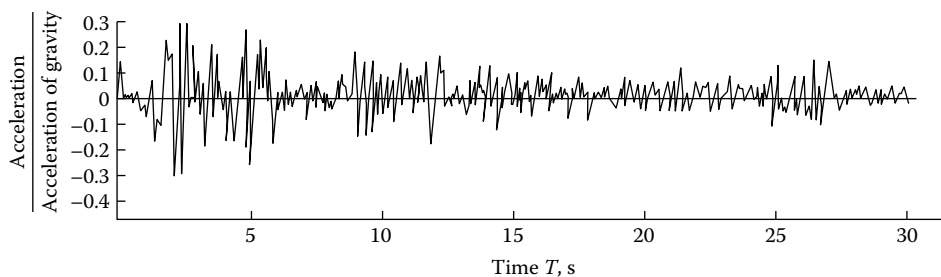


**FIGURE 5.20** Examples of SDOF systems: (a) elevated water tank.

(continued)



**FIGURE 5.20 (continued)** (b) Restaurant atop tall concrete core. Note from Figure 5.19, the acceleration =  $26.25 \text{ ft/s}^2$  for  $T = 0.5 \text{ s}$  and  $\beta = 0.05$  (water tank), and the acceleration =  $11.25 \text{ ft/s}^2$  for  $T = 1.00 \text{ s}$  and  $\beta = 0.10$  (restaurant).



**FIGURE 5.21** Recorded ground acceleration: El Centro earthquake.

for the tank and restaurant are 5% and 10% of the critical damping, respectively. From Figure 5.19, the acceleration for the tank structure is  $26.25 \text{ ft/s}^2$ , giving a horizontal force in kips, equal to the mass of the tank, times the acceleration. Thus  $F = 720/32.2 \times 26.25 = 587$  kip. The acceleration for the second structure from Figure 5.19 is  $11.25 \text{ ft/s}^2$ , and the horizontal force in kip would be equal to the mass at the top times the acceleration. Thus  $F = 2400/32.2 \times 11.25 = 838.51$  kip.

The two structures can then be designed by applying the seismic loads at the top and determining the associated forces, moments, and deflection. The lateral load, evaluated by multiplying the response-spectrum acceleration by the effective mass of the system, is referred to as base shear, and its evaluation forms one of the major tasks in earthquake analysis.

In the examples, Single-Degree-of-Freedom, SDOF structures were chosen to illustrate the concept of spectrum analysis. A multistory building, however, cannot be modeled as a SDOF system

because it will have as many modes of vibration as its Degrees-of-Freedom, DOFs which are infinite for a real system. However, for practical purposes, the distributed mass of a building may be lumped at discrete levels to reduce the DOFs to a manageable number. In multistory buildings, the masses are typically lumped at each floor level.

Thus, in the 2D analysis of a building, the number of modes of vibration corresponds to the number of levels, with each mode having its own characteristic frequency. The actual motion of a building is a combination of its natural modes of vibration. During vibration, the masses vibrate in phase with the displacements as measured from their initial positions, always having the same relationship to each other. Therefore, all masses participating in a given mode pass the equilibrium position at the same time and reach their extreme positions at the same instant.

Using certain simplifying assumptions, it can be shown that each mode of vibration behaves as an independent SDOF system with a characteristic frequency. This method, called the modal superposition method, consists of evaluating the total response of a building by statistically combining the response of a finite number of modes of vibration.

A building, in general, vibrates with as many mode shapes and corresponding periods as its DOFs. Each mode contributes to the base shear, and for elastic analysis, this contribution can be determined by multiplying a percentage of the total mass, called effective mass, by an acceleration corresponding to that modal period. The acceleration is typically read from the response spectrum modified for a damping associated with the structural system. Therefore, the procedure for determining the contribution of the base shear for each mode of a MDOF structure is the same as that for determining the base shear for a SDOF structure, except that an effective mass is used instead of the total mass. The effective mass is a function of the lumped mass and deflection at each floor with the largest value for the fundamental mode, becoming progressively less for higher modes. The mode shape must therefore be known in order to compute the effective mass.

Because the actual deflected shape of a building consists of a combination of its modal shapes, higher modes of vibration also contribute, although to a lesser degree, to the structural response. These can be taken into account through the use of the concept of a participation factor. Further mathematical explanation of this concept is deferred to a later section, but suffice it to note that the base shear for each mode is determined as the summation of products of effective mass and spectral acceleration at each level. The force at each level for each mode is then obtained by distributing the base shear in proportion to the product of the floor weight and displacement. The design values are then computed using modal combination methods, such as the complete quadratic combination (CQC) or the square root of sum of the squares (SRSS), the preferred method being the former.

### 5.2.13.2 Response-Spectrum Concept

Earthquake response spectrum gives engineers a practical means of characterizing ground motions and their effects on structures. Introduced in 1932, it is now a central concept in earthquake engineering that provides a convenient means to summarize the peak response of all possible linear SDOF systems to a particular ground motion. It also provides a practical approach to apply the knowledge of structural dynamics to the design of structures and the development of lateral force requirements in building codes.

A plot of the peak value of response quantity as a function of the natural vibration period  $T_n$  of the system (or a related parameter such as circular frequency  $\omega_n$  or cyclic frequency  $f_n$ ) is called the response spectrum for that quantity. Each such plot is for SDOF systems having a fixed damping ratio  $\beta$ . Often times, several such plots for different values of  $\beta$  are included to cover the range of damping values encountered in actual structures. Whether the peak response is plotted against  $f_n$  or  $T_n$  is a matter of personal preference. In this chapter, we use the later because engineers are more comfortable in using natural period rather than natural frequency because the



period of vibration is a more familiar concept and one that is intuitively appealing. Although a variety of response spectra can be defined depending on the chosen response quantity, it is almost always the acceleration response spectrum, a plot of pseudo-acceleration, against the period  $T_n$  for a fixed damping  $\beta$ , is most often used in the practice of earthquake engineering. A similar plot of displacement  $u$  is referred to as the deformation spectrum, while that of velocity  $\dot{u}$  is called a velocity spectrum.

It is worth while to note that only the deformation  $u(t)$  is needed to compute internal forces. Obviously, then, the deformation spectrum provides all the information necessary to compute the peak values of deformation and internal forces. The pseudo-velocity and pseudo-acceleration response spectrum are important, however, because they are useful in studying characteristics of response spectra, constructing design spectra, and relating structural dynamics results to building codes.

### 5.2.13.3 Deformation Response Spectrum

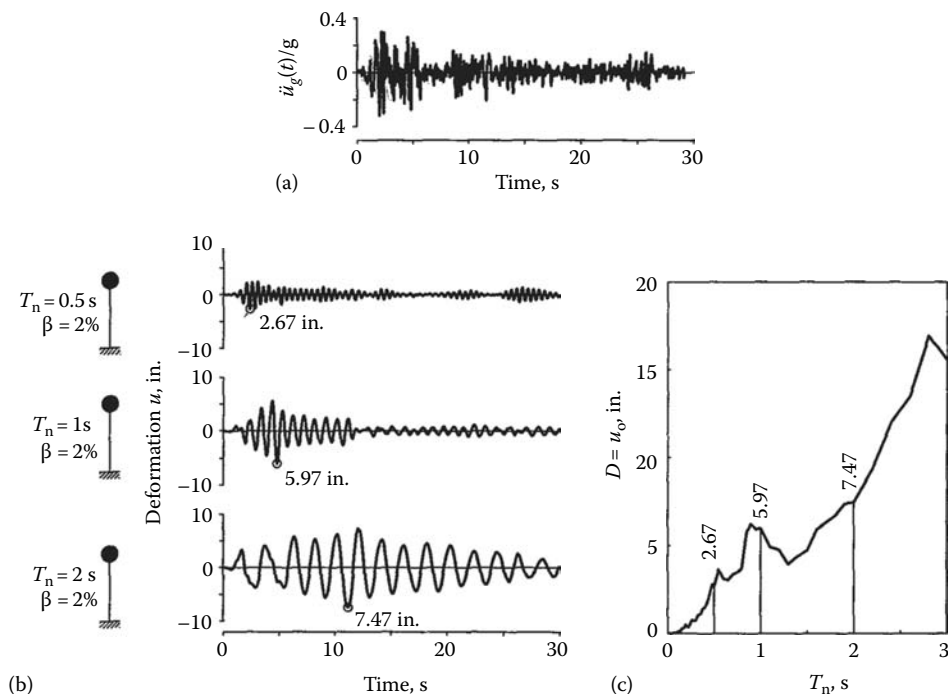
To explain the procedure for determining the deformation response spectrum, we start with the spectrum developed for El Centro ground motion, which has been studied extensively in textbooks (see Ref. 104). The acceleration is shown in Figure 5.22a. The deformation induced by this ground motion in three SDOF systems spectrum of varying periods is presented in Figure 5.22b. For each system, the peak value of deformation is determined from the deformation history.

The peak deformations are

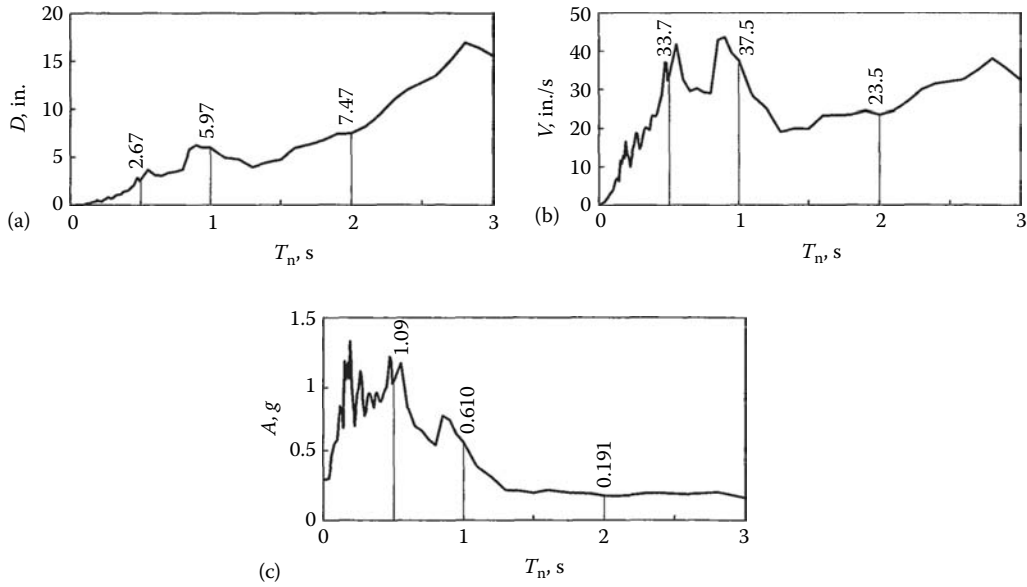
$u_o = 2.67$  in. for a system with natural period  $T_n = 0.5$  s and damping ratio  $\beta = 2\%$

$u_o = 5.97$  in. for a system with  $T_n = 1$  s and  $\beta = 2\%$

$u_o = 7.47$  in. for a system with  $T_n = 2$  s and  $\beta = 2\%$



**FIGURE 5.22** (a) Ground acceleration; (b) deformation response of three SDOF systems with  $\beta = 2\%$  and  $T_n = 0.5, 1$ , and  $2$  s; and (c) deformation response spectrum for  $\beta = 2\%$ .



**FIGURE 5.23** Response spectra ( $\beta = 2\%$ ) for El Centro ground motion: (a) deformation response spectrum, (b) pseudo-velocity response spectrum, and (c) pseudo-acceleration response spectrum.

The  $u_o$  value so determined for each system provides one point on the deformation response spectrum. Repeating such computations for a range of values of  $T_n$  while keeping  $\beta$  constant at 2% provides the deformation response spectrum shown in Figure 5.23a. The spectrum shown is for a single damping value,  $\beta = 2\%$ . However, a complete response spectrum would include such spectrum curves for several values of damping.

#### 5.2.13.4 Pseudo-Velocity Response Spectrum

The pseudo-velocity response spectrum is a plot of  $V$  as a function of the natural vibration period  $T_n$ , or natural vibration frequency  $f_n$ , of the system. For a given ground motion, the peak pseudo-velocity  $V$  for a system with natural period  $T_n$  can be determined from the following equation using the deformation  $D$  of the same system from the response spectrum of Figure 5.23b:

$$V = \omega_n D = \frac{2\pi}{T_n} D$$

As an example, for a system with  $T_n = 0.5$  s and  $\beta = 2\%$ ,  $D = 2.67$  in.:

$$V = \omega_n D = \frac{2\pi}{T_n} D = \left( \frac{2\pi}{0.5} \right) 2.67 = 33.7 \text{ in./s}$$

Similarly, for  $T_n = 1.0$  s and  $\beta = 2\%$ ,  $D = 5.97$  in.:

$$V = \left( \frac{2\pi}{1} \right) 5.97 = 37.5 \text{ in./s}$$

And, for  $T_n = 2.0$  s and the same damping  $\beta = 2\%$ ,  $D = 7.47$  in.:

$$V = \left( \frac{2\pi}{2} \right) 7.47 = 23.5 \text{ in./s}$$

These three values of peak pseudo-velocity  $V$  are identified in Figure 5.23b. Repeating such computations for a range of values of  $T_n$  while keeping  $\beta$  constant at 2% provides the pseudo-velocity spectrum shown in Figure 5.23b. The prefix “pseudo” is used for  $V$  because  $V$  is not equal to the peak velocity, although it has the same units for velocity.

#### 5.2.13.5 Pseudo-Acceleration Response Spectrum

It has been stated many times in this chapter that the base shear is equal to the inertia force associated with the mass  $m$  undergoing acceleration  $A$ . This acceleration  $A$  is generally different from the peak acceleration of the system. It is for this reason that  $A$  is called the peak pseudo-acceleration; the prefix “pseudo” is used to avoid possible confusion with the true peak acceleration, just as we did for velocity  $V$ . The pseudo-acceleration response spectrum is a plot of acceleration  $A$  as a function of the natural vibration period  $T_n$ , or natural vibration frequency  $f_n$ , of the system. For a given ground motion, peak pseudo-acceleration  $A$  for a system with natural period  $T_n$  and damping ratio  $\zeta$  can be determined from the following equation using the peak deformation  $D$  of the system from the response spectrum:

$$A = \omega_n^2 D = \left( \frac{2\pi}{T_n} \right)^2 D$$

As an example, for a system with  $T_n = 0.5$  s and  $\beta = 2\%$ ,  $D = 2.67$  in.:

$$A = \omega_n^2 D = \left( \frac{2\pi}{T_n} \right)^2 D = \left( \frac{2\pi}{0.5} \right)^2 2.67 = 1.09g$$

where  $g = 386 \text{ in./s}^2$

Similarly, for a system with  $T_n = 1$  s and  $\zeta = 2\%$ ,  $D = 5.97$  in.:

$$A = \left( \frac{2\pi}{T_n} \right)^2 D = \left( \frac{2\pi}{1} \right)^2 5.97 = 0.610g$$

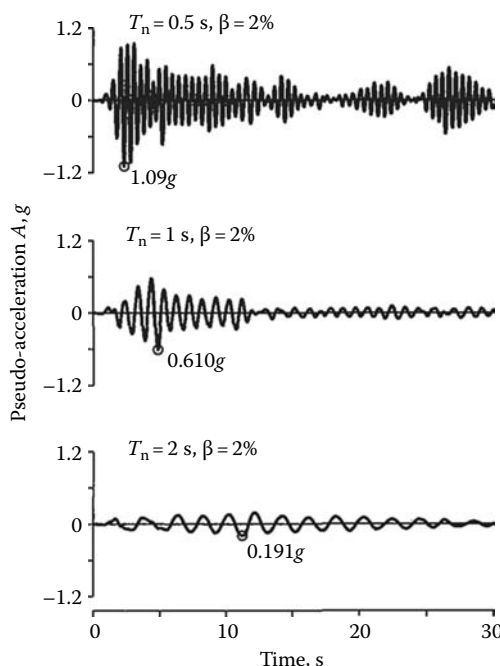
And, for a system with  $T_n = 2$  s and the same damping  $\zeta = 2\%$ ,  $D = 7.47$  in.:

$$A = \left( \frac{2\pi}{2} \right)^2 7.47 = 0.191g$$

The three values  $T_n$  of pseudo-acceleration,  $A$ , are shown in Figure 5.24. Repeating similar computations for a range of  $T_n$  values, while keeping  $\beta$  constant at 2% yields the pseudo-acceleration spectrum shown in Figure 5.23c.

#### 5.2.13.6 Tripartite Response Spectrum: Combined Displacement–Velocity–Acceleration (DVA) Spectrum

It was shown in the previous section that each of the deformation, pseudo-velocity, and pseudo-acceleration response spectra for a given ground motion contain the same information, no more and no less. The three spectra are simply distinct ways of displaying the same information on structural



**FIGURE 5.24** Pseudo-acceleration response of SDOF systems to El Centro ground motion.

response. With a knowledge of one of the spectra, the other two can be derived by algebraic operations using the procedure given in the previous section.

If each of the spectra contains the same information, why do we need three spectra? There are two reasons. One is that each spectrum directly provides a physically meaningful quantity: The deformation spectrum provides the peak deformation of a system, the pseudo-velocity spectrum gives the peak strain energy stored in the system during the earthquake, and pseudo-acceleration spectrum yields directly the peak value of the equivalent static force and base shear. The second reason lies in the fact that the shape of the spectrum can be approximated more readily for design purposes with the aid of all three spectral quantities rather than any one of them alone. For this purpose, a combined plot showing all three of the spectral quantities is especially useful. This type of plot was developed for earthquake response spectra for the first time by A.S. Veletsos and N.M. Newmark in 1960.

In an integrated *DVA* spectrum, the vertical and horizontal scales for  $V$  and  $T_n$  are standard logarithmic scales. The two scales for  $D$  and  $A$  sloping at  $+45^\circ$  and  $-45^\circ$ , respectively, to the  $T_n$ -axis are also logarithmic scales but not identical to the vertical scale. The pairs of numerical data for  $V$  and  $T_n$  that were plotted in Figure 5.23b on linear scales are replotted in Figure 5.25 on logarithmic scales. For a given natural period  $T_n$ , the  $D$  and  $A$  values can be read from the diagonal scales. As an example, for  $T_n = 2$  s, Figure 5.25 gives  $D = 7.47$  in. and  $A = 0.191g$ . The four-way plot is a compact presentation of the three—deformation, pseudo-velocity, and pseudo-acceleration—response spectra, for a single plot of this form replaces the three plots.

The benefit of the response spectrum in earthquake engineering may be recognized by the fact that spectra for virtually all ground motions strong enough to be of engineering interest are now computed and published soon after they are recorded. From these we can get a reasonable idea of the kind of motion that is likely to occur in future earthquakes. It should be noted that for a given ground motion response spectrum, the peak value of deformation, pseudo-velocity, and base shear in any linear SDOF can be readily read from the spectra without resorting to dynamic analyses. This is because the computationally intensive dynamic analysis has been completed in generating the response spectrum.

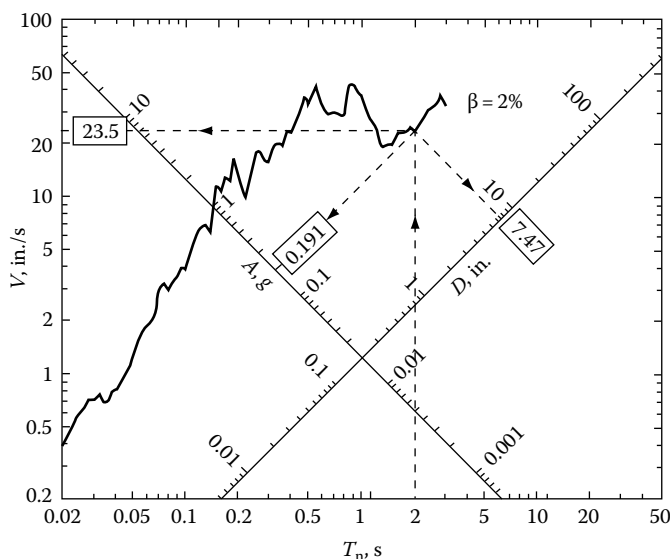


FIGURE 5.25 Combined DVA response for El Centro ground motion;  $\beta = 2\%$ .

Given these advantages doesn't it make good sense to have geotechnical engineers provide tripartite response spectrum rather than just acceleration spectrum, when site specific studies are commissioned?

Tripartite response spectra for four seismic events characterized as earthquakes A, B, C, and D for a downtown Los Angeles site are shown in Figure 5.26. Response spectrum A is for a maximum capable earthquake of magnitude 8.25 occurring at San Andreas fault at a distance of 34 miles while B is for a magnitude 6.8 earthquake occurring in Santa Monica (Hollywood) fault at a distance of 3.7 miles from the site. Response spectra C and D are for earthquakes with a 10% and 50% probability of being exceeded in 50 years, respectively.

The response spectrum tells us that the forces experienced by buildings during an earthquake are not just a function of the quake, but are also their dynamic response characteristics to the quake. The response primarily depends on the period of the building being studied. A great deal of single-mode information can be read directly from the response spectrum. Referring to Figure 5.27, the horizontal axis of the response spectrum expresses the period of the building during affected by the quake. The vertical axis shows the velocity attained by this building during the quake. The diagonal axis running up toward the left-hand corner reads the maximum accelerations to which the building is subjected. The axis at right angles to this will read the displacement of the building in relation to the support. Superimposed on these tripartite scales are the response curves for an assumed 5% damping of critical. Now let us see how various buildings react during an earthquake described by these curves.

If the building to be studied had a natural period of 1 s, we would start at the bottom of the chart at  $T = 1$  s, and reference vertically until we intersect the response curve. From this intersection, point A, we travel to the extreme right and read a velocity of 16 in./s. Following a displacement line diagonally down to the right, we find a displacement of 2.5 in. Following an acceleration line down to the left, we see that it will experience an acceleration of 0.25g. If we then move to the 2 s period, point B, in the same sequence, we find that we will have the same velocity of 16 in./s, a displacement of 4 in., and a maximum acceleration of 0.10g. If we then move to 4 s, point C, we see a velocity of 16 in./s, a displacement of 10 in., and an acceleration of 0.06g. If we run all out to 10 s, point D, we find a velocity of 7 in./s, a displacement of 10 in. the same as for point C, and an acceleration of 0.01g. Notice that the values vary widely, as started earlier, depending on the period of building exposed to this particular quake.

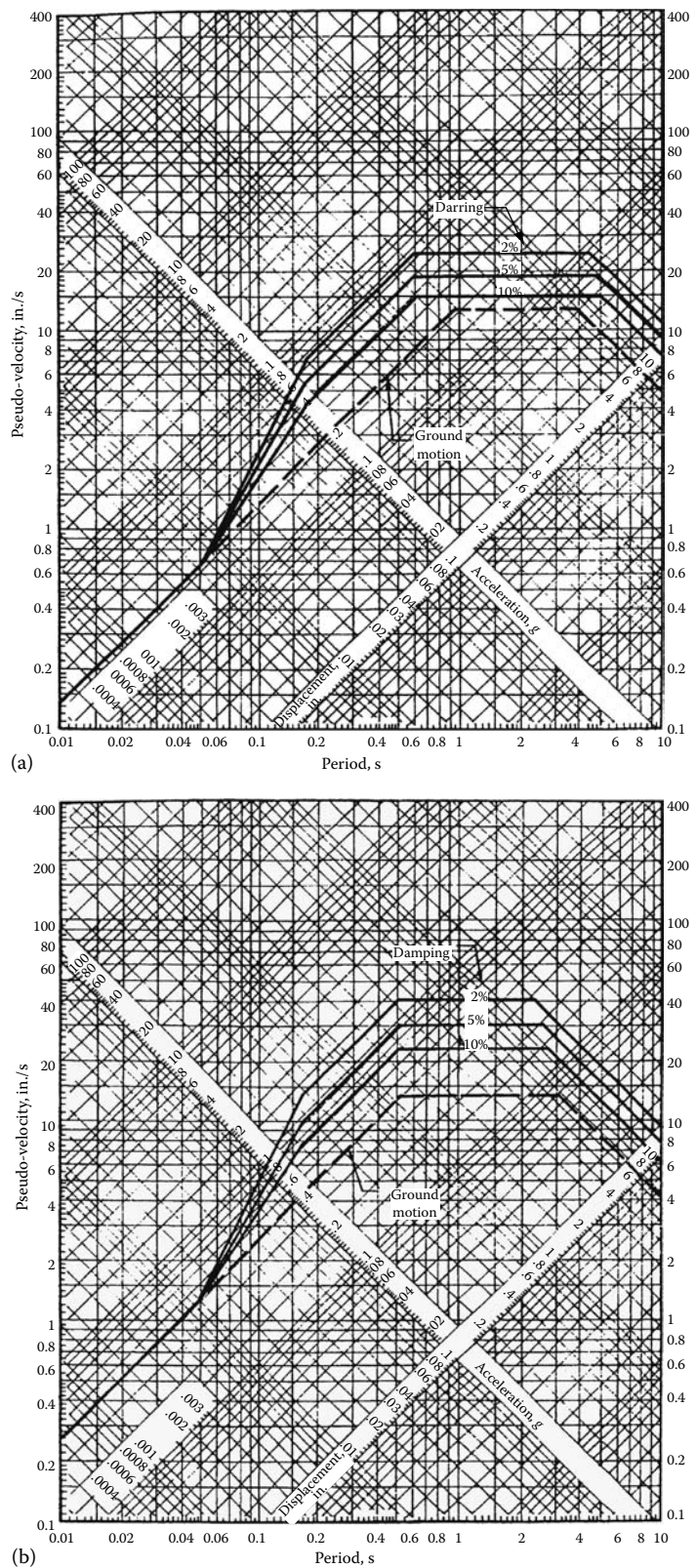


FIGURE 5.26 Tripartite site-specific response spectra: (a) earthquake A, (b) earthquake B,

(continued)

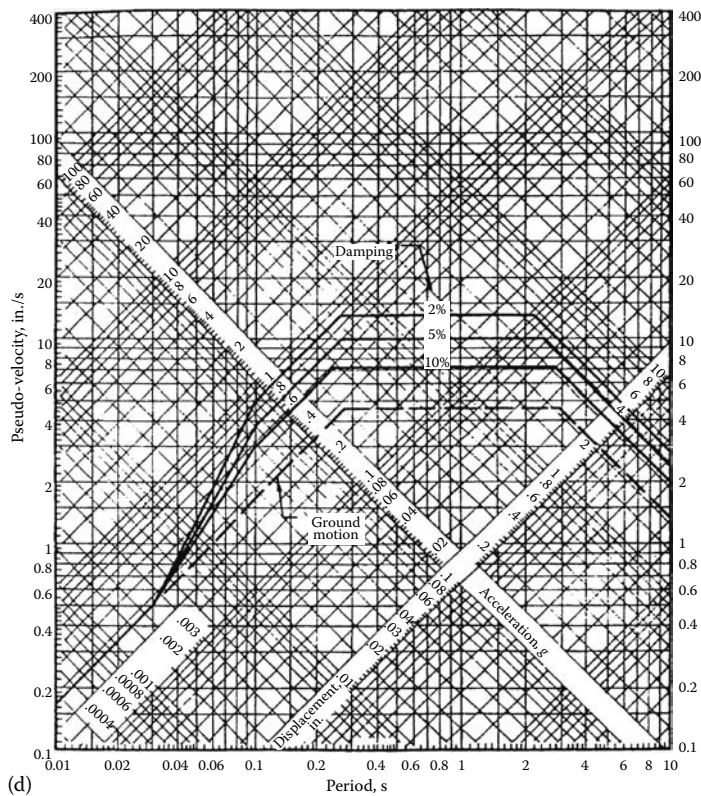
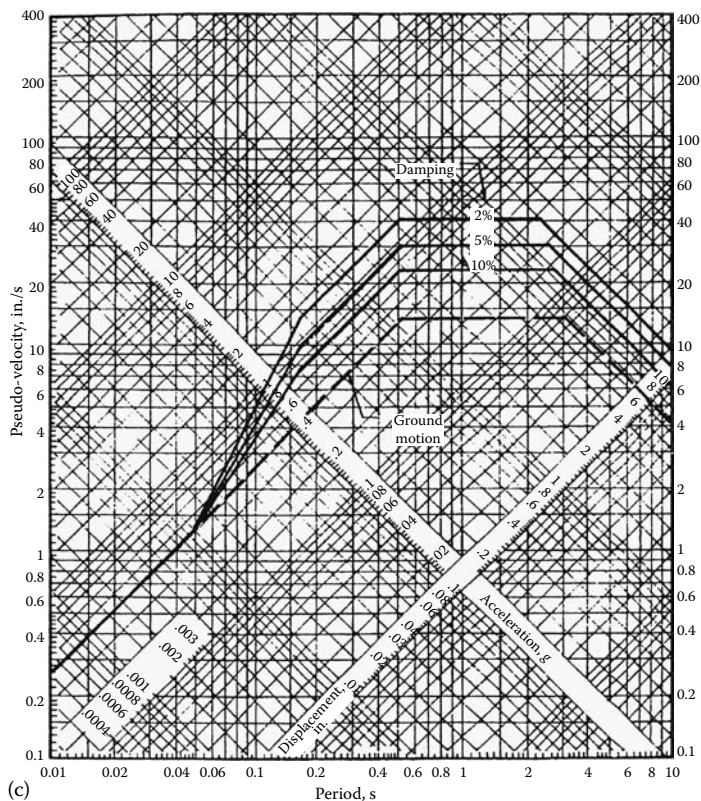


FIGURE 5.26 (continued) (c) earthquake C, and (d) earthquake D.

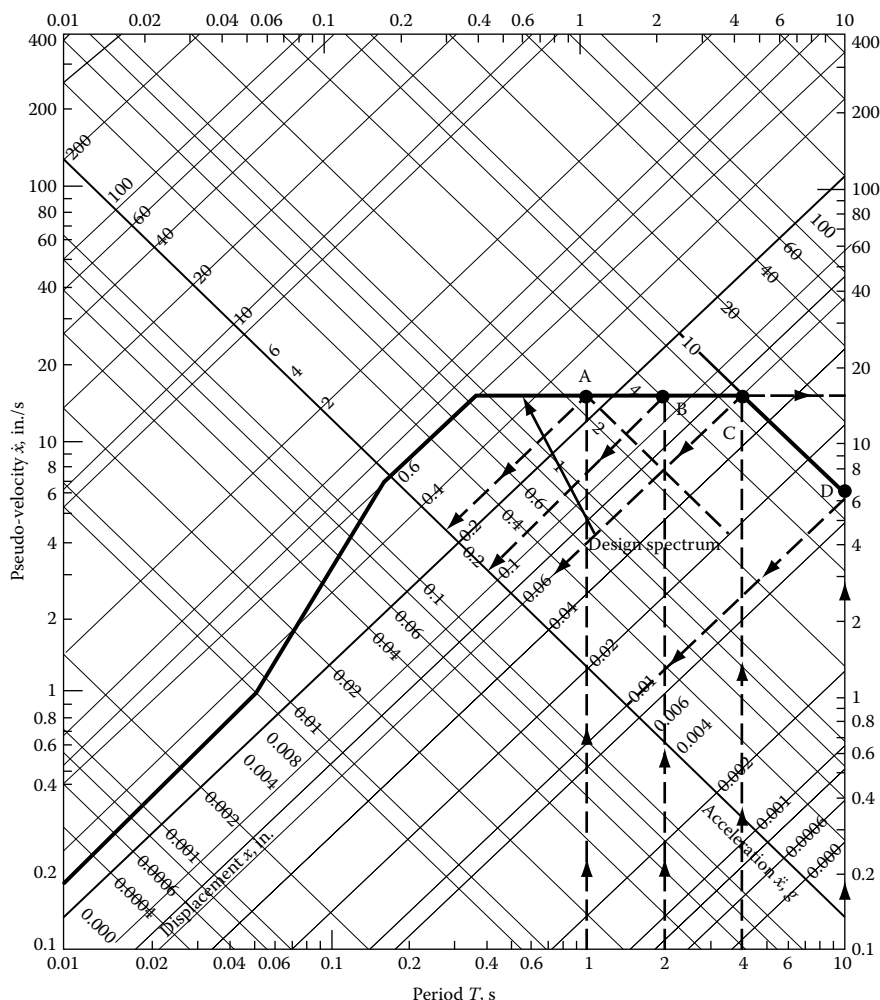


FIGURE 5.27 Velocity, displacement, and acceleration readout from response spectra.

### 5.2.13.7 Characteristics of Response Spectrum

We now study the important properties of earthquake response spectra. For this purpose, we use once again an idealized response spectrum for El Centro ground motion shown in Figure 5.28. The damping,  $\beta$ , associated with the spectrum is 5%. The period  $T_n$  plotted on a logarithmic scale covers a wide range,  $T_n = 0.01 - 10$  s.

Consider a system with a very short period, say 0.03 s. For this system, the pseudo-acceleration  $A$  approaches the ground acceleration while the displacement  $D$  is very small. There is a physical reasoning for this trend: For purposes of dynamic analysis, a very short period system is extremely stiff and may be considered essentially rigid. Such a system would move rigidly with the ground as if it is a part of the ground itself. Thus its peak acceleration would be approximately equal to the ground acceleration as shown in Figure 5.29.

Next, we examine a system with a very long period, say  $T_n = 10$  s. The acceleration  $A$ , and thus the force in the structure, which is related to  $mA$ , would be small. Again there is a physical reasoning for this trend: A very long period system is extremely flexible. The mass at top is expected to remain stationary while the base would move with the ground below (see Figure 5.29).

Based on these two observations, and those in between the two periods (not examined here), it is logical to divide the spectrum into three period ranges. The long-period region to the right of point D,



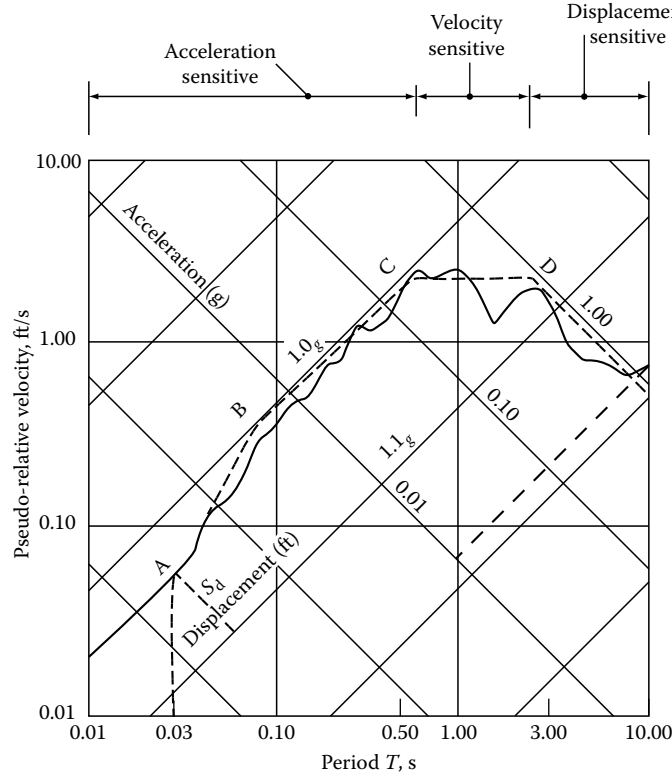


FIGURE 5.28 Idealized response spectrum for El Centro ground motion.

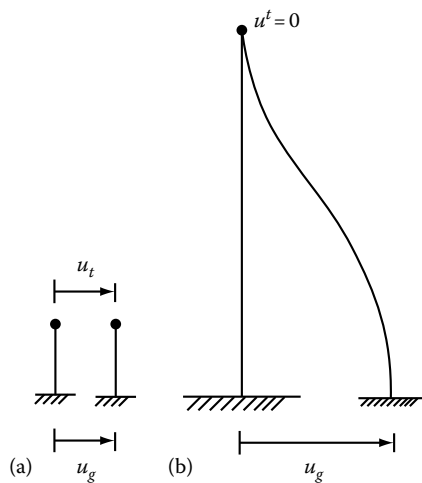


FIGURE 5.29 Schematic response of rigid and flexible systems. (a) Rigid system, acceleration at top is nearly equal to the ground acceleration; (b) flexible system, structural response is most directly related to ground displacement.

is called the displacement-sensitive region because structural response is most directly related to ground displacement. The short-period region to the left of point C, is called the acceleration-sensitive region because structural response is most directly related to ground acceleration. The intermediate

period region between points C and D, is called the velocity-sensitive region because structural response appears to be better related to ground velocity than to other ground motion parameters.

The preceding discussion has brought out the usefulness of the four-way logarithmic plot of the combined deformation, pseudo-velocity, and pseudo-acceleration response spectra. These observations would be difficult to discover from the three individual spectra.

We now turn to damping, which has significant influence on the earthquake response spectrum by making the response much less sensitive to the period. Damping reduces the response of a structure, as expected, and the reduction achieved with a given amount of damping is different in the three spectral regions. In the limit as  $T_n \rightarrow \infty$ , damping again does not affect the response because the structural mass stays still while the ground underneath moves. Among the three period regions, the effect of damping tends to be greatest in the velocity-sensitive region of the spectrum. In this spectral region, the effect of damping depends on the ground motion characteristics. If the ground motion is harmonic over many cycles as it was in the Mexico City earthquake of 1985, the effect of damping would be especially large for systems near resonance.

The motion of structure and the associated forces could be reduced by increasing the effective damping of the structure. The addition of dampers achieves this goal without significantly changing the natural vibration periods of the structure. Viscoelastic dampers have been used in many structures; for example, 10,000 dampers were installed throughout the height of each tower of the now nonexistent World Trade Center in New York City to reduce wind-induced motion to within a comfortable range for the occupants. In recent years, there is a growing interest in developing dampers suitable for structures in earthquake-prone regions. Because the inherent damping in most structures is small, their earthquake response can be reduced significantly by the addition of dampers. These can be especially useful in improving the seismic safety of an existing structure.

### 5.3 AN OVERVIEW OF 2006 IBC

Chapter 16 of the 2006 International Building Code (IBC), entitled Structural Design, addresses seismic provisions in a single section (Section 1613), as opposed to multiple sections of the 2003 IBC.

The most significant change in the 2006 IBC is the removal of large portions of text related to the determination of snow, wind, and seismic loads. All technical specifications related to these loads are incorporated into 2006 IBC through reference to 2005 edition of ASCE 7 Standard, Minimum Design Loads for Buildings and Other Structures. However, certain portions are still retained in the 2006 IBC particularly those related to local geology, terrain, and other environmental issues that many building officials may wish to consider when adapting the 2006 IBC provisions to local conditions.

An update of 2009 IBC provisions is given in Chapter 9 of this book.

#### 5.3.1 OCCUPANCY CATEGORY

This replaces “Seismic Use Group” of the 2003 IBC, and is used directly to determine importance factors for snow, wind, and seismic designs.

A confusion related to the Occupancy Category III designation of 2003 IBC has been clarified. It now applies to covered structures whose primary occupancy is public assembly with an occupant load greater than 300. In the 2003 IBC, it was not clear if the term “one area” defined in that edition, meant a single room, a number of connected rooms, or a complete floor, etc. The statement regarding the nature of occupancy was unclear and inadvertently included a large number of commercial buildings where an occupant load of more than 300 people is not unusual. Thus, the clarification permits Occupancy Category II for typical commercial buildings.

Although 2006 IBC has eliminated much of the confusion regarding how to treat large projects having only a small, isolated portion with high occupant load, it behooves the engineers to verify their assumptions with the owners, architect, peer reviewers, and building officials. If the building in question is classified as Occupancy Category Type II, then  $I_w = 1.0$  and  $I_E = 1.25$ ; if on the other hand the building is classified as Occupancy Category Type I, then  $I_w = 0.87$  or  $0.77$  and  $I_E = 1.0$ .

**TABLE 5.3**  
**Occupancy Category of Buildings and Importance Factors**

Nature of Occupancy	Occupancy Category	Importance Factor		
		$I_E$	$I_{W1}$	$I_{W2}$
Buildings and other structures that represent a low hazard to human life in the event of failure, including, but not limited to <ul style="list-style-type: none"> <li>• Agricultural facilities</li> <li>• Certain temporary facilities</li> <li>• Minor storage facilities</li> </ul>	I	1.0	0.87	0.77
All buildings and other structures except those listed in Occupancy Categories I, III, and IV	II	1.0	1.0	1.0
Buildings and other structures that represent a substantial hazard to human life in the event of failure, including, but not limited to <ul style="list-style-type: none"> <li>• Buildings and other structures where more than 300 people congregate in one area</li> <li>• Buildings and other structures with day care facilities with a capacity greater than 150</li> <li>• Buildings and other structures with elementary school or secondary school facilities with a capacity greater than 250</li> <li>• Buildings and other structures with a capacity greater than 500 for colleges or adult education facilities</li> <li>• Health care facilities with a capacity of 50 or more resident patients, but not having surgery or emergency treatment facilities</li> <li>• Jails and detention facilities</li> </ul>	III	1.25	1.15	1.15
Buildings and other structures, not included in Occupancy Category IV, with potential to cause a substantial economic impact and/or mass disruption of day-to-day civilian life in the event of failure, including, but not limited to <ul style="list-style-type: none"> <li>• Power generating stations<sup>a</sup></li> <li>• Water treatment facilities</li> <li>• Sewage treatment facilities</li> <li>• Telecommunication centers</li> </ul>				
Buildings and other structures not included in Occupancy Category IV (including, but not limited to, facilities that manufacture, process, handle, store, use, or dispose of such substances as hazardous fuels, hazardous chemicals, hazardous waste, or explosives) containing sufficient quantities of toxic or explosive substances to be dangerous to the public if released.				
Buildings and other structures containing toxic or explosive substances shall be eligible for classification as Occupancy Category II structures if it can be demonstrated to the satisfaction of the authority having jurisdiction by a hazard assessment as described in Section 1.5.2 that a release of the toxic or explosive substances does not pose a threat to the public.				
Buildings and other structures designated as essential facilities, including, but not limited to <ul style="list-style-type: none"> <li>• Hospitals and other health care facilities having surgery or emergency treatment facilities</li> <li>• Fire, rescue, ambulance, and police stations and emergency vehicle garages</li> <li>• Designated earthquake, hurricane, or other emergency shelters</li> <li>• Designated emergency preparedness, communication, and operation centers and other facilities required for emergency response</li> </ul>	IV	1.5	1.15	1.15

**TABLE 5.3 (continued)**  
**Occupancy Category of Buildings and Importance Factors**

Nature of Occupancy	Occupancy Category	Importance Factor		
		$I_E$	$I_{W1}$	$I_{W2}$
<ul style="list-style-type: none"> <li>• Power generating stations and other public utility facilities required in an emergency</li> <li>• Ancillary structures (including, but not limited to, communication towers, fuel storage tanks, cooling towers, electrical substation structures, fire water storage tanks or other structures housing or supporting water, or other fire-suppression material or equipment) required for the operation of Occupancy Category IV structures during an emergency</li> <li>• Aviation control towers, air traffic control centers, and emergency aircraft hangars</li> <li>• Water storage facilities and pump structures required to maintain water pressure for fire suppression</li> <li>• Buildings and other structures having critical national defense functions</li> </ul>				

Buildings and other structures (including, but not limited to, facilities that manufacture, process, handle, store, use, or dispose of such substances as hazardous fuels, hazardous chemicals, or hazardous waste) containing highly toxic substances where the quantity of the material exceeds a threshold quantity established by the authority having jurisdiction.

Buildings and other structures containing highly toxic substances shall be eligible for classification as Occupancy Category II structures if it can be demonstrated to the satisfaction of the authority having jurisdiction by a hazard assessment as described in Section 1.5.2 that a release of the highly toxic substances does not pose a threat to the public. This reduced classification shall not be permitted if the buildings or other structures also function as essential facilities.

*Source:* From ASCE 7-05, Table 1.1.

*Note:*  $I_E$  = seismic importance factor.  $I_{W1}$  = wind importance factor, non-hurricane prone regions and hurricane prone regions with  $V = 85\text{--}100$  mph, and Alaska.  $I_{W2}$  = wind importance factor, hurricane prone regions with  $V > 100$  mph.

<sup>a</sup> Cogeneration power plants that do not supply power on the national grid shall be designated Occupancy Category II.

Occupancy categories are given in Table 5.3 (ASCE 7-05, Table 1-1). Note Table 5.3 gives the importance factors for both wind and seismic designs.

### 5.3.2 OVERTURNING, UPLIFTING, AND SLIDING

The provisions regarding design against overturning, uplifting, and sliding applies to both wind and seismic designs. This is clarified in a new section (Section 1604.9, Counteracting Structural Actions).

### 5.3.3 SEISMIC DETAILING

The requirement that the lateral force-resisting system meet seismic-detailing provisions even when wind load effects are greater than seismic load effects is not now. However, to emphasize this requirement, a new section (Section 1604.10, Wind and Seismic Detailing) is added to the general design requirement of Section 1604.

### 5.3.4 LIVE-LOAD REDUCTION IN GARAGES

Live-load reduction in passenger vehicle garages is prohibited for floor-framing members. However, a maximum of 20% reduction is permitted for members supporting two or more levels. Thus, floor members of a garage are designed for an unreduced live load of 40 psf (as set forth in the 2006 IBC, Table 1607.1), and columns and walls supporting loads from two or more levels are designed for a reduced live load of  $0.8 \times 40 = 32$  psf, rounded down to 30 psf.

### 5.3.5 TORSIONAL FORCES

A clarification is made regarding the increase in forces resulting from torsion due to eccentricity between the center of the application of lateral forces and the center of the rigidity of the lateral force-resisting system. Because flexible diaphragms cannot transmit torsion, an exception is made to the torsion provision required for buildings with rigid diaphragms.

### 5.3.6 PARTITION LOADS

The live load for partitions in office buildings or any other buildings where partition locations are subject to change and where the specified live load is less than or equal to 80 psf has been reduced from 20 to 15 psf.

## 5.4 ASCE 7-05 SEISMIC PROVISIONS: AN OVERVIEW

Before discussing the seismic provisions of ASCE 7-05, it is perhaps instructive to briefly dwell on their evolution. In the United States, the code development process for seismic provisions is less than 80 years old. In 1926, the Pacific Coast Building Officials published the first edition of the UBC with nonmandatory seismic provisions that appeared only in an appendix. They included only a few technical requirements consisting of design for a minimum base shear equal to approximately 10% of the building's weight on soft soil sites, and 3% of the building's weight on rock or firm soil sites.

Since then, building code provisions for seismic resistance have evolved on a largely empirical basis. Following the occurrence of damaging earthquakes, engineers investigated the damage, tried to understand why certain buildings and structures performed in an unsatisfactory manner, and developed recommendations on how to avoid similar vulnerabilities. Examples include limitations on the use of unreinforced masonry in regions anticipated to experience strong ground shaking, requirements to positively anchor concrete and masonry walls to floor and roof diaphragms, and limitations on the use of certain irregular building configurations.

The focus of seismic code development has traditionally been on California, the region where the most U.S. earthquakes have occurred. Periodically, recommendations were published in the form of a best practice guide, the Recommended Lateral Force Requirements and Commentary, or more simply, the blue book, because it traditionally had a blue cover.

In 1971, the San Fernando earthquake demonstrated that the code provisions in place at the time were inadequate and that major revision was necessary. To accomplish this, the Applied Technology Council (ATC) was founded to perform the research and development necessary to improve the code. This effort culminated in 1978, with the publication of ATC3.06, a report titled Tentative Recommended Provisions for Seismic Regulation of Buildings. The Structural Engineers Association of California (SEAOC) incorporated many of the recommendations in that report into the 1988 edition of the UBC. Perhaps more important, however, was that the publication of this report coincided with the adoption of the National Earthquake Hazards Reduction Program (NEHRP).

Although NEHRP provisions were first published in 1985, they were not formally used as the basis of any model building codes until the early 1990s. Prior to that time, these codes had adopted seismic provisions based on the American National Standards Institute's (ANSI) publication ANSI

A58.1 (later ASCE-7), which had been based on SEAOC recommendations. In 1993, the American Society of Civil Engineers (ASCE) revised its ASCE-7 standard to include seismic provisions that closely mirrored the NEHRP document.

Currently, there is a concerted effort to maintain a single model code for the entire United States. This is the IBC, developed by the International Code Council, a coalition of the Building Officials Code Administrators International, International Conference of Building Officials, and Southern Building Code Conference International. The model building code, the IBC-06, has incorporated major national standards such as AISC, ACI, and the seismic provisions of ASCE 7-05 “by preference.” The ASCE-7 is used as a reference for load combinations; seismic, wind, and snow loads. AISC is a reference for steel design, ACI 318 is a reference for concrete design, ACI 530 is a reference for masonry design, and the National Design Specifications are a reference for wood construction. The seismic section of the 2006 IBC is only 24 pages long. It is not a stand-alone document, and has ASCE-05 embedded throughout the seismic section. Therefore, instead of wading through IBC provisions, the user can go directly to ASCE-7. IBC allows one to do so.

The seismic design provisions presented in the following sections are based on ASCE 7-05. Since IBC 2006 has adapted this document by reference, the design provisions given here apply equally to 2006 IBC. Therefore, although for simplicity, only ASCE-05 is referenced in the following text, it is understood that the provisions are also applicable to 2006 IBC.

Engineers who design and detail structures for many areas of the United States with low seismic risk have not had the pleasure to deal with design and detailing requirements that apply to moderate and high seismic zones on the west coast. But that has changed due to major revisions of seismic provisions published in ASCE 7-05 and its predecessor ASCE 7-02.

Traditionally, the magnitude of the seismic force and the level of seismic detailing were strictly a function of structure location. With the latest seismic design provisions, these are now a function of

1. Structure location
2. Nature of the structure’s occupancy
3. Type of soil the structure rests upon

Does this affect the design of a structure in a low seismic-risk zone? You bet. Consider, for example, the design of an essential facility such as a hospital in Charlotte, North Carolina, on a site with a soft soil profile. These two factors—the nature of the building’s occupancy and the type of soil it rests upon—could place the structure in an SDC (Seismic Design Category) equivalent to that for seismic zones 3 or 4, indicating high seismic risk. This, in turn, triggers a whole host of seismic-detailing requirements, as explained later in this section. Design ground-motion parameters are determined from mapped values of  $S_s$  and  $S_1$ . The mapped contours of these parameters attain high values in the vicinity of seismic sources that are judged capable of generating large earthquakes. The spectral response accelerations  $S_s$  and  $S_1$  are specified on the seismic hazard maps prepared by the United States Geological Survey (USGS). The short period is at 0.2 s and is for  $S_s$ , and at 1 s period,  $S_1$ . The maps are for 5% of critical damping for Site Class B, soft rock, commonly found in the U.S. west coast.

SDC triggers the seismic design requirements including the choice of analysis procedure, the required level of strength and detailing, and the permissible irregularities and the height of buildings. The detailing and other seismic restrictions are now dependent on the soil characteristics at the site of the structure. The SDC for the building is established based on the occupancy category of the building and the short period response acceleration,  $S_{DS}$ , and the 1 s period response,  $S_{D1}$ , at the building site.

The mapped spectral accelerations  $S_s$  and  $S_1$  for Site Class B are modified to other site conditions by using site coefficients  $F_a$  and  $F_v$ . The modified values denoted as  $S_{MS}$  and  $S_{M1}$  are the maximum considered earthquake (MCE), which has a 2% probability of occurrence in 50 years corresponding approximately to a 2500-year recurrence interval. The design response spectral accelerations  $S_{DS}$  and  $S_{D1}$  are simply the two-third values of  $S_{MS}$  and  $S_{M1}$ . The reason for the two-third reduction is as follows.

Traditionally, for seismic design, engineers on the U.S. west coast have used ground acceleration, with a 10% probability of occurrence in 50 years corresponding to a 475-year recurrence interval. In coastal California, a 2500-year earthquake is considered the largest possible earthquake and, it is the considered opinion of the engineering community that a building with proper seismic details designed for an earthquake of 475-year recurrence interval, has a margin of safety of 1.5 against collapse in an MCE event. In other parts of the United States, however, notably in the New Madrid fault area, a 2500-year earthquake may be as much as four-to-five times the 475-year earthquake. Therefore, a building designed in California for a 475-year earthquake has a good chance of not collapsing under a 2500-year earthquake, whereas its counterpart in the New Madrid area may not have this chance. To keep a uniform margin against collapse, the 2005 ASCE-7 uses a 2500-year earthquake spectral response acceleration for all the areas of the United States. To bring the design up to par with the current practice of designing with a 1.5 margin against collapse, a two-third value (the reciprocal of 1.5) of the MCE is used in the design. This is the rationale for taking the two-third values of  $S_{MS}$  and  $S_{MI}$  to arrive at the design response accelerations  $S_{DS}$  and  $S_{DI}$ .

## 5.5 AN OVERVIEW OF CHAPTER 11 OF ASCE 7-05, SEISMIC DESIGN CRITERIA

Chapter 11 of ASCE 7-05 includes introductory material required for establishing seismic design requirements for structures assigned to SDC A through E. It defines how to construct a general design response spectrum by using acceleration parameters  $S_S$  and  $S_I$ , and explains the procedures for establishing the seismic importance factor,  $I_E$ , and the SDC A through F. The limitation for siting SDC E and F buildings is given in the final sections of Chapter 11 followed by the requirements for the investigation of the building site for potential geologic and seismic hazards.

Tucked in-between the introductory material and the requirements of geotechnical investigation, are the seismic design requirements for SDC A buildings. If the building being designed is assigned to SDC A, the designer is not required to comply with the requirements of other seismic chapters.

### 5.5.1 SEISMIC GROUND-MOTION VALUES

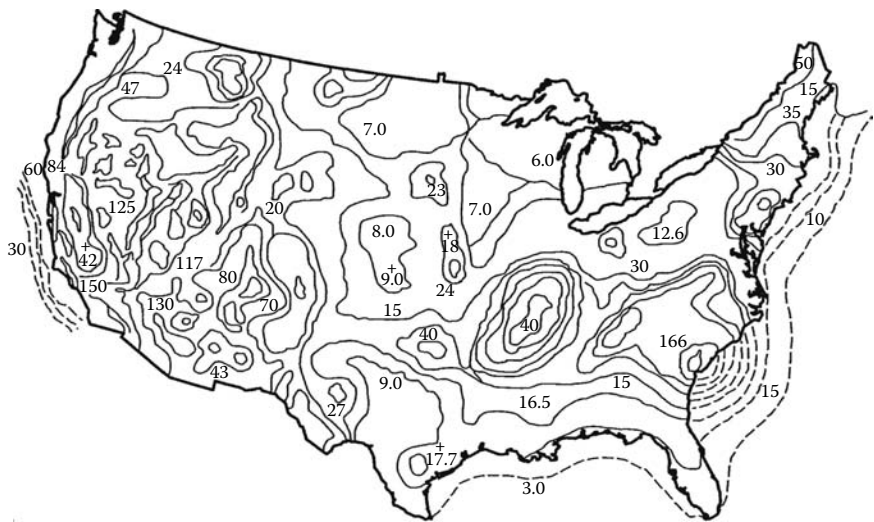
Two parameters  $S_S$  and  $S_I$  play a key role in the determination of ground motion values used in seismic design. These are derived using the maps given in the ASCE provisions or by accessing Web-based information. For many buildings designed using equivalent lateral force (ELF) procedure, the modified values of these key parameters denoted as  $S_{DS}$  and  $S_{DI}$  are directly used in seismic design. The ASCE procedure also provides for the development of a general response spectrum, which may be used in the modal analysis procedure.

The seismicity maps showing the contours of 5%-damped 0.2 and 1 s spectral acceleration values for the MCE ground motions are based on the 2002 USGS probabilistic maps. These maps incorporate improved earthquake data in terms of updated fault parameters (such as slip rates, recurrence time, and magnitude) and additional attenuation parameters, also referred to as ground motion prediction equations. The interpolated ground motion for the conterminous 48 states by latitude and longitude are calculated using a closer grid spacing in areas of known fault regions.

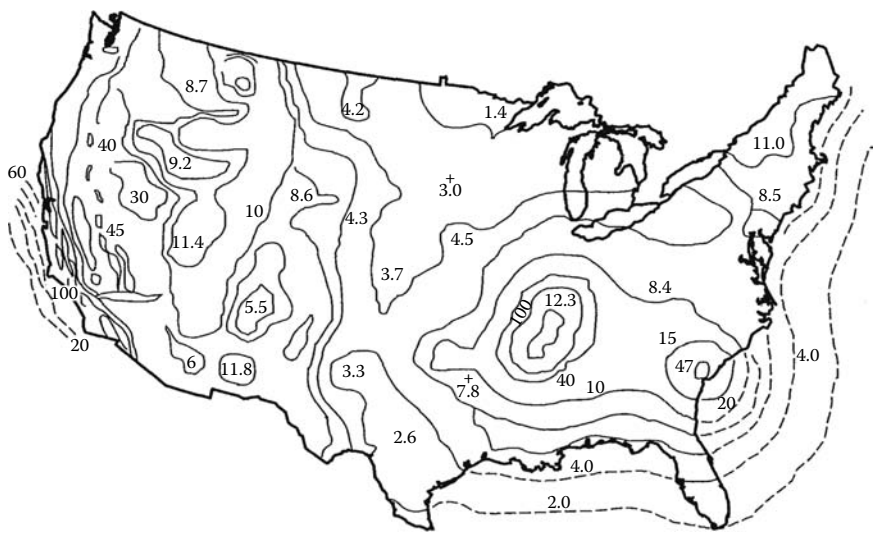
$S_S$  is the mapped value of the 5%-damped Maximum Considered Earthquake, MCE spectral response acceleration, for short-period structures founded on Class B, firm rock, sites. Note that MCE is the most severe earthquake considered in the ASCE 7-05 Standard. The short-period acceleration

has been determined at a period of 0.2 s. This is because 0.2 s is reasonably representative of the shortest effective period of buildings and structures that are designed by the ASCE provisions considering the effects of soil compliance, foundation rocking, and other factors typically neglected in structural analysis.

Similarly,  $S_1$  is the mapped value of the 5%-damped MCE spectral response acceleration at a period of 1 s on Site Class B. The spectral response acceleration at periods other than 1 s can typically be derived from the acceleration at 1 s. Consequently, these two response acceleration parameters,  $S_s$  and  $S_1$ , are sufficient to define an entire response spectrum for the period range of importance for most buildings. See Figures 5.30 and 5.31 for ground motion acceleration values  $S_s$  and  $S_1$ .



**FIGURE 5.30** MCE ground motion for the United States, 0.2s. Spectral response acceleration,  $S_s$ , as a percent of gravity, site class B with 5% critical damping.



**FIGURE 5.31** MCE ground motion for the United States, 1.0s. Spectral response acceleration,  $S_1$ , as a percent of gravity, site class B with 5% critical damping.



### 5.5.1.1 Site Coefficients $F_a$ and $F_v$

To obtain acceleration response parameters that are appropriate for sites with characteristics, other than those for  $S_B$  sites, it is necessary to modify the  $S_s$  and  $S_1$  values. This modification is preformed with the use of two coefficients,  $F_a$  and  $F_v$  (see Tables 5.4 and 5.5), which scale the  $S_s$  and  $S_1$  values determined for firm rock sites to values appropriate for other site conditions, respectively. The MCE spectral response accelerations adjusted for site class effects are designated  $S_{MS}$  and  $S_{M1}$ , respectively, for short-period and 1 s-period responses.

As stated previously, structural design is preformed for earthquake demands that are two-thirds of the maximum considered earthquake response spectra. Two additional parameters,  $S_{DS}$  and  $S_{D1}$ , are used to define the acceleration response spectrum for this design level event. These are taken, respectively, as the two-thirds of the maximum considered earthquake values,  $S_{MS}$  and  $S_{M1}$ , and completely define a design response spectrum for sites of any characteristics.

Strong-motion recordings obtained on a variety of geologic deposits during the Loma Prieta earthquake of October 17, 1989 provided an important basis for the development of the site coefficients  $F_a$  and  $F_v$ . The measured peak acceleration of about 0.08–0.1g at the rock sites was amplified 2–3 times to 0.2g or 0.3g at the soft soil sites. The response spectral accelerations at short periods

**TABLE 5.4**

**Site Coefficient,  $F_a$**

Site Class	Mapped MCE Spectral Response Acceleration Parameter at Short Period				
	$S_s'' \leq 0.25$	$S_s = 0.5$	$S_s = 0.75$	$S_s = 1.0$	$S_s \geq 1.25$
A	0.8	0.8	0.8	0.8	0.8
B	1.0	1.0	1.0	1.0	1.0
C	1.2	1.2	1.1	1.0	1.0
D	1.6	1.4	1.2	1.1	1.0
E	2.5	1.7	1.2	0.9	0.9
F	See Section 11.4.7, ASCE 7–05				

Source: ASCE 7-05, Table 11.4-1.

Note: Use straight-line interpolation for intermediate values of  $S_s$ .

**TABLE 5.5**

**Site Coefficient,  $F_v$**

Site Class	Mapped MCE Spectral Response Acceleration Parameter at 1 s Period				
	$S_1'' \leq 0.1$	$S_1 = 0.2$	$S_1 = 0.3$	$S_1 = 0.4$	$S_1 \geq 0.5$
A	0.8	0.8	0.8	0.8	0.8
B	1.0	1.0	1.0	1.0	1.0
C	1.7	1.6	1.5	1.4	1.3
D	2.4	2.0	1.8	1.6	1.5
E	3.5	3.2	2.8	2.4	2.4
F	See Section 11.4.7, ASCE 7-05				

Source: ASCE 7-05.

Note: Use straight-line interpolation for intermediate values of  $S_1$ .

(~0.2 or 0.3 s) were also amplified on average by factors of 2 or 3. At longer periods between about 0.5 and 1.5 or 2 s, the amplifications or response spectra on the soft clay site relative to rock were even greater, ranging from about 3 to 6 times.

### 5.5.1.2 Site Class

A set of six site classifications, *A* through *F*, based on the average properties of the upper 100 ft of soil profile are defined in ASCE-05 Table 20.3-1. Since, in practice, geotechnical investigations are seldom conducted to depths of 100 ft, ASCE-7 allows the geotechnical engineers to determine site class based on site-specific data and professional judgment.

The site class should reflect the soil conditions that will affect the ground motion input to the structure or a significant portion of the structure. For structures receiving substantial ground motion input from shallow soils (e.g., structures with shallow spread footings, laterally flexible piles, or structures with basements where it is judged that substantial ground-motion input to the structure may come through the side walls), it is reasonable to classify the site on the basis of the top 100 ft (30 m) of soils below the ground surface. Conversely, for structures with basements supported on firm soils or rock below soft soils, it is reasonable to classify the site on the basis of the soil or rock below the mat, if it can be justified that the soils contribute very little to the response of the structure.

Buildings on sloping bedrock sites and/or having highly variable soil deposits across the building area require careful study since the input motion may vary across the building (e.g., if a portion of the building is on rock and the rest is over weak soils). Site-specific studies including 2D or 3D modeling may be appropriate in such cases to evaluate the subsurface conditions, and site and superstructure response. Other conditions that may warrant site-specific evaluation include the presence of low shear wave velocity soils below a depth of 100 ft (30 m), location of the site near the edge of a filled-in basin, or other subsurface or topographic conditions with strong 2D and 3D site response-effects.

### 5.5.1.3 Design Response Spectrum

Where a site-specific ground motion response spectrum is not used, the design response spectrum curve is developed as shown in Figure 5.32, and as follows.

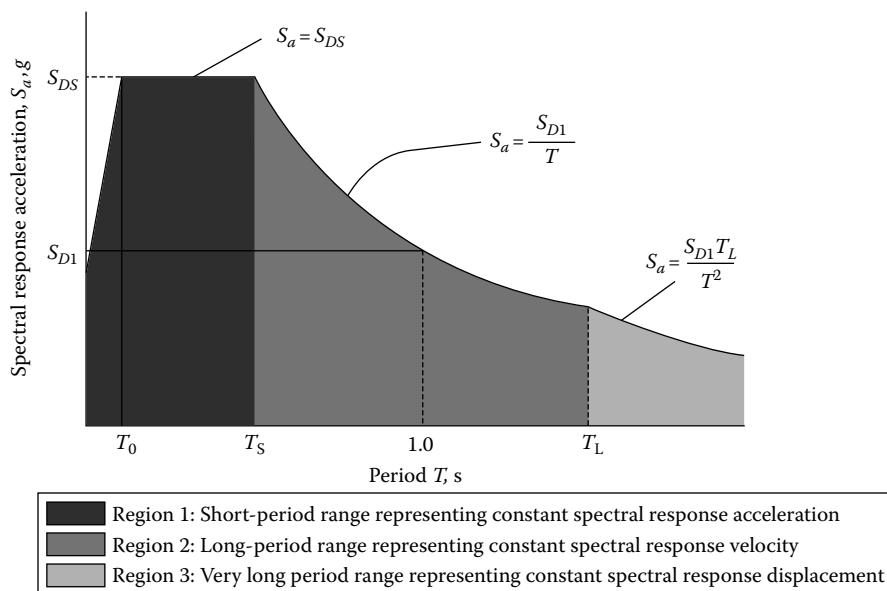


FIGURE 5.32 Design response spectrum.

1. For periods less than  $T_0$ , the design spectral response acceleration,  $S_a$ , shall be taken as

$$S_a = S_{DS} \left( 0.4 + 0.6 \frac{T}{T_0} \right)$$

2. For periods greater than or equal to  $T_0$  and less than or equal to  $T_s$ , the design spectral response acceleration,  $S_a$ , shall be taken equal to  $S_{DS}$ .
3. For periods greater than  $T_s$ , and less than or equal to  $T_L$ , the design spectral response acceleration,  $S_a$ , shall be taken as

$$S_a = \frac{S_{D1}}{T}$$

4. For periods greater than  $T_L$ ,  $S_a$  shall be taken as

$$S_a = \frac{S_{D1} T_L}{T^2}$$

where

$S_{DS}$  is the design spectral response acceleration parameter at short periods

$S_{D1}$  is the design spectral response acceleration parameter at 1 s period

$T$  is the fundamental period of the structure, s

$$T_0 = 0.2(S_{D1}/S_{DS})$$

$$T_s = S_{D1}/S_{DS}$$

$T_L$  is the long-period transition period

To assist engineers in preliminary designs, response spectrum curves for site class C and D, for selected cities in the United States are given in Section 5.5.8. The response curves are for site class C and D.

### 5.5.2 EQUIVALENT LATERAL FORCE PROCEDURE

Design base shear is the total lateral force or shear at the base of the building also equal to the sum of the seismic design forces at each level of a building. The symbol  $V$  is used to represent the base shear. For the purpose of calculating the base shear, the base of the building is the level at which the earthquake forces are considered to be imparted to the structure or the level at which the structure, as a dynamic vibrator, is supported.

The formula for determining the base shear,  $V = C_s W$ , is given as a percentage of the weight,  $W$ , of the building. It is given in the same form as the well-known, classic dynamic equilibrium formula,  $F = ma$ , with an upper and lower bound limits.

The seismic base shear,  $V$ , in a given direction shall be determined in accordance with the following equation:

$$V = C_s W$$

where

$C_s$  is the seismic response coefficient

$W$  is the effective seismic weight

The seismic response coefficient,  $C_s$ , shall be determined in accordance with

$$C_s = \frac{S_{DS}}{\left(\frac{R}{I}\right)}$$

where

$S_{DS}$  is the design spectral response acceleration parameter in the short period range

$R$  is the response modification factor

$I$  is the occupancy importance factor

The value of  $C_s$  computed need not exceed the following:

$$C_s = \frac{S_{D1}}{T\left(\frac{R}{I}\right)} \quad \text{for } T \leq T_L$$

$$C_s = \frac{S_{D1}T_L}{T^2\left(\frac{R}{I}\right)} \quad \text{for } T > T_L$$

$C_s = 0.044 S_{DS}I$  (2006 IBC Supplement 2, and 2009 IBC)

$C_s$  shall not be less than

$$C_s = 0.01$$

In addition, for structures located where  $S_1$  is equal to or greater than 0.6g,  $C_s$  shall not be less than

$$C_s = \frac{0.5S_1}{\left(\frac{R}{I}\right)}$$

where  $I$  and  $R$  are as defined earlier

$S_{D1}$  is the design spectral response acceleration parameter at a period of 1.0 s,

$T$  is the fundamental period of the structure

$T_L$  is long-period transition period

$S_1$  is the mapped maximum considered earthquake spectral response acceleration parameter

Step by step for procedure for determination of base shear,  $V$  follows

### Step 1: Determine $S_s$ and $S_1$

The parameters  $S_s$  and  $S_1$  represent the MCE, 5%-damped, spectral acceleration parameters at short periods (0.2s) and 1 s period. Use the ASCE 7-05 mapped values or obtain the values for  $S_s$  and  $S_1$  directly through Web-based information.  $S_s$  and  $S_1$  represent the maximum ground-motion acceleration values on rock, associated with an earthquake that is expected to occur once in every 2475 years, usually rounded to 2500 years.

**TABLE 5.6**  
**Importance Factors**

Occupancy Category	$I$
I or II	1.0
III	1.25
IV	1.5

Source: ASCE 7-05, Table 11.5.1.

### Step 2: Determine the importance factor, $I$

The importance factor reflects the relative importance assigned to a building based on its occupancy category. In a conceptual sense, it indicates the performance expected of the building during and after an earthquake. In an attempt to achieve the desired performance, the design base shear is increased 25% for those in Occupancy Category III, and 50% for those in Occupancy Category IV (see Table 5.6).

**Step 3:** Determine site class

The site is assigned a Site Class  $S_A$ ,  $S_B$ ,  $S_C$ ,  $S_D$ ,  $S_E$ , or  $S_F$  based on soil properties for the top 100 ft of soil profile. Generic description of soil profiles are as follows:

$S_A$  is the hard rock (found east of Rocky Mountains).

$S_B$  is the soft rock (found west of Rocky Mountains, note this is also the basis for  $S_S$  and  $S_1$  maps).

$S_C$  is the very dense soil, soft rock.

$S_D$  is the stiff soil (also default classification).

$S_E$  is the soft soil profile.

$S_F$  is the poor soil.

In North American practice, typically structural engineers do not participate in deciding the site class: it is the project geotechnical engineer who determines the site class. If not classified, then ASCE 7-05 permits the use of Site Class  $S_D$  in seismic calculations.

**Step 4:** Adjustment of MCE spectral response acceleration parameters

$S_S$  and  $S_1$  are modified to account for site class effects by using short-period site coefficient,  $F_a$ , and 1 s period coefficient,  $F_v$ , respectively. The modified values are denoted as  $S_{MS}$  and  $S_{M1}$ . The subscript M stands for “modified values.” Thus

$$S_{MS} = F_a S_S$$

$$S_{M1} = F_v S_1$$

Use Tables 5.4 and 5.5 for determining the values of  $F_a$  and  $F_v$ , respectively.

**Step 5:** Determine design spectral acceleration parameters,  $S_{DS}$  and  $S_{D1}$ 

As explained previously, the design earthquake forces are determined the MCE spectral acceleration parameters,  $S_{MS}$  and  $S_{M1}$  as two-thirds of. The purpose is to scale down ground motion values to a 10% probability of being exceeded in 50 years. These represent ground motion values expected to occur once every 475 years, generally rounded to 500 years. The subscript D in  $S_{DS}$  and  $S_{D1}$  stands for “design values.” Thus

$$S_{DS} = 2/3 S_{MS}$$

$$S_{D1} = 2/3 S_{M1}$$

**Step 6:** Determine the building period  $T_a$ 

$T_a$  represents the fundamental period of vibration of the building calculated by using approximate formulas. The subscript  $a$  distinguishes the approximate value from that calculated by using more exact methods such as dynamic analysis procedures. The latter is typically denoted as  $T_b$ .

The appropriate period formulas are

1.  $T_a = C_t(h_n)^x = 0.016(h_n)^{0.9}$  (moment-resisting concrete frame building)
2.  $T_a = 0.02(h_n)^{0.75}$  (concrete shear wall building)

See Table 5.7 for values of  $C_t$  and  $x$ .

Alternately, for shear wall buildings, the more complicated formula 12.8.10 of ASCE 7-05 may be used. The well-known formula  $T_a = 0.1N$ , where  $N$  is the number of stories, is also permitted. However, for buildings such as apartments and hotels with story heights less than 10 ft, the formula  $T_a = 0.1N$  is not permitted.

$T_b$ , the fundamental period of vibration determined from a dynamic analysis, is generally larger than  $T_a$ . To prevent the misuse of  $T_b$ , resulting from using a too sharp pencil, Table 5.8 (ASCE 7-05, Table 12.8.1) stipulates the following upper limits for  $T_b$ :

$$T_b \leq C_u T_a$$

The values of the coefficient  $C_u$  that is a function of  $S_{D1}$  are as follows:

$$S_{D1} \geq 0.4, \quad C_u = 1.4$$

$$S_{D1} \geq 0.3, \quad C_u = 1.4$$

$$S_{D1} \geq 0.2, \quad C_u = 1.5$$

$$S_{D1} \geq 0.15, \quad C_u = 1.6$$

$$S_{D1} \geq 0.1, \quad C_u = 1.7$$

It should be noted, however, that there is no upper limit on  $T_b$  for calculating story-drift limitations. Also we are permitted to use the redundancy factor  $\rho = 1$  for the determination of building drift.

**Step 7:** Determine the response modification coefficient,  $R$

The  $R$  value shown in Table 5.9, is a rating of the ability of the structural system to resist earthquake ground motion without collapse. It encompasses, among other things, the detailing employed to

**TABLE 5.7**  
**Values of Approximate Period Parameters  $C_t$  and  $\alpha$**

Structure Type	$C_t$	$\alpha$
Moment-resisting frame systems in which the frames resist 100% of the required seismic force and are not enclosed or adjoined by components that are more rigid and will prevent the frames from deflecting where subjected to seismic forces		
Concrete moment-resisting frames	0.016 (0.0466) <sup>a</sup>	0.9
		0.5
All other structural systems	0.02	0.75

Source: Adapted from ASCE 7-05, Table 12.8.2.

**TABLE 5.8**  
**Coefficient for Upper Limit on Calculated Period**

Design Spectral Response Acceleration Parameter at 1 s, $S_{D1}$	Coefficient $C_u$
$\geq 0.4$	1.4
0.3	1.4
0.2	1.5
0.15	1.6
$\leq 0.1$	1.7

Source: ASCE 7-05, Table 12.8.1

**TABLE 5.9**  
**Design Coefficients and Factors for Seismic Force–Resisting Systems: ASCE 7-05**

	Response Modification Coefficient	System over Strength Factor	Deflection Amplification Factor	Structural System Limitations and Building Height (ft) Limit				
				SDC				
Seismic Force–Resisting System	$R$	$\Omega_o$	$C_d$	B	C	D	E	F
<b>A. Bearing wall systems</b>								
Special reinforced concrete shear walls	5	$2^{1/2}$	5	NL	NL	160	160	100
Ordinary reinforced concrete shear walls	4	$2^{1/2}$	4	NL	NL	NP	NP	NP
<b>B. Building frame systems</b>								
Special reinforced concrete shear walls	6	$2^{1/2}$	5	NL	NL	160	160	100
Ordinary reinforced concrete shear walls	5	$2^{1/2}$	$4^{1/2}$	NL	NL	NP	NP	NP
<b>C. Moment-resisting frame systems</b>								
Special reinforced concrete moment frames	8	3	$5^{1/2}$	NL	NL	NL	NL	NL
Intermediate reinforced concrete moment frames	5	3	$4^{1/2}$	NL	NL	NP	NP	NP
Ordinary reinforced concrete moment frames	3	3	$2^{1/2}$	NL	NP	NP	NP	NP
<b>D. Dual systems with special moment frames capable of resisting at least 25% of prescribed seismic forces</b>								
Special reinforced concrete shear walls	7	$2^{1/2}$	$5^{1/2}$	NL	NL	NL	NL	NL
Ordinary reinforced concrete shear walls	6	$2^{1/2}$	5	NL	NL	NP	NP	NP
<b>E. Dual systems with intermediate moment frames capable of resisting at least 25% of prescribed seismic forces</b>								
Special reinforced concrete shear walls	$6^{1/2}$	$2^{1/2}$	5	NL	NL	160	100	100
Ordinary reinforced concrete shear walls	$5^{1/2}$	$2^{1/2}$	$4^{1/2}$	NL	NL	NP	NP	NP
<b>F. Shear wall–frame interactive system</b>								
With ordinary reinforced moment frames and ordinary reinforced concrete shear walls	$4^{1/2}$	$2^{1/2}$	4	NL	NL	NP	NP	NP
<b>G. Cantilevered column systems</b>								
Special reinforced concrete moment frames	$2^{1/2}$	$1^{1/4}$	$2^{1/2}$	35	35	35	35	35
Intermediate reinforced concrete moment frames	$1^{1/2}$	$1^{1/4}$	$1^{1/2}$	35	35	NP	NP	NP
Ordinary reinforced concrete moment frames	1	$1^{1/4}$	1	35	NP	NP	NP	NP

Source: Adapted from ASCE 7-05, Table 12.2-1.

Note: NL, no height limit; NP, not permitted. For buildings with flexible diaphragms,  $\Omega_o = (\Omega_o - 0.5)$ . Heights are measured from the level at which the horizontal ground motions are considered to be imparted to the structure.

enhance the ductility of connections. The values of  $R$  along with other seismic coefficients and factor are given again in Tables 5.10 through 5.15 in a more compact format.

**Step 8:** Calculate the base shear,  $V$

Now that all of the coefficients for  $C_s$  are determined, we calculate the base shear,  $V$  by the relation  $V = C_s W$ . see Section 5.6.7 for calculation of seismic weight  $W$ .

**TABLE 5.10**  
**Ordinary Reinforced Concrete Moment Frames: Seismic Factors**

System	Height Limit
1. Stand-alone system: $R = 3$ , $\Omega_o = 3$ , and $C_d = 2.5$	NL for SDC A or B NP for SDC C and above
2. Interactive with ordinary reinforced concrete shear walls: $R = 4.5$ , $\Omega_o = 2.5$ , and $C_d = 4$	NL for SDC A and B NP for SDC C and above
3. Cantilevered column system: $R = 1$ , $\Omega_o = 1.25$ , and $C_d = 1$	NL for SDC A 35 ft for SDC B NP for SDC C and above

**TABLE 5.11**  
**Intermediate Reinforced Concrete Moment Frames: Seismic Factors**

System	Height Limit
1. Stand-alone system: $R = 5$ , $\Omega_o = 3$ , and $C_d = 2.5$	NL for SDC A, B, or C NP for SDC D, E, or F
2. Dual system with special reinforced concrete shear walls: $R = 6$ , $\Omega_o = 2.5$ , and $C_d = 5$	NL for SDC A, B, or C 160 ft for SDC D 100 ft for SDC E or F
3. Dual system with ordinary reinforced concrete shear walls: $R = 5.5$ , $\Omega_o = 2.5$ , and $C_d = 4.5$	NL for SDC A, B, or C NP for SDC D, E, or F
4. Cantilevered column system: $R = 1.5$ , $\Omega_o = 1.25$ , and $C_d = 1.5$	NL for SDC A 35 ft for SDC B or C NP for SDC D, E, or F

**TABLE 5.12**  
**Special Reinforced Concrete Moment Frames: Seismic Factors**

System	Height Limit
1. Stand-alone system: $R = 8$ , $\Omega_o = 3$ , and $C_d = 5.5$	NL for SDC A, B, C, D, E, or F
2. Dual system with special reinforced concrete shear walls: $R = 8$ , $\Omega_o = 2.5$ , and $C_d = 6$	NL for SDC A, B, C, D, E, or F
3. Dual system with ordinary reinforced concrete shear walls: $R = 7$ , $\Omega_o = 2.5$ , and $C_d = 6$	NL for SDC A, B, or C NP for SDC D, E, or F
4. Cantilevered column system: $R = 2.5$ , $\Omega_o = 1.1/4$ , and $C_d = 2.5$	NL for SDC A 35 ft for SDC B and above



**TABLE 5.13**  
**Ordinary Reinforced Concrete Shear Walls: Seismic Factors**

System	Height Limit
1. Bearing wall: $R = 4$ , $\Omega_o = 2.5$ , and $C_d = 4$	NL for SDC A, B, or C NP for SDC D, E, or F
2. Building frame: $R = 4$ , $\Omega_o = 2.5$ , and $C_d = 4.5$	NL for SDC A or B NP for SDC C and above
3. Dual system with special moment frame: $R = 7$ , $\Omega_o = 2.5$ , and $C_d = 6$	NL for SDC A or B NP for SDC C and above
4. Dual system with intermediate moment frame: $R = 5.5$ , $\Omega_o = 2.5$ , and $C_d = 4.5$	NL for SDC A or B NP for SDC C and above
5. Interactive system with ordinary moment frame: $R = 4.5$ , $\Omega_o = 2.5$ , and $C_d = 4$	NL for SDC A or B NP for SDC C and above

**Table 5.14**  
**Special Reinforced Concrete Shear Walls: Seismic Factors**

System	Height Limit
1. Bearing wall: $R = 5$ , $\Omega_o = 2.5$ , and $C_d = 5$	NL for SDC A, B, or C 160 ft for SDC D, E, or F
2. Building frame: $R = 6$ , $\Omega_o = 2.5$ , and $C_d = 5$	NL for SDC A, B, or C 160 ft for SDC D or E 100 ft for SDC F
3. Dual system with special moment frame capable of resisting at least 25% of prescribed seismic forces: $R = 7$ , $\Omega_o = 2.5$ , and $C_d = 5.5$	NL for SDC A and above
4. Dual system with intermediate moment frame capable of resisting at least 25% of prescribed seismic forces: $R = 6.5$ , $\Omega_o = 2.5$ , and $C_d = 5$	NL for SDC A, B, or C 160 ft for SDC D 100 ft for SDC E or F

### 5.5.2.1 Parameters $S_S$ and $S_1$

The first step is to determine the two parameters  $S_S$  and  $S_1$ . Precise values of the two parameters are difficult to determine in congested areas of the maps given in ASCE 7-05. To obviate this problem, a software program that calculates the special parameters from the latitude and longitude of a specific location is available on the USGS Web site at <http://earthquake.usgs.gov/research/hazmaps>.

The latitude and longitude for a specific location may be found from Web sites such as


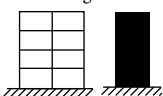
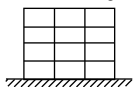
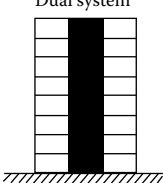
<http://www.terraser.com>  
<http://stevemorse.org/jcal/latlon.php>  
<http://www.batchgeocode.com/lookup/>  
<http://geocoder.us>  
<http://www.infosports.com/m/map.htm>

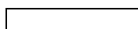
As an example, a site on “Las Vegas Boulevard and Harmon Avenue” in Las Vegas, Nevada, with a latitude of  $36^\circ$  and a longitude of  $115^\circ$ , has Web-based values for  $S_a$  and  $S_1$  are as follows:

$$S_S = 0.5534g$$

$$S_1 = 0.1713g$$

**TABLE 5.15**  
**Permitted Building Systems for Different SDC**

Basic seismic force resisting system			SDC						Seismic parameters	
			A	B	C	D	E	F	R	C <sub>d</sub>
Bearing wall 	Ordinary reinforced concrete shearwall								4	4
	Special reinforced concrete shearwall					160	160	100	5	5
Building frame 	Ordinary reinforced concrete shearwall								5	4.5
	Special reinforced concrete shearwall					160	160	100	6	5
Moment-resisting frame 	Ordinary frame								3	2.5
	Moment-resisting frame								5	4.5
	Special frame								8	5.5
Dual system 	With intermediate moment frame	Ordinary shearwall							5.5	4.5
		Special shearwall				160	100	100	6	5
	With special moment frame	Ordinary shearwall							6.5	5
		Special shearwall							7	5.5

 Permitted with the indicated height limit (if any)

 Not permitted

### 5.5.2.2 Site-Specific Ground Motion Analysis

The site-specific design response spectrum is estimated using a probabilistic seismic hazard analysis (PSHA) together with a site response analysis, if necessary, for the site profile. The site-specific response spectra for design should not be less than 80% of the general response spectra of ASCE 7-05 for the site.

The objective in conducting a site-specific ground motion analysis is to develop ground motions that are determined with higher confidence for the local seismic and site conditions than can be determined from national ground motion maps and the general procedure. Accordingly, such studies must be comprehensive and incorporate current scientific interpretations. Because there is typically more than one scientifically credible alternative for models and parameter values used to characterize seismic sources and ground motions, it is important to formally incorporate these uncertainties in a site-specific probabilistic analysis. For example, uncertainties may exist in seismic source location, extent and geometry; maximum earthquake recurrence rate; choices for ground motion attenuation relationships; and local site conditions including soil layering and dynamic soil properties as well as possible 2D or 3D wave propagation effects. The use of peer review for a site-specific ground motion analysis is encouraged.

Near-fault effects on horizontal response spectra include (1) directivity effects that increase ground motions for periods of vibration greater than  $\sim 0.5$  s for fault rupture propagating toward the site and (2) directionality effects that increase ground motions for periods greater than  $\sim 0.5$  s in the direction normal (perpendicular) to the strike of the fault.

ASCE 7-05 requires that site-specific geotechnical investigations and dynamic site response analysis be preformed for sites having Site Class F soils. For purposes of obtaining data to conduct a site response analysis, site-specific geotechnical investigations should include borings with sampling, standard penetration tests for sandy soils, cone penetrometer tests, and/or other subsurface investigative techniques and laboratory soil testing to establish the soil types, properties, and layering and the depth to rock or rock-like material. For very deep soil sites, the depth of investigation need not necessarily extend to bedrock but to a depth that may serve as the location of input motion for a dynamic site response analysis. It is desirable to measure shear wave velocities in all soil layers. Alternatively, shear wave velocities may be estimated based on shear wave velocity data available for similar soils in the local area or through correlations with soil types and properties.

Development of a site-specific design response spectrum requires reviewing seismological and geological data and performing engineering analyses. ASCE 7-05 allows the development of a site-specific design spectrum using PSHA and site response analysis. However, as noted above, the design spectrum for structural analysis may not be less than 80% of the general response spectrum developed using Section 11.4 of ASCE 7.05.

The development of the site-specific spectra typically involve the following steps:

1. Select previously recorded time histories of acceleration and scale the records to match the estimate bedrock motions.
2. Perform site response analyses to estimate the response of the site soils to the bedrock motions.

A PSHA considers all potential earthquake sources that may contribute to strong ground shaking at a specific site. Magnitude, distance, and the probability of occurrence are all factored into the computation. Typically, PSHA data generated by the USGS is used for the purpose. Next, rock outcrop motions (i.e., spectral ordinates) are selected for a probability of exceedance of 2% in 50 years and multiplied the values by two-thirds as per the ASCE 7-05.

### 5.5.3 IMPORTANCE FACTOR AND OCCUPANCY CATEGORY

#### 5.5.3.1 Importance Factor, $I_E$

The purpose of this factor,  $I_E$  (referred to as  $I$  without the subscript E in ASCE 7-05), is to specifically improve the capability of certain types of buildings such as essential facilities and structures containing substantial quantities of hazardous materials, to function during and after design earthquakes. This is achieved by introducing an importance factor of 1.25 for Occupancy Category III structures and 1.5 for Occupancy Category IV structures. This factor is intended to reduce the ductility demands and result in less damage. When combined with the more stringent drift limits, the result is the improved performance of such facilities (see Table 5.3 for importance factors).

Although a value of  $I$  greater than unity has the effect of reducing the ductility expected of a structure, however, added strength due to higher design forces by itself is not sufficient to ensure superior seismic performance. Connection details that assure ductility, quality assurance procedures, and limitations on building deformation are also important to improve the functionality and safety in critical facilities and those with high-density occupancy. Consequently, the reduction in the damage potential of critical facilities is also addressed by using more conservative drift controls and by providing special design and by detailing requirements and material limitations. The assignment of

the importance factor,  $I_E$ , is not the sole responsibility of the structural engineer. It is a decision to be made concurrently with the building owners, architects, and building officials.

### 5.5.3.2 Occupancy Categories

The expected performance of structures is controlled by the assignment of each structure to one to four occupancy categories (see Tables 5.16 and 5.17). The ASCE provisions specify progressively more conservative strength, drift control, system selection, and detailing requirements for structures contained in four groups, in order to attain minimum levels of earthquake performance suitable to the individual occupancies.

In terms of post-earthquake recovery and redevelopment, certain types of occupancies are vital to public needs. These special occupancies are identified and given specific recognition. In terms of disaster preparedness, regional communication centers identified as critical emergency services should be in a higher classification than retail stores, office buildings, and factories.

Specific consideration is given to essential facilities required for post-earthquake recovery. Also included are structures that contain substances deemed to be hazardous to the public. It is at the discretion of the authority having jurisdiction that structures are required for post-earthquake response and recovery.

Although the AISC provisions explicitly require design for only a single level of ground motion, it is expected that structures designed and constructed in accordance with these requirements will generally be able to meet a number of performance criteria, when subjected to earthquake ground motions of differing severity. Occupancy Category I, II, or III structure located where the mapped

**TABLE 5.16**  
**SDC Based on Short-Period Response**  
**Acceleration Parameter**

Value of $S_{DS}$	Occupancy Category		
	I or II	III	IV
$S_{DS} < 0.167$	A	A	A
$0.167 \leq S_{DS} < 0.33$	B	B	C
$0.33 \leq S_{DS} < 0.50$	C	C	D
$0.50 \leq S_{DS}$	D	D	D

Source: ASCE 7-05, Table 11.6.1.

**TABLE 5.17**  
**SDC Based on 1 s-Period Response**  
**Acceleration Parameter**

Value of $S_{D1}$	Occupancy Category		
	I or II	III	IV
$S_{D1} < 0.067$	A	A	A
$0.067 \leq S_{D1} < 0.133$	B	B	C
$0.133 \leq S_{D1} < 0.20$	C	C	D
$0.20 \leq S_{D1}$	D	D	D

Source: ASCE 7-05, Table 11.6.2.

spectral response acceleration parameter at 1 s period,  $S_1$ , is greater than or equal to 0.75 shall be assigned to SDC E. Occupancy Category IV structure located where the mapped spectral response acceleration parameter at 1 s period,  $S_1$ , is greater than or equal to 0.75 shall be assigned to SDC F. All other structures shall be assigned to a SDC based on their occupancy category and the design spectral response acceleration parameters,  $S_{DS}$  and  $S_{D1}$ . Each building and structure shall be assigned to the more adverse SDC, irrespective of the fundamental period of vibration of the structure,  $T$ .

**Protected access for Occupancy Category IV:** Where operational access to an Occupancy Category IV structure is required through an adjacent structure, the adjacent structure shall conform to the requirements for Occupancy Category IV structure. Where operational access is less than 10ft from an interior lot line or another structure on the same lot, protection from potential falling debris from adjacent structures shall be provided by the owner of the Occupancy Category IV structure.

The value for Occupancy Category III building, which includes buildings that with an occupancy greater than 5000 and college buildings with a capacity greater than 500 students, is now 1.25, while in previous codes it has been 1.0. There is a new emphasis in attempting to control the amount of ductility demand for these occupancies.

#### 5.5.4 SEISMIC DESIGN CATEGORY

The earthquake limit state is based upon system performance, not member performance, and considerable energy dissipation through repeated cycles of inelastic straining is assumed. The reason is the large demand exerted by the earthquake and the associated cost of providing enough strength to maintain linear elastic response in ordinary buildings.

However, structures that include facilities with critical post-earthquake operations—such as hospitals, fire stations, and communication centers—must not only survive without collapse, but must also remain operational after an earthquake. Therefore, in addition to life safety, damage control is also a design consideration for structures deemed vital to post-earthquake function. The current requirements of achieving this goal are to increase the magnitude of design forces by a factor of 1.25 or 1.5 depending upon the nature of occupancy. For certain structures such as nuclear facilities, yielding cannot be tolerated and as such, the design needs to be based on forces determined by elastic analysis.

ASCE-7 establishes five SDCs that are the keys for establishing design requirements for any building or structure. The SDC A, B, C, D, E, or F is established, using the short-period and 1 s period response parameters,  $S_{DS}$  and  $S_{D1}$ , and the occupancy category.

SDC A represents structures in regions where anticipated ground motions are minor, even for very long return periods. For such structures, ASCE-7 requires only that a complete lateral force-resisting system be provided and that all elements of the structure be tied together. A nominal design base shear equal to 1% of the weight of the structure is used to proportion the lateral system.

SDC B includes structures in regions of seismicity where only moderately destructive ground shaking is anticipated. In addition to the requirements for SDC A, structures in SDC B must be designed for forces determined using ASCE 7-05 seismic maps.

SDC C includes buildings in regions where moderately destructive ground shaking may occur. The use of some structural systems is limited and some nonstructural components must be specifically designed for seismic resistance.

SDC D includes structures located in regions expected to experience destructive ground shaking, but not located very near major active faults. In SDC D, severe limits are placed on the use of some structural systems and irregular structures must be subjected to dynamic analysis techniques as part of the design process.

**TABLE 5.18**  
**SDC Based on  $S_{D1}$  and  $S_1$**

Nature of Occupancy (Typical Examples)	Occupancy Category	Importance Factors	$S_{D1}$				$S_1$ $S_1 \geq 0.75$
			$S_{D1} < 0.067$	$0.067 \leq S_{D1} < 0.133$	$0.133 \leq S_{D1} < 0.20$	$0.20 \leq S_{D1}$	
Agricultural, temporary facilities and minor storage facilities	I	$I_W = 0.83$ or $0.77$ $I_E = 1.0$	A	B	C	D	E
Typical residential and office buildings	II	$I_W = 1.0$ $I_E = 1.0$	A	B	C	D	E
Schools, colleges, fire and police stations, detention facilities, and buildings containing toxic substance	III	$I_W = 1.15$ $I_E = 1.25$	A	B	C	D	E
Hospitals, health care facilities, and designated emergency shelters	IV	$I_W = 1.15$ $I_E = 1.50$	A	C	D	D	F

SDC E includes structures in regions located very close to major active faults and SDC F includes Occupancy Category IV structures in these locations. Very severe limitations on systems, irregularities, and design methods are specified for SDC E and F. For the purpose of determining if a structure is located in a region that is very close to a major active fault, ASCE-7 uses a trigger of mapped MCE spectral response acceleration at 1 s periods,  $S_1$  of 0.75g or more regardless of the structure's fundamental period. The mapped short-period acceleration,  $S_S$ , is not used for this purpose because short-period response accelerations do not tend to be affected by near-source conditions as strongly as do response accelerations at longer periods.

See Tables 5.16 and 5.17 for SDCs. The same information is given in Tables 5.18 and 5.19 in a different format.

### 5.5.5 DESIGN REQUIREMENTS FOR SDC A BUILDINGS

SDC A represents structures in regions where anticipated ground motions are minor, even for very long return periods. For such structures, the ASCE provisions require only that a complete seismic force-resisting system be provided and that all elements of the structure be tied together. A nominal design force equal to 1% of the weight of the structure is used to proportion the lateral system.

It is not considered necessary to specify seismic-resistant design on the basis of an MCE ground motion for SDC A structures because the ground motion computed for the areas where these

**TABLE 5.19**  
**SDC Based on  $S_{Ds}$  and  $S_1$**

Nature of Occupancy (Typical Examples)	Occupancy Category	Importance Factors	$S_{Ds}$				$S_1$ $S_1 \geq 0.75$
			$S_{Ds} < 0.167$	$0.167 \leq S_{Ds} < 0.33$	$0.33 \leq S_{Ds} < 0.5$	$0.5 \leq S_{Ds}$	
Agricultural, temporary facilities and minor storage facilities	I	$I_W = 0.87$ or $0.77$ $I_E = 1.00$	A	B	C	D	E
Typical residential and office buildings	II	$I_W = 1.00$ $I_E = 1.00$	A	B	C	D	E
Schools, colleges, fire and police stations, detention facilities, and buildings containing toxic substances	III	$I_W = 1.15$ $I_E = 1.25$	A	B	C	D	E
Hospitals, health care facilities, and designated emergency shelters	IV	$I_W = 1.15$ $I_E = 1.50$	A	C	D	D	F

structures are located is determined more by the rarity of the event with respect to the chosen level of probability than by the level of motion that would occur if a small but close earthquake actually did occur. However, it is desirable to provide some protection against earthquakes and many other types of unanticipated loadings. Thus, the requirements for SDC A provide a nominal amount of structural integrity that will improve the performance of buildings in the event of a possible but rare earthquake even though it is possible that the ground motions could be large enough to cause serious damage or even collapse.

The integrity is provided by a combination of requirements. First, a complete load path for lateral forces must be designed for a lateral force based on a 1% acceleration of the mass. The minimum connection forces specified for SDC A must also be satisfied.

The 1% value has been used in other countries as a minimum value for structural integrity. For many structures, design for the wind loadings specified in the local building codes normally will control the lateral force design when compared to the minimum integrity force on the structure. However, many low-rise, heavy structures or structures with significant dead loads resulting from heavy equipment may be controlled by the 1% acceleration. Also, minimum connection forces may exceed structural forces due to wind in some structures.

The minimum lateral force for SDC A structures is a structural integrity issue related to the load path. It is intended to specify design forces in excess of wind loads in heavy low-rise construction.

The design calculation is simple and easily done to ascertain if it governs or the wind load governs. The ASCE 7-05 provision requires a nominal lateral force,  $F_X$ , equal to 1% of the gravity load assigned to a story to assure general structural integrity.

The complete list of seismic design requirements are as follows:

- Analyze the structure for the effect of static lateral forces,  $F_X$ , applied independently in each of the two orthogonal directions.
- Apply the static forces,  $F_X$ , at all levels simultaneously.
- Determine the force,  $F_X$ , at each level by using the following equation:

$$F_X = 0.01W_X$$

where

$F_X$  is the design lateral force applied at level  $X$

$W_X$  is the portion of the dead load,  $D$ , located or assigned to level  $X$

- Connect all parts of the structure to form a continuous load path to the lateral force-resisting system.
- Tie any smaller portion of the structure to the remainder of the structure with connections capable of transmitting at least 5% of the portion's weight.
- Provide a positive connection for resisting a horizontal force acting parallel to each horizontal member such as slab, beam, girder, or truss. The connection shall be adequate to transfer a minimum horizontal force equal to 5% of the dead plus live load vertical reaction.
- Anchor concrete walls at the roof and all floors. Design the anchors for a horizontal force equal to 5% of the wall weight, but no less than 280 lb per linear foot.

Because of the very low seismicity associated with sites with  $S_{DS} < 0.25$  and  $S_{D1} < 0.10$ , it is considered appropriate for SDC A buildings to require only a complete seismic force-resisting system, a good quality of construction materials, and adequate ties and anchorage as specified in this section. SDC A buildings will be constructed in a large portion of the United States that is generally subject to strong winds but low earthquake risk. Those promulgating construction regulations for these areas may wish to consider many of the low-level seismic requirements as being suitable to reduce the windstorm risk. Since the seismic provisions consider only earthquakes, no other requirements are prescribed for SDC A buildings. Only a complete seismic force-resisting system ties, and wall anchorage are required.

Construction qualifying under SDC A may be built with no special detailing requirements for earthquake resistance. Special details for ductility and toughness are not required in SDC A.

**Lateral forces:** SDC A buildings are not designed for resistance to any specific level of earthquake ground shaking as the probability that they would ever experience shaking of sufficient intensity to cause life threatening damage is very low so long as the structures are designed with basic levels of structural integrity. Minimum levels of structural integrity are achieved in a structure by assuring that all elements in the structure are tied together so that the structure can respond to shaking demands in an integral manner and also by providing the structure with a complete seismic force-resisting system. It is believed that structures having this level of integrity would be able to resist, without collapse, the very infrequent earthquake ground shaking that could affect them. In addition, requirements to provide such integrity provide collateral benefit with regard to the ability of the structure to survive other hazards such as high windstorms, tornadoes, and hurricanes.

The procedure outlined for SDC A buildings is intended to be a simple approach to ensuring both that a building has a complete seismic force-resisting system and that it is capable of sustaining



at least a minimum level of lateral force. In this analysis procedure, a series of static lateral forces equal to 1% of the weight at each level of the structure is applied to the structure independently in each of the two orthogonal directions. The structural elements of the seismic force-resisting system then are designed to resist the resulting forces in combination with other loads under the load combinations specified by the building code.

The selection of 1% of the building weight as the design force for SDC A structures is somewhat arbitrary. This level of design lateral force is consistent with prudent requirements for the lateral bracing of structures to prevent inadvertent buckling under gravity loads. It is also sufficiently small as to not present an undue burden on the design of structures in zones of very low seismic activity.

The seismic weight  $W$  is the total weight of the building and that part of the service load that might reasonably be expected to be attached to the building at the time of an earthquake. It includes permanent and movable partitions and permanent equipment such as mechanical and electrical equipment, piping, and ceilings. The normal human live load is taken to be negligibly small in its contribution to the seismic lateral forces. Buildings designed for storage or warehouse usage should have at least 25% of the design floor live load included in the weight,  $W$ . Snow loads up to 30 psf are not considered. Freshly fallen snow would have little effect on the lateral force in an earthquake; however, ice loading would be more or less firmly attached to the roof of the building and would contribute significantly to the inertia force. For this reason, the effective snow load is taken as the full snow load for those regions where the snow load exceeds 30 psf with the proviso that the local authority having jurisdiction may allow the snow load to be reduced up to 80%. The question of how much snow load should be included in  $W$  is really a question of how much ice buildup or snow entrapment can be expected for the roof configuration or site topography, and this is a question best left to the discretion of the local authority having jurisdiction.

**Connections:** For SDC A, 5% is always greater than 0.133 times  $S_{DS}$ .

**Anchorage of concrete or masonry walls:** The intent is to ensure that out-of-plane inertia forces generated within a concrete or masonry wall can be transferred to the adjacent roof or floor construction. The transfer can be accomplished only by reinforcement or anchors.

### 5.5.6 GEOLOGIC HAZARDS AND GEOTECHNICAL INVESTIGATION

This section, which applies to buildings assigned to SDC C through F, tells us limitations for siting buildings and requirements of geotechnical investigation report.

- **SDC E or F.** Siting of a structure assigned to SDC E or F is not permitted where there is a known potential for an active fault to cause rupture of the ground surface at the structure.
- **SDCs C through D.** For these buildings, a geotechnical investigation report is required. The report shall include an evaluation of the following potential geologic and seismic hazards:
  - a. Slope instability
  - b. Liquefaction
  - c. Differential settlement
  - d. Surface displacement due to faulting or lateral spreading

The report shall contain recommendations for appropriate foundation designs or other measures to mitigate the effects of the previously mentioned hazards. Where deemed appropriate by the authority having jurisdiction, a site-specific geotechnical report is not required where prior evaluations of nearby sites with similar soil conditions provide sufficient direction relative to the proposed construction.

- **Additional geotechnical investigation report requirements for SDCs D through F.** The report shall include the following:
  1. Determination of lateral pressures on basement and retaining walls due to earthquake motions.
  2. Potential for liquefaction and soil strength loss evaluated for site peak ground accelerations, magnitudes, and source characteristics consistent with the design earthquake ground motions. Peak ground acceleration is permitted to be determined based on a site-specific study taking into account soil amplification effects or, in the absence of such a study, peak ground accelerations shall be assumed equal to  $S_s/2.5$ .
  3. Assessment of potential consequences of liquefaction and soil strength loss—including the estimation of differential settlement, lateral movement, lateral loads on foundations, and the reduction in foundation soil-bearing capacity—increases in lateral pressures on retaining walls, and the flotation of buried structures.
  4. Discussion of mitigation measures such as, but not limited to, ground stabilization, the selection of appropriate foundation type and depths, the selection of appropriate structural systems to accommodate anticipated displacements and forces, or any combination of these measure and how they shall be considered in the design of the structure.

### 5.5.7 BASE SHEAR FOR PRELIMINARY DESIGN

The comparison of computer results with approximate analysis techniques and presolved problems is an effective way of catching flawed designs that may arise from errors due to computer modeling. This is beneficial particularly for students entering the structural engineering profession. They are often bewildered by and unprepared to deal with the building codes and standards.

Therefore, generalizations such as “the seismic base shear for an SDC C, 14-story reinforced concrete building located in downtown Boston is approximately equal to 1.58% of the weight of the building” would be of great assistance in ensuring that you are in the right ball park. Such general statements or tables would be useful for quick peer reviews and back of the envelope calculations. Because the base shear is not only a province of the seismicity of the site, but also depends on other interrelated factors such as:

- Building fundamental period that in turn depends on its height and the structural system chosen for the building
- Response modification factor,  $R$
- Properties of the soil on which it rests upon

it is unwieldy if not impossible to generate an all-encompassing table. Instead, we present here two simplified tables, one for Site Class D, Table 5.20, and the other for Site Class C, Table 5.21.

The tables are referenced to 48 selected cities in the USA shown in Figure 5.33. The parameters chosen in the preparation of tables are

- Building height,  $h_n = 160$  ft
- Building period,  $T_a = 1.22$  s,  $T_b$  (noted as  $T_B$  in tables) =  $C_u T_a$
- Site class C or D as noted in the tables
- Response modification factor,  $R = 4$
- Importance factor,  $I_E = 1.0$

Approximate base shear values given in the tables as a percent of the building weight are based on an approximate fundamental period,  $T_a$ , calculated for a 160 ft tall building, using an average of the periods determined by using the formulas given in ASCE 7-05, Section 12.8.2.1. With the exception of ordinary moment frames, all other systems up to 160 ft tall are permitted in buildings assigned to SDC D and lower. Hence the choice of  $h_n = 160$  ft in the tables.

TABLE 5.20  
Approximate Base Shear as a Percent of Building Weight: Site Class D

#	City	Map Location (Latitude, Longitude)	Site Class	$S_s$	$S_1$	$F_a$	$F_v$	$S_{MS}$ (g)	$S_{M1}$ (g)	$S_{DS}$ (g)	$S_{D1}$ (g)	SDC	$T_L$ , Long-Period Transition (Informational Purposes)	$C_u T_A$	$C_s$ , Base Shear as a Percentage of Building Weight	#
1	New York, New York	40° 47' N 73° 58' W	D	0.364	0.070	1.509	2.400	0.549	0.169	0.366	0.113	C	6	1.51	2.30%	1
2	Los Angeles, California	34° 3' N 118° 14' W	D	2.176	0.729	1.000	1.500	2.176	1.093	1.451	0.729	D	12	1.26	14.94%	2
3	Chicago, Illinois	41° 53' N 87° 38' W	D	0.162	0.059	1.600	2.400	0.260	0.142	0.173	0.095	B	12	1.53	1.93%	3
4	Houston, Texas	29° 59' N 95° 22' W	D	0.090	0.038	1.600	2.400	0.144	0.091	0.096	0.060	A	12	1.53	1.00%	4
5	Philadelphia, Pennsylvania	39° 53' N 75° 15' W	D	0.266	0.059	1.587	2.400	0.422	0.142	0.282	0.094	B	6	1.53	1.93%	5
6	Phoenix, Arizona	33° 26' N 112° 1' W	D	0.180	0.061	1.600	2.400	0.288	0.147	0.192	0.098	B	6	1.53	2.00%	6
7	San Antonio, Texas	29° 32' N 98° 28' W	D	0.103	0.030	1.600	2.400	0.165	0.073	0.110	0.049	A	6	1.53	1.00%	7
8	San Diego, California	32° 44' N 117° 10' W	D	1.573	0.613	1.000	1.500	1.573	0.919	1.049	0.613	D	8	1.26	12.56%	8
9	Dallas, Texas	32° 51' N 96° 51' W	D	0.118	0.050	1.600	2.400	0.188	0.121	0.125	0.081	B	12	1.53	1.64%	9
10	San Jose, California	37° 22' N 121° 56' W	D	1.500	0.600	1.000	1.500	1.500	0.900	1.000	0.600	D	8	1.26	12.30%	10
11	Detroit, Michigan	42° 25' N 83° 1' W	D	0.118	0.044	1.600	2.400	0.190	0.106	0.126	0.070	B	12	1.53	1.44%	11
12	Indianapolis, Indiana	39° 44' N 86° 17' W	D	0.203	0.086	1.600	2.400	0.325	0.207	0.217	0.138	C	12	1.46	2.82%	12
13	Jacksonville, Florida	30° 30' N 81° 42' W	D	0.151	0.064	1.600	2.400	0.242	0.152	0.161	0.102	B	8	1.53	2.10%	13
14	San Francisco, California	37° 46' N 122° 26' W	D	1.502	0.731	1.000	1.500	1.502	1.097	1.001	0.731	D	12	1.26	14.98%	14

15	Columbus, Ohio	40° 0' N 82° 53' W	D	0.145	0.058	1.600	2.400	0.232	0.140	0.155	0.093	B	12	1.53	1.90%	15
16	Austin, Texas	30° 18' N 97° 42' W	D	0.082	0.033	1.600	2.400	0.131	0.079	0.087	0.053	A	12	1.53	1.00%	16
17	Memphis, Tennessee	35° 3' N 90° 0' W	D	1.130	0.316	1.048	1.768	1.184	0.559	0.790	0.372	D	12	1.26	7.63%	17
18	Baltimore, Maryland	39° 11' N 76° 40' W	D	0.163	0.050	1.600	2.400	0.261	0.121	0.174	0.081	B	6	1.53	1.64%	18
19	Fort Worth, Texas	32° 50' N 97° 3' W	D	0.14	0.049	1.600	2.400	0.183	0.118	0.122	0.079	B	12	1.53	1.61%	19
20	Charlotte, North Carolina	35° 13' N 80° 56' W	D	0.318	0.106	1.546	2.377	0.491	0.251	0.328	0.168	C	8	1.41	3.44%	20
21	El Paso, Texas	31° 48' N 106° 24' W	D	0.336	0.108	1.531	2.367	0.514	0.256	0.343	0.171	C	6	1.40	3.49%	21
22	Milwaukee, Wisconsin	42° 57' N 87° 54' W	D	0.110	0.045	1.600	2.400	0.176	0.109	0.117	0.073	B	12	1.53	1.48%	22
23	Seattle, Washington	47° 39' N 122° 18' W	D	1.306	0.444	1.000	1.556	1.306	0.691	0.870	0.460	D	6	1.26	9.44%	23
24	Boston, Massachusetts	42° 22' N 71° 2' W	D	0.282	0.068	1.574	2.400	0.445	0.163	0.296	0.109	B	6	1.51	2.23%	24
25	Denver, Colorado	39° 45' N 104° 52' W	D	0.210	0.055	1.600	2.400	0.337	0.133	0.225	0.089	B	4	1.53	1.80%	25
26	Louisville- Jefferson County, Kentucky	38° 11' N 85° 44' W	D	0.247	0.103	1.600	2.389	0.395	0.245	0.263	0.164	C	12	1.41	3.36%	26
27	Washington, District of Columbia	38° 51' N 77° 2' W	D	0.153	0.050	1.600	2.400	0.244	0.121	0.163	0.081	B	8	1.53	1.64%	27
28	Nashville- Davidson, Tennessee	36° 7' N 86° 41' W	D	0.331	0.129	1.535	2.283	0.508	0.295	0.339	0.197	C	12	1.36	4.03%	28
29	Las Vegas, Nevada	36° 5' N 115° 10' W	D	0.554	0.171	1.357	2.115	0.752	0.362	0.501	0.241	D	6	1.31	4.94%	29
30	Portland, Oregon	45° 36' N 122° 36' W	D	0.907	0.317	1.137	1.767	1.031	0.559	0.687	0.373	D	16	1.26	7.65%	30

(continued)

TABLE 5.20 (continued)  
Approximate Base Shear as a Percent of Building Weight: Site Class D

#	City	Map Location (Latitude, Longitude)	Site Class	$S_s$	$S_1$	$F_a$	$F_v$	$S_{MS}$ (g)	$S_{M1}$ (g)	$S_{DS}$ (g)	$S_{D1}$ (g)	SDC	$T_L$ Long-Period Transition (Informational Purposes)	$C_u T_A$	$C_S$ Base Shear as a Percentage of Building Weight	#
31	Oklahoma City, Oklahoma	35° 24' N 97° 36' W	D	0.354	0.076	1.516	2.400	0.537	0.182	0.358	0.121	C	12	1.49	2.49%	31
32	Tucson, Arizona	32° 7' N 110° 56' W	D	0.282	0.080	1.575	2.400	0.444	0.192	0.296	0.128	B	6	1.48	2.62%	32
33	Albuquerque, New Mexico	35° 3' N 106° 37' W	D	0.571	0.172	1.343	2.112	0.767	0.363	0.511	0.242	D	6	1.31	4.96%	33
34	Long Beach, California	33° 49' N 118° 9' W	D	1.693	0.644	1.000	1.500	1.693	0.966	1.129	0.644	D	8	1.26	13.20%	34
35	Atlanta, Georgia	33° 39' N 84° 26' W	D	0.218	0.084	1.600	2.400	0.348	0.202	0.232	0.134	C	12	1.47	2.75%	35
36	Fresno, California	36° 46' N 119° 43' W	D	0.488	0.219	1.410	1.962	0.688	0.430	0.459	0.287	D	12	1.27	5.87%	36
37	Sacramento, California	38° 31' N 121° 30' W	D	0.629	0.251	1.297	1.898	0.816	0.477	0.544	0.318	D	12	1.26	6.51%	37
38	New Orleans, Louisiana	29° 59' N 90° 15' W	D	0.111	0.048	1.600	2.400	0.177	0.115	0.118	0.077	B	12	1.53	1.57%	38
39	Cleveland, Ohio	41° 24' N 81° 51' W	D	0.179	0.051	1.600	2.400	0.286	0.123	0.191	0.082	B	12	1.53	1.67%	39
40	Kansas City, Missouri	39° 7' N 94° 35' W	D	0.127	0.058	1.600	2.400	0.204	0.140	0.136	0.094	B	12	1.53	1.90%	40

41	Omaha, Nebraska	41° 18' N 95° 54' W	D	0.118	0.042	1.600	2.400	0.188	0.100	0.125	0.066	B	12	1.53	1.38%	41
42	Oakland, California	37° 49' N 122° 19' W	D	1.500	0.600	1.000	1.500	0.900	1.000	0.600	D	D	8	1.26	12.30%	42
43	Miami, Florida	25° 48' N 80° 16' W	D	0.051	0.020	1.600	2.400	0.082	0.047	0.055	0.031	A	8	1.53	1.00%	43
44	Tulsa, Oklahoma	36° 12' N 95° 54' W	D	0.159	0.067	1.600	2.400	0.255	0.160	0.170	0.107	B	12	1.52	2.20%	44
45	Minneapolis, Minnesota	44° 53' N 93° 13' W	D	0.060	0.027	1.600	2.400	0.096	0.065	0.064	0.043	A	12	1.53	1.00%	45
46	Colorado Springs, Colorado	38° 49' N 104° 43' W	D	0.203	0.058	1.600	2.400	0.324	0.139	0.216	0.093	B	4	1.53	1.90%	46
47	Irvine, California	33° 40' N 117° 47' W	D	1.476	0.522	1.000	1.500	1.476	0.783	0.984	0.522	D	8	1.26	10.79%	47
48	Raleigh, North Carolina	35° 52' N 78° 47' W	D	0.202	0.079	1.600	2.400	0.323	0.189	0.215	0.126	B	8	1.48	2.59%	48

Note:  $h_n = 160$  ft.  $I_E = 1.0$ .  $T_a = 1.22$  s (see text). Site Class = D (Stiff soil, see ASCE 7-05, Chapter 20).  $R = 4.0$ . For systems with differing  $R$  values, multiply base shear by the ratio  $(4.0/R)$ . Ordinary moment frame not permitted for buildings assigned to SDC C and higher.

TABLE 5.21  
Approximate Base Shear as a Percent of Building Weight: Site Class C

#	City	Map Location (Latitude, Longitude)	Site Class	$S_s$	$S_1$	$F_a$	$F_v$	$S_{MS}$ (g)	$S_{M1}$ (g)	$S_{DS}$ (g)	$S_{D1}$ (g)	SDC	$T_U$ , Long- Period Transition (Informational Purposes)	$C_u T_A$	$C_s$ , Base Shear as a Percentage of Building Weight		#
															Weight	%	
1	New York, New York	40° 47' N 73° 58' W	C	0.364	0.070	1.200	1.700	0.437	0.120	0.291	0.080	B	6	1.53	1.63%		1
2	Los Angeles, California	34° 3' N 118° 14' W	C	2.176	0.729	1.000	1.300	2.176	0.948	1.451	0.632	D	12	1.26	12.95%		2
3	Chicago, Illinois	41° 53' N 87° 38' W	C	0.162	0.059	1.200	1.700	0.195	0.101	0.130	0.067	A	12	1.53	1.00%		3
4	Houston, Texas	29° 59' N 95° 22' W	C	0.090	0.038	1.200	1.700	0.108	0.064	0.072	0.043	A	12	1.53	1.00%		4
5	Philadelphia, Pennsylvania	39° 53' N 75° 15' W	C	0.266	0.059	1.200	1.700	0.319	0.100	0.213	0.067	B	6	1.53	1.37%		5
6	Phoenix, Arizona	33° 26' N 112° 1' W	C	0.180	0.061	1.200	1.700	0.216	0.104	0.144	0.069	B	6	1.53	1.42%		6
7	San Antonio, Texas	29° 32' N 98° 28' W	C	0.103	0.030	1.200	1.700	0.124	0.052	0.083	0.034	A	6	1.53	1.00%		7
8	San Diego, California	32° 44' N 117° 10' W	C	1.573	0.613	1.000	1.300	1.573	0.796	1.049	0.531	D	8	1.26	10.89%		8
9	Dallas, Texas	32° 51' N 96° 51' W	C	0.118	0.050	1.200	1.700	0.141	0.086	0.094	0.057	A	12	1.53	1.00%		9
10	San Jose, California	37° 22' N 121° 56' W	C	1.500	0.600	1.000	1.300	1.500	0.780	1.000	0.520	D	8	1.26	10.66%		10
11	Detroit, Michigan	42° 25' N 83° 1' W	C	0.118	0.044	1.200	1.700	0.142	0.075	0.095	0.050	A	12	1.53	1.00%		11
12	Indianapolis, Indiana	39° 44' N 86° 17' W	C	0.203	0.086	1.200	1.700	0.244	0.146	0.163	0.098	B	12	1.53	2.00%		12

13	Jacksonville, Florida	30° 30' N 81° 42' W	C	0.151	0.064	1.200	1.700	0.181	0.108	0.121	0.072	B	8	1.53	1.49%	13
14	San Francisco, California	37° 46' N 122° 26' W	C	1.502	0.731	1.000	1.300	1.502	0.951	1.001	0.634	D	12	1.26	12.98%	14
15	Columbus, Ohio	40° 0' N 82° 53' W	C	0.145	0.058	1.200	1.700	0.174	0.099	0.116	0.066	A	12	1.53	1.00%	15
16	Austin, Texas	30° 18' N 97° 42' W	C	0.082	0.033	1.200	1.700	0.098	0.056	0.065	0.037	A	12	1.53	1.00%	16
17	Memphis, Tennessee	35° 3' N 90° 0' W	C	1.130	0.316	1.000	1.484	1.130	0.469	0.753	0.313	D	12	1.26	6.41%	17
18	Baltimore, Maryland	39° 11' N 76° 40' W	C	0.163	0.050	1.200	1.700	0.196	0.086	0.130	0.057	A	6	1.53	1.00%	18
19	Fort Worth, Texas	32° 50' N 97° 3' W	C	0.114	0.049	1.200	1.700	0.137	0.083	0.091	0.056	A	12	1.53	1.00%	19
20	Charlotte, North Carolina	35° 13' N 80° 56' W	C	0.318	0.106	1.200	1.694	0.381	0.179	0.254	0.119	B	8	1.49	2.45%	20
21	El Paso, Texas	31° 48' N 106° 24' W	C	0.336	0.108	1.200	1.692	0.403	0.183	0.269	0.122	B	6	1.49	2.50%	21
22	Milwaukee, Wisconsin	42° 57' N 87° 54' W	C	0.110	0.045	1.200	1.700	0.132	0.077	0.088	0.051	A	12	1.53	1.00%	22
23	Seattle, Washington	47° 39' N 122° 18' W	C	1.306	0.444	1.000	1.356	1.306	0.602	0.870	0.401	D	6	1.26	8.22%	23
24	Boston, Massachusetts	42° 22' N 71° 2' W	C	0.282	0.068	1.200	1.700	0.339	0.116	0.226	0.077	B	6	1.53	1.58%	24
25	Denver, Colorado	39° 45' N 104° 52' W	C	0.210	0.055	1.200	1.700	0.253	0.094	0.168	0.063	B	4	1.53	1.28%	25
26	Louisville- Jefferson County, Kentucky	38° 11' N 85° 44' W	C	0.247	0.103	1.200	1.697	0.296	0.174	0.197	0.116	B	12	1.50	2.39%	26
27	Washington, District of Columbia	38° 51' N 77° 2' W	C	0.153	0.050	1.200	1.700	0.183	0.086	0.122	0.057	A	8	1.53	1.00%	27

(continued)



TABLE 5.21 (continued)  
Approximate Base Shear as a Percent of Building Weight: Site Class C

#	City	Map Location (Latitude, Longitude)	Site Class	S <sub>s</sub>	S <sub>1</sub>	F <sub>a</sub>	F <sub>v</sub>	S <sub>MS</sub> (g)	S <sub>M1</sub> (g)	S <sub>DS</sub> (g)	S <sub>D1</sub> (g)	SDC	T <sub>v</sub> Long- Period Transition (Informational Purposes)	C <sub>u</sub> T <sub>A</sub>	C <sub>S</sub> Base Shear as a Percentage of Building Weight	#
28	Nashville- Davidson, Tennessee	36° 7' N 86° 41' W	C	0.331	0.129	1.200	1.671	0.397	0.216	0.265	0.144	C	12	1.45	2.94%	28
29	Las Vegas, Nevada	36° 5' N 115° 10' W	C	0.554	0.171	1.178	1.629	0.653	0.279	0.435	0.186	C	6	1.38	3.81%	29
30	Portland, Oregon	45° 36' N 122° 36' W	C	0.907	0.317	1.037	1.483	0.940	0.469	0.627	0.313	D	16	1.26	6.42%	30
31	Oklahoma City, Oklahoma	35° 24' N 97° 36' W	C	0.354	0.076	1.200	1.700	0.425	0.129	0.284	0.086	B	12	1.53	1.77%	31
32	Tucson, Arizona	32° 7' N 110° 56' W	C	0.282	0.080	1.200	1.700	0.338	0.136	0.225	0.091	B	6	1.53	1.86%	32
33	Albuquerque, New Mexico	35° 3' N 106° 37' W	C	0.571	0.172	1.172	1.628	0.669	0.280	0.446	0.187	C	6	1.37	3.83%	33
34	Long Beach, California	33° 49' N 118° 9' W	C	1.693	0.644	1.000	1.300	1.693	0.837	1.129	0.558	D	8	1.26	11.44%	34
35	Atlanta, Georgia	33° 39' N 84° 26' W	C	0.218	0.084	1.200	1.700	0.261	0.143	0.174	0.095	B	12	1.53	1.95%	35
36	Fresno, California	36° 46' N 119° 43' W	C	0.488	0.219	1.200	1.581	0.585	0.346	0.390	0.231	D	12	1.32	4.73%	36
37	Sacramento, California	38° 31' N 121° 30' W	C	0.629	0.251	1.148	1.549	0.722	0.389	0.481	0.259	D	12	1.30	5.31%	37

38	New Orleans, Louisiana	29° 59' N 90° 15' W	C	0.111	0.048	1.200	1.700	0.133	0.081	0.089	0.054	A	12	1.53	1.00%	38
39	Cleveland, Ohio	41° 24' N 81° 51' W	C	0.179	0.051	1.200	1.700	0.214	0.087	0.143	0.058	A	12	1.53	1.00%	39
40	Kansas City, Missouri	39° 7' N 94° 35' W	C	0.127	0.058	1.200	1.700	0.153	0.099	0.102	0.066	A	12	1.53	1.00%	40
41	Omaha, Nebraska	41° 18' N 95° 54' W	C	0.118	0.042	1.200	1.700	0.141	0.071	0.094	0.047	A	12	1.53	1.00%	41
42	Oakland, California	37° 49' N 122° 19' W	C	1.500	0.600	1.000	1.300	1.500	0.780	1.000	0.520	D	8	1.26	10.66%	42
43	Miami, Florida	25° 48' N 80° 16' W	C	0.051	0.020	1.200	1.700	0.062	0.033	0.041	0.022	A	8	1.53	1.00%	43
44	Tulsa, Oklahoma	36° 12' N 95° 54' W	C	0.159	0.067	1.200	1.700	0.191	0.113	0.127	0.076	B	12	1.53	1.56%	44
45	Minneapolis, Minnesota	44° 53' N 93° 13' W	C	0.060	0.027	1.200	1.700	0.072	0.046	0.048	0.031	A	12	1.53	1.00%	45
46	Colorado Springs, Colorado	38° 49' N 104° 43' W	C	0.203	0.058	1.200	1.700	0.243	0.099	0.162	0.056	A	4	1.53	1.00%	46
47	Irvine, California	33° 40' N 117° 47' W	C	1.476	0.522	1.000	1.300	1.476	0.679	0.984	0.452	D	8	1.26	9.27%	47
48	Raleigh, North Carolina	35° 52' N 78° 47' W	C	0.202	0.079	1.200	1.700	0.242	0.134	0.161	0.089	B	8	1.53	1.83%	48

Note:  $h_n = 160$  ft.  $I_E = 1.0$ .  $T_s = 1.22$  s (see text). Site Class = C (Very dense soil and soft rock, see ASCE 7-05, Chapter 20).  $R = 4.0$ . For systems with differing  $R$  values, multiply base shear by the ratio  $(4.0/R)$ . Ordinary moment frame not permitted for buildings assigned to SDC C and higher.



**FIGURE 5.33** Locations of cities cited in Tables 5.20, 5.21 and Figure 5.34.

The period  $T_a$  (denoted as  $T_A$  in the tables) is calculated as follows

- For a concrete moment frame

$$\begin{aligned} T_a &= C_t(h_n)^x \\ &= 0.016 \times (160)^{0.9} = 1.54 \text{ s} \end{aligned}$$

- For all other structural systems

$$T_a = 0.02 \times (160)^{0.75} = 0.90 \text{ s}$$

$$\text{Average } T_a = (1.54 + 0.9)/2 = 1.22 \text{ s}$$

The period used in the calculation of base shears given in the tables has been multiplied by  $C_u$  where  $C_u$  varies from 1.4 to 1.7, depending on the SDC of the building.

### 5.5.8 DESIGN RESPONSE SPECTRUM FOR SELECTED CITIES IN THE U.S.A.\*

As stated previously, where a site-specific design response spectrum is not used, the design response curve is developed by using ASCE 7-05 Equations 11.4-5 through 11.4-7. To assist engineers in their preliminary designs, design response curves for 48 selected cities in the USA, shown in Figure 5.33 are presented in Figure 5.34. The curves are developed for site class is C and D.

\* The author would like to acknowledge his gratitude to Mr. Michael Y. Stavropoulos, project engineer, DeSimone Consulting Engineers, Las Vegas, Nevada, for preparing the tables and graphs of this section.

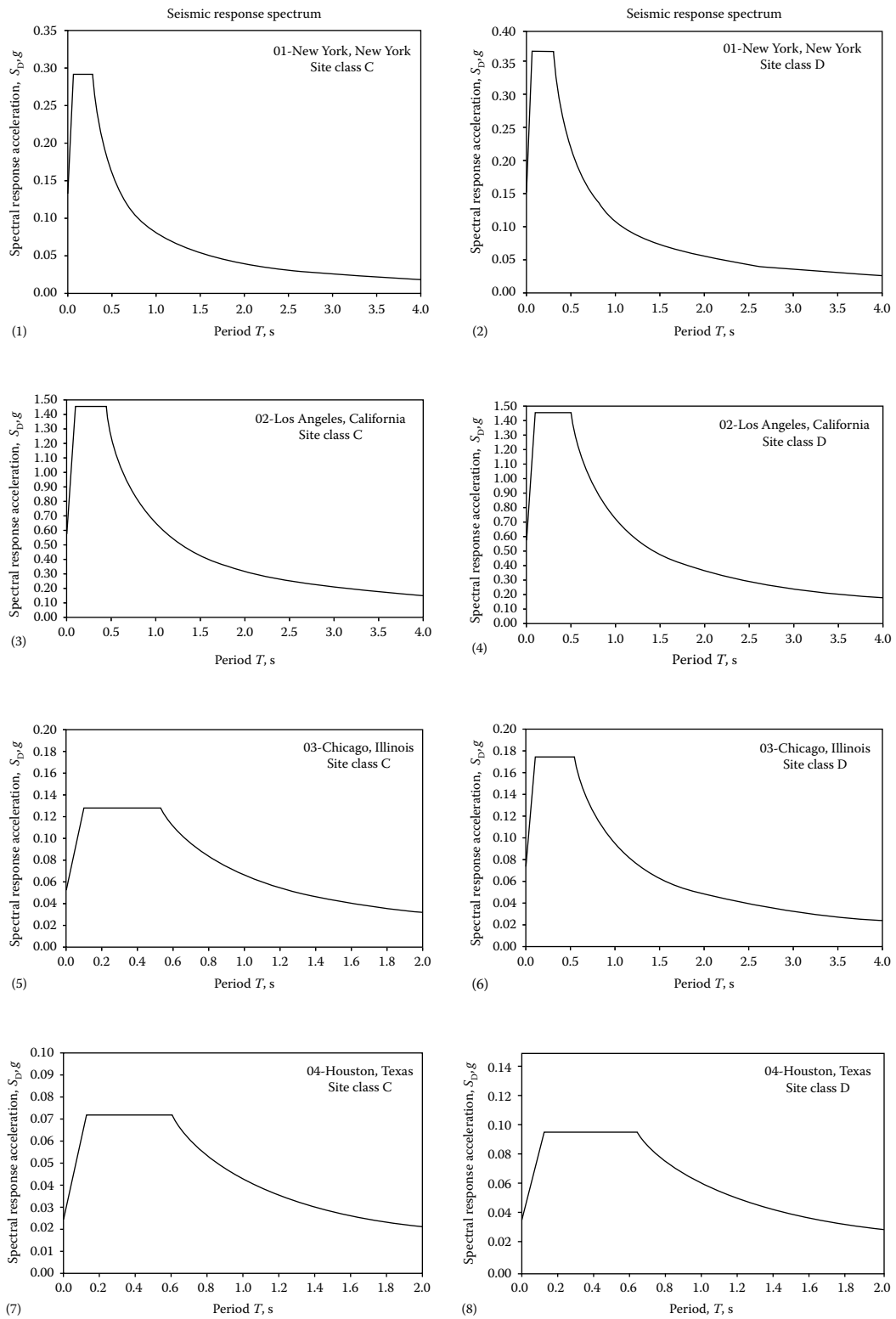


FIGURE 5.34 Design response spectrum for selected cities in the United States.

(continued)

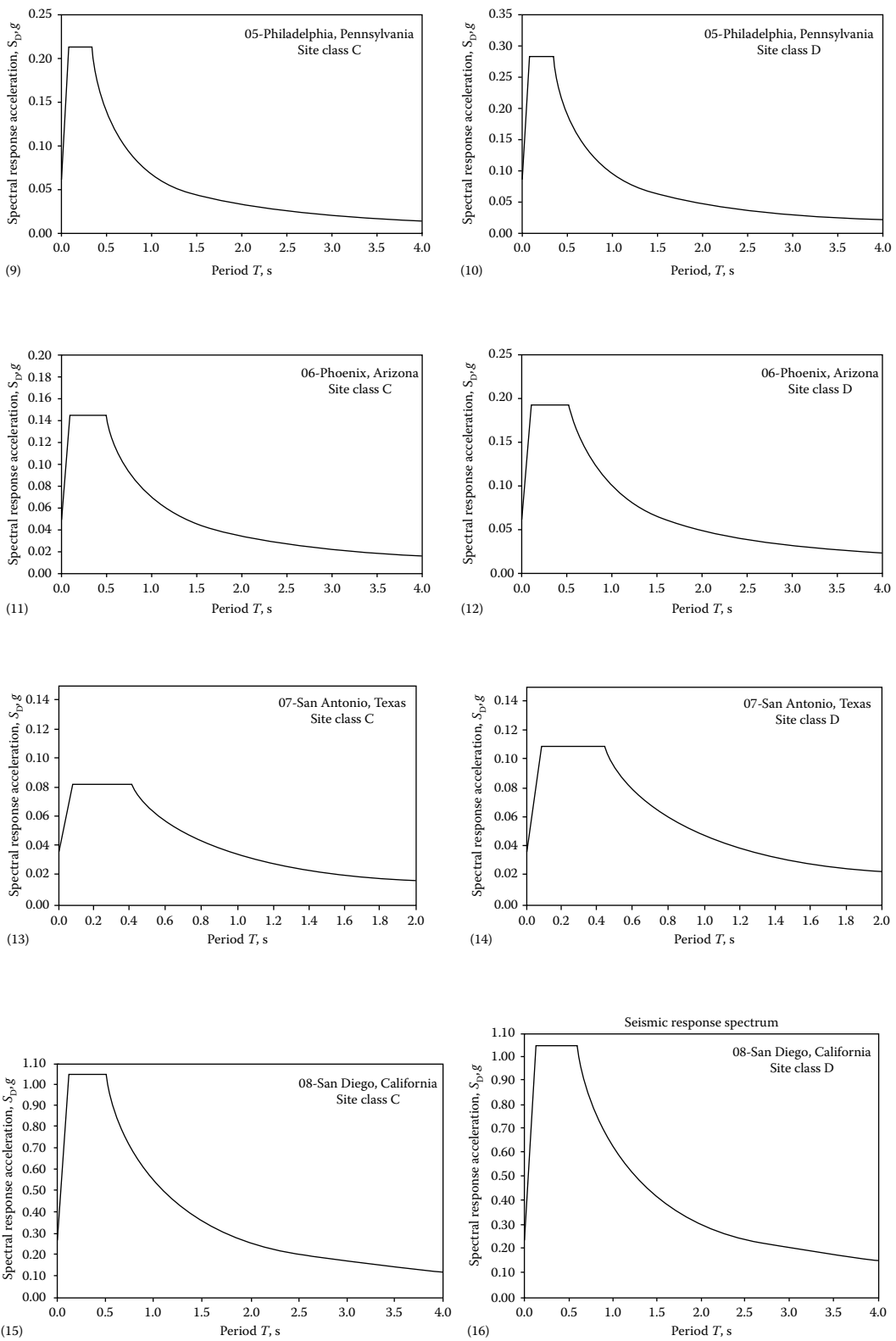


FIGURE 5.34 (continued)

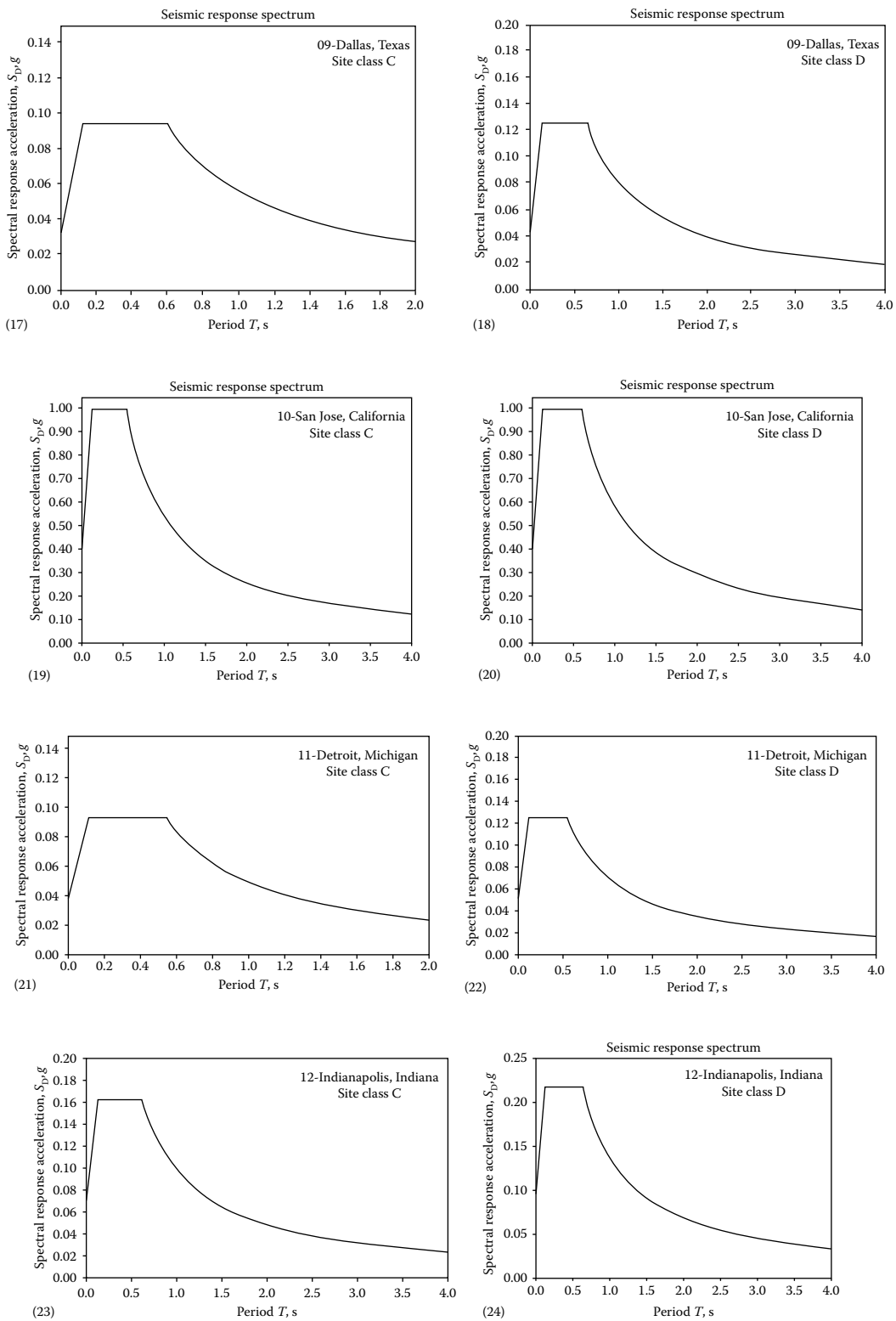


FIGURE 5.34 (continued)

(continued)

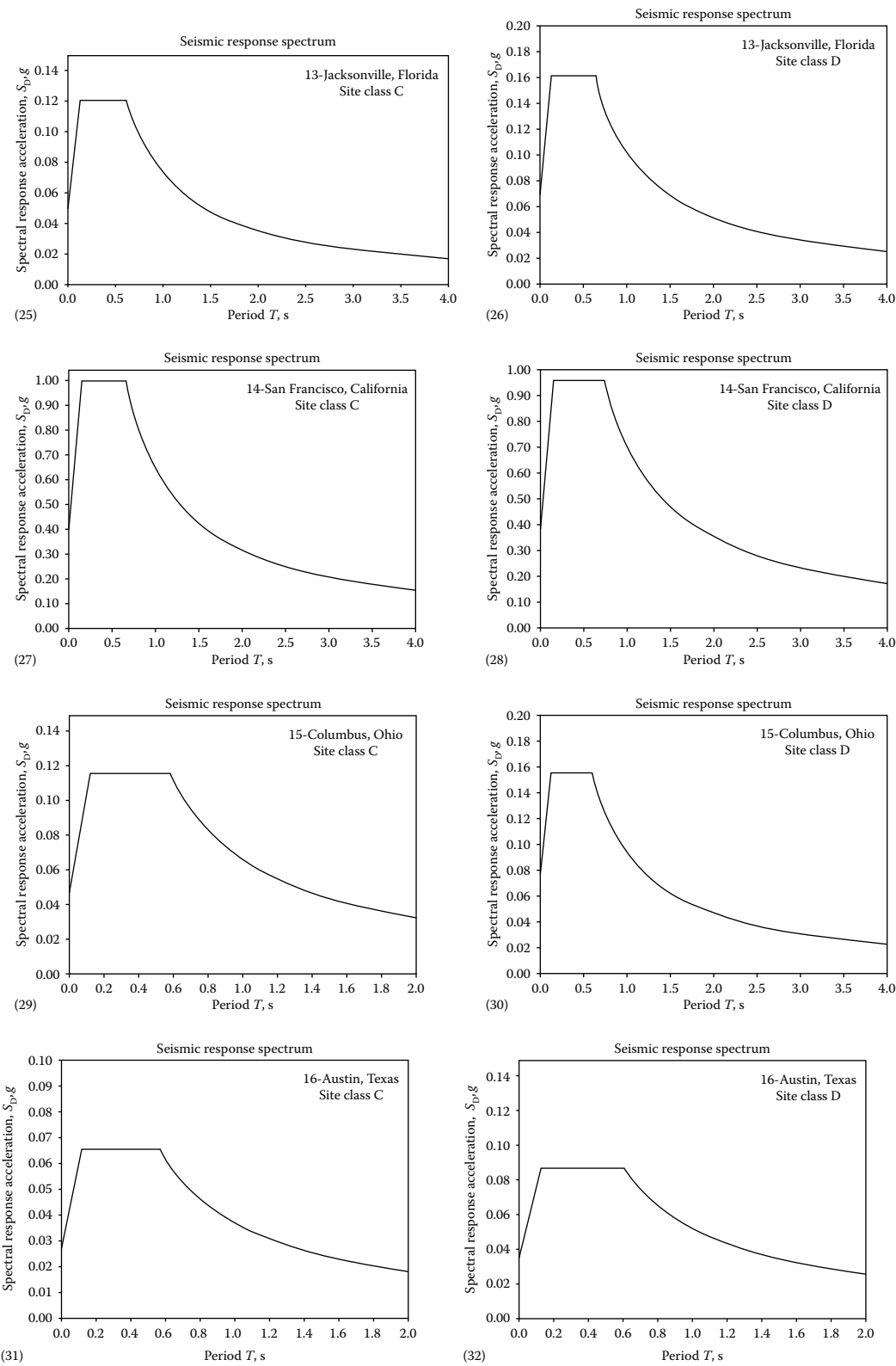


FIGURE 5.34 (continued)

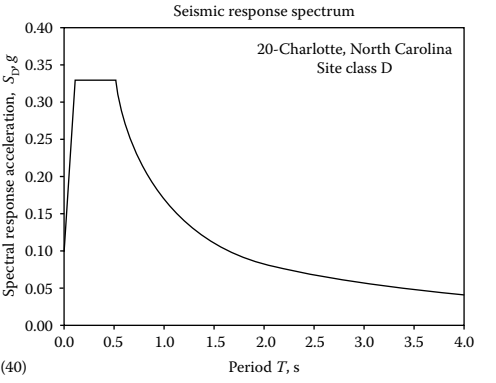
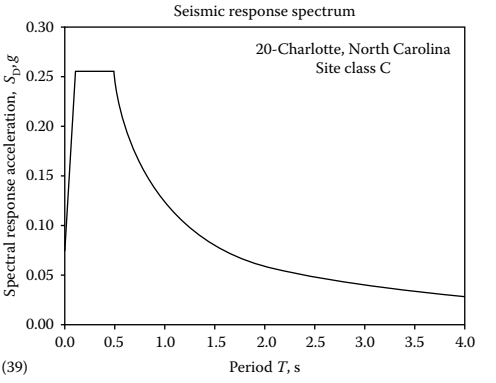
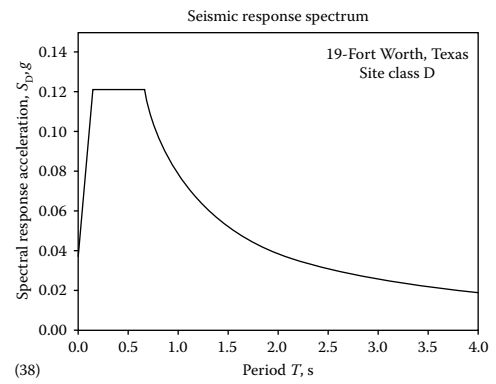
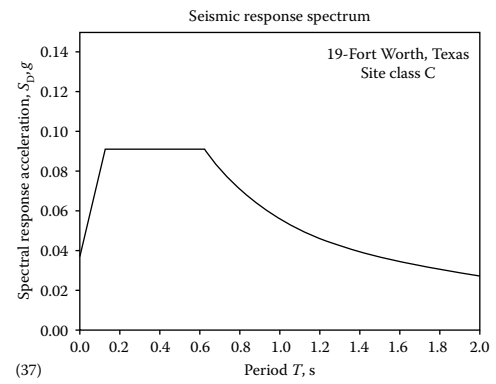
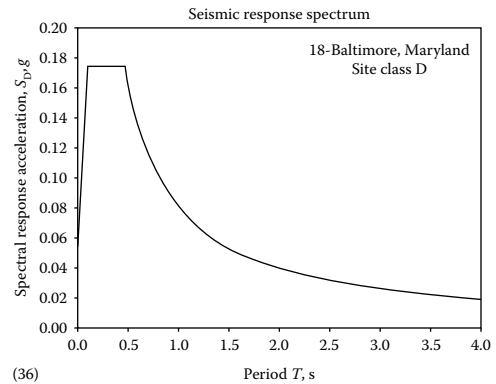
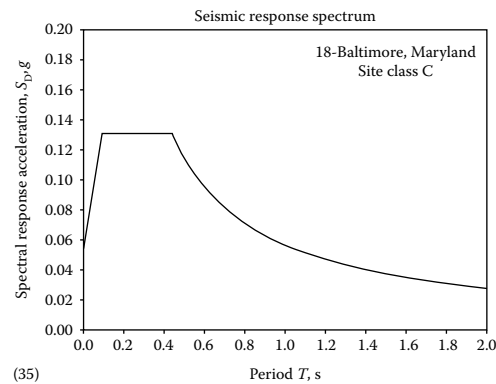
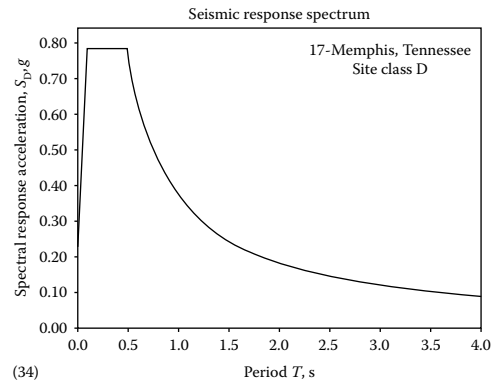
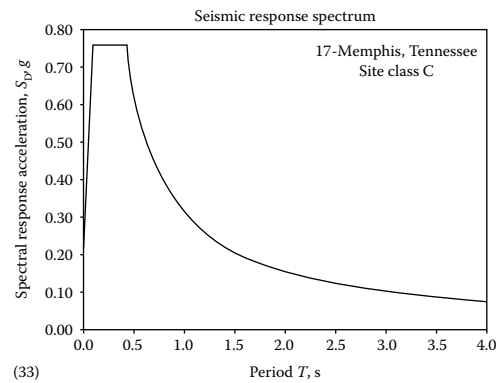


FIGURE 5.34 (continued)

(continued)



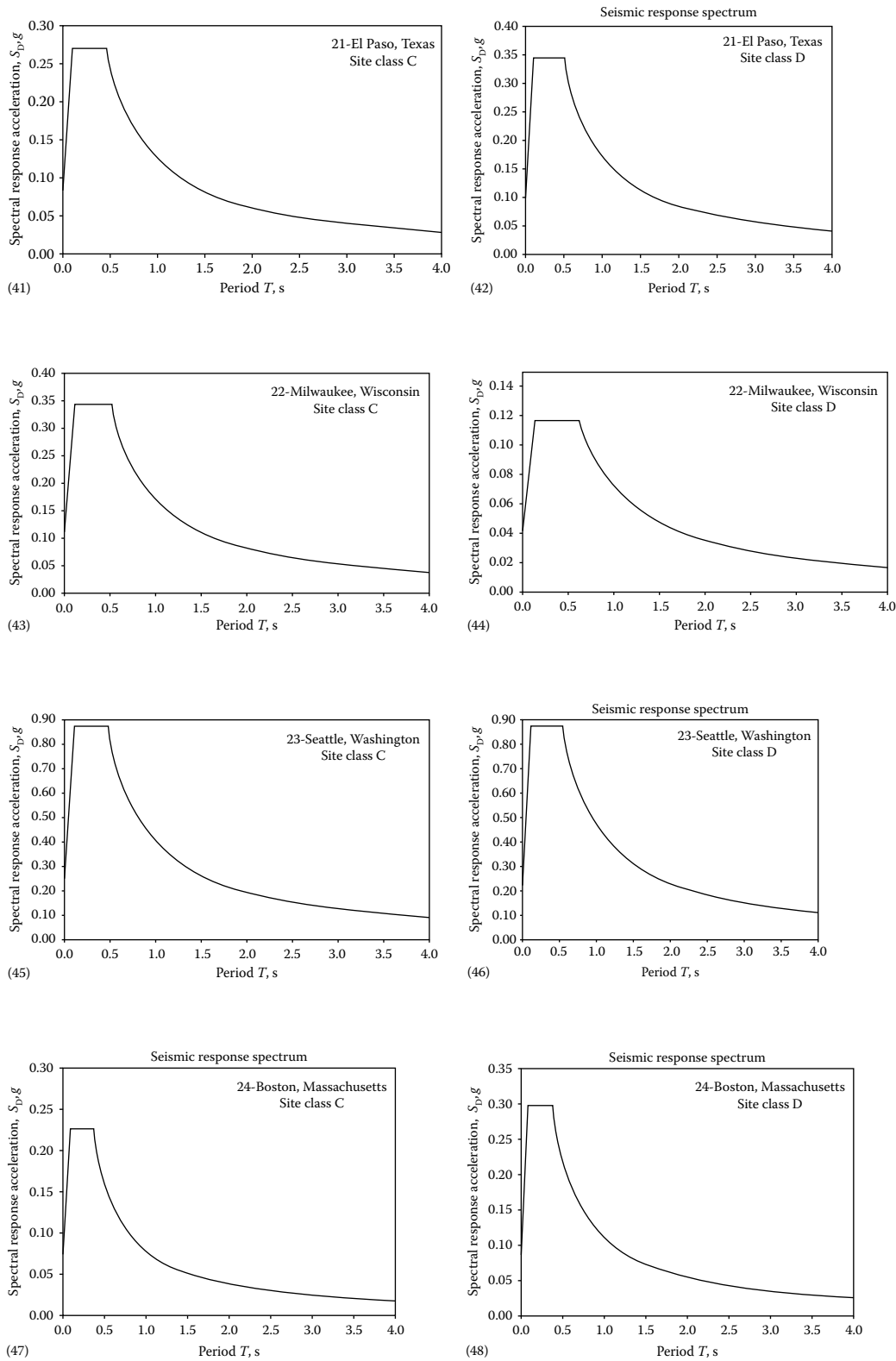


FIGURE 5.34 (continued)

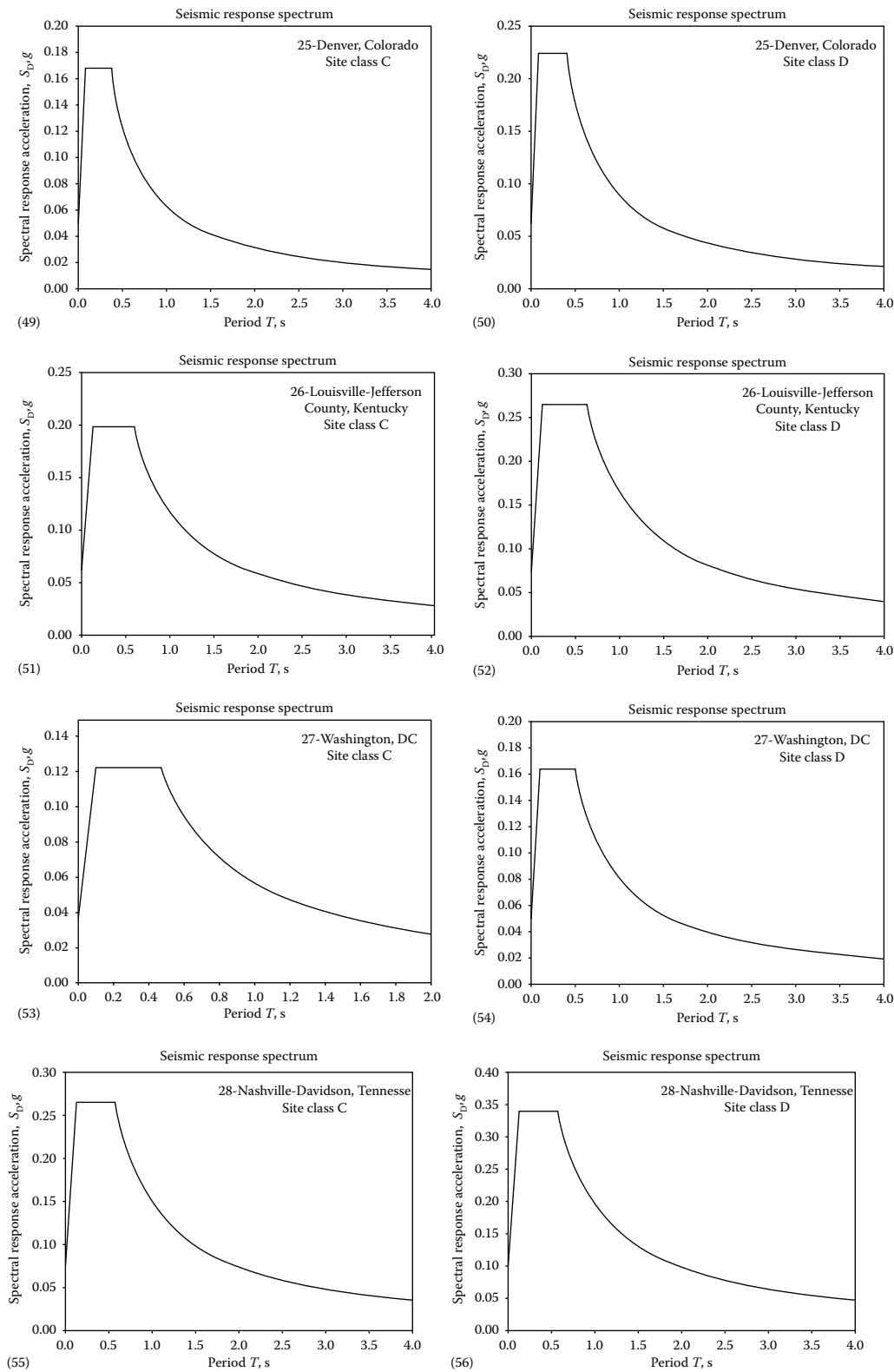


FIGURE 5.34 (continued)

(continued)

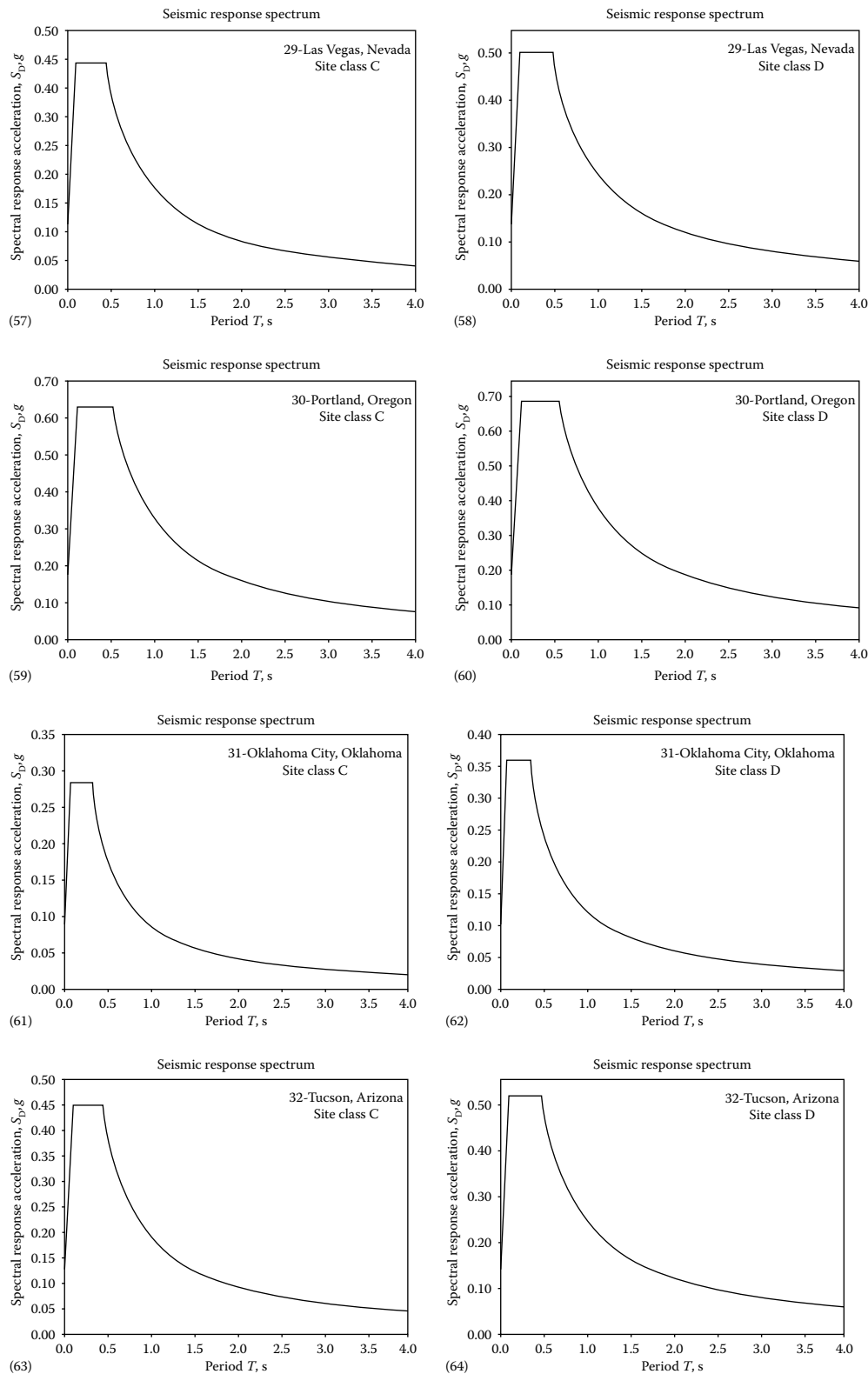


FIGURE 5.34 (continued)

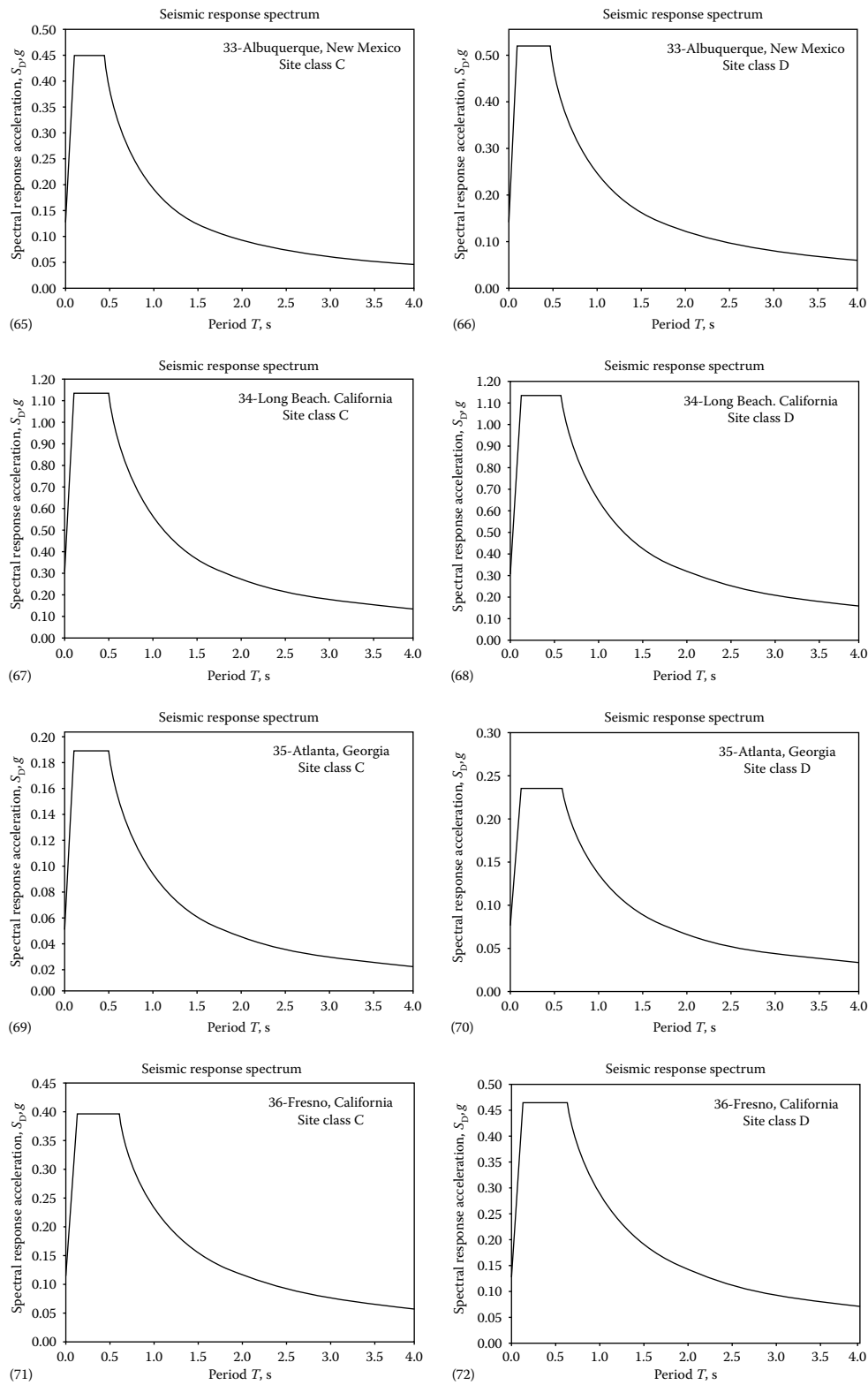


FIGURE 5.34 (continued)

(continued)

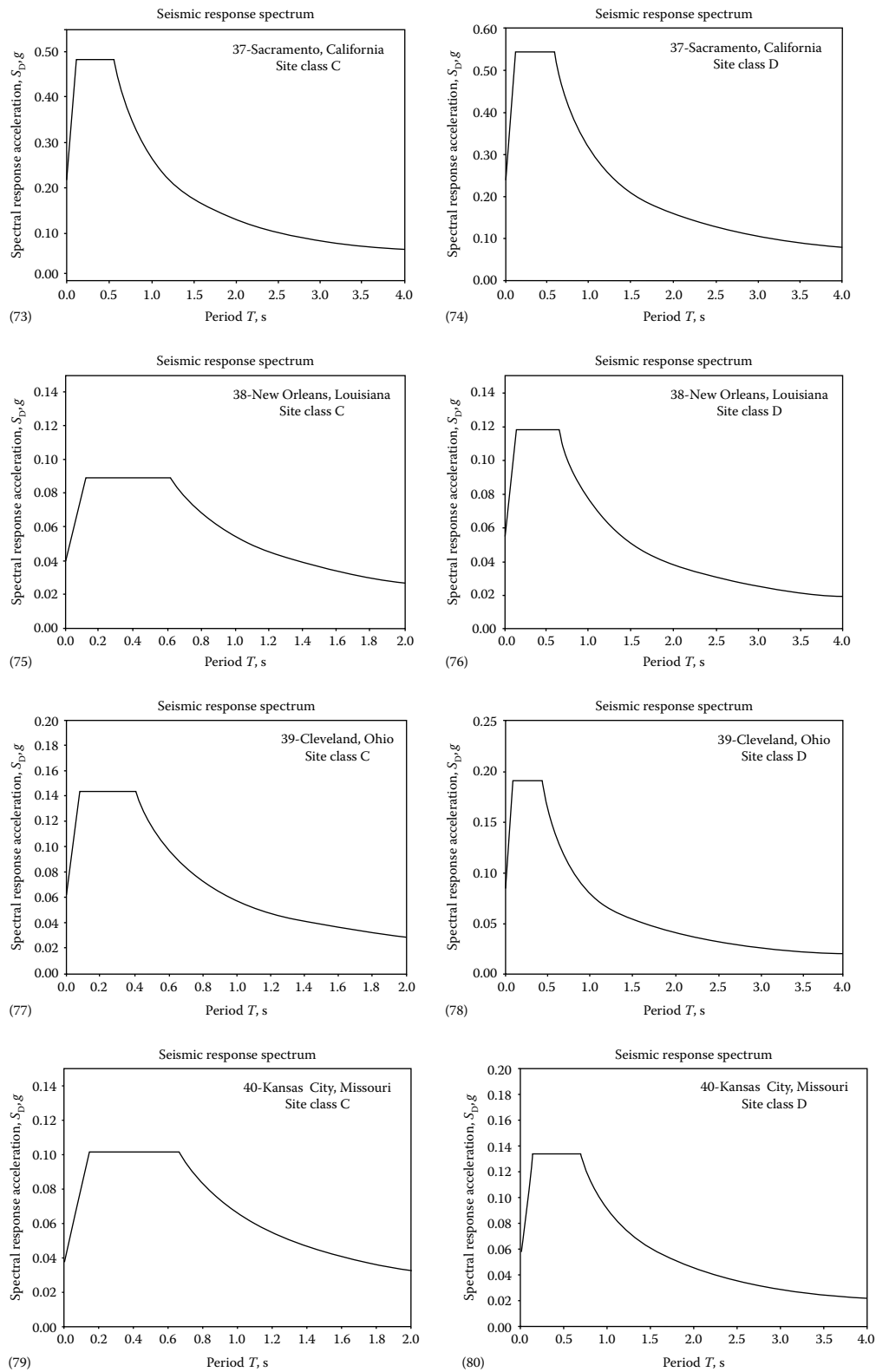


FIGURE 5.34 (continued)

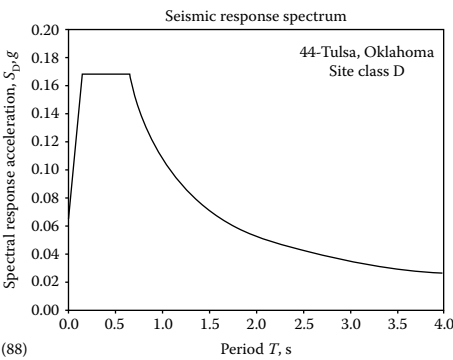
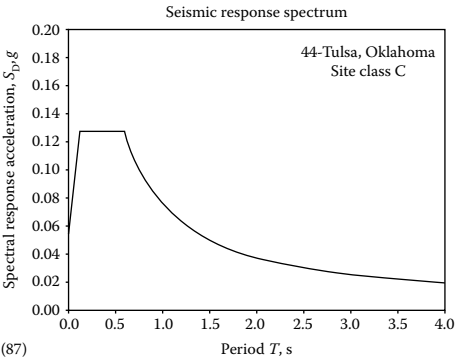
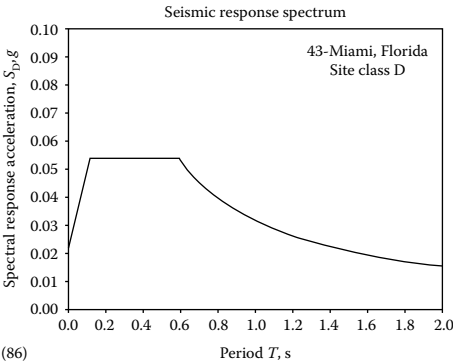
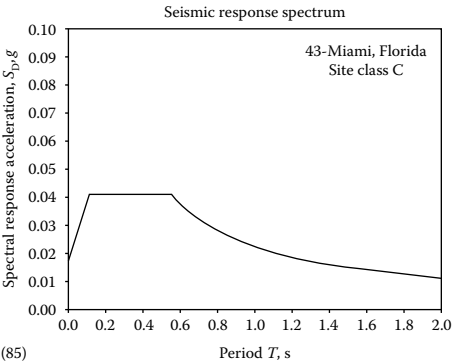
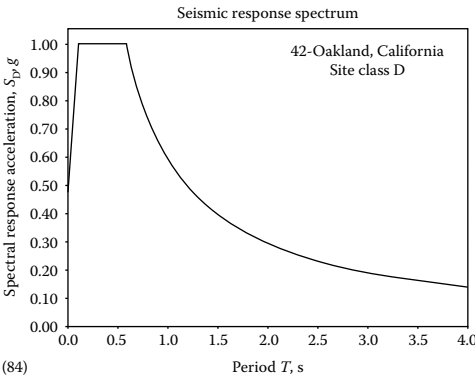
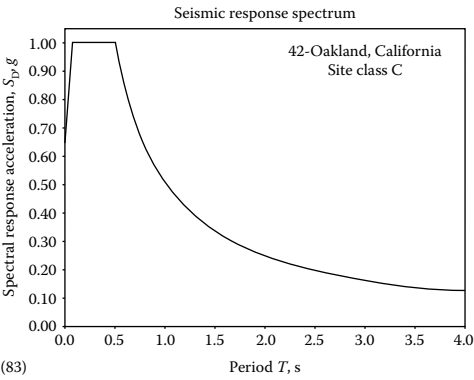
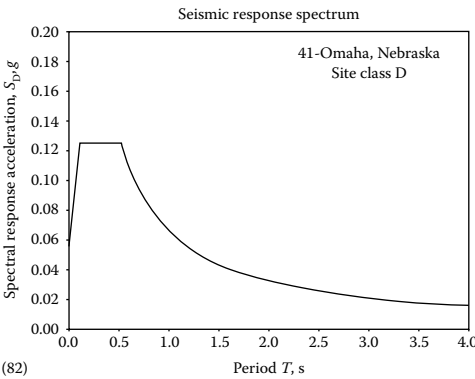
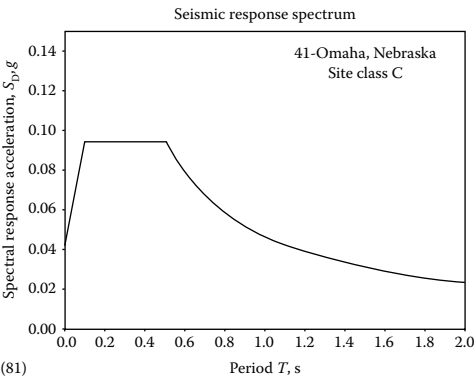


FIGURE 5.34 (continued)

(continued)

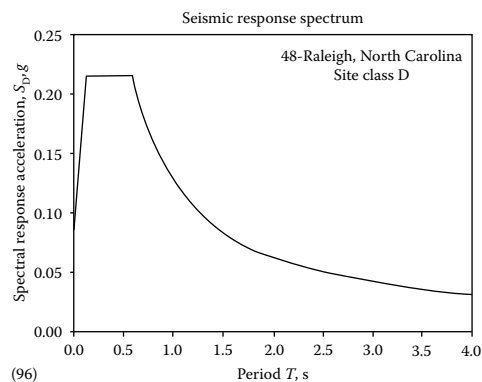
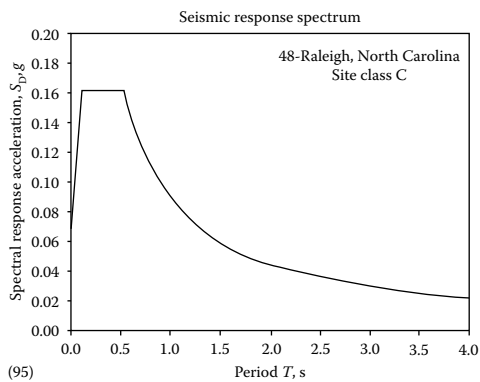
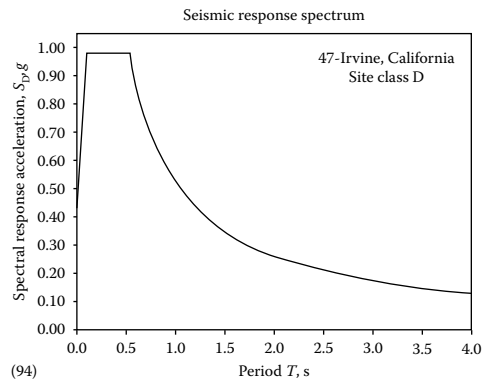
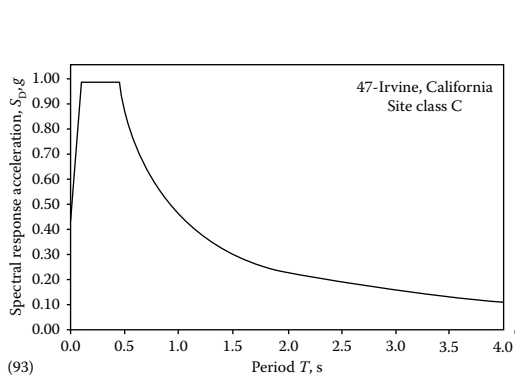
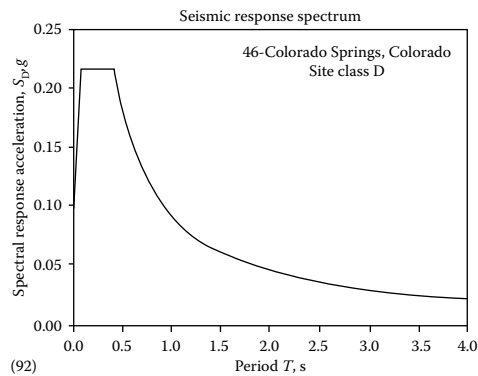
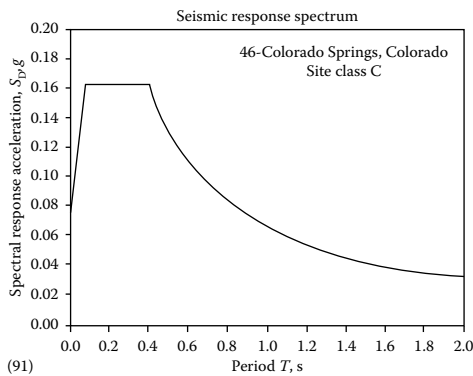
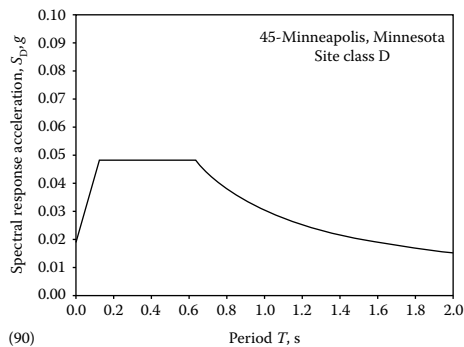
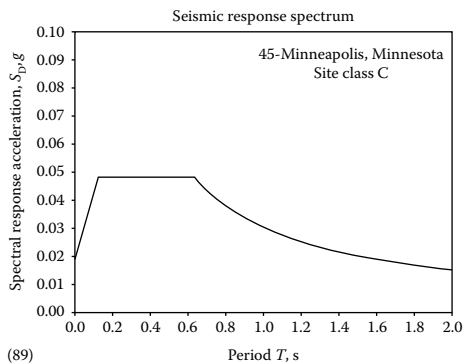


FIGURE 5.34 (continued)

## 5.6 AN OVERVIEW OF CHAPTER 12 OF ASCE 7-05, SEISMIC DESIGN REQUIREMENTS FOR BUILDING STRUCTURES

The requirements of Chapter 12 of ASCE 7-05 apply to buildings assigned to SDC B, C, D, E, or F. For SDC A buildings, the requirements given in Chapter 11 are deemed sufficient: No need for the designers to go in to the seismic design requirements given in Chapter 12.

### 5.6.1 SEISMIC DESIGN BASIS

**Basic requirements:** As stated many times in this work, the first and foremost requirement is for the building structure to include complete lateral and vertical force-resisting systems capable of providing adequate strength, stiffness, and energy-dissipation capacity to withstand the design ground motions within the prescribed limits of deformation and strength demand. The design ground motions shall be assumed to occur along any horizontal direction of a building structure. The adequacy of the structural systems shall be demonstrated through the construction of a mathematical model and the evaluation of this model for the effects of design ground motions.

**Member design, connection design, and deformation limit:** Individual members, including those not part of the seismic force-resisting system, shall be provided with adequate strength to resist the shears, axial forces, and moments. Connections shall develop the strength of the connected members or the forces determined by the analysis. The deformation of the structure shall not exceed the prescribed limits where the structure is subjected to the design seismic forces.

**Continuous load path and interconnection:** A continuous load path, or paths, with adequate strength and stiffness shall be provided to transfer all forces from the point of application to the final point of resistance. All parts of the structure shall be interconnected to form a continuous path to the seismic force-resisting system, and the connections shall be capable of transmitting the seismic force,  $F_p$ , induced by the parts being connected. Any smaller portion of the structure shall be tied to the remainder of the structure with elements having a design strength capable of transmitting a seismic force of 0.133 times the short-period design spectral response acceleration parameter,  $S_{DS}$ , times the weight of the smaller portion or 5% of the portion's weight, whichever is greater. Connection design forces need not exceed the maximum forces that the structural system can deliver to the connection.

**Connection to supports:** A positive connection for resisting a horizontal force acting parallel to the member for each beam, girder, or truss is provided either directly to its supporting elements or to slabs designed to act as diaphragms. Where the connection is through a diaphragm, then the member's supporting element must also be connected to the diaphragm. The connection shall have minimum design strength of 5% of the dead plus live load reaction (same as the SDC A requirements).

**Foundation design:** The foundation shall be designed to resist the forces developed and accommodate the movements imparted to the structure by the design ground motions. Include in the foundation design criteria the dynamic nature of the forces, the expected ground motion, the design basis for strength and energy-dissipation capacity of the structure, and the dynamic properties of the soil.

### 5.6.2 STRUCTURAL SYSTEM SELECTION

Select a system that conforms to one of the types shown in AISC Table 12.12.1. If you want to use a system that is not in the table, you may do so, but the catch is you are required to backup the seismic performance of your system with analytical and test data that establish its energy-dissipation capacity and dynamic performance. The seismic coefficients,  $R$ ,  $\Omega_o$ , and  $C_d$ , used for your system should be the same as for the system being duplicated.

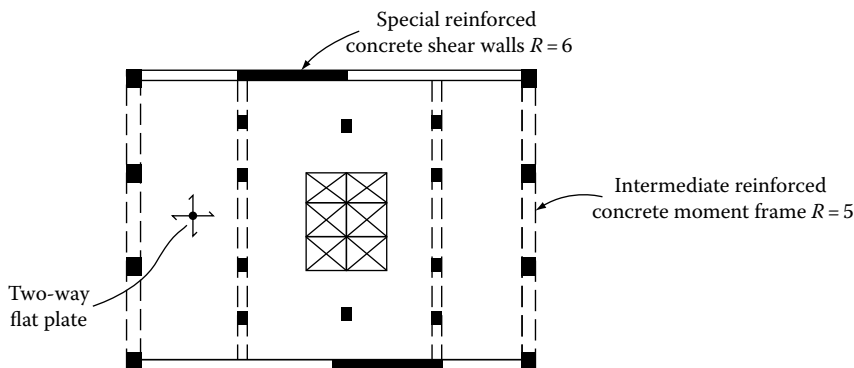


Note that all systems indicated in the table may be used for SDC B buildings without height limits, except for cantilevered column systems that have a height limit of 35 ft.

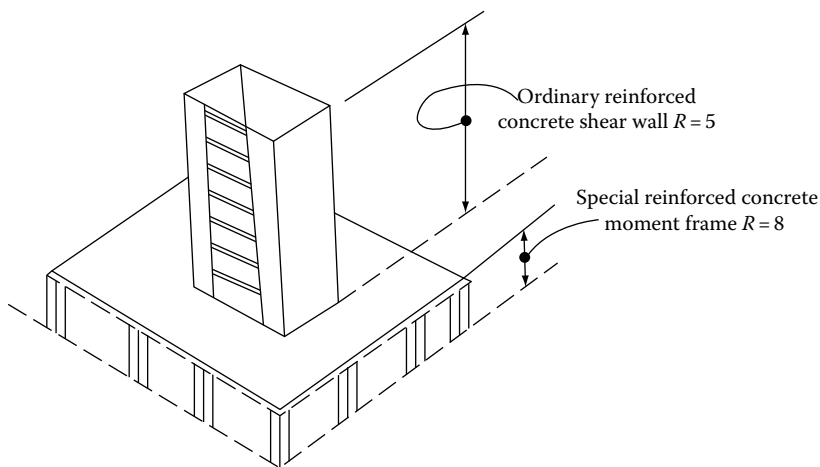
**Combinations of framing systems along two orthogonal axes:** Different seismic force-resisting systems are permitted to be used to resist seismic forces along each of the two orthogonal axes of the structure. Where different systems are used, the respective  $R$ ,  $C_d$ , and  $\Omega_o$  coefficients shall apply to each system (see Figure 5.35).

**Combinations of framing systems in the same direction:** Where different seismic force-resisting systems are used in combination to resist seismic forces in the same direction of structural response, other than those combinations considered as dual systems, the more stringent system limitation shall apply.

**$R$ ,  $C_d$ , and  $\Omega_o$  values for vertical combinations:** The value of the response modification coefficient,  $R$ , used for design at any story shall not exceed the lowest value of  $R$  that is used in the same direction at any story above that story (see Figure 5.36). Likewise, the deflection amplification factor,  $C_d$ , and the system overstrength factor,  $\Omega_o$ , used for the design at any story shall not be less than the largest value of this factor that is used in the same direction at any story above that story.



**FIGURE 5.35** Different systems used along two orthogonal axes; use appropriate value of  $R$  for each system.



**FIGURE 5.36** Different systems used over the height of a structure. The response modification coefficient,  $R$ , for any story above, shall not exceed the lowest value, in the direction under consideration.

A two-stage equivalent lateral-force procedure is permitted to be used with structures having a flexible upper portion above a rigid lower portion, provided that the design of the structure complies with the following:

1. The stiffness of the lower portion must be at least 10 times the stiffness of the upper portion.
2. The period of the entire structure shall not be greater than 1.1 times the period of the upper portion considered as a separate structure fixed at the base.
3. The flexible upper portion shall be designed as a separate structure using the appropriate values of  $R$  and  $\rho$ .
4. The rigid lower portion shall be designed as a separate structure using the appropriate values of  $R$  and  $\rho$ . The reactions from the upper portion shall be those determined from the analysis of the upper portion amplified by the ratio of the upper portion over  $R/\rho$  of the lower portion. This ratio shall not be less than 1.0.

**$R$ ,  $C_d$ , and  $\Omega_o$  values for horizontal combinations:** Where the combination of different structural systems is used to resist lateral forces in the same direction, the value of  $R$  used for design in that direction shall not be greater than the least value of any of the systems utilized in that direction. Resisting elements are permitted to be designed using the least value of  $R$  for the different structural systems found in each independent line of resistance if the following three conditions are met: (1) Occupancy Category I or II building, (2) two stories or less in height, and (3) the use of light-frame construction or flexible diaphragms. The value of  $R$  used for the design of diaphragms in such structures shall not be greater than the least value for any of the systems utilized in the direction.

The deflection amplification factor,  $C_d$ , and the system over the factor,  $\Omega_o$ , in the direction under consideration at any story shall not be less than the largest value of this factor for the  $R$  factor used in the same direction being considered.

**Combination framing detailing requirements:** Structural components common to different framing systems used to resist seismic motions in any direction shall be designed using the detailing requirements required by the highest modification coefficient,  $R$ , of the connected framing systems.

**System-specific requirements:** The structural framing shall also comply with the following system-specific requirements of this section:

- *Dual system.* For a dual system, the moment frames shall be capable of resisting at least 25% of the design forces. The total seismic force resistance is to be provided by the combination of the moment frames and the shear walls or frames in proportion to their rigidities.
- *Cantilever column systems.* The load on individual cantilever column elements calculated in accordance with the applicable load combinations shall not exceed 15% of the design strength of the column to resist axial loads alone. The foundation and other elements used to provide overturning resistance at the base of cantilever column elements shall have the strength to resist the load combinations with overstrength factor.
- *Inverted pendulum-type structures.* Supporting columns or piers of inverted pendulum-type structures shall be designed for bending moment calculated at the base determined using the ELF procedure and varying uniformly to a moment at the top equal to one-half the calculated bending moment at the base.

### 5.6.3 DIAPHRAGMS

The structural analysis shall consider the relative stiffness of diaphragms and the vertical elements of the seismic force-resisting system. Unless a diaphragm can be idealized as either flexible or rigid the structural analysis shall explicitly include the consideration of the stiffness of the

diaphragm by modeling semirigid diaphragm. Diaphragms of concrete slabs with span-to-depth ratios of 3 or less in structures that have no horizontal irregularities are permitted to be idealized as rigid. They may be idealized as flexible where the computed maximum in-plane deflection of the diaphragm under lateral load is more than two times the average story drift of adjoining vertical elements of the seismic force-resisting system of the associated story under equivalent tributary lateral load. The loadings used for this calculation shall be based on ELF procedures.

### 5.6.3.1 Irregularities

Structures assigned to SDC E or F having extreme torsional, soft story, weak story, or extreme weak story irregularity shall not be permitted. Structures assigned to SDC D having extreme weak story irregularity shall not be permitted. Structures in SDCs B and C with extreme weak story irregularity shall not be over two stories or 30 ft (9 m) in height, unless the weak story is capable of resisting load combinations with overstrength factor,  $\Omega_o$ .

Columns, beams, trusses, or slabs supporting discontinuous walls or frames of structures having out-of-plane or in-plane discontinuity in vertical lateral force-resisting element irregularity shall have the design strength to resist the maximum axial force that can develop in accordance with the load combinations with overstrength factor. The connections of such discontinuous elements to the supporting members shall be adequate to transmit the forces for which the continuous elements were required to be designed.

For structures assigned to SDC D, E, or F and having any horizontal structural irregularity except Type A or in-plane discontinuity in vertical lateral force-resisting element irregularity, the design forces shall be increased 25% for connections of diaphragms to vertical elements. Collectors and their connections also shall be designed for these increased forces unless they are designed for the load combinations with overstrength factor.

### 5.6.4 SEISMIC LOAD EFFECTS AND COMBINATIONS

The letter E of the English language is the notation used for representing the earthquake loads. In general, it represents the combination of horizontal and vertical effects of earthquake loads. Thus,  $E = E_h + E_v$ . Used in conjunction with other suffixes, it represents the whole spectrum of earthquake effects shown below:

- Horizontal load without redundancy factor:  $E_h = Q_E$
- Horizontal load including redundancy factor:  $E_h = \rho Q_E$
- Vertical load:  $E_v = \pm 0.2 S_{DS} D$
- Maximum horizontal load including overstrength factor  $\Omega_o$ :  $E_{mh} = \Omega_o E_h$
- Maximum effect of both horizontal and vertical loads including overstrength factor:  

$$E_m = E_{mh} \pm E_v = \Omega_o Q_E \pm 0.2 S_{DS} D$$

The symbol E encompasses the axial, shear, flexural, and torsional forces resulting from both horizontal and vertical seismic forces. Until recently (1997), vertical accelerations, although were recognized as effecting the seismic response, were not codified in seismic design. Now it is required for structures in SDC B and above. It should be noted that when calculating the maximum seismic loads,  $E_m$ , the overstrength factor,  $\Omega_o$ , is applied only to horizontal forces,  $Q_E$ , by assuming the redundancy factor equal to 1.0. In summary, earthquake load effects are as follows:

- **Without overstrength factor**

$$\begin{aligned} E &= E_h \pm E_v \\ &= \rho Q_E \pm 0.2 S_{DS} D \end{aligned}$$

- **With overstrength factor,  $\Omega_o$**

$$\begin{aligned} E_m &= E_{mh} \pm E_v \\ &= \Omega_o Q_E \pm 0.2 S_{DS} D \end{aligned}$$

- **Load combinations without overstrength factor**

$$(1.2 + 0.2 S_{DS}) D + \rho Q_E + L \text{ (compression controlled)}$$

$$(0.9 - 0.2 S_{DS}) D + \rho Q_E \text{ (tension controlled)}$$

- **Load combinations with overstrength factor,  $\Omega_o$**

$$(1.2 + 0.2 S_{DS}) D + \Omega_o Q_E + L \text{ (compression controlled)}$$

$$(0.9 - 0.2 S_{DS}) D + \Omega_o Q_E \text{ (tension controlled)}$$

The reader is referred to ASCE 7-05, Section 12.4.2.3 for load combinations including snow load,  $S$ , and lateral earth pressure, ground water pressure, or pressure due to bulk materials,  $H$ .

During an earthquake, the building in addition to moving back and forth, also moves up and down albeit not with the same intensity. When subjected to downward accelerations, the resulting vertical forces are additive to the gravity forces, and the opposite is true when the building is subjected to vertically upward accelerations. Hence the plus-or-minus sign ( $\pm$ ), for the forces associated with the vertical accelerations.

A comment on the determination of  $E_{mh}$ , the horizontal force that includes the overstrength factor,  $\Omega_o$ . The value of  $E_{mh}$  need not exceed the maximum force that can develop in the element as determined by a rational, plastic mechanism analysis or nonlinear response analysis utilizing realistic expected values of material strengths. And finally in structures assigned to SDC D, E, or F, horizontal cantilever structural components shall be designed for a minimum net upward force of 0.2 times the dead load.

### 5.6.5 DIRECTION OF LOADING

The directions of the application of seismic forces used in the design shall be those which will produce the most critical load effects.

**SDC B.** For structures assigned to SDC B, the design seismic forces are permitted to be applied independently in each of two orthogonal directions and orthogonal interaction effects are permitted to be neglected.

**SDC C.** Structures assigned to SDC D and above, which have nonparallel systems irregularity, shall use one of the following procedures:

1. *Orthogonal combination procedure.* The structure shall be analyzed using the equivalent lateral force analysis procedure, the modal response spectrum analysis procedure, or the linear response history procedure. With the loading applied independently in any two orthogonal directions and the most critical load effect due to the direction of the application of seismic forces on the structure is permitted to be assumed to be satisfied if components and their foundations are designed for the following combination

of prescribed loads: 100% of the forces for one direction plus 30% of the forces for the perpendicular direction; the combination requiring the maximum component strength shall be used.

2. *Simultaneous application of orthogonal ground motion.* The structure shall be analyzed using the linear response history procedure or the nonlinear response history procedure with orthogonal pairs of ground motion acceleration histories applied simultaneously.

**SDCs D through F.** Any column or wall that forms part of two or more intersecting seismic force-resisting systems and is subjected to axial load due to seismic forces acting along either principal plan axis equaling or exceeding 20% of the axial design strength of the column or wall shall be designed for the most critical load effect due to the application of seismic forces in any direction. Either of the two previous procedures, a or b, are permitted to be used to satisfy this requirement.

### 5.6.6 ANALYSIS PROCEDURE

Three types of analysis are permitted based on the SDC of the structure, structural system, dynamic properties, and regularity:

1. ELF procedure
2. Model response spectrum analysis
3. Linear elastic and nonlinear time-history procedures

Today (2009), model response analysis is by far the most common procedure.

### 5.6.7 MODELING CRITERIA

**Foundation modeling:** For purposes of determining seismic loads, it is permitted to consider the structure to be fixed at the base. Alternatively, where foundation flexibility is considered, it shall be in accordance with Section 12.13.3 or Chapter 19 of ASCE 7-05.

**Effective seismic weight:** The effective seismic weight,  $W$ , of a structure shall include the total dead load and other loads listed below:

1. In areas used for storage, a minimum of 25% of the floor live load (floor live load in public garages and open parking structures need not be included)
2. Where provision for partitions is required in the floor load design, the actual partition weight or a minimum weight of 10 psf (0.48 kN/m<sup>2</sup>) of floor area, whichever is greater
3. Total operating weight of permanent equipment
4. Where the flat roof snow load exceeds 30 psf, 20% of the uniform design snow load regardless of actual roof slope

**Structural modeling:** A mathematical model of the structure shall be constructed for the purpose of determining member forces and structure displacements resulting from applied loads and any imposed displacements or  $PA$  effects. The model shall include the stiffness and strength of elements that are significant to the distribution of forces and deformations in the structure and represent the spatial distribution of stiffness throughout the structure.

Structures that have horizontal structural irregularity Type 1a, 1b, 4, or 5 of Table 12.3-1 of ASCE 7-05 shall be analyzed using a 3D representation. Where a 3D model is used, a minimum of three dynamic DOFs consisting of translation in two orthogonal plan directions and torsional

rotation about the vertical axis shall be included at each level of the structure. Where the diaphragm have not been classified as rigid or flexible, the model shall include the representation of the diaphragm's stiffness characteristics and such additional dynamic DOFs are required to account for the participation of the diaphragm in the structure's dynamic response.

**Interaction effects:** Moment-resisting frames that are enclosed or adjoined by elements that are more rigid and not considered to be part of the seismic force-resisting system shall be designed so that the action or failure of those elements will not impair the vertical load and seismic force-resisting capability of the frame. The design shall provide for the effect of these rigid elements on the structural system at structural deformations corresponding to the design story drift ( $\Delta$ ). In addition, the effects of these elements shall be considered where determining whether a structure has one or more of the irregularities.

### 5.6.8 MODAL ANALYSIS

**Number of modes:** The analysis shall include a sufficient number of modes to obtain a combined modal mass participation of at least 90% of the actual mass in each of the orthogonal horizontal directions of response considered by the model.

**Modal response parameters:** The value for each design parameter of interest, including story drifts, support forces, and individual member forces for each mode of response, shall be computed using the properties of each mode and the response spectra divided by the quantity  $R/I$ . The value for displacement and drift quantities shall be multiplied by the quantity  $C_d/I$ .

**Combined response parameters:** The value calculated for the various modes shall be combined using either the SRSS or the CQC method. The CQC method shall be used for each of the modal values or where closely spaced modes that have significant cross-correlation of translations and torsional response.

**Scaling design values of combined response:** A base shear ( $V$ ) shall be calculated in each of the two orthogonal horizontal directions using the calculated fundamental period of the structure  $T$  in each direction except where the calculated fundamental period exceeds  $C_u T_a$ , then  $C_u T_a$  shall be used in lieu of  $T$  in that direction. When the combined response for the modal base shear ( $V_l$ ) is less than 85% of the calculated base shear ( $V$ ) using the ELF procedure, the forces, but not the drifts, shall be multiplied by  $0.85V/V_l$ , where  $V$  is the ELF procedure base shear and  $V_l$  is the base shear from modal combination.

**Horizontal shear distribution:** The distribution of horizontal shear shall be based on the relative lateral stiffness of the vertical resisting elements and diaphragm. The amplification of torsion is not required where accidental torsional effects are included in the dynamic analysis model.

**$P\Delta$  Effects:** The  $P\Delta$  effects shall be determined by using the index procedure or by including the effects in an automated analysis.

**Soil structure interaction reduction:** A soil structure interaction reduction is permitted where determined using procedures as outlined in Chapter 19 of ASCE 7-05, and generally accepted procedures approved by authority having jurisdiction.

### 5.6.9 DIAPHRAGMS, CHORDS, AND COLLECTORS

**Diaphragm design.** Diaphragms shall be designed for both the shear and bending stresses resulting from design forces. At diaphragm discontinuities, such as openings and reentrant corners, the design shall assure the dissipation or transfer of edge (chord) forces combined with other forces in the diaphragm within shear and tension capacity of the diaphragm.

**Diaphragm design forces:** Floor and roof diaphragms shall be designed to resist design seismic force from the structural analysis, but shall not be less than that determined in accordance with the following equation:

$$F_{px} = \frac{\sum_{i=x}^n F_i}{\sum_{i=x}^n W_i} W_{px}$$

where

$F_{px}$  is the diaphragm design force at level  $x$

$F_i$  is the design force applied to level  $i$

$W_i$  is the weight tributary to level  $i$

$W_{px}$  is the weight tributary to the diaphragm at level  $x$

The force determined from the above equation need not exceed  $0.4S_{DS}IW_{px}$ , but shall not be less than  $0.2S_{DS}IW_{px}$ .

Where the diaphragm is required to transfer design seismic force from the vertical resisting elements below the diaphragm due to offsets in the placement of the elements or to changes in relative lateral stiffness in the vertical elements, these forces,  $V_{px}$ , shall be added to those determined from the above equation.

The redundancy factor,  $\rho$ , applies to the design of diaphragms in structures assigned SDC D, E, or F. For floor inertial forces, the redundancy factor shall equal 1.0. For the transfer forces,  $V_{px}$ , the redundancy factor,  $\rho$ , shall be the same as that used for the structure. For SDC D and above structures that have any of the horizontal irregularities other than nonparallel system irregularity, the design forces shall be increased by 25% for the connection of diaphragms to vertical elements and to collectors and for the connection of collectors to the vertical elements. A similar increase is required if the building has a vertical irregularity of in-plane discontinuity in vertical lateral force-resisting elements.

**Collector elements:** Collector elements shall be provided that are capable of transferring the seismic forces originated in other portions of the structure to the element providing the distance to those forces.

**Collector elements requiring load combinations with overstrength factor for SDCs C through F:** In structures assigned to SDC C, D, E, or F, collector elements, splices, and their connections to resisting elements shall resist the load combinations with overstrength.

## 5.6.10 STRUCTURAL WALLS AND THEIR ANCHORAGE

**Design for out-of-plane forces:** Structural walls and their anchorage shall be designed for a force normal to the surface equal to  $0.45S_{DS}I$  times the weight of the structural wall. The interconnection of structural wall elements and connections supporting framing system shall have sufficient ductility, rotational capacity, or sufficient strength to resist shrinkage, thermal changes, and differential foundation settlement when combined with seismic forces.

**Anchorage of concrete structural walls:** The anchorage of concrete walls to supporting construction shall provide a direction connection capable of resisting the greater of the following:

1.  $F_p = 0.8S_{DS}IW_p$  [lb/ft]
2.  $F_p = 400S_{DS}I$  [lb/ft]
3.  $F_p = 280$  lb/ft

Structural walls shall be designed to resist bending between anchors where the anchor spacing exceeds 4 ft.

**Anchorage of concrete structural walls to flexible diaphragms:** In addition to the requirements given in the previous paragraphs, the anchorage of concrete or masonry structural walls to flexible diaphragms in structures assigned to SDC C, D, E, or F shall have the strength to develop the out-of-plane force given by the following:

$$F_p = 0.8S_{DS}IW_p$$

where

$F_p$  is the design force in the individual anchors

$S_{DS}$  is the design spectral response acceleration parameter at short periods

$I$  is the occupancy importance factor

$W_p$  is the weight of the wall tributary to the anchor

### 5.6.11 DRIFT AND DEFORMATION

**Story-drift limit:** The design story drift ( $\Delta$ ) shall not exceed the allowable story drift ( $\Delta_a$ ) as obtained from Table 5.22 (Table 12.12-1 of ASCE 7-05), for any story. For structures with significant

**TABLE 5.22**  
**Allowable Story Drift,  $\Delta_a^{a,b}$**

Structure	Occupancy Category		
	I or II	III	IV
Structures, other than masonry shear wall structures, four stories or less with interior walls, partitions, ceilings and exterior wall systems that have been designed to accommodate the story drifts	$0.025h_{sx}^c$	$0.020h_{sx}$	$0.015h_{sx}$
Masonry cantilever shear wall structures <sup>d</sup>	$0.010h_{sx}$	$0.010h_{sx}$	$0.010h_{sx}$
Other masonry shear wall structures	$0.007h_{sx}$	$0.007h_{sx}$	$0.007h_{sx}$
All other structures	$0.020h_{sx}$	$0.015h_{sx}$	$0.010h_{sx}$

Source: ASCE 7-05, Table 12.12-1.

<sup>a</sup>  $h_{sx}$  is the story height below level  $x$ .

<sup>b</sup> For seismic force-resisting systems comprised solely of moment frames in SDCs D through F, the allowable story drift shall comply with the requirements of Section 12.12.1.1 of ASCE 7-05.

<sup>c</sup> There shall be no drift limit for single-story structures with interior walls, partitions, ceilings, and exterior wall systems that have been designed to accommodate the story drifts. The structure separation requirement of Section 12.12.3 of ASCE 7-05 is not waived.

<sup>d</sup> Structures in which the basic structural system consists of masonry shear walls designed as vertical elements cantilevered from their base or foundation support that are so constructed that moment transfer between shear walls (coupling) is negligible.



torsional deflections, the maximum drift shall include torsional effects. For structures assigned to SDC C, D, E, or F having torsional or extreme torsional irregularity, the design story drift,  $\Delta$ , shall be computed as the largest difference of the deflections along any of the edges of the structure at the top and bottom of the story under consideration.

**Moment frames in structures assigned to SDCs D through F:** For seismic force-resisting systems comprised solely of moment frames in structures assigned to SDCs D, E, or F, the design story drift ( $\Delta$ ) shall not exceed  $\Delta_u/\rho$  for any story.

**Diaphragm deflection:** The calculated deflection in the plane of the diaphragm shall not exceed the permissible deflection of the attached elements. The permissible deflection shall be that deflection that will permit the attached element to maintain its structural integrity under the individual loading and continue to support the prescribed loads.

**Building separation:** All portions of the structure shall be designed and constructed to act as an integral unit in resisting seismic forces unless separated structurally by a distance sufficient to avoid damaging contact under total deflection:

$$\delta_x = \frac{c_d \delta_{xe}}{I}$$

**Deformation compatibility for SDCs D through F:** For structures assigned to SDC D, E, or F, every structural component not included in the seismic force-resisting system in the direction under consideration shall be designed to be adequate for the gravity load effects and the seismic forces resulting from displacement to the design story drift  $\Delta = \frac{c_d \delta_{xe}}{I}$ .

**Exception:** Reinforced concrete frame members not designed as part of the seismic force-resisting system shall comply with Section 21.9 of ACI 318-05.

Where determining the moments and shears induced in components that are not included in the seismic force-resisting system in the direction under consideration, the stiffening effects of adjoining rigid structural and nonstructural elements shall be considered and a rational value of member and restraint stiffness shall be used.

## 5.6.12 FOUNDATION DESIGN

**Foundation load-deformation characteristics:** Where foundation flexibility is included for the linear analysis procedures, the load-deformation characteristics of the foundation-soil system (foundation stiffness) shall be modeled. The linear load-deformation behavior of foundations shall be represented by an equivalent linear stiffness using soil properties that are compatible with the soil strain levels associated with the design earthquake motion. The strain-compatible shear modulus,  $G$ , and the associated strain compatible shear wave velocity,  $v_s$ , needed for the evaluation of equivalent linear stiffness shall be determined using the a site-specific study. A 50% increase and decrease in stiffness shall be incorporated in dynamic analyses unless smaller be justified based on field measurements of dynamic soil properties or direct measurements of dynamic foundation stiffness. The largest values of response shall be used in design.

**Reduction of foundation overturning:** Overturning effects at soil-foundation interface are permitted to be reduced by 25% for foundations of structures that satisfy both the following conditions:

1. The structure is designed in accordance with the ELF analysis.
2. The structure is not an inverted pendulum or cantilevered column-type structure.

Overturning effects at the soil–foundation interface are permitted to be reduced by 10% for foundations of structures designed in accordance with the modal analysis requirements.

#### 5.6.12.1 Foundation Requirements for Structures Assigned to Seismic Design Category C

**Pole-type structures:** Where construction employing posts or poles as columns embedded in the earth or embedded in concrete footings in the earth is used to resist lateral loads, the depth of embedment required for posts or poles to resist seismic forces shall be determined by means of the design criteria established in the foundation investigation report.

**Foundation ties:** Individual pile caps, drilled piers, or caissons shall be interconnected by ties. All ties shall have a design strength in tension or compression at least equal to a force equal to 10% of  $S_{DS}$  times the larger pile cap or column design dead plus factored live load unless it is demonstrated that equivalent restraint will be provided by reinforced concrete beams within slabs on grade or reinforced concrete slabs on grade or confinement by competent rock, hard cohesive soils, very dense granular soils, or other approved means.

**Pile anchorage requirements:** Where required for resistance to uplift forces, anchorage of steel pipe (round HSS sections), concrete-filled steel pipe, or H piles to the pile cap shall be made by means other than concrete bond to the bare steel section.

**Exception:** The anchorage of concrete-filled steel pipe piles is permitted to be accomplished using deformed bars developed into the concrete portion of the pile.

#### 5.6.12.2 Foundation Requirements for Structures Assigned to Seismic Design Categories D, E, or F

The design and construction of concrete foundation components shall conform to the requirements of ACI 318-05, Section 21.8, except as modified as follows:

**Pole-type structures:** Where construction employing posts or poles as columns embedded in the earth or embedded in concrete footings in the earth is used to resist lateral loads, the depth of embedment required for posts or poles to resist seismic forces shall be determined by means of the design criteria established in the foundation investigation report.

**Foundation ties:** Individual pile caps, drilled piers, or caissons shall be interconnected by ties. In addition, individual spread footings founded on soil as Site Class E or F soil shall be interconnected by ties. All ties shall have a design strength in tension or compression at least equal to a force equal to 10% of  $S_{DS}$  times the larger pile cap or column factored dead plus factored live load unless it is demonstrated that equivalent restraint will be provided by reinforced concrete beams within slabs on grade or reinforced concrete slabs on grade or confinement by competent rock, hard cohesive soils, very dense granular soils, or other approved means.

**General pile design requirement:** Piling shall be designed and constructed to withstand deformations from earthquake ground motions and structure response. Deformations shall include both free-field soils strains (without the structure) and deformations induced by lateral pile resistance to structure seismic forces, all as modified by soil–pile interaction.

**Batter piles:** Where vertical and batter piles act jointly to resist foundation forces as a group, these forces shall be distributed to the individual piles in accordance with their relative horizontal and vertical rigidities and the geometric distribution of the piles within the group.

**Pile anchorage requirements:** The design of the anchorage of piles into the pile cap shall consider the combined effect of axial forces due to uplift and bending moments due to fixity to the pile cap. For piles required to resist uplift forces or provide rotational restraint, anchorage into the pile cap shall be capable of developing the following:

1. In the case of uplift, the lesser of the nominal tensile strength of the longitudinal reinforcement in a concrete pile, the nominal tensile strength of a steel pile, 1.3 times the pile pullout resistance, or the axial tension force resulting from the load combinations with overstrength. The pile pullout resistance shall be taken as the ultimate frictional or adhesive force that can be developed between the soil and the pile plus the pile weight.
2. In the case of rotational restraint, the lesser of the axial and shear forces and moments resulting from the load combinations with overstrength factor  $\Omega_o$  or the development of the full axial, bending, and shear nominal strength of the pile.

**Splices of pile segments:** Splices of pile segments shall develop the nominal strength of the pile section, but the splice need not develop the nominal strength of the pile in tension, shear, and bending where it has been designed to resist axial and shear forces and moments from the load combinations with overstrength factor.

**Pile–soil interaction:** Pile moments, shears, and lateral deflections used for design shall be established considering the interaction of the shaft and soil. Where the ratio of the depth of embedment of the pile to the pile diameter or width is less than or equal to 6, the pile is permitted to be assumed to be flexurally rigid with respect to the soil.

**Pile group effects:** Pile group effects from soil on lateral pile nominal strength shall be included where pile center-to-center spacing in the direction of lateral force is less than eight pile diameters or widths. Pile group effects on vertical nominal strength shall be included where pile center-to-center spacing is less than three pile diameters or widths.

## 5.7 ASCE 7-05, SEISMIC DESIGN: AN IN-DEPTH DISCUSSION

The seismic provisions of ASCE 7-05, like its predecessors, present criteria for the design and construction of new structures subject to earthquake ground motions. The goal is to minimize the hazard to life for all structures, to increase the expected performance of structures having a substantial public hazard due to occupancy or use as compared to ordinary structures, and to improve the capability of essential facilities to function after an earthquake. To this end, ASCE 7-05 provides the minimum criteria considered prudent for the protection of life safety in structures subject to earthquakes.

Some structural and nonstructural damages can be expected as a result of the “design ground motions” because the provisions allow inelastic energy dissipation in the structural system. For ground motions in excess of the design levels, the intent is for the structure to have a low likelihood of collapse.

It must be emphasized that absolute safety and no damage even in an earthquake event with a reasonable probability of occurrence cannot be achieved for most structures. However, a high degree of life safety, albeit with some structural and nonstructural damages, can be achieved economically in structures by allowing inelastic energy dissipation in the structure. The objective therefore is to set forth the minimum requirements to provide reasonable and prudent life safety. For most structures designed and constructed according to the ASCE 7-05 provisions, it is expected that structural damage from even a major earthquake would likely be repairable, but the damage may not be economically repairable.

Where damage control is desired, the design must provide not only sufficient strength to resist the specified seismic loads but also the proper stiffness to limit the lateral deflection. The damage to nonstructural elements may be minimized by the proper limitation of deformations; by careful attention to detail; and by providing the required clearances for exterior cladding, glazing, partitions, and wall panels. The nonstructural elements can be separated or floated free and

allowed to move independently of the structure. If these elements are tied rigidly to the structure, they should be protected from deformations that can cause cracking. Otherwise, one must expect damage to these nonstructural elements. It should be recognized, however, that major earthquake ground motions can cause deformations much larger than the specified drift limits in the provisions.

Where prescribed wind loading governs the stress or drift design, the resisting system still must conform to the special requirements for seismic force-resisting systems. This is required in order to resist, in a ductile manner, potential seismic loading in excess of the prescribed loads.

A proper, continuous load path is an obvious design requirement for equilibrium, but experience has shown that it often is overlooked and that significant damage and collapse can result. The basis for this design requirement is twofold:

1. To ensure that the design has fully identified the seismic force-resisting system and its appropriate design level
2. To ensure that the design basis is fully identified for the purpose of future modifications or changes in structure.

*The ASCE 7-05 commentaries on the seismic provisions of Chapters 11 and 12 do not attempt to explain the earthquake provisions in great detail. Instead, the reader is referred to two sources: (1) NEHRP, 2003 edition commentary and (2) SEAOC 1999 Blue Book. Much of the material given in the following sections is based on these two references. They are included here in a doctored-up format to assist design professionals seeking a deeper understanding of the basis and limits of the seismic provisions.*

### 5.7.1 SEISMIC DESIGN BASIS

Structural design for acceptable seismic resistance includes

1. The selection of gravity and seismic force-resisting systems that are appropriate to the anticipated intensity of ground shaking.
2. The layout of these systems such that they provide a continuous, regular, and redundant load path capable of ensuring that the structures act as integral units in responding to ground shaking.
3. The proportioning of the various members and connections such that adequate lateral and vertical strength and stiffness is present to limit damage in a design earthquake to acceptable levels.

The proportioning of structural elements (sizing of individual members, connections, and supports) is typically based on the distribution of internal forces computed based on linear elastic response spectrum analyses using response spectra that are representative of, but substantially reduced from, the anticipated design ground motions. As a result, under the severe levels of ground shaking anticipated in many regions of the nation, the internal forces and the deformation produced in most structures will substantially exceed the point at which elements of the structures start to yield or buckle and behave in an inelastic manner. This approach can be taken because historical precedent and the observation of the behavior of structures that have been subjected to earthquakes in the past demonstrates that if suitable structural systems are selected and structures are detailed with appropriate levels of ductility, regularity, and continuity, it is possible to perform an elastic design of structures for reduced forces and still achieve acceptable performance. Therefore, the ASCE provisions adopt the approach of proportioning structures such that under prescribed design lateral forces that are significantly reduced, by the response modification coefficient  $R$ , from those

that would actually be produced by a design earthquake, they will not deform beyond a point of significant yield. The elastic deformations calculated under these reduced design forces are then amplified by the deflection amplification factor  $C_d$  to estimate the expected deformations likely to be experienced in response to the design ground motion. Considering the intended structural performance and acceptable deformation levels, the story-drift limits are prescribed for the expected (amplified) deformations.

The term “significant yield” is not the point where first yield occurs in any member but, rather, is defined as that level causing the complete plastification of at least the most critical region of the structure. A concrete frame reaches significant yield when at least one of the sections of its most highly stressed component reaches its strength. This requirement contemplates that the design includes a seismic force-resisting system with redundant characteristics wherein significant structural overstrength above the level of significant yield can be obtained by plastification at other points in the structure prior to the formation of a complete mechanism. Significant yield is the level where plastification occurs at the most heavily loaded element in the structure, shown as the lowest yield hinge on the load-deflection diagram. With increased loading, causing the formation of additional plastic hinges, the capacity increases until a maximum is reached. The overstrength capacity obtained by this continued inelastic action provides the reserve strength necessary for the structure to resist the extreme motions of the actual seismic forces that may be generated by the design ground motion.

## 5.7.2 STRUCTURAL SYSTEM SELECTION

For purposes of seismic analyses and design, cast-in-place concrete systems may be grouped into categories shown in Tables 5.10 through 5.14. Although as many as 15 systems are shown there in, they all stem from a basic list of 5. These are

1. Ordinary reinforced concrete moment frames
2. Intermediate reinforced concrete moment frames
3. Special reinforced concrete moment frames
4. Ordinary reinforced concrete shear walls
5. Special reinforced concrete shear walls

Ordinary shear walls and ordinary moment frames represent structures in regions where anticipated ground motions are minor, even for very long return periods. In fact, most of the buildings in the United States are built using these two systems, which may be called as work horse of the building industry. Ordinary shear walls may comprise of planar solid walls, coupled shear walls, or 3D core walls.

Intermediate moment frames, as the name implies, are those with seismic details somewhere in-between ordinary and special moment frames. Their detailing imparts limited ductility to the system allowing their use in regions of moderate seismicity.

The current ACI 318-08, like its predecessors, does not distinguish intermediate shear walls from ordinary shear walls in cast-in-place concrete systems. The detailing requirements specified for ordinary shear walls are deemed sufficient to provide for the limited ductility required in regions of moderate seismicity. Hence, they are permitted in buildings assigned to SDCs A, B, and C.

Special moment frames and special shear walls are detailed to respond with a high degree of ductility when subjected to design earthquakes, and hence they are the only systems permitted in regions of high seismicity (SDC D and above) without height limits.

### 5.7.2.1 Bearing Wall System

In this system, support for all or major portions of the vertical loads are provided by bearing walls. Shear walls provide seismic force resistance. In general, this system has comparably lower values

of  $R$  than the other systems due to the frequent lack of redundancy for the vertical and horizontal load supports.

### 5.7.2.2 Building Frame System

In this system, gravity loads are carried primarily by a complete space frame supported on columns rather than by bearing walls. Some minor portions of the gravity load may be carried on bearing walls, but the amount so carried should not represent more than a few percent of the building area. Lateral resistance is provided by structural walls. It is a good practice to provide for continuity and to have the full anchorage of longitudinal reinforcement and stirrups over the full length of beams and girders framing into columns. With this detail, the frame becomes capable of providing a nominal secondary line of resistance even though the components of the seismic force-resisting system are designed to carry all of the seismic force.

The mere presence of a load bearing wall does not necessarily mean that a building should be classified as a bearing wall system. Where there is doubt as to the type of system, the final decision should be made through consultation with the building official.

### 5.7.2.3 Moment Frame System

A moment frame is a system that has an essentially complete space frame for resisting gravity loads. The primary lateral resistance is provided by moment-resisting frames composed of columns with interacting beams or girders. Moment-resisting frames may be either ordinary, intermediate, or special moment frames as required by the SDCs.

*Special moment frames* are for high-end seismic design. They must meet all the stringent design and ductile-detailing requirements. They are appropriate for structures anticipated to experience large inelastic demands. For this reason, they are required in zones of high seismicity with large anticipated ground shaking accelerations. In zones of lower seismicity, the inherent overstrength in typical structural designs is such that the anticipated inelastic demands are somewhat reduced, and less ductile systems may be safely employed. For buildings in which these special designs and detailing requirements are not used, lower  $R$  values are specified indicating that ordinary framing systems do not possess as much toughness.

### 5.7.2.4 Dual System

This system consists of a 3D space frame with columns and beams providing primary support for gravity loads. Primary lateral resistance is supplied by structural walls. The frame, as a redundant lateral force-resisting system, acts as a backup. The moment frame is required to be capable of resisting at least 25% of the specified seismic force. This percentage mandated in ASCE 7-05 is based on judgment. The walls acting together with the moment frame must be capable of resisting all of the design seismic force. The following analyses are required for dual systems:

1. The frame and shear walls must resist the prescribed lateral seismic force in accordance with their relative rigidities considering fully the interaction of the walls and the moment frames as a single system. This analysis must be made considering the relative rigidities of the elements and torsion in the system. Deformations imposed upon members of the moment frame by their interaction with the shear walls must be considered in this analysis.
2. The moment frame must be designed to have a capacity to resist at least 25% of the total required lateral seismic force including torsional effects.

As stated previously, the dual system design mandates that the frames have a capacity to carry at least 25% of the design lateral forces independently of the shear walls. The design lateral forces are

the design base shears distributed along the height of the building in a manner prescribed by the ASCE 7-05. For the secondary analysis of the frame alone, no computation of base shears or periods is necessary. The lateral force at every floor is simply one-quarter of the lateral force determined for the combined shear wall-frame system.

A lateral load analysis of a typical dual system will show that almost the entire shear is carried by the shear walls at the base, whereas the frames work the hardest in the upper stories. If columns of frames are designed using the results of the wall-frame analysis, they would be quite frail near the base of the structure where they are needed the most. The 25% backup frame requirements ensures that the columns will be sufficiently strong and stiff near the base. The secondary frame analysis for 25% of the design lateral forces typically governs the design of lower level columns.

### 5.7.3 SPECIAL REINFORCED CONCRETE SHEAR WALL

One of the items that stands out in Table 5.14 is the specific height limits imposed for buildings depending upon their SDC. The table limits the height of special reinforced concrete shear walls in bearing wall systems to 160 ft for buildings in SDCs D and E, and to 100 ft for those in SDC F. The limits are the same for walls used as part of building frame systems. The lateral systems for buildings above these heights are limited to moment frame systems or dual frame systems. The height restrictions apply across the board to special reinforced shear walls irrespective of whether the wall is a planar wall, a coupled wall interconnected with energy absorbing coupling beams, or a 3D core wall. The prescriptive provisions of the ASCE 7-05 do not differentiate between planar walls, coupled walls, and core walls.

In researching the origin of the 160 ft height limit, one learns that the first mention of this limit made in early 1950s was based on the reach of the fire-fighting equipment available at that time, and not on engineering principles. During the 1980s, the 160 ft limit was increased to 240 ft for building frame systems. This 50% height limit, however, has been receded and we are back to the 160 ft limit for both bearing wall and building frame systems.

Today (2008), with the thrust of performance-based design, it appears that engineers particularly those practicing in the West Coast of United States are suggesting that these height restrictions are not absolute and can be exceeded for a variety of building geometrics, including core wall and coupled wall systems dominated by a more ductile response than that associated with a planar shear wall. An in-depth discussion of this trend is given in Chapter 9.

### 5.7.4 DETAILING REQUIREMENTS

As with other materials, the main consideration in reinforced concrete construction for earthquake resistance is the proper detailing of members and connections. The bulk of the detailing requirements are contained in ACI 318-05/08 with its commentary adding the valuable discussion of the rationale behind detailing requirements. A brief summary of design requirements are as follows:

**SDCs A and B.** Special details for ductility and toughness are not required for buildings assigned to SDC A or B. Since ordinary frames are permitted only in SDCs A and B, they are not required to meet any particular seismic requirements. However, attention should be paid to the often overlooked requirement of integrity joint reinforcement.

**SDC C.** A frame used as part of the seismic force-resisting system in SDC C is required to have certain details that are intended to help sustain the integrity of the frame when subjected to deformation reversals into the nonlinear range of response. Such frames must have attributes of intermediate moment frames. Structural walls of buildings in SDC C are to be designed in accordance with the requirements of the first 20 chapters of ACI 318-05/08.

Two sets of moment frame detailing requirements are defined: one for “regions of high seismic risk” and the other for “regions of moderate seismic risk.” The “regions” are made equivalent to SDCs

in which “high risk” means SDCs D and E and “moderate risk” means SDC C. These two frames are labeled the “special moment frame” and the “intermediate moment frame,” respectively.

The level of inelastic energy absorption of the two frames is not the same. Hence, the concept of  $R$  factors is not the same for these two frames. In spite of the fact that the  $R$  factor for the intermediate frame is less than the  $R$  factor of the special frame, the use of the intermediate frame is not permitted in the higher SDCs (SDC D, E, or F). On the other hand, the seismic provisions encourage the consideration of the more stringent detailing practices for the special frame in SDC C because the reward for the use of the higher  $R$  factor can be weighed against the higher cost of the detailing requirements. It should be noted that the intermediate frame may be part of a dual system in SDC C.

The difference in the performance basis of the requirements for the two types of frames may be summarized as follows.

1. The shear strength of beams and columns must not be less than that required when the member has yielded at each end in flexure. For the special frame, strain hardening and other factors are considered by raising the effective tensile strength of the bars to 125% of specified yield. For the intermediate frame, an escape clause is provided in that the calculated shear using double the prescribed seismic force may be substituted. Both types require the same minimum amount and maximum spacing of transverse reinforcement throughout the member.
2. The shear strength of joints is limited and special provisions for anchoring bars in joints exist for special moment frames but not for intermediate frames. Both frames require transverse reinforcement in joints although less is required for the intermediate frame.
3. Closely spaced transverse reinforcement is required in regions of potential hinging (typically the ends of beams and columns) to control the lateral buckling of longitudinal bars after the cover has spalled. The spacing limit is slightly more stringent for columns in the special frame.
4. The amount of transverse reinforcement in regions of hinging for special frames is tied to the concept of providing enough confinement of the concrete core to preserve a ductile response. These amounts are not required in the intermediate frame and, in fact, for beams, stirrups may be used in lieu of hoops.
5. The special frame must follow the strong column/weak beam rule. Although this is not required for the intermediate frame, it is highly recommended for multistory construction.
6. The maximum and minimum amounts of reinforcement are limited to prevent rebar congestion and to assure a non-brittle flexural response. Although the precise limits are different for the two types of frames, a great portion of practical, buildable designs will satisfy both.
7. The minimum amounts of continuous reinforcement to account for moment reversals are required by placing lower limits on the flexural strength at any cross section. Requirements for the two types of frames are similar.
8. Locations for splices of reinforcement are more tightly controlled for the special frame.
9. In addition, the special frame must satisfy numerous other requirements beyond the intermediate frame to assure that member proportions are within the scope of the present research experience on seismic resistance and that analysis, design procedures, qualities of the materials, and inspection procedures are at the highest level of the state of the art.

**SDCs D through F.** The design requirements for structures assigned to SDC D, E, or F are quite extensive to be listed here. For this reason, extensive design examples are given in Chapter 6.

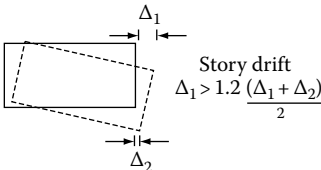
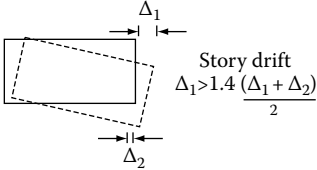
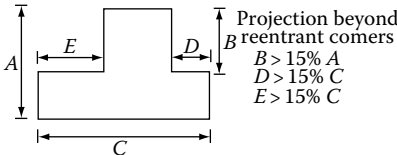
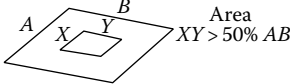
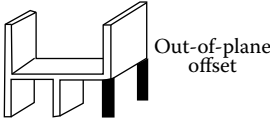
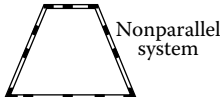
### 5.7.5 BUILDING IRREGULARITIES

Prior to the 1988 UBC, building codes published a list of irregularities defining the conditions, but provided no quantitative basis for determining the relative significance of a given irregularity.



However, starting in 1988, seismic codes have attempted to quantify irregularities by establishing geometrically or by the use of building dimensions, the points at which the specific irregularity becomes an issue as to require extra analysis and design considerations over and above those of the equivalent lateral procedure. The code requirements for determining the presence of irregularity, and the required methods to compensate for it, have now become complex, as can be seen in a graphic interpretation of the irregularities given in Tables 5.23 and 5.24. Observe that the remedial measures range from a simple requirement of a dynamic distribution of lateral forces (e.g., mass irregularity), to special load combination of gravity and seismic forces (e.g., out-of-plane offset irregularity).

**TABLE 5.23**  
**Horizontal Irregularities**

Types of Irregularity	Graphic Interpretation	Remedial Measures	SDC Application
1a. Torsional irregularity	 <p>Story drift <math>\Delta_1 &gt; 1.2 \frac{(\Delta_1 + \Delta_2)}{2}</math></p>	1 2 3 4 5	D through F C through F B through F C through F D through F
1b. Extreme torsion irregularity	 <p>Story drift <math>\Delta_1 &gt; 1.4 \frac{(\Delta_1 + \Delta_2)}{2}</math></p>	6 1 3 2 4 5	E and F D B through D C and D C and D D
2. Reentrant corner irregularity	 <p>Projection beyond reentrant corners <math>B &gt; 15\% A</math> <math>D &gt; 15\% C</math> <math>E &gt; 15\% C</math></p>	1 5	D through F D through F
3. Diaphragm discontinuity irregularity	 <p>Area <math>XY &gt; 50\% AB</math></p>	1 5	D through F D through F
4. Out-of-plane offsets irregularity	 <p>Out-of-plane offset</p>	1 7 3 5	D through F B through F B through F D through F
5. Nonparallel systems irregularity	 <p>Nonparallel system</p>	8 3 5	C through F B through F D through F


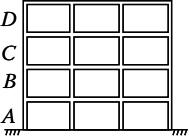

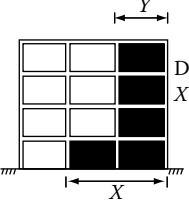
Source: ASCE 7-05, Table 12.3-1.

#### Remedial measures

1. Increase design forces determined by static procedure by 25% for connection of diaphragms to vertical elements and to collectors, and for connections of collectors to the vertical elements. Collectors and their connections also shall be designed for these increased forces unless they are designed for load combinations with overstrength factor  $\Omega_o$  (ASCE 7-05, Section 12.3.3.4).

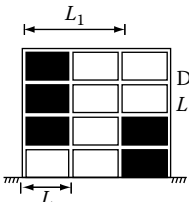
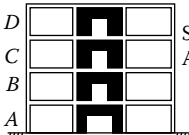
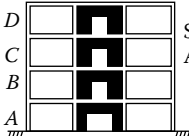
- 2. Multiply,  $M_{ta}$ , the torsional moment due to accidental torsion by a torsional amplification  $A_t = \left( \frac{\delta_{max}}{1.2\delta_{ave}} \right)^2 \leq 3.0$  (ASCE 7-05, Section 12.8.4.3).
- 3. Perform a 3D dynamic analysis with due consideration for diaphragm stiffness. Use cracked section properties for concrete elements. Include  $P\Delta$  effects (ASCE 7-05, Section 12.7.3).
- 4. Compute story drift,  $\Delta$ , as the largest difference of the deflections along any of the edges of the structure at the top and bottom of the story under consideration (ASCE 7-05, Section 12.12.1).
- 5. Use model analysis or more rigorous procedure (ASCE 7-05, Table 12.6.1).
- 6. Not permitted (NP) (ASCE 7-05, Section 12.3.3.1).
- 7. Design columns, beams, trusses, or slabs supporting discontinuous walls or frames to resist maximum axial forces determined by using the following load combinations with the overstrength factor  $\Omega_o$ :  
 $(1.2 + 0.2S_{DS})D + \Omega_o Q_E + L + 0.2S$   
 $(0.9 - 0.2S_{DS})D + \Omega_o Q_E + 1.6H$   
(ASCE 7-05, Section 12.3.3.3)
- 8. Use  $100x + 30y$ , if you are using ELF or modal analysis. Use simultaneous application of load, if you are analyzing the structure using a linear or nonlinear response history procedure (ASCE 7-05, Section 12.5.3).
- 9. Maximum height limit 30 ft or two stories, unless the weak story is capable of resisting a seismic force  $= \Omega_o$  times the design force (ASCE 7-05, Section 12.3.3.2).

TABLE 5.24  
Vertical Irregularities

Type of Irregularity	Graphic Interpretation	Remedial Measures	SDC Application
1a. Stiffness irregularity (soft story)	 <p>Stiffness <math>A &lt; 70\% B</math> or <math>A &lt; 80\% \frac{(B + C + D)}{3}</math></p>	5	D through F
1b. Stiffness irregularity (extreme soft story)	 <p>Stiffness <math>A &lt; 60\% B</math> or <math>A &lt; 70\% \frac{(B + C + D)}{3}</math></p>	6 5	E and F D through F
2. Weight (mass) irregularity	 <p>Mass <math>B &gt; 150\%</math> Mass A</p>	5	D through F
3. Vertical geometric irregularity	 <p>Dimension <math>X &gt; 130\% Y</math></p>	5	D through F

(continued)

**TABLE 5.24 (continued)**  
**Vertical Irregularities**

Type of Irregularity	Graphic Interpretation	Remedial Measures	SDC Application
4. In-plane discontinuity in vertical lateral force-resisting systems	 <p>Dimension <math>L_1 &gt; L</math></p>	7 1 5	B through F D through F D through F
5a. Discontinuity in lateral strength (weak story)	 <p>Shear strength <math>A &lt; 80\% B</math></p>	6 5 6	E and F D through F D through F
5b. Discontinuity in lateral strength (extreme weak story)	 <p>Shear strength <math>A &lt; 65\% B</math></p>	9 5	B and C D through F

Source: ASCE 7-05, Table 12.3-2.

#### Remedial measures

1. Increase design forces determined by static procedure by 25% for connection of diaphragms to vertical elements and to collectors, and for connections of collectors to the vertical elements. Collectors and their connections also shall be designed for these increased forces unless they are designed for load combinations with overstrength factor  $\Omega_o$  (ASCE 7-05, Section 12.3.3.4).
2. Multiply,  $M_{ta}$ , the torsional moment due to accidental torsion by a torsional amplification  $A_x = \left( \frac{\delta_{max}}{1.2\delta_{ave}} \right)^2 \leq 3.0$  (ASCE 7-05, Section 12.8.4.3).
3. Perform a 3D dynamic analysis with due consideration for diaphragm stiffness. Use cracked section properties for concrete elements. Include  $P\Delta$  effects (ASCE 7-05, Section 12.7.3).
4. Compute story drift,  $\Delta$ , as the largest difference of the deflections along any of the edges of the structure at the top and bottom of the story under consideration (ASCE 7-05, Section 12.12.1).
5. Use model analysis or more rigorous procedure (ASCE 7-05, Table 12.6.1).
6. Not permitted (NP) (ASCE 7-05, Section 12.3.3.1).
7. Design columns, beams, trusses, or stabs supporting discontinuous walls or frames to resist maximum axial forces determined by using the following load combinations with the overstrength factor  $\Omega_o$ :
 
$$(1.2 + 0.2S_{DS})D + \Omega_o Q_E + L + 0.2S$$

$$(0.9 - 0.2S_{DS})D + \Omega_o Q_E + 1.6H$$
 (ASCE 7-05, Section 12.3.3.3).
8. Use  $100x + 30y$ , if you are using ELF or modal analysis. Use simultaneous application of load, if you are analyzing the structure using a linear or nonlinear response history procedure (ASCE 7-05, Section 12.5.3).
9. Maximum height limit 30 ft or two stories, unless the weak story is capable of resisting a seismic force =  $\Omega_o$  times the design force (ASCE 7-05, Section 12.3.3.2).

#### 5.7.5.1 Plan or Horizontal Irregularity

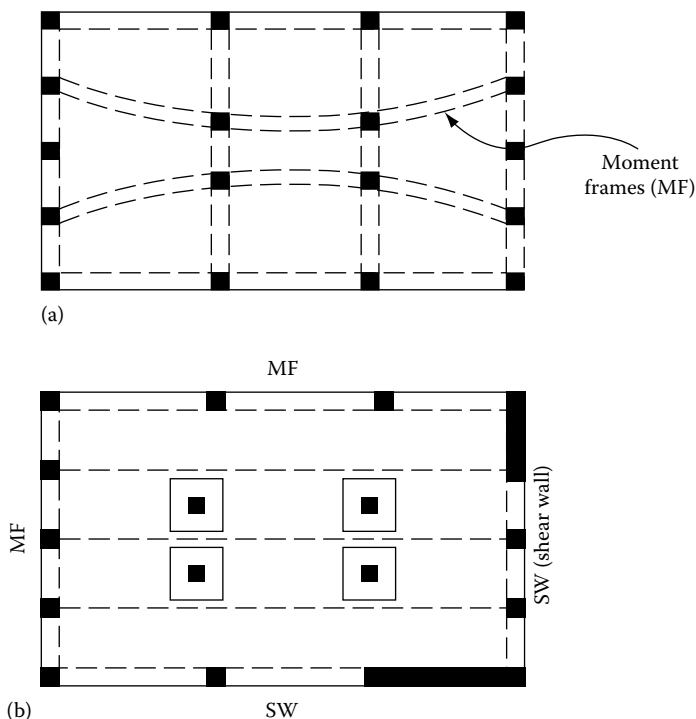
Table 5.23 indicates under what circumstances a building must be designed as having a plan irregularity. A building may have a symmetrical geometric shape without reentrant corners or wings but still be classified as irregular in plan because of the distribution of mass or vertical seismic force-resisting elements. Torsional effects in earthquakes can occur even when the static centers of mass and resistance coincide. For example, ground motion waves acting with a skew with respect to the

building axis can cause torsion. Cracking or yielding in a nonsymmetrical fashion can also cause torsion. These effects can also magnify the torsion due to eccentricity between the static centers. For this reason, buildings having an eccentric dimension perpendicular to the direction of the seismic force should be classified as irregular. The vertical-resisting components may be arranged so the static centers of mass and resistance are within the limitations given above and still be unsymmetrically arranged so the prescribed torsional forces would be unequally distributed to the various components. Torsional irregularities are subdivided into two categories, with a category of extreme irregularity. Extreme torsional irregularities are prohibited for structures located very close to major active faults and should be avoided, when possible, in all structures.

There is a second type of the distribution of vertical-resisting components that, while not being classified as irregular, does not perform well in earthquakes. This arrangement is termed a core-type building with the vertical components of the seismic force-resisting system concentrated near the center of the building. Better performance has been observed when the vertical components are distributed near the perimeter of the building. In recognition of the problems leading to torsional instability, a torsional amplification factor is prescribed in the ASCE provisions.

A building having a regular configuration can be square, rectangular, or circular. A square or rectangular building with minor reentrant corners would still be considered regular, but large reentrant corners creating a crucifix form would be classified as an irregular configuration. The response of the wings of this type of building is generally different from the response of the building as a whole, and this produces higher local forces than would be determined by analysis. Other plan configurations such as H-shapes that have a geometrical symmetry would also be classified as irregular because of the response of the wings.

Significant differences in stiffness between portions of a diaphragm at a level are classified as irregularities since they may cause a change in the distribution of seismic forces to the vertical components and create torsional forces not accounted for in the normal distribution considered for a regular building. Examples of plan irregularities are illustrated in Figures 5.6 and 5.37.



**FIGURE 5.37** (a) Highly redundant structure and (b) not-so-redundant structure.

Where there are discontinuities in the path of lateral force resistance, the structure can no longer be considered “regular.” The most critical of the discontinuities is the out-of-plane offset of vertical elements of the seismic force-resisting elements. Such offsets impose vertical and lateral load effects on horizontal element that are, at the least, difficult to provide for adequately.

Where vertical elements of the lateral force-resisting system are not parallel to or symmetric about major orthogonal axes, the static lateral force procedures cannot be applied and, thus, the structure must be considered to be “irregular.”

### 5.7.5.2 Vertical Irregularity

Table 5.24 indicates under what circumstances a structure must be considered to have a vertical irregularity. Vertical irregularities affect structural response and induce loads at the irregularity levels that are significantly different from the distribution assumed in the ELF procedure.

A building would be classified as irregular if the ratio of mass to stiffness in adjoining stories differs significantly. This might occur when a heavy mass, such as a swimming pool, is placed at one level while the floors above or below have typical floor loads. A comparative stiffness ratio between stories is given as a bench mark to exempt structures from being designed as having a vertical irregularity.

Another type of vertical irregularity is created by unsymmetrical geometry with respect to the vertical axis of the building. The building may have a geometry that is symmetrical about the vertical axis and still be classified as irregular because of significant horizontal offset in the vertical elements of the lateral force-resisting system at one or more levels. An offset is considered to be significant if the ratio of the larger dimension to the smaller dimension is more than 130%. The building would also be considered irregular if the smaller dimensions were below the larger dimensions, thereby creating an inverted pyramid effect.

Weak story irregularities occur whenever the strength of a story to resist lateral demands is significantly less than that of the story above. This is because buildings with this configuration tend to develop all of their inelastic behavior at the weak story. This can result in a significant change in the deformation pattern of the building, with most earthquake-induced displacement occurring within the weak story. This can result in extensive damage within the weak story and even instability and collapse. Note that an exception has been provided in which there is considerable overstrength of the “weak” story.

The soft story irregularity is subdivided into two categories with an extreme soft story category. Like weak stories, soft stories can lead to instability and collapse. Buildings with extreme soft stories are prohibited on sites located very close to major active faults (see Table 5.24 for the schematics of vertical irregularities and remedial measures).

### 5.7.6 REDUNDANCY

Redundancy provisions were first introduced into building codes and standards via the 1997 UBC. Since their original inception, the redundancy provisions created much controversy with respect to their interpretation and implementation. The debate centered mainly on the following issues:

- A sliding redundancy value as was proposed originally, based on the force in only one of the elements of the system, was too precise and not technically justified.
- A better approach to determining redundancy is to base it on whether the loss or removal of an important component within the system would result in more than a 33% reduction in story strength, or would the resulting system have an extreme torsional irregularity (horizontal structural irregularity Type 1b, ASCE 7-05, Table 12.3-1).

- Checking redundancy throughout the entire building height is not necessary. Only those stories resisting more than 35% of the base shear in the direction of interest need to be checked.
- Well-distributed perimeter systems should automatically qualify for a redundancy value of 1.0—specifically, those structures that are regular in plan at all levels.

Now it seems that the issue is settled with the ASCE 7-05 permitting the redundancy factor to be taken as 1.0 for

1. Structures assigned to SDC B or C
2. Drift calculation and  $P\Delta$  effects
3. Design of nonstructural components
4. Design of nonbuilding structures that are not similar to buildings
5. Design of collector elements, splices, and their connections for which the load combinations with overstrength factor are used
6. Design of members or connections where the load combinations with overstrength are required for design
7. Diaphragm loads determined using Equation 12.10-1 of ASCE 7-05
8. Structures with damping systems

It should be noted that the lack of redundancy exists when the failure of a component results in the failure of the entire system. Therefore, a logical way to determine the lack of redundancy is to check whether a component's failure results in an unacceptable amount of the loss of story strength or in the development of extreme torsional irregularity.

In the ASCE 7-05,  $\rho = 1.0$  or 1.3, depending on whether or not an individual element can be removed from the lateral force-resisting-system without

1. Causing the remaining structure to suffer a reduction of story strength of more than 33%
2. Creating an extreme torsional irregularity

Additionally, the redundancy factor,  $\rho$ , is 1 for the following cases:

1. *Moment frames*: The loss of moment resistance at the beam-to-column connections at both ends of a single beam would not result in more than a 33% reduction in story strength, nor does the resulting system have an extreme torsional irregularity (see Table 5.25 for additional ASCE 7-05 comments, and Figure 5.37 for conceptual plans of a highly redundant and not-so-highly redundant buildings).
2. *Shear walls or wall pier with a height-to-length ratio of greater than 1.0*: The removal of a shear wall or wall pier with a height-to-length ratio greater than 1.0 within any story, or collector connections thereto, would not result in more than a 33% reduction in story strength, nor does the resulting system have an extreme torsional irregularity.

### 5.7.7 SEISMIC LOAD COMBINATIONS

Some elements of properly detailed structures are not capable of safely resisting ground shaking demands through inelastic behavior. To ensure safety, these elements must be designed with sufficient strength to remain elastic. The  $\Omega_o$  coefficient approximates the inherent overstrength in typical structures having different seismic force-resisting systems. The special seismic loads, factored by the  $\Omega_o$  coefficient, are an approximation of the maximum force these elements are ever likely to

**TABLE 5.25**  
**Requirements for Each Story Resisting More Than 35% of the Base Shear**

Lateral Force–Resisting Element	Requirement
Moment frames	Loss of moment resistance at the beam-to-column connections at both ends of a single beam would not result in more than a 33% reduction in story strength, nor does the resulting system have an extreme torsional irregularity (horizontal structural irregularity Type 1b)
Shear walls or wall pier with a height-to-length ratio of greater than 1.0	Removal of a shear wall or wall pier with a height-to-length ratio greater than 1.0 within any story, or collector connections thereto, would not result in more than a 33% reduction in story strength, nor does the resulting system have an extreme torsional irregularity (horizontal structural irregularity Type 1b)
Cantilever columns	Loss of moment resistance at the base connections of any single cantilever column would not result in more than a 33% reduction in story strength, nor does the resulting system have an extreme torsional irregularity (horizontal structural irregularity Type 1b)
Other	No requirements

Source: Adapted from ASCE 7-05, Table 12.3-3.

experience. ASCE 7-05 permits the special seismic loads to be taken as less than the value computed by applying the  $\Omega_o$  coefficient to the design seismic forces when it can be shown that the yielding of other elements in the structure will limit the amount of load that can be delivered to the element. A case in point is the axial load induced in a column of a moment-resisting frame from the shear forces in the beams that connect to this column. The axial loads due to lateral seismic action need never be taken greater than the sum of the shears in these beams at the development of a full structural mechanism, considering the probable strength of the materials and strain-hardening effect. For frames controlled by beam hinge-type mechanisms, this would typically be  $2M_p/L$ , where for steel frames,  $M_p$  is the expected plastic moment capacity of the beam as defined in the AISC seismic specifications. For concrete frames,  $M_p$  is the probable flexural strength of the beams.  $L$  is the clear span length for both steel and concrete beams. In the context of seismic design, the term capacity means the expected or median-anticipated strength of the element, considering potential variation in material yields strength- and strain-hardening effects. When calculating the capacity of elements for this purpose, material strengths should not be reduced by capacity or resistance factors.

### 5.7.7.1 Seismic Load Effect

The factor of  $0.2S_{DS}$  placed on the dead load account for the effects of vertical acceleration. The  $0.2S_{DS}$  factor on dead load is not intended to represent the total vertical response. The concurrent maximum response of vertical and horizontal accelerations is unlikely and, therefore, the direct addition of responses is not considered.

The  $\rho$  factor relates to the redundancy inherent in the seismic force–resisting system and is, in essence, a reliability factor, penalizing designs that are likely to be unreliable due to the concentration of the structure’s resistance to lateral forces in a relatively few elements. However, it should be noted that there is very little research that speaks directly of the merits of redundancy in buildings for seismic resistance.

### 5.7.7.2 Seismic Load Effect with Overstrength

The seismic load effect with overstrength is intended to address those situations where the failure of an isolated, individual, brittle element can result in the loss of a complete seismic force-resisting system or in instability and collapse.

This somewhat arbitrary factor attempts to quantify the maximum force that can be delivered to sensitive elements based on historic observation that the real force that could develop in a structure may be three to four times the design levels. The use of the  $\Omega_o$  coefficient provides an estimate of the maximum forces likely to be experienced by an element.

Most structures designed with a given seismic force-resisting system will fall within a range of overstrength values. Since the purpose of the  $\Omega_o$  factor is to estimate the maximum force that can be delivered to a component that is sensitive to overstress, the values of this factor are intended to be representative of the larger values in this range for each system.

While overstrength can be quite beneficial in permitting structures to resist actual seismic demands that are larger than those for which they have been specifically designed, it is not always beneficial. Some elements incorporated in structures behave in a brittle manner and can fail in an abrupt manner if substantially overloaded. The existence of structural overstrength results in a condition where such overloads are likely to occur, unless they are specifically accounted for in the design process.

One case where structural overstrength should specifically be considered is in the design of column elements beneath discontinuous braced frames and shear walls, such as that occurs at vertical in-plane and out-of-plane irregularities. Overstrength in shear walls could cause the buckling failure of such columns with resulting structural collapse. Columns subjected to tensile loading in which splices are made are another example of a case where the seismic effect with overstrength should be used.

Although the most common cases in which structural overstrength can lead to an undesirable failure mode are identified in the ASCE provisions, not all such conditions are noted. Therefore, designers should be alert to conditions where the isolated independent failure of any element can lead to a condition of instability or collapse and should use the seismic effect with overstrength for the design of such elements. Other conditions that may warrant such a design approach include the design of transfer structures beneath discontinuous lateral force-resisting elements and the design of diaphragm force collectors to shear walls and braced frames, when these are the only methods of transferring force to these elements at a diaphragm level.

### 5.7.7.3 Elements Supporting Discontinuous Walls or Frames

The purpose of the special load combinations is to protect the gravity load-carrying system against possible overloads caused by overstrength of the lateral force-resisting system. Either columns or beams may be subject to such failure; therefore, both should include this design requirement. Beams may be subject to failure due to overloads in either the downward or upward directions of force. Examples include reinforced concrete beams or unbraced flanges of steel beams or trusses. Hence, the provision has been limited simply to downward force, but instead to the larger context of vertical load. The connections between the discontinuous elements and the supporting members shall be adequate to transmit the forces for which the discontinuous elements were required to be designed.

### 5.7.8 DIRECTION OF LOADING

Earthquake forces act in both principal directions of the building simultaneously, but the earthquake effects in the two principal directions are unlikely to reach their maxima simultaneously. A reasonable and adequate method for combining them is to require that structural elements be designed for 100% of the effects of seismic forces in one principal direction combined with 30% of the effects of seismic forces in the orthogonal direction.

Orthogonal effects are typically negligible for beams, girders, slabs, and other horizontal elements that are essentially one-directional in their behavior, but they may be significant in columns or other vertical members that participate in resisting earthquake forces in both principal directions of



the building. For two-way slabs, orthogonal effects at slab-to-column connections can be neglected provided the moment transferred in the minor direction does not exceed 30% of that transferred in the orthogonal direction and there is adequate reinforcement within lines one and one-half times the slab thickness on either side of the column to transfer all the minor direction moment.

### 5.7.9 ANALYSIS PROCEDURES

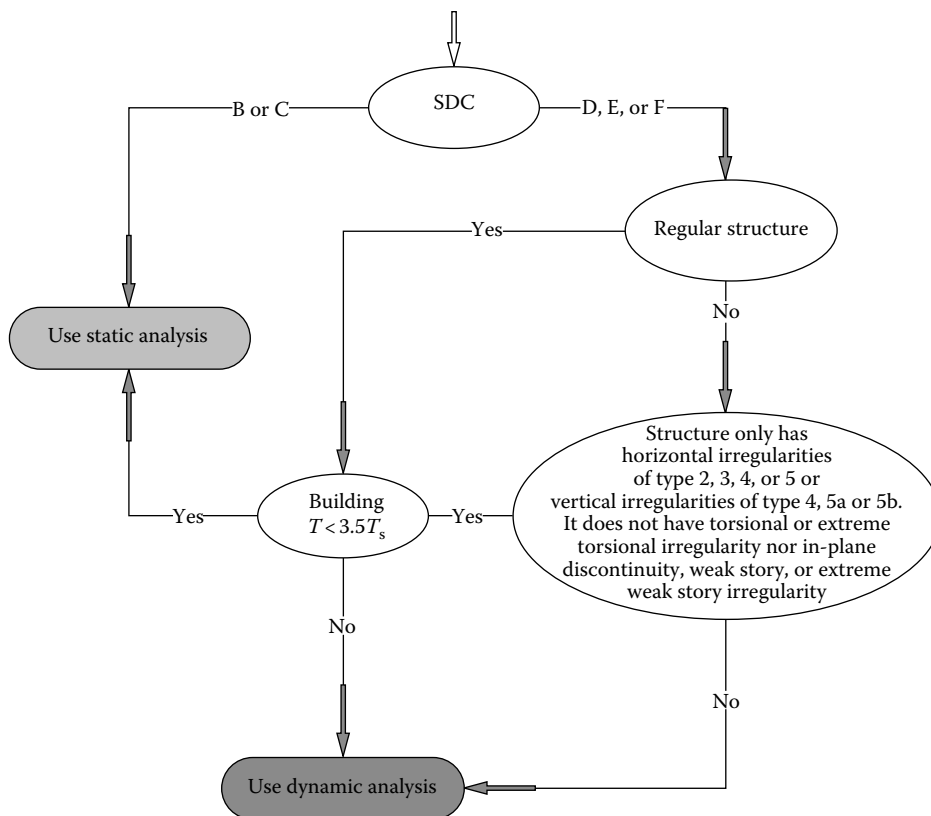
A flow chart of permitted analysis procedures, developed from ASCE 7-05, Table 12.6-1 (Table 5.26 of this chapter), is shown in Figure 5.38.

**TABLE 5.26**  
**Permitted Analytical Procedures**

SDC	Structural Characteristics	ELF Analysis Section 12.8	Modal Response Spectrum Analysis Section 12.9	Seismic Response History Procedures Chapter 16
<b>B and C</b>	Occupancy Category I or II buildings of light-framed construction not exceeding three stories in height	P	P	P
	Other Occupancy Category I or II buildings not exceeding two stories in height	P	P	P
	All other structures	P	P	P
<b>D through F</b>	Occupancy Category I or II buildings of light-framed construction not exceeding three stories in height	P	P	P
	Other Occupancy Category I or II buildings not exceeding two stories in height	P	P	P
	Regular structures with $T < 3.5T_s$ and all structures of light-frame construction	P	P	P
	Irregular structures with $T < 3.5T_s$ and having only horizontal irregularities Type 2, 3, 4, or 5 of Table 12.2-1 of ASCE 7-05 or vertical irregularities Type 4, 5a, or 5b of Table 12.3-1 of ASCE 7-05	P	P	P
	All other structures	NP	P	P

Source: ASCE 7-05, Table 12.6-1.

Note: P, permitted; NP, not permitted.



**FIGURE 5.38** Permitted analysis procedures for seismic design. (Developed from ASCE 7-05, Table 12.6-1.)

The modal superposition method is a general procedure for linear analysis of the dynamic response of structures. In various forms, modal analysis has been widely used in the earthquake-resistant design of special structures such as very tall buildings, offshore drilling platforms, dams, and nuclear power plants for a number of years; however, its use has become more common for ordinary structures as well because of the advent of high-speed, desktop computers and the availability of relatively inexpensive structural analysis software capable of performing 3D modal analyses. When modal analysis is specified by the ASCE provisions, a 3D analysis generally is required except in the case of highly regular structures or structures with flexible diaphragms.

The ELF procedure and the response spectrum procedure are both based on the approximation that the effects of yielding can be adequately accounted for by the linear analysis of the seismic force-resisting system for the design spectrum, which is the elastic acceleration response spectrum reduced by the response modification factor,  $R$ . The effects of the horizontal component of ground motion perpendicular to the direction under consideration in the analysis, the vertical component of ground motion, and torsional motions of the structure are all considered in the same simplified approaches in the two procedures. The main difference between the two procedures lies in the distribution of the seismic lateral forces over the height of the building. In the modal analysis procedure, the distribution is based on properties of the natural vibration modes, which are determined from the mass and stiffness distribution. In the ELF procedure, the distribution is based on simplified formulas that are appropriate for regular structures. Otherwise, the two procedures are subject to the same limitations.

The simplifications inherent in the ELF procedure result in approximations that are likely to be inadequate if the lateral motions in two orthogonal directions and the torsional motion are strongly coupled. Such would be the case if the buildings were irregular in its plan configuration

or if it had a regular plan, but its lower natural frequencies were nearly equal. The modal analysis method includes a general model that is more appropriate for the analysis of such structures. It requires at least three DOFs per floor: two for translational motion and one for torsional motion.

The methods of modal analysis can be generalized further to model the effect of diaphragm flexibility, soil-structure interaction, etc. In the most general form, the idealization would take the form of a large number of mass points, each with six DOFs (three translational and three rotational) connected by generalized stiffness elements.

The ELF procedure and the response spectrum procedure are all likely to err systematically on the unsafe side if story strengths are distributed irregularly over height. This feature is likely to lead to the concentration of ductility demands in a few stories of the building. The nonlinear static (or the so-called pushover) procedure is a method to more accurately account for irregular strength distribution. However, it also has limitations and is not particularly applicable to tall structures or structures with relatively long fundamental periods of vibration.

The actual strength properties of the various components of a structure can be explicitly considered only by a nonlinear analysis of dynamic response by the direct integration of the coupled equations of motion. This method has been used extensively in earthquake research studies of inelastic structural response. If the two lateral motions and the torsional motion are expected to be essentially uncoupled, it would be sufficient to include only one DOF per floor, for motion in the direction along which the structure is being analyzed; otherwise at least three DOFs per floor, two translational and one torsional, should be included. It should be recognized that the results of a nonlinear response history analysis of such mathematical structural models are only as good as the models chosen to represent the structure vibrating at amplitudes of motion large enough to cause significant yielding during strong ground motions. Furthermore, reliable results can be achieved only by calculating the response to several ground motion–recorded accelerograms and/or simulated motions, and examining the statistics of response.

It is possible with presently available computer programs to perform 2D and 3D inelastic analyses of reasonably simple structures. The intent of such analyses could be to estimate the sequence in which components become inelastic and to indicate those components requiring strength adjustments so as to remain within the required ductility limits. It should be emphasized that with the present state of the art in analysis, there is not one method that can be applied to all types of structures. Further, the reliability of the analytical results is sensitive to

1. The number and appropriateness of the input motion records
2. The practical limitations of mathematical modeling including interacting effects of inelastic elements
3. The nonlinear solution algorithms
4. The assumed hysteretic behavior of members

Because of these sensitivities and limitations, the maximum base shear produced in an inelastic analysis should not be less than 80% of that required by ELF.

The least rigorous analytical procedure that may be used in determining the design seismic forces and deformations in structures depends on the SDC and the structural characteristics (in particular, regularity). Except for structures assigned to SDC A, the ELF procedure is the minimum level of analysis except that a more rigorous procedure is required for some SDCs D, E, and F structures. The modal analysis procedure adequately addresses vertical irregularities of stiffness, mass, or geometry.

The ELF procedure is adequate for most regular structures; however, the designer may wish to employ a more rigorous procedure for those regular structures where the ELF procedure is likely to be inadequate such as in the following cases:

1. Structures with irregular mass and stiffness properties in which case the simple equations for the vertical distribution of lateral forces may lead to erroneous results.
2. Structures (regular or irregular) in which the lateral motions in two orthogonal directions and the torsional motion are strongly coupled.
3. Structures with the irregular distribution of story strengths leading to the possible concentration of ductility demand in a few stories of the building.

In such cases, a more rigorous procedure that considers the dynamic behavior of the structure should be employed.

Many of the standard procedures for the analysis of forces and deformations in structures subjected to earthquake ground motion are listed below in order of increasing rigor and expected accuracy:

1. ELF procedure
2. Response spectrum (modal analysis) procedure
3. Linear response history procedure
4. Nonlinear static procedure, involving the incremental application of a pattern of lateral forces and the adjustment of the structural model to account for progressive yielding under load application (pushover analysis)
5. Nonlinear response history procedure, involving the step-by-step integration of the coupled equations of motion

Each procedure becomes more rigorous if effects of soil–structure interaction are considered.

### 5.7.9.1 Equivalent Lateral-Force Procedure

**Design base shear,  $V$ :** The corner stone of seismic analysis is the ELF procedure. It incorporates all the basic ideas of seismic design. The design base shear, as set forth by the following equation:

$$V = C_s W$$

is the starting point. It is given as a seismic response coefficient,  $C_s$ , times the effective seismic weight of the structure,  $W$ . The effective seismic weight, as shown in Figure 5.39, is the total weight of the building and other gravity loads that might reasonably be expected to be acting on the building at the time of an earthquake. It includes permanent and movable partitions and permanent equipments such as mechanical and electrical equipment, piping, and ceilings. The human live load is taken to be negligibly small in this contribution to the seismic lateral forces. Buildings intended for storage or warehouse occupancy must have at least 25% of the design floor live load included in the calculation of  $W$ .

Freshly fallen snow has little effect on the lateral force, but ice firmly attached to the roof of a building would contribute significantly to the inertia force. For this reason, effective snow load is taken as the full design snow load for those regions where the snow load exceeds 30 psf, with the provision that the local authority having jurisdiction may allow a reduction of up to 80%. The magnitude of snow load to be included in the calculation of  $W$  depends on how much ice buildup or snow entrapment is expected for the roof configuration and site topography. ASCE 7-05 requires the inclusion of a fixed 20% of the flat roof snow load in  $W$ , where the flat roof snow load exceeds 30 psf. When the flat roof snow load is lower, no portion of it needs to be included in  $W$ .

The ELF procedure is intended to provide a relatively straightforward design approach where complex analyses are not warranted. However, given the widespread use of computer-assisted analysis, the limitations on the application of the ELF procedure is not burdensome.



taken any larger than a coefficient  $C_u$  times the approximate period calculated. Reasonable mathematical rules should be followed such that the increase in period allowed by the  $C_u$  coefficient is not taken advantage of when the structure does not merit it. Note that for purposes of drift analysis only, the upper bound limitation on the computed fundamental period  $T$  of the building does not apply. It may be noted that larger values of  $C_u$  are permitted as the design spectral response acceleration parameter, at 1 s,  $S_{D1}$ , of a location decreases. This is because buildings in area with lower lateral-force requirements are thought likely to be more flexible. Higher values of  $C_u$  for lower values of  $S_{D1}$  also result in less dramatic changes from prior practice in lower rise areas. It is generally accepted that the equations for  $T_a$  are tailored to fit the types of construction common in areas with high lateral-force requirements. It is unlikely that buildings in lower seismic risk areas would be designed to produce as high a drift level as allowed by ASCE 7-05, due to stability ( $P\Delta$ ) considerations and wind requirements.

**Vertical distribution of seismic forces:** The distribution of lateral forces over the height of a structure is quite complex because these forces are the result of superposition of a number of natural modes of vibration. The relative contributions of these vibration modes to the total forces depends on a number of factors including the shape of the earthquake response spectrum, the natural periods of vibration of the structure, and the shapes of vibration modes that, in turn, depend on the distribution of mass and stiffness over the height.

It is well known that the influence of modes of vibration higher than the fundamental mode is small in the earthquake response of short-period structures and that, in regular structures, the fundamental vibration mode departs little from a straight line. It has been demonstrated that although the earthquake response of long-period structures is primarily due to the fundamental natural mode of vibration, the influence of higher modes of vibration can be significant and, in regular structures, the fundamental vibration mode lies approximately between a straight line and a parabola with the vertex at the base. Thus, the value of index  $k = 2$  is appropriate for structures having a fundamental period of vibration of 2.5 s or longer. Linear variation of  $k$  between 1 at a 0.5 s period and 2 at a 2.5 s period provides the simplest possible transition between the two extreme values (see ASCE Eq. 12.8–12).

**Horizontal shear distribution:** The story shear in any story is the sum of the lateral forces acting at all levels above that story. Story  $x$  is the story immediately below level  $x$ . Reasonable and consistent assumptions regarding the stiffness of concrete elements may be used for analysis in distributing the shear force to such elements connected by a horizontal diaphragm. Similarly, the stiffness of moment frames will establish the distribution of the story shear to the vertical resisting elements in that story.

**Inherent and accidental torsion:** The torsional moment to be considered in the design elements in a story consists of two parts:

1.  $M_e$ , the moment due to eccentricity between centers of mass and resistance for that story, which is computed as the story shear times the eccentricity perpendicular to the direction of applied earthquake forces
2.  $M_{ta}$ , commonly referred to as “accidental torsion,” which is computed as the story shear times the “accidental eccentricity,” equal to 5% of the dimension of the structure (in the story under consideration) perpendicular to the applied earthquake forces

The computation of  $M_{ta}$  in this manner implies that the dimension of the structure is the dimension in the story where the torsional moment is being computed and that all the masses above that story should be assumed to be displaced in the same direction at one time (e.g., first, all of them to the left and, then, to the right).

Dynamic analyses assuming linear behavior indicate that the torsional moment due to eccentricity between centers of mass and resistance may significantly exceed  $M_t$ . However, such dynamic magnification is not included in the ASCE 7-05 partly because its significance is not well understood for structures designed to deform well beyond the range of linear behavior.

Accidental torsion is intended to cover the effects of several factors that have not been explicitly considered in the design. These factors include the rotational component of ground motion about a vertical axis; unforeseeable differences between computed and actual values of stiffness, yield strengths, and dead-load masses; and unforeseeable unfavorable distributions of dead- and live-load masses.

The way in which the story shears and the effects of torsional moments are distributed to the vertical elements of the seismic force-resisting system depends on the stiffness of the diaphragms relative to vertical elements of the system.

Where the diaphragm stiffness in its own plane is sufficiently high relative to the stiffness of the vertical components of the system, the diaphragm may be assumed to be indefinitely rigid for purposes of analysis. Then, in accordance with compatibility and equilibrium requirements, the shear in any story is to be distributed among the vertical components in proportion to their contributions to the lateral stiffness of the story while the story torsional moment produces additional shears in these components that are proportional to their contributions to the torsional stiffness of the story about its center of resistance. This contribution of any component is the product of its lateral stiffness and the square of its distance to the center of the resistance of the story. Alternatively, the story shears and torsional moments may be distributed on the basis of a 3D analysis of the structure, consistent with the assumption of linear behavior.

Where the diaphragm in its own plane is very flexible relative to the vertical components, each vertical component acts nearly independently of the rest. The story shear should be distributed to the vertical components considering these to be rigid supports. The analysis of the diaphragm acting as a continuous horizontal beam or truss on rigid supports leads to the distribution of shears. Because the properties of the beam or truss may not be accurately computed, the shears in vertical elements should not be taken to be less than those based on "tributary areas." Accidental torsion may be accounted for by adjusting the position of the horizontal force with respect to the supporting vertical elements.

There are some common situations where it is obvious that the diaphragm can be assumed to be either rigid or very flexible in its own plane for purposes of distributing story shear and considering torsional moments. For example, a solid monolithic reinforced concrete slab, square or nearly square in plan, in a structure with slender moment-resisting frames may be regarded as rigid. For other situations, the design forces should be based on an analysis that explicitly considers diaphragm deformations and satisfies equilibrium and compatibility requirements. Alternatively, the design forces could be based on the envelope of the two sets of forces resulting from both extreme assumptions regarding the diaphragms—rigid or very flexible.

Where earthquake forces are applied concurrently in two orthogonal directions, the 5% displacement of the center of mass should be applied along a single orthogonal axis of the building chosen to produce the greatest effect. The eccentricity need not be applied simultaneously along two axes (i.e., in a diagonal direction). Most diaphragms of light-framed construction are somewhere between rigid and flexible for analysis purpose, that is, they are semirigid. Such diaphragm behavior is difficult to analyze when considering the torsion of the structure. As a result, it is believed that the consideration of the amplification of the torsional moment is a refinement that is not warranted for light-framed construction. The intent is not to amplify the actual, that is, the calculated torsion component, but only the component due to accidental torsion. There is no theoretical justification to further increase design forces by amplifying both components together.

**Overturning:** The structure must be designed to resist overturning moments statically consistent with the design story shears. In the current 2005 ASCE 7-05 provisions, there is no modification

factor,  $T$ , to reduce the moment to account for the effects of higher mode except at the soil–foundation interface. A 25% reduction is allowed in overturning values if the analysis is performed by using ELF procedure and a 10% reduction if the analysis is by modal response method. However, no reduction is permitted for cantilevered column-type structures.

**$P\Delta$  effects:** The  $P\Delta$  effects in a given story are due to the eccentricity of the gravity load above that story. If the story drift due to the lateral forces were  $\Delta$ , the bending moments in the story would be augmented by an amount equal to  $\Delta$  times the gravity load above the story. The ratio of the  $P\Delta$  moment to the lateral-force story moment is designated as a stability coefficient,  $\phi$ . If the stability coefficient  $\phi$  is less than 0.10 for every story, the  $P\Delta$  effects on story shears and moments and member forces may be ignored. If, however, the stability coefficient  $\phi$  exceeds 0.10 for any story, the  $P\Delta$  effects on story drifts, shears, member forces, etc. for the entire structure must be determined by a rational analysis.

The  $P\Delta$  procedure effectively checks the static stability of a structure based on its initial stiffness. There is justification for using the  $P\Delta$  amplifier as based on elastic stiffness because

1. Many structures display strength well above the strength implied by code-level forces. This overstrength likely protects structures from stability-related failures.
2. The likelihood of a failure due to instability decreases with the increased intensity of expected ground shaking. This is due to the fact that the stiffness of most structures designed for extreme ground motion is significantly greater than the stiffness of the same structure designed for lower intensity shaking or for wind. Since damaging, low-intensity earthquakes are somewhat rare, there would be little observable damage.

**Drift determination:** In the ASCE 7-05, for the first time, allowable drifts are based on building occupancy category (see Table 5.22). The more significant (or “essential”) the occupancy, the more restrictive the allowable story drift. For Occupancy Category IV buildings (essential facilities), the allowable story drift has been reduced by a factor of two relative to recent versions of the UBC. The current requirement specifies an allowable story drift of 0.01, while the UBC value was 0.02. Depending on the selected building system, this can have a significant effect on the seismic design.

The design story drift is the difference of the deflections,  $\delta_x$ , at the top and bottom of the story under consideration. The deflections,  $\delta_x$ , are determined by multiplying the deflections,  $\delta_{xe}$  (determined from an elastic analysis), by the deflection amplification factor,  $C_d$ . The elastic analysis is to be made for the seismic force–resisting system using the prescribed seismic design forces and considering the structure to be fixed at the base. Stiffness other than those of the seismic force–resisting system should not be included since they may not be reliable at higher inelastic strain levels.

The deflections are to be determined by combining the effects of the joint rotation of members, shear deformations between floors, the axial deformations of the overall lateral resisting elements, and the shear and flexural deformations of shear walls. Centerline dimensions between the frame elements often are used for analysis, but clear-span dimensions with the consideration of joint panel zone deformation also may be used.

The term “drift” has two connotations: story drift and absolute displacement.

1. “Story drift” is the maximum lateral displacement within a story (i.e., the displacement of one floor relative to the floor below caused by the effects of seismic loads).
2. “Absolute displacement” is the lateral deflection of any point in the structure relative to the base. This is not “story drift” and is not to be used for drift control or stability considerations since it may give a false impression of the effects in critical stories. However, it is important when considering seismic separation requirements.



There are many reasons for controlling drift: one is to control member inelastic strain and the other stems from stability considerations. The stability of members under elastic and inelastic deformations is a direct function of both axial loading and bending of members. A stability problem is resolved by limiting the drift on the vertical load-carrying elements and the resulting secondary moment from this axial load and deflection, that is, the  $P\Delta$  effect. Under small lateral deformations, secondary stresses are normally within tolerable limits. However, larger deformations with heavy vertical loads can lead to significant secondary moments from the  $P\Delta$  effects in the design. The drift limits indirectly provide upper bounds for these effects.

Another reason for drift control is to restrict damage to partitions, elevator shafts, stair enclosures, glass, and other fragile nonstructural elements. The design of some nonstructural components that span vertically in the structure can be complicated when supports for the element do not occur at horizontal diaphragms. Therefore, story drift must be accommodated in the elements that will actually distort. For example, a glazing system supported by precast concrete spandrels must be designed to accommodate the full story drift, even though the height of the glazing system is only a fraction of the floor-to-floor height. The condition arises because the precast spandrels will behave as rigid bodies relative to the glazing system and therefore, all the drift must be accommodated by the joint between the precast spandrel and the glazing unit.

The determination of design story drift involves the following steps:

1. Determine the lateral deflections at the various floor levels by an elastic analysis of the building under the design base shear. The lateral deflection at floor level  $x$ , obtained from this analysis, is termed  $\delta_{xe}$ . The subscript “e” stands for elastic analysis.
2. Amplify  $\delta_{xe}$  by the deflection amplification factor,  $C_d$ . The resulting quantity,  $C_d\delta_{xe}$ , is an estimated design earthquake displacement at floor level  $x$ . ASCE 7-05 requires this quantity to be divided by the importance factor,  $I_E$ , because the forces under which the  $\delta_{xe}$  displacement is computed are already amplified by  $I_E$ . Since drift limits are tighter for buildings in higher occupancy categories, this division by  $I_E$  is important. Without it, there would be a double tightening of drift limitations for buildings with seismic importance factors greater than one. The quantity  $C_d\delta_{xe}/I_E$  at floor level  $x$  is  $\delta_x$ , the adjusted design earthquake displacement.
3. Calculate the design story drift  $\Delta_x$  for story  $x$  (the story below floor level  $x$ ) by deducting the adjusted design earthquake displacement at the bottom of story  $x$  (floor level  $x - 1$ ) from the adjusted design earthquake displacement at the top of story  $x$ :

$$\Delta_x = \delta_x - (\delta_{x-1})$$

The  $\Delta_x$  values must be kept within limits, as given in Table 5.22 (ASCE 7-05, Table 12.12-1).

Three items are worth noting:

1. The design story drift must be computed under the strength-level design earthquake forces irrespective of whether member design is done using the strength design or the allowable stress design load combinations. Note this comment does not apply to reinforced concrete structures that are designed by ultimate strength method.
2. The redundancy coefficient,  $p$ , is equal to 1.0 for the computation of the design story drift.
3. For determining compliance with the story drift limitations, the deflections,  $\delta_x$ , may be calculated as indicated previously using design forces corresponding to the fundamental period of the structure,  $T$ , calculated without the limit,  $T < C_u T_a$ . The same model for the seismic force-resisting system used in determining the deflections must be used for determining  $T$ . The waiver does not pertain to the calculation of drifts for determining  $P\Delta$  effects on member forces, overturning moments, etc. If  $P\Delta$  effects are significant, the design story drift must be increased by the resulting incremental factor.

The  $P\Delta$  effects in a given story are due to the eccentricity of the gravity load above the story. If the design story drift due to the lateral forces is  $\Delta$ , the bending moments in the story are augmented by an amount equal to  $\Delta$  times the gravity load above the story. The ratio of the  $P\Delta$  moment to the lateral-force story moment is designated as the stability coefficient. If the stability coefficient,  $q$ , is less than 0.10 for every story, then the  $P\Delta$  effects on story shears and moments and member forces, etc. must be determined by a rational analysis. However, with the availability of computer programs that take into consideration  $P\Delta$  effects automatically within the analysis, hand calculations of  $q$ , for determining whether  $P\Delta$  is significant, are rarely necessary.

$P\Delta$  effects are much more significant in buildings assigned to low-seismic design categories than in buildings assigned to high-seismic design categories. This is because lateral stiffness of buildings is typically greater for higher seismic design categories.

The design story drift limits reflect consensus judgment taking into account the goals of drift control outlined above. In terms of life safety and damage control objectives, the drift limits should yield a substantial, though not absolute, measure of safety for well-detailed and constructed brittle elements. To provide a higher performance standard, the drift limit for structures contained in the four occupancy categories are progressively more stringent in order to attain minimum levels of earthquake performance suitable to the individual occupancies. It should be emphasized that the drift limits,  $\Delta_a$ , are story drifts and, therefore, are applicable to each story (i.e., they must not exceed in any story even though the drift in other stories may be well below the limit).

Stress or strength limitations imposed by design level forces may provide adequate drift control for low-rise buildings. However, it is expected that the design of moment-resisting frames and tall, narrow shear wall buildings will be governed at least in part by drift considerations. In areas having large design spectral response accelerations,  $S_{DS}$  and  $S_{D1}$ , it is expected that seismic drift considerations will predominate for buildings of medium height. In areas having low design spectral response accelerations and for very tall buildings in areas with large design spectral response accelerations, wind considerations generally will generally control. However, as stated many times in this chapter, the detailing of members must comply with the governing seismic provisions.

Due to probable first mode drift contributions, the ELF procedure may be too conservative for drift design of very tall moment-frame buildings. It is suggested for these buildings, where the first mode would be responding in the constant displacement region of a response spectrum (where displacements would be essentially independent of stiffness), that the response spectrum procedure be used for design even when not required, the reason being economy.

Building separations are necessary between two adjoining buildings or parts of the same building, with or without frangible closures, for the purpose of permitting the adjoining buildings or parts to respond independently to earthquake ground motion. Unless all portions of the structure have been designed and constructed to act as a unit, they must be separated by seismic joints. For irregular structures that cannot be expected to act reliably as a unit, seismic joints should be used to separate the building into units whose independent response to earthquake ground motion can be predicted.

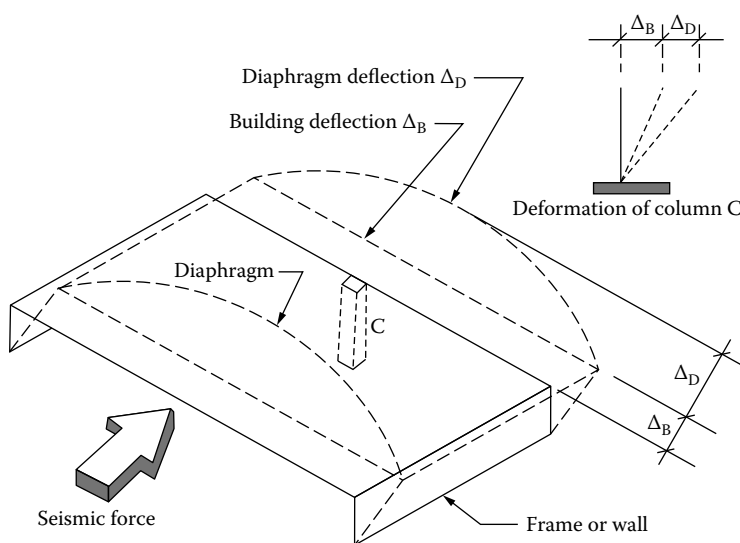
The separation should be sufficient to avoid damaging contact under total deflection to prevent interference and possible destructive hammering between buildings. It is recommended that the distance be equal to the statistical sum of the lateral deflections,  $\delta_x$ , of the two units. This involves increasing separations with height. If the effects of hammering can be shown not to be detrimental, these distances can be reduced.

**Deformation compatibility:** The ASCE 7-05 requires that for buildings in SDC D, E or F, all structural framing elements and their connections, not required by design to be part of the lateral force-resisting system, must be designed and/or detailed to be adequate to maintain the support of gravity loads when subjected to the expected deformations caused by seismic forces. Important features of deformation compatibility requirements are

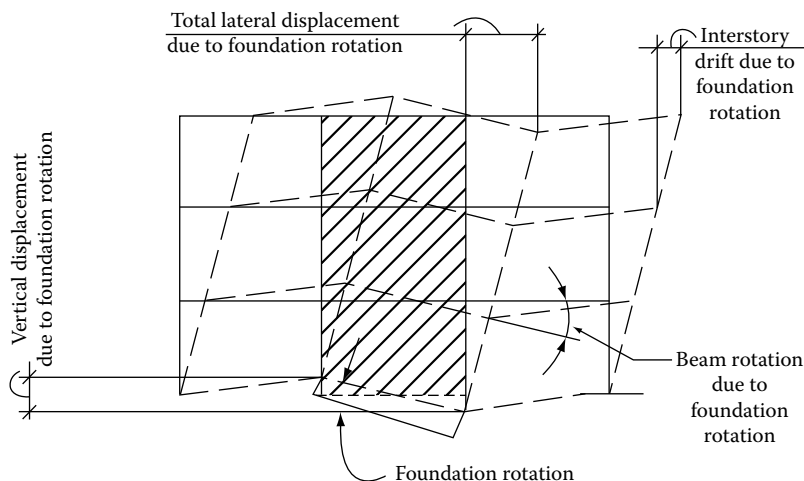
1. Expected deformations must be greater of the maximum inelastic response displacement,  $\delta_v$ , considering  $P\Delta$  effects and deformation induced by a story drift of 0.0025 times the story height.
2. When computing expected deformations, stiffening effects of those elements not part of the lateral force-resisting system must be neglected.
3. Forces induced by expected deformations may be considered factored forces.
4. In computing forces, the restraining effect of adjoining rigid structures and nonstructural elements must be considered.
5. For concrete elements that are not part of the lateral force-resisting system, assigned flexural and shear stiffness properties must not exceed one-half of gross section properties, unless a rational cracked section analysis is performed.
6. Additional deformations that may result from foundation flexibility and diaphragm deflection must be considered.

The deformation compatibility requirements for SDC D, E, or F buildings provide a means of protecting elements of the structure that are not part of the seismic force-resisting system. The fact that many elements of the structure are not intended to resist seismic forces and are not detailed for such resistance does not prevent them from actually providing this resistance and becoming severely damaged. Hence the compatibility requirements. Of particular concern are the shears that can be induced in structural components that are not part of the lateral force-resisting system since sudden shear failures have been catastrophic in past earthquakes.

The ASCE provisions encourage the use of intermediate or special detailing in beams and columns that are not part of the lateral force-resisting system. In return for better detailing, such beams and columns are permitted to be designed to resist moments and shears from unamplified deflections. This reflects observations that well-detailed components can accommodate large drifts by responding inelastically without losing significant vertical load-carrying capacity. It should be noted that diaphragm and foundation deformations must be included in checking compatibility requirements (see Figures 5.40 and 5.41).



**FIGURE 5.40** Column deformation for use in compatibility considerations. Deformation of column = building deflection  $\Delta_B$  + diaphragm deflection  $\Delta_D$ . (Adapted from SEAOC Blue Book, 1999 edition.)



**FIGURE 5.41** Deformation compatibility consideration of foundation flexibility. (Adapted from SEAOC Blue Book, 1999 edition.)

### 5.7.9.2 Modal Response Spectrum Analysis

To proceed with an equivalent static analysis of a structure, we need to determine only the two characteristic values of the design acceleration response parameters,  $S_{D1}$  and  $S_{D5}$ . This is because the base shear equations, discussed previously, are directly related to these parameters. However, for buildings and structures requiring modal analysis procedures, it is necessary to develop an acceleration graph, commonly referred to as an acceleration spectrum, because design acceleration values are required for an entire range of building periods. In a modal analysis, we attempt to capture the multimodal response of a building by statistically combining its individual modal responses. Therefore, accelerations corresponding to an entire range of building periods are required in performing the dynamic analysis.

Modal analysis is applicable for calculating the linear response of complex, MDOF structures and is based on the fact that the response is the superposition of the responses of individual natural modes of vibration, each mode responding with its own particular pattern of deformation (the mode shape), with its own frequency (the modal frequency), and with its own modal damping. The response of the structure, therefore, can be modeled by the response of a number of SDOF oscillators with properties chosen to be the representative of the mode and the degree to which the mode is excited by the earthquake motion. For certain types of damping, this representation is mathematically exact and, for structures, numerous full-scale tests and analyses of earthquake response structures have shown that the use of modal analysis, with viscously damped SDOF oscillators describing the response of the structural modes, is a reasonably accurate approximation for the analysis of linear response.

The ELF procedure is simply a first mode application of this technique, which assumes all of the structure's mass is active in the first mode. The purpose of modal analysis is to obtain the maximum response of the structure in each of its important modes, which are then summed in an appropriate manner. This maximum modal response can be expressed in several ways. In practice, the SRSS or the CQC is used for this purpose. Once the story shears and other response variables for each of the important modes are determined and combined to produce design values, the design values are used in basically the same manner as the ELFs.

The SRSS of the modal quantities is typically used for its simplicity and its wide familiarity. In general, it gives satisfactory results, but it is not always a conservative predictor of the earthquake response inasmuch as more adverse combinations of modal quantities than are given by this method of combination can occur. The most common instance where combination by the use of the SRSS is

unconservative occurs when two modes have very nearly the same natural period. In this case, the responses are highly correlated and the designer should consider combining the modal quantities more conservatively. The CQC technique provides somewhat better results than the SRSS method for the case of closely spaced modes.

Although modal analysis procedure is more accurate, the ASCE 7-05 limits the reduction of base shear that can be achieved by modal analysis compared to the use of the ELF procedure. Some reduction, where it occurs is thought to be justified because the modal analysis gives a somewhat more accurate representation of the earthquake response. Some limit to the reduction permitted as a result of the calculation of longer natural periods is necessary because the actual periods of vibration may not be as long, even at moderately large amplitudes of motion, due to the stiffening effects of structural elements not a part of the seismic force-resisting system and of nonstructural components. The limit is imposed by the comparison of 80% of the base shear value computed using the ELF procedure. Where modal analysis predicts response quantities corresponding to a total base shear less than 80% of that which is computed by using the ELF procedure, all response results must be sealed up to that level.

For many structures, including low-rise structures and structures of moderate height, three modes of vibration in each direction are nearly always sufficient to determine design values of the earthquake response of the structure. For high-rise structures, however, more than three modes may be required to adequately determine the forces for design. Therefore, a simple rule that the combined participating mass of all modes considered in the analysis should be equal to or greater than 90% of the effective total mass in each of two orthogonal horizontal directions is provided in the ASCE 7-05 provisions.

**Concept of model participation factors:** The modal participation factor for each mode may be defined as a constant always less than unity, by which the actual masses of the system are multiplied to give the effective masses for the mode under consideration. Simply stated, model participation factor defines the degree to which that mode participates in the total vibration. The more nearly the lateral loads are similar to the corresponding amplitudes of the characteristic shape, the greater is the participation. In fact, if loads at all floors were proportional to the product of the floor mass and the amplitude of a certain mode at that floor, the response would be entirely in that mode and in that mode alone.

A review of the participation factors for the first few modes will give an indication if more modes are required to capture the essential dynamic behavior of the building. The sum of participation factors for all the modes at a particular story equals unity. Also, the sum of all the modal base shear participation factors will equal unity. Most codes make a general statement that all modes having a significant contribution to the total structural response should be included in the analysis. This requirement is deemed satisfied if the sum of the participation factors for the modes considered is at least equal to 90% of unity.

As stated previously, combining modes in 3D analysis becomes substantially more complex than in a 2D analysis. It is therefore desirable to plot mode shapes to confirm the validity of the computer model and check the possibility of data input errors. The concept of participation factors is also more difficult to interpret in 3D analysis because for each direction of applied seismic forces there will be three components of motion, two transitional and one rotational about the vertical axis.

### 5.7.10 DIAPHRAGMS, CHORDS, AND COLLECTORS

Diaphragms are designed as deep beams that distribute the lateral loads from their origin to the components where such forces are resisted. Therefore, they are subjected to shears and bending moments while the collector elements are subjected to direct stresses. The deformations of the diaphragms must be minimized in some cases because they could overstress the walls to which the diaphragms are connected. The amount of deflection permitted in the diaphragm must be related to the ability of the walls to deflect (normal to the direction of force application) without failure.

A detail commonly overlooked by many engineers is the requirement to tie the diaphragm together so that it acts as a unit. Wall anchorages tend to tear off the edges of the diaphragm; thus, the ties must be extended into the diaphragm so as to develop adequate anchorage. During the San

Fernando earthquake, seismic forces from the walls caused separations in roof diaphragms in several industrial buildings.

Where openings occur in shear walls or diaphragms, temperature “trim bars” alone do not provide adequate reinforcement. The chord stresses must be provided for and the chords anchored to develop the chord stresses by embedment. The embedment must be sufficient to take the reactions without overstressing the material.

#### 5.7.10.1 Diaphragms for SDC A

No specific requirements are given for the design of diaphragms of buildings in SDC A, other than a general statement that “every structure and portion thereof, including nonstructural components shall be designed and constructed to resist the effects of earthquake motions.”

#### 5.7.10.2 Diaphragms for SDCs B through F

The determination of design forces for diaphragms of buildings in SDC B and above is somewhat involved although their responses are conceptually considered quite simply as that of a deep beam subjected to bending and shear forces. The difficulty is in the proper identification and design of load path that must be provided for delivering the inertia forces generated at the roof and floor levels to the vertical lateral load-resisting elements. Additionally, the seismic loads resulting from structural analysis must be compared to the minimum requirements of the provisions, and often increased by 25% for the design of connections of diaphragms to vertical elements and to collectors, and for connections of collectors to the vertical elements. Alternately, load combinations that include the overstrength factor  $\Omega_o$  may be used. In addition to the inertia loads generated at the floor and roof levels, one must consider the shear forces that result from the transfer of seismic force from the vertical-resisting elements above the diaphragm. Added to these seemingly arbitrary requirements, one must be cautious when applying the redundancy factor,  $\rho$ . It applies only to the portion of diaphragm load resulting from the transfer of vertical-resisting elements, and not for the inertia forces generated at the floor and roof levels. Thus, diaphragm design that starts off as a simple design of a deep beam ends up being quite a challenging and demanding piece of work.

#### 5.7.10.3 General Procedure for Diaphragm Design

In its role as a distributor of seismic loads to vertical lateral supports, the floor or roof surface acts as a diaphragm essentially responding as a horizontal beam, spanning between lateral support points. It may engage beam elements at the perimeter transverse to the direction of load as top and bottom *chords* or flanges. In this case, the bending moment can be resolved into a tension and compression couple and considered resisted by the beam elements while the shear is resisted by the diaphragm surface. In the absence of such flange elements to resist the moment couple, the floor or roof must act as a deep plate resisting both bending and shear forces. Either types of diaphragm behavior requires the effective transfer of bending and shear forces in the plane of the roof or floor, necessitating careful the detailing of connections between the diaphragm and the lateral support system.

*Collectors* are elements of the floor or roof structures that serve to transmit lateral forces from their location of origin to the vertical seismic force-resisting elements (e.g., walls or moment frames) of the building. Typically, collectors transfer earthquake forces in axial tension or compression. When a collector is a part of the gravity force-resisting system, it is designed for seismic axial forces along with the bending moment and shear force from the applicable gravity loads acting simultaneously with seismic forces.

When subjected to lateral forces corresponding to a design earthquake, most buildings are expected to undergo inelastic, nonlinear behavior. Typically, the structural elements of a building that are intended to perform in the nonlinear range are the vertical elements of the seismic force-resisting system, such as structural walls or moment frames. For the intended seismic response to occur, other parts of the seismic-force path, particularly collectors and their connections to the vertical seismic

force-resisting elements, should have the strength to remain essentially elastic during an earthquake. It is for this reason that ACI 318-08, Section 21.11 mandates the design of collectors and their connections in buildings assigned to SDC D and higher, for seismic forces amplified by a factor,  $\Omega_o$ . The amplification factor ranges between 2 and 3 depending upon the type of seismic system.

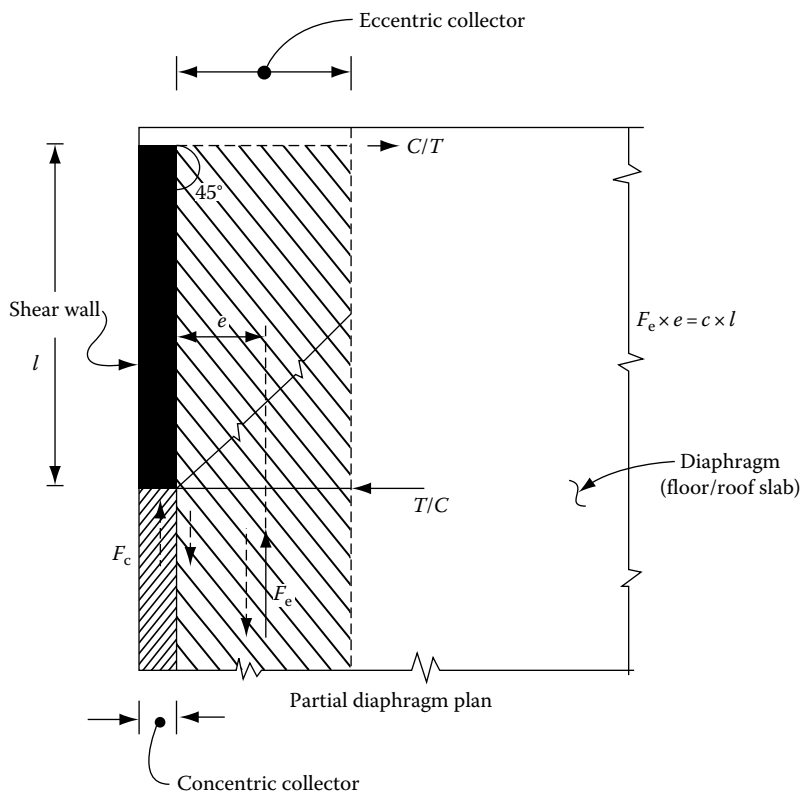
The intent of the  $\Omega_o$  amplification factor, as stated previously, is to allow for the likely overstrength of the vertical seismic force-resisting elements so that major yielding does not occur in collectors and their connections prior to yielding and inelastic response at the vertical elements of the building's seismic force-resisting system.

Two values of compressive stress index calculated for the factored forces on the gross section of the structural diaphragm are used to determine whether confining reinforcement is required. A compressive stress index of  $0.2f'_c$  is permitted when design forces are not amplified. If they are, then a higher index of  $0.5f'_c$  is used. Because the integrity of the entire structure depends on the ability of the collector to resist substantial compressive force under severe cyclic loading, transverse reinforcement is required to provide the confinement for the concrete and the reinforcement.

### 5.7.10.3.1 Eccentric Collectors

The following discussion illustrates a method for collector design where only a part of the seismic load is resisted by the reinforcement directly in line with the shear wall. The balance of seismic force is resisted by reinforcing bars placed along the side of the wall. The slab shear-friction capacity at the wall-slab interface provides for the transfer of seismic forces to the wall.

Observe when this occurs, there is an eccentricity between the resultant of collector force in the slab and the shear wall reaction (see Figure 5.42). This eccentricity can create secondary stresses in the slab-transfer region adjacent to the wall. For a complete and consistent load path design, the



**FIGURE 5.42** Eccentric collector:  $F_c$  is the axial force concentric to wall and  $F_e$  is the axial force eccentric to wall.

effect of seismic force eccentricity in this “diaphragm segment” must be evaluated to determine that adequate reinforcement is provided to resist the induced stresses.

A key design issue is to determine the effective width of slab adjacent to the shear wall that is used to resist collector forces. Where a narrow effective width is assumed, eccentric force effects become small, but more reinforcement may be required to drag the collector forces in line with the wall. On the other hand, if a wide slab width is used more force can be transferred through the slab, reducing reinforcing bar congestion at the end of the wall; however, secondary stresses caused by force eccentricity would be larger. In the absence of definitive guide lines, the author recommends a 45° dispersion line to determine the effective slab width. A schematic design strategy is shown in Figure 5.42.

As inferred many times in this chapter, the term “diaphragm” in seismic design applies to a horizontal element that transfers earthquake-induced inertial forces to vertical elements of the lateral force-resisting systems. To do so requires a collective action of diaphragm components including chords, collectors, and ties. In buildings, typically floors and roofs provide for the diaphragm action by connecting building masses to the primary vertical elements of the lateral force-resisting system.

A chord is a component of a diaphragm provided at each edge to develop the axial force due to bending. It may consist of either a continuous beam or of a combination of wall, frame, or a segment of the slab assumed to act as a chord element. At reentrant corners, diaphragm chords are extended beyond the corners, a distance sufficient to develop the accumulated diaphragm boundary stresses into the diaphragm.

For the purpose of analysis, diaphragms are classified as either flexible or rigid depending upon their in-place deformation relative to the average interstory drift of the vertical lateral force-resisting elements of the story immediately below the diaphragm level. If the deformation of the diaphragm is twice the average interstory drift of the story below the diaphragm, then the diaphragm is considered flexible. If it is less, it is classified as rigid.

A diaphragm collector may be defined as a horizontal element furnished to transfer accumulated diaphragm shear forces to the vertical lateral force-resisting element. Its primary purpose is to deliver diaphragm forces that are in excess of the forces transferred directly to the vertical element.

#### 5.7.10.3.2 Diaphragm Design Summary: Buildings Assigned to SDC C and Higher

##### Step 1:

- Evaluate the diaphragm inertial force  $F_{px}$  at the floor and roof levels by the following formula (ASCE 7-05, Equation 12.10.1):

$$F_{px} = \frac{\sum_{i=x}^n F_i}{\sum_{i=x}^n W_i} W_{px}$$

where

$F_{px}$  is the diaphragm design force at level  $x$

$F_i$  is the design force applied to level  $i$

$W_i$  is the weight tributary to level  $i$

$W_{px}$  is the weight tributary to the diaphragm at level  $x$

$F_{px}$  need not exceed  $0.4S_{DS}IW_{px}$  but shall not be less than  $0.2S_{DS}IW_{px}$ .

- Observe that additional shear forces resulting from the transfer of vertical seismic elements or changes in their relative stiffness must be added to  $F_{px}$ . These additional forces shall be multiplied by the redundancy factor,  $\rho$ , equal to that used in the design of the structure. Observe that  $F_{px}$  computed from the above equation is typically larger than force  $F_x$  determined by the following equation (ASCE 7-05, Equation 12.8-11):

$$F_x = C_{vx}V$$



where

$C_{vx}$  is the vertical distribution factor, which is calculated from  $\frac{W_x h_x^k}{\sum_{i=1}^n W_i h_i^k}$  (ASCE 7-05, Equation 12.8-12)

$V$  is the total design lateral force often referred to as base shear (kip or kN)

$W_i$  and  $W_x$  are the portion of the total gravity load of the structure ( $W$ ) located or assigned to level  $i$  or  $x$

$h_i$  and  $h_x$  are the height (ft or m) from the base to level  $i$  or  $x$

$k$  is an exponent related to the structure period as follows:

For structures having a period of 0.5 s or less,  $k = 1$ .

For structures having a period of 2.5 s or more,  $k = 2$ .

For structures having a period between 0.5 and 2.5 s,  $k$  shall be 2 or shall be determined by linear interpolation between 1 and 2.

The formula for  $F_{px}$  allows for a higher mode participation that can result in larger forces at individual diaphragm levels than predicted by the equation for  $F_x$ .

**Step 2:** Perform a 3D lateral load analysis of the building by applying  $F_{px}$  at the floor and roof levels. Include torsion but ignore its effect if it reduces shear in the vertical lateral load-resisting elements.

**Step 3:** Determine the net shear in the vertical elements due to  $F_{px}$  equal to the difference in shears resisted by the vertical elements immediately above and below the level of the diaphragm being designed. Conceptually, the shear forces may be considered as reactions to the inertial forces of the diaphragm at that level.

**Step 4:** Determine a set of equivalent loads at the diaphragm level that is in equilibrium with the shear forces determined in Step 3. Use both force and moment equilibrium conditions. The equivalent loads may be determined as a combination of primary action due to  $F_{px}$  and a secondary action due to torsional effects. Refer to the numerical example given below.

**Step 5:**

- Using the equivalent loads, determine the shear and bending moment at critical sections of the diaphragm.
- Compute the shear per unit length to check the shear capacity of the diaphragm. Provide collectors, also referred to as drag beams, to carry the shear that is in excess of force transferred directly into the vertical elements.

**Step 6:** Calculate the ultimate shear capacity of the diaphragm as follows.

$$\begin{aligned} V_u &= \phi(V_c + V_s) \\ &= \phi A_{cv}(2\sqrt{f'_c} + \rho_n f_y) \end{aligned}$$

Note that the strength reduction factor for shear,  $\phi$ , in diaphragm designs must not exceed the value used for the shear design of vertical elements of lateral force-resisting systems.

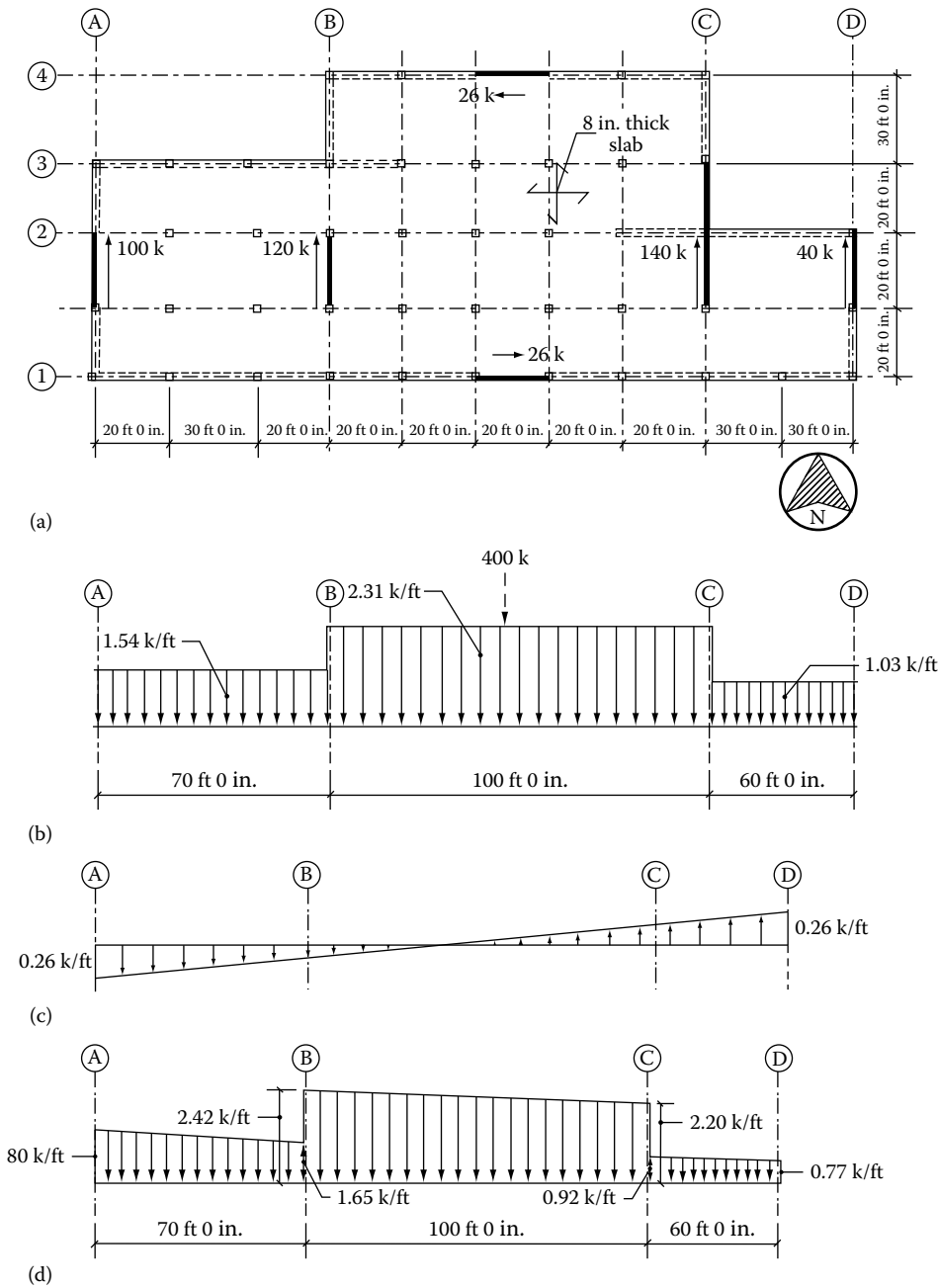
**Step 7:**

- Check perimeter beams (or equivalent widths of slab assumed to act as beams) and their connections for diaphragm chord forces.
- Extend chords at reentrant corners, if any, to develop the forces calculated at the critical sections.

5.7.10.3.3 Diaphragm Design Example

**Given:** A typical floor plan of a concrete building is shown in Figure 5.43a. The building’s lateral load-resisting system consists of special reinforced concrete shear walls in both directions. The floor framing is an 8-in.-thick, two-way slab system.

The wall forces above and below the given diaphragm have been determined by performing a 3D analysis assuming rigid diaphragms for the floors and roof. The differences between the two shears,



**FIGURE 5.43** Diaphragm design example: (a) floor plan, (b) equivalent loads due to primary diaphragm action, (c) equivalent loads due to torsional effects, (d) final equivalent loads (= (b) + (c)),

(continued)

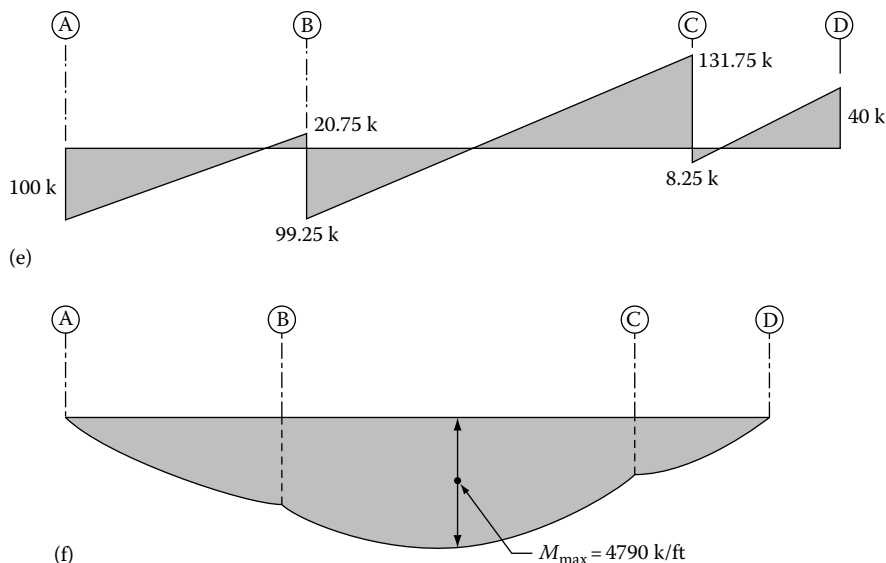


FIGURE 5.43 (continued) (e) shear diagram, and (f) bending moment diagram.

which may be considered as reactions to the diaphragm inertial loads, are shown in Figure 5.43b. The shears in the E–W walls are due to torsional effects.

In designing the shear walls for seismic loads, it was determined that their nominal shear strength was less than the shear corresponding to the development of the nominal flexural strength. Therefore, a strength reduction factor  $\phi = 0.60$  was used for the shear design of the walls. And, because ACI 318-08 Section 9.3.4(b) mandates the value of  $\phi$  for the shear design of diaphragms not to exceed the value used for the shear design of walls, we use  $\phi = 0.60$ .

**Required:** Diaphragm analysis including design of collectors and chords.

### Solutions

**Equivalent loads:** These may be determined by considering the diaphragm inertial forces as a consequence of two actions. The first, the primary action, results from the inertial force  $F_{px}$  distributed along the length of the diaphragm in proportion to its mass. The second is due to the eccentricity of  $F_{px}$  with respect to the center of the stiffness of the walls. This action results in a set of equal and opposite loads that establish moment equilibrium between the inertial forces and the reactions.

Observe that the mass per unit area of floors and roof is typically constant over the entire area. Therefore,  $F_{px}$  may be distributed along the length of the diaphragm in the same proportion as its width. For the example problem, as shown in Figure 5.43c,

$$\text{Total area of diaphragm} = 60 \times 70 + 90 \times 100 + 40 \times 60 = 15,600 \text{ ft}^2$$

$$\text{Inertial force per unit area} = \frac{400}{15,600} = 0.0256 \text{ kip-ft}^2$$

$$\text{Load per unit length of segment A} = 0.0256 \times 60 = 1.54 \text{ kip-ft}$$

$$B = 0.0256 \times 90 = 2.31 \text{ kip-ft}$$

$$C = 0.0256 \times 40 = 1.03 \text{ kip-ft}$$

If we were to draw a bending moment diagram corresponding to the primary equivalent loads shown in Figure 5.43b, it would be seen that the moment diagram will not close. For example, the moment at D due to reactions at A, B, and C

$$\begin{aligned} M_D &= 100 \times 23 + 120 \times 160 + 140 \times 60 \\ &= 50,600 \text{ kip-ft} \end{aligned}$$

And the moment due to the equivalent inertial loads

$$\begin{aligned} M_D &= 1.54 \times 70 \left( \frac{70}{2} + 160 \right) + 2.31 \times 100(50 + 60) \\ &= 48,267 \text{ kip-ft} \end{aligned}$$

Thus, there is a moment gap of  $50,600 - 48,267 = 2,333$  kip-ft calculated at grid D. Observe that the gap is the same for the entire length of diaphragm.

To close the gap, we modify the distribution of the primary equivalent load. This is done by determining an equal and opposite inertia force due to the secondary action, and superimposing the same on the primary action. The secondary action is a self-equilibrating system resulting only in an applied moment.

For the example problem, the moment gap of 2333 kip-ft is closed by imposing a triangular distribution of equal and opposite inertia forces as shown in Figure 5.43c. If  $w_T$  is the maximum value at the ends

$$\frac{w_T}{2} \times \frac{L}{2} \times \frac{2L}{3} = 2333 \text{ kip-ft}$$

or

$$w_T = 0.26 \text{ kip-ft/ft}$$

The final equivalent load for determining the design shear force and bending moments is shown in Figure 5.43c.

**Diaphragm design for shear forces:** In determining the shear capacity of diaphragms, the value for  $\phi$ , the capacity reduction factor, should not exceed the value used in the design of vertical elements of the lateral load-resisting systems (see ACI 318-08, Section 9.3.4(b)). For the example problem,  $\phi$  for shear wall design is given as 0.6. Therefore,  $\phi$  for diaphragm shear design should not exceed 0.6. Use  $\phi = 0.6$ .

The shear capacity per feet length of a concrete slab without shear reinforcement is given by

$$\begin{aligned} \phi V_c &= \phi 2\sqrt{f'_c}bt \\ &= 0.6 \times 2\sqrt{4000 \times 12 \times 8} \\ &= 7286 \text{ lbs} \\ &= 7.3 \text{ kip-ft} \end{aligned}$$

Grid	A	B	B	C	C	D
		Left	Right	Left	Right	
Diaphragm width, ft	60	60	90	90	40	40
Ultimate shear force, kip	100	20.75	99.25	131.75	8.25	40
Unit shear per feet of diaphragm	1.67	0.35	1.10	1.46	0.20	1.0

**FIGURE 5.44** Summary of unit shears.

Referring to the bending moment and shear force diaphragms given in Figure 5.43e and f, and the summary of unit shears given in Figure 5.44 it is observed that the maximum ultimate shear flow equal to 1.67 kip-ft occurs in the diaphragm at line A. This is less than the capacity 7.3 kip-ft. Therefore, by calculations, no shear reinforcement is required. However, provide #4 @ 18 in. the N–S direction at mid-depth of slab for a width equal to 5 ft from grid A.

**Collector (drag-strut) design:** To keep the maths simple, the drag strut along line A will be designed by conservatively ignoring the shear transferred to the 5 ft-long wall at the slab–wall interface. Therefore, the entire shear of 100 kip must be delivered as axial forces to the shear wall by the drag beams on grid A. Let us assume the drag beams are 18 in. wide  $\times$  18 in. deep. Using a seismic amplification factor,  $\Omega_o = 2.5$ , the design axial compression and tension at the two ends of the 5 ft-wall is

$$\begin{aligned} T_u = C_u &= \Omega_o \times 100/2 \\ &= 2.5 \times 100/2 = 125 \text{ kip} \end{aligned}$$

$$A_s \text{ tension} = 125/0.9 \times 60 = 2.315 \text{ in.}^2$$

$$\text{Provide four \#7, } A_s, \text{ provided} = 2.4 \text{ in.}^2 > 2.315 \text{ in.}^2$$

The compressive stress in the drag beam is equal to  $125/18 \times 18 = 0.386 \text{ ksi} = 386 \text{ psi}$ .

Comparing this to the index stress  $= 0.5f'_c = 0.5 \times 4000 = 2000 \text{ psi}$ , we observe that transverse reinforcement in the collectors need not satisfy the confinement requirement given in ACI 318-08, Section 21.9.6.4(c). However, as a nominal transverse reinforcement, we use #4 @ 12, two-legged, closed stirrups.

**Chord design:** Determine the design tension  $T_u$  and compression  $C_u$  from the relation  $T_u = C_u = M_u/\text{Slab width}$

$$T_u = C_u, \text{ Span BA} = 1244/60 = 20.74 \text{ kip } A_s = 20.74/0.9 \times 60 = 0.39 \text{ in.}^2, \text{ provide two \#6}$$

$$\text{BC} = 1244/90 = 13.82 \text{ kip } A_s = 13.82/0.9 \times 60 = 0.26 \text{ in.}^2, \text{ provide two \#5}$$

$$\text{CB} = 90/90 = 15.92 \text{ kip } A_s = 15.92/0.9 \times 60 = 0.30 \text{ in.}^2, \text{ provide two \#5}$$

$$\text{CD} = 90/40 = 35.82 \text{ kip } A_s = 35.82/0.9 \times 60 = 0.67 \text{ in.}^2, \text{ provide two \#6}$$

The maximum moment for chord design occurs between grids B and C. The corresponding chord tension force is given by

$$\begin{aligned} T_u &= 4790/90 = 53.22 \text{ kip} \\ A_s &= T_u/\phi f_y = 53.22/0.9 \times 60 = 0.98 \text{ in.}^2 \end{aligned}$$

Provide two #7 reinforcements giving  $A_s = 2 \times 0.6 = 1.2 \text{ in.}^2$ , for chord action in the spandrel beams between grids B and C. At reentrant corners extend the beams and reinforcement one-bay into the slab.

The maximum compressive force  $C_u$  occurs in span BC, and is equal to

$$C_u = T_u = 52.22 \text{ kip}$$

Assuming a 24 in.  $\times$  24 in. spandrel beam, the compressive stress due to chord action is equal to  $52.22/24 \times 24 = 0.096 \text{ ksi} = 96 \text{ psi}$ , which is less than  $0.2 f'_c = 0.2 \times 4000 = 800 \text{ psi}$ . Therefore, by calculations, no additional transverse reinforcement is required in the chord beams. However, provide a nominal reinforcement of #4 @ 12, two-legged stirrups for the entire span.

### 5.7.11 CATALOG OF SEISMIC DESIGN REQUIREMENTS

The seismic design requirements given in the ASCE 7-05 are cascading, meaning that what applies to a lower SDC building also applies to buildings in higher SDCs. For example, if analysis using bidirectional lateral loads is required for an SDC B building, they are also a requirement for SDCs C through F buildings. In other words, what applies to SDC A applies to SDCs B through F, what applies to SDC C applies to SDCs D through F, and so on.

#### 5.7.11.1 Buildings in SDC A

1. Determine a pseudo-seismic lateral force at each level by using the following equation:

$$F_x = 0.01 w_x$$

where

$F_x$  is the design lateral force applied at story  $x$

$w_x$  is the portion of the total dead load of the structure,  $D$ , located at or assigned to level  $x$

This minimum base shear equal to 1% of the seismic weight of the structure applies to all buildings irrespective of SDC. The term  $w_x$  applies only to the dead load of the floor. It is a revision to ASCE 7-02 provision in which  $w_x$  included a list of other loads such as 25% of the floor live load in a storage structure, partition load, the weight of permanent equipment, and 20% of the flat roof snow load. The load  $F_x$  does not represent a seismic-related calculation, but rather meant to provide a certain level of strength relative to the mass of the structure to ensure structural integrity.

2. Apply the static lateral force  $F_x$  independently in two orthogonal directions. The lateral forces in each direction shall be applied at all levels simultaneously. Orthogonal combination procedure of applying 100% of the forces in one direction plus 30% in the perpendicular direction is not required. Similarly, simultaneous applications of orthogonal ground motions are not warranted.
3. Interconnect all parts of the structure to provide a continuous load path. Tie any smaller portion of the structure to the remainder of the structure with connections having a lateral design strength not less than 5% of the portion's weight.
4. Provide connections at supports for each beam, girder, or truss for resisting a horizontal force acting parallel to the member. The connections shall have a minimum design strength of 5% of the dead plus live load reaction.
5. Anchor concrete walls to the roof and all floors to provide lateral support for the wall. The connection shall be capable of resisting a horizontal force equal to 5% of the wall weight but not less than 280 lb/linear foot.

6. The following combinations of factored loads using strength design are applicable. Only the more common dead, live, wind, and earthquake loads are given here.
  - a.  $1.4D$
  - b.  $1.2D + 1.6L + 0.5L_r$
  - c.  $1.2D + 1.6L_r + (L + 0.8W)$
  - d.  $1.2D + 1.6W + L + 0.5L_r$
  - e.  $1.2D + 1.0E + L$
  - f.  $0.9D + 1.6W$
  - g.  $0.9D + 1.0E$

In the above equations, the term  $E$  refers to the effect of earthquake loads as determined by applying a horizontal load of  $F_x$  equal to 1% of the building dead load at each level. Vertical effects,  $E_v$ , of the seismic loads, design coefficients, and seismic factors such as response modification coefficient  $R$ , over strength factors  $\Omega_o$ , and deflection amplification factor,  $C_d$ , are not of concern in the design of structures assigned to SDC A.

7. Just about any structural system that has a continuous load path is permitted for buildings assigned to SDC A. You are not restricted to the list given in ASCE 7-05, Table 12.2.1. The structural members and connections need only to be designed for the forces determined from the prescribed analysis. The non-ductile detailing requirements given in the first 20 chapters of ACI 318-05/08 are presumed to be sufficient to provide the necessary strength and ductility for buildings assigned to SDC A.
8. For SDC A buildings, ASCE 7-05 provisions do not require the structural design of diaphragms, chords, and collectors. This is not so for buildings in SDCs B through F.
9. There is no requirement to increase the design loads due to horizontal and vertical structural irregularities. Extreme irregularities are not prohibited. This is not the case for buildings assigned to SDCs B through F.
10. There is no requirement to multiply the torsional moment by a torsional amplification factor.
11. There is not requirement to compute the story drift,  $\Delta$ , along the building edges.
12. Elements supporting discontinuous walls or frames need not be designed for load combinations along the overstrength factor  $\Omega_o$ .
13. There is no height limit for buildings exhibiting extreme weak story irregularity.

### 5.7.11.2 Buildings in SDC B

SDCs B and C buildings will be constructed in the largest portion of the United States. Earthquake-resistant requirements are increased appreciably over SDC A requirements, but they still are quite simple compared to present requirements in areas of high seismicity or for buildings assigned to SDC C and higher. The SDC B requirements specifically recognize the need to design diaphragms, provide collectors, and reinforce around openings. These requirements may seem elementary and obvious but, because they are not specifically covered in many codes, some engineers totally neglect them.

SDC B includes Occupancy Categories I through III structures in regions of moderate seismicity. Structures in this category must be designed for the calculated forces in addition to the requirements of SDC A. The design requirements are

1. Instead of lateral force,  $F_x = 0.01w_x$  at each level, we now use a rational procedure to determine the total design seismic force and its distribution over the height of the building. Typically the ELF procedure or a dynamic procedure is used for this purpose.
2. The building structure shall include complete lateral and vertical force-resisting systems capable of providing adequate strength stiffness and *energy-dissipating capacity* to withstand the design ground motions without exceeding prescribed limits of deformation and strength demand.

3. The directions of the application of seismic forces used in the design shall be those that will produce the most critical effects. However, the application of seismic forces independently in two orthogonal directions (as for SDC A buildings) is deemed sufficient. Similarly, orthogonal effects are permitted to be neglected.
4. The connections shall develop the strength of the connected members or the forces determined from seismic analysis. Adequate strength shall be provided in individual members to resist the shears, moment, and axial forces determined from seismic analysis.

The analysis of a structure and the provision of a design ground motion alone do not make a structure earthquake resistant; additional design requirements are necessary to provide adequate earthquake resistance in structures. Experienced seismic designers normally fill these requirements, but because some were not formally specified, they often are overlooked by inexperienced engineers.

Probably the most important single requirement of an earthquake-resistant structure is that it be tied together to act as a unit. This is important not only in earthquake-resistant design, but also is an indispensable strategy in resisting high winds, floods, explosion, progressive failure, and even such hazards as foundation settlement. Hence, the requirement that all parts of the building (or unit if there are separation joints) be so tied together. Any part of the structure must be tied to the rest to resist a force of  $0.133S_{DS}$  (but not less than 0.05) times the weight of the smaller portion. In addition, beams must be tied to their supports or columns and columns to footings for a minimum of 5% of the dead and live load reactions.

The connections shall be capable of transmitting the seismic force,  $F_p$ , induced by the parts being connected. Any small portion of the structure shall be tied to the main structure with connections capable of delivering a seismic force equal to  $0.33S_{DS}$  times the weight of the smaller portion, or 5% of the portion weight, whichever is greater.

5. Extreme weak story irregularity is permitted for SDC B buildings not over two stories or 30 ft in height. The height limit does not apply where the extreme weak story is capable of resisting a total seismic force equal to  $\Omega_0$  times the design force.
6. There is no requirement to increase the diaphragm forces due to horizontal or vertical irregularities.
7. Torsional moment due to accidental torsion need not be amplified.
8. Perform a 3D dynamic analysis for structures exhibiting torsional irregularity, extreme torsional irregularity, out-of-plane irregularity, or nonparallel-systems irregularity.
9. There is no requirement to compute the story drift,  $\Delta$ , along the building edges.
10. Extreme torsional irregularity, extreme soft story irregularity, or extreme weak story irregularity are not prohibited.
11. Design the elements supporting discontinuous walls or frames for load combinations using the overstrength factor  $\Omega_o$ .
12. Perform a 3D dynamic analysis with due consideration for diaphragm stiffness. Use cracked section properties for concrete elements. Include  $P\Delta$  effects.
13. There is no need to multiply,  $M_{ta}$ , the torsional moment due to accidental torsion by a torsional amplification  $A_x = (\delta_{\max}/1.2\delta_{\text{ave}})^2 \leq 3.0$ .

### 5.7.11.3 Buildings in SDC C

The requirements for SDC C are more restrictive than those for SDCs A and B. Also, a nominal interconnection between pile caps and caissons is required. SDC C includes Occupancy Categories I through III structures in regions of severe seismicity. The design requirements are:

1. All requirements SDCs A and B also apply to SDC C.
2. A geotechnical investigation shall be conducted and a report shall be submitted that includes an evaluation of the following potential geologic and seismic hazards:



- a. Slope instability
- b. Liquefaction
- c. Differential settlement
- d. Surface displacement due to faulting or lateral spreading

The report shall contain recommendations for appropriate foundation designs or other measures to mitigate the effects of the previously mentioned hazards. Where deemed appropriate by the authority having jurisdiction, a site-specific geotechnical report is not required where prior evaluations of nearby sites with similar soil conditions provide sufficient direction relative to the proposed construction.

3. Foundations:

**Pole-type structures.** Where construction employing posts or poles as columns embedded in the earth or embedded concrete footings in the earth is used to resist lateral loads, the depth of embedment required for posts or poles to resist seismic forces shall be determined by means of the design criteria as established in the foundation investigation report.

**Foundation ties.** Individual pile caps, drilled piers, or caissons shall be interconnected by ties. All ties shall have a design strength in tension or compression at least equal to a force equal to 10% of  $S_{DS}$  times the larger pile cap or column factored dead plus factored live load unless it is demonstrated that equivalent restraint will be provided by reinforced concrete beams within slabs on grade or reinforced concrete slabs on grade or confinement by competent rock, hard cohesive soils, very dense granular soils, or other approved means.

**Pile anchorage requirements.** Where required for resistance to uplift forces, the anchorage of steel pipe (round HSS sections), concrete-filled steel pipe, and H piles to the pile cap shall be made by means other than concrete bond to the base steel section.

**Exception.** The anchorage of concrete-filled steel pipe piles is permitted to be accomplished using deformed bars developed into the concrete portion of the pile.

4. Increase design forces determined by static procedure by 25% for connections of diaphragms to vertical elements and to collectors, and for connections of collectors to the vertical elements. Collectors and their connections also shall be designed for these increased forces unless they are designed for load combinations with the overstrength factor  $\Omega_o$  (Section 12.3.3.4).
5. Multiply,  $M_{ta}$ , the torsional moment due to accidental torsion by a torsional amplification

$$A_x = \frac{(\delta_{\max})^2}{1.2\delta_{\text{ave}}} \leq 3.0.$$

6. Compute story drift,  $\Delta$ , as the largest difference of the deflections along any of the edges.
7. Use  $100x+30y$ , if you are using ELF or modal analysis. Use the simultaneous application of load, if you are analyzing the structure using a linear or nonlinear response history procedure.

#### 5.7.11.4 Buildings in SDC D

SDC D requirements compare roughly to present design practice in California seismic areas for buildings other than schools and hospitals. All moment-resisting frames of concrete must meet ductility requirements. Interaction effects between structural and nonstructural elements must be investigated. Foundation interaction requirements are increased.

SDC D includes Occupancy Categories I through IV structures in regions of high seismicity, but not located close to a major fault, as well as Occupancy Category IV structures in regions of somewhat less severe seismicity. The use of some structural systems is restricted in this design category and dynamic analysis must be used for the design of irregular structures. The design requirements are

1. All requirements of SDCs A through C also apply to SDC D.
2. Additional geotechnical investigation report requirements shall include
  - a. The determination of lateral pressures on basement and retaining walls due to earthquake motions.
  - b. The potential for liquefaction and soil strength loss evaluated for site peak ground accelerations, magnitudes, and source characteristics consistent with the design earthquake ground motions. Peak ground acceleration is permitted to be determined based on a site-specific study taking into account soil amplification effects or, in the absence of such a study, peak ground accelerations shall be assumed equal to  $S_s/2.5$ .
  - c. The assessment of potential consequences of liquefaction and soil strength loss, including the estimation of differential settlement, lateral movement, lateral loads on foundations, the reduction in foundation soil-bearing capacity, increases in lateral pressures on retaining walls and the flotation of buried structures.
  - d. The discussion of mitigation measures such as, but not limited to, ground stabilization, the selection of appropriate foundation type and depths, the selection of appropriate structural systems to accommodate anticipated displacements and forces, or any combination of these measures and how they shall be considered in the design of the structure.
3. A special moment frame that is used but not required by ASCE 7-05, Table 12.2.1 shall not be discontinued and supported by a more rigid system with a lower response coefficient  $R$ , unless the building height is limited to two stories, and a 25% increase in loads is taken in the design of diaphragm elements.
4. Vertical irregularity Type 5b of Table 5.24 (ASCE 7-05, Table 12.3-2) shall not be permitted.
5. For structures having a horizontal structural irregularity of Type 1a, 1b, 2, 3, or 4 in Table 5.23 (ASCE 7-05, Table 12.3-1) or a vertical structural irregularity of Type 4 in Table 5.24 (ASCE 7-05, Table 12.3-2), the design forces shall be increased 25% for connections of diaphragms to vertical elements and to collectors, and for connections of collectors to the vertical elements. Collectors and their connections also shall be designed for these increased forces unless they are designed for the load combinations with the overstrength factor  $\Omega_o$ .
6. Horizontal structural components shall be designed for a net upward force of 0.2 times the dead load in addition to the other applicable load combinations.
7. Redundancy factor,  $\rho$ , shall equal 1.3 unless one of the two conditions is met, whereby  $\rho$  is permitted to be taken as 1.0:
  - a. Each story resisting more than 35% of the base shear in the direction of interest shall comply with ASCE 7-05, Table 12.3-3.
  - b. Structures that are regular in plan at all levels provided that the seismic force-resisting systems consist of at least two bays of seismic force-resisting perimeter framing on each side of the structure in each orthogonal direction at each story resisting more than 35% of the base shear. The number of bays for a shear wall shall be calculated as the length of shear wall divided by the story height or two times the length of shear wall divided by the story height for light-framed construction.
8. Foundations: The anchorage of the pile into the pile cap should be conservatively designed to allow energy-dissipating mechanisms, such as rocking, to occur in the soil without the structural failure of the pile. Precast prestressed concrete piles are exempt from the concrete special moment frame column confinement requirements since these requirements were never intended for slender, precast prestressed concrete elements and will result in unbuildable piles. These piles have been proven through cyclic testing to have adequate performance with substantially less confinement reinforcing than required by ACI 318. Therefore, a transverse steel ratio reduced from that required in frame columns is permitted in concrete piles. It should be noted that confinement provided by the soil improves the behavior of concrete piles.

The design and construction of concrete foundation components shall confirm to the requirements of ACI 318, Section 21.8, except as modified here in:

**Pole-type structures:** Where construction employing posts or poles as columns embedded in the earth or embedded concrete footings in the earth is used to resist lateral loads, the depth of embedment required for posts or poles to resist seismic forces shall be determined by means of the design criteria as established in the foundation investigation report.

**Foundation ties:** Individual pile caps, drilled piers, or caissons shall be interconnected by ties. In addition, individual spread footings founded on soil defined in ASCE 7-05 Chapter 20 as Site Class E or F shall be interconnected by ties. All ties shall have a design strength in tension or compression at least equal to a force equal to 10% of  $S_{DS}$  times the larger pile cap or column factored dead plus factored live load unless it is demonstrated that equivalent restraining will be provided by reinforced concrete beams within slabs on grade or reinforced concrete slabs on grade or confinement by competent rock, hard cohesive soils, very dense granular soils, or other approved means.

**General pile design requirement:** Piling shall be designed and constructed to withstand deformations from earthquake ground motions and structure responses. Deformations shall include both free-field soils strains (without the structure) and deformations induced by lateral pile resistance to structure seismic forces, all as modified by soil–pile interaction.

**Batter piles:** Batter piles and their connections shall be capable of resisting forces and moments from the load combinations with the overstrength factor of ASCE 7-05 Section 12.4.3.2 or 12.14.3.2.2. Where vertical and batter piles act jointly to resist foundation forces as a group, these factors shall be distributed to the individual piles in accordance with their relative horizontal and vertical rigidities and the geometric distribution of the piles within the group.

Batter pile systems that are partially embedded have historically performed poorly under strong ground motions. Difficulties in examining fully embedded batter piles have led to uncertainties as to the extent of damage for this type of foundation. Batter piles are considered as limited ductile systems and should be designed using the special seismic load combinations.

#### 5.7.11.5 Buildings in SDC E

SDC E includes Occupancy Categories I through III structures located close to major active fault that is defined as a region with  $S_1 \geq 0.75g$ . Severe restrictions are placed on the use of some structural systems, irregular structures, and analysis methods. The design requirements are

1. All requirements of SDCs A through D also apply to SDC E.
2. Siting of a structure is prohibited where there is a known potential for an active fault to cause the rupture of the ground surface at the structure.

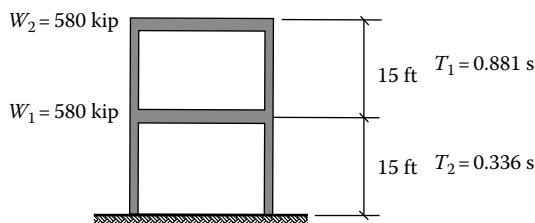
#### 5.7.11.6 Buildings in SDC F

SDC F includes Occupancy Category IV structures located close to major active fault (regions where  $S_1 \geq 0.75g$ ). As in SDC E structures, severe restrictions are placed on the use of some structural systems, irregular structures, and analysis methods. The design requirements are

1. All requirements of SDCs A through E also apply to SDC F.
2. There are no additional requirements for SDC F buildings designed using reinforced concrete. (The two limitations given in ASCE 7-05 Sections 12.2.5.8 and 12.2.5.9 apply to ordinary and intermediate moment frames in steel.)

### 5.8 SEISMIC DESIGN EXAMPLE: DYNAMIC ANALYSIS PROCEDURE (RESPONSE SPECTRUM ANALYSIS) USING HAND CALCULATIONS

The illustration of dynamic analysis procedure using hand calculations for buildings taller than, say, two or three stories becomes unwieldy. Therefore, in the following example, a planar frame of a two-story building shown in Figure 5.45 is selected. To keep the explanation simple, infinitely large



**FIGURE 5.45** Two-story example: dynamic analysis hand calculations.

values are assumed for the flexural stiffness of the beams and the axial stiffness of the columns. Thus, the lateral deflection of the frame results from column flexure only.

**Given:**

A two-story, 30-ft-tall concrete building with a floor-to-floor height of 15 ft  
 Structural system: special moment-resisting frame (SMRF) system  
 Cracked moment of inertia of columns  $I_{cr} = 12,000 \text{ in.}^4$  for each column  
 Seismic dead load  $W = 580 \text{ kip/floor} = 2 \times 580 = 160 \text{ kip}$  for the entire building  
 Modules of the elasticity of concrete  $E = 4000 \text{ ksi}$

The procedure consists of determining

- Modal periods  $T_1$  and  $T_2$
- Mode shapes corresponding to  $T_1$  and  $T_2$
- Modal mass and participation factors for each mode
- Modal base shears

To help us understand how static base shear is used to scale dynamic shear, the remainder of this solution consists of determining

- Static base shear using ELF procedure
- Scaling of dynamic results
- Distribution of modal base shear in each mode

**Seismic design data:**

MCE spectral response acceleration:

At short period:  $S_s = 1.5$

At 1 s-period:  $S_1 = 0.6$

Seismic importance factor  $I = 1.0$

Soil type =  $S_D$

Site coefficient  $F_a = 1.0$

Site coefficient  $F_v = 1.5$

Modified at short-period response,  $S_{MS} = F_a S_s = 1 \times 1.5 = 1.5$

Modified 1 s-period response,  $S_{M1} = F_v S_1 = 1.5 \times 0.6 = 0.9$

Design spectral response acceleration parameters at 5% damping:

At short period:  $S_{DS} = 2/3 S_{MS} = 2/3 \times 1.5 = 1.0$

At 1 s-period:  $S_{D1} = 2/3 S_{M1} = 2/3 \times 0.9 = 0.6$

For a SMRF,  $R = 8$  and  $C_d = 6.5$ , where  $R$  and  $C_d$  are response modification and deflection factor, respectively. SDC based on both  $S_{DS}$  and  $S_{D1}$  is D for the example building.

**Determine mass matrix [m]**

$$m = W/g = 580/386.4 = 1.5 \text{ kip-s}^2/\text{in.}$$

$$[m] = \begin{bmatrix} 1.5 & 0 \\ 0 & 1.5 \end{bmatrix}$$

**Determine stiffness matrix:** Stiffness  $K$  of each column is given by

$$K = \frac{12EI}{h_s^3}$$

where

$I$  is the total moment of inertia of all columns at level  $i$

$h_s$  is the story height

$E$  is the modulus of elasticity of concrete

$$K = \frac{12EI}{h_s^3} = \frac{12 \times 4,000 \times 12,000}{(12 \times 15)^3}$$

$$= 98.76 \text{ kip/in. for each column, use } 100 \text{ kip/in.}$$

Therefore, stiffness matrix  $[K] = 200 \begin{bmatrix} 2 & -1 \\ -1 & 1 \end{bmatrix}$

**Find the determinant of the matrix**

$$\begin{aligned} & [K] - \omega^2[m] \\ [K] - \omega^2[m] &= \begin{bmatrix} 400 & -200 \\ -200 & 200 \end{bmatrix} - \omega^2 \begin{bmatrix} 1.5 & 0 \\ 0 & 1.5 \end{bmatrix} \\ &= \begin{bmatrix} 400 - 1.5\omega^2 & -200 \\ -200 & 200 - 1.5\omega^2 \end{bmatrix} \end{aligned} \quad (5.1)$$

This matrix is of the form

$$\begin{bmatrix} a_{11} & a_{12} \\ a_{21} & a_{22} \end{bmatrix} \quad (5.2)$$

The determinant of Equation 5.2 is given by

$$a_{11}a_{22} - a_{21}a_{12} \quad (5.3)$$

Substituting the elements of the matrix in Equation 5.1 into Equation 5.3, we get the determinant equal to

$$(400 - 1.5\omega^2)(200 - 1.5\omega^2) - (-200)(-200)$$

Setting the determinant to zero yields a quadratic equation in  $\omega_i^2$ . Thus

$$2.25\omega^4 - 900\omega^2 + 40,000 = 0$$

$$\omega^4 - 400\omega^2 + 17,777.7 = 0$$

Solve for the two roots of this characteristic equation. Label these roots  $\omega_1^2$  and  $\omega_2^2$ , with  $\omega_1$  being smaller of the two.  $\omega_1$  and  $\omega_2$  are called the circular natural frequencies of the system. In mathematical terminology,  $\omega_1^2$  and  $\omega_2^2$  are called the eigenvalues.

$$\omega_i^2 = \frac{400 \mp \sqrt{400^2 - 4 \times 17,777.7}}{2}$$

$$\omega_1^2 = 50.9, \quad \omega_1 = 7.134 \text{ rad/s}$$

$$\omega_2^2 = 349, \quad \omega_2 = 18.68 \text{ rad/s}$$

The period  $T$  is equal to  $\frac{2\pi}{\omega}$

**Determine periods**

$$T_1 = \frac{2\pi}{7.134} = 0.881 \text{ s}$$

$$T_2 = \frac{2\pi}{18.68} = 0.336 \text{ s}$$

**Find mode shapes:** Substitute  $\omega_i^2$  back into the first or second of the characteristic equation to obtain the ratio  $\phi_{11}/\phi_{21}$ . This ratio defines the natural mode or mode shape corresponding to the natural frequency  $\omega_1$ .

$$\begin{bmatrix} 400 - 1.5(50.9) & -200 \\ -200 & 100 - 1.5(50.9) \end{bmatrix} \begin{bmatrix} \phi_{11} \\ \phi_{21} \end{bmatrix} = \begin{bmatrix} 0 \\ 0 \end{bmatrix}$$

$$(400 - 1.5 \times 50.9)\phi_{21} = 200\phi_{11} = 1.618\phi_{11}$$

$$\phi_{21} = 1.0, \quad \phi_{11} = 0.618$$

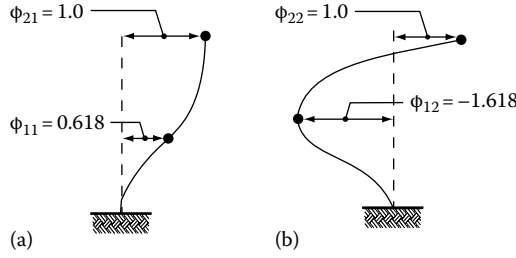
Similarly, by substituting  $\omega_2^2$  back into either the first or second of the characteristic equation, we obtain the mode shape corresponding to the frequency  $\omega_2$ :

$$\begin{bmatrix} 400 - 1.5 \times 349 & -200 \\ 200 & 100 - 1.5 \times 349 \end{bmatrix} \begin{bmatrix} \phi_{12} \\ \phi_{22} \end{bmatrix} = \begin{bmatrix} 0 \\ 0 \end{bmatrix}$$

$$(400 - 1.5 \times 349)\phi_{22} = 200\phi_{12}$$

$$\phi_{22} = -0.618\phi_{12}$$

$$\phi_{22} = 1, \quad \phi_{12} = -1.618$$



**FIGURE 5.46** Vibration modes, two-story example: (a) first mode and (b) second mode.

In mathematical terminology, natural modes  $\begin{bmatrix} \phi_{11} & \phi_{12} \\ \phi_{21} & \phi_{22} \end{bmatrix}$  shown in Figure 5.46 are called eigenvectors.

The portion of the base shear contributed by the  $m$ th mode,  $V_m$ , shall be determined by the following equations:

$$V_m = C_{Sm} W_m$$

$$W_m = \frac{\left( \sum_{i=1}^n \omega_i \phi_{im} \right)^2}{\sum_{i=1}^n \omega_i \phi_{im}^2}$$

where

$C_{Sm}$  is the modal seismic design coefficient determined below

$W_m$  is the effective modal gravity load

$\omega_i$  is the portion of the total gravity load of the structure at level  $i$

$\phi_{im}$  is the displacement amplitude at the  $i$ th level of the structure when vibrating in its  $m$ th mode

**Determine modal mass and participation factors for each mode:** Using the notation

$$L_m = \sum_{i=1}^n \frac{w_i}{g} \phi_{im}$$

and

$$M_m = \sum_{i=1}^n \frac{w_i}{g} \phi_{im}^2$$

$$L_1 = \sum_{i=1}^2 \frac{w_i}{g} \phi_{i1}$$

$$= 1.5 \text{ [kip-s}^2\text{/in.]} \times (\phi_{11} + \phi_{21})$$

$$= 1.5(0.618 + 1.0)$$

$$= 2.426 \text{ kip-s}^2\text{/in.}$$

$$M_1 = \sum_{i=1}^2 \frac{w_i \phi_{i1}^2}{g}$$

$$\begin{aligned}
 &= 1.5 \text{ [kip-s}^2\text{/in.]} \times (\phi_{12}^2 + \phi_{21}^2) \\
 &= 1.5(-1.618 + 1) \\
 &= 2.073 \text{ kip-s}^2\text{/in.}
 \end{aligned}$$

$$\begin{aligned}
 L_2 &= \sum_{i=1}^2 \frac{w_i \phi_{im}}{g} \\
 &= 1.5 \text{ [kip-s}^2\text{/in.]} \times (\phi_{12} + \phi_{22}) \\
 &= 1.5(-1.618 + 1) \\
 &= -0.9270 \text{ kip-s}^2\text{/in.}
 \end{aligned}$$

$$\begin{aligned}
 M_2 &= \sum_{i=1}^2 \frac{w_i \phi_{i2}}{g} \\
 &= 1.5 \text{ [kip-s}^2\text{/in.]} \times (\phi_{12}^2 + \phi_{22}^2) \\
 &= 1.5(-1.618^2 + 1.0^2) \\
 &= 5.43 \text{ kip-s}^2\text{/in.}
 \end{aligned}$$

**Determine effective weight and participating mass for each mode**

$$\begin{aligned}
 W_1 &= \frac{L_1^2 g}{M_1} \\
 &= \frac{2.426^2 \times 386.4}{2.073} \\
 &= 1098 \text{ kip}
 \end{aligned}$$

$$\begin{aligned}
 W^2 &= \frac{L_2^2 g}{M_2} \\
 &= \frac{(0.927)^2 \times 386.4}{5.43} \\
 &= 61.15 \text{ kip, use 61 kip}
 \end{aligned}$$

$$\begin{aligned}
 \sum_{i=1}^2 W_i &= W_1 + W_2 \\
 &= 1098 + 61 \\
 &= 1159 \text{ kip}
 \end{aligned}$$

$$\text{PM}_1 = \frac{1098}{2 \times 580} = 0.95$$

This means that 95% of the total mass participates in the first mode.



$PM_2 = \frac{61}{2 \times 580} = 0.052$  means that 5.2% of the total mass participates in the second mode. Since  $PM_1 = 95\%$  is greater than 90% of the total mass, the consideration of just the first mode would have been sufficient, per most building codes, to capture the dynamic response of the example building.

**Modal seismic design coefficients,  $C_{Sm}$**

$$C_{Sm} = \frac{S_{am}}{(R/I_E)}$$

where  $S_{am}$  is the modal design spectral response acceleration at period  $T_m$  determined from either the general design response spectrum or a site-specific response spectrum.

In the example considered here, the general procedure for determining the spectral acceleration,  $S_{am}$ , will be followed.

$$\text{For } T \geq T_s, \quad S_a = \frac{S_{D1}}{T}$$

$$T_0 < T < T_s, \quad S_a = S_{DS}$$

$$T \leq T_0, \quad S_a = 0.6S_{DS} \frac{T}{T_0} + 0.4S_{DS}$$

where

$$T_s = \frac{S_{D1}}{S_{DS}} \quad \text{and} \quad T_0 = 0.2T_s$$

For the example problem,

$$T_s = \frac{0.6}{1.0} = 0.6 \text{ s}$$

$$T_0 = 0.2 \times 0.6 = 0.12 \text{ s}$$

Mode 1:  $T_1 = 0.881 \text{ s}$ . This is greater than  $T_s = 0.6 \text{ s}$ . Therefore,

$$C_s = \frac{S_{D1}}{T \left( \frac{R}{I} \right)} = \frac{0.6}{0.881 \times \frac{8}{1}} = 0.0851g$$

Mode 2:  $T_2 = 0.336 \text{ s}$ . This is greater than  $T_0$  and less than  $T_s$ . Therefore,

$$C_s = \frac{S_{DS}}{\left( \frac{R}{I} \right)} = \frac{1.0}{8} = 0.125g$$

**Base shear using modal analysis**

$$V_m = C_{Sm} W_m = \frac{I_m^2}{M_m} C_{Sm}$$

Mode 1:  $V_1 = 0.0851 \times 1477 = 125.7 \text{ kip}$

Mode 2:  $V_2 = 0.127 \times 61 = 7.7 \text{ kip}$

The modal base shear may be combined by taking the SRSS of each of the modal values or by the CQC technique. The SRSS method is used here:

$$\begin{aligned} V_t &= (125.7^2 + 7.7^2)^{1/2} \\ &= 125.9 \text{ kip, say, } 126 \text{ kip} \end{aligned}$$

**Design base shear using ELF product:** For the example considered, we have

$$S_{DS} = 1.0$$

$$S_{DI} = 0.6$$

$$S_1 = 0.6$$

$$R = 8$$

$$I = 1.0$$

Approximate fundamental period

$$T_a = C_t(h_n)^x$$

$$C_t = 0.016 \text{ for a moment-resisting concrete frame system}$$

$$x = 0.9$$

$$h_n = \text{total height} = 30 \text{ ft}$$

$$T_a = 0.016 \times (30)^{0.9} = 0.34 \text{ s}$$

$$T_b = 0.881 \text{ s established from modal analysis should not exceed the approximate fundamental period, } T_a, \text{ by more than a factor } C_u$$

For this example problem,  $S_{DI} = 0.6 > 0.4$ . Therefore

$$C_u = 1.4$$

$$T_{\max} = 1.4 \times 0.34 = 0.48 \text{ s}$$

$$\text{Base shear } V = \frac{S_{DI} I}{R T} W = \frac{0.6 \times 1 \times 1160}{8.0 \times 0.48} = 181.3 \text{ kip}$$

$$\text{Max } V = \frac{S_{DS} I}{R} W = \frac{1.0 \times 1.0 \times 1160}{8} = 145 \text{ kip}$$

$$\text{Min } V = 0.044 S_{DS} I W = 0.044 \times 1.0 \times 1 \times 1160 = 51 \text{ kip}$$

$$\text{Min } V \text{ for buildings in SDC E or F} = 0.5 S_1 I W = \frac{0.5 \times 0.6 \times 1 \times 1160}{8} = 43.5 \text{ kip}$$

However, this is not applicable to the example problem since it is in SDC D.

$V = 145 \text{ kip}$  governs.

**Scaling of elastic response parameters for design:** The dynamic base shear,  $V_i$ , should be scaled up when it is less than 85% of the static base shear  $V$ . However, it is permissible to use a fundamental period  $T = C_u C_u T_a$  in the calculation of base shear using the equivalent static procedure, instead of  $T = C_u T_a$ .

The new period  $T = 1.4 \times 1.4 \times 0.34 = 0.67$  s. The revised base shear for  $T = 0.67$  is calculated as follows:

$$V = \frac{S_{DS} I_E}{RT} W = \frac{0.6 \times 1 \times 1160}{8 \times 0.67} = 130 \text{ kip (controls)}$$

$$\text{Max } V = \frac{S_{DS} I_E}{R} W = \frac{1 \times 1 \times 1160}{8} = 145 \text{ kip}$$

$$\text{Min } V = 0.044 S_{DS} I_E W = 0.044 \times 1 \times 1160 = 51 \text{ kip}$$

For buildings in SDC E or F

$$\text{Min } V = \frac{0.5 S_1 I_E}{R} W = \frac{0.5 \times 0.6 \times 1 \times 1160}{8} = 43.5 \text{ kip}$$

This is not applicable to the design example, since it is in SDC D.

Use  $V = 130$  kip.

The modal base shear  $V_i = 126$  kip is not less than 85% of the static base shear  $V = 130$  kip. Therefore, modal base shear need not be scaled up by a factor equal to

$$0.85 \frac{V}{V_i}$$

Therefore, use the following shear values derived earlier for modal distribution:

$$V_1 = 125.7 \text{ kip}$$

$$V_2 = 7.7 \text{ kip}$$

**Distribution of base shear:** Lateral force at level  $x$  (levels 1 and 2, in our example), for mode  $m$  (modes 1 and 2) is calculated as follows:

$$F_m = C_{xm} / V_m$$

$$C_m = \frac{W_x \phi_{xm}}{\sum_{i=1}^n W_i \phi_{im}}$$

where

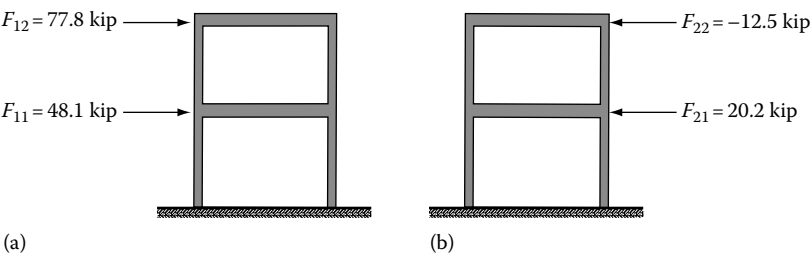
$C_{xm}$  is the vertical distribution factor at the  $x$ th level in the  $m$ th mode

$V_m$  is the total design lateral force or shear at the base in the  $m$ th mode

$W_i$  and  $W_x$  are the portion of the gravity load of the building at level  $i$  and  $x$

$\phi_{im}$  is the displacement amplitude at the  $i$ th level of building when vibrating in its  $m$ th mode

$\phi_{xm}$  is the displacement amplitude at the  $x$ th level of the building when vibrating in its  $m$ th mode



**FIGURE 5.47** Distribution of modal shears: (a) first mode and (b) second mode.

The distribution of modal base shear shown in Figure 5.47 is calculated as follows:

Level	Weight $w_i$	$\phi_i$	$w_i\phi_i$	$F = \frac{w_i\phi_{im}}{\sum w_i\phi_{im}} \times V_m$
<b>Mode 1</b>		<b><math>V_m = V_1 = 125.7</math> kip</b>		
2	580	$\phi_{12} = 1.0$	580	$F_{12} = 77.8$ kip
1	580	$\phi_{11} = 0.618$	358.4	$F_{11} = 48.1$ kip
			$\Sigma = 938.4$	$\Sigma = 125.9$ kip
<b>Mode 2</b>		<b><math>V_m = V_2 = 7.7</math> kip</b>		
2	580	$\phi_{22} = 1.0$	580	$F_{22} = -12.5$ kip
1	580	$\phi_{21} = -1.618$	-938.4	$F_{21} = 20.2$ kip
			$\Sigma = -358.4$	$\Sigma = 7.7$ kip

**5.9 ANATOMY OF COMPUTER RESPONSE SPECTRUM ANALYSES  
(IN OTHER WORDS, WHAT GOES ON IN THE BLACK BOX)**

Now that we have learned the fundamentals of dynamic analysis, perhaps it is instructive to study a couple of computer dynamic-analysis results. This will enhance our understanding of the modal superposition process that takes place in the computer, in the black box.

The examples presented illustrate the modal analysis method. In the first part of each example, the analysis is performed to determine the base shear for each mode using given building characteristics and ground motion spectra. In the second part, the story forces, accelerations, and displacements are calculated for each mode, and are combined statistically using the SRSS combination. The following equations are used in the analysis procedure.

The base shear is determined from

$$V_m = \alpha_m S_{am} W$$

where

- $V_m$  is the base shear contributed by the  $m$ th mode
- $\alpha_m$  is the modal base shear participation factor for the  $m$ th mode
- $S_{am}$  is the spectral acceleration for the  $m$ th mode determined from the response spectrum
- $W$  is the total weight of the building including dead loads and applied portions of other loads

The modal base shear participation factor,  $\alpha_m$ , for the  $m$ th mode is determined from

$$\alpha_m = \frac{\left( \sum_{i=1}^n \frac{w_i}{g} \phi_{im} \right)^2}{\sum_{i=1}^n \frac{w_i}{g} \sum_{i=1}^n \frac{w_i}{g} \phi_{im}^2}$$

The story modal participation,  $PF_{xm}$ , for the  $m$ th mode is determined from

$$PF_{xm} = \left( \frac{\sum_{i=1}^n \frac{w_i}{g} \phi_{im}}{\sum_{i=1}^n \frac{w_i}{g} \phi_{im}^2} \right) \phi_{xm}$$

where

$PF_{xm}$  is the modal participation factor at level  $x$  for the  $m$ th mode

$w_i/g$  is the mass assigned to level  $i$

$\phi_{im}$  is the amplitude of the  $m$ th mode at level  $i$

$\phi_{xm}$  is the amplitude of the  $m$ th mode at level  $x$

$n$  is the level  $n$  under consideration

The modal story lateral displacement,  $\delta_{xm}$ , is determined from

$$\delta_{xm} = PF_{xm} S_{am}$$

where

$\delta_{xm}$  is the lateral displacement at level  $x$  for the  $m$ th mode

$S_{am}$  is the spectral acceleration for the  $m$ th mode determined from the response spectrum

$T_m$  is the period of vibration at the  $m$ th mode

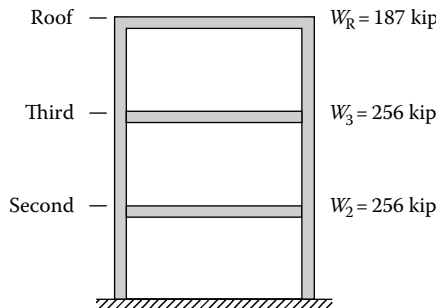
### Example 1: Three-story building

**Given:** The example is illustrated in Figure 5.48.

Weights and masses:

$$W_R = 187 \text{ kip}$$

$$m_R = \frac{187}{32.2} = 5.81 \text{ kip-s}^2/\text{ft}$$



**FIGURE 5.48** Three-story building example: dynamic analysis.

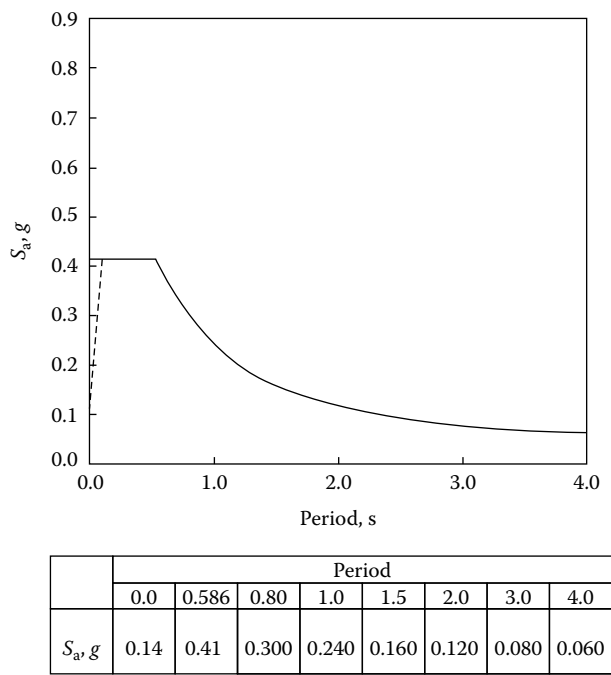


FIGURE 5.49 Three-story building: response spectrum.

$$W_2 = W_3 = 236 \text{ kip}$$

$$m_2 = m_3 = \frac{236}{32.2} = 7.33 \text{ kip-s}^2/\text{ft}$$

Periods

$$T_1 = 0.964 \text{ s}$$

$$T_2 = 0.356 \text{ s}$$

$$T_3 = 0.182 \text{ s}$$

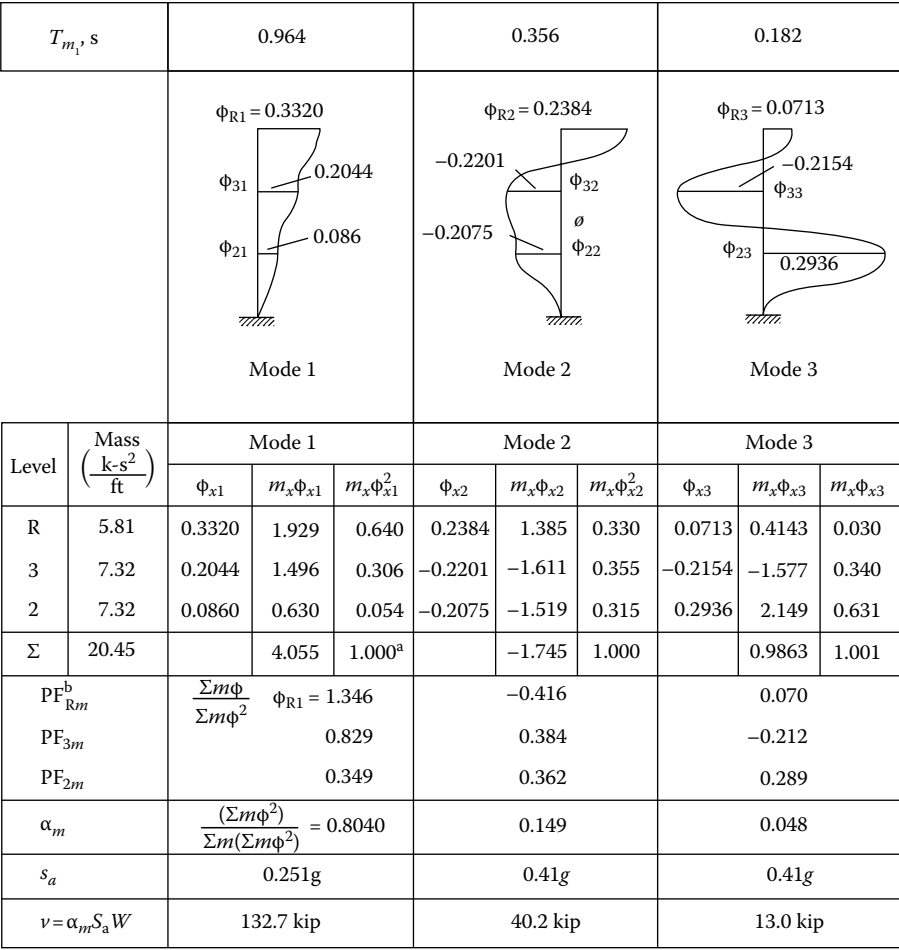
**Spectral acceleration:** From the response spectrum of Figure 5.49, the spectral accelerations are

- $S_{a1} = 0.251g$  for mode 1
- $S_{a2} = 0.41g$  for mode 2
- $S_{a3} = 0.251g$  for mode 3

Required:

1. Modal analysis to determine base shears
2. Story forces, overturning moments, accelerations, and displacements for each mode
3. SRSS combinations

**Solution:** The results of the modal analysis are shown in Figures 5.50 through 5.52. It should be noted that higher modes of response become increasingly important for taller or irregular buildings. For the regular three-story building, the first mode dominates the lateral response as shown in



<sup>a</sup> The mode shapes have been normalized by the computer program so that  $\Sigma m \phi^2 = 1.0$

<sup>b</sup> Note that the sum of the modal participation factors  $\Sigma_{m=1}^3 PF_{xm} = 1.0$  and the sum of modal base shear participation factors  $\Sigma_{m=1}^3 \alpha_m = 1.0$

FIGURE 5.50 Three-story building: modal analysis to determine base shears.

the comparison of the modal story shears and the SRSS story shears in Figure 5.51. For example, if only the first mode shears had been used for analysis, we would have obtained 89% of the SRSS shear at the roof, 99% at the third floor, and 95% at the second floor. While the second mode shear at the roof is 50% of the first mode shear, when combined on SRSS basis, the first mode accounts for 79% of the SRSS response, with 20% for the second mode and 0.6% for the third mode. These percentages are 91%, 8%, and 1% at the base. The effective modal weight factor,  $\alpha_m$ , also shows the relative importance of each mode. In this example, with  $\alpha_1 = 0.804$ ,  $\alpha_2 = 0.149$ , and  $\alpha_3 = 0.048$ , this indicate that 80.4% of the building mass participation is in the first mode, 14.9% in the second, and 4.8% in the third.

Example 2: Seven-story building

Given: See the seven-story building illustration in Figure 5.53.

Level	PF <sub>xm</sub>	$\frac{m_x \phi_{xm}}{\sum m_x \phi_{xm}}$	F <sub>xm</sub> (k)	V <sub>xm</sub> (k)	$\Delta OTM_{xm}$ (ft-k)	$OTM_{xm}$ (ft-k)	$a_{xm} = \frac{F_{xm}}{w_x}$	$\delta_{xm}$ (in.)	$\Delta_{xm}$ (in.)
R	1.346	0.476	63.2	63.2	772	0	0.337	3.065	1.182
3	0.829	0.369	48.9	112.1	1233	772	0.208	1.892	1.101
2	0.349	<u>0.155</u>	20.6	132.7	1416	2005	0.087	0.791	0.791
		1.000				3421			
(a) Mode 1									
R	-0.416	-0.793	-31.9	-31.9	-389	0	-0.171	-0.212	0.407
3	0.384	0.923	37.1	5.2	57	-389	-0.157	0.195	0.011
2	0.362	<u>0.870</u>	35.0	40.2	429	-332	-0.148	0.184	0.184
		1.000				97			
(b) Mode 2									
R	0.070	0.420	5.5	5.5	67	0	-0.029	0.0094	0.037
3	-0.212	-1.599	-20.8	-15.3	-168	67	-0.087	-0.028	0.066
2	0.289	<u>2.179</u>	28.3	13.0	139	-101	0.118	0.038	0.038
		1.000				38			
(c) Mode 3									
R			71.0	71.0	867	0	0.379	3.072	1.251
3			64.8	113.3	1246	867	0.275	1.893	1.094
2			49.5	139.3	1486	2035	0.208	0.812	0.813
						3423			
(d) SRSS combination									

FIGURE 5.51 Three-story building: modal analysis to determine story forces, accelerations, and displacements.

Level	Mode 1				Mode 2		Mode 3	
	V <sub>SRSS</sub>	V <sub>1</sub>	V <sub>1</sub> /V <sub>SRSS</sub>	(V <sub>1</sub> /V <sub>SRSS</sub> ) <sup>2</sup>	V <sub>2</sub>	(V <sub>2</sub> /V <sub>SRSS</sub> ) <sup>2</sup>	V <sub>1</sub>	(V <sub>3</sub> /V <sub>SRSS</sub> ) <sup>2</sup>
R	71.0	63.2	0.89	0.79	-31.9	0.202	5.5	0.006
3	119.3	112.1	0.989	0.98	5.2	0.002	-15.3	0.018
2	139.3	132.7	0.953	0.91	40.2	0.083	13.0	0.009

FIGURE 5.52 Three-story building: comparison of modal story shears and the SRSS story shears.

Weights and masses

$$W_R = 1410 \text{ kip}$$

$$m_R = \frac{W_R}{g} = \frac{1410}{32.2} = 43.79 \text{ kip-s}^2/\text{ft}$$

$$W_7 = W_6 = W_5 = W_4 = W_3 = 1460 \text{ kip}$$

$$m_7 = m_6 = m_5 = m_4 = m_3 = \frac{1460}{32.2} = 45.34 \text{ kip-s}^2/\text{ft}$$

$$W_2 = 1830 \text{ kip}$$

$$m_2 = \frac{1830}{32.2} = 56.83 \text{ kip-s}^2/\text{ft}$$



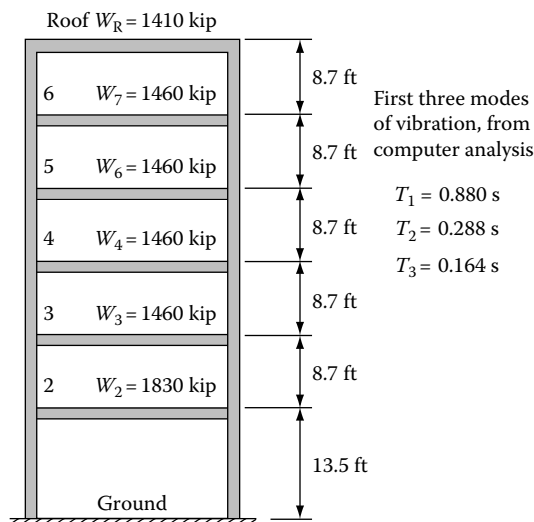


FIGURE 5.53 Seven-story building example: dynamic analysis.

#### Periods:

$$T_1 = 0.880 \text{ s}$$

$$T_2 = 0.288 \text{ s}$$

$$T_3 = 0.164 \text{ s}$$

**Spectral accelerations:** From the response spectrum of Figure 5.53a through c, the spectral accelerations are

$$S_{a1} = 0.276 g$$

$$S_{a2} = 0.500 g$$

$$S_{a3} = 0.500 g$$

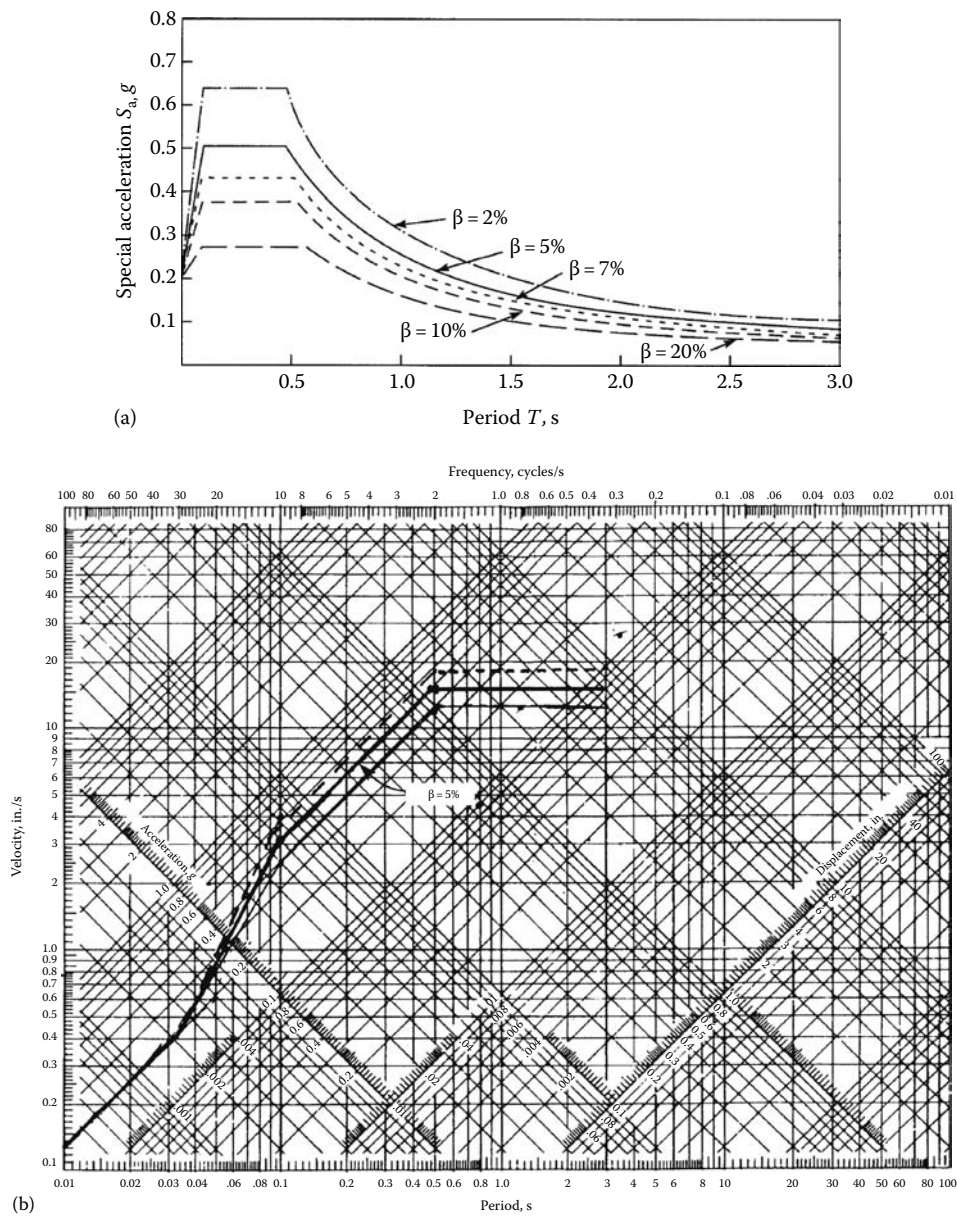
Observe that all three parts of Figure 5.54 contain the same information related to the acceleration response,  $S_a$ . Only the format is different. Figure 5.54a shows the building periods and spectral accelerations in a format similar to that in 1997 UBC and IBC-03. Figure 5.54b is a tripartite response spectrum with additional values for displacements and velocities. Figure 5.54c shows the building periods and response accelerations in tabular format.

It should be noted that in the computer program used for the calculation of the eigenvalues, each mode is normalized for a value of  $\sum_g^w \phi_2 = 1.0$ . In some programs,  $\phi$  is normalized to 1.0 at the uppermost level.

#### Required:

1. Modal analysis to determine base shears
2. First, second, and third mode forces and displacements
3. Modal analysis summary

**Solution:** From the modal analysis results shown in Figure 5.55, the sum of the participation factors,  $PF_{xm}$  and  $\alpha_m$ , add up to 1.08 and 0.986, respectively. These values being close to 1.0 indicate that most of the modal participation is included in the three modes considered in the example. The story accelerations and the base shears are combined by the SRSS. The modal base shears are 2408, 632, and 200 kip for the first, second, and third modes, respectively. These are used in Figure 5.59 to determine story forces. The SRSS base shear is 2498 kip.



	Spectral Acceleration, $S_a(g)$											
$T/\beta$	0.1	0.48	0.50	0.80	1.0	1.75	1.5	1.75	2.0	2.25	2.5	3.0
2%	0.64	0.64	0.59	0.37	0.30	0.24	0.20	0.17	0.15	0.13	0.17	0.10
5%	0.50	0.50	0.48	0.30	0.24	0.192	0.16	0.137	0.12	0.107	0.096	0.08
7%	0.44	0.44	0.44	0.28	0.22	0.18	0.15	0.13	0.11	0.10	0.09	0.07
10%	0.38	0.38	0.38	0.25	0.20	0.16	0.13	0.11	0.10	0.09	0.08	0.066
20%	0.27	0.27	0.27	0.20	0.16	0.12	0.10	0.09	0.08	0.07	0.06	0.05

FIGURE 5.54 Response spectrum for seven-story building example: (a) acceleration spectrum, (b) tripartite diagram, and (c) response spectra numerical representation.

Level	$\frac{w}{g}$ $\left(\frac{\text{k}\cdot\text{s}^2}{\text{ft}}\right)$	Mode 1				Mode 2				Mode 3				SRSS $a_x(g)$
		$\phi_1$	$\frac{w}{g}\phi_1$	$\frac{w}{g}\phi_1^2$	$a_1(g)$	$\phi_2$	$\frac{w}{g}\phi_2$	$\frac{w}{g}\phi_2^2$	$a_2(g)$	$\phi_3$	$\frac{w}{g}\phi_3$	$\frac{w}{g}\phi_3^2$	$a_3(g)$	
Roof	43.78	0.0794	3.48	0.276	0.362	0.0747	3.27	0.744	-0.235	0.0684	2.99	0.205	0.120	0.448
7	45.34	0.0745	3.38	0.252	0.340	0.0411	1.86	0.076	-0.129	-0.0040	-0.18	0.001	-0.007	0.364
6	45.34	0.0666	3.02	0.201	0.304	-0.0042	-0.19	0.001	0.013	-0.0644	-2.92	0.188	-0.113	0.325
5	45.34	0.0558	2.53	0.141	0.254	-0.0471	-2.14	0.101	0.148	-0.0630	-2.86	0.180	-0.111	0.314
4	45.34	0.0425	1.93	0.082	0.194	-0.0718	-3.26	0.234	0.226	-0.0023	-0.10	0.000	-0.004	0.298
3	45.34	0.0279	1.27	0.035	0.127	-0.0697	-3.16	0.220	0.219	0.0604	2.74	0.166	0.0106	0.275
2	56.83	0.0149	0.85	0.013	0.068	-0.0467	-2.65	0.124	0.147	0.0677	3.85	0.261	0.0119	0.201
1	—	0	0	0	0	0	0	0	0	0	0	0	0	0
$\Sigma$	327.31		16.46	1.000			-6.27	1.000			3.52	1.001		
$\text{PF}_{\text{roof}}$		$\frac{16.46}{1.000}$	$\frac{(0.0794)}{1.000} = 1.31$			$\frac{-6.37}{1.000}$	$\frac{(0.0747)}{1.000} = -0.47$			$\frac{3.52}{1.001}$	$\frac{(0.0684)}{1.001} = 0.24$	$\Sigma = 1.08$		
$\alpha$		$\frac{(16.46)^2}{(327.31)(1.000)} = 0.828$				$\frac{(-6.27)^2}{(327.31)(1.000)} = 0.120$				$\frac{(3.52)^2}{(927.31)(1.001)} = 0.038$	$\Sigma = 0.986$			
$T$		0.880 s				0.288 s				0.164 s				
$S_a$		0.276 g				0.500 g				0.500 g				
$a_{\text{roof}}$		$(1.31)(0.276) = 0.362\text{ g}$				$(-0.47)(0.500) = -0.235\text{ g}$				$(0.24)(0.500) = 0.120\text{ g}$			0.448	
$V$		$(0.828)(0.276)(10.539) = 2,408\text{ kip}$				$(0.12)(0.500)(10.539) = 632\text{ kip}$				$(0.038)(0.500)(10.539) = 200\text{ kip}$			2,498 kip (SRSS)	
$V/W$		0.229				0.060				0.019			0.237	
$W = \Sigma \left(\frac{w}{g}\right) \times g = 327.31 \times 32.2 = 10,539\text{ kip} = \text{Building weight}$														
$A_G = 0.20\text{ g site PGA}$														
$\beta = 0.05\text{ damping factor}$														

FIGURE 5.55 Seven-story building: modal analysis to determine base shears.

**Story forces, accelerations, and displacements:** Figures 5.55 through 5.58 are set up in a manner similar to the static design procedure described previously. In the static lateral procedure,  $Wh/\sum Wh$  is used to distribute the force on the assumption of a straight line mode shape. In the dynamic analysis, the more representative  $W\phi/\sum W\phi$  distribution is used to distribute the forces. The story shears and overturning moments are determined in the same manner for each method. Modal story accelerations are determined by dividing the story force by the story weight. Modal story displacements are calculated from the accelerations and the period by using the following equations:

$$\delta_{xm} = PF_{xm} S_{am} \left( \frac{T_m}{2\pi} \right)^2 g$$

where

$\delta_{xm}$  is the lateral displacement at level  $x$  for mode  $m$

$S_{am}$  is the spectral displacement for mode  $m$  calculated from response spectrum

$T_m$  is the modal period of vibration

$T_1 = 0.880 \text{ s}$													
Modal Base Shear $V_1 = 2408 \text{ kip}$													
(1)	(2)	(3)	(4)	(5)	(6)	(7)	(8)	(9)	(10)	(11)			
Story	$\phi$	$h \text{ ft}$	$\Delta h \text{ ft}$	$w \text{ kip}$	$\frac{w\phi}{\sum w\phi}$	$F \text{ kip}$ ( $V_1 \times (6)$ )	$V \text{ kip}$ $\sum (7)$	$\Delta OTM$ k-ft (4)–(8)	$OTM \text{ k-ft}$ $\sum (9)$	Acceleration g (7) $\div$ (5)	$\delta^* \text{ ft}$	$\Delta \delta \text{ ft}$	
Roof	0.0794	65.7		1,410	0.211	508			0	0.360	0.228		
			8.7				508	4,420				0.014	
7	0.7450	57.0		1,460	0.205	494			4,420	0.338	0.214		
			8.7				1,002	8,717				0.022	
6	0.0666	48.3		1,460	0.184	443			13,137	0.303	0.192		
			8.7				1,445	12,572				0.031	
5	0.0558	59.6		1,460	0.154	371			25,709	0.254	0.161		
			8.7				1,816	15,799				0.039	
4	0.0425	30.9		1,460	0.117	282			41,508	0.193	0.122		
			8.7				2,098	10,253				0.042	
3	0.0279	22.2		1,460	0.077	185			59,761	0.127	0.080		
			8.7				2,283	19,862				0.057	
2	0.0149	13.5		1,830	0.052	125			79,623	0.068	0.043		
			13.5				2,408	32,508				0.043	
Ground	0	0		0	0	0			112,131	0	0		
				$\sum$	1.000	2408		112,191					

$$\begin{aligned}
 * \text{ Displacement } \delta_{x1} &= \frac{g}{4\pi^2} \times T_1^2 \times \frac{F}{W} \\
 &= \frac{32}{4\pi^2} \times 0.88^2 \times \text{acceleration} \\
 &= 0.632 \times \text{acceleration}
 \end{aligned}$$

**FIGURE 5.56** Seven-story building: first-mode forces and displacements.

$T_2 = 0.288 \text{ s}$												
Modal base shear $V_2 = 632 \text{ kip}$												
(1)	(2)	(3)	(4)	(5)	(6)	(7)	(8)	(9)	(10)	(11)		
Story	$\phi$	$h \text{ ft}$	$\Delta h \text{ ft}$	$w \text{ kip}$	$\frac{w\phi}{\Sigma w\phi}$	$F \text{ kip}$ ( $V_2 \times$ (6)	$V \text{ kip}$ $\Sigma (7)$	$\Delta \text{OTM}$ k-ft (4) $\times$ (8)	$\text{OTM}$ k-ft $\Sigma (9)$	Acceleration g (7)+(5)	$\delta^* \text{ ft}$	$\Delta \delta \text{ ft}$
Roof	0.0747	65.7		1410	0.522	-330			0	0.234	-0.016	
			8.7				-330	-2871				0.007
7	0.0411	57.0		1460	0.297	-188			-2871	-0.129	-0.009	
			8.7				-518	-4507				0.010
6	-0.0042	48.3		1460	0.030	19			-7378	0.013	0.001	
			8.7				-499	-4341				0.009
5	-0.0471	39.6		1460	0.341	216			-11719	0.148	0.010	
			8.7				-283	-2462				0.005
4	-0.0718	30.9		1460	0.520	329			-14181	0.225	0.015	
			8.7				46	400				0.000
3	-0.0697	22.2		1460	0.504	319			-13781	0.219	0.015	
			8.7				365	3176				0.005
2	-0.0467	13.5		1830	0.423	267			-10605	0.146	0.010	
			13.5				632	8532				0.010
Ground	0	0							-2073	0	0	
				$\Sigma$	0.999	632		-2073				

$$\begin{aligned}
 * \text{ Displacement } \delta_{x2} &= \frac{g}{4\pi^2} \times T_2^2 \times \frac{F}{w} \\
 &= \frac{32}{4\pi^2} \times 0.288^2 \times \text{acceleration} \\
 &= 0.068 \times \text{acceleration}
 \end{aligned}$$

**FIGURE 5.57** Seven-story building: second-mode forces and displacements.

Modal interstory drifts are calculated by taking the difference between the values of adjacent stories. The values shown in Figures 5.56 through 5.58 are summarized in Figure 5.59.

The fundamental period of vibration as determined from a computer analysis is 0.88 s. The periods of the second and third modes of vibration are 0.288 and 0.164 s, respectively. From Figures 5.56 through 5.58 using a response curve with 5% of critical damping ( $\beta = 0.05$ ), it is determined that the second and third mode spectral accelerations (0.500g) are 80% greater than the first mode spectral acceleration (0.276g). On the basis of mode shapes and modal participation factors, modal story forces, shears, overturning moments, acceleration, and displacements are determined.

Figure 5.59a shows story forces obtained by multiplying the story acceleration by the story mass. The shapes of story force curves (Figure 5.59a) are quite similar to the shapes of the acceleration curves (Figure 5.59d), because the building mass is essentially uniform.

Figure 5.59b shows story shears that are a summation of the modal story forces in Figure 5.59a. The higher modes become less significant in relation to the first mode because the forces tend to cancel each other due to the reversal of direction. The SRSS values do not differ substantially from the first mode values.

Figure 5.59c shows the building overturning moments. Again, the higher modes become somewhat less significant because of the reversal of force direction. The SRSS curve is essentially equal to the first mode curve.

$T_3 = 0.164 \text{ s}$												
Modal base shear $V_3 = 200 \text{ kip}$												
(1)	(2)	(3)	(4)	(5)	(6)	(7)	(8)	(9)	(10)	(11)		
Story	$\phi$	$h \text{ ft}$	$\Delta h \text{ ft}$	$w \text{ kip}$	$F \text{ kip}$		$V \text{ kip}$	$\Delta \text{OTM}$		Acceleration	$\delta^* \text{ ft}$	$\Delta \delta \text{ ft}$
					$\frac{w\phi}{\sum w\phi}$	$(V_3) \times$		k-ft (4)	OTM			
						(6)	$\sum (7)$	$\times (8)$	$\sum (9)$	$g (7) \div (5)$		
Roof	0.0684	65.7		1410	0.849	170			0	0.121	0.003	
			8.7				170	1479				0.003
7	-0.0040	57.0		1460	-0.051	-10			1479	-0.007	0.000	
			8.7				160	1392				0.003
6	-0.0644	48.3		1460	-0.830	-166			2871	-0.114	-0.003	
			8.7				-6	-52				0.000
5	-0.0630	39.6		1460	-0.813	-163			2819	-0.112	-0.003	
			8.7				-169	-1470				0.003
4	-0.0023	30.9		1460	-0.028	-6			1349	-0.004	0.000	
			8.7				-175	-1523				0.002
3	0.0604	22.2		1460	0.778	156			-174	0.107	0.002	
			8.7				-19	-165				0.001
2	0.0677	13.5		1830	1.094	219			-339	0.120	0.003	
			13.5				200	2700				0.003
Ground	0	0							2361	0	0	
				$\Sigma$	0.999	200		2361				

\* Displacement  $\delta_{x3} = -\frac{g}{4\pi^2} \times T_3^2 \times \frac{F}{W}$

$= \frac{32}{4\pi^2} \times 0.64^2 \times \text{acceleration}$

$= 0.022 \times \text{acceleration}$

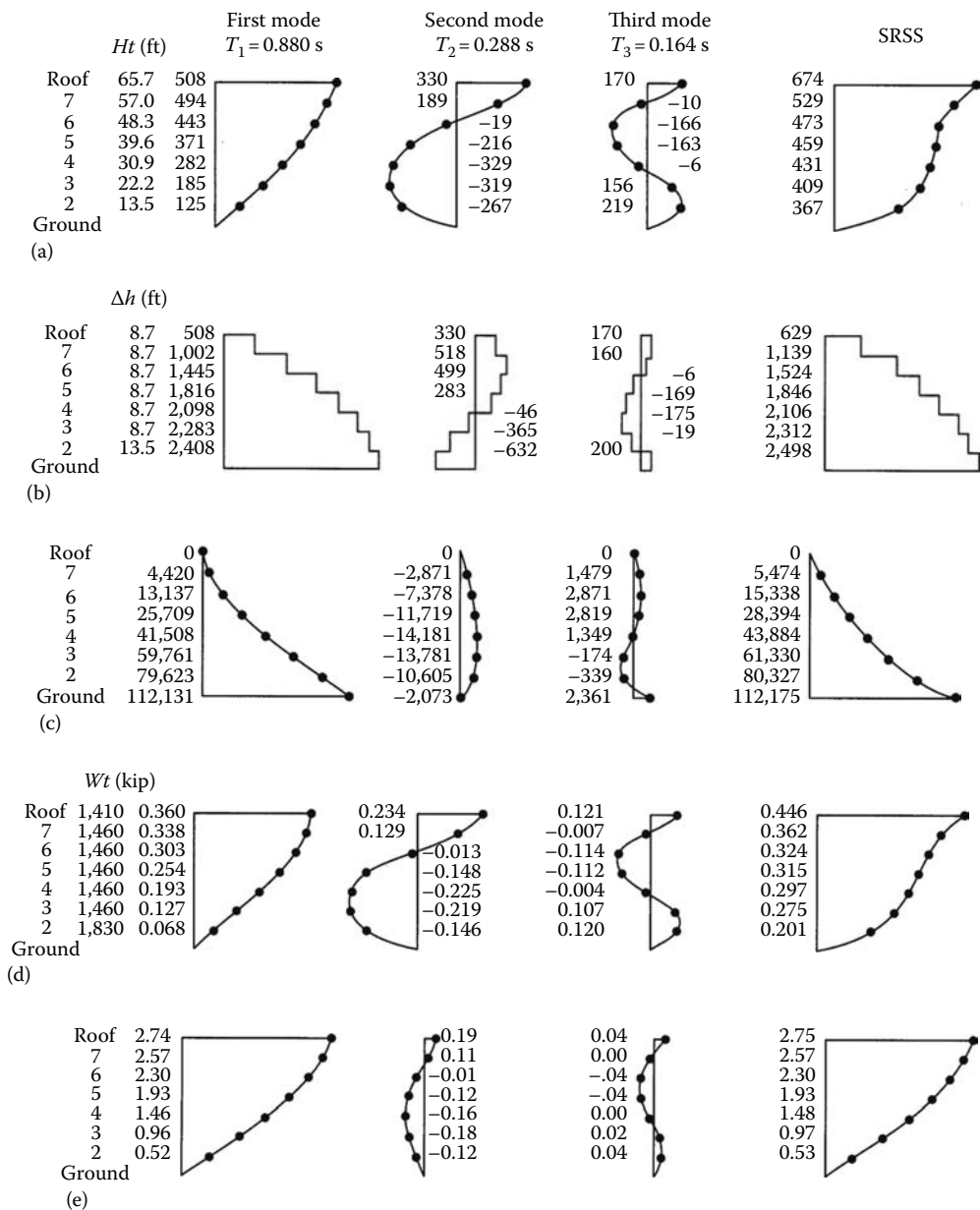
FIGURE 5.58 Seven-story building: third-mode forces and displacements.

Figure 5.59d shows story accelerations. Observe that the second and third modes do play a significant role in the structure’s maximum response. While the shape of an individual mode is the same for displacements and accelerations, accelerations are proportional to displacements divided by the squared value of the modal period, which accounts for the greater accelerations in the higher modes. The shape of the SRSS combination of the accelerations is substantially different from the shapes of any of the individual modes because it accounts for the predominance of the various modes at different story levels.

Figure 5.59e shows the modal displacements. Observe that the fundamental mode predominates, while the second and third mode displacements are relatively insignificant. The SRSS combination does not differ greatly from the fundamental mode. It should be noted that for taller and irregular buildings, the influence of the higher modes becomes larger.

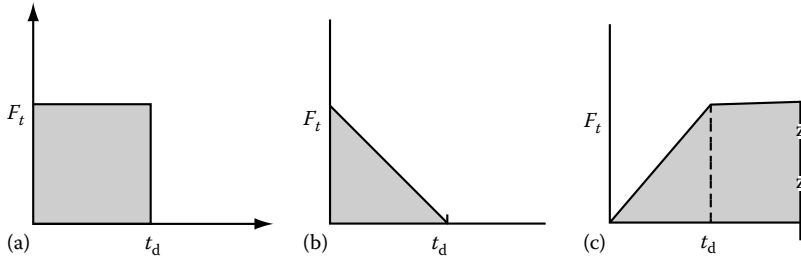
5.10 DYNAMIC RESPONSE CONCEPT

In this section, we explain the dynamic response concept of simple systems by using basic principles of physics and the most elementary mathematics. We will begin by introducing the concept of dynamic load factor, DLF, and time-load function,  $F_t$ . Simply stated, DLF is the ratio of the dynamic

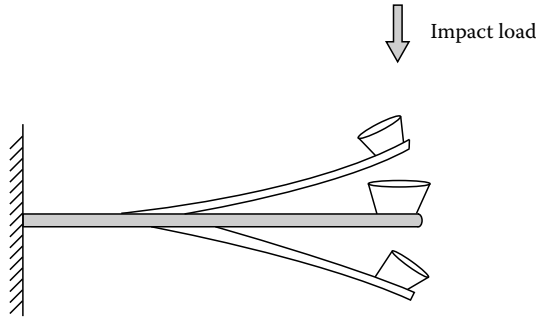


**FIGURE 5.59** Seven-story building, modal analysis summary: (a) modal story forces, kip; (b) modal story shears, kip; (c) modal story overturning moments, kip-ft; (d) modal story accelerations, g; and (e) modal lateral displacement, inches.

response (such as deflection of an elastic system) to the static response. In a static problem, the time-variation of the load has no effect on the response since it is assumed that the load is applied in a gradual manner. However, in dynamic problems, the time it takes to apply the load has considerable influence on the structural behavior, and thus must be given consideration in the analysis. Shown in Figure 5.60 are some examples of time-load function,  $F_t$ , in which load variation is graphed with respect to time  $t$ .



**FIGURE 5.60** Time-load functions. (a) Rectangular pulse (b) triangular pulse and (c) constant force with finite rise time. *Note:*  $F_t$  = Load function,  $t_d$  = time function.



**FIGURE 5.61** Dynamic response of a cantilever. *Note:* Dynamic Load Factor, DLF, is equal to 2.0 for a load applied instantaneously.

Consider a cantilever beam shown in Figure 5.61 with an empty container of weight  $W_D$  at the free end. Ignoring the self weight of the beam and using common notions, the deflection of the cantilever due to the self weight  $W_D$  of the container is given by

$$\Delta_c = \frac{W_D L^3}{3EI}$$

Let the container be filled with water of weight  $W_w$ , flowing gradually, say, drop-by-drop, into the container. The additional deflection due to the weight of water  $W_w$  is

$$\Delta_w = \frac{W_w L^3}{3EI}$$

Instead of a drop-by-drop loading, if all water is suddenly gushed into the container instantly, (as in Figure 5.60c, in which  $t_d = 0$ ), the cantilever deflection will no longer be the same as the static deflection,  $\Delta_w$ . We know by intuition, it will be larger than  $\Delta_w$ . In our case it can be proved that it is two times the static deflection,  $\Delta_w$ . Hence  $DLF = 2$ . The cantilever not only moves downward, but also springs up, and then down and continues to do so about its static position. In other words, the cantilever when subject to a sudden load exhibits a dynamic response by vibrating typically in a sinusoidal manner. But for the effects damping, it would continue to do so indefinitely as shown schematically in Figure 5.61.

Conceptually, the behavior of buildings experiencing earthquakes is similar to the vibratory motions of our cantilever. However, earthquake ground motions are erratic; they are neither harmonic nor periodic but vary arbitrarily with time and last no more than a few seconds, although it many have seemed like eternity for those experiencing the trauma.



To analyse for the effect of erratic ground motions, analytically it is permitted to interpret the response of a dynamic system as a sum of the responses to individual impulses. An impulsive force is defined as a large force that acts for a very short time of finite duration.

Some examples of impulsive force are

1. A step force that jumps suddenly from zero to  $F_t$  and stays constant at that value.
2. Ramp or linearly increasing force.
3. Step force with finite rise time. This is of interest because in reality a force can never be applied suddenly but has a finite rise,  $T_r$ .
4. Rectangular pulse force.
5. Half-cycle sine pulse.
6. Triangular pulse.

A design response spectrum characterizing the maximum response of single-degree of systems to a given ground acceleration can be determined by superposition of selected impulsive forces corresponding to the acceleration. This is possible because ground accelerations can be replaced by effective force:

$$F_t = M \times a$$

where

$F_t$  is the effective force at time  $t$

$M$  is the mass of the structure

$a$  is the ground acceleration at time  $t$

Note the deflection load factor, DLF, also varies with time. However, in structural engineering we are interested in the maximum design values (such as displacements, stresses, etc). Therefore, the DLF for the cantilever for design purposes is two. The DLF for other common time-load functions are shown in Figure 5.62.

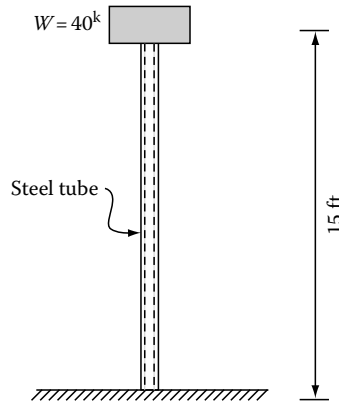
Lest it be forgotten, it is worthwhile to repeat that when we use response spectra to obtain design values for single-degree-of-freedom systems it is not necessary to amplify the design values by the DLF because the computationally intensive dynamic analysis have been completed in generating the response spectra. Somebody else has done all the hardwork for us.

### 5.10.1 DIFFERENCE BETWEEN STATIC AND DYNAMIC ANALYSES

In this section, we will point out an important difference between the response of structures to seismic excitation and to a fixed value static force. In the static case, the stress in a member would decrease, obviously, by increasing the member size, and thus its section modules. In the case of earthquake

Load function	Rectangular pulse	Symmetrical triangular pulse	Constant force with finite rise time
Ratio $t_d/T$	5/4	2	1/5
DLF	2.0	1.75	Very nearly 2.0

**FIGURE 5.62** Dynamic load factor, DLF, for common time-load functions.  $t_d$  = time duration of pulse,  $T$  = fundamental period of the system to which load is applied.



**FIGURE 5.63** Cantilever column with weight at top.

excitation, the increase in member size resulting in higher stiffness shortens the natural vibration period that may have the effect of increasing the equivalent static force. Whether the stress decreases or increases by increasing the size of the member depends on the increase in section modulus,  $S$ , and the increase in the equivalent static force that in turn depends on the response spectrum.

### Example

#### Given:

A 15 ft tall cantilever, an 8 in. nominal diameter standard steel pipe supporting a 40 kip weight at the top as shown in Figure 5.63. The properties of the column are

$$I = 106 \text{ in.}^4$$

$$S = 24.5 \text{ in.}^3$$

$$\text{Weight } W = 43.39 \text{ lb/ft}$$

$$E = 29,000 \text{ ksi}$$

#### Required:

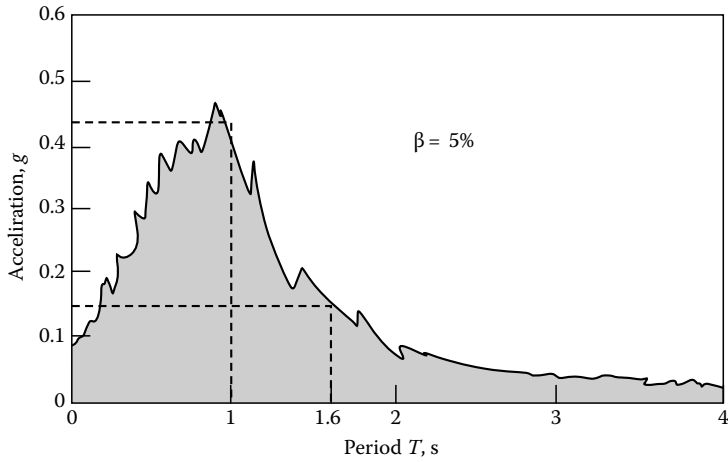
1. Determine the peak deformation and bending stress in the cantilever column using the seismic ground motion, acceleration response spectrum, for a damping  $\beta = 5\%$ , shown in Figure 5.64.
2. Repeat the calculations using a bigger section, a 12 in. diameter standard pipe. Discuss the pros and cons of using a bigger pipe.

#### Solution:

1. The weight of pipe at  $43.39 \text{ plf} = 15 \times 43.39 = 650 \text{ lbs}$ . Compared to the load of 40 kip at the top of the cantilever, the self weight of the column is small, and therefore, can be ignored. The lateral stiffness of the column is

$$k = \frac{3EI}{h^3} = \frac{3 \times 29,000 \times 106}{(15 \times 12)^3} = 1.584 \text{ kip/in.}$$

$$\text{Mass at top} = \frac{w}{g} = \frac{40}{386} = 0.104 \text{ kip-s}^2/\text{in.}$$



**FIGURE 5.64** Acceleration response spectrum.

The natural vibration frequency is given by

$$\omega_n = \sqrt{\frac{k}{m}} = \sqrt{\frac{1.584}{0.104}} = 3.91 \text{ rad}$$

$$\text{Period } T_n = \frac{2\pi}{\omega_n} = \frac{2 \times 3.14}{3.91} = 1.6 \text{ s}$$

From the response spectrum curve (Figure 5.64) for  $T_n = 1.6 \text{ s}$ , acceleration  $a = 0.15g$   
The peak value of the equivalent static force is

$$v = \frac{a}{g} w = 0.15 \times 40 = 6 \text{ kip}$$

The bending moment at the base of the column is

$$6 \times 15 = 90 \text{ kip-ft}$$

$$\text{Bending stress } f_b = \frac{90 \times 12}{24.5} = 44.08 \text{ ksi}$$

2. Because the bending stress is relatively high, the designer elects to try a bigger pipe, a 12 in. diameter standard pipe. Let us verify if the resulting bending stress situation gets any better.

The properties of the new column are

$$I = 279 \text{ in.}^4$$

$$S = 43.8 \text{ in.}^3$$

$$\text{Weight} = 49.56 \text{ lb/ft}$$

As before, we ignore the self weight of the column.

The lateral stiffness in the new column is

$$k = \frac{3EI}{h^3} = \frac{3 \times 29,000 \times 279}{(15 \times 12)^3} = 4.17 \text{ kip/in.}$$

Mass at top = 0.104 kip-s<sup>2</sup>/in., as before

The natural vibration frequency is

$$\omega_n = \sqrt{\frac{k}{m}} = \sqrt{\frac{4.17}{0.104}} = 6.33 \text{ rad}$$

$$\text{Period } T_n = \frac{2\pi}{\omega_n} = \frac{2 \times 3.14}{6.33} = 0.992 \text{ s} \approx 1.0 \text{ s.}$$

From the response spectrum curve (Figure 5.64) for  $T_n = 1 \text{ s}$ , acceleration  $a = 0.43g$ .

The peak value of the equivalent static force is

$$v = \frac{a}{g} w = 0.43 \times 40 = 17.2 \text{ kip}$$

The bending moment at the base of the column is

$$17.2 \times 15 = 258 \text{ kip-ft}$$

$$\text{Bending stress } f_b = \frac{258 \times 12}{43.8} = 70.68 \text{ ksi}$$

that is about 60% more than the calculated value for the 8 in. diameter pipe.

The above example gives us an insight into the adage: “in seismic design, increasing stiffness of the structural system may not always be desirable.”

The concept of designing with sufficient strength has been viewed traditionally as a key to more effectively control the behavior of buildings. However, in certain instances, the benefits associated with an increase in strength may be small or even have a negative impact. The doctored-up example given here is not intended to discount strength as an important design consideration but rather to allude to the possible negative impacts. Keep in mind, the excessive strength of the yielding element will impose more demand on the brittle components along the lateral load path. A better design strategy would be to increase ductility; treat ductility as a wealthy person treats money—you can’t have too much of it.

### 5.10.2 DYNAMIC EFFECTS DUE TO WIND LOADS

Perhaps the reader will recall that in Chapter 4, a brief statement was made regarding the effect of wind gusts on dynamic response of tall buildings. It was stated that the load on a building due to a wind gust is a dynamic load if the period of the gust is shorter than the fundamental period of the building. Conversely, if the gust period is same as, or higher than, the building’s period, it is a static load.

Consider, for example, a tall building with a period,  $T_B$ , of 5 s (frequency of 0.166 Hz) subject to a constant wind pressure of 30 psf, and then suddenly to a 1 s gust of 15 psf. A 1 s gust simply means that wind pressure has increased to  $30 + 15 = 45 \text{ psf}$  in a time-period of 1 s. In other words the 30 psf

of constant pressure has increased to 45 psf, with the increase taking place in a short time interval of 1 s, and remains at 45 psf for the time duration of interest. Using the notion  $T_g$  for the gust period, the ratio  $T_g/T_B = 1/5$ , the corresponding maximum DLF for this case is 1.9, very close to the case of a suddenly applied load (Figure 5.62).

Next we consider the same increase in the wind load but we assume that the increase occurs over a fairly long time-interval of, say, 16.6 s. As can be seen in Figure 5.67, for the ratio  $T_g/T_B = 16.16/5 = 3.33$ , the maximum DLF is close to unity, signifying that the dynamic effect can, in fact, be ignored for this case. For the in-between values of  $T_g/T_B$ , the value of DLF is some where between 1.9 and 1.0.

The concept of DLF presented above for wind gust is equally applicable to seismic design, except the load-time function is based on support acceleration. Therefore, the specific time load functions studied in the above paragraphs may also be used to explain seismic behavior, if the time function is represented as a variation in ground acceleration.

### 5.10.3 SEISMIC PERIODS

Every building has a set of periods in which it “wants” to oscillate when set in motion by seismic ground motions or wind gusts. The period of vibrations are based on buildings mass and stiffness characteristics. The longest period of the system, and, more specifically, the inverse of the fundamental period is the natural frequency.

In seismic design, the closer the frequency of an earthquake is to the natural frequency of a building, the more energy is introduced into the building structure. Buildings with shorter fundamental periods attract higher forces as the code-based or site-specific response spectrum exhibits higher accelerations at shorter periods.

Conversely, taller buildings because of longer fundamental period tend to attract lower seismic forces. For wind design, the opposite behavior is observed. Longer fundamental periods are indicative of buildings that are more susceptible to dynamic amplification effects from wind gusts and result in higher design forces. In order to investigate the magnitudes of these wind and seismic effects, the fundamental period of the building must first be determined.

Most designers are familiar with the use of the fundamental period of the structure,  $T$ , in conjunction with calculating the seismic response coefficient,  $C_s$ , for base shear determination using the ELF procedure. The most straightforward method for determining the building period is to use the empirical formulas for the calculation of the approximate building period,  $T_a$ , presented in Chapter 12 of ASCE 7-05.

The equations are based on data from several instrumented buildings subjected to ground motion during seismic events. The formulas are intentionally skewed to represent a conservative (short) estimation of the fundamental building period. Shorter building periods result in higher and more conservative base shears.

If desired, the approximate period,  $T_a$ , may be used for the strength design and checking the drift limits of the building. However, this practice typically results in significantly overly conservative results. Therefore, ASCE 7-05 allows us the use of a “properly sustained analysis” in today’s practice means the use of software programs to perform an eigenvalue analysis to determine the mode shapes and periods of a building. It is important to note that the periods determined using an eigenvalue analysis are significantly longer than those determined using the approximate equations. This discrepancy is primarily due to two factors. First, the analytical model does not include the stiffening effect of the nonstructural infill, cladding, and the lateral resistance of “gravity-only” columns, beams, and slabs. Second, as previously noted, the approximate equations are skewed to provide shorter periods.

For strength design, ASCE 7-05 caps the maximum building period to the approximate building period,  $T_a$ , multiplied by the factor,  $C_u$ , from ASCE 7-05 Table 12.8-1. The cap is intended to prevent the so-called “sharp-pencil effects” resulting from erroneous assumptions used in the “properly substantiated analysis.” However, for the determination of seismic drift, ASCE 7-05 removes the cap and allows the engineer to use the building period resulting from analysis without restriction.

## 5.11 DYNAMIC ANALYSIS THEORY

A good portion of the loads that occur in buildings can be considered static, requiring static analysis only. Although almost all loads except dead loads are transient, meaning that they change with time, it is customary to treat them as static. For example, lateral loads imposed by transient wind pulses are usually treated as static loads and even in earthquake design, one of the acceptable methods of design, particularly for buildings with regular configuration, is to use an equivalent static force procedure. Under these circumstances, the analysis of a structure reduces to a single solution for a given set of static loads. Although the equivalent static method is a recognized method, most building codes typically mandate dynamic analysis for certain types of buildings such as those with irregular configurations. It is therefore necessary, particularly in seismic design, to have a thorough understanding of dynamic analysis concept.

Consider a building subjected to lateral wind loads. Although wind loads are dynamic, in typical design practice, except in the case of slender buildings, wind loads are considered as equivalent static loads. The variation of wind velocity with time is taken into account by including a gust factor in the determination of wind loads. Therefore, for a given set of wind loads, there is but one unique solution.

Now consider the same building, instead of being buffeted by wind, subjected to ground motions due to an earthquake. The input shaking causes the foundation of the building to oscillate back and forth in a more or less horizontal plane. The building would follow the movement of the ground without experiencing lateral loads if the ground oscillation took place very slowly over a long period of time. The building would simply ride to the new displaced position. On the other hand, when the ground moves suddenly as in an earthquake, building mass, which has inertia, attempts to prevent the displacement of the structure.

Therefore, lateral forces are exerted on the mass in order to bring it along with the foundation. This dynamic action maybe visualized as a group of horizontal forces applied to the structure in proportion to its mass, and to the height of the mass above the ground.

These earthquake forces are considered dynamic, because they vary with time. Since the load is time-varying, the response of the structure, including deflections, axial and shear forces, and bending moments, is also time-dependent. Therefore, instead of a single solution, a separate solution is required to capture the response of the building at each instant of time for the entire duration of an earthquake. Because the resulting inertia forces are a function of building accelerations, which are themselves related to the inertia forces, it is necessary to formulate the dynamic problem in terms of differential equations.

### 5.11.1 SINGLE-DEGREE-OF-FREEDOM SYSTEMS

Consider a portal frame, shown in Figure 5.65, consisting of an infinitely stiff beam supported by flexible columns that have negligible mass as compared to that of the beam. For horizontal motions,

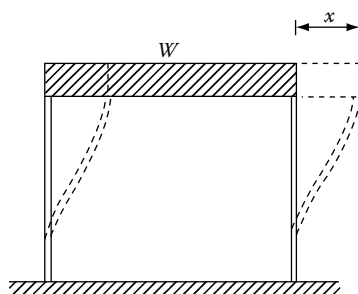
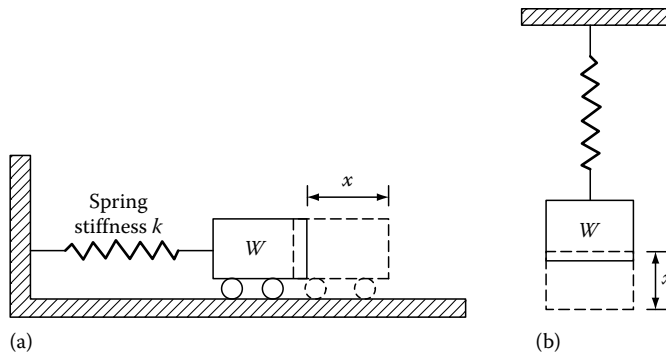


FIGURE 5.65 Single-bay single-story portal frame.



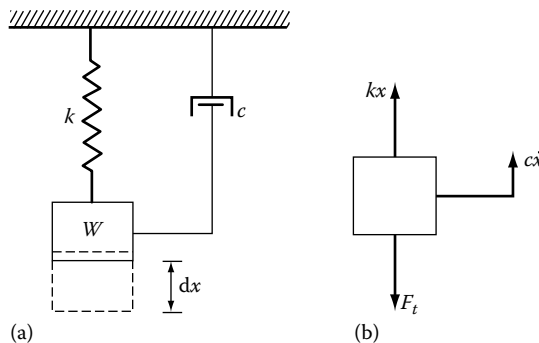
**FIGURE 5.66** Analytical models for SDOF system: (a) model in horizontal position and (b) model in vertical position.

the structure can be visualized as a spring-supported mass, as shown in Figure 5.66a, or as a weight  $W$  suspended from a spring, as shown in Figure 5.66b. Under the action of gravity force on  $W$ , the spring will extend by a certain amount  $x$ . If the spring is very stiff,  $x$  is small, and vice versa. The extension  $x$  can be related to the stiffness of the spring  $k$  by the relation

$$x = \frac{W}{k} \quad (5.4)$$

The spring constant or spring stiffness  $k$  denotes the load required to produce the unit extension of the spring. If  $W$  is measured in kip and the extension in inches, the spring stiffness will have a dimension of kip per inch. The weight  $W$  comes to rest after the spring has extended by the length  $x$ . Equation 5.4 expresses the familiar static equilibrium condition between the internal force in the spring and the externally applied force  $W$ .

If a vertical force is applied or removed suddenly, vibrations of the system are produced. Such vibrations, maintained by the elastic force in the spring alone, are called free or natural vibrations. The weight moves up and down, and therefore is subjected to an acceleration  $\ddot{x}$  given by the second derivative of displacement  $x$ , with respect to time  $t$ . At any instant  $t$ , there are three forces acting on the body: the dynamic force equal to the product of the body mass and its acceleration, the gravity force  $W$  acting downward, and the force in the spring equal to  $W + kx$  for the position of weight shown in Figure 5.67. These are in a state of dynamic equilibrium given by the relation



**FIGURE 5.67** Damped oscillator: (a) analytical model and (b) forces in equilibrium.

$$\frac{W}{g} \ddot{x} = W - (W + kx) = -kx \quad (5.5)$$

The preceding equation of motion is called Newton's law of motion and is governed by the equilibrium of inertia force that is a product of the mass  $W/g$  and acceleration  $\ddot{x}$ , and the resisting forces that are a function of the stiffness of the spring.

The principle of virtual work can be used as an alternative to derive Newton's law of motion. Although the method was first developed for static problems, it can be readily applied to dynamic problems by using D'Alembert's principle. The method establishes dynamic equilibrium by including inertial forces in the system.

The principle of virtual work can be stated as follows: For a system in equilibrium, the work done by all the forces during a virtual displacement is equal to zero. Consider a damped oscillator subjected to a time-dependent force  $F_t$ , as shown in Figure 5.67. The free-body diagram of the oscillator subjected to various forces is shown in Figure 5.62b.

Let  $\delta x$  be the virtual displacement. The total work done by the system is zero and is given by

$$m\ddot{x} \delta \dot{x} + c\dot{x} \delta x + kx \delta x - F_t \delta x = 0 \quad (5.6)$$

$$(m\ddot{x} + c\dot{x} + kx - F_t) \delta x = 0 \quad (5.7)$$

Since  $\delta x$  is arbitrarily selected

$$m\ddot{x} + c\dot{x} + kx - F_t = 0 \quad (5.8)$$

This is the differential equation of motion of the damped oscillator.

The equation of motion for an undamped system can also be obtained from the principle of conservation of energy. It states that if no external forces are acting on the system, and there is no dissipation of energy due to damping, then the total energy of the system must remain constant during motion and consequently, its derivative with respect to time must be equal to zeros.

Consider again the oscillator shown in Figure 5.67 without the damper. The two energies associated with this system are the kinetic energy of the mass and the potential energy of the spring.

The kinetic energy of the spring

$$T = \frac{1}{2} m \dot{x}^2 \quad (5.9)$$

where  $x$  is the instantaneous velocity of the mass.

The force in the spring is  $kx$ ; work done by the spring is  $kx \delta x$ . The potential energy is the work done by this force and is given by

$$V = \int_0^x kx \delta x = \frac{1}{2} kx^2 \quad (5.10)$$

The total energy in the system is a constant. Thus

$$\frac{1}{2} m \dot{x}^2 + \frac{1}{2} kx^2 = \text{constant } c_0 \quad (5.11)$$



Differentiating with respect to  $x$ , we get

$$m\ddot{x} + kx\dot{x} = 0 \quad (5.12)$$

Since  $\dot{x}$  cannot be zero for all values of  $t$ , we get

$$m\ddot{x} + kx = 0 \quad (5.13)$$

which has the same form as Equation 5.5. This differential equation has a solution of the form

$$x = A \sin(\omega t + \alpha) \quad (5.14)$$

$$x = \omega A \cos(\omega t + \alpha) \quad (5.15)$$

where

$A$  is the maximum displacement

$\omega A$  is the maximum velocity

Maximum kinetic energy is given by

$$T_{\max} = \frac{1}{2} m(\omega A)^2 \quad (5.16)$$

Maximum potential energy is

$$V_{\max} = \frac{1}{2} kA^2 \quad (5.17)$$

Since  $T = V$ ,

$$\frac{1}{2} m(\omega A)^2 = \frac{1}{2} kA^2$$

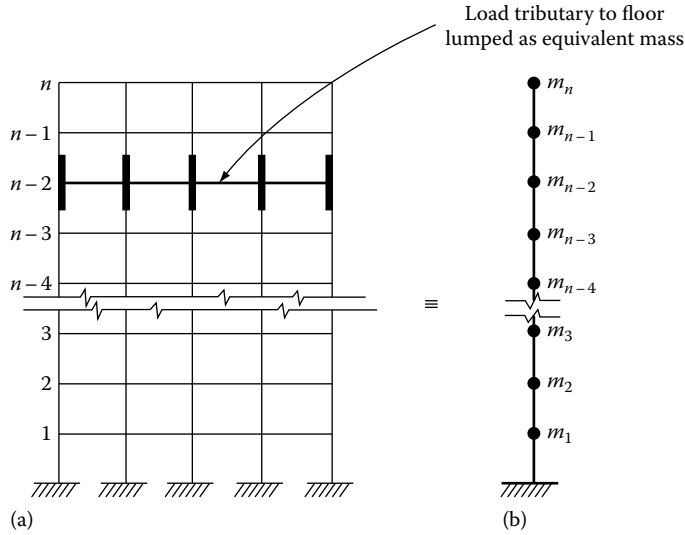
or

$$\omega = \sqrt{\frac{k}{m}} \quad (5.18)$$

which is the natural frequency of the simple oscillator. This method, in which the natural frequency is obtained by equating maximum kinetic energy and maximum potential energy, is known as Rayleigh's method.

### 5.11.2 MULTI-DEGREE-OF-FREEDOM SYSTEMS

In these systems, the displacement configuration is determined by a finite number of displacement coordinates. The true response of a multi-degree system can be determined only by evaluating the inertia effects at each mass particle because structures are continuous systems with an infinite number of DOF. Although analytical methods are available to describe the behavior of such systems, these are limited to structures with uniform material properties and regular geometry. The methods are complex, requiring the formulation of partial differential equations. However, the analysis is greatly simplified by replacing the entire displacement of the structure by a limited number of



**FIGURE 5.68** MDOF: (a) multistory analytical model with lumped masses.

displacement components, and assuming the entire mass of the structure is concentrated in a number of discrete points.

Consider a multistory building with  $n$  DOFs, as shown in Figure 5.68. The dynamic equilibrium equations for undamped free vibration can be written in the general form

$$\begin{bmatrix} m_{11} & m_{12} & m_{13} & \dots & m_{1n} \\ m_{21} & m_{22} & m_{23} & \dots & m_{2n} \\ m_{31} & m_{32} & m_{33} & \dots & m_{3n} \\ \vdots & \vdots & \vdots & \ddots & \vdots \\ m_{n1} & m_{n2} & m_{n3} & \dots & m_{nn} \end{bmatrix} \begin{bmatrix} \ddot{x}_1 \\ \ddot{x}_2 \\ \ddot{x}_3 \\ \vdots \\ \ddot{x}_n \end{bmatrix} + \begin{bmatrix} k_{11} & k_{12} & k_{13} & \dots & k_{1n} \\ k_{21} & k_{22} & k_{23} & \dots & k_{2n} \\ k_{31} & k_{32} & k_{33} & \dots & k_{3n} \\ \vdots & \vdots & \vdots & \ddots & \vdots \\ k_{n1} & k_{n2} & k_{n3} & \dots & k_{nn} \end{bmatrix} \begin{bmatrix} x_1 \\ x_2 \\ x_3 \\ \vdots \\ x_n \end{bmatrix} = 0$$

Writing the equations in matrix form

$$[M]\{\ddot{x}\} + [K]\{x\} = 0 \quad (5.18a)$$

where

$[M]$  is the mass or inertia matrix

$\{\ddot{x}\}$  is the column vector of accelerations

$[K]$  is the structure stiffness matrix

$\{x\}$  is the column vector of displacements of the structure

If the effect of damping is included, the equations of motion would be out of the form

$$[M]\{\ddot{x}\} + [C]\{\dot{x}\} + [K]\{x\} = \{P\} \quad (5.18b)$$

where

$[C]$  is the damping matrix

$\{\dot{x}\}$  is the column vector of velocity

$\{P\}$  is the column vector of external forces

General methods of solutions of these equations are available, but tend to be cumbersome. Therefore, in solving seismic problems, simplified methods are used; the problem first is solved by neglecting damping. The absence of precise data on damping does not usually justify a more rigorous treatment. Neglecting damping results in dropping the second term, and limiting the problem to free vibrations results in dropping the right-hand side of Equation 5.18b. The resulting equations of motion will become identical to Equation 5.18a. During free vibrations, the motions of the system are simple harmonic, which means that the system oscillates about the stationary position in a sinusoidal manner; all masses follow the same harmonic function, having similar angular frequency,  $\omega$ . Thus,

$$\begin{aligned}x_1 &= a_1 \sin \omega_1 t \\x_2 &= a_2 \sin \omega_2 t \\&\vdots \\x_n &= a_n \sin \omega_n t\end{aligned}$$

Or in matrix notation,

$$\{x\} = \{a_n\} \sin \omega_n t$$

where

$\{a_n\}$  represents the column vector of modal amplitudes for the  $n$ th mode

$\omega_n$  is the corresponding frequency

Substituting for  $\{x\}$  and its second derivative  $\{\ddot{x}\}$  in Equation 5.19 results in a set of algebraic expressions:

$$-\omega_n^2 [M] \{a_n\} + [K] \{a_n\} = 0 \quad (5.18c)$$

Using a procedure known as Cramer's rule, the preceding expressions can be solved for determining the frequencies of vibrations and relative values of amplitudes of motion  $a_{11}$ ,  $a_{12}$ , ...,  $a_n$ . The rule states that nontrivial values of amplitudes exist only if the determinant of the coefficients of  $a$  is equal to zero because the equations are homogeneous, meaning that the right-hand side of Equation 5.21 is zero. Setting the determinant of Equation 5.21 equals to zero, we get

$$\begin{bmatrix} k_{11} - \omega_1^2 m_{11} & k_{12} - \omega_1^2 m_{12} & k_{13} - \omega_1^2 m_{13} & \dots & k_{1n} - \omega_1 m_{1n} \\ k_{21} - \omega_2^2 m_{21} & k_{22} - \omega_2^2 m_{22} & k_{23} - \omega_2^2 m_{23} & \dots & k_{2n} - \omega_2 m_{2n} \\ k_{31} - \omega_3^2 m_{31} & k_{32} - \omega_3^2 m_{32} & k_{33} - \omega_3^2 m_{33} & \dots & k_{3n} - \omega_3 m_{3n} \\ \vdots & \vdots & \vdots & \vdots & \vdots \\ k_{n1} - \omega_n^2 m_{n1} & k_{n2} - \omega_n^2 m_{n2} & k_{n3} - \omega_n^2 m_{n3} & \dots & k_{nn} - \omega_n m_{nn} \end{bmatrix} = 0 \quad (5.18d)$$

With the understanding that the values for all the stiffness coefficients  $k_{11}$ ,  $k_{12}$ , etc. and the masses  $m_1$ ,  $m_2$ , etc. are known, the determinant of the equation can be expanded, leading to a polynomial expression in  $\omega^2$ . The solution of the polynomial gives one real root for each mode vibration. Hence, for a system with  $n$  DOFs,  $n$  natural frequencies are obtained. The smallest of the values obtained is called the fundamental frequency and the corresponding mode, the fundamental or first mode.

In mathematical terms, the vibration problem is similar to those encountered in stability analyses. The determination of frequency of vibrations can be considered similar to the determination of critical loads, while the modes of vibration can be likened to the evaluation of buckling modes.

Such types of problems are known as eigenvalue, or characteristic value, problems. The quantities  $\omega^2$ , which are analogous to critical loads, are called eigenvalues, or characteristic values, and in a broad sense can be looked upon as unique properties of the structure similar to geometric properties such as area or moment of inertia of individual elements.

Unique values for characteristic shapes, on the other hand, cannot be determined because the substitution of  $\omega^2$  for a particular mode into the dynamic equilibrium equation (Equation 5.18c) results in exactly  $n$  unknowns for the characteristic amplitudes  $x_1, \dots, x_n$  for that mode. However, it is possible to obtain relative values for all amplitudes in terms of any particular amplitude. We are, therefore, able to obtain the pattern or the shape of the vibrating mode, but not its absolute magnitude. The set of modal amplitudes that describe the vibrating pattern is called eigenvector or characteristic vector.

### 5.11.3 MODAL SUPERPOSITION METHOD

In this method, the equations of motions are transformed from a set of  $n$  simultaneous differential equations to a set of  $n$  independent equations by the use of normal coordinates. The equations are solved for the response of each mode, and the total response of the system is obtained by superposing individual solutions. Two concepts are necessary for the understanding of the modal superposition method: (1) the normal coordinates and (2) the property of orthogonality.

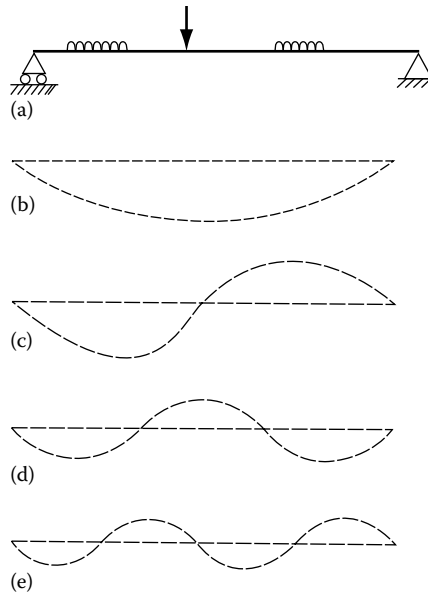
### 5.11.4 NORMAL COORDINATES

In a static analysis, it is common to represent structural displacements by a Cartesian system of coordinates. For example, in a planar system, coordinates  $x$  and  $y$  and rotation  $q$  are used to describe the position of a displaced structure with respect to its static position. If the structure is restrained to move only in the horizontal direction and if rotations are of no consequence, only one coordinate  $x$  is sufficient to describe the displacement. The displacements can also be identified by using any other independent system of coordinates. The only stipulation is that a sufficient number of coordinates are included to capture the deflected shape of the structure. These coordinates are commonly referred to as generalized coordinates and their number equal the number of DOFs of the system. In dynamic analysis, however, it is advantageous to use free-vibration mode shapes known as normal modes to represent the displacements. While a mathematical description of normal modes and their properties may be intriguing, there is nothing complicated about their concept. Let us indulge in some analogies to bring home the idea. For example, normal modes may be considered as being similar to the primary colors red, blue, and yellow. None of these primary colors can be obtained as a combination of the others, but any secondary color such as green, pink, or orange can be created by combining the primary colors, each with a distinct proportion of the primary colors. The proportions of the primary colors can be looked upon as scale factors, while the primary colors themselves can be considered similar to normal modes. To further reinforce the concept of generalized coordinates, recall beam bending problems in which the deflection curve of a beam is represented in the form of trigonometric series. Considering the case of a simply supported beam subjected to vertical loads, as shown in Figure 5.64, the deflection  $y$ , at any point can be represented by the following series:

$$y = a_1 \frac{\sin \pi x}{l} + a_2 \frac{\sin 2\pi x}{l} + a_3 \frac{\sin 3\pi x}{l} \quad (5.19)$$

Geometrically, this means that the deflection curve can be obtained by superposing simple sinusoidal shown in Figure 5.69.

The first term in Equation 5.19 represents the full-sine curve, the second term, the half-sine, etc. The coefficients  $a_1, a_2, a_3$ , etc. represent the maximum ordinates of the curves, while the numbers 1, 2, 3, etc., the number of waves or mode shapes. By determining the coefficients  $a_1, a_2, a_3$ , etc., the series can represent the deflection curve to any desired degree of accuracy, depending on the number of terms considered in the series.

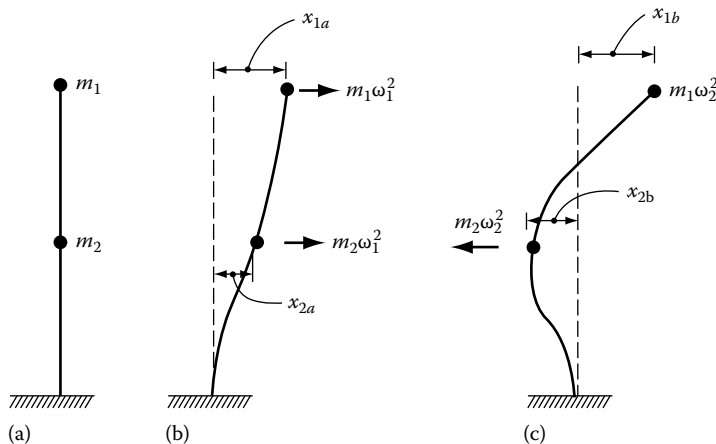


**FIGURE 5.69** Generalized displacement of a simply supported beam: (a) loading, (b) full-sine curve, (c) half-sine curve, (d) one-third-sine curve, and (e) one-fourth-sine curve.

### 5.11.5 ORTHOGONALITY

This force–displacement relationship is rarely used in static problems, but is of great significance in structural dynamics. This is best explained with an example shown in Figure 5.70.

Consider a two-story, lumped-mass system subjected to free vibrations. The system's two modes of vibrations can be considered as elastic displacements due to two different loading conditions, as shown in Figure 5.70b and c. We will use a theorem known as Betti's reciprocal theorem to demonstrate the derivation of orthogonality conditions. This theorem states that the work done by one set of loads on the deflections due to a second set of loads is equal to the work done by the second set of loads acting on the deflections due to the first. Using this theorem with reference to Figure 5.70, we get



**FIGURE 5.70** Two-story lumped-mass system illustrating Betti's reciprocal theorem: (a) lumped model, (b) forces during first mode of vibration, and (c) forces acting during second mode of vibration.

$$\omega_1^2 m_1 x_{1b} + \omega_1^2 m_2 x_{2b} = \omega_2^2 m_1 x_{1a} + \omega_1^2 m_2 x_{2a} \quad (5.20)$$

This can be written in matrix form

$$\omega_1^2 \begin{bmatrix} m_1 & 0 \\ 0 & m_2 \end{bmatrix} \begin{bmatrix} x_{1b} \\ x_{2b} \end{bmatrix} = \omega_2^2 \begin{bmatrix} m_1 & 0 \\ 0 & m_2 \end{bmatrix} \begin{bmatrix} x_{1a} \\ x_{2a} \end{bmatrix} \quad (5.21)$$

or

$$(\omega_1^2 - \omega_2^2) \{x_b\}^T [M] \{x_a\} = 0$$

If the two frequencies are not the same, that is,  $\omega_1 \neq \omega_2$ , we get

$$\{x_b\}^T [M] \{x_a\} = 0 \quad (5.22)$$

This condition is called the orthogonality condition, and the vibrating shapes,  $\{x_a\}$  and  $\{x_b\}$ , are said to be orthogonal with respect to the mass matrix,  $[M]$ . By using a similar procedure, it can be shown

$$\{x_a\}^T [k] \{x_b\} = 0 \quad (5.23)$$

The vibrating shapes are therefore orthogonal with respect to the stiffness matrix as they are with respect to the mass matrix. In the general case of the structures with damping, it is necessary to make a further assumption in the modal analysis that the orthogonality condition also applies for the damping matrix. This is for mathematical convenience only and has no theoretical basis. Therefore, in addition to the two orthogonality conditions mentioned previously, a third orthogonality condition of the form

$$\{x_a\}^T c \{x_b\} = 0 \quad (5.24)$$

is used in the modal analysis.

To bring out the essentials of the normal mode method, it is convenient to consider the dynamic analysis of a two-DOF system. We will first analyze the system by a direct method and then show how the analysis can be simplified by modal superposition method.

Consider a two-story dynamic model of a shear building shown in Figure 5.71a through c, subject to free vibrations. The masses  $m_1$  and  $m_2$  at levels 1 and 2 can be considered connected to each other and to the ground by two springs having stiffnesses  $k_1$  and  $k_2$ . The stiffness coefficients are mathematically equivalent to the forces required at levels 1 and 2 to produce unit horizontal displacements relative to each level.

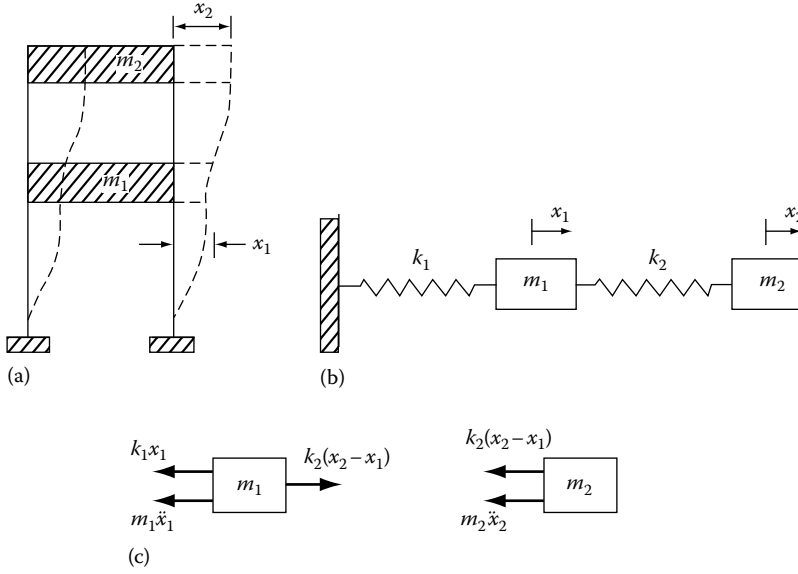
It is assumed that the floors, and therefore the masses  $m_1$  and  $m_2$ , are restrained to move in the direction  $x$  and that there is no damping in the system. Using Newton's second law of motion, the equations of dynamic equilibrium for masses  $m_1$  and  $m_2$  are given by

$$m_1 \ddot{x}_1 = -k_1 x + k_2 (x_2 - x_1) \quad (5.25)$$

$$m_2 \ddot{x}_2 = -k_2 (x_2 - x_1) \quad (5.26)$$

Rearranging terms in these equations gives

$$m_1 \ddot{x}_1 + (k_1 + k_2) x_1 - k_2 x_2 = 0 \quad (5.27)$$



**FIGURE 5.71** Two-story shear building, free vibrations: (a) building with masses, (b) mathematical model, and (c) free-body diagram with masses.

$$m_2\ddot{x}_2 - k_2x_1 + k_2x_2 = 0 \quad (5.28)$$

The solutions for the displacements  $x_1$  and  $x_2$  can be assumed to be of the form

$$x_1 = A \sin(\omega t + \alpha) \quad (5.29)$$

$$x_2 = B \sin(\omega t + \alpha) \quad (5.30)$$

where

$\omega$  represents the angular frequency

$\alpha$  represents the phase angle of the harmonic motion of the two masses

$A$  and  $B$  represent the maximum amplitudes of the vibratory motion

The substitution of Equations 5.29 and 5.30 into Equations 5.27 and 5.28 gives the following equations:

$$(k_1 + k_2 - \omega^2 m_1)A - k_2 B = 0 \quad (5.31)$$

$$k_2 A + (k_2 - \omega^2 m_2)B = 0 \quad (5.32)$$

To obtain the solution for the nontrivial case of  $A$  and  $B \neq 0$ , the determinant of the coefficients of  $A$  and  $B$  must be equal to zero. Thus,

$$\begin{bmatrix} (k_1 + k_2 - \omega^2 m_1) & -k_2 \\ -k_2 & (k_2 - \omega^2 m_2) \end{bmatrix} = 0 \quad (5.33)$$

The expansion of the determinant gives the relation

$$(k_1 + k_2 - \omega^2 m_1)(k_2 - \omega^2 m_2) - k_2^2 = 0 \quad (5.34)$$

or

$$m_1 m_2 \omega^4 - m_1 k_2 + m_2 (k_1 + k_2) \omega^2 + k_1 k_2 = 0 \quad (5.35)$$

The solution of this quadratic equation yields two values for  $\omega^2$  of the form

$$\omega_1^2 = \frac{-b + \sqrt{b^2 - 4ac}}{2a} \quad (5.36)$$

$$\omega_2^2 = \frac{-b - \sqrt{b^2 - 4ac}}{2a} \quad (5.37)$$

where

$$a = m_1 m_2$$

$$b = -[m_1 k_2 + m_2 (k_1 + k_2)]$$

$$c = k_1 k_2$$

As mentioned previously, the two frequencies  $\omega_1$  and  $\omega_2$ , which can be considered intrinsic properties of the system, are uniquely determined.

The magnitudes of the amplitudes  $A$  and  $B$  cannot be determined uniquely, but can be obtained in terms of ratios  $r_1 = A_1/B_1$  and  $r_2 = A_2/B_2$  corresponding to  $\omega_1^2$  and  $\omega_2^2$ , respectively. Thus,

$$r_1 = \frac{A_1}{B_1} = \frac{k_2}{k_1 + k_2 - \omega_1^2 m_1} \quad (5.38)$$

$$r_2 = \frac{A_2}{B_2} = \frac{k_2}{k_1 + k_2 - \omega_2^2 m_1} \quad (5.39)$$

The ratios  $r_1$  and  $r_2$  are called the amplitude ratios and represent the shapes of the two natural modes of vibration of the system.

Substituting the larger angular frequency  $\omega_1$  and the corresponding ratio  $r_1$  in Equations 5.29 and 5.30, we get

$$x_1' = r_1 B_1 \sin(\omega_1 t + \alpha_1) \quad (5.40)$$

$$x_2' = B_1 \sin(\omega_1 t + \alpha_1) \quad (5.41)$$

These expressions describe the first mode of vibration, also called the fundamental mode. Substituting the larger angular frequency  $\omega_2$  and the corresponding ratio  $r_2$  in Equations 5.29 and 5.30, we get

$$x_1'' = r_2 B_2 \sin(\omega_2 t + \alpha_2) \quad (5.42)$$



$$x_2'' = B_2 \sin(\omega_2 t + \alpha_2) \quad (5.43)$$

The displacements  $x_1''$  and  $x_2''$  describe the second mode of vibration. The general displacement of the system is obtained by summing the modal displacements:

$$x_1 = x_1' + x_1''$$

$$x_2 = x_2' + x_2''$$

Thus, for systems having two DOFs, we are able to determine the frequencies and mode shapes without undue mathematical difficulties. Although the equations of motions for multi-degree systems have similar mathematical form, solutions for modal amplitudes in terms of geometrical coordinates become unwieldy. The use of orthogonal properties of mode shapes makes this laborious process unnecessary. We will demonstrate how the analysis can be simplified by using the modal superposition method. Consider again the equations of motion for the idealized two-story building discussed in the previous section. As before, damping is neglected, but instead of free vibrations, we will consider the analysis of the system subject to time-varying force functions  $F_1$  and  $F_2$  at levels 1 and 2. The dynamic equilibrium for masses  $m_1$  and  $m_2$  is given by

$$m_1 \ddot{x}_1 + (k_1 + k_2)x_1 - k_2 x_2 = F_1 \quad (5.44)$$

$$m_2 \ddot{x}_2 - k_2 x_1 + k_2 x_2 = F_2 \quad (5.45)$$

These two equations are interdependent because they contain both the unknowns  $x_1$  and  $x_2$ . These can be solved simultaneously to get the response of the system, which was indeed the method used in the previous section to obtain the values for frequencies and mode shapes. The modal superposition method offers an alternate procedure for solving such problems. Instead of requiring the simultaneous solution of the equations, we seek to transform the system of interdependent or coupled equations into a system of independent or uncoupled equations. Since the resulting equations contain only one unknown function of time, solutions are greatly simplified. Let us assume that solution for the preceding dynamic equations is of the form

$$x_1 = a_{11}z_1 + a_{12}z_{12} \quad (5.46)$$

$$x_2 = a_{21}z_1 + a_{22}z_2 \quad (5.47)$$

What we have done in the preceding equations is to express displacement  $x_1$  and  $x_2$  at levels 1 and 2 as a linear combination of properly scaled values of two independent modes. For example,  $a_{11}$  and  $a_{12}$ , which are the mode shapes at level 1, are combined linearly to give the displacement  $x_1$ ;  $z_1$  and  $z_2$  can be looked upon as scaling functions. Substituting for  $x_1$  and  $x_2$  and their derivatives  $\dot{x}_1$  and  $\dot{x}_2$  in the equilibrium Equations 5.44 and 5.45, we get

$$m_1 a_{11} \ddot{z}_1 + (k_1 + k_2) a_{11} z_1 - k_2 a_{21} z_1 - m_1 a_{12} \ddot{z}_2 + (k_1 + k_2) a_{12} z_2 - k_2 a_{22} z_2 = F_1 \quad (5.48)$$

$$m_2 a_{21} \ddot{z}_1 - k_2 a_{11} z_1 + k_2 a_{21} z_1 + m_2 a_{24} \ddot{z}_2 - k_2 a_{12} z_2 + k_2 a_{22} z_2 = F_2 \quad (5.49)$$

We seek to uncouple Equations 5.44 and 5.45 by using the orthogonality conditions. Multiplying Equations 5.48 by  $a_{11}$  and Equations 5.49 by  $a_{21}$ , we get

$$\begin{aligned} m_1 a_{11}^2 \ddot{z}_1 + (k_1 + k_2) a_{11}^2 z_1 - k_2 a_{11} a_{21} z_1 + m_1 a_{11} a_{12} \ddot{z}_2 \\ + (k_1 + k_2) a_{11} a_{12} z_2 - k_2 a_{11} a_{22} z_2 = a_{11} F_1 \end{aligned} \quad (5.50)$$

$$\begin{aligned}
& m_1 a_{21}^2 \ddot{z}_1 - k_2 a_{11} a_{21} z_1 + k_2 a_{21}^2 z_1 + m_2 a_{21} a_{22} \ddot{z}_2 - k_2 a_{12} a_{21} z_2 \\
& + k_2 a_{21} a_{22} z_2 = a_{21} F_2
\end{aligned} \tag{5.51}$$

Adding the preceding two equations, we get

$$(m_1 a_{11}^2 + m_2 a_{21}^2) \ddot{z}_1 + \omega_1^2 (m_1 a_{11}^2 + m_2 a_{21}^2) z_1 = a_{11} F_1 + a_{21} F_2 \tag{5.52}$$

Similarly, multiplying Equations 5.48 and 5.49 by  $a_{12}$  and  $a_{22}$  and adding, we obtain

$$(m_1 a_{12}^2 + m_2 a_{22}^2) \ddot{z}_2 + \omega_2^2 (m_1 a_{12}^2 + m_2 a_{22}^2) z_2 = a_{12} F_1 - a_{22} F_2 \tag{5.53}$$

Equations 5.52 and 5.53 are independent of each other and are the uncoupled form of the original system of coupled differential equations. These can be further written in a simplified form by making use of the following abbreviations:

$$M_1 = m_1 a_{11}^2 + m_2 a_{21}^2 \tag{5.54}$$

$$M_2 = m_1 a_{12}^2 + m_2 a_{22}^2$$

$$K_1 = \omega_1^2 M_1 \tag{5.55}$$

$$K_2 = \omega_2^2 M_2$$

$$P_1 = a_{11} F_1 + a_{21} F_2 \tag{5.56}$$

$$P_2 = a_{12} F_1 - a_{22} F_2$$

where

$M_1$  and  $M_2$  are called the generalized masses

$K_1$  and  $K_2$  are the generalized stiffnesses

$P_1$  and  $P_2$  are the generalized forces

Using these notations, each of the Equations 5.52 and 5.53 takes the form similar to the equations of motion of a SDOF system:

$$M_1 \ddot{z}_1 + k_1 z_1 = P_1 \tag{5.57}$$

$$M_2 \ddot{z}_2 + k_2 z_2 = P_2 \tag{5.58}$$

The solution of these uncoupled differential equations can be found by any of the standard procedures given in textbooks on vibration analysis. In particular, Duhamel's integral provides a general method of solving these equations irrespective of the complexity of the loading function. However, in seismic analysis, usually a response spectrum is used instead of a forcing function to obtain the maximum values of the response corresponding to each modal equation. The direct superposition of modal maximum would, however, give only an upper limit for the total system that, in many engineering problems, would be too conservative. To alleviate this problem, approximations based on probability considerations are generally employed. One method employs the so-called root mean square procedure, also called the SRSS method. As the name implies, a probable maximum value is obtained by evaluating the SRSS of the modal quantities. Although this method is simple and widely used, it is not always a conservative predictor of earthquake response because more severe combinations of modal quantities can occur, as for example, when two modes have nearly the same natural period. In such cases, it is more appropriate to use the CQC procedure.

The aim of this section is to bring out the essentials of structural dynamics as related to seismic design of buildings. A certain amount of mathematical presentation has been unavoidable. Lest the reader lose the physical meaning of the various steps, it is worthwhile to summarize the essential features of dynamic analysis.

The dynamic analysis of buildings is performed by idealizing them as MDOF systems. The dead load of the building together with a percentage of live load (estimated to be present during an earthquake) is considered as lumped masses at each floor level. In a planar analysis, each mass has one DOF corresponding to lateral displacement in the direction under consideration, while in a 3D analysis, it has three DOF corresponding to two translational and one torsional displacements. Free vibrations of the buildings are evaluated, without including the effect of damping. The damping is taken into account by modifying the design response spectrum. The dynamic model representing a building has the number of mode shapes equal to the number of DOF of the model. Mode shapes have the property of orthogonality, which means that no given mode shape can be constructed as a combination of others, yet any deformation of the dynamic model can be described as a combination of its mode shapes, each multiplied by a scale factor. Each mode shape has a natural frequency of vibration. The mode shapes and frequencies are determined by solving for the eigenvalues. The total response of the building to a given response spectrum is obtained by statistically summing a predetermined number of modal responses. The number of modes required to adequately determine the design forces is a function of the dynamic characteristics of the building. Generally, for regular buildings, 6–10 modes in each direction are considered sufficient. Since each mass responds to earthquakes in more than one mode, it is necessary to evaluate effective modal mass values. These values indicate the percentage of the total mass that is mobilized in each mode. The acceleration experienced by each mass undergoing various modal deformations is determined from the response spectrum, which has been adjusted for damping. The product of the acceleration for a particular mode, multiplied by the effective modal mass for that mode, gives the static equivalent of forces at each discrete level. Since these forces do not reach their maximum values simultaneously, statistical methods such as SRSS or CQC are used for the combinations. The resulting forces are used as design static forces.

## 5.12 SUMMARY

A detailed analysis of the structure for the expected ground motions does not by itself make a building earthquake resistant. Additional design requirements over and above those indicated by the analysis are necessary to provide a consistent degree of earthquake resistance in buildings. The more severe the expected seismic ground motion, the more stringent these additional design requirements should be. It should be noted that not all of the necessary design requirements are explicit in the seismic provisions of ASCE 7-05, and although experienced seismic design engineers account for them, engineers lacking experience in the design and construction of earthquake-resistant structures often overlook them. Additionally, it should be kept in mind that considerable uncertainties exist regarding

1. Dynamic characteristics of future earthquake motions expected at a building site
2. Soil–structure–foundation interaction
3. Actual response of buildings when participation of nonstructural elements is taken into consideration
4. Mechanical characteristics of structural materials, particularly when they undergo significant cyclic straining in the inelastic range

It should be noted that the overall inelastic response of a structure is very sensitive to the inelastic behavior of its critical regions, and this behavior is influenced, in turn, by the detailing of these regions.

Although it is possible to counteract the consequences of these uncertainties by increasing the level of design force, it is considered more feasible and appropriate to provide a building system with

the largest energy dissipation consistent with the maximum tolerable deformations of nonstructural components and equipment. This energy-dissipation capacity, which is denoted simplistically as “ductility,” is extremely sensitive to the detailing. Therefore, in order to achieve such a large energy-dissipation capacity, it is essential that stringent design requirements be used for detailing the structural as well as the nonstructural components and their connections. Furthermore, it is necessary to have good quality control of materials and competent inspection. The importance of these factors has been clearly demonstrated by the building damage observed after both moderate and severe earthquakes.

It should be kept in mind that a building’s response to seismic ground motion most often does not reflect the designer’s or analyst’s original conception or the modeling of the structure on paper. What is reflected is the manner in which the building was constructed in the field. The detailing requirements should be related to the expected earthquake intensities and the importance of the building’s function and/or the density and type of occupancy. The greater the expected intensity of earthquake ground shaking and the more important the building function or the greater the number of occupants in the building, the more stringent the design and detailing requirements should be. Hence the concept of SDCs, which relate to the design ground motion severities, given by the spectral response acceleration coefficients  $S_{DS}$  and  $S_{DI}$ .

Since earthquakes can occur almost anywhere, some measure of earthquake resistance in the form of reserve ductility and redundancy should be built into the design of all structures to prevent catastrophic failures. The magnitude of inertial forces induced by earthquakes essentially depends on the building mass, ground acceleration, and the dynamic response of the structure. The shape and proportion of a building have a major effect on the distribution of earthquake forces as they work their way through the building. If irregular features are unavoidable, as in most practical cases, special design considerations are required to account for load transfer at abrupt changes in structural resistance.

Two approaches are recognized in modern codes for estimating the magnitude of seismic loads. The first approach, termed the ELF procedure, uses a simple method to take into account the properties of the structure and the foundation material. The second is a dynamic analysis procedure in which the modal responses are combined in a statistical manner to find the maximum values of the building response. Note that the level of force experienced by a structure during a major earthquake is much larger than the forces determined from either the static or dynamic analysis usually employed in the design. However, by prescribing detailing requirements, the structure is relied upon to sustain post-yield displacements without collapse.

The complex and random nature of ground motion makes it necessary to work with a more general characterization of ground motion. This is achieved by using earthquake response spectra to postulate the intensity and vibration content of ground motion at a given site. The duration of ground motion, although important, is not used explicitly in establishing design criteria at present (2009).

Earthquakes “load” structures indirectly. As the ground displaces, a building will follow and vibrate. The vibration produces deformations with associated strains and stresses in the structure. The computation of dynamic response to earthquake ground shaking is complex. As a simplification, the concept of a response spectrum is used in practice. A response spectrum for specific earthquake ground motion does not reflect the total time history of response, but only approximates the maximum value of response for simple structures to that ground motion. The design response spectrum is a smoothed and normalized approximation for many different ground motions, adjusted at the extremes for characteristics of larger structures.

Multistory buildings are analyzed as MDOF systems. They are represented by lumped masses at story intervals along the height of a vertically cantilevered pole. Each mode of the building system is represented by an equivalent SDOF system using the concept of generalized mass and stiffness. With the known period, mode shape, mass distribution, and acceleration, one can compute the deflected shape, story accelerations, forces, and overturning moments. Each predominant mode is analyzed separately, and by using either the SRSS or CQC method, the peak modal responses are combined to give a reasonable value between an upper bound as the absolute sum of the modes and a lower bound as the maximum value of a single mode.

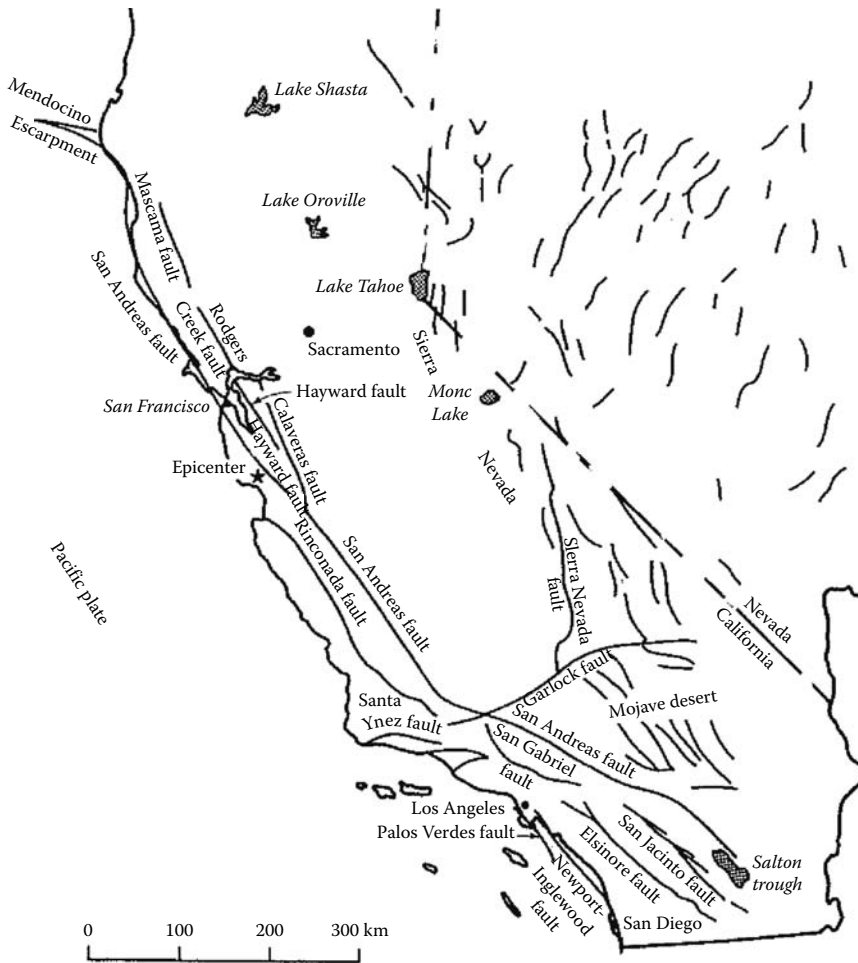


FIGURE 5.72 Major earthquake faults in California.

The time-history analysis technique represents the most sophisticated method of dynamic analysis for buildings. In this method, the mathematical model of the building is subjected to full range of accelerations for the entire duration of earthquake by using earthquake records that represent the expected earthquake at the base of the structure. The equations of motion are integrated by using computers to obtain a complete record of acceleration, velocity, and displacement of each lumped mass. The maximum value is found by scanning the output record. Even with the availability of sophisticated computers, the use of this method is restricted to the design of special structures such as nuclear facilities, military installations, and base-isolated structures.

In seismic design, nearly elastic behavior is interpreted as allowing some structural elements to slightly exceed specified yield stress on the condition that the elastic linear behavior of the overall structure is not substantially altered. For a structure with a multiplicity of structural elements forming the lateral force-resisting system, the yielding of a small number of elements will generally not affect the overall elastic behavior of the structure if excess load can be distributed to other structural elements that have not exceeded their yield strength.

Although for new buildings, the ductile design approach is quite routine, seismic retrofitting of existing non-ductile buildings with poor confinement details is generally extremely expensive. Therefore, it is necessary to formulate an alternative method that attempts a realistic assessment of

damage resistance of the building. One method, discussed in Chapter 7, is based on the concept of trade-off between ductility and strength. In other words, structural systems of limited ductility may be considered valid in seismic design, provided they can resist correspondingly higher forces. In this method, the concept of the inelastic demand ratio is used to describe the ability of the structural elements to resist stresses beyond yield stress.

California is the highest earthquake risk area in the contiguous United States. Several large, well-known, active faults run through the states—for example, the San Andreas, Hayward, and Newport-Inglewood (see Figures 5.68 through 5.72). They have been the cause of destructive earthquakes in the past and will be the sources of future destructive shocks.

Since the 1906 San Francisco earthquake (8.3 on the Richter scale), California has not experienced a major destructive quake with magnitude greater than 8.0. Such earthquakes, therefore, can be characterized as low-probability, high-loss events. However, damaging earthquakes with magnitudes greater than 6.5 occur in California on the average of every 4 years.

Today we have a reasonably good understanding of earthquakes, their effects, and their damage potential. We still are unable to predict when the next earthquake will occur. However, the effects of earthquakes on buildings are predictable. In the recent earthquakes, the kinds of damage that affected homes in 1906 occurred again. This damage can be prevented.

Engineers today have the knowledge and skills to evaluate the risks to all types of buildings. We can also design and strengthen buildings to withstand the strongest earthquake, making it possible to live and work in earthquake country and have peace of mind.



---

# 6 Seismic Design Examples and Details

In Chapter 5, we learned in minute detail the seismic provisions of ASCE 7-05 along with the reasoning behind these provisions. In this chapter, we apply this knowledge to seismic design examples that occur in our day-to-day engineering practice.

We use ACI 318-05 seismic provisions to present methods for the design of connections and structural members. Recent advances and revisions given in ACI 318-08 are addressed at the end of this chapter. The design of connections for special moment frames, shear walls, and other seismic load-resisting elements, including chords and collectors required to resist high-demand cyclic loads, are also discussed.

In keeping with the stated objective of this work, namely, to promote the understanding of the behavior of structures, we begin with a recap of the reasons for providing ductility, which in turn results in a higher level of energy dissipation or toughness in a structure (Section 6.1). We then examine why and how certain design techniques are used to promote inelastic behavior in a structure (Section 6.2). We then proceed to discuss the reasons for providing the so-called integrity reinforcement, the purpose of which is to limit damage to structures in the event of unexpected overloads (Section 6.3). This is followed by a review of strength design with applicable load and strength-reduction factors (Section 6.4). A comprehensive discussion of detailing requirements is then provided for

- Intermediate moment-resisting frames (IMRFs) and two-way slab frames (Section 6.5)
- Special moment-resisting frames (SMRFs) (Section 6.6)
- Shear walls (Section 6.7)
- Frame members not designed to resist earthquake forces (Section 6.8)
- Diaphragms (Section 6.9)
- Foundations (Section 6.10)

Design examples for the previously stated structural systems are provided toward the end of this chapter (Section 6.11). The chapter concludes with a presentation of typical details normally used in North American practice (Section 6.12).

## 6.1 SEISMIC DESIGN RECAP

For buildings in regions of low seismic risk, that is, for buildings assigned to seismic design category (SDC) A or B, the design provisions given in the first 20 chapters of the ACI code are considered sufficient. Hence there are no requirements for special ductile detailing for walls or moment frames. For buildings in regions of moderate seismic risk, that is, for buildings assigned to SDC C, there is no special ductile detailing required for cast-in-place shear walls. However, some ductile detailing requirements are required for moment frames including flat slab frames. For buildings assigned to SDC D, E, or F, a high degree of ductile detailing is required for both shear walls and moment frames.

Given the ready availability of computer programs, the analysis of a building is the easy part, and, in a broad sense, is the same for all SDCs. The detailing requirements, particularly at the beam–column joint of moment frames and the boundary elements of shear walls, are what set the designs apart.



It is likely that a building assigned to SDC A or B will never experience seismic forces that would result in an inelastic excursion of the building. For these buildings, a safe and economic design is achieved by using an appropriate margin of safety against gravity and lateral overloads.

In ultimate strength design, also referred to as strength design, or load resistance factor design (LRFD), the margin of safety is achieved by the use of load factors and strength-reduction factors. A structure designed by this method is believed to have an adequate margin of safety against overloads. In other words, the probability of yielding of the structure is considered very low. Structural deflections under lateral loads are expected to be elastic and thus fully recoverable. For example, a very tall building, say, at a height of 1400 ft, on a windy day may experience as much as 3 ft of lateral deflection at the top, but would not endure any permanent deflection. The elastic design used in the sizing of structural members for these loads assures that after the winds have subsided, the building would come back to its pre-wind plumbness without any permanent deflection.

Such is not the case for buildings in moderate-to-high seismic-risk zones, that is, buildings assigned to SDC C, D, or F. It is true that they too respond elastically under the most severe of wind conditions because the design is meant to keep the structure elastic under the generally predictable wind loads. However, the lateral loads that we use in elastic seismic designs are but a fraction of the highly unpredictable seismic loads. We know only so much as past earthquakes have taught us: The magnitudes of lateral loads experienced by buildings under intense earthquakes are so large that an elastic design under these loads is not economically feasible. The building designed to perform elastically in a large seismic event will have structural members so large costing so much more that society has accepted the risk of buildings going beyond their elastic limit, with the stipulation that they do not crumble or collapse. In other words, a building may be utterly damaged beyond repair and may never be occupied again, but if it stays up and ensures the safety of the occupants of the building during and immediately after a large earthquake, it is deemed to have performed adequately under present seismic codes.

The collapse of a building is generally preventable if brittle failure of its members and connections is prevented. In other words, during a code-stipulated earthquake, the structural elements may bend and twist to their hearts' content, but may not snap. The intent, then, is to build ductility into the structure so that it will absorb energy, and thus prevent the sudden breaking up of members that would result in a collapse.

Therefore, buildings in regions of high seismic risk, typically those assigned to SDC C, D, E, or F, are detailed to have ductility. The degree of detailing is entirely dependent on the severity of the seismic risk. This is the very reason why a building assigned to SDC D, E, or F, is designed to be more ductile than its counterpart that has been assigned to SDC A, B, or C. The vast difference in design requirements may be appreciated by studying Tables 6.1 and 6.2, which gives a comparison of non-seismic and seismic design criteria for moment frames and shear walls.

Seismic design using the ASCE 7-05 provisions entails the following steps:

1. The determination of earthquake forces for a seismic event having a 10% probability of occurrence in 50 years, is commonly referred to as design earthquake. This includes
  - a. The calculation of the base shear corresponding to the computed or estimated fundamental period of vibration of the structure.
  - b. The distribution of the base shear over the height of the building.
2. The analysis of the structure for the lateral forces calculated in step 1, as well as forces induced by gravity and wind loads. The results are used to design structural members and story drift ratios and overall deflections.
3. The design of members and joints for the most unfavorable combination of gravity and lateral loads, including the design and detailing of members and their connections to ensure their ductile behavior.
4. The verification of inter-story drift using magnified elastic displacements.

**TABLE 6.1**  
**Design Criteria Comparison, ACI 318-05, Moment Frames**

Member	Type of Checks/ Design	Ordinary Moment- Resisting Frames	Intermediate Moment- Resisting Frames	Special Moment- Resisting Frames
Frame column	Column design: Flexure and axial loads	Ultimate load combinations $1\% < \rho < 8\%$	Ultimate load combinations $1\% < \rho < 8\%$	Ultimate load combinations. Column capacity $\geq \frac{6}{5}$ beam capacity with $\alpha = 1.0$ , $\Sigma M_c \geq \frac{6}{5} \Sigma M_g$ $1\% < \rho < 6\%$
	Column design: Shear	Ultimate load combinations	Modified ultimate load combination (earthquake loads doubled). Column capacity $\phi = 1.0$ and $\alpha = 1.0$	Ultimate load beam capacity combinations with $\phi = 1.0$ and $\alpha = 1.25$
Frame beam	Beam design: Flexure	Ultimate load combinations	Ultimate load combinations	Ultimate load combinations
	Beam min. moment requirements	No requirement	$M_{uEND}^+ \geq \frac{1}{3} M_{uEND}^-$ $M_{uSPAN}^+ \geq \frac{1}{5} M_{uEND}^+$ $M_{uSPAN}^+ \geq \frac{1}{5} M_{uEND}^-$	$\rho_{max} \leq 0.025$ $M_{uEND}^- \geq \frac{1}{2} M_{uEND}^+$ $M_{uSPAN}^+ \geq \frac{1}{4} M_{uEND}^+$ $M_{uSPAN}^- \geq \frac{1}{4} M_{uEND}^-$
	Beam design: Shear	Ultimate load combinations	Modified ultimate load combinations (earthquake loads doubled). Beam capacity shear ( $V_p$ ) with $\alpha = 1.0$ and $\phi = 1.0$ plus $V_{D+L}$	Beam shear capacity $\geq$ plastic shear ( $V_p$ ) with $\alpha = 1.25$ and $\phi = 1.0$ plus $V_{D+L}$ (ult). $V_c = 0$ , if $V_p \geq \frac{V_{total}}{2}$ , and axial compressive force $< \frac{A_g f_c}{20}$ .
Beam-column joint	Shear design	No requirement	No requirement	Shear capacity of joint area, $A_j \geq$ beam plastic shear capacity ( $V_p$ ) with $\alpha = 1.25$ and $\phi = 1.0$
	Beam/column ratios	No requirement	No requirement	Column capacity based on uniaxial capacity under axial loads from ultimate load combinations $\geq$ beam capacity with $\alpha = 1.0$

*Note:* To assure adequate flexural ductility in critical regions, ACI 318-08, like its predecessors, specifies a factor  $\alpha = 1.25$  as the ratio of ultimate tensile strength to actual yield strength of the reinforcement.

The above steps are carried out in each principal direction of the building assuming that the design lateral forces act nonconcurrently in each of these directions. However, for buildings that are sensitive to torsional oscillations and/or are characterized by significant irregularities, orthogonal effects need to be considered. This requirement is deemed to be satisfied if the design is based on the more severe combination of 100% of the prescribed seismic forces in one direction in addition to 30% of the forces in the perpendicular direction.

**TABLE 6.2**  
**Design Criteria Comparison, ACI 318-05, Shear Walls**

Type of Check/Design	Ordinary Shear Wall <sup>a</sup>	Special Shear Wall
Flexure design	Ultimate load combinations No special ductile detailing	Ultimate load combinations Boundary elements as required by displacement-based or stress-based design
Shear design	Ultimate load combinations; no special requirement	$\phi = 0.6$ (shear controlled), $\phi = 0.75$ (flexure controlled) $\phi_{\text{diaphragm}} \leq \phi_{\text{shear wall}}$

<sup>a</sup> ACI 318-08, like its predecessors, does not save a classification for intermediate cast-in-place shear wall. It considers the detailing requirements given for ordinary shear walls as sufficient to provide a degree of toughness that is consistent with the seismic risk associated to SDC C and lower.

## 6.2 DESIGN TECHNIQUES TO PROMOTE DUCTILE BEHAVIOR

Experience has shown that reinforced concrete members achieve ductility when certain limits are placed on steel in tension and on concrete in compression. Reinforced concrete beams with common proportions can possess ductility under monotonic loading even greater than common steel beams in which buckling may be a limiting factor. However, providing stability and resistance to reversed inelastic strains requires special detailing. Thus the essence of seismic detailing is to prevent premature shear failures in members and joints, the buckling of compression bars, and the crushing of concrete. It is not sufficient to have only strength capability; there must also be special details to actualize the inelastic behavior of the seismic-resisting elements to ensure that the system remains stable at deformations corresponding to maximum expected ground motion. Vertical loads must be supported even when maximum elastic deformations are exceeded. In other words, inelastic yielding is allowed in resisting seismic loads as long as yielding does not impair the vertical load capacity of the structure.

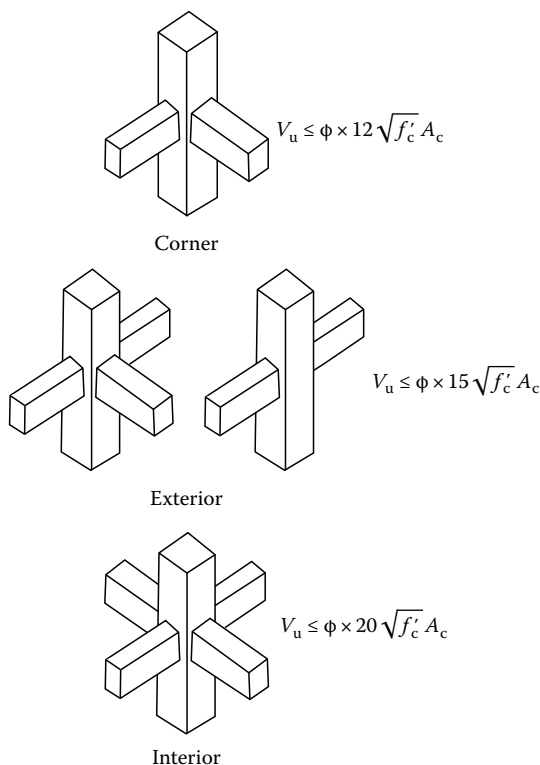
Why shear reinforcement in a beam–column joint? Because the mechanism of shear failure in a joint is different from shear-flexure failure in beams; the nominal shear capacities are considerably higher than the values the designers in the non-seismic areas are accustomed to. For example, following are the ACI 318-05 permitted ultimate shear stress values in joints, as shown in Figure 6.1:

1.  $\phi 20\sqrt{f'_c}$  for joints confined on all four sides
2.  $\phi 15\sqrt{f'_c}$  for joints confined on three sides or two opposite sides
3.  $\phi 12\sqrt{f'_c}$  for all other cases

Compare this to the value of  $\phi 4\sqrt{f'_c}$  allowed for punching shear in flat slabs without shear reinforcement, and  $\phi 6\sqrt{f'_c}$  for the same with shear reinforcement. The relatively high values for joint shear allowed in seismic design may give the wrong impression that joint shear will not be a problem in sizing of columns in high seismic zones. This is not the case. Even with the very high shear stresses permitted, joint shear most often controls the size of frame columns. Also note that shear reinforcement extending through the beam–column joint is required even though no increase in shear capacity is credited for its presence.

Why a strong column–weak beam? The reason is to prevent a story mechanism. This is achieved by assuring that, at each beam–column joint, the flexural resistance of columns is substantially (20%) more than the flexural strength of beams. In calculating the nominal flexural strength of columns, the effect of column axial loads should be included.

Why minimum positive reinforcement? The reason for minimum positive moment at beam ends is because actual seismic loads are much larger than what we calculate for design purposes and



**FIGURE 6.1** Shear strength of joints.

more importantly they reverse in direction. The bending moment and shear at beam ends, therefore, can be positive or negative at different points in time. Simple elastic analysis and typical ultimate load combinations cannot possibly give reliable results. Therefore, it is necessary to provide a minimum capacity for positive moments at the ends as well as negative moments at midspans.

Why closely spaced ties? To ensure that a plastic hinge develops in frame beams, it is necessary (1) to attain yielding of reinforcement well before concrete fails in compression and (2) to provide transverse reinforcement at close intervals to confine the concrete core within the longitudinal reinforcement.

Closely spaced ties enhance the ductility of concrete by allowing large compression strains to develop in concrete without spalling. The ties prevent the buckling of longitudinal bars. A buckled or kinked bar has a tendency to fracture when the bar straightens in tension under load reversals. Therefore, in seismic detailing, it is necessary to use seismic hooks in the ties. This is because when the concrete cover spalls, the hoops may themselves be exposed and lose their confining capacity. Therefore, the ties must be anchored into the confined zone of concrete permitting the structure to survive even after responding inelastically during strong earthquakes. In essence, the members must be designed and detailed with prior realization of the inevitability of inelastic response by promoting a relatively benign ductile response rather than an undesirable brittle response. This is typically achieved by ensuring that members have inelastic energy-dissipation characteristics, through yielding of reinforcement as opposed to the shearing or the crushing of concrete.

The vertical elements designed to partake in energy dissipation should have proper confinement such that the vertical load-carrying capacity is not compromised. The seismic provisions encourage the formation of beam hinges rather than column hinges to prevent story mechanisms. To ensure adequate flexural ductility in critical regions of beams, ACI 318-05 specifies a factor of 1.25 as the ratio of ultimate tensile strength to actual yield strength of the reinforcement. Also, the amount by

which the actual yield strength can exceed the minimum specified value is limited to 18,000 psi. The joints of frames are designed for shears corresponding to the development of maximum beam moments, assuming the longitudinal reinforcement is stressed to 1.25 times the specified yield strength. This is to allow for the effects of strain hardening and for the possibility of actual yield strengths exceeding the specified minimum values.

Why diagonal reinforcement in deep coupling beams? Coupling beams designed as conventional flexural members with stirrups, and with some shear resistance allocated to concrete, are unsuitable for energy dissipation by the formation of plastic hinges at the beam ends, as implied for typical frame beams. The relatively short beam between the walls has a tendency to divide itself into two triangular parts if the shear force associated with the flexural overstrength of the beam cannot be effectively transmitted by the vertical stirrups.

This consideration has led to the use of diagonal reinforcement in relatively deep coupling beams. The shear resistance is provided by the diagonal tension and compression in the reinforcement. This results in a very ductile behavior that can then sustain large deformations imposed on the beams during seismic inelastic excursions.

Why boundary elements in special reinforced concrete walls? Boundary elements are required at the vertical edges of walls to provide proper confinement of concrete at these locations. ACI 318-05 permits two methods for determining the confinement requirements. In the first method, the strain at the extreme fiber of the wall is compared to a threshold value when the wall is subjected to a lateral displacement corresponding to a displacement likely to occur in a large earthquake, that is, the magnified elastic displacements. The second method is based on the calculated compressive stress at the extreme fibers. In either case, transverse reinforcement similar to that required for a frame column is required to prevent the buckling of the longitudinal reinforcement due to cyclic load reversals.

Why heavy transverse reinforcement in frame columns? The amount of transverse reinforcement provided in columns is controlled by four design requirements: (1) shear strength; (2) lateral support of compression reinforcement to prevent buckling; (3) confinement of highly stressed compression zones, both in potential plastic hinge regions and along the full height of columns; and (4) prevention of bond strength loss within column vertical bar splices.

1. Shear resistance: Some or all of the design force  $V$  must be resisted by the transverse reinforcement in the form of spiral or circular hoops and column ties. The approach to shear design in potential plastic hinge regions is different from that for other parts of the column.
2. Lateral support for compression reinforcement: Anti-buckling reinforcement should be provided in the plastic hinge regions of frame columns in the same manner as for the end regions of frame beams. The design of transverse reinforcement in between the end regions is as for non-seismic designs. However, the minimum spacing requirements for shear strength or confinement of compression reinforcement generally govern the spacing.
3. Confinement of concrete: Confinement is essential to preserve adequate rotational ductility in potential plastic hinge regions of columns. The lengths of potential plastic hinge regions in columns are generally smaller than in beams partly because column moments vary along the story height with a relatively large gradient. Therefore, the region of a frame column subjected to tension yielding of reinforcement is somewhat limited. The calculated reinforcement is required for the entire plastic region, with only one-half of this required in between.
4. Transverse reinforcement at lapped splices: Splicing of reinforcement in structural members is not a requirement but a necessity for building practical structures. This is commonly achieved by overlapping parallel bars. Force transmission from one bar to the next occurs through the response of surrounding concrete. However, when large forces are to be transmitted by bond, splitting of concrete may develop resulting in cracks. To mobilize a load path for the force transmission through the cracked concrete, a shear friction reinforcement, in the form of transverse reinforcement, is required at lapped splices.

It is most important to design and detail the reinforcement in members and their connections to ensure their ductile behavior and thus allow the structure to sustain, without collapse, the severe distortions that may occur during a major earthquake. This requirement—intended to ensure adequate ductility in structural elements—represents the major difference between the design requirements for conventional, non-earthquake-resistant structures and those located in regions of high seismic risk, or assigned to SDC C, D, E, or F.

### 6.3 INTEGRITY REINFORCEMENT

The goal of structural integrity is the following: If a structure or part of a structure is subjected to an abnormal loading, or if a primary element sustains damage from an unanticipated event, tying the members together should result in confining the resulting damage to a relatively small area. Requirements for structural integrity included in Sections 7.13 and 13.3.8.5 of the ACI 318-05, focus on the structural detailing of cast-in-place concrete. Basically, the prescribed amounts of longitudinal reinforcement must be continuous over the support or the reinforcing bars that terminate at discontinuous ends of a member must be anchored with hooks.

Since accidents and misuse are normally unforeseeable events, they cannot be defined precisely. Similarly, providing general structural integrity to a structure is a requirement that cannot be stated in simple terms. The code's performance provision—"a structure shall be effectively tied together to improve integrity of the overall structure"—requires considerable judgment on the part of the design engineer. Opinions among engineers differ on the effectiveness of a general structural integrity solution for a particular framing system. However, the code does set forth specific examples of certain reinforcing details for cast-in-place joists, beams, and two-way slab constructions.

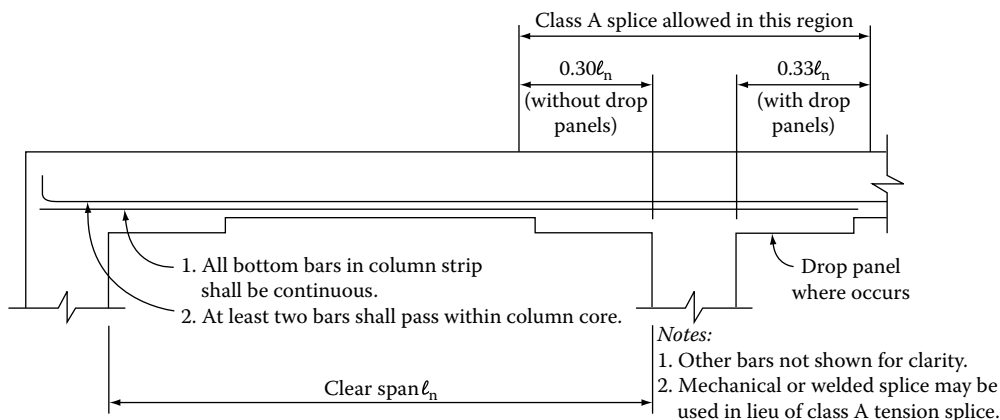
With damage to a support, top reinforcement that is continuous over the support will tend to tear out of the concrete. It will not provide the catenary action needed to bridge the damaged support unless it is confined by stirrups. By making a portion of the bottom reinforcement in beams continuous over supports, a catenary action can be provided. By providing some continuous top and bottom reinforcement in edge or perimeter beams, an entire structure can be tied together. Also, continuous ties provided in perimeter beams of a structure will toughen the exterior portion of a structure, should an exterior column be severely damaged.

Provisions for integrity reinforcement, first introduced in ACI 318-89, require continuous reinforcement in beams around the perimeter of the structure. The required minimum is one-sixth of the tension reinforcement for negative moment at the support and one-fourth of the tension reinforcement for positive moment at the midspan. In either case, a minimum of two bars is required. Continuity in rebars is achieved by providing class A tension lap splices and mechanical or welded splices in cast-in-place joists and beams.

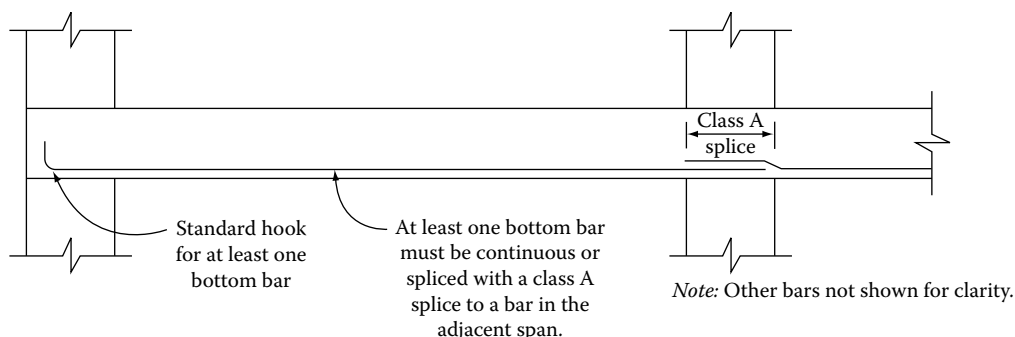
**Two-way slabs:** In a two-way slab construction, all bottom bars within the column strip in each direction must be lap-spliced with class A tension laps. See Figure 6.2 for locations where the lap splices are permitted. At least two of the bottom bars in the column strip must pass within the core of the columns and be anchored at exterior supports.

**Joists:** At least one reinforcing bar at the bottom of a rib is to be continuous over supports or the bar must be spliced with a class A tension lap splice to a bar in the adjacent span. At discontinuous ends of joists, anchorage of at least one bottom bar must be provided with a standard hook (Figure 6.3).

**Beams:** Beams are categorized as either perimeter or nonperimeter beams. A spandrel beam would be a perimeter beam. The detailing of top and bottom bars and of stirrups in perimeter beams is impacted by the structural integrity provisions. At least one-sixth of the  $-A_s$  required for negative-factored moment at the face of supports, and one-quarter of the  $+A_s$  required for positive-factored moment at midspan are to be made continuous around the perimeter of the structure. Closed stirrups are also required in perimeter beams. It is not necessary to place closed stirrups within the



**FIGURE 6.2** Structural integrity reinforcement in flat slabs without beams.



**FIGURE 6.3** Structural integrity reinforcement in joists.

joists. It is permissible to provide continuity of the top and bottom bars by splicing the top bars at midspan and the bottom bars at or near the supports. Lap-splicing with class A tension lap splices is also required (Figure 6.4).

For nonperimeter beams, the engineer has two choices to satisfy the structural integrity requirements: (1) provide closed stirrups or (2) make at least one-quarter of the  $+A_s$  required for positive-factored moment at midspan continuous. Splicing the prescribed number of bottom bars over the supports with class A tension lap splices is acceptable. At discontinuous ends of nonperimeter beams, the bottom bars must be anchored with standard hooks (Figure 6.5). In all cases, mechanical or welded splices may be used instead of class A tension lap splices.

## 6.4 REVIEW OF STRENGTH DESIGN

Concrete structures are commonly designed in the United States using the ultimate strength method. Since the American Concrete Institute published ACI 318-71, the term “ultimate” has been dropped, so that what used to be referred to as ultimate-strength design is now simply called strength design. In this approach, structures are proportioned such that their ultimate capacity is equal to or greater than the required ultimate strength. The required strength is based on the most critical combination

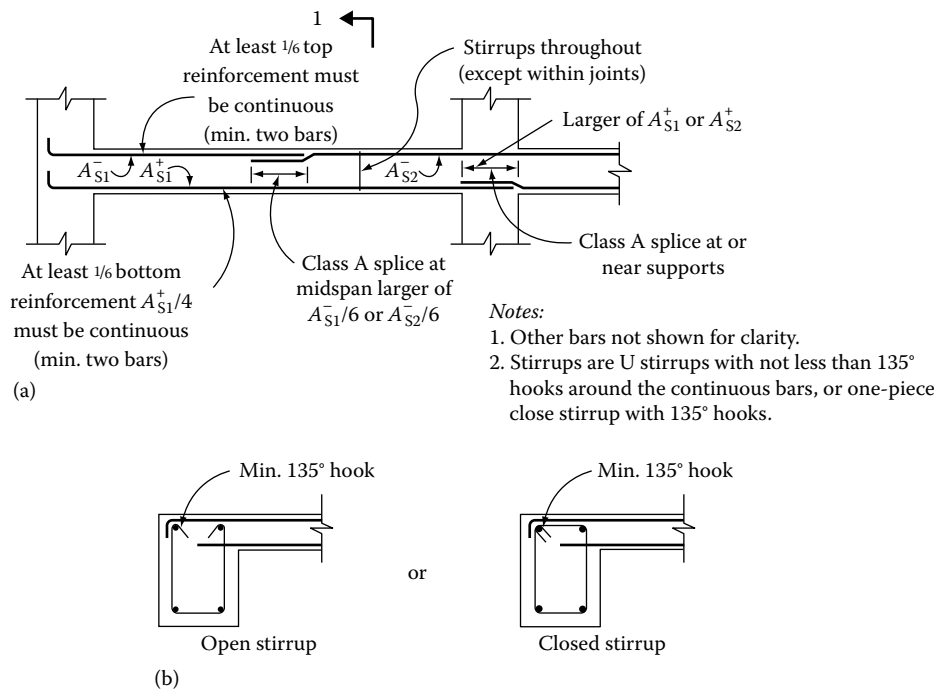


FIGURE 6.4 Integrity reinforcement in perimeter beams: (a) perimeter beam elevation and (b) Section 1.

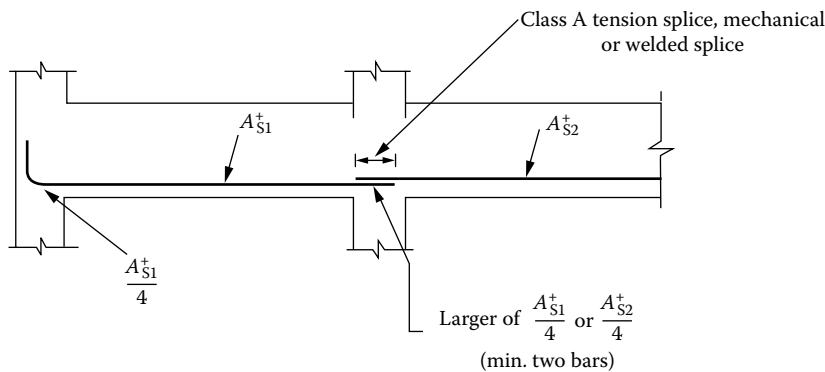


FIGURE 6.5 Integrity reinforcement in beams other than perimeter beams.

of factored loads, obtained by multiplying specified service loads by appropriate load factors. The capacity of an element, on the other hand, is obtained by applying a strength-reduction factor  $\phi$  to the nominal resistance of the element. Load factors are intended to take into account the variability in the magnitude of the specified loads. Lower load factors are used for types of loads that are less likely to vary significantly from the specified values. To allow for the lesser likelihood of certain types of loads occurring simultaneously, reduced load factors are specified for some loads when considered in combination with other loads.



### 6.4.1 LOAD COMBINATIONS

For the most common dead load  $D$ , live load  $L$ , roof live load  $L_r$ , wind load  $W$ , and earthquake load  $E$ , the simplified load combinations of ACI 318-08 are

$$U = 1.4D \quad (6.1)$$

$$U = 1.2D + 1.6L + 0.5L_r \quad (6.2)$$

$$U = 1.2D + 1.6L_r + (1.0L \text{ or } 0.8W) \quad (6.3)$$

$$U = 1.2D + 1.6W + 1.0L + 0.5L_r \quad (6.4)$$

$$U = 1.2D + 1.0E + 1.0L \quad (6.5)$$

$$U = 0.9D + 1.6W \quad (6.6)$$

$$U = 0.9D + 1.0E \quad (6.7)$$

The designer is referred to ACI 318-05, Section 9.2, for load combinations that include loads due to

1.  $H$  = weight and pressure of soil, water in soil, or other materials
2.  $F$  = weight and pressures of fluids
3.  $T$  = temperature, creep, shrinkage, differential settlement
4.  $R$  = rain load
5.  $S$  = snow load

ACI 318-05 permits a reduction of 50% on the load factor for  $L$ , except for garages, areas occupied as places of public assembly, and all areas where the live load,  $L$ , is greater than 100 lb/ft<sup>2</sup>.

The load factor of 1.6 for wind is based on the premise that the designers will be using wind loads determined by the provisions of ASCE 7-05, which includes a factor for directionality that is equal to 0.85 for buildings. Therefore, the corresponding load factor for wind, which was 1.3 prior to ACI 318-02, is increased to 1.6 ( $1.3/0.85 = 1.53$  rounded up to 1.6). Use of a previous wind load factor of 1.3 is permitted when wind load is obtained from other sources that do not include the directionality factor.

### 6.4.2 EARTHQUAKE LOAD $E$

A reduced load factor of 1.0 for earthquake forces is used because recent standards such as ASCE 7 have converted earthquake forces to strength level beginning with the 2002 edition.

Within the 2005 edition of the ASCE 7,  $E$  is defined as earthquake load in Section 2.2 and as the seismic load effect in Section 12.4.2. This second definition is a better description of what the term  $E$  actually represents because  $E$  is combined with other load effects (dead, live, snow, etc.) via a load combination for member design. It is not simply the force in the member as a result of a seismic load case.

The basic load combinations as stated in ASCE 7-05 (Section 2.3) that deal with the LRFD seismic load cases are as follows:

$$1.2D + 1.0E + L + 0.2S \quad (6.8)$$

$$0.9D + 1.0E \quad (6.9)$$

Note that cases that include  $H$  (lateral earth pressure) and  $F$  (fluid) load effects are not shown for simplicity.

The seismic load effect,  $E$ , has both a horizontal and vertical component. These are defined in ASCE 7-05, Section 12.4. The vertical component,  $E_v$ , is defined as  $E_v = 0.2S_{DS}D$ , where  $S_{DS}$  is the design spectral response acceleration parameter at short periods.

The horizontal component,  $E_h$ , is defined as  $E_h = \rho Q_E$ . The redundancy factor,  $\rho$ , is incorporated into this component to ensure that the building's seismic load-resisting system (SLRS) will have redundancy built into it for high seismic applications. Redundancy is demonstrated when a system is able to form a large number of plastic hinges, in a progressive fashion. This ensures that no one member will carry the bulk of the seismic resistance of the system and that the building as a whole will exhibit ductile behavior. It varies for different SDCs. For SDCs A, B, and C, it is 1.0. For SDCs D, E, and F, it is usually 1.3.

Separating the vertical and horizontal components and substituting into the load equations above results in the following expressions:

$$(1.2 + 0.2S_{DS})D + \rho Q_E + L + 0.2S \quad (6.10)$$

$$(0.9 - 0.2S_{DS})D + \rho Q_E \quad (6.11)$$

The ASCE 7-05 no longer uses the phraseology “special seismic load combinations,” as is done by 2006 IBC, Section 1605.4. Instead ASCE 7-05 prescribes an equation for  $E_m$ , the seismic load effect including overstrength factor,  $\Omega_o$ , that is to be used in ASCE 7-05, Chapter 2 Load Combinations.

$E_m$  is given by

1. For load combination in which seismic effects are additive to gravity loads

$$E_m = E_{mh} + E_v = \Omega_o Q_E + E_v \quad (6.12)$$

2. For load combination in which seismic effects counteract gravity loads

$$E_m = E_{mh} - E_v = \Omega_o Q_E - E_v \quad (6.13)$$

Note that in the load combinations, the overstrength factor,  $\Omega_o$ , is substituted for the redundancy factor,  $\rho$ .

Although defined elsewhere in the text, for convenience we repeat the definitions for earthquake-related effects,  $E$ .

$E_m$  = Seismic load effect including overstrength factor

$E_{mh}$  = Effect of horizontal seismic forces including structural overstrength

$E_v$  = Vertical seismic load effect

The horizontal seismic load effect with overstrength factor,  $E_{mh}$ , shall be determined in accordance with the following equation:

$$E_{mh} = \Omega_o Q_E \quad (6.14)$$

where  $Q_E$  is the effect of horizontal seismic forces from  $V$  or  $F_p$ . Where required such effects shall result from application of horizontal forces simultaneously in two different directions at right angles to each other.  $\Omega_o$  is the overstrength factor.

Exceptions: The value of  $E_{mh}$  need not exceed the maximum force that can develop in the element as determined by a rational, plastic mechanism analysis or nonlinear response analysis utilizing realistic expected values of material strengths.

A list of situations in which the use of overstrength factor,  $\Omega_o$ , is mandated by the ASCE 7-05 are

1. Cantilever systems (Section 12.2.5.2)
2. Elements supporting discontinuous walls or frames (Section 12.3.3.3)
3. Collector elements (Section 12.10.2.1 seismic category C and higher)
4. Batter piles (Section 12.13.6.4)
5. Pile anchorage requirement for uplift (Section 12.13.6.5)

The referenced sections are from the ASCE 7-05.

#### 6.4.2.1 Load Combination for Verifying Building Drift

Lateral deflections, commonly referred to as drifts, are of concern in serviceability checking arising primarily from the effects of wind. Drift limits in common usage for building design are on the order of 1/600–1/400 of the building or story height. These limits generally are sufficient to minimize damage to cladding and nonstructural walls and partitions. Smaller drift limits may be appropriate if the cladding is brittle. An absolute limit on inter-story drift such as 3/8 in. (10 mm), may also need to be imposed to limit damage to nonstructural partition cladding and glazing. Significantly larger drifts are permissible if special details are provided to accommodate larger deformations. When checking drifts for wind, it should be kept in mind that many components can accept deformations that are significantly larger.

The use of factored wind load in checking serviceability is excessively conservative. The load combination with an annual probability of 0.05 of being exceeded (20 year recurrence interval), which can be used for checking short-term effects, is given in Chapter C, Appendix C of the ASCE 7-05, as follows:

$$D + 0.5L + 0.7W \quad (6.15)$$

Typically, in practice, the lateral deflection of a building due to dead load,  $D$ , and live load,  $L$ , is not considered. Therefore, verifying lateral deflection due to 70% of wind loads calculated by method 2, or by wind tunnel procedure is deemed sufficient for practical purposes.

#### 6.4.3 CAPACITY REDUCTION FACTORS, $\phi$

In concrete buildings, the capacity of a structural element is calculated by applying a strength-reduction factor,  $\phi$ , to the nominal strength of the element. The factor  $\phi$  is intended to take into account the variations in material strength and the uncertainties in the estimation of the nominal member strength, the nature of the expected failure mode, and the importance of a member to the overall safety of the structure.

The values of the strength-reduction factor given in the ACI 318-05 are

- $\phi = 0.90$  for tension-controlled sections (no change from the 1999 edition). This typically results in a 10% reduction in the flexural rebars as compared to designs performed using the ACI 318-99
- $\phi = 0.70$  for spirally reinforced compression members
- $\phi = 0.65$  for other compression-controlled reinforced members
- $\phi = 0.75$  for shear and torsion
- $\phi = 0.65$  for bearing on concrete (except for posttensioned anchorage zones and strut-and-tie models)

$\phi = 0.85$  for posttensioned anchorage zones

$\phi = 0.75$  for strut-and-tie models

For pretensioned members, see ACI Section 9.3.2.7.

However, an exception to the value of  $\phi = 0.75$  in shear design is specified for structures designed in high seismic zones. For shear capacity calculations of structural members other than joints, a value of  $\phi = 0.60$  is to be used when the nominal shear strength of a member is less than the shear corresponding to the development of the nominal flexural strength of the member. For shear in joints and diagonally reinforced coupling beams,  $\phi = 0.85$ . The above exception applies mainly to brittle members such as low-rise walls, portions of walls between openings, or diaphragms that are impractical to reinforce to raise their nominal shear strength above nominal flexural strength for the pertinent loading conditions.

Reference is made in the remainder of this chapter to various equations and sections given in ACI 318.

Unless specifically stated otherwise, it is understood, that these refer to ACI 318-05.

## 6.5 INTERMEDIATE MOMENT-RESISTING FRAMES

### 6.5.1 GENERAL REQUIREMENTS: FRAME BEAMS

The general requirements for frame beams of intermediate moment frames (IMFs) given in ACI 318-05, Sections 21.12.2 and 21.12.3, are as follows:

- Reinforcement details in a frame member shall satisfy the requirements given in Section 21.12.4 if the factored compressive axial load  $\leq A_g f'_c / 10$ .
- If the factored compressive axial load  $> A_g f'_c / 10$ , frame reinforcement details shall satisfy the requirements given in Section 21.12.5, unless the member has spiral reinforcement in accordance with Equation 6.5.
- If a two-way slab system without beam is treated as part of the lateral force-resisting system, reinforcement details in any span-resisting moments caused by lateral forces shall satisfy the requirements given in Section 21.12.6.
- Design shear strength of beams, columns, and two-way slabs resisting earthquake effects shall not be less than either.
- The sum of the shear forces associated with the development of nominal moment strengths of the member at each restrained end of the clear span and the shear force calculated for factored gravity loads.
- The maximum shear force obtained from design load combinations that include earthquake effects, with the shear force from earthquake effects assumed to be twice that prescribed by the governing code for earthquake-resistant design.

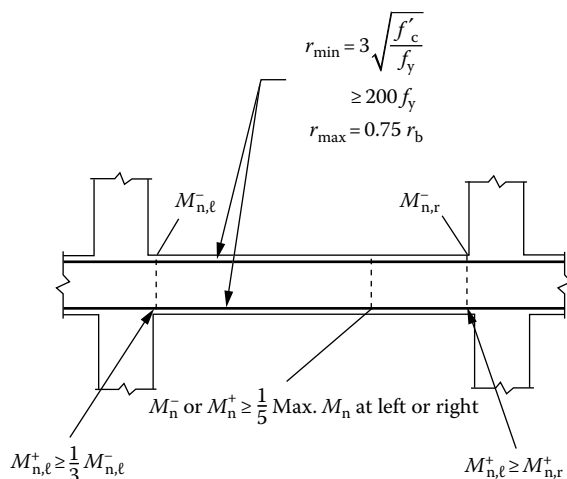
### 6.5.2 FLEXURAL AND TRANSVERSE REINFORCEMENT: FRAME BEAMS

The flexural and transverse reinforcement requirements for frame beams given in Sections 21.12.4.1 through 21.12.4.3 are as follows:

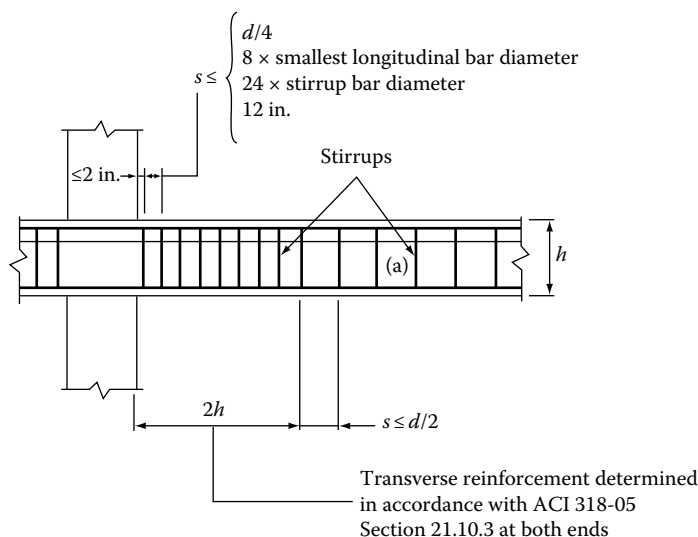
- Positive moment strength at joint face is greater than or equal to one-third negative moment strength provided at that face of the joint.
- Neither the negative nor the positive moment strength at any section along the member length shall be less than one-fifth the maximum moment strength provided at the face of either joint.
- Stirrups shall be provided at both ends of the member over a length equal to  $2h$  from the face of the supporting member toward midspan.

- The first stirrup shall be located not more than 2 in. from the face of the supporting member.
- Maximum stirrup spacing shall not exceed
  - $d/4$
  - $8 \times$  the diameter of the smallest longitudinal bar
  - $24 \times$  the diameter of the stirrup bar
  - 12 in.
- Stirrups shall be spaced at not more than  $d/2$  throughout the length of the member.
- Stirrups shall be spaced at not more than  $d/2$  throughout the length of the member.

Refer to Figures 6.6 and 6.7 for details regarding schematic flexural and transverse reinforcements for frame beams.



**FIGURE 6.6** IMRF: flexural reinforcement requirements for frame beams.



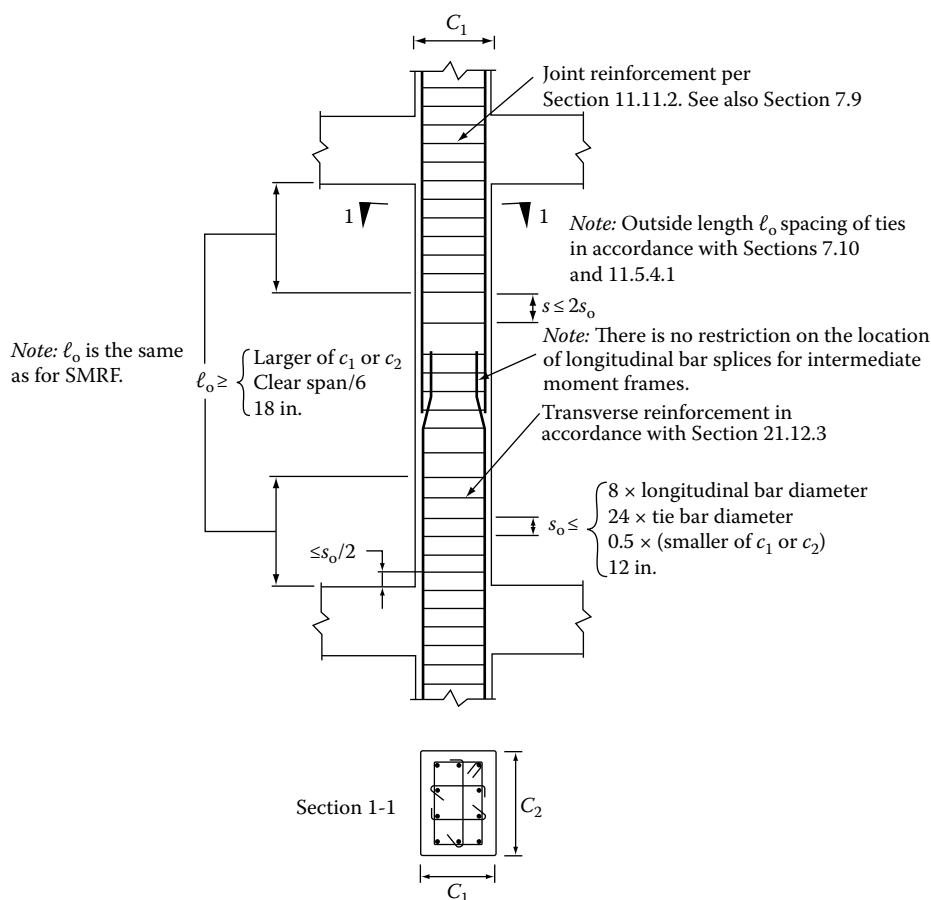
**FIGURE 6.7** IMRF: transverse reinforcement requirements for frame beams.

### 6.5.3 TRANSVERSE REINFORCEMENT: FRAME COLUMNS

The transverse reinforcement requirements for frame columns given in Sections 20.12.5.1 through 20.12.5.4 are as follows:

- Maximum tie spacing shall not exceed  $s_o$  over a length  $\ell_o$  measured from each joint face. Spacing  $s_o$  shall not exceed the smallest of
  - $8 \times$  the diameter of the smallest longitudinal bar
  - $24 \times$  the diameter of the tie bar
  - The minimum member dimension/2
  - 12 in.
- The length  $\ell_o$  shall not be less than the largest of
  - Clear span/6
  - The maximum cross-sectional dimension of member
  - 18 in.
- The first tie shall be located no farther than  $s_o/2$  from the joint face
- Joint reinforcement shall conform to Section 11.11.2
- Tie spacing outside of length  $\ell_o$  shall not exceed  $2s_o$

Figure 6.8 provides a schematic interpretation of these requirements.



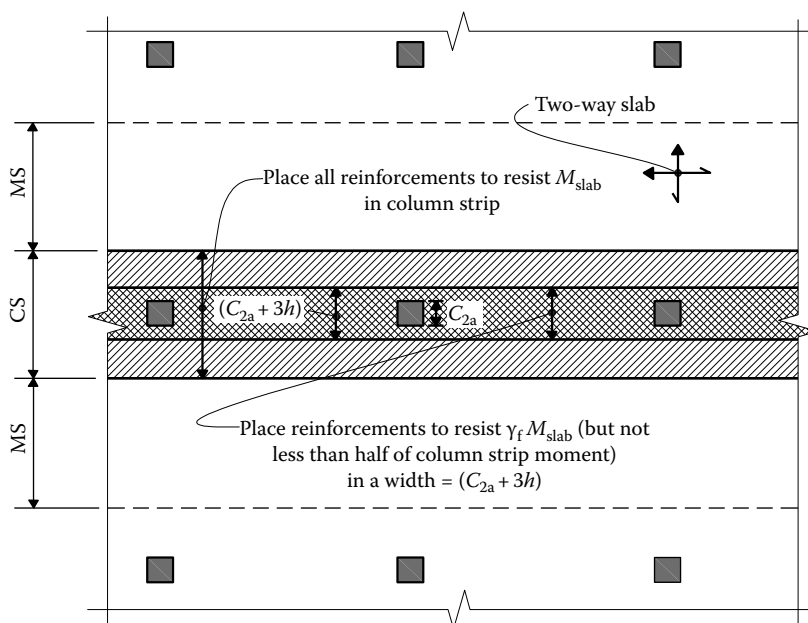
**FIGURE 6.8** IMRF: transverse reinforcement requirements for frame columns.

### 6.5.4 DETAILING REQUIREMENTS FOR TWO-WAY SLAB SYSTEMS WITHOUT BEAMS

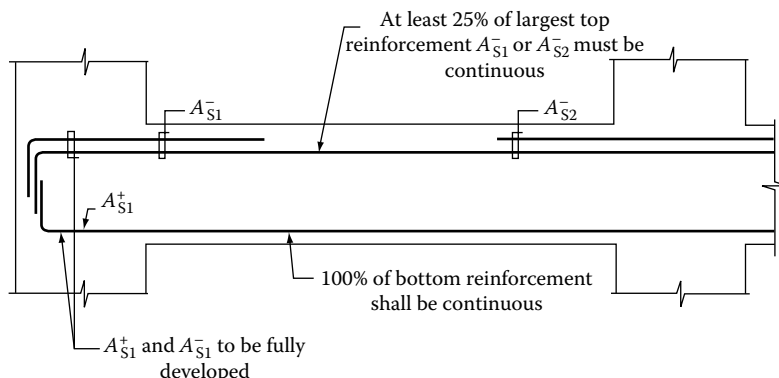
The detailing requirements given in Sections 21.12.6.1 through 21.12.6.7 may be summarized as follows:

- All reinforcements provided to resist  $M_s$  shall be placed within the column strip defined in Section 13.2.1.
- Reinforcements to resist  $\gamma_f M_s$  shall be placed within the effective slab width defined in Section 13.5.3.2.
- Not less than one-half of the column strip reinforcement at the support shall be placed within the effective slab width defined in Section 13.5.3.2.
- Not less than one-quarter of the top reinforcement at the support in the column strip shall be continuous throughout the span.
- All bottom reinforcement in the column strip shall be continuous or spliced with class A splices. At least two of the column strip bottom bars shall pass within the column core and shall be anchored at exterior supports.
- Not less than one-half of all bottom reinforcements at midspan shall be continuous and shall develop its yield strength at the face of the support as defined in Section 13.6.2.5.
- At discontinuous edges of the slab, all top and bottom reinforcements at the support shall be developed at the face of the support as defined in Section 13.6.2.5.

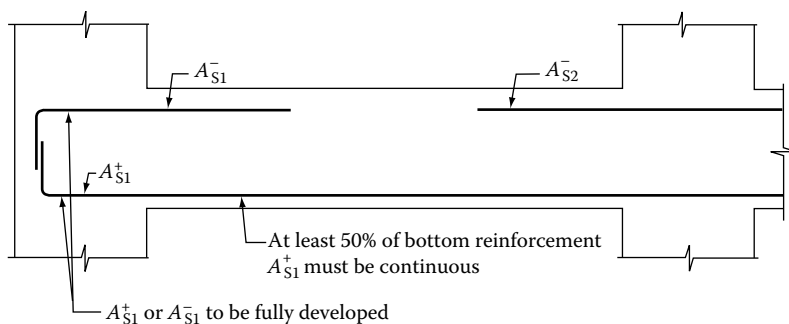
Refer to Figures 6.9 through 6.11 for pictorial representations of these items.



**FIGURE 6.9** Seismic detailing requirements for two-way slabs in areas of moderate seismic risk; flat slab-beams not permitted in UBC zones 3 and 4, or for buildings assigned to SDC C, D, E, or F.



**FIGURE 6.10** Seismic detailing requirements for two-way slabs in areas of moderate seismic risk: column strip.



**FIGURE 6.11** Seismic detailing requirements for two-way slabs in areas of moderate seismic risk: middle strip.

## 6.6 SPECIAL MOMENT-RESISTING FRAMES

### 6.6.1 GENERAL REQUIREMENTS: FRAME BEAMS

The general requirements for the design and detailing of SMRFs given in Sections 21.3.1.1 through 21.3.1.4 are summarized as follows:

- Factored axial compressive forces  $\leq A_g f'_c / 10$
- Clear span  $\geq 4 \times$  effective depth
- Width-to-depth ratio  $\geq 0.3$
- Width  $\geq 10$  in.
- Width  $\leq$  width of supporting member (measured on a plane perpendicular to the longitudinal axis of the flexural member) + distances on each side of the supporting member not exceeding three-fourths of the depth of the flexural member

See Figure 6.12 for schematics of general requirements.



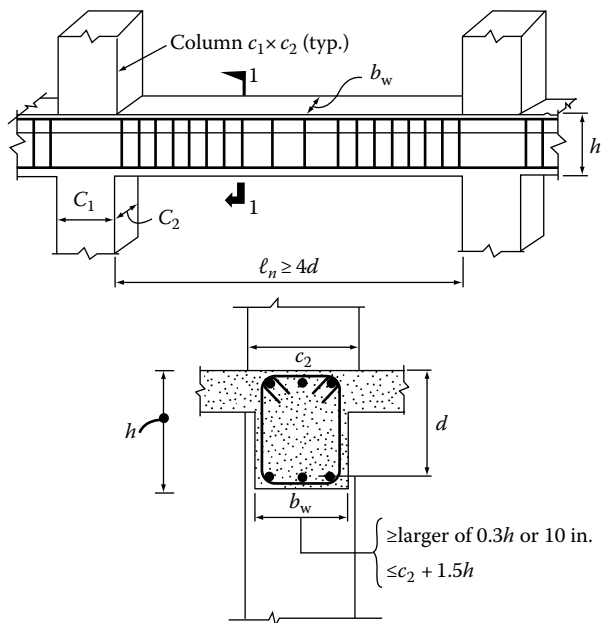


FIGURE 6.12 Frame beam: general requirements, special moment frame.

### 6.6.2 FLEXURAL REINFORCEMENT: FRAME BEAMS

The requirement for flexural reinforcement, referring to the width limitation, effectively eliminates the use of flat slabs as frame beams in areas of high seismicity or for buildings assigned to SDC D, E, or F.

Structural requirements for flexural reinforcements and their splices given in Sections 21.3.2.1 through 21.3.2.4 for frame beams are as follows:

- Minimum reinforcement shall not be less than

$$\frac{3\sqrt{f'_c}}{f_y} \times b_w d \quad \text{and} \quad \frac{200b_w d}{f_y} \quad (6.16)$$

at any section, top or bottom, unless provisions of Section 10.5.3 are satisfied.

- The reinforcement ratio,  $\rho$ , shall not exceed 0.025.
- At least two bars must be provided continuously at both the top and the bottom of the section.
- Positive moment strength at joint face shall be greater than one-half the negative moment strength provided at the face of the joint.
- Neither the negative nor the positive moment strength at any section along the member length shall be less than one-quarter the maximum moment strength provided at the face of either joint.
- Lap splices of flexural reinforcement are permitted only if hoop or spiral reinforcements are provided over the lap length. Hoop and spiral reinforcement spacing shall not exceed
  - $d/4$ .
  - 4 in.
- Lap splices are not permitted.
  - Within joints.
  - Within a distance of  $2h$  from the face of the joint.

- At locations where analysis indicates flexural yielding caused by inelastic lateral displacement of the frame.
- Mechanical splices shall conform to Section 21.2.6 and welded splices shall conform to Section 21.2.7.1.

### 6.6.3 TRANSVERSE REINFORCEMENT: FRAME BEAMS

The requirements for transverse reinforcement (hoops and stirrups) in frame beams given in Sections 21.3.3.1 through 21.3.3.6 and Section 21.3.4 are summarized as follows:

- Hoops are required in the following regions of framed members:
  - Over a length equal to  $2h$  from the face of the supporting member toward midspan at both ends of the flexural member.
  - Over lengths equal to  $2h$  on both sides of the section where flexural yielding may occur in connection with inelastic lateral displacements of the frame.
- Where hoops are required, the spacing shall not exceed
  - $d/4$ .
  - $8 \times$  the diameter of the smallest longitudinal bar.
  - $24 \times$  the diameter of hoop bars.
  - 12 in.
- The first hoop shall be located not more than 2 in. from the face of the supporting member.
- Where hoops are required, longitudinal bars on the perimeter shall have lateral support conforming to Section 7.10.5.3.
- Where hoops are not required, stirrups with seismic hooks at both ends shall be spaced at a distance not more than  $d/2$  throughout the length of the member.
- Stirrups or ties required to resist shear shall be hoops over lengths of members in Sections 21.3.3., 21.4.4, and 21.5.2.
- Hoops in flexural members shall be permitted to be made up of two pieces of reinforcement: a stirrup having seismic hooks at both ends and closed by a crosstie. Consecutive crossties engaging the same longitudinal bar shall have their  $90^\circ$  hooks at opposite sides of the flexural member. If the longitudinal bars secured by the crossties are confined by a slab on only one side of the flexural frame member, the  $90^\circ$  hooks of the crossties shall be placed on that side.
- Transverse reinforcement must also be proportioned to resist the design shear forces.

Figures 6.13 and 6.14 show transverse reinforcement schematics for frame beams.

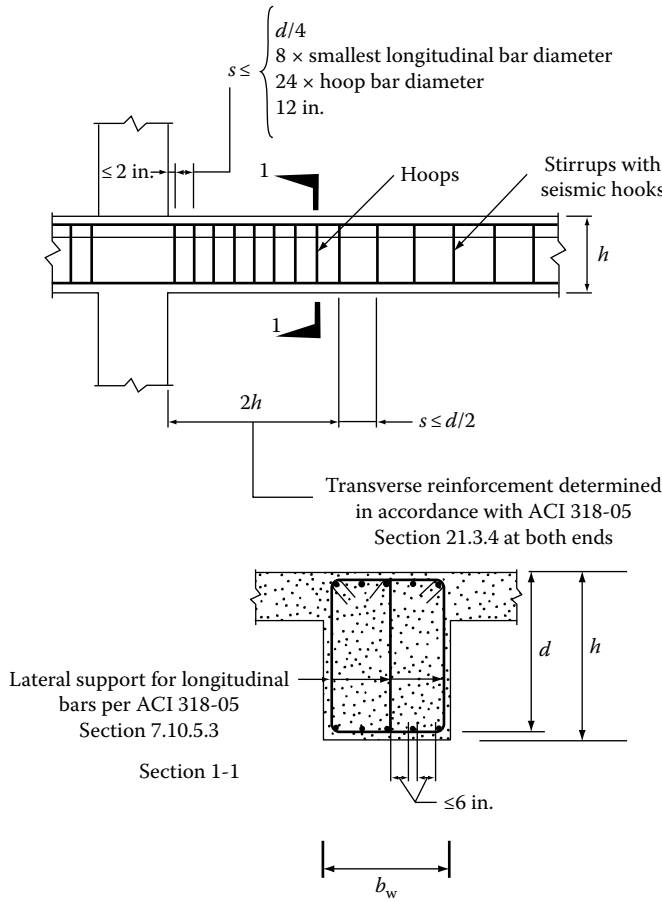
### 6.6.4 GENERAL REQUIREMENTS: FRAME COLUMNS

The requirements given in Section 21.4 are summarized as follows:

- Factored axial compressive force  $> A_g f'_c / 10$ .
- Shortest cross-sectional dimension measured on a straight line passing through the geometric centroid  $\geq 12$  in.
- Ratio of the shortest cross-sectional dimension to the perpendicular dimension  $\geq 0.4$ .

### 6.6.5 FLEXURAL REINFORCEMENT: FRAME COLUMNS

Refer to Figures 6.15 and 6.16 for schematic details and minimum requirements of transverse reinforcement.



**FIGURE 6.13** Frame beam: transverse reinforcement requirements, special moment frame.

- The flexural strengths of columns shall satisfy the following:

$$\sum M_c \geq (6/5) \sum M_g \quad (6.17)$$

where

$\sum M_c$  is the sum of moments at the faces of the joint, corresponding to the nominal flexural strength of the columns framing into that joint. Column flexural strength shall be calculated for the factored axial force, consistent with the direction of the lateral forces considered, resulting in the lowest flexural strength.

$\sum M_g$  is the sum of moments at the faces of the joint, corresponding to the nominal flexural strength of the girders framing into that joint. In T-beam construction, slab reinforcement within an effective slab width defined in Section 8.10 shall contribute to flexural strength.

- If Equation 21.1 is not satisfied, the lateral strength and stiffness of the columns shall not be considered when determining the strength and stiffness of the structure, and the columns shall conform to Section 21.11. Also, the columns must have transverse reinforcement over their full height as specified in Sections 21.4.4.1 through 21.4.4.3.
- The reinforcement ratio  $\rho_g$  shall not be less than 0.01 and shall not exceed 0.06.

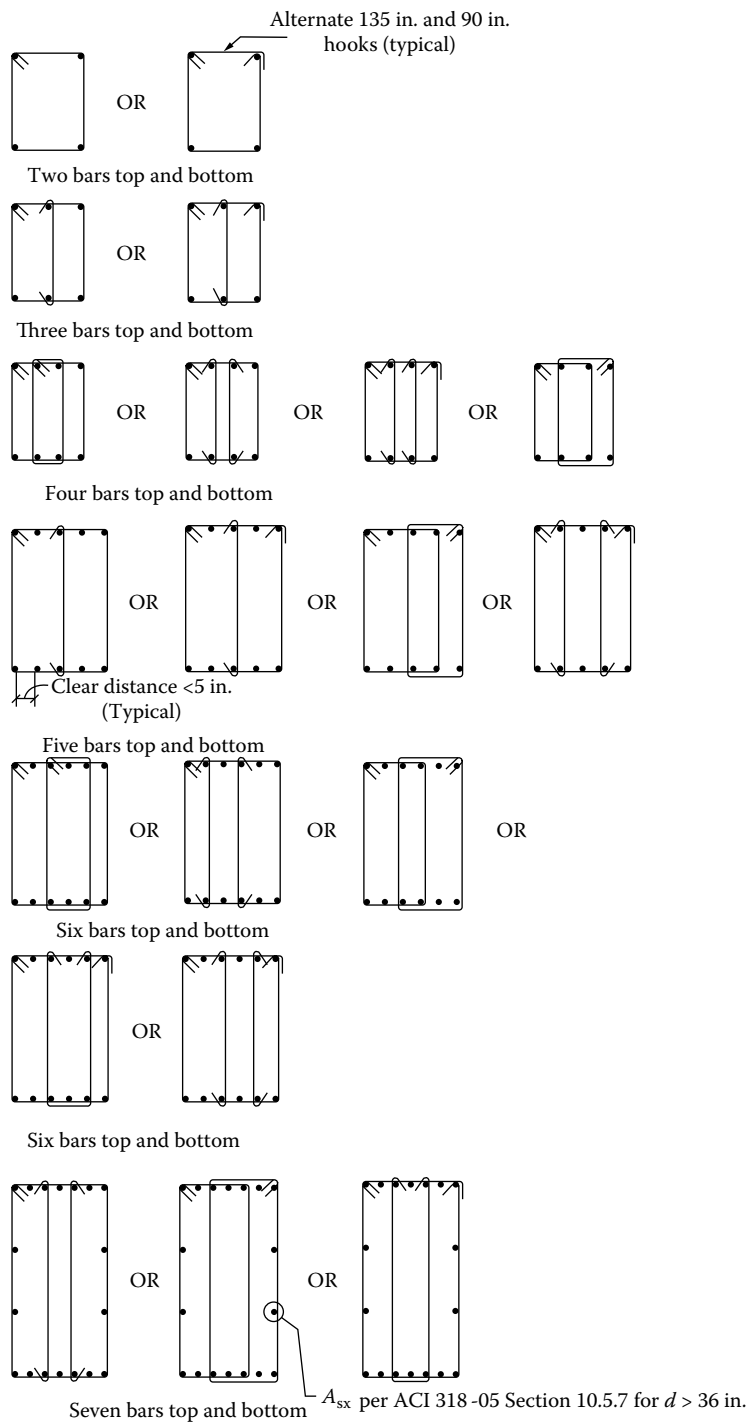


FIGURE 6.14 Arrangement of hoops and cross-ties: frame beams; special moment frame.

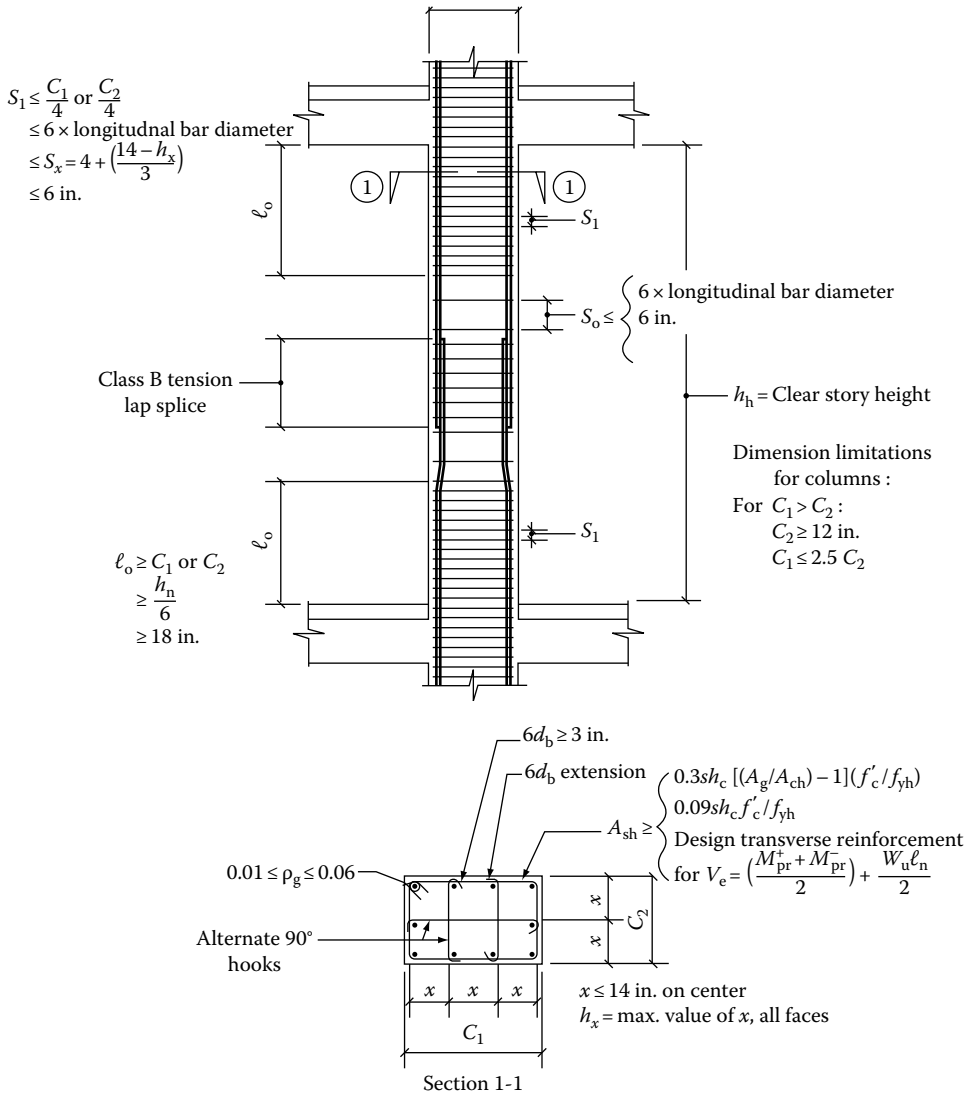
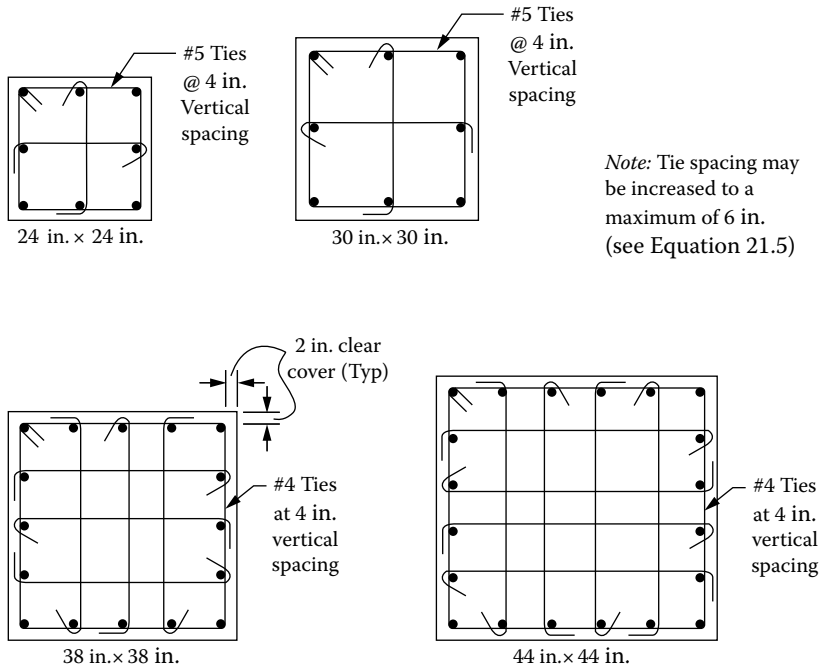


FIGURE 6.15 Frame column: detailing requirements, special moment frame.

- Mechanical splices shall conform to Section 21.2.6 and welded splices shall conform to Section 21.2.7.1. Lap splices are permitted only within the center half of the member length, must be tension lap splices, and shall be enclosed within transverse reinforcement conforming to Sections 21.4.4.2 and 21.4.4.3.

### 6.6.6 TRANSVERSE REINFORCEMENT: FRAME COLUMNS

- The transverse reinforcement requirements discussed in the following need to be provided only over a length  $\ell_o$  from each joint face and on both sides of any section where flexural yielding is likely to occur. The length  $\ell_o$  shall not be less than
  - The depth of member at joint face or at section where flexural yielding is likely to occur.
  - Clear span/6.
  - 18 in.



**FIGURE 6.16** Examples of minimum transverse reinforcement in frame columns of SMRF. *Note:*  $f'_c = 5$  ksi,  $f_y = 60$  ksi. Vertical spacing of ties = 4 in. Ties #5 for 24 in. × 24 in. and 30 in. × 30 in. columns. #4 for 38 in. × 38 in. and 44 in. × 44 in. columns.

- Ratio of spiral or circular hoop reinforcement  $\rho_s$  shall not be less than that given by

$$\rho_s = 0.12 \frac{f'_c}{f_{yh}} \geq 0.45 \left( \frac{A_g}{A_c} - 1 \right) \frac{f'_c}{f_{yh}}. \quad (6.18)$$

- Total cross-sectional area of rectangular hoop reinforcement for confinement  $A_{sh}$  shall not be less than that given by the following two equations:

$$A_{sh} = 0.3(s h_c f'_c / f_{yh}) [(A_g / A_{ch}) - 1], \quad (6.19)$$

$$A_{sh} = 0.09 s h_c f'_c / f_{yh}. \quad (6.20)$$

- Transverse reinforcement shall be provided by either single or overlapping hoops. Crossties of the same bar size and spacing as the hoops are permitted, with each end of the crosstie engaging a peripheral longitudinal reinforcing bar. Consecutive crossties shall be alternated end for end along the longitudinal reinforcement.
- Equations 21.3 and 10.6 need not be satisfied if the design strength of the member core satisfies the requirement of the design loading combinations, including the earthquake effects.

If the thickness of the concrete outside of the confining transverse reinforcement is greater than 4 in., additional transverse reinforcement shall be provided at a spacing of less than or equal to 12 in. Concrete cover on the additional reinforcement is less than or equal to 4 in.

- Transverse reinforcement shall be space at distances not exceeding
  - The minimum member dimension/4
  - $6 \times$  the longitudinal bar diameter
  - $s_x$

where  $4 \text{ in.} \leq s_x = 4 + 14 - h x / 3 \leq 6 \text{ in.}$

- Crossties or legs of overlapping hoops shall not be spaced more than 14 in. on center in the direction perpendicular to the longitudinal axis of the structural member. Vertical bars shall not be farther than 6 in. clear from a laterally supported bar.

Where transverse reinforcement as required in Sections 21.4.4.1 through 21.4.4.3 is no longer required, the remainder of the column shall contain spiral or hoop reinforcements spaced at distances that shall not exceed

- $6 \times$  the longitudinal bar diameter.
- 6 in.
- Transverse reinforcement must also be proportioned to resist the design shear forces.
- Columns supporting reactions from discounted stiff members, such as walls, shall have transverse reinforcements as specified in Sections 21.4.4.1 through 21.4.4.3 over their full height, if the factored axial compressive force related to earthquake effects is greater than  $A_g f'_c / 10$ . This transverse reinforcement shall extend into the discounted member for at least the development length of the largest longitudinal reinforcement in the column in accordance with Section 21.5.4.
- If the lower end of the column terminates on a wall, transverse reinforcement per Sections 21.4.4.1 through 21.4.4.3 shall extend into the wall for at least the development length of the largest longitudinal bar in the column at the point of termination.
- If the column terminates on a footing or mat, transverse reinforcement per Sections 21.4.4.1 through 21.4.4.3 shall extend at least 12 in. into the footing or mat.

Schematic details of reinforcement for ductile frames are shown in Figure 6.17.

### 6.6.7 TRANSVERSE REINFORCEMENT: JOINTS

The transverse reinforcement requirements for joints of SMRFs given in Sections 21.5.2.1 through 21.5.2.3 are as follows:

- Transverse hoop reinforcement required for column ends per Section 21.4.4 shall be provided within a joint, unless structural members confine the joint as specified in Section 21.5.2.2.
- Where members frame into all four sides of a joint and each member width is at least three-fourth the column width, the transverse reinforcement within the depth of the shallowest member may be reduced to one-half of the amount required per Section 21.4.4.1. The spacing of the transverse reinforcement required in Section 21.4.4.2(b) shall not exceed 6 in. at these locations.
- Transverse reinforcement per Section 21.4.4 shall be provided through the joint to confine longitudinal beam reinforcements outside the column core if a beam framing into the joint does not provide such confinement.

### 6.6.8 SHEAR STRENGTH OF JOINT

The shear strength requirements for joints in SMRFs given in Sections 21.5.3.1 and 21.5.3.2, are summarized as follows:

- For normal weight concrete, the nominal shear strength of the joint shall not exceed the following forces:
  - For joints confined on all four faces  $20\sqrt{f'_c} A_j$
  - For joints confined on three faces or on two opposite faces  $15\sqrt{f'_c} A_j$
  - For other joints  $12\sqrt{f'_c} A_j$

where  $A_j$  is the effective cross-sectional area within a joint in a plane parallel to the plane of the reinforcement generating shear in the joint. The overall depth shall be the overall depth

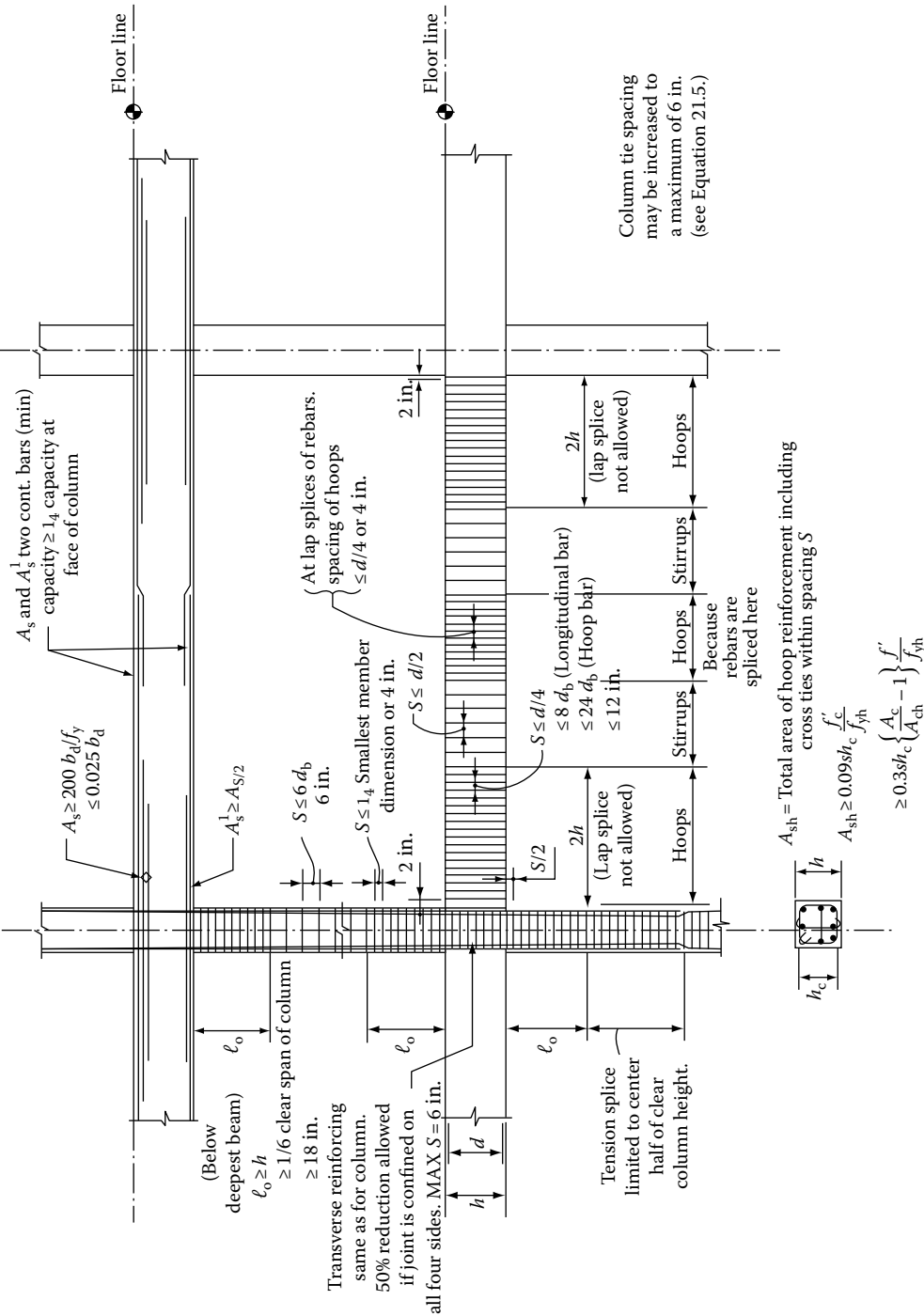


FIGURE 6.17 Ductile frame, SMRF: schematic reinforcement detail.



of the column. Where a beam frames into a support of larger width, the effective width of the joint shall not exceed the smaller of

1. Beam width plus the joint depth.
  2. Twice the smaller perpendicular distance from the longitudinal axis of the beam to the column side.
- A joint is considered confined if the confining members frame into all faces of the joint. A member is considered to provide confinement at the joint if the framing member covers at least three-fourth of the joint face.
  - For lightweight aggregate concrete, the nominal shear strength of the joint shall not exceed three-fourth of the limits given in Section 21.5.3.1.

### 6.6.9 DEVELOPMENT OF BARS IN TENSION

The criteria for the development of bars in tension are given in Sections 21.5.4.1 through 21.5.4.4 and are as follows:

- For normal weight concrete, the development length  $\ell_{dh}$  for a bar with a standard 90° degree hook shall not be less than the largest of
  - $8 \times$  the diameter of the bar
  - 6 in.
  - $f_y d_b / (65 \sqrt{f'_c})$

For bar sizes No. 3 through No. 11. The 90° hook shall be located within the confined core of a column or boundary element.

- For lightweight aggregate concrete, the development length  $\ell_{dh}$  for a bar with a standard 90° hook shall not be less than the largest of
  - $10 \times$  the diameter of the bar
  - 7.5 in.
  - $1.25 f_y d_b / (65 \sqrt{f'_c})$

For bar sizes No. 3 through No. 11. The 90° hook shall be located within the confined core of a column or boundary element.

- For bar sizes No. 3 through No. 11, the development length  $\ell_d$  for a straight bar shall not be less than
  - $2.5 \ell_{dh}$  if the depth of the concrete cast in one lift beneath the bar  $\leq 12$  in.
  - $3.5 \ell_{dh}$  if the depth of the concrete cast in one lift beneath the bar  $> 12$  in.
- Straight bars terminated at a joint shall pass through the confined core of a column or boundary element. Any portion of the straight embedment length column or boundary element. Any portion of the straight embedment length not within the confined core shall be increased by a factor of 1.6.
- For epoxy-coated reinforcement, the development lengths in Sections 21.05.4.1 through 21.5.4.3 shall be multiplied by
  - 1.5 for straight bars with cover less than  $3d_b$  or clear spacing less than  $6d_b$ .
  - 1.2 for all other straight bars.
  - 1.2 for bars terminating in a standard hook.

## 6.7 SHEAR WALLS

### 6.7.1 MINIMUM WEB REINFORCEMENT: DESIGN FOR SHEAR

The requirements for minimum web reinforcement and design for shear strength of shear walls are given in Sections 21.7.2.1 through 21.7.4.5 and are summarized as follows:

- The required amounts of vertical and horizontal web reinforcement depend on the magnitude of the design shear force  $V_u$ :

- For  $V_u \leq A_{cv}\sqrt{f'_c}$  :

Vertical reinforcement ratio  $\geq 0.0012$  for No. 5 bars or smaller

$\geq 0.0015$  for No. 6 bars or larger

Horizontal reinforcement ratio  $\geq 0.0020$  for No. 5 bars or s

$\geq 0.0025$  for No. 6 bars or larger.

- For  $V_u \leq A_{cv}\sqrt{f'_c}$  :  
 $\rho_v \geq 0.0025$   
 $\rho_n \geq 0.0025$ .
- Reinforcement spacing each way shall not exceed 18 in.
- Reinforcement provided for shear strength shall be continuous and shall be distributed across the shear plane.
- For  $V_u \leq A_{cv}\sqrt{f'_c}$ , two curtains of reinforcement must be provided.
- All continuous reinforcement in structural walls shall be anchored or spliced in accordance with the provisions for reinforcement in tension in Section 21.5.4.
- The nominal shear strength  $V_n$  of structural walls shall not exceed

$$V_n = A_{cv}(\alpha_c\sqrt{f'_c} + \rho_n f_y) \quad (6.21)$$

where

$$\alpha_c = 3.0 \text{ for } h_w/l_w \leq 1.5$$

$$= 2.0 \text{ for } h_w/l_w \geq 2.0$$

$\alpha_c$  varies linearly between 3.0 and 2.0 for  $h_w/l_w$  between 1.5 and 2.0.

- The value of  $h_w/l_w$  used for determining  $V_n$  for segments of a wall shall be the larger of the ratios for the entire wall and the segment of wall considered.
- Walls shall have distributed shear reinforcement in two orthogonal directions in the plane of the wall, if  $h_w/l_w \leq 2.0$ ,  $\rho_v \geq \rho_n$ .
- Nominal shear strength of all wall piers sharing a common lateral force shall not be assumed to exceed  $8A_{cv}\sqrt{f'_c}$ , where  $A_{cv}$  is the total cross-sectional area, and the nominal shear strength of any one of the individual wall piers shall not be assumed to exceed  $10A_{cp}\sqrt{f'_c}$ , where  $A_{cp}$  is the cross-sectional area of the pier considered.
- Nominal shear strength of horizontal wall segments and coupling beams shall be assumed not to exceed  $10A_{cp}\sqrt{f'_c}$ , where  $A_{cp}$  is the cross-sectional area of a horizontal wall segment or coupling beam.

## 6.7.2 BOUNDARY ELEMENTS

The boundary element requirements for shear walls given in Sections 21.7.6.2 through 21.7.6.4 are as follows:

- Compression zones of walls or wall piers that are effectively continuous over their entire height and designed to have a single critical section for flexure and axial loads shall be reinforced with special boundary elements

$$c \geq l_w/600(\delta_u/h_w) \quad (6.22)$$

where  $\delta_u/h_w \geq 0.007$ .

- Special boundary element reinforcement shall extend vertically from the critical section a distance not less than the larger of  $l_w$  or  $M_u/4V_u$ .
- Structural walls not designed by the provisions of Section 21.7.6.2 shall have special boundary elements at boundaries and around openings of structural walls where the maximum extreme fiber compressive stress, corresponding to factored forces including earthquake effects, exceeds  $0.2f'_c$ .
- Special boundary elements may be discontinued where the calculated compressive strength is less than  $0.15f'_c$ .
- Stresses shall be calculated using a linearly elastic model and gross-section properties.
- Where special boundary elements are required per Sections 21.7.6.2 or 21.7.6.3, the following shall be satisfied:
  - The boundary element shall extend horizontally from the extreme compression fiber a distance not less than the larger of  $c - 0.1l_w$  and  $c/2$ .
  - In flanged sections, the boundary element shall include the effective flange width in compression and shall extend at least 12 in. into the web.
  - Special boundary element transverse reinforcement shall satisfy the requirements given in Sections 21.4.4.1 through 21.4.4.3; Equation 21.3 alone need not be satisfied.
  - Special boundary element transverse reinforcement at the base of the wall shall extend into the support at least the development length of the largest longitudinal bar in the special boundary element. If the special boundary element terminates on a footing or mat, the special boundary element transverse reinforcement shall extend at least 12 in. into the footing or mat.
  - Horizontal reinforcement in the web shall be anchored to develop the specified yield strength,  $f_y$ , within the confined core of the boundary element.
  - Mechanical splices and welded splices of longitudinal reinforcement of boundary elements shall conform to Sections 21.2.6 and 21.2.7, respectively.

Although boundary elements may not be required by calculations, Section 21.6.6.5 stipulates certain requirements as follows:

- Where special boundary elements are not required per Sections 21.7.6.2 or 21.7.6.3, the following shall be satisfied:
  - Boundary transverse reinforcement shall satisfy the requirements given in Sections 21.4.4.1(c), 21.4.4.3, and 21.7.6.4(c) if the longitudinal reinforcement ratio at the wall boundary is greater than  $400/f_y$ . The maximum longitudinal spacing of transverse reinforcement in the boundary shall not exceed 8 in.
  - Horizontal wall reinforcement terminating at the ends of structural walls without boundary elements shall have a standard hook engaging in U-stirrups having the same size and spacing as, and spliced to, the horizontal reinforcement when  $V_u \geq A_{cv}\sqrt{f'_c}$ .

### 6.7.3 COUPLING BEAMS

The design requirements for coupling beams given in Sections 21.7.7.1 through 21.7.7.4 are as follows:

- Coupling beams with aspect ratio  $l_n/d \geq 4$  shall satisfy the requirements of Equation 21.3, except the provisions of Sections 21.3.1.3 and 21.3.1.4 (a) shall not be required if it can be shown by analysis that the beam has adequate lateral stability.
- Coupling beams with aspect ratio  $l_n/d \geq 4$  shall be permitted to be reinforced with two intersecting groups of diagonally placed bars symmetrical about the midspan.

- Coupling beams with aspect ratio  $l_n/d \geq 2$  and  $V_u > 4\sqrt{f'_c} b_w d$  shall be reinforced with two intersecting groups of diagonally placed bars symmetrical about the midspan, unless it can be shown that loss of stiffness and strength of the coupling beams will not impair the vertical load carrying capacity of the structure, or the egress from the structure, or the integrity of nonstructural components and their connections to the structure.
- Coupling beams reinforced with two intersecting groups of diagonally placed bars symmetrical about the midspan shall satisfy the following:
  - A minimum of four bars is required in each group of diagonally placed bars. Each diagonal group of bars is assembled in a core having sides measured to the outside of transverse reinforcement greater than or equal to  $b_w/2$  perpendicular to the plan of the beam and  $b_w/5$  in the plane of the beam and perpendicular to the diagonal bars.
  - The nominal shear strength  $V_n$  is determined from the following:

$$V_n = 2A_{vd}f_y \sin \alpha \leq 10\sqrt{f'_c} b_w d$$

- Each group of diagonally reinforced bars shall be enclosed in transverse reinforcement satisfying the requirements given in Sections 21.4.4.1 through 21.4.4.3. The minimum concrete cover required in Section 7.7 shall be assumed on all four sides of each group of diagonally placed reinforcing bars for purposes of computing  $A_g$  in Equations 10.6 and 21.3.
- The diagonally placed bars shall be developed for tension in the wall.
- The diagonally placed bars shall be considered to contribute to the nominal flexural strength of the coupling beam.
- Reinforcement conforming to Sections 11.8.9 and 11.8.10 shall be provided as a minimum parallel and transverse to the longitudinal axis of the beam.

## 6.8 FRAME MEMBERS NOT DESIGNED TO RESIST EARTHQUAKE FORCES

Detailing requirements for frame members not designed to resist earthquake forces are given in Sections 21.11.2 and 21.11.3. The requirements given in Section 21.11.2 are for frame members expected to experience only moderate excursions into inelastic range during design earthquake motions. Those given in Section 21.11.3 are for members expected to experience nearly the same magnitude of inelastic deformations as members designed to resist earthquake motions. If  $M_u \leq \phi M_n$  and  $V_u \leq \phi V_n$ , the members are designed according to Section 21.11.2 (Case 1). If  $M_u \geq \phi M_n$  and  $V_u \geq \phi_2 V_n$ , the detailing requirements are more stringent, that is, nearly the same as those specified for members proportioned to resist forces induced by earthquake motions (Case 2).

Case 1:  $M_u \leq \phi M_n$  and  $V_u \leq \phi V_n$

- Factored gravity axial force  $\leq A_g f'_c / 10$ .
  - Satisfy detailing requirements given in Section 21.3.2.1.
  - Provide stirrups spaced not more than  $d/2$  throughout the length of the member.
- Factored gravity axial force  $> A_g f'_c / 10$ .
  - Satisfy detailing requirements given in Sections 21.4.3, 21.4.4.1(c), 21.4.4.3 and 21.4.5.
  - Maximum longitudinal spacing of ties shall be  $s_o$  for the full column height.
  - Spacing  $s_o$  shall not be more than the smaller of six diameters of the smallest longitudinal bar enclosed or 6 in.
- Factored gravity axial force  $> 0.35P_o$ .
  - Satisfy detailing requirements given in Section 21.11.2.2.
  - Provide transverse reinforcement  $\geq$  one-half of that required per Section 21.4.4.1.
  - Maximum longitudinal spacing of ties shall be  $s_o$  for the full column height.
  - Spacing  $s_o$  shall not be more than the smaller of six diameters of the smallest longitudinal bar or 6 in.

Case 2:  $M_u \geq \phi M_n$  or  $V_u \geq \phi_2 V_n$  or induced moments not calculated:

- Materials shall satisfy the requirements given in Sections 21.2.4 and 21.2.5. Mechanical and welded splices shall satisfy the requirements given in Sections 21.2.6 and 21.2.7.1, respectively.
- Factored gravity axial force  $\leq A_g f'_c / 10$ .
  - Satisfy detailing requirements given in Sections 21.3.2.1 and 21.3.4.
  - Provide stirrups spaced not more than  $d/2$  throughout the length of the member.
- Factored gravity axial force  $> A_g f'_c / 10$ .
  - Satisfy detailing requirements given in Sections 21.4.4., 21.4.5, and 21.5.2.1.

## 6.9 DIAPHRAGMS

### 6.9.1 MINIMUM THICKNESS AND REINFORCEMENT

The minimum thickness and reinforcement requirements for diaphragms as given in Sections 21.9.4 and in 21.9.5.1 through 21.9.5.5 are as follows:

- Concrete slabs and composite topping slabs serving as structural diaphragms to transmit earthquake forces shall not be less than 2 in. thick.
- Topping slabs over precast floor or roof elements, acting as structural diaphragms and not relying on composite action with the precast elements to resist earthquake forces, shall not be less than 2 1/2 in. thick.
- For structural diaphragms:
  - Minimum reinforcement shall be in conformance with Section 7.12.
  - Spacing of nonprestressed reinforcement shall not exceed 18 in.
  - Where welded wire fabric is utilized to resist shear forces in topping slabs over precast floor and roof elements, the wires parallel to the span of the precast elements shall be spaced not less than 10 in. center.
  - Reinforcement provided for shear strength shall be continuous and shall be distributed uniformly across the shear plane.
  - In diaphragm chords or collectors utilizing bonded prestressing tendons as primary reinforcement, the stress due to design seismic forces shall not exceed 60,000 psi.
  - Precompression from unbonded tendons shall be permitted to resist diaphragm design forces if a complete load path is provided.
- Structural truss elements, struts, ties, diaphragm chords, and collector elements shall have transverse reinforcement in accordance with Sections 21.4.4.1 through 21.4.4.3 over the length of the element where compressive stresses exceed  $0.2f'_c$ . Special transverse reinforcement may be discontinued where the compressive stress is less than  $0.15f'_c$ . Stresses shall be calculated for the factored forces using a linearly elastic model and gross-section properties.
- All continuous reinforcement in diaphragms, trusses, struts, ties, chords, and collector elements shall be anchored or spliced in accordance with the provisions for reinforcement in tension as specified in Section 21.5.4.
- Type 2 splices are required where mechanical splices are used to transfer forces between the diaphragm and the vertical components of the lateral force-resisting system.

### 6.9.2 SHEAR STRENGTH

The shear strength requirements for diaphragms given in Section 21.9 are summarized as follows:

- Nominal shear strength  $V_n$  of structural diaphragms shall not exceed

$$V_n = A_{cv}(2\sqrt{f'_c} + \rho_n f_y). \quad (6.23)$$

- The nominal shear strength of cast-in-place composite-topping slab diaphragms and cast-in-place noncomposite-topping slab diaphragms on a precast floor or roof shall not exceed

$$V_n = A_{cv}\rho_n f_y \quad (6.24)$$

where  $A_{cv}$  is based on the thickness of the topping slab. The required web reinforcement shall be distributed uniformly in both directions.

- Nominal shear strength shall not exceed  $8A_{cv}\sqrt{f'_c}$ , where  $A_{cv}$  is the gross cross-sectional area of the diaphragm.

### 6.9.3 BOUNDARY ELEMENTS

A summary of boundary element requirements for diaphragms given in Sections 21.9.8.1 through 21.9.8.3 are given as follows:

- Boundary elements of structural diaphragms shall be proportioned to resist the sum of the factored axial forces acting in the plane of the diaphragm and the force obtained by dividing the factored moment at the section by the distance between the boundary elements of the diaphragm at the section.
- Splices of tensile reinforcement in chords and collector elements of diaphragms shall develop the specified yield strength,  $f_y$  of the reinforcement. Mechanical and welded splices shall conform to Sections 21.2.6 and 21.2.7, respectively.
- Reinforcement for chords and collectors at splices and anchorage zones shall have either of the two following requirements:
  - A minimum spacing of 3 longitudinal bar diameters, but not less than 1½ in., and a minimum concrete cover of 2½ longitudinal bar diameters, but not less than 2 in.
  - Transverse reinforcement per Section 11.5.5.3, except as required in Section 21.9.5.3.

## 6.10 FOUNDATIONS

### 6.10.1 FOOTINGS, MATS, AND PILES

The structural requirements for footings, foundation mats, and piles are given in Sections 21.10.2.1 through 21.10.2.5 and in Section 22.10. They are summarized as follows:

- Longitudinal reinforcement of columns and structural walls resisting earthquake-induced forces shall extend into the footing, mat, or pile cap, and shall be fully developed for tension at the interface.
- Columns designed assuming fixed end conditions at the foundation shall comply with Section 21.10.2.1.
- If longitudinal reinforcement of a column requires hooks, the hooks shall have a 90° bend and shall be located near the bottom of the foundation with the free end of the bars oriented toward the center of the column.
- Transverse reinforcement in accordance with Section 21.4.4 shall be provided below the top of a footing when columns or boundary elements of special reinforced concrete structural walls have an edge located within one-half the footing depth from an edge of a footing. The transverse reinforcement shall extend into the footing a distance greater than or equal to the smaller of
  - The depth of the footing, mat, or pile cap.
  - The development length in tension of the longitudinal reinforcement.

- The flexural reinforcement shall be provided in the top of a footing, mat, or pile cap supporting columns or boundary elements of special reinforced concrete structural walls subjected to uplift forces from earthquake effects. Flexural reinforcement shall not be less than that required per Section 10.5.
- The use of structural plain concrete in footings and basement walls is prohibited, except for specific cases cited in Section 22.10.

### 6.10.2 GRADE BEAMS AND SLABS-ON-GRADE

The requirements for grade beams and slabs-on-grade given in Sections 21.10.3.1 through 21.10.3.4 are summarized as follows:

- Grade beams acting as horizontal ties between pile caps or footings shall have continuous longitudinal reinforcement that shall be developed within or beyond the supported column. At all discontinuities, the longitudinal reinforcement must be anchored within the pile cap or footing.
- Grade beams acting as horizontal ties between pile caps or footings shall be proportioned such that the smallest cross-section dimension is greater than or equal to the clear spacing between connected columns divided by 20, but need not be greater than 18 in.
- Closed ties shall be provided at a spacing that shall not exceed the lesser of one-half the smallest orthogonal cross-section dimension or 12 in.
- Grade beams and beams that are part of the lateral-force-resisting system shall conform to Section 21.3.
- Slabs-on-grade that resist seismic forces from columns or walls that are part of the lateral-force-resisting system shall be designed as structural diaphragms per Section 21.9.
- The design drawings shall clearly state that the slab-on-grade is a structural diaphragm and is part of the lateral-force-resisting system.

### 6.10.3 PILES, PIERS, AND CAISSONS

The requirements for piles, piers, and caissons are given in Sections 21.10.4.2 through 21.10.4.7. They are summarized as follows:

- Piles, piers, and caissons resisting tension loads shall have continuous longitudinal reinforcement over the length resisting the design tension forces. The longitudinal reinforcement shall be detailed to transfer tensile forces between the pile cap and the supported structural members.

## 6.11 DESIGN EXAMPLES

Several design examples are given in the following sections to explain the provisions of the ACI 318-05. The examples range from ordinary moment-resisting frames (OMRFs, sometimes referred to as non-seismic frames) to coupled shear walls with diagonal beams, applicable to designs in high seismic zones.

An attempt is made to keep the numerical work simple. For example, the tension-controlled flexural reinforcement,  $A_s$ , is calculated by using the relation.

$$A_s = \frac{M_u}{a_u d}$$

with  $a_u$  typically taken at 4.0 or 4.1, for  $f'_c = 4000$  psi and  $f_y = 60,000$  psi. Other similar shortcuts are used throughout. The designer is referred to standard reinforced concrete design handbooks for more precise design calculations.

### 6.11.1 FRAME BEAM EXAMPLE: ORDINARY REINFORCED CONCRETE MOMENT FRAME

**Given:** Figure 6.18 shows frame beam B3 of an ordinary moment frame (OMF) of a building located in an area of low seismicity corresponding to UBC 1997 seismic zone 0 or 1. The seismic characteristics of the building site are  $S_s = 0.14g$  and  $S_1 = 0.03g$ . The building has been analyzed using a commercially available three-dimensional analysis program. Cracked section properties have been input for the members; for beams,  $I_{\text{eff}} = 0.5I_g$ ; for columns,  $I_{\text{eff}} = 0.7I_g$ ; and for shear walls,  $I_{\text{eff}} = 0.5I_g$ . Rigid diaphragms and rigid-end offsets have been assumed, consistent with the assumptions commonly used in practice. The analysis automatically has taken the effect of  $P\Delta$  into consideration. The analysis results for beam B3 are as follows:

Dead load  $D$

At supports:  $M = -150$  kip-ft,  $V = 40$  kip

At midspan:  $M = 90$  kip-ft,  $V = 0$

Live load  $L$

At supports:  $M = -20$  kip-ft,  $V = 12$  kip

At midspan:  $M = 15$  kip-ft,  $V = 0$

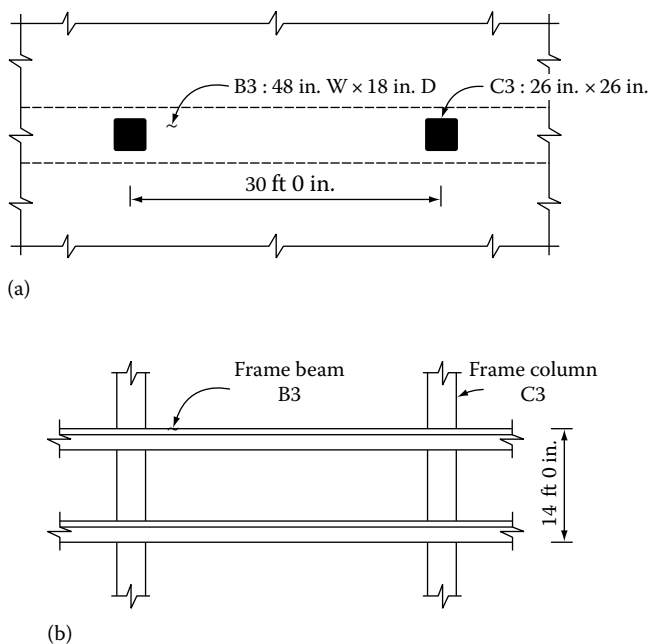
Wind  $W$

At supports:  $M = \pm 95$  kip-ft,  $V = \pm 18$  kip

**Required:** Design and a schematic reinforcement detail for B3 using the provisions of ACI 318-05.

**Solution:** The ultimate design load combinations consisting of dead, live, and wind loads are shown in Table 6.2.

**Check limitations on beam section dimensions:** According to ACI 318-05 Section 21.2.1.2, the provisions of Chapters 1 through 18 and Chapter 22 are adequate to provide a threshold of toughness expected of structures assigned to ordinary categories. These are structures in regions of low seismic risk, corresponding approximately to UBC zones 0 and 1, or assigned to SDC A or B.



**FIGURE 6.18** Frame beam and column example; OMF: (a) plan and (b) elevation.



No dimensional limitations are specified for frame beams of buildings assigned to SDC A or B. Thus, the given dimensions of 48 in. wide  $\times$  18 in. deep for the example beam is acceptable. Note that beam depth of 18 in. satisfies the minimum requirements specified in ACI 318-05/08 Table 9.5(a) for non-prestressed beams and slabs.

**Calculate the required flexural reinforcement:** At support:  $-M_u = 315$  kip-ft (load combination 4, see Table 6.3).

$$-A_s = 312/4.1 \times 15.25 = 4.99 \text{ in.}^2$$

Use five #9 at top, giving  $-A_s = 5.0 \text{ in.}^2$

At midspan:  $+M_u = 152$  kip-ft (load combination 1)

$$+A_s = 148/4.1 \times 15.25 = 2.36 \text{ in.}^2$$

Use five #7 at bottom, giving  $+A_s = 3.0 \text{ in.}^2$

The reinforcement ratios provided are

$$P_{\text{top}} = 5 \times 1/48 \times 15.25 = 0.0068 \text{ and}$$

$$P_{\text{top}} = 5 \times 0.6/48 \times 15.25 = 0.0041$$

These are more than the minimum required per Section 10.5, and, by inspections, less than the maximum permitted per Section 10.3.3.

**Shear design:** The maximum factored shear force  $V_u$  is 88.8 kip, as calculated in load combination (Table 6.3). Assume an equivalent factored uniform load  $w_u$  equal to  $88.8/27.43 = 3.19$  kip/ft<sup>3</sup> where 27.83 ft is the clear span for B3.

At critical section distance  $d$  from the face of columns,  $V_u = 88.8 - (15.25/12) \times 3.19 = 84.75$  kip.

$$\begin{aligned} V_c &= 2\sqrt{f'_c} b_w d \\ &= 2\sqrt{4000} \times 48 \times 15.25/1000 \end{aligned}$$

Since  $V_u$  is greater than  $\phi V_c/2 = 0.75 \times 93/2 = 34.87$  kip, and is less than  $\phi V_c = 0.75 \times 93 = 69.75$  kip, the required shear reinforcement is governed by the minimum specified in Section 11.5.5. Assuming #3 stirrups with four vertical legs, the required spacing  $s$  is

**TABLE 6.3**

**Design Bending Moments and Shear Forces for Frame Beam B3: OMF**

Load Case		Location		Bending Moment (kip-ft)	Shear Force (kip)
1	1.4D	Support		210	56
		Midspan		126	0
2	1.2D + 1.6LL	Support		148	67.2
		Midspan		132	0
3	1.2D + 0.8W	Support	Max	256	62.4
			Min	104	33.6
		Midspan		108	0
4	1.2D + 1.6W + 1.0L	Support	Max	312	88.8
			Min	8	31.2
		Midspan		123	0
5	0.9D + 1.6W	Support	Max	287	64.8
			Min	-17	7.2
		Midspan		81	0

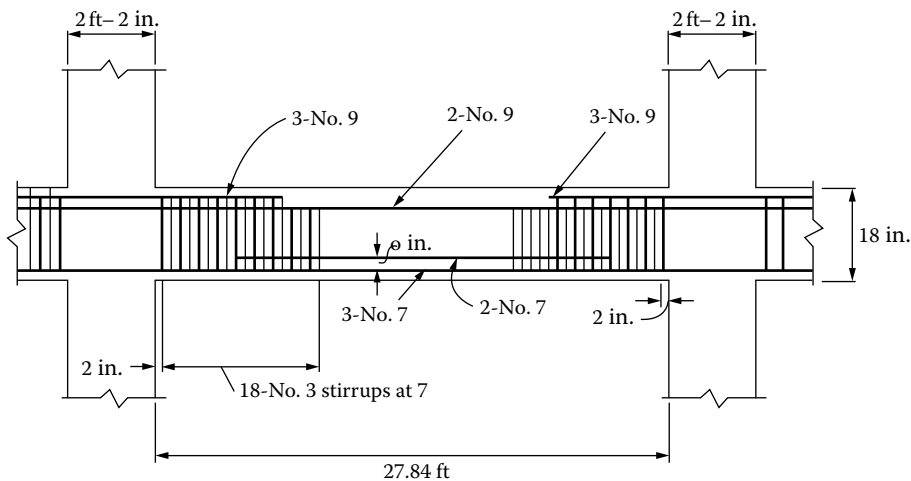
$$s = A_v f_y / 50 b_w$$
$$= 4 \times 0.11 \times 60,000 / 50 \times 48 = 11 \text{ in.}$$

The maximum spacing of shear reinforcement, according to Section 11.5.4, is  $d/2 = 15.25/2 = 7.6$  in. or 21 in. Thus, the governing spacing of stirrups is 7.6 in. According to Section 11.5.5.1, stirrups may be discontinued at sections where  $V_u \leq V_c/2$ . For the example beam, this occurs at about 10.0 ft from the face of the column. Provide 18 #3, four-legged stirrups at 7 in. spacing at each end. First place the stirrup 2 in. from the face of the support. For the remainder of the center span, provide #3 stirrups at 12 in. spacing (see Figure 6.19).

6.11.2 FRAME COLUMN EXAMPLE: ORDINARY REINFORCED CONCRETE MOMENT FRAME

**Given:** Values of axial loads, bending moments, and shear forces obtained for three load combinations for column C3 are given in Table 6.4.

**Required:** Design and a schematic reinforcement detail for column C3 using provisions of ACI 318-05/08.



**FIGURE 6.19** Design example, frame beam; OMF. For this example problem, although by calculations no shear reinforcement is required in the midsection of the beam, it is good practice to provide #3 four-legged stirrups at 15 in. spacing.

**TABLE 6.4**  
**Design Axial Forces, Bending Moments, and Shear Forces for Frame Column C3: OMF**

Load Case	Axial Force (kip)	Bending Moment (kip-ft)	Shear Force (kip)
1	2440	0	0
2	1830	±268	±30
3	1350	±273	±52

**Solution:** Similar to frame beams of OMF, frame columns must satisfy the design provisions of ACI Chapters 1 through 18 and Chapter 22, the last of which refers to structural plane concrete and has limited impact on the design of our column.

Since in the ACI 318 there are no dimensional limitations specified for frame columns OMF, the given column dimensions of 26 in.  $\times$  26 in. are acceptable.

From an interaction diagram not shown here, a 26 in.  $\times$  26 in. column with 12 # 11 vertical bars has been found to be adequate for the ultimate load combinations given in Table 6.5. The reinforcement ratio of  $(12 \times 1.56)/(26 \times 26) \times 100 = 2.7\%$  is within the maximum and minimum limits of 1% and 8%. Thus, the design of column C3 is suitable. Note that for columns in buildings assigned to SDC D, E, or F, the maximum ratio for longitudinal steel is 6%.

**Design for shear:** The shear design of a frame column of OMF is no different from that of a non-frame column. The shear strength of column is verified using ACI Equation 11.4 for members subject to axial compression:

$$\begin{aligned} V_c &= 2(1 + N_u/2000A_g) \sqrt{f'_c} b_w d \\ &= 2(1 + 1,350,000/2000 \times 26 \times 26) \sqrt{4000} \times 26 \times 22/1000 \\ &= 145 \text{ kip} \end{aligned}$$

Observe that  $N_u$  is the smallest axial force corresponding to the largest shear force  $V_u^- \pm 52$  kip (see Table 6.4).

Since  $V_u = 52$  kip  $< \phi V_c/2 = 0.75 \times 145/2 = 54.38$  kip, column tie requirements must satisfy the requirements given in Section 7.10.5. Using #4 ties, the minimum vertical spacing of ties is given by the smallest of

- $16 \times$  the diameter of vertical bars  $= 16 \times 1.41 = 22.5$  in.
- $48 \times$  the diameter of tie bars  $= 48 \times 0.5 = 24$  in.
- The least column dimension  $= 26$  in.

**TABLE 6.5**  
**Design Bending Moments and Shear Forces for B2: Special Moment Frame**

Load Case	Location	Bending Moment (kip-ft)	Shear Force (kip)
Dead load, $D$	Support	-120	35
	Midspan	+90	0
Live load, $L$	Support	-20	10
	Midspan	9	0
Seismic, $Q_E$	Support	$\pm 600$	$\pm 60$
<b>Load Combinations</b>			
1. $U = 1.4D + 1.7L$	Support	-202	66
	Midspan	+141.3	0
2. $U = 1.2D + F_1L + 1.0E$ , where $E = \rho Q_E + 0.2S_{DS}D$ . Since $F_1 = 0.5$ , $\rho = 1.0$ , and $S_{DS} = 1.0$ , $U = 1.2D + 0.5L + Q_E + 0.2D$ $= 1.4D + 0.5L + Q_E$	Support	-778	114
	Midspan	130.5	60
3. $U = 0.9D - 1.0E = 0.9D + \rho Q_E - 0.2S_{DS}D$ $U = 0.7D + Q_E$	Support	516	-35.5
	Midspan	63	-60

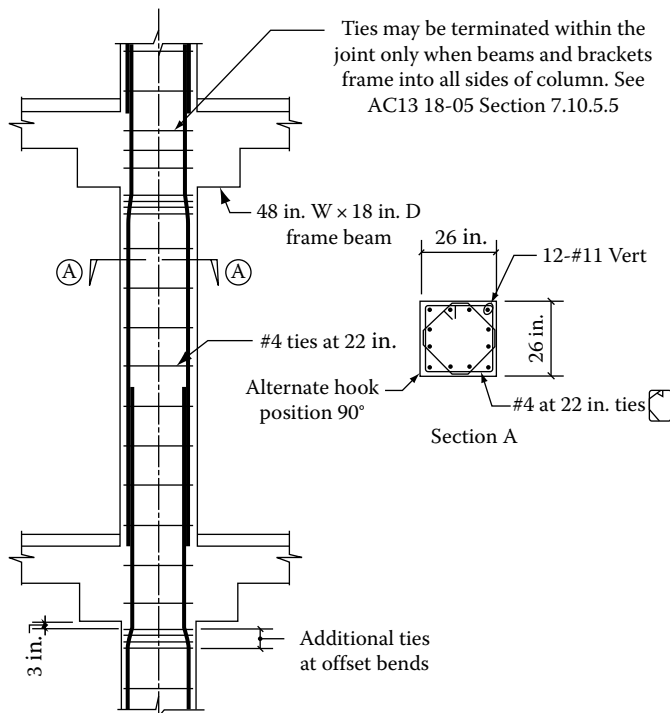


FIGURE 6.20 Design example, frame column; OMF.

Use #4 ties at 22 in. Observe that at least #4 ties are required for vertical bars of sizes #11, 14, and 18, and for bundled vertical bars. See Figure 6.20 for column reinforcement.

6.11.3 FRAME BEAM EXAMPLE: INTERMEDIATE REINFORCED CONCRETE MOMENT FRAME

**Given:** A beam 24 in. wide x 26 in. deep as shown in Figure 6.21. The beam is part of the lateral resisting system that consists of an intermediate reinforced concrete moment frame.

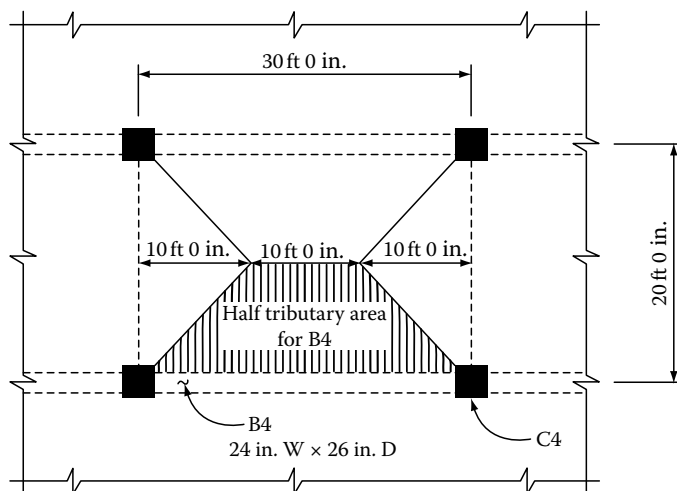


FIGURE 6.21 Frame beam and column example; IMF.

Ultimate design values are as follows:

Support moment  $-M_{ul} = 376$  kip-ft

$-M_{ur} = 188$  kip-ft

Midspan moment  $+M_u = 157$  kip-ft

Clear span  $= 30 - 30/12 = 27.50$  ft.

Shear force due to seismic  $= 50$  kip

Shear force due to gravity loads  $= 63$  kip

$f'_c = 4000$  psi  $f_y = 60,000$  psi

Nominal moments ( $\phi = 1$ ) are as follows:

At supports:  $-M_{nl} = 418$  kip-ft

$-M_{nr} = 209$  kip-ft

**Required:** Design and schematic of reinforcement for beam B4 using the provisions of ACI 318-05/08.

**Solution:**

At left support,  $-A_{s, \text{left}} = 376/4 \times 23.5$   
 $= 4.0 \text{ in.}^2$

Use four #9 at top giving  $-A_{s, \text{left}} = 4.0 \text{ in.}^2$

At right support,  $-A_{s, \text{right}} = 188/4 \times 23.5$   
 $= 2.01 \text{ in.}^2$

Use two #9 at top, giving  $-A_{s, \text{right}} = 2.0 \text{ in.}^2$

Use four #6 at bottom, giving  $+A_s = 4 \times 0.44 = 1.76 \text{ in.}^2$

Actual moment capacity  $= 1.76/1.67 \times 157 = 165$  kip-ft

Verify minimum strength requirements

1. At joint face, positive moment  $-\Phi M_n^-/3$ .
2. At any section along the beam, both positive and negative moments  $-\Phi M_n^-/5$ .

For item 1 above, positive moment strength criteria are satisfied because  $165 \text{ kip-ft} > 376/3 = 125 \text{ kip-ft}$ .

For item 2, both positive and negative moment criteria are satisfied along the beam, because two #9 bars are continued at top and four #6 are continued at bottom. The flexural capacity of 188 kip-ft provided at top and 165 kip-ft at bottom are greater than  $376/5 = 75 \text{ kip-ft}$ .

**Shear design:** The designer is given the following two options for determining the factored design shear force (ACI 318-05, Section 21.12.3):

1. Use the nominal moment strength of the member and the gravity load on it to determine the design shear force. Assume that nominal moment strengths ( $\phi = 1.0$ ) are developed at both ends of its clear span. Use statics to evaluate the shear associated with this condition. Add the effect of the factored gravity loads  $W_D$  and  $W_L$  to obtain the total design shear.

Observe that the procedure is the same as for frame beams of SMRF. The only difference is that for an IMF, nominal moment  $M_n$ , and not probable moment  $P_{mr}$ , is used as the beam ends.

2. Use a factored design shear  $V_u$  based on load combinations that include earthquake effects  $E$ , where  $E$  is taken to be twice that prescribed by the governing code.

For the example problem, we use the first option. Shear force associated with nominal moments  $M_{nl}$  and  $M_{nr}$  is equal to  $M_{nl} + M_{nr}/l_n$ .

$$V = 418 + 219/(30 - 30/12) = 28 \text{ kip}$$

Shear force due to factored gravity load  $= 63$  kip.

Design shear force =  $28 + 63 = 91$  kip.

$$V_c = 2\sqrt{f'_c} b_w d = 2\sqrt{4000} \times 26 \times 23.5/1000 = 77.3 \text{ kip}$$

Assuming #3 stirrups, the required spacing  $s$  is

$$s = A_v f_y d / V_s = 2 \times 0.11 \times 60 \times 23.5 / (91 / 0.85 - 77.3) = 10.4 \text{ in.}$$

Maximum spacing of stirrups over a length equal to  $2h = 2 \times 26 = 52$  in. from the face of the supports is the smallest of

- $d/4 = 23.5/4 = 5.9$  in. (Controls)
- $8 \times$  the diameter of smallest longitudinal bar  $8 \times 1 = 8.0$  in.
- $24 \times$  the diameter of stirrup bar  $= 24 \times 0.375 = 9.0$  in.
- 12 in.

Observe that the allowable maximum spacing is the same as for the frame beams of SMRFs. However, hoops and crossties with seismic hooks are not required for frame beams of IMFs.

Provide 12 #3 stirrups at each end spaced at 5 in. on centers. Place the first stirrup 2 in. from the face of each column. For the remainder of the beam, the maximum spacing of stirrups is  $d/2 = 23.5/2 = 11.8$  in. Use 11 in. spacing. Figure 6.22 provides a schematic reinforcement layout.

#### 6.11.4 FRAME COLUMN EXAMPLE: INTERMEDIATE REINFORCED CONCRETE MOMENT FRAME

**Given:** A 30 in.  $\times$  30 in. frame column of an intermediate reinforced concrete moment frame. The column has been designed with 10 #11 longitudinal reinforcement to satisfy the ultimate axial load and moment combinations.

The ultimate design shear force due to earthquake loads  $E = 35$  kip. The smallest axial load,  $N_u$ , corresponding to the shear force, = 1040 kip.

$$f'_c = 4000 \text{ psi} \quad f_y = 60,000 \text{ psi}$$

Clear height of the column = 11.84 ft

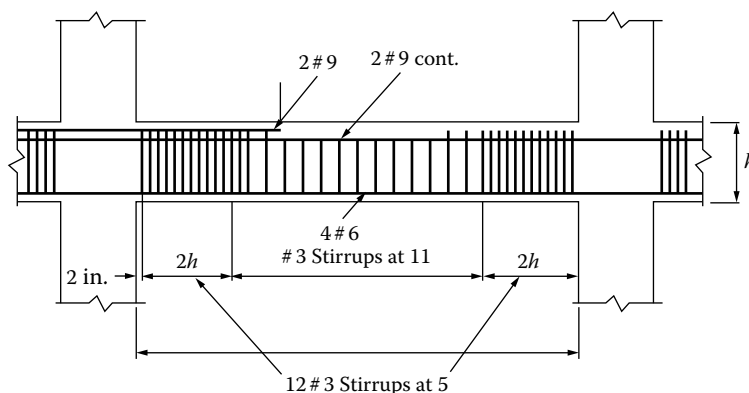


FIGURE 6.22 Design example, frame beam; IMF.

**Required:** Seismic design and a schematic reinforcement detail for column C4 using the provisions given in Section 21.10 of ACI 318-05.

**Check limitations on column cross-sectional dimensions:** No limitations are specified in ACI 318-05. Therefore, the given dimensions of 30 in.  $\times$  30 in. for the column are acceptable.

**Design for bending and axial loads:** The statement of the problem acknowledges that the column has been designed for the governing load combinations with 10 #11 vertical reinforcement. The reinforcement ratio (equal to  $15.6/(30 \times 30) \times 100 = 1.74\%$ ) is within the allowable range of 1%–8%.

**Design for shear:** Similar to that for beams, the shear design of columns in IMFs is based on providing a threshold of toughness. The design shear in columns may be determined by using either of the two options similar to those given earlier for beams. The first choice is to use the shear associated with the development of nominal moment strengths of column at each end of the clear span. The second is to double the earthquake effect  $E$  when calculating ultimate design load combinations that include the earthquake effect  $E$ .

The ultimate shear force  $E$  due to earthquake is equal to 35 kip, as given in the statement of the problem. Using the second option, the design shear force  $V_u$  is equal to  $2 \times E = 2 \times 35 = 70$  kip. The shear capacity of the column is

$$\begin{aligned} V_c &= 2\sqrt{f'_c} b_w d \\ &= 22\sqrt{4000}/1000 \times 30 \times 23.5 = 89 \text{ kip.} \end{aligned}$$

The shear capacity may also be calculated by taking advantage of the axial compression present in the column by using the equation

$$\begin{aligned} V_c &= 2(1 + N_u/2000A_g)\sqrt{f'_c} b_w d \\ &= 2(1 + 1,040,000/2000 \times 30 \times 30)\sqrt{4000} \times 30 \times 23.5/1000 \\ &= 141 \text{ kip} \end{aligned}$$

In the above equation,  $N_u$  is the smallest axial load and is equal to 1040 kip corresponding to the largest shear force on the column (as given in the statement of the problem).

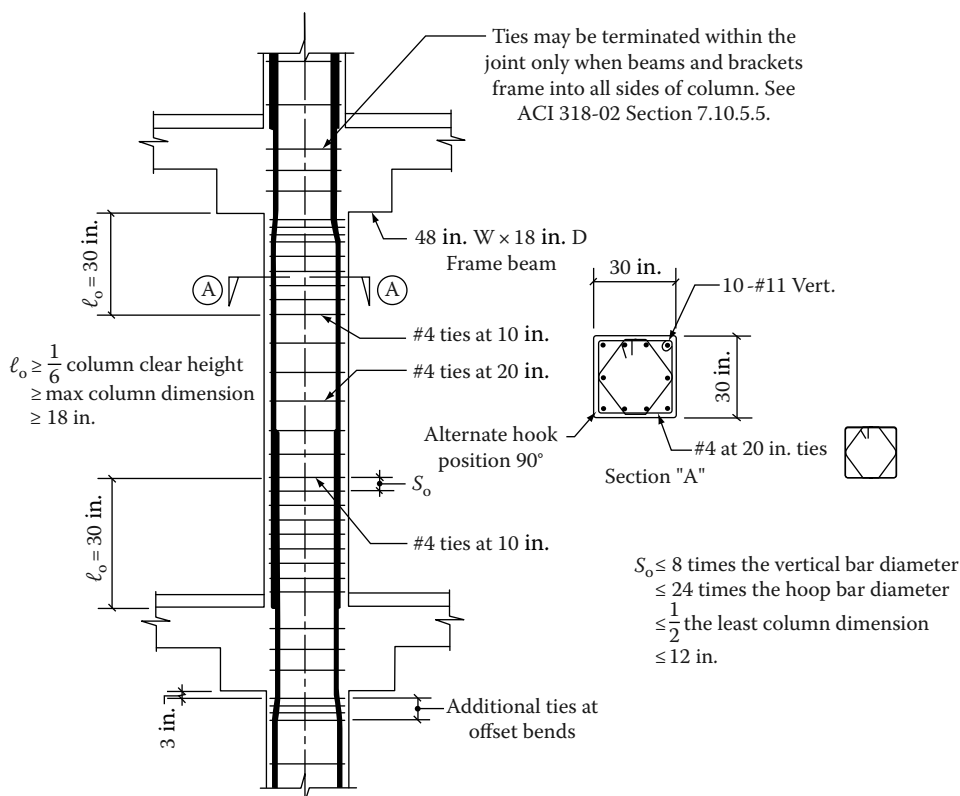
Since  $V_u = 70 \text{ kip} < 141/2 = 70.5 \text{ kip}$ , column tie requirements given in Section 7.10.5 would have sufficed: However, frame columns of IMFs are required to have a minimum threshold of toughness. Hence the requirements given in Section 21.10.4.

To properly confine the concrete core in the plastic hinge length region  $\ell_o$ , and to maintain lateral support of column vertical bars, transverse reinforcement requirements for frame columns of IMF are as follows:

- $8 \times$  the diameter of the smallest vertical bar of column  $= 8 \times 1.41 = 11.3 \text{ in.}$   $\leftarrow$  controls
- $24 \times$  the diameter of the tie bar  $= 24 \times 0.5 = 12 \text{ in.}$
- One-half the least column dimension  $= 30/2 = 15 \text{ in.}$
- 12 in.

The plastic hinge length  $\ell_o$  is the largest of

- One-sixth of the column clear height  
 $= 11.84/6 \times 12 = 24 \text{ in.}$



**FIGURE 6.23** Design example, frame column; OMF. Note:  $l_o$  is the same as for columns of SMRF. There is no requirement to splice column bars at mid-height.

- Maximum cross-sectional dimension of the columns  
= 30 in. ← controls
- 18 in.

Use #4 ties and cross-ties at 10 in. spacing within the  $l_o$  region. In between  $l_o$ , provide ties at 20 in. spacing. Figure 6.23 provides a schematic reinforcement layout of column vertical bar and ties.

### 6.11.5 SHEAR WALL EXAMPLE: SEISMIC DESIGN CATEGORY A, B, OR C

Although ACI 318-05 specifies certain seismic design and detailing requirements for IMFs there are no requirements for shear walls in buildings assigned to SDC A, B, or C. For these buildings, ACI considers that the requirements given in Chapters 1 through 18 and Chapter 22 are sufficient to provide a degree of toughness that is consistent with the seismic risk associated with buildings assigned to SDC C and lower.

The design procedure for a reinforced shear wall subjected to bending and axial loads is a two-step process. First generate an axial load–moment interaction diagram for the shear wall of given dimensions and concrete strength, with various percentages of reinforcement. This is done by taking successive choices of neutral axis distance measured from one face of the wall, and then calculating the axial force  $P_u$  and the corresponding moment  $M_u$ . Each sequence of calculations is repeated until the complete interaction diagram is obtained. The next step is the selection of reinforcement that satisfies the design requirement under loads and moments equal to or larger than the factored loads and moments. The formulation is based on the principles of ultimate strength design with a



linear strain diagram that limits the concrete strain at the extremity of the section to 0.003. With the general availability of computers it is no longer tedious to establish axial load–moment interaction diagrams. Therefore, design for axial loads and moments are not discussed further in this section.

**Given:** A shear wall 24 ft long and 12 in. thick with a floor-to-floor height of 14 ft.

Compressive strength of concrete  $f'_c = 4000$  psi

Yield strength of reinforcing bars  $f_y = 60$  ksi

Maximum factored shear force  $V_u = 500$  kip

Vertical reinforcement as determined for bending and axial loads = four #7 at 9 in. vertical at each end, and #6 at 15 in. vertical in between each face (see Figure 6.24).

**Required:** Shear design using the provisions of ACI 318-05.

**Solution:**

**Shear design:**

$$\begin{aligned} V_c &= 2\sqrt{f'_c} h_d \\ &= 2\sqrt{4000} \times 12 \times 0.8 \times 24 \times 12/1000 = 350 \text{ kip} \end{aligned}$$

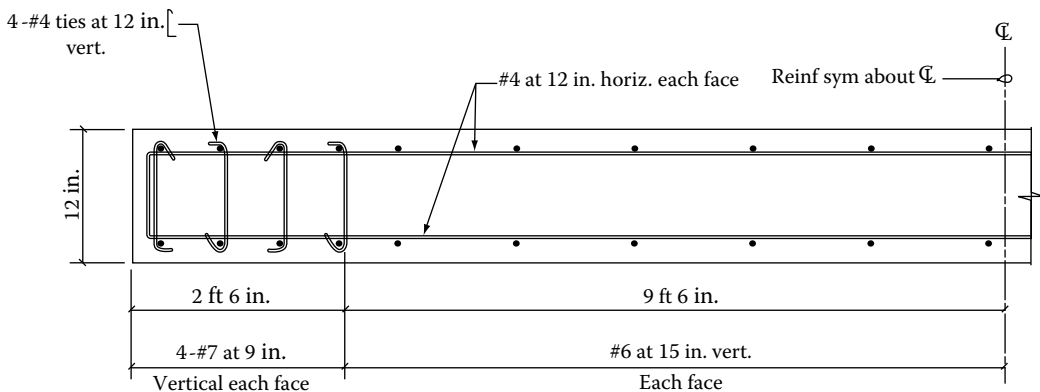
Observe that Equation 11.10.4 permits  $d$  to be taken equal to  $0.8l_w = 0.8 \times 24 \times 12 = 230$  in. for the design of horizontal shear forces in the plane of the wall. A larger value of  $d$  equal to the distance from the extreme compression fiber to the centerline of tension reinforcement determined by a strain compatibility analysis is also permitted.

The maximum factored shear force  $V_u$  is 500 kip, as given in the statement of the problem. Since  $V_u = 500 \text{ kip} > \phi V_c/2 = 0.75 \times 350/2 = 131.25 \text{ kip}$ , provide horizontal reinforcement given by

$$V_s = A_v f_y d / s_2$$

Assuming two layers of #4 horizontal reinforcement, one layer at each face

$$S_2 = 2 \times 0.22 \times 60 \times 230 / (500/0.75 - 350)$$



**FIGURE 6.24** Shear wall: low-to-moderate seismic zones (SDC A, B, or C). Note: Vertical reinforcement of #7 @ 9 in. at each end is enclosed by lateral ties, since the reinforcement area of eight #7 vertical bars equal to  $8 \times 0.6 = 4.8 \text{ in.}^2$  is greater than 0.01 times the area of concrete  $= 12 \times 30 = 360 \text{ in.}^2$  (see ACI 318-05 Section 14.3.6).

However, the maximum spacing of horizontal reinforcement must not exceed

- $l_w/5 = 24 \times 12/5 = 57.6$  in.
- $3h = 3 \times 12 = 36$  in.
- 18 in. (Controls)

Section 11.10.9.2 requires a ratio  $\rho_h$  of horizontal reinforcement to be not less than 0.0025.

Therefore, use two layers of #4 horizontal bars at 12 in. spacing, giving  $\rho_h = 0.0028 > 0.0025$ .

At any horizontal section, the shear strength  $V_n$  must not exceed  $10 \sqrt{f'_c} h_d = 10 \sqrt{4000} \times (12 \times 230) / 1000 = 1746$  kip

$$\begin{aligned} V_n &= V_c = V_s \\ &= 350 + 2 \times 0.20 \times 60 \times 230 / 12 \\ &= 810 \text{ kip} < 1746 \text{ kip} \end{aligned}$$

Section 11.10.9.4 requires the area of vertical shear reinforcement to gross concrete area of horizontal section, denoted by  $\rho_n$  to be not less than

$$\begin{aligned} \rho_n &= 0.0025 + 0.5(2.5 - h_w/l_w) (\rho_h - 0.0025) \\ &= 0.0025 + 0.5(2.5 - 14 \times 12/24 \times 12)(0.0028 - 0.0025) \\ &= 0.0028 \quad (\text{Controls}) \end{aligned}$$

Note that  $h_w$  = wall height = 14 ft;  $l_w$  = wall length = 24 ft.

- $\rho_n \geq 0.0025$
- $\rho_n$  need not be greater than the required horizontal shear reinforcement

Thus,  $\rho_n = 0.0028$ .

The spacing of vertical shear reinforcement, according to Section 11.10.9.5, must not exceed

- $l_w/3 = 24 \times 12/3 = 96$  in.
- $3h = 3 \times 12 = 36$  in.
- 18 in.

For two curtains of #6 vertical bars spaced at 15 in. centers,  $\rho_n = 2 \times 0.44 / 12 \times 15 = 0.0049$  is acceptable.

The provided horizontal and vertical reinforcements satisfy the minimum reinforcement ratios  $\rho_h$  and  $\rho_n$  given in Sections 14.3.2 and 14.3.3.

### 6.11.6 FRAME BEAM EXAMPLE: SPECIAL REINFORCED CONCRETE MOMENT FRAME

**Given:** Beam B2: 28 in. wide  $\times$  33 in. deep clear span  $l_n = 25.17$  ft (Table 6.5)

$$f'_c = 4000 \text{ psi}; f_y = 60,000 \text{ psi}$$

Ultimate design values at support:

$$\begin{aligned} M_u &= 788 \text{ kip-ft} \\ V_u &= 114 \text{ kip} \\ V_e &= 129.6 \text{ kip} \end{aligned}$$

$V_e$  is the design shear corresponding to the development of the probable moment strength of the member (see ACI 318-05, 21.3.4.1 and 21.4.5.1).

The axial force in B2 is negligible.

**Required:** Schematic design and detail of frame beam B2 using the provisions of ACI 318-05.

**Solution:**

**Check limitations on section dimensions:** The factored axial compressive force on B2 is negligible. Therefore, B2 may be designed as a flexural member.

- $l_n/d = (28 \times 12) - 34/30.5 = 10.0 > 4$ . (Section 21.3.1.2)
- Width/depths =  $28/33 = 0.85 > 0.3$  (Section 21.3.1.3)
- Width = 28 in.  $> 10$  in. (Section 21.3.1.4)  
 $< \text{width of supporting column}$   
 $+ (1.5 \times \text{beam depth})$   
 $< 34 + 1.5 \times 33 = 83.5 \text{ in. (Section 21.3.1.5)}$

**Calculate required flexural reinforcement:**

At support:  $-M_u = 778 \text{ kip-ft}$

$$-A_s = 778/4.24 \times 30.5 = 6.02 \text{ in.}^2$$

Use six #9 top

$$\phi M_n = -778 \text{ kip-ft}$$

$$+M_u = 516 \text{ kip-ft}$$

$$+A_s = 516/4.1 \times 30.5 = 4.12 \text{ in.}^2$$

Use six #8 bottom,  $A_s = 4.74 \text{ in.}^2$

$$\phi M_n = 516 \times 4.74/4.12 = 594 \text{ kip-ft}$$

At midspan:  $M_u = +141.3 \text{ kip-ft}$

$$A_s = 141.3/4.1 \times 30.5 = 1.13 \text{ in.}^2$$

$$\begin{aligned} A_{s(\min)} &= 3\sqrt{f'_c} b_w d / f_y \\ &= 3\sqrt{4000} \times 28 \times 30.5 / 60,000 = 2.70 \text{ in.}^2 \quad (10.3) \end{aligned}$$

$$\begin{aligned} A_{s(\min)} &= 200 b_w d / f_y \\ &= 200 \times 28 \times 30.5 / 60,000 = 2.84 \text{ in.}^2 \quad (\text{Controls}) \quad (\text{Section 21.3.2.1}) \end{aligned}$$

$$\begin{aligned} A_{s(\max)} &= \rho_{\max} b_w d \\ &= 0.025 \times 28 \times 30.5 \\ &= 21.3 \text{ in.}^2 \end{aligned}$$

$> 2.84 \text{ in.}^2$  OK (Section 21.3.2.1)

Use three #9 giving  $A_s = 3.0 \text{ in.}^2$

**Verify minimum strength requirements:**

1. At joint face, for positive movement  $\geq \frac{-M_u}{2}$ .
2. At any section along the beam, for both positive and negative moments  $\geq \frac{-M_u}{4}$  (21.3.2.2).
  - a. Positive moment strength criteria are satisfied because 594 kip-ft  $> \frac{778}{4} = 389$  kip-ft.
  - b.  $-M_u/4 = \frac{778}{4} = 194.5$  kip-ft. This can be satisfied by providing two #9 top bars and two #8 bottom bars. However, the minimum reinforcement requirement is 2.84 in.<sup>2</sup>. Therefore, provide continuous three #9 top bars and four #8 bottom bars, giving  $A_s = 3.00$  in.<sup>2</sup> and 3.16 in.<sup>2</sup>, respectively, which are greater than  $A_{s(\min)} = 2.84$  in.<sup>2</sup>.

Observe that this also automatically fulfills the requirement that at least two bars be continuous at both the top and the bottom of the beam (Section 21.3.2.1).

**Shear design:** It is worth mentioning again that the values for shear obtained from lateral analysis at the beam ends do not play a primary role in determining the shear reinforcement. This is because the method of determining shear forces in beams of special moment frames is based on the premise that plastic hinges may form at regions near the supports. The shear forces are thus computed using statistics, based on the assumption that moments of opposite sign corresponding to the probable moment strength,  $M_{pr}$ , act at the beam ends. Additionally, a shear force corresponding to the factored gravity load is added to the shear derived from the probable moment to determine the design shear forces.

The probable moment,  $M_{pr}$ , is determined by using (1) a stress of  $1.25f_y$  in the tensile reinforcement and (2) a strength-reduction factor  $\phi$  equal to 1.0. In determining the shear strength of a frame beam, both contributions provided by concrete,  $V_c$ , and reinforcing steel,  $V_s$ , are taken into account. However,  $V_c$  is to be taken as zero when both of the following conditions are met: (1) The earthquake-induced shear force (calculated using the probable moment  $M_{pr}$  and  $\phi = 1$ ) is greater than or equal to 50% of the maximum required shear strength. (2) The factored axial compressive force in the beam, including earthquake effects, is less than  $A_g f'_c / 20$ .

The second condition reflects the necessity of increasing the shear reinforcement in the case of little or no axial load.

The following equation may be used to compute  $M_{pr}$ :

$$M_{pr} = A_s (1.25 f_y) \left( d - \frac{a}{2} \right)$$

where

$$a = \frac{A_s (1.25 f_y)}{0.85 f'_c b}$$

Returning to example problem, for six #9 top bars,  $A_s = 6$  in.<sup>2</sup>.

$$a = \frac{6 \times 1.25 \times 60}{0.85 \times 4 \times 28} = 4.73 \text{ in.}$$

$$\begin{aligned} M_{pr} &= 6 \times 1.25 \times 60 \left( 30.5 - \frac{4.73}{2} \right) \\ &= 12,661 \text{ kip-in.} = 1055 \text{ kip-ft} \end{aligned}$$

For six #8 bottom bars,  $A_s = 4.74 \text{ in.}^2$

$$a = \frac{4.74 \times 1.25 \times 60}{0.85 \times 4 \times 28} = 3.73 \text{ in.}$$

$$\begin{aligned} M_{pr} &= 4.74 \times 1.25 \times 60 \left( 30.5 - \frac{3.73}{2} \right) \\ &= 10,179 \text{ kip-in.} = 848 \text{ kip-ft} \end{aligned}$$

The shear forces corresponding to  $M_{pr}$  at each end (positive at one end and negative at the other) are computed from a free body diagram of the beam. Added to these are the shear forces due to factored gravity loads to obtain the design shear force,  $V_e$ , at each end of the beam.

The following data will be used to determine the uniformly distributed gravity load on the frame beam.

Area of trapezoid tributary to B4 = 360 ft<sup>2</sup>

Dead load of slab assuming a thickness of 7.5 in.

$$= \frac{7.5}{12} \times 0.15 \times 360 = 33.75 \text{ kip}$$

$$\text{Dead load of B2} = \frac{28 \times 33}{144} \times 0.15 \times 25.17 = 24.22 \text{ kip}$$

Superimposed dead load at 20 psf for partitions and 15 psf for ceiling, mechanical, and floor finishes =  $\frac{35 \times 360}{100} = 12.60 \text{ kip}$

Total  $D_L = 70.57 \text{ kip}$

$$\text{Live load at 50 psf} = \frac{50 \times 360}{100} = 18.0 \text{ kip}$$

$$\text{Equivalent dead load} = \frac{70.57}{25.17} = 2.8 \text{ kip-ft}$$

$$\text{Equivalent live load} = \frac{18}{25.17} = 0.72 \text{ kip-ft}$$

$$\begin{aligned} \text{Factored gravity load} &= 1.4D = 0.5L \text{ (load combination 2)} \\ &= 1.4 \times 2.8 + 0.5 \times 0.72 \\ &= 4.3 \text{ kip-ft} \end{aligned}$$

Therefore,

$$w_u = 4.3 \text{ kip-ft}$$

The maximum combined designed shear force,  $V_e$ , equal to 129.6 kip, is larger than the shear force value of 114 kip obtained from load combination 2, based on structural analysis. To determine whether the shear strength,  $V_c$ , provided by the concrete can be used in calculating the shear resistance, two checks are preformed:

- Determine whether earthquake-induced shear force based on  $M_{pr}$  is larger than 50% of the total shear  $V_c$ .
- Determine whether the compressive axial force in the beam is less than  $A_g f'_c / 20$ . (For example, it is given in the statement of the problem that axial compressive force in the beam is negligible.)

If both of these criteria are satisfied, then  $V_c$  must be assumed to be equal to zero (Section 21.3.4.2). For example:

$$\begin{aligned}\text{Shear force due to plastic moments at each end of beam} &= \frac{848+1055}{25.17} = 75.6 \text{ kip} \\ \text{Design shear force } V_c &= \text{shear due to } M_{pr} + \text{gravity shear} \\ &= 75.6 + 4.3 \times 25.17/2 = 129.6 \text{ kip}\end{aligned}$$

Since 74.6 kip is greater than 50% of 129.6 = 64.8 kip, and the axial compressive force is negligible,  $V_c = 0$ .

Design shear,  $V_u$ , is equal to

$$V_u = 129.6 = \phi V_u + \phi V_s$$

Since  $V_c = 0$ ,  $V_u = \phi V_s$ , and  $V_s = V_u/\phi = 129.6/0.85 = 152.5$  kip, the spacing  $s$  of #4 hoops (closed stirrups) with four legs is given by

$$\begin{aligned}s &= \frac{A_v f_y d}{V_s} = \frac{0.2 \times 4 \times 60 \times 30.5}{152.5} \\ &= 9.6 \text{ in.}\end{aligned}$$

Observe that four legs are required because longitudinal beams bars on the perimeter are to have lateral confinement conforming to Section 7.10.5.3; every corner and alternate bar must have lateral support provided by the corner of a tie with an included angle of not more than  $135^\circ$ , and no bar shall be farther than 6 in. clear on each side along the tie from such a laterally supported bar.

Additionally, 135 hooks are required for hoops and ties. The maximum spacing of hoops within the plastic hinge length, equal to a distance of 2 times the beam depth,  $2h = 2 \times 33 = 66$  in., is the smaller of

- $\frac{d}{4} = \frac{30.5}{4} = 7.6$  in.
- $8 \times$  the diameter of the smallest longitudinal bar  $= 8 \times 1 = 8$  in. (Section 21.3.3.2)
- $24 \times$  the diameter of hoop bar  $= 24 \times 0.5 = 12$  in.

Use nine #4 hoops at each end of the beam spaced 7.5 in. apart. Place the first loop 2 in. from the face of support, as required per Section 21.3.3.2.

Hoops are required only in plastic hinge length; stirrups with seismic hooks at both ends may be used elsewhere along the beam length. Additionally, the shear strength contribution  $V_c$  of the beam concrete may be used in calculating the shear resistance.

At a distance 6.6 in. from the face of support

$$\begin{aligned}V_u &= 129.6 - \left[ \frac{66}{12} \times 4.3 \right] = 106 \text{ kip} \\ V_c &= 2\sqrt{f'_c b_w d} \\ &= 2 \times \sqrt{4000} \times \frac{28 \times 30.5}{1000} = 108 \text{ kip} \\ V_s &= \frac{V_u}{\phi} - V_c \\ &= \frac{106}{0.85} - 108 = 16.7 \text{ kip}\end{aligned}$$

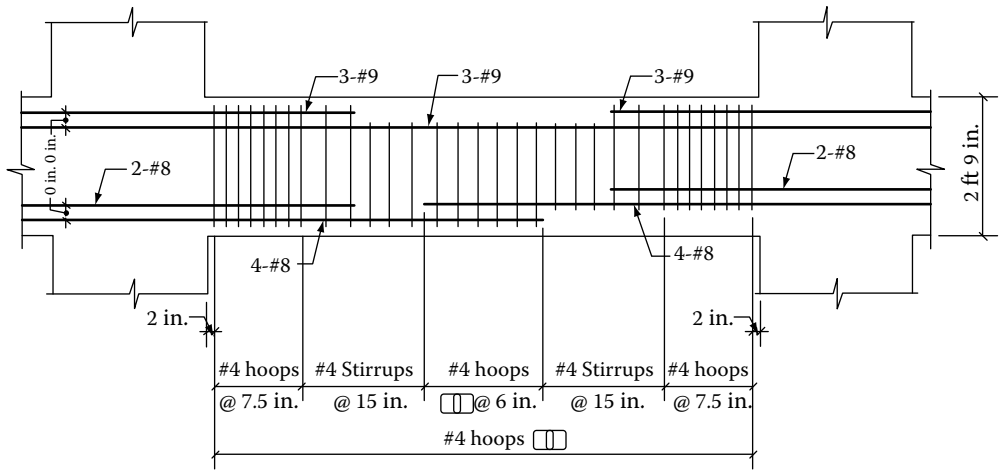


FIGURE 6.25 Design example, frame beam; special moment frame.

The required stirrup spacing of two-legged #4 stirrups is

$$s = \frac{A_v f_y d}{V_s}$$
$$= \frac{0.2 \times 2 \times 60 \times 30.5}{16.7} = 43.8$$

The maximum allowable spacing is  $d/2 = 30.5/2 = 15.25$  in. (Section 21.3.3.4).

Use 15 in. spacing for the portion of the beam bounded between the plastic hinge length and the bottom bar splice at the center. Use 6 in. spacing for the length of splice (Figure 6.25).

### 6.11.7 FRAME COLUMN EXAMPLE: SPECIAL REINFORCED CONCRETE MOMENT FRAME

**Given:** A 34 in.  $\times$  34 in. column (column C2) with 10 # 11 vertical reinforcement (see Figure 6.26). The column has been verified for the axial loads and bending moments resulting from the following ultimate load combinations.

Load Combination	$P_u$ (kip)	$M_u$ (kip-ft)	$V_u$ (kip)
1	2372	0	0
2	2180	400	80
3	1050	-400	-80

Beam moments framing into the column:  $M_{g, \text{left}} = 848$  kip-ft

$$-M_{g, \text{right}} = -1055 \text{ kip-ft}$$

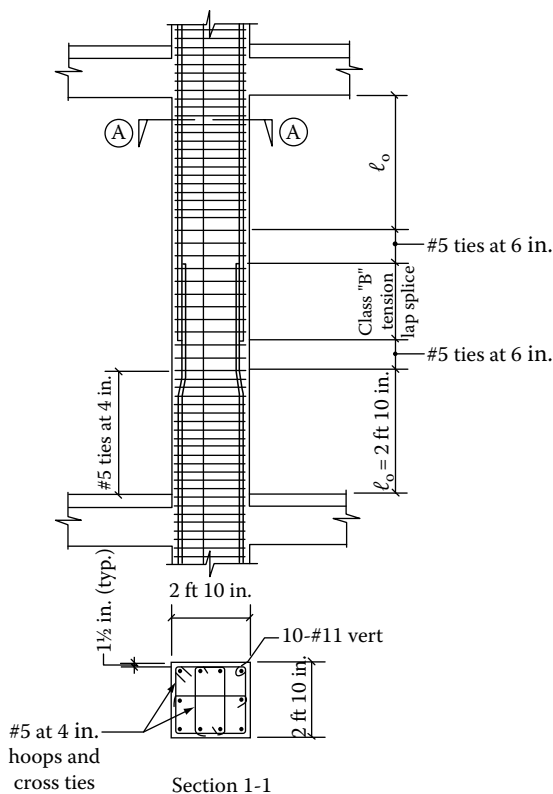
The nominal flexural strength of column at the beam-column joint.

Above the joint = 1769 kip-ft

Below the joint = 1819 kip-ft

Clear height of column = 13 ft – beam depth

$$= 13 - \frac{33}{12} = 10.25 \text{ ft}$$



**FIGURE 6.26** Design example, frame column; special moment frame.

$$f'_c = 5000 \text{ psi}, \quad f_y = 60,000$$

**Required:** Design and a schematic reinforcement detail for C2 using the provisions of ACI 318-05.

**Solution:**

**Check limitations on section dimensions:**

- The index axial force that delineates a frame column from a frame beam is given by

$$\frac{A_g f'_c}{10} = \frac{34 \times 34 \times 5}{10} = 578 \text{ kip} \quad (\text{Section 21.4.1})$$

Since the factored axial loads given in load combinations exceed the index value, C2 may be designed as a column.

- A column cross-sectional dimension of 34 in. > 12 in. is acceptable. (Section 21.4.1)
- A ratio of column cross-sectional dimensions =  $34/34 = 1.0 > 0.4$  is acceptable. (Section 21.4.2)

**Design for bending and axial loads:** The  $34 \times 34$  in. column with 10 #11 vertical bars is adequate for the combined bending and axial loads as stated in the problem. Reinforcement ratio  $\rho_g = (10 \times 156)/(34 \times 34) \times 100 = 1.35\%$  is within the allowable range of 1.0%–6.0% (Section 21.4.3.1).



**Minimum flexural strength of columns:** The sum of the nominal flexural strengths of columns at a joint must be greater than or equal to 6/5 the sum of the nominal flexural strengths of girders framing into that joint.

$$\sum M_c \geq \frac{6}{5} \sum M_g$$

When computing the nominal flexural strengths of T-beams, top slab reinforcement with in an effective width of beam as defined in Section 8.10 must be included if the slab reinforcement is developed at the critical section for flexure. For the example problem, it is assumed that the top slab reinforcement is not developed at the critical bending region. Therefore, its contribution may be ignored in computing  $M_g$ .

$$\sum M_g = 1055 + 848 = 1903 \text{ kip-ft, and } \sum M_c = 1815 + 1769 = 3584 \text{ kip-ft.}$$

Checking Equation 21.1

$$\sum M_c = 3584 > \frac{6}{5}(1903) = 2283 \text{ kip-ft is acceptable}$$

Therefore, the lateral strength and stiffness of a column can be considered when evaluating the strength and stiffness of the structure. If these strong column–weak beam criteria are not satisfied, then any positive contribution of the column to the strength and stiffness is to be ignored. Negative impacts of ignoring the stiffness and strength of the column must, however, be taken into account. For example, if ignoring the strength and stiffness of the column results in a decrease in torsional effects, the decrease should not be considered in the analysis.

**Design for shear:** The method of determining design for shear forces in columns is similar to that for beams. It takes into consideration the likelihood of the formation of plastic hinges in regions near the ends of columns. This region, denoted as  $\ell_o$ , is the largest of

- The depth of member = 34 in. (Controls)
- The clear span/6 =  $(13 \times 12 - 33)/6 = 20.5$  in. (Section 21.4.4)
- 18 in.

To maintain lateral support of column vertical bars and to confine the concrete core in the region  $\ell_o$ , transverse reinforcement requirements are as follows:

- One-fourth of the minimum member dimension =  $34/4 = 8.5$  in.
- $6 \times$  times the diameter of the longitudinal reinforcement =  $6 \times 1.41 = 8.46$  in.
- $s_x = 4 + \left( \frac{14 - h_x}{3} \right)$  but not greater than 6 in. or less than 4 in.

$$= 4 + \left( \frac{14 - 10}{3} \right) = 5.33 \text{ in. but use } s_x = 4 \text{ in. (Controls)}$$

From Figure 6.26, it is seen that  $h_x = 10$  in. < 14 in. (Section 21.4.4.3)

**Determine the area of hoops and crossties:** Assuming 4 in. vertical spacing,

$$A_{sh} = \frac{0.3s_h f'_c}{f_{yh}} \left[ \left( \frac{A_g}{A_{ch}} \right) - 1 \right]$$

$$= \frac{0.3 \times 4 \times 30.5 \times 5}{60} \left( \frac{34 \times 34}{961} \right) - 1 = 0.62 \text{ in.}^2 \quad (21.3)$$

$$\begin{aligned} A_{sh} &= \frac{0.09 s_{hc} f'_c}{f_{yh}} \\ &= \frac{0.09 \times 4 \times 30.5 \times 5}{60} = 0.92 \text{ in.}^2 \end{aligned} \quad (21.4)$$

Using #5 hoops with two crossties in the longitudinal and one in the transverse direction,

$$\begin{aligned} A_{sh} &= 4 \times 0.31 = 1.24 \text{ in.}^2 \text{ in the longitudinal direction} \\ A_{sh} &= 3 \times 0.31 = 0.93 \text{ in.}^2 \text{ in the transverse direction} \end{aligned}$$

this is larger than 0.92 required by Equation 21.4. Use #5 hoops and crossties at 4 in. vertical spacing as shown in Figure 6.26.

**Verify confining reinforcement for shear:** In the previous step, we determined transverse reinforcement required for confining column concrete and for providing lateral support to column vertical bars. In this step, we check if this reinforcement is adequate to resist shear forces resulting from the probable flexural strengths  $M_{pr}$  at each end of a column.

The positive probable flexural strength of the beam framing to the left face of column at third level is 848 kip-ft. The negative probable strength on the right face is 1055 kip-ft. Assuming that the flexural reinforcement for the beam below the level under consideration is the same, the design strength  $V_e$  is given by

$$V_e = \frac{\frac{2(848 + 1055)}{2}}{\left(13 - \frac{33}{12}\right)} = 186 \text{ kip}$$

$$V_u = V_e = \phi(V_c + V_s)$$

Since the factored axial forces are greater than  $A_g f'_c / 20$ , the shear strength,  $V_c$ , of concrete may be included in calculating the capacity of column shear. For simplicity, we use  $V_c = 2\sqrt{f'_c} bd$ , although for members subjected to axial compression (as is the case for the example column), Equation 11.4 permits higher shear values in concrete.

$$V_c = \frac{2\sqrt{5000} \times 34 \times (34 - 3)}{1000}$$

$$= 149 \text{ kip}$$

$$V_s = \frac{A_v f_y d}{s} = \frac{1.24 \times 60 \times 31}{4} = 577 \text{ kip}$$

Shear capacity  $\phi V_n = \phi(V_c + V_s)$

$$= 0.85(149 + 577)$$

$$= 617 \text{ kip} > 186 \text{ kip}$$

Therefore, #5 hoops and crossties provided at spacings of 4 in. for confinement over a length of  $\ell_o = 34$  in. at column ends is also adequate for design shear.

The midlength of the column between the plastic hinging lengths must be provided with hoop reinforcement not exceeding a spacing of 6 times the diameter of the longitudinal bar  $= 6 \times 1.56 = 9.36$  in. or 6 in. In our case, the spacing of 6 in. governs. Therefore, provide #5 hoops and crossties at 6 in. for the midlength of the column. See Figure 6.26 for a schematic layout of reinforcement.

### 6.11.8 BEAM–COLUMN JOINT EXAMPLE: SPECIAL REINFORCED CONCRETE FRAME

To ensure that the beam–column joint of SMRFs have adequate shear strength, an analysis of the beam–column panel zone is preformed to determine the shear forces generated in the joint. This is then checked against allowable shear stress.

The joint analysis is done in the major and the minor directions of the column. The procedure involves the following steps:

- The determination of panel zone design for shear force.
- The determination of effective area of the joint.
- The verification of panel zone shear stress.

**The determination of panel zone shear force:** Consider the free body stress condition of a typical beam–column intersection showing the forces  $P_u$ ,  $V_u$ ,  $M_u^L$ , and  $M_u^R$  (Figure 6.26). The force  $V_u^h$ , the horizontal panel zone shear force, is to be calculated.

The forces  $P_u$  and  $V_u$  are the axial force and shear force, respectively, from the column framing into the top of the joint. The moments  $M_u^L$  and  $M_u^R$  are the beam moments framing into the joint. The joint shear force  $V_u^h$  is calculated by resolving the moments into compression  $C$  and tension  $T$  forces. The location of  $C$  or  $T$  is determined by the direction of the moment using basic principles of ultimate strength design. Noting that  $T_L = C_L$  and  $T_R = C_R$ ,  $V_u^h = T_L + T_R - V_u$ .

The moments and the  $C$  and  $T$  forces from beams that frame into the joint in a direction that is not parallel to the major or minor directions of the column are resolved along the direction that is investigated.

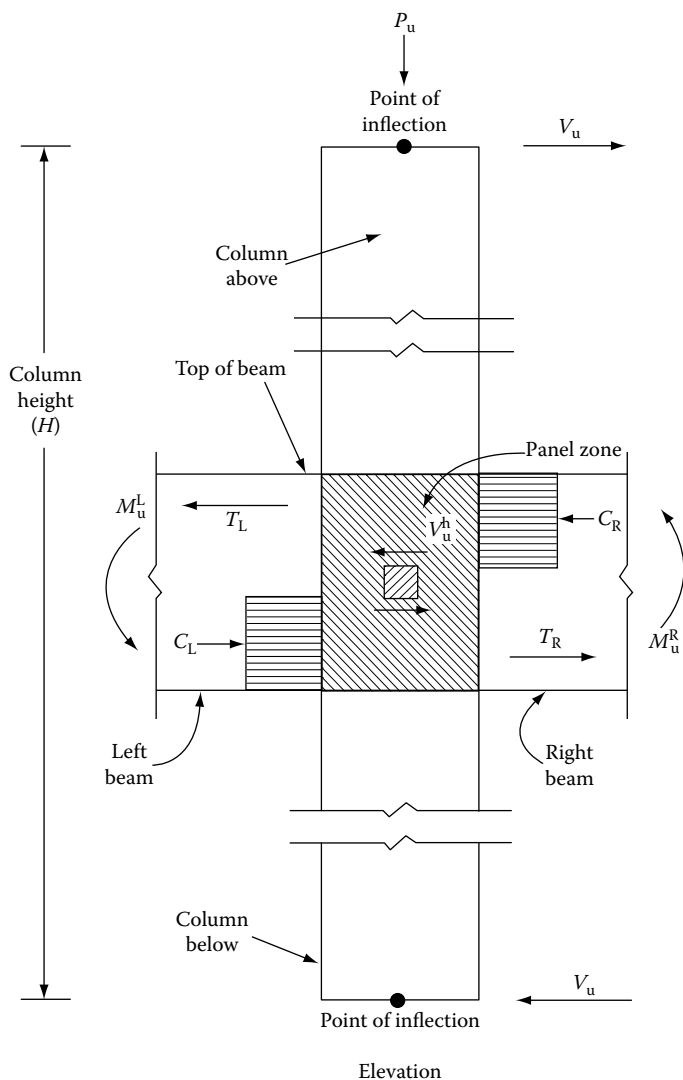
In the design of SMRFs, the evaluation of the design shear force is based on the moment capacities (with reinforcing steel overstrength factor  $\alpha$  and no  $\phi$  factors) of the beams framing into the joint. The  $C$  and  $T$  forces are based on these moment capacities. The column shear force  $V_u$  is calculated from the beam moment capacities as follows:

$$V_u = \frac{M_u^L + M_u^R}{H}$$

It should be noted that the points of inflection shown in Figure 6.27 are taken as midway between actual lateral support points for the columns.

The effects of load reversals, as illustrated in Cases 1 and 2 of Figure 6.28, are investigated and the design is based on the maximum of joint shears obtained from the two cases.

**Determine the effective area of joint:** The joint area that resists the shear forces is assumed to be always rectangular. The dimensions of the rectangle correspond to the major and minor dimensions of the column below the joint, except that if the beam framing into the joint is very narrow, the width of the joint is limited to the depth of the joint plus the width of the beam. The area of the joint is assumed not to exceed the area of the column below. It should be noted that if the beam frames into the joint eccentrically, the above assumptions may be nonconservative.

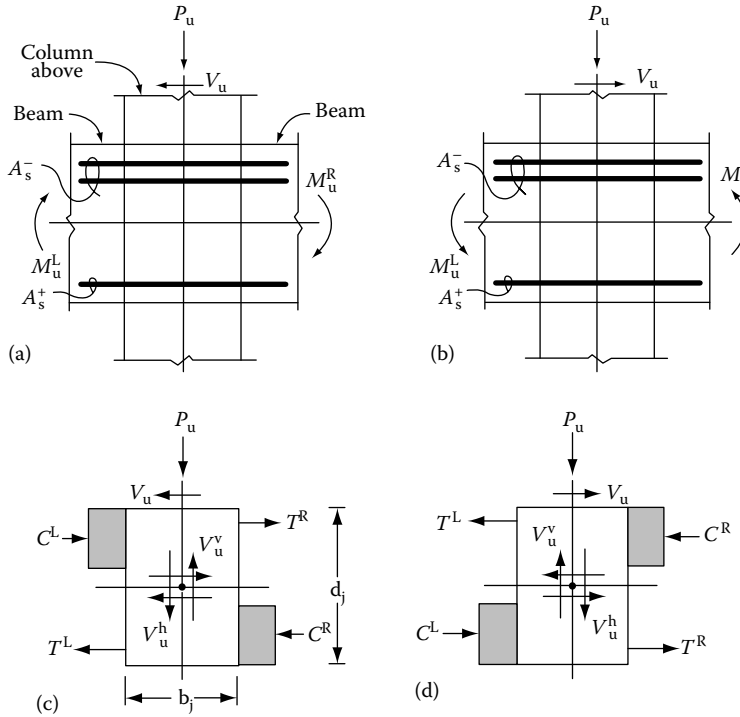


**FIGURE 6.27** Column panel shear forces.

**Given:** A frame column joint

- Beam: 28 in. wide  $\times$  33 in. deep
- Column: 34 in.  $\times$  34 in. Floor-to-floor height = 10.23 ft
- Beam top reinforcement, six #9 top
- Beam bottom reinforcement, eight #8 bottom
- Beam moment  $M_u^L = 1055$  kip-ft
- Beam moment  $M_u^R = 186$  kip-ft
- Beam confined on two faces:
  - $f'_c = 5000$  psi,  $f_y = 60,000$  psi

Confining reinforcement through the joint of a frame column is required no matter how low the calculated shear force is. This is to ensure the ductile behavior of the joint and to allow it to maintain its load-carrying capacity even after possible spalling of concrete outside of transverse reinforcement.



**FIGURE 6.28** Beam-column joint analysis: (a) forces and moments, case 1; (b) forces and moments, case 2; (c) resolved forces, case 1; and (d) resolved forces, case 2.

The design shear force is determined by subtracting the column shear force from the tensile force in the top beam reinforcement and the compressive force at the bottom of the beam on the opposite face of the column. The stress in the beam reinforcement is taken as  $1.25 f_y$  (Section 21.5.1.1).

$$T_L \text{ due to six \#9} = A_s \times 1.25 f_y = 6 \times 1.0 \times 1.25 \times 60 = 450 \text{ kip}$$

$$C_R \text{ due to six \#8} = 6 \times 0.79 \times 1.25 \times 60 = 356 \text{ kip}$$

Column horizontal shear force,  $V_h$ , is obtained by assuming a point of contraflexure at mid-height of column and by moment equilibrium condition at the frame joint.

$$\begin{aligned} V_h &= \frac{M_u^L + M_u^R}{H} \\ &= \frac{1055 + 186}{13} = 95.46 \text{ kip, use 96 kip} \end{aligned}$$

The net shear force is  $T_L + C_R - V_h = 450 + 356 - 96 = 710 \text{ kip}$ .

The example column joint is confined on two opposite faces as given in the statement of the problem. Therefore,

$$\begin{aligned} \phi V_c &= 15 \sqrt{f'_c} A_j \\ &= \frac{15 \sqrt{5000} \times 34 \times 34}{1000} = 1226 \text{ kip} > 620 \text{ kip} \quad (\text{Section 21.5.3}) \end{aligned}$$

Note that  $A_j$  = effective cross-sectional area within the joint equal to the joint depth times an effective width. The effective width is the smaller of

- Beam width + joint depth =  $28 + 34 = 62$  in.
- Beam width + twice the smaller distance from beam edge to column edge equal to  $28 + 2 \times 3 = 34$  in.

Observe the joint shear is a function of effective cross-sectional area  $A_j$  of the joint and the square root of the concrete compressive strength  $\sqrt{f'_c}$  only. If the net shear exceeds the nominal shear strength  $\phi V_c$  (equal to  $20\sqrt{f'_c}A_j$ ,  $15\sqrt{f'_c}A_j$ , or  $12\sqrt{f'_c}A_j$ , depending on the confinement provided at the joint), then the designer has no choice but to increase  $f'_c$  of concrete and/or the size of columns.

A column face is considered confined by a beam if the beam width is equal to at least 75% of the column width. (No mention is made in ACI 318-02 for the required depth of beam.) When joints are confined on all four sides, transverse reinforcement within the joint required per Section 21.4.4 may be reduced by 50%. Hoop spacing is permitted to a maximum of 6 in (see Figure 6.29).

### 6.11.9 SPECIAL REINFORCED CONCRETE SHEAR WALL

**Given:** A shear wall that is part of a lateral load-resisting system of a 10-story building located in a high seismic zone that has the following seismic characteristics:

$S_1$  = maximum considered earthquake, 5% damped, spectral response acceleration at a period of  $1\text{ s} = 0.85g$

$S_s$  = maximum considered earthquake, 5% damped, spectral response acceleration at short periods =  $1.80g$

Site class =  $D$  (as determined by project geotechnical engineer)

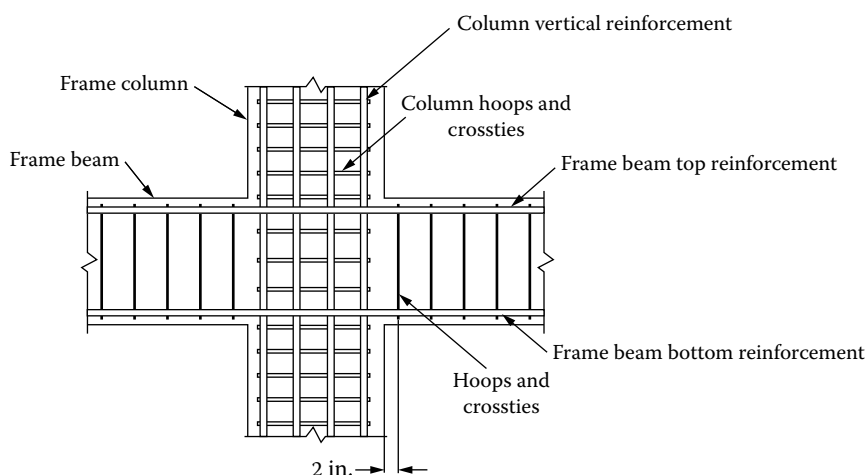
Seismic design category,  $SDC = D$

Reliability/redundancy factor,  $\rho = 1.0$

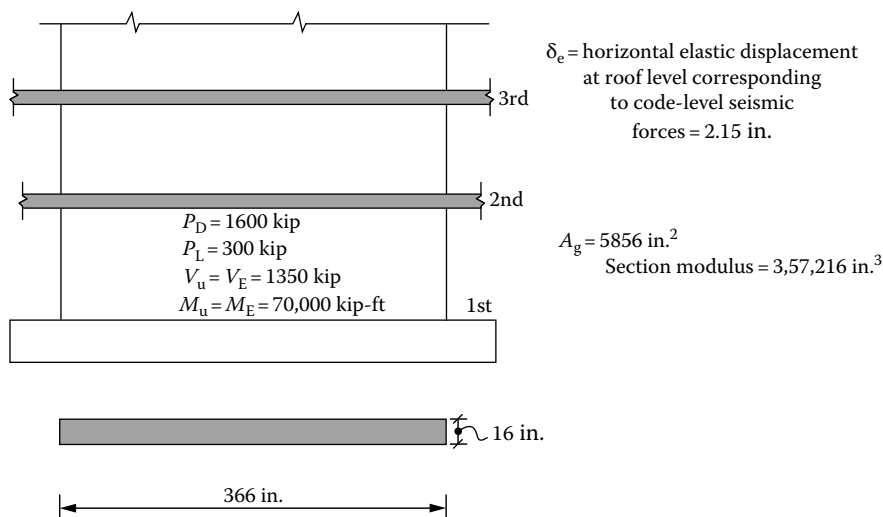
Seismic importance factor,  $I_E = 1.0$

Specified compressive strength of concrete  $f'_c = 5000$  psi

Specified yield strength of reinforcement  $f_y = 60$  ksi



**FIGURE 6.29** Beam–column joint; special moment frame. Transverse reinforcing in the joint is the same as for the frame column. A 50% reduction is allowed if the joint is confined on all the four faces. Maximum spacing of transverse reinforcement is equal to 6 in.



**FIGURE 6.30** Design example; partial shear wall elevation and plan.

Figure 6.30 shows a partial elevation and plan of the wall along with the ultimate axial forces and moments due to gravity and lateral loads. The dead load,  $P_D$ , includes the self-weight of the wall.  $P_L$  is the reduced live load. Also shown therein are the section properties of the wall and the horizontal displacement  $\delta_e$  equal to 2.15 in. at the roof level. The displacement is the lateral elastic deflection due to design basis code level earthquake loads. As will be seen presently, this displacement multiplied by the  $C_d$  factor is used to determine the requirements for detailing boundary elements.

The wall has been analyzed using the following assumptions:

- The base of the wall is fixed
- The effective section properties of the wall are based on a cracked section
- The flexural rigidity =  $0.5E_cI_g$
- The shear rigidity =  $0.4E_cA_w$
- The actual rigidity =  $E_cA_g$

It should be noted that a computer analysis is almost always necessary to determine the building's response. This is because it is mandated in recent seismic codes to consider variables such as uncracked and cracked concrete section properties and some soil or foundation deformation beneath the structure's base.

#### Required:

- The calculation of ultimate design loads and moments using ASCE 7-05 load combinations.
- The preliminary sizing of the wall using a rule-of-thumb approach.
- The design of wall for shear.
- The design of wall for combined axial load and bending moment.
- The determination of boundary element requirements using both stress index and displacement-based methods.
- The design of boundary elements.
- The schematics showing reinforcement layout.
- The design shall be in accordance with ACI 318-05.

**Solution:****Load Combinations:**

1.  $1.2D + 1.0E + f_1L = f_2S$
2.  $0.9D = 1.0E$

For compression check,  $E = \rho Q_E + 0.25_{DS}D$

For tension check,  $E = \rho Q_E - 0.25_{DS}D$

$\rho = 1$  and  $S_S = 1.80$  as given in the statement of the problem

$S_{MS} = F_a S_S$ ,  $F_a = 1.0$  for site class  $D$  with  $S \geq 1.25 = 1.0$   $S_S = 1.80$

$S_{DS} = 2/3 S_{MS} = 2/3 \times 1.80 = 1.20$

Factored axial load,  $P_u$ , for compression check

$$P_u = 1.2 (1600) + 1.0 (1 \times 0 \times 0.2 \times 1.20 \times 1600) + 300 + 0 = 2604 \text{ kip}$$

Factored axial load,  $P_u$ , for tension check

$$P_u = 0.9 \times 1600 - 1 \times 0 - 0.2 \times 1.2 \times 1600 = 1056 \text{ kip}$$

The two sets of design forces and moments for the example are

$$\begin{array}{ll} P_u = 2604 \text{ kip} & P_u = 1056 \text{ kip} \\ M_u = 71,000 \text{ kip-ft} & M_u = 71,000 \text{ kip-ft} \\ V_u = 1400 \text{ kip} & V_u = 1400 \text{ kip} \end{array}$$

**6.11.9.1 Preliminary Size Determination**

Since the length of the wall has been set at 30.5 ft, only the thickness  $t$  is adjusted to limit shear stress. The maximum shear stress allowed per Section 21.7.4.4 is  $8\sqrt{f'_c}$ , but experience has shown that limiting shear stress between  $3\sqrt{f'_c}$  and  $5\sqrt{f'_c}$  usually results in an economical wall design. For the example walls, using  $4\sqrt{f'_c} = 4\sqrt{5000} = 283$  psi as the limiting shear stress, the required wall thickness equals  $t = 135,000 / (30 \times 12 \times 283) = 13.25$  in.

However, because of boundary element considerations we will use 16 in. as the wall thickness.

A few thoughts about preliminary sizing of shear walls. An estimate of wall length and thickness based on a reasonable shear stress using only the base shear may not be adequate for resisting design moments. The resulting area of vertical boundary reinforcement may be too high, quickly leading to unworkable details. Thus, it is prudent to verify that the wall thickness determined on the basis of shear stress is also thick enough to allow room for placement of reinforcing steel and concrete.

**6.11.9.2 Shear Design**

Shear design using ACI 318-05 requirements is quite straightforward. Typically, the shear demand is taken directly from the lateral analysis without having to go through load combinations because, most often, horizontal shear resulting from gravity loads is negligible unless, of course, the building is highly irregular with built-in  $P\Delta$  effects. For the example wall,  $V_u = V_E = 1350$  kip as obtained from a lateral analysis performed by using the ultimate earthquake loads.

Next, the required horizontal reinforcement is calculated from the usable shear capacity equation

$$\phi V_n = \phi A_{CV} (\alpha_c \sqrt{f'_c} + \rho_n f_y)$$

where

$V_n$  is the nominal shear capacity

$\phi$  is the strength-reduction factor = 0.6 (see Section 9.3.4)

$A_{CV}$  is the gross area of wall equal to its length times the thickness



$\alpha_c$  is the coefficient defining the relative contribution of concrete strength to wall strength, typically taken as equal to 2.0. (Note that Section 21.7.4.1 permits  $\alpha_c = 3.0$  for squat walls with  $h_w/l_w \leq 2.0$ , and a linear variation between 3.0 and 2.0 for intermediate values of  $h_w/l_w$ .)

The controlling ratio for the design of wall pier is based on the larger of overall dimensions of the wall or a segment of the wall. It is permitted to use  $\alpha_c = 2.0$  in all cases.)

$\rho_n$  is the ratio of area horizontal reinforcement to gross concrete area perpendicular to it

$f'_c$  is the specified compressive strength of concrete, psi

$f_y$  is the specified yield strength of reinforcement, psi

For the example wall, the shear demand

$$V_u = V_E = 1350 \text{ kip}$$

Assuming #5 at 15 horizontal reinforcement, each face

$$\rho_n = 0.31 \times 2 \times 12 / 16 \times 12 \times 15 = 0.0026$$

$$\begin{aligned} \phi V_n &= 0.6 \times 16 \times 366 / 1000 (2\sqrt{5000} + 0.0026 \times 60,000) \\ &= 1045 \text{ kip} < 1350 \text{ kip} \quad \text{NG} \end{aligned}$$

Try #6 at 12 horizontal, each face

$$\rho_n = 0.44 \times 12 / 16 \times 12 = 0.0046$$

$$\begin{aligned} \phi V_n &= 0.6 \times 16 \times 366 / 1000 (2\sqrt{5000} + 0.0046 \times 60,000) \\ &= 1467 > V_u = 1350 \text{ kip} \end{aligned}$$

Use #6 at 12 horizontal, each face

Check for minimum horizontal reinforcement

$$\rho_n \geq 0.0025$$

Check for maximum allowable nominal shear strength

$$V_n \not\leq 8A_{CV}\sqrt{f'_c}$$

$$\begin{aligned} 8A_{CV}\sqrt{f'_c} &= 8 \times 16 \times 366 / 1000 \sqrt{5000} \quad (\text{Section 21.7.2}) \\ &= 3312 \text{ kip} > 1350 / 0.6 = 2250 \text{ kip} \quad (\text{Section 21.7.4.4}) \end{aligned}$$

### 6.11.9.3 Shear Friction (Sliding Shear)

The shear design performed in the previous section is intended to prevent diagonal tension failures rather than direct shear transfer failures. Direct shear transfer failure, also referred to as sliding shear failure, can occur by the sliding of two vertical segments of a wall at weak sections such as at construction joints. The shear resistance is verified by using the equation

$$V_n = A_{vf} f_y \mu \quad (11.25)$$

where

$A_{vf}$  is the area of shear friction reinforcement, in.<sup>2</sup> that crosses the potential sliding plane

$\mu$  is the coefficient of friction = 1.0 for a normal weight concrete surface roughened to 1/4 in. amplitude.

Additionally, ACI 318-05 permits permanent net compression across the shear plane as additive to the resistance provided by shear friction reinforcement. For the example shear wall, we will conservatively ignore the beneficial effect of compression.

As will be seen presently, the vertical reinforcement,  $A_{vf}$ , required to satisfy the governing axial load and moment combination is equal to

$$\begin{aligned} A_{vf} &= 32 \text{ \# } 11 \text{ plus } 36 \text{ \# } 7 \\ &= 32 \times 1.56 + 36 \times 0.60 \\ &= 71.5 \text{ in.}^2 \end{aligned}$$

The sliding shear resistance  $V_n = 71.5 \times 60 \times 1 = 4290 \text{ kip}$

$$\phi V_n = 0.65 \times 4290 = 2788 \text{ kip} > 1350 \text{ kip}$$

Therefore, the wall is acceptable for sliding shear

Section 11.7.5 limits the shear friction strength to  $0.2f'_c A_c$  or  $800A_c$  in.-lb, where  $A_c$  is the area of concrete resisting shear transfer.

For the example wall

$$V_n = 0.2f'_c A_c = 0.2 \times 5000 \times 16 \times 366 / 1000 = 5836 \text{ kip}$$

$$V_n = 800A_c = 800 \times 16 \times 366 / 1000 = 4685 \text{ kip} \leftarrow \text{controls}$$

$$\phi V_n = 0.65 \times 4685 = 3045 \text{ kip} > 1350 \text{ kip}$$

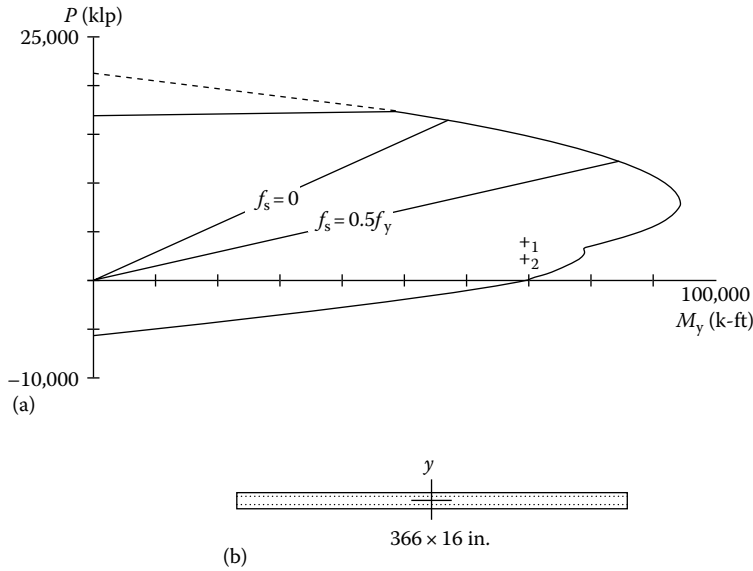
#### 6.11.9.4 Longitudinal Reinforcement

The design of vertical reinforcement to resist a given set of axial loads and bending moments is typically a trial-and-error procedure. Give a wall section and an assumed reinforcement layout, the section is checked from the governing axial load and bending moment combinations. Although hand calculations and spreadsheet approaches are possible, the most desirable and expedient method is to use a computer program such as PCACOL developed by Portland Cement Association.

Figure 6.31 shows an interaction diagram for the wall with 16 #11 placed near the wall boundaries and #7 at 9, each face, in between the boundaries for a total  $A_{vf}$ —71.5 in.<sup>2</sup>. Figure 6.31 is a printed screen output of the PCACOL run. Points 1 and 2 that lie within the interaction curve represent the governing loads. Point 1 is for  $P_u = 2604 \text{ kip}$  and  $M_u = 71,000 \text{ kip-ft}$ , and point 2 is for  $P_u = 1056 \text{ kip}$  and  $M_u = 71,000 \text{ kip-ft}$ . Since both points lie within the interaction curve, the example wall is acceptable for the ultimate axial load and moment combinations.

#### 6.11.9.5 Web Reinforcement

Section 21.7.2.1 requires a uniform distribution of both horizontal shear reinforcement,  $P_n$ , and vertical reinforcement,  $P_v$ . Further, to control the width of inclined cracks due to shear, a minimum



**FIGURE 6.31** (a) Shear wall load/moment interaction diagram and (b) cross section of wall.

reinforcement ratio equal to 0.0025 and a maximum spacing of 18 in. is specified for both  $P_n$  and  $P_u$ . However, a reduction in the reinforcement ratio is permitted if the design shear force,  $V_u$ , is less than  $A_c \sqrt{f'_c}$ .

The minimum ratios of  $P_u$  if  $V_u \leq A_c \sqrt{f'_c}$  (see Section 14.3) are

- 0.0020 for #5 and smaller bars, with  $f_y \geq 60,000$  psi
- 0.0025 for other bars
- 0.0020 for welded fabric not larger than W31 or D31

The minimum ratios of  $P_v$  (vertical reinforcement) for the same condition are

- 0.0012 for #5 and smaller bars, with  $f_y \geq 60,000$  psi
- 0.0015 for other bars
- 0.0010 for welded wire fabric not larger than W31 or D31

In seismic design, the vertical reinforcement at the bottom few stories of a shear wall is typically controlled by bending requirements. The upper levels are likely to be controlled by the ACI 318-02 minimum reinforcement ratio of 0.0025.

For the example wall,

$$A_{cv} \sqrt{f'_c} = 2 \times 366 \times 16 / 1000 \sqrt{5000} / 1000 = 414 \text{ kip} < V_u = 1400 \text{ kip}$$

The minimum horizontal reinforcement

$$\begin{aligned} &= 0.0025 \times b \times t \\ &= 0.0025 \times 16 \times 12 \\ &= 0.48 \text{ in.}^2 \end{aligned}$$

Use #5 at 15 giving a steel area =  $2 \times 0.31 \times 12/15 = 0.496 \text{ in.}^2$   
 $> 0.48 \text{ in.}^2$

Section 21.7.2.2 requires at least two curtains of reinforcement if the factored shear force  $V_u$  exceeds  $2A_{CV}\sqrt{f'_c}$ .

For the example wall,

$$2A_{CV}\sqrt{f'_c} = 2 \times 366 \times 16/1000 \sqrt{5000}/1000 = 828 \text{ kip}$$

Since  $V_u = 1350 \text{ kip}$  is greater than 828 kip, we use two layers of #5 at 15. The reason for two layers of reinforcement is to place web reinforcement close to the wall surface to inhibit fragmentation of concrete in the event of a severe cracking of concrete during an earthquake.

### 6.11.9.6 Boundary Elements

#### 6.11.9.6.1 Stress Index Procedure

This method is quite straightforward (Section 21.7.6.3). A stress index of  $0.2f'_c$  is used as a benchmark for the maximum extreme fiber compressive stress corresponding to factored forces that include gravity and earthquake effects. If the calculated compressive stress is less than the index value, special boundary elements are not required. If not, detailing of boundary elements in accordance with Section 21.7.6.4 is required. The compressive stresses are calculated for the factored axial forces and bending moments using a linear elastic model and gross-section properties.

For the example wall,

$$A_g = 366 \times 16 = 5856 \text{ in.}^2$$

$$I_g = 16 \times 366^3/12 = 65,370,528 \text{ in.}^4$$

$$S_{yy} = 65,370,528/183 = 357,216 \text{ in.}^3$$

$$P_u/A_g + M_u/S_{yy} = 2604/5856 + 71,000 \times 12/357,216$$

$$= 0.445 + 2.385 = 2.83 \text{ ksi} > 0.2f'_c$$

$$= 0.2 \times 5000$$

$$= 1.0 \text{ ksi}$$

Therefore, boundary elements are required by the stress-index procedure.

#### 6.11.9.6.2 Displacement-Based Procedure

In this procedure (Section 21.7.6.2), the neutral axis depth  $c$ , which is directly related to the strain at the extreme compression fiber, is used as an index to determine whether or not boundary elements are required. Boundary zone detailing is required if

$$c > l_w/600(\delta_u/h_w) \quad (21.8)$$

where

$c$  is the distance from the extreme compression fiber to the neutral axis

$l_w$  is the length of entire wall or wall-pier (segment)

$\delta_u$  is the design displacement at the top of a wall or segment equal to elastic displacement,  $\delta_e$ , due to code level seismic forces multiplied by  $C_d$ , the deflection amplification factor given in governing codes

$h_w$  is the height of entire wall or wall segment

The displacement-based approach is founded on the assumption that the inelastic response of the wall is due to flexural yielding at a critical section, typically at its base. Given this proviso, the method of determining whether or not boundary elements are required is as follows:

- Analytically displace the wall at the top equal to the design displacement,  $\delta_u$ . This displacement is equal to the elastic displacement,  $\delta_e$ , calculated for code seismic loads, multiplied by a deflection amplification factor,  $C_d$ . Thus,  $\delta_u = \delta_e \times C_d$ .
- Calculate the strain in the extreme compression fiber of the wall corresponding to the horizontal displacement of  $\delta_u$ . Since the strain is related to the depth of neutral axis,  $c$ , it is used indirectly for evaluating the strain. Equation 21.8 of ACI 318/05 is used to calculate  $c$ . The depth  $c$  may be considered, in a conceptual sense, as an index depth of neutral axis for comparing against the actual depth calculated for the largest ultimate load,  $P_u$ , and the corresponding moment,  $M_u$ .
- Next, compute the neutral axis depth  $c$ , using a linear strain distribution (Section 10.2), or by assuming yielding of all vertical reinforcement in compression or tension. The latter is recommended by the 1999 Blue Book of the Structural Engineers Association of California (SEAOC). The depth  $c$  is calculated for the factored axial force and nominal moment strength consistent with the displacement,  $\delta_u$ , at the top of the wall resulting in the largest neutral axis depth.
- If the calculated value of  $c$  is greater than the index value, then special boundary elements detailed are similar to those of a ductile column.

For the example wall, we have the following two load combinations:

$$P_u = 2470 \text{ kip}$$

$$P_u = 1056 \text{ kip}$$

$$M_u = 70,000 \text{ kip-ft}$$

$$M_u = 70,000 \text{ kip-ft}$$

$$V_u = 1350 \text{ kip}$$

$$V_u = 1350 \text{ kip}$$

Using the PCACOL column design program, the depth of the neutral axis was found to be 108 in.

The term  $\delta_u$  is design displacement defined as the lateral displacement expected for the design-based earthquake. It is invariably larger than the elastic displacement,  $\delta_e$ , calculated for code-level forces applied to a linear elastic model. Although the analysis may consider the effects of cracked sections, torsion,  $P\Delta$  forces, and foundation flexibility, it does not account for the expected inelastic response. Thus,  $\delta_u$  is calculated by multiplying  $\delta_e$  by a deflection amplification factor  $C_d$  given in the governing codes or standards. For example, ASCE 7-05 and IBC-06 specify  $C_d = 5.5$  and  $6.5$  for special reinforced concrete moment frames and dual systems consisting of SMRF and special reinforced concrete walls. For the example problem, having a building system of special reinforced concrete wall,  $C_d = 5.0$ , by both ASCE and IBC.

The elastic deflection  $\delta_e$  of the shear wall at the roof level = 2.15 in., as obtained from a linear elastic analysis of the building under code-prescribed seismic forces. This is given in the statement of the problem.

Therefore

$$\delta_u = \frac{C_d \delta_e}{I_E} = \frac{5 \times 2.15}{1} = 10.75 \text{ in.}$$

$$\frac{\delta_u}{h_w} = \frac{10.75}{18 \times 12} = 0.0076 > 0.007 (\text{min})$$

$$c = \frac{l_w}{600 \left( \frac{h_w}{l_w} \right)} = 366 / (600 \times 0.0076) = 80.26 \text{ in.} < 108 \text{ in.}$$

Special boundary elements are therefore required. It is interesting to note that for the example wall, both the stress index and the strain index methods lead to the same conclusion, namely, that boundary elements are required. This may not be the case in all designs. A more likely scenario would be for the stress index method to show that boundary elements are required, while the strain method does not. Although ACI 318-05 does not require both criteria to be satisfied, many engineers choose to detail the boundary zones as required by the stress index method. Keep in mind, in seismic design, more is less!

#### 6.11.9.6.3 Reinforcement Details

Irrespective of the method used to determine whether or not special boundary elements are required, the detailing is performed according to Sections 21.6.6.4 through 21.6.6.6, and is summarized as follows:

- The required width of boundary element is given by the larger of  $c - 0.1l_w$  and  $c/2$
- Where required, special boundary elements are extended from the critical section a distance not less than  $l_w$  or  $M_u/4V_u$

For the example wall, the width of boundary element is the larger of

$$C = 0.1 l_w = 108 - 0.1 \times 366 = 71.4 \text{ in.} \leftarrow \text{controls}$$

$$c/2 = 108/2 = 54 \text{ in.}$$

Considering the placement of vertical bars, detail a boundary element for a width of 75 in. (Figure 6.32).

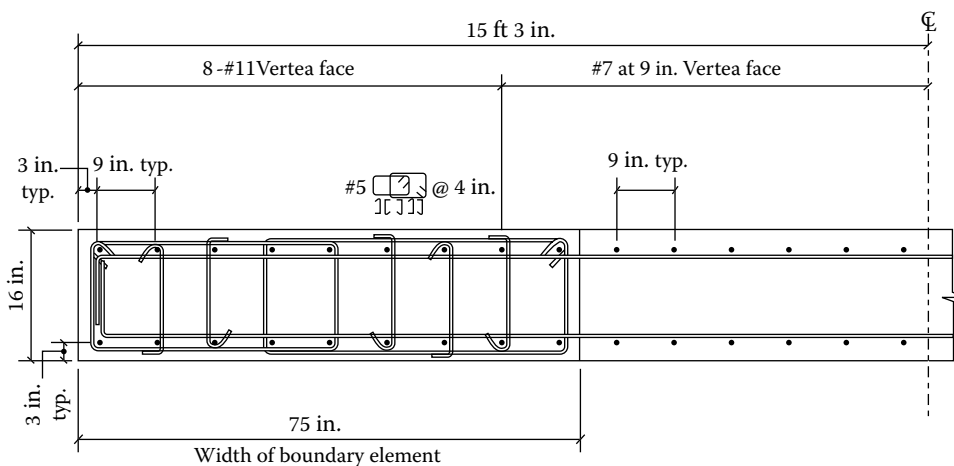


FIGURE 6.32 Shear wall example; schematic reinforcement.

The vertical extension of the boundary element must not be less than

$$l_w = 366 \text{ in.} \quad \text{or} \quad \leftarrow \text{controls}$$

$$M_u/4V_u = 71,000 \times 12/1400 = 608.6 \text{ in.}$$

**The confinement of 16 × 75 in. boundary elements:**

**Confinement perpendicular to the wall:** The maximum allowable spacing of hoops and crossties, assuming #5 bars,

$$\begin{aligned} S_{\max} &= 0.25 \times \text{minimum member dimensions} \\ &= 0.25 \times 16 = 4 \text{ in.} \quad (\text{Controls}) \\ &= 6 \times \text{diameter of longitudinal bar} \\ &= 6 \times 1.41 = 8.5 \text{ in.} \\ &= s_x = 4 + (14 - b_x/3) = 4 + (14 - 10/3) = 5.33 \text{ in.} \end{aligned}$$

The required cross-sectional area of confining reinforcement  $A_{sh}$ , in the 16 × 75 in. boundary elements, using  $s = 4$  in., is given by

$$A_{sh} = 0.09 s h_c f'_c / f_y$$

where  $h_c$  is the cross-sectional dimension of boundary element measured center-to-center of confining reinforcement.

In our case,  $h_c = 16 - (3 + 3) + 1.41 + 0.625 = 12$  in.

$$A_{sh} = 0.09 \times 4 \times 12 \times 5/60 = 0.36 \text{ in.}^2$$

No. 5 hoops with two legs provide  $A_{sh} = 2 \times 0.31 = 0.62 \text{ in.}^2 > 0.36 \text{ in.}^2$

**Confinement parallel to the wall:**

$$h_c = 75 - (3 + 3) + 1.41 + 0.625 = 71 \text{ in.}$$

$$A_{sh} = 0.09 \times 4 \times 71 \times 5/60 = 2.14 \text{ in.}^2$$

With two hoops consisting of two legs each, and five crossties,

$$A_{sh} \text{ provided} = 9 \times 0.31 = 2.79 \text{ in.}^2 > 2.13 \text{ in.}^2$$

In most designs, special boundary elements may not be required by calculations for the entire height of walls. However, to prevent the buckling of boundary longitudinal elements even in cases where they are not done by design, Section 21.7.6.5 requires transverse ties not exceeding a vertical spacing of 8 in., if the vertical reinforcement ratio is greater than  $400/f_y$ . The transverse reinforcement shall consist of either single or overlapping hooks. As in ductile columns, crossties are permitted. For calculating the ratio  $400/f_y$ , only the reinforcement within the wall boundary element is included.

Using the most common value of  $f_y = 60,000$  psi, the ratio  $400/f_y = 400/60,000 = 0.0067$ . If the ratio of vertical reinforcement is greater than this value, then hoops supplemented with crossties are required. What if the ratio of vertical bars placed in between the boundary zones is greater than 0.0067? Do they also need to be tied? Yes, but only if the vertical reinforcement ratio is greater than 0.01, or where the vertical reinforcement is required as a compression reinforcement (see Section 14.3.6). A schematic placement of reinforcement is shown in Figure 6.33.

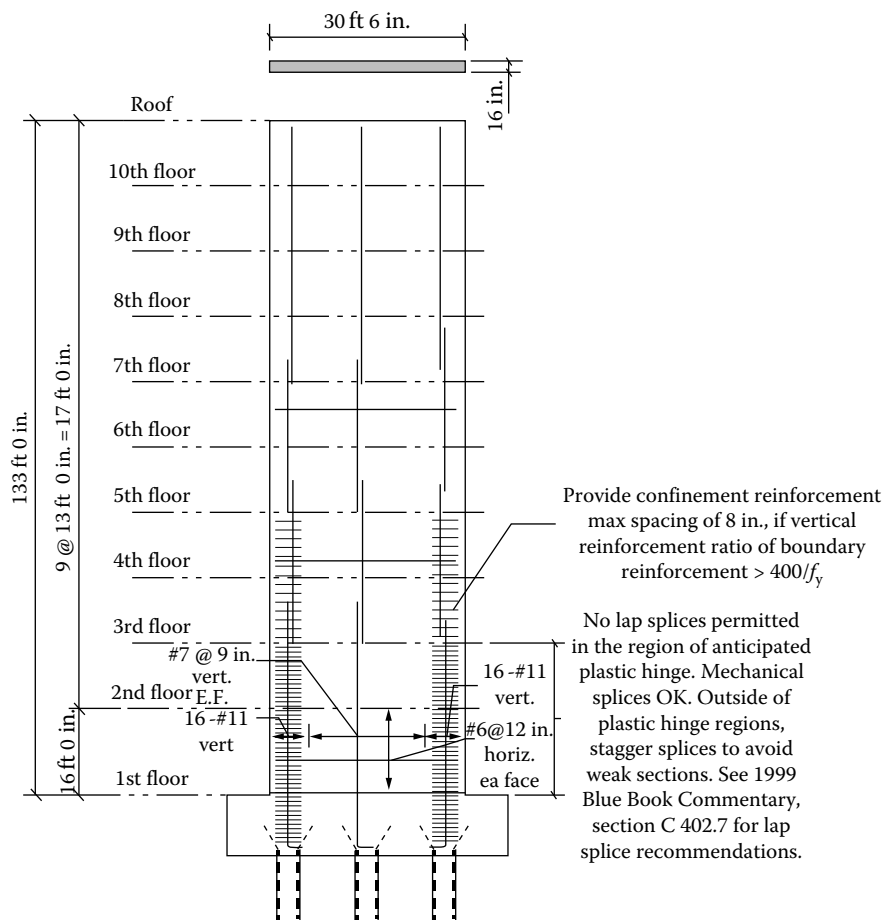


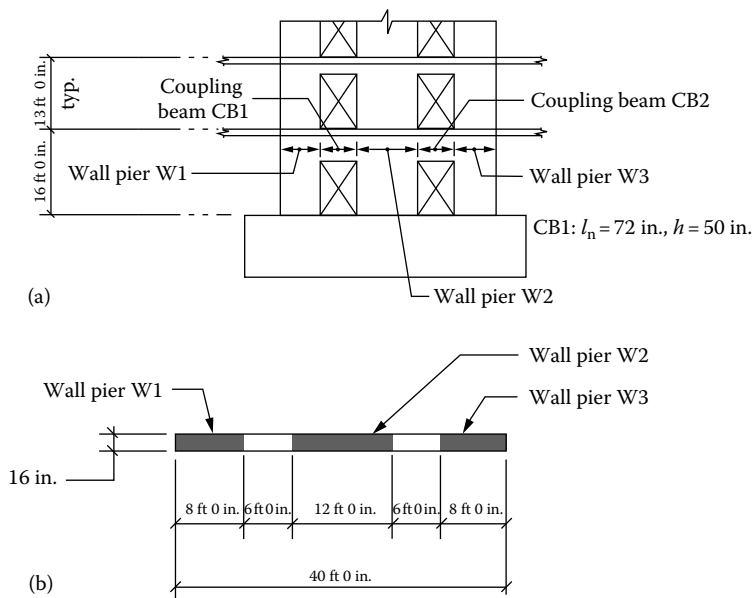
FIGURE 6.33 Wall elevation showing schematic placement of reinforcement.

#### 6.11.10 SPECIAL REINFORCED CONCRETE COUPLED SHEAR WALLS

**Given:** A 40-ft-long by 16-in.-thick shear wall with openings as shown in Figure 6.34. The shear wall forms part of a lateral load-resisting system of a 10-story concrete building located in a high seismic zone. A computer analysis has been performed for the building using code-prescribed lateral forces and gravity loads. The analysis typically has provided moment and shear forces for each coupling beam, and moments, shear forces, and axial forces for each wall segment commonly referred to as wall pier. In modeling the shear walls, effective section properties, rather than gross properties, are used as required by most current codes.

The first step in design is the determination of ultimate design values, generally the  $P_u$ ,  $M_u$ , and  $V_u$  using code-specified load combinations. Typically, the design of an element such as a wall pier or a coupling beam is verified for a number of design load combinations. This is because several lateral load analyses are performed to account for changes in load directions, minimum eccentricities in each direction, uplift and downward effects of seismic loads, etc. The computation of design values using different load combinations that includes several lateral load analyses is indeed a major task invariably necessitating the use of computers. Without dwelling on this





**FIGURE 6.34** Coupled shear walls: (a) partial elevation and (b) plan.

further, we will proceed with the design of coupling beam CB1 and wall pier W1 by presupposing the following ultimate design values:

CB1	$V_u = 300$ kip
	$M_u = 12,000$ kip-ft, left end
	$M_u = 8$ kip-ft, right end
Wall pier W1	$P_u = 1500$ kip
	$V_u = 210$ kip
	$M_u = 45,000$ kip-ft

**Required:**

1. Coupling beam design
  - a. The design of diagonal reinforcement
  - b. The design of transverse reinforcement
  - c. Schematic section through coupling beam
2. The design of wall pier W1
  - a. The design for shear
  - b. The design for combined flexure and axial loads
  - c. Determine boundary element requirements using
    - i. The stress-index procedure
    - ii. The displacement-based procedure
    - iii. The schematic layout of reinforcement

The design shall be in accordance with ACI 318-05.

**Solution:**

**6.11.10.1 Coupling Beams**

**6.11.10.1.1 Diagonal Reinforcement**

Two simultaneous criteria establish whether diagonal reinforcement is required in coupling beam.

1. Clear length-to-span ratio, often referred to as the aspect ratio of the beam, is less than 2, i.e.,  $l_n/h < 2.0$
2. The factored shear force,  $V_u$ , is greater than  $4\sqrt{f'_c} A_{cp}$

For the example coupling beam CB1, we have

$$f'_c = 4000 \text{ psi}, f_y = 60,000 \text{ psi}, A_{cp} = b \times h = 16 \times 50 = 800 \text{ in.}^2$$

$$V_u = \phi V_n = 210 \text{ kip}, l_n = 72 \text{ in.}$$

$$l_n/h = 72/50 = 1.44 < 2 \text{ (Aspect ratio criterion)}$$

$$V_u = 210 \text{ kip} > 4\sqrt{4000} \times 800/1000 = 203 \text{ kip} (V_u \text{ criterion})$$

Therefore, because of both the aspect ratio and the  $V_u$  criteria, diagonal reinforcement must be provided.

Observe that if either of the criteria was not satisfied, we would have had the option of designing the beam CB1 without the diagonal reinforcement. We could have used conventional horizontal reinforcement to resist flexure and vertical stirrups to resist shear. However, research has shown that diagonal reinforcement improves coupling beam performance, even at lower shear stress level (see SEAOC's 1999 Blue Book Commentary, Section C 407.7).

In some buildings it may be impractical to use diagonal reinforcement. Do the designers have any fallback position? Yes, they do. The requirements given in Section 21.6.7.3 for diagonal reinforcement may be waived if coupling beams are not used as part of the lateral force resisting system. Such beams are permitted at locations where damage to these elements does not impair vertical load-carrying capacity or egress of the structure, or integrity of nonstructural components and their connections to the structure.

Returning to the example problem, the equation that determines the area of diagonal reinforcement  $A_{vd}$  is given by

$$V_n = 2A_{vd}f_y \sin \alpha \leq 10\sqrt{f'_c} A_{cp} \quad (6.10)$$

This can be written as

$$A_{vd} = \phi V_n / 2\phi f_y \sin \alpha = V_n / 2\phi f_y \sin \alpha$$

where

$\alpha$  is the angle between the diagonal reinforcement and the longitudinal axis of the coupling beam (Figure 6.35).

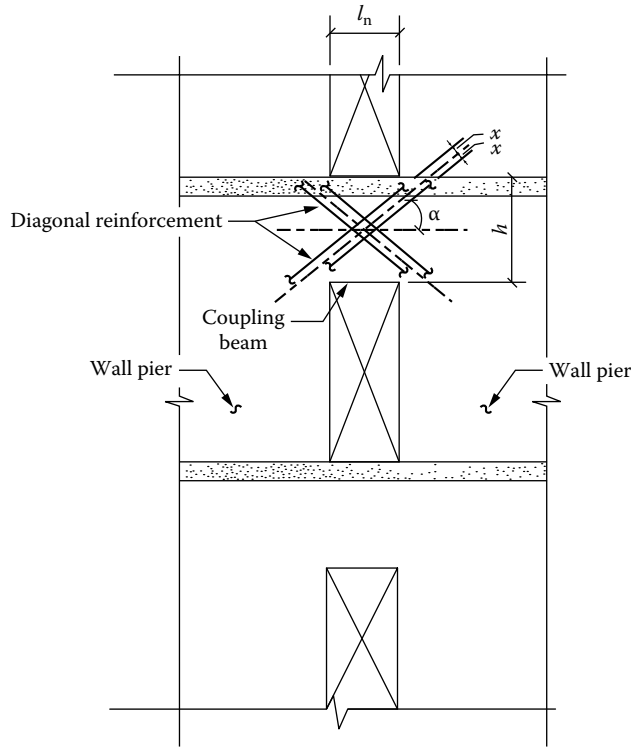
$A_{vd}$  is the area of diagonal reinforcement in each diagonally reinforced beam.

It should be noted that diagonally oriented reinforcement is effective only if the bars are placed with a reasonably large inclination angle  $\alpha$ . So, diagonally reinforced coupling beams are restricted to beams having an aspect ratio  $l_w/h < 4.0$ . This ratio approximately corresponds to  $\alpha = 13^\circ$ . Therefore, for beams with a geometry that results in  $\alpha$  less than about  $13^\circ$ , ACI 318-05 does not permit diagonal reinforcement.

Each diagonal element is reinforced similar to a column consisting of longitudinal and transverse reinforcements. The column cage must consist of at least four longitudinal bars, with core dimensions measured to the outside of the transverse reinforcement not less than  $b_w/2$  and  $b_w/5$ . It should be noted that, in practice, minimum required reinforcement clearance often controls the thickness of walls. Typically, a wall thickness of 16 in. or larger is required for the detailing of diagonally reinforced coupling beams.

The required area of longitudinal reinforcement,  $A_{vd}$ , is calculated as follows:

$$A_{vd} = V_u / 2\phi f_y \sin \alpha$$



**FIGURE 6.35** Geometry for calculating  $\alpha$ , the angle between the diagonal reinforcement and the longitudinal axis of the coupling beam. *Note:*  $\tan \alpha = h/2 - x/\cos \alpha / l_n/2$  (solve for  $\alpha$  by trial and error).

This is the same as Equation 2.19, written in a different form. An upper limit of  $10\sqrt{f'_c} A_{cp}$  is imposed for the nominal capacity  $V_n = V_u/\phi$ . For the example problem, the upper limit is equal to

$$10\sqrt{f'_c}/\Phi A_{cp} = 10\sqrt{4000} \times 800/1000 \times 0.75 = 675 \text{ kip}$$

This is greater than the design value of  $V_u = 210$  kip.

Referring to Figure 4.47, we have  $\tan \alpha = h - \frac{2x}{\cos \alpha} / l_n$ . This is a transcendental equation, best solved by trial and error.

Try  $\alpha = 30^\circ$ :  $\tan \alpha = \tan 30^\circ = 0.577$ ,  $\cos 30^\circ = 0.866$

$$\frac{h - \frac{2x}{\cos \alpha}}{l_n} = \frac{50 - \frac{2 \times 6}{0.866}}{72} = 0.50$$

$\tan \alpha = \tan 30^\circ = 0.577$ . Compared to 0.50, this is not close enough.

Try  $\alpha = 28^\circ$ ,  $\tan 28^\circ = 0.552$ ,  $\cos 28^\circ = 0.883$

$$\frac{h - \frac{2x}{\cos \alpha}}{l_n} = \frac{50 - \frac{2 \times 6}{0.866}}{72} = 0.506 \quad \tan \alpha = 0.552$$

Again, not close enough.

Try  $\alpha = 27^\circ$ ,  $\tan 27^\circ = 0.509$ ,  $\cos 27^\circ = 0.891$

$$\frac{h - \frac{2x}{\cos \alpha}}{l_n} = \frac{50 - \frac{2 \times 6}{0.891}}{72} = 0.507 \quad \tan \alpha = 0.509$$

Use  $\alpha = 27^\circ$ ,  $\sin \alpha = 0.459$

$$A_{vd} = \frac{V_u}{2\phi f_y \sin \alpha}$$

$$= \frac{210}{2 \times 0.75 \times 60 \times 0.459} = 5.0 \text{ in.}^2$$

Use four #10 diagonal reinforcements giving  $A_{vd} = 4 \times 1.27 = 5.08 \text{ in.}^2$

#### 6.11.10.1.2 Transverse Reinforcement

The requirements of transverse reinforcement given below are the same as for frame columns of SMRFs.

$$A_{sh} = 0.3 \left( sh_c \frac{f'_c}{f_{yh}} \right) \left[ \frac{A_g}{A_{ch}} - 1 \right] \quad (21.3)$$

$$A_{sh} = 0.09 sh_c \frac{f'_c}{f_y} \quad (21.4)$$

The maximum spacing limits of transverse reinforcement, also referred to as ties, are once again the same as for frame columns. According to Section 21.4.4.2, the limits are

1. One-quarter the minimum member dimensions
2.  $6 \times$  the diameter of diagonal reinforcement

$$3. \quad s_x = 4 + \left( \frac{14 - h_x}{3} \right)$$

$s_x$  should not be less than 4 in. nor can it exceed 6 in., i.e.,  $4 \text{ in.} \leq s_x \leq 6 \text{ in.}$

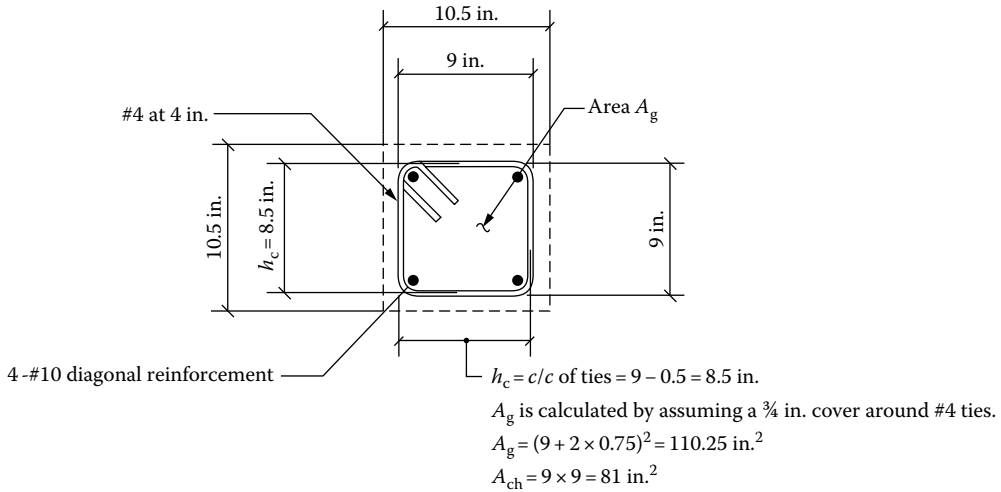
For the diagonally reinforced CB1 we have

1.  $\frac{b_w}{4} = \frac{16}{4} = 4 \text{ in.} \leftarrow$  controls
2.  $6d_b = 6 \times 1.27 = 7.62 \text{ in.}$
3.  $s_x = 4 + \left( \frac{14 - 14}{3} \right) = 4 \text{ in.}$

Substituting the controlling value of 4.0 in. for the spacing  $s$  in Equations 21.3 and 21.4, we get

$$A_g = (9 + 2 \times 0.75)(9 + 2 \times 0.75) = 110.25 \text{ in.}^2$$

Note that  $A_g$  is calculated assuming a minimum cover of  $3/4$  in. around the diagonal core (Figure 6.36).



**FIGURE 6.36** Parameters for calculating diagonal beam reinforcement.

By Equation 21.3,

$$A_{sh} = 0.3 \left( 4 \times 8.5 \times \frac{4}{60} \right) \left[ \frac{110.25}{81} - 1 \right]$$

$$= 0.246 \text{ in.}^2 \leftarrow \text{controls}$$

By Equation 21.4,

$$A_{sh} = 0.09 \times 4 \times 8.5 \times \frac{4}{60} = 0.204 \text{ in.}^2$$

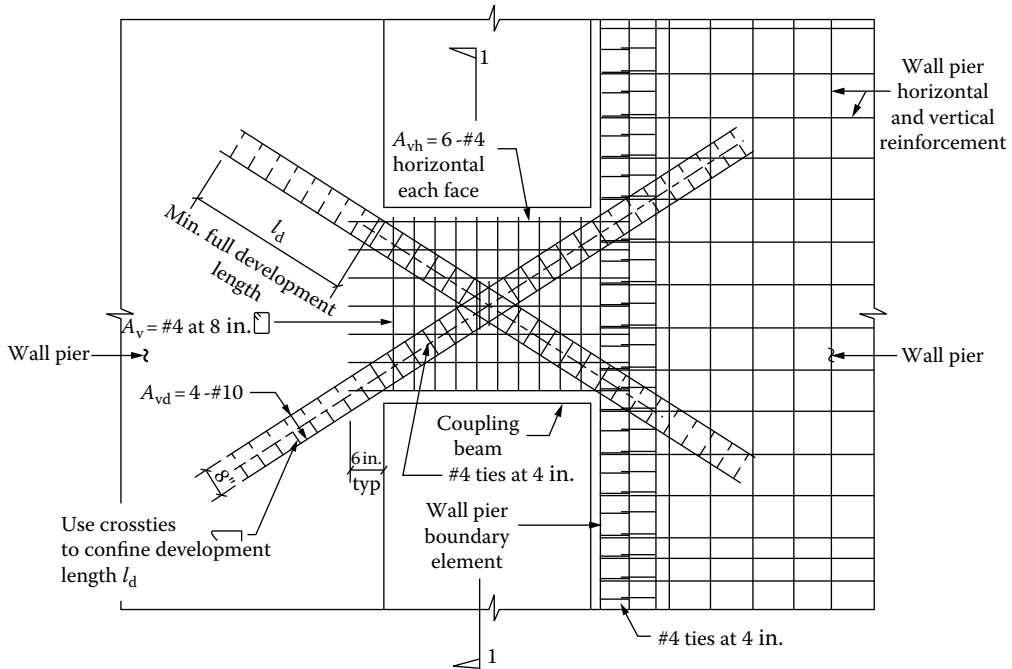
A single #4 loop around four diagonal bars with two legs gives  $A_{sh} = 0.40 \text{ in.}^2$ . Hence, #4 ties at 4 in. spacing are acceptable for the bursting steel requirements.

Note that in our example, the core dimensions of diagonal reinforcement are the same in both directions. In a general case, with differing cross-section dimensions,  $A_{sh}$  is calculated for each direction.

As per Section 21.7.7.4(d), diagonal bars are required to be developed for tension into the wall piers. This is shown in Figure 6.37 where the diagonal bars extend a distance of  $l_d$  beyond the face of the wall pier. Instead of loops, crossties are used along the development length and at the intersection of diagonal bars at the center of diagonal beams.

In addition to the reinforcement calculated thus far, supplemental horizontal and vertical reinforcements are required per Sections 11.8.4 and 11.8.5. The intent of additional reinforcement is to contain the concrete outside the diagonal cores, in case the concrete is damaged by earthquake loading. Since the diagonal reinforcement is designed to resist the entire shear and flexure in the coupling beam, additional transverse and longitudinal reinforcements act primarily as a basketing reinforcement to contain concrete that may spall. It is not necessary to develop the horizontal bars into wall piers.

The minimum reinforcement,  $A_v$ , perpendicular to the longitudinal axis of the coupling beam (meaning vertical reinforcement) shall not be less than  $A_v \geq 0.0025 b_w s$  (Section 11.8.4). The area of horizontal (longitudinal) reinforcement,  $A_{vh}$ , shall not be less than  $0.0015 b_w s_2$ , and  $s_2$  shall not exceed  $d/5$  or 12 in. (Section 11.8.5).



**FIGURE 6.37** Coupling beam with diagonal reinforcement. Each diagonal reinforcement must consist of at least four bars with closely spaced ties. Use wider closed ties or crossties at central intersection. Use crossties to confine development length  $l_d$ .

For the example beam, assuming #4 at eight loops as vertical reinforcement,

$$A_v = \frac{0.2 \times 2 \times 12}{8} = 0.60 \text{ in.}^2 > 0.0025b_ws = 0.0025 \times 16 \times 8 = 0.32 \text{ in.}^2$$

Assuming six #4 horizontal bars at each face,

$$A_{vh} \geq 0.0025b_w \times h = 0.0025 \times 16 \times 50 = 2 \text{ in.}^2 < 6 \times 2 \times 0.2 = 2.4 \text{ in.}^2$$

A schematic section of the coupling beam is shown in Figure 6.38.

### 6.11.10.2 Wall Piers

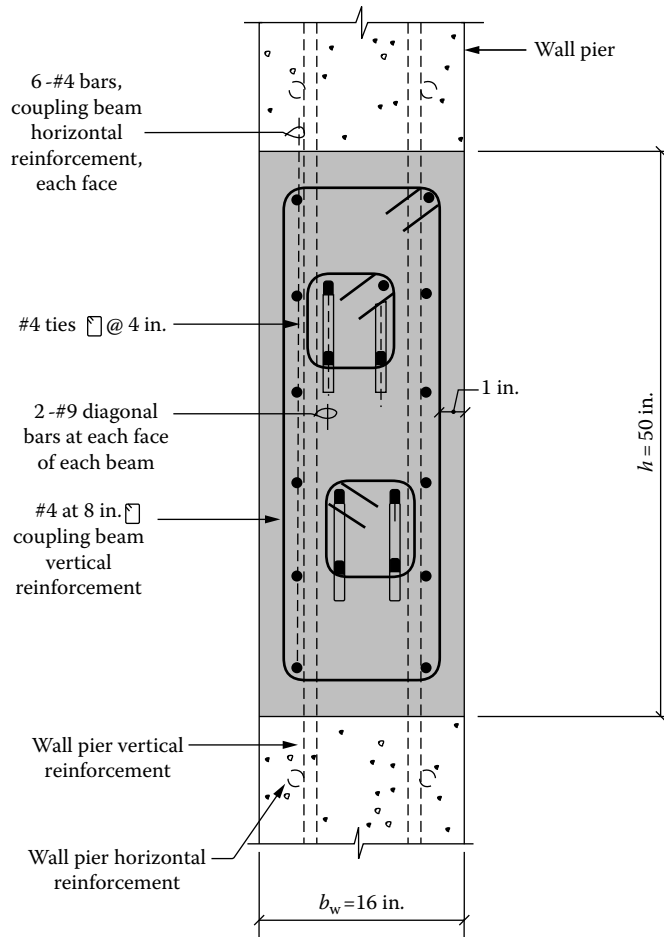
#### 6.11.10.2.1 Shear Design

For the example pier W1,  $V_u = 300$  kip. The parameter  $\alpha_c$ , the coefficient defining the relative contribution of concrete shear strength to the total shear strength of wall, may be conservatively assumed to be equal to 2.0. However, if the designer chooses to calculate  $\alpha_c$ , it should be based on the ratio  $h_w/l_w$ , taken as the larger for the individual wall pier and the entire wall (see Section 21.7.4.2).

For the example wall pier, the overall  $h_w/l_w = 133/40 = 3.325$  and the individual wall pier  $h_w/l_w = 15/8 = 1.875$ .

Thus, the ratio 3.325 controls the determination of  $\alpha$ , giving  $\alpha = 2.0$ .

$$\phi V_n = \phi A_{cv} (\alpha_c \sqrt{f'_c} + \rho_n f_y) \quad (21.7)$$



**FIGURE 6.38** Section 1.1. Schematic section through coupling beam. The purpose of this sketch is to ensure that the wall is thick enough for the proper placement of wall and diagonal beam reinforcement and concrete.

Try #5 at 15 horizontal, each face.

$$\rho_n = \frac{0.31 \times 2 \times 12}{16 \times 12 \times 15} = 0.0026$$

$$A_{CV} = 8 \times 12 \times 16 = 1536 \text{ in.}^2$$

$$\begin{aligned} \phi V_n &= 0.6 \times 1536 (2\sqrt{4000} + 0.0026 \times 60,000) \\ &= 260 \text{ kip} < V_u = 300 \text{ kip} \quad \text{NG} \end{aligned}$$

Try #6 at 15 horizontal, each face.

$$\rho_n = \frac{0.44 \times 2 \times 12}{16 \times 12 \times 15} = 0.0037$$

$$\begin{aligned} \phi V_n &= 0.6 \times 1536 (2\sqrt{4000} + 0.0037 \times 60,000) \\ &= 320 \text{ kip} > 300 \text{ kip} \end{aligned}$$

Use #6 at 15 horizontal, each face.

$$\rho_n = 0.0037 > \rho_{\min} = 0.0025$$

Check for maximum allowable nominal strength.

$$V_n \nless 10A_{cv}\sqrt{f'_c} = \frac{10 \times 1536}{1000} \sqrt{4000} = 971 \text{ kip}$$

$$V_n = \frac{320}{0.6} = 533 \text{ kip} < 971 \text{ kip}$$

#### 6.11.10.2.2 Shear Friction (Sliding Shear)

To determine the sliding shear resistance, we need to know the area of vertical reinforcement  $A_{vf} = 22.24 \text{ in.}^2$ , which will be used to check the sliding shear.

The sliding shear resistance is given by

$$V_n = A_{vf}f_y\mu$$

Using  $\mu = 1.0\lambda$ , where  $\lambda = 1$  for normal weight concrete, and  $A_{vf} = 22.4 \text{ in.}^2$ ,

$$V_n = 22.4 \times 60 \times 1 = 1334.4 \text{ kip} > 300 \text{ kip}$$

Section 11.7.5 limits shear friction strength to  $0.2 f'_c A_c$  or  $800 A_c$ . For the example wall pier,

$$V_n = 0.2 f'_c A_c = \frac{0.2 \times 4000 \times 16 \times 8 \times 12}{1000}$$

$$= 1228 \text{ kip} > 300 \text{ kip}$$

$$V_n = 800 A_c = \frac{800 \times 16 \times 8 \times 12}{1000} = 1228 \text{ kip} > 300 \text{ kip}$$

Therefore, wall pier W1 is acceptable for sliding shear

#### 6.11.10.2.3 Longitudinal Reinforcement

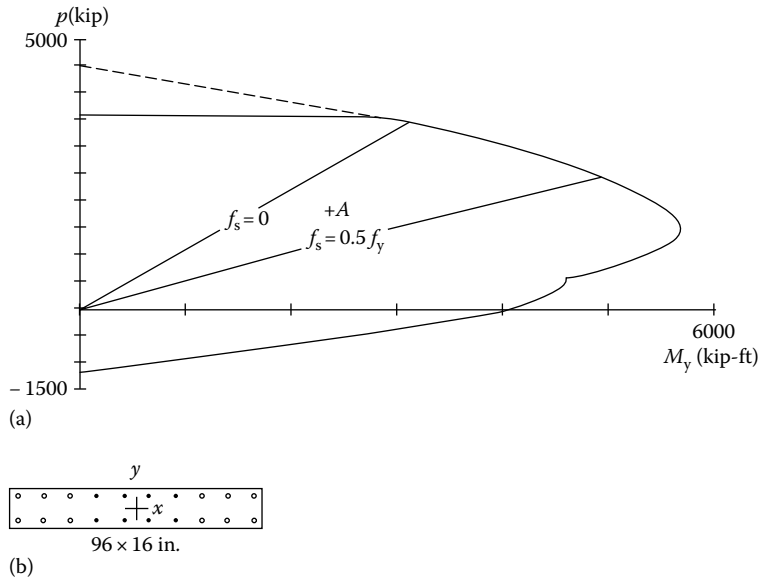
Factored axial forces and moments for the design of W1 are as follows:

$$P_u = 1200 \text{ kip}$$

$$M_u = 25,200 \text{ kip-in} = 2100 \text{ kip-ft}$$

Figure 6.39 shows the arrangement of vertical reinforcement in wall pier W1 along with the interaction diagram. Six #11 rebars are placed near the wall boundary zones, with #6 at 10 at each face in between the boundary elements. The interaction point A, corresponding to  $P_u = 1200 \text{ kip}$ ,  $M_u = 210 \text{ kip}$ , is well within the interaction curve, justifying the design of W1 for the combined axial load and building moments.





**FIGURE 6.39** (a) Wall pier W1, load/moment interaction diagram and (b) cross section of wall pier W1.

#### 6.11.10.2.4 Web Reinforcement

The minimum vertical reinforcement ratio  $\rho_v$  per Section 21.7.2.1 is 0.0025. However, Section 14.3 permits a reduction in  $\rho_v$  if  $V_u > 2A_{CV}\sqrt{f'_c}$ .

For the example wall pier W1,

$$V_u = 210 \text{ kip} > \frac{96 \times 16 \sqrt{4000}}{1000} = 97 \text{ kip}$$

Therefore, minimum  $\rho_v = 0.0025$

$$\begin{aligned} \rho_v \text{ provided at \#6 at eight, each face} &= \frac{0.44 \times 2 \times 12}{8 \times 16 \times 12} \\ &= 0.0069 \\ &> 0.0025 \end{aligned}$$

Section 21.7.2.2 requires at least two curtains of reinforcement, for both  $\rho_v$  and  $\rho_n$ , if  $V_u = 2A_{CV}\sqrt{f'_c}$ .

For the example wall pier W1,

$$V_u = 210 \text{ kip} > 2A_{CV}\sqrt{f'_c} = \frac{2 \times 96 \times 16 \sqrt{4000}}{1000} = 194.3 \text{ kip}$$

Therefore, two curtains of #6 at eight at each face are acceptable.

#### 6.11.10.2.5 Boundary Elements

The design of wall segments for flexure is identical to that for a conventional solid wall. However, in designing boundary elements, a question comes up as to whether to use the displacement-based

approach or the stress-index method. Section 21.7.6.2 limits the use of displacement-based approach to walls that are continuous from the base of the structure to the top of the wall and designed to have a single critical section for flexure and axial loads. A coupled shear wall as a whole is typically not designed to have a single critical section for flexure and axial loads because plastic hinges may form in the coupling beams as well as at the base of each pier. Therefore, by this interpretation, displacement-based design is not permitted for wall piers.

However, if the makeup of the wall is considered as an assemblage of independent wall piers, then it can be argued that each wall pier is continuous and is designed to have a single critical section at its base for flexure and axial loads. Using this interpretation, the evaluation of special boundary elements may be based on the displacement-based method of comparing neutral axis depths.

Faced with this uncertainty, what is the best way to tackle wall pier designs? Keeping in mind that “more is less” in seismic design, I recommend the use of the more conservative stress-index method. However, for the purpose of illustration, the example wall pier W1 will be designed using both methods.

**Stress index procedure:** For the example wall pier W1,  $A_g = 96 \times 16 = 1356 \text{ in.}^2$ , and the combined compressive stress for the factored axial load and bending moments is

$$\begin{aligned}\frac{P_u}{A_g} + \frac{M_u}{S_{y-y}} &= \frac{1200}{1356} + \frac{2100 \times 12}{24576} \\ &= 0.78 + 1.02 = 1.8 \text{ ksi}\end{aligned}$$

This is greater than  $0.2f'_c = \frac{0.2 \times 4000}{1000} = 0.80 \text{ ksi}$ .

Therefore, boundary elements are required by the stress-index procedure.

**Displacement-based procedure:** Boundary zone detailing is required if the depth of the neutral axis  $c$  from the extreme compression fiber is greater than an index depth as given by

$$c > \frac{l_w}{600 \left( \frac{\delta_u}{h_w} \right)} \quad (21.8)$$

For the example wall W1, the value of  $c$  calculated by using the PCACOL program is equal to 40.63 in.

The elastic deflection  $\delta_e$  is equal to 1.97 in. at the roof, as given in the statement of the problem.

The design displacement  $\delta_u = C_d \delta_e = 5.5 \times 1.97 = 10.85 \text{ in.}$

$$\frac{\delta_u}{h_w} = \frac{10.85}{133 \times 12} = 0.0068 < 0.007$$

Therefore,  $c = \frac{96}{600 \times 0.007} = 22.86 \text{ in.}$

The value of  $c = 40.63 \text{ in.}$  calculated using the PCACOL program is greater than the index value of 22.86 in. Therefore, boundary elements are required by the displacement-based procedure.

**Reinforcement details:** The required width of a boundary element is the larger of

$$c - 0.1l_w = 40.63 - 0.1 \times 96 = 31 \text{ in.} \leftarrow \text{controls}$$

$$\frac{c}{2} = \frac{40.63}{2} = 20.31 \text{ in.}$$

Considering the placement of the vertical bars, confine 36 in. width of wall at both ends of the wall pier.  
The vertical extension must not be less than

$$l_w = 96 \text{ in. (Controls)}$$

$$\frac{M_n}{4V_n} = \frac{2100 \times 12}{4 \times 210} = 30 \text{ in.}$$

Although the boundary element need not extend more than 96 in., we choose to extend it to the full height of the first floor.

**The confinement of 16 × 36 in. boundary elements:**

**Confinement perpendicular to the wall:** Minimum allowable spacing of hoops and crossties is given by

$$s_{\max} = 0.25 \times \text{the minimum member dimension}$$

$$= 0.25 \times 16 = 4 \text{ in. (Controls)}$$

$$= 6 \times \text{the diameter of longitudinal bar}$$

$$= 6 \times 1.41 = 8.5 \text{ in.}$$

$$= 4 + \left( \frac{14 - h_x}{3} \right) = 4 + \left( \frac{14 - 11.91}{3} \right) = 4.7 \text{ in.}$$

Note that crossties are not used in this example because

$$h_x = 16 - (3 + 3) + 1.41 + 0.5 = 11.91 < 14 \text{ in.}$$

The required cross-sectional area of confining reinforcement using  $s = 4 \text{ in.}$  is given by

$$A_{sh} = 0.09 s h_c \frac{f_c}{f_y} \quad (21.9)$$

where

$h_c$  is the cross-sectional dimension of boundary element measured center-to-center of confining reinforcement.

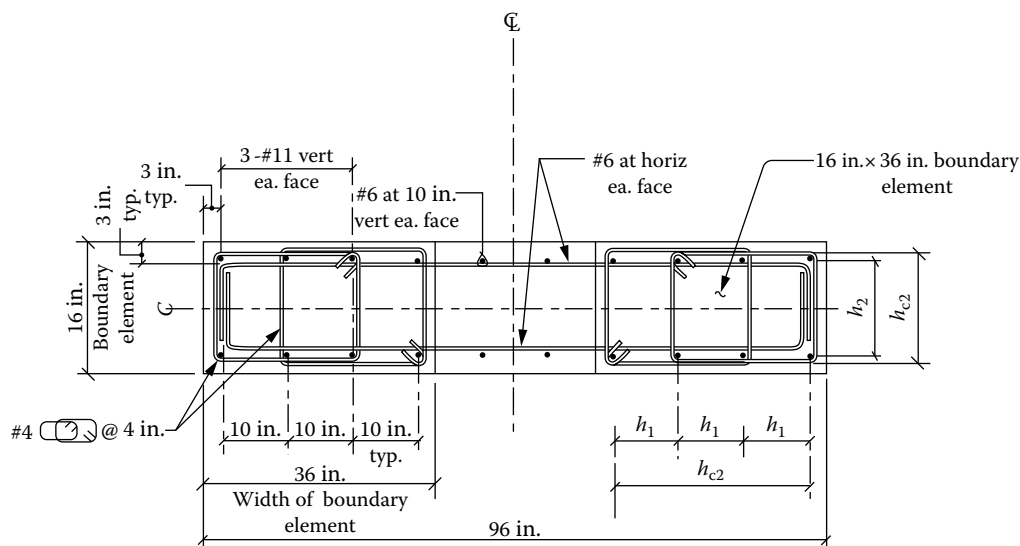
In our case,  $h_c = 16 - (3 + 3) + 1.41 + 0.5 = 11.91 \text{ in.}$

$$A_{sh} \text{ required} = 0.09 \times 4 \times 12 \times \frac{4}{60} = 0.29 \text{ in.}^2$$

No. 4 hoops with two legs provide  $A_{sh} = 2 \times 2.0 = 4.0 \text{ in.}^2 > 0.29 \text{ in.}^2$

**Confinement parallel to the wall:**

$$h_c = 33 - (3 + 3) + 1.41 + 0.625 = 29 \text{ in.}$$



$$A_{sh} = 0.09 \times 4 \times 29 \times \frac{4}{60} = 0.7 \text{ in.}^2$$

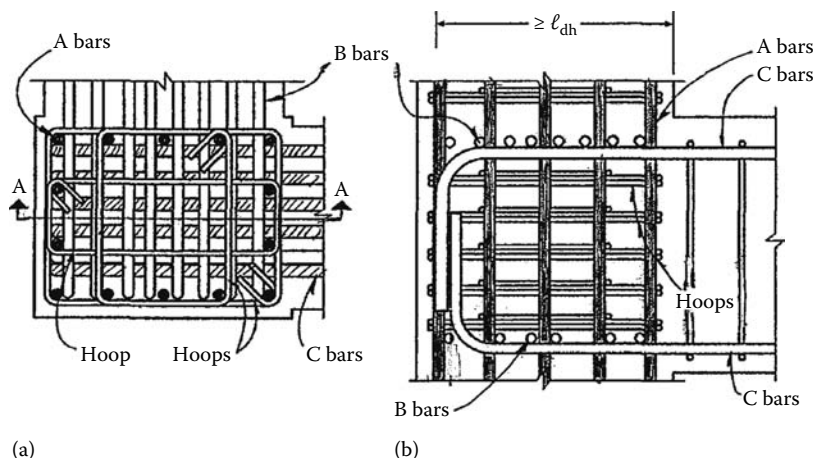
With two hoops,  $A_{ch \text{ provided}} = 4 \times 0.2 = 0.8 \text{ in.}^2 > 0.7 \text{ in.}^2$

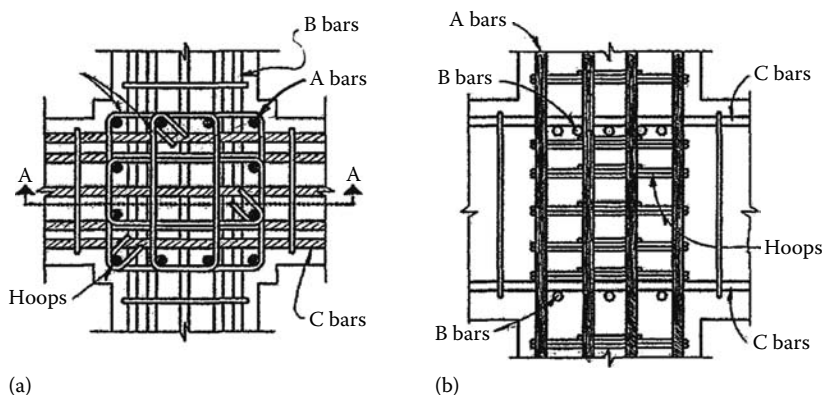
Figure 6.40 shows a schematic layout of reinforcement in wall pier W1.

The analysis and design performed thus far does not consider post-elastic behavior of coupled walls, nor does it explain how a plastic analysis may be performed for seismic forces when the elements of the wall are yielding. This type of postyield analysis is not required by ACI 318-05 but is recommended in the 1999 Blue Book, *Recommended Lateral Force and Commentary*, published by the SEAOC. The designer is referred to Chapter 4 of this reference for further details.

## 6.12 TYPICAL DETAILS

Details typically used in the North American practice are given in Figures 6.41 through 6.47. Ample description is given in each figure to make it self-explanatory.





**FIGURE 6.42** Interior joint detailing; schematics: (a) plan and (b) section.

### 6.13 ACI 318-08 UPDATE

There are many revisions in ACI 318-08. For example, the design engineer is required to assign exposure categories and classes based on the severity of the anticipated exposure of structural members to achieve durability. Requirements are included to select effective stiffness for determining lateral deflections. A new simple procedure helps determine if compression members are considered braced or unbraced. Provisions are introduced for design of headed stud assemblies. Design and detailing requirements are correlated with the SDCs given in the 2006 IBC. The use of high strength confining steel is permitted to help reduce congestion. The beneficial effect of supplementary reinforcement and anchor reinforcement on the capacity of anchors is quantified.

#### 6.13.1 OUTLINE OF MAJOR CHANGES

- The correlation of design requirements for earthquake-resistant structures with the SDCs used in the ASCE/SEI 7-05 and the 2006 IBC.
- New requirements for headed shear stud reinforcement, headed deformed bars, stainless steel bars, and high-strength steel bars.
- Licensed design professional to prescribed new exposure categories and classes for durability requirements.
- Strength test based on three 4 in.  $\times$  8 in. cylinders or two 6 in.  $\times$  12 in. cylinders.
- A 12 month limit set on historical data used to qualify mixture proportions.
- Enhanced structural integrity with Class B lap splices and continuous top and bottom structural integrity reinforcement passing through column core.
- Modeling procedure for evaluation of lateral displacements.
- Simple procedure to define braced and unbraced compression members.
- Design provisions for headed stud assemblies as shear reinforcement for slabs and footings.
- Decreased allowable concrete compression stress immediately after prestress transfer.
- Reorganized and enhanced provisions for earthquake-resistant structures in order of increasing SDC.
- Use of supplementary reinforcement and anchor reinforcement to enhance the capacity of anchors.
- Ductility requirements for anchors in seismic zones.
- Unified handling of lightweight concrete in design equations.
- ACI 332 referenced for residential cast-in-place footings, foundation walls, and slabs-on-ground for one- and two-family dwellings and town homes.

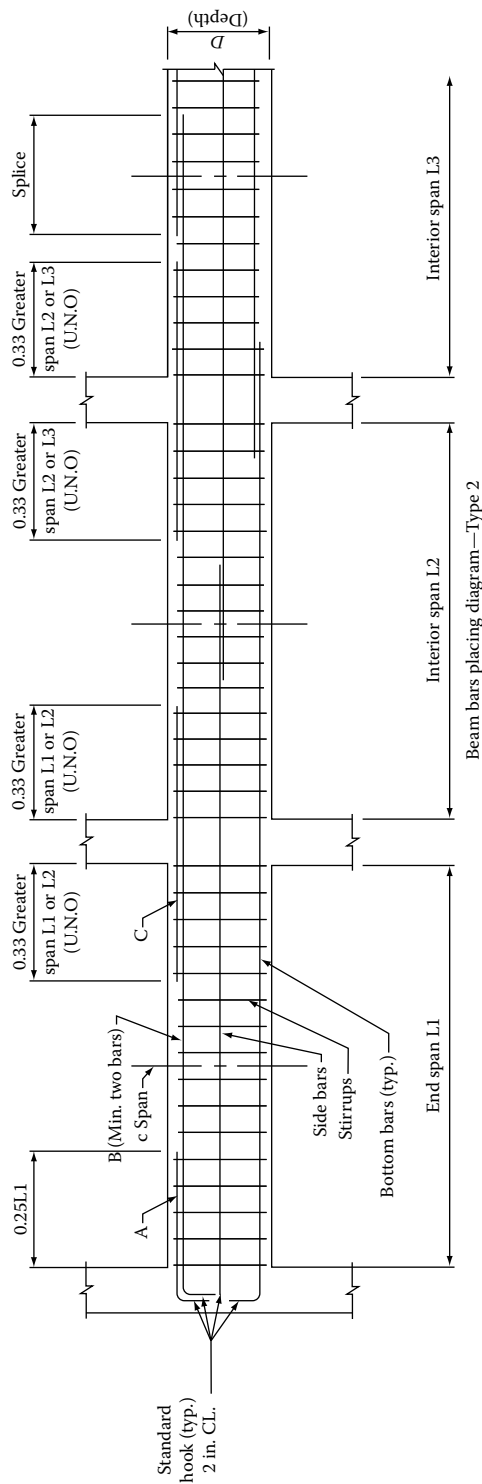


FIGURE 6.43 Beam bar placement.

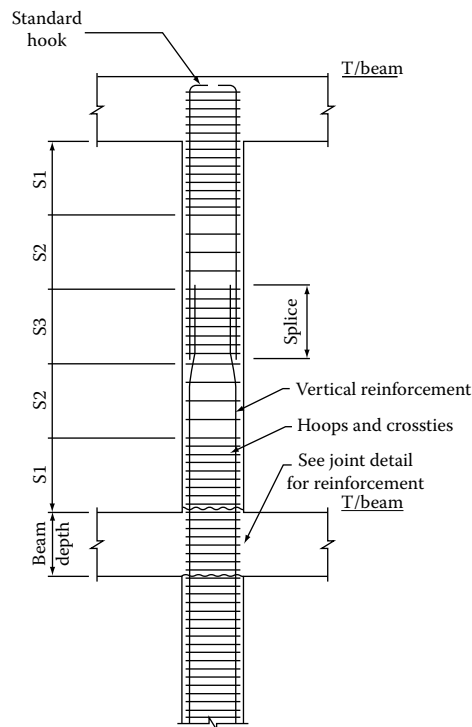


FIGURE 6.44 SDC D, E, or F: Frame columns.

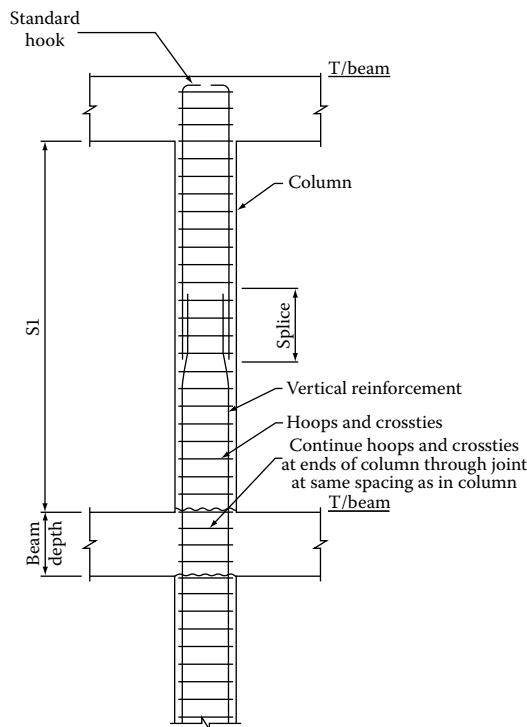


FIGURE 6.45 SDC D, E, or F: Gravity columns in which induced moments and shears due to deformation compatibility, combined with factored gravity moments and shears do not exceed design moments and shears.

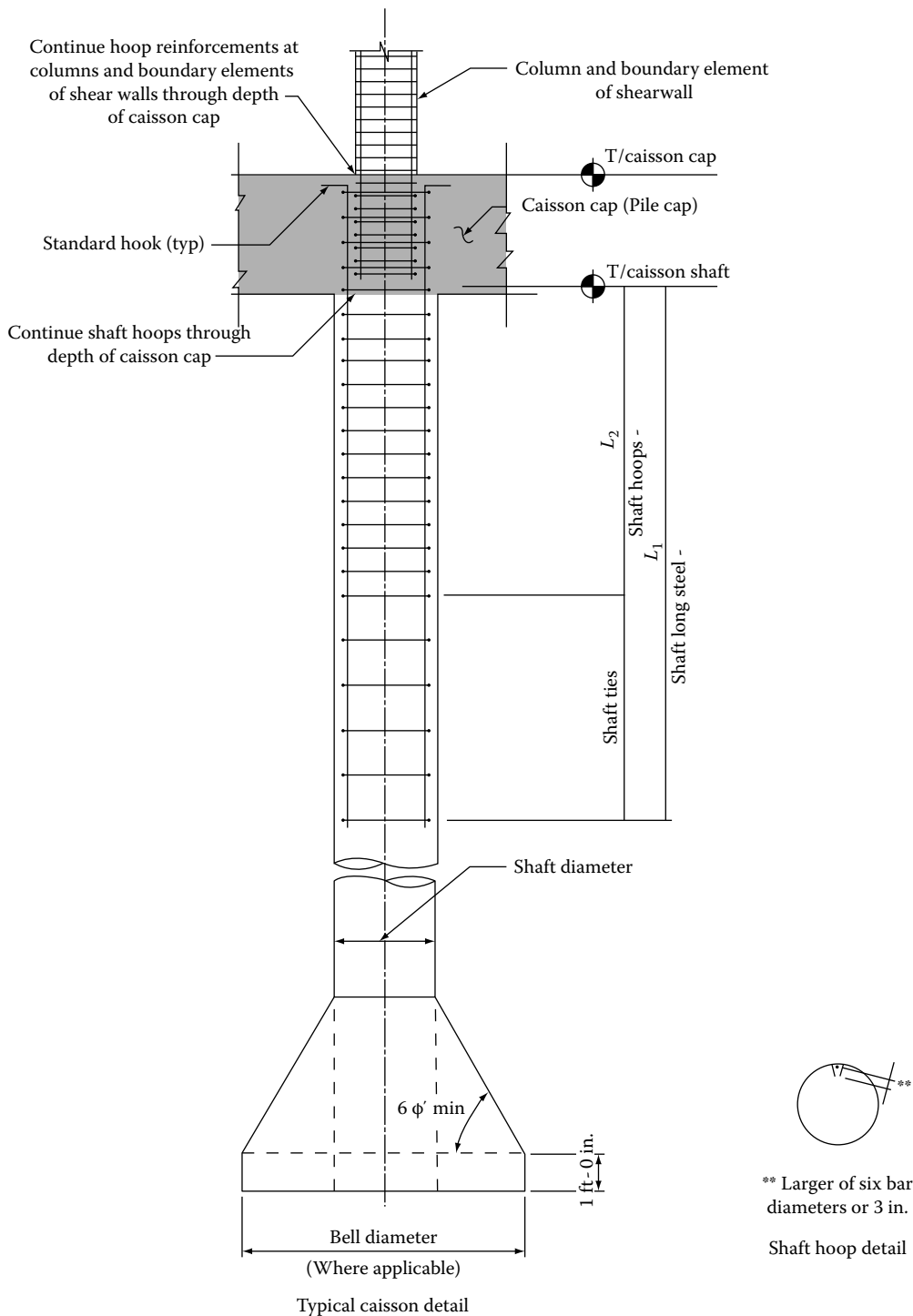


FIGURE 6.46 Typical caisson detail.





- Modified load factors for required test load.
- New design requirements for SDCs.
- Alternative reinforcement scheme for coupling beams.
- Increased design yield strength for confinement reinforcement to help reduce congestion.
- Revisions to boundary element confinement requirements.

### 6.13.2 SUMMARY OF CHAPTER 21, ACI 318-08

In 2008, provisions of Chapter 21, Earthquake-Resistant Structures, have been revised and reformatted to present seismic requirements in order of increasing SDC. A brief description of selected topics is given in the following sections.

As stated previously, the provisions relate detailing requirements to type of structural framing and SDC. SDCs relate to considerations of seismic hazard level, soil type, occupancy, and use, while the SDC is regulated by the legally adopted general building code.

The design and detailing requirements depict the level of energy dissipation (or toughness) assumed in the computation of the design earthquake forces. The degree of required toughness, and therefore, the level of detailing, increases for structures progressing from SDC A through SDC F. It is essential that structures assigned to higher SDCs possess a higher degree of toughness. It is permitted, however, to design for higher toughness in the lower SDCs and take advantage of the lower design force levels.

The provisions of Chapters 1 through 19 and Chapter 22 are considered adequate for structures assigned to SDC A (corresponding to the lowest seismic hazard). For structures assigned to SDC B, additional requirements apply.

Structures assigned to SDC C may be subjected to moderately strong ground shaking while structures assigned to SDC D, E, or F may be subjected to strong ground shaking. The seismic-force-resisting system for buildings assigned to SDC D, E, or F is generally provided by special moment frames, special structural walls, or a combination of the two. Additionally, these structures are also required to satisfy requirements for continuous inspection of diaphragms and trusses, foundations, and gravity-load-resisting elements that are not designated as part of the seismic-force-resisting system. These provisions have been developed to provide the structure with adequate toughness for the high demands expected for these SDCs.

Where special systems are used for structures in SDC B or C, it is not required to satisfy the deformation compatibility requirements, although it should be verified that members not designated as part of the seismic-force-resisting system will be stable under design displacements. The toughness requirements refer to the concern for the structural integrity of the entire seismic-force-resisting system at lateral displacements anticipated for ground motions corresponding to the design earthquake.

### 6.13.3 ANALYSIS AND PROPORTIONING OF STRUCTURAL MEMBERS

Unless convincing evidence is developed, the maximum specified compressive strength of lightweight concrete to be used in structural design calculations is limited to 5000 psi, primarily because of the lack of experimental and field data on the behavior of members made with lightweight concrete subjected to displacement reversals in the nonlinear range.

### 6.13.4 REINFORCEMENT IN SPECIAL MOMENT FRAMES AND SPECIAL STRUCTURAL WALLS

Use of longitudinal reinforcement with strength substantially higher than that assumed in design will lead to higher shear and bond stresses at the time of development of yield moments. These conditions may lead to brittle failures in shear or bond and should be avoided even if such failures may occur at higher loads than those anticipated in design. Therefore, a ceiling of 18,000 psi is placed on the actual yield strength,  $f_y$ , of the steel.

The requirement for a tensile strength larger than a yield strength of the reinforcement,  $f_{yt} \geq 1.25f_y$ , is based on the assumption that the capability of a structural member to develop inelastic rotation capacity is a function of the length of the yield region along the axis of the member. The restrictions on the values of  $f_y$  and  $f_{yt}$  apply to all types of transverse reinforcements, including spirals, circular hoops, rectilinear hoops, and crossties. The restrictions on the values of  $f_y$  and  $f_{yt}$  for computing nominal shear strength are intended to limit the width of shear cracks.

### 6.13.5 MECHANICAL SPLICES IN SPECIAL MOMENT FRAMES AND SPECIAL STRUCTURAL WALLS

In a structure undergoing inelastic deformations during an earthquake, the tensile stresses in reinforcement may approach the tensile strength of the reinforcement. The requirements for Type 2 mechanical splices are intended to avoid a splice failure when the reinforcement is subjected to expected stress levels in yielding regions. Type 1 splices are not required to satisfy the more stringent requirements for Type 2 splices, and may not be capable of resisting the stress levels expected in yielding regions.

### 6.13.6 WELDED SPLICES IN SPECIAL MOMENT FRAMES AND SPECIAL STRUCTURAL WALLS

Welding of crossing reinforcing bars can lead to local embrittlement of the steel. If welding of crossing bars is used to facilitate fabrication or placement of reinforcement, it should be done only on bars added for such purposes. The prohibition of welding crossing reinforcing bars does not apply to bars that are welded with welding operations under continuous, competent control as in the manufacture of welded wire reinforcement.

### 6.13.7 ORDINARY MOMENT FRAMES, SDC B

The provisions for beam reinforcement are intended to improve continuity in the framing members thereby improve lateral force resistance and structural integrity; these provisions do not apply to slab-column moment frames. The provisions for columns are intended to provide additional toughness to resist shear for columns with proportions that would otherwise make them more susceptible to shear failure under earthquake loading.

### 6.13.8 INTERMEDIATE MOMENT FRAMES

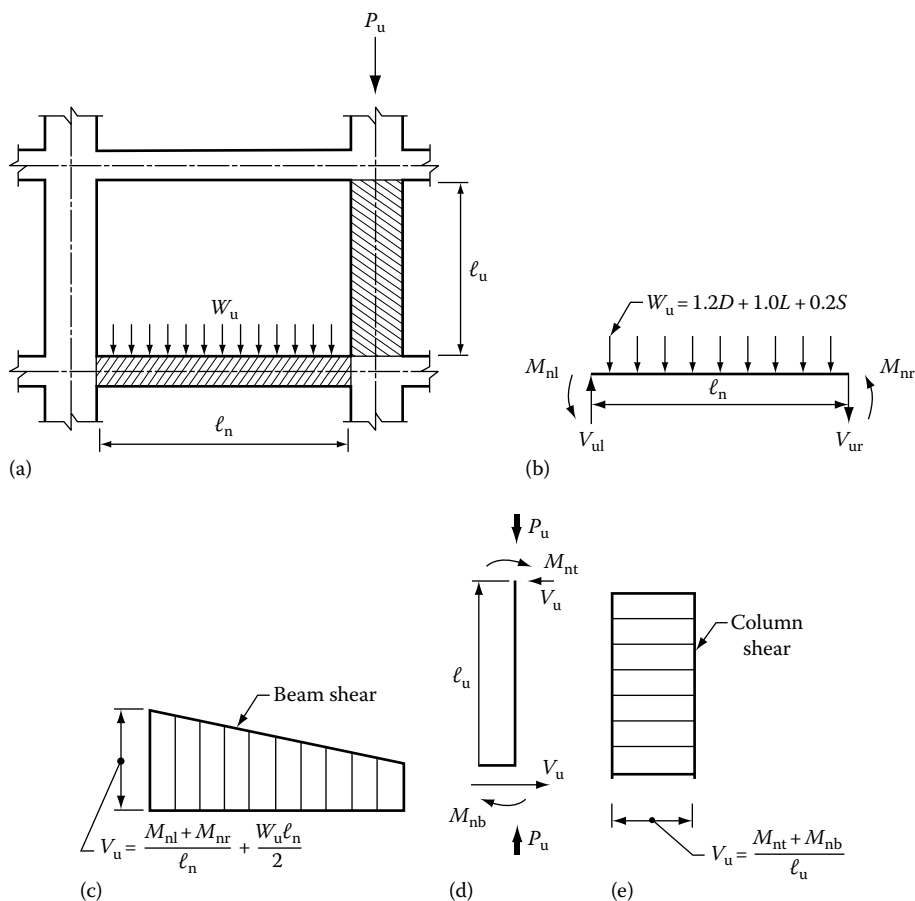
The objective of using the lesser of factored shear force given by

1.  $V_u = M_{nl} + M_{nr}/\ell_n + W_u\ell_n/2$
2.  $E = 2E$  in all design load combination

is to reduce the risk of failure in shear in beams and columns during an earthquake.

Note that the factored shear force is determined from the nominal moment strength of the member and the gravity load on it (see Figure 6.48 for design shear requirements). To determine the maximum beam shear, it is assumed that its nominal moment strengths ( $\theta = 1.0$ ) are developed simultaneously at both ends of its clear span. The shear associated with this condition  $[(M_{nl} + M_{nr})/\ell_n]$  is added algebraically to the shear for the beam.

In the determination of the design shear for a column, the factored axial force,  $P_u$ , should be chosen to develop the largest moment strength of the column. In all applications of the first option, shears are required to be calculated for moments, acting both clockwise and counterclockwise. To provide beams with a threshold level of toughness, transverse reinforcement at the ends of the beam is required to be hoops.



**FIGURE 6.48** Design shears for IMFs: (a) moment frame, (b) loads on frame beams, (c) beam shear, (d) loads on frame columns, and (e) column shear.

Discontinuous structural walls and other stiff members can impose large axial forces on supporting columns during earthquakes. The specified transverse reinforcement is to improve the column toughness under anticipated demands. The factored axial compressive force related to earthquake effect should include the factor  $\Omega_o$ .

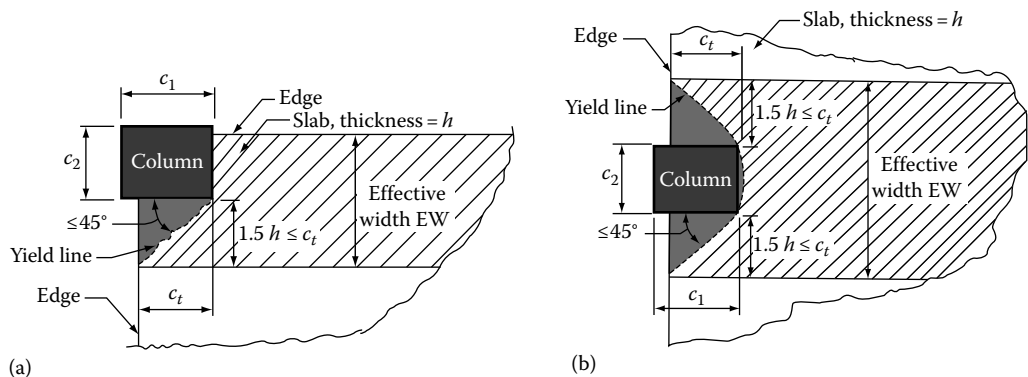
### 6.13.9 TWO-WAY SLABS WITHOUT BEAMS

Reinforcement details for two-way slabs designed as slab-beams of a moment-resisting frame are shown in Figures 6.49 through 6.51.

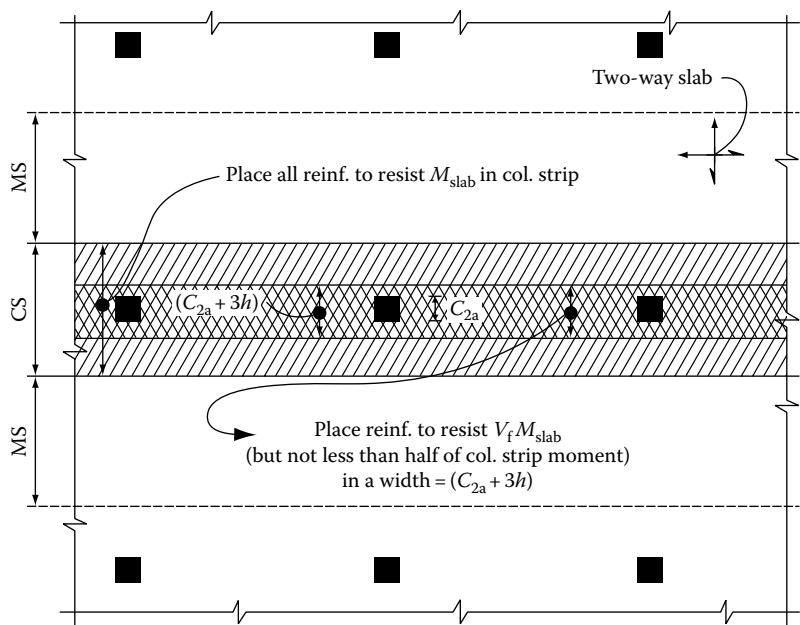
The moment  $M_{slab}$  refers to that portion of the factored slab moment that is balanced by the supporting members at a joint. Only a fraction of the moment equal to  $r_f M_{slab}$  is assigned to the slab effective width.

### 6.13.10 FLEXURAL MEMBERS (BEAMS) OF SPECIAL MOMENT FRAMES

Any frame member subjected to a factored axial compressive force exceeding  $(A_g f'_c / 10)$  under any load combination is considered as a flexural member. However, since the seismic behavior of frame beams having length-to-depth ratios of less than 4 is significantly different from the behavior of



**FIGURE 6.49** Two-way slabs: Effective width concept placement for reinforcement: (a) corner column and (b) interior column.

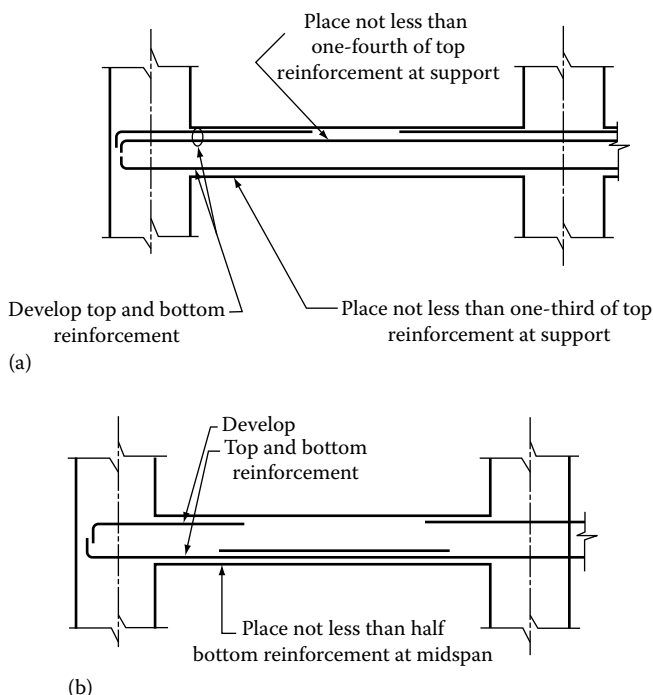


**FIGURE 6.50** Reinforcement placement in two-way slabs without beams. (Applies to both top and bottom reinforcement.) Note:  $h$  = slab thickness.

relatively slender member beams with length-to-depth ratios less than 4, they are not permitted as flexural members of special moment frames. These geometric constraints were derived from practice and research on reinforced concrete frames resisting earthquake-induced forces. The specified limits on effective width  $b_w$  as shown in Figure 6.52, recognize that the maximum effective beam width depends principally on the column dimensions rather than on the depth of the beam.

### 6.13.11 TRANSVERSE REINFORCEMENT

Transverse reinforcement is required primarily to confine the concrete and maintain lateral support of the reinforcing bars in regions where yielding is expected. Because spalling of the concrete shell



**FIGURE 6.51** Two-way slabs: Arrangement of reinforcement in (a) column and (b) middle strips.

is anticipated during strong ground motions, especially at and near regions of flexural yielding, all web reinforcement should be provided in the form of closed hoops.

### 6.13.12 SHEAR STRENGTH REQUIREMENTS

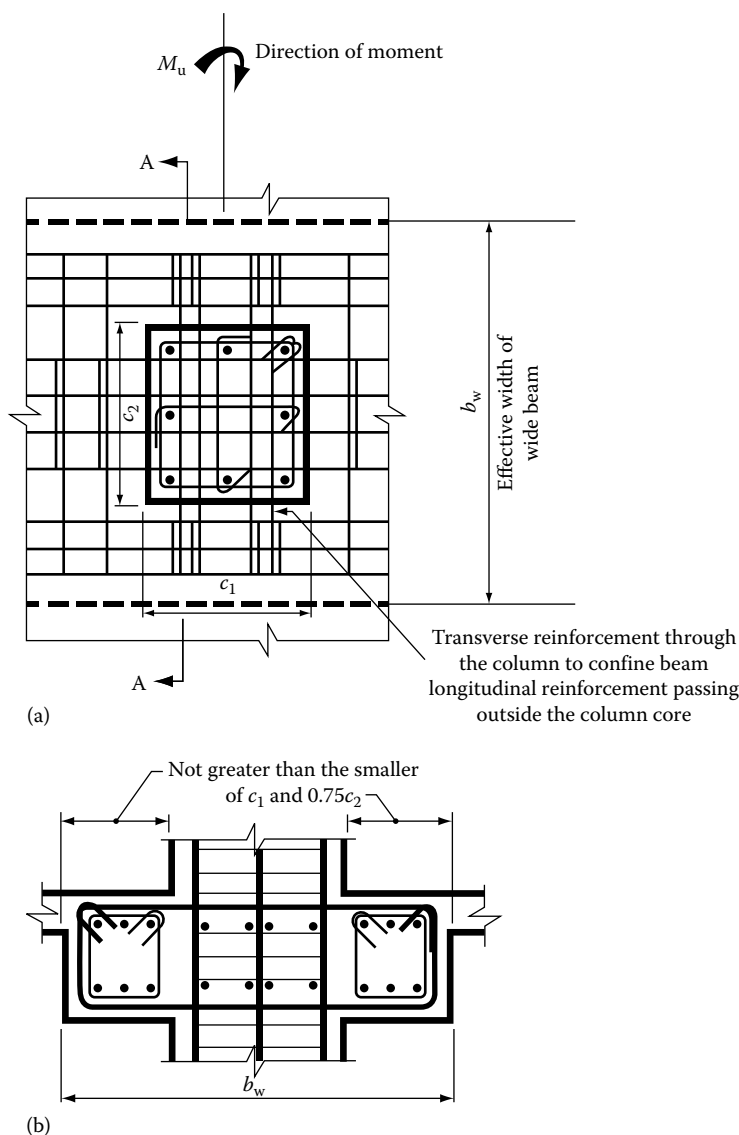
Because the actual yield strength of the longitudinal reinforcement may exceed the specified yield strength and because strain hardening of the reinforcement is likely to take place at a joint subjected to large rotations, required shear strengths are determined using a stress of at least  $1.25f_y$  in the longitudinal reinforcement.

It has been known quite convincingly for some time that reinforced concrete members subjected to cyclic loading require more shear reinforcement to ensure a flexural failure as opposed to a shear failure. Thus, the contribution of concrete-to-shear strength is neglected in shear design. The added conservatism is deemed necessary in locations where potential flexural hinges may occur.

### 6.13.13 SPECIAL MOMENT FRAME MEMBERS SUBJECTED TO BENDING AND AXIAL LOADS

The intent of minimum flexural strength of columns,  $\sum M_{nc} \geq (6/5)\sum M_{nb}$ , is to reduce the likelihood of yielding in columns that are considered as part of the seismic-force-resisting system. If columns are not stronger than beams framing into a joint, there is a likelihood of inelastic action due to flexural yielding at both ends of all columns in a given story. This would result in a column failure mechanism that can lead to building collapse.

When determining the nominal flexural strength of a girder section in negative bending region (top in tension), longitudinal reinforcement contained within an effective flange width of a top slab that acts monolithically with the girder increases the girder strength. Accounting for the top reinforcement placed within the effective flange widths gives reasonable estimates of girder negative bending strengths.



**FIGURE 6.52** Definition of effective width of wide beams for placement of transverse reinforcement: (a) plan and (b) Section A-A.

The lower limit of the area of longitudinal reinforcement is to control time-dependent deformations and to have the yield moment exceed the cracking moment. The upper limit reflects concern for steel congestion, load transfer from floor elements to column, and the development of high shear stresses.

Spalling of concrete, which is likely to occur near the ends of the column in frames of typical configuration, makes lap splices in these locations vulnerable. If lap splices are to be used at all, they should be located near the mid-height where stress reversal is likely to be limited to a smaller stress range than at locations near the joints. Transverse reinforcement is required along the lap-splice length because of the uncertainty in moment distributions along the height and the need for confinement of lap splices subjected to stress reversals. Additional reasons for providing the transverse reinforcement are concerned with confining the concrete and providing lateral support to the longitudinal reinforcement.

A minimum length is stipulated over which closely spaced transverse reinforcement is required at the member ends, where flexural yielding normally occurs. The length should be increased by 50% or more in locations, such as the base of the building, where axial loads and flexural demands may be high.

The requirement that spacing not exceed one-quarter of the minimum member dimension,  $d/4$ , is to obtain adequate concrete confinement. The requirement that spacing not exceed six bar diameters,  $6d_b$ , is intended to restrain longitudinal reinforcement buckling after spalling. The 4 in. spacing is for concrete confinement. This limit may be relaxed to a maximum of 6 in. if the spacing of crossties or legs of overlapping hoops is less than 8 in.

Columns supporting discontinued stiff members, such as walls, may develop considerable inelastic response. Therefore, it is required that these columns have the specified reinforcement throughout their length.

The unreinforced shell may spall as the column deforms to resist earthquake effects. Separation of portions of the shell from the core caused by local spalling creates a falling hazard. The additional reinforcement is required to reduce the risk of portions of the shell falling away from the column.

#### 6.13.14 SHEAR STRENGTH REQUIREMENTS FOR COLUMNS

The moment at a frame joint is typically limited by the flexural strength of the beams framing into the joint. Where beams frame into opposite sides of a joint, the combined strength is the sum of the negative moment strength of the beam on one side of the joint and the positive moment strength of the beam on the other side of the joint. Moment strengths are to be determined using a strength-reduction factor of 1.0 and reinforcing steel stress equal to at least  $1.25f_y$  (see Figure 6.53 for design shear requirements for columns and beams).

#### 6.13.15 JOINTS OF SPECIAL MOMENT FRAMES

The development of inelastic rotations at the faces of joints of reinforced concrete frames is associated with strains in the flexural reinforcement well in excess of the yield strain. Consequently, joint shear force generated by the flexural reinforcement is calculated for stress of  $1.25f_y$  in the reinforcement.

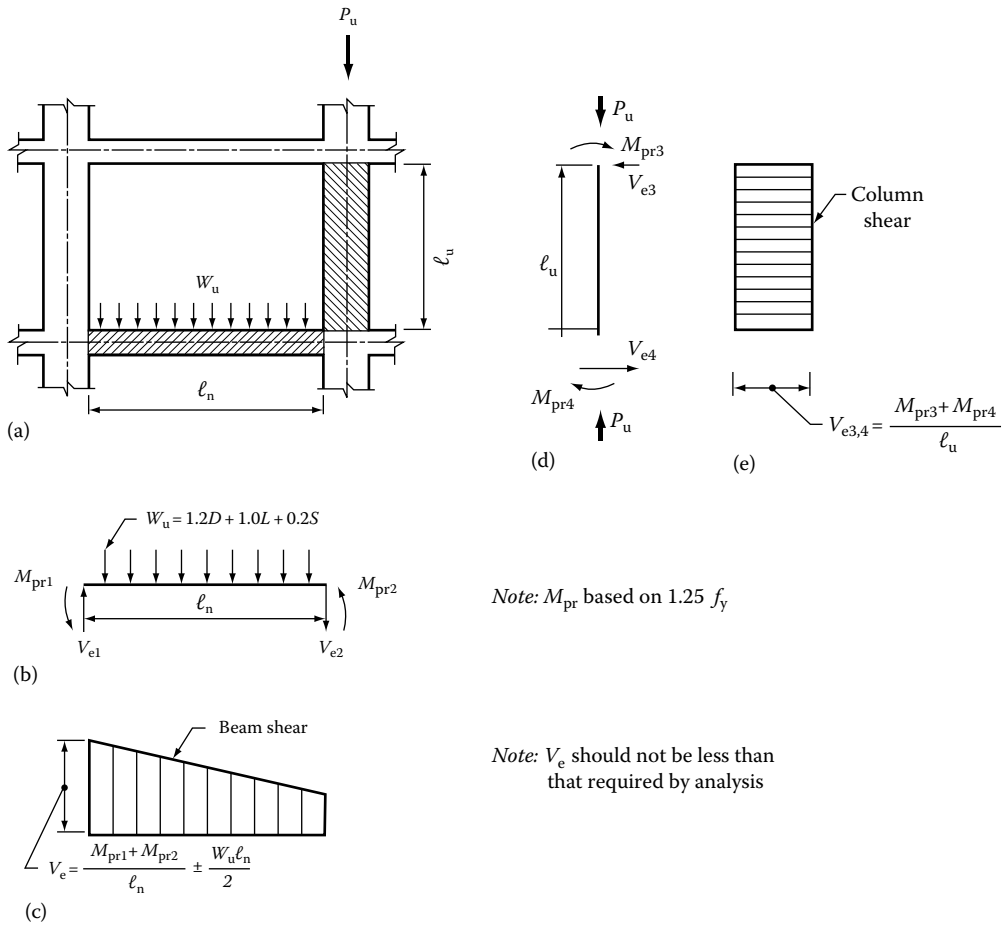
#### 6.13.16 SPECIAL STRUCTURAL WALLS AND COUPLING BEAMS

The minimum web reinforcement ratio of  $\rho_t$  and  $\rho_l \geq 0.0025$  are the same as in the preceding provisions. The uniform distribution requirement of the shear reinforcement is related to the intent to control the width of inclined cracks. The requirement for two layers of reinforcement in walls carrying substantial design shears is based on the observation that, under ordinary construction conditions, the probability of maintaining a single layer of reinforcement near the middle of the wall section is quite low. Furthermore, the presence of reinforcement close to the surface tends to inhibit the fragmentation of the concrete in the event of severe cracking during an earthquake.

Because actual forces in the longitudinal reinforcement of structural walls may exceed calculated forces, reinforcement should be developed or spliced to reach the yield strength of the bar in tension. At locations where yielding of longitudinal reinforcement is expected, a 1.25 multiplier is applied to account for the likelihood that the actual yield strength exceeds the specified yield strength of the bar, as well as the influence of strain hardening and cyclic load reversals. Where transverse reinforcement is used, development lengths for straight and hooked bars may be reduced as permitted elsewhere in ACI 318-08, because closely spaced transverse reinforcement improves the performance of splices and hooks subjected to repeated inelastic demands.

The nominal shear strength is given by  $V_n = A_{cv}(\alpha_c \lambda \sqrt{f'_c} P_t f_y)$  in which the term  $\alpha_c \lambda$  is usually taken as 2.0. For a rectangular section without openings, the term  $A_{cv}$  refers to the gross area of the cross section rather than to the product of the width and the effective depth.





**FIGURE 6.53** Design shears for special moment frames: (a) moment frame, (b) loads on frame beams (same as for IMFs), (c) beam shear, (d) loads on frame columns, and (e) column shear.

If the factored shear force at a given level in a structure is resisted by several walls or several piers of a perforated wall, the average unit shear strength assumed for the total available cross-sectional area is limited to  $8\sqrt{f'_c}$  with the additional requirement that the unit shear strength assigned to any single pier does not exceed  $10\sqrt{f'_c}$ . The upper limit of strength to be assigned to any one member is imposed to limit the degree of redistribution of shear force.

### 6.13.17 SHEAR WALL DESIGN FOR FLEXURE AND AXIAL LOADS

Strength in a shear wall is determined considering both the applied axial and lateral forces. In flanged shear walls such as L, T, and C sections, reinforcement concentrated in boundary elements and distributed in flanges and webs should be included in the strength computations based on a strain compatibility analysis. The foundation supporting the wall should be designed to develop the wall boundary and web forces.

Where wall sections intersect to form L-, T-, C-, or other cross-sectional shapes, the influence of the flange on the behavior of the wall should be considered by selecting appropriate flange widths. To simplify design, a single value of effective flange width based on an estimate of the effective tension flange width is used in both tension and compression.

### 6.13.18 BOUNDARY ELEMENTS OF SPECIAL STRUCTURAL WALLS

There are two design approaches for evaluating detailing requirements at wall boundaries that are the same as in the previous publications. The first approach follows from a displacement-based approach. The equation  $c \geq l_w/600 (\delta_u/h_w)$  assumes that special boundary elements are required to confine the concrete where the strain at the extreme compression fiber of the wall exceeds a critical value when the wall is displaced to the design placement. The horizontal dimension of the special boundary element is intended to extend at least over the length where the compression strain exceeds the critical value. The height of the special boundary element is based on upper bound estimates of plastic hinge length and extends beyond the zone over which concrete spalling is likely to occur. The lower limit of 0.007 on the quantity  $\delta_u/h_w$  requires moderate wall deformation capacity for stiff buildings.

The neutral axis depth  $c$  in the above equation is the depth calculated using linear strain requirements corresponding to the development of nominal flexural strength of the wall when displaced in the same direction as  $\delta_u$ . The axial load is the factored axial load that is consistent with the design load combination that produces the design displacement  $\delta_u$ .

In the second procedure, the gravity loads and the maximum shear and moment induced by earthquakes are used to calculate compressive stresses at critical regions of the wall. Under this loading, the compressed boundary at the critical section is assumed to resist the tributary gravity load plus the compressive resultant associated with the bending moment.

Recognizing that this loading condition may be repeated many times during the strong motion, the concrete is required to be confined where the calculated compressive stresses, including those due to bending, exceed a nominal critical value equal to  $0.2 f'_c$ . The bending stress is calculated for the factored forces assuming linear response of the gross concrete section. The benchmark compressive stress of  $0.2 f'_c$  is used only as an index value and does not necessarily describe the actual state of stress that may develop at the critical section under the anticipated earthquake intensity.

Cyclic load reversals may lead to the buckling of boundary longitudinal reinforcements even in cases where the demands on the boundary of the wall do not require special boundary elements. For walls with moderate amounts of boundary longitudinal reinforcement, reinforcement ratios greater than  $400/f_y$  ties are required to inhibit buckling. The longitudinal reinforcement ratio is intended to include only the reinforcement at the wall boundary.

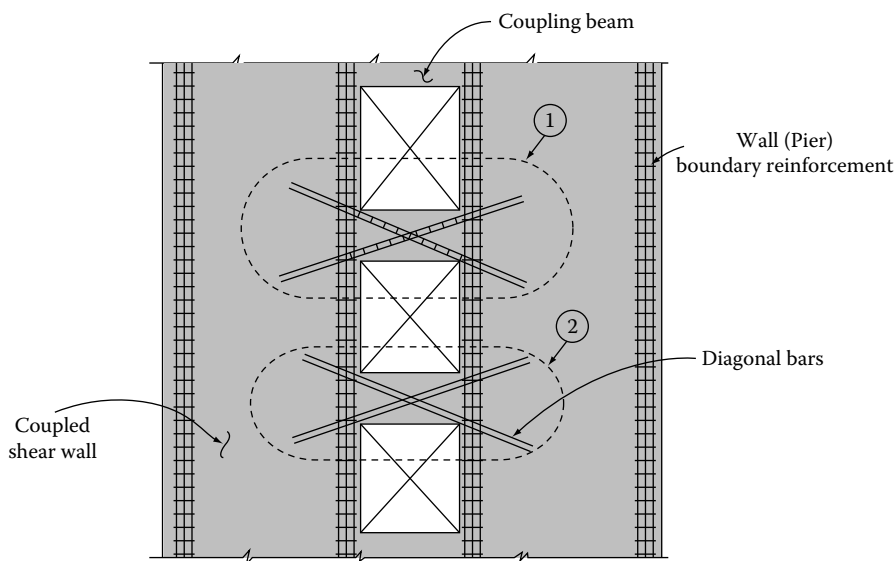
The addition of hooks or U-stirrups at the ends of horizontal wall reinforcement provides anchorage so that the reinforcement will be effective in resisting shear forces. It will also tend to inhibit the buckling of the vertical edge reinforcement. In walls with low in-plane shear, the development of horizontal reinforcement is not necessary.

### 6.13.19 COUPLING BEAMS

The addition of coupling beams between shear walls increases stiffness while providing for excellent energy dissipation. Oftentimes, coupling beams are deep in relation to their clear span resulting in their design being controlled by shear. They may be susceptible to strength and stiffness deterioration under severe earthquake loading.

Because diagonally oriented reinforcement is effective only if the bars are placed with large inclination, diagonally reinforced coupling beams are restricted to beams having an aspect ratio of  $\ell_n/h < 4$ . However, coupling beams of intermediate aspect ratio may be reinforced according to requirements for flexural members of special moment frames.

Diagonal bars are typically placed symmetrically in two or more layers within the beam cross section. The diagonal bars are intended to provide for the entire shear and the corresponding moment strength of the beam; designs deriving their moment strength from combinations of diagonal and longitudinal bars are not covered in the 2008 ACI provisions.



**FIGURE 6.54** Diagonal reinforcement in coupling beams. Detail 1: ACI 318-05 required confinement of individual diagonals. Detail 2: As an option, ACI 318-08 allows full-depth confinement of diagonals.

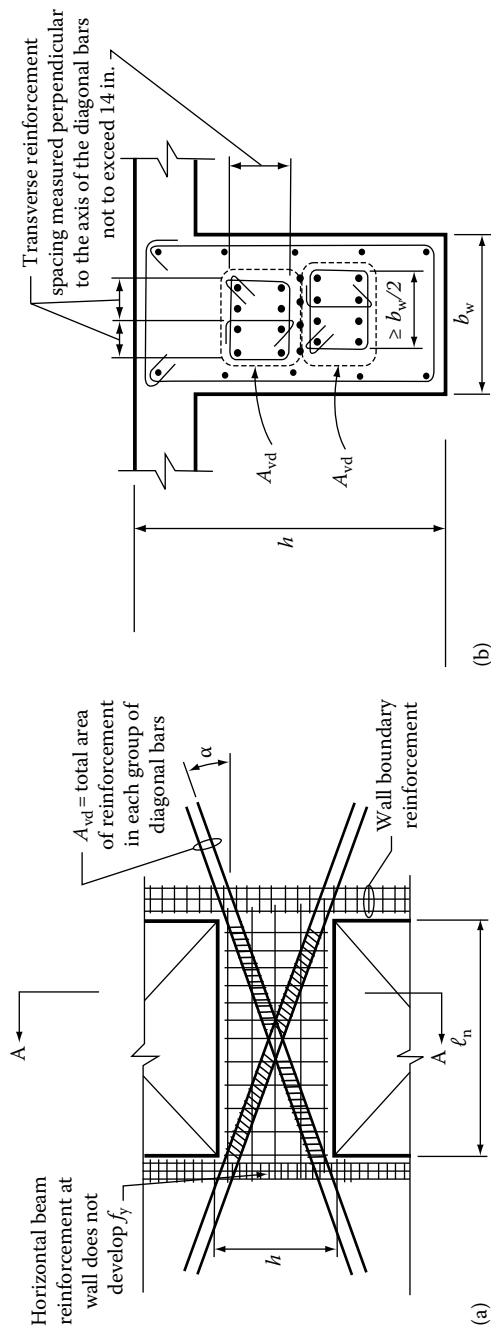
As prescribed by ACI 318-05, the individual diagonals are to be confined by transverse reinforcement, with the remainder of the beam reinforced by nominal transverse and longitudinal reinforcements. These beams may be quite challenging to construct particularly in two areas. The first area is where the diagonals intersect. Here it is difficult to install confining ties with in the complex geometry because of the criss-crossing diagonals. The second area of difficulty is where the diagonals intersect the walls at a steep angle presenting confinement challenges. The optional detail prescribed in the 2008 ACI, is expected to be more economical because of savings in labor cost.

Two options for confining the diagonal reinforcement are described in the 2008 ACI, (see Figure 6.54). In the first, each diagonal element consists of a cage of longitudinal and transverse reinforcements as shown in Figure 6.55. Each cage contains at least four diagonal bars and confines a concrete core. The requirement on side dimensions of the cage and its core is to provide adequate toughness and stability to the cross section when the bars are loaded beyond yielding. The minimum dimensions and required reinforcement clearances may control the wall width. Revisions were made in the 2008 code to relax the spacing of transverse reinforcement confining the diagonal bars, to clarify that confinement is required at the intersection of the diagonals, and to simplify the design of the longitudinal and transverse reinforcements around the beam perimeter; beams with these new details are expected to perform acceptably.

The second option for the confinement of the diagonals introduced in the 2008 code is to confine the entire beam cross section instead of confining the individual diagonals (see Figure 6.56). This option simplifies the field-placement of hoops, which can otherwise be difficult where diagonal bars intersect each other or enter the wall boundary.

When coupling beams are not used as part of the lateral-force-resisting system, the requirements for diagonal reinforcement may be waived.

Beams reinforced as described above have adequate ductility at shear forces exceeding  $10\sqrt{f'_c}b_wd$ . Consequently, the use of  $10\sqrt{f'_c}A_{cw}$  provides an acceptable upper limit.



**FIGURE 6.55** Coupling beam diagonal reinforcement. Detail 1: Confinement of individual diagonals: (a) elevation and (b) section.

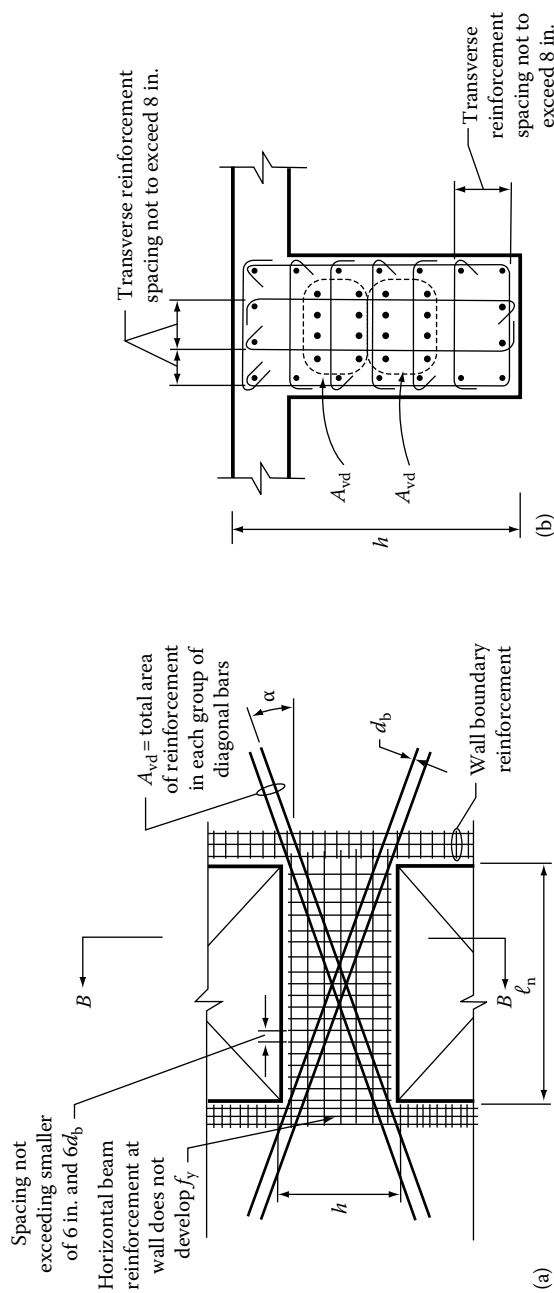


FIGURE 6.56 Coupling beam diagonal reinforcement. Detail 2: Full-depth confinement of diagonals: (a) elevation and (b) section.

---

# 7 Seismic Rehabilitation of Existing Buildings

Seismic rehabilitation is a classic mitigation strategy not unlike preventive medicine. The core argument for the seismic rehabilitation of buildings is that rehabilitated buildings will provide increased protection of life and property in future earthquakes, thereby resulting in fewer casualties and less damage than would otherwise be the case. More earthquake-resistant buildings will mean fewer deaths and injuries in an event and therefore lower demand on emergency medical services, urban search and rescue teams, fire and law enforcement personnel, utilities, and the providers of emergency shelter. In the commercial sector, less damage to structures will mean enhanced business survival and continued ability to serve customers and maintain market shares. More specifically, for commercial enterprises seismic rehabilitation will better protect physical and financial assets; reduced inventory loss; shorten the business interruption period; avoid the need for relocation; and minimize secondary effects on suppliers, shippers, and other businesses involved in support services or product cycles. For governments, if their structures come through an earthquake with little or no damage, public officials can better respond to the immediate and long-term demands placed on them by the event. In short, seismic rehabilitation as a preevent mitigation strategy will improve postevent response by lessening life loss, injury, damage, and disruption.

Seismic rehabilitation also will help achieve other important goals that contribute to business and community well-being. For example, seismic rehabilitation will

- Reduce community, economic, and social impacts.
- Minimize the need for getting disaster assistance as seeking loans or grants.
- Help to protect historic buildings, structures, or areas that represent unique community values that provide the residents with a sense of their unique histories.
- Minimize impacts on critical community services such as hospitals and medical care facilities.
- Support the community's postearthquake need to return to a pattern of normal activities by helping to ensure the early reopening of business and civic facilities. In addition to reducing demands for immediate assistance, seismic rehabilitation restores normal activities as soon as possible thus contributing greatly to the psychological well-being of a community.
- Minimize the many and often subtle direct and indirect socioeconomic impacts of earthquakes, some of which emerge slowly but often last a long time. Help marginal businesses to reopen, thus, strengthening a community's economic and social fabric.
- Reduce the environmental impacts of earthquakes. These include, for example, the need to dispose of large quantities of debris, the release of asbestos in damaged buildings, and the contamination of the air and water with spilled hazardous materials.

In sum, the rehabilitation of existing buildings significantly reduces future losses and, in economic terms, can be considered an investment to protect assets currently at risk.

Earthquake-vulnerable buildings exist nationwide, but the earthquake hazard is not uniform across the country. Moreover, awareness of the earthquake hazard, the precursor to any action, varies even more than the hazard itself. Therefore, tackling the earthquake-vulnerable building problem takes place in an incredibly diverse set of geographic, social, economic, and political environments.

Further complicating the situation is the fact that no two buildings ever seem to present exactly the same problems. Each building has its own earthquake-vulnerability profile—location, architecture, structural system, occupancy, economic role, and financing. In other words, each building has its own story.

In sum, the intent of this chapter is to explain seismic rehabilitation and to offer a set of approaches or “models,” as given in ASCE/SEI 41-06 document.

Seismic rehabilitation of a building entails costs as well as disruption of its usage. In fact, the effects of a rehabilitation program are similar to those of an earthquake because strengthening, in terms of cost and the need to vacate the structure while strengthening is underway is analogous to building repair after an earthquake. The crucial difference is that strengthening occurs at a specified time and no deaths or injuries will occur during the process.

In a seismic rehabilitation study, it is convenient to classify the damage within a building in two categories, structural and nonstructural. Structural damage refers to degradation of the building’s support system, such as frames and walls, whereas nonstructural damage is any damage that does not affect the integrity of the building’s physical support system. Examples of nonstructural damage are chimneys that collapse, broken windows or ornamental features, and collapsed ceilings. The type of damage a building experiences depends on its structural characteristics, age, configuration, construction, materials, site conditions, proximity to neighboring buildings, and the type of non-structural elements.

An earthquake can cause a building to experience four types of damage:

1. The entire building collapses.
2. Portions of the building collapse.
3. Components of the building fail and fall.
4. Entry–exit routes are blocked, preventing evacuation and rescue.

Any of the above may result in unacceptable risk to human lives. It can also mean loss of property and interruptions of use or normal function.

Another type of damage that should be included in the rehabilitation study is the structural damage from the pounding action that results when two insufficiently separated buildings collide. This condition is particularly severe when the floor levels of the two buildings do not match, because the stiff floor framing of one building can badly damage the more fragile walls or columns of its neighbor.

A rehabilitation objective may be achieved by implementing a variety of measures, including

1. Local modification of deficient components
2. Removal or partial mitigation of existing irregularities
3. Global stiffening
4. Global strengthening
5. Reduction of mass
6. Seismic isolation
7. Installation of supplemental energy dissipation devices

Failure of nonstructural architectural elements can also create life-threatening hazards. For example, windows may break or architectural cladding such as granite veneer or precast with insufficient anchorage may separate from the building, causing injury to pedestrians. Consequently, a seismic retrofit program should explore techniques for dealing with nonstructural components such as veneers, light fixtures, glass doors and windows, raised computer access floors, and ceilings. Similarly, damage to mechanical and electrical components can impair building functions that may be essential to life safety (LS) and seismic strengthening should be considered for components such as mechanical and electrical equipment, ductwork and piping, elevators, emergency power systems, communication systems, and computer equipment.

## 7.1 CODE-SPONSORED DESIGN

The forces experienced by a structure during a major earthquake are much greater than the design forces. Usually, it is neither practical nor economically feasible to design a building to remain elastic during a major seismic event. Instead, the structure is designed to remain elastic at a reduced force level. By prescribing detailing requirements, engineers can rely upon the structure to sustain postyield displacements without collapse when subjected to higher levels of ground motion. The rationale for designing with lower forces is based on the premise that the special ductile detailing of the components is adequate to allow for additional deformation without collapse. Historically, this approach has produced buildings with a strength capacity adequate for the scaled-down seismic forces and, more important, with adequate performance characteristics beyond the elastic range. It is the consensus of the structural engineering profession that a building properly designed to both code-specified forces and detailing requirements will have an acceptable level of LS during a major seismic event.

The ability of a member to undergo large deformations beyond the elastic range is termed ductility. The same property in a building that allows it to absorb earthquake-induced damage and yet remain stable may be considered, in a conceptual sense, similar to ductility. Ductile structures may deform excessively under load, but they remain by and large intact. This characteristic prevents total structural collapse and provides protection to occupants of buildings. Therefore, providing capacity for displacement beyond the elastic range without collapse is a primary goal.

Aside from this implicit philosophy, no explicit earthquake performance objectives are stated in most building codes. However, building structures designed in conformance with modern codes such as the IBC-06 are expected to

1. Resist low-level earthquakes without damage
2. Resist moderate-level earthquakes without structural damage, while possibly experiencing some nonstructural damage
3. Resist high-level earthquakes of intensity equal to the strongest experienced or forecast for the building site without collapse, while possibly experiencing some structural or non-structural damage

It is expected that structural damage, even in a major earthquake, will be limited to a repairable level for structures that meet these requirements. However, conformance to these provisions does not ensure that significant structural damage will not occur in the event of a large earthquake. Therefore, additional requirements are given in the code to provide for structural stability in the event of extreme structural deformations.

The protection of life rather than prevention and repairability of damage is the primary purpose of the code; the protection of life is thus reasonably provided for but not with complete assurance.

## 7.2 ALTERNATE DESIGN PHILOSOPHY

Although earthquake performance objectives are implicit in building codes, significant questions linger. Is the philosophy of inferring the behavior adequate to define the expected earthquake performance? Can the performance be actually delivered? Should the earthquake response objectives be explicitly stated in building codes? Is it feasible to make an existing nonductile building conform to current detailing and ductility provisions? If not, what level of upgrade will provide for minimum LS? How much more strengthening is required to achieve an “immediate occupancy rating?”

Explicit answers to these and similar questions cannot be found in current building codes. Although a set of minimum design loads are prescribed, the loads may not be appropriate for seismic performance verification and upgrade design because

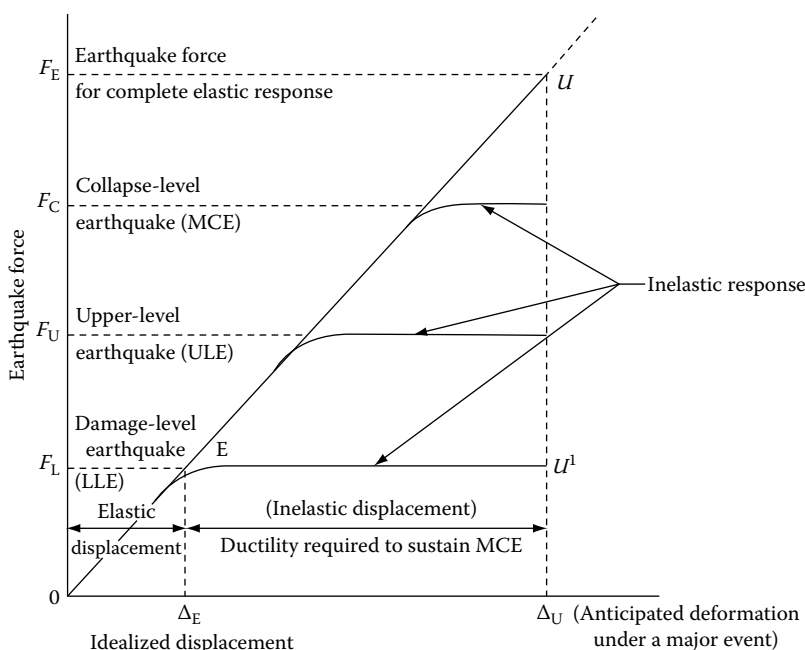


1. The code provisions do not provide a dependable or established method to evaluate the performance of noncode compliant structures.
2. They are not readily adaptable to a modified criterion, such as one that attempts to limit damage.
3. Since the primary purpose is protection of LS, the code does not address some building owners' business concerns such as protection of property, the environment, or business operations.

To overcome these shortcomings, a procedure that uses a two-phase design and analysis approach has been in use for some time. The technique explicitly requires verification of serviceability and survival limit states by using two distinct design earthquakes; one that defines the threshold of damage and the other that defines collapse. The serviceability level earthquake is normally characterized as an earthquake that has a maximum likelihood of occurring once during the life of the structure. The collapse threshold is typically associated with the maximum earthquake that can occur at the building site in the presently known tectonic framework. This characterization can vary, however, to suit the specifics of the project, such as the nature of the facility, associated risk levels, and the threshold of damageability.

The principle behind the two-phase approach may be explained by recalling the primary goal in seismic design, which is to provide capacity for displacement beyond the elastic range. Any combination of elastic and inelastic deformations is possible to attain this goal. For example, we could design a structural system that would remain elastic throughout the displacement range. This system would have a high elastic strength but low ductility. Conversely, it is entirely possible to have a system with relatively low elastic strength but high ductility, meeting the same design objective of remaining stable. It may be easier to understand the methodology if it is recognized that a specific earthquake excitation causes about the same displacement in a structure whether it responds elastically or with any degree of inelasticity.

Figure 7.1 shows the behavior of an idealized structure subjected to three levels of earthquake forces  $F_L$ ,  $F_U$ , and  $F_C$  corresponding to lower-level, upper-level, and collapse-level earthquakes.



$\Delta_U$  = Anticipated deformation irrespective of ductility that can be achieved as a combination of elastic deflection  $OE$  + inelastic deformation  $EU^1$  or by a totally elastic response of  $OE + EU$ .

**FIGURE 7.1** Idealized earthquake force–displacement relationships.

Also shown is an earthquake force  $F_E$  experienced by the structure if it were to remain completely elastic. The structure designed using the lower-level earthquake force  $F_L$  deforms elastically from 0 to  $E$  and inelastically from  $E$  to  $U$ . The same structure designed using the force  $F_U$  needs to deform 0 to  $U$ , responding elastically all through the displacement range. Both systems are capable of attaining the anticipated deformation of  $\Delta_U$ . However, a building designed using the force  $F_L$  will require a more ductile system than a building designed for the fully elastic force  $F_E$ . More importantly, it will suffer heavier damage should the postulated event occur. Nevertheless, both systems achieve the primary goal: Both remain stable without collapse under the expected deformation  $\Delta_U$ . Therefore, it is possible to design the structure using any level of force between  $F_L$  and  $F_E$  with the understanding that a corresponding ductility is developed by the detailing of the system. For example, a structure designed for the force level  $F_U$  requires a higher strength but less ductility than if it were designed for force level  $F_L$ . Hence, it is a matter of choice as to how much strength can be traded off for ductility and, conversely, ductility traded for strength. Expressed another way, structural systems of limited ductility may be considered valid, provided they are capable of resisting correspondingly higher seismic forces.

This is the approach used in the seismic retrofit design of existing buildings. Since buildings of pre-1970 vintage do not have the required ductile detailing, the purpose is to establish the strength levels that can be traded off in part, for lack of required ductility.

### 7.3 CODE PROVISIONS FOR SEISMIC UPGRADE

Building codes deal primarily with the design of new buildings. For seismic upgrade, the primary use of these documents is for determining existing building capacity. They do not, in general, provide guidance for evaluating and upgrading the seismic resistance of existing buildings.

Most codes allow existing buildings to use their current lateral-load-resisting systems if only trivial changes to the structure are proposed and the building's use remains unchanged. Codes require upgrading of buildings when major changes or tied-in additions are planned, and when the proposed alterations reduce the existing lateral-load-resisting capacity. A lateral-load upgrade may also be required if the proposed changes move the building into the categories of "essential" or "hazardous" facilities.

The seismic provisions of the IBC-06 attempt to be more specific by quantifying the meaning of "significant change." It requires that the addition itself be compliant with the code for new construction, and requires a seismic upgrade of the existing building if the addition increases the seismic forces in any existing structural member by more than 5% unless that member is already strong enough to comply with the code. Similarly, the addition is not allowed to weaken the seismic capacity of any existing structural member to a level below that specified for new construction. However, there remain some questions as to how to interpret these provisions.

When building codes prescribe full compliance with their current seismic provisions, they are rarely explicit in telling users what measures to take to upgrade the building. There are exceptions, of course. On the U.S. west coast, San Francisco's building code requires upgrading of existing structures to 75% of the strength required by the code for new construction. On the east coast, the *Commonwealth of Massachusetts Building Code* offers an elaborate path for determination of required remedial measures. In some cases it allows lower seismic forces than those used for new construction. In some regions of high seismic activity, state and local codes and ordinances may require a seismic upgrade even for buildings that are not undergoing renovation. Perhaps the best known of these is California's Senate Bill 1953, a seismic retrofit ordinance adopted on February 24, 1994, in the wake of the Northridge earthquake. It required more than 450 acute care facilities to submit seismic evaluation and compliance plans showing how the facilities will withstand a code-level earthquake, defined as a seismic event with a 10% probability of being exceeded in 100 years.

In general, the process for seismic upgrade is somewhat disorderly. It is not uncommon to have one engineer declare that a building needs a complete seismic upgrade, while another states that none is needed. Sometimes the owner will “shop” for an engineer in whose opinion an upgrade is not needed and is willing to justify this interpretation of the code to building officials.

These real-life observations lead to the conclusion that guidance on this issue from an authoritative source is sorely needed. One source—the ASCE/SEI 41-06 publication, discussed shortly—attempts to fill the void.

As compared to seismic upgrade of existing structures, design of a new structure for proper seismic performance is a “cinch.” This is because most structural characteristics important to seismic performance including ductility, strength, deformability, continuity, configuration, and construction quality can be designed and, to a certain extent, controlled.

Seismic rehabilitation of existing structures poses a completely different problem. First, until recently, there was no clear professional consensus on appropriate design criteria. That changed substantially with the publication of FEMA 356, *Prestandard and Commentary on the Seismic Rehabilitation of Buildings*. Second, the building codes for new construction are not directly applicable because they incorporate levels of conservatism and performance objectives that may not be appropriate for use on existing structures due to economic limitations. Third, the material strengths and ductility characteristics of an existing structure will, in general, not be well defined. And finally, the details and quality of construction are frequently unknown and, because the structure has been in service for some time, deterioration and damage are often a concern.

The successful seismic upgrade of an existing structure therefore requires a thorough understanding of the existing construction, its limiting strength and deformation characteristics, qualification of the owner’s economic and performance objectives, and selection of an appropriate design criterion to meet these objectives, and must also be acceptable to the building officials. Most of the time it includes the selection of retrofit systems and detailing that can be installed within the existing structure.

## 7.4 BUILDING DEFORMATIONS

The basic design procedure for new structures consists of the selection of lateral forces appropriate for design purposes, and then providing a complete, appropriately detailed, lateral-force-resisting system to carry these forces from the mass levels to the foundations. Although deformations are checked, experience has shown that new structures with modern materials and ductile detailing can sustain large deformations while experiencing limited damage. Older structures, however, do not have the advantage of this inherent ductility. Therefore, control of deformations becomes an extremely important issue in the design of seismic retrofits.

Determination of the deformations expected in a structure, when subjected to the design earthquake, is the most important task in seismic rehabilitation design. There are three types of deformations that must be considered and controlled in a seismic retrofit design. These are

1. Global deformations
2. Elemental deformations
3. Interstructural deformations

Although they are all interrelated, for purposes of seismic upgrade it is convenient to consider each of these separately.

*Global deformations* are the only type explicitly controlled by the building codes and are typically considered by reviewing interstory drift. The basic concern is that large interstory drifts can result in  $P\Delta$  instabilities. Control of interstory drift can also be used as a means of limiting damage to nonstructural elements of a structure. However, it is less effective than elemental or interstructural deformations in limiting damage to individual structural elements.

*Elemental deformation* is the amount of seismic distortion experienced by an individual element of a structure such as a beam, column, shear wall, or diaphragm. Building codes have very

few provisions that directly control these deformations. They rely on ductility to ensure that individual elements will not fail at the global deformation levels predicted for the structure. In existing structures with questionable ductility, it is therefore critical to evaluate the deformation of each element and to ensure that expected damage to the element is acceptable. This requirement extends to elements not normally considered as participating in the lateral-force-resisting system. A glaring example that is attracting much attention after the Northridge earthquake is the punching shear failure of flat slabs at interior columns, resulting from excessive rotation at the slab–column joint. Often, the slab system is not considered to participate in the lateral-force-resisting system. In fact, building codes indirectly prohibit the use of flat slab–frames in the lateral system of buildings in high seismic zones. However, in relatively flexible buildings such as those without shear walls, when flat slabs “go for a ride,” they bend and twist. In doing so, they fail if they do not have adequate ductility. Therefore it is very important to limit the rotational deformation of these joints to prevent a punching shear failure.

*Interstructural deformations* are those that relate to the differential movement between elements of the structure. Failures that result from lack of such control include failures of masonry walls that have not been anchored to diaphragms and failures resulting from bearing connections slipping off beam seats. Building codes control these deformations, which may cause separation of one element from another, by requiring interconnection of all portions of structures. A similar technique should be considered in the retrofit of an existing structure.

Code methodologies rely on elastic dynamic analysis using base shears that are reduced by response modification coefficient  $R$  and then they are scaled up or down to 85% of base shear values computed on the basis of an equivalent lateral-load procedure. Therefore, design forces are significantly smaller than those likely to be experienced by the building. However, when it comes to deformations, it is explicitly recognized that the predicted elastic levels of deformation, termed  $\delta_{xe}$  are quite small compared to the actual deformations that may be experienced by the building. Hence, the amplified deformations  $\delta_x = C_d \delta_{xe} / I_s$  are specified in the codes to evaluate the effects of seismic deformation. It is even more important to use a similar approach in evaluating existing structural elements in a retrofitted structure, because pre-1971 buildings rarely have the required ductility.

## 7.5 COMMON DEFICIENCIES AND UPGRADE METHODS

Seismic upgrade of buildings typically involves strengthening of their horizontal and vertical lateral-load-resisting elements. This can be done by reinforcing the existing elements, or by adding new elements. If the existing lateral-load-resisting structure is grossly deficient, it can be replaced. Whenever buildings are upgraded to resist a larger seismic load, their foundations must be checked for the new loading, and be reinforced if necessary.

Prime candidates for renovation and strengthening are

- Buildings with irregular configurations, such as those with abrupt changes in stiffness, large floor openings, very large floor heights, reentrant corners in plan, and soft stories.
- Buildings with walls of unreinforced masonry, which tend to crack and crumble under severe ground motions.
- Buildings with inadequate diaphragms lacking ties between walls and floors or roofs.
- Buildings with nonductile concrete frames, in which shear failures at beam–column joints and column failures are common.
- Concrete buildings with insufficient lengths of bar anchorage and splices.
- Concrete buildings with flat-slab framing, which can be severely affected by large story drifts.
- Buildings with open storefronts.
- Buildings with clerestory conditions.
- Buildings with elements that tend to fail during ground shaking: Examples are unreinforced masonry parapets and chimneys, and nonstructural building elements, which may fall, blocking exits and injuring people.

### 7.5.1 DIAPHRAGMS

The floors and roofs of buildings must act as a diaphragm—a deep horizontal beam capable of transferring lateral load generated by the floor/roof mass to the vertical elements resisting lateral loads. To do so it must have

1. The ability to resist horizontal shear forces, meaning that it must possess a certain degree of strength and rigidity in its plane. In other words, it must be able to function as a web of the horizontal beam that neither breaks nor deflects excessively under horizontal load.
2. Flanges at opposite ends of the diaphragm perpendicular to the applied forces. These flanges, called chords, must be attached to the diaphragm's web with connections capable of transmitting the seismic forces.
3. Drag struts, also called collector elements, to deliver the seismic load from the diaphragm to the vertical lateral-load-resisting elements. However, drags are required only when the horizontal distribution of load among the walls or frames depends on the types of floor and roof diaphragms in the building. Flexible systems are assumed to distribute lateral loads to the walls or frames in proportion to their tributary areas. In contrast, rigid diaphragms are assumed to distribute lateral loads to the walls or frames in proportion to their relative rigidities. Rigid diaphragms can distribute horizontal forces by developing torsional resistance. This is helpful in buildings with irregular wall layout. Flexible diaphragms are considered too supple to work in torsion. The majority of real-life floor structures fall between the two categories; engineering judgment is required to predict the behavior of these semirigid or semiflexible diaphragms. However, prevailing practice allows the assumption of rigid diaphragms for concrete slabs, unless diaphragm span to depth are very large, typically in excess of three.

The type and function of existing diaphragms must be evaluated prior to making a decision on how to strengthen the vertical lateral-load-resisting elements of the building. For example, it is unwise to add shear walls in an asymmetric manner if this introduces additional torsion into the existing diaphragm and may lead to its possible distress. If shear walls are placed in the interior of the building, collector elements must be present in the diaphragm to carry the inertial forces to them.

Methods of strengthening diaphragms depend on their composition and the nature of their weaknesses. Deficiencies of existing diaphragms typically fall into two categories: insufficient strength or stiffness and the absence of chords and collectors. Replacing a diaphragm, which involves taking out the building floor, is reserved for the most critical conditions.

#### 7.5.1.1 Cast-in-Place Concrete Diaphragms

Cast-in-place diaphragms are sturdy elements that rarely require a major upgrade except at their connections to the chord. However, common deficiencies at diaphragm openings or plan irregularities include inadequate shear capacity, inadequate chord capacity, and excessive shear stresses.

Two alternatives may be effective in correcting the deficiencies: either improve strength and ductility, or reduce demand. Providing additional reinforcement and encasement may be an effective measure to strengthen or improve individual components. Increasing the diaphragm thickness may also be effective, but the added weight may overload the footings and increase the seismic loads. Lowering seismic demand by providing additional lateral-force-resisting elements, introducing additional damping, or base isolating the structure may also be effective rehabilitation measures.

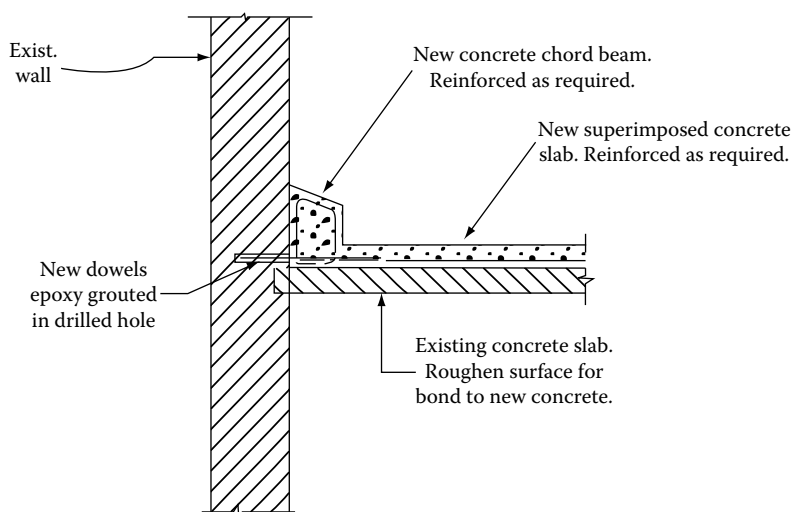
Inadequate shear capacity of concrete diaphragms may be mitigated by reducing the shear demand on the diaphragm by providing additional vertical lateral-force-resisting elements or by increasing the diaphragm capacity by adding a concrete overlay. The addition of a concrete overlay is usually quite expensive, since this requires the removal of existing partitions and floor finishes and may require the strengthening of existing beams and columns to carry the added dead load.

Adding supplemental vertical lateral-force-resisting elements will provide additional benefits by reducing demand on other elements that have deficiencies.

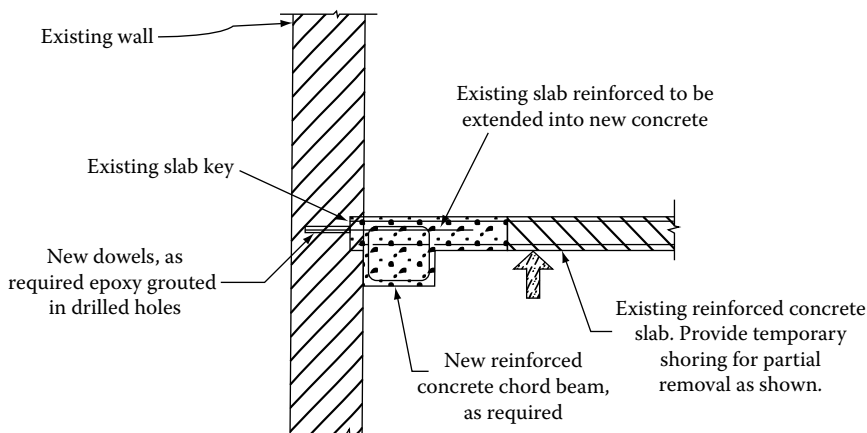
Increasing the chord capacity of existing concrete diaphragms can be realized by adding new concrete or steel members or by improving the continuity of existing members. A common method for increasing the chord capacity of a concrete diaphragm with the addition of a new concrete member is shown in Figures 7.2 and 7.3. This member can be placed above or below the diaphragm. Locating the chord below the diaphragm will typically have less impact on floor space. Shown in Figure 7.4 is a method of strengthening chord capacity of diaphragms around existing openings while Figure 7.5 shows addition of collectors at reentrant corners of a diaphragm.

The following measures may be effective in rehabilitating chord and collector elements:

1. Strengthening the connection between diaphragms and chords and collectors
2. Strengthening steel chords or collectors with steel plates attached directly to the slab with embedded bolts or epoxy and strengthening slab chord or collectors with added reinforcing bars
3. Adding chord members



**FIGURE 7.2** Superimposed diaphragm slab at an existing concrete wall.



**FIGURE 7.3** Diaphragm chord for existing concrete slab.

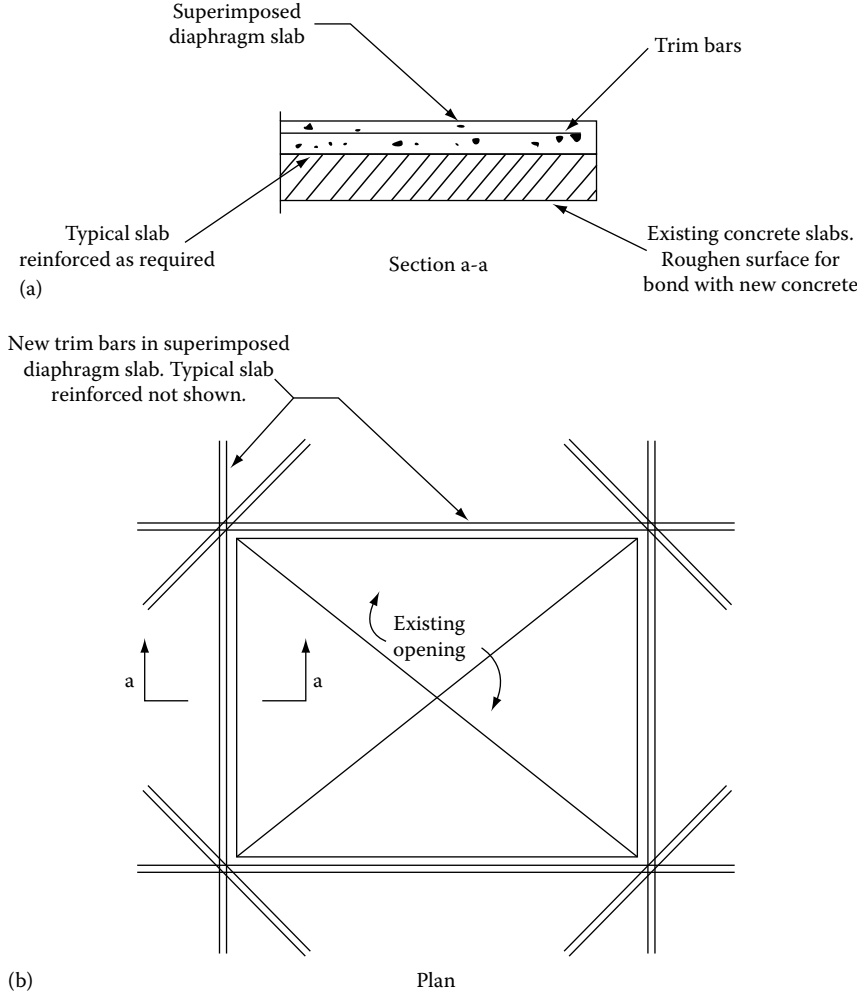


FIGURE 7.4 Strengthening of openings in a superimposed diaphragm; (a) section, (b) plan.

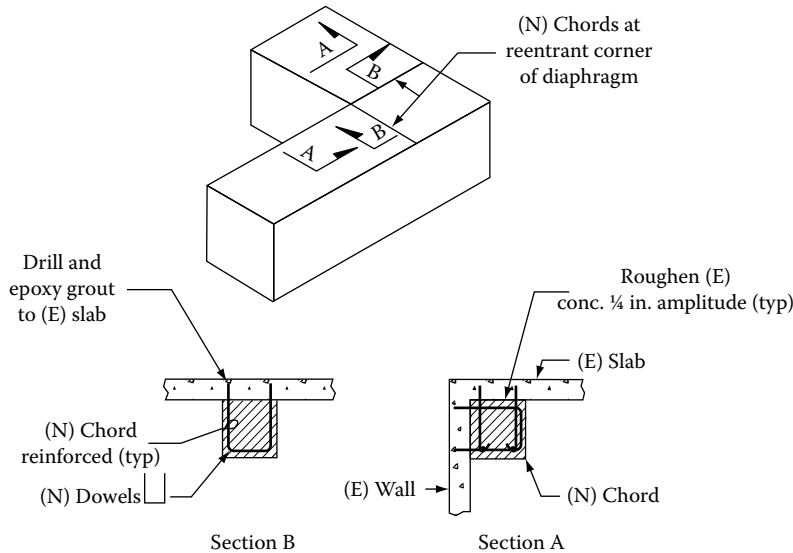


FIGURE 7.5 New chords at reentrant corners.

### 7.5.1.2 Precast Concrete Diaphragms

Common deficiencies of precast concrete diaphragms include inadequate shear capacity, inadequate chord capacity, and excessive shear stresses at diaphragm openings or plan irregularities. Existing precast concrete slabs constructed using precast tees or cored planks commonly have inadequate shear capacity. Frequently, limited shear connectors are provided between adjacent units, and a minimal topping slab with steel mesh reinforcement is placed over the planks to provide an even surface to compensate for irregularities in the precast elements. The composite diaphragm may have limited shear capacity.

Strengthening the existing diaphragm is generally not cost effective. Adding a reinforced topping slab is generally not feasible because of the added weight. Adding mechanical connectors between units is generally not practical, because the added connectors are unlikely to have sufficient stiffness, compared to the topping slab, to resist an appreciable load. The connectors would therefore need to be designed for the entire shear load assuming the topping slab fails. The number of fasteners, combined with edge distance, typically makes this impractical. The most cost-effective approach is generally to reduce the diaphragm shear forces through the addition of supplemental shear walls or braced frames.

Inadequate chord capacity in a precast concrete deck can be mitigated by adding new concrete or steel members, as discussed earlier for a cast-in-place concrete diaphragm. A new chord member can be added above or below the precast concrete deck. Excessive stresses at diaphragm openings or plan irregularities in precast concrete diaphragms can also be mitigated by introducing drag struts, as described earlier for cast-in-place concrete diaphragms.

## 7.5.2 SHEAR WALLS

The problems that are most difficult to fix are those caused by the irregular configuration of a building (e.g., abrupt changes in stiffness, soft stories, large floor openings, and reentrant floor corners). These cases may require the addition of vertical or horizontal rigid structural elements, as well as strengthening of existing foundations or addition of new ones.

There are several approaches to increasing the capacity of existing concrete shear walls. These are discussed in the following sections.

### 7.5.2.1 Increasing Wall Thickness

Wall thickness is increased by applying reinforced concrete to the wall surface. Shotcrete, a mixture of aggregate, cement, and water sprayed by a pneumatic gun at high velocity, is widely used for strengthening walls because it bonds well with concrete. Some prefer application by the dry mix method (sometimes called gunite) because the slump and stiffness can be better controlled by the nozzle operator and because gunite is applied at higher nozzle velocities, it promotes superior bonding.

Concrete shear walls that lack ductility may fail by crushing of their boundary elements, horizontal sliding along construction joints due to shear, or diagonal cracking caused by combined flexure and shear. Among the most common areas of damage are the coupling beams. These can be repaired by through-bolted side plates extending onto the faces of the walls. Short and rigid piers between walls openings also tend to attract an inordinate amount of seismic loading and are therefore prone to damage.

The key to shotcreting walls lies in the surface preparation of the wall because existing concrete may be counted as part of the strengthened wall. All loose and cracked concrete must be removed from the existing wall, and its surface cleaned and roughened by sandblasting or other means. To assure composite action, the overlay is mechanically connected to the wall by closely spaced shear dowels. In addition, steel reinforcement placed in shotcrete is developed at the ends by grouted-in dowels or by continuation into an adjacent overlay space. This involves drilling through the perimeter beams or columns, filling the drilled openings with epoxy, and splicing the bars with those in the adjoining overlay areas. If the existing wall openings must be filled, the infill should be connected to the roughened edges of the opening with perimeter dowels set in epoxy.



When interior shotcreting is used, attention must be directed toward stabilizing the exterior walls and any exterior ornamental element of the structure. These may have to be tied back into the new shotcrete by drilled-in dowels set at regular intervals. Dowels placed in exterior elements that are exposed to moisture should be given a measure of corrosion protection, such as galvanizing.

In cases where it is desirable not to increase the wall size, the outer course of bricks can be removed and replaced with shotcrete. The same can be done with interior shotcreting, except that any members framing into the wall may have to be shored during this operation. The added bonus of this approach is that the vertical load on the existing wall foundations changes very little, and they may not require the otherwise necessary enlargement.

### **7.5.2.2 Increasing Shear Strength of Wall**

Increasing the shear strength of the web of a shear wall by casting additional reinforced concrete adjacent to the wall web may be an effective rehabilitation measure. The new concrete should be at least 4 in. thick, contain horizontal and vertical reinforcements, and be properly bonded to the existing web of the shear wall. The use of composite fiber sheets, epoxied to the concrete surface, is another method of increasing the shear capacity of a shear wall. The use of confinement jackets as a rehabilitation measure for wall boundaries may also be effective in increasing both the shear capacity and deformation capacity of coupling beams and columns supporting discontinuous shear walls.

### **7.5.2.3 Infilling between Columns**

Where a discontinuous shear wall is supported on columns that lack either sufficient strength or deformation capacity, making the wall continuous by infilling the opening between these columns may be an effective rehabilitation measure. The infill and existing columns should be designed to satisfy all the requirements for the new wall construction, including any strengthening of the existing columns required by adding a composite fiber jacket or a concrete or steel jacket for strength and increased confinement. The opening below a discontinuous shear wall may also be infilled with steel bracing. The bracing members should be sized to satisfy all design requirements for new construction and the columns should be strengthened with steel or a concrete jacket. All of these rehabilitation measures require an evaluation of the wall foundation, diaphragms, connections between existing structural elements, and any elements added for rehabilitation purposes.

Adding new shear walls or braced frames conforming to current code detailing provisions is among the most common steps taken to strengthen the lateral-load-resisting systems of buildings. The new walls and frames can either (1) complement the existing elements or (2) be designed as the sole means of providing vertical rigidity to the building. In the first case, analysis of comparable rigidities must be done to determine what percentage of the total lateral loading the new construction will carry. In the second case, the existing rigid elements that are now considered to be nonstructural must be checked for inelastic deformation compatibility. In any case, new foundations must be provided under the new elements and dowels placed around them for proper transfer of loads.

A common complication of adding shear walls and braced frames is that they tend to interfere with the building layout, circulation, or fenestration. Quite often, shear walls with openings or braced frames of unusual configurations may be needed to accommodate window or door openings. In some rare cases, exterior buttresses or counterforts may be considered.

### **7.5.2.4 Addition of Boundary Elements**

Addition of boundary members may be an effective measure in strengthening shear walls or wall segments that have insufficient flexural strength. These members may be either cast-in-place reinforced concrete elements or steel sections. In both cases, proper connections should be made between the existing wall and the added members. The shear capacity of the rehabilitated wall should be reevaluated.

### 7.5.2.5 Addition of Confinement Jackets

Increasing the confinement at wall boundaries with the addition of a steel or reinforced concrete jacket may be effective in improving the flexural deformation capacity of a shear wall. The minimum thickness for a concrete jacket should be 3 in. A composite fiber jacket may be used to improve the confinement of concrete in compression.

### 7.5.2.6 Repair of Cracked Coupling Beams

Cracked coupling beams can be repaired by adding side plates extending on the faces of the walls. In this procedure, the plates are attached with both epoxy adhesive and anchor bolts. The plates may be attached to only one face of the wall or can be placed at both faces for extra strength, with the opposite plates through-bolted together. Another possibility for improving coupling beams is by using composite fiber wrap. This method is least intrusive because the wrapping and the epoxy combined are only 0.25 in. thick.

### 7.5.2.7 Adding New Walls

Adding new shear walls at a few strategic locations can be a very cost-effective approach to a seismic retrofit. The new wall is connected to the adjoining frame by drilled-in dowels. Its foundations are similarly doweled into the existing column footings. To accommodate wall shrinkage, the wall can stop short some distance—2 in., for example—from the existing concrete at the top. The space can be filled later with nonshrink grout.

### 7.5.2.8 Precast Concrete Shear Walls

Precast concrete shear wall systems may suffer from some of the same deficiencies as cast-in-place walls. These may include inadequate flexural capacity, inadequate shear capacity with respect to flexural capacity, lack of confinement at wall boundaries, and inadequate splice lengths for longitudinal reinforcement in wall boundaries. Deficiencies unique to precast wall construction are inadequate connections between panels, to the foundation, and to floor or roof diaphragms.

The rehabilitation measures previously described for concrete buildings may also be effective in rehabilitating precast concrete shear walls. In addition, the following rehabilitation measures may be effective:

- *Enhancement of connections between adjacent or intersecting precast wall panels.* Mechanical connectors such as steel shapes and various types of drilled-in anchors, cast-in-plane strengthening methods, or a combination of the two may be effective in strengthening connections between precast panels. Cast-in-place strengthening methods include exposing the reinforcing steel at the edges of adjacent panels, adding vertical and transverse reinforcement, and placing new concrete.
- *Enhancement of connections between precast wall panels and foundations.* Increasing the shear capacity of the wall panel-to-foundation connection by using supplemental mechanical connectors or a cast-in place overlay with new dowels into the foundation may be effective rehabilitation measures. Increasing the overturning moment capacity of the panel-to-foundation connection by using drilled-in dowels within a new cast-in-place connection at the edges of the panel is another effective rehabilitation measure. Adding connections to adjacent panels is also an effective rehabilitation measure, eliminating some of the forces transmitted through the panel-to-foundation connection.

## 7.5.3 INFILLING OF MOMENT FRAMES

In many cases, the existing concrete skeleton is stiffened by filling in the space between the beams and columns with masonry or cast-in-place concrete. These infill walls can be a cost-effective method of increasing the lateral strength and rigidity of the building.

Designers should avoid counting on some of the infill walls in structural analysis but not on others, because the stiffness of the frames filled with this nonstructural masonry will increase, whether the designers realize this fact or not. In an earthquake, these panels attract large lateral forces and are damaged, or the perimeter columns, beams, and their connections fail. When a frame, however well designed, is filled with rigid material, however brittle and weak, the fundamental behavior of this structural element is changed from that of a frame to that of a shear wall.

Rehabilitation measures commonly used for concrete frames with masonry infills may also be effective in rehabilitating concrete frames with concrete infills. Additionally, application of shotcrete to the face of an existing wall to increase the thickness and shear strength may be effective. For this purpose, the face of the existing wall should be roughened, a mat of reinforcing steel doweled into the existing structure, and shotcrete applied to the desired thickness.

#### 7.5.4 REINFORCED CONCRETE MOMENT FRAMES

Earthquake damage sometimes results in sheared-off columns that formerly were parts of a frame. Typically, the concrete cover is spalled, column bars buckled, and concrete inside broken up. Most problems in concrete frames involve bar splices and failures of beam–column joints that lack confinement and in which reinforcement is stopped prematurely.

Many old buildings with flat-slab and flat-plate floor systems, even those constructed after 1973 (and presumably reflecting the post-San Fernando earthquake code changes), are vulnerable to earthquakes.

Methods available for strengthening traditional concrete frames include encasing the beam–column joints in steel or high-strength fiber jackets. One such design uses jackets consisting of four U-shaped corrugated-metal parts, two around the beam and two around the column. The column jackets are bolted to the end of the beam, the pieces are welded together, and the space between the jackets and the frame is filled with grout.

Frame joints damaged during earthquakes can be repaired with epoxy injection, and badly fractured concrete can be removed and replaced. To minimize shrinkage, the replacement concrete should be made with shrinkage-compensating (type K) cement, or should utilize a shrinkage-reducing admixture. Frame members that have been pushed out of alignment during an earthquake should be jacked back into the proper position before repair. Damaged columns can also be strengthened with fiber-reinforced wraps or other methods of exterior concrete confinement. This is common practice for seismic strengthening of buildings and bridge columns in California. Another structural issue that requires consideration is the transfer of load from the floor diaphragms to the frames and walls. This may require new drag struts. These elements can be added by attaching new concrete or structural steel sections to the underside of existing floors. They are typically placed against cleaned and roughened concrete surfaces and anchored to the floors and to frames by drilled-in dowels or through bolts.

Connections between new and existing materials should be designed to transfer the forces anticipated for the design load combinations. Where the existing concrete frame columns and beams act as boundary elements and collectors for the new shear wall or braced frame, these should be checked for adequacy, considering strength, reinforcement development, and deformability. Diaphragms, including drag struts and collectors, should be evaluated and rehabilitated to ensure a complete load path to the new shear wall or braced frame element, if necessary.

Another method of seismic rehabilitation is to jacket existing beams, columns, or joints with new reinforced concrete, steel, or fiber-wrap overlays. The new materials should be designed and constructed to act compositely with the existing concrete. Where reinforced concrete jackets are used, the design should provide detailing to enhance ductility and the jackets should be designed to provide increased connection strength and improved continuity between adjacent components.

Posttensioning existing beams, columns, or joints using external posttensioned reinforcement is an effective strategy of seismic rehabilitation. Posttensioned reinforcement should be unbounded within a distance equal to twice the effective depth from sections where inelastic action is expected. Anchors should be located away from regions where inelastic action is anticipated, and be designed considering possible force variations due to earthquake loading.

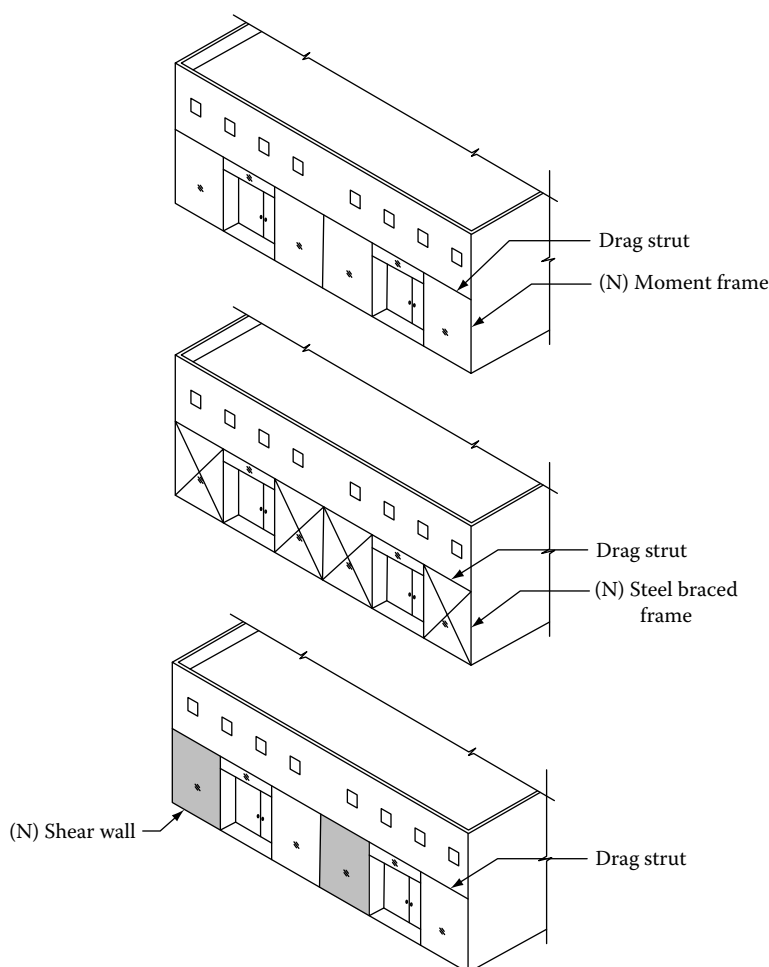
### 7.5.5 OPEN STOREFRONT

The deficiency in a building with an open storefront is the lack of a vertical line of resistance along one or two sides of a building. This results in a lateral system that is excessively soft at one end of the building, causing significant torsional response and potential instability.

The most effective method of correcting this deficiency is to install a new stiff vertical element in the line of the open-front side or sides. If the open-front appearance is desired, the steel frames may be located directly behind the storefront windows. Shear walls may also be used to provide adequate strength. In both cases collectors are required to adequately distribute the loads from the diaphragm into the vertical lateral-load-resisting element. Adequate anchorage of vertical elements into the foundation is also required to resist overturning forces. Steel moment frames instead of brace frames can also be utilized to provide adequate strength, provided that inelastic deformations of the frame under severe seismic loads are carefully considered to ensure that displacements are controlled. Common methods for upgrading buildings with open storefronts are shown in Figure 7.6.

### 7.5.6 CLERESTORY

A clerestory, typically designed to produce an open airy feeling, can result in significant discontinuity in a horizontal diaphragm. A common method of correcting the diaphragm discontinuity is to add a



**FIGURE 7.6** Common methods for upgrading buildings with open storefronts.

horizontal steel truss. Steel members can be designed to transfer diaphragm shears while minimizing the visual obstruction of the clerestory.

An alternate approach is to reduce the demands on the diaphragm through the addition of new vertical lateral-force-resisting elements such as shear walls or braced frames.

### 7.5.7 SHALLOW FOUNDATIONS

The following rehabilitation measures may be considered for shallow foundations:

1. Enlarging the existing footing to resist the design loads. Care must be taken to provide adequate shear and moment transfer capacity across the joint between the existing footing and the additions.
2. Underpinning the existing footing, removing of unsuitable soil underneath and replacing it with concrete, soil cement, or another suitable material. Underpinning should be staged in small increments to prevent endangering the stability of the structure. This technique may be used to enlarge an existing footing or to extend it to a more competent soil stratum.
3. Providing tension hold-downs to resist uplift. Tension ties consisting of soil and rock anchors with or without prestress may be drilled and grouted into competent soils and anchored in the existing footing. Piles or drilled piers may also be effective in providing tension hold-downs for existing footings.
4. Increasing the effective depth of the existing footing by placing new concrete to increase shear and moment capacity. The new concrete must be adequately doweled or otherwise connected so that it is integral with the existing footing. New horizontal reinforcement should be provided, if required, to resist increased moments.
5. Increasing the effective depth of a concrete mat foundation with a reinforced concrete overlay. This method involves placing an integral topping slab over the existing mat to increase shear and moment capacity.
6. Providing pile supports for concrete footings or mat foundations. Adding new piles may be effective in providing support for existing concrete footing or mat foundations, provided the pile locations and spacing are designed to avoid overstressing the existing foundations.
7. Changing the building structural characteristics to reduce the demand on the existing elements. This may be accomplished by removing mass or height from the building or adding other elements such as energy dissipation devices to reduce the load transfer at the base. New shear walls or braces may be provided to reduce the demand on foundations.
8. Adding new grade beams to tie existing footings together when soil conditions are poor. This method is useful for providing fixity to column bases, and to distribute lateral loads between individual footings, pile caps, or foundation walls.
9. Grouting techniques to improve existing soil.

### 7.5.8 REHABILITATION MEASURES FOR DEEP FOUNDATIONS

The following rehabilitation measures may be considered for deep foundations:

1. Providing additional piles or piers to increase the load-bearing capacity of the existing foundations.
2. Increasing the effective depth of a pile cap by adding concrete and reinforcement to its top. This method is effective in increasing its shear and moment capacity, provided the interface is designed to transfer loads between the existing and new materials.
3. Improving the soil adjacent to an existing pile cap by injection-grouting.

4. Increasing the passive pressure bearing area of a pile cap by addition of new reinforced concrete extensions.
5. Changing the building system to reduce the demands on the existing elements by adding new lateral-load-resisting elements.
6. Adding batter piles or piers to the existing pile or pier foundation to increase resistance to lateral loads. It should be noted that batter piles have performed poorly in recent earthquakes when liquefiable soils were present. This is especially important to consider near-wharf structures and in areas with a high water table.
7. Increasing tension tie capacity from a pile or pier to the superstructure.

## **7.5.9 NONSTRUCTURAL ELEMENTS**

### **7.5.9.1 Nonload-Bearing Walls**

The performance of buildings with nonstructural walls that adversely affect the seismic response of a building may be improved by removing and replacing them with walls constructed of relatively flexible materials such as gypsum board sheathing or modifying the wall connections so that they will not resist lateral loads. Removal and replacement of existing hollow clay tile, concrete, or brick masonry partitions is the preferred method of addressing the inadequate out-of-plane capacity of nonstructural partitions. Alternatively, steel strongbacks can provide the out-of-plane support. Steel members are installed at regular intervals and secured to the masonry with drilled and grouted anchors. The masonry spans between the steel members, which span either vertically between floor diaphragms or horizontally between columns. A third method for mitigating masonry walls with inadequate out-of-plane capacity is to provide a structural overlay. The overlay may be constructed of plaster with welded wire mesh reinforcement or concrete with reinforcing steel or welded wire mesh. This approach is used at times merely to provide containment of the masonry. Nonstructural masonry walls are frequently used as firewalls around means of egress. Egress walls with deficient out-of-plane capacity can fail, resulting in rubble blocking the egress. Containment of the masonry with a plaster or concrete overlay can maintain egress, although the walls may need to be replaced following a major seismic event.

### **7.5.9.2 Precast Concrete Cladding**

Precast concrete cladding panels with rigid connections may not have the flexibility or ductility to accommodate large building deformations. Failure of the connection may result in heavy panels falling away from the building. Complete correction of this deficiency is likely to be costly, since numerous panel connections would need to be modified to accommodate anticipated building drifts. This may require removal and reinstallation or replacement of the panels. A more economical solution is to install redundant flexible/ductile connections that will keep the panels from falling, should the existing connections fail.

Improper design or installation of precast concrete cladding may also be more than just a connection problem. The cladding may act as an unintended lateral-load-resisting element, should the connections be rigid or insufficient gaps are present between panels. Correcting this deficiency can be accomplished by installing occasional seismic joints in the panels to minimize their stiffness or by stiffening the existing lateral-force-resisting system.

If an entirely new precast cladding system is installed, the connections should be designed to

- Carry gravity loads of precast panels
- Transfer the in-plane and out-of-plane inertia forces of the panels into the building
- Isolate the panels from the inelastic drift likely to be experienced by the building in a large earthquake

### 7.5.9.3 Stone or Masonry Veneers

Stone or masonry veneers may become falling hazards unless their anchorage can accommodate the inelastic deformation of the building. Removal and replacement by veneer with adequate anchorage is one option. A second option is to decrease the deformation of the supporting wall by adding stiffness to the structure.

### 7.5.9.4 Building Ornamentation

Building ornamentation such as parapets, cornices, signs, and other appendages are another potential falling hazard during strong ground shaking. Unreinforced masonry parapets with heights greater than 1½ times their width are particularly vulnerable to damage. Parapets are commonly retrofitted by providing bracing back to the roof framing.

Cornices and other stone or masonry appendages may be retrofitted by installing drilled and grouted anchors at regular intervals. Sometimes they may be replaced with a lightweight substitute material such as plastic, fiberglass, or metal.

### 7.5.9.5 Acoustical Ceiling

Unbraced suspended acoustical tile ceilings are significantly more flexible than the floors or roofs to which they are attached. The ceilings sway independently from the floor or roof, typically resulting in their connections being broken. This deficiency can be reduced by stiffening the suspended ceiling system with diagonal wires between the ceiling grid and the structural floor or roof members. Vertical compression struts are also required at the location of the diagonal wires to resist the upward component of force caused by the lateral loads. Current code standards can be used for the upgrade of existing ceiling systems.

## 7.6 SEISMIC REHABILITATION OF EXISTING BUILDINGS, ASCE/SEI 41-06

The document *Seismic Rehabilitation of Existing Buildings (ASCE/SEI 41-06)* specifies nationally applicable provisions for the seismic rehabilitation of buildings. Seismic rehabilitation is defined as improving the seismic performance of structural and/or nonstructural components of a building by correcting deficiencies identified in a seismic evaluation. Seismic evaluation is defined as a process or methodology of evaluating deficiencies in a building, which prevent the building from achieving a selected Rehabilitation Objective.

This standard consists of two parts: Provisions, which contain the technical requirements, and Commentary, intended to explain the provisions.

It is expected that most buildings rehabilitated in accordance with this standard would perform within the desired levels when subjected to the design earthquakes. However, compliance with this standard does not guarantee such performance; rather, it represents the current standard of practice in designing to attain this performance.

The procedure contained in this standard are specifically applicable to the rehabilitation of existing buildings and, in general, are more appropriate for that purpose than are new building codes. New building codes are primarily intended to regulate the design and construction of new buildings; as such, they include many provisions that encourage or require the development of designs with features important for good seismic performance, including regular configuration, structural continuity, ductile detailing, and materials of appropriate quality. Many existing buildings were designed and constructed without these features and contain characteristics such as unfavorable configuration and poor detailing and preclude application of building code provisions for their seismic rehabilitation.

This standard is intended to be generally applicable to seismic rehabilitation of all buildings regardless of importance, occupancy, historic status, or other classifications of use. However, application of these provisions should be coordinated with other requirements that may be in effect, such as ordinances governing historic structures or hospital construction. In addition to the direct effects of ground shaking, this standard also addresses the effects of local geologic site hazards such as liquefaction.

This standard is arranged such that there are four analysis procedures that can be used, including the linear static procedure (LSP) and nonlinear dynamic procedure (NDP). These linear analyses procedures are intended to provide a conservative estimate of building response and performance in an earthquake, though they are not always accurate. Since the actual response of buildings to earthquakes is not typically linear, the nonlinear analysis procedure should provide a more accurate representation of building response and performance. In recognition of the improved representation of building behavior when nonlinear analysis is conducted, the nonlinear procedures have less conservative limits on permissible building response compared to linear procedures. Building that is found to be seismically deficient based on linear analysis may comply with this standard if a nonlinear analysis is performed. Therefore, performing a nonlinear analysis can minimize or eliminate unnecessary seismic rehabilitation and potentially lower construction costs.

In addition to techniques for increasing the strength and ductility of systems, this standard provides techniques for reducing seismic demand, such as the introduction of isolation or damping devices.

However, once the decision to rehabilitate a building has been made, this standard can be referenced for detailed engineering guidance on how to conduct a seismic rehabilitation analysis and design. Featured in this standard are descriptions of damage states in relation to specific performance levels. These descriptions are intended to aid design professionals and owners in selecting appropriate performance levels.

### 1. Design basis

Provisions of ASCE/SEI 41-06 for seismic rehabilitation are based on a performance-based design methodology that differs from seismic design procedures for the design of new buildings currently specified in national building codes and standards.

The framework in which these requirements are specified is purposefully broad so that Rehabilitation Objectives can accommodate buildings to different types, address a variety of performance levels, and reflect the variation of seismic hazards across the United States and U.S. territories. The provisions are based primarily on and are intended to supersede *FEMA 356: Prestandard and Commentary on the Seismic Rehabilitation of Buildings*.

### 2. Rehabilitation process

The steps for establishing seismic rehabilitation process are typically in the order in which they would be followed in the rehabilitation process. Figure 6.1 depicts the rehabilitation process written for voluntary rehabilitations. However, it can also be used as a guide for mandatory rehabilitations.

Prior to embarking on a rehabilitation program, an evaluation should be performed to determine whether the building, in its existing condition, has the desired seismic performance capability. ASCE 31 contains an evaluation methodology that may be used for this purpose. It should be noted, however, that a building may meet certain performance objectives using the methodology of ASCE 31, but may not meet those same performance objectives when an evaluation is performed using the procedures of ASCE/SEI 41-06. This is largely because ASCE 31 is specifically intended to accept somewhat greater levels of damage within each performance level than permitted by ASCE/SEI 41-06. This is consistent with the historic practice of evaluating existing buildings for slightly lower criteria than those used for design of new buildings. ASCE 31 typically quantifies this difference with the use of a 0.75 factor on demands. This essentially lowers the reliability of achieving the selected performance level from about 90% to about 60%. This practice minimizes the need to rehabilitate structures with relatively modest deficiencies relative to the desired performance level.

### 3. Initial considerations

The process of building rehabilitation will be simplified and made more efficient if information that significantly affects the rehabilitation design is obtained and considered prior to beginning the process.

The building owners' skip and the design team should be aware of the range of costs and impacts of rehabilitation, including both the variation associated with different rehabilitation objectives



and the potential additional costs often associated with seismic rehabilitation, such as other LS upgrades, hazardous material removal, work associated with the Americans with Disabilities Act, and nonseismic building remodeling.

Seismic hazards other than ground shaking may exist at the building site. The risk and possible extent of damage from geologic site hazards identified should be considered before undertaking rehabilitation aimed solely at reducing damage due to seismic shaking. In some cases it may be feasible to mitigate the site hazard or rehabilitate the building and still meet the selected performance level. In other cases, the risk due to site hazards may be so extreme and difficult that to control the rehabilitation is neither cost-effective nor feasible.

There are many ways to reduce seismic risk, whether the risk is to property, LS, or postearthquake use of the building. The occupancy of vulnerable buildings can be reduced, redundant facilities can be provided, and nonhistoric buildings can be demolished and replaced. The risks posed by nonstructural components and contents can be reduced. Seismic site hazards other than shaking can be mitigated.

Most often, however, when all alternatives are considered, the options of modifying the building to reduce the risk of damage should be studied. Such corrective measures include stiffening or strengthening the structure, adding local components to eliminate irregularities or tie the structure together, reducing the demand on the structure through the use of seismic isolation or energy dissipation devices, and reducing the height or mass of the structure.

#### 4. Selection of rehabilitation objective

The concepts and terminology of performance-based design are relatively new. The terminology used for target building performance levels is intended to represent goals of design. In most events, designs targeted at various damage states may only determine relative performance. Variations in actual performance could be associated with unknown geometry and member sizes in existing buildings, deteriorations of materials, incomplete site data, variation of ground motion that can occur within a small area, and incomplete knowledge and simplifications related to modeling and analysis.

The determination of the rehabilitation objective differs depending on whether the rehabilitation is mandated or voluntary. For voluntary building rehabilitation, the building owner selects a seismic rehabilitation of the building. In a mandated rehabilitation project, the rehabilitation objective is typically stipulated directly by local code or ordinance.

Building performance can be described qualitatively in terms of the safety afforded to building occupants during and after the event. These performance characteristics are directly related to the extent of damage that would be sustained by the building.

The extent of damage to a building is categorized as a building performance level. A broad range of target building performance levels may be selected when determining Rehabilitation Objectives.

Probabilistic earthquake hazard levels frequently used and their corresponding mean return periods (the average number of years between events of similar severity) are as follows:

Earthquake Having Probability of Exceedance	Mean Return Period (Years)
50%/50 year	72
20%/50 year	225
10%/50 year	474
2%/50 year	2475

These mean return periods are typically rounded to 75, 225, 500, and 2500 years, respectively.

The rehabilitation objective selected as a basis for design will determine, to a great extent, the cost and feasibility of any rehabilitation project, as well as the benefit to be obtained in terms of

**TABLE 7.1**  
**Rehabilitation Objectives**

		Target Building Performance Levels			
		Operational Performance Level (1-A)	Immediate Occupancy Performance Level (1-B)	Life Safety Performance Level (3-C)	Collapse Prevention Performance Level (5-E)
Earthquake hazard level	50%/50 year	a	b	c	d
	20%/50 year	e	f	g	h
	BSE-1 (~10%/50 year)	i	j	k	l
	BSE-2 (~2%/50 year)	m	n	o	p

Source: ASCE/SEI 41-06 Table C1-1.

<sup>a</sup> Each cell in the above matrix represents a discrete rehabilitation objective.

<sup>b</sup> The rehabilitation objectives in the matrix above may be used to represent the three specific rehabilitation objectives defined in Sections 1.4.1 through 1.4.3, as follows:

Basic safety objective (BSO)	k and p
Enhanced objectives	k and m, n, or o
	p and i or j
	k and p and a, b, e, or f
	m, n, or o alone
Limited objectives	k alone
	p alone
	c, d, g, h, or l alone

improved safety, reduction in property damage, and interruption of use in the event of future earthquakes. Table 7.1 indicates the range of rehabilitation objectives that may be used.

### 5. Basic safety objectives (BSO)

The BSO is intended to approximate the earthquake risk to LS traditionally considered acceptable in the United States. Buildings meeting the BSO are expected to experience little damage from relatively frequent, moderate earthquakes, but significantly more damage and potential economic loss from the most severe and infrequent earthquakes that could affect them. The level of damage and potential economic loss experienced by buildings rehabilitated to the BSO may be greater than that expected in properly designed and constructed new buildings.

### 6. Enhanced rehabilitation objectives

Rehabilitation that provides building performance exceeding that of the BSO is termed an enhanced objective. Enhanced rehabilitation objectives can be obtained by designing for higher target building performance levels or by designing using higher earthquake hazard levels, or a combination of these methods.

### 7. Limited rehabilitation objectives

Rehabilitation that provides building performance less than that of the BSO is termed a limited objective. Limited rehabilitation objectives may be achieved using reduced rehabilitation, or partial rehabilitation.

Rehabilitation that addresses the entire building structural and nonstructural systems, but uses a lower seismic hazard or lower target building performance level than the BSO, is termed reduced rehabilitation objective.

Rehabilitation that addresses a portion of the building without rehabilitating the complete lateral-force-resisting system is termed partial rehabilitation.

The objectives of limited rehabilitation are

1. The rehabilitation measures shall not result in a reduction in the performance level of the existing building.
2. The rehabilitation measures shall not create a new structural irregularity or make an existing structural irregularity more severe.
3. The rehabilitation measures shall not result in an increase in the seismic forces to any component that is deficient in capacity to resist such forces.
4. All new or rehabilitated structural components shall be specially detailed and connected to the existing structure in compliance with seismic standards.

### **8. Intended (or expected) building performances**

Building performance is a combination of the performance of both structural and nonstructural components. It is described in Table 7.1 with approximate limiting levels of structural and nonstructural damage that may be expected of buildings rehabilitated to the levels defined earlier. On average, the expected damage would be less. Similarly structural performance descriptions given in Tables 7.2 and 7.3 for vertical and horizontal elements are estimates rather than precise predictions and variation among buildings of the same intended building performance must be expected.

This targeted building performance is discrete damage states selected from among the infinite spectrum of possible damage states that buildings could experience during an earthquake. The particular damage states identified as expected building performances have been selected because they have readily identifiable consequences associated with the postearthquake disposition of the building that are meaningful to the building community. These include the ability to resume normal functions within the building, the advisability of postearthquake occupancy, and the risk to LS.

Due to inherent uncertainties in prediction of ground motion and analytical prediction of building performance, some variation in actual performance should be expected. Compliance with the methodology of ASCE/SEI 41-06 should not be considered a guarantee of performance.

ASCE/SEI-06 endorses the use of performance-based design solutions for seismic rehabilitation of buildings. The chosen performance of the building may vary from preventing collapse to a near-perfect building that would survive an expected earthquake without a scratch. The standard allows owners to select their desired performance objective and permits designers to choose their own approaches to achieve the desired results rather than strictly adhering to the prescriptive requirements of codes. Instead of dictating how to achieve a given design goal, performance-based design emphasizes the goals that must be met and sets the criteria for acceptance. This way, engineers are free to innovate without running afoul of specific code provisions, within certain limits.

The SEI 41-06 outlines criteria and methods for ensuring the desired performance of buildings at various performance levels selected by the owners with input from their design professionals. The guidelines allow owners to select a level of seismic upgrade that not only protects lives, a goal of all building codes, but also protects their investment.

SEI 41-06 is a radical departure from current practice in that it seeks to provide the structural engineering profession with tools to explicitly, rather than implicitly, design for multiple, specifically defined, levels of performance. These performance levels are defined in terms of specifically limiting damage states, against which a structure's performance can be objectively measured. Recommendations are developed as to which performance levels should be attained by buildings of different occupancies and use. This tiered specification of performance levels at predetermined earthquake hazard levels becomes the design performance objective and a basis for design. It recognizes the importance of the performance of all the various component systems to the overall building performance and defines a uniform methodology of design to obtain the desired performance.

**TABLE 7.2**  
**Structural Performance Levels and Damage<sup>a,b,c</sup>—Vertical Elements**

Elements	Type	Structural Performance Levels		
		Collapse Prevention (S-5)	Life Safety (S-3)	Immediate Occupancy (S-1)
Concrete frames	Primary	Extensive cracking and hinge formation in ductile elements. Limited cracking and/or splice failure in some nonductile columns. Severe damage in short columns.	Extensive damage to beams. Spalling of cover and shear cracking (<1/8 in. width) for ductile columns. Minor spalling in nonductile columns. Joint cracks <1/8 in. wide.	Minor hairline cracking. Limited yielding possible at a few locations. No crushing (strains below 0.003).
	Secondary	Extensive spalling in columns (limited shortening) and beams. Severe joint damage. Some reinforcing buckled.	Extensive cracking and hinge formation in ductile elements. Limited cracking and/or splice failure in some nonductile columns. Severe damage in short columns.	Minor spalling in a few places in ductile columns and beams. Flexural cracking in beams and columns. Shear cracking in joints <1/16 in. width.
	Drift	4% transient or permanent.	2% transient; 1% permanent.	1% transient; Negligible permanent.
Concrete walls	Primary	Major flexural and shear cracks and voids. Sliding at joints. Extensive crushing and buckling of reinforcement. Failure around openings. Severe boundary element damage. Coupling beams shattered and virtually disintegrated.	Some boundary element stress, including limited buckling of reinforcement. Some sliding at joints. Damage around openings. Some crushing and flexural cracking. Coupling beams: extensive shear and flexural cracks; some crushing, but concrete generally remains in place.	Minor hairline cracking of walls, <1/16 in. wide. Coupling beams experience cracking <1/8 in. width.
	Secondary	Panels shattered and virtually disintegrated.	Major flexural and shear cracks. Sliding at joints. Extensive crushing. Failure around openings. Severe boundary element damage. Coupling beams shattered and virtually disintegrated.	Minor hairline cracking of walls. Some evidence of sliding at construction joints. Coupling beams experience cracks <1/8 in. width. Minor spalling.
	Drift	2% transient or permanent.	1% transient; 0.5% permanent.	0.5% transient; Negligible permanent.
Precast concrete connections	Primary	Some connection failures but no elements dislodged.	Local crushing and spalling at connections, but no gross failure of connections.	Minor working at connections; cracks <1/16 in. width at connections.
	Secondary	Same as primary.	Some connection failures but no elements dislodged.	Minor crushing and spalling at connections.

(continued)

**TABLE 7.2 (continued)**  
**Structural Performance Levels and Damage<sup>a,b,c</sup>—Vertical Elements**

Elements	Type	Structural Performance Levels		
		Collapse Prevention (S-5)	Life Safety (S-3)	Immediate Occupancy (S-1)
Foundations	General	Major settlement and tilting.	Total settlements <6 in. and differential settlements <1/2 in. in 30 ft.	Minor settlement and negligible tilting.

Source: ASCE SEI 41-06 Table C1-3.

<sup>a</sup> Damage states indicated in this table are provided to allow an understanding of the severity of damage that may be sustained by various structural elements where present in structures meeting the definitions of the structural performance levels. These damage states are not intended for use in postearthquake evaluation of damage or for judging the safety of, or required level of repair to, a structure following an earthquake.

<sup>b</sup> Drift values, differential settlements, crack widths, and similar quantities indicated in these tables are not intended to be used as acceptance criteria for evaluating the acceptability of a rehabilitation design in accordance with the analysis procedures provided in this standard; rather, they are indicative of the range of drift that typical structures containing the indicated structural elements may undergo when responding within the various structural performance levels. Drift control of a rehabilitated structure may often be governed by the requirements to protect nonstructural components. Acceptable levels of foundation settlement or movement are highly dependent on the construction of the superstructure. The values indicated are intended to be qualitative descriptions of the approximate behavior of structures meeting the indicated levels.

<sup>c</sup> For limiting damage to frame elements of infilled frames, refer to the rows for concrete or steel frames.

**TABLE 7.3**  
**Structural Performance Levels and Damage<sup>a,b</sup>—Horizontal Elements**

Element	Structural Performance Levels		
	Collapse Prevention (S-5)	Life Safety (S-3)	Immediate Occupancy (S-1)
Concrete diaphragms	Extensive crushing and observable offset across many cracks.	Extensive cracking (<1/4 in. width). Local crushing and spalling.	Distributed hairline cracking. Some minor cracks of larger size (<1/8 in. width).
Precast diaphragms	Connections between units fail. Units shift relative to each other. Crushing and spalling at joints.	Extensive cracking (<1/4 in. width). Local crushing and spalling.	Some minor cracking along joints.

Source: ASCE SEI 41-06 Table C1-4.

<sup>a</sup> Damage states indicated in this table are provided to allow an understanding of the severity of damage that may be sustained by various structural elements where present in structures meeting the definitions of the structural performance levels. These damage states are not intended for use in postearthquake evaluation of damage or for judging the safety of, or required level of repair to, a structure following an earthquake.

<sup>b</sup> Drift values, differential settlements, crack widths, and similar quantities indicated in these tables are not intended to be used as acceptance criteria for evaluating the acceptability of a rehabilitation design in accordance with the analysis procedures provided in this standard; rather, they are indicative of the range of drift that typical structures containing the indicated structural elements may undergo when responding within the various structural performance levels. Drift control of a rehabilitated structure may often be governed by the requirements to protect nonstructural components. Acceptable levels of foundation settlement or movement are highly dependent on the construction of the superstructure. The values indicated are intended to be qualitative descriptions of the approximate behavior of structures meeting the indicated levels. Concrete Diaphragms.

### 7.6.1 OVERVIEW OF PERFORMANCE LEVELS

SEI 41-06 sets forth a menu of four rehabilitation objectives associated with four earthquake hazard levels. The rehabilitation objectives are

- Operational performance
- Immediate occupancy (IO) performance
- LS performance
- Collapse prevention (CP) performance

Each of these performance levels is associated with defined levels of damage to structural, architectural, mechanical, and electrical building components as well as tenant furnishings. The designer is referred to SEI-41 Tables C1.3 through C1.7 for an overview of where each performance level falls within the overall spectrum of possible damage states. From these tables, the designer may infer, for example, a building designed for top-of-the-line performance using higher earthquake hazard levels is likely to come out scratch-free, delivering performance well above the code minimum for LS level. On the other hand, much less is expected of a building rehabilitated to a CP performance level. It is deemed to have fulfilled its obligations if it remains standing during and after a large earthquake: Any other damage or loss is acceptable.

The four levels of earthquake levels hazard recognized in the development of design performance objectives are

1. Frequent earthquakes, having a 50% chance of exceedence in 30 years (43 year mean return period)
2. Occasional earthquakes, having a 50% chance of exceedence in 50 years (72 year mean return period)
3. Rare earthquakes, having a 10% change of exceedence in 50 years (475 year mean return period) also called basic safety earthquake (BSE-1) and design basis earthquake (DBE)
4. Very rare earthquakes, having a 10% chance of exceedence in 100 years (950 year return period) also called basic safety earthquake (BSE-2) and maximum considered earthquake (MCE)

In order to execute a performance-based design, a series of design parameters and acceptance criteria are given for each performance level for the various structural and nonstructural components. Design response parameters are defined at an element level in terms of element forces, interstory drifts, and plastic rotations. These can be derived from a structural analysis of building response to a particular design earthquake. Acceptance criteria are the limiting values for design parameters in order to attain a given performance level. For example, if interstory drift ratio is a design parameter used for a certain class of building, acceptance criteria would be the drift ratios defined for each performance level. Typical drift ratios normally considered in design are 0.020 for the near collapse level, 0.015 for the LS level, 0.01 for the operational level, and 0.005 for the fully operational level. A wide variety of potential design parameters may need to be defined including deformation, strength, and energy-based parameters. The purpose of SEI 41-06 is to provide a consensus-backed, professionally accepted, nationally applicable, and seismic rehabilitation standard. It can be used as a tool by design professionals, a reference document by building regulatory officials, and a foundation for the future development and implementation of building code provisions and standards related specifically to existing buildings. The absence of such a standard has been the primary barrier to widespread seismic upgrading of buildings in the United States.

In new buildings, the structural system can be controlled to fit a set of preconditions or a configuration to satisfy the design objectives prescribed by building codes. The degree of nonlinear behavior can be designed to be consistent throughout the structural system, allowing a single seismic reduction factor,  $R$ , to be used for the entire building.

Experience in seismic design over the past 100 years has shown that buildings designed to resist ground shaking from an earthquake with a 10% chance of exceedence in 50 years, at a LS level of performance, have been able to resist the strongest earthquake without collapse. This experience has given structural engineers enough confidence to design new structures in which ductile details are specified, properties of materials used in construction are controlled, and stringent requirements of testing and inspection are specified.

Assessing the seismic vulnerability of existing buildings is an entirely different problem. This is because, for existing buildings, structural details and the properties of materials must be confirmed or assumed from available information augmented by testing and inspection. Conservative assumptions consistent with the quality of the information available must be made prior to seismic evaluation. The engineer has no control over the structural system or its configuration. The existing building may not fit prescriptive details to permit code-type analysis. Nonlinear behavior of the components of the structural system will probably not be consistent. Thus, the properties of each component must be separately studied. Because of the inconsistent levels of reserve capacity in existing buildings and the differences between the 10% in a 50-year earthquake and the maximum considered earthquake (MCE) in various regions of the country, it is inappropriate that rehabilitated buildings be designed to resist a single level of earthquake shaking. Therefore, using an entirely different approach, SEI-41 provides a basis of rehabilitation designs for a variety of structural performance levels, ranging from enhanced performance to CP. It emphasizes the idea that seismic rehabilitation should be directed to controlling deformation in order to minimize damage. Use of all existing seismic resistance is permitted in the evaluation. Acceptance criteria tailored to recognize the deformation capacity of all existing as well as enhanced or new components are provided.

The seismic loads used in the evaluation are based on a suite of USGS-developed acceleration maps including four key maps. Two of these are BSE-1 maps of acceleration response spectra having a 10% probability of exceedence in 50 years. The other two are BSE-2 maps of acceleration response spectra for the MCE—modified 2% probability of exceedence in 50 year maps: Both BSE-1 and BSE-2 maps are given for 0.2 s period (short period) and 1 s period buildings.

### 7.6.2 PERMITTED DESIGN METHODS

Two methods are permitted by SEI 41-06: a simplified method and a systematic method. The simplified approach is for the rehabilitation design of small buildings of regular configuration, and is intended to fulfill limited objectives. Partial rehabilitation measures that seek to eliminate high-risk building deficiencies such as exterior falling hazards are included in the technique.

The systematic rehabilitation method discussed at length in this section is applicable to any building. It is a component- and element-based design. In this method, global seismic response of the building is sought with unreduced seismic loads (that is, with a global  $R$ -factor of unity). In the seismic evaluation, all components and seismic elements are considered with their individual deformation and force-resisting characteristics. It is a deformation-based design with the explicit rather than tacit acknowledgment that seismic elements and components behave in a nonlinear manner.

Any of the following analysis procedures may be used in the rehabilitation study and upgrade design:

- *Linear static procedure (LSP)*. This procedure replaces the equivalent lateral force procedure included in most seismic design codes. It incorporates techniques for considering the nonlinear response of individual seismic elements. The distribution of forces is similar to equivalent lateral force procedures for new buildings.
- *Linear dynamic procedure (LDP)*. In this method, the modeling and acceptance criteria are similar to those of LSP. However, calculations are carried out using modal spectra analysis or time history analysis using response spectra or time-history records that are not modified to account for inelastic response for distribution of forces.

- *Nonlinear static procedure (NSP)*. This method is frequently referred to as a pushover analysis. It has been in use for some time without specific guidance from building codes and standards regarding modeling assumptions and acceptance criteria. This is now alleviated to some extent because previously FEMA 356 and currently SEI 41-06 have set forth specific procedures.
- *Nonlinear dynamic procedure (NDP)*. The modeling approaches and acceptance criteria for this method are similar to those of NSP. It differs from NSP in that response calculations are made using inelastic time history dynamic analysis to determine distribution of forces and corresponding internal forces and system displacements. Peer review by an independent engineer with experience in seismic design and nonlinear procedures is recommended because this method requires assumptions that are not included in SEI 41-06.

### 7.6.3 SYSTEMATIC REHABILITATION

The process of arriving at a systematic rehabilitation design includes the following steps:

1. Determination of seismic ground motions
2. Determination of as-built conditions
3. Classification of structural components into primary and secondary components
4. Setting up of analytical models and determination of design forces
5. Ultimate load combinations; combined gravity, and seismic demand
6. Component capacity calculations,  $Q_{CE}$  and  $Q_{CL}$
7. Capacity versus demand comparisons
8. Development of seismic strengthening strategies

First, the seismic hazard for the site is established by determining the probable ground shaking (spectral acceleration) from either seismic hazard maps or a site-specific investigation. Other site hazards such as liquefaction, lateral spreading, and land sliding are determined from site reconnaissance, existing documentation, or a subsurface investigation.

The desired performance level is then established. This requires close communication with the client using damage descriptions for each performance level as a tool to get ideas across. The damage descriptions associated with each performance level can be used to inform and assist the client to make a decision of the preferred performance level.

Next, an analysis is performed after classifying building components as either primary or secondary. This distinction is required because the acceptance criteria are different for each type of component. The primary components are parts of the building's lateral-force-resisting system, whereas the secondary components are those not required for lateral-force resistance, although they may actually resist some lateral forces. The analysis is performed by considering general requirements such as  $P\Delta$  effects, torsion, overturning, continuity, integrity of elements, and building separations. Cracked properties as given in Table 7.4 are used for concrete buildings.

New or modified components are evaluated using the same standards as existing components, and the designs are completed by comparing capacities with demands for each component. The components and connections are redesigned where demand exceeds capacity and analysis is iterated to confirm the design. Nonstructural components are verified for the performance level and rehabilitation objective selected.

It should be noted that selection of a rehabilitation strategy follows confirmation of seismic deficiencies. From among many possible strategies, the strategy most likely to meet requirements is selected. Some possible strategies are modification of components, removal of irregularities and discontinuities, global strengthening and stiffening, mass reduction, seismic isolation, and energy dissipation.



**TABLE 7.4**  
**Effective Stiffness Values<sup>a</sup>**

Component	Flexural Rigidity	Shear Rigidity	Axial Rigidity
Beams—Nonprestressed	$0.5 E_c I_g$	$0.4 E_c A_w$	—
Beams—Prestressed	$E_c I_g$	$0.4 E_c A_w$	—
Columns with compression due to design gravity loads $\geq 0.5 A_g f_c'$	$0.7 E_c I_g$	$0.4 E_c A_w$	$E_c A_g$
Columns with compression due to design gravity Loads $\leq 0.3 A_g f_c'$ or with tension	$0.5 E_c I_g$	$0.4 E_c A_w$	$E_s A_s$
Walls—Uncracked (on inspection)	$0.8 E_c I_g$	$0.4 E_c A_w$	$E_c A_g$
Walls—Cracked	$0.5 E_c I_g$	$0.4 E_c A_w$	$E_c A_g$
Flat slabs—Nonprestressed	See Section 6.5.4.2	$0.4 E_c A_g$	—
Flat slabs—Prestressed	See Section 6.5.4.2	$0.4 E_c A_g$	—

Source: ASCE/SEI 41-06 Table 6.5.

<sup>a</sup> It shall be permitted to take  $I_g$  for T-beams as twice the value of  $I_g$  of the web alone. Otherwise,  $I_g$  shall be based on the effective width as defined in Section 6.3.1.3. For columns with axial compression falling between the limits provided, linear interpolation shall be permitted. Alternatively, the more conservative effective stiffnesses shall be used.

### 7.6.3.1 Determination of Seismic Ground Motions

Two characteristic earthquakes, referred to as BSE-1 and BSE-2, are of particular importance. These generally correspond to return periods of 474 and 2475 years, respectively, and are commonly referred to as earthquakes with a 10% chance of exceedence in 50 years and a 2% chance of exceedence in 50 years, respectively. At sites close to major faults, the probabilistic estimates of ground motion are capped by deterministic ones. The engineer has three choices for determining the acceleration response spectra corresponding to these earthquakes: (1) use spectral response acceleration contour maps developed by the USGS, available from the FEMA distribution center, and online; (2) use CD-ROM available from the USGS; or (3) engage a geotechnical engineer to develop site-specific response spectra based on the geologic, seismologic, and soil characteristics associated with the specific site. For some sites option three may be the only permitted method. However, to define as precise a seismic demand as possible, it is common practice to engage a geotechnical engineer to perform a site-specific study for developing response spectra corresponding to specific return periods. The geotechnical report also typically addresses other seismic hazards such as liquefaction, lateral spreading, or potential for land sliding at the site.

It should be noted that the acceleration response spectra for earthquake hazard levels corresponding to probabilities of exceedence other than the BSE-1 and BSE-2 earthquakes can be determined by the following procedures specified in ASCE/SEI 41-06.

### 7.6.3.2 Determination of As-Built Conditions

In this step the following tasks are performed:

- Field observation
- Review of available documents, including plans, specifications geotechnical reports, shop drawings, test records, and maintenance histories

- Review of information regarding material standards and construction practices for location and date of construction
- Destructive and nondestructive testing of selected building components for determination of material properties and configuration of details
- Interviews with people knowledgeable about the building (i.e., owners, tenants, maintenance personnel, architects, engineers, and builders)

As a measure of the knowledge gained from this investigation, engineers assign a numerical value to the knowledge coefficient  $k$ . ( $k = 1.0$  if the available information is reliable; if not,  $k = 0.75$ .)

### 7.6.3.3 Primary and Secondary Components

Before setting up the analytical model, structural components are classified as either primary or secondary. Primary components are those that provide the structure's basic lateral resistance. Secondary components are those that do not, and as such are permitted to experience more damage and displace more than the primary components. Additionally, components are further classified as either deformation-controlled, if they are capable of sustaining the loads when strained inelastically, or force-controlled, if they are not capable of sustaining load when strained inelastically.

### 7.6.3.4 Setting Up Analytical Model and Determination of Design Forces

An analytical model of the building is set up to represent the structure's dynamic behavior. Although two-dimensional models may be adequate, current practice is to use three-dimensional models to account for torsion, plan, and vertical irregularities, and nonuniform distribution of building mass. Only the primary components are modeled, with the stipulation that the secondary elements, if used in the model, cannot exceed 25% of the total structural stiffness. If they do, then some of the secondary components must be reclassified as primary components.

#### 7.6.3.4.1 Calculation of Building Period

The building period,  $T$ , is calculated by using either the modal analysis procedure, method 1, or empirical equations, method 2.

Method 1 is the preferred method. The fundamental period  $T$  is obtained by an eigenvalue analysis using the analytical model. This is the more commonly used method, particularly in seismic vulnerability studies.

In method 2, the period  $T$  is determined using the following equation:

$$T = C_t h_n^x \quad (7.1)$$

where

$C_t = 0.018$  for concrete moment frames  
 $= 0.020$  for all other framing systems

$h_n = 0.035$  height, in feet, above shear base to the building roof  
 $= 0.90$  for concrete moment frames  
 $= 0.75$  for all other systems

However, there is a major difference worthy of note between building code procedures for new buildings and the ASCE/SEI 41-06 approach. Unlike the code stipulation, there is no maximum limit on period calculated using method 1. The intent of this omission is to encourage the use of more advanced analysis such as computer dynamic analysis. It is believed that sufficient controls on analysis and acceptance criteria are present within the ASCE/SEI 41-06 standard to provide reasonably conservative results even though there is no upper limit for the period obtained by method 1.

#### 7.6.3.4.2 Determination of Base Shear (Pseudolateral Load)

The base shear, also referred to as pseudolateral force, for use in the design of new components and in the verification of existing components of the lateral-force-resisting system is given by

$$V = C_1 C_2 C_m S_a W \quad (7.2)$$

where

$V$  is the pseudolateral load (the base shear)

$C_1$  is the modification factor that accounts for the difference in the structure's elastic and inelastic displacement amplitude. Its value is equal to 1.0 for  $T > 1.0$  s. (See ASCE/SEI 4-06 Section 3.3.1.3 for additional information.)

$C_2$  is the modification factor that represents the effect of strength and stiffness degradation of the components on maximum displacement response. For periods greater than 0.7 s,  $C_2 = 1.0$

$C_m$  is the effective mass factor to account for higher modal mass participation: 1.0 if building fundamental period  $T$  is greater than 1.0 s or if the building is one or two stories

= 0.9 for three or more story concrete frame buildings

= 0.8 for three or more story concrete shear wall or pier-spandrel buildings

$S_a$  is the response spectrum acceleration at the fundamental period and damping ratio of the building

$W$  is the effective seismic weight of the building, including the total dead load and applicable portions of other gravity loads listed below:

- In storage and warehouse occupancies, a minimum of 25% of floor live load.
- Where an allowance for partition load is included in the floor load design (the actual partition weight) or a minimum weight of 10 psf of floor area, whichever is greater.
- The total operating weight of permanent equipment.
- The effective snow load equal to 20% of the design snow load if design snow load exceeds 30 psf. If not, the effective snow load may be taken to be zero.

#### 7.6.3.4.3 Vertical Distribution of Base Shear

The lateral force  $F_x$ , applied at any level  $x$ , is determined in accordance with the following equations:

$$F_x = C_{vx} V \quad (7.3)$$

$$C_{vx} = \frac{w_x h_x^k}{\sum_{i=1}^n w_i h_i^k} \quad (7.4)$$

where

$C_{vx}$  is the vertical distribution factor

$V$  is the pseudolateral force (base shear)

$w_i$  and  $w_x$  are the portion of the total gravity load of the building  $W$  located or assigned to level  $i$  or  $x$

$h_i$  and  $h_x$  are the height in feet from the base to level  $i$  or  $x$

$k$  is an exponent related to the building period as follows:

If the building period is 0.5 s or less,  $k = 1$ .

If the buildings period is 2.5 s or more,  $k = 2$ .

Linear interpretation is used for intermediate values of the period  $T$ .

#### 7.6.3.4.4 Diaphragm Design Force $F_{px}$

Floor and roof diaphragms should be designed to resist the combined effects of the inertial force  $F_{px}$  calculated at the diaphragm level combined with the horizontal forces resulting from offsets in the vertical seismic elements above and below the diaphragm. The design force shall not be less than

$$F_{px} = \frac{\sum_{i=x}^n F_i}{\sum_{i=x}^n w_i} + \rho v_{px}. \quad (7.5)$$

The first term of the above equation need not exceed  $0.4S_{DS}IW_{px}$ , but shall not be less than  $0.20S_{DS}IW_{pn}$

where

$v_{px}$  is the forces due to transfer of vertical resisting elements above the diaphragm or changes in relative lateral stiffness in the vertical elements

$F_{px}$  is the total diaphragm inertial force at level  $x$

$F_i$  is the lateral load at level  $i$

$w_i$  is the portion of the effective seismic weight  $w$

$w_{px}$  is the portion of the effective seismic weight  $w$  located at or assigned to floor level  $x$

$\rho$  is the redundancy factor applicable to diaphragms in SDC D, E, or F buildings

#### 7.6.3.5 Ultimate Load Combinations: Combined Gravity and Seismic Demand

In this step the earthquake actions  $Q_E$  obtained in step 4 for the unreduced response spectra are combined with the gravity actions,  $Q_G$ , to determine the demand imposed on the component. When the effects of gravity and seismic loads are additive, an upper bound value for gravity loads is estimated by using the following load combinations:

$$Q_G = 1.1(Q_D + Q_L + Q_s) \quad (7.6)$$

And when the effects of gravity and seismic loads are counteracting, a lower bound value of the gravity load is estimated by using 90% of the dead load:

$$Q_G = 0.9Q_D \quad (7.7)$$

where

$Q_D$  is the dead load action

$Q_L$  is the effective live load action equal to 25% of the unreduced design live load but not less than the actual live load

$Q_s$  is the effective live load action equal to 20% of the design snow where the design snow load exceeds 30psf. No part of the load need be included if the design snow load is less than 30psf.

Next, the gravity and seismic loads are combined together to determine the demand using the following equations:

For deformation-controlled actions:

$$Q_{UD} = Q_G \pm Q_E \quad (7.8)$$

For force-controlled actions:

$$Q_{UF} = Q_G \pm \frac{Q_E}{C_1 C_2 J} \quad (7.9)$$

where

$Q_{UD}$  is the deformation-controlled demand due to gravity loads and earthquake loads

$Q_{UF}$  is the force-controlled demand due to gravity loads in combination with earthquake loads

$J$  is the coefficient used to estimate the actual forces delivered to force-controlled components by other yielding components. The values of  $J$  are

- $J = 2.0$  in zones of high seismicity
- $= 1.5$  in zones of moderate seismicity
- $= 1.0$  in zones of low seismicity

Alternatively,  $J$  may be taken as the smallest demand capacity ratio (DCR) for the components in the load path delivering force to the component being designed. The minimum value of  $J$ , the force-delivery reduction factor, is 1.0. See Section 7.6.3.4.2 for  $C_1$  and  $C_2$ . The reader is referred to SEI 41-06, Section 3.4 for further definition of terms used in this section.

### 7.6.3.6 Component Capacity Calculations $Q_{CE}$ and $Q_{CL}$

ASCE/SEI 41-06 specifies two different equations for evaluating component capacities depending upon whether the action of the component is deformation-controlled ( $Q_{CE}$ ) or force-controlled ( $Q_{CL}$ ). The subscript  $E$  in  $Q_{CE}$  stands for expected capacity, whereas  $L$  in  $Q_{CL}$  stands for lower-bound capacity. The subscript  $C$  in both  $Q_{CE}$  and  $Q_{CL}$  stands for capacity. The terminology of “design actions” is used to define forces and moments in the components due to seismic and gravity effects.

The two types of actions—deformation-controlled actions and force-controlled actions—are defined to distinguish a ductile behavior from a brittle behavior.

#### 7.6.3.6.1 Deformation-Controlled Actions

Deformation-controlled actions in simple terms refer to forces and moments in a component that has recognizable nonlinear deformation characteristics. Because of possible anticipated nonlinear response, the design forces and moments in the component are permitted to exceed their capacity. The acceptance criteria, discussed presently in Section 7.6.3.7, take this overload into account through the use of an  $m$ -factor, which in a conceptual sense is an indirect measure of the nonlinear deformation capacity of the component.

Some examples of deformation-controlled actions for concrete components are as follows:

- Beams controlled by flexure
- Beams controlled by shear
- Beams controlled by inadequate splicing along the span
- Beams controlled by inadequate embedment into the beam column joint
- Columns controlled by flexure

#### 7.6.3.6.2 Force-Controlled Actions

Force-controlled actions differ from deformation-controlled actions in that they do not have a recognizable inelastic response. Therefore, demands for force-controlled actions must not exceed the calculated capacity (i.e., there are no  $m$ -factors in the acceptance criteria). It should be noted, however, that the calculated design force (demand) itself is reduced by the  $C_1$ ,  $C_2$ ,  $C_m$ , and  $J$  factors before demand is compared to capacity.

An ideal procedure for determining the magnitude of force-controlled actions is by identifying an inelastic limit state for the component and then, by statics, evaluation of the corresponding

force-controlled action. For example, seismic shear in a frame beam is determined from equilibrium considerations of a free-body diagram of the beam with a moment equal to the expected moment strength plus gravity moments.

However, it is acceptable to determine force-controlled actions from Equation 7.9, where it is not possible to identify a well-defined limit state.

#### 7.6.3.6.3 Capacity $Q_{CE}$ of Concrete Beam

**Given:** A reinforced concrete frame beam in a building built in the year 1980. The beam has the following properties:  $b = 30$  in.,  $h = 48$  in.,  $d = 45$  in., with 5 #11 top bars, ASTM A615, grade 60, at the negative zones.

$$f_c = 4 \text{ ksi}, \quad f_y = 60 \text{ ksi}$$

**Required:** The expected capacity  $Q_{CE}$  of the beam.

**Solution:** Reinforcement  $f_{ye}$ : From Table 7.5 (ASCE/SEI 41-06 Table 6.1), the default lower bound yield strength for ASTM A615, grade 60 reinforcement = 60 ksi. From Table 7.7 (ASCE/SEI 41-06 Table 6.4), the factor to translate lower-bound material properties to expected strength material properties = 1.25. Therefore, the expected strength of the reinforcement

$$f_{ye} = 60 \times 1.25 = 75 \text{ ksi}$$

From Table 7.6 (ASCE/SEI 41-06 Table 6.3), the default lower-bound compressive strength of structural concrete in beams built in 1980 varies from 3 to 5 ksi, with an average value of 4 ksi. From Table 7.7, the adjustment factor = 1.50. Therefore

$$f'_{ce} = 1.50 \times 4 = 6 \text{ ksi}$$

#### 7.6.3.7 Capacity versus Demand Comparisons

In this step, the component capacities are compared with the demand due to earthquake and gravity loads. If the capacity of a component exceeds the demand imposed on it by the seismic and gravity load combinations, the component is judged to satisfy the performance criteria. If not, a more refined technique such as a pushover analysis is performed before declaring the component deficient.

Two equations are given in ASCE/SEI 41-06 for verifying the acceptance criteria.

$$\text{For deformation-controlled actions: } mkQ_{CE} \geq Q_{UD}. \quad (7.10)$$

$$\text{For force-controlled actions: } kQ_{CL} \geq Q_{UF}. \quad (7.11)$$

where

$m$  is the modifier given in Tables 7.8 through 7.14 that takes into account the expected ductility of the component associated with the action being verified at the selected structural performance level

$Q_{CE}$  is the expected strength of the component at the deformation level under consideration for deformation-controlled actions

$k$  is the knowledge factor defined in Section 6.10

$Q_{CL}$  is the lower-bound strength of a component for force-controlled actions

$Q_{UD}$  is the deformation-controlled demand due to gravity and earthquake loads

$Q_{UF}$  is the force-controlled demand due to gravity and earthquake loads

Numerical values of  $m$  are given in SEI 41-06 for steel, concrete, masonry, and wood components. Values are given separately for linear and nonlinear procedures. An abbreviated version of the tables of  $m$ -values for use in linear procedures is given here for the following components:

TABLE 7.5  
Default Lower-Bound Tensile and Yield Properties of Reinforcing for Various ASTM Specifications and Periods<sup>a</sup>

ASTM Designation <sup>c</sup>	Steel Type	Year Range	Structural <sup>b</sup>		Intermediate <sup>b</sup>		Hard <sup>b</sup>				
			ASTM Grade	33	40	40,000	50,000	60	65	70	75
			Minimum Yield (psi)	33,000	40,000	40,000	50,000	60,000	65,000	70,000	75,000
Minimum Tensile (psi)			55,000	70,000	80,000	90,000	75,000	80,000	100,000		
A15	Billet	1911–1966	x	x	x	—	—	—	—	—	
A16	Rail <sup>d</sup>	1913–1966	—	—	x	—	—	—	—	—	
A61	Rail <sup>d</sup>	1963–1966	—	—	—	x	—	—	—	—	
A160	Axle	1936–1964	x	x	x	—	—	—	—	—	
A160	Axle	1965–1966	x	x	x	x	—	—	—	—	
A185	WWF	1936–present	—	—	—	—	x	—	—	—	
A408	Billet	1957–1966	x	x	x	—	—	—	—	—	
A431	Billet	1959–1966	—	—	—	—	—	—	—	x	
A432	Billet	1959–1966	—	—	—	x	—	—	—	—	
A497	WWF	1964–present	—	—	—	—	—	—	x	—	
A615	Billet	1968–1972	—	x	x	x	—	—	—	x	
A615	Billet	1974–1986	—	x	x	x	—	—	—	—	
A615	Billet	1987–present	—	x	x	x	—	—	—	x	
A616 <sup>e</sup>	Rail <sup>d</sup>	1968–present	—	—	—	—	—	—	—	—	
A617	Axle	1968–present	—	x	x	x	—	—	—	—	
A706	Low-alloy	1974–present	—	—	—	x	x	—	x	—	
A955	Stainless	1996–present	—	x	x	x	x	—	—	x	

Source: ASCE/SEI 41-06 Table 6-2.

<sup>a</sup> An entry of “x” indicates the grade was available in those years.

<sup>b</sup> The terms structural, intermediate, and hard became obsolete in 1968.

<sup>c</sup> ASTM steel is marked with the letter “W.”

<sup>d</sup> Rail bars are marked with the letter “R.”

<sup>e</sup> Bars marked “s” (ASTM 616) have supplementary requirements for bend tests.

<sup>f</sup> ASTM A706 has a minimum tensile strength of 80 ksi, but not less than 1.25 times the actual yield strength.

**TABLE 7.6**  
**Default Lower-Bound Compressive Strength of Structural Concrete (psi)**

Time Frame	Footings	Beams	Slabs	Columns	Walls
1900–1919	1000–2500	2000–3000	1500–3000	1500–3000	1000–2500
1920–1949	1500–3000	2000–3000	2000–3000	2000–4000	2000–3000
1950–1969	2500–3000	3000–4000	3000–4000	3000–6000	2500–4000
1970–present	3000–4000	3000–5000	3000–5000	3000–10000	3000–5000

Source: ASCE/SEI 41-06 Table 6-3.

**TABLE 7.7**  
**Factors to Translate Lower-Bound Material Properties to Expected Strength Material Properties**

Material Property	Factor
Concrete compressive strength	1.50
Reinforcing steel tensile and yield strength	1.25
Connector steel yield strength	1.50

Source: ASCE/SEI 41-06 Table 6-4.

1. Reinforced concrete beams (Table 7.8, ASCE/SEI 41-06 Table 6–11)
2. Reinforced concrete columns (Table 7.9, ASCE/SEI 41-06 Table 6–12)
3. Reinforced concrete beam–column joints (Table 7.10, ASCE/SEI 41-06 Table 6–13)
4. Two-way slabs and slab–column connections (Table 7.11, ASCE/SEI 41-06 Table 6–15)
5. Reinforced concrete shear wall and associated components controlled by flexure (Table 7.12, ASCE/SEI 41-06 Table 6–20)
6. Reinforced concrete shear walls and associated components controlled by shear (Table 7.13, ASCE/SEI 41-06 Table 6–21)
7. Reinforced concrete infilled frames (Table 7.14, ASCE/SEI 41-06 Table 6–17)

### 7.6.3.8 Development of Seismic Strengthening Strategies

If all of the components in the structure meet the basic acceptance criteria associated with their actions, no further analysis is necessary, and the building can be judged to meet the evaluation criteria. If not, typically a more refined study (including, perhaps, a pushover analysis) would be considered before deciding on a seismic rehabilitation program. The final evaluation should be based on a review of the qualitative and quantitative results. The evaluating engineer is urged to consider the issues carefully, to refrain from penalizing the building due to fine technical points beyond those contained in the FEMA 356 evaluation methodology, and to visualize the building in its ultimate condition in an earthquake, being aware of the risks of brittle failure and buckling. Due consideration should be given to the mitigating influences of good workmanship, structural integrity, and the strengths and redundancies that are not explicitly considered to be part of the lateral-force-resisting system. Most important, engineering judgment based on sound seismic design principles should be exercised before pronouncing a building unsafe. The questions that review engineers should ask themselves before declaring a building noncompliant are many. Some of these are

1. What if the material properties are higher than assumed in the analysis?
2. What if we allow for a small amount of rocking and sliding at the base to absorb excess earthquake energy with little harm to structure?



**TABLE 7.8**  
**Numerical Acceptance Criteria for Linear Procedures—Reinforced**  
**Concrete Beams**

			<i>m</i> -Factors <sup>a</sup>				
			Performance Level				
			Component Type				
			IO	Primary		Secondary	
Conditions				LS	CP	LS	CP
<b>1. Beams controlled by flexure<sup>b</sup></b>							
$\frac{\rho - \rho'}{\rho_{bal}}$	Transverse reinforcement <sup>c</sup>	$\frac{V}{b_w d \sqrt{f'_c}}$					
≤ 0.0	C	≤ 3	3	6	7	6	10
≤ 0.0	C	≥ 6	2	3	4	3	5
≥ 0.5	C	≤ 3	2	3	4	3	5
≥ 0.5	C	≥ 6	2	2	3	2	4
≤ 0.0	NC	≤ 3	2	3	4	3	5
≤ 0.0	NC	≥ 6	1.25	2	3	2	4
≥ 0.5	NC	≤ 3	2	3	3	3	4
≥ 0.5	NC	≥ 6	1.25	2	2	2	3
<b>2. Beams controlled by shear<sup>b</sup></b>							
Stirrup spacing ≤ <i>d</i> /2			1.25	1.5	1.75	3	4
Stirrup spacing > <i>d</i> /2			1.25	1.5	1.75	2	3
<b>3. Beams controlled by inadequate development or splicing along the span<sup>b</sup></b>							
Stirrup spacing ≤ <i>d</i> /2			1.25	1.5	1.75	3	4
Stirrup spacing > <i>d</i> /2			1.25	1.5	1.75	2	3
<b>4. Beams controlled by inadequate embedment into beam–column joint<sup>b</sup></b>							
			2	2	3	3	4

Source: ASCE/SEI 41-06 Table 6-7.

<sup>a</sup> Linear interpolation between values listed in the table shall be permitted.

<sup>b</sup> Where more than one of the conditions 1 through 4 occurs for a given component, use the minimum appropriate numerical value from the table.

<sup>c</sup> “C” and “NC” are abbreviations for conforming and nonconforming transverse reinforcement. A component is conforming if, within the flexural plastic hinge region, hoops are spaced at  $\leq d/3$ , and if, for components of moderate and high ductility demand, the strength provided by the hoops ( $V_s$ ) is at least three-fourths of the design shear. Otherwise, the component is considered nonconforming.

<sup>d</sup>  $V$  is the design shear force calculated using limit-state analysis procedures in accordance with Section 6.4.2.4.1.

- What if we use gross properties for concrete components, particularly for *T*- and *I*-shaped beams?
- For a moment frame building, what if we reanalyze the frame using different size rigid joints in the frame model? Does inclusion of an elastic spring to represent the stiffness of the joint result in a more favorable demand/capacity ratio?
- What if we use slightly higher values for the ductility factor  $m$  in verifying the acceptance criteria?

**TABLE 7.9**  
**Numerical Acceptance Criteria for Linear Procedures—Reinforced**  
**Concrete Columns**

			<i>m</i> -Factors <sup>a</sup>					
			Performance Level					
			Component Type					
			IO	Primary		Secondary		
Conditions		LS		CP	LS	CP		
<b>1. Columns controlled by flexure<sup>b</sup></b>								
$\frac{P}{A_g f'_c d}$	Transverse reinforcement <sup>c</sup>	$\frac{V}{b_w d \sqrt{f'_c}}$						
≤ 0.1	C	≤3	2	3	4	4	5	
≤ 0.1	C	≥6	2	2.4	3.2	3.2	4	
≥ 0.4	C	≤3	1.25	2	3	3	4	
≥ 0.4	C	≥6	1.25	1.6	2.4	2.4	3.2	
≤ 0.1	NC	≤3	2	2	3	2	3	
≤ 0.1	NC	≥6	2	2	2.4	1.6	2.4	
≥ 0.4	NC	≤3	1.25	1.5	2	1.5	2	
≥ 0.4	NC	≥6	1.25	1.5	1.75	1.5	1.75	
<b>2. Columns controlled by shear<sup>b,f</sup></b>								
Hoop spacing ≤ <i>d</i> /2, or $\frac{P}{A_g f'_c} \leq 0.1$			—	—	—	2	3	
Other cases			—	—	—	1.5	2	
<b>3. Columns controlled by inadequate development or splicing along the clear height<sup>b,f</sup></b>								
Hoop spacing ≤ <i>d</i> /2			1.25	1.5	1.75	3	4	
Hoop spacing > <i>d</i> /2			—	—	—	2	3	
<b>4. Columns with axial loads exceeding 0.70 <i>P</i><sub>o</sub><sup>b,f</sup></b>								
Conforming hoops over the entire length			1	1	2	2	2	
All other cases			—	—	—	1	1	

Source: ASCE/SEI 41-06 Table 6-12.

<sup>a</sup> Linear interpolation between values listed in the table shall be permitted.

<sup>b</sup> Where more than one of the conditions 1 through 4 occurs for a given component, use the minimum appropriate numerical value from the table.

<sup>c</sup> “C” and “NC” are abbreviations for conforming and nonconforming transverse reinforcement. A component is conforming if, within the flexural plastic hinge region, hoops are spaced at ≤  $d/3$ , and if, for components of moderate and high ductility demand, the strength provided by the hoops ( $V_h$ ) is at least three-fourths of the design shear. Otherwise, the component is considered nonconforming.

<sup>d</sup>  $P$  is the design axial force in the member. Alternatively, use of axial loads determined based on a limit-state analysis shall be permitted.

<sup>e</sup>  $V$  is the design shear force calculated using limit-state analysis procedures in accordance with Section 6.4.2.4.1.

<sup>f</sup> To qualify, columns must have transverse reinforcement consisting of hoops. Otherwise, actions shall be treated as force-controlled.

**TABLE 7.10**  
**Numerical Acceptance Criteria for Linear Procedures—Reinforced**  
**Concrete Beam—Column Joints**

			<i>m</i> -Factors <sup>a</sup>				
			Performance Level				
			Component Type				
			Primary <sup>b</sup>		Secondary		
Conditions			IO	LS	CP	LS	CP
<b>1. Interior joints<sup>c,d</sup></b>							
$\frac{P}{A_g f'_c}$	Transverse reinforcement <sup>e</sup>	$\frac{V}{V_n}$					
≤ 0.1	C	≤ 1.2	—	—	—	3	4
≤ 0.1	C	≥ 1.5	—	—	—	2	3
≥ 0.4	C	≤ 1.2	—	—	—	3	4
≥ 0.4	C	≥ 1.5	—	—	—	2	3
≤ 0.1	NC	≤ 1.2	—	—	—	2	3
≤ 0.1	NC	≥ 1.5	—	—	—	2	3
≥ 0.4	NC	≤ 1.2	—	—	—	2	3
≥ 0.4	NC	≥ 1.5	—	—	—	2	3
<b>2. Other joints<sup>c,d</sup></b>							
$\frac{P}{A_g f'_c}$	Transverse reinforcement <sup>e</sup>	$\frac{V}{V_n}$					
≤ 0.1	C	≤ 1.2	—	—	—	3	4
≤ 0.1	C	≥ 1.5	—	—	—	2	3
≥ 0.4	C	≤ 1.2	—	—	—	3	4
≥ 0.4	C	≥ 1.5	—	—	—	2	3
≤ 0.1	NC	≤ 1.2	—	—	—	2	3
≤ 0.1	NC	≥ 1.5	—	—	—	2	3
≥ 0.4	NC	≤ 1.2	—	—	—	1.5	2.0
≥ 0.4	NC	≥ 1.5	—	—	—	1.5	2.0

Source: ASCE/SEI 41-06 Table 6-13.

<sup>a</sup> Linear interpolation between values listed in the table shall be permitted.

<sup>b</sup> For linear procedures, all primary joints shall be force-controlled; *m*-factors shall not apply.

<sup>c</sup> *P* is the design axial force on the column above the joint calculated using limit-state analysis procedures in accordance with Section 6.4.2.4. *A<sub>g</sub>* is the gross cross-sectional area of the joint.

<sup>d</sup> *V* is the design shear force and *V<sub>n</sub>* is the shear strength for the joint. The design shear force and shear strength shall be calculated according to Sections 6.4.2.4.1 and 6.4.2.3, respectively.

<sup>e</sup> “C” and “NC” are abbreviations for conforming and nonconforming transverse reinforcements. A joint is conforming if hoops are spaced at ≤ *h<sub>c</sub>*/3 within the joint. Otherwise, the component is considered nonconforming.

Although SEI 41-06 has procedures to answer some of these questions the author recommends that a parametric study of the acceptance criteria be undertaken before declaring the building noncomplaint. This recommendation should not be constructed as sanctioning indiscriminate manipulation of the ASCE/SEI 41-06 procedure, but as a reminder for engineers to use that nonquantifiable,

**TABLE 7.11**  
**Numerical Acceptance Criteria for Linear Procedures—**  
**Two-Way Slabs and Slab–Column Connections**

		<i>m</i> -Factors <sup>a</sup>				
		Performance Level				
		Component Type				
		Primary		Secondary		
Conditions		IO	LS	CP	LS	CP
<b>1. Slabs controlled by flexure, and slab–column connections<sup>b</sup></b>						
$\frac{V_g}{V_oC}$	Continuity reinforcement <sup>d</sup>					
≤0.2	Yes	2	2	3	3	4
≥0.4	Yes	1	1	1	2	3
≤0.2	No	2	2	3	2	3
≥0.4	No	1	1	1	1	1
<b>2. Slabs controlled by inadequate development or splicing along the span<sup>b</sup></b>						
		—	—	—	3	4
<b>3. Slabs controlled by inadequate embedment into slab–column joint<sup>b</sup></b>						
		2	2	3	3	4

Source: ASCE/SEI 41-06 Table 6-15.

<sup>a</sup> Linear interpolation between values listed in the table shall be permitted.

<sup>b</sup> Where more than one of the conditions 1 through 3 occurs for a given component, use the minimum appropriate numerical value from the table.

<sup>c</sup>  $V_g$  = the gravity shear acting on the slab critical section as defined by ACI 318 (ACI 2002);  $V_o$  = the direct punching shear strength as defined by ACI 318.

<sup>d</sup> Under the heading “Continuity Reinforcement,” use “Yes” where at least one of the main bottom bars in each direction is effectively continuous through the column cage. Where the slab is post-tensioned, use “Yes” where at least one of the post-tensioning tendons in each direction passes through the column cage. Otherwise, use “No.”

mysterious branch of engineering often called the art of design. It should be kept in mind that no matter how sophisticated an analysis is, it is hard to justify that its seismic behavior will be satisfactory if it has large vertical and horizontal discontinuities. Experience has taught time and again that unfavorable seismic characteristics arise in a poorly balanced structural system. The seismic retrofit should, then, focus on removing irregularities and discontinuities.

In the evaluation and upgrading of an existing structure, it is sometimes difficult to identify an existing lateral-force-resisting system. Innovative analytical procedures and reliance on existing materials and systems that are not generally considered for new construction are required to determine the load paths and capacities of the existing structures. When an existing structure is not adequate to resist the prescribed lateral forces, strengthening of the existing lateral-force-resisting system will be required.

The selection of an appropriate strengthening technique for the upgrading of an existing building that does not comply with the acceptance criteria will depend upon the type of structural systems

TABLE 7.12

### Numerical Acceptance Criteria for Linear Procedures—Reinforced Concrete Shear Walls and Associated Components Controlled by Flexure

			<i>m</i> -Factors <sup>a</sup>				
			Performance Level				
			Component Type				
Conditions			IO	Primary		Secondary	
				LS	CP	LS	CP
<b>1. Shear walls and wall segments</b>							
$\frac{(A_s - A'_s)f_y + p^b}{t_w l_w f'_c}$		$\frac{V^c}{t_w l_w \sqrt{f'_c}}$	Confined boundary <sup>d</sup>				
≤0.1	≤3	Yes	2	4	6	6	8
≤0.1	≥6	Yes	2	3	4	4	6
≥0.25	≤3	Yes	1.5	3	4	4	6
≥0.25	≥6	Yes	1.25	2	2.5	2.5	4
≤0.1	≤3	No	2	2.5	4	4	6
≤0.1	≥6	No	1.5	2	2.5	2.5	4
≥0.25	≤3	No	1.25	1.5	2	2	3
≥0.25	≥6	No	1.25	1.5	1.75	1.75	2
<b>2. Columns supporting discontinuous shear walls</b>							
Transverse reinforcement <sup>c</sup>							
Conforming			1	1.5	2	n.a.	n.a.
Nonconforming			1	1	1	n.a.	n.a.
<b>3. Shear wall coupling beams<sup>f</sup></b>							
Longitudinal reinforcement and transverse reinforcement <sup>g</sup>		$\frac{V^c}{t_w l_w \sqrt{f'_c}}$					
Conventional longitudinal		≤3	2	4	6	6	9
Reinforcement with conforming transverse reinforcement		≥6	1.5	3	4	4	7
Conventional longitudinal		≤3	1.5	3.5	5	5	8
Reinforcement with nonconforming transverse reinforcement		≥6	1.2	1.8	2.5	2.5	4
Diagonal reinforcement		n.a.	2	5	7	7	10

Source: ASCE/SEI 41-06 Table 6-20.

<sup>a</sup> Linear interpolation between values listed in the table shall be permitted.

<sup>b</sup> *P* is the design axial force in the member. Alternatively, use of axial loads determined based on a limit-state analysis shall be permitted.

<sup>c</sup> *V* is the design shear force calculated using limit-state analysis procedures in accordance with Section 6.7.2.4.

<sup>d</sup> Requirements for a confined boundary are the same as those given in ACI 318 (ACI 2002).

<sup>e</sup> Requirements for conforming transverse reinforcement in columns are: (1) hoops over the entire length of the column at a spacing ≤*d*/2, and (2) strength of hoops *V<sub>s</sub>* ≥ required shear strength of column.

<sup>f</sup> For secondary coupling beams spanning <8 ft, 0 in., with bottom reinforcement continuous into the supporting walls, secondary values shall be permitted to be doubled.

<sup>g</sup> Conventional longitudinal reinforcement consists of top and bottom steel parallel to the longitudinal axis of the coupling beam. Conforming transverse reinforcement consists of: (1) closed stirrups over the entire length of the coupling beam at a spacing ≤*d*/3, and (2) strength of closed stirrups *V<sub>s</sub>* ≥ three-fourths of required shear strength of the coupling beam.

**Table 7.13**  
**Numerical Acceptance Criteria for Linear Procedures—Reinforced Concrete**  
**Shear Walls and Associated Components Controlled by Shear**

		<i>m</i> -Factors				
		Performance Level				
		Component Type				
Conditions		IO	Primary		Secondary	
			LS	CP	LS	CP
<b>1. Shear walls and wall segments</b>						
All shear walls and wall segments <sup>a</sup>		2	2	3	2	3
<b>2. Shear wall coupling beams<sup>b</sup></b>						
Longitudinal reinforcement	$\frac{V^d}{t_w l_w \sqrt{f'_c}}$					
and transverse reinforcement <sup>c</sup>						
Conventional longitudinal	≤3	1.5	3	4	4	6
Reinforcement with conforming	≥6	1.2	2	2.5	2.5	3.5
Transverse reinforcement						
Conventional longitudinal	≤3	1.5	2.5	3	3	4
Reinforcement with nonconforming	≥6	1.2	1.2	1.5	1.5	2.5
transverse reinforcement						

Source: ASCE/SEI 41-06 Table 6-21.

<sup>a</sup> The shear shall be considered to be a force-controlled action for shear walls and wall segments where inelastic behavior is governed by shear and the design axial load is greater than 0.15  $A_g f'_c$ . It shall be permitted to calculate the axial load based on a limit-state analysis.

<sup>b</sup> For secondary coupling beams spanning <8 ft, 0 in., with bottom reinforcement continuous into the supporting walls, secondary values shall be permitted to be doubled.

<sup>c</sup> Conventional longitudinal reinforcement consists of top and bottom steel parallel to the longitudinal axis of the coupling beam. Conforming transverse reinforcement consists of: (1) closed stirrups over the entire length of the coupling beam at a spacing  $\leq d/3$ , and (2) strength of closed stirrups  $V_s \geq$  three-fourths of required shear strength of the coupling beam.

<sup>d</sup> For the purpose of determining  $m$ ,  $V$  is the coupling beam expected shear strength.

in the existing building and the nature of the deficiency. In some cases, the selection may be influenced by other than structural considerations. For example, a requirement that the building be kept operational during the structural modifications may dictate that the modification be restricted to the periphery of the building. On the other hand, it may be possible to temporarily relocate the occupants of a building that is to be upgraded. This, of course, provides more latitude in the selection of appropriate and cost-effective strengthening techniques. In many cases, seismic upgrading is accomplished concurrently with functional alterations, renovation, and/or energy retrofits. In these cases, the selected structural modification scheme should be the one that best suits the requirements of all the proposed alterations.

Determination of the seismic capacity of a structure includes consideration of all elements, structural and nonstructural, which contribute to the resistance of lateral forces.

Physical properties are generally obtained from available data; otherwise, assumptions and/or tests must be made. The analysis must include the evaluation of the most rigid elements resisting the initial lateral forces, as well as the more flexible elements that resist the lateral distortions after

**TABLE 7.14**  
**Numerical Acceptance Criteria for Linear Procedures—Reinforced Concrete**  
**Infilled Frames**

Conditions	<i>m</i> -Factors <sup>a</sup>				
	Performance Level				
	Component Type				
	IO	Primary		Secondary	
		LS	CP	LS	CP
<b>1. Columns modeled as compression chords<sup>b</sup></b>					
Columns confined along entire length <sup>c</sup>	1	3	4	4	5
All other cases	1	1	1	1	1
<b>2. Columns modeled as tension chords<sup>b</sup></b>					
Columns with well-confined splices, or No splices	3	4	5	5	6
All other cases	1	2	2	3	4

Source: ASCE/SEI 41-06 Table 6.17.

- <sup>a</sup> Interpolation shall not be permitted.
- <sup>b</sup> If load reversals will result in both conditions 1 and 2 applying to a single column, both conditions shall be checked.
- <sup>c</sup> A column may be considered to be confined along its entire length where the quantity of hoops along the entire story height including the joint is equal to three-quarters of that required by ACI 318 (ACI 2002) for boundary components of concrete shear walls. The maximum longitudinal spacing of sets of hoops shall not exceed either  $h/3$  or  $8d_b$ .

the rigid elements yield or fail. Consideration must also be given to the interaction of various combinations of the structural framing systems and elements, which will contribute to the resistance of the lateral loads.

The results of the detailed structural analysis will identify the deficiencies with respect to the acceptance criteria of the various structural components and systems. These results should be carefully reviewed in the development of alternative upgrade concepts unless justification can be shown for a single solution. Each concept should be developed to the extent that will permit a reasonable cost estimate to be made. The extent of removal of existing construction should be considered, including the sizes and locations of new, replaced, or strengthened structural members. Typical structural connections with schematic details for upgrading nonstructural elements should be included in the study.

The following general considerations should be addressed in the development of the design concepts:

- Structural systems
- Configuration
- Horizontal diaphragms
- Eccentricity
- Deformation compatibility
- Foundations
- Basic isolation and passive energy dissipation

7.6.3.8.1 *Structural Systems*

The development of the structural upgrading concepts requires a complete understanding of the existing vertical and lateral-load-resisting systems of the existing building. The designer must be

able to determine the consequences that the removal, addition, or modification of any structural or nonstructural element will have on the performance of the strengthened building.

An evaluation of the existing vertical load-carrying structural system should be made to determine the effects that the seismic upgrading may have on the performance of the building to resist gravity loads. Vertical load-resisting elements such as columns and framing systems may also be affected by seismic upgrading. If these framing elements are not used for the lateral-force-resisting system, they must be analyzed for deformation compatibility. This analysis should include the effects of the lateral displacements due to extreme seismic motion on the vertical load-carrying capacity of the vertical structural elements.

#### 7.6.3.8.2 *Configuration*

Severe problems may arise if the existing building is highly irregular in plan configuration or is composed of units with incompatible seismic response characteristic. An example is a flexible steel moment frame building connected to a relatively low rigid concrete shear wall building. If the resulting problem cannot be resolved by strengthening or upgrading the connection between two units, consideration should be given to separating them with a seismic joint. Each unit should have a complete system for resisting vertical as well as lateral loads. Structural members bridging the joint with sliding supports on the adjacent unit should be avoided. The criteria for new building separations apply to existing buildings. Seismic joints should provide for the three-dimensional uncoupled response of each of the separate units of a building, but need not extend through the foundations.

#### 7.6.3.8.3 *Diaphragms*

In most buildings, the horizontal framing systems (i.e., floors and roofs) will participate in the lateral-force-resisting system as diaphragms in addition to supporting the gravity loads. As part of the seismic upgrade, the floor and roof systems may require modifications (e.g., new topping or horizontal bracing), which will add to the dead load; thus, the capacity of the modified system must be evaluated for the new loading conditions. Every upgraded building should have either a rigid or a semirigid horizontal floor diaphragm. Roof diaphragms may be flexible or semiflexible.

#### 7.6.3.8.4 *Eccentricity*

Provisions should be made for the increase in shear resulting from the horizontal torsional moment due to an eccentricity between the center of mass and the center of rigidity. In the development of upgrading concepts, when the vertical shear-resisting elements must be strengthened, supplemented, or replaced with new elements, consideration should be given to the location of new or strengthened elements so as to reduce eccentricity between the center of rigidity and the center of mass.

#### 7.6.3.8.5 *Deformation Compatibility*

The compatibility of the deformation characteristics of existing elements and the new strengthening elements should be considered. When lateral forces are applied to a building, they will be resisted by the elements in proportion to their relative rigidities. If the structure is to be strengthened to resist seismic forces, the new structural elements must be more rigid than the existing elements if they are to take a major portion of the lateral forces and reduce the amount of force that is taken by the existing elements. Both the relative rigidities and strengths of all lateral-force-resisting elements must be considered.

Special consideration must be given in determination of relative rigidities of (1) concrete components: cracked versus uncracked; (2) shear walls: participation of intersecting walls (e.g., effective flange widths) and the effects of openings; and (3) steel frames: participation of concrete floor slab and framing, and infill walls. Structural elements that are not part of the lateral-force-resisting system should be evaluated for the effects of the deformation that occurs in the lateral-force-resisting system. Brittle elements are particularly susceptible to damage if they are forced to conform to the deformations of the lateral-force resisting system. In order to protect these elements from the possibility of being subjected to large distortions, provisions should be made to allow the structural



system to distort without forcing distortion on the brittle elements. A good example is the isolation of a masonry wall from the slab soffit. When rigid walls are locked in between columns, a similar method of isolation may be required at each end of the wall.

#### 7.6.3.8.6 Foundations

If the seismic upgrade adds weight or redistributes the gravity loads, the foundations must be analyzed for the additional gravity loads combined with the horizontal and overturning forces associated with the seismic lateral force. Existing foundation ties that do not provide for adequate load transfer must be strengthened or replaced, unless proper justification can be provided for waiving the deficiency.

#### 7.6.3.8.7 Base Isolation

Design strategies that significantly modify the dynamic response of a structure at or near the ground level are generically termed base isolation. This is usually achieved by introduction of additional flexibility at the base of the structure. The objective is to force the entire superstructure to respond to vibratory ground motion as a rigid body with a new fundamental mode based on the stiffness of the isolation devices. This strategy is particularly effective for short buildings (i.e., buildings with a fundamental mode less than about 1 s). For these buildings, it is feasible with the isolation devices to develop a new fundamental mode with a period of about 2–3 s. For most sites (e.g., those with a predominant site period less than 1 s), the new fundamental mode period will occur beyond the portion of the response spectrum that is subject to dynamic amplification and the response of the structures will be greatly reduced.

A typical base isolation installation consists of large pads of natural or synthetic rubber layers bonded to steel plates in a sandwich assembly or sliding bearings with either a flat or a single curvature spherical sliding surface made of polytetrafluoroethylene (PTFE) or PTFE-based composites in contact with polished stainless steel. The isolator assembly, as well as all connecting elements and building services, must be capable of resisting the design spectral displacement corresponding to the new fundamental mode (some installations have base isolation assemblies that can deflect elastically up to 24 in.). Certain base isolation assemblies may have a lead core or other device to increase damping and thus decrease the response at the isolator. Because of the uncertainties associated with ground motion predictions, seismic base isolators are designed with fail-safe provisions to arrest the motion of the building to development of instability due to excessive displacement of the isolator. Base isolation can be an effective strategy to reduce the seismic response of a building, provided careful consideration is given to the amplitude and frequency content of the expected ground motion, the design of the pipes and conduits providing services to accommodate the expected displacements, and provision of fail-safe mechanisms as described above. The ability of base isolation to reduce seismic response is even more attractive in application to existing buildings with inadequate seismic resistance.

However, in addition to the considerations just described, installation of base isolation in an existing building entails accurate determination of the magnitude and location of the vertical loads, a rigid diaphragm above the isolators to collect and distribute the lateral loads, and careful underpinning and jacking of the existing structure in order to effect a systemic transfer of the existing foundation loads to the base isolation device.

#### 7.6.3.8.8 Passive Energy Dissipation

An effective means of providing substantial damping is through hysteretic energy dissipation. Some structures, for example, properly designed ductile steel and concrete frames, exhibit additional damping and reduced dynamic response as a result of the limited yielding of structural steel or concrete reinforcement.

In addition to the damping inherent in a ductile structure, passive energy-dissipating systems designed to increase structural damping have been in use for some time. This is an emerging

technology that provides an alternate approach to conventional stiffening and strengthening schemes. The primary use of energy-dissipation devices is to reduce earthquake displacements in structure. These devices will also reduce the force in the structure, provided the structure is responding elastically, but would not be expected to reduce force in structures that are responding beyond yield.

Further discussion of base isolation and passive energy dissipation techniques is found in Chapter 8.

#### 7.6.3.8.9 Conclusions

Before concluding this section, perhaps it is beneficial to reflect on some of the performance characteristics offered in ASCE/SEI 41-06, particularly those at the top-of-the-line performance levels. It is the opinion of many engineers that high-end building performance cannot be promised or achieved with 100% certainty. Top-of-the-line-performance implies a near-perfect earthquake-proof building. Therefore, building owners and the public are likely to ask for it more frequently. Ask they should, but with the understanding that there is no such thing as earthquake-proof buildings, only earthquake-resistant buildings. It is therefore the structural engineers' responsibility to make this fact clear to the owners and to the public so that their expectations for building performance do not exceed those implied in the ASCE/SEI 41-06 performance definition. Although major advances have been made in analytical capability and in the synthesizing of experimental and earthquake performance data, prediction of building performance relative to future earthquakes is still a risky and dangerous business. Thus, seismic rehabilitation continues to challenge the very core of conventional thinking.

Generally seismic retrofit should be considered only if its entire cost is less than 70%–80% of replacement cost. It should be noted that it is impossible to bring an existing structure into conformance with current code requirements. Therefore, the cost assigned to the retrofit should not outweigh the seismic performance expected of the building.

It behooves the designer to consider more than one seismic retrofit strategy. One of these should be a conventional one. This ensures that designers are not carried away with a high-tech new approach when a more conventional retrofit strategy is more cost-effective.

Seismic retrofit design is invariably more expensive than new construction design. The extra design effort required for retrofit design should be communicated to the owner at the onset of the project. The cost of the retrofit design should be pegged to the complexity of the analysis required. Many designers do not assign sufficient design hours to projects that require NSP or NDP. The cost of developing and implementing material test recommendations should be considered at the start of the project. It is recommended that material test results be available to the designer before the design development phase is started. The design basis should already be stated and discussed with the owner and peer reviewers at the onset of the project.

It is emphasized that a number of parameters used in ASCE/SEI 41-06 remain a matter of discussion and research. It must remain at the discretion of engineers to modify the parameters they deem appropriate. Agreement on key issues must be reached with peer reviewers as the analysis progresses.

### 7.6.4 ASCE/SEI 41-06: DESIGN EXAMPLE

#### 7.6.4.1 Dual System: Moment Frames and Shear Walls

**Given:** An existing 15-story office building located in downtown Los Angeles, California. The lateral system consists of moment frames and shear walls. The building was built in 1972 and suffered cosmetic damage during the 1994 Northridge earthquake. The damage was repaired by patching spalled concrete. No seismic evaluations were made at the time of repairs.

In 2008, the building is being acquired by new owners who desire an assessment of the building's expected seismic performance. A structural engineer has been hired to evaluate the seismic vulnerability of the building, and, if required, to come up with a seismic upgrade scheme. The selected

design objective, as desired by the owners, is that the building should be operational after a major earthquake, i.e., the performance criterion is IO.

The engineer has selected the following components for a preliminary seismic evaluation:

1. Frame beams
2. Frame columns
3. Shear walls
4. Diaphragm components
5. Frame column-to-foundation connections

However, to keep the explanation simple, seismic evaluation of only one frame beam is presented assuming the following.

Typical frame beam is the same as the beam explained in Section 7.6.3.6.3. Its Capacity is equal to 2101 k-ft.

$Q_E$  is the Action due to unreduced earthquake loads (i.e.,  $R = 1$ ), determined using a LDP. In our case, the beam action is bending. Assume  $M_E = Q_E = 3820$  kip-ft.

$Q_D$  is the Dead-load action (i.e., dead load moment). Assume  $Q_D = M_D = 580$  kip-ft.

$Q_L$  is the Effective live load action (equal of 25% of unreduced design live load, but not less than actual live load). Assume  $Q_L = M_L = 145$  kip-ft.

$Q_S$  is the Effective snow load contribution. Assume there is no snow load,  $Q_S = 0$ .

**Required:** The buildings seismic evaluation, and possibly an upgrade scheme that meets the requirements of ASCE/SEI 41-06 for enhanced performance objectives. Verify the acceptability of the typical frame beam by considering only the bending action.

### Solution:

**Step 1:** is the determination of the characteristics of the ground motion likely to be experienced at the building site, because ground motions are the most common cause of earthquake damage. Consequently, rehabilitation objectives are commonly established using earthquake ground shaking hazards, typically defined on a probabilistic basis. Performance characteristics that are functions of the severity of specified earthquakes are directly related to the extent of damage sustained by the building.

As stated earlier, owners of the building desire to have an evaluation of seismic vulnerability of the building. And, if required, a seismic rehabilitation design for an enhanced performance objective. Their intent is to have the building operational during and after seismic events postulated for IO. The engineer has, in nontechnical terms, described to the owners the broad range of expected building performances in terms of possible damage to both structural and nonstructural building components. Communication with the owner in lay terms is perhaps the most important step in a seismic rehabilitation study. The owners of our subject building are now well informed about probable postearthquake scenarios. Because retrofit objective is IO, they expect the following performance after the seismic retrofit, if any.

- Overall damage to the building to be light
- Structure to have no permanent lateral displacement
- Structure's original strength and stiffness to remain substantially unchanged
- Minor cracking in facade partitions and ceilings
- Minor local yielding of structural elements at a few places, without fracture
- Elevators and fire protection system remaining operable
- In terms of nonstructural components, equipment and contents to be generally secure, but perhaps not operable due to mechanical failure or lack of utilities

Prediction of building performance in a future earthquake is a dangerous and risky business. Consider, for example, the top-of-the-line performance as set forth in SEI 41-06. There, it implies that a building designed for IO is likely to come out scratch-free after a high seismic event, giving the wrong impression that the building is earthquake-proof. We as structural engineers understand that buildings designed using the principle of ductile design is earthquake-resistant and not earthquake-proof. This important difference should be brought to the attention of building owners.

Table 7.1 (SEI 41-06 Table C1-1) displays in a matrix format the characteristics of ground motion for three distinct earthquakes, represented by notations  $k + p + e$ . These are

- BSE-1 earthquake with a 10% probability in 50 years (mean return period of 474 years, rounded to 500 years, used in most seismic standards)
- BSE-2 earthquake with a 2% probability in 50 years (mean recurrence interval of 2475 years, rounded to 2500 years)
- An earthquake with a 20% probability in 50 years (mean recurrence interval of 225 years)

For the example building, we assume that the project geotechnical engineer has, after conducting site-specific studies, developed an acceleration response spectra for the earthquakes listed earlier. Since the methodology of seismic evaluation is the same for all postulated earthquakes (except for numerical values of demand, and  $m$  factors), we will verify the performance of the frame beam for only BSE-2 earthquake. This shortcut is to keep the explanation simple.

**Step 2:** is the determination of as-built conditions in order to arrive at a value for the reliability coefficient  $k$ . The building that is fairly old, built in 1972; for simplicity we will assume that as-built information pertinent to its seismic performance, including construction documents and material test reports is not available. Further a visual survey has indicated that there are site-related concerns such as pounding from neighboring structures. Because of the absence of as-built information, the engineer is not able to gain a comprehensive knowledge and understanding of the behavior of structural components. Therefore, a value of  $k = 1.0$  cannot be used in the analyses.  $k$  is a reliability coefficient used to reduce the component strength value for existing components. Because  $k$  is less than 1.0, there is a need to reduce the computed strength values of the component when making demand capacity comparisons. For our example, we will assume  $k = 0.9$ .

**Step 3:** the classification of the structural members into primary and secondary components, is a straightforward task. In a moment frame building, both frame beams and columns are classified as primary because they are essential for providing the structure's basic lateral resistance. This step also includes the classification of the response of lateral-resisting components into either deformation-controlled or force-controlled actions. In our case the flexural action of the frame beams is deformation-controlled. However, the classification of frame columns subject to combined compression and bending is not so obvious. It could be either deformation-controlled or force-controlled, depending on the ratio of axial load in the column and its axial strength.

**Step 4:** entails setting up the analytical model; calculating the building period; and determining the base shear, its vertical distribution up the building height, and the forces in the floor and roof diaphragms. This task—an everyday occurrence in a design office—does not (here) require explanation except to point out that

1. If an LSP is used for seismic analysis, then the base shear  $V$ , also referred to as the pseudolateral load, is calculated using the unreduced spectral acceleration  $S_a$  without an upper limit on the building period,  $T$ .
2. If an LDP such as a modal superposition is used, then the analysis is carried out using a response spectrum that is not reduced to account for the anticipated inelastic response of the building (i.e.,  $R = 1.0$ ).

The purpose of an LSP or LDP is to determine the distribution of forces and deformations induced in a structure by the design ground motion. Although an LSP is permitted for simple buildings less than 100 ft in height, prevailing practice in most design offices is to use an LDP with modal superposition method. Hence, we will assume that the forces and moments in the frame beam given earlier have been evaluated by performing linear dynamic analyses for each of the three response spectra selected for the study.

**Step 5:** is where the seismic and gravity loads are combined to determine  $Q_{UD}$ , the demand imposed on elements due to seismic and gravity loads. Because the actions of both the frame beams and frame columns of the example building are considered to be deformation-controlled, we use the following equation to calculate the demand:

$$Q_{UD} = Q_G \pm Q_E$$

If, on the other hand, the action of an element under consideration is force-controlled, the corresponding equation for verifying the acceptance criteria would have been

$$Q_{UF} = Q_G \pm \frac{Q_E}{C_1 C_2 J}$$

where

$Q_{UF}$  is the design action due to combinations of gravity and seismic loads

$J$  is the coefficient that estimates the maximum earthquake force that a component can sustain and deliver to other components

The maximum value of  $J$  is 2. It is calculated by the relation

$J = 1$  in zones of low seismicity

$J = 1.5$  in zones of moderate seismicity

$J = 2$  in zones of high seismicity

$C_1$  and  $C_2$  = modification coefficients explained earlier in Section 7.6.3.5

**Step 6:** is where the component capacities  $Q_{CE}$  or  $Q_{CL}$  are calculated, depending upon whether the action considered is deformation- or force-controlled. We will not dwell on this here, because it was explained in detail in the previous section.

Returning to the example, since the bending of the frame beam is categorized as a deformation-controlled action, the demand  $Q_{UD}$  when the effects of gravity and seismic loads are additive is given by

$$\begin{aligned} Q_{UD} &= Q_G + Q_E \\ &= 1.1 (Q_D + Q_L + Q_S) + Q_E \\ &= 1.1 (580 + 145 + 0) + 3820 \\ &= 797.5 + 3820 \\ &= 4617.5 \text{ kip-ft} \end{aligned}$$

**Step 7:** is the final step, in which the acceptance criterion is verified for each component. As stated previously although we earmarked six distinct components for seismic assessment, to keep the presentation simple we check here the acceptance criterion for the frame beam only.

In step 3 it was determined that the limit state for the example beam was flexure. Beam flexure (and for that matter, beam shear) with negligible axial loads is considered as deformation-controlled action.

The expected flexural capacity of the beam,  $Q_{CE}$ , as calculated in Section 7.6.3.6.3 is equal to 2101 k-ft. In step 1, we determined the reliability coefficient,  $K$ , as equal to 0.9. We now determine from Table 7.8 the  $m$  factor for our beam for IO performance level. For this purpose we assume the following conditions:

1.  $\frac{\rho - \rho'}{\rho_{bal}} > 0.5$
2. The transverse reinforcement in the beam is not in conformance with ductile detailing
3. The ratio  $\frac{V}{b_w d \sqrt{f'_c}} < 3.0$

(See Table 7.8 for definitions of terms in the equations above).

Using the assumed conditions, the  $m$  factor (component modification factor to account for the expected ductility) for our example beam from Table 7.8 is 2.0.

Therefore, the flexural capacity for comparison with the demand is

$$mkQ_{CE} = 2 \times 0.9 \times 2101 = 3781 \text{ kip-ft.}$$

The demand/capacity ratio is

$$\frac{Q_{UD}}{mkQ_{CE}} = \frac{4617.5}{3781} = 1.22$$

The demand  $Q_{UD}$  from step 6 is 4617.5 kip-ft, which is greater than the expected capacity of 3781 kip-ft, indicating noncompliance. However, before judging the beam as unsafe, a similar evaluation is made for other actions of the beam and the analysis repeated for the other seismic resisting elements. The results are reviewed, keeping in mind that values of  $m$  are only approximate indicators of seismic performance. Reevaluation of the building using nonlinear analysis procedures with reevaluated gravity and lateral loads using a sharp pencil is a prudent course of action before deciding on seismic rehabilitation.

The procedure for evaluating acceptance criteria is conceptually the same for other components of the moment frame, such as columns, panel zones, beam column connections, and column-to-foundation connections.

Suppose the objective of the seismic evaluation of our example building is basic LS, instead of IO. Does the procedure for seismic study differ from the preceding procedure for IO performance? What if the target performance is CP instead of IO?

The procedure is generally the same, irrespective of the selected target performance. The differences are in ground motions used in the analysis and in the values of the  $m$ -factors used in the acceptance criteria.

The  $m$ -factors corresponding to LS and CP are larger than those for IO. For instance,  $m$  for LS would equal 3, instead of 2, for the deformation-controlled beam studied in the illustrative example.

It is perhaps worth recalling that collapse prevention refers to the building in the postearthquake damage state that is on the verge of partial or total collapse but has not yet collapsed. Substantial damage to the structure has occurred, with considerable loss of stiffness and strength in the lateral-force-resisting system. However, all significant components of the gravity-load-resisting system continue to function.

If the building does not collapse, some engineers may wrongly consider that the LS objective has been met. The LS performance level includes a margin of safety against collapse for the lower-level

earthquake. Significant risk of injury from falling structural debris may exist. It may not be practical to repair the structure and it may not be safe for reoccupancy, because aftershock activity may induce collapse.

To satisfy the limited safety objective of CP, the building must be evaluated for a single earthquake chosen from a range of specified earthquake hazard levels. Building Safety Earthquake-2 (BSE-2) with a 2% probability of occurrence in 50 years, is one example. See Table 7.1 for other specified earthquakes.

### 7.6.5 SUMMARY OF ASCE/SEI 41-06

The purpose is to predict for a design earthquake, the force and deformation demands on the various components of the structure. The analysis allows for the evaluation of the acceptability of structural behavior (performance) through a series of demand versus capacity (D/C) checks.

SEI 41-06 permits both linear and nonlinear analysis procedures for evaluation of existing construction and evaluation of rehabilitated construction. Whether or not it is applicable to design of new construction is a matter of discussion with the building official. It describes rehabilitation strategies, which include

- Global modifications such as
- Increasing stiffness and strength by adding new elements
- Increasing damping using supplemental damping devices
- Isolating the structure from seismic ground motions by using seismic isolation
- Decreasing mass
- Local modification of components consisting of
- Local strengthening or weakening
- Jacketing

The LSP is similar to the equivalent lateral procedure included in most building codes. However, the pseudolateral loads  $V = C_1 C_2 C_m S_a W$  incorporate techniques for considering the nonlinear response of individual elements and components, and is based on the unreduced spectral acceleration  $S_a$ .

The LDP may be used on either linear modal spectral analysis or linear time history analysis. In both cases, the results are modified with coefficients similar to those in the LSP. The acceptability criteria are the same as for LSP, including separating force- and displacement-controlled actions. The acceptance of performance is judged on a component action level. Each component action is defined as either deformation-controlled or force-controlled.

Permissible levels of inelastic displacement or strength demand are defined for each performance level.

In an NSP the analytical model consists of all elements having significant strength or stiffness. An analysis, commonly referred to as pushover analysis, is performed to develop the relationship between lateral forces and displacement at the roof or other convenient locations.

The elements that do not have significant lateral resistance can be designated secondary and removed from the model. Generally, a computer program with nonlinear analysis capability is used or a linear analysis with incremental loading is performed. Static lateral loads are applied incrementally and the element properties are adjusted for yielding or failure. The seismic global displacement demand is determined and deformation-controlled components are judged acceptable if their gravity plus earthquake deformation demand is less than or equal to the expected permissible deformation capacity given in tabular form in the standard.

## 7.7 FIBER-REINFORCED POLYMER SYSTEMS FOR STRENGTHENING OF CONCRETE BUILDINGS

Composite materials made of fibers in a polymeric resin—also known as fiber-reinforced polymers (FRP)—have come into use as an alternative to traditional strengthening techniques such as steel plate bonding, section enlargement, and external posttensioning. This technique has been used to strengthen many bridges and buildings around the world, and was first applied to concrete columns in Japan for providing additional confinement. The development of codes and standards for externally bonded FRP systems is ongoing in Europe, Japan, Canada, and the United States. Within the last 10 years, several documents related to the use of FRP materials in concrete structures have been published.

The FRP systems come in a variety of forms including wet layup and precured systems. Wet layup systems consist of dry unidirectional or multidirectional fiber sheets impregnated with a saturating resin on-site. The saturating resin along with the compatible primer and putty is used to bond the FRP fabric to the concrete surface.

Prepregnation systems consist of uncured unidirectional or multidirectional fiber sheets or fabrics that are prepregged with a saturating resin in the manufacturing facility. They are bonded to the concrete surface with or without an additional resin application, depending upon specific system requirements.

Precured systems consist of a wide variety of manufactured composite shapes. The precured shapes are typically bonded to the concrete surface by an adhesive along with a primer and putty. There are three common types of precured systems:

- Unidirectional laminate sheets typically delivered to the site as thin ribbon strips coiled on a roll
- Multidirectional grids, also typically delivered to the site coiled on a roll
- Shell segments cut longitudinally so they can be opened and fitted around columns, beams, or other components of buildings

### 7.7.1 MECHANICAL PROPERTIES AND BEHAVIOR

Unlike steel reinforcement, FRP materials do not exhibit plastic behavior when loaded in tension. The stress–strain relationship is linearly elastic until failure, which is sudden and can be catastrophic.

The tensile property of the FRP material is governed by the type of fiber and its orientation and quantity. The tensile property of an FRP system should be characterized as a composite, based on not just the material properties of the individual fibers, but also on the efficiency of the fiber–resin system, the fabric design, and the method used to create the composite. The mechanical properties should be based on the testing of laminate samples with known fiber content.

Externally bonded FRP systems should not be used as compression reinforcement. There has been very little testing to validate their use in resisting compressive forces. The failure mode for FRP laminates subjected to longitudinal compression can include transverse tensile, fiber microbuckling, or shear failure.

The FRP materials subject to a constant load over time suddenly fail after a period referred to as endurance time, also referred to as creep–rupture. In general, carbon fibers are the least susceptible to creep–rupture, aramid fibers are moderately susceptible, and glass fibers are the most susceptible.

Many FRP systems exhibit reduced mechanical properties after exposure to certain environmental factors, including temperature, humidity, and chemicals. The tensile properties reported by the manufacturers are based on tests conducted in a laboratory and do not reflect the effects of environmental exposure. Therefore, the properties should be adjusted to account for the anticipated service environment.



### 7.7.2 DESIGN PHILOSOPHY

The design of FRP systems is based on traditional reinforced concrete design principles. The FRP strengthening systems are designed to resist tensile forces while maintaining strain compatibility with the concrete substrate. Unlike mild steel reinforcement, FRP systems should not rely on resist compressive forces. However, it is permissible for the FRP tension reinforcement to experience compression due to changes in moment patterns or moment reversals, as in members subjected to seismic forces, with the proviso that the compressive strength of the FRP system is neglected in calculating the member capacities.

In FRP design, certain limits are imposed to guard against collapse of the structure, should bond or some other type of failure occur due to vandalism, fire, or other causes. The designer is referred to the ACI committee 440 recommendations for further details.

### 7.7.3 FLEXURAL DESIGN

An increase in the flexural strength of a concrete member can be achieved by bonding FRP reinforcement to its tension face with fibers oriented along the member's length. Although higher strength increases are reported in test results, an increase of up to 40% of the original flexural strength is considered reasonable in view of ductility and serviceability limits.

Flexural strengthening using FRP systems are not recommended for enhancing flexural capacity of members in the expected plastic regions. Cases in point are the plastic hinge regions of ductile moment frames resisting seismic loads. For such cases, the effect of cyclic load reversal on the FRP system should be investigated.

## 7.8 SEISMIC STRENGTHENING DETAILS

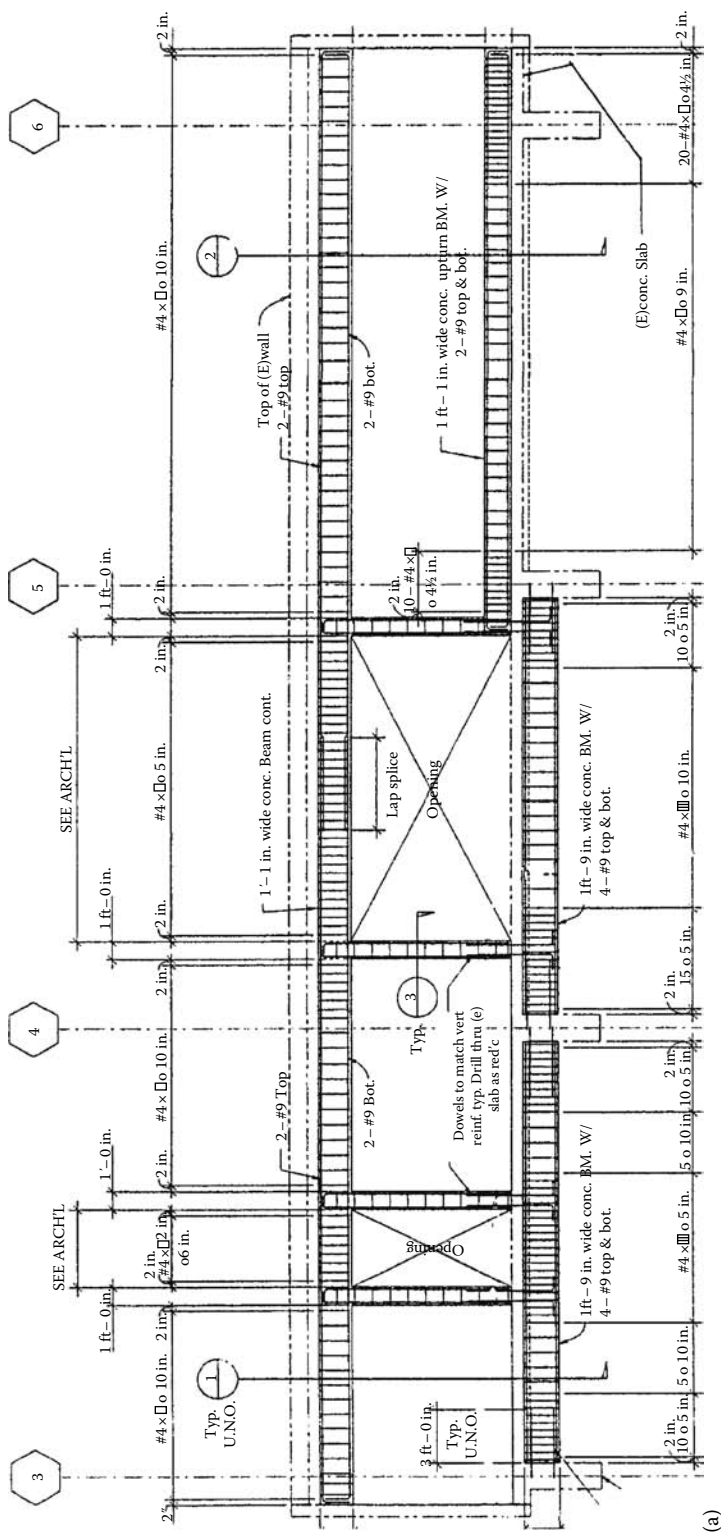
A thorough understanding of existing construction and seismic retrofit objectives acceptable to owners and to the building official is an important consideration before a seismic retrofit is undertaken. The importance of considering global and elemental deformations at expected levels of seismic forces, not at code or design levels, cannot be overstressed. This is because even with the use of amplification factors, the deformations are at best an approximation, particularly when applied to complex multistory and multi-degree-of-freedom systems. It should be kept in mind that detailing in existing buildings often does not meet the requirements of new construction, and that the strength and stiffness of existing elements may not be comparable with new upgraded systems and elements. Thus, verification of elements for deformation compatibility becomes even more important. This criterion is secondary only to the requirement of providing a continuous load path that is sufficiently stiff and strong to resist realistic earthquake forces. Suggested rehabilitation measures listed by deficiencies are given in subsequent paragraphs.

1. *Load path.* Add elements to complete the load path. This may require adding new shear walls or frames to fill gaps in existing shear walls or frames that are not continued to the foundation. It also may require the addition of elements throughout the building to pick up loads from diaphragms that have no path into existing vertical elements.
2. *Redundancy.* Add new lateral-force-resisting elements in locations where the failure of a single element will cause instability in the building. The added lateral-force resisting elements should be of comparable stiffness to the elements they are supplementing.
3. *Vertical irregularities.* Provide new vertical lateral-force-resisting elements to eliminate vertical irregularity. For weak stories, soft stories, and vertical discontinuities, add new elements of the existing type.
4. *Plan irregularities.* Add lateral-force-resisting bracing elements that will support major diaphragm segments in a balanced manner. Verify whether it is possible to allow the irregularity to remain and instead strengthen those structural elements that are overstressed.

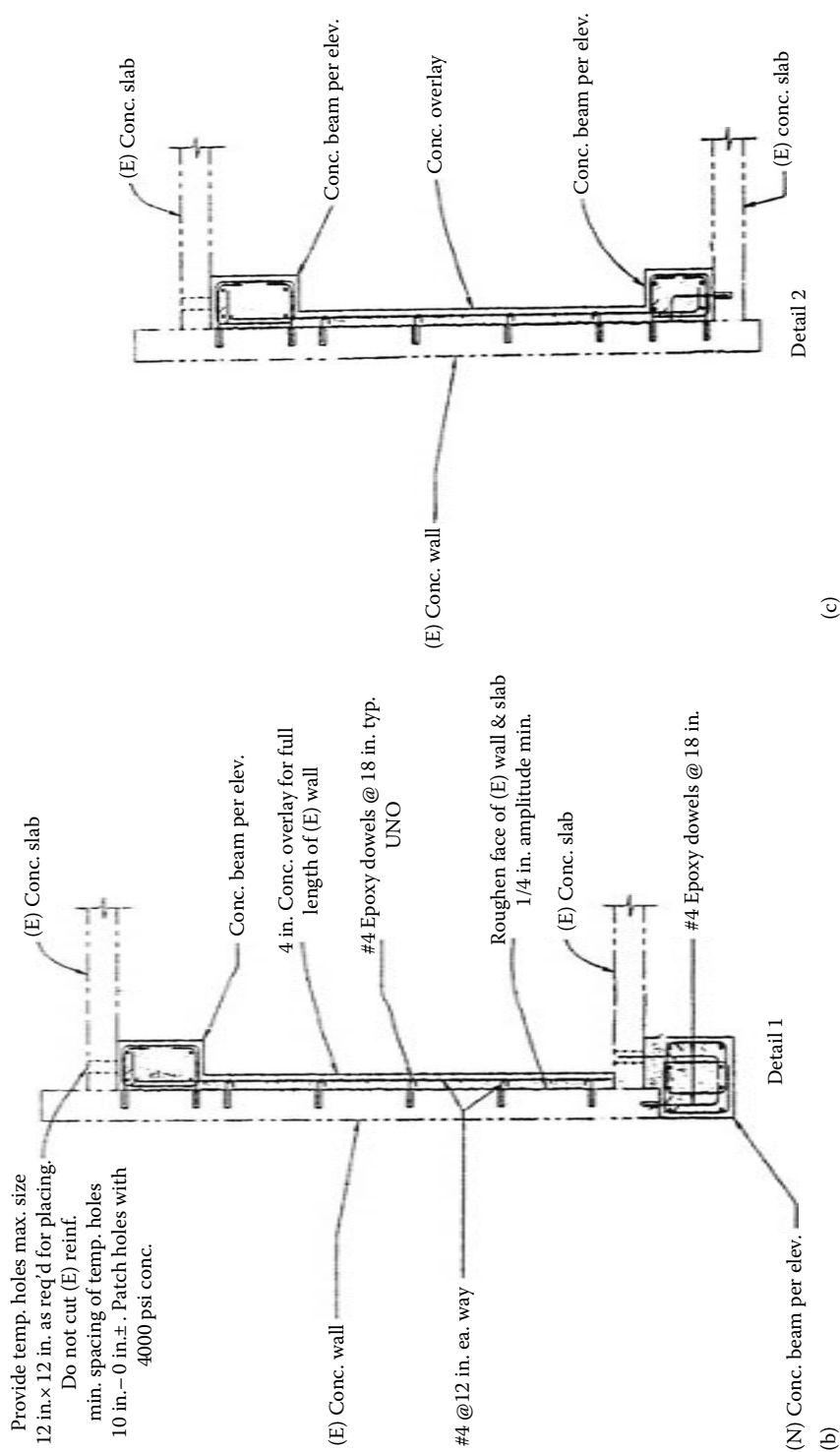
5. *Adjacent buildings.* Add braced frames or shear walls to one or both buildings to reduce the expected drifts to acceptable levels. With separate structures in a single building complex, it may be possible to tie them together structurally to force them to respond as a single unit. The relative stiffness of each structure and the resulting force interactions must be determined to ensure that additional deficiencies are not created. Pounding can also be eliminated by demolishing a portion of one building to increase the separation.
6. *Lateral load path at pile caps.* Typically, deficiencies in the load path at the pile caps are not a LS concern. However, if it is determined that there is a strong possibility of a LS hazard, piles and pile caps may be modified, supplemented, repaired, or, in the most severe condition, replaced in their entirety.
7. *Deflection compatibility.* Add vertical lateral-force-resisting elements to decrease the drift demand on the columns, or increase ductility of the columns. Jacketing the columns with steel or concrete is one way to increase their ductility.
8. *Drift.* The most direct mitigation approach is to add properly placed and distributed stiffening elements—new moment frames, braced frames, or shear walls—that can reduce the interstory drifts to acceptable levels. Alternatively, the addition of energy dissipation devices to the system may reduce the drift.
9. *Frame and nonductile concerns.* Add properly placed and distributed stiffening elements, such as shear walls, to supplement the moment frame system with a new lateral-force-resisting system. For eccentric joints, columns and beams may be jacketed to reduce the effective eccentricity. Jackets may also be provided for shear critical columns.
  - Short captive columns. Columns may be jacketed with steel or concrete such that they can resist the expected forces and drifts. Alternatively, the expected story drifts can be reduced throughout the building by infilling openings or adding shear walls.
10. *Cast-in-place concrete shear walls; Shear stress.* Add new shear walls and/or strengthen the existing walls to satisfy seismic demand criteria. New and strengthened walls must form a complete, balanced, and properly detailed lateral-force-resisting system for the building. Special care is needed to ensure that the connection of the new walls to the existing diaphragm is appropriate and of sufficient strength such that yielding will occur in the wall first. All shear walls must have sufficient shear and overturning resistance.
  - Overturning. Lengthening or adding shear walls can reduce overturning demand.
  - Coupling beams. Strengthen the walls to eliminate the need to rely on the coupling beam. The beam should be jacketed only as a means of controlling debris. If possible, the existing opening should be infilled.
  - Boundary component detailing. Splices may be improved by welding bars together after exposing them. The shear transfer mechanism can be improved by adding steel studs and jacketing the boundary components.

### 7.8.1 COMMON STRATEGIES FOR SEISMIC STRENGTHENING

Techniques for strengthening or upgrading existing buildings will vary according to the nature and extent of the deficiencies, the configuration of the structural systems, and the structural materials used in construction. Typical details commonly used for seismic upgrading of structural members and systems are given in Figures 7.7 through 7.19 to provide guidelines to engineers. Many of the details shown are adapted from the technical manual TM 5-809-10-12 published by the Departments of the U.S. Army, Navy, and Air Force. In using these details, it should be kept in mind that designers' judgment and ingenuity in addressing specific situations is an important prerequisite for appropriate use of these details.

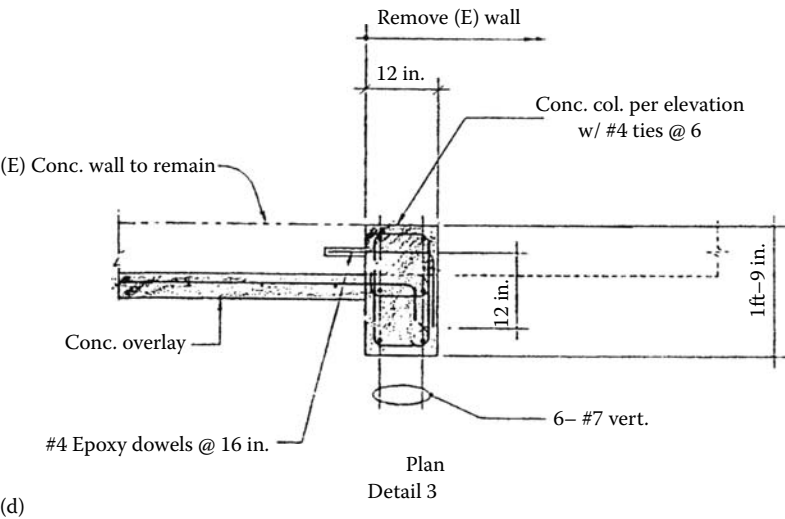


**FIGURE 7.7** (N) openings in an (E) 3-story concrete shear wall building. The seismic upgrade consisted of providing concrete overlay to restore shear capacity of walls and adding boundary elements around (N) openings: (a) wall elevation.

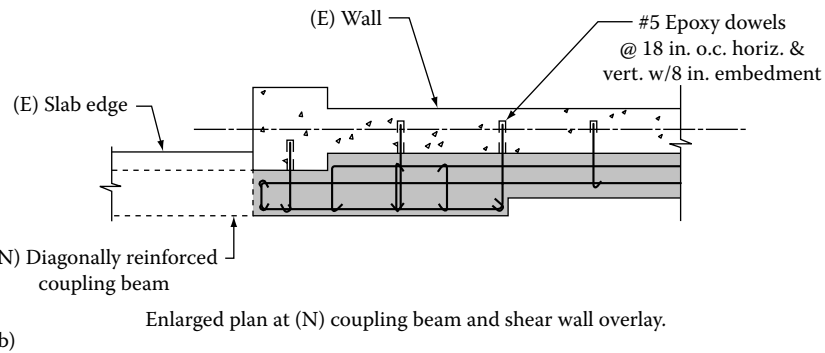
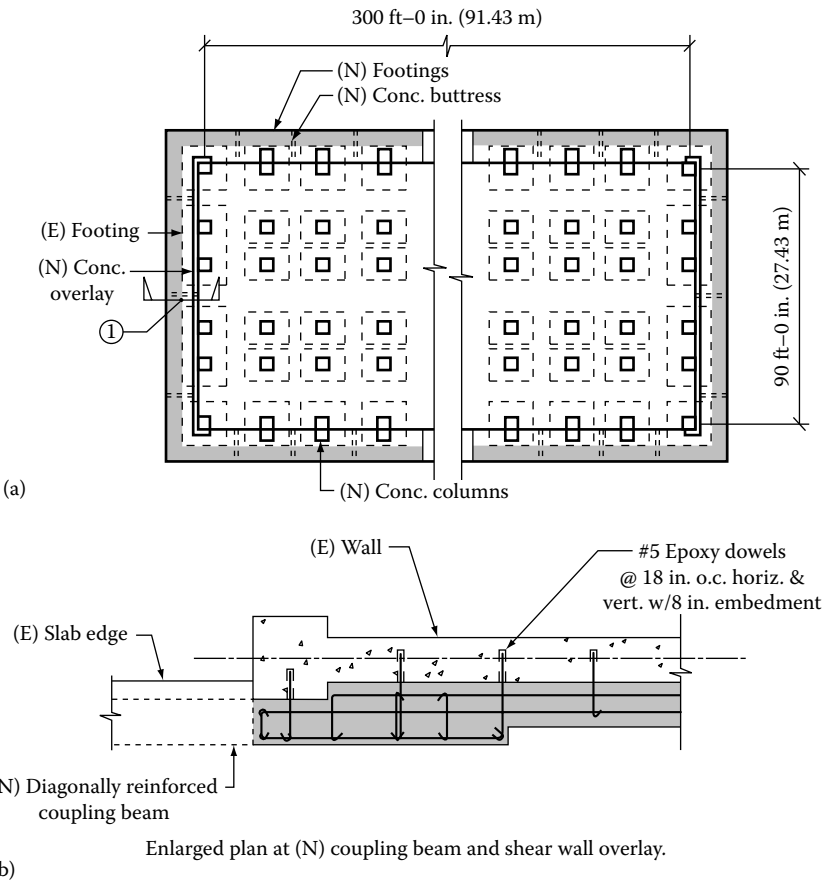


**FIGURE 7.7 (continued)** (b) concrete overlay with (N) beam below (E) slab; (c) concrete overlay with (N) beam above (E) slab.

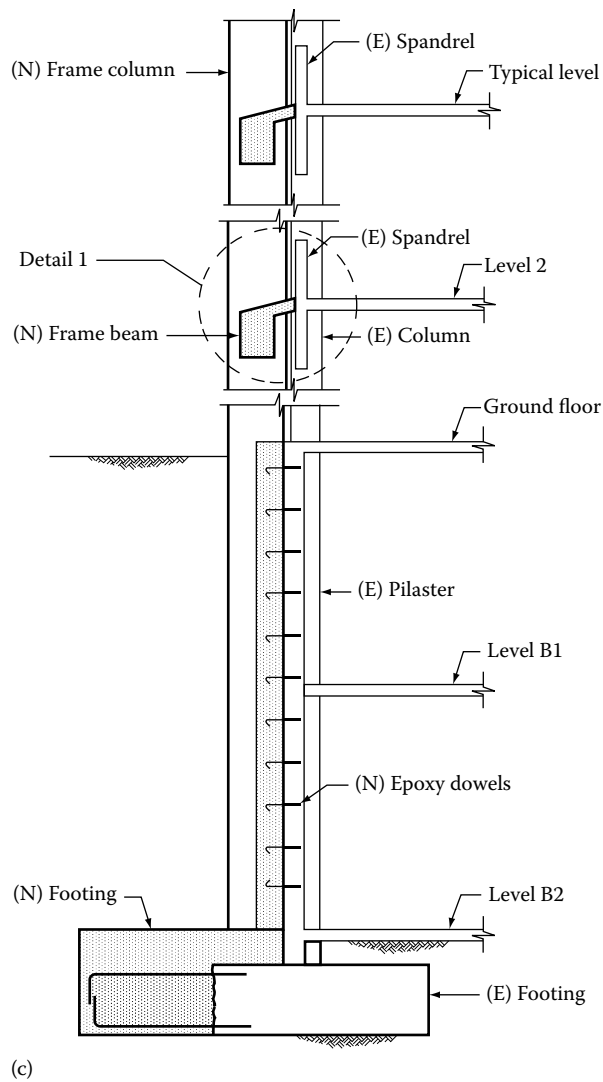
(continued)



**FIGURE 7.7 (continued)** (d) Plan detail at (N) boundary element. *Note:* (E), existing, (N), new.

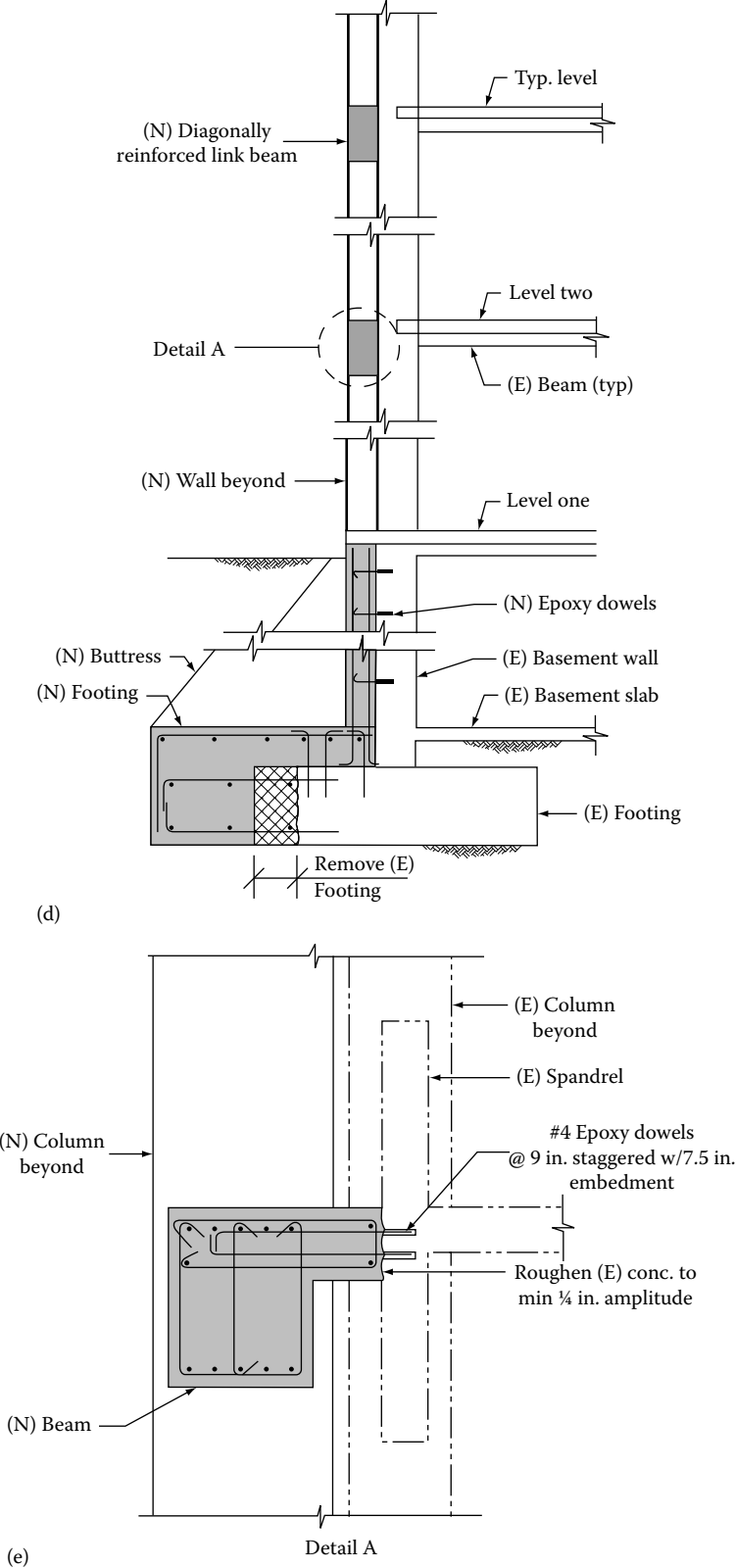


**FIGURE 7.8** Seismic upgrade of a concrete hospital building with an external concrete moment frame. Modifications were restricted to the periphery of the building to keep the building operational. (a) Plan showing (N) foundations, (N) concrete overlay in the transverse direction, and (N) moment frames in the longitudinal direction. (b) Enlarged plan at (N) coupling beam and shear wall overlay.

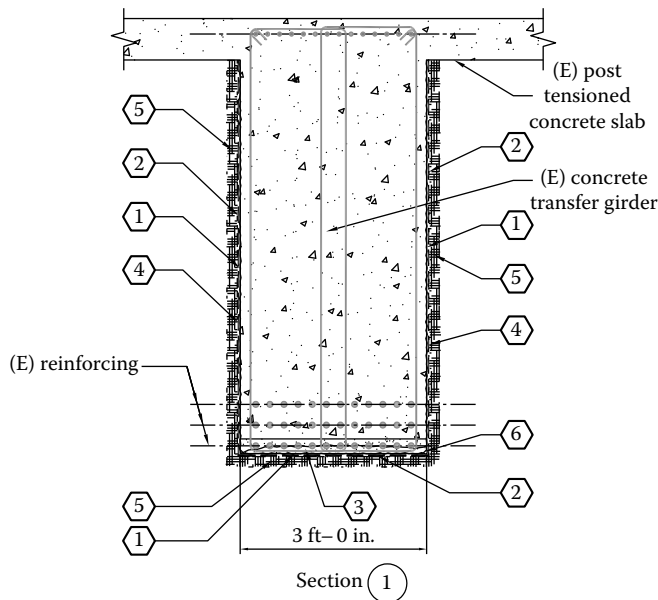
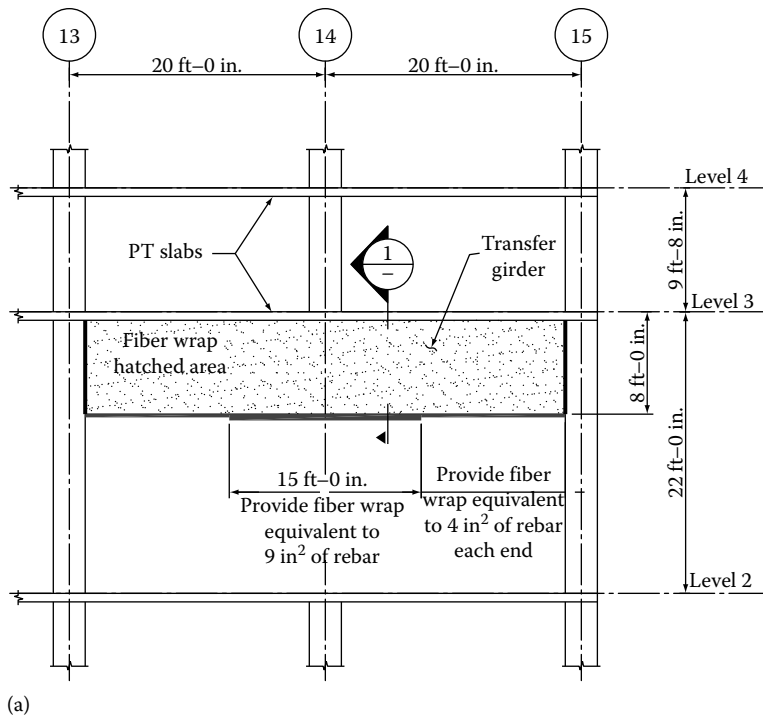


**FIGURE 7.8 (continued)** (c) Section through longitudinal frame.

(continued)



**FIGURE 7.8 (continued)** (d) Section through transverse wall. (e) Connection between (N) and (E) frame.



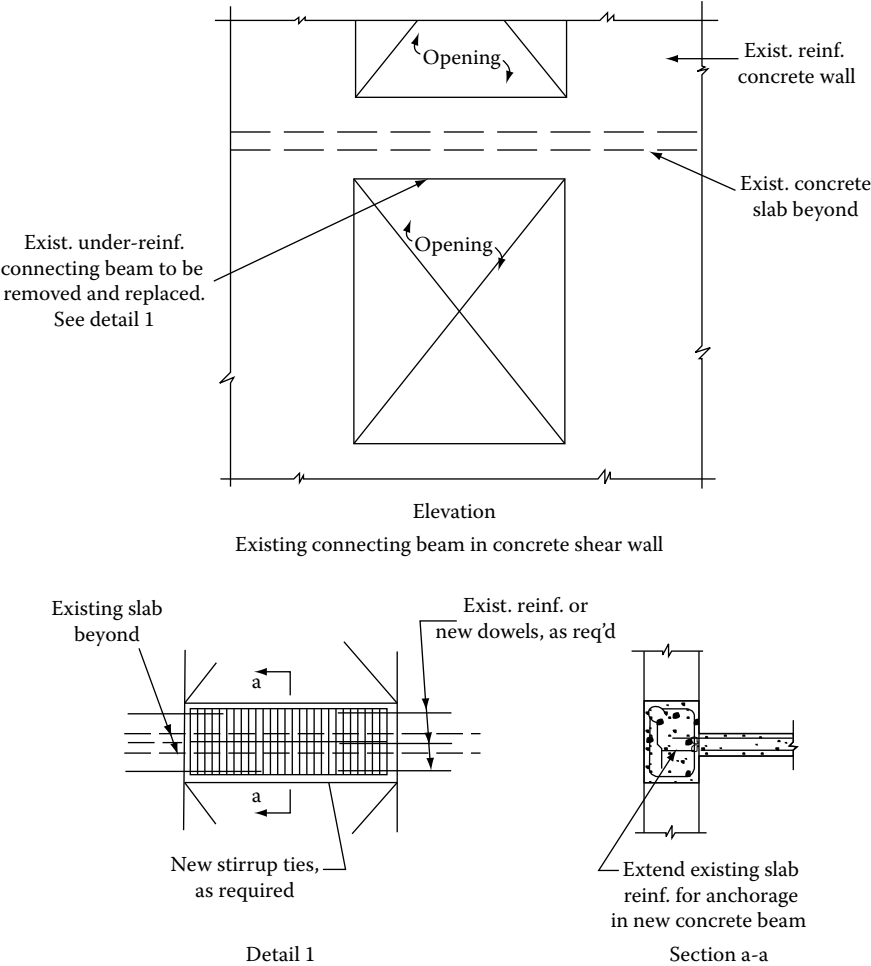
Suggested repair procedure:

1. Sand blast girder soffit and sides.
2. Install fiber wrap material at the bottom and sides of the girder for the entire length.
3. Design fiber wrap at the bottom of the girder to compensate for the rebars as specified by the Engineer of Record (EOR). See elevation (a).
4. The fiber wrap at the sides of the girder shall provide a tensile strength equal to 3 kip/in. width.
5. Fireproof fiber wrap material as required.
6. Ensure that a minimum chamfer of  $\frac{3}{4}$  in. exists at corners. If not, provide a radius as required by the fiber wrap design.

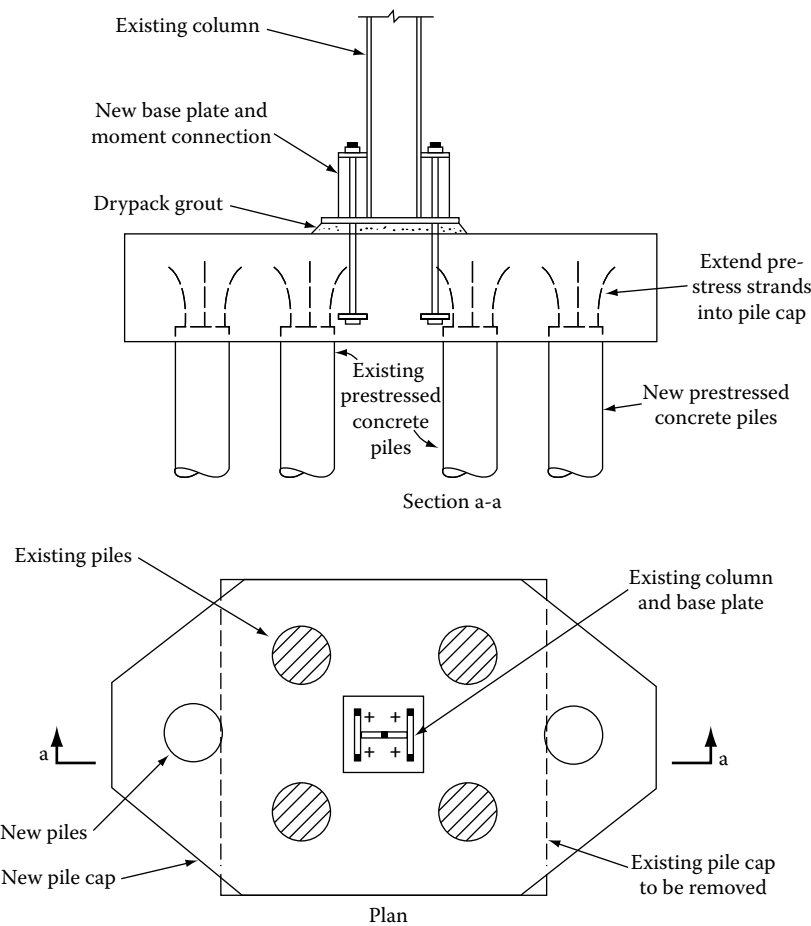
(b)

**FIGURE 7.9** Fiber wrap of a transfer girder: (a) elevation and (b) section.

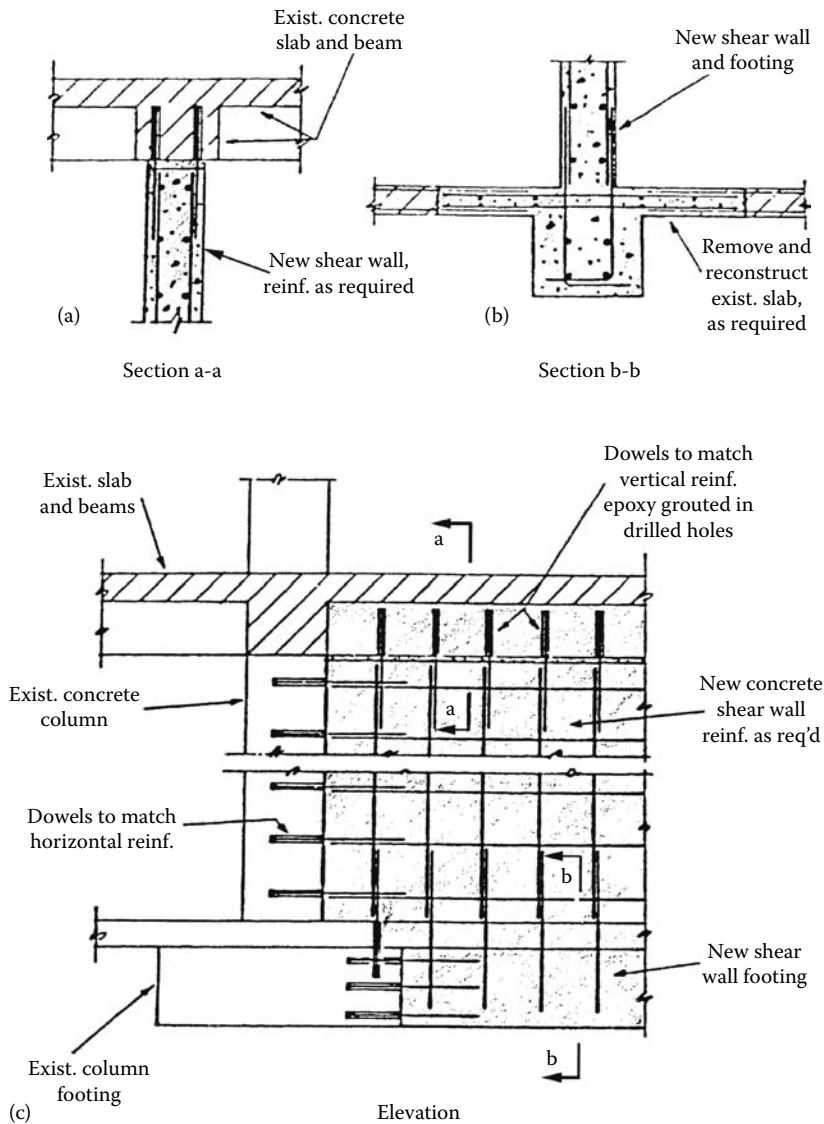




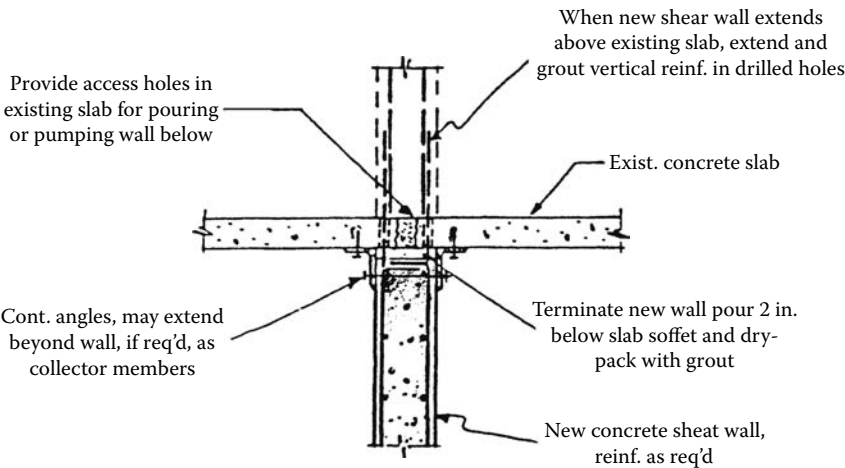
**FIGURE 7.10** Strengthening of existing connecting beams in reinforced concrete walls.



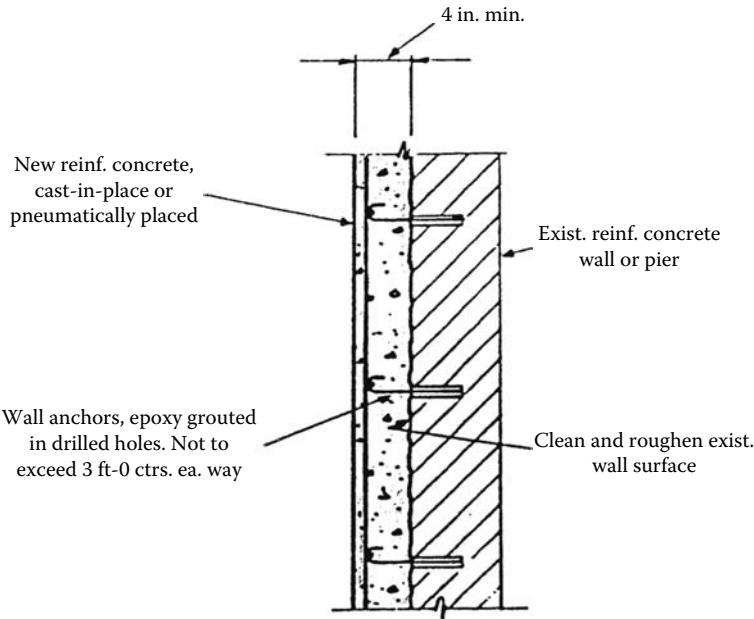
**FIGURE 7.11** Upgrading of an existing pile foundation. Add additional piles or piers, remove, replace, or enlarge existing pile caps. *Note:* Existing framing to be temporarily shored to permit removal of existing pile cap and column base plate. Drive new piles; weld new base plate and moment connection to column; pour new pile cap; and drypack under base plate.



**FIGURE 7.12** Strengthening of an existing concrete frame building by adding (N) a reinforced concrete shear wall: (a) section a-a; (b) section b-b, and (c) elevation.



**FIGURE 7.13** New concrete shear wall at existing slab.



**FIGURE 7.14** Strengthening of existing reinforced concrete wall or piers.

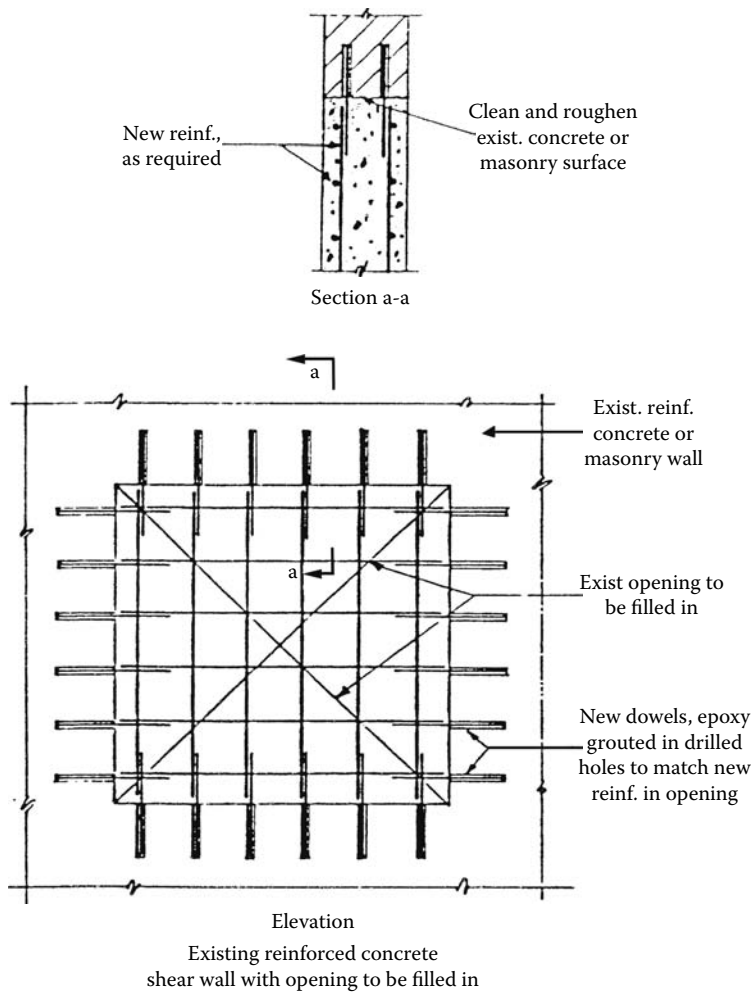


FIGURE 7.15 Strengthening of existing reinforced concrete walls by filling in openings.

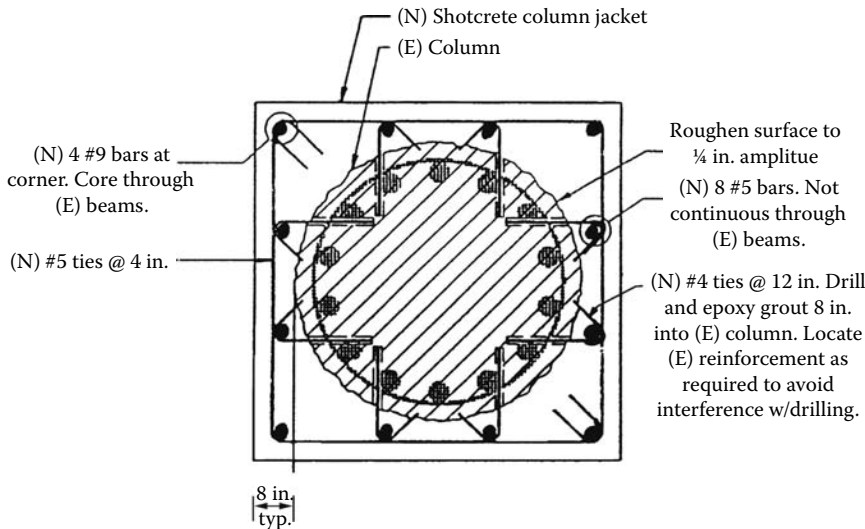


FIGURE 7.16 Jacketing of circular column.

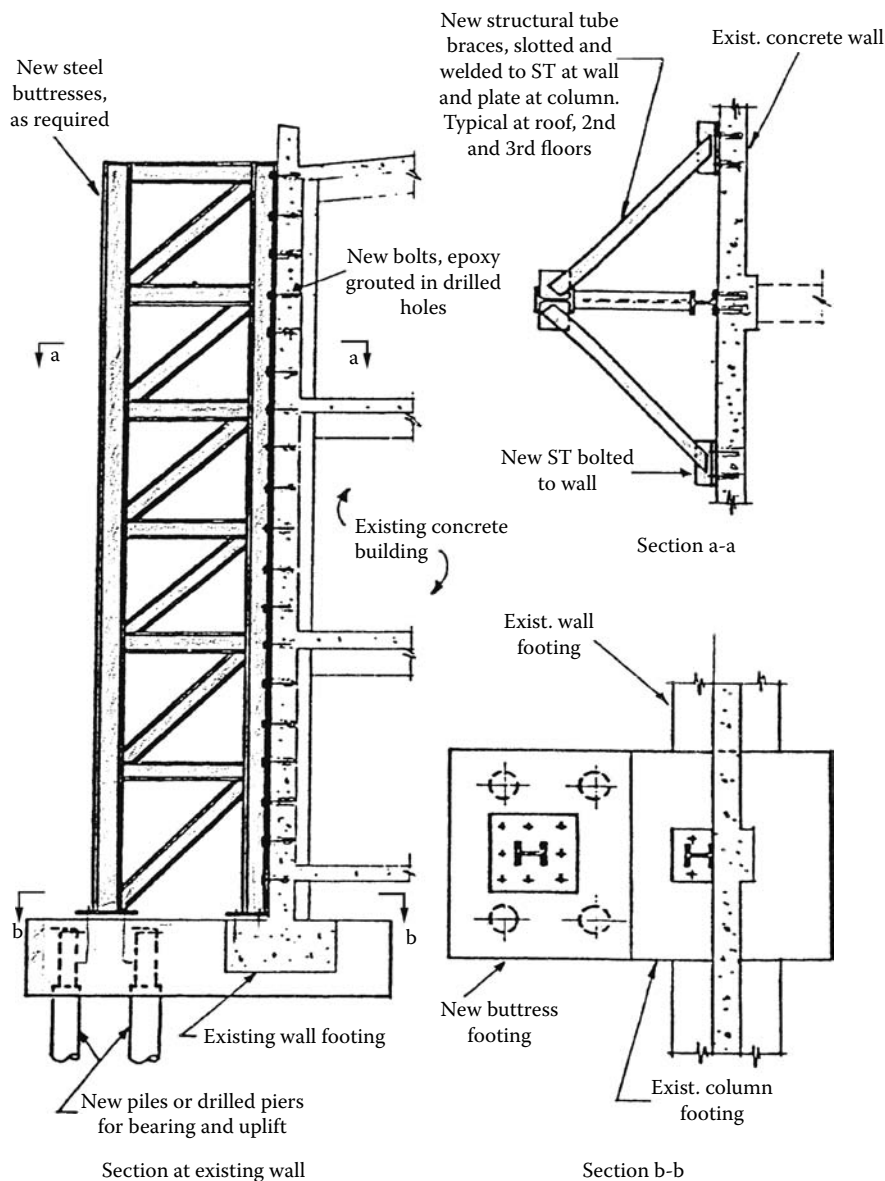
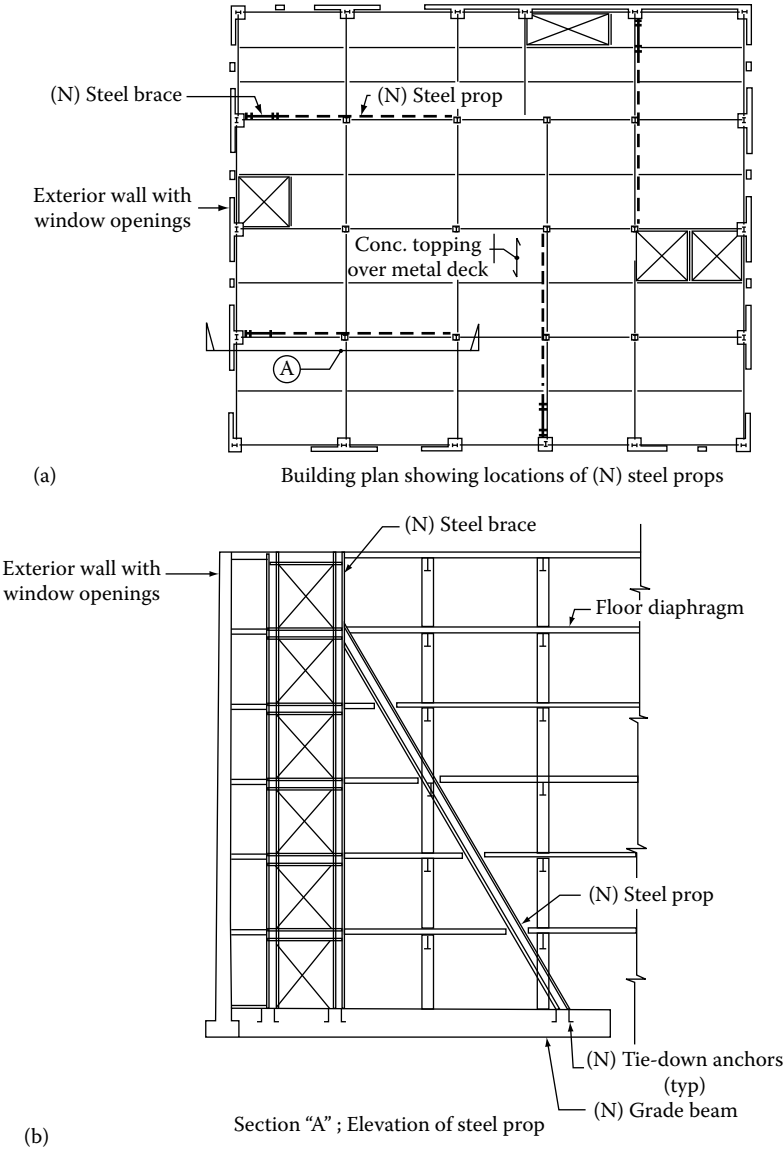


FIGURE 7.17 Braced structural steel buttresses to strengthen an existing reinforced concrete building.



**FIGURE 7.18** (a) Building plan showing locations of (N) steel props. (b) Section A; elevation of (N) steel prop.

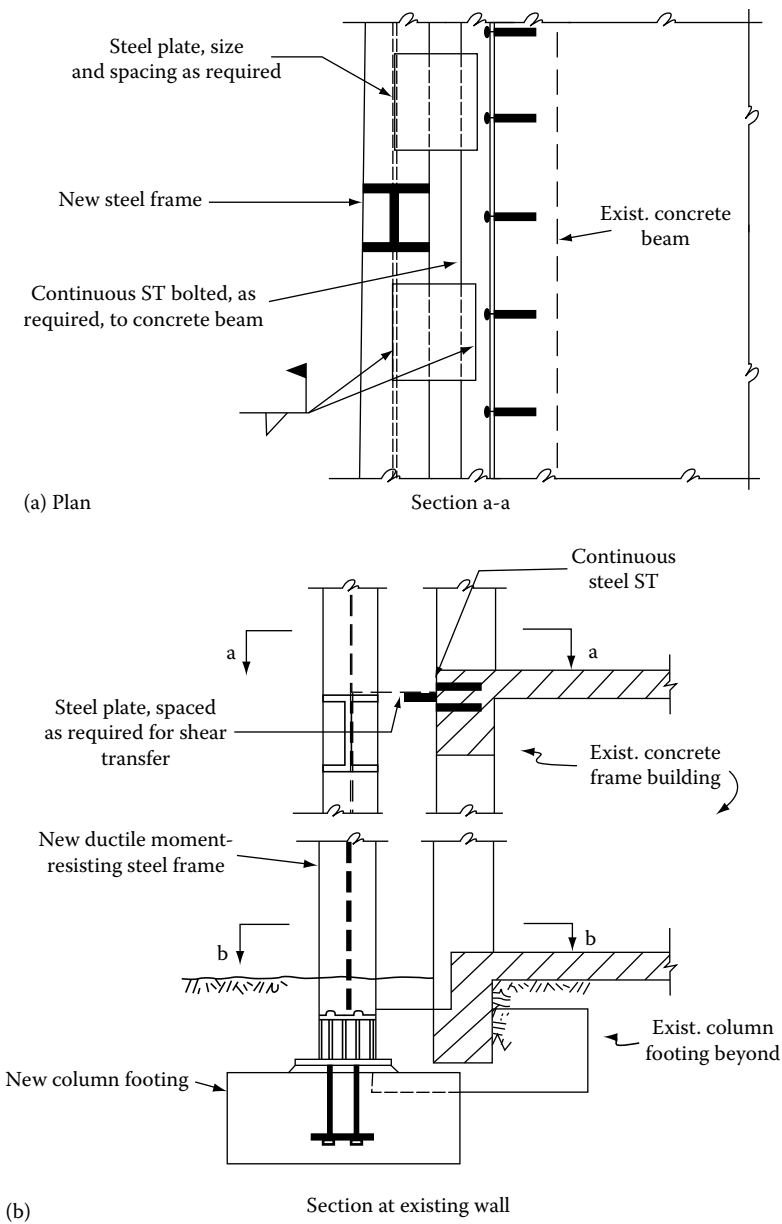


FIGURE 7.19 Upgrading an existing building with external frames.

(continued)



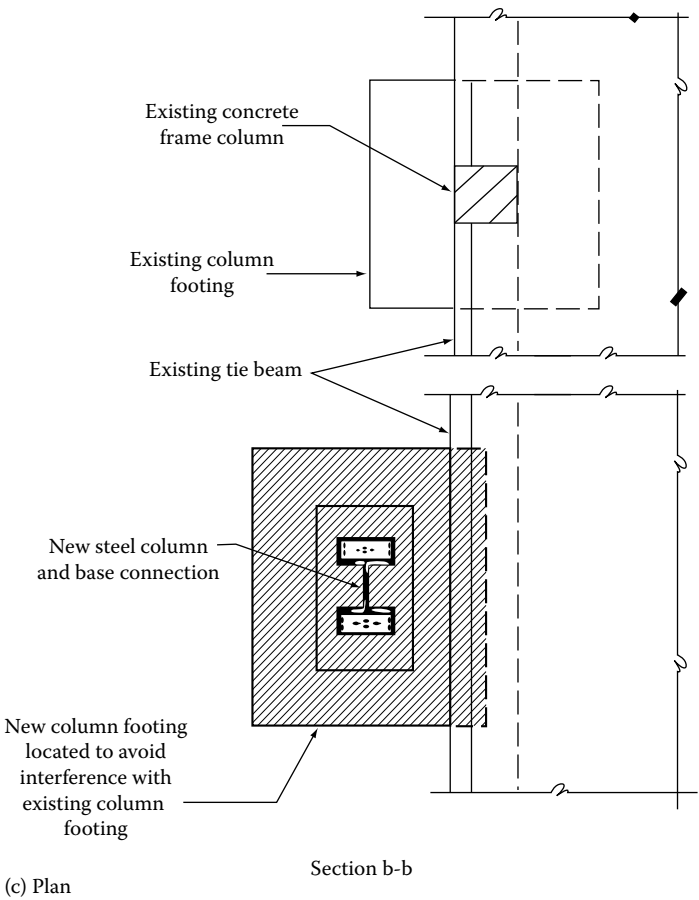


FIGURE 7.19 (continued)

---

# 8 Tall Buildings

While the world is full of interesting structures, large and small, old and modern, the most eye-catching and the ones that instill the greatest sense of wonder in the onlooker are the modern skyscrapers. They are monuments of power and prestige, supreme achievements in engineering and design, comforting landmarks, testimonials to the human spirit, and public relations at the highest level. When considering skyscrapers, until recently, the observer was drawn to great cities such as New York and Chicago. Today, after a century during which New York and Chicago went unchallenged as home to the world's tallest modern buildings, the crown has been snatched first by Kuala Lumpur's twin Petronas Towers, then by Taipei's 101 Tower, and recently by the Burj Dubai, the 162 floor, mostly residential concrete tower in Dubai.

In New York, the Empire State Building was completed in 1931 and with 102 stories stood at no less than 1250 ft height (see Figure 8.1). Among the many astonishing features of the building is the fact that it has no less than 73 elevators, although not all traverse the full height. Amazingly it was built in the relatively short period of 410 days. After the completion of the Empire State Building, architects began to explore more extensive use of materials such as glass and metal to replace the traditional masonry cladding of the building. The ultimate expression of the trend were the twin towers of the World Trade Center (WTC), as shown in Figure 8.2, which became the world's tallest building in 1972 with each tower reaching up to 1368 ft and to 1727 ft with the addition of TV and other antennas. Sadly these towers are not with us because of the infamous terrorist attack on September 11, 2001.

To turn to the world's tallest towers, it might be surprising to find that the three highest towers in the world lie outside of China and the United States. In Kuala Lumpur, the capital of Malaysia, are the Petronas Towers standing side by side at a height of 1483 ft (see Figure 8.3). The accolade of the world's tallest building, not accounting for yet to be completed Burj Tower, goes to Taipei 101 Tower, which stands at 1671 ft in Taipei, the capital of Taiwan.

The Burj Dubai shown in Figure 8.4 is a super-tall skyscraper in Dubai, the United Arab Emirates. The tower is composed of a Y-shaped floor plan with setbacks occurring at each segment in an upward-spiraling pattern, decreasing the cross section of the tower as it reaches toward the sky.

Tall buildings have fascinated humans from the beginning of civilization as evidenced by the pyramids of Giza, Egypt; the Mayan temples of Tikal, Guatemala; and the Kutub Minar of Delhi, India. The motivation behind their construction was primarily for creating monumental rather than human habitats. By contrast, contemporary tall buildings are primarily a response to the demand by commercial activities, often developed for corporate organizations as prestige symbols in city centers.

The feasibility of tall buildings has always depended upon the available materials and the development of the vertical transportation necessary for moving people up and down the buildings. The ensuing growth that has occurred from time to time may be traced back to two major technical innovations that occurred in the middle to the end of the nineteenth century: the development of wrought iron and subsequently steel, and the incorporation of the elevator in high-rise buildings. The introduction of elevators made the upper floors as attractive to lease as the lower ones and, as a result, made the taller buildings financially successful.

During the last 120 years, three major types of structures have been employed in tall buildings. The first type was used in the cast iron buildings of the 1850 to 1910, in which the gravity load was carried mostly by the exterior walls. The second generation of tall buildings, which began with the 1883 Home Insurance Building, Chicago, and includes the 1913 Woolworth Building and the 1931



**FIGURE 8.1** Empire State Building, New York City.



**FIGURE 8.2** World Trade Center Twin Towers, New York City.



**FIGURE 8.3** Petronas Towers, Kuala Lumpur.



(a)



(b)

**FIGURE 8.4** Burj Dubai.

Empire State Building, are frame structures, in which a skeleton of welded or riveted steel columns and beams runs through, often encased in cinder concrete, and the exterior is a nonbearing curtain wall. Most high-rises erected since the 1960s use a third type of structure, in which the perimeter structure of these buildings resembles tubes consisting of either closely spaced columns or widely spaced megacolumns with braces. Inside the perimeter structure, a core, made of steel, concrete, or a combination of the two, contains many of the services such as elevators, stairwells, mechanical equipment, and toilets.

The art of designing tall buildings in windy climates is to bestow them with enough strength to resist forces generated by windstorms and enough stiffness or energy dissipation so that people working on upper floors are not disturbed by the buildings' periodic swaying.

In seismic regions of the world, including the most severe areas of California, the effects of earthquakes are relatively small for tall buildings. For example, using the provisions of ASCE 7-05, the calculated base shear for a 60-story steel moment frame building located in downtown Los Angeles, California, would be as little as 1% of its mass, as compared to 9% for a five-story building. However, the taller building would move considerably more than its five-story counterparts. Stiffness and ductility considerations rather than strength would govern the design.

The intent in seismic design then is to limit building movements, not so much to reduce perception of motion but to maintain the building's stability and prevent danger to pedestrians due to breakage and falling down of nonstructural elements.

## 8.1 HISTORICAL BACKGROUND

Throughout the recorded history of buildings, perhaps nothing is more captivating than the human aspiration to create increasingly tall structures. Pride seems to have been the prime motivation for the building of such ancient structures as the Tower of Babel, the Colossus of Rhodes, the pyramids of Egypt, the Mayan temples of Mexico, and the Kutub Minar of India. Ego and competition still play a part in determining the height of a building, but various other social and economic factors, such as increase in land values and higher density of population, have also contributed to an increase in the number of tall buildings all over the world. Until recently, what was considered as an American urban phenomenon can now be seen even in open country. The skylines of the world's cities are continually being pierced by distinct and identifiable tall buildings as impressive as mountain ranges. Reaching upward continues to be the challenge and goal.

The ancient tall structures, which can be considered as prototypes of present-day high-rise buildings were protective or symbolic in nature and were infrequently used as human habitats. Structures such as the Egyptian pyramids and the Mayan temples primarily served more as monuments than as space enclosures. Throughout history, humans had to make use of the available building materials. The Pyramid of Cheops, for example, was built by piling huge masonry blocks one on top of another to a peak of 481 ft (146.7 m), equivalent to a modern 40-story office building. The two basic materials, masonry and timber, used in construction through early centuries had their limitations. The spans that timber and stone could bridge, either as beams, lintels, or arches, were limited. Wood was neither strong enough for large structures, nor did it possess fire-resisting characteristics. Brick and stone masonry, in spite of their excellent strength and fire resistance, suffered from the drawback of weight. The mass of masonry required to carry the weight of a structure was too great to allow anything but a token usable space within it. The percentage of area taken up by vertical structural elements, that is, columns, walls, and braces, was inordinately large when compared to the gross floor area at the base. This percentage was at a maximum value for the pyramids.

Masonry construction reached its zenith in 1891 with the construction of the 17-story, 210 ft (64 m) Monadnock Building in Chicago (see Figure 8.5), an impressive structure that has gained historic landmark status. Gravity and the overturning moment caused by wind are resisted solely by the load-bearing masonry walls, which are 7 ft (2.13 m) thick at ground level. The area occupied by the walls of this building is 15% of the gross area at the ground floor.

In 1885, an American engineer named William LeBaron Jenny became the creator of the modern skyscraper when he realized that an office building could be constructed using totally different materials. He chose structural steel and incorporated it into a revolutionary system that was to make possible the soaring office towers that now symbolize the modern metropolis. Instead of relying on heavy masonry walls to support the weight of upper floors, Jenny had the ingenious idea of supporting the gravity loads of the 10-story Home Insurance Building in Chicago on a steel framework.



**FIGURE 8.5** Monadnock Building, Chicago.

The appropriateness of a steel skeleton for this purpose was acknowledged almost immediately. Its emergence was further influenced by factors such as economic expansion, the financial and institutional character of American business, and the intense use of urban land in central business districts. Still, very few buildings above 10 stories were built.

Two technological developments, the elevator and modern metal frame construction, removed the then prevailing limitations on height of the buildings, and the race for tallness was on. Competition to be the leading metropolis as judged by building heights, developed between Chicago and New York. By the turn of the century, the downtown business district around Wall Street in New York had achieved the status of the nation's foremost financial center. The great demand for office space saw the construction of several 20-story steel-skeleton buildings in this area.

In 1913, the Woolworth building (see Figure 8.6) was the first to reach 60 stories, soaring up 792 ft (242 m) in lower Manhattan. This Gothic cathedral style building is still in vigorous use after 70 years of service and the installation of air conditioning and automatic elevators. There was a temporary lull in high-rise construction during World War I, but activity picked up with renewed vigor after the war. Many excellent structures were built in New York, such as the 66-story, 950 ft (290 m) 60 Wall Tower Building; 71-story, 927 ft (283 m) Cities Service Building; and 77-story, 1046 ft (319 m) Chrysler Building (see Figure 8.7).

The demand for tall buildings increased because large corporations recognized the advertising and publicity advantages of connecting their names with imposing high-rise office buildings even though their operations required a relatively small percentage of floor space. The surplus space was leased out to eager business tenants, making the investment in high-rise development not only a source of publicity and pride but also a sound financial investment as an income generator.

The collapse of the financial market during the depression put an end to speculative high-rises, and only in the late 1940s in the wake of World War II did a new era of high-rise building set in. With the population doubling in almost every generation and production growing at an even faster



**FIGURE 8.6** Woolworth Building, New York City.



**FIGURE 8.7** Chrysler Building, New York City.



**FIGURE 8.8** Sears Tower, Chicago.

pace, developers could scarcely keep up with the demand for space. In the frenzy of new building, the race for height ended for the time being, in 1930, with the construction of the Empire State Building in New York City. This building, measured 1250 ft (381 m) without the 222 ft (67.7 m) television antenna (added later), taller than the 984 ft (300 m) Eiffel Tower in Paris, which was the highest structure of the nineteenth century. In 1968, the John Hancock Center in Chicago rose to a height of 1127 ft (344 m) plus 344 ft (105 m) of television antennas. The World Trade Center in New York City rose higher than the Empire State Building, to an awe-inspiring height of 1350 ft (412 m). In 1974, however, the 110-story Sears Tower in Chicago shown in Figure 8.8 took the crowning title as the world's tallest building at 1450 ft (442 m).

Whether the next assault will be on the American skyline remains to be seen. Perhaps the fabled King Kong will make his next climb atop a high-rise building again in New York. Builders have no doubt that such behemoths could be constructed, and they believe that a strong economy, a strong demand for office space, and strong popular or political support will once again sow the seeds of competitiveness for super-tall structures.

Earlier, high-rises tended to be prismatic in shape, but today even the most conservative architects are designing buildings with a touch of flamboyance. Owners and developers, who were once suspicious of daring designs, have come to expect them. In response, current architecture is producing buildings from 3 to as many as 10 sides, as well as round buildings. Some buildings proudly express on their surfaces, bold structures, and others are clad in smooth architectural curtain walls. Some consist of a single tower; others of two, sometimes identical twins, looking at each other in perpetual challenge.

The current flamboyance in architecture has not deterred the structural engineer from coming up with economical support systems. In fact, it has stimulated the profession to give almost total freedom in the architecture of high-rise structures. Today, with the use of computers, buildings are planned and designed which have little or no historic precedent. New structural systems are



conceived and applied to extremely tall buildings in a practical demonstration of the engineer's confidence in the predictive ability of the analysis, the methods used, and the reliability of computer solutions. Computers have made once difficult calculations easy, allowing the engineer to experiment with new configurations in an overall effort to reduce the structural cost.

Compared to advances in other engineering disciplines, the increase in the height of buildings brought about the structural innovation and computer technology is only modest; compare the height of the Empire State Building, which was completed in 1931 using a semirigid connection in a record time of 18 months from preliminary architectural drawings to the skyscrapers built today, such as the 110-story Sears Tower or the twin towers of the World Trade Center. What is more important in the present context is the significant decrease in structural materials the engineer has been able to achieve because of innovative design techniques. Before examining the reasons for the steady decrease in the material quantities, it is instructive to follow the development of twentieth-century high-rise architecture because structural quantities are closely related to the architecture of the building.

## 8.2 REVIEW OF HIGH-RISE ARCHITECTURE

The architecture of the United States in the twentieth century can be traced to several nineteenth-century roots principally to the advent of new forms of structural and other materials so strikingly displayed in the building technology of the American skyscraper. This has allowed greater scope of aesthetic expression and innovation in architectural practice.

The nineteenth century was one of the most technically inventive centuries. It witnessed the application of new techniques and of new mechanical means in virtually every human activity. It became clear in time that the innovation in architecture would come from those who grasped the possibilities of the new materials and techniques. Revolutionary methods of building with wood were developed in the 1830s to meet the demands for speedy construction and to overcome the shortage of skilled labor. Cast iron was developed into a building material lighter and more adaptable than masonry, and combined with other inventions, notably the elevator, paved the way for tall buildings unprecedented not only for height but ease of construction.

In Chicago, during the later part of the nineteenth century, a school of architects of whom Louis Sullivan and Frank Lloyd Wright were the most famous members, originated a new American style of domestic architecture. Their ideas were ignored for more than a decade in America, but were taken up abroad and developed into the so-called International Style. The International Style was also influenced by the German Bauhaus school, founded by Walter Adolf Gropius, and by the abstract artists interested in using pure forms for buildings. This style was the architectural response to the machine age. Simplicity meant elegance derived from "pure" forms. Display of the structural muscle beyond the tightly stretched curtain wall was widely accepted as the "in thing." Structures designed in this era incorporated three distinct elements of the new style: (1) a new vocabulary of forms borrowed largely from abstract art, consisting of planes, lines, and rectangles without ornaments or moldings; (2) the representation of interior space and exterior façade as a cohesive unit; and (3) the use of new structural materials such as steel and concrete.

The new style, with its angular forms, plane surfaces, and lack of conventional ornament, met with some resistance from the public, which tended to regard it as bare and inhuman. But by the middle of the twentieth century the style had become dominant across the country. Bold use of modern construction methods and structural materials became common. Noteworthy among the latter are glass tinted to reduce glare; glass brick designed to admit additional light while preventing glare and furnishing effective insulation against heat, cold and noise; artificial stone; plastics; chromium, aluminum, and other metals; and above all steel and concrete.

The early stages of American architecture lacked truly monumental structures. The monumental idea was gradually added to American architectural forms, reaching its apex with the construction of the Rockefeller Center in New York City (see Figure 8.9). The center represented a new concept of



**FIGURE 8.9** Rockefeller Center, New York City.

building a city within a city, containing a towering 60-story structure surrounded by a number of smaller high-rise office buildings and recreational facilities. This complex of skyscrapers has exercised increased influence since 1931, the year work on the Center was started. The building represents a departure in architectural thinking from a single-use, single-building concept to multiuse, multi-complex structures on a community scale. Because of that practical example, American architectures have responded more and more creatively to such demands and integration of city and surrounding region. Another example of multibuilding planning is the now nonexistent World Trade Center in New York City that consisted of twin 110-story towers and four smaller buildings grouped around a plaza.

From 1950 to the mid-1960s, the International Style of architecture was embraced by prominent American architects and resulted in sleek boxlike glass and concrete or steel high-rises which integrated the concept of purity of design into the architecture of the structure. Notable examples are the Seagram Building (1950) and the Whitney Museum (1966), both in New York City, and the John Hancock Center (1968) in Chicago, as shown in Figure 8.10.

During the mid-1960s a reaction developed to the International Style that emphasized greater freedom of design. Figuratively speaking, the concept of glass box was beginning to shatter. It was no longer wrong to hide a structure behind a more aesthetic exterior. The building and construction industry saw the advent of new forms of structural and other materials which allowed greater scope for aesthetic expression and innovation. Within the last two decades many major cities have had imaginative new shapes thrusting above their skylines using plan shapes that are other than prismatic. American corporations have built a new generation of flamboyant head-quarter buildings that are altering the urban skyline and bringing new vigor to cities. Many are spectacle buildings—giant architectural logos that draw enormous public attention and increased revenues to the companies that build them. These grand new buildings are emerging as good investments, serving not only as advertising symbols and marketing tools but also as sources of above-market rents for excess office space. The distinguishing architectural features for this new generation of buildings are sculptural shapes at their tops and elaborate detailing at their bases.



**FIGURE 8.10** John Hancock Center, Chicago.

### 8.3 FUNCTIONAL REQUIREMENTS

Building configurations vary copiously with their derivation seemingly at random, and at times even whimsical. In reality however, the configuration tries to simultaneously satisfy the requirements of

1. The land on which the building is sited
2. The building program as mandated by the developer
3. Appearance as desired by the architect

The first is due to constraints of site geometry and location, the second relates to the planning and occupancy needs, and the third depicts the designers desires for physical images that express the aspirations of the building owner, users, and of course, the designers themselves.

Buildings of the 1950s and 1960s responded to the functionalist ideas of the 1920s that the aesthetic and utilitarian aspects of the building are to be simultaneously satisfied. Such an idea is still being practiced, although currently functionalism is being hotly disputed. For a building to be successful, it should

1. Create a friendly and inviting image that has positive values to building owners, users, and observers.
2. Fit the site, providing proper approaches with a congenial layout for people to live, work, and play.
3. Be energy-efficient, providing interior space with controllable climate.
4. Allow flexibility in office layout with easily divisible space.
5. Offer space oriented to provide best views.
6. Most of all, the building must make economic sense, without which none of the development would be a reality.



**FIGURE 8.11** Chicago skyline.

## 8.4 DEFINITION OF TALL BUILDINGS

It is difficult to distinguish the characteristics of a building which categorize it as tall. After all, the outward appearance of tallness is a relative matter. In a typical single-story neighborhood, a five-story building may appear tall. A 50-story building in a city may be called a high-rise, but the citizens of a small town may point proudly to their skyscraper of six stories. In large cities, such as Chicago and Manhattan, and now in United Arab Republic, with a vast number of tall buildings, a structure must pierce the sky around 100–120 stories if it is to appear tall in comparison with its immediate neighbors (Figure 8.11). A tall building cannot be defined in specific terms related to height or number of floors. There is no consensus on what constitutes a tall building or at what magic height, number of stories or proportion a building can be called tall. Perhaps the dividing line should be drawn where the design of the structure moves from the field of statics into the field of structural dynamics.

From the structural design point of view, it is simpler to consider a building as tall when its structural analyses and design are in some way affected by the lateral loads, particularly the sway caused by such loads. Sway or drift is the magnitude of the relative lateral displacement between a given floor and the one immediately below it. As the height increases, the forces of nature particularly due to wind, begin to dominate. Therefore, structural framework for super-tall buildings is developed around concepts associated entirely with resistance to turbulent wind.

## 8.5 LATERAL LOAD DESIGN PHILOSOPHY

In contrast to vertical loads that may be assumed to increase linearly with height, lateral loads are quite variable and increase rapidly with height. For example, under a uniform wind load the overturning moment at the base varies in proportion to the square of the height of the building, while the lateral deflection varies as the fourth power. As for their lower brethren, there are four factors to consider in the design of tall buildings: strength, rigidity, stability, and, nowadays, legality. While the strength requirement is the dominant factor, as height increases, the rigidity and stability requirements also take on a dominant role, and often control the design. There are basically two ways to satisfy rigidity and stability requirements. The first is to increase the size of members above and beyond the strength requirements. However, this approach has its own limits, beyond which it becomes either impractical or uneconomical. The second and more elegant approach is to change

the configuration of the structure into something that is inherently more rigid and stable. It is of significance to note that there are no reports of completed tall buildings having collapsed because of wind loads. Analytically, it can be shown that a tall building under the action of wind will reach a state of collapse by the so-called  $P\Delta$  effect, in which the eccentricity of the gravity load increases to such a magnitude that it brings about crushing of columns as a result of large axial loads. Therefore, an important stability criterion is to assure that predicted wind loads will be below the load corresponding to the stability limit. The second consideration is to limit the lateral deflection to a level that will ensure that architectural finishes and partitions are not damaged. Although less severe than the collapse of the main structure, the floor-to-floor deflection normally referred to as the inter-story drift nevertheless has to be limited because of the cost of replacing the windows and the hazard to pedestrians of falling glass.

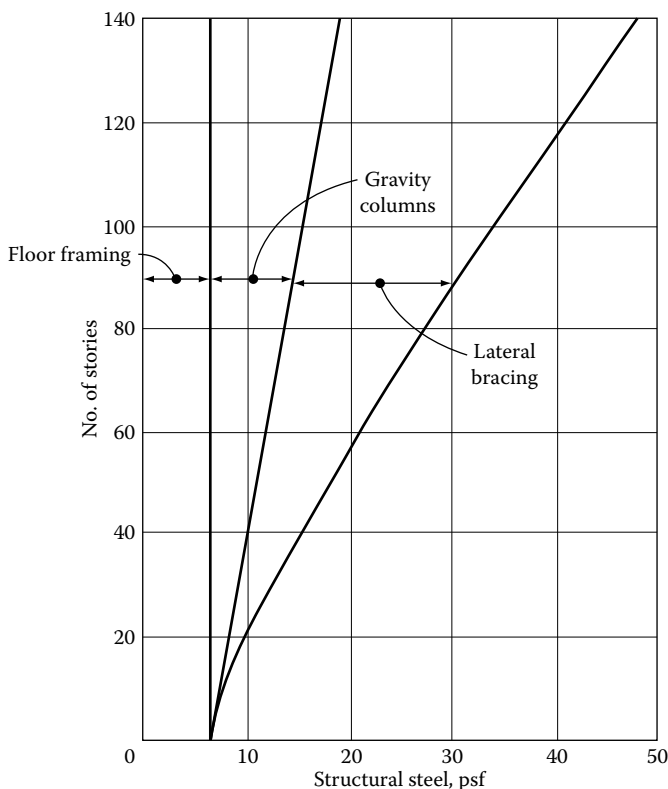
Slender high-rise buildings should be designed to resist the dynamic effects of vortex shedding by adjusting the stiffness and other dynamic properties of the structure such that the frequency of vortex shedding does not correspond to the natural frequency of the structure. Lateral deflections and accelerations of the buildings' top floors should be considered from the standpoint of serviceability and occupant comfort. Peak acceleration at the top floors of the building resulting from frequent windstorms should be limited to minimize possible perception of motion by the occupants. In earthquake-resistant designs it is necessary to prevent outright collapse of buildings under severe earthquakes while limiting the nonstructural damage to a minimum during frequent earth tremors. The building should be designed to have a reserve of ductility to sustain gravity loads under large inelastic deformations during severe seismic activity.

## 8.6 CONCEPT OF PREMIUM FOR HEIGHT

If there were no lateral loads such as wind or earthquake, any high-rise building could be designed primarily for gravity loads. Such a design would not impose any premium for height. Since there is no way to circumvent the gravity loads resulting from dead and live loads, the minimum possible material for a building of any number of stories cannot be less than that required for gravity loads alone. Qualitatively, from the structural point of view, this corresponds to the most efficient or optimum system. Ideally, the structure needs to be designed for gravity loads only, whereas the stresses caused by lateral loads will automatically be limited to any overstress permitted for transient loads.

When a low- or mid-rise building is designed for gravity loads, it is very likely that the structure can carry the lateral loads without a premium. This is not so for high-rises because the required resistance to overturning moment combined with the necessity of limiting lateral deflections among other requirements will almost always require additional material over and above that required for gravity load alone. Assuming equal bay sizes, the material quantities required for gravity floor framing in low- and high-rise structures are essentially identical; it makes no difference in the required quantities whether the floor being framed is at the second level of a low-rise building or at the 70th level of a high-rise building. The quantity of material required for floor framing is a function of the column-to-column span and not the building height. However, the material required for the vertical gravity system, such as columns and walls, increases in the ratio  $(n + 1)/2$ , where  $n$  is the number of floors. This is because these elements are designed not just for the loads from the particular floor, but also for the loads from above.

The quantity of material required for resisting lateral loads is even more pronounced and would soon far outstrip all other structural costs if only rigid frame action is used for tall buildings. The graph shown in Figure 8.12 illustrates this concept. Lateral loads begin to show dominance at about 50 stories and become increasingly important with greater height. Above 50 stories, lateral bracing often makes the difference between an economical and an expensive solution. The objective is to arrive at a bracing system that keeps the additional material required for lateral loads to a minimum.



**FIGURE 8.12** Concept of premium for height.

## 8.7 RELATIVE STRUCTURAL COST

The structural cost typically accounts for 20%–30% of the overall building cost. For buildings above 50 stories, the cost of lateral bracing works out, at most, one-third of the structural cost. Therefore, compared to the total building cost, lateral cost is in the range of 7%–10%. It is of interest to note that the cost of exterior cladding alone can be half as much or may even be in excess of total structural cost, depending upon its complexity and composition. The heating, ventilating, and air conditioning system often stands out in the cost picture.

Tall buildings must offer savings in areas other than the structural system for economical purposes. Therefore, mere optimization of structure to carry the intended loads with minimum material may not always result in a reduction in the overall cost. The goal then, is to examine impact of structural system on other features such as increased or decreased floor-to-floor height and leasability of floors.

The technique of optimization is not new for structural engineers. Engineering decisions have always included considerations of optimum structures, usually by minimizing quantity of concrete and reinforcement, and by using repetitive formwork in concrete structures. Each building with its own singular structural system is of course, a response to a unique set of circumstances brought about by the real estate market, zoning laws, client priorities, and architects' tastes and fantasies. It is this singularity that has given impetus to the innovations in the art of structural engineering.

## 8.8 FACTORS FOR REDUCTION IN THE WEIGHT OF STRUCTURAL FRAME

Historically, the unit weight of structural framing members in terms of, say, average weight per square foot of floor area appears to be progressively decreasing over the years. For example, a survey of tall steel buildings built over the past 40 years will verify that today it is possible to build

a 100-story building with perhaps no more than 30 psf (4137 Pa) of steel as compared to the 42 psf (2011 Pa) used for the Empire State Building in the 1930s. The reasons for this gradual decrease are manifold, as given in the following list.

1. Innovative design concepts. For medium high-rise buildings in the range of 30–40 stories, other factors being equal, the lateral load design methodology, although important, will not make a dramatic impact in the weight of structural framing materials. For taller buildings, the ingenuity of lateral design makes a big difference in the material quantities. Therefore, structural engineers are continually seeking better and more efficient methods of resisting the lateral loads. Some of the common approaches are (a) increase the effective width of subsystems to resist the overturning moment; (b) design systems such that the components interact in the most efficient manner; (c) use interior or exterior bracing for the full width of the building; (d) arrange floor framing in such a way that all or most of the gravity loading is directly carried by the primary lateral-load-carrying components; (e) manipulate the dispersion of materials in composite construction consisting of concrete and structural steel in a manner such that both materials are used to their best advantage; (f) minimize the bending induced by lateral loads in the primary components; (g) employ truss action to eliminate bending in columns and spandrels; (h) slope exterior columns if architecturally acceptable to reduce drift; (i) use rounded plan shapes to reduce the magnitude of wind pressure; (j) arrange closely spaced columns at the building exterior to support most or all of the gravity and lateral loads; (k) suspend floors from a central core such that the total gravity load acting on the core will induce enough hold-down forces to counteract the overturning moment; (l) use an interior-braced core that interacts with exterior columns via belt and outrigger trusses; and (m) use exterior steel plate curtain wall to resist lateral forces.

All these methods essentially strive to obtain a structure that behaves like a cantilever of the ground with a minimum of secondary effects. A building system that utilizes columns located ideally at the perimeter of the building and tied together in such a manner that only axial loads are induced in the columns results in one of the most optimal solutions for lateral bracing.

2. Use of high-strength low-alloy steels. Today it is a common practice to use 50 ksi (345 MPa) steel in most composite floor-framing systems, gravity columns, and not too infrequently in lateral-load-resisting elements.
3. Increased use of welding as compared to bolting, which effects a savings in the range of 8%–15% in the weight of steel.
4. Increased use of composite construction. Steel and concrete are being mixed and matched to give the most cost-effective solutions.
5. Account for interactions between structural elements which were considered minor and thus neglected in precomputer era.
6. Gradual increase in member capacities based on research and successful past performance.
7. A reduction in the weight of other construction materials. Heavy interior partition walls are a thing of the past. Drywall partitions weighing considerably less is the norm. Exterior masonry has given way to more slick-looking glass curtain walls. Even when the building exterior is clad in stone, reduction in weight is achieved with lighter backup materials. Changes in stone fabrication methods and finishings have made the use of relatively thin  $7/8$  to  $1^{3/8}$  in. (20–35 mm) stone sections feasible. Heavy masonry or concrete backup has given way to much lighter systems, such as aluminum mullions that incorporate stone in curtain wall systems. Increased use of prefabricated steel backup truss is yet another innovation that has reduced the weight of exterior skin.

In concrete construction, major factors responsible for reducing reinforcement and concrete quantities are

1. New framing techniques, such as skip joist construction in which every other joist is eliminated, have caught on with a consequent reduction in the weight of floor framing.
2. Increased use of mechanical couplers for transferring compression and tensile forces.
3. Use of welded cage for column ties, beam stirrups, etc., resulting in reduction of reinforcement.
4. Use of high-strength concrete; 6,000 psi (41,370 kPa) to 10,000 psi (98,950 kPa) strengths are quite common.
5. Use of lightweight aggregate typically reduces 10–20 psf (479–958 Pa) in the dead load of the structure. The resulting savings in mild steel reinforcement is approximately 10%–15%.
6. Most fire codes do not require as great a thickness of slabs when structural lightweight concrete is used. Typically a thickness of at least 1/2 in. (12.5 mm) of concrete can be taken off from floor slabs without reducing the fire rating.
7. Use of 75 ksi (517 MPa) steel reinforcement.

Because of the factors noted above, a typical glass curtain wall skyscraper weighs 8–9 lb/ft<sup>3</sup> (1.25–1.41 kN/m<sup>3</sup>) as compared to 15 lb/ft<sup>3</sup> (2.35 kN/m<sup>3</sup>) for buildings built in the 1940s.

## 8.9 DEVELOPMENT OF HIGH-RISE ARCHITECTURE

The high-rise architecture of the United States in the twenty and twenty-first centuries shows such a wide diversification as to defy distinct classification. Nevertheless, its development can be traced, perhaps somewhat imprecisely, in five phases.

In the first stage attributed to the early 1940s before the advent of air conditioning and fluorescent light fixtures, the building form was controlled by the need for natural daylight and ventilation and thus required a form somewhat similar to the layout of contemporary apartments and hotels. The building width was limited to ensure that light and air reached all parts of the building. A building width of say, 55–60 ft (16.7–18.3 m) with office spaces on either side of a double-loaded corridor was common. To achieve more leasable space in a given rectangular or square block, plan forms with a central core and radiating wings were conceived. Still, the plan form did not allow for maximization of available site area. The limited width of floor plan usually resulted in a relatively closely spaced column layout of 20–25 ft (6.1–7.6 m). The building usually had heavy masonry cladding that added enormously to the dead load and, in a manner of speaking, helped structural design, by increasing the hold-down force to counteract uplift effects of loads. Also, light-gauge metal deck and sprayed-on fireproofing had not come about. The required fireproofing was achieved by enclosing the structural steel beams and columns with an envelope of cast-in-place concrete, thereby increasing the stiffness enormously, which in turn limited the wind drift. Instead of realizing the benefits of the composite nature of steel and concrete, early designs penalized the design of steel members by requiring the weight of surrounding concrete to be treated as additional dead load.

The second phase is the result of interactions between the desire to create an increasing amount of rentable area in a given space and the advent of air conditioning and fluorescent lighting. This period is also characteristic of the modern movement in architecture stressing the aesthetic value of simplicity in façade treatment by using simple cubic shapes, such as rectangles, squares, circles, and sometimes ovals. The curtain wall was stretched tightly over the skin while the building shot up toward the sky in one regular prismatic shape. In keeping with the International Style, it was not offensive—in fact, it was highly promoted to display the structural muscle. Glass boxes with exposed structural steel or concrete constituted the backbone of the International Style.

The third of high-rise architectural development is a result of interaction between marketing experts and a mild boredom of the architectural community toward the repetitive nature of the



boxes on the cityscapes. The simplest prismatic shape has only four corners, and therefore could offer at best four corner offices. Even those corner offices more than likely displayed corner columns positioned in the most logical location. From the point of view of leasing there was no great advantage in having many corner offices with views on two sides. Now, however, corner offices have become the most sought after lease space almost overnight, and the demand appears to be on the increase. In an overbuilt high-rise market, it is a well-proven fact that corner office providing unobstructed views bring in more rental dollars or facilitate earlier leasing of space than a single-view office. Whether or not the views have improved over the period is debatable; at least in the urban setting it is more than likely that one has nothing to look at but the curtain wall of another high-rise building. Thanks to the marketing experts, irrespective of the quality of view, it appears that corner office are still perceived as the most desirable lease space by corporations and small renters alike. To capture this market, the trend in high-rise floor planning is to create as many corner offices as possible. This is achieved by undulating the exterior by providing nicks, notches, and other contortions at the perimeter of the building. Sometimes to create visual identity and interest, setbacks are provided at intermediate levels. An otherwise simple plan is sliced and diced creating vertical lines to emphasize the verticality of the buildings while simultaneously providing for additional corner offices.

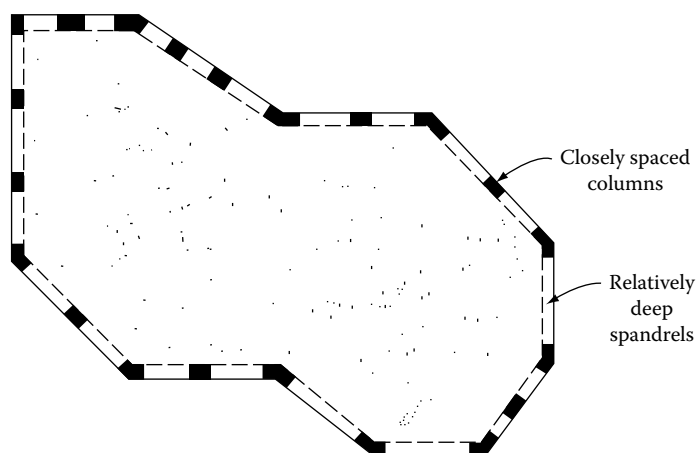
A fourth phase known as postmodern architecture is currently sweeping through the profession, bringing in daringly articulated buildings. These buildings not only have stepbacks, angles, notches, and curves, but the resulting articulations are so severe as to preclude the use of any one type of structural system. This phase of office design, which began around 1970, is considered primarily an aesthetic reaction to the cubism period. This reaction has evolved gradually in three stages. First, the flat roof, which is all that is necessary from the functional point of view of the 1950s and 1960s, started receiving architectural attention to gain identity in the city skyline. Today, many building tops sport either a peaked roof, a pyramid, a dome, or any combination of these. The second stage is characterized by the creation of elaborate entrances to the building in an effort to give it a street-level identity. The third stage is a continuation in the battle for identity. Articulations at the extremities are no longer sufficient to create a building's identity. The whole architectural façade needs to proclaim the identity of the building. To this end, terracing of building plans, cutouts, slicing and dicing, and overhanging features are added to the buildings throughout its height.

The fifth phase can be looked upon as a modification of the current building shapes in the energy conservation context. We are witnessing buildings suitable for natural daytime lighting with courtyards, light wells, and skylights. Energy conservation efforts have brought about an understanding of spaces as a whole, especially in relation to how light influences the space. Instead of depending totally on mechanical heating and cooling and electric light, architects are considering the possible solar controls outside and in as an integral part of both engineering and architectural design. Lighting design is not evaluated from an electrical engineering standpoint only, but from the various light sources outside the building as well.

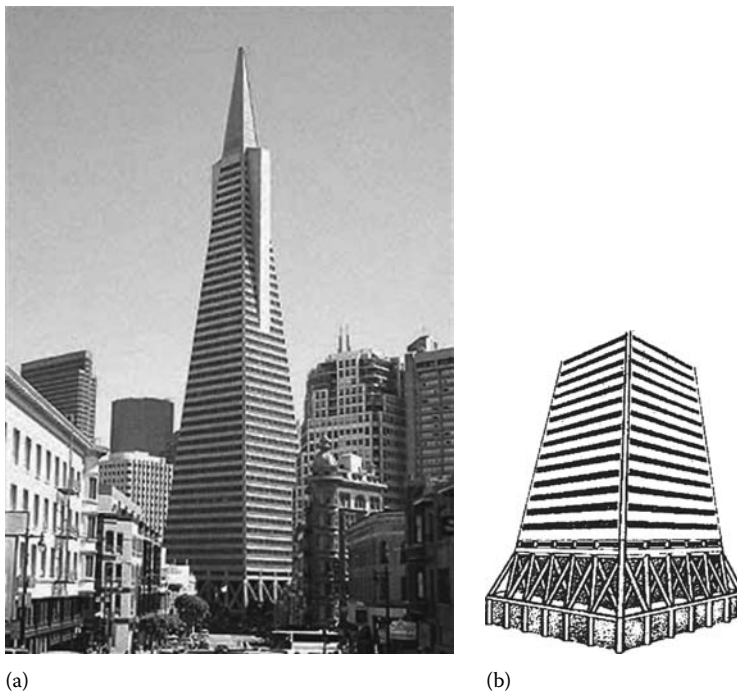
It is of interest to trace the development of structural systems corresponding to the previously mentioned architectural trends. As stated earlier, ancient monuments such as the pyramids required very little attention in terms of lateral load resistance, as did the early 10-story high-rises of the 1870s. The high-rises prior to the advent of air conditioning and fluorescent lights were of limited width and could accommodate interior columns at a relatively close spacing of 20–25 ft. Deep girders were moment-connected across the columns to create a rigid frame for providing lateral stiffness and stability. Often the rigid frame action was supplemented by using cross braces around utility cores. In addition to this bracing, the heavy masonry partitions and exterior cladding used in these buildings added a form of passive support to the stability of the building. Because rigid frame action and bracing across limited width of core are somewhat inefficient for tall buildings, the quantity of material used in these buildings were relatively high; for example, the Empire State Building used 42 psf of structural steel (2011 Pa) in the gross area of the building as compared to the 33 psf (1580 Pa) in the Sears Tower.

The International Style of architecture, which started with the second phase of high-rises, disrobed the building of its heavy partitions and cladding. Also, leasing requirements demanded column-free space between the central core and exterior columns. Even when the building exterior was clad in stone, relatively lightweight backup systems using stones which were only  $7/8$  to  $1\frac{3}{8}$  in. (20–32 mm) thick were commonly employed. Thus the built-in heavy gravity loads which could be counted on for resisting overturning moments in the design of the first phase of high rises were no longer available to perform the holding down function. The combination of long-span moment frames and bracing systems, when placed within the confines of the service core, were therefore no longer economical for modern tall buildings. A natural structural response to the economic requirements was to move the bracing from the interior to the exterior of the building, thereby creating maximum separation between the windward and leeward walls. To make the separation structurally effective, that is, to make the windward and leeward walls work as integral parts of a three-dimensional system, it was necessary to introduce a shear-resisting element between the two faces of the building. This was achieved either by providing diagonal bracing between the exterior columns or by a system of closely spaced columns and deep spandrels along the building periphery. Thus a new concept termed a “tubular system” was introduced into the structural vocabulary (see Figure 8.13). The tube immediately freed up the economical height restrictions of moment frames. Note the simplicity of the system, which was first introduced by the late Dr. Fazlur Khan of the architectural and engineering firm of Skidmore, Owings, and Merrill; it neither required invention of new materials nor new framing or erection techniques. It employed the very basic elements of high-rise structures, namely, beams and columns, and by strategically manipulating their locations, a very economical structural system has been found almost overnight. Also, the system did not require new methods of analysis other than encouraging the engineer to think in three dimensions. The emergence of the tube as the most logical form for high-rise structures is reflected by the innumerable examples of such buildings built in almost every growing metropolis throughout the world. The tube structure was suited admirably to the International Style. Buildings were prismatic with compact plan forms and, therefore, did not penalize the efficiency of the framed tubes.

The radical departure from the pure prismatic shapes occurred over a period of time. First, the building top, which was invariably flat in keeping with the “less is more” norm, began to take on new forms, giving identity to buildings in an otherwise anonymous cityscape. Perhaps the best example of this is the headquarters building of the Transamerica Corporation in San Francisco. Here the architect used sloped-column approach to create a 48-story American version of the pyramid (see Figure 8.14).



**FIGURE 8.13** Tubular system: Closely spaced exterior columns interconnected with deep spandrels.

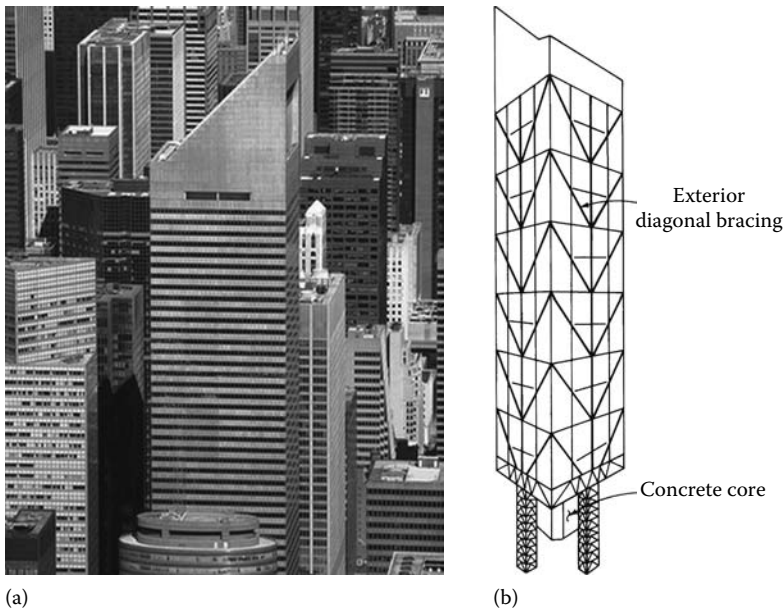


**FIGURE 8.14** (a) Transamerica Tower, San Francisco, California. (b) Transamerica Tower, schematic.

The third phase of high-rise architectural development with its many corner offices did not entirely preclude the use of a tube system because the basic prismatic shape of the building was still being preserved for almost the entire height of the building. The seemingly restrictive form of the tube, which was confined to square and rectangular shapes, very quickly found application in nonprismatic shapes. The tube was so benign to engineers that they could even rupture it without paying a significant penalty in structure, as long as the discontinuity was filled in with another structural element.

Then came the period where elaborate entrances and tops to the buildings were created to identify the building at the base and on the skyline. None of these changes, namely, seductive tops, the undulations of the exterior or the appendages to the building entrance, precluded the development of the structural logic so brilliantly conceived by Fazlur Khan. The tube system, either with its rhythmic columns connected by a pattern of deep exterior spandrels or as an exterior braced tube with its bold diagonals on the building face, could still be used for buildings of this period. Whether the diagonals were expressed on the building face as in the John Hancock Tower in Chicago, or were hidden behind a smooth glass wall as in the Citicorp Building in Manhattan (Figure 8.15), was of course, a matter of how strongly the architect felt about preserving the International Style; the structural logic was still the same.

The current state of high-rise architecture is characterized by the use of articulated sculptured forms. Owners and developers are demanding, and the public has come to expect these daring shapes. Buildings are designed not to express the pure form of the structural elements but to express the technological progress by creating façades that appear to be structural feats. The goal is the expression of the architectural envelope, not the structure. Today's bracing design required to limit the sway or wind drift of the building calls for ingenuity not in terms of visualizing a single pure structural system but in combining several systems to make the dramatic design concepts of the architect an economic reality. The work of the structural engineer comes in refinements to proven structural schemes with particular attention to details.



**FIGURE 8.15** City Corp Building, New York City.

Logical structural solutions which could be used in the earlier versions are no longer sufficient to take into account the structural discontinuities. In fact, there no longer is a single system applicable for the entire height. In keeping up with the architectural slicing and dicing, engineers have to follow suit. In a manner of speaking, they cut a brace here, introduce a partial tube there, and so on. In other words, dissimilar structural systems are ushered around the building façade without undue regard to the one next to, above, or below it. The challenge is in interconnecting different systems to achieve overall continuity. For example, the building configuration may permit the use of perimeter bracing for the bottom 10 floors, the next 10 floors could accommodate a framed-tube solution, and so on.

In spite of the cacophony of external forms currently accepted as architectural styles, large, many-sided prismatic shapes with hints of flamboyance are still dominating the architectural vocabulary because they have the backing of large corporations seeking prestigious symbols. As stated earlier, the tube is still the workhorse of the structural systems, as demonstrated by its use in a large number of buildings. With these practical displays of the tube characteristics, is it not conceivable that this is the most logical solution for all high-rises? Should not the proven economy of this system put an end forever to the search by engineers for a suitable system on each project? The questions are perhaps deceptively simple. To be sure, the tube system is very economical, but even with its adaptability, it requires a certain amount of structural discipline that restricts the use of free-form architecture. The current flamboyance in architecture has necessitated that several schemes be studied and comparatively priced before the adoption of a final scheme. There are several reasons for this.

First, every building is a unique response to a particular set of conflicting demands. For example, architecturally it may be desired to have a sculptured profile without structural bracing at the perimeter. And because of the desired size of vision panels, depth of spandrels may have to be limited. Interior beams and girders working efficiently for gravity loads may require expensive penetrations for passages or air conditioning ducts or may require an increase in the floor-to-floor height. Suboptimizing of the structure without due regard to the opposing demands of other disciplines may eventually result in an increase in the total cost of building. Therefore, less efficient structural systems often need to be studied in the interest of bringing in the total project cost within the allotted budget.

### 8.9.1 ARCHITECT–ENGINEER COLLABORATION

In structural engineering practice, one of the foremost requirement is for the architect and the engineer to participate in the conceptional stages of the project in order to come up with an economical building. Although there is a general awareness in the architectural community about the concept of premium for height, there is insufficient understanding of the structural engineering discipline that is so integral a part of architecture, mainly because the necessary engineering information is not accessible in a concise form. However, it is necessary for the architect to understand structural concepts because structural cost accounts for 20%–30% of a building cost and, therefore, has profound influence on design, aesthetics, and manipulation of resources to deliver a project that the owner and architect have in mind. Even in today's postmodern architectural environment with its hint of antitechnology there is a need for the architects to assume the traditional role as master builders, not in the sense that they learn how to design and analyze structural elements, but they should develop an appreciation of general flow of forces in the building frame. Although it is impossible and indeed unnecessary to know all aspects of structural analysis, architects should be able to grasp the idea of unit quantity of material required for a particular system such as “pounds per square foot” of the structure, just as they would know “watts per square foot” and “Btus per square foot” as related to electrical energy efficiency of the building.

It is perhaps of interest to explore the idea of different structural systems and their impact on the economy and architecture of high-rise structure. To this end, a critical appraisal of structural systems of a 62-story building is presented in this section. In particular, the study will focus on certain aspects of exterior tube columns such as their size, location, number, and effect on the interior layout of the offices. This study is partly based on the work done by the author as a principle with the firm of Walter P. Moore and Associates. The building to be discussed was scheduled for construction in Houston during the year 1982–1983. The study was undertaken because a review of a typical floor plan of the project from marketing, leasing, and space planning considerations, raised concerns about the size and location of columns. The leasing market was very soft, requiring all prudent concerns to be addressed before committing the finances to the project.

The main purpose of this section is to give an overview of the many possible structural solutions that are normally considered in the development of a high-rise project. Details of structural analyses are not given and only passing remarks are made on the behavior of each structural system. Design for seismic loads was not a consideration.

### 8.9.2 SKY SCRAPER PLURALISM

A building structure particularly that of a tall building can be said to have at least two aims of equal importance: the technical and the aesthetic. The first aim, the technical function, is to stand upright, secure from collapse or excessive deformation. The structure accomplishes this by withstanding loads and transferring them, through the building components, to the ground. The second aim, the aesthetic function, mainly in the architect's domain, is to act as a potent and meaningful visual vehicle that can become a convincing and recognizable medium of architectural expression. Both the technical and the aesthetic functions of a building structure must be satisfied simultaneously if the structure is to be more than just an assemblage of answers to various technical problems.

There is little disagreement among engineers with regard to the theory of statics for it is mathematically and scientifically founded and logical in its composition. The word “static” comes from the Greek word *statikos*, meaning “to make something stand still.” The idea of statics is based on the principle that buildings and building elements “shall stand still.” This is the foundation for our understanding of structures. If beams, columns, and arches cannot be held in place when loaded, they are of little value.

Structures are subject to a variety of conditions that they must endure: winds and snow loads, the weight of components, inhabitants and equipment, and in many parts of the world to seismic

ground motions. To be sure that the building can withstand such loads without severe deformation or collapse, theoretical and practical analysis must be performed beforehand. Statics is part of the theory applied for this purpose.

Structural theory is universal while architecture varies according to time and place. The forces that are transferred from the beam to the column are the same, whether at the limestone Doric Aphaian temple at Aegina outside Pireus from the fifth century BC or at Sears Tower in Chicago from 1974.

### 8.9.3 STRUCTURAL SIZE

In his discussion of different types of bridges, Palladio wrote that all bridges could have an unlimited span, as long as their internal proportions remained constant. Palladio was actually wrong. Over a certain span, his bridges, and for that matter all bridges, would collapse.

If we imagine a freely supported beam with a cross section of 3 ft-3 in.  $\times$  3 ft-3 in. (1 m  $\times$  1 m) and a length of 33 ft (10 m), then double the dimensions so that the cross section becomes 6 ft-6 in.  $\times$  6 ft-6 in. (2 m  $\times$  2 m) and the length 66 ft (20 m), we will see that the actual weight increases by the factor of 8. The strength of the beam is proportional to the increase in the cross section and thus increases four times, but the weight is proportional to the volume and is multiplied eight times. If we continue to proportionally increase the dimensions of the beam, it will eventually fail owing to its own weight.

The first person to discover that maximum span widths do exist was Galileo Galilei. In his work written in 1638, Galileo discusses a number of examples that show that the size of an object or a building has an important influence on the economic use of construction materials. Certain types of constructions are only feasible within a certain range of size.

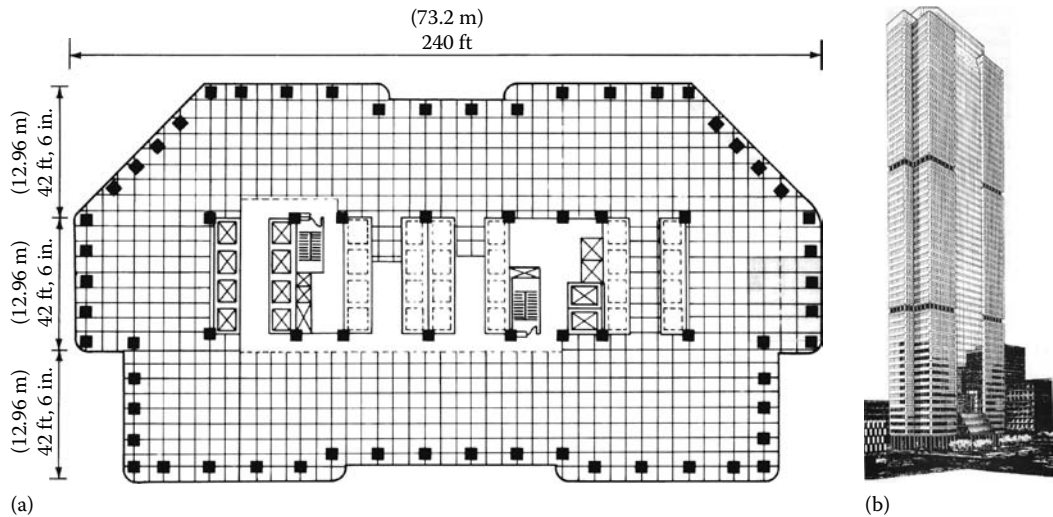
In the animal world, we can see exactly how the phenomenon has manifested itself. Large animals such as the elephant and the buffalo have massive bone structures and move slowly in relation to their weight, while an antelope with its spindly bone structure can move quickly. Dinosaurs with their colossal bones are long since extinct, perhaps because they became too heavy, too slow, and lost the battle for survival against smaller and quicker species.

To summarize, one can conclude that the size of every structural system has its upper and lower limits. The challenge then for architects and engineers lies in finding the structural system that is best suited to the overall scope of the project.

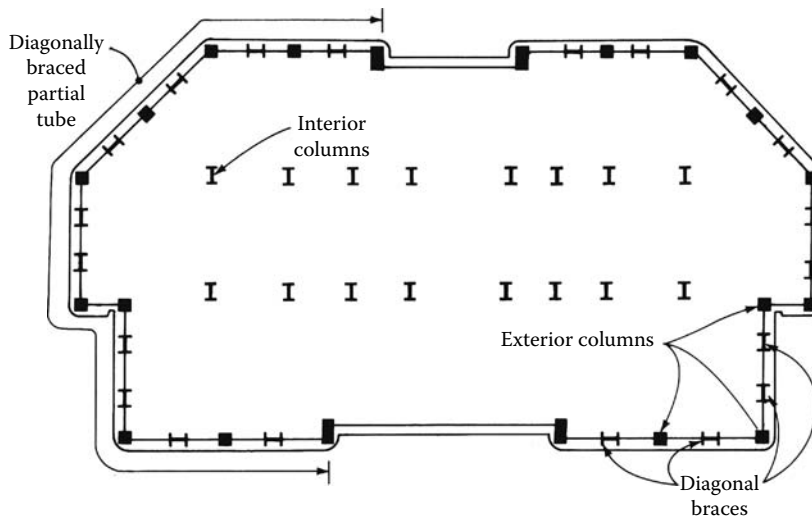
## 8.10 STRUCTURAL SCHEME OPTIONS

A schematic elevation and typical floor plan are shown in Figure 8.16a and b. The building has 1.7 million sq ft (157,935 m<sup>2</sup>) of office space, with 62 floors extending above a landscaped plaza and a two-level basement below an entire city block. The building is relatively slender, with a height-to-width ratio of approximately 6:1. The floor plan is compact, with a length-to-width ratio of approximately 2:1. Relatively stiff elements are used parallel to the short face to resist wind on the perpendicular faces. This is achieved by selecting a framed tube with columns at approximately 10 ft (3.0 m) centers along the short faces and 15 ft (4.58 m) along the long faces. A deep spandrel connecting the perimeter columns completes the framed tube systems.

The building may be conceived in steel, concrete, or a combination of the two, known as a composite system, utilizing the advantages of both concrete and structural steel: concrete for stiffness and steel for speed of construction. One of the methods of composite construction popular in certain parts of North America uses small, wide flange shapes as exterior erection columns with a planned initial growth of 10–12 floors, which are subsequently enclosed in reinforced concrete. The exterior spandrels consist of rolled wide flange beam shapes. The composite tube system was chosen for this building based on comparative studies preformed on similar projects that were under construction at the time the project was being designed.



**FIGURE 8.16** Structural system study: 62-story building. (a) Plan and (b) elevation.

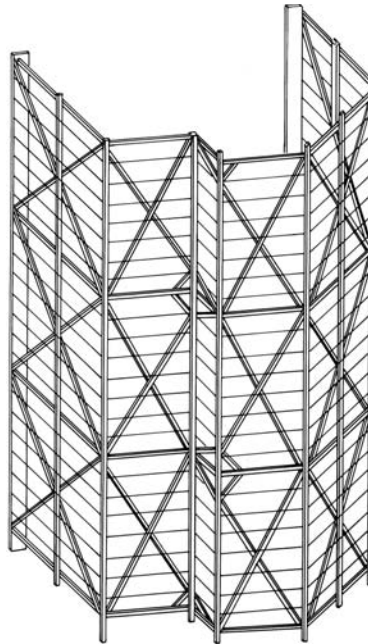


**FIGURE 8.17** Exterior braced tube: plan.

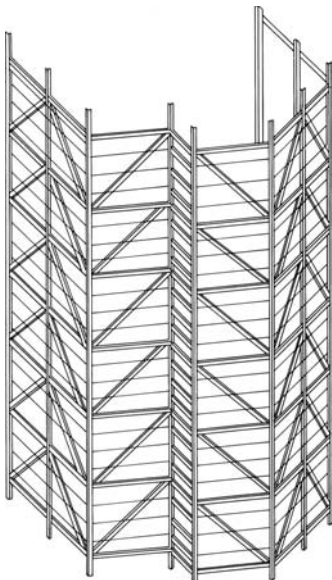
The structural schemes presented in this section may be broadly classified into three categories. The first consists of cross-bracing schemes, the second framed tubes with deep spandrels and closely spaced columns, and the third an assortment of schemes ranging from those utilizing shear wall frame interaction to a 14-column scheme interconnected with Vierendeel trusses spanning the full width of the building. A brief description of each scheme is given as follows:

### 1. Cross-bracing systems

- a. Exterior-braced tube. An all-steel scheme which consists of a series of eight-story-high exterior X braces is utilized to wrap around the two short faces and a significant portion of the flange faces, as shown in Figures 8.17 and 8.18. It was not necessary to wrap the entire perimeter with braces; the center portion of the two broad faces could



**FIGURE 8.18** Isometric of exterior braced tube.



**FIGURE 8.19** Isometric view of four-story high braced tube.

be kept free of vision-impairing columns and braces. The column-free areas would provide for views, thus enhancing the leasability of the building. Note the bracing follows the exterior contour of the building including its in-and-out modulations.

As an alternative to X-bracing, a four-story-high brace was also appraised, as shown in Figure 8.19. To achieve frame action, moment connections are used on the undulating faces. As in the previous scheme, no columns or braces were anticipated behind the all-glass face.

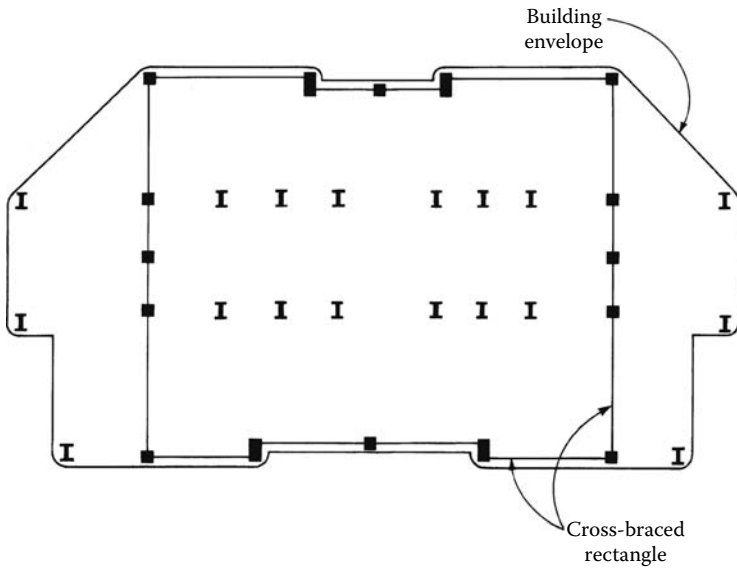
- b. Interior-braced tube. In this scheme, for purposes of structural bracing, the plan may be considered as though it is a rectangle. Note that the bracings penetrate the interior space, creating somewhat of a restriction on the leasability, as shown in Figures 8.20 and 8.21. As a trade-off, the two short faces are unobstructed by braces or closely spaced columns.
- c. Braced and framed tube combination. The proposed scheme is evident from Figures 8.22 and 8.23. A framed tube working with cross bracing at the extremities provides the required structural action.

## 2. Framed tube systems

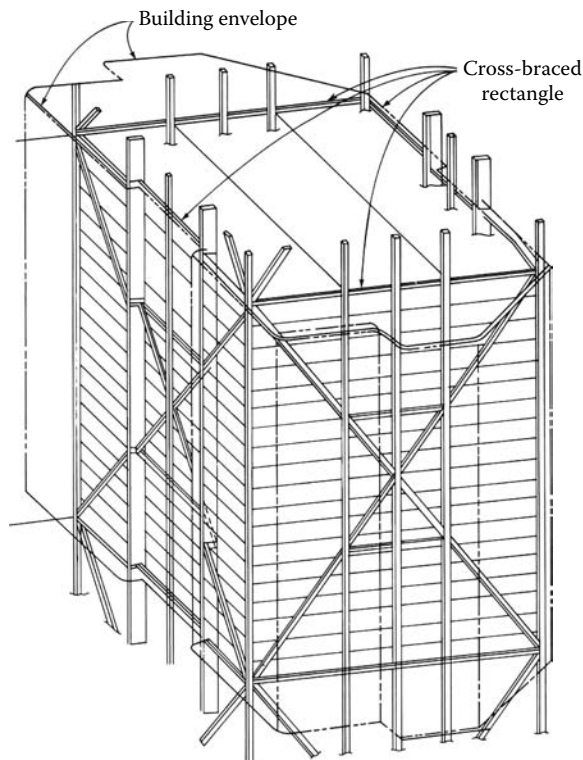
- a. In this scheme, the framed tube columns occur at 10 and 15 ft (3 and 4.58 m) spacings. The exterior columns are spaced at approximately 10 ft (3 m) centers on the short faces and are opened up to 15 ft (4.58 m) centers on the long faces (see Figure 8.24). In this scheme identified as scheme 4,  $40 \times 38$  in. ( $1016 \times 965$  mm) composite columns are used on the exterior. Scheme 5 is identical to scheme 4 with the exception that smaller composite columns  $40 \times 27$  in. ( $1016 \times 686$  mm) are used in an effort to provide more



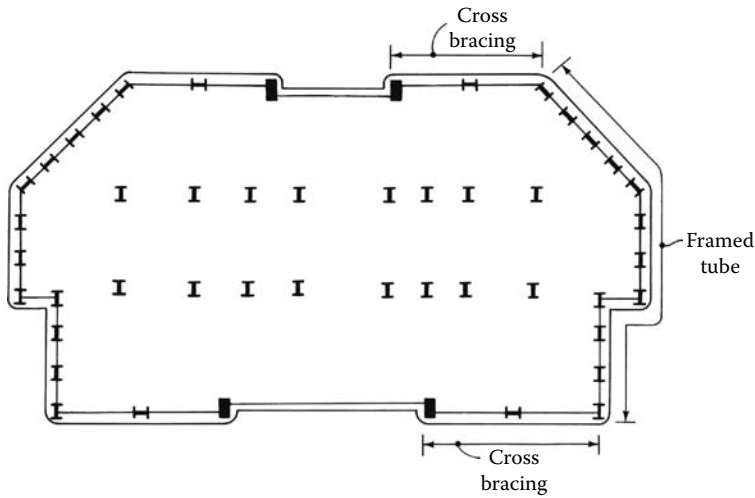
flexibility in the layout of office space adjacent to windows. An all-steel scheme which would give the smallest size of columns  $36 \times 20$  in. ( $914 \times 508$  mm) is used in scheme 6. Note the actual size of finished steel column with the required fireproofing and finishing tends to approach the size of composite columns.



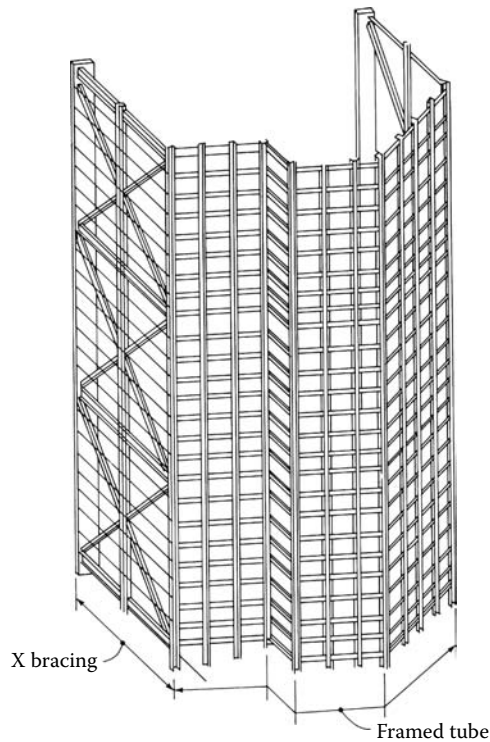
**FIGURE 8.20** Interior cross bracing system: plan.



**FIGURE 8.21** Isometric of interior cross bracing system.

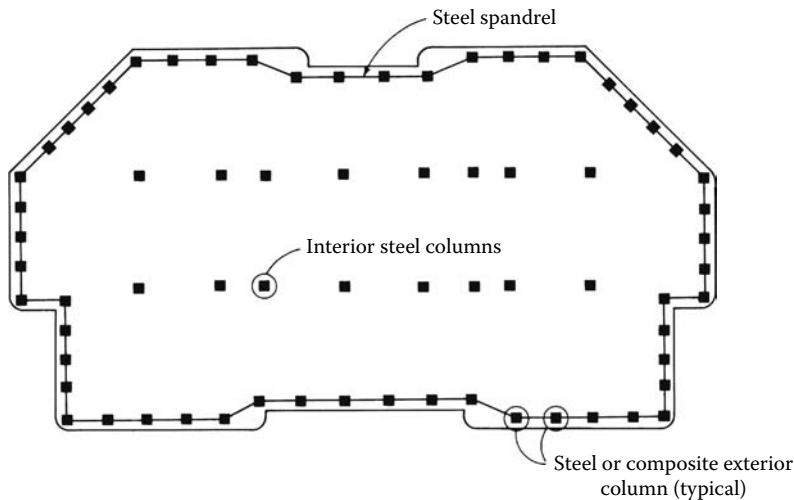


**FIGURE 8.22** Interacting framed tube and braced frame.

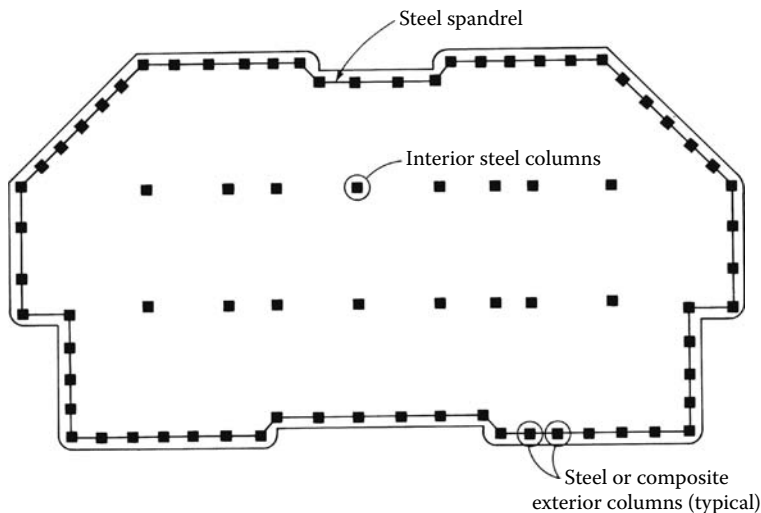


**FIGURE 8.23** Isometric of framed tube and brace frame.

- b. In this scheme, the framed tube columns are at a 10 ft (3 m) spacing around the perimeter (see Figure 8.25). Although many buildings have been built using a 10 ft (3 m) column spacing, and in some cases even smaller, such as at 3 ft 4 in. spacing used in the now nonexistent World Trade Center Towers, New York, of late close spacing of columns has fallen out of favor.

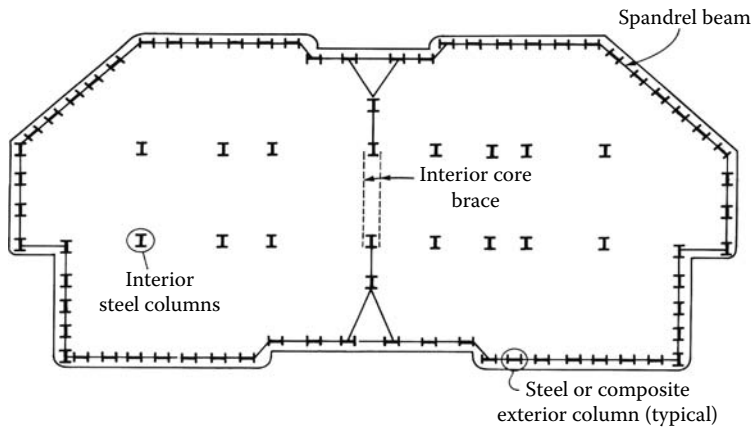


**FIGURE 8.24** Framed tube with 10 and 15 ft column spacing.



**FIGURE 8.25** Framed tube with 10 ft column spacing.

- c. Twin tubes with 10 ft (3 m) column spacing. The efficiency of a framed tube is to a great extent dependent on the so-called shear lag phenomenon. When the plan shape of the building is oblong, it so happens that for lateral loads on the long faces, the flange columns do not fully participate in resisting the lateral loads. A technique to minimize this problem is to use a minimum number of interior columns in the lease space (two in this building), creating a rigid frame across the middle of the floor plan. The oblong tube is, therefore, made structurally more efficient by making it work as though it is a bundled tube, as shown in Figure 8.26. As noted earlier, to achieve structural efficiency, interior layout has to be compromised because of the presence of columns. Scheme 9 was engineered with an all-steel structure, while scheme 10 used composite columns. The typical exterior column sizes were  $33 \times 20$  in. ( $838 \times 508$  mm) and  $45 \times 27$  in. ( $1143 \times 686$  mm), respectively.

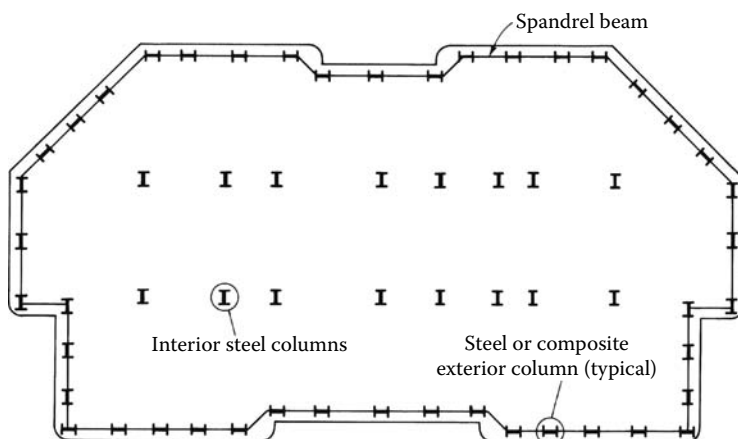


**FIGURE 8.26** Twin-tube system with 10 ft column spacing.

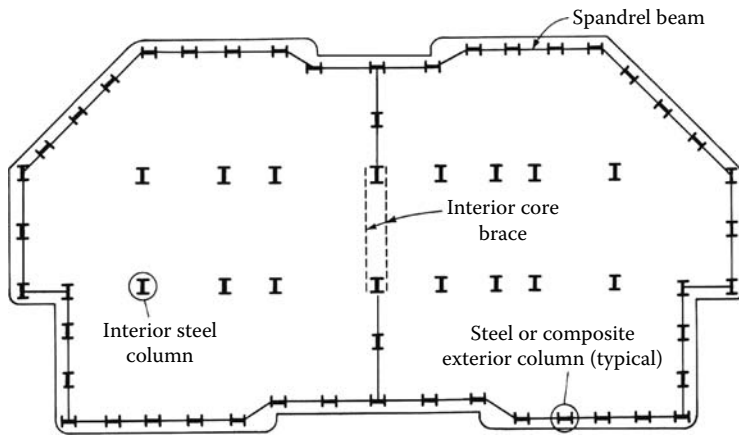
- d. Framed tube with 15 ft (4.58 m) column spacing. The columns are spaced approximately 15 ft (4.50 m) on the center around the building perimeter, as shown in Figure 8.27. The size of typical exterior columns for steel and composite schemes (schemes 11 and 12) were  $40 \times 22$  in. ( $1016 \times 559$  mm) and  $48 \times 36$  in. ( $1219 \times 914$  mm), respectively.
- e. Twin tubes with 15 ft (4.58 m) column spacing. The structural concept is similar to schemes 9 and 10 with the exception that columns are spaced on approximately 15 ft (4.58 m) centers around the perimeter, as shown in Figure 8.28. The size of typical exterior column for steel and composite schemes (schemes 13 and 14) were  $36 \times 20$  in. ( $914 \times 508$  mm) and  $40 \times 36$  in. ( $1016 \times 914$  mm), respectively.
- f. Framed tube with 20 ft (6.1 m) column spacing. The structural analysis for this column spacing shown in Figure 8.29 confirmed that the column spacing was too large to make this scheme economically feasible. Built-up steel spandrels of the order of 40 in. (1016 mm) in depth were required at the perimeter to limit sway.

The exterior column sizes for steel and composite schemes (schemes 13 and 14) were  $45 \times 24$  in. ( $1143 \times 610$  mm) and  $60 \times 36$  in. ( $1524 \times 914$  mm), respectively.

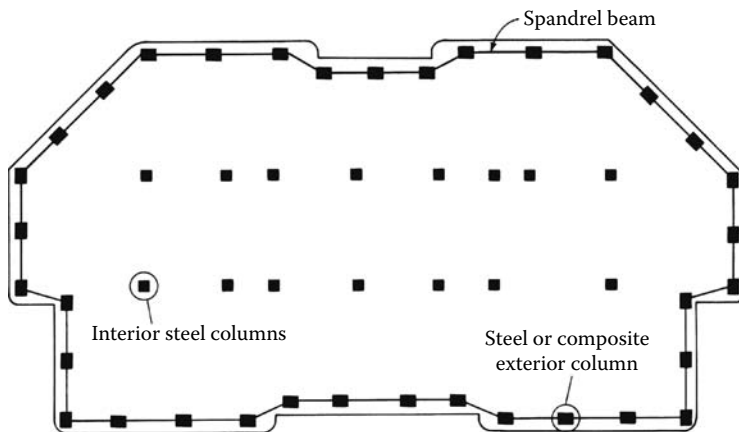
- g. Twin tubes with 20 ft (6.1 m) column spacing. The column layout is shown in Figure 8.30. The shear lag phenomenon predominant in the single tube solution is improved



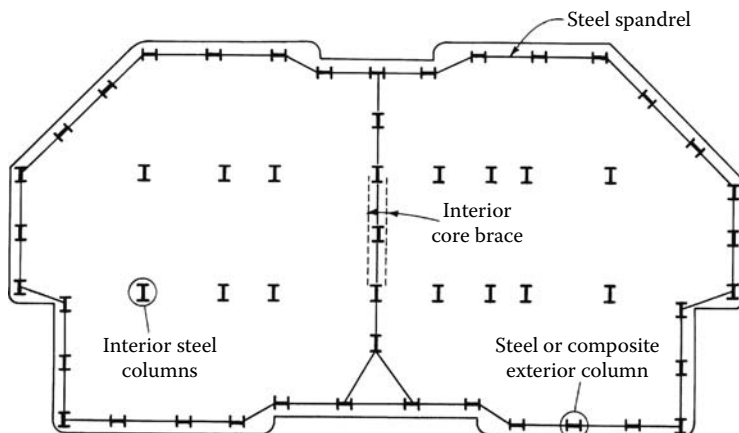
**FIGURE 8.27** Framed tube with 15 ft column spacing.



**FIGURE 8.28** Twin-tube system with 15 ft column spacing.



**FIGURE 8.29** Framed tube with 20 ft column spacing.



**FIGURE 8.30** Twin-tube system with 20 ft column spacing.

considerably because of bundling of tubes. For the steel scheme (scheme 17), the column size is  $42 \times 24$  in. ( $1067 \times 610$  mm), while for the composite scheme (scheme 18) the column size worked out to be  $57 \times 32$  in. ( $1448 \times 813$  mm).

### 3. Nontubular schemes

- a. Shear wall frame interaction. Closely spaced columns and deep spandrels on the short faces constitute efficient moment frames, as shown in Figure 8.31. These acting together with interior shear walls provide for the lateral load resistance. Scheme 19, which uses steel columns for moment frames, requires  $36 \times 20$  in. ( $914 \times 508$  mm) columns on the short faces while for scheme 20 the corresponding composite column size is  $40 \times 27$  in. ( $1016 \times 686$  mm). Both schemes require  $20 \times 17$  in. ( $508 \times 432$  mm) columns on long faces.
- b. Moment frames and braced cores. A steel scheme that uses core bracing and moment-connected frames at each column line along the width of the building was analyzed as a possible solution, although it was intuitively clear that this would not work. However, the efficiency was improved in this scheme by providing interior columns as shear links at every other floor, as shown in Figure 8.32. Although the interior columns are

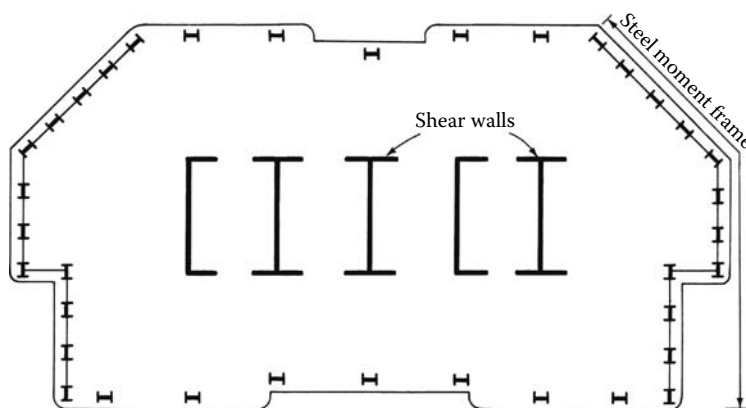


FIGURE 8.31 Shear wall frame interacting system.

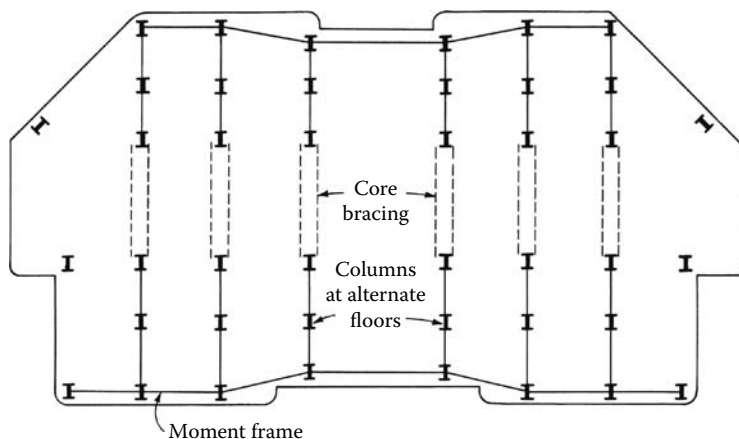


FIGURE 8.32 Moment frame and braced core system.

not continuous, they provide considerable resistance to the bending deformation of the girders by effectively reducing their span by half. The presence of interior columns at every other floor was objectionable from leasing considerations but was only included in the study for comparative purposes.

- c. Outrigger and belt walls. The idea of engaging belt and outrigger walls to the perimeter columns in order to improve the lateral load resistance of tall buildings has been known for some time. In fact this system is most popular in the design of super-tall and ultra-tall buildings. The stiffening effect of outrigger and belt walls is akin to a moment-resistant spring which tends to induce a reversal of curvature in the cantilever bending of the core walls. Using certain simplified assumptions, it is shown in Chapter 3, that the outrigger walls can be located at levels other than their optimum locations without unduly decreasing their efficiency.

The desired architectural elevation in the initial stages of the project appeared to allow for placing of outrigger and belt trusses at levels 20 and 40, along four column lines (see Figure 8.33). Although structural efficiency is increased by the addition of these trusses, note that interior space planning is compromised at two levels. In buildings which cannot make use of these floors as mechanical floors, usually there is a strong objection to their presence.

On this project, levels 20 and 40 were dedicated as premium lease spaces with an extra high floor-to-floor height; clearly the outrigger and belt trusses were architecturally unacceptable but were included in the structural study for comparative purposes.

- d. Jumbo column scheme. This scheme, shown in Figure 8.34, was investigated at a conceptual level only. It is based on the idea that an efficient structural solution results by transferring all gravity loads to wind-resisting columns. The columns, as in framed and braced tubes, work most efficiently when placed at maximum a distance apart and connected by a shear-resisting system so that they work as compression and tension members of a giant truss with a depth equal to the entire building width. For this building, Vierendeel and/or interior diagonal trusses spanning the full width of the building were envisaged as the shear-resisting elements. A majority of the gravity loads are channeled to the 14 jumbo columns. Four relatively small columns are introduced at the building perimeter to simplify gravity framing and to eliminate long cantilevers.

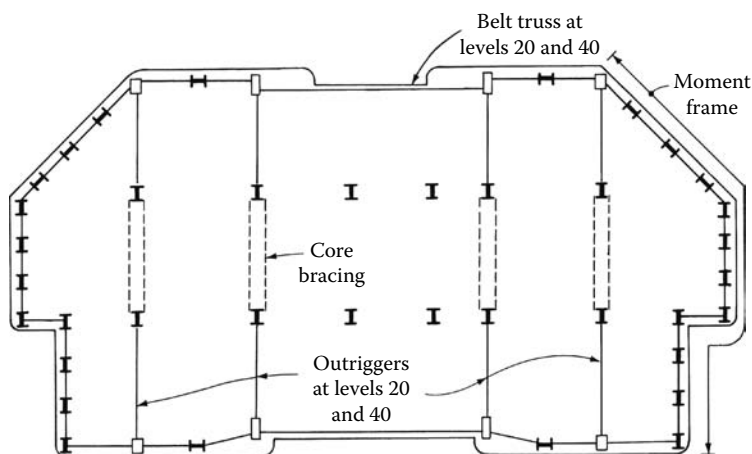
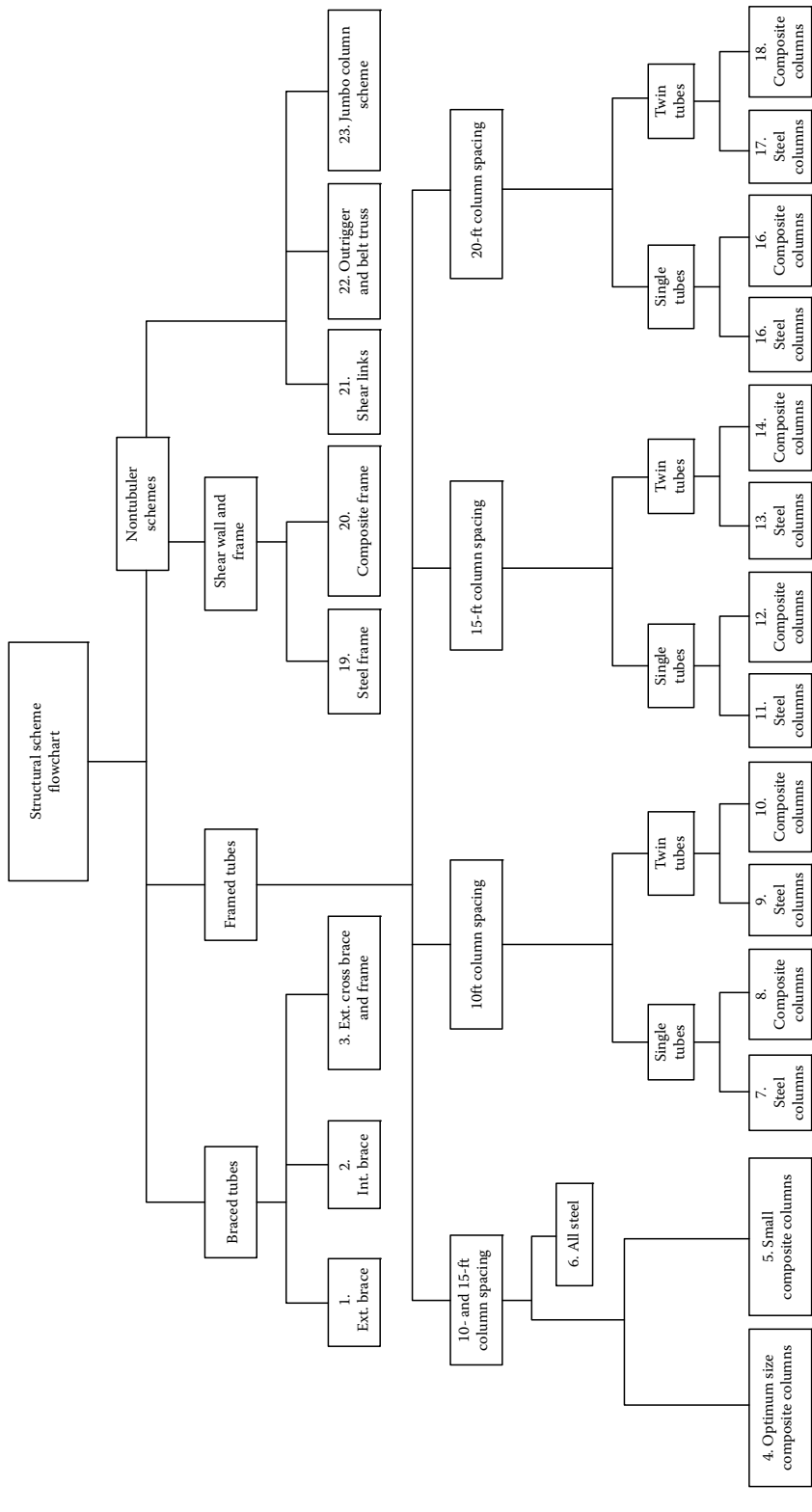


FIGURE 8.33 Outrigger and belt truss system: schematic plan.



(a)

FIGURE 8.34 Jumbo column scheme.

(continued)



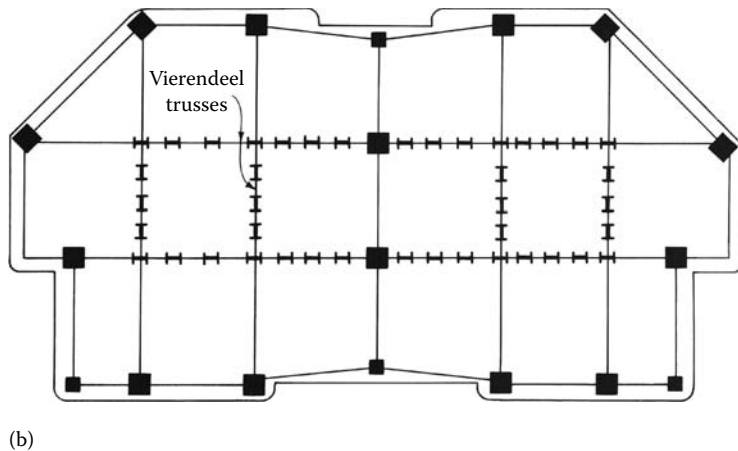


FIGURE 8.34 (continued)

### 8.10.1 SPACE EFFICIENCY OF HIGH-RISE BUILDING COLUMNS

A high-rise building essentially consists of vertical elements such as columns, walls and braces, and horizontal surfaces for floor structure. Depth of floors although quite important from the overall economic considerations, does not pose undue limitations on the architectural space planning. After the initial discussion of the project during which ceiling and floor-to-floor heights, required cavity for air-conditioning ducts, lights, and sprinkler system were discussed, the beam and girder depths hardly evoke the emotional discussion that pursues the determination of location and size of vertical elements. In a manner of speaking, the size of floor beams and girders become almost inconsequential because it literally hides in the ceiling cavity and escapes the scrutiny of any number of consultants, architects, interior space planners, marketing experts, lease space consultants, and, of course, the developer who is looking for maximization of rental space. While it is possible that seemingly alike columns of two buildings may have different sizes, it appears from an overall perspective, in comparison to floor area, the area taken up by vertical structural elements does not differ significantly from one scheme to another and for that matter, from one high-rise to another. Irrespective of its location, material used, and the system employed, the finished size of vertical elements appears to vary within a very narrow band, say to within 1% of the gross ground floor area. Would it not be of interest to explore this rather interesting phenomenon historically and as it relates to modern high-rise buildings?

The size and density of structural elements in a modern tall building are strikingly less than in the buildings of former centuries. Real estate market considerations and aesthetic principles have motivated us to continuously push this trend further. Let us examine this tendency as it applies to contemporary high-rise buildings. First we define a term, “structural plan density index,” as the total area of vertical structural elements divided by the gross floor area of the footprint of the building at ground level. It is of interest to observe that historically, this ratio has been decreasing. Monumental structures such as the pyramids of Egypt and more recently the Washington Monument did not require usable spaces within and, therefore, the structural plan density index is close to 100 for these structures. This ratio is reduced to 50 for the Taj Mahal in India and 25 for St. Peter’s in Rome. The 17-story, 210 ft (64 m) Monadnock Building constructed in Chicago in 1891 sports 7 ft (2.13 m) thick masonry walls at ground floor, taking up as much as 15% of the floor area at ground level. Contemporary high-rises, because of their lightweight construction, improved high-strength materials, and innovative structural techniques require a rather modest 2%–4% of the gross area of ground floor; the higher percentage is most often found in buildings using shear walls for resisting lateral loads. The Sears Tower in Chicago supported by 112 steel built-up columns varying in size from  $39 \times 39$  in. to  $39 \times 24$  in. ( $990 \times 990$  mm to  $990 \times 610$  mm) at ground level takes up no more than 2% of the ground floor area.

With the above comparisons as a guide, it is of interest to study the plan density index for the structural schemes of the 64-story building examined in detail earlier. The comparison is shown in Table 8.1. It is assumed in this study that structural steel columns are articulated to rectangular shapes with an allowance of 2 1/2 in. (64 mm) for fireproofing and drywall construction at each face.

### 8.10.2 STRUCTURAL COST AND PLAN DENSITY COMPARISON

All in all, including slight variations of certain schemes, a total of 23 alternative schemes were evaluated. See Figure 8.34a. Structural costs were calculated on the basis of unit prices for the in-place structural steel and concrete. It was assumed that additional construction time required for one scheme versus another had negligible effect on cost comparisons. During the early design stages, cross-bracing schemes were comparatively priced on an earlier architectural version of the tower but were ruled out by the owners in preference to a tubular scheme. Therefore, these schemes were not priced in the final comparison. Table 8.1 shows a summary of the structural cost comparison in which the relative cost of the base scheme is considered as 1.0. The comparison is based on unit prices obtained in the early part of 1983 in the Houston construction market, which was soft. It is seen from the table that the framed tube option dominates the economic picture, with a relative cost index varying from a low of 0.97 to a high of 1.30 depending upon the exterior column spacing and the material used for the column. The study clearly demonstrates that the Houston version of composite construction, which utilizes exterior composite columns and steel spandrel beams, is more economical than an all-steel scheme, irrespective of the column spacing. The twin-tube scheme with the 10 ft (3 m) spacing worked out to be the most economical.

**TABLE 8.1**  
**Structural Cost and Column Density Comparison**

Scheme No.	Column Spacing, ft	Exterior Column Type	Relative Structural Cost	Plan Density Index
<b>Framed Single Tubes</b>				
4	10 and 15	Composite	1.00	2.5
5	10 and 15	Composite	1.06	1.95
6	10 and 15	Structural steel	1.10	1.87
7	10	Composite	0.97	2.13
8	10	Structural steel	1.09	2.57
11	15	Structural steel	1.18	1.83
12	15	Composite	1.04	2.39
15	20	Structural steel	1.30	1.76
16	20	Composite	1.09	2.38
<b>Twin Tubes</b>				
9	10	Structural steel	1.01	2.07
10	10	Composite	0.96	2.50
13	15	Structural steel	1.12	1.68
14	15	Composite	1.01	2.14
17	20	Structural steel	1.26	1.73
18	20	Composite	1.07	2.15
<b>Nontubular Schemes</b>				
19	Shear walls and steel frame		1.15	2.66
20	Shear walls and composite frame		1.10	2.66
21	Shear links		1.32	1.28
22	Outrigger and belt trusses		1.20	1.36
23	14 jumbo columns		1.24	2.15

The scheme which employed a combination of 10 and 15 ft (3 and 4.58 m) columns spacing was well in line with the most economical scheme. At the other end of the comparative scale, schemes that depart from the compact tube concept add a distinct premium to the structural cost. It is likely that further refinements of these schemes would have reduced the premium, but not to a level where they would compete with the base scheme. The study demonstrates that the base scheme chosen for this project is just as economical as the most economical scheme. Minor revisions such as reduction in size and relocation of certain columns are feasible to improve the leasability without paying undue penalty in the structural cost.

The plan density index, which is a reflection of the size of vertical elements is seen in this study to vary over a slight range from a low of 1.28 to a maximum of 2.66. Maximum economy is achieved by maintaining this index around 2.5. Whether or not it is justified to incur an additional cost of about 30% of the structural cost to reduce this index to around 1.8 is a matter to be decided for each project by the building owners and/or developers. However, from the study it appears that the premium for reducing the size of vertical elements is a way out of proportion to the planning flexibility gained by use of smaller columns.

## 8.11 SUMMARY OF BUILDING TECHNOLOGY

Ancient tall buildings such as the Egyptian pyramids and Mayan temples were primarily solid structures serving as monuments rather than as space enclosures. Contemporary tall buildings by contrast are conceived to serve as space enclosures, although the sheer magnitude and audacity in scale of some tall buildings may give them the dubious title of monuments. Refinement from solid structures to space enclosures in itself does not change the basic issues of providing overall structural stability. The issues are the same, but the method of achieving the required structural action has changed considerably.

In the early monumental buildings it was unnecessary to consider the spatial interaction between subsystems because there was no subsystem to speak of. Massiveness of the structure provided for the stability of the buildings without requiring much ingenuity on the part of the structural engineer. The size and density of structural elements in a modern tall building are strikingly less than in the buildings of former centuries. Structural technology has allowed and real estate market and aesthetic principals have motivated us continuously to push this trend to further limits.

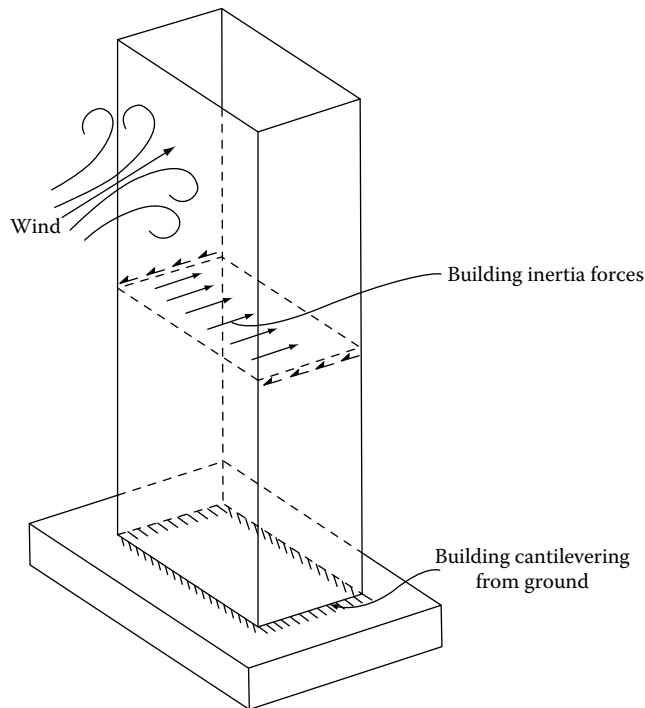
The high-rise building technology can be thought of as a progressive reduction of material quantity used within the space enclosed by the building. Physically, it can be pictured as progressive hollowing of the solidified interior of the building. For a tall building to be successful, it has to satisfy concurrently the requirements of site, building program, and above all make economic sense. From structural design considerations, a building can be considered tall when the effect of lateral loads are overwhelmingly reflected in its design. Lateral deflections of tall buildings due to wind and earthquake loads should be limited to prevent damage to both structural and nonstructural elements. The accelerations at the top floors during frequent windstorms should be kept within acceptable limits to minimize discomfort to the building occupants.

The trend today in high-rise architecture is to have free forms that fulfill the dual function of creating an exciting exterior and at the same time provides interior spaces that are highly desirable to lessees. The structural engineer, who at one time dominated the process of determining building form, no longer considers the domination a necessity. Instead, with the immense analytical backup provided by the computers, the structural engineer has set architecture in a manner of speaking, free of structural restraints. Needless to say, free-form architecture has demanded closer scrutiny of the proven systems, challenging the engineer to either modify the proven system or to come up with new structural solutions altogether. Although it is possible to arrive at a number of structural solutions which are readily applicable to high-rise buildings, the final scheme may well depend on how best it meets other nonstructural requirements. Optimization of structural systems is thus a task to be studied together with other building disciplines.

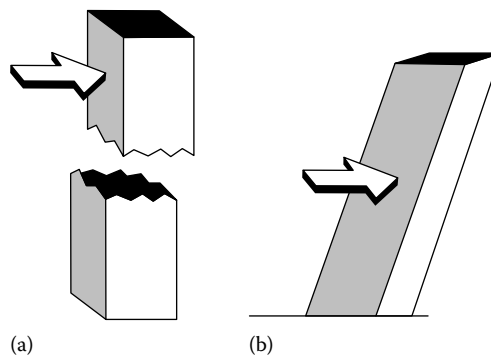
## 8.12 STRUCTURAL CONCEPTS

Although shape plays a large role in how the building behaves under wind and seismic loads, few engineers are given the opportunity (and rightly so, otherwise all our buildings would be prismatic and would either be square or round) to influence the shape of the building. Instead, their role is confined to optimization of the structure for the particular shape which the architect and the owners provide.

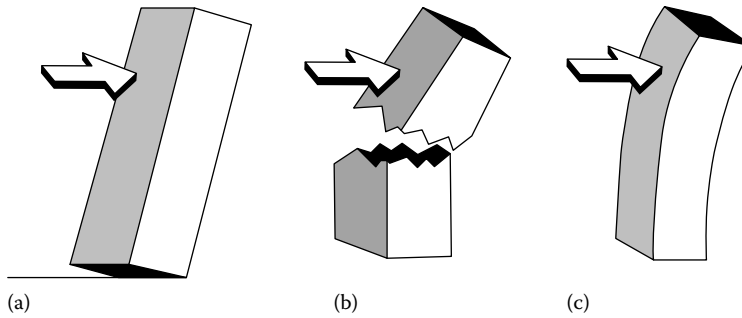
The key idea in conceptualizing the structural system for a narrow tall building is to think of it as a column cantilevering from the earth (Figure 8.35). The laterally directed force generated, either due to wind blowing against the building or due to the inertia forces induced by ground shaking, tends both to snap it (shear), and push it over (bending). Therefore, the building must have a system to resist shear as well as bending. In resisting shear forces, the building must not break by shearing off (Figure 8.36), and in general must not strain beyond the limit of elastic recovery. Similarly, the system resisting the



**FIGURE 8.35** Structural concept of tall building.



**FIGURE 8.36** Building shear resistance: (a) building must not break and (b) building must not have excessive shear deflection.



**FIGURE 8.37** Bending resistance of building: (a) building must not overturn, (b) columns must not fail in tension or compression, and (c) bending deflection must not be excessive.

bending must satisfy three needs (Figure 8.37). The building must not overturn from the combined forces of gravity and lateral loads due to wind or seismic effects; it must not break by premature failure of columns either by crushing or by excessive tensile forces; and its bending deflection in general should not exceed the limit of elastic recovery. In addition, a building in seismically active regions must be able to resist earthquake forces without losing its vertical load-carrying capacity.

In the structure's resistance to bending and shear, a tug-of-war ensues that sets the building in motion, thus creating a third engineering problem: motion perception or vibration. If the building sways and accelerates too much, human comfort is sacrificed, or more importantly, nonstructural elements may break resulting in expensive damage to the building contents and causing danger to the pedestrians.

A perfect structural form to resist the effects of bending, shear, and excessive vibration is a system possessing vertical continuity ideally located at the farthest extremity from the geometric center of the building. A concrete chimney is perhaps an ideal, if not an inspiring engineering model for a rational super-tall structural form. The quest for the best solution lies in translating the ideal form of the chimney into a more practical skeletal structure.

### 8.13 BENDING AND SHEAR RIGIDITY INDEX

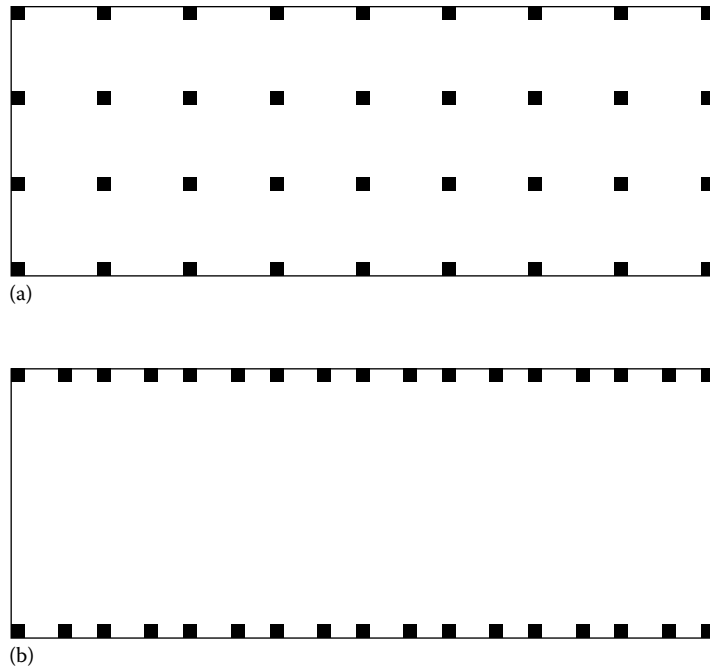
With the proviso that a tall building is a column cantilevering from earth, it is evident that all columns should be at the edges of the plan. Thus the plan shown in Figure 8.38b would be preferred over the plan in Figure 8.38a. Since this arrangement is not always possible, it is of interest to study how the resistance to bending is affected by the arrangement of columns in plan. We will use two parameters: Bending Rigidity Index (BRI) and Shear Rigidity Index (SRI).

The ultimate possible bending efficiency would manifest in a square building which concentrates all the building columns into four corner columns, as shown in Figure 8.39a, as compared to numerous columns of traditional buildings of the 1930s (Figure 8.39b). Since this plan has maximum efficiency, it is assigned the ideal BRI of 100. The BRI is the total moment of inertia of all the building columns about the centroidal axes participating as an integrated system.

A traditional tall building of the 1980s and 1990s has closely spaced exterior columns and long clear spans to the elevator core to the exterior, in an arrangement called a “tube.” If only the perimeter columns are used to resist the lateral loads, the BRI for this arrangement is 33. An example of this plan type is the now nonexistent World Trade Center in New York City (Figure 8.39c).

The Sears Tower in Chicago uses all its columns as part of the lateral system in a configuration called a “bundled tube.” It also has a BRI of 33 (Figure 8.39d).

The Citicorp Tower (Figure 8.39e), uses all of its columns as part of its lateral system, but because columns could not be placed in the corners, its BRI is reduced to 31. If these columns were moved to the corners, the BRI would be increased to 56 (Figure 8.39f). Because there are eight columns in the core supporting the gravity loads, the BRI falls short of 100.



**FIGURE 8.38** Building plan forms: (a) uniform distribution of columns and (b) columns concentrated at the edges.

The plan of Bank of Southwest Tower, a proposed building in Houston, Texas, approaches the realistic ideal for bending rigidity with a BRI of 63 (Figure 8.39g). The corner columns are split and displaced from the corners to allow generous views from the office interiors.

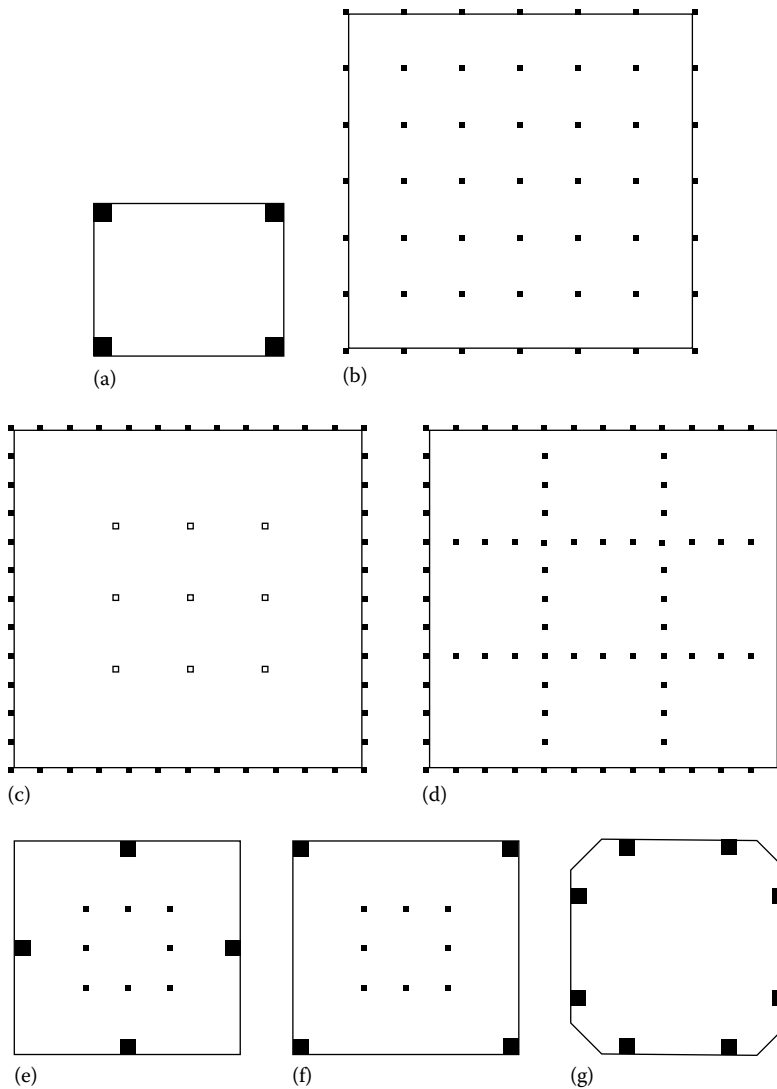
As stated earlier, in order for the columns to work as elements of an integrated system, it is necessary to interconnect them with an effective shear-resisting system. Let us look at some of the possible solutions and their relative SRI.

The ideal shear system is a plate or wall without openings which has an ultimate SRI of 100 (Figure 8.40a). The second-best shear system is a diagonal web system with an angle of  $45^\circ$  which has an SRI of 62.5 (Figure 8.40b). A more typical bracing system which combines diagonals and horizontals but uses more material is shown in Figure 8.40c. Its SRI depends on the slope of the diagonals and has a value of 31.3 for the most usual brace angle of  $45^\circ$ .

The most common shear systems are rigidly joined frames, as shown in Figure 8.40d through g. The efficiency of a frame as measured by its SRI depends on the proportions of members' lengths and depths. A frame, with closely spaced columns, like those shown in Figure 8.40e through g, has a high shear rigidity and doubles up as an efficient bending configuration. The resulting configuration is called a “tube” and is the basis of structural design for innumerable tall buildings.

In designing lateral bracing systems, it is important to distinguish between a “wind design” and a “seismic design.” The lateral system must be designed for forces generated by wind or seismic loads, whichever is greater. However, since the actual seismic forces, when they occur, are likely to be much larger than code-prescribed forces, buildings in high seismic zones, even when wind forces govern the design, must be detailed and proportioned to satisfy seismic requirements. The requirements get progressively more stringent as the Seismic Design Category, SDC, gets progressively higher.

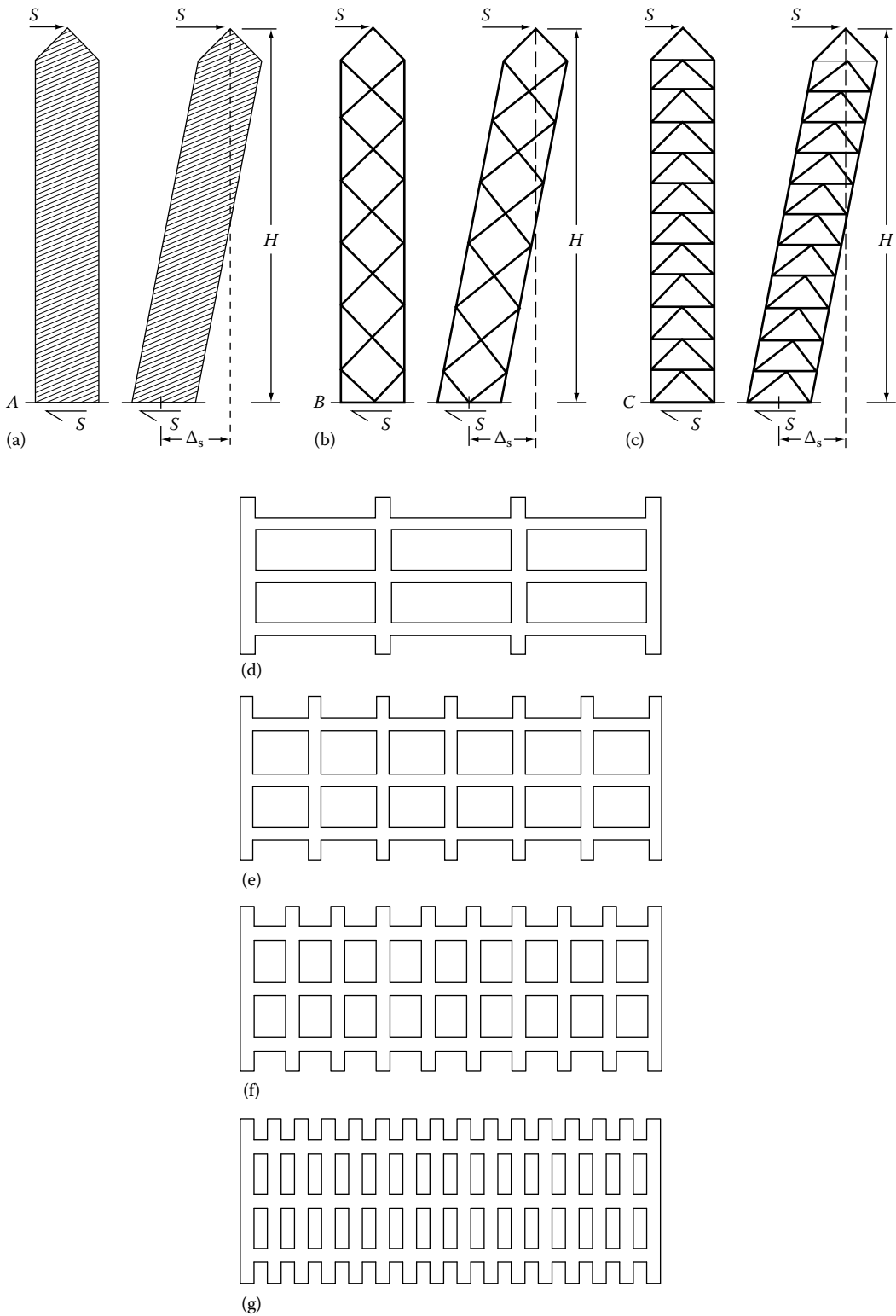
Building structural design is governed by codes that specify the minimum loads that a building must have the strength to resist. However, in planning a new building, or in retrofitting an existing



**FIGURE 8.39** Column layout and BRI: (a) square building with corner columns, BRI = 100; (b) traditional building of the 1930s, (c) modern tube building, BRI = 33; (d) Sears Towers, BRI = 33; (e) City Corp Tower, BRI = 31; (f) building with corner and core columns, BRI = 56; and (g) Bank of Southwest Tower, BRI = 63.

facility, an owner may request enhanced requirements in its design for events that are not anticipated in the building codes. Defense facilities, nuclear power plants, and overseas embassies are just a few examples where special strengthening features are requested by building owners in the design and engineering of their facilities. Therefore, designers must consider project-specific needs and owner expectations when determining design loads.

The effects of earthquake are relatively small for very tall buildings in all regions of the world, including the seismic area of California. The flexibility of a very tall building of, say, 50-plus stories generally allows the building to sway back and forth to the ground motions without developing forces nearly as large as those produced by design wind loads. Therefore, even in a severe seismic area, tall building design is generally controlled by wind loads. However, even then as stated previously, the detailing of the building components and connections should conform to seismic design requirements.



**FIGURE 8.40** Tall building shear systems (a) shear wall system; (b) diagonal web system; (c) web system with diagonals and horizontals; (d–g) rigid frames.



## 8.14 CASE STUDIES

Having noted that a building must have a system to resist both lateral bending and shear, in addition to the ever-present gravity loads, let us take a trip around the world to explore how prominent engineers have exploited this concept. Although some of the case studies include run-of-the-mill designs that a large number of engineers solve on a day-to-day basis, others are once-in-a-lifetime high-profile projects, even daring in their engineering solutions. Many are examples of buildings constructed or proposed in seismically inactive regions, requiring careful examination of their ductile behavior and reserve strength capacity before they are applied in seismically active regions.

The main purpose of this section is to introduce the reader to various structural systems normally considered in the design of tall buildings. Presently, it will be seen that design trend is toward using composite systems that include such components as mega-frames, interior and exterior super-braced frames, and spine structures. The case studies highlight those aspects of conceptualization that are timeless constants of the design process and are as important for understanding structural design as is the latest computer software. The case histories are based on information contained in various technical publications and periodicals. Frequent use is made of personal information obtained from structural engineers of record.

### 8.14.1 EMPIRE STATE BUILDING, NEW YORK, CITY, NEW YORK

We start our world tour in New York City to pay homage to the Empire State Building, which was the tallest building in the world for more than 40 years, from the day of its completion in 1931 until 1972 when the Twin Towers of New York's World Trade Center exceeded its 1280 ft (381 m) height by almost 120 ft (37 m). The structural steel frame consisting of moment and braced frames with riveted joints was designed to carry 100% of the gravity and wind loads. The concrete encasement of steel members, although neglected in strength analysis, stiffened the frame considerably against wind loads. Measured frequencies of the building have estimated the actual stiffness at 4.8 times the stiffness of the bare frame. A schematic elevation of the structural framing is shown in Figure 8.41.

### 8.14.2 SOUTH WALKER TOWER, CHICAGO, ILLINOIS

This tower, 946 ft (288.4 m) in height, has a changing geometry with the east face rising in a single plane from street level to 65th floor whereas the other three faces change shape. In the 14th level, the structure is basically a trapezoid in plan  $135 \times 225$  ft ( $41.15 \times 68.6$  m) overall. The building steps back at the 15th floor on three faces to provide 10 corner offices on each floor. There are additional setbacks at the 47th floor. At the 51st floor, the saw tooth shape is dropped and the tower becomes an octagon in plan with 70 ft (21.4 m) long sides. The slenderness ratio of the structures is 7.25:1. The schematic floor plans at various levels are shown in Figure 8.42.

The core shear walls in the tower's lower floors carry much of the lateral loading with shear wall-frame interaction. There are four main shear walls—two I-shapes and two C-shapes—on a typical floor. These interact with the perimeter columns and perimeter spandrel beams through girders that span from core to the perimeter.

The girders have 39 in. (1.0 m)-deep haunches at the columns. Spandrels are 36 in. (0.92 m) deep. Core wall concrete design strength varies from 8000 psi (55.12 MPa) at the base to 4000 psi (27.6 MPa) at the upper levels.

There is a 40–48 ft (12.2–14.63 m) span between the core and the perimeter. The spacing between the perimeter columns is fairly short, about 14 ft (4.3 m), except at two corners where the spacing is 32 ft (9.76 m). Column loads range from 12,000 to 30,000 kip (53,376 to 133,440 kN). Concrete strengths range from 12,000 to 4,000 psi (82.74 to 27.58 MPa).

The largest columns, which are  $5 \times 5$  ft contain 52 #18, grade 75 rebars. The original design for the floor system had 16 in. (406.4 mm)-deep mild steel reinforced joist with 4 in. (101.6 mm) thick slabs. This was changed to a posttensioned system with a 10 in. (254 mm)-deep joist and a 4.5 in. thick slab.

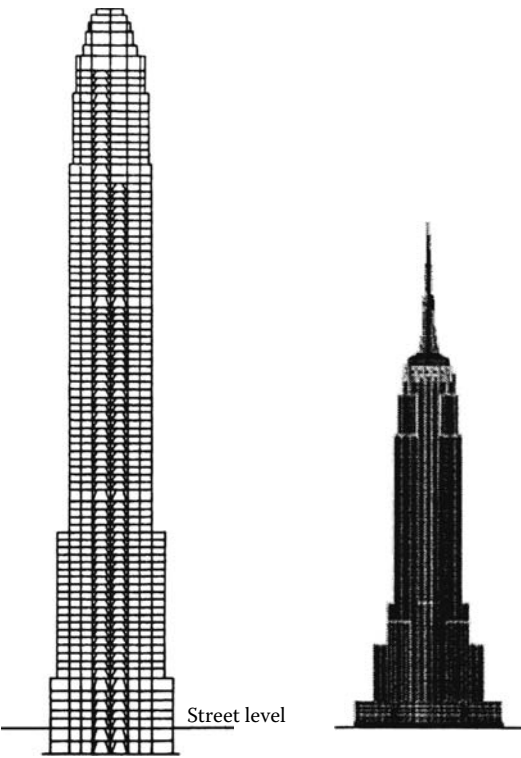


FIGURE 8.41 Empire State Building, New York City.

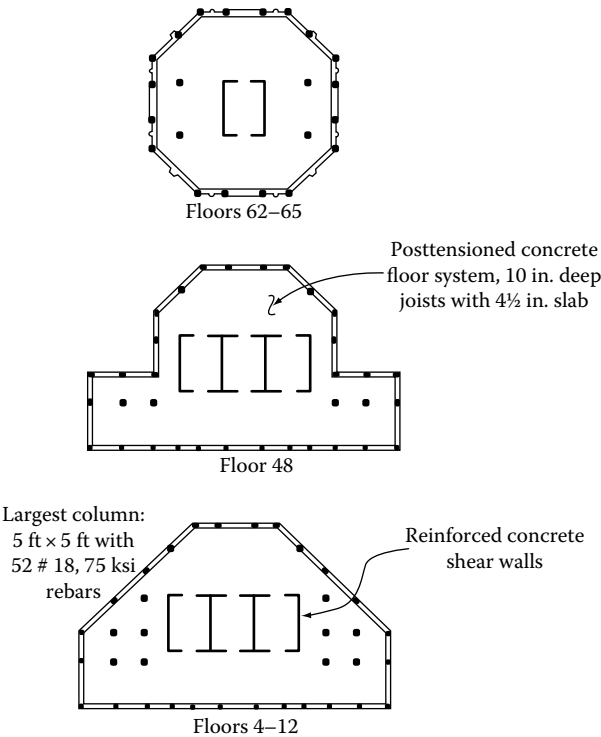
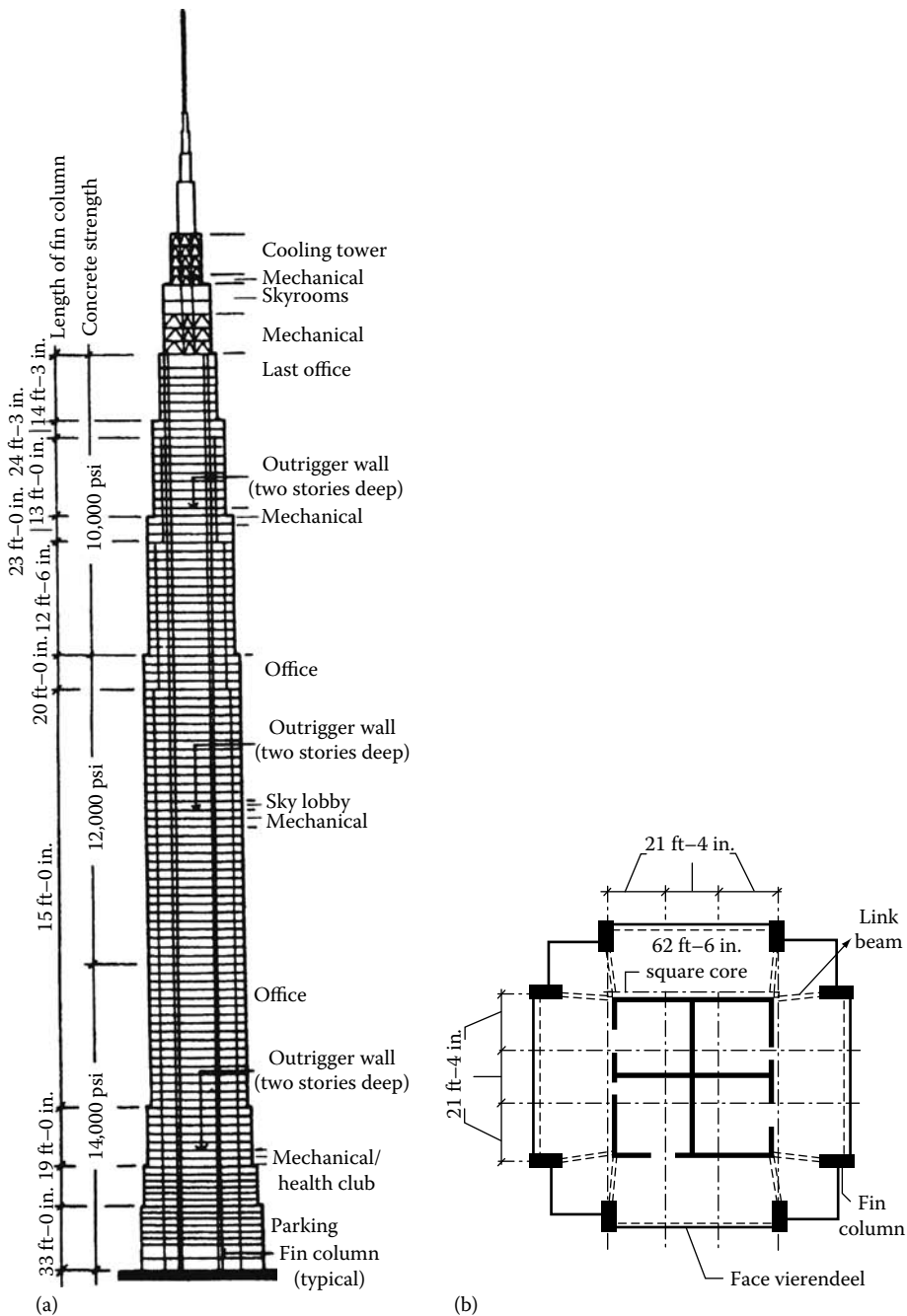


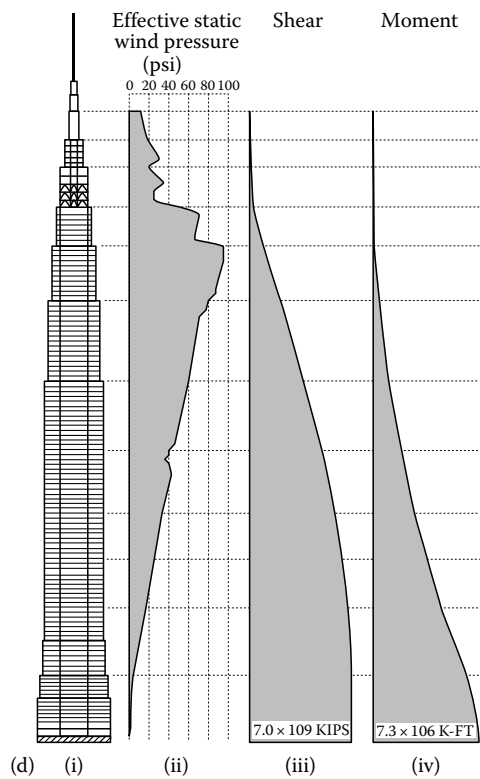
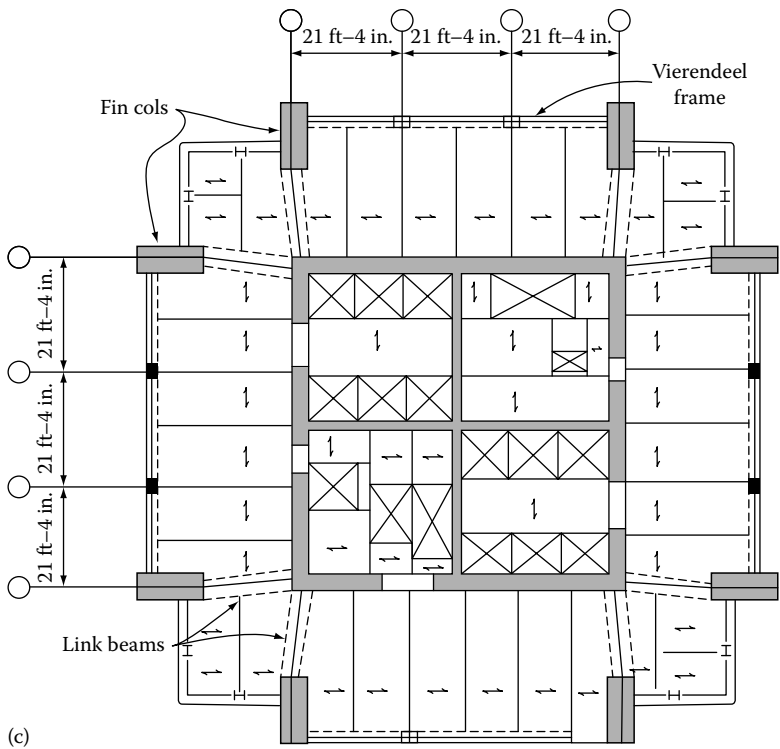
FIGURE 8.42 South Walker Tower, Chicago, Illinois.

### 8.14.3 MIGLIN-BEITLER TOWER, CHICAGO, ILLINOIS

The proposed Miglin-Beitler Tower, designed by the New York Office of Thornton-Tomasetti Engineers, will rise to the height of 1486.5 ft (453 m) at the upper skyroom level, 1584.5 ft (483 m) at the top of the mechanical areas, and finally to 1999.9 ft (609.7 m) at the tip of the spire. An elevation and the schematic plan of the proposed building are shown in Figure 8.43.



**FIGURE 8.43** Miglin-Beitler Tower, Chicago: (a) elevation and (b) plan;



**FIGURE 8.43 (continued)** (c) typical floor framing plan, and (d) lateral loads (i) building elevation (ii) effective static wind pressure (iii) shear force and (iv) overturning moment.

The structural system consists of five major components, as shown in Figure 8.44.

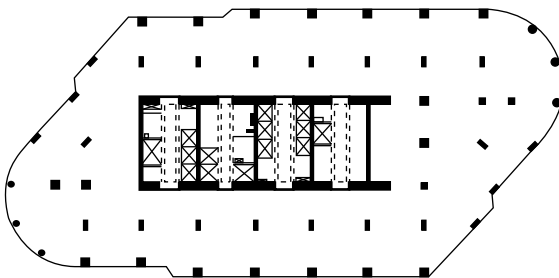
1. A 62 ft 6 in.  $\times$  62 ft 6 in. (19  $\times$  19 m) concrete core with walls varying from a maximum thickness of 3 ft (0.91 m) to a minimum thickness of 1 ft 6 in. (0.46 m).
2. A conventional structural steel composite floor system consisting of 18 in. (0.46 m)-deep rolled steel sections spaced 10 ft (3.05 m) on center with 3 in. (74 mm)-deep corrugated



(a)



(b)

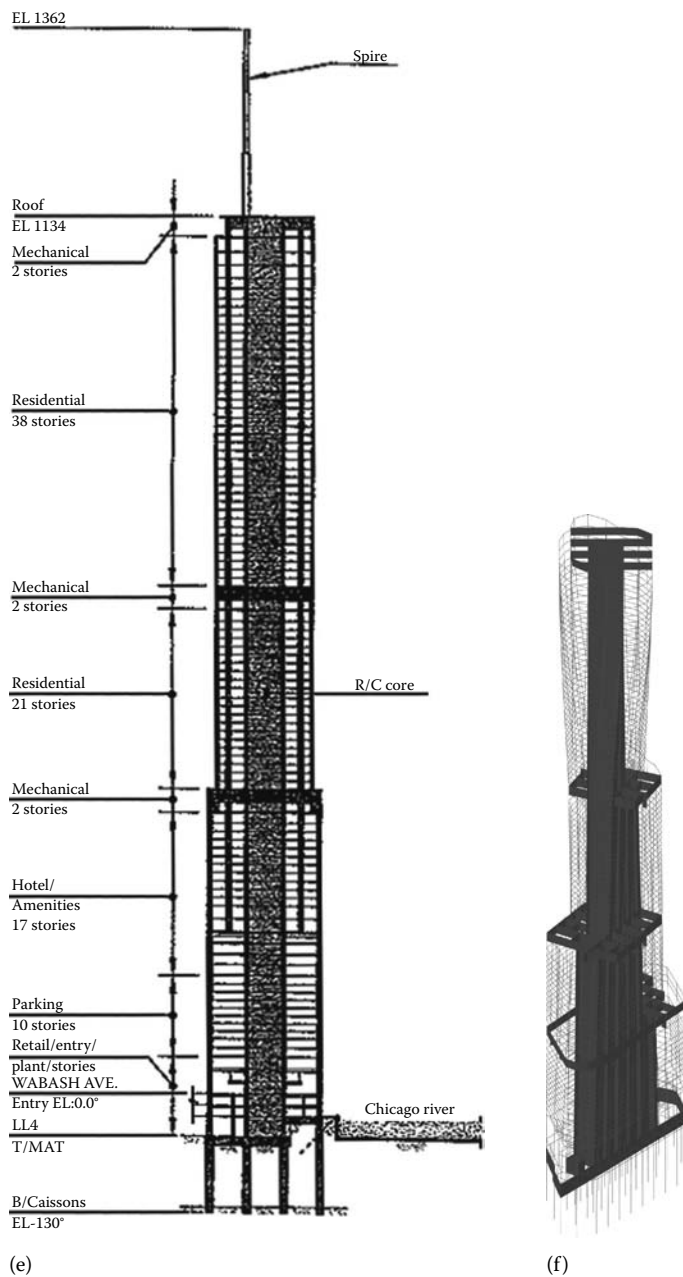


(c)



(d)

**FIGURE 8.44** Trump Tower, Chicago: (a) architectural rendering, (b) photograph, (c) 20th floor framing plan, (d) schematic elevation,



**FIGURE 8.44 (continued)** (e) schematic section, and (f) schematic 3-D.

metal deck and a 3 1/2 in. (89 mm)-thick normal-weight concrete topping. The steel floor system is supported on light steel erection columns that allow the steel construction to proceed 8–10 floors ahead of concrete operation.

- Concrete fin columns, each of which encases a pair of steel erection columns located at the face of the building. These fin columns, which extend 20 ft (6.10 m) beyond the 140 × 140 ft (42.7 × 42.7 m) footprint of the building, vary in dimension from 6 1/2 × 33 ft (2.0 × 10 m) at the base, 5 1/2 × 15 ft (1.68 × 4.6 m) at the middle, to 4 1/2 × 13 ft (1.38 × 4 m) near the top.

4. Concrete link beams that interconnect the four corners of the core to the eight fin columns at every floor. These beams tie the fin columns to the core, thus engaging the full structural width of the building to resist lateral loads. In addition to the link beams at each floor, there are three two-story-deep outrigger walls located at the 16th, 56th, and 91st stories. These outrigger walls further enhance the structural rigidity by linking the exterior fin columns to the concrete core.
5. Exterior Vierendeel trusses comprising a horizontal spandrel and two columns at each of the 60 ft (18.3 m) faces on the four sides of the building. These Vierendeels supplement the lateral force resistance and also improve the torsional resistance of the structural system. Additionally, these trusses transfer gravity loads to the exterior columns, thus minimizing uplift forces.

The proposed foundation system is rock caissons varying in diameter from 8 to 10 ft (2.44–3.0 m). The caisson will have a straight shaft steel casing and will be embedded into rock at a minimum of 6 ft (1.88 m). The length of these caissons is 95 ft (29 m). A 4 ft (1.22 m)-thick concrete mat will tie the caissons and provide a means for resisting the shear forces at the base of the building. The bottom of the mat will be cast in a two-directional groove pattern to engage the soil in shear. Passive pressure on the edge of the mat and on the projected side surface of the caisson will provide additional resistance to shear at the base.

#### 8.14.4 TRUMP TOWER, CHICAGO, ILLINOIS

With a 2.6 million sq ft of occupied space, the Trump Tower located in the downtown Chicago area, close to Lake Michigan, stands as the tallest reinforced concrete building in the United States. Reaching a height of 1134 ft (1362 ft including the spire), above grade the structure includes condominiums, service apartments, health club, parking, and retail functions. The foundation for the tower consists of 10 ft diameter caissons drilled approximately 130 ft deep, 6 ft into bedrock, and filled with 10,000 psi concrete. In the core of the building, there exists a 10 ft thick, 4700 cubic yard mat slab using 10,000 psi self-consolidating concrete (SCC). Reinforced concrete pile caps and grade beams over the caissons surrounding the mat slab are to distribute the loads imposed by the building's columns. Typical floor consists of "flat slab" construction significantly reducing the height required between floors.

As is common to all tall buildings, a central concern is the forces generated by wind on tall structures. During the design phase, wind tunnel tests were conducted using models to see how the structure would perform particularly to learn more about the vortex shedding phenomenon.

Challenges for this construction include the floors where setbacks occur, columns spaced at 30 ft intervals supporting flat plate 9 in. thick floors, and the slender north–south orientation of the building with an aspect ratio of 14 to 1. The setback locations occur at the 16th, 29th, and 51st floors and at the top of the building. On each of these floors there is a system of shear walls, outriggers, and belt walls that transfer the load from columns above each setback to those below.

To overcome the consolidation problems of concrete during placement of as much as 3000 t of rebar in the three-story transfer level at 29, SCC with a compressive strength of 12,000–16,000 psi was specified.

A climbing protection panel (CPP) windscreen system, which extends 10 ft above the top deck, protecting works and materials on the top three floors of construction was used. The system prevents debris from blowing off the building onto the downtown sidewalks below. The windscreen also helps workers deal with the icy temperatures and winds occurring in the windy city.

Forms for the flat-plate floors are a drop-head system with no single part of the system weighing more than 33 lb. Workers assemble the shores and beams from below, then the panels are dropped into place from above. When the forms can be stripped, the panels and beams are removed, while

the shores remain in position until the slab reaches the proper strength. With the exception of transfer floors, a one floor per week construction cycle was maintained on floors ranging in size from 35,000 to 45,000 ft<sup>2</sup>.

The project required 180,000 cubic yards of concrete. The concrete requirements include

- 10,000 psi compressive strength for the caissons.
- 10,000 psi SCC for the mat slab with in-place concrete temperature not to exceed 170°F and differential temperature between the center of the slab and its extremities not to exceed 40°F.
- A range of 8,000 psi to 12,000 psi for columns and core walls.
- 5000 psi for floors.
- 12,000 psi and 16,000 psi SCC for transfer floors with an average of  $E_c$  of 6200 ksi. It is believed to be the first application of 16,000 psi SCC pumped and placed to an elevation up to 650 ft above grade.

High strength concrete is now defined by ACI Committee 363, High-Strength Concrete as concrete with a minimum strength of 800 psi.

The two biggest challenges for the concrete included developing SCC mixes that could make the high strengths required and meet specifications where modulus of elasticity was considered as important as compressive strength.

For the entire project, the challenge was to produce high-strength, high-modulus mixes, consistency between loads, and slump spreads of 28 in. that allowed the SCC to move approximately 50 ft from the point of placement. All this while still maintaining the restrictive temperature controls on the mixtures, both at the time of placement and during the initial curing period. Designing an SCC mix for good pumpability was especially important for the 16,000 psi placements at the upper transition floor levels.

The average measured values for the modulus of elasticity,  $E_c$ , were 6,200 ksi or greater for 12,000 psi concrete and 7,200 ksi for the 16,000 psi concrete—well within the expected limits.

The architectural and structural design is by Skidmore, Owings and Merrill (SOM), Chicago.

#### 8.14.4.1 Vital Statistics

- Building height: 1134 ft (approximately 100 stories)
- Height to the top of the spire: 1362 ft
- Square feet of occupied space: 2.6 million
- Residential floors: 472 luxury condominiums spanning 60 floors
- Hotel floors: 286 five-star condominium guest rooms on 17 floors
- Parking levels: 12
- Volume of concrete: 180,000 cubic yards
- Volume of high-strength SCC: 14,000 cubic yards
- Rebar: 25,000 t (about 20 psf of occupied space)
- Formwork: 4.5 million sq ft

#### 8.14.5 JIN MAO TOWER, SHANGHAI, CHINA

This building consists of a 1381 ft (421 m) tower and an attached low-rise podium for a total gross building area of approximately 3 million sq ft (278,682 m<sup>2</sup>). The building includes 50 stories of office space topped by 36 stories of hotel space with two additional floors for a restaurant and an observation deck. Parking for automobiles and bicycles is located below grade. The podium consists of retail spaces as well as an auditorium and exposition spaces.

The superstructure is a mixed use of structural steel and reinforced concrete with many major structural members composed of both steel and concrete. The primary components of the lateral



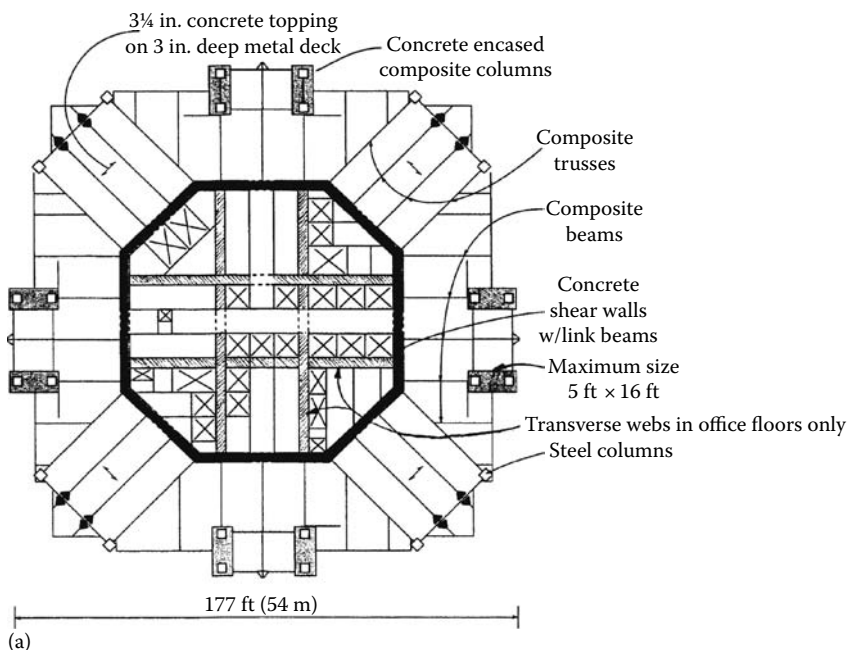
system include a central reinforced concrete core linked to exterior composite megacolumns by outrigger trusses (Figure 8.45). A central shear wall core houses the primary building functions including elevators, mechanical fan rooms, and washrooms. The octagon-shaped core, nominally 90 ft (27.43 m) from centerline to centerline of perimeter flanges, is present from the foundation to level 87. Flanges of the core typically vary from 38 in. (84 cm) thick at the foundation to 18 in. (46 cm) at level 87 with concrete strengths varying from 7500 to 5000 psi (51.71 to 34.5 MPa). Four 18 in. (46 cm)-thick interconnecting core wall webs exist through the office floors. The central area of the core is open throughout the hotel floor, creating an atrium that leads into the spire with a total height of approximately 675 ft (206 m). The size of composite megacolumns varies from  $5 \times 16$  ft ( $1.5 \times 4.88$  m) with a concrete strength of 7500 psi (51.71 MPa) at the foundation to  $3 \times 11$  ft ( $0.91 \times 3.53$  m) with a concrete strength of 5000 psi (34.5 MPa) at level 87.

The shear wall core is directly linked to the exterior composite megacolumns by structural steel outrigger trusses. The outrigger trusses resist lateral loads by maximizing the effective depth of the structure. Under bending, the building acts as a vertical cantilever with tension in the windward columns and compression in the leeward columns. Gravity load framing minimizes uplift in the exterior composite megacolumns. The octagon-shaped core provides exceptional torsional resistance, eliminating the need for any exterior belt or frame systems to interconnect exterior columns.

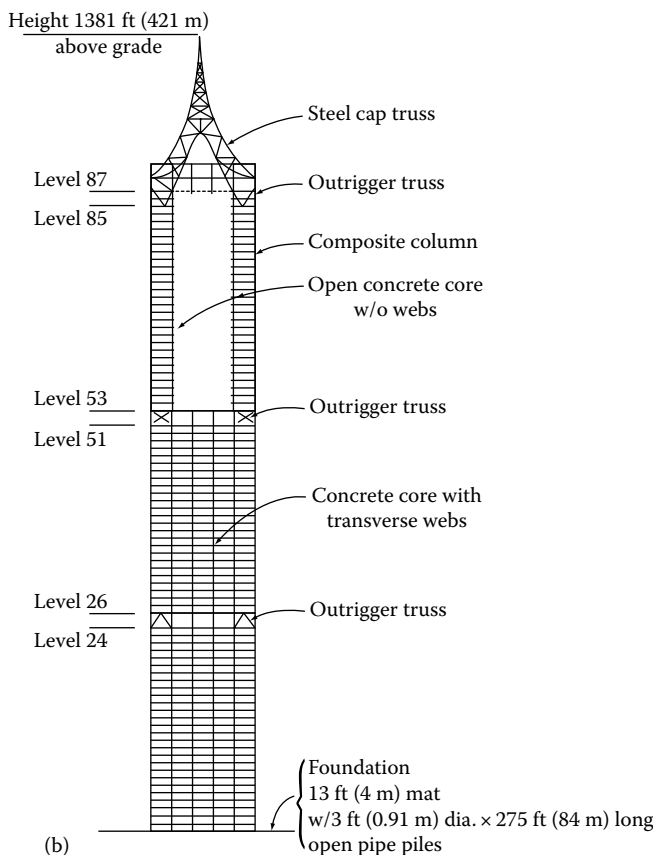
The outrigger trusses are located between levels 24 and 26, 51 and 53, and 85 and 87. The outrigger truss system between levels 85 and 87 is capped with a three-dimensional steel space that provides for the transfer of lateral loads between the core and the exterior composite columns. It also supports gravity loads of heavy mechanical spaces located in the penthouse floors.

The structural elements for resisting gravity loads include eight structural steel built-up columns. Composite wide-flange beams and trusses are used to frame the floors. The floor-framing elements are typically 14 ft 6 in. (4.4 m) at the center with a composite 3 in. (7.6 cm)-deep metal deck and a  $3\frac{1}{4}$  in. (8.25 cm)-thick normal-weight concrete topping slab spanning between the steel members.

The foundation system for the Tower consists of high-capacity piles capped with a reinforced concrete mat. High-water conditions required the use of a 3 ft 3 in. (1 m)-thick, 100 ft (30 m)-deep, continuous reinforced concrete slurry wall diaphragm along the 0.5 mile (805 m) perimeter of the site.



**FIGURE 8.45** Jin Mao Tower, Shanghai, China: (a) typical office floor framing plan;



**FIGURE 8.45 (continued)** (b) structural system elevation.

The high-capacity pile system consists of a 3 ft (0.91 m)-diameter structural steel open-pipe pile with a 7/8 in. (2.22 cm)-thick wall typically spaced 9 ft (2.75 m) on center capped by a 13 ft (4 m)-deep reinforced concrete mat. Since soil conditions at the upper strata are so poor, the piles were driven into a deep, stiff sand layer located approximately 275 ft (84 m) below grade. The individual design-pile capacity is 1650 kip (7340 kN).

Strength design of the structure is based on a 100 year wind with a basic wind speed of 75 mph for a 10 min average time. The wind speed corresponds to a design wind pressure of approximately 14 psf (0.67 kN/m<sup>2</sup>) at the bottom of the building and 74 psf (3.55 kN/m<sup>2</sup>) at the top of the spire. Exterior wall-design pressures are in excess of 100 psf (4.8 kN/m<sup>2</sup>) at the top of the building.

Wind speeds can average 125 mph (56 m/s) at the top of the building over a 10 min time period during a typhoon event. The earthquake ground accelerations compare to 1994 UBC zone 2A. The overall building drift index for a 50 year return wind with a 2.5% structural damping is 1/1142. This increases to 1/887 for a future developed condition in which two tall structures are proposed adjacent to the Jin Mao Building. The drift index based on specific Chinese code-defined winds, which are equivalent to a 3000 year wind, is 1/575.

The structural design for the tower is governed by its dynamic behavior under wind and not by its strength or its overall or inter-story drift. The calculated fundamental translational periods are 5.7 s for each principal axis. The torsional period is 2.5 s.

In a force-balance and aeroelastic wind-tunnel study, the accelerations at the top floors were evaluated using a value of 1.5% for structural damping. The accelerations measured in the wind tunnel were between 9 and 13 mg for a 10 year return period, and between 3 and 5 mg for a 1 year return

period—well within the generally accepted range of 20–25 mg for a 10 year return. Only the passive characteristics of the structural system including its inherent mass, stiffness, and damping are required to control the dynamic behavior. Therefore, no mechanical damping systems are used.

Since the central core and composite megacolumns are interconnected by outrigger trusses at only three 2-story levels, the stresses in the trusses due to differential shortening of the core relative to the composite columns were of concern. Therefore, concrete stress levels in the core and megacolumns were controlled in an attempt to reduce relative movements. To further reduce the adverse effect of differential shortening, slotted connections were used in the trusses during the construction period of the building. Final bolting with hard connections was done after completion of construction to relieve the effect of differential shortening occurring during construction. The architecture and structural engineering of the building is by the Chicago office of Skidmore, Owings, and Merrill.

#### 8.14.6 PETRONAS TOWERS, MALAYSIA

Two 1476 ft (450 m) towers, 33 ft (7 m) taller than Chicago's Sears Tower, and a sky bridge connecting the twin towers characterize the buildings in Kuala Lumpur, Malaysia (Figure 8.46a and b).

The towers have 88 numbered levels but are in fact equal to 95 stories when mezzanines and extra tall floors are considered. In addition to 6,027,800 ft<sup>2</sup> (560,000 m<sup>2</sup>) of office space, the project includes 1,501,000 ft<sup>2</sup> (140,000 m<sup>2</sup>) of retail and entertainment space in a six-story structure linking the base of the towers, plus parking for 7000 vehicles in five below-ground levels.

The lateral system for the towers is of reinforced concrete consisting of a central core, perimeter columns, and ring beams using concrete strengths up to 11,600 psi (80 MPa). The foundation system consists of pile and friction barrette foundations with a foundation mat.

The typical floor system consists of wide-flange beams spanning from the core to the ring beams. A 2 in. deep composite metal deck system with a 4 1/4 in. (110 mm) concrete topping completes the floor system.

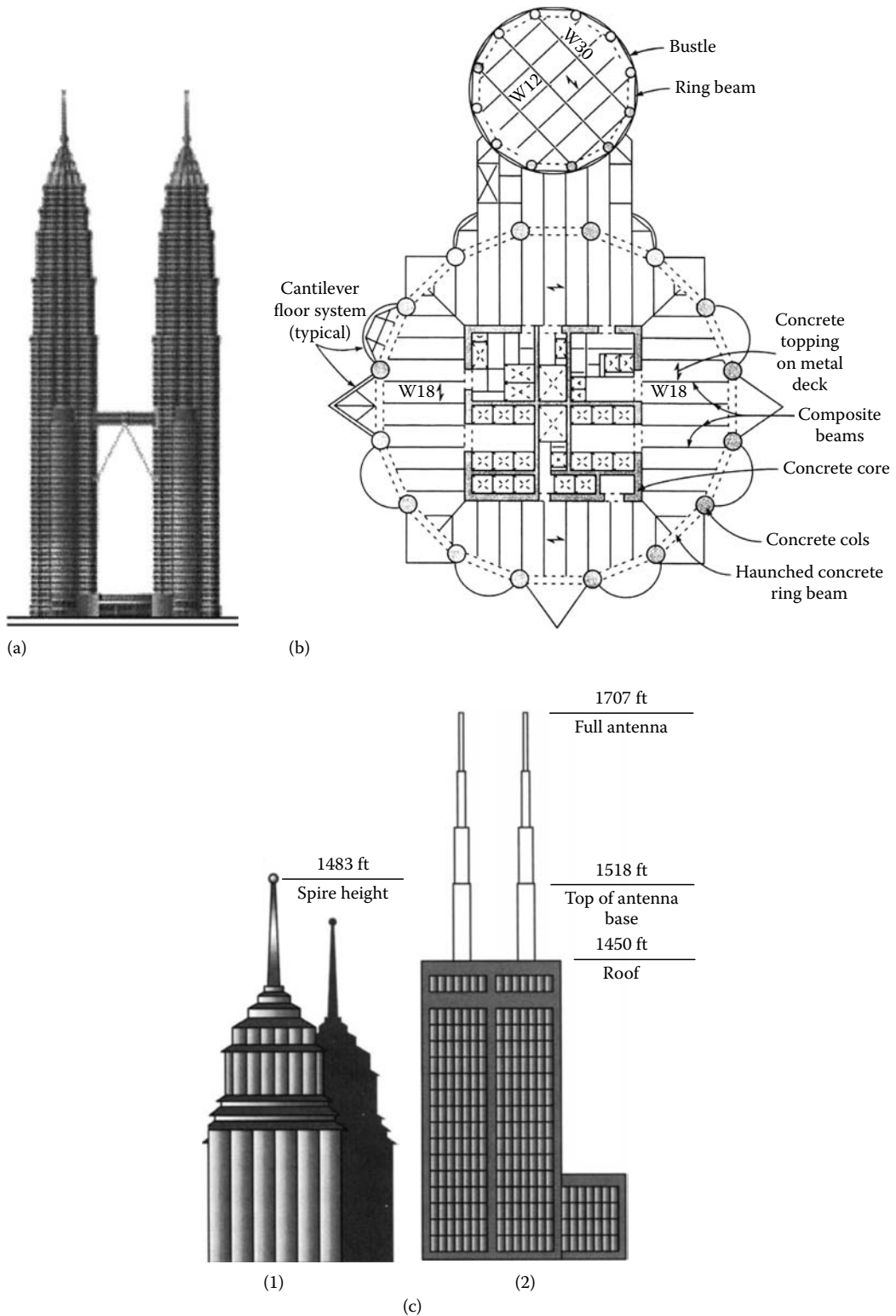
Architecturally, the towers are cylinders 152 ft (46.2 in.) in diameter formed by 16 columns. The façade between columns has pointed projections alternating with arcs, giving unobstructed views through glass and metal curtain walls on all sides. The floor plate geometry is composed of two rotated and superimposed squares overlaid with a ring of small circles. The towers have setbacks at levels 60, 72, 82, 85, and 88 and circular appendages at level 44. Concrete perimeter framing is used up to level 84. Above this level, steel columns and ring beams support the last few floors and a pointed pinnacle.

The towers are slender with an aspect ratio of 8.64 (calculated to level 88). The design wind speed in Kuala Lumpur area is based on 65 mph (35.1 m/s) peak, 3 s gusts at 33 ft (10 m) above grade for a 50 year return. In terms of the old U.S. standard of fastest mile wind, the corresponding wind speed is about 52 mph (28.1 m/s).

The mass and stiffness of concrete are taken advantage of in resisting lateral loads, whereas the advantages of speed of erection and long-span capability of structural steel are used in the floor framing system. The building density is about 18 lb/cu ft (290 kg/m<sup>3</sup>).

As is common for tall buildings of high aspect ratios, the towers were wind-tunnel tested to determine dynamic characteristics of the building in terms of occupant perception of wind movements and acceleration on the upper floors. The 10 year return period acceleration is in the range of 20 mg, within the normally accepted criterion of 25 mg. The periods for the primary lateral modes are about 9 s, while the torsional mode has a period of about 6 s. The drift index for lateral displacement is of the order of 1/560.

Because the limestone bedrock lies 200 ft (60 m) to more than 330 ft (100 m) below dense salty sand formation, it was not feasible to extend the foundations to bedrock. A system of drilled friction piers was designed for the foundation, but barrettes (slurry-wall concrete segments) proposed as an alternative system by the contractor were installed. A 14.8 ft (4.5 m)-thick mat supports the 16



**FIGURE 8.46** Petronas Towers, Malaysia. (a) Elevation and (b) structural system plan. (c) Height comparison: (1) Petronas Towers and (2) Sears Tower, Chicago.

tower columns and 12 bustle columns. The floor corners of alternating right angles and arcs are cantilevered from the perimeter ring beams. Haunched ring beams varying from 46 in. (1.17 m) deep at columns to 31 in. (0.78 m) at midspan are used to allow for ductwork in office space outside of the ring beams. A similar approach with a midspan depth of 31 in. (0.78 m) is used in the bustles. The haunches are used primarily to increase the stiffness of the ring beams.

The central core for each tower houses elevators, exit stairs, and mechanical services, while the bustles have solid walls. The core and bustle walls carry about half the overturning moment at the foundation level.

Each core is 75 ft (23 m) square at the base, rising in four steps to  $62 \times 72$  ft ( $18.8 \times 22$  m). Inner walls are a constant 14 in. (350 mm) thick while outer walls vary from 30 to 14 in. (750 to 350 mm). The concrete strength varies from 11,600 to 5,800 psi (80 to 40 MPa).

To increase the efficiency of the lateral system, the interior core and exterior frame are tied together by a two-story-deep outrigger truss at the mechanical equipment room (level 38). A Vierendeel type of truss with three levels of relatively shallow beams connected by a midpoint column is used to give flexibility in the planning of building occupancy.

The tower floors (Figure 8.12b), typically consist of composite metal deck with concrete topping varying from 4 1/2 in. (110 mm) in offices to 8 in. (200 mm) on mechanical floors, including a 2 in. (53 mm)-deep composite metal deck. Wide-flange beams frame the floors at spans up to 42 ft (12.8 m), and are W18 or shallower on most floors to provide room for ductwork, sprinklers, and lights.

Cantilevers for the points beyond the ring beams are 3.28 ft (1 m)-deep prefabricated steel trusses. For the arcs, the cantilevers are beams propped with kickers back to the columns. Trusses and beams are connected to tower columns by embedded high-strength bolts. The structural engineering is by Thornton-Tomasetti Engineers, and Ranhill Bersekutu Sdn. Bhd.

Although the Sears Tower's 110 stories dwarf the Malaysian twin skyscrapers' 88 floors (Figure 8.46c), an engineering panel from the Council on Tall Buildings and Urban Habitat says that the Sears Tower is no longer the world's tallest building. This panel, which sets international building height standards, contends that the Petronas Towers' 242 ft high ornamental spires are part of their height while the radio antennas of the Sears Tower are not. This is because traditionally the measurement from ground-floor entrance to the highest original structural point has been the criterion for assessing the height of skyscrapers for over a quarter of a century. Executives of the Chicago skyscrapers disagree, and say their building is actually 35 ft taller if the radio bases are considered as part of the height.

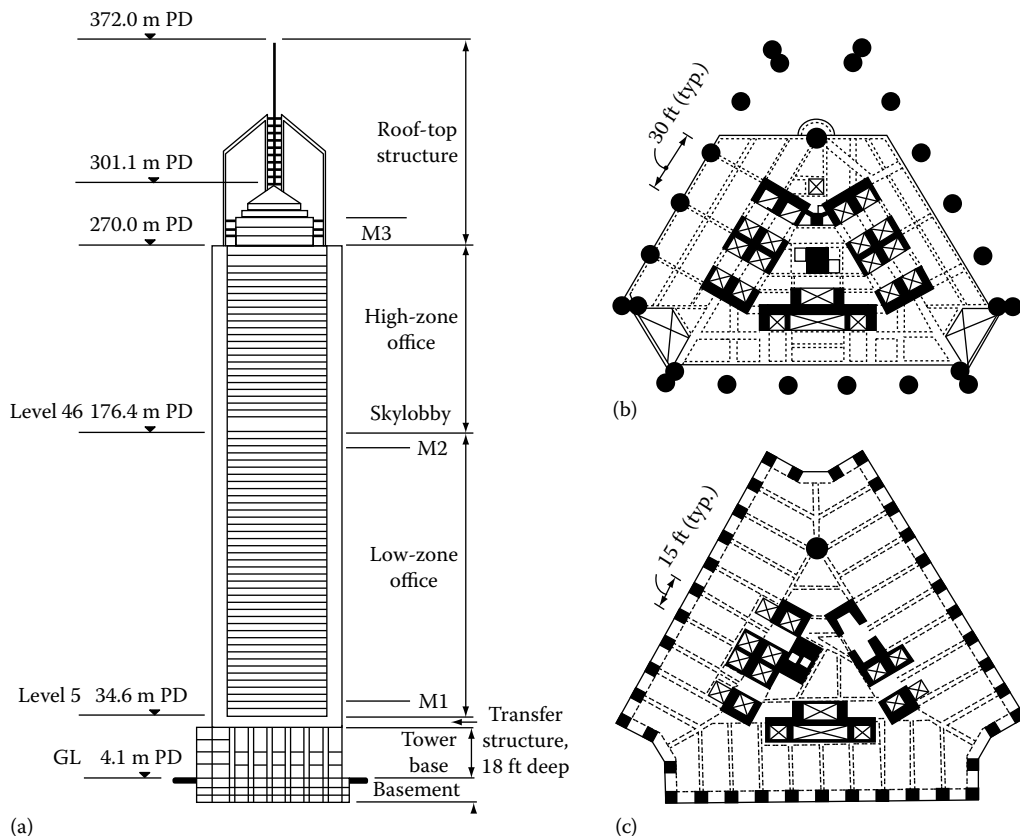
### 8.14.7 CENTRAL PLAZA, HONG KONG

The building has 78 stories, with the highest office floor at 879 ft (268 m) above ground. Including the tower mast, the building is 1207.50 ft (368 m) tall (Figure 8.47). The building has a triangular floor plate with a sky lobby on the 46th floor. The triangular design consisting of a typical floor area of 23,830 ft<sup>2</sup> (2214 m<sup>2</sup>) (Figure 8.48b and c) was preferred over a more traditional square or rectangular plan because the triangular shape has very few dead corners and offers more views from the building interiors.

The tower consists of three sections: (1) a 100 ft (30.5 m)-tall tower base forming the main entrance and public circulation spaces; (2) a 772.3 ft (235.4 m)-tall tower section containing 57 office floors, a sky lobby, and five mechanical floors; and (3) a top section consisting of six mechanical floors and a 334 ft (102 m)-tall tower mast.

The triangular building shape is not truly triangular because its three corners are chamfered to provide better internal office layout. The building façade is clad in insulated glass. The mast is constructed of structural steel tubes with diameters up to 6.1 ft (2 m).

The triangular core design provides a consistent structural and building services configuration. A column-free office space, with 30.84–44.3 ft (9.4–13.5 m) depth is provided between the core and the building perimeter.



**FIGURE 8.47** Central Plaza, Hong Kong: (a) elevation; (b, c) floor plans.

To enhance the spatial quality of the tower at the base, the 15 ft (4.6 m) column grid of the tower is transformed to a 30 ft (9.2 m) column grid by eliminating every other column. An 18 ft (5.5 m)-deep transfer girder facilitates column termination.

The building site is typical of a recently reclaimed area in Hong Kong with sound bedrock lying between 82 and 132 ft (25 and 40 m) below ground level. This is overlaid by decomposed rock and marine deposits with the top 33–50 ft (10–15 m) consisting of a fill material. The allowable bearing pressure on sound rock is of the order of 480 t/ft<sup>2</sup> (5.0 kN/m<sup>2</sup>). The maximum water table is about 6.1 ft (2 m) below ground level.

Wind loading is the major lateral load criterion in Hong Kong, which is situated in an area subject to typhoon winds. The local wind design is based on a mean hourly wind speed of 100 mph (44.7 m/s), corresponding to a 3 s gust of 158 mph (70.5 m/s). The resulting lateral design pressure is 86 psf (4.1 kN/m<sup>2</sup>) at 656 ft (200 m) above ground level.

The basement consisting of a diaphragm slurry wall extends around the whole site perimeter and is constructed down to and grouted into rock. The diaphragm wall design allowed for the basement to be constructed by the “top-down” method. This method typically has the following features:

1. Simultaneous construction of superstructure and basement, thus reducing the time required for construction
2. Use of basement floor slabs for bracing of diaphragm walls, thereby reducing lateral tiebacks
3. Construction of a watertight box within the site enabling installation of hand-dug caissons, traditional in some countries outside of North America

The lateral system for the tower above the transfer girder consists of external façade frames acting as a tube. These consist of closely spaced 4.93 ft (1.5 m)-wide columns at 15 ft (4.6 m) centers and 3.6 ft (1.1 m)-deep spandrel beams. The floor-to-floor height is 11.82 ft (3.6 m). The core shear walls carry approximately 10% of the lateral load above the transfer level. The transfer girder located at the perimeter is 18 ft (5.5 m) deep by 9.2 ft (2.8 m) wide. The increased column spacing, together with the elimination of spandrel beams in the tower base, results in the external frame no longer being able to carry the entire lateral load acting on the building. Therefore, the wind shears are transferred to the core through the diaphragm action of a 3.28 ft (1 m)-thick slab located at the transfer level. Structural engineering for the project is by Ove Arup and Partners.

The building is 78-stories with the highest office floor at 879 ft (268 m) above ground. Including the tower mast, the building is 1207.50 ft (368 m) tall (Figure 8.47). The building has a triangular floor plate with a sky lobby on the 46th floor.

The triangular design consisting of a typical floor area of 23,830 sq ft (2214 m<sup>2</sup>) was preferred over a more traditional square or rectangular plan, because the triangular shape has very few dead corners and offers more views from the building interiors.

The tower consists of three sections: (1) a 100 ft (30.5 m) tall tower base forming the main entrance and public circulation spaces; (2) a 772.3 ft (235.4 m) tall tower section containing 57 office floors, a sky lobby and five mechanical floors; and (3) a top section consisting of six mechanical floors and a 334 ft (102 m) tall tower mast.

The triangular building shape is not truly triangular because its three corners are cut off to provide better internal office layout. The building façade is clad in insulated glass. The mast is constructed of structural steel tubes with diameter up to 6.1 ft (2 m).

The triangular core design (Figure 8.47) provides a consistent structural and building services configuration. A column-free office space, with 30.84–44.3 ft (9.4–13.5 m) depth is provided between the core and the building perimeter.

To enhance the spatial quality of the tower at the base, the 15 ft (4.6 m) column grid of the tower is transformed to 30 ft (9.2 m) column grid by eliminating every other column. An 18 ft (5.5 m) deep transfer girder facilitates column termination.

The building site is typical of a recently reclaimed area in Hong Kong with sound bed rock lying between 82 and 132 ft (25 and 40 m) below ground level. This is overlaid by decomposed rock and marine deposits with the top 33–50 ft (10–15 m) consisting of a fill material. The allowable bearing pressure on sound rock is of the order of 480 t/sq ft (5.0 kN/m<sup>2</sup>). The maximum water table is about 6.1 ft (2 m) below ground level.

Wind loading is the major lateral load criterion in Hong Kong, which is situated in an area susceptible to typhoon winds. The local wind design is based on a mean hourly wind speed of 100 mph (44.7 m/s), a 3 s gust of 158 mph (70.5 m/s) and gives rise to a lateral design pressure of 86 psf (4.1 kN/m<sup>2</sup>) at 656 ft (200 m) above ground level.

The basement consisting of a diaphragm slurry wall extends around the whole site perimeter and is constructed down to and grouted to the rock. The diaphragm wall design allowed for the basement to be constructed by the “top-down” method. This method has three fundamental advantages:

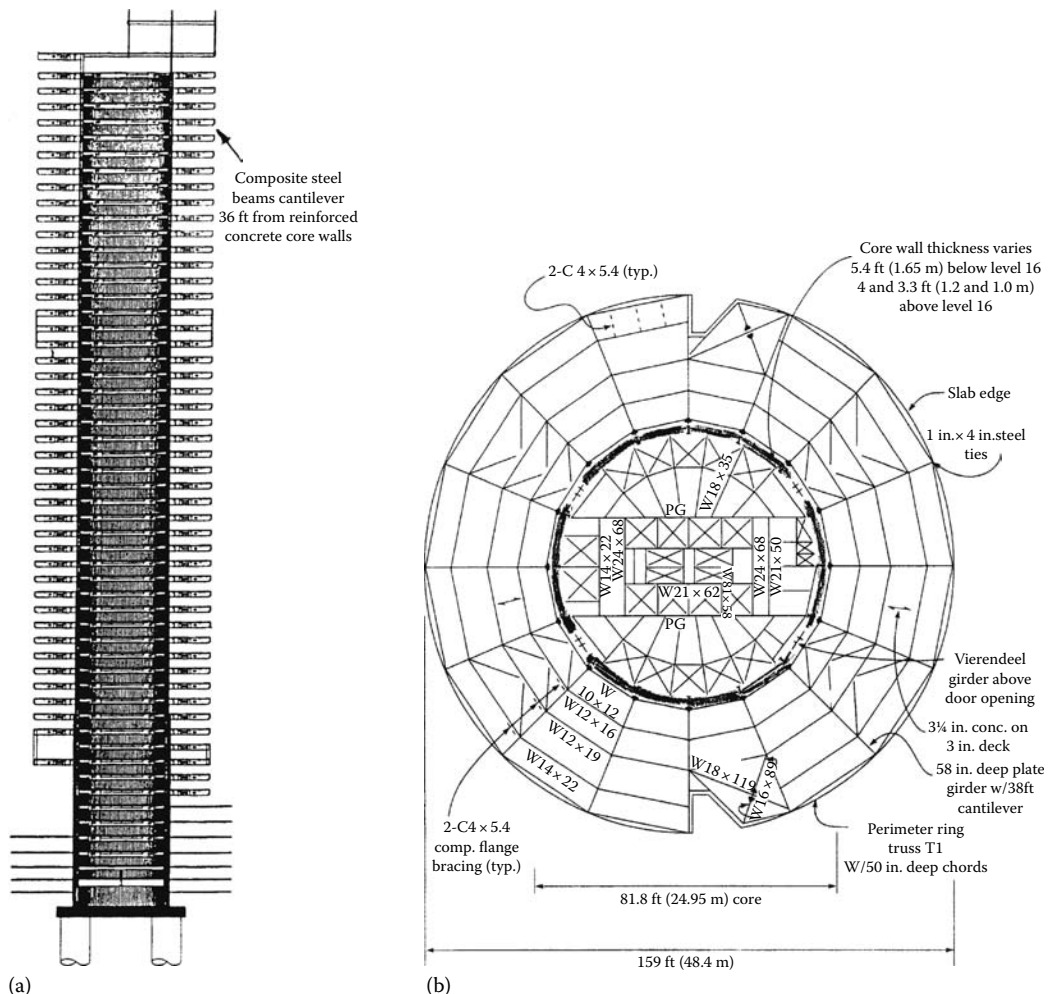
1. It allows for simultaneous construction of superstructure and basement thus reducing time required for construction.
2. Basement floor slabs are used for bracing of diaphragm walls thereby reducing lateral tie-backs.
3. Creates a watertight box within the site enabling installation of hand dug caissons, traditional in Hong Kong.

The lateral system for the tower above the transfer girder consists of external façade frames acting as a tube. These consist of closely spaced 4.93 ft (1.5 m) wide columns at 15 ft (4.6 m) centers and

3.6 ft (1.1 m) deep spandrel beams. The floor-to-floor height is 11.82 ft (3.6 m). The core shear walls carry approximately 10% of the lateral load above the transfer level. The transfer girder located at the perimeter is 18 ft (5.5 m) deep  $\times$  9.2 ft (2.8 m) wide, allowing alternate columns to be dropped from the façade, thereby opening up public area at ground level. The increased column spacing together with the elimination of spandrel beams in the tower base, results in the external frame no longer being able to carry the lateral loads acting on the building. Therefore, the wind shears are transferred to the core through the diaphragm action of 3.258 ft (1 m) thick slab located at the transfer level. The wind shear is taken out from the core at the lowest basement level, where it is transferred to the perimeter diaphragm walls. In order to reduce large shear reversals in the core walls, the floor slabs and beams are separated horizontally from the core walls at certain levels. Structural engineering is by Ove Arup and Partners.

### 8.14.8 SINGAPORE TREASURY BUILDING

This 52-story office tower, shown in Figure 8.48a, is unique in that every floor in the building is cantilevered from an inner cylindrical, 82 ft (25 m)-diameter core enclosing the elevator and service areas (Figure 8.48b). Radial beams cantilever 38 ft (11.6 m) from the reinforced concrete core wall.



**FIGURE 8.48** Singapore Treasury Building, Singapore: (a) schematic section and (b) typical floor framing plan.



Each cantilever girder is welded to a steel erection column embedded in the core wall. To reduce relative vertical deflections of adjacent floors, the steel beams are connected at their free ends by a  $1 \times 4$  in. ( $25 \times 100$  mm) steel tie hidden in the curtain wall. A continuous perimeter ring-truss at each floor minimizes relative deflections of adjacent cantilevers on the same floor produced by uneven distribution of live load. Additionally the vertical ties and the ring beam provide a backup system for the cantilever beams.

Since there are no perimeter columns, all gravity and lateral loads are resisted solely by the concrete core. The thickness of core walls varies from 3.3 ft (1.0 m) at the top to 4 ft (1.2 m) at the 16th floor, and remains at 5.4 ft (1.65 m) below the 16th floor. The fundamental vibration period of this cylindrical tower is 5.6 s. Its foundation has six 8.0 m diameter reinforced concrete caissons 35 m long, equally spaced on a 23.5 m diameter circle, which transfer building loads to rock mainly via skin friction. Tops of caissons are connected by a 2.9 m thick reinforced concrete mat. The structural engineering is by LeMessurier Consultants, Cambridge, Massachusetts, and Ove Arup and Partners, Singapore.

#### 8.14.9 CITY SPIRE, NEW YORK CITY

This 75-story office and residential tower, with a height-to-width ratio of 10:1, was one of the most slender buildings, concrete or steel, at the time it was built. The critical wind direction is from the west, which produces maximum crosswind response. Wind studies indicated possible problems of vortex shedding as well as occupant perception of acceleration. This possibility was eliminated by adding mass and stiffness to the building.

The main structural system consists of shear walls connected to exterior jumbo columns with staggered rectangular concrete panels. The structure is subdivided into nine major structural subsystems with setbacks and column transfers as evident from the plans shown in Figure 8.49a through d. The structural design is by Robert Rosenwasser Associates, New York.

#### 8.14.10 NCNB TOWER, NORTH CAROLINA

This building is an 870 ft (265.12 m)-tall, concrete office building with a 100 ft (30.5 m) crown of aluminum spires (Figure 8.50). The building has a 12 ft 8 in. (3.87 m) floor-to-floor height and a 48 ft (14.63 m) column-free span from the perimeter to core.

The structural system for resisting lateral loads consists of a reinforced concrete perimeter tube with normal-weight concrete ranging in strength from 8000 psi (55.16 MPa) near the building's base to 6000 psi (41.37 MPa) at the top. Typical column sizes range from  $24 \times 38$  in. ( $0.61 \times 0.97$  m) at the base to  $24 \times 24$  in. ( $0.61 \times 0.61$  m) at the top. The floor system (Figure 8.50) consists of a  $4\frac{3}{8}$  in. (118 mm)-thick lightweight concrete slab supported on 18 in. (458 mm)-deep posttensioned beams spaced at 10 ft (3.05 m) on centers. Lightweight concrete was used to reduce the building weight and to achieve the required fire rating for the floor system.

The tower's columns are spaced 10 ft (3.05 m) on center and are connected by 40 in. (1.01 m)-deep spandrel beams. The building has a square plan at the base, but above the 13th floor it resembles a square set over a slightly larger cross, with the four major corners recessed and its four major faces bowed slightly outward. To maintain tube action between the 13th and 43rd floors, engineers used L-shaped Vierendeel trusses to continue the tube around the corners. Instead of transfer girders at the building step-backs, the building's column-and-spandrel structure is used to create multilevel Vierendeel trusses on the building's main façades. These Vierendeels transfer loads using another set of Vierendeel trusses perpendicular to the façade at the edges of recessed corners. Differential shortening between the core and perimeter columns was a concern during design because the core columns will be under significantly higher stresses than the closely spaced perimeter columns. To compensate for this, the core columns were constructed slightly longer than the perimeter columns.

Both standard and lightweight concrete were used simultaneously. The normal-weight concrete was used for the perimeter columns, which ranged in size from  $24 \times 38$  in. ( $6.10 \times 965$  mm) at the

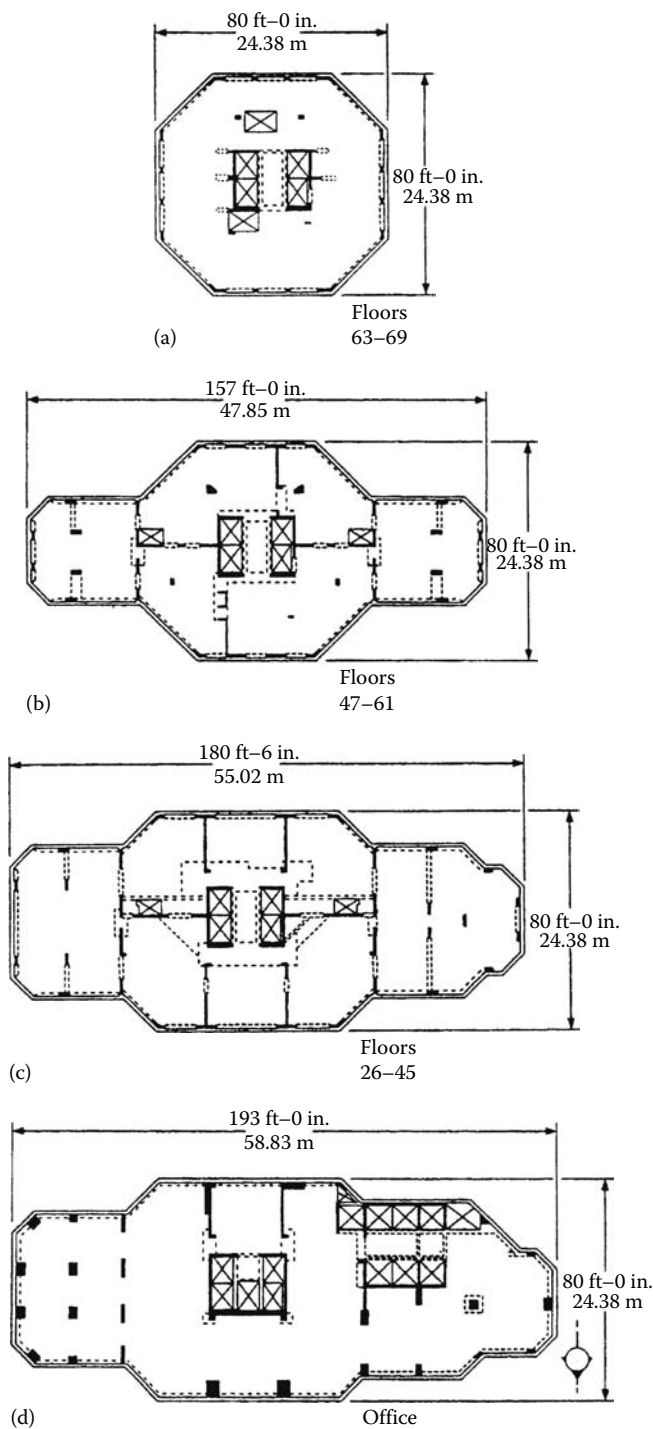
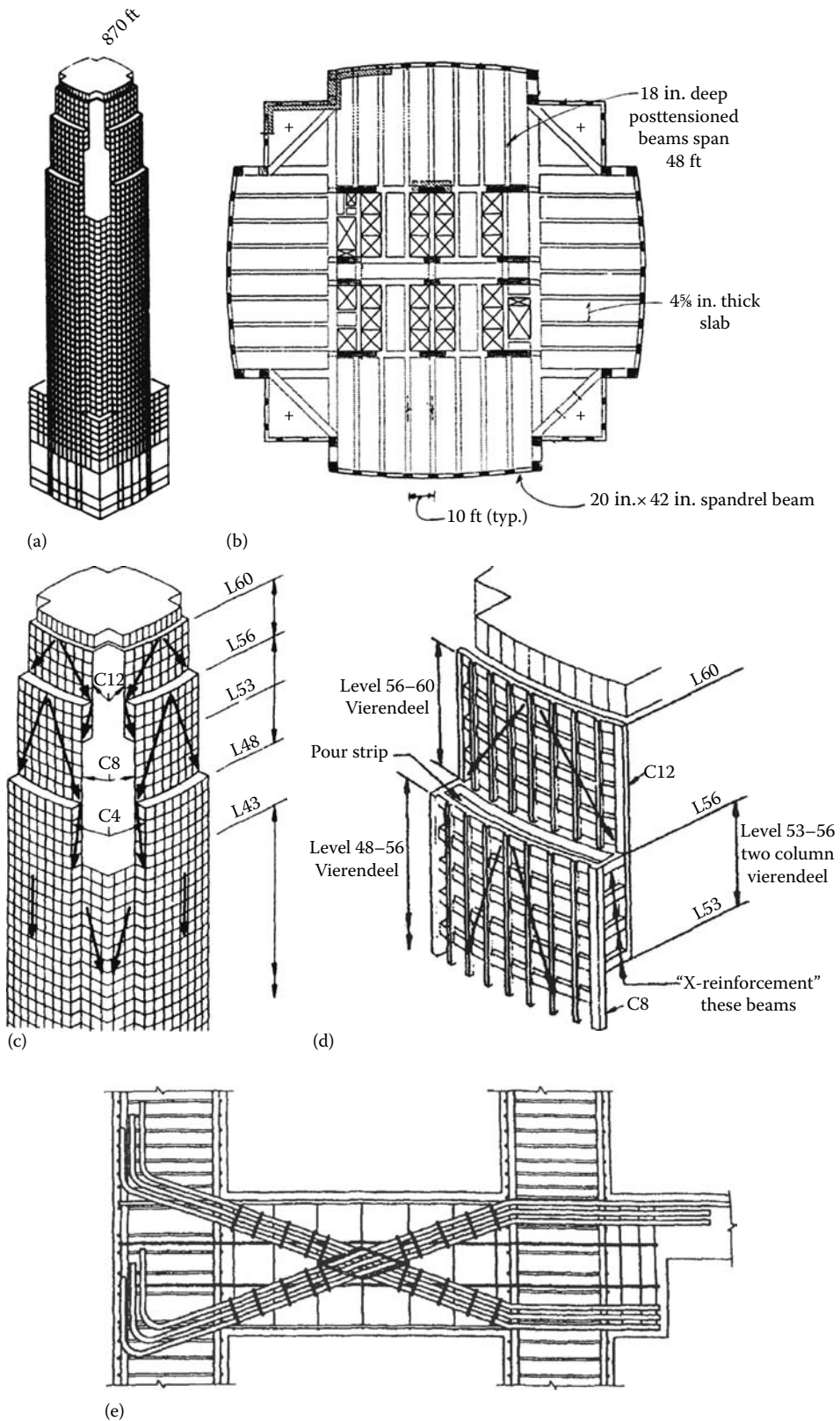


FIGURE 8.49 City Spire, New York City.



**FIGURE 8.50** NCNB Tower, North Carolina.

bottom to  $24 \times 24$  in. ( $610 \times 610$  mm) at the top, as well as for the core columns, ranging from  $2 \times 18$  ft ( $0.61 \times 3.5$  m) at the base to  $2 \times 3$  ft ( $0.61 \times 0.92$  m) at the top.

Normal-weight concrete was also used for posttensioned spandrels at the perimeter of each floor, but 5000 psi (34.5 MPa) lightweight concrete was used for the  $4 \frac{5}{8}$  in. (118 mm)-thick floor slabs and the 18 in. (0.46 m)-deep posttensioned beams. The two types of concrete were poured in quick succession and puddled to avoid a cold joint.

The foundation system for the Tower consists of high-capacity caissons under the perimeter columns and a reinforced concrete mat for the core columns. The high-capacity caissons were designed for a total end-bearing pressure of 150ksf (7182 kN/m<sup>2</sup>) and skin friction of 5ksf (240 kN/m<sup>2</sup>). The high bearing pressure required that the caissons be advanced through the fractured and layered rock zones into high-quality bedrock. Full-length casing was provided to prevent intrusion of soil and ground water into the drilled hole and for the safety of inspectors.

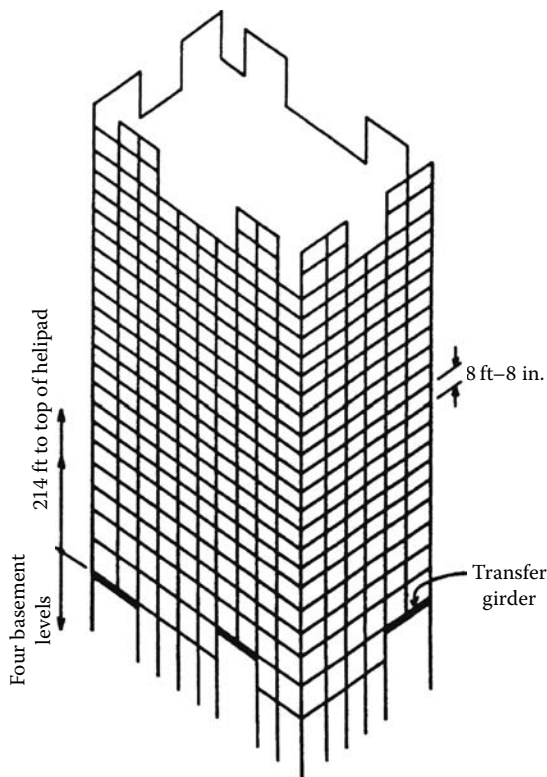
The core columns are supported on a foundation mat bearing on partially weathered rock. The mat dimensions are  $83 \times 93 \times 8$  ft ( $25.3 \times 28.35 \times 2.44$  m). The average total sustained bearing pressure under the mat is equal to 20ksf (958 kN/m<sup>2</sup>). The reported fundamental period of the building is 5.3 s. The building completed in the year 1992 was designed by Walter P. Moore and Associates, Inc., Houston, Texas.

#### 8.14.11 MUSEUM TOWER, LOS ANGELES, CALIFORNIA

This 22-story residential building, shown in Figure 8.51, consists of a tubular ductile concrete frame with perimeter columns spaced at 13 ft (8.96 m) centers interconnected with upturned spandrel beams. The exterior frame is of exposed painted concrete.



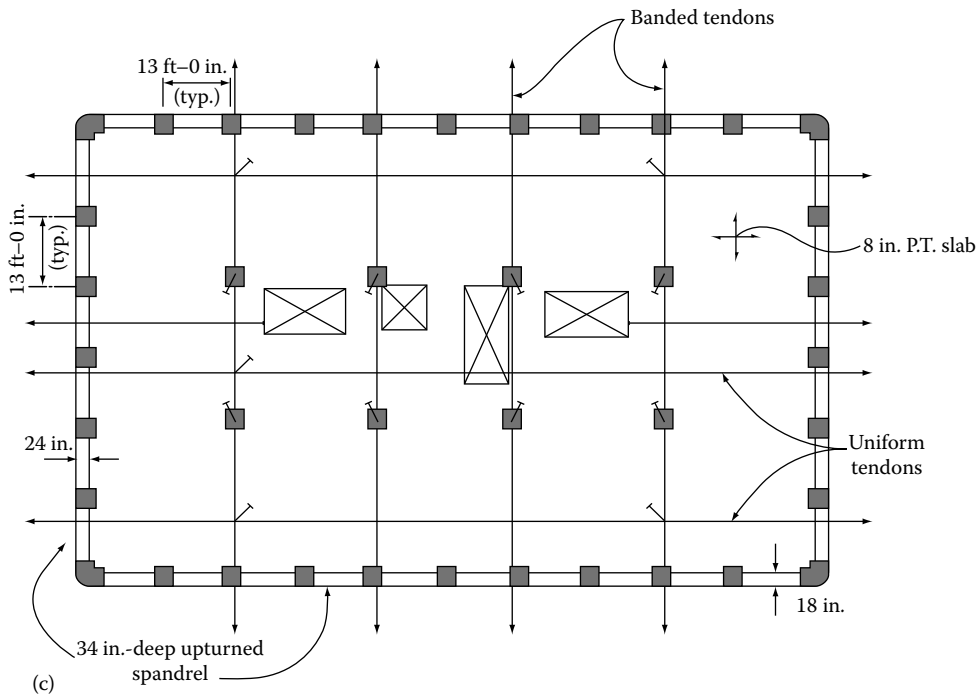
(a)



(b)

**FIGURE 8.51** Museum Tower, Los Angeles: (a) building elevation; (b) lateral bracing system;

(continued)



**FIGURE 8.51 (continued)** (c) typical floor framing plan.

The gravity system for the typical floor consists of an 8 in. (203 mm)-thick posttensioned flat plate with banded and uniform tendons running in the short and long directions of the building, respectively, as shown in Figure 8.51.

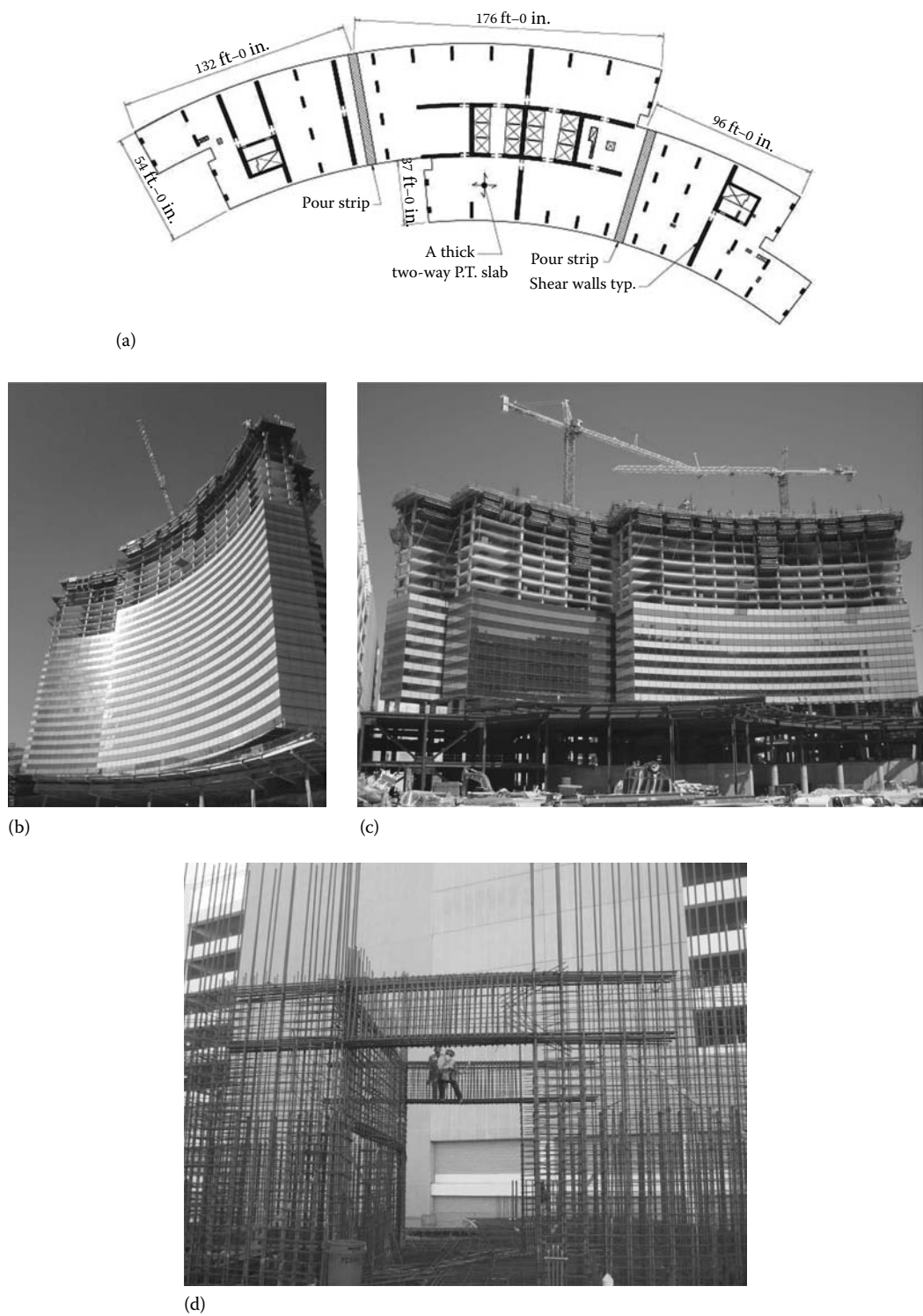
Although the building is regular both in plan and elevation and is less than 240 ft (78 m) in height, because of transfers at the base (Figure 8.51), a dynamic analysis using site-specific spectrum was used in the seismic design. The dynamic base shear was scaled down to a value corresponding to the static base shear. To preserve the dynamic characteristics of the building, the spectral accelerations were scaled down without altering the story masses. The structural design is by John A. Martin & Associates, Inc., Los Angeles, California.

#### 8.14.12 MGM CITY CENTER, VDARA TOWER, LAS VEGAS, NEVADA

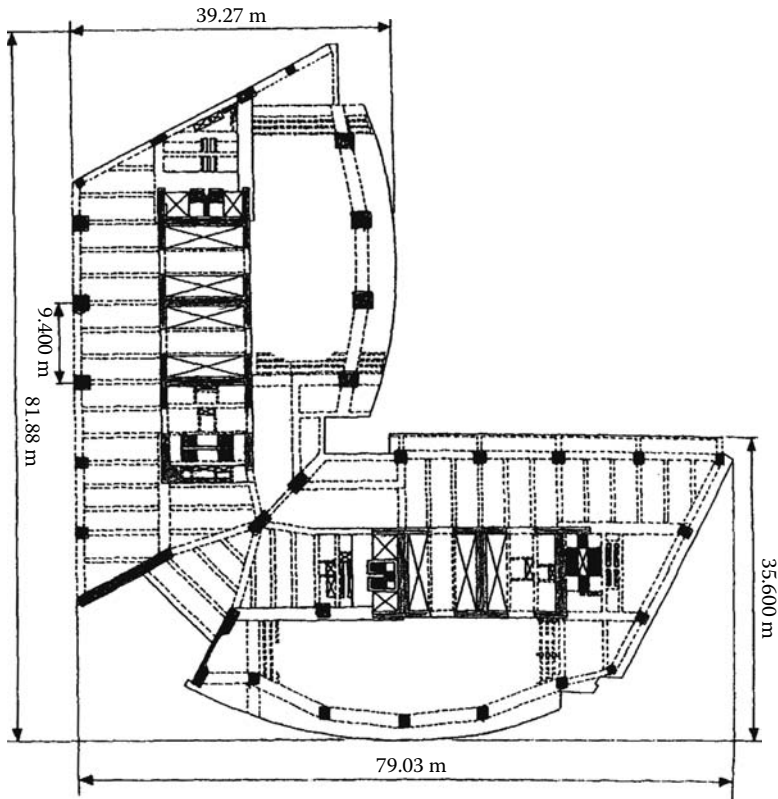
Located in Las Vegas on a 66-acre downtown site, this 57-story 1.5 million sq ft, mixed use project contains 1500-unit condominium hotel tower, retail areas, spa facilities, restaurants, back-of-the-house areas and parking. Construction completion is slated for December 2009.

The floor framing consists of 8 in. thick, posttensioned flat plate system with two pour strips, as shown in Figure 8.52a. The lateral system consists of cast-in-place reinforced concrete shear walls in both directions. Adjacent shear walls are interconnected with reinforced concrete link beams, some reinforced with diagonally intersecting rebars. The foundation system consists of mat foundation supported on 48 in. diameter drilled piers for the cores, and continuous pile caps also with 48 in. diameter piles for the typical gravity columns.

Construction photograph of typical building elements are shown in Figure 8.52b through d. The structural engineering is by DeSimone Consulting Engineers.



**FIGURE 8.52** Vdara tower; MGM Block B, Las Vegas, Nevada: (a) floor plan and (b–d) construction photos.



**FIGURE 8.53** City Bank Plaza, Hong Kong.

#### 8.14.13 CITYBANK PLAZA, HONG KONG

This 41-story building shown in Figure 8.53 is 772 ft (220 m)-tall with a four level below grade basement. The lateral loads are resisted by the internal core shear walls acting together with perimeter columns using outriggers at two levels. The floor system consists of 20 in. (508 mm)-deep one-way joist system spanning 31 ft (9.45 m) from the core to the exterior columns. The interior core walls are 40–48 in. (1.0–1.2 m) thick at the base while the columns are  $6.25 \times 10$  ft ( $1.9 \times 3$  m), spaced typically at 31 ft (9.4 m). Typical story height is 12.8 ft (3.9 m).

Because part of the building is seated above an entry way to a neighboring development, the perimeter columns rake outward along one face of the building over a one-story height. The resulting lateral forces are resisted by a prestressed beam system tied back to the cores, prestressing being applied in stages as construction progressed.

The building designed by Arup and Partners was completed in the year 1992.

#### 8.14.14 TRUMP TOWER, NEW YORK

This is a 58-story, 664 ft (202 m) tall building with a three level below grade construction. The lateral load system consists of a concrete shear core linked to perimeter columns via concrete out-rigger walls. The shear walls are 18 in. (457 mm)-thick at ground floor and the columns are  $32 \times 32$  in. ( $0.82 \times 0.82$  m) spaced at 24 to 40 ft (7.31 to 12.2 m). Various story heights, 9.5, 12, and 16 ft (2.89, 3.65, and 4.88 m) are used to accommodate residential, offices, and retail spaces.

Because the tower is a multiuse building, several column transfers are used. Through the 38 condominium levels, loads are carried by 52 concrete columns and concrete walls around the service core. At roof level, two outrigger walls 18 in. (450 mm) thick and 20 ft (6 m) deep link the core perimeter columns on two opposite sides to reduce lateral displacement in that direction. Extended shear walls do the same job in the other direction.

Below the 20th floor a system of transfer girders, 18–24 in. (450–600 mm) and 24 ft (7.3 m) deep allows for the transfer of 52 columns to only 8 columns through the 13 office levels. Because the transfer girders span between the interior core and exterior columns, they also act as outrigger walls to further control lateral displacement. The outriggers are pierced by openings for ducts, pipes, and doors.

Another transfer system comprising of two inclined columns in the form of an A frame exists between the 7th and 11th floor. The purpose is to open up the atrium space by removing two columns below the 7th level.

The 11,700 sq ft (10.87 m<sup>2</sup>) residential floors consisting of 16 in. (400 mm)-deep waffle slab and 7.5 in. (190 mm) flat slab were poured on a 2 day cycle. The reported fundamental period of the building is 5.2 s.

The foundation system consists of spread footings bearing on Manhattan mica schist. The building was completed in 1982. Structural engineering was by the Office of Irwin G. Cantor. Schematics are shown in Figure 8.54.

#### **8.14.15 TWO PRUDENTIAL PLAZA, CHICAGO, ILLINOIS**

The structural system for this 912 ft (278 m) tall, 64-story building, shown in Figure 8.55, consists of interacting core shear walls with the perimeter frame. Additionally, at levels 39 and 59 the interior shear walls are tied to the exterior columns via outrigger walls to control wind drift and reduce the overturning moment in the core shear walls. The outrigger wall at level 39 is story-deep at 16.5 ft (5.03 m) between levels 39 and 40, while the one at level 59 is 5 ft 5 in. (1.68 m) deep.

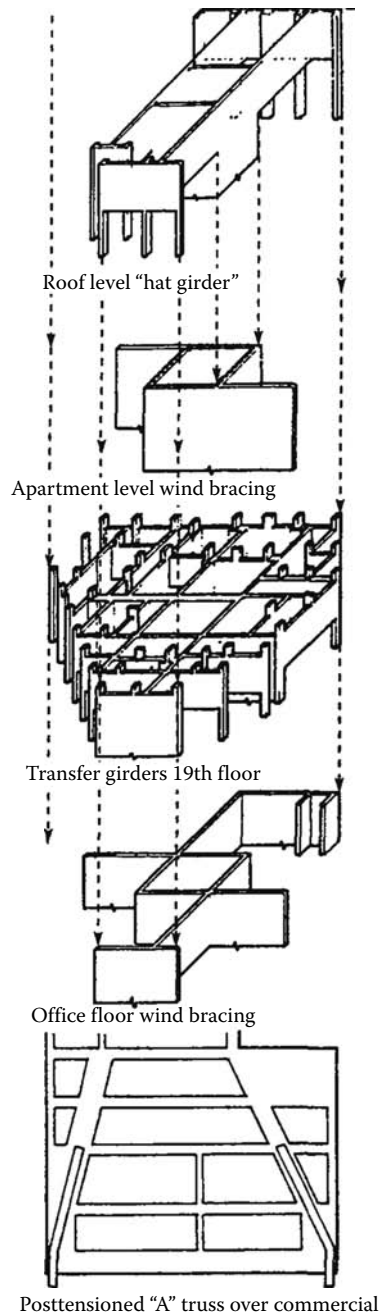
The building is rectangular at the lower levels, 122 ft 6 in. by 132 ft 8 in. (27.4 by 40.4 m) in plan, but becomes a square at the 59th floor due to a series of setbacks on the north and south faces. Above the 59th floor, the building starts tapering to form a “cone head,” which is topped by an 82 ft (25 m) architectural spire. The top elevation of the spire is 1000 ft (304.8 m).

The lateral stiffness in each direction is mainly provided by the four shear walls located in the core of the building. Their depth is 45 ft 4 in. (13.8 m). The flanges are 33 in. (838 mm) thick and the webs are 24 and 15 in. (610 and 380 mm)-thick for the interior and exterior walls, respectively. The south shear wall drops off at level 27 whereas the north wall does the same at level 40. The middle walls continue all the way to floor 59. The flanges of walls are connected together in the north–south direction by 27 in. (686 mm)-deep link beams.

The columns at the east and west faces are spaced at 20 ft (6.1 m) centers, whereas on the north and south faces they are spaced at 30 ft (9.15 m). The typical exterior column size varies from 35 × 45 in. (890 × 1140 mm) at the lower floors to 24 × 24 in. (600 × 600 mm) at the top floors. A maximum concrete strength of 12,000 psi (84 MPa) was used for columns and shear walls at the lower floors. The concrete strength was reduced to 6000 psi (42 MPa) at the upper floors.

The floor beams have a clear span of approximately 40 ft (12 m) from the perimeter columns to the shear wall core. Typical floor beam size is 38 in. (965 mm) by 24 in. (610 mm)-deep. Floor framing consist of a 6 in. (150 mm) thick normal-weight concrete slab with a clear span of 16 ft 10 in. (5.13 m) between the floor beams, spaced at 20 ft (6.1 m) centers. In addition to carrying the gravity load, the floor beams carry some of the wind shear from the shear walls to the outside columns. At the 40th and 59th floors the core is tied to the outside columns at two locations with the help of outrigger walls to control the wind drift and reduce the overturning moment in the core shear walls. The beams are full story deep at 16 ft 6 in. (5.03 m) between floors 39 and 40 and 5 ft 5 in. (1.68 m) at floor 59.





**FIGURE 8.54** Trump Tower, New York City.

The foundation consists of straight shaft caissons up to 10 ft (3 m) in diameter. These caissons rest on the bedrock, which is about 100 ft (30 m) below the existing ground level. The allowable bearing capacity is 200 t/sq ft (18 MPa). To fully utilize this capacity, (8000 psi) 56-MPa concrete was used in caissons. In the parking garage adjacent to the main tower, belled caissons were used. These caissons extend to hardpan about 70 ft (21 m) below existing grade. The allowable bearing capacity for this hardpan is about 36 t/sq ft (3.4 MPa). The structural design is by CBM Inc., Houston, Texas.

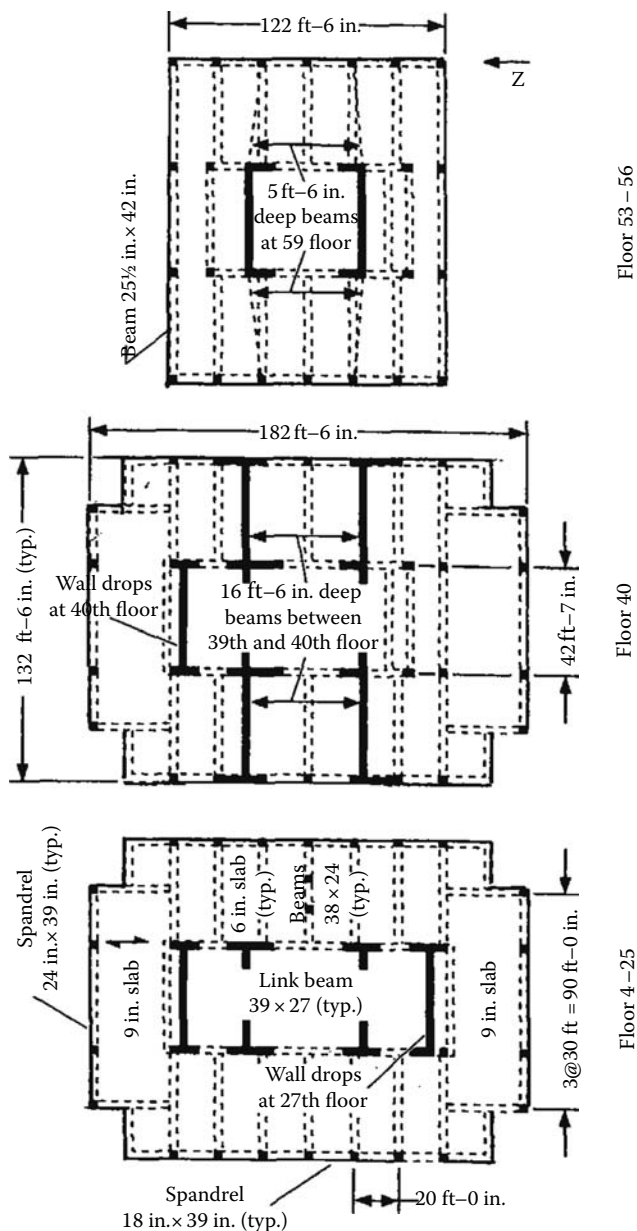
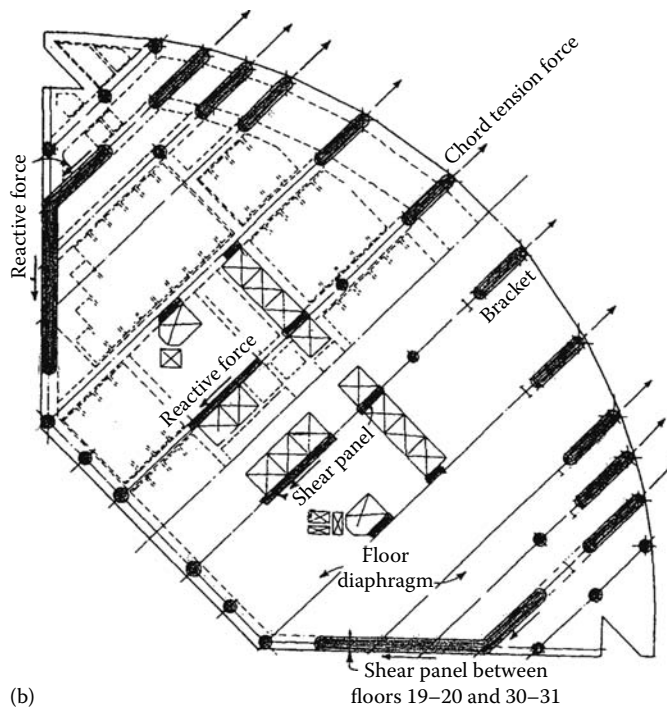
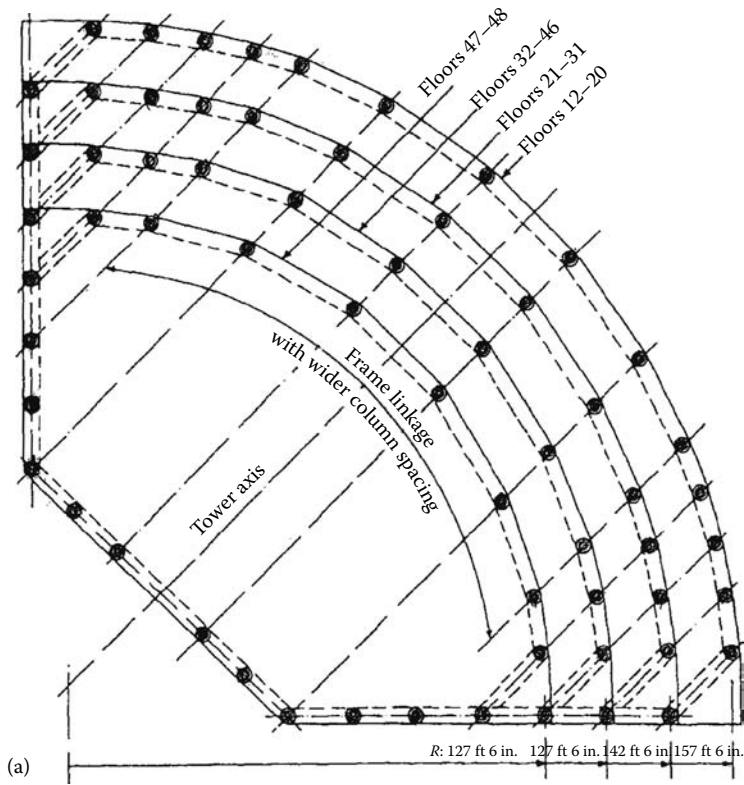


FIGURE 8.55 Two Prudential Plaza, Chicago.

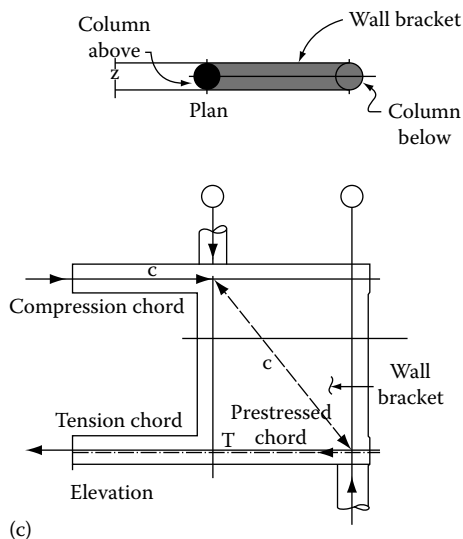
#### 8.14.16 CENT TRUST TOWER, MIAMI, FLORIDA

The building schematically shown in Figure 8.56 consists of a 48-story, 585 ft (178 m) tall office tower set on top of an 11-story parking structure. The office tower is a chamfered quarter circle in plan with three 15 ft (4.6 m) step backs at the circular face, as it rises up. The lateral loads are resisted by an interacting system of perimeter partial tubes and interior shear walls.

The typical floor framing consists of 20.5 in. (520 mm) deep pan joists spanning 35 ft (10.7 m) between 48 ft (14.6 m)-long haunch girders. Depth of haunch girders varies from 32 in. (813 mm) at the ends and matches the pan joist depth of 20.5 in. (520 mm) at the middle.



**FIGURE 8.56** Cent Trust Tower, Miami, Florida. (a) Schematic plan, (b) shear wall layout, and



**FIGURE 8.56 (continued)** (c) column transfer.

The step barks at the circular face of the building occur at floors 20, 31, and 46. Conventional girders are used to transfer columns at level 46, but at floors 20 and 31, a one-story deep wall acting as a bracket does the same job. Figure 8.56 shows the resolution of forces due to gravity load transfer. The tension chords at the bottom of the wall are prestressed with an effective force of 2500 k at levels 19 and 30. Where the bracket aligns with interior shear walls, the compression and tension forces resulting from the gravity load transfer are directly resisted by the walls. For the other brackets, these forces are indirectly transferred to the shear walls by the in-plane diaphragm action of thickened floor slabs (7.5 in. thick at levels 19 and 30 as compared to 4.5 in. thick for typical floors).

Each of the interior shear walls is transferred to two columns at the 10th floor of the garage to facilitate traffic flow. Typical columns in the garage are 42 × 74 in. (1067 × 1880 mm) rectangular, and 54 to 42 in. (1372 to 1067 mm) in diameter. Tower columns vary from 42 in. (1067 mm) diameter at lower floors to 30 in. (762 mm) diameter at the top. Spandrel beams are 36 in. deep in the tower but vary in depth at the garage floors from 54 in. (1372 mm) at three straight sides to 32 in. (813 mm) along the area due to headroom requirements.

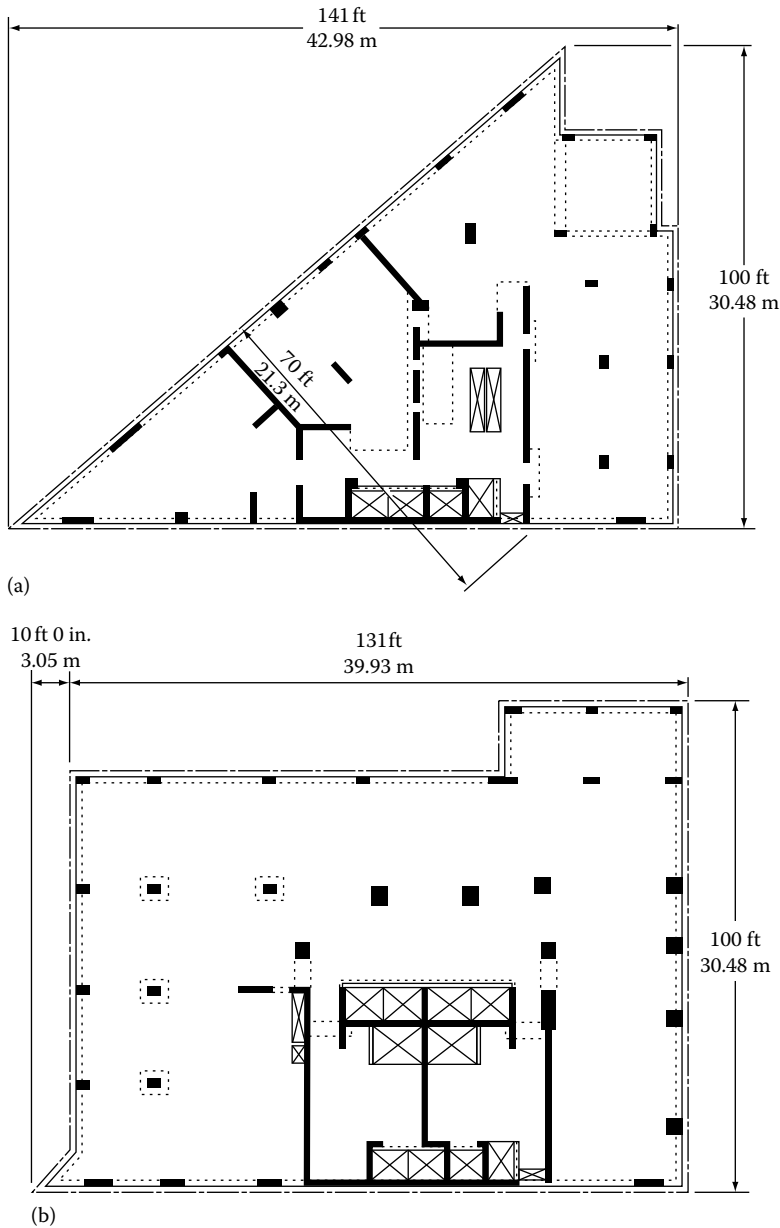
The tower is supported on a 7–8 ft (2.1–2.44 m) thick mat bearing on 14 × 14 in. (350 × 350 mm) precast piles. Garage columns are founded on spread footings. The structural engineering is by CBM Inc. Houston, Texas.

#### 8.14.17 METROPOLITAN TOWER, NEW YORK CITY

This is a 68-story, 716 ft (218 m)-tall building completed in the year 1985. The lateral load resisting system consists of coupled shear walls interacting with perimeter frames. The size and spacing of exterior columns vary, as shown in Figure 8.57. The perimeter spandrel beam is 20 in. (508 mm) deep. The floor framing consists of an 8.5 in. (216 mm)-thick flat slab.

The building has an L-shaped commercial base for the bottom 18 stories, with a 46-story triangular condominium tower sitting atop. Two more stories occur above the 46th story for housing mechanical equipment. The typical floor-to-floor height for the condos is 9 ft 8 in. (2.96 m) while for the commercial floors it is 11 ft 4 in. (3.45 m).

To keep an efficient column grid in the commercial floors, a two-story reinforced concrete mechanical floor is used to transfer column loads from the triangular upper plan of the building's upper tower to the L-shaped base. In effect, the transfer level acts as a foundation at the sky for the upper tower.



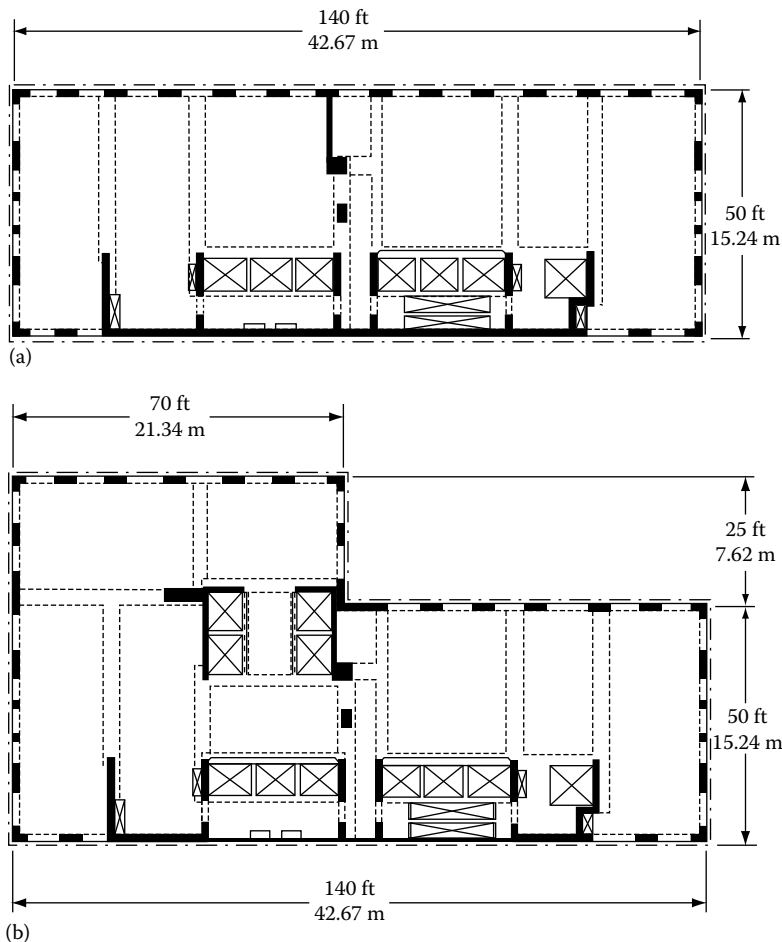
**FIGURE 8.57** Metropolitan Tower, New York City. (a,b) Framing plans.

Transfer girders at this level are 13 ft (4 m)-deep and were cast in two stages, the bottom 2 to 3 ft (600 to 900 mm) being cast first to serve as support for the remainder of the concrete in the second pour.

The foundation consists of spread footings on rock, with a bearing capacity of 40 t/sq ft (4 MPa). The structural design is by Robert Rosenwasser Associates.

#### 8.14.18 CARNEGIE HALL TOWER, NEW YORK CITY

The lateral load resisting system for this 757 ft (230.7 m)-tall 62-story building, shown in Figure 8.58, is a bundled tube, consisting of two side-by-side concrete tubes. With plan dimensions of



**FIGURE 8.58** Carnegie Hall Tower, New York City. (a,b) Framing plans.

50 × 75 ft (15.2 × 22.9 m), the building's height-to-width ratio is approximately 10, making it one of the most slender buildings.

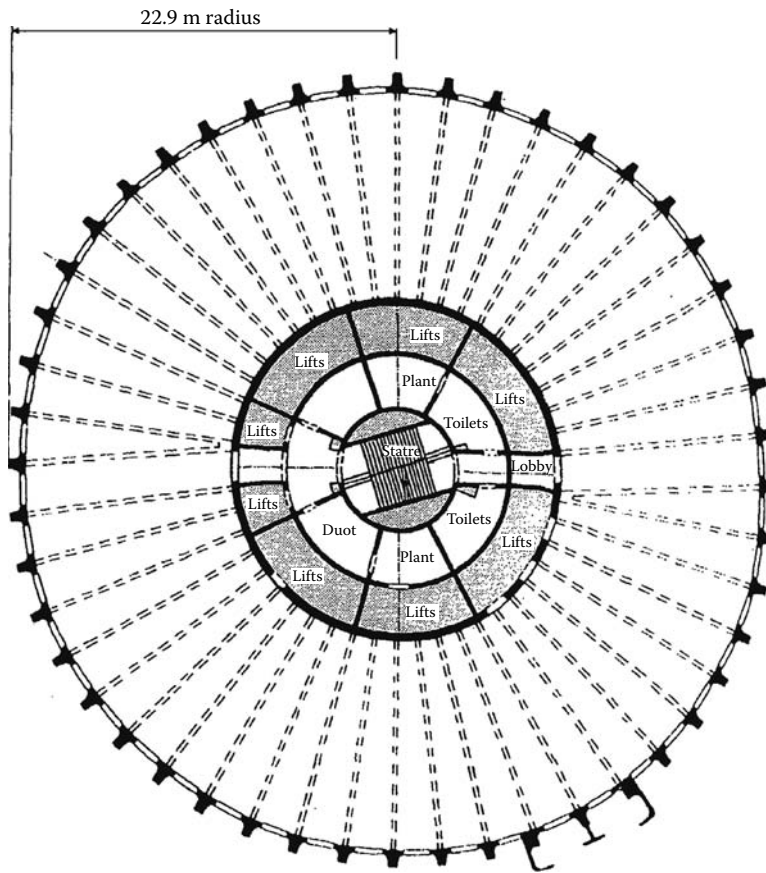
The floor system consists of a one- and two-way 9 in. (230 mm) slab spanning between 18 in. (457 mm)-deep interior beams of various span and spacing, as shown in Figure 8.61. The spandrel beams connecting the tube columns are 30 in. (762 mm) deep. Typical story height is 12 ft (3.66 m).

The reported periods of the building are 4.8 s; east–west direction, 3 s; and north–south direction 2 s torsion. The foundation consists of spread footings on rock with a bearing capacity of 40 t/sq ft (4 MPa). Structural engineering is by Robert Rosenwasser Associates.

#### 8.14.19 HOPEWELL CENTER, HONG KONG

The structural system for this 708 ft (216 m)-tall, 64-story building (see Figure 8.59) consists of a perimeter tube formed by 48 columns at a spacing of 10 ft (3 m) linked by a 66 in. (1670 mm)-deep spandrel beam. Some resistance to lateral loads is also provided by the interior shear walls.

Radial beams span the 40 ft (12.3 m) distance between the perimeter columns and the interior core walls. The depth is 27 in. (686 mm) including the slab thickness of 5.9 in. (100 mm). The perimeter columns spaced radially at 10 ft (3 m) are 4.75 × 4.0 ft (1.45 × 1.22 m) at the ground floor. The shear walls are 30 in. (762 mm) thick at the base. The tower is founded on spread footings sitting on



**FIGURE 8.59** Hopewell Center, Hong Kong. Schematic Plan.

granite very close to ground level, at levels varying between the underside of basement and the third floor. The structural engineering of the building completed in 1980 is by Ove Arup and Partners.

#### 8.14.20 COBALT CONDOMINIUMS, MINNEAPOLIS, MINNESOTA\*

This mixed use development consists of 150,000 sq ft of residential and 45,000 sq ft of commercial space plus parking for both condo residents and retail customers. Built in 2006 the building uses an innovative structural system consisting of precast, prestressed trusses (see Figure 8.60a through c).

The floor framing system is hollow core precast planks, supported on precast, prestressed, open-web trusses. The trusses are a full story tall, and are located on every other floor. The trusses are spaced at 41 ft-0 in. o.c., and are located at party walls between condominium units. Floors without trusses are free of interior structure, only having columns at the building exterior. The chords of the trusses are an inverted T shape, with ledges that provide bearing for the precast plank. Solid precast concrete slabs are used around the perimeter of the tower to allow extensions of the slab edge for balconies. The slabs have insulation embedded to reduce their weight.

The lateral system is precast concrete shear walls, located mainly at the stair and elevator shafts. Wind controlled the design of the lateral system. Grouted splice sleeves were used at the base connections to the foundation, in order to resist the uplift forces. The hollow core floors were designed as rigid diaphragms.

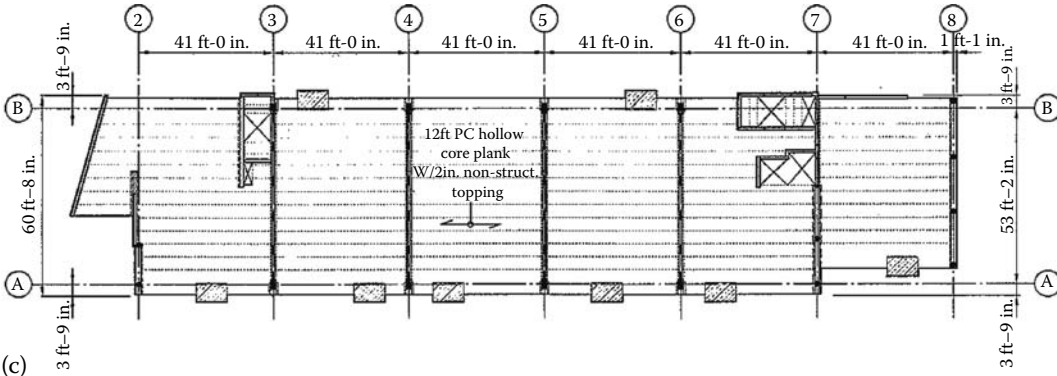
\* The author wishes to acknowledge is gratitude to Mr. Tim Morey, PE of Ericksen Roed & Associates for providing information on this project.



(a)



(b)



(c)

**FIGURE 8.60** Cobalt Condominiums, Minneapolis, Minnesota: (a) photograph of completed building, (b) erection of prestressed precast truss, (c) eighth floor framing plan, *(continued)*



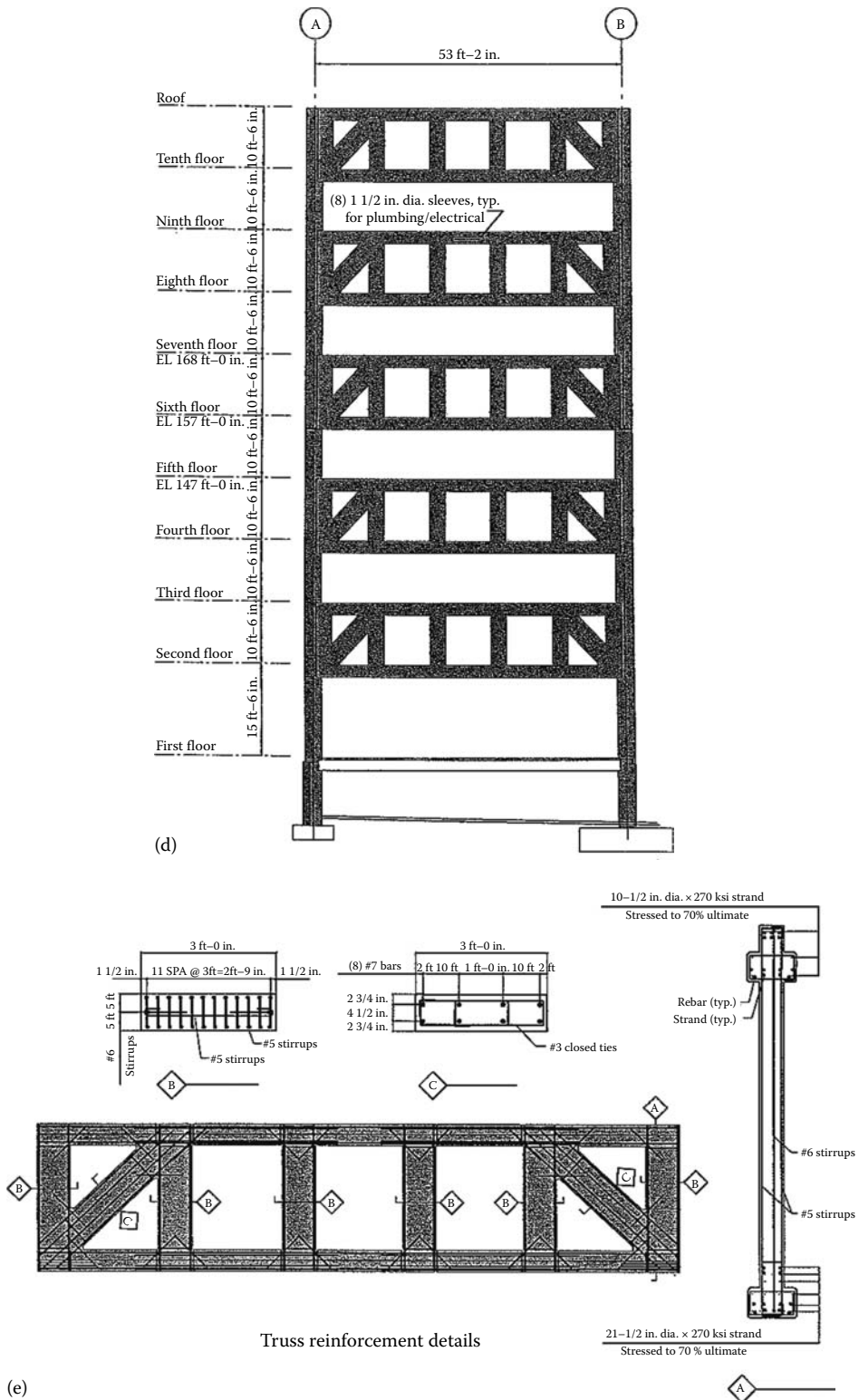


FIGURE 8.60 (continued) (d) interior truss, and (e) truss reinforcement details.

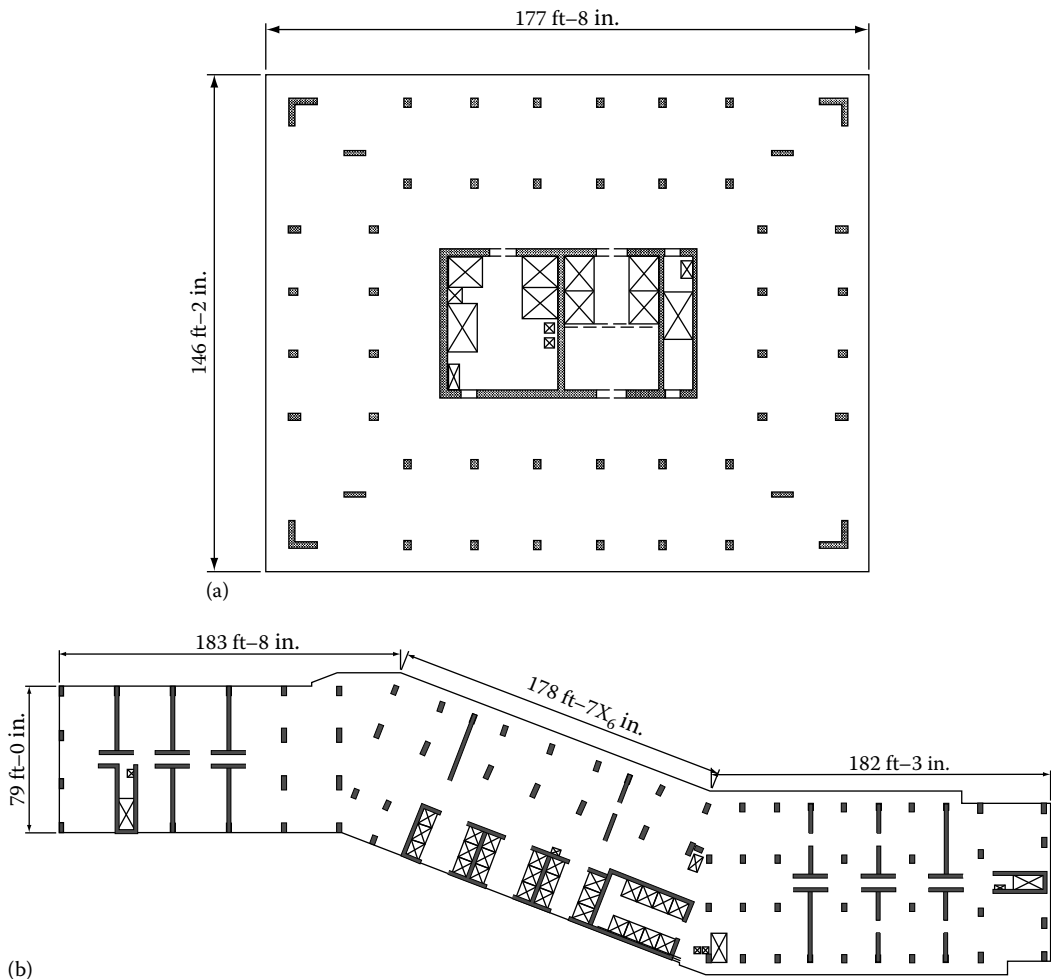
The truss system was especially well-suited for the Cobalt project because the small number of columns created large open areas on all levels, particularly so at the street level retail space, and the below grade parking.

The foundation system is primarily conventional spread footings. Drilled concrete piers were used in some locations around the perimeter due to close proximity to existing city streets. Cast-in-place basement walls enclosed the one level of below grade parking.

The tallest building to date (2008) using the system is a 14-story building, Oak Park Terrace, in Oak Park, IL. Structural engineering for both the projects is by Ericksen Roed & Associates.

#### 8.14.21 THE COSMOPOLITAN RESORT & CASINO, LAS VEGAS, NEVADA\*

The Cosmopolitan Resort & Casino shown schematically in Figure 8.61a through e, is a high-density, ultra-compact, mixed-use development that combines city-living with all the amenities of a full-scale gaming resort. The project packs nearly 7 million sq ft of functional space into a narrow eight-and-a-half



**FIGURE 8.61** The Cosmopolitan Resort & Casino, Las Vegas, Nevada. (a) East tower, (b) West tower, *(continued)*

\* The author wishes to acknowledge his gratitude to Heinz Kuo, project engineer, Rani Athelon, Project Manager and David Sze, S.E., Associate, DeSimone Consulting Engineers, Las Vegas, Nevada, for providing information on this project.



(c)



(d)



(e)



(f)

**FIGURE 8.61 (continued)** (c–f) project photographs.

acre lot, and will consist of two concrete towers rising from a six story steel podium structure. The podium houses a 5 acre pool deck, a 75,000sq ft casino, a 150,000sq ft convention and meeting space, a 1,800 seat theater, a 50,000sq ft spa and salon and over 300,000sq ft of entertainment space. Five basement levels beneath the podium are used for underground garage parking. Above the podium, the East and West Towers rise to a height of 654 and 662 ft, respectively.

One of the foremost challenges was to create as much open and unobstructed space in the podium below the residential towers as possible. The two towers are sprawled over roughly 25% of the podium floor map—sitting on top of key, central areas of the podium. Since the towers use a typical concrete flat plate construction, with columns and walls spaced anywhere from 18ft-6in. to 30ft-0in. apart, the towers' columns and walls would have disrupted a considerable amount of convention, meeting, retail, and casino space where they run through the podium.

The solution was to create a “sky mat” at approximately 100 ft above grade, at podium levels four and five. All of the tower gravity columns and almost all but a few of the elevator core walls are terminated at the sky mat to create open spaces in the podium below. The 6 ft-0 in. thick sky mat was poured in three separate lifts above the podium deck. Each lift was designed to sustain the weight

of the concrete already poured and the weight of the subsequent lift of wet concrete. Staging the concrete pour for the sky mat facilitated savings in construction shoring.

The sky mat served to transfer the towers' gravity loads and overturning forces down to the foundation. The towers' shear forces are transferred out to the perimeter podium walls by a reinforced 12 in. thick composite deck. The sky mat is supported on concrete-filled steel box columns. There are 75 box columns supporting the sky mat for the West Tower. Forty-eight box columns support the sky mat for the East Tower. The box columns vary in dimensions from 3 ft-0 in. to 4 ft-0 in. and were fabricated in Japan using grade 65 plates, varying in thickness from 1 in. to 4 1/2 in. The box columns were shipped and erected in segments—the heaviest of which was 35 ft long and weighed 85 kip (without concrete).

Composite steel shear walls are used as the lateral system for the podium. The walls are located at the perimeter of the podium to allow greater operational functionality and architectural flexibility within the podium structure. However, placing the walls adjacent to the property line caused tight site constraints.

The Cosmopolitan subterranean garage levels, having to provide enough space for 3800 cars over a narrow plan, required one of the deepest digs in Las Vegas history. Slurry walls were employed to retain the 60 ft of soil pressure surrounding the subterranean garage. In addition, the slurry wall panels were extended 40 ft below the foundation to cut off ground water flow beneath the project substantially reducing the dewatering demands for the lifetime of the building.

In selecting the foundation system, due consideration was given to avoid the post-construction differential settlement that has been problematic for other large construction along the Strip. Therefore, a mat foundation with micropiles installed at peak bearing stress areas was selected.

The Cosmopolitan is expected to open in December 2009. Structural engineering is by DeSimone Consulting Engineers, Las Vegas, Nevada.

#### **8.14.22 ELYSIAN HOTEL AND PRIVATE RESIDENCES, CHICAGO, ILLINOIS**

This project, under construction at the time of writing (2009), is a 638,000 sq ft of mixed-use space with retail, parking, hotel, and condominium functions located on E. Walton Place, just minutes from Chicago's iconic Magnificent Mile. The west side of the site consists of a four-story (60 ft tall) steel structure above grade containing retail facilities, office, restaurant, fitness, pool, and an open motor courtyard. To serve residents and hotel visitors, four levels of below grade parking are provided under the courtyard. A 61-story (685 ft tall) reinforced concrete tower structure marks the east side of the site. A one-level basement, 16 ft deep, will be constructed under the tower for mechanical and office usages and the ground level will contain lobby, retail, and service facilities. There will be five stories of hotel amenity space such as a spa, a restaurant, meeting rooms, and ball room facilities. The next 19 stories will contain hotel room space with balconies. Mechanical floors are provided at levels 27 and 28 and above the penthouse level. The tower columns are transferred at level 28 with a 6 ft-0 in. thick slab to accommodate the building set back at the east and west sides of level 29. Residential condominium space is provided in the upper portion of the tower at level 29 through 59. Column transfers at level 51, 52, 57, and 59 are supported by posttensioned concrete beams or thickened slabs. A Tuned Liquid Damper (TLD), consisting of four reinforced concrete tanks with water, is located at the top of the building to control building accelerations. The Elysian Hotel and Private Residences is one of the first residential buildings in the United States to integrate a TLD into the structural design. Additionally, the superstructure will be clad with insulated precast concrete panels and metal panels.

##### **8.14.22.1 Foundations**

The foundations for the columns and walls are founded on belled caissons bearing on hardpan clay with an allowable bearing capacity of 32 ksf. High-strength 8000 psi concrete was specified. The caisson shafts range in size from 2 ft-6 in. to 7 ft-0 in. with bell sizes from 4 ft-0 in. to 20 ft-0 in. To limit total and differential settlements, special construction sequence have been considered.

The center core shear walls are supported with a 12 ft-0 in. thick mat foundation that are supported by a group of eight caissons with 7 ft-0 in. shafts and 20 ft-0 in. bells. The caissons resist lateral base shears from the core shear walls. Reinforcing for the mat consists of #11 top and bottom reinforcing bars and #9 shear reinforcing bars. An 8000 psi mix design was specified for strength. Megacolumns, 6 ft-0 in. by 10 ft-6 in. located at the north and south perimeter sides, are supported by mega grade beams 12 ft-0 in. wide by 16 ft-0 in. deep. A total of 228-#11 reinforcing bars are provided for the bottom and 114-#11 for the top reinforcing. Shear reinforcing consisted of #7 bars with 14 legs. Because of the thickness of the mat and mega grade beams, concerns for the heat of hydration and maximum differential temperature between the center of the members and their surfaces became apparent. To prevent unwanted cracking, mass concrete provisions were specified. These included the maximum temperature during the curing process and maximum temperature gradient between the center of the members and the surfaces. A self-consolidating, low heat of hydration mix design was provided by the contractor to satisfy these provisions. Thermal sensors were used to monitor the temperatures within the members for a specified time period.

Four levels of parking are located at the west side of the site. The lowest level is 47 ft below grade. Because of lateral earth pressures at this depth, 30 in. thick reinforced concrete slurry walls were designed with 4000 psi concrete. The walls provide lateral earth support for the below grade parking while also supporting the gravity loads from the low-rise steel building above. Under the footprint of the tower on the east side, a one-level basement has 14 in. thick perimeter reinforced concrete walls to resist lateral earth pressures and transfer lateral base shear from the tower superstructure to the soil.

During construction, the temporary earth retention system for the below grade parking structure consisted of four levels of internal steel pipe bracing with wide flange whalers. These members braced the concrete slurry walls until the permanent 10 in. two-way reinforced concrete flat slabs were constructed at each level. The pipe bracing spanned diagonally at the corners and 122 ft in the north-south direction. Steel sheeting was installed at the tower basement perimeter and large diameter pipes were used to brace the sheeting internally. The bracing spanned 96 ft in the north-south direction. All the temporary earth retention systems were designed by the contractor.

#### **8.14.22.2 Floor Systems**

A 10 in. two-way reinforced flat slab with drop panels is used at the four levels of below grade parking under the courtyard. The floor plate has dimensions of 121 ft  $\times$  121 ft. The concrete strength is 6000 psi. The slab resists horizontal earth pressures acting simultaneously with vertical gravity loads.

The typical hotel level floor plate is 97 ft in the north-south and 126 ft in the east-west directions. The typical condominium floor plate is 86 ft in the north-south and 112 ft in the east-west directions. Columns are located only at the perimeters that help create open, column-free space between the perimeter and center core walls. An 8 in. two-way, posttensioned concrete flat plate supports typical residential live loads. The slab spans 34 ft from perimeter to core wall and 50 ft between concrete outrigger walls. The concrete strength is 5000 psi. Slab deflections were limited to the span divided by 360 for live loads, or the span divided by 240 for total long-term sustained loads after partitions are installed. Perimeter slab deflections were limited to 1/2 in. or less where it supports the precast building façade.

The transfer slab at east and west sides of the concrete core at level 28 is a 6 ft-0 in. thick two-way conventionally reinforced flat plate. Seven concrete columns on each side of the core are transferred from above which support 29 condominium levels. The slab is reinforced with #11 bars at the top and bottom along with #9 bars shear reinforcing at the columns were required for punching shear resistance. For constructability purposes, the transfer slab was poured in two separate sections. The first was a 2 ft-0 in. thick bottom section followed by the remaining 4 ft-0 in. thick top section several days later. The first 2 ft-0 in. thick bottom portion was designed by the contractor with post-tensioning to assist in supporting the wet weight of the remaining 4 ft-0 in. thick pour section. The project Engineers of Record, Halvorson and Partners (HP) designed the slab portions to behave compositely by adding vertical shear reinforcing throughout the slab footprint to transfer horizontal

shear forces. The top of the slab was intentionally roughened per ACI requirements to provide shear friction between the two pours and the concrete strength is 6000psi for both pours. HP also evaluated the effects of the posttensioning on the slab behavior for the final condition where the composite slab sections together resist the applied transfer column forces. Close communication and coordination with the contractor was needed for the construction of level 28 to be successful.

A full-story transfer beam is located from level 5 to 7, with dimensions of 5 ft-8 in. wide by 19 ft-6 in. deep, to support two transferred columns. The columns support floor framing from level 8 to 58. A high-strength concrete of 12,000psi is provided and reinforcing consists of #11 top and bottom bars with #7 shear reinforcing.

#### **8.14.22.3 Gravity System**

The perimeter-reinforced concrete columns and the interior core walls comprise the gravity system. All cladding will be supported directly by the perimeter-reinforced concrete columns and selected floor slabs.

#### **8.14.22.4 Lateral System**

The lateral load resisting system consists of an 18 in. thick central reinforced concrete shear wall surrounding the core elements and four reinforced concrete “megacolumns” located on the north and south sides of the tower. The central shear wall has out dimensions of 21 ft-6 in. in the north–south and 56 ft-6 in. in the east–west directions. The mega-columns are 6 ft-0 in. by 10 ft-6 in. at the base and transition in size throughout the height of the building. Outrigger shear walls in the north–south direction connect the core to the mega-columns. These walls start at level 7 and terminate at level 40 on the south side and level 51 on the north side to create open spaces for the top condominium units. The walls beginning at Level 7 allow for flexibility in the space layout for the hotel functions. Reinforced concrete link beams will be provided at the openings in the shear walls. The widths of the link beams typically match the thickness of the shear walls at the central building core. Link beams between the core and the outrigger walls are typically wider than the walls. Lateral forces are resisted by the Outrigger-Braced system in the north–south direction and the central shear walls in the east–west direction. The concrete strength for the mega-columns, core shear walls, outrigger walls, and link beams transitions from 12,000psi at the base to 8,000psi to 6,000psi to 5,000psi at the top of the building. Overall building drift is  $H/800$  at the roof of the building yielding a relatively stiff building. The calculated building periods are as follows:

- First Mode, East–West direction: 4.37 s
- Second Mode, North–South direction: 3.87 s
- Third Mode, Torsion: 2.9 s

#### **8.14.22.5 Tuned Liquid Damper\***

Wind tunnel testing was conducted for the building by the Boundary Layer Wind Tunnel Laboratory (BLWTL) at the University of Western Ontario. Wind and dynamic effects governed the structural design of this residential building due to its slender nature. The building minimum width-to-height ratio is greater than 7. The building stiffness alone was determined to be insufficient in bringing accelerations within acceptable limits without increasing costs substantially and yielding impractical architectural space layouts. With the assistance of the BLWTL, Halvorson and Partners studied options for different combinations of structural stiffness and damping to develop a cost-effective structural solution that incorporates a TLD at the top of the building. The TLD is the latest approach to controlling motion in tall, slender buildings offering low cost, low maintenance, and high performance over a broad range of wind conditions. The Elysian is one of the first residential towers in the United States to incorporate this technology. Water-filled concrete tanks fitting the central core wall

---

\* The author would like to acknowledge his gratitude to Mr. Timothy W. Laken, SE, PE, Senior Project Engineer, and Bob Halvorson P.E. founder of Halvorson Partners, Chicago, for providing information on this project.

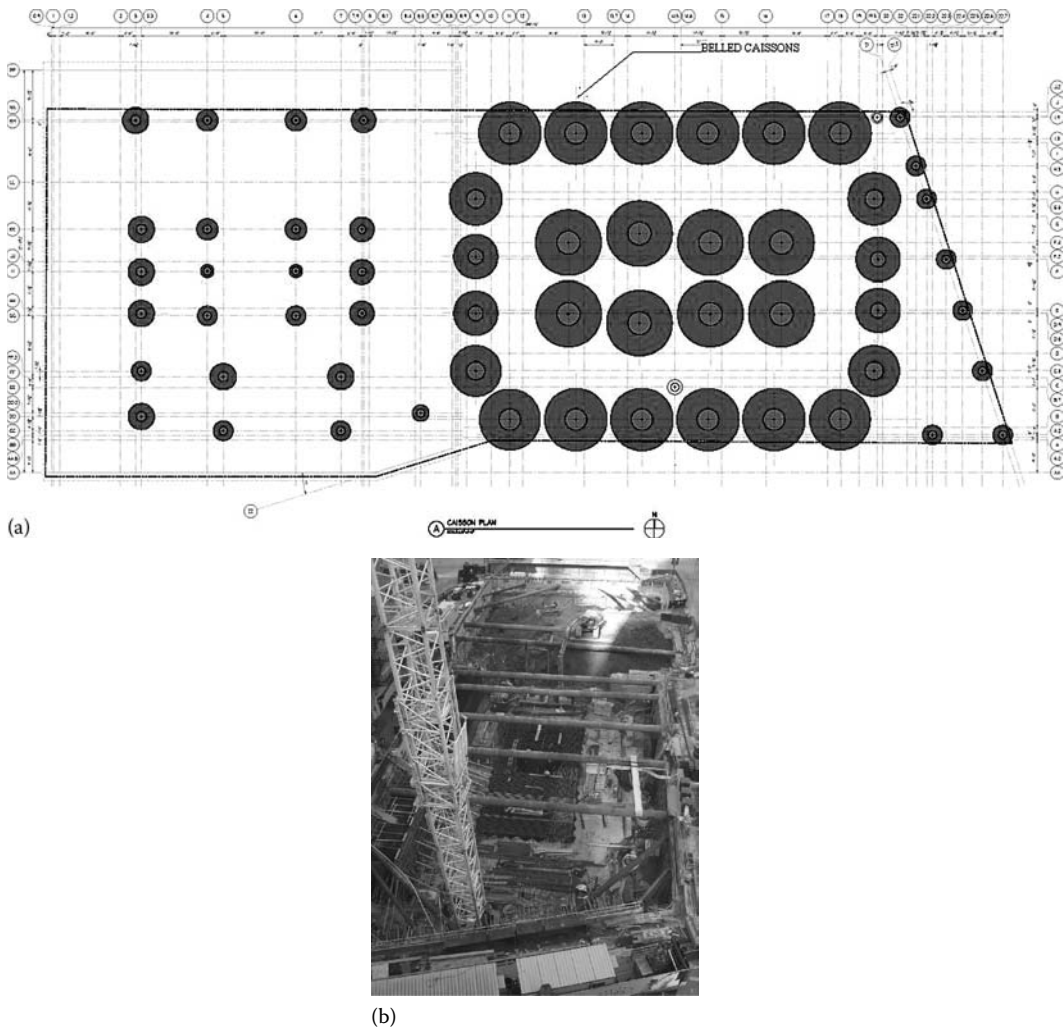
footprint will be located at the top of the building. The movement of the water will be controlled with internal steel baffles that produce a sloshing effect. The water motion works opposite to the building motion to control accelerations produced from wind forces. The Elysian's TLDs will be tuned in two directions to mitigate motion perception.

The structural engineering for the project is by Halvorson Partners, Chicago, Illinois.

Schematic plans, elevations, and photographs are shown in Figure 8.62.

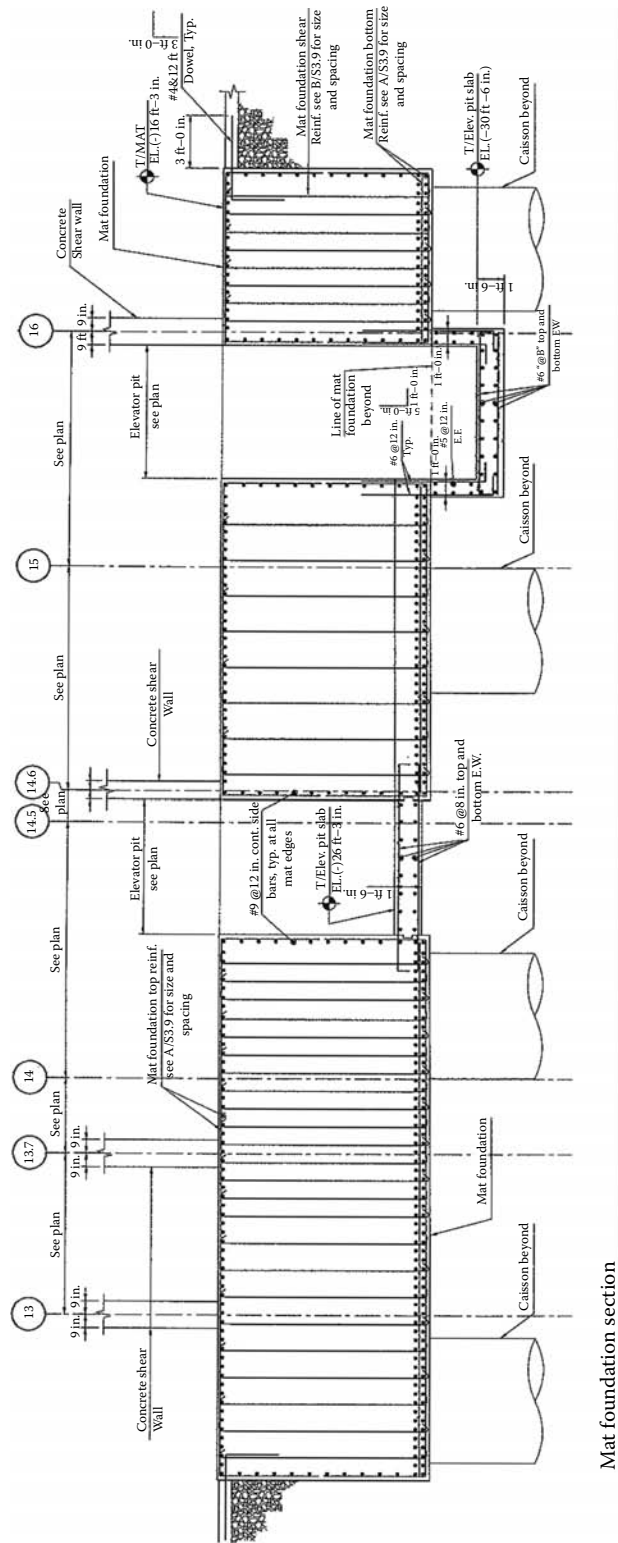
### 8.14.23 SHANGRI-LA NEW YORK (610 LEXINGTON AVENUE), NEW YORK\*

The Shangri-La New York hotel project, located at 610 Lexington Avenue, is a 67-story luxury condominium/condominium hotel located in midtown Manhattan at the corner of Lexington Avenue and 53rd Street. The 300,000sq ft building contains two-and-a-half below grade levels, a



**FIGURE 8.62** Elysian Hotel and Private Residences, Chicago. (a) Schematic foundation plan, (b) foundation bracing system,

\* The author wishes to acknowledge his gratitude to Mr. A. Christopher Cerino, Associate Principal, DeSimone Consulting Engineers, New York for providing information on this project.



Mat foundation section  
Scale: 1/4 in. = 1 ft-0 in.

(c)

FIGURE 8.62 (continued) (c) mat foundation,

(continued)



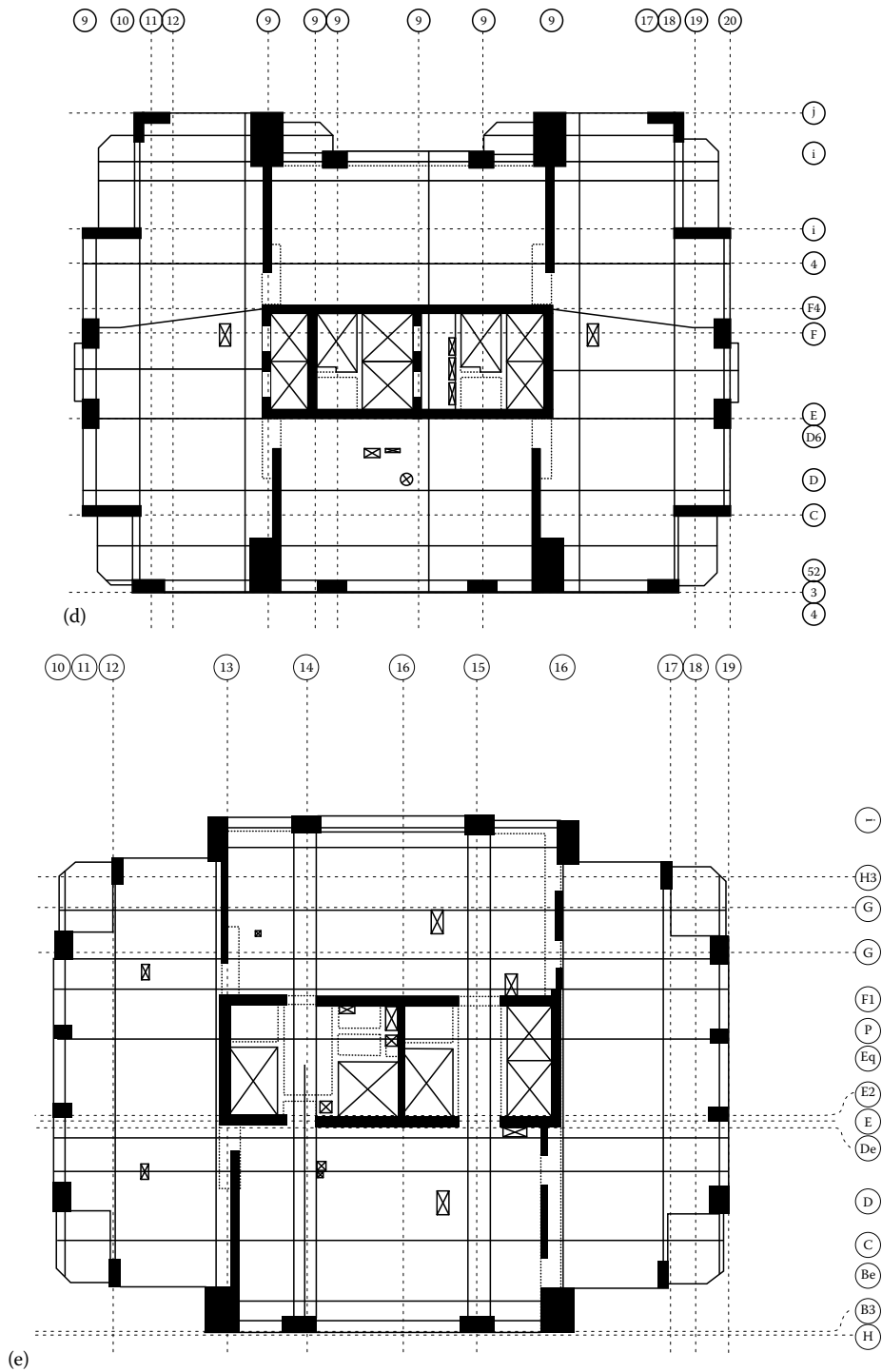


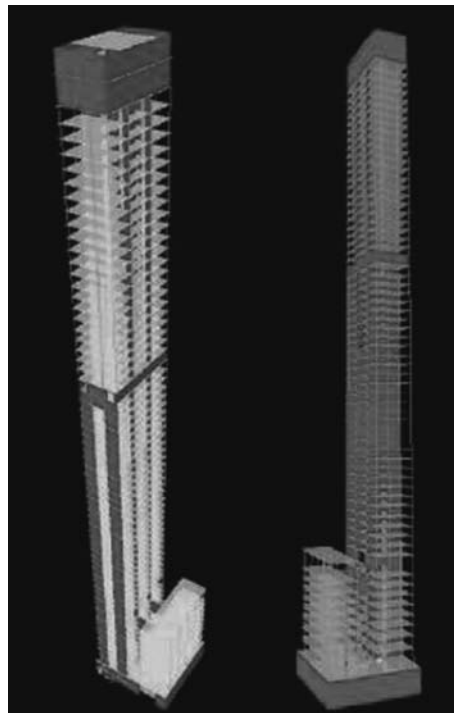
FIGURE 8.62 (continued) (d) levels 5–10 post-tensioning plan, and (e) levels 30–34 post-tensioning plan.

10-story tower located at the east end of the site and a 67-story tower covering the west side of the site. Construction planning required extensive complex land-use agreements with adjacent property owners to ensure the new building would have minimal impact on the surrounding properties. Constructed on the former site of a YWCA, the building is in close proximity to many notable landmarks including the Seagram Building and Lever House. The project was further complicated by New York's ULURP (Uniform Land Use Review Procedure) and Landmarks approval process and the location of two MTA subway lines adjacent to the site under Lexington Avenue and 53rd Streets. With stringent zoning restrictions to the north due to the city of Manhattan's sky exposure plane and to east due to a "light and air" easement for the southern office tower, most of the available zoning floor area had to be compressed into the western portion of the site. With a tiny 3500 sq ft tower footprint available (43 ft wide, 80 ft long), the building will rise 709 ft giving the structure a very slender aspect ratio of 16.5:1. To overcome this challenge, the design implements the first use of vertically posttensioned shear walls in New York City. In addition, the tower uses a three-story hat truss, a one-story belt truss, and a two-story rigid link at the top podium level, thereby reducing the effective cantilever length of the tower. Dual, symmetric, folded pendulum tuned mass dampers are also utilized to control the building's lateral response.

The tower gravity frame consists of a 10 in. (250 mm) conventionally reinforced cast-in-place concrete flat plate that spans from core to perimeter. In order to avoid the need to puddle the vertical concrete, the slabs will be cast as high-strength concrete in accordance with ACI's 1.4 reduction factor. The lateral frame, as mentioned previously, utilizes vertically posttensioned concrete shear walls supplemented by concrete belt and hat walls, as shown in Figure 8.63a and b.



(a)



(b)

**FIGURE 8.63** Shangri La New York City (610 Lexington Avenue), New York City. (a) Schematic elevation, (b) structural system consists of (1) 10 in. thick conventionally reinforced concrete slab, (2) posttensioned shear walls, (3) concrete belt and hat walls,

(continued)

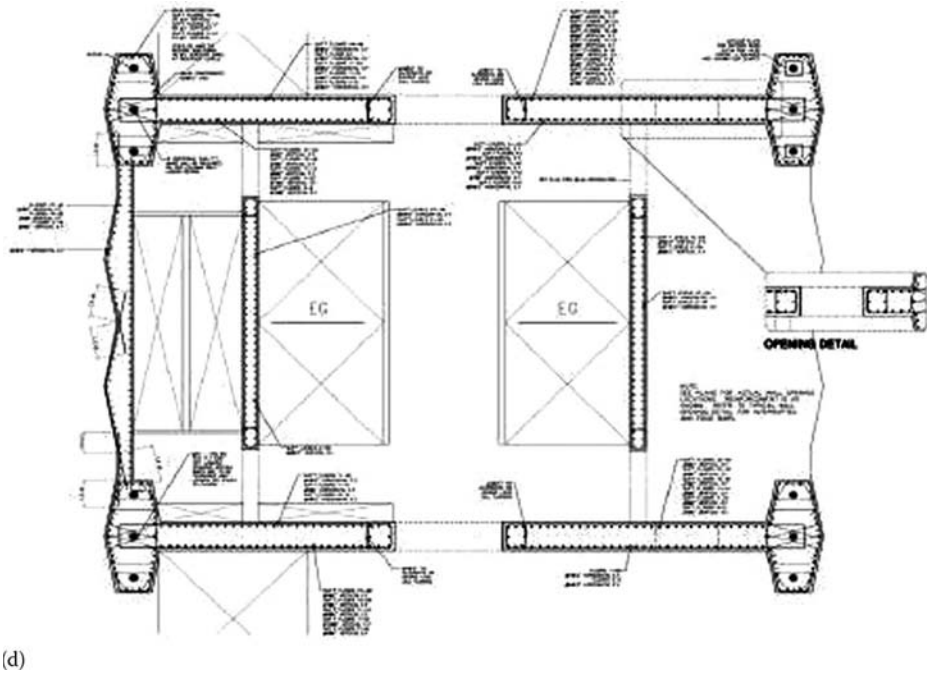
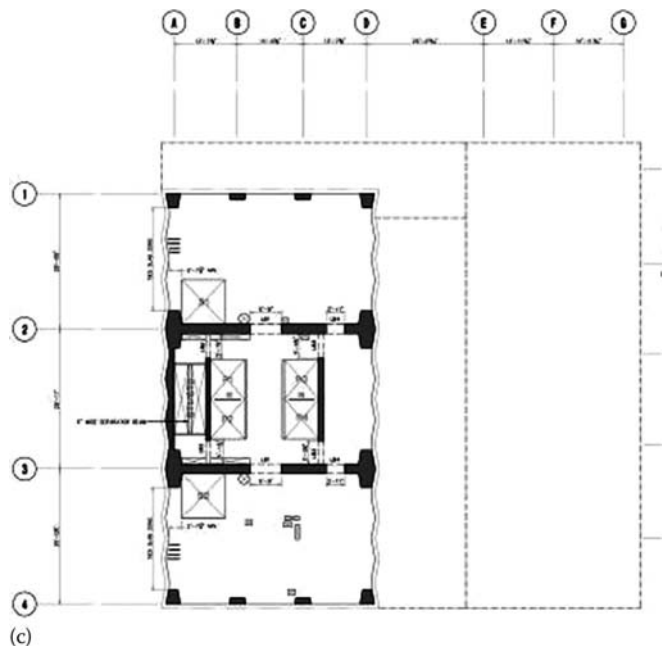
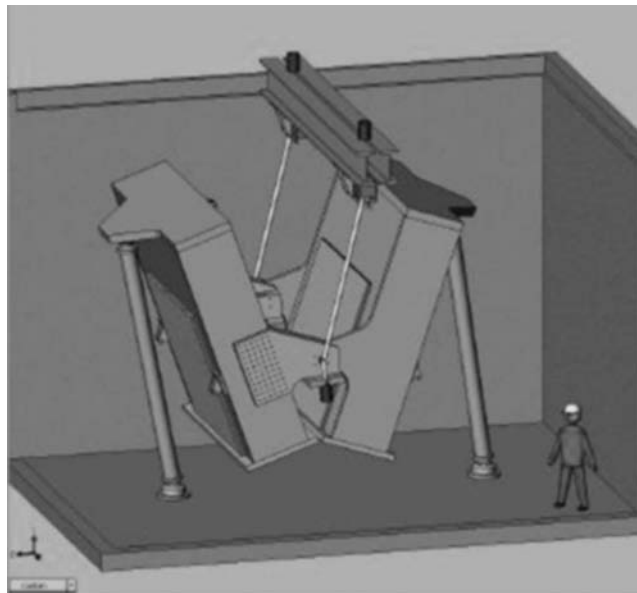
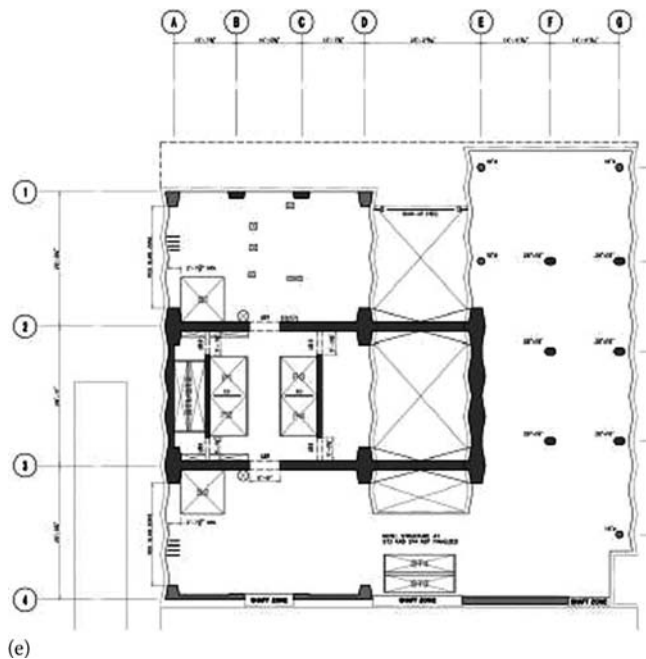


FIGURE 8.63 (continued) (c) typical floor framing plan, (d) core framing details,



**FIGURE 8.63 (continued)** (e) high-rise tower connection to 10-story podium, (f) schematics of folded pendulum tuned mass damper, TMD; two 375 t TMDs will be located on either side of the core, below the roof parapet.

High-strength concrete, up to 12 ksi (8.6 MPa) is used. The reinforced concrete core is bounded on the East and West sides by four large bulb elements. In the design wind condition these elements see a substantial amount of tension force. The vertical posttensioning of the bulbs, accomplished with three 150 ksi post-grouted #24 bars (3 in. diameter) in each bulb, eliminated net tension in these elements and the adjacent wall segments, allowing the use of an unreduced moment of inertia in the lateral load analysis of the building. While the additional compressive force was critical to

the building's performance, mild vertical reinforcing needed to be increased to cover this addition to the gravity load case. Because the post-tensioning force acts along the centroid of the wall, it induces a countering force to compensate the  $PA$  effects.

As stated previously, the tower is structurally attached to the relatively stiff 10-story low-rise building on the east side of the site (see Figure 8.50c and d). The structural link, in a manner of speaking, serves as a flying buttress that reduces the effective length of the slender portion of the tower, thereby reducing the lateral deflections considerably.

To decrease the possibility of perception of wind-related building motions, a target building response acceleration of 15 mg, under a wind recurrence interval of 10 years, was established by the engineers of this five-star hotel. However, initial wind tunnel measurements indicated possible peak accelerations of as much as 25 mg with an assumed damping of 2.0%. Therefore, various damping techniques were studied, including slosh tanks, a conventional tuned mass damper, and a folded pendulum tuned mass damper. Because of the tight space limitations around the other equipment in the top of the tower, a folded pendulum TMD (because it requires the least space) was chosen. However, there was not enough central space for the damper. Alternatively, symmetrical spaces to the north and south of the core were designated as damper zones and the original single TMD was then split into two. The dampers selected for the project shown schematically in Figure 8.50e, consist of two 325 t folded pendulum tuned mass dampers located at the top on either side of the elevator core. The dampers increased the damping value to 4% from the assumed value of 2.0%. In addition to being used as a lateral load reducing device, the resulting building response was reduced to 16 mg, slightly higher than the target of 15, but well within the industry standards.

The foundations consist of mats and spread footings bearing on and socketed into 40 t/sq ft Manhattan bedrock. Similar to the bulbs, the core mat is then anchored to the bedrock using multiple groups of #24 bars grouted into the rock below.

Structural schematics and photographs are shown in Figure 8.63.

The structural engineering is by DeSimone Consulting Engineers, New York.

#### **8.14.24 MILLENNIUM TOWER, 301 MISSION STREET, SAN FRANCISCO, CALIFORNIA\***

When completed in 2008, at 645 ft, this project will be the tallest reinforced concrete building situated in a seismic zone 4 region, the fourth tallest structure in the City of San Francisco, and the tallest residential building in the United States, west of Chicago. The tower has 58 occupied floors and combined with an adjacent 12-story tower and a podium provides over 1,150,000 sq ft of space for condominiums and recreational amenities. See Figure 8.64 for structural schematics and photographs.

The tower's lateral system is comprised of 36-in. thick concrete shear wall core and partial perimeter special moment resisting frames (SMRF). Laterally the building is a dual system with a cast-in-place shear wall core connected with outriggers to the perimeter columns comprising the primary system, and a total of 10 single-bay moment frames at the perimeter comprising the backup system.

The tower is supported by a 10 ft thick mat foundation resting on 954-130-t 14-in. square precast piles, each approximately 80 ft in length. There is only one basement below the tower, and the piles were needed to transfer the loads down, through a soft clay layer, to denser material located at about 75 ft below the street level. This was done simply to reduce overall settlement, as more would have occurred if the intermediate clay layer had been loaded more directly.

There are three outrigger trusses that connect the interior core with perimeter super-columns at three intermediate levels. In order to reduce the required floor-to-floor heights, shallow steel link beams are used within the shear wall core as coupling beams, in lieu of deeper diagonally reinforced concrete beams, and the floor framing is entirely a cast-in-place posttensioned flat plate system.

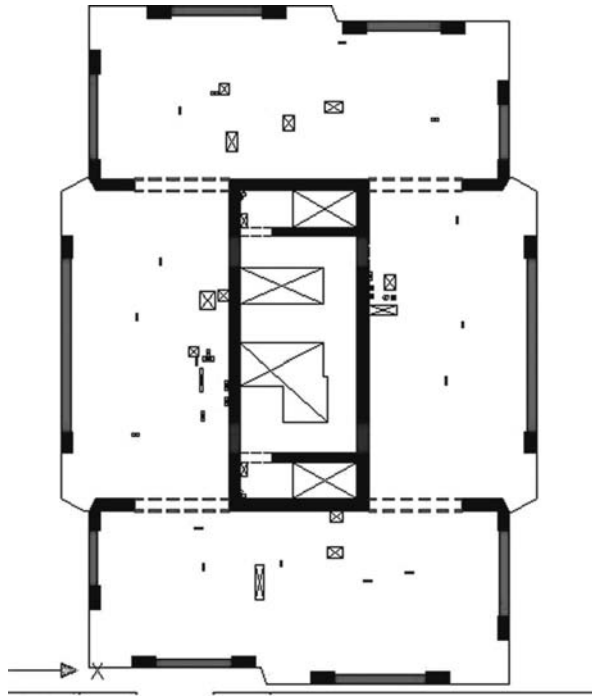
---

\* The author wishes to acknowledge his gratitude to Mr. Derrick D. Roorda, S.E., Senior Associate Principal, DeSimone Consulting Engineers, San Francisco, for providing information on this project.

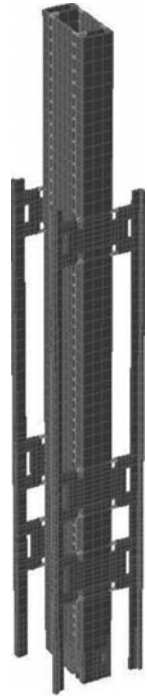
It was shown in Chapter 3 that the optimum location for a three-outrigger system is at the one-quarter, one-half and three-quarter heights. However, the outriggers in this building are not located in the structurally optimum positions. Rather, they represent a structural solution that is optimized around an architectural design. The engineers kept the outriggers out of the expensive four-unit



(a)



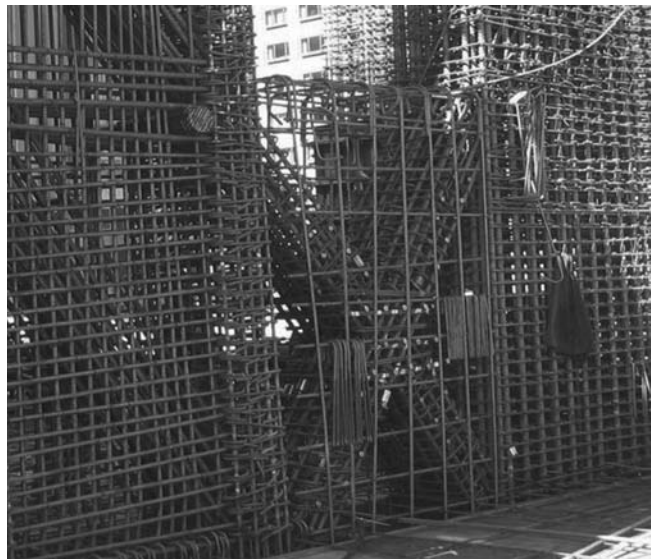
(b)



(c)



(d)



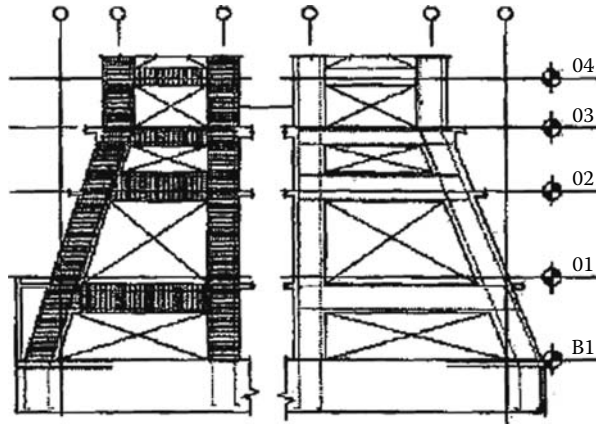
(e)

**FIGURE 8.64** Millennium Tower, 310 Mission Street, San Francisco, California: (a) Architectural rendering, (b) building plan, (c) isometric of shear walls and outriggers, (d) construction photograph, (e) outrigger reinforcement.

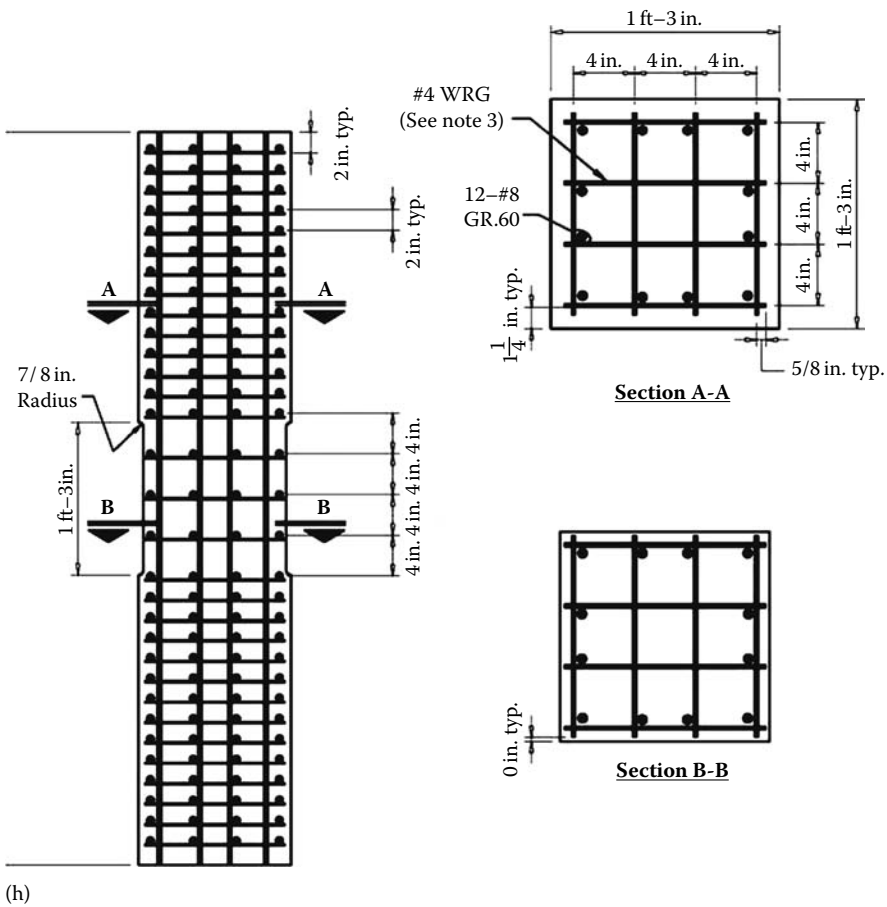
*(continued)*



(f)

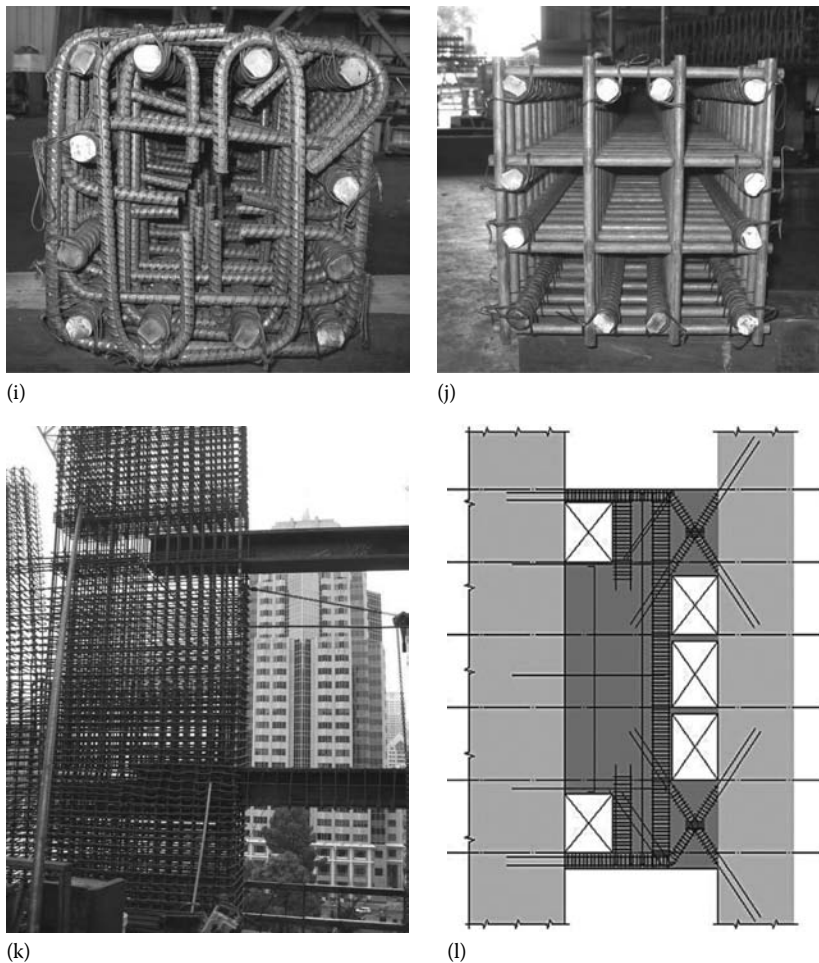


(g)



(h)

**FIGURE 8.64 (continued)** (f) building section, (g) sloping columns, (h) test specimens.



**FIGURE 8.64 (continued)** (i) conventional hoops and ties, (j) welded reinforcement grid, (k) photograph of link beams, and (l) details of outrigger reinforcement.

plans at the top of the building, and pushed them down so that two of them are located in the relatively inexpensive (see Figure 8.64a) 9 unit plans.

Closely spaced ties in columns and walls posed a challenge to the placement of the high-strength 10ksi concrete needed for this project. To alleviate some of this congestion, the engineers specified a system of welded reinforcement grid (WRG) that eliminated all hooks, significantly reduced the volume of rebar, and decreased overall labor costs. A successful laboratory test program was implemented to demonstrate the adequacy of this product for use on the project.

The design of this building utilizes 10ksi concrete and 75 ksi reinforcing rebars. Even with these high-strength materials, the reinforcing ratios in the columns and shear walls were so dense that alternative systems had to be employed to allow for successful concrete placement.

Structural steel link beams were in lieu of diagonally reinforced concrete beams, special WRG was used for confinement, and SCC was specified. These features relieved congestion and permitted properly consolidated concrete to be placed more reliably and also allowed faster construction.

The lateral system is comprised of a rectangular shear wall core with concrete SMRFs located at the building perimeter, as shown in Figure 8.64c, thus qualifying the lateral system as a dual system.

In the long direction of the building, the concrete box comprising of elevator cores has adequate stiffness for the design level earthquake. However, in the short direction it is not adequate on its



own. Therefore, large super-columns were introduced at the perimeter of the building and connected to the shear wall core with perforated outriggers at three locations up the height of the building, as shown in Figure 8.64d. The outrigger perforations allow pedestrian access around the entire core at each level. Without these openings all residential units adjacent the outriggers would have been two level-units, which was not acceptable to the building owner.

Each of the outriggers is comprised of two distinct elements. The first, providing connection to the shear wall core, is a multiple-story, solid concrete element. The second, connecting the solid portion to the super-column, is a pair of diagonally reinforced link beams.

The diagonally reinforced link beams were designed for the demands obtained from performing a response spectrum analysis. A capacity design approach was utilized to design both the solid portion of the outrigger, as well as the connection to the core. The maximum probable shear capacity of the link beams was calculated, and the results were used as design forces for the rest of the outrigger and for the design of the connection to the core. The resulting outrigger rebar detail is shown schematically in Figure 8.64d.

The super-columns were also designed using the same capacity design approach. Axial loads corresponding to the maximum probable shear capacity of the link beams were added to the tributary gravity loads in order to determine the design strength of the columns. This approach was slightly conservative since it assumes that all of the outriggers would reach their maximum capacity at the same time. With the higher mode effects of tall building response, this condition is unlikely to occur.

At the high-end of the tower, the SMRF attracted very little lateral load (about 5%–8% of base shear) away from the shear wall core. The requirement to design the SMRF of a dual system for 25% of the base shear as specified in the then governing code, controlled the design of the SMRFs.

Since higher mode effects are so prevalent in a building of this height, the typical procedure of applying 25% of static base shear to the SMRF was deemed to be not adequate. Therefore, studies were performed where the core was given various reduced stiffness and response spectrum analyses were performed. The resulting force distribution in the frames was monitored in an attempt to envelope the possible mode shapes and force distributions. However, it was found that in order for the frames to attract 25% for the base shear, the core stiffness had to be reduced to less than half of what the design stiffness was, and the building had to drift to more than twice the coded allowed displacement. The study made a good case to show that the 1997 UBC-specified requirement of 25% of base shear for the design frames is too high. More research is needed in this area to reduce this apparent conservatism inherent in the code. This trend is becoming more apparent in other “core only” buildings being designed in San Francisco.

However, for this project, since the 1997 UBC (the governing code in San Francisco at the time of design) required the frames to be designed for 25% of the base shear, the engineers adhered to the code.

Mechanical systems in residential buildings are generally confined to small areas adjacent the interior stair and elevator core. For this reason, such buildings can often be built with shorter floor-to-floor heights than office buildings. For this project, a 9 ft-7 in. floor-to-floor height was desired for the lower levels, which allowed only 21 in. for link beams above the door openings into the core. Since diagonally reinforced concrete link beams would not fit within the dimensional constraint, steel beams were used.

The concrete shear walls and the outrigger super-columns required large amounts of tension reinforcement. For example, the base of the super-column was reinforced with 152-#14 (75 ksi) rebar resulting in a reinforcement ratio of 6%, the code maximum. However, the vertical steel reinforcement only comprises about half of the total reinforcing volume in these elements.

The ACI 318 requirements for column and boundary element confinement (bursting) reinforcing are directly proportional to the concrete strength. For 10 ksi and grade 75 ties, the requirements is #5 bars at 4 in. o.c. vertically and about 6 in. o.c. horizontally. Full-scale pre-construction mockups constructed for the project showed that conventional ties with hooks could be built with this spacing, and the placement of concrete was possible, although quite challenging.

At the request of the contractor, the project structural engineers allowed the use of WRG system. This system allows for quick erection and greatly reduces reinforcing congestion in confined zones, thus ensuring proper concrete consolidation.

In order to demonstrate that the product was acceptable for 10,000psi concrete used on this project, a testing program was developed. A group of specimens constructed similarly to the portion of the shear wall core that is expected to undergo the largest strain demand was selected. The specimens had the same vertical reinforcing ratio, concrete strength, reinforcing bar strengths, and volumetric confinement ratio. The resulting specimens resembled a reinforced 15 in. square column, as shown in Figure 8.64f. The concrete specimens all exhibited ductile behavior and the performance of the WRG system was deemed a success.

At the ground level of the south side of the building, there exists a porte cochere having a minimum width and height for car clearance. To accommodate this feature, two SMRF columns were transferred, one column about 18 ft to the west and another one 15 ft to the east from level 3 to the basement floor. While the slope of the two frames is not that great, 55 stories of column load transferred from the building above would create a horizontal force component of significant magnitude. Since the sloping columns produce horizontal loads in opposite directions under gravity loads, the gravity horizontal force component was resolved by building up the slab between the frames at level 3.

The structural engineering for the project is by the San Francisco office of DeSimone Consulting Engineers.

#### 8.14.25 AL BATEEN TOWERS, DUBAI, UAE

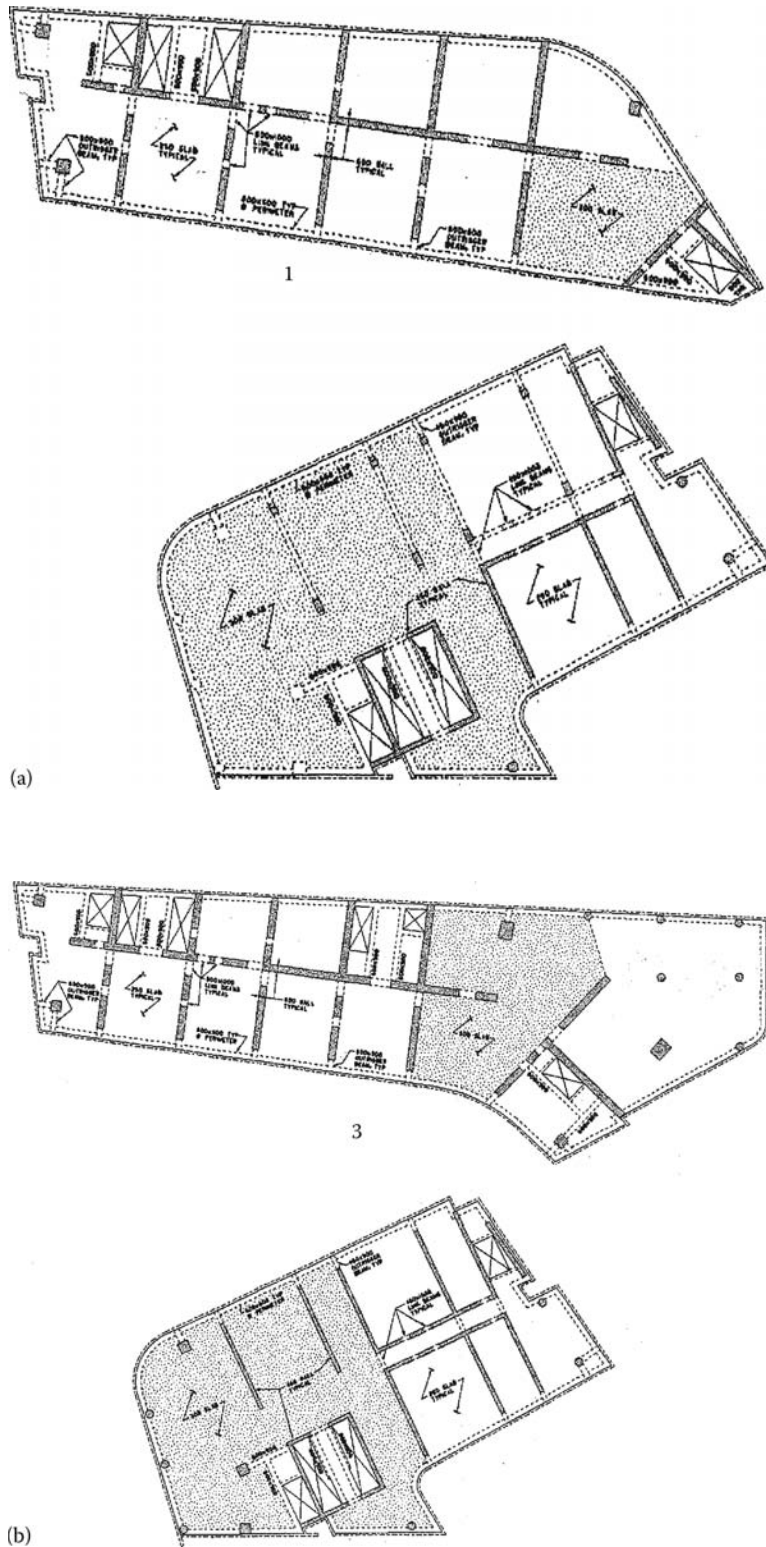
Al Bateen project in Dubai, United Arab Emirates, designed by structural engineers LeMessurier Consultants is under construction in Dubai Marina. The project consists of a 49-story residential tower and a separate 26-story hotel tower both on top of a four-story podium structure. Two stories of below grade parking occur beneath the podium structure. Above the podium, a nine-story mechanical parking structure will be built.

The residential tower is 670 ft (204 m) to the roof of the penthouse with a mechanical room and parapet of approximately 50 ft (15 m) atop, giving a total building height of 718 ft (219 m). The hotel tower is 377 ft (115 m) to the roof of the penthouse with a mechanical room and parapet of approximately 30 ft (7 m) for a total building height of 400 ft (122 m). The structural frame for the towers consists of cast-in-place reinforced concrete two-way slabs supported on concrete columns and shear walls. Beams are used to support larger slab spans and to frame out around openings. Spandrel beams are used at the perimeter edge of the slab. Figure 8.65a through d show the typical floor framing plans.

Some of the typical dimensions of the structural framing system are as follows:

Slab thickness	9.8–11.8 in. (250–300 mm)
Coupling beams	(Wall width) × 39.4 in. (1000 mm)
Slab edge beam	23.62 × 23.62 in. (600 × 600 mm)
Slab edge support beam	23.62 × 35.5 in. (600 × 900 mm)
Concrete shear walls	
Residential tower	
Base to second floor	39.4 in. (1000 mm)
3rd to 16th floor	31.5 in. (800 mm)
17th to roof	23.62 in. (600 mm)
Hotel tower	17.72 in. (450 mm)

Open lobby space exists on the first floors of both the residential and hotel towers. Thus, full-story reinforced concrete deep beams with a depth of 18 ft (5.5 m) and a width of 3.28 ft (1 m) are used at the second floor to transfer the gravity and lateral loads from the shear walls above.



**FIGURE 8.65** Al Bateen Towers, Dubai, UAE: (a) upper residential and hotel tower framing plans, (b) mid-residential and hotel room framing plans.

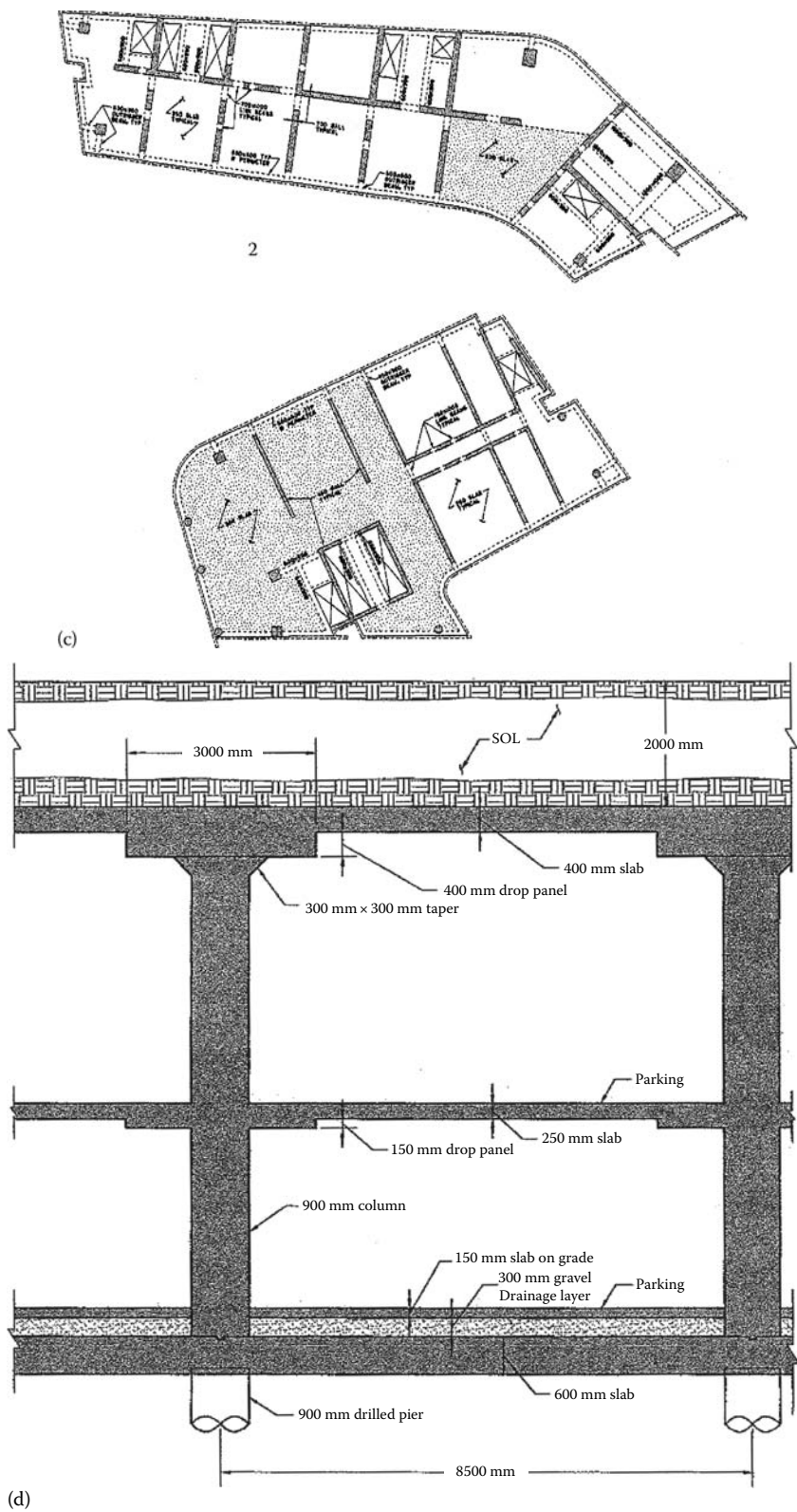
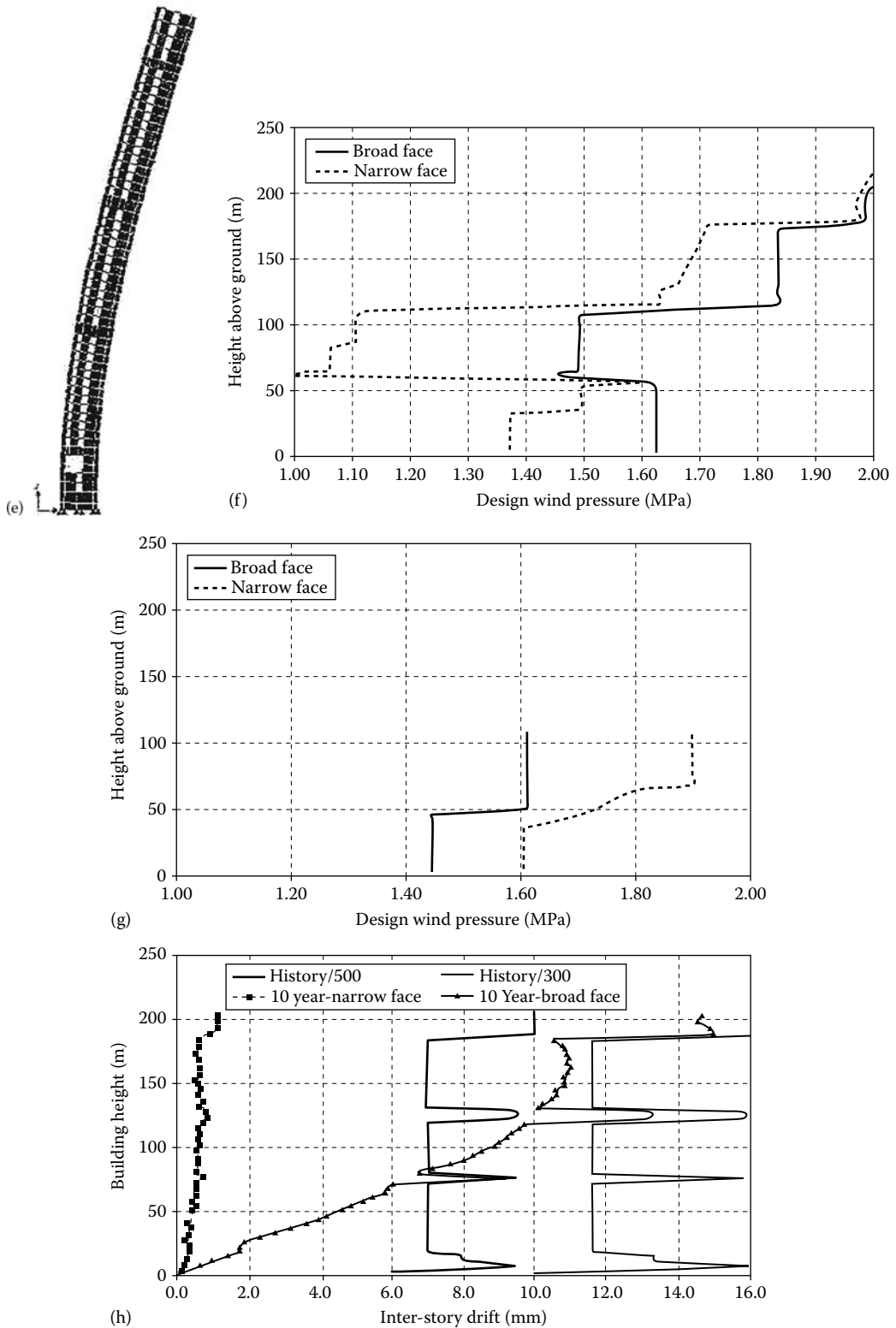


FIGURE 8.65 (continued) (c) lower-residential and hotel room framing plans, (d) garage section. (continued)



**FIGURE 8.65 (continued)** (e) residential deflected shape (wind on broad face), (f) residential tower effective applied wind pressure versus height, (g) hotel tower effective applied wind pressure versus height, and (h) residential tower, 10-year inter-story drift.

The two levels of below grade parking are supported by a flat slab system with drop panels. An allowance for the dead load of a 6.5 ft (2 m) depth of soil above the parking garage has been provided for in the design. The slab at ground floor is 15.5 in. (400 mm) thick with drop panels of same thickness. The Basement Level B1 slab is 9.85 in. (250 mm) with 5.9 in. (150 mm) drop panels and the Basement Level B2 slab is a 5.9 in. (150 mm) slab on grade. The flat slabs are supported by 35.5 in. (900 mm) columns spaced in a  $27.9 \times 27.9$  ft ( $8.5 \times 8.5$  m) grid. Figure 8.65 shows the flat slab system for the garage.

Lateral loads due to wind and earthquake acting in the short direction on the residential tower are resisted by five shear walls parallel to the direction of loading and one shear at an angle of  $36^\circ$  for a total of six shear walls. These six shear walls also resist torsion resulting from lateral loads. The average length of shear walls that span the short direction of the residential tower is 57.5 ft (17.5 m).

Lateral loads acting in the long direction of the residential tower are resisted by a single shear wall located at approximately the center of the building. This shear wall is made up of a 190.5 ft (50 m) length that is parallel to the direction of loading and a 39.4 ft (12 m) length at a  $36^\circ$  angle from the direction of loading. Full-story reinforced concrete outrigger beams are used in the short direction at the 16th, 30th, and 46th floors of the residential tower and have depths of 18.9 ft (5.75 m), at the top two floors and 14.75 ft (4.5 m) at the 16th level. With the outrigger beams, Figure 8.65 shows a schematic elevation of a typical shear wall elevation at the 16th level. The foundation system consists of a mat slab supported on drilled piers.

The following dead and live loads used in analysis reflect the expected use of the two towers:

Dead loads	
Partition allowance	20 psf (1.0 kPa)
75 mm floor finish allowance	38 psf (1.8 kPa)
HVAC, ceiling lights allowance	80 psf (0.5 kPa)
Live loads	
Public spaces	100 psf (4.8 kPa)
Residential areas	40 psf (1.9 kPa)
Mechanical areas	150 psf (7.2 kPa)
Stairs and exits	100 psf (4.8 kPa)

#### 8.14.25.1 Wind Loads

Wind loads were determined from British Standard BS6399-2, 1997 Code of Practice for Wind Loads using the directional method of Section 3. The following properties were used to calculate the design wind pressures:

Open terrain coastal wind speed, $V_b$	45 m/s (100 mph)
Upwind distance from sea to site	<0.1 km (at sea)
Building type factor, $K_b$	1.0

The maximum wind load for each of the principal building axes was used. The applied wind pressure is also a function of height above ground level, angle of the wall relative to the wind direction, and area of the loaded surface as given in Section 3 of BS 6399-2, 1997. For purposes of calculating the wind loads, the towers were divided into parts (strips) per Section 2.2.3.2 of BS6399-2 using the diagonal dimension of each strip. Figure 8.65 show the calculated wind pressures for the residential and hotel towers. The wind pressures represent combined effect of pressure on the windward wall and suction on the leeward wall.

The following lists the calculated wind base shears for the 50 year wind load:

Residential tower (broad face)	6,003 kip (26,700 kN)
Residential tower (narrow face)	1,731 kip (7,700 kN)
Hotel tower (broad face)	1,956 kip (8,700 kN)
Hotel tower (narrow face)	1,439 kip (6,400 kN)

### 8.14.25.2 Seismic Loads\*

Seismic loads were determined using the Equivalent Later Procedure, ELF, given in UBC-97 (Uniform Building Code 1997 Edition). The following seismic properties were used:

Seismic zone	2a
Soil site	C
Importance factor	1.0
$C_t$	0.488
$R$ (shear walls)	4.5
Natural period, $T = C_t(h_n)^{3/4}$	
Residential tower	2.63 s
Hotel tower	1.67 s
Seismic weight	
Residential tower	314,748 kip (1,400,000 kN)
Hotel tower	164,118 kip (730,000 kN)

A dynamic response spectrum analysis was performed using the UBC-97 response spectrum. The dynamic results were scaled to obtain 90% of the static base shear, as permitted by the Code.

Shear walls were modeled with shell elements having both out-of-plane bending and in-plane membrane properties. No stiffness reduction modifiers were applied to shear walls for serviceability checks because typically no cracking is expected under service loads. To confirm this, concrete stresses over the height of the residential tower resulting from a 50 year wind load were calculated. These were compared to the direct tensile strength calculated by the ACI 318-05 equation  $F_{ct} = 6.7f_c^{0.5}$  and the modulus of rupture by the equation  $f_r = 7.5f_c^{0.5}$ . As observed in Figure 8.65a and b, the calculated stresses are typically well within the rupture strength.

The transfer girders located on the second floor of both towers were modeled with shell elements. This was done to provide continuity between the shear walls and transfer girders. No stiffness reduction was taken for these elements. All other beams including shear wall coupling beams were modeled using frame elements and were assigned stiffness reduction modifiers of 0.5 for shear and 0.35 for bending.

Figure 8.65a and b show the maximum inter-story drift due to a 10 year wind load for both the residential and hotel towers, respectively. Also shown are the Dubai Municipality inter-story drift limit of 1/500. It is seen from Figure 8.65c that the residential tower does not meet the 1/500 criterion above the 19th floor. However it satisfies an inter-story drift limit of 1/300 over the entire tower height, which was considered by the engineers to be satisfactory. The reasoning is the drifts at upper levels are primarily due to tower bending and not due to shear deformations and thus would not adversely affect the performance of the curtain wall system. It was also anticipated that architectural detailing of the nonstructural components would be designed to accommodate an inter-story drift of 1/300.

### 8.14.26 SRZ TOWER, DUBAI, UAE

A preliminary analysis and design performed by structural engineers, Lemessurier Consultants, Cambridge, MA on a proposed tower called SRZ Tower, to be located on Sheikh Zayed Road in Dubai, United Arab Emirates is given in this section. The development consists of a 63-story office tower with a high slenderness ratio of 19:1, in the transverse direction.

\* The author wishes to acknowledge his gratitude to Mr. M.V. Ravindra, President and CEO, LeMessurier Consultants, Cambridge, Massachusetts for providing information on this project.

The Tower floor plan is approximately  $131 \times 92$  ft ( $40 \times 28$  m). The typical floor-to-floor height is 13 ft (4 m) and the tower will have an overall height of approximately 870 ft (265 m) to the top of the wind sail. The structural frame for the tower will consist of cast-in-place reinforced concrete two-way slabs supported on reinforced concrete columns and a reinforced concrete core. The reinforced concrete core is approximately  $75 \times 45$  ft ( $22.9 \text{ m} \times 13.8 \text{ m}$ ). A beam will span from column D-1 around the perimeter of the building to column E-7 (see Figure 8.66). For typical floors, beams will frame between columns D-1, D-2, E-1, and the corner of the reinforced concrete core at grid-line E-2. These beams will allow for the slab to be removed so that local staircases between floors can be more easily provided at any time throughout the life of the building. The typical floor plans are shown in Figure 8.66a and b.

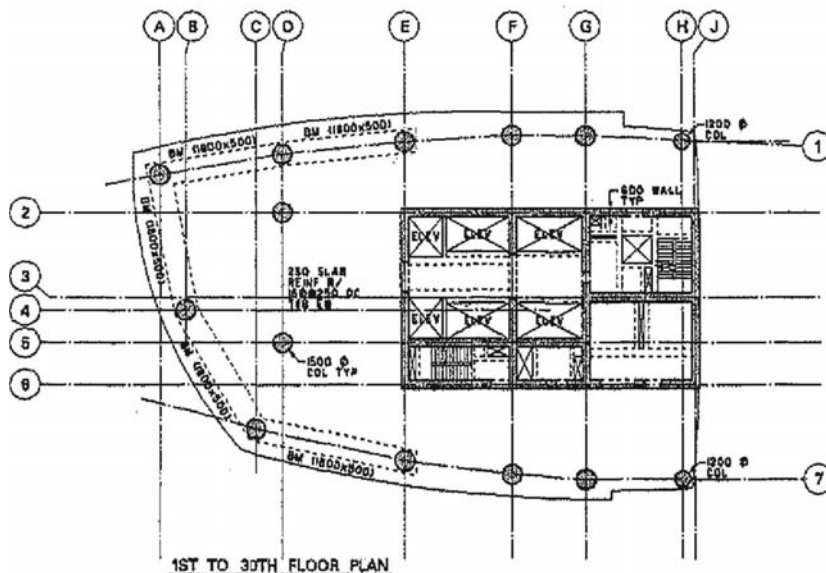
Some of the commonly used dimensions of the structural systems of the Tower are as follows:

Slab thickness	9.84 in. (250 mm)
Reinforced concrete core wall thickness	23.6 (600)
Coupling beams (reinforced concrete core)	$39.4 \times 23.6$ in. ( $1000 \times 600$ mm)
Perimeter beams	$19.68 \times 71$ in. ( $500 \times 1800$ mm)
Columns	Vary from $59 \times 59$ in. ( $1500 \times 1500$ mm) to $35.5 \times 35.5$ in. ( $900 \times 990$ mm)

In addition to the reinforced concrete core and moment frames, two steel outriggers are used on column lines E, F and G at the tower mid-height (floor 31–32) and at the top of the tower (mechanical floor) to stiffen the building in the transverse direction. A representative elevation is shown in Figure 8.66b.

#### 8.14.26.1 Wind Loads

Wind loads were determined from the British Standard BS6399-2, 1997 “Code of Practice for Wind Loads” using the directional method of Section 3. The following properties were used to calculate the design wind pressures:

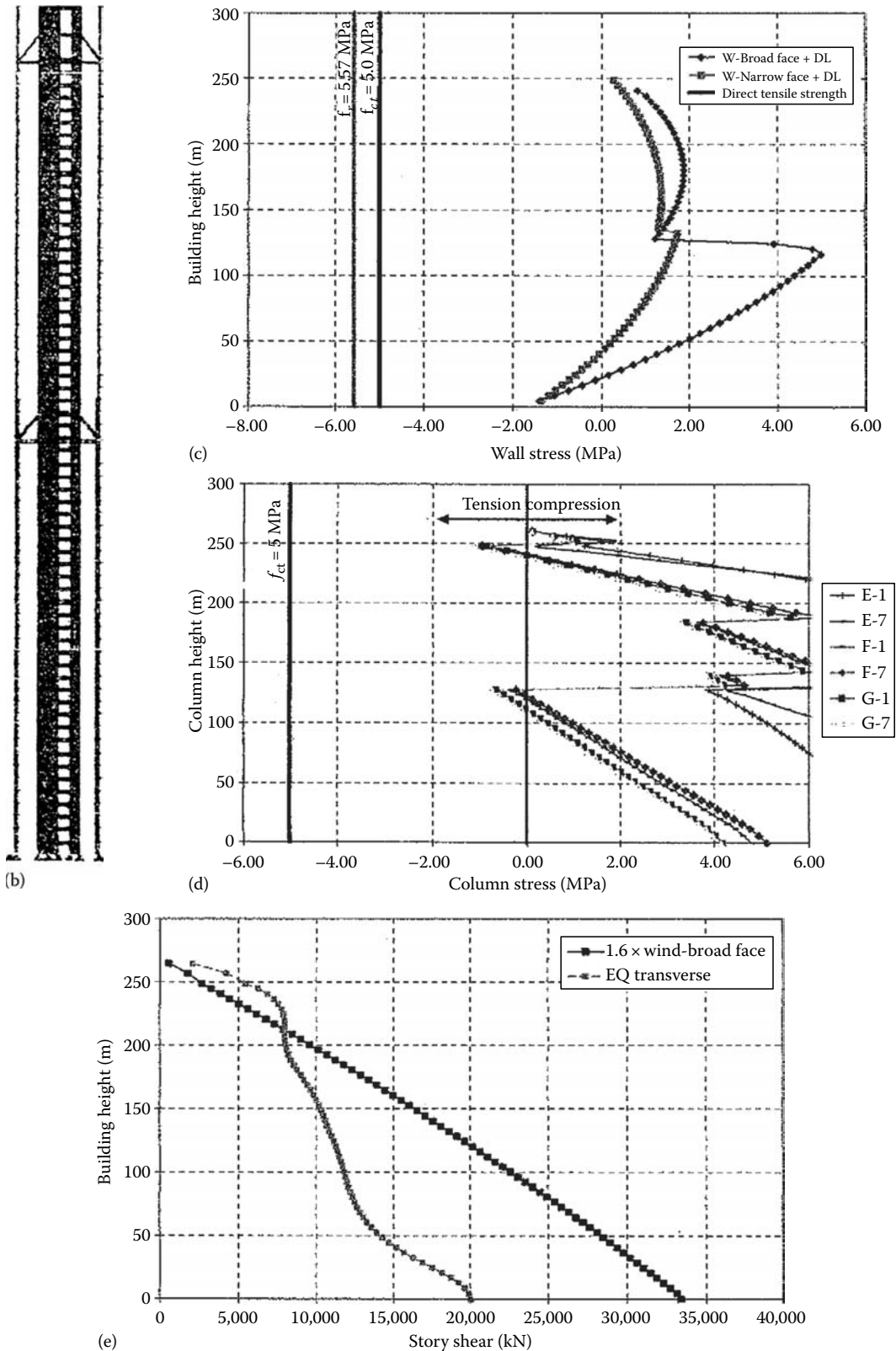


(a)

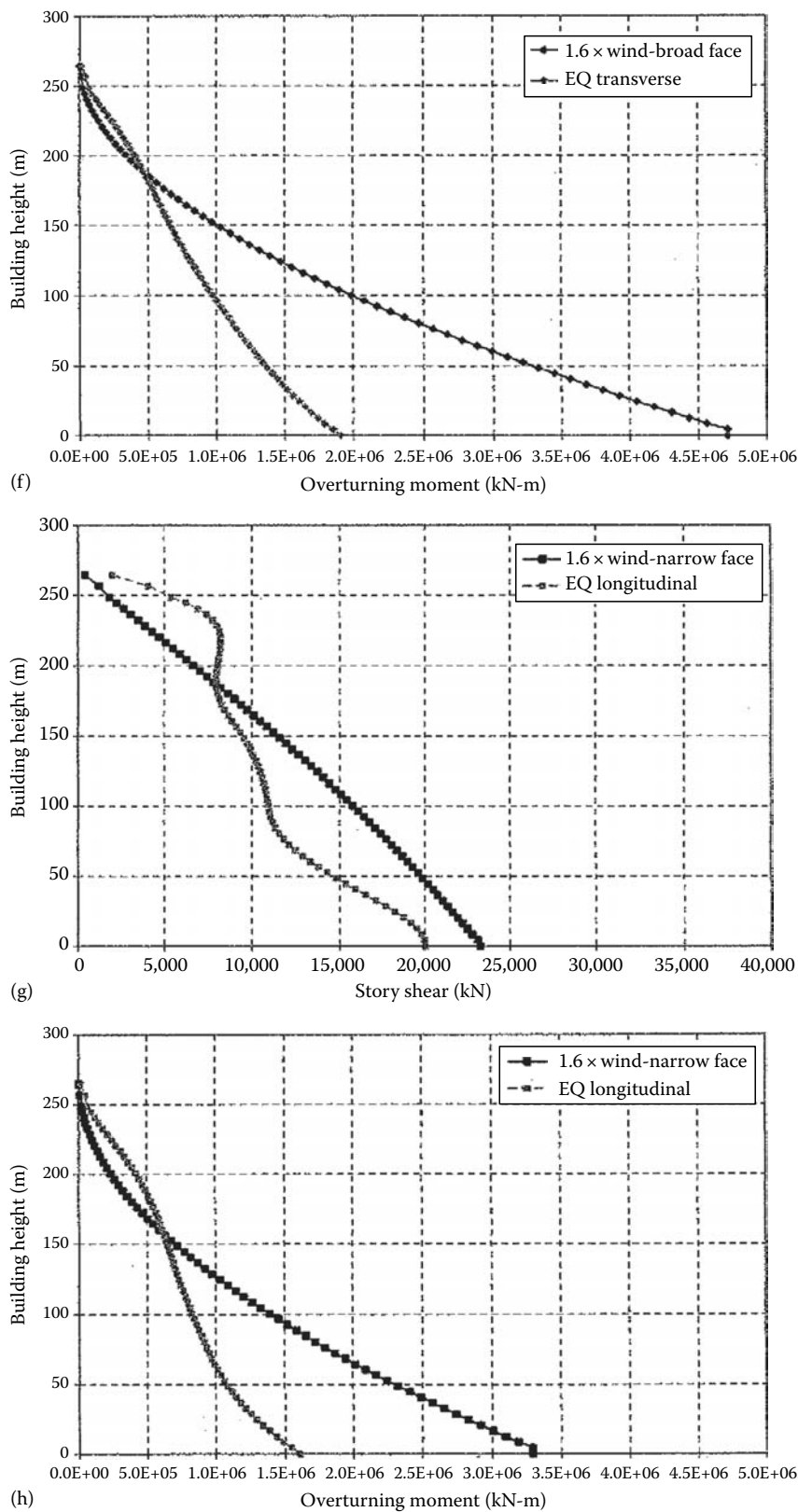
**FIGURE 8.66** SRZ Tower, Dubai, UAE: (a) 1st to 30th floor plan.

(continued)





**FIGURE 8.66 (continued)** (b) E-line elevation, (c) maximum stress in reinforced concrete core, (d) maximum stress in outrigger columns, (e) story shear (transverse direction).



**FIGURE 8.66 (continued)** (f) overturning moment (transverse direction), (g) story shear (longitudinal direction), and (h) overturning moment (longitudinal direction).

Open terrain costal wind speed, $V_b$	45 m/s (100 mph)
Upwind distance from sea to site	1.0 km
Building type factor, $K_b$	1.0
Dynamic augmentation factor, $C_r$	1.5

The tower was analytically divided into six parts to determine the diagonal dimension of the loaded area “a.” These values were used in calculating the design wind pressure at each floor. Using a single value of “a” for each zone results in slightly conservative deflection results throughout the building height.

The following lists the calculated wind base shears and overturning moments for a 50 year design wind load:

Broad face (transverse direction)	
$V_{base}$	4700 kip (20,900 kN)
$M_{overturning}$	$2.17 \times 10^6$ k-ft ( $2.95 \times 10^6$ kN m)
Narrow face (longitudinal direction)	
$V_{base}$	3282 kip (14,600 kN)
$M_{overturning}$	$1.118 \times 10^6$ k-ft ( $1.52 \times 10^6$ kN m)

It is expected that wind tunnel tests will be performed to determine more accurate wind loads.

#### 8.14.26.2 Seismic Loads

Seismic loads were determined using the 1997 edition of the Uniform Building Code (UBC 1997). The equivalent lateral force procedure, ELF, was used to obtain seismic base shears using the following seismic properties.

Seismic zone	2a
Soil site	C
Importance factor	1.0
$C_t$	0.488
$R$ (shear walls)	4.5
Natural period, $T = C_t(h_n)^{3/4}$	3.16 s

The following are the estimated seismic weight and base shears:

Seismic weight	252,698 kip (1,124,000 kN)
Equivalent static base shear	5002 kip (22,250 kN)

A response spectrum analysis on the 3D model was used for both strength and serviceability design of the building. The response spectrum results were scaled to give 90% of the static base shear.

#### 8.14.26.3 Computer Model

The walls of the reinforced concrete core were modeled with shell elements having both out-of-plane bending and in-plane membrane properties. No stiffness reduction modifiers were applied to shear walls for wind serviceability checks because no cracking was expected. Graphs of concrete stress over the tower height resulting from the service wind loads and a lower bound dead load are shown in Figure 8.66. As per ACI 318-5, the direct tensile strength was calculated by the equation  $f_{ct} = 6.7f_c^{0.5}$ , and modulus of rupture by the equation  $f_t = 7.5f_c^{0.5}$ . As shown in Figure 8.66 no cracking is expected in the reinforced concrete core under service wind loads. Similarly no cracking is expected in the outrigger columns and therefore no stiffness reduction modifiers were applied.

The shell elements were given a stiffness modifier of 0.7 for seismic strength and serviceability checks. No cracking is expected in the reinforced concrete core due to seismic loading. All coupling beams of the reinforced concrete core were modeled using shell elements having both out-of-plane bending and in-plane membrane properties, and were assigned stiffness reduction modifiers of 0.5 for shear and 0.35 for bending.

#### 8.14.26.4 Building Behavior

Figure 8.66a through d present the story shears and overturning moments for ultimate lateral forces acting in both of the principle directions of the tower. The analysis indicated that for both the transverse and longitudinal directions the seismic forces will control the strength design at the top of the building while ultimate wind forces will control the strength design at the bottom of the building.

#### 8.14.26.5 Wind\*

Serviceability limits of the structural response to wind loads were checked using a 10 year wind load. The 10 year wind load was taken as 90% of the 50 year load based on Equation D.1 in Annex D of BS639-2 1997. A deflection limit of  $H/500$  was used to check building deflections. The analysis indicated that the proposed structure meets the deflection requirement throughout the height of the tower in the longitudinal direction, but not so in the transverse direction above the 23rd level. This was considered acceptable for reasons.

Noting that the main purpose for adopting a drift criteria is to limit damage to the building façade, partitions, interior finishes (nonstructural components) and also to limit the secondary loading effects due to  $P-\Delta$  effects, it is of interest to examine the components that contribute to the overall story drift of a building. The two major contributions to story drift are racking (shear) and chord (bending) drifts. The summation of the two gives the overall story drift. The racking drift is the component that induces significant loads into the building nonstructural components. In this building, due to the high slenderness ratio of the reinforced concrete core in the transverse direction (19:1), the chord drifts are large as compared to shear deflections. Hence it was determined that the nonstructural components can be designed and detailed to accommodate the building's racking drifts rather than the overall drift. Additionally, because the lateral system satisfies the industry standard of a maximum story drift of 12.5 mm, the design was judged to be satisfactory.

#### 8.14.27 THE FOUR SEASONS HOTEL AND TOWER, MIAMI, FLORIDA

This 789 ft tall tower is a mixed-use building that includes a five-star hotel, condominiums, office space, and a 900 car parking garage. The complex consists of three distinct buildings that stand independent of each other: a 67-story high rise tower attached to a 15-story lower rise, an 8-story podium, and a 7-story parking garage.

The office building has clear spans ranging from 40 to 50 ft. A posttensioned cast-in-place concrete slab 12 in. thick is used for the floor system. The building's lateral system consists of a tube-in-tube system with coupled shear walls on the interior acting as the interior tube and frames on the buildings façade acting as a perimeter tube.

Interior core shear walls vary in thickness from 18 in. to 30 in. and are linked by beams, which are up to 36 in. deep. Four-foot wide columns at 15 ft center to center with spandrel beams varying in depth from 4 to 2 ft comprise the perimeter frame. The interior core is connected to the exterior frame using outrigger walls and link beams.

For a design wind speed of 150 mph, wind tunnel studies showed that the maximum equivalent static pressure would be 170 psf as compared to the code prescribed pressure of 120 psf.

---

\* The author wishes to acknowledge his gratitude to Mr. M.V. Ravindra, President and CEO, LeMessurier Consultants, Cambridge, Massachusetts for providing information on this project.

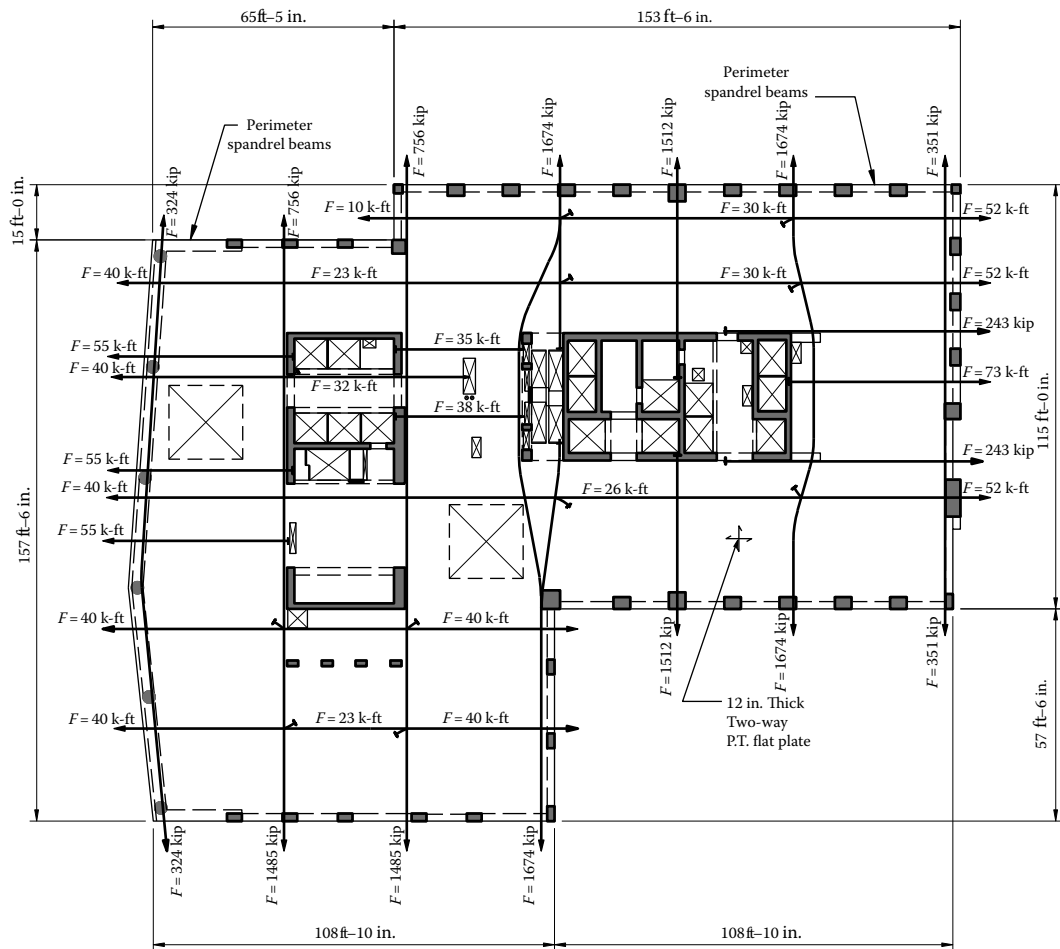
To support column loads, of up to 16,500 kip a foundation system consisting of 109 six ft diameter, 125 ft-long side friction drilled shafts was used. The length of the socket, the region in which the side friction was developed, varied from 30–40 ft. The capacity of drilled shafts was verified using Osterberg Cell, a test that loads the shaft using hydraulic jacks.

Concrete strengths ranged from 6,000 psi on the upper floors to 10,000 psi on the lower floors. Modulus of elasticity of concrete in the vertical members also needed special consideration. Typical concrete that uses granite aggregate provides a modulus of elasticity equal to or greater than ACI 318 prescribed formulation. However, the project's local concrete was a limestone-based aggregate, which exhibits a lower modulus of elasticity. Therefore, an appropriate combination of granite and limestone aggregates was used in the mix design after a series of tests were performed to determine concrete modulus.

The Four Seasons project is the first posttensioned slab building to use a self-climbing formwork system for the core shear walls. The construction schedule and the requirement of maintaining a plumb core for 800 ft, made this system called the “Peri Formwork” efficient.

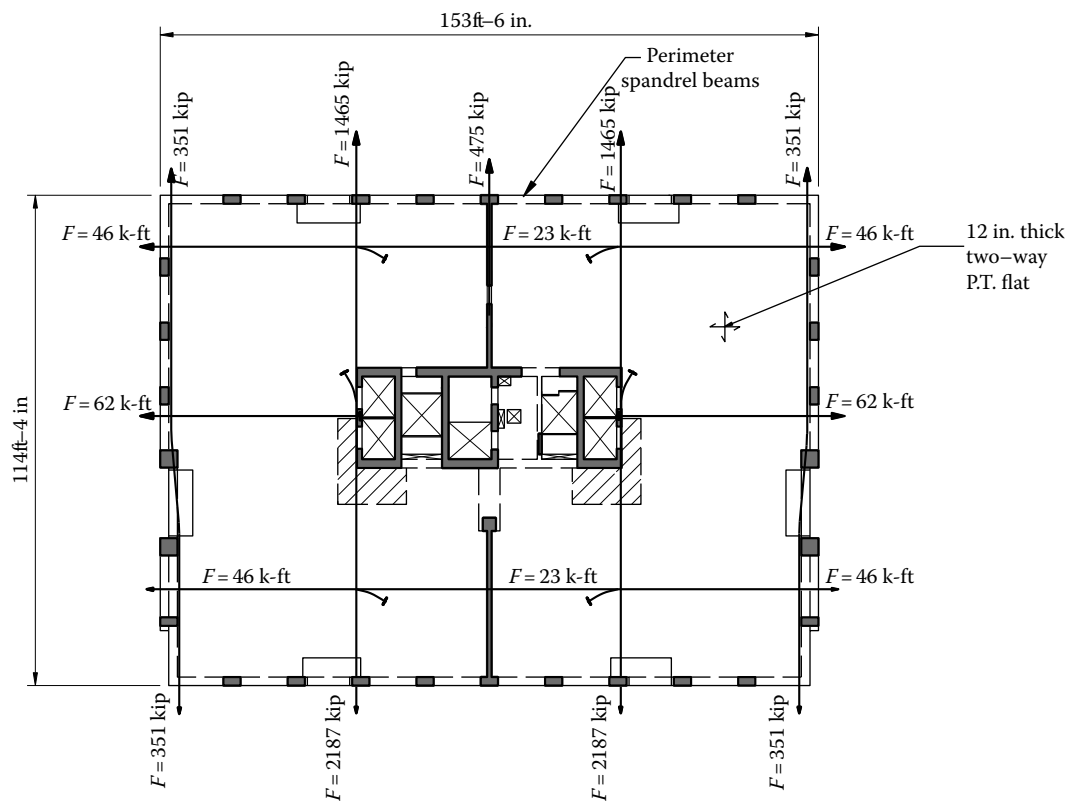
The structural schematics and photographs are shown in Figure 8.67a and e.

The structural engineering for the project is by DeSimone Consulting Engineers, Miami, Florida.



(a)

**FIGURE 8.67** The Four Seasons hotel and tower, Miami, Florida: (a) lower level framing plan.



Note: Mild Steel Reinforcement not shown for clarity.

(b)

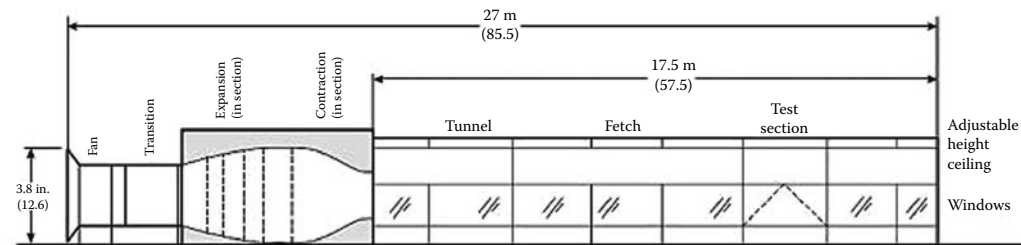


(c)

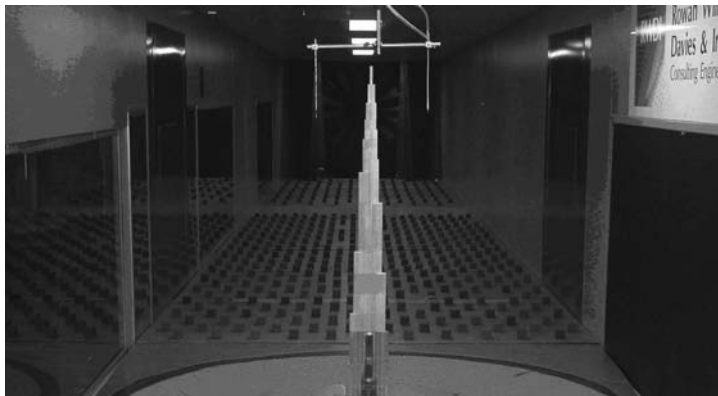
FIGURE 8.67 (continued) (b) upper level framing plan; and (c) photograph.

### 8.14.28 BURJ DUBAI

The Burj Dubai meaning “The Tower of Dubai” in Arabic, is now the tallest building in the world. At the time of publication of this book (2009), the building’s height had reached 818 m (2684 ft) totaling 162 floors, making it more than 1000 ft taller than the Taipei 101 building in Taipei, Taiwan, the previous tallest building. The frame is of reinforced concrete with a structural steel spire at the top. The multi-use skyscraper consisting of 3 million sq ft (280,000 m<sup>2</sup>) is utilized for retail, a hotel, residential, and office. Schematic plans, elevations, wind study models, and photographs are shown in Figure 8.68a through f.



(a) 1.9 × 2.4 m boundary layer wind tunnel facility



(b)



(c)

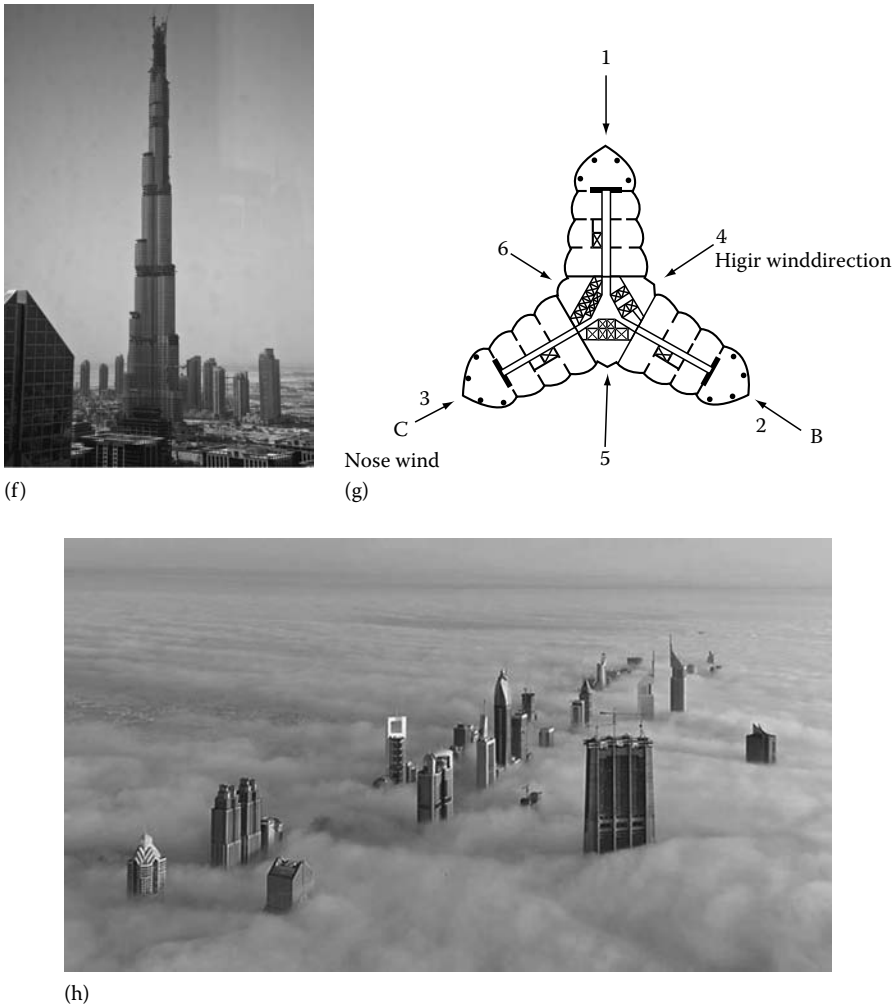


(d)



(e)

**FIGURE 8.68** Burj Dubai: (a) Boundary-layer wind-tunnel facility, (b) wind tunnel high frequency force balance model, (c) wind tunnel aeroelastic model, (d) wind tunnel cladding model, (e) pedestrian level wind study.



**FIGURE 8.68 (continued)** (f) photograph, (g) schematic floor plan showing six major wind directions, and (h) view from top of Burj Dubai.

Before describing the structural system for Burj Dubai, perhaps it is interesting to examine the increasing trend toward constructing structural concrete super-tall buildings. Some of the advantages associated for this preference are as follows:

- The mass and rigidity of concrete provides increased dampening effect compared to steel, reducing forces on super-tall buildings due to wind.
- Improvements in concrete mixes, including strength and modulus of elasticity ( $E_c$ ), have made high-rise construction more attractive. SCC too is increasing in use.
- Structural concrete is fire resistant.
- By using “flat plate” floor construction methods, the distance between floors is minimized.
- Modern forming system for both vertical and floor construction greatly increase the speed of construction.
- Advancements in concrete pumping technology, including the introduction of placing booms, make easy, fast delivery of concrete possible, freeing tower cranes for other work.



The building system may be described as a “buttressed core system.” The three wings in the “Y” pattern brace the core structure. Like the horizontal root system of a tree, the buttresses support the structure and reduce torsional forces on the core regardless of the direction of the wind. For the Burj Dubai, the columns are in line to the top of the structure. There is no transfer of columns. As the building floor plan diminishes in size, column lines terminate at the top of walls below. There are 27 such reductions in floor size to control wind shear and vortex shedding. To increase lateral resistance and strength of the frame, concrete outrigger walls are placed every 30 floors.

The building is supported by 194 caissons, 5 ft in diameter and approximately 150 ft deep. The soils in the region have high chloride and high sulfate contents and are composed of silt-formed calcium type rock. The caissons depend on skin friction—the resistance between the concrete caisson and the surrounding soil—to provide the necessary support. High-performance, dense concrete resists the high sulfate soils.

Resting on the caissons is a 12 ft thick mat cast with SCC placed in three lifts. The core structure, the buttresses, and the columns are all supported by the mat. The core walls start at 26 in. thick, diminishing to a 20-in. thickness at the top of the structure. Floor thickness for the floors are typically 8 in. thick and mechanical floors are 12 in. thick. There is no posttension (PT) reinforcement used anywhere in the building.

For super-tall buildings the modulus of elasticity,  $E_c$ , of concrete is as important as its compressive strength. Normal weight concrete has an  $E_c$  of 2000 to 6000 ksi, with the requirements for the Burj being 6300 ksi at 90 days. Since the quality of aggregate material has much to do with  $E_c$ , the engineers decided to specify the  $E_c$  they required and let the contractor be responsible for the mix details.

When there are hundreds of concrete placements over the course of construction, shrinkage and creep, occurring at different rates over time, can be critical to a building like the Burj Dubai. For that reason it was decided to use one mix for all the vertical work on a given floor level, keeping surface-to-volume ratios the same for columns and core walls by making column and wall thickness equal. This way shrinkage and creep would be the same and have minimal influence on the structure. Most of the mixes are “triple blends” including Portland cement, fly ash, and silica fume. They have a relatively high fine aggregate fraction as well as containing up to 650 lb/cubic yards of cementitious content. Flowability is increased with polycarboxylate superplasticizers while keeping water–cement (w/c) ratios below 0.32 for higher strength concretes. Although some vibration was used during casting, the concrete could be considered to be SCC. Three-quarter inch maximum aggregate was used up to the 100th floor and 9/16 in. at higher elevations to reduce pumping pressures. Significant amounts of ice were added to keep concrete temperatures between 75°F to 90°F. Even with placements conducted at night, ambient temperatures could be up to 105°F from daily highs of 120°F in the middle of summer.

Concrete cube strengths (which are approximately 80% of the cylinder strength) specified for building elements includes the following:

- Caissons: 9000 psi minimum strength.
- Mat slab: SCC with 6000 psi minimum cube strength.
- Core walls and columns below the 126th floor and floors 154 and 155: 11,600 psi minimum strength.
- Floors: 5000 psi minimum strength. According to the design engineers, column and core walls mixes specified for 11,600 psi compressive strengths were actually developing at an average 56-day strength of 15,000 psi with a modulus of 7,000 psi.

Core walls were constructed with self-rising or “jump forms” with the concrete placing boom mounted on the top of the forms. The boom advanced as the forms move upward.

Winds in the region did not permit the use of table forms for floor construction, so workers used handset forming system for the floor construction.

The concrete pump for the project could develop as much as 5500 psi pressure on the material, although 3000 psi is all that's needed for this project; the rest being reserved capacity. At the placing boom, the pressure is approximately 50 psi to ensure safe delivery.

To clean the pipe line, rubber balls are placed in the line at the top, the line is capped and air is pumped in behind the ball, pushing approximately 15 yards of concrete down the pipe (assisted by gravity) where it is diverted into ready-mix trucks.

As stated earlier, the structural system is "Y" shaped in plan to reduce the wind forces on the tower. The structural system is described as a "buttressed" core (Figure 8.68). Each wing, with its own concrete corridor walls and perimeter columns, buttresses the others via a six-sided central core, or hexagonal hub resulting in a tower that is stiff laterally and torsionally. All the common central core, wall, and column elements are aligned: There are no major transfers of columns or walls.

Each tier of the building sets back in a spiral stepping pattern up the building. The building stepping is accomplished by aligning columns above with walls below to provide a smooth load path for vertical loads.

The setbacks are organized such that the tower's width changes at each setback. As discussed earlier, the advantage of the stepping and shaping is to reduce the effect of vortex shedding caused by across wind.

The center hexagonal reinforced concrete core walls provide the torsional resistance of the structure similar to a closed tube. These walls are buttressed by the wing walls and hammerhead walls, which behave as the webs and flanges of a beam to resist the wind shears and moments. Outriggers at the mechanical floors allow the exterior columns to participate in the lateral load resistance of the structure; hence, all of the vertical concrete is utilized to support both gravity and lateral loads. The reinforced concrete structure was designed in accordance with the requirements of ACI 318-02 Building Code Requirements for Structural Concrete.

To reduce the effects of differential column shortening due to creep, between the perimeter columns and interior walls, the perimeter columns were sized such that the self-weight gravity stress on the perimeter columns matched the stress on the interior corridor walls. The five sets of outriggers, distributed up the building, tie all the vertical load-carrying elements together, further ensuring uniform gravity stresses, hence reducing differential creep movements. Since the shrinkage in concrete occurs more quickly in thinner walls or columns, the perimeter column thickness of 600 mm (24 in.) matched the typical corridor wall thickness to achieve similar volume-to-surface ratios. This balance design ensures the column and walls will generally shorten at the same rate due to concrete shrinkage.

The top section of the tower consists of a structural steel spire using a diagonally braced lateral system. The structural steel spire was designed for gravity, wind, seismic, and fatigue in accordance with the requirements of AISC Load and Resistance Factor Design Specification for Structural Steel Buildings (1999). The exterior exposed steel is protected with a flame-applied aluminum finish.

The three-dimensional analysis model used for design consisted of the reinforced concrete walls, link beams, slab, mat and supporting piles, and the spire structural steel system. From lateral wind loading analysis, the building deflections were found to be well below commonly used criteria. The dynamic analysis indicated the first mode is lateral sidesway with a period of 11.3 s. The second mode is a perpendicular lateral sidesway with a period of 10.2 s. Torsion is the fifth mode with a period of 4.3 s.

The permitting authority in Dubai specifies Dubai as a UBC97 Zone 2a seismic region with a seismic zone factor  $Z = 0.15$  and soil profile  $S_e$ . The seismic analysis consisted of a site-specific response spectra analysis. Seismic loading typically did not govern the design of the reinforced concrete tower structure. Seismic loads did govern the design of the reinforced concrete podium buildings and the tower structural steel spire.

The tower foundation consists of a pile-supported mat 3.7 m (12 ft) thick and was poured utilizing SCC. The mat was constructed in four separate pours (three wings and the center core). Each pour occurred over at least a 24 h period. Reinforcement was typically at 12 in. (300 mm) spacing.

The tower mat is 3.7 m (12 ft) thick and therefore, in addition to durability, limiting peak temperature was an important consideration. The concrete mix for the mat incorporated 40% fly ash and a water–cement ratio of 0.34.

The tower mat is supported by 194 bored cast-in-place piles. The piles are 5 ft (1–5 m) in diameter and approximately 141 ft (43 m) long, with a design capacity of 3000 t each. The pile load test indicated a capacity of over 6000 t. The SCC concrete was placed by the tremie method using polymer slurry. The friction piles are supported in the naturally cemented calcisiltite/conglomeritic calcisiltite formations, developing an ultimate pile skin friction of 250–350 kPa (2.6 to 3.6 t/ft<sup>2</sup>).

It was determined the maximum long-term settlement over time would be about a maximum of 80 mm (31 in.).

When the construction was at Level 135, the average foundation settlement was 30 mm (1.2 in.).

The groundwater in which the Burj Dubai substructure is constructed is particularly severe, with chloride concentrations of up to 45% and sulfates of up to 6%. The chloride and sulfate concentrations found in the groundwater are even higher than the concentration in sea water. Accordingly, the primary consideration in designing the piles and mat foundation was durability. The concrete mix cube strength for the piles was a 8700 psi (60 MPa) mix based on a triple blend with 25% fly ash, 7% silica fume, and water–cement ratio of 0.32. The concrete was also designed as a fully SCC, incorporating a viscosity-modifying admixture with a slump flow of  $675 \pm 75$  mm ( $26.6 \pm 3$  in.) to limit the possibility of defects during construction.

Owing to the aggressive conditions present due to the extremely corrosive ground water, a rigorous program of anti-corrosion measures was required to ensure the durability of the foundations. Measures implemented included specialized waterproofing systems, increased concrete cover, the addition of corrosion inhibitors to the concrete mix, stringent crack control design criteria, and an impressed current cathodic protection system utilizing titanium mesh.

As is common to tall buildings, the wind tunnel program included rigid-model force balance tests, full multi-degree of freedom aeroelastic model studies, measurements of localized pressures, pedestrian wind environment studies, and wind climatic studies. Wind tunnel models accounted for the cross-wind effects of wind-induced vortex shedding on the building (Figure 8.68). The aeroelastic and force balance studies used models mostly at 1:500 scale.

To determine the wind loading on the main structure, wind tunnel tests were undertaken early in the design using the high-frequency force-balance technique. The wind tunnel data were then combined with the dynamic properties of the tower in order to compute the tower's dynamic response and the overall effective wind force distributions at full scale. For the Burj Dubai, the results of the force balance tests were used as early input for the structural design and the detailed shape of the tower and allowed parametric studies to be undertaken on the effects of varying the tower's stiffness and mass distribution.

The building has essentially six important wind directions. The principal wind directions are when the wind is blowing into Nose A, Nose B, and Nose C (see Figure 8.68). The other three directions are when the wind blows in between two wings, (Tail A, Tail B, and Tail C). It was noticed that the force spectra for different wind directions showed less excitation in the important frequency range for wind impacting the pointed or nose end of a wing than from the opposite tail direction.

Several rounds of force balance tests were undertaken as the geometry of the tower evolved and was refined architecturally. The three wings were set back in a clockwise sequence, with the A wing setting back first. After each round of wind tunnel testing, the data were analyzed and the building was reshaped to minimize wind effects. Toward the end of design more accurate aeroelastic model tests were initiated. An aeroelastic model is flexible in the same manner as the real building, with properly scaled stiffness, mass, and damping. The aeroelastic tests were able to model several of the higher translational modes of vibration. These higher modes dominated the structural response and design of the tower except at the very base, where the fundamental modes controlled. Based on the results of the aeroelastic models, the predicted building motions were found to be within the

International Organization for Standardization (ISO 6899, 1984) recommended values without the need for auxiliary damping (2.0 percent of gravity for a 10-year wind return period).

The tower is constructed utilizing both a vertical and horizontal compensation program. For vertical compensation, each story is being constructed incorporating a modest increase in the typical floor-to-floor height.

For horizontal compensation, the building is “recentered” with each successive jump of the center hexagonal core. The recentering compensation will correct for all gravity-induced sideways effects (elastic, differential foundation settlement, creep, and shrinkage) which occur up to the casting of each story.

The reinforced concrete link beams transfer the gravity loads at the setbacks including the effects of creep and shrinkage, and interconnect the shear walls for lateral loads. The link beams were designed by the requirements of ACI 318-02, Appendix A, for strut and tie modeling. Strut and tie modeling permitted the typical link beams to remain relatively shallow.

The design of the concrete for the vertical elements is determined by the requirements for a compressive strength of 10 MPa (1.5 ksi) at 10h to permit the construction cycle and a design strength/modulus of 80 MPa, (11.6 ksi) as well as ensuring adequate pumpability and workability. The ambient conditions in Dubai vary from a cool winter to an extremely hot summer, with maximum temperatures occasionally exceeding 50°C. To accommodate the different rates of strength development and workability loss, the dosage and retardation level is adjusted for the different seasons.

Ensuring pumpability to reach world record heights is probably the most difficult concrete design issue, particularly considering the high summer temperatures. Four separate basic mixes were developed to enable reduced pumping pressure as the building gets higher.

The concrete mix contains 13% fly ash and 10% silica fume with a maximum aggregate size of 20 mm (3/4 in.). The mix is virtually self-consolidating with an average slump flow of approximately 600 mm (24 in.).

The walls are formed using automatic self-climbing formwork system. The circular nose columns are formed with steel forms. Wall reinforcement is prefabricated on the ground in 26 ft (8 m) sections to allow fast placement.

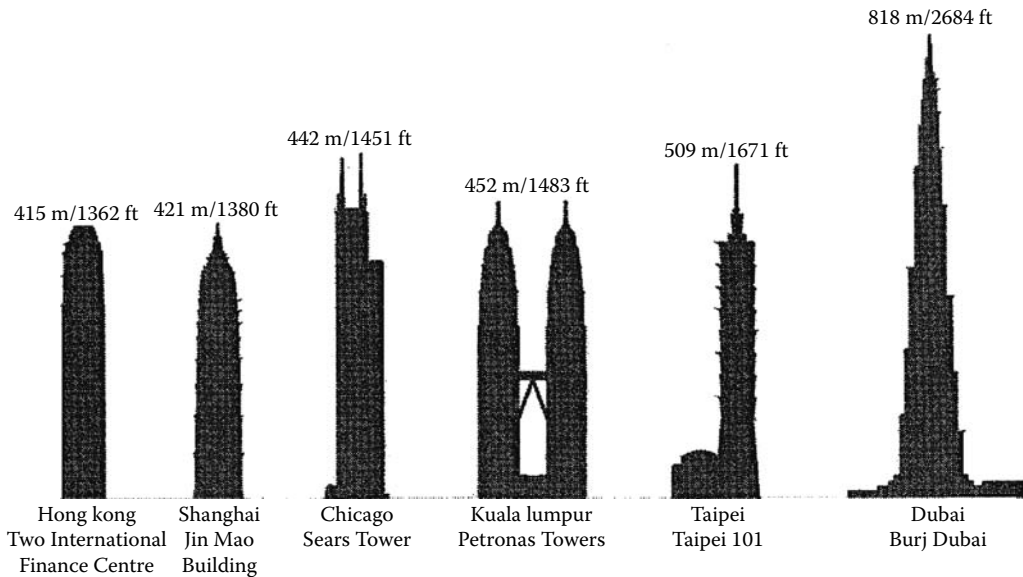
The construction sequence for the structure has the central core and slabs being cast first, in three sections; the wing walls and slabs follow behind; and the wing nose columns and slabs follow behind these. Concrete is pumped to heights of 600 m (1970 ft) in a single stage.

## 8.15 FUTURE OF TALL BUILDINGS

September 11, 2001, has not marked the end of the skyscraper era. Already there is talk of America reclaiming the crown with several of the recent proposals for the WTC site in Manhattan involving world-beating structures. But the race for tallness is happening not in America. Instead the action is in the Far East and UAE. The past 10 or 15 years (from the mid-1990s to, say, 2010) marks the tall building era of the Far East. Of the world’s ten tallest buildings, eight are in Asia (Figure 8.69).

What is the motivation behind the race? To be candid, the reasons are the same today as they were some 70 years ago: height now, as then, is an exhibition of technology and power. Nothing is more expressive than an upright symbol, particularly the one with high-tech items such as pressurized double-decker elevators, external damping devices to reduce sway caused by windstorms, and fiber optics incorporated into curtain walls that transform buildings into giant billboards. Tall buildings become instant icons, putting their cities on the map.

Given humanity’s competitive nature, it is hard to believe that Burj Dubai at 2684 ft (818 m) will wear the crown long. The quest for the title of world’s tallest building is alive and well. This begs the question, in its search for the sky how tall can buildings go? Answer: No limit is in sight, at least from structural considerations. Humanity has an obsession with building super-tall structures, particularly when humans can live and work in them. While there are indeed lessons to be



**FIGURE 8.69** Comparative heights of several of the world's tallest buildings.

learned from the WTC catastrophe, the skyscraper will remain viable well into the foreseeable future. The race for the clouds obscures the preformed changes taking place in the design and construction of skyscrapers: A new generation model is energy efficient, radically designed, and an essential component of urban design.

What part will concrete play in super-tall buildings? It is very likely residential buildings will continue to use structural concrete. Commercial high-rise buildings mostly will be composite structures with structural concrete cores and super-columns consisting of high-strength steel structural steel shapes encased in super strong reinforced concrete. Outrigger and belt truss systems will continue to play their traditional roles in optimizing the lateral bracing.

The Chrysler building in New York, completed in 1930 was the first to surpass the 300 m (984 ft) mark, the point at which the Council on Tall Buildings and Urban Habitat, CTBHU, defines a building as being *Supertall*. In the 80 years since its completion, only 37 buildings have achieved this same status and only 18 cities can today boast of being home to a supertall building. However, there are already several projections indicating that the numbers of superfall buildings in the world will have more than doubled by the end of year 2015.

The emphasis on a growing number of these supertall projects is to search for appropriate environmental responses as a design motivation. It is the buildings green credentials and environmental friendliness that is demanding attention rather than its height. The goal is to exploit on-site energy from renewable sources and take every opportunity to reduce energy consumption.

Looking ahead, future projects are expected to focus on green building and leadership in energy and environmental design (LEED) certification. Energy elements, to name a few, will include the use of insulated concrete forms for shear walls, roof top solar arrays, low E windows, ultra-efficient HVAC systems, and engineered lighting plans.

The success of supertall buildings constructed thus far is a testimony to technical ability of architects, developers and engineers. Making the yet unborn supertall buildings, supergreen and eco-friendly is the newest challenge.

---

# 9 Special Topics

## 9.1 DAMPING DEVICES FOR REDUCING MOTION PERCEPTION

Engineers have learned from building occupants and owners, and from wind-tunnel studies, that designing a tall building to meet a given drift limit under code-specified equivalent static loads is not enough to make occupants comfortable during windstorms. However, they have only limited control over three intrinsic factors, namely, the height, the shape, and the mass that influence the dynamic response of buildings. Additionally, the behavior of a tall building subjected to dynamic loads such as wind or seismic activity is difficult to predict with any accuracy because of the uncertainty associated with the evaluation of a building's damping and stiffness, as well as the complicated nature of loading.

The present state of the art is such that an estimate of structural damping can be made with a plus or minus accuracy of only 30% until the building is constructed and the nonstructural elements are fully installed. It is well known that wind-induced building response is inversely proportional to the square root of total damping, consisting of aerodynamic plus structural damping. So, if damping is quadrupled (increased by four times), a 50% response reduction is achieved, and if damping is doubled, the dynamic response is reduced by 25%. Because of the inherent damping of a building responding elastically to wind loads is in the range of 0.5%–1.5% of the critical response, it is impractical to increase the damping to, say, four times as much by use of modified structural materials.

Suppression of excessive vibrations can be dealt with limited success in a variety of ways. Additional stiffness can be provided to reduce the vibration period of a building to a less sensitive range. Changes in mass of a building can be effective in reducing excessive wind-induced excitation. Aerodynamic modifications to the building's shape, if agreeable to the building's owner and architect, can result in reduced vibrations caused by wind. However, these traditional methods can be implemented only up to a point beyond which the solutions may become unworkable because of other design constraints such as cost, space, or aesthetics. Therefore, to achieve reduction in response, a practical solution is to supplement the damping of the structure with a mechanical damping system external to the building's structure.

### 9.1.1 PASSIVE VISCOELASTIC DAMPERS

Figure 9.1 shows schematic of a viscoelastic polymer damper. This type of damper was first used in the now nonexistent World Trade Center Towers, conceived in the 1960s, constructed in the early 1970s, and destroyed by terrorists on September 11, 2001. These buildings were designed with viscoelastic dampers distributed at approximately 10,000 locations in each building. The dampers extended between the lower chords of the floor joists and gusset plates mounted on the exterior columns beneath the stiffened seats (Figures 9.2 and 9.3).

Viscoelastic dampers dissipate energy through deformation of polymers sandwiched between relatively stationary steel plates. Their energy dissipation depends on both relative shear deformation of the polymer and relative velocity within the device. The device is typically used to reduce occupants' perception of wind-induced motions. It does not require constant operational monitoring and is not dependent on electric power.

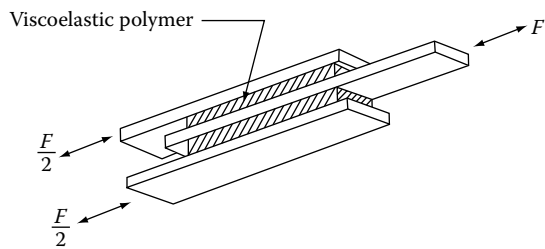


FIGURE 9.1 Schematics of viscoelastic damper.

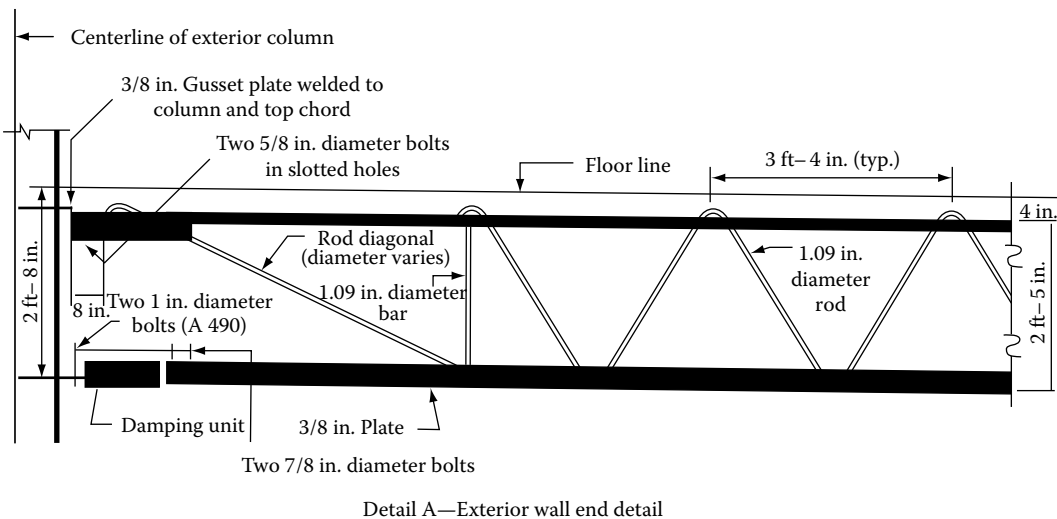
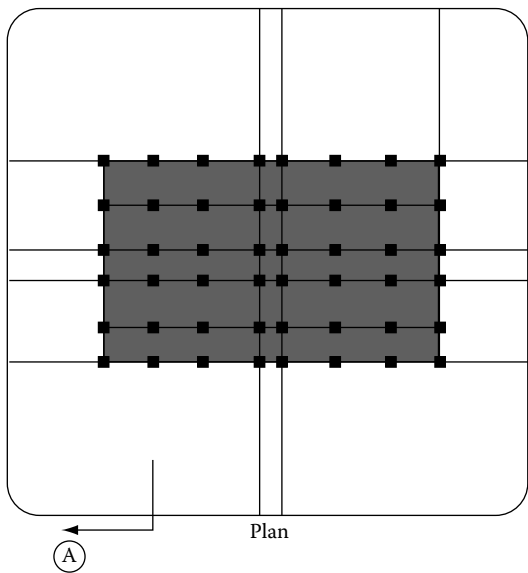
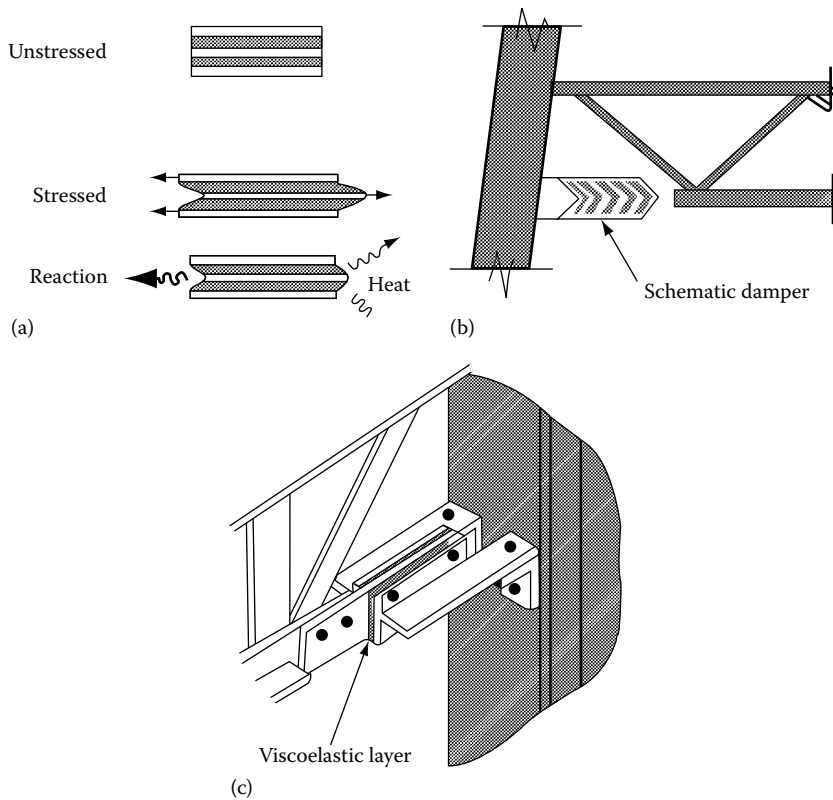


FIGURE 9.2 Viscoelastic dampers in World Trade Center Towers.



**FIGURE 9.3** Viscoelastic dampers, schematics.

The Columbia Seafirst Center, a 76-story building in Seattle, built in 1984 is another example of using this technology to reduce occupant perception of wind-induced building motion. The dampers used in this building consist of steel plates coated with a polymer compound. The plates are sandwiched between a system of relatively stationary plates. As the building sways under the action of wind loads, the steel plates which are attached to structural members are subjected alternately to compression and tension. In turn, the viscoelastic polymer subjected to shearing deformations absorbs and dissipates much of the strain energy into heat, thus reducing wind-induced motions.

### 9.1.2 TUNED MASS DAMPER

A typical application of a tuned mass damper (TMD) consists of a heavy mass installed near a building's top in such a way that it tends to remain still while the building moves beneath it. This strategy allows the mass at the top to transmit its inertial force to the building in a direction opposite to the motions of the building itself, thereby reducing the building's oscillations.

The mass itself weighs only a small fraction, 0.25%–0.70%, of the building's total weight, which corresponds to about 1%–2% of first modal mass. “Tuned” simply means the mass can be adjusted to move in a fundamental period equal to the building's natural period so that it will be more effective in counteracting the building oscillations. In addition to the initial tuning when it is first installed, the TMD may be fine-tuned as the building period changes with time. The period may



increase as the building occupancy changes, as nonstructural partitions are added, or as elements contributing to nonstructural stiffness “loosen up” after initial windstorms.

Thus a TMD may be considered as a small damped mass of single-degree-of-system riding “piggyback” atop a building. Although its mass is a small fraction of the building’s mass, its vibration characteristics are adjusted to mimic those of the building’s. For example, if a tall building sways, say, 24 in. to the right at a fundamental frequency of 0.16 Hz, the TMD is designed to move to the left at the same frequency. The idea of using the inertia of a floating mass to tame the sway of a tall building is not entirely new. In fact, the invention of the TMD as an energy-dissipative vibration absorber is credited to Frahm, who developed the concept in 1909. The theory was later described by Den Hartog in his classic textbook in 1956, and since then has been applied in automotive and aircraft engines to reduce vibrations. Since the wind force–time relationship is not harmonic (sinusoidal), the basic ideas developed by Den Hartog have been modified in building applications to account for the random nature of wind.

When activated during windstorms, the TMD becomes free-floating by rising on a nearly frictionless film of oil. To dissipate energy, the TMD must be allowed to move with respect to the building. In the earlier TMDs installed in tall buildings, springlike devices connecting the mass to the building pull the building back to center, as the building sways away from its equilibrium position. The mass is also connected to the building with a damping device, in the form of a hydraulic actuator, which is controlled to provide a predetermined percentage of critical damping. This limits the lateral displacements of the mass relative to the building.

The TMD’s advantages become academic in a power failure. It needs electricity to work and if that is lost in a heavy windstorm, when the TMD would most be needed, it would not work. So it is advisable to have the TMD wired to an emergency power system.

During a major windstorm, the mass will move in relation to the building some 2–5 ft. The system is controlled to activate when a predetermined building lateral acceleration occurs. This motion is registered on an accelerometer and, if the allowable limit is reached, the mass is activated automatically.

#### 9.1.2.1 Citicorp Tower, New York

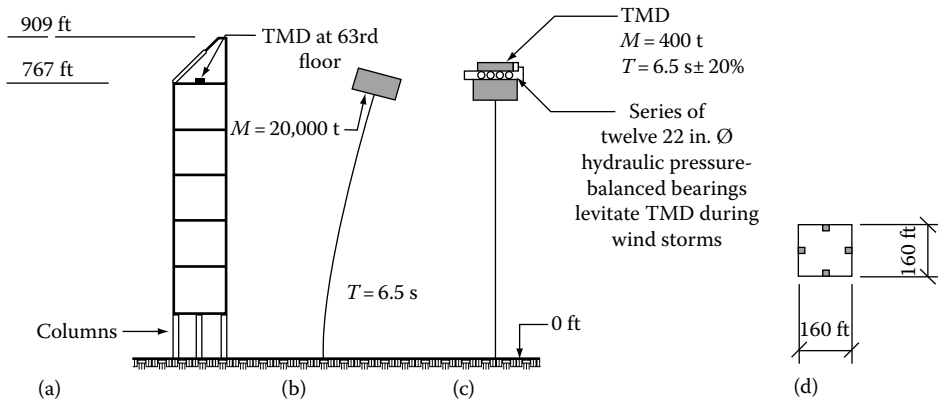
The Citicorp Tower, shown in Figure 9.4, consists of a unique structural system of perimeter-braced tubes elevated on four 112 ft-high columns and a central core. It rises approximately 914 ft above grade. The tower is square in cross section with plan dimensions of approximately  $157 \times 157$  ft. The top 140 ft portion of the tower slopes downward from north to south.

The TMD designed for the building consists of a concrete block  $29 \times 29 \times 9$  ft that weighs 410t (820 kip). It is attached to the building with two nitrogen-charged pneumatic spring devices and two hydraulic actuators that are controlled to provide damping to the TMD and linearize the “springs.” One set counters north–south building dynamic motion and the other set counters east–west motion. The spring stiffness, and thereby the TMD frequency, is adjusted (tuned) by changing the pneumatic pressure. It also has an antiyaw device to prevent twisting of the block and snubbers to prevent excessive motion of the block.

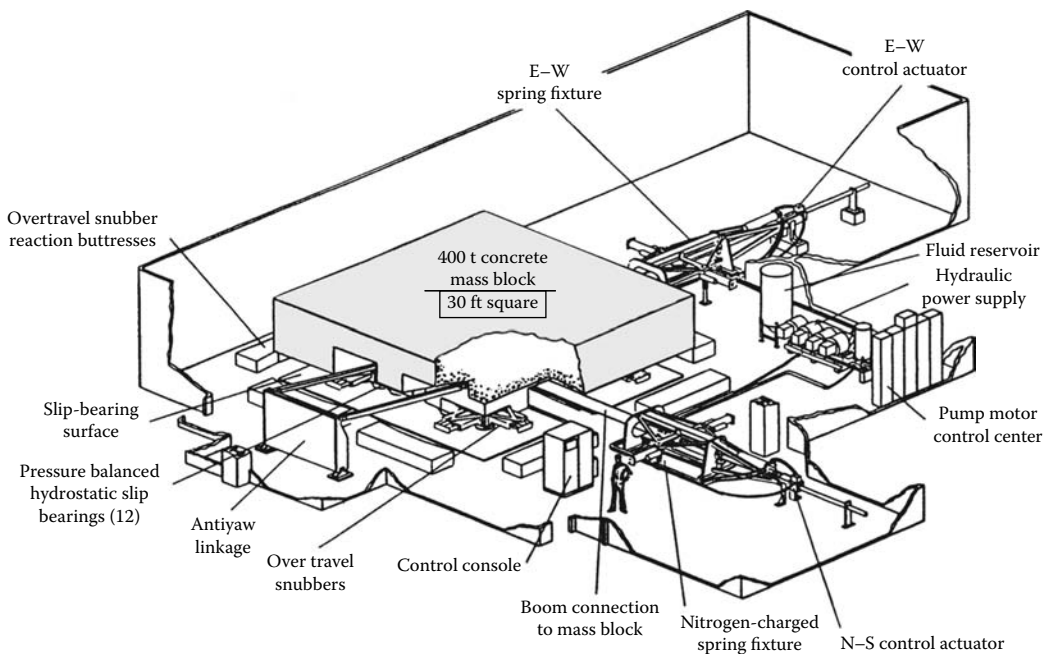
The TMD is capable of a 45 in. operating stroke in each orthogonal direction. The operating period is adjustable independently in each axis. The mass block is supported with twelve 22 in.-diameter pressure-balanced bearings connected to a hydraulic pump.

The block positioned at the building’s 63rd floor (780 ft high) represents approximately 2% of first-period modal mass of the building. The motions of the block are controlled by pneumatic devices and servohydraulics resulting in a system that has the characteristics of a spring–mass–damper system, as shown schematically in Figure 9.5.

To dissipate energy, the TMD is allowed to move with respect to the building. It is continuously on standby, and is designed to start up automatically whenever the accelerations exceed a predetermined value. The TMD kicks in whenever the accelerations for two successive cycles of build-



**FIGURE 9.4** Tuned mass damper (TMD) for City Corp, New York: (a) building elevation, (b) first-mode response, (c) TMD atop the building, and (d) plan.



**FIGURE 9.5** Schematics of TMD, City Corp Center, New York.

ing motion exceed 3 milli- $g$  (1 milli- $g$  =  $1/1000$  of acceleration due to gravity, therefore, 3 milli- $g$  corresponds to an acceleration of approximately  $1.16 \text{ in./s}^2$ ).

The system continues to operate as long as building motions continue and stops only a half-hour after the last pair of building cycles for which maximum acceleration is greater than 0.75 milli- $g$ . The TMD provides the building with an effective structural damping of about 4% of critical. This is a significant increase above the inherent damping estimated to be just under 1% of critical. Since wind-induced accelerations of a building are approximately proportional to the inverse of the square root of the damping, when in operation the TMD reduces the building sway oscillations by over 40%.

The Citicorp TMD is installed on the 63rd floor. At this elevation, the building may be represented by a single-degree-of-freedom system with a modal mass of 40,000 kip resonating biaxially at a 6.8 s period with a critical damping factor of 1%. The TMD is designed with a moving mass of 820 kip, biaxially resonant with a period of  $6.7 \text{ s} \pm 20\%$ , and an adjustable damping of 8%–14% of critical. Observe that the moving mass represents approximately 2% of the first-period modal mass, which typically corresponds to about 0.6%–0.7% of the total mass.

### 9.1.2.2 John Hancock Tower, Boston, Massachusetts

The TMD for the John Hancock Mutual Life Insurance Co.'s glass-clad landmark in Boston is somewhat different from that for Citicorp Tower. It was added as an afterthought to prevent occupant discomfort. Second, Hancock Tower is rectangular in plan and consists of moment frames unlike Citicorp's diagonally braced frame (Figures 9.6 and 9.7). Because of the building's shape, location, and vibration properties, its dynamic wind response is mainly in the east–west direction and in torsion about its vertical axis. There is a TMD near each end of an upper floor. They are tuned to a vibration period of approximately 7.5 s. The total east–west moving mass represents about 1.4% of the building first-mode generalized mass, while in the twist direction the moving masses represents about 2.1% of the building's generalized torsional inertia. The dampers, then, move only in an east–west direction and work together to resist sway motions in the short direction, or in opposition to stabilize torsional rotations of the building. They are located 220 ft apart, and when moving in opposition act in effect as a 220 ft lever arm to resist twisting. Hancock's dampers each have a 300 t mass consisting of lead blocks contained in a steel coffer box. They also activate at 3 milli-g of acceleration. In operation the masses may move up to 6 ft with an operating cycle of about 7.5 s. Each mass block is supported on sixteen 22 in. diameter pressure-balanced bearings connected to a hydraulic pump.

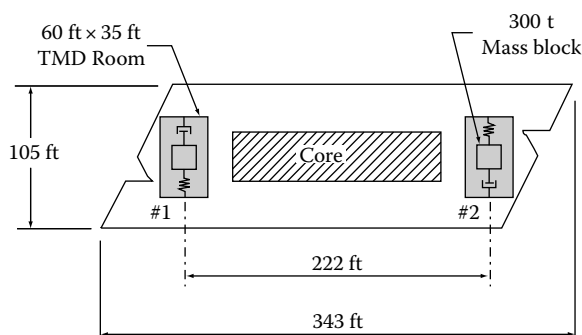


FIGURE 9.6 Dual TMD: John Hancock Tower, Boston, MA.

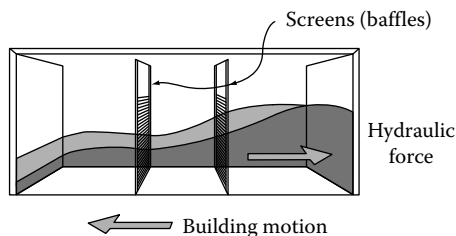


FIGURE 9.7 Sloshing water damper, schematics.

The TMDs in both the Citicorp and John Hancock towers are used only to assure occupants' comfort. Their beneficial effects in reducing wind-induced dynamic forces are not relied upon for structural integrity under extreme wind loads.

Both the John Hancock Tower and Citicorp Tower TMDs are called passive-powered because, although the reduction in the buildings sway response comes from the inertial force of the dampers, initially power is required to activate the masses. The sliding masses installed in these towers cannot move until their oil bearings are pressurized to levitate the masses.

### 9.1.2.3 Design Considerations for TMD

There are a number of practical considerations in the design of the TMD. One of these is the need to limit the motions of the TMD mass under very high wind loading that occur in the design storm or under ultimate load conditions. One way of doing this is to use a nonlinear hydraulic damper in the TMD. By employing such a damper, the motions of the TMD mass can be greatly reduced under very high wind loading conditions or under strong seismic excitation. A further safeguard against excessive TMD motion is to install hydraulic buffers around the mass. When the mass comes into contact with the buffers, high velocities are quickly reduced.

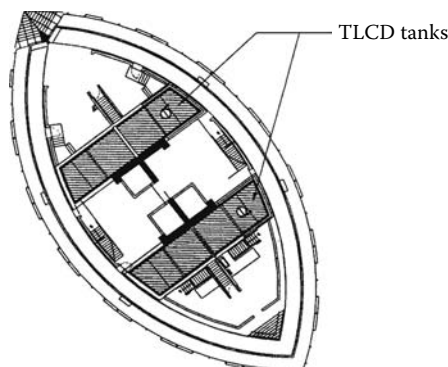
Both the Citicorp and John Hancock TMD systems have sensors and feedback and electronic control systems, but these were designed to make the TMD operate like a passive-TMD. TMDs can in principle be readily converted to be an active system by incorporating sensors and feedback systems that can drive the TMD mass to produce more effective damping than is possible in a purely passive mode. As a result, a larger effective damping can be obtained from a given mass. This approach has been used in several commercially available ready-to-install systems. The TMD is thus made more efficient, a benefit to be weighed against the increased cost, complexity, and maintenance requirements that are entailed with an active system.

### 9.1.3 SLOSHING WATER DAMPER

A simple sloshing type of damper consists of a tuned rectangular tank filled to a certain level with water (Figure 9.5b). The tuning of the system consists of matching the tank's natural period of wave oscillation to the building's period by appropriate geometric design of the tank. If obstacles such as screens and baffles are placed in the tank, dissipation of the waves takes place when water sloshes across these obstructions resulting in a behavior similar to that of a TMD, and the result is again that the tank behaves as a TMD. However, analysis indicates that a sloshing water tank does not make efficient use of the water mass as a tuned liquid column damper.

### 9.1.4 TUNED LIQUID COLUMN DAMPER

A tuned liquid column damper (TLCD) is in many ways similar to a TMD that uses a heavy concrete block or steel as the tuned mass. The difference is that the mass is now water or some other liquid. The damper is essentially a tank in the shape of a U. It has two vertical columns connected by a horizontal passage and filled up to a certain level with water or other liquid. Within the horizontal passage, screens or a partially closed sluice gate are installed to obstruct flow of water, thus dissipating energy due to motion of water. The TLCD is mounted near the top of a building, and when the building moves, the inertia of the water causes the water to oscillate into and out of the columns, traveling in the passage between them. The columns of water have their own natural period of oscillation which is determined purely by the geometry of the tank. If this natural period is close to that of the building's period then the water motions become substantial. Thus the building's kinetic energy is transferred to the water. However, as the water moves past the screens or the partially open sluice gate in the horizontal portion of the tank, the drag of these obstacles to the flow dissipates the energy of the motion. The end result is added damping to reduce building oscillations.



**FIGURE 9.8** Tuned liquid column dampers, TLCD, Wall Center, Vancouver, BC.

#### 9.1.4.1 Wall Center, Vancouver, British Columbia

Figure 9.8 shows the plan for the mechanical penthouse of a building called Wall Center, a 48-story residential tower in Vancouver, BC. From wind-tunnel tests, predicted 10 year accelerations were in the range of 40 milli-g, depending on the structural systems considered in the preliminary design. To minimize occupants' perception of motion due to wind excitations, a limit of 15 milli-g was chosen as the design criterion for a 10 year acceleration. A damper using water serves a dual purpose by also providing a large supply of water high up in the tower for fire suppression. Initially, a sloshing water damper was considered but the TLCD was found preferable due to its greater efficiency in using the available water mass. The design turned out to be a remarkably economical solution considering the saved cost of having to install a high-capacity water pump and emergency generator in the base of the building as initially required by fire officials. The total mass required was on the order of 600 t which corresponds to a large volume of water. However, sufficient space was available. Also a helpful factor was that the motions of the tower were primarily in one direction only. Therefore only motions in one direction needed to be damped, which simplified the design. Figure 9.9 illustrates the TLCD design consisting of two identical U-shaped concrete tanks. Since the building was concrete, it was relatively easy to incorporate the tanks into the design and to construct them as a simple addition to the main structure. The structural design is by Glotman Simpson Engineers, Vancouver, BC, Canada. The design of the TLCD is by Rowan, Williams, Davis, and Irwin, Inc., Guelph, ON, Canada.

#### 9.1.4.2 Highcliff Apartment Building, Hong Kong

Another example of a tall building that uses TLMD to control accelerations and provide enhanced structural performance during typhoon conditions, is the 73-story Highcliff apartment building in Hong Kong, one of the windiest places on earth. The building soars to a height of 705 ft (215 m) with an astonishing slenderness ratio of 20:1. A unique structural system that incorporates all vertical elements as part of the lateral system, in combination with a series of tuned liquid mass dampers, ensures the safety and comfort of the buildings occupants.

Photographs of the building are shown in Figure 9.10. The structural engineering is by the Seattle firm of Magnusson Klemencic Associates.

#### 9.1.5 SIMPLE PENDULUM DAMPER

The principal feature of the system shown in Figure 9.11 is a mass block slung from cables with adjustable lengths. The mass typically represents approximately 1.5%–2% of the building's generalized mass in the first mode of vibration. The mass is connected to hydraulic dampers that dissipate energy while reducing the swinging motions of the pendulum.

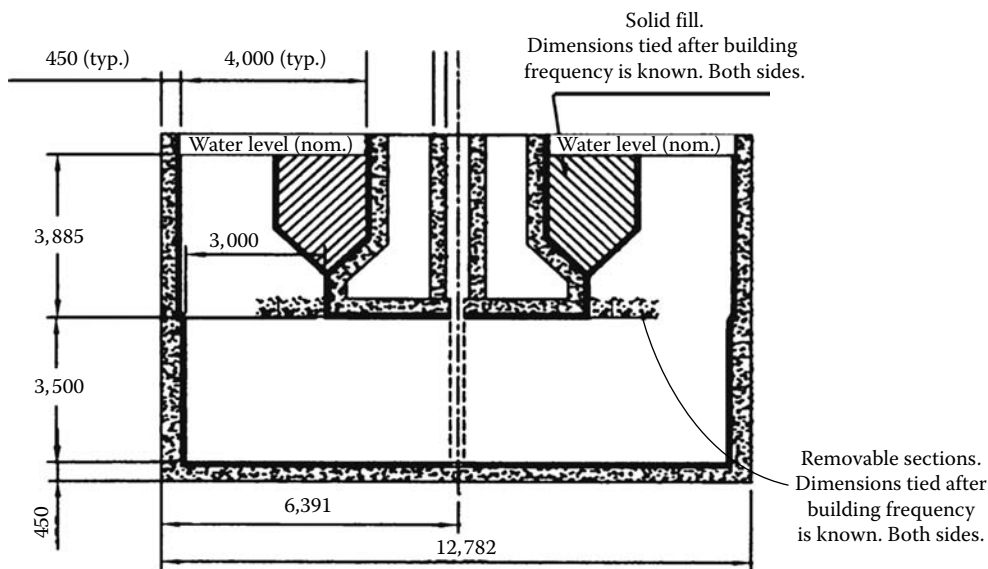


FIGURE 9.9 TLCD, Wall Center, Vancouver, BC.

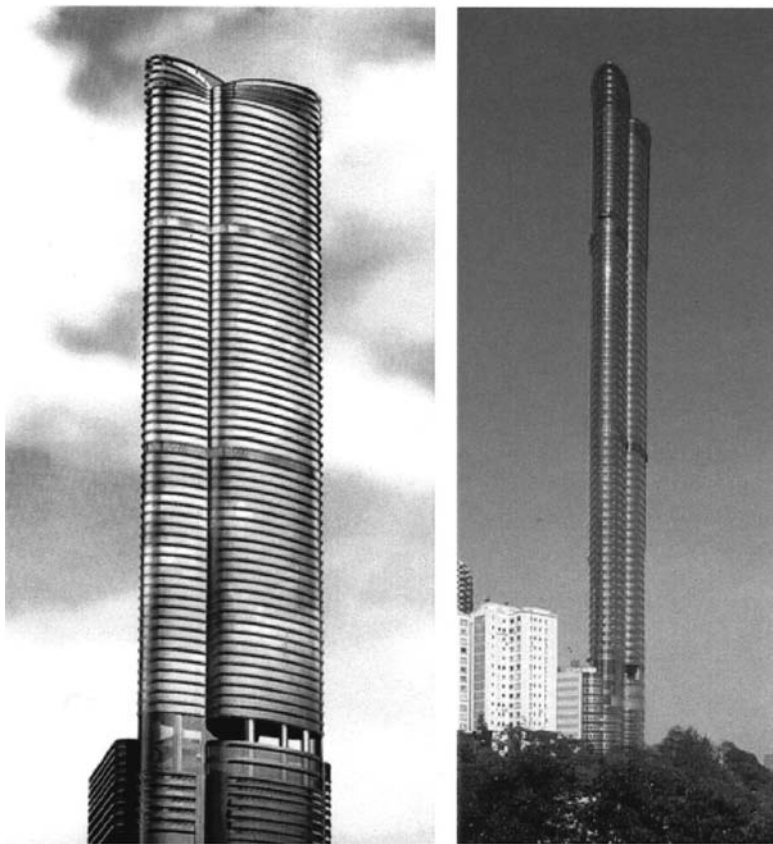
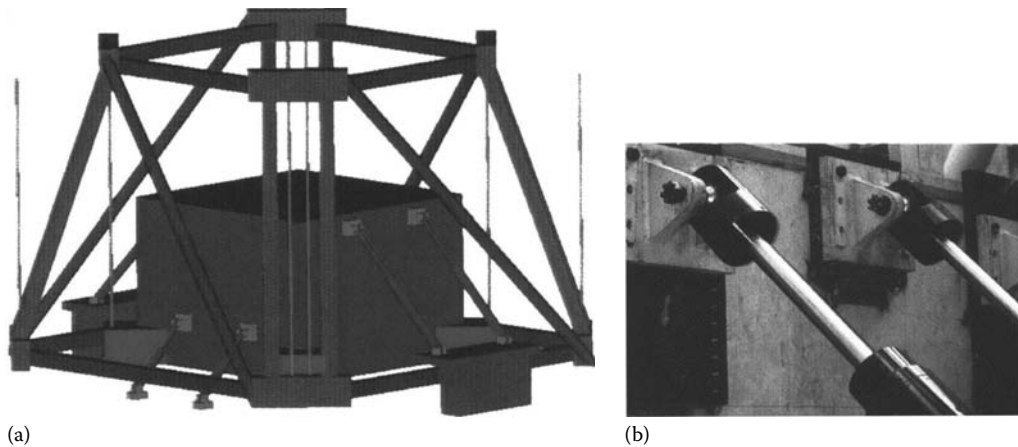


FIGURE 9.10 Highcliff apartments, Hong Kong.

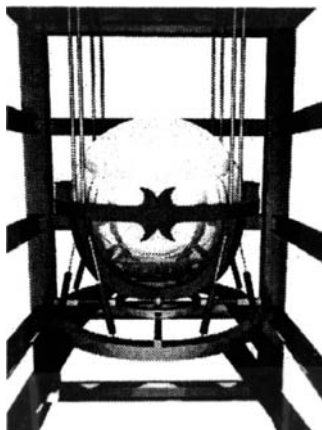


**FIGURE 9.11** (a) Simple pendulum damper. (b) Hydraulic dampers attached to mass block.

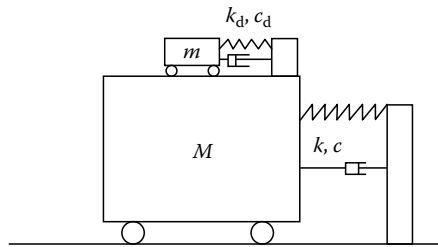
The adjustable frame is used as a tuning device to tailor the natural period of vibration of the pendulum. The frame can be moved up and down and clamped on the cables to allow the natural period of the pendulum to be adjusted. The mass is connected to an antiyaw device to prevent rotations about a vertical axis. Below the mass there is a bumper ring connected to hydraulic buffers to prevent travel beyond the hydraulic cylinder's stroke length.

#### 9.1.5.1 Taipei Financial Center

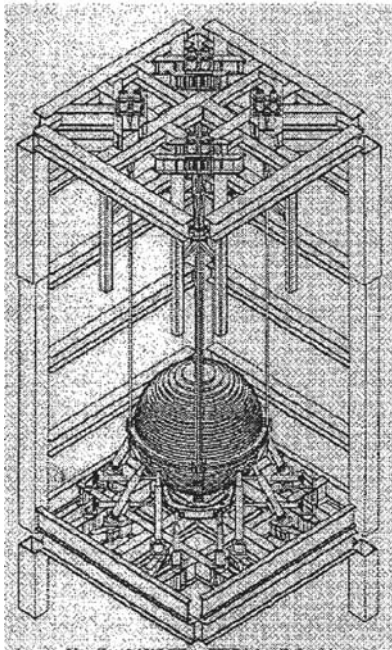
An example of a tuned mass pendulum damper (TMPD) architecturally expressed as a building feature is shown in Figures 9.12 and 9.13. At a height of 1667 ft (508 m), consisting of 101 stories, the building, called Taipei Financial Center, is poised to steal the crown from the twin Malaysian Petronas Towers as the tallest building in the world. A special space has been allocated for the TMPD near the top of the building and people will be able to walk around it and view it from a variety of angles. The TMPD, consisting of a 730t steel ball, will be brightly colored, and special lighting effects are planned. The architecture of the building is by C.Y. Lee and Partners, Taiwan; structural engineering is by Evergreen Consulting Engineering, Inc., Taipei, Taiwan, and Thornton-Tomasetti Engineers, New York; and the design of the TMPD is by Motioneering, Inc.,



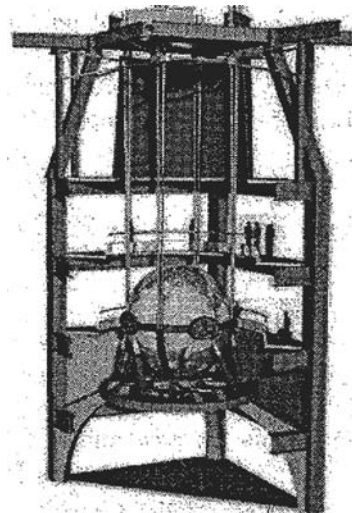
**FIGURE 9.12** Spherical tuned mass pendulum damper, TMPD, Taipei Financial Center.



(a)



(b)



(c)

**FIGURE 9.13** Taipei 101, tuned mass pendulum damper: (a) TMPD, (b) TMPD principle, and (c) schematics.

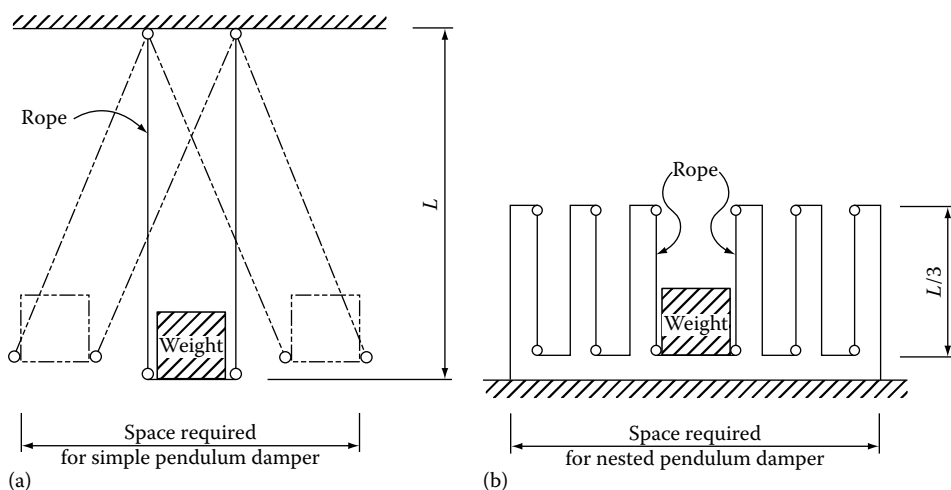
a company in Ontario, Canada, that specializes in designing and supplying damping systems for dynamically sensitive structures.

### 9.1.6 NESTED PENDULUM DAMPER

In situations where the height available in a building is insufficient to allow installation of a simple pendulum system, a nested TMD may be designed as illustrated in Figure 9.14. The design shown is for a North American residential tower. The total vertical space occupied by the damper, which has a natural period of about 6 s and a mass of 600 t, is less than 25 ft (7.62 m), as compared to 30 ft (9.14 m) required for a simple pendulum. The design of the damper is by Rowan, Williams, Davis, and Irwin, Inc., Guelph, ON, Canada.

A nested pendulum damper is installed at the top of the 70-story, 971 ft-tall Landmark Tower, Yokohama, Japan. The damper requires only a one-story-high space, and is semi-actively controlled. Wind-induced lateral accelerations are expected to be reduced at least 60%. The damper design is by Mitsubishi Heavy Industries, Ltd., Tokyo, Japan.





**FIGURE 9.14** (a) Simple pendulum damper. (b) Nested pendulum damper.

## 9.2 SEISMIC ISOLATION

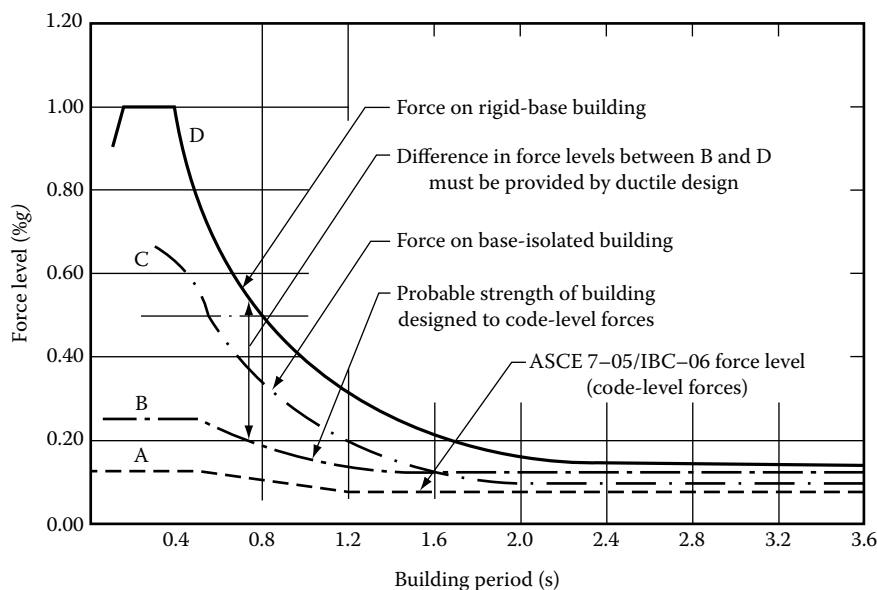
Seismic isolation is a viable design strategy that has been used for seismic rehabilitation of existing buildings and in the design of a number of new buildings. In general, this system will be applicable to the rehabilitation and design of buildings whose owners desire superior earthquake performance and can afford the special costs associated with the design, fabrication, and installation of seismic isolators. The concepts are relatively new and sophisticated, and require more extensive design and detailed analysis than do most conventional schemes. In California, peer review of these new concepts is required for all designs that use seismic isolation.

Conceptually, isolation reduces response of the superstructure by “decoupling” the building from seismic ground motions. Typical isolation systems reduce seismic forces transmitted to the superstructure by lengthening the period of the building and adding some amount of damping. Added damping is an inherent property of most isolators, but may also be provided by supplemental energy dissipation devices installed across the isolation interface. Under favorable conditions, the isolation system reduces drift in the superstructure by a factor of at least two—and sometimes by as much as a factor of five—from that which would occur if the building were not isolated. Accelerations are also reduced in the structure, although the amount of reduction depends on the force–deflection characteristics of the isolators and may not be as significant as the reduction of drift.

Reduction of drift in the superstructure protects structural components and elements as well as nonstructural components sensitive to drift-induced damage. Reduction of acceleration protects nonstructural components that are sensitive to acceleration-induced damage.

To understand the design principles for base-isolated buildings, consider Figure 9.15, which shows four distinct response curves A, B, C, and D. Let us examine the design of a building, say, some five stories tall, with a fixed-base fundamental period of 0.6 s. Curve A, the lowest, shows lateral design demand resulting from loads prescribed in building codes such as IBC 2005. (ASCE 7-05) Curve B, the second lowest, represents the probable strength of the structure. This strength is generally greater than the design strength because of several factors. This is because

1. Actual material strengths are almost always higher than those assumed in design.
2. Use of load factors typically overestimates the actual loads imposed on the structure.
3. Some conservatism is used in sizing of structural members.



**FIGURE 9.15** Design concept for base-isolated buildings.

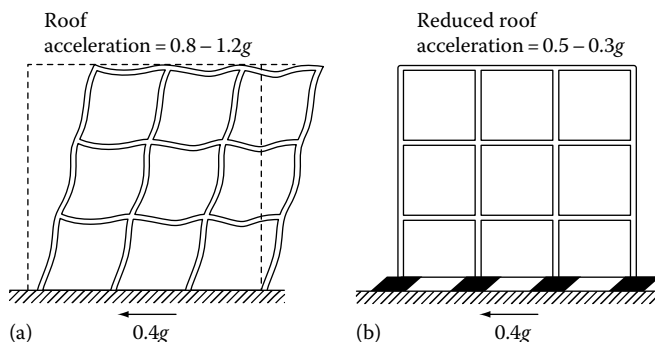
4. Designs are often based on drift limits.
5. Members are designed to have at least some ductility. It is estimated that the probable strength of a structure designed to code-level forces is about 1.5–2.0 times larger than the design strength.

Curve D at the top shows the forces our fixed-base building would experience if it were to remain elastic for the entire duration of a design earthquake. However, in earthquake-resistant design, it is assumed that the lateral-force-resisting system will make excursions well into the nonlinear inelastic capacities of the structural materials. Therefore, typical buildings are designed to resist only a fraction of the full linear elastic demands of major earthquakes. Heavy reliance is placed on special prescribed details to provide ductility for the extreme nonlinear inelastic demands. The difference between the linear elastic demand, Curve D, and the probable capacity of the building, Curve B, conceptually represent the magnitude of energy dissipation expected of the structure.

Let us compare this to the energy dissipation required of the building, if it is seismically isolated. The elastic forces experienced by a seismically isolated building are significantly reduced for two reasons. First, the flexibility of the base isolators shifts the period of the building toward the low end of the spectrum. For instance, our example building with a fixed-base period of 0.6 s would probably now have a period in the neighborhood of, say, 2–2.5 s. The drop in the elastic design force, as seen in the graph, is considerable.

The second factor contributing to the reduction in force level is the additional damping provided by the dampers. Depending on the type of base isolator and supplemental viscous damper (if any) chosen for the building, the damping may increase from a generally assumed value of 5% of critical to as much as 20% or more. Together, these two factors help to reduce the ductility demand expected of the structure during a large seismic event. In fact, it is quite likely that our base-isolated structure may never be pushed beyond its elastic limit. In other words, in the 2.0–2.5 period range, the probable strength of the building is very nearly the same as the maximum unreduced elastic demand.

Therefore, the building need not take excursions into nonlinear inelastic range, and can remain elastic for the entire duration of a design earthquake.



**FIGURE 9.16** Comparison of response of fixed-base and base-isolated building: (a) fixed-base and (b) base-isolated.

In simple terms, seismic isolation involves placing a building on isolators that have large flexibility in the horizontal plane (Figure 9.16). The system consists of

- A flexible mounting to increase the building period which, in turn, reduces seismic forces in the structure above.
- A damper or energy dissipater to reduce relative deflections between a building and the ground it rests upon.
- A mounting that is sufficiently rigid to control the building lateral deflection during minor earthquakes and windstorms.

Flexibility can be introduced at the base of a building by many devices. These include

- Elastomeric bearings
- Rollers
- Sliding plates
- Cable suspension
- Sleeved piles
- Rocking foundations

However, decrease in base shear due to lengthening of a building's period comes at a price; the flexibility at the base gives rise to large relative displacements across the flexible mount. Hence, the necessity of providing additional damping at the base-isolation level.

While a flexible mounting is required to isolate a building from seismic loads, its flexibility under frequently occurring wind and minor earth tremors is undesirable. Therefore, the device at the base must be stiff enough at these loads, such that the building's response is as if it were on a fixed base.

Generally one isolator per column is used. However, more than one isolator may be required in certain type of buildings. For isolation of shear walls, one or more isolators are used at each end, and if the wall is long, isolators may be placed along its entire length, the spacing depending upon the spanning ability of the wall between the isolators.

### 9.2.1 SALIENT FEATURES

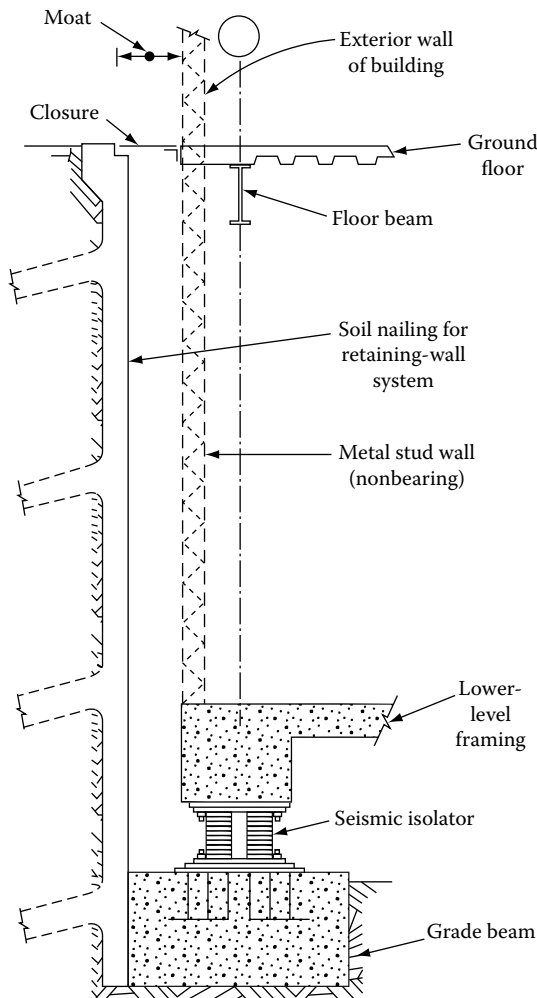
It is important to consider the following features in the design of base-isolated buildings.

1. Access for inspection and replacement of bearings should be provided at bearing locations.
2. Stub-walls or columns to function as backup systems should be provided to support the building in the event of isolator failure.

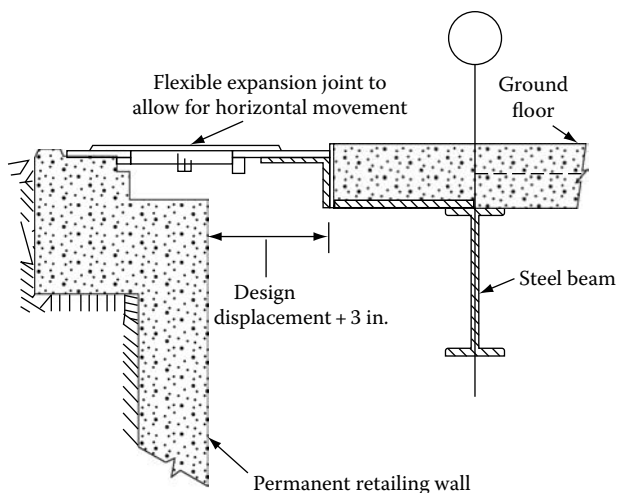
3. A diaphragm capable of delivering lateral loads uniformly to each bearing is preferable. If the shear distribution is unequal, the bearings should be arranged such that larger bearings are under stiffer elements.
4. A moat to allow free movement for the maximum predicted horizontal displacement must be provided around the building (Figures 9.17 and 9.18).
5. The isolator must be free to deform horizontally in shear and must be capable of transferring maximum seismic forces between the superstructure and the foundation.
6. The isolators should be tested to ensure that they have lateral stiffness properties that are both predictable and repeatable. The tests should show that over a wide range of shear strains, the effective horizontal stiffness and area of the hysteresis loop are in agreement with values used in the design.

When earthquakes occur, the elastomeric bearings used for base isolation are subjected to large horizontal displacements, as much as 15 in. or greater in a 10-story steel-framed building. They must therefore be designed to carry the vertical loads safely at these displacements.

Isolation systems should be considered if the desired performance objective is immediate occupancy (IO). Conversely, isolation will likely not be an appropriate design strategy if the desired



**FIGURE 9.17** Moat around base-isolated building.



**FIGURE 9.18** Moat detail at ground level.

performances objective is collapse prevention (CP). In general, isolation systems provide significant protection to the building structure, nonstructural components, and contents, but at a cost that precludes practical application when the budget and design objectives are modest.

### 9.2.2 MECHANICAL PROPERTIES OF SEISMIC ISOLATION SYSTEMS

A seismic isolation system is the collection of all individual seismic isolators and may be composed entirely of one type of seismic isolator, a combination of different types of seismic isolators, or a combination of seismic isolators acting in parallel with energy dissipation devices (i.e., a hybrid system).

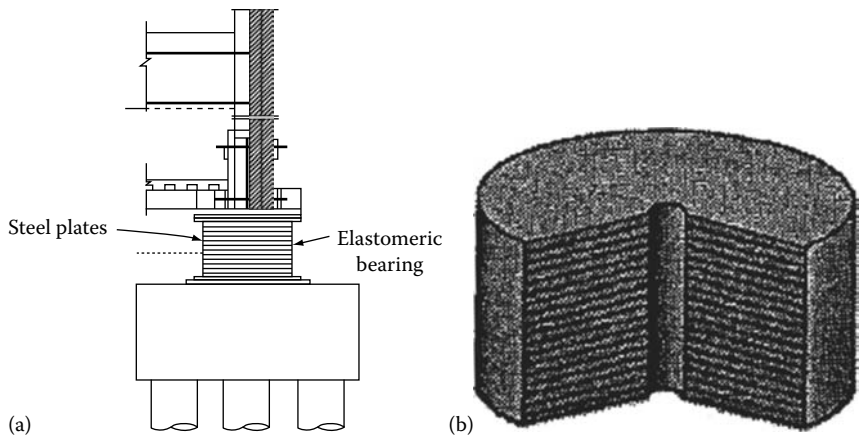
The most popular devices for seismic isolation in the United States may be classified as either elastomeric or sliding. Examples of elastomeric isolators include high-damping rubber bearings (HDR), low-damping rubber bearings (RB), or low-damping rubber bearings (LRB) with a lead core. Sliding isolators include flat assemblies or those with a curved surface, such as the friction-pendulum system (FPS).

### 9.2.3 ELASTOMERIC ISOLATORS

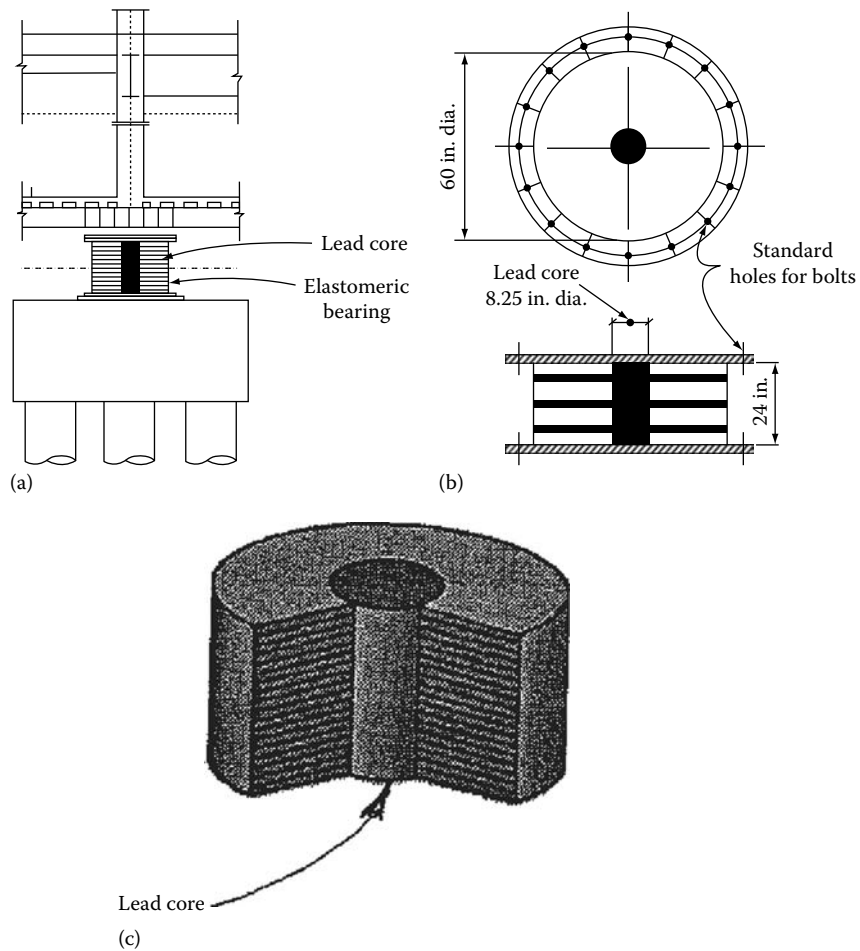
Elastomeric bearings are a common means for introducing flexibility into structure. They consist of thin layers of natural rubber that are vulcanized and bonded to steel plates. Natural rubber exhibits a complex mechanical behavior that can be described simply as a combination of viscoelastic and hysteretic behavior. Low-damping natural rubber bearings exhibit essentially linearly elastic and linearly viscous behavior at large shear strains. The effective damping is typically less than or equal to 0.07 for shear strains in the range 0–2.0.

Lead-rubber bearings are generally constructed of low-damping natural rubber with a preformed central hole into which a lead core is press-fitted (see Figures 9.19 and 9.20). Under lateral deformation, the lead core deforms in almost pure shear, yields at low levels of stress of approximately 1160–1450 psi (8–10 MPa) in shear at normal temperature), and produces hysteretic behavior that is stable over many cycles. Unlike mild steel, lead recrystallizes at normal temperature (about 20°C), so that repeated yielding does not cause fatigue failure. Lead-rubber bearings generally exhibit characteristic strength that ensures rigidity under service loads.

High-damping rubber bearings are made of specially compounded rubber that exhibits effective damping between 0.10 and 0.20 of critical. The increase in effective damping of high-damping rubber is achieved by the addition of chemical compounds that may also affect other mechanical properties of rubber.



**FIGURE 9.19** Elastomeric isolators: (a) high-damping rubber bearing made by bonding rubber sheets to steel plates and (b) high-damping rubber bearing.



**FIGURE 9.20** (a) Lead-rubber bearing under interior columns. (b) Lead-rubber bearing for an interior column for a five-story steel frame building: approximate dimensions. (c) Natural rubber bearing with press-fit lead core.

Scragging is the process of subjecting an elastomeric bearing to one or more cycles of large amplitude displacement. The scragging process modifies the molecular structure of the elastomer and results in a more stable hysteresis at strain levels lower than that to which elastomer was scragged. Although it is usually assumed that the scragged properties of an elastomer remain unchanged with time, recent studies suggest that partial recovery of unscragged properties is likely. The extent of this recovery is dependent on the elastomer compound.

#### 9.2.4 SLIDING ISOLATORS

Sliding isolators with either a flat or a single-curvature spherical sliding surface are typically made of PTFE or PTFE-based composites in contact with polished stainless steel. The shape of the sliding surface allows large contact areas that, depending on the materials used, are loaded to average bearing pressures in the range 1,015–10,150 psi (7–70 MPa).

Sliding isolators tend to limit the transmission of force to an isolated structure to a predetermined level. While this is desirable, the lack of significant restoring force can result in significant variations in the peak displacement response, and can result in permanent offset displacements. To avoid these undesirable features, sliding isolators are typically used in combination with a restoring force mechanism.

Combined elastomeric-sliding isolation systems have been used in buildings in the United States. Japanese engineers have also used elastomeric bearings in combination with mild steel elements designed to yield in strong earthquakes and enhance the energy dissipation capability of the isolation systems.

Details of a spherical sliding system commonly referred to as a FPS is shown in Figures 9.21 through 9.24. Figure 9.25 shows a schematic of base-isolation devices acting in conjunction with viscoelastic dampers.

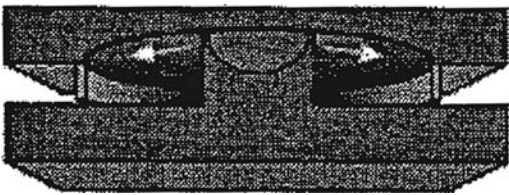
#### 9.2.5 SEISMICALLY ISOLATED STRUCTURES: ASCE 7-05 DESIGN PROVISIONS

The procedures and limitations for the design of seismically isolated structures is determined considering zoning, site characteristics, vertical acceleration, cracked section properties of concrete and masonry members, seismic use group, configuration, structural system, and height. Both the lateral force-resisting system and the isolation system must be designed to resist the deformations and stresses produced by the effects of ground motions. The stability of the vertical load-carrying elements of the isolation system must be verified by analysis and tested for lateral seismic displacement equal to the total maximum displacement. All portions of the structure, including the structure above the isolation system, must be assigned a seismic use group based on ASCE 7-05 provisions with an occupancy importance factor taken as 1.0 regardless of its seismic use group categorization. Each structure must be designated as being regular or irregular on the basis of the structural configuration above the isolation system.

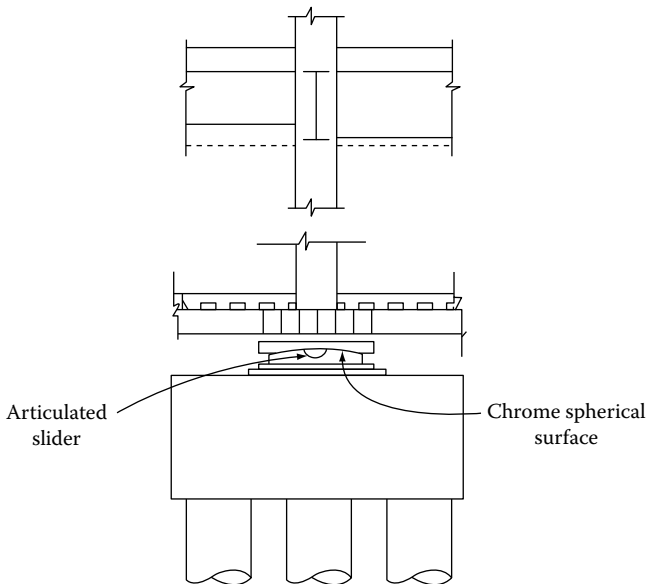
Three procedures are permissible: static analysis, response spectrum analysis, and time–history analysis. The static analysis procedure is generally used to start the design process and to calculate benchmark values for key design parameters (displacement and base shear) evaluated using either response spectrum or time–history analysis procedures.

The static analysis procedure is straightforward. However, the procedure cannot be used when the spectral demands cannot be adequately characterized using the assumed spectral shape. Typically this occurs in

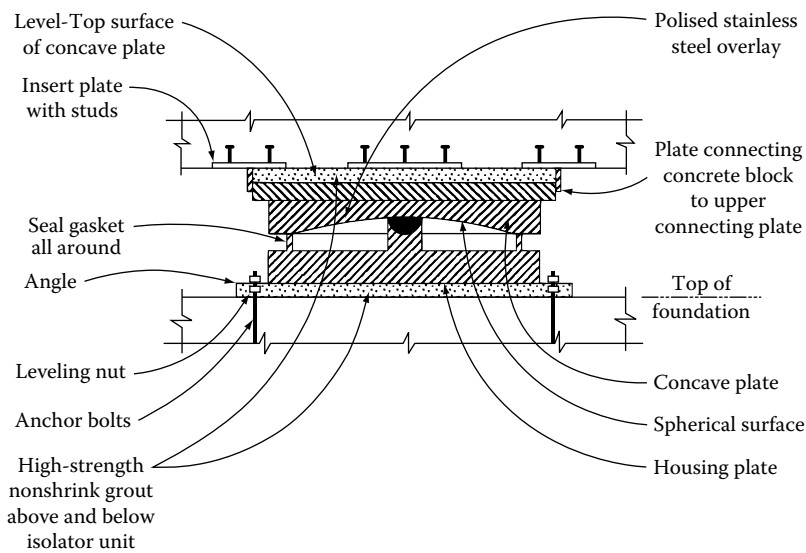
1. Isolated buildings located in the near field
2. Isolated buildings on soft soil sites
3. Long-period isolated buildings (beyond the constant velocity domain)



**FIGURE 9.21** Single stage friction pendulum.

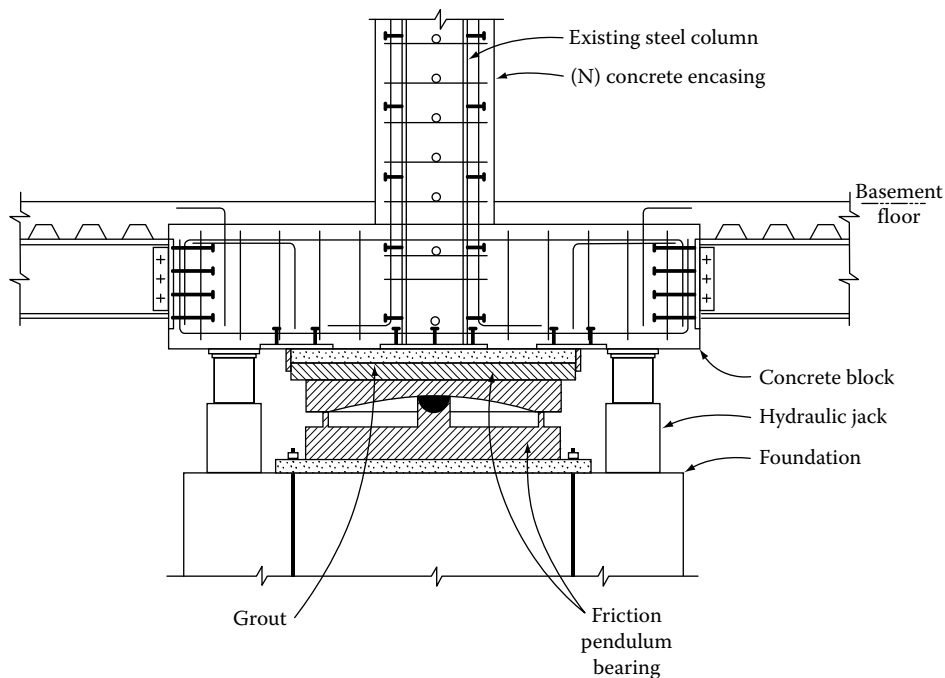


**FIGURE 9.22** Sliding bearing: friction pendulum system base-isolation.

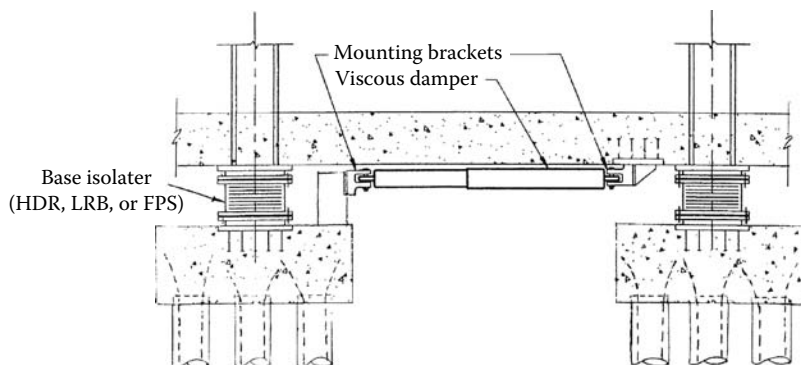


**FIGURE 9.23** Friction pendulum system, details.





**FIGURE 9.24** Installation details, FPS under existing interior columns.



**FIGURE 9.25** Base isolator operating in concert with viscous damper.

Further, the static procedure cannot be used for nonregular superstructures or for highly nonlinear isolation systems.

Response spectrum analysis is permitted for the design of all isolated buildings except for those buildings located on very soft soil sites (for which site-specific spectra should be established), buildings supported by highly nonlinear isolation systems for which the assumptions implicit in the definitions of effective stiffness and damping break down, or buildings located in the very near field of major active faults where response spectrum analysis may not capture pulse effects adequately.

Time-history analysis is the default analysis procedure: It must be used when the restrictions set forth on static and response spectrum analysis cannot be satisfied, and may be used for the analysis of any isolated building. Arguably the most detailed of the analysis procedures, the results of time-history analysis must be carefully reviewed to avoid any gross design errors.

### 9.2.5.1 Equivalent Lateral Force Procedure

This procedure is permitted when the following restrictions are met:

1. The structure is located at a site with  $S_1$  less than or equal to 0.60g.
2. The structure is located on a class A, B, C, or D site.
3. The structure above the isolation interfaces is less than or equal to four stories or 65 ft (19.8 in.) in height.
4. The effective period of the isolated structure at maximum displacement  $T_m$  is less than or equal to 3.0s.
5. The effective period of the isolated structure at the design displacement  $T_p$  is greater than three times the elastic, fixed-base period of the structure above the isolation system.
6. The structure above the isolation system is of regular configuration.
7. The isolation system meets all the following criteria:
  - a. The effective stiffness of the isolation system at the design displacement is greater than one-third of the effective stiffness at 20% of the design displacement.
  - b. The isolation system is capable of producing a restoring force such that the lateral force at the total design displacement  $D_T$  is at least 0.025  $w$  greater than the lateral force at 50% of the total design displacement.
  - c. The isolation system has force–deflection properties that are independent of the rate of loading.
  - d. The isolation system has force–deflection properties that are independent of vertical load and bilateral load.
  - e. The isolation system does not limit maximum considered earthquake displacement to less than  $S_{M1}/S_{D1}$  times the total design displacement.

### 9.2.5.2 Lateral Displacements

There are as many as six definable displacements in base-isolation terminology. Three of these are defined in Figures 9.26 and 9.27, while the others, related to certain prescribed formulas, are explained in the text.

**Design displacement:** The isolation system must be designed and constructed to withstand design lateral earthquake displacements  $D_D$ , calculated to occur in the direction of each of the main horizontal axes of the structure in accordance with the following equation:

$$D_D = gS_{D1}T_D / 4\pi^2 B_D \quad (17.5-1)$$

where

$g$  is the acceleration due to gravity—the units for  $g$  are in./s<sup>2</sup> (mm/s<sup>2</sup>) if the units of the design displacement,  $D_D$  are in. (mm)

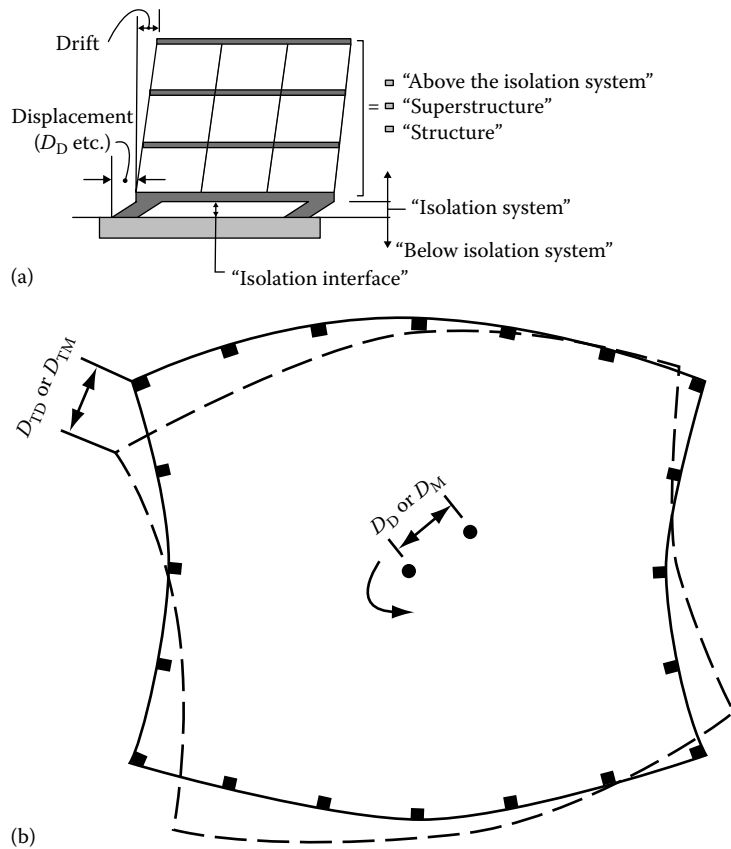
$S_{D1}$  is the design 5% damped spectral acceleration parameter at 1 s period in units of g-s, as determined

$T_D$  is the effective period of seismically isolated structure in seconds, at the design displacement in the direction under consideration, as prescribed by Equation 17.5-2

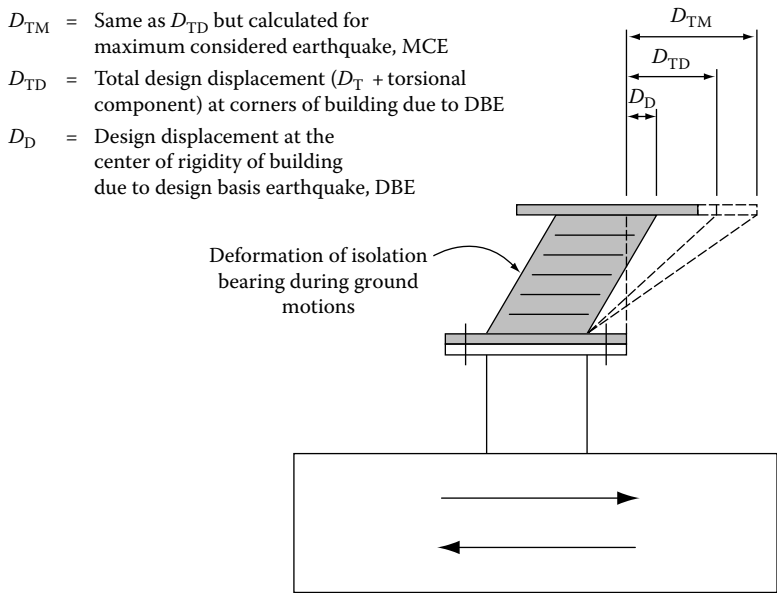
$B_D$  is the numerical coefficient related to the effective damping of the isolation system at the design displacement,  $\beta_D$ , as set forth in Table 17.5-1

The equation numbers given here correspond to those in Chapter 17 of ASCE 7-05.

**Effective period at design displacement:** The effective period of the isolated structure at design displacement  $T_D$  shall be determined using the deformational characteristics of the isolation system in accordance with the following equation:



**FIGURE 9.26** (a) Base isolation: ASCE 7-05 nomenclature. (b) Isolator displacements: ASCE 7-05 definitions.



**FIGURE 9.27** Isolator displacement terminology.

$$T_D = 2\pi \sqrt{\frac{W}{k_{D\min}g}} \quad (17.5-2)$$

where

$T_D$  is the effective period of the isolated structure at design displacement  $D_D$

$W$  is the effective seismic weight of the structure above the isolation interface

$K_{D\min}$  is the minimum effective stiffness in kip/in. (kN/mm) of the isolation system at the design displacement in the horizontal direction under consideration

$g$  is the acceleration due to gravity

**Maximum lateral displacement:** The maximum displacement of the isolation system  $D_M$  in the most critical direction of horizontal response can be calculated in accordance with the formula:

$$D_M = \frac{gS_{M1}T_M}{4\pi^2 B_M} \quad (17.5-3)$$

where

$g$  is the acceleration due to gravity

$S_{M1}$  is the maximum considered 5% damped spectral acceleration at 1 s period, in units of g-s

$T_M$  is the effective period, in s, of seismic-isolated structure at the maximum displacement in the direction under consideration, as prescribed by Equation 17.5-4

$B_M$  is the numerical coefficient related to the effective damping of the isolation system at the maximum displacement  $\beta_M$ , as set forth in Table 17.5-1

**Effective period at maximum displacement:** The effective period of the isolated structure,  $T_M$ , at maximum displacement  $D_M$  shall be determined using the deformational characteristics of the isolation system in accordance with the equation:

$$T_M = 2\pi \sqrt{\frac{W}{k_{M\min}g}} \quad (17.5-4)$$

where

$W$  is the effective seismic weight of the structure below the isolation interface

$k_{M\min}$  is the minimum effective stiffness in kip/in (kN/mm), of the isolation system at the maximum displacement in the horizontal direction under consideration, as prescribed by Equation 17.8-6

$g$  is the acceleration due to gravity

**Total lateral displacement:** The total design displacement  $D_{TD}$  and the total maximum displacement  $D_{TM}$  of elements of the isolation system includes additional displacement due to actual and accidental torsion calculated from the spatial distribution of the lateral stiffness of the isolation system and the most disadvantageous location of mass eccentricity. The total design displacement  $D_{TD}$  and the total maximum displacement  $D_{TM}$  of elements of an isolation system with uniform spatial distribution of lateral stiffness shall not be taken less than that prescribed by the following equations:

$$D_{TD} = D_D \left[ 1 + y \frac{12e}{b^2 + d^2} \right] \quad (17.5-5)$$

$$D_{TM} = D_M \left[ 1 + y \frac{12e}{b^2 + d^2} \right] \quad (17.5-6)$$

**Exception:** The total design displacement,  $D_{TD}$ , and the total maximum displacement,  $D_{TM}$ , are permitted to be taken as less than the value prescribed by Equations 17.5-5 and 17.5-6, respectively, but not less than 1.1 times  $D_D$  and  $D_M$ , respectively, provided the isolation system is shown by calculation to be configured to resist torsion accordingly.

where

$D_D$  is the design displacement at the center of rigidity of the isolation system in the direction under consideration, as prescribed by Equation 17.5-1

$D_M$  is the maximum displacement at the center of rigidity of the isolation system in the direction under consideration, as prescribed by Equation 17.5-3

$y$  is the distance between the centers of rigidity of the isolation system and the element of interest measured perpendicular to the direction of seismic loading under consideration

$e$  is the actual eccentricity measured in plan between the center of mass of the structure above the isolation interface and the center of rigidity of the isolation system, plus accidental eccentricity, in ft (mm), taken as 5% of the longest plan dimension of the structure perpendicular to the direction of force under consideration

$b$  is the shortest plan dimension of the structure, in ft (mm), measured perpendicular to  $d$

$d$  is the longest plan dimension of the structure

### 9.2.5.3 Minimum Lateral Forces for the Design of Isolation System and Structural Elements at or below Isolation System

The isolation system, the foundation, and all structural elements below the isolation system shall be designed and constructed to withstand a minimum lateral seismic force,  $V_b$ , using all of the appropriate provisions for a nonisolated structure where

$$V_b = k_{D \max} D_D \quad (17.5-7)$$

where

$k_{D \max}$  is the maximum effective stiffness, in kip/in. (kN/mm), of the isolation system at the design displacement in the horizontal direction under consideration as prescribed by Equation 17.8-3.

$V_b$  is the minimum lateral seismic design force or shear on elements of the isolation system or elements below the isolation system

$D_D$  is the design displacement, in in. (mm), at the center of rigidity of the isolation system in the direction under consideration, as prescribed by Equation 17.5-1

$V_b$  shall not be taken as less than the maximum force in the isolation system at any displacement up to and including the design displacement

### 9.2.5.4 Minimum Lateral Forces for the Design of Structural Elements above Isolation System

The structure above the isolation system shall be designed and constructed to withstand a minimum shear force  $V_s$  using all of the appropriate provisions for a nonisolated structure where

$$V_s = \frac{k_{D \max} D_D}{R_t} \quad (17.5-8)$$

where

$k_{D\max}$  is the maximum effective stiffness of the isolation system at the design displacement in the horizontal direction under consideration

$D_D$  is the design displacement at the center of rigidity of the isolation system in the direction under consideration

$R_I$  is the numerical coefficient related to the type of lateral force-resisting system above the isolation system

The  $R_I$  factor shall be based on the type of lateral force-resisting system used for the structure above the isolation system and shall be three-eighths of the  $R$  value of a nonisolated structure with an upper-bound value not exceeding 2.0 and a lower-bound value not less than 1.0.

**Limits on  $V_s$ :** The value of  $V_s$  shall not be taken as less than the following conditions:

1. The lateral seismic force of a fixed-base structure of the same weight  $W$ , and a period equal to the isolated period  $T_D$
2. The base shear corresponding to the factored design wind load
3. The lateral seismic force required to fully activate the isolation system (e.g., the yield level of a softening system, the ultimate capacity of a sacrificial wind-restraint system, or the breakaway friction level of a sliding system) factored by 1.5

**Vertical distribution of  $V_s$ :** The total force shall be distributed over the height of the structure above the isolation interface in accordance with the following equation:

$$F_x = \frac{V_s w_x h_x}{\sum_{i=1}^n w_i h_i} \quad (17.5-9)$$

where

$F_x$  is the lateral force at level  $x$

$V_s$  is the total lateral seismic design force or shear on elements above the isolation system

$w_x$  is the portion of  $W$  that is located at or assigned to level  $i$ ,  $n$ , or  $x$ , respectively

$h_x$  is the height above the base level  $i$ ,  $n$ , or  $x$ , respectively

$w_i$  is the portion of  $W$  that is located at or assigned to level  $i$ ,  $n$ , or  $x$ , respectively

$h_i$  is the height above the base level  $i$ ,  $n$ , or  $x$ , respectively

At each level designated as  $x$ , the force  $F_x$  shall be applied over the area of the structure in accordance with the mass distribution at the level.

### 9.2.5.5 Drift Limits

The maximum story drift of the structure above the isolation system shall not exceed  $0.015h_{sx}$ . The drift shall be calculated by the ASCE 7-05 Equation 12.8-15 with the  $C_d$  factor of the isolated structure equal to the  $R_I$  factor defined in Section 17.5.4.2.

### 9.2.5.6 Illustrative Example: Static Procedure

Up to this point we have discussed the basic principles of seismic isolation and the equivalent lateral force (ELF) procedure of ASCE 7-05. Although not discussed here, it should be noted that a dynamic analysis is mandatory for most buildings because buildings that meet the requirements for the use of ELF procedure such as regularity are indeed rare, even in high seismic zones. However, the design principles are best understood by working through a static example, as given in the following section. Ample interpretation of ASCE 7-05 provisions is repeated to present the solution in a stand-alone format (Table 9.1).

**TABLE 9.1**  
**Lower-Bound Limits on Dynamic Procedures Specified in Relation to ELF Procedure Requirements**

Design Parameter	ELF Procedure	Dynamic Procedure	
		Response Spectrum	Response History
Design displacement— $D_D$	$D_D = (g/4\pi^2)(S_{D1}T_D/B_D)$	—	—
Total design displacement— $D_T$	$D_T \geq 1.1D$	$\geq 0.9D_T$	$\geq 0.9D_T$
Maximum displacement— $D_M$	$D_M = (g/4\pi^2)(S_{M1}T_M/B_M)$	—	—
Total maximum displacement— $D_{TM}$	$D_{TM} \geq 1.1D_M$	$\geq 0.8D_M$	$\geq 0.8D_M$
Design shear— $V_b$ (moat size) (at or below the isolation system)	$V_b = k_{D \max} D_D$	$\geq 0.9V_b$	$\geq 0.9V_b$
Design shear— $V_s$ (“regular” superstructure)	$V_s = k_{D \max} D_D/R_1$	$\geq 0.8V_s$	$\geq 0.6V_s$
Design shear— $V_s$ (“irregular” superstructure)	$V_s = k_{D \max} D_D R_1$	$\geq 1.0V_s$	$\geq 0.8V_s$
Drift (calculated using $R_1$ for $C_d$ )	$0.015h_{sx}$	$0.015h_{sx}$	$0.020h_{sx}$

**Given:** A new four-story hospital building is located in the outskirts of Los Angeles, California. The owners of the facility have desired a building of superior earthquake performance and are willing to incur the special costs associated with the design, fabrication, and installation of seismic isolators. A target building performance level of immediate occupancy or better is sought.

The structure is expected to outperform a comparable fixed-base building in moderate and large earthquakes. The intent is to limit damage to the structure and its contents by using seismic isolation that, in effect, permits an elastic response of the structure, while limiting the floor accelerations to low levels even in a large earthquake.

### Building characteristics

- A single basement, four-story, regular configuration concrete building. The building has no vertical or plan irregularities. The lateral system is a dual system consisting of special reinforced concrete shear walls and special moment frames capable of resisting at least 25% of prescribed seismic force.
- Response modification coefficient  $R = 7$  (ASCE 7-05, Table 12.2-1).
- Building is located in the outskirts of Los Angeles, California.
- From seismic hazard maps  $S_s = 1.5g$  and  $S_1 = 0.60g$  for the building site.
- Importance factor  $I = 1.0$ . Observe that the importance factor  $I$  for a seismic-isolated building is taken as 1.0, regardless of the occupancy category, since there is no design ductility demand on the structure.
- Building period calculated as a fixed-base building = 0.9 s.
- Building plan dimensions are  $120 \times 120$  ft.
- Calculated distance between the center of mass and the center of rigidity is 5 ft at each floor and at the roof.
- The project geotechnical engineer has established the building site as site class D.
- Building weight for seismic design = 7200 kip.
- The project structural engineer has established that, to achieve immediate occupancy performance goals, the isolation system should provide effective isolated periods of  $T_D = 2.5$  and  $T_M = 3.0$  s, and a damping of 20% of the critical. A margin of  $\pm 15\%$  variation in stiffness of isolators from the mean values is considered acceptable.

**Required:** A preliminary design using the provisions of ASCE 7-05 for base isolation of the building. For purposes of illustration, an FPS, is selected as the base-isolation system. It should

be noted that, in practice, building ownership, particularly if it is a public entity, requires that the design accommodate alternative systems to secure competitive bids. However, for illustration purposes, we will consider only the FPS, it being understood that other isolation systems such as high-damping rubber and lead-rubber isolators are equally viable alternatives.

As part of preliminary design determine

- Minimum design displacements  $D_D$  and  $D_M$  under the design basis earthquake (DBE) and the maximum considered earthquake (MCE) and total displacements  $D_{TD}$  and  $D_{TM}$  which include effects of torsion
- Base shear  $V_b$  for designing the structure below the isolation surface
- Base shear  $V$  for designing the structure above the isolation surface
- Maximum dimension of the isolators

**Solution:** The restrictions placed on the use of the static lateral response procedures effectively require dynamic analysis for most isolated structures. Therefore one might ask, “Why perform, in this day and age of computers, a static analysis of a building with a sophisticated system such as base isolation?” The answer is quite simple: to establish a minimum level of design forces and displacement. Lower-bound limits on design displacements and design forces are specified in ASCE 7-05 as a percentage of the values prescribed by the static procedure. These lower-bound limits on key design parameters ensure consistency in the design of isolated structures and serve as a safety net against gross undersign.

As mentioned previously, seismic isolation, also referred to as base isolation, is a design concept based on the premise that a structure can be substantially “decoupled” from potentially damaging earthquake ground motions. By decoupling the structure from ground shaking, isolation reduces the level of response in the structure from a level that would otherwise occur in a conventional fixed-base building. Typically, decoupling is accomplished using an isolation system that makes the effective period of the isolated structure several times greater than the period of the structure above the isolation system.

In our case, the four-story example building with a fixed-base period of 0.9 s and a standard damping of 5% would have experienced a first-mode acceleration of 0.48 g (see Figure 9.15). By decoupling the building from the ground, the period of the building is expected to increase to 2.7 s. Additionally, the base isolation is counted upon to increase the damping from a standard 5% to about 20% of the critical. Together, these two factors reduce the first-mode acceleration to 0.12 g, as shown in Figure 9.15.

The underlying philosophy behind isolated structures may be characterized as a combination of primary performance objective for fixed-base buildings, which is the provision of life safety in a major earthquake, and the additional performance objective of damage protection, an attribute provided by isolated structures. The design criteria are then a combination of life safety and damage protection goals summarized as follows:

Two levels of earthquake, DBE and MCE, are typically considered in the design of isolated structures. The DBE is the same level of ground shaking as that recommended for design of fixed-base structures. The MCE is a higher level of earthquake ground motion defined as the maximum level of ground shaking that may be expected at the building site within the known geological framework.

The isolators must be capable of sustaining loads and displacements corresponding to the MCE without failure.

The structure above the isolation system must remain “essentially elastic” for the DBE.

From the criteria given above, it is seen that the performance objectives and design requirements for fixed-base and isolated buildings vary significantly. The performance objective for fixed-base construction is life safety in a DBE; the intent is to prevent substantial loss of life rather than control damage. For isolated buildings, the performance objectives are

1. Minimal to no damage in the design earthquake (thus providing life safety)
2. A stable isolation system in the maximum capable earthquake



The performance of an isolated building in a DBE will likely be much better (less interstory drift, smaller floor accelerations) than its fixed-base counterpart. Further, isolated buildings can be designed to provide continued function following a design earthquake: a level of performance that is very difficult to achieve with conventional fixed-base construction.

Fixed-base buildings are generally designed using large response modification factors to reduce elastic spectral demands to a design level, a strategy predicated on significant inelastic deformation of the framing system and damage to nonstructural building element. Such buildings are checked for response in the design earthquake only; there is no design check for the MCE. In contrast, isolated buildings are designed using a dual-level approach, namely, the framing system is designed to remain essentially elastic (no damage) in the design earthquake, and the isolators are designed (and tested) to remain stable in the MCE.

The subject building is a concrete dual system building. Using the post-earthquake scenario given in ASCE/SEI 41-06 as a guide, our building is expected to have

- No permanent drift. Structure substantially retains original strength and stiffness.
- Transient drift less than 0.5%.
- Negligible damage to nonstructural components.
- Minor hairline cracking in concrete walls, less than 1/16 in. wide. No crushing of concrete.
- Some evidence of sliding at construction joints.
- Coupling beams experience cracks less than 1/8 in. width.
- Minor settlement and negligible tilting of foundations.
- Diaphragm experiences hairline cracking. Some minor cracks of larger size but less than 1/8 in.
- Cladding connections may yield. No failure.
- Some cracked panes in glazing. None broken.
- Negligible damage in stairs and fire escapes.
- Elevators operate.
- Fire alarm systems and electrical equipment functional.
- Computer units undamaged and operable.

Before proceeding with the illustrative example, certain design requirements touched upon briefly in the preceding sections will be explained in greater detail. The purpose is to delve into the design intent behind these provisions.

#### 9.2.5.6.1 Effective Stiffness of Isolators

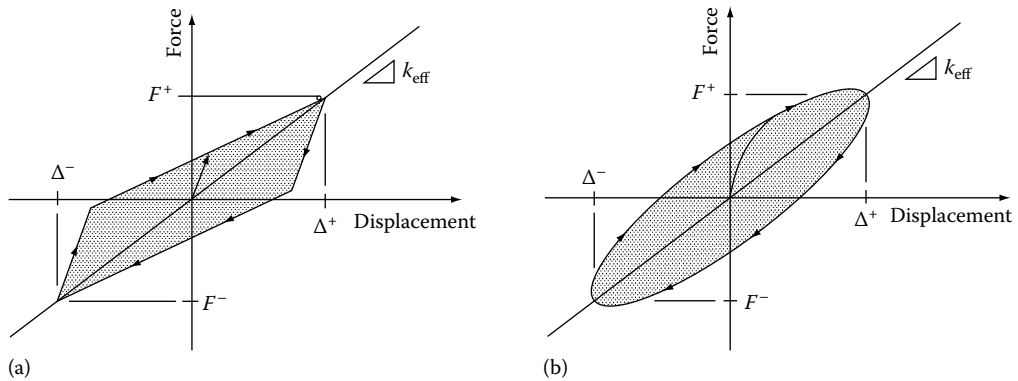
Typically, isolation systems are nonlinear, meaning that their effective stiffness is displacement- and/or velocity-dependent, as shown by an idealized force–deflection relationship in Figure 9.28.

The effective stiffness  $k_{\text{eff}}$  of a seismic isolator is calculated using the forces in the isolator at the maximum and minimum displacements, as given in the following equation:

$$k_{\text{eff}} = \frac{|F^+| + |F^-|}{|\Delta^+| + |\Delta^-|}$$

where  $F^+$  and  $F^-$  are the positive and negative forces at  $\Delta^+$  and  $\Delta^-$ , respectively.

For isolators whose properties are independent of velocity, the forces in the isolator at the maximum and minimum displacements will generally be maximum and minimum forces, respectively. For isolators whose properties exhibit velocity dependence, the forces in the isolator at the maximum and minimum displacements will generally be less than the maximum and minimum forces, respectively. However, it is usually assumed that maximum and minimum forces in an isolator are



**FIGURE 9.28** Idealized force–displacement relationship for base-isolation systems: (a) hysteretic system and (b) viscous system.

attained at maximum and minimum displacements, respectively. For most types of isolators, this assumption is reasonable.

The deformational characteristics of an isolation system determine (1) the design displacements and (2) the maximum forces transmitted to the isolated structure. Deformational characteristics are represented by the effective (secant) stiffness of the isolation system. Recognizing that force–displacement hysteresis of an isolation system may change over the course of an earthquake, the maximum effective stiffness is used to calculate the maximum force transmitted by the isolators, and the minimum effective stiffness is used to calculate the fundamental period of the isolated building. The reason for using minimum effective thickness is to arrive at a conservative estimate of the design displacement. The limiting values are generally established in the design phase and are required to be confirmed by testing.

Effective stiffness of the isolation system is determined from the force–displacement (hysteresis) loops based on the results of cyclic testing of a selected sample of isolator. The values of maximum effective stiffness and minimum effective stiffness can be calculated, as shown in Figure 9.28, for both design and maximum displacement levels.

#### 9.2.5.6.2 Effective Damping

The effective damping  $b_{\text{eff}}$  is used to quantify the energy dissipation furnished by the isolation system. The maximum effective stiffness of the isolation system is used to provide a lower-bound, that is, conservative, estimate of the effective damping.

For the purpose of design, energy dissipation is characterized as an equivalent viscous damping. The following equation defines the equivalent viscous damping  $\beta_{\text{eff}}$  for a single isolator:

$$b_{\text{eff}} = \frac{2}{\pi} \frac{E_{\text{loop}}}{k_{\text{eff}} (|\Delta^+| + |\Delta^-|)^2}$$

where

$b_{\text{eff}}$  is the effective damping of the isolation system and isolator unit

$E_{\text{loop}}$  is the area enclosed by the force–displacement loop of a single isolator in a complete cycle of loading to maximum positive and maximum negative displacement,  $\Delta^+$  and  $\Delta^-$

$\Delta^+$  is the maximum positive displacement of isolator during prototype testing

$\Delta^-$  is the maximum negative displacement of isolator during prototype testing

### 9.2.5.6.3 Total Design Displacement

The design of isolated structures must consider additional displacements due to actual and accidental eccentricity, similar to those prescribed for fixed-base structures. Equations given below provide a simple means to combine translational and torsional displacement in terms of the gross plan dimensions of the building (i.e., dimensions  $b$  and  $d$ ), the distance from the center of the building to the point of interest (i.e., dimension  $y$ ), and the actual plus the accidental eccentricity, as follows:

$$D_{TD} = D_D \left[ 1 + y \frac{12e}{b^2 + d^2} \right]$$

$$T_{TM} = D_M \left[ 1 + y \frac{12e}{b^2 + d^2} \right]$$

where  $e$  is the sum of the actual and accidental eccentricities.

Notice that the design displacement  $D_D$  at the center of the building has been modified to account for additional displacement at the corners or edges of the building due to torsion. It is assumed that the stiffness of the isolation system is distributed in plan proportional to the distribution of the supported weight of the building.

Smaller values of  $D_{TD}$  can be used for design if the isolation system is configured to resist torsion (e.g., if stiffer isolator units are positioned near the edges and corners of the building). However, the minimum value of  $D_{TD}$  is set equal to  $1.1 D_D$  for all types of isolation systems. The total displacement  $D_{TM}$  is calculated in a manner similar to the calculation of  $D_{TD}$ . The eccentricity  $e$  used for calculating torsional displacements is the actual eccentricity of the isolation system plus an allowance of 5% of the width of building to account for accidental torsion. The parameter  $y$  is the distance between the center of rigidity of the isolation system and farthest corners of the building.

It should be noted that the stiffness values  $K_{D \min}$  and  $K_{M \min}$  are not known to the designer during the preliminary design stage, but are derived from the known or expected values of periods of the building. Since the expected periods may not turn out to be equal to the final values, the derived stiffness values are also preliminary. After completing a satisfactory preliminary design, typically prototype isolators are tested to obtain values of  $K_{D \min}$ ,  $K_{D \max}$ ,  $K_{M \min}$ , and  $K_{M \max}$ .

### 9.2.5.6.4 Minimum Design Lateral Forces

**9.2.5.6.4.1 Isolation System and Structural Elements at or below Isolation Interface** The design actions for elements at or below the isolation interface are based on the maximum forces delivered by the isolation system during the DBE. The building's foundation, the isolation system, and all structural elements at or below the isolation interface are required to be designed and constructed to withstand a minimum lateral force.

$$V_b = K_{D \max} D_D$$

The maximum force  $V_b$  is the product of the maximum stiffness of the isolation system at the design displacement  $K_{D \max}$  and the design displacement  $D_D$ . The design force  $V_b$  represents strength level forces.

The previous equation for  $V_b$  is for use in regions of high seismicity, such as the uniform building code, UBC zone 4, wherein the difference between the total design displacement and the total maximum displacement is relatively small; that is, if a supporting element was designed for DBE forces at the strength level, it is probable that such a supporting element could resist the forces associated with the MCE without failure.

There are significant differences in values of  $M_M$  between regions of high and low seismicity: Values of  $M_M$  may be less than 1.25 in regions of high seismicity, but may exceed 2.5 in regions of low seismicity. As such, in a region of low seismicity, a supporting element designed for DBE-induced forces may be unable to sustain forces associated with the MCE without significant distress or failure. Therefore, in these regions it may be prudent to consider MCE-level forces to check the design of the isolation system and the structural elements at or below the isolation interface.

Isolation interface is the boundary between the upper portion of the building, which is isolated, and the lower portion, which is rigidly attached to the foundation or ground. The isolation interface can be assumed to pass through the midheight of elastomeric bearings or the sliding surface of sliding bearings. Observe that the isolation interface need not be a horizontal plane, but could change elevation if the isolators are positioned at different elevations throughout the building.

The isolation system includes the isolator units, connections of isolator units to the structural system, and all structural elements required for isolator stability. Isolator units include bearings that support the building's weight and provide lateral flexibility. Typically, isolation system bearings provide damping and wind restraint as an integral part of the bearing. Isolator systems may also include supplemental damping devices. For example, an FPS of basic isolation may include viscous dampers.

Structural elements that are required for structural stability include all structural elements necessary to resist design forces at the connection of the structure to isolator units. For example, a column segment and a beam immediately above an isolator constitute elements of the isolation system because they are necessary to resist forces due to the lateral earthquake displacement of the isolators.

**9.2.5.6.4.2 Structural Elements above Isolation System** The design of the framing above the isolation system is based on the maximum force delivered by the isolation system divided by a response reduction factor,  $R_I$ . The values assigned to  $R_I$  reflect system overstrength only and no expected ductility demand. By using these values for  $R_I$ , a significant measure of damage control is afforded in the design earthquake, since the structure remains essentially elastic.

The minimum base shear for the design of the structure above the isolation is given by

$$V_s = K_{D_{\max}} D_D / R_I$$

Three limits are imposed for the calculation of  $V_s$ .

- $V_s$  should not be less than the base shear required for a fixed-base structure of the same weight  $w$  and a period equal to the isolated period.
- $V_s$  should not be less than the total shear corresponding to the design wind load. (In wind design, engineers seldom use the term “base shear” to define the total shear due to wind. However, base shear and total shear are one and the same.)
- $V_s$  should not be less than 150% of the lateral seismic force required to fully activate the system.

Thus there are three lower-bound limits set on the minimum seismic shear to be used for the design of the framing above the isolation system. The first limit requires design base shear to be at least that of a fixed-base building of comparable period. The second limit ensures that the elements above the isolation system remain elastic during a design windstorm. The third limit is designed to prevent the elements above the isolation system from deforming inelastically before the isolation system is activated.

**9.2.5.6.4.3 Vertical Distribution of  $V_s$**  The vertical distribution of the seismic base shear is similar to that used for fixed-base buildings, namely, a distribution that approximates the first-mode shape of a fixed-base building. This distribution conservatively approximates the inertia force distributions measured from time-history analyses.

**Continuation of illustrative problem:** The effective periods  $T_D$  and  $T_M$  of the isolated building are

$$T_D = 2\pi \sqrt{\frac{W}{K_{D\min}g}}$$

$$T_D^2 = \frac{4\pi^2 W}{K_{D\min}g}$$

$$T_D = 2.5 \text{ s} \quad (\text{given})$$

$$W = 7200 \text{ kip} \quad (\text{given})$$

$$g = 386.4 \text{ in./s}^2$$

$$\begin{aligned} K_{D\min} &= \frac{4\pi^2 W}{T_D^2 g} \\ &= \frac{4 \times \pi^2 \times 7200}{2.5^2 \times 386.4 \text{ in./s}^2} \\ &= 117.7 \text{ kip/in.}, \quad \text{say, } 118 \text{ kip/in.} \end{aligned}$$

Similarly

$$\begin{aligned} K_{M\min} &= \frac{4 \times \pi^2 \times 7200}{3^2 \times 386.4} \quad T_M = 3 \text{ s} \quad (\text{given}) \\ &= 81.7 \text{ kip/in.}, \quad \text{say, } 82 \text{ kip/in.} \end{aligned}$$

As stated in the problem, a  $\pm 15\%$  variation in stiffness from the mean values is permitted. Therefore, use a factor of 0.85 to determine  $K_{D\max}$  and  $K_{M\max}$ .

$$K_{D\max} = \frac{1.15 \times 118}{0.85} = 159.5 \text{ kip/in.}, \quad \text{say, } 160 \text{ kip/in.}$$

$$K_{M\max} = \frac{1.15 \times 82}{0.85} = 111 \text{ kip/in.}$$

From ASCE-05, Table 17.5-1, for a 20% effective damping, that is,  $B_D$  or  $B_M = 20\%$ , the value of damping coefficient  $B = 1.5$ .

Observe that the same damping coefficient is applied to both DBE and MCE events. The value of  $F_v$  as a function of site class and mapped 1 s period MCE spectral acceleration is given in Table 11.4.2 of ASCE7-05. From this table, for site class D and  $S_1 = 0.60 > 0.50$ , we get

$F_v = 1.5$ . The spectral response acceleration  $S_{M1}$  at a period of 1 s, adjusted for site class D, is equal to

$$\begin{aligned} S_{M1} &= F_v S_1 \\ &= 1.5 \times 0.6 \\ &= 0.9g \end{aligned}$$

The design spectral response acceleration  $S_{D1}$  is given by

$$\begin{aligned} S_{D1} &= 2/3 S_{M1} \\ &= 2/3 \times 0.9 \\ &= 0.6g \end{aligned}$$

Similarly

$$\begin{aligned} S_s &= 1.5 \\ S_{MS} &= F_a S_s \\ &= 1 \times 1.5 \\ &= 1.5 \\ S_{DS} &= 2/3 \times 1.5 \\ &= 1.0g \end{aligned}$$

The minimum design displacements are obtained as follows:

$$\begin{aligned} D_D &= \left( \frac{386.4}{4\pi^2} \right) \frac{0.60 \times 2.5}{1.5} \\ &= 9.79 \text{ in.} \\ D_M &= \left( \frac{386.4}{4\pi^2} \right) \frac{0.9 \times 3}{1.5} \\ &= 17.62 \text{ in.} \end{aligned}$$

The eccentricity for calculating torsional effects is equal to the actual eccentricity plus 5% of the building width. Thus

$$\begin{aligned} e &= 60 + 0.05 \times 120 \times 12 \\ &= 132 \text{ in.} \end{aligned}$$

The displacements including the torsional effects are

$$\begin{aligned}
 D_{TD} &= D_D \left( 1 + y \frac{12e}{b^2 + d^2} \right) \\
 &= 9.79 \left\{ 1 + \frac{120}{2} \frac{132}{(120^2 + 120^2)} \right\} \\
 &= 12.48 \text{ in.}
 \end{aligned}$$

$$\begin{aligned}
 D_{TM} &= 17.62 \times 1.275 \\
 &= 22.47 \text{ in.}
 \end{aligned}$$

$$\begin{aligned}
 V_b &= K_{D\max} D_D \\
 &= 160 \times 9.79 \\
 &= 1566.4 \text{ kip}
 \end{aligned}$$

Given a seismic weight of  $W = 7200 \text{ kip}$ , the seismic base shear coefficient for the design of isolation system and structural elements below it corresponds to

$$1566.4/7200 = 0.218 \text{ or } 21.8\% \text{ of gravity.}$$

Before calculating the base shear for the superstructure, we need to calculate  $R_I$ . However,  $R_I$  need not be greater than 2.0.

Therefore

$$\begin{aligned}
 R_I &= 3/8 R = 3/8 \times 7 = 2.657 > 2.0 \\
 R_I &= 2.0 \\
 V_s &= K_{D\max} D_D / R_I \\
 &= V_b / 2 \\
 &= 1566.4 / 2 \\
 &= 783.2 \text{ kip or } 783.2/7200 \times 100 = 10.9\% \text{ of gravity.}
 \end{aligned}$$

Using the equivalent lateral procedure of ASCE 7-05, we now calculate the base shear required for a fixed-base structure of weight  $W = 7200 \text{ kip}$ , and a period  $T = T_D = 2.5 \text{ s}$ , equal to the period of the isolated building.

$$\begin{aligned}
 1. \quad V &= \frac{S_{DS}}{\left( \frac{R}{I} \right)} W \\
 &= \frac{1}{\left( \frac{7}{1} \right)} W = 0.143W = 14.3\%g
 \end{aligned}$$

$$\begin{aligned}
 2. V_{\max} &= \frac{S_{D1}}{T \left( \frac{R}{I} \right)} W \\
 &= \frac{0.6}{2.5 \times 7} W = 0.034W = 3.4\%g
 \end{aligned}$$

$$\begin{aligned}
 3. V_{\min} &= 0.01W \\
 &= 1.0\%g
 \end{aligned}$$

$$\begin{aligned}
 4. V_{\min} &= \frac{0.5S_1}{\left( \frac{R}{I} \right)} \\
 &= \frac{0.5 \times 0.6}{\left( \frac{7}{1} \right)} = 0.043W = 4.3\%g
 \end{aligned}$$

The base shear  $V_{\min} = 4.3\%g$ , obtained from the fourth equation yields the design base shear for the fixed-based building. However, a base shear equal to 10.9% of gravity, obtained from the calculations for a base-isolated building controls the design of the subject building. Using this base shear, the structural elements above the isolation system are designed by applying the appropriate provisions of a nonisolated structure.

#### 9.2.5.6.5 Preliminary Design of Friction Pendulum System, FPS

Recall that the period  $T$  of a pendulum is inversely proportional to the square root of its length, and does not depend on the mass  $m = w/g$ . Similarly, the period of the FPS depends only on the square root of its radius  $R$  of the dish and not the supported mass of the building above. To increase the period of a pendulum we increase the length; to increase the apparent period of the building we increase the radius of the dish.

If the weight of the building above is  $W$ , and the radius of FPS dish is  $R$ , then the horizontal stiffness of the isolator is given by

$$k_h = W/R$$

The period of the isolated system is a function of its radius  $R$  only, and is given by

$$T = 2\pi \sqrt{\frac{R}{g}}$$

For our building, the effective isolated period  $T_D = 2.5$  s, as given in the statement of the problem.

Therefore

$$2.5 = 2\pi \sqrt{\frac{R}{386.4}} \quad \text{giving}$$

$$R = 61.23 \text{ in.}$$



The effective stiffness of a FPS is given by

$$K_{\text{eff}} = \frac{W}{R} + \frac{\mu W}{D}$$

where the new term  $\mu$  is the friction coefficient.

The friction coefficient  $\mu$  for an FPS may be assumed to be independent of velocity for pressures of 20 ksi or more. The damping  $\beta$  provided by the system is given by

$$\beta = \frac{2}{\pi} \frac{\mu}{\mu + \frac{D}{R}}$$

Assuming  $\mu = 0.06$  and a design displacement of 10 in., the effective damping is calculated from

$$\begin{aligned} \beta_{\text{eff}} &= \frac{2 \times 0.06}{\pi \left( 0.06 + \frac{10}{61.23} \right)} \\ &= 0.10 \quad \text{or} \quad 10\% \text{ of the critical} \end{aligned}$$

The selected value of  $D = 10$  in. satisfies the minimum code displacement of  $D_D = 9.79$  in., calculated earlier for  $T = 2.5$  s,  $\beta = 20\%$ , and  $B = 1.5$ .

The effective stiffness is calculated from

$$\begin{aligned} K_{\text{eff}} &= W/R + \mu W/D \\ &= 7200 / 61.23 + 0.06 \times 7200 / 10 = 161 \text{ kip/in.} \end{aligned}$$

This is almost exactly the same as  $K_{D_{\text{max}}}$  of 160 kip/in. derived earlier. Therefore, no further iterations are necessary.

With regard to the example problem, the following observations are appropriate for preliminary design purposes.

- An FPS of approximately 5 ft radius is required underneath each column.
- The required stiffness of each FPS is approximately equal to 100 kip/in.
- A moat about 23 in. around the building is required to accommodate the calculated displacement  $D_{\text{TM}} = 22.47$  in.
- The torsional contribution to the displacement is equal to  $D_{\text{TM}} - D_{\text{M}}$ . In our case this is equal to  $(22.47 - 17.62) = 4.85$  in. A possible solution to reducing the torsion contribution is to use a stiffer FPS at the building perimeter.
- As mentioned previously, other competing isolation systems are generally evaluated to achieve competitive bids. Usually a performance type of specifications for a base-isolation system accompanies structural drawings to encourage competitive bids.

#### 9.2.5.6.6 Triple Pendulum Bearing

So far our discussion has been confined to a conventional, “single pendulum bearing” in which the bearing surfaces maintain constant friction, lateral stiffness, and dynamic period irrespective of the expected earthquake motion. This is inline with the current design practice of designing the

isolation system to have sufficient displacement capacity to meet the demands of the maximum credible earthquake (MCE) (an event having a 2% probability of occurrence in 50 years, corresponding approximately to a 2500 year recurrence interval). While the design meets the objectives of MCE, its performance is less than optimum for the DBE which is two-thirds of the MCE spectrum. Moreover, the performance of the isolation system in more frequent events of smaller magnitude is typically not considered in the design process of base isolation. Generally, low-level shaking is not a design issue in terms of strength or displacement capacity. However, it can be a performance issue. Isolation systems designed with sufficient damping and flexibility for larger earthquakes may not activate in more frequent minor events. To overcome this issue, a new type of FPS referred to as an adaptive or smart seismic isolation system has recently (2006) been introduced. Developed by Earthquake Protection Systems (EPS), the new device permits the isolation system to be separately optimized for low intensity, design level, and maximum ground motions. To satisfy the dual requirement of controlling displacements in large earthquakes while still maintaining good performance in low-to-moderate earthquakes one needs to design an isolation system that

1. Is very stiff with low damping at low-level shaking
2. Softens with increasing damping in the DBE
3. Softens even more and increases damping in the MCE
4. Stiffens beyond MCE

This methodology has been incorporated by EPS in a new device referred to as triple pendulum bearing system which has three independently designed friction pendulum bearings incorporated in a single pendulum bearing. The properties of each of the bearing's three pendulums are chosen to become sequentially active as the earthquake motions become stronger.

The triple pendulum bearing's inner isolator consists of an inner slider along two inner concave spherical surfaces. Properties of the inner pendulum are chosen to reduce structure shear forces that occur during service-level earthquakes.

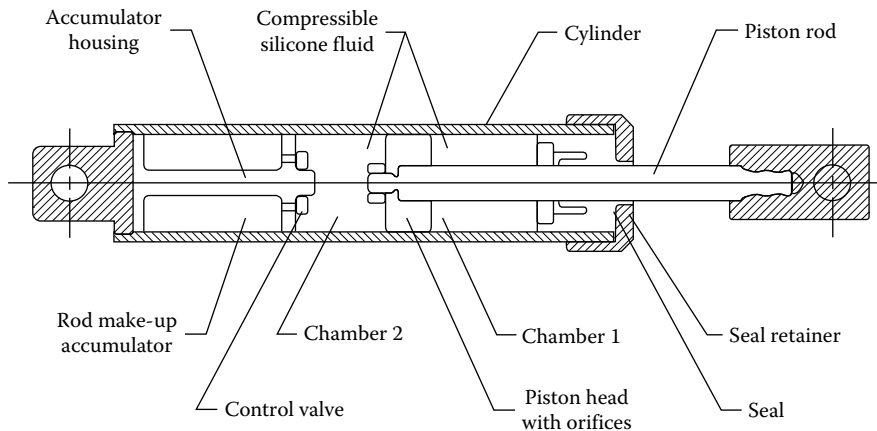
The two slider concaves, sliding along the two main concave surfaces, comprise of two more isolators designed to minimize the structure shear forces that occur during the DBE. And, finally the properties of the pendulum are chosen to minimize bearing displacements that occur during the maximum credible earthquake.

According to the manufacturer, when designed for a severe maximum credible earthquake, the plan dimensions of the triple pendulum bearing are approximately 60% that of the single pendulum bearing.

### 9.3 PASSIVE ENERGY DISSIPATION

Passive energy dissipation is an emerging technology that enhances the performance of a building by adding damping (and in some cases, stiffness) to the building. The primary use of energy dissipation devices is to reduce earthquake displacement of the structure. Energy dissipation devices will also reduce force in the structure, provided the structure is responding elastically, but would not be expected to reduce force in structure that is responding beyond yield.

For most applications, energy dissipation provides an alternative approach to conventional stiffening and strengthening schemes, and would be expected to achieve comparable performance levels. In general, these devices are expected to be good candidates for projects that have a target building performance level of life safety or perhaps immediate occupancy, but would be expected to have only limited applicability to projects with a target building performance level of collapse prevention. Other objectives may also influence the decision to use energy dissipation devices, since these devices can also be useful for control of building response to small earthquakes and wind loads.



**FIGURE 9.29** Fluid viscous damper consisting of a piston in a damping housing filled with a compound of silicone or similar type of fluid.

A wide variety of passive energy dissipation devices are available, including fluid viscous dampers, viscoelastic materials, and hysteretic devices. Ideally, energy dissipation devices dampen earthquake excitation of the structure that would otherwise cause higher levels of response and cause damage to components of the building. Under favorable conditions, energy dissipation devices reduce drift of the structure by a factor of about 2 to 3 (if no stiffness is added) and by larger factors if the devices also add stiffness to the structure.

Unlike base isolation, passive energy dissipation does not intercept earthquake energy entering the structure. It allows earthquake energy into the building. However, the energy is directed toward energy dissipation devices located within the lateral resisting elements. Earthquake energy is transformed into heat by these devices and dissipated into the structure.

A fluid viscous damper shown in Figure 9.29 is one such energy dissipation device. It dissipates energy by forcing a fluid through an orifice, similar to the shock absorbers of an automobile. The fluid used is usually of high viscosity, such as a silicone. The unique feature of these devices is that their damping characteristics, and hence the amount of energy dissipated, can be made proportional to the velocity. The response of a fluid viscous damper is considered to be out of phase with those due to seismic activity. This is because the damping force provided by the device varies inversely with the dynamic lateral displacements of a building. To understand the concept, consider a building shaking laterally back and forth during a seismic event. The stress in a lateral-load-resisting element such as a frame-column is at its maximum when the building deflection is also at maximum. This is also the point at which the building reverses direction to move back in the opposite direction. The damping force of a fluid viscous damper will drop to zero at this point of maximum deflection. This is because the damper stroking velocity goes to zero as the building reverses direction. As the building moves back in the opposite direction, a maximum damper force occurs at the maximum velocity which happens when the building goes through its normal upright position. This is also the point when the stresses in the lateral-load-resisting elements are at a minimum. Therefore, the damping provided by the device varies from a maximum to a minimum as the building moves from an at-rest position to its maximum lateral deflection position. This out-of-phase response is considered a desirable feature in seismic designs.

## 9.4 PRELIMINARY ANALYSIS TECHNIQUES

Simply defined, structural analysis is a mathematical process by which the engineer verifies the adequacy of the structure with respect to its strength and stiffness. It is not always possible to obtain rigorous mathematical solutions for building engineering problems. In fact, rigorous analytical

solutions can be obtained only for certain simplified cases. High-rise structural problems, like most other practical engineering problems, involve complex material property, and loading and boundary conditions. The engineers introduce assumptions and idealizations deemed necessary to make the problem mathematically manageable, but still capable of providing sufficiently accurate solutions and satisfactory results from the point of view of safety and economy. They establish a link between the real physical system and the mathematically feasible solution by providing an analytical model, which is the symbolic designation for the substitute idealized system, including all the assumptions imposed on physical problems. Modeling techniques, therefore, can be defined as a way to reduce, synthesize, and properly represent the structural system.

The basic principles and mathematical relationships used in the design and analysis of tall buildings are not unique to this type of construction. Virtually all of the fundamental relationships are based on the normal assumptions of elastic design which form the backbone of the study of the strength of materials. Although the form of certain relationships is somewhat modified, their application to the analysis and design of high-rise buildings will not impose undue difficulty.

Two major types of problems are encountered by the engineer engaged in the design of tall buildings: (1) review of a set of completed working drawings and (2) the actual design, starting from the preliminary stages. The review of a completed design consists of the determination of the stresses and deflections under appropriate conditions of loading in order to confirm their compliance with the design criteria and applicable codes. The strength of a member under all loading conditions, bending, shear, torsion, axial, and bond must be determined to exceed the minimum strength requirements. It should be apparent that in order to review the design, the dimensions and material properties of all structural elements that are used in the makeup of the tall building, together with knowledge of the loads to which the structure is subjected, must be known.

The task of checking the work of another engineer is done to ensure that the design satisfies the safety requirements, as specified in the applicable codes. Although there is no uniform procedure for carrying out this work, a balance must be maintained between checking for safety compliance and the avoidance of malicious damage to the reputation of another engineer. The check should be carried out in a climate of mutual understanding. The checker must recognize that he or she has no duty to comment on the choice of design, only on its validity and its satisfactory compliance with applicable codes. It is a mistake to concentrate on the minute accuracy of the calculations when time can be saved by assessing the soundness of the structure.

The design of a building, on the other hand, consists of selecting and proportioning member sizes in which the stresses do not exceed the permissible values under any combination of loads. The design also includes the study of the deformation characteristics to assure that the building meets applicable serviceability criteria. In common with other types of design, member sizes in a tall building are arrived at from a trial-and-error procedure. In the design of a member, several adjustments of the trial section are normally required before a satisfactory solution is found. Of course, it is just as important to adjust members that are found to be excessively conservative.

At the schematic stages of architectural design, overall options associated with different space forms of the building are thought through with due consideration given to the basic relationship of the building to the available site, environmental conditions, intended use of the building, and other performance criteria. The architectural task at this stage is to organize and orient various space components such as service cores, stairs, elevator cores, and mechanical rooms. These are arranged around the typical floor plan configuration, with the understanding that it works around a typical floor, it is relatively easy to force the arrangement to work at other nontypical levels. The various components are organized around the typical floor to achieve maximum efficiency, measured in terms of the gross to net leasable floor space. A structural appraisal is made of the general geometry of the building, especially the height-to-width ratio, function of the structure, whether it is a single-use or multiuse project, whether there is a basement, parking, or other requirements that may necessitate transfer of large vertical elements, limitations on layout and sizes of structural members, head room, and span requirements. The process of preparing structural system alternatives starts simultaneously with due

regard to choice of construction materials, availability of building materials, and local workmanship. Generally speaking, the economy of a structure depends to a great extent upon the design criteria and framing layout adopted but to a far lesser extent upon the detailed design of structural members. Although the decision on the framing may be somewhat subjective, it should have the backing of at least some preliminary economic comparison. While the analytical phase of structural engineering is based on physical sciences, designing remains essentially an art for which knowledge of structural analysis, imagination, judgment, and experience are prerequisites.

It is difficult, if not impossible, to outline the thought process that would go through a structural engineer's mind when he or she conceptualizes the structure at the schematic level. It is very likely that more than one solution may present itself at this stage, and proper guidance to the architect may require knowledge of relative cost and construction procedures on the part of the structural engineer. The point is that one does not really make a lot of calculations or hard-line drawings at this stage, but guides the architect with enough confidence obtained through experience. What is needed is a thorough knowledge of the structural systems to augment the creative thinking of the architect by concentrating on the design evolution of the whole rather than becoming entangled in premature consideration of consequential details of the parts. The key to successful application of structural design ideas at schematic stages of architectural design rests in being able to look at the big picture first without getting bogged down by the details.

Although for optimum results a comprehensive interactive approach between architectural and engineering fields is necessary, there is a growing tendency for the architect to initiate a space form and then to have the engineer find a way to technically implement the form. This idea appears to stem from the premise that building forms, like pure art, need to be developed without the restriction imposed by engineering disciplines. The results have often been very daring and interesting building forms.

Even in today's high-tech computer-oriented world with all its sophisticated design capability, there still is a need to perform approximate analysis of structures. First, it provides a basis for selecting preliminary member sizes because the design of a structure, no matter how simple or complex begins with a tentative selection of members. With the preliminary sizes, an analysis is made to determine if design criteria are met. If not, an analysis of the modified structure is made to improve its agreement with the requirements, and the process is continued until a design is obtained within the limits of acceptability. Starting the process with the best possible selections of members results in a rapid convergence of the iterative process to the desired solution.

Second, because of the ever-increasing cost of labor and building materials, it is almost mandatory for the structural engineer to compare several designs before choosing the one most likely to be the best from the points of view of structural economy and how well it minimizes the premium required by the mechanical, electrical, and curtain wall systems. Of the myriad structural systems which present themselves as possibilities, only two or three schemes may be worthy of further refinement requiring full-blown computer solutions. Approximate methods are all that may be required to logically arrive at cost figures and to sort out the few final contenders from among the innumerable possibilities. It is very time consuming, costly, and indeed unnecessary to undertake a complete sophisticated analysis for all the possible schemes. Preliminary designs are therefore very useful in weeding out the weak solutions.

Sophisticated computer analyses are indispensable in reducing the number of inaccuracies caused by hand analysis techniques and are being used routinely in everyday engineering practice. Although such computer analyses may intimidate the structural engineer by virtue of their unbelievable amount of documentation and output, the prudent engineer will always verify the reasonableness of the computer analysis by using approximate hand-calculated values for forces, moments, and deflections. Approximate analysis is, therefore, a powerful tool in providing the engineer with (1) a basis for preliminary sizing of members, (2) an orderly method for evaluating several schemes to select the most likely one for further study, and (3) methods for obtaining approximate values of forces, moments, and deflections to check on the validity of the computer solutions.

Having established the need for preliminary analysis techniques, what then are the techniques available for the structural engineer? The techniques are many and range from sophisticated solutions satisfying both compatibility and equilibrium conditions requiring lengthy calculations to simple ones based on considerations of equilibrium alone.

In this section, we will consider the analysis of structural systems subjected to lateral loads only, it being assumed that the reader is familiar with approximate methods of gravity analysis.

In the lateral load analysis of buildings, wind and earthquake forces are treated as equivalent static loads and are reduced to a series of horizontal concentrated loads applied to the building at each floor level. Portal and cantilever methods offer quick ways of analysis of a rigid bent with unknown sizes. The idea behind both these methods of analysis is based on the well-observed characteristics of portal frames, namely, that the points of contraflexure in beams and columns tend to form near the center of each column and girder segment. For purposes of analysis, the inflection points are assumed to occur exactly at the center of each member.

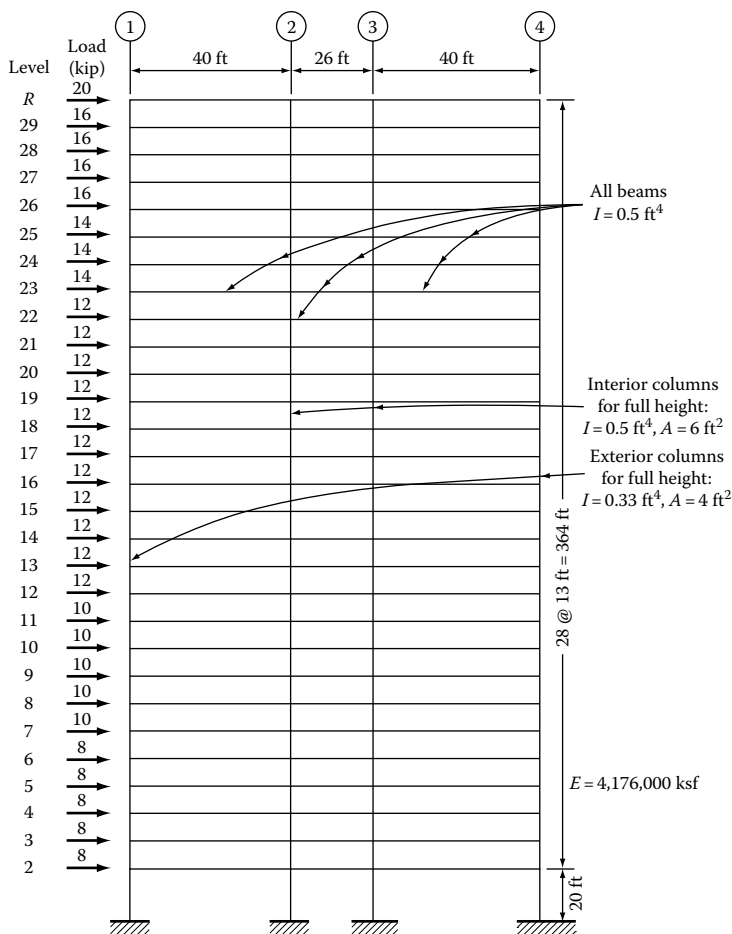
In the portal method, a wind bent is treated as a series of consecutive single-bay portal frames in the determination of axial stresses in the columns due to overturning effect. Interior columns are considered as part of two such portals and the direct compression arising from the overturning effect of the leeward column of one portal is offset by the direct tension arising from the overturning effect on the windward column of the adjacent portal. If the widths of different portals are unequal, the distribution of wind shear resisted by each portal can be assumed proportional to the aisle widths to maintain the interior column free of direct stress. Alternately, the column shears can be assumed to be unaffected by aisle widths resulting in axial stresses in the interior columns. With the shears in each column known and the points of contraflexure preestablished, the moments in beams and columns are determined. Simple statics will yield axial and shear forces in beams and columns.

In the cantilever method, as the name implies, the building is analyzed as a cantilever standing on end fixed to the ground level. The overturning moment is assumed to be resisted by the axial compression of all columns on the leeward side of the neutral axis and tension on all columns on the windward side of the neutral axis. The neutral axis for the cantilever frame is determined as the centroid of the areas of columns in the bent, and the axial forces in the columns due to overturning are assumed to be proportional to their distances from the neutral axis. As in the portal method, the points of inflection are assumed to occur at midheight of columns and midspan of girders. From the known axial forces in columns and the locations of the points of contraflexure, moments in columns and girders are obtained. These methods are considered in some detail in the sections that follow. Applications of the methods for manual calculations of deflection of frames and tube structures are illustrated by example problems.

*It is important to emphasize that in the structural analysis field, as in many others, the use of computers and commercially available computer programs rule the world. The back of the envelope, hand calculations given earlier for posttensioned members, and presently for frame analysis and later for torsion analysis, are not substitutes for computer analysis. They are given here with an eye to stressing the basics and to serve as procedures for checking computer out put. The goal is to assist young engineers who analyze complex structures using computer techniques, to understand what computers are doing and why they are doing it.*

#### 9.4.1 PORTAL METHOD

In this method, it is assumed that (1) points of contraflexure are located at midpoints of girders and columns and (2) the shear in columns is distributed in a rational manner. Under the second category, some engineers assume that the shear in exterior columns equals one-half of the shear in an interior column, while some assume that the shear is distributed in proportion to the tributary bay width. For unequal bays, the former assumption results in direct stresses in the interior columns equal to the difference in girder shears on either side of the column. The latter assumption keeps the interior columns free from direct stresses.



**FIGURE 9.30** Example frame; dimensions and properties.

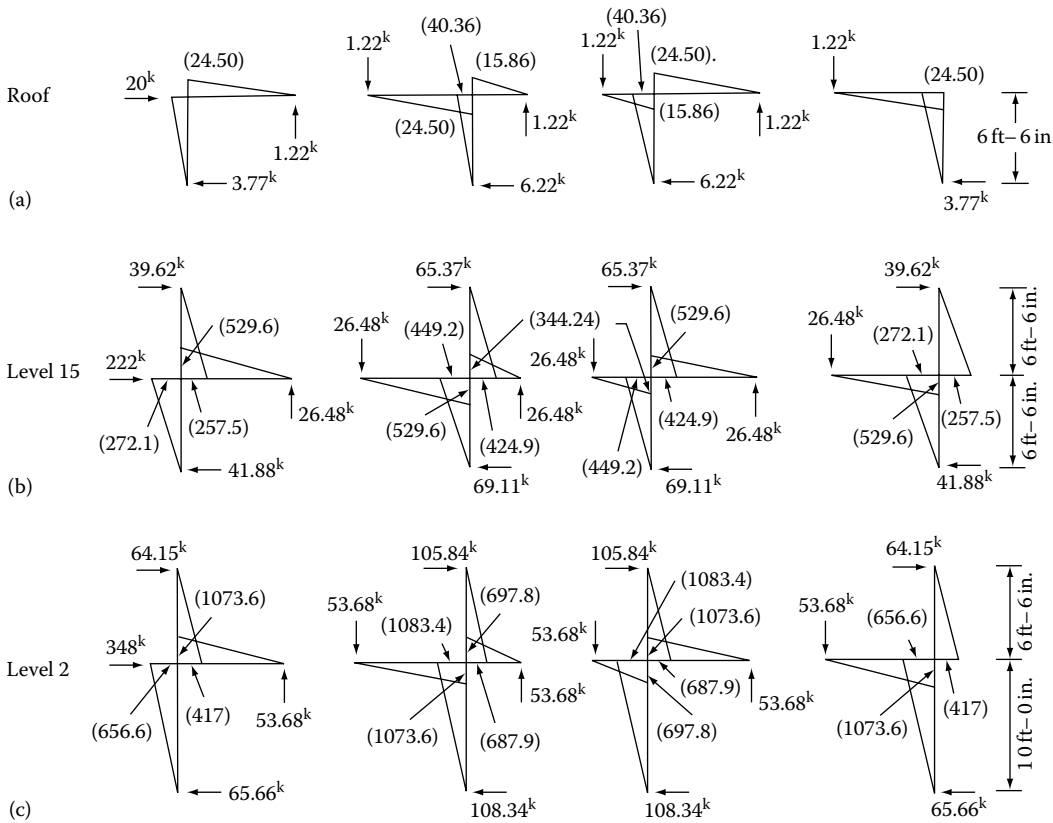
We will now consider the application of the portal method to a 30-story frame shown in Figure 9.30, consisting of two equal exterior bays and a smaller interior bay. Table 9.2 lists the lateral loads assumed in the analysis. The procedure is as follows. Distribute the accumulated story shears to each column in proportion to the aisle widths to keep the interior columns free of direct stresses. Calculate the moments in the top and bottom of each column as a product of the known shear in the column and one-half of the story height. Next, starting at the upper left corner of the frame, write the girder moments where the column and girder moments are the same. Since the points of contraflexure are assumed at the center of girder, the moments at each end are equal but opposite in sign. Determine the girder shears by the relation that shear multiplied by half of span lengths equals girder end moment. Next the direct stresses at the exterior columns are written directly from girder shears. The results for the example frame are shown in Figure 9.31.

#### 9.4.2 CANTILEVER METHOD

The frame analysis for horizontal loads by the so-called cantilever method is obtained by assuming that (1) inflection points, that is, hinges form at midspan of each beam and at midheight of each column and (2) the unit direct stresses in the columns vary as the distance from the frame centroidal axis. Its forces will vary as the distance from the center of gravity of the bent. Using these

**TABLE 9.2**  
**Lateral Loads for 30-Story Building Shown in Figure 9.30**

Level	Story Shear (kip)	Accumulated Shear (kip)	Level	Story Shear (kip)	Accumulated Shear (kip)
<i>R</i>	20	20	15	12	222
29	16	36	14	12	234
28	16	52	13	12	246
27	16	68	12	12	258
26	16	84	11	10	268
25	14	98	10	10	278
24	14	112	9	10	288
23	14	126	8	10	298
22	12	138	7	10	308
21	12	150	6	8	316
20	12	162	5	8	324
19	12	174	4	8	332
18	12	186	3	8	340
17	12	198	2	8	348
16	12	210			

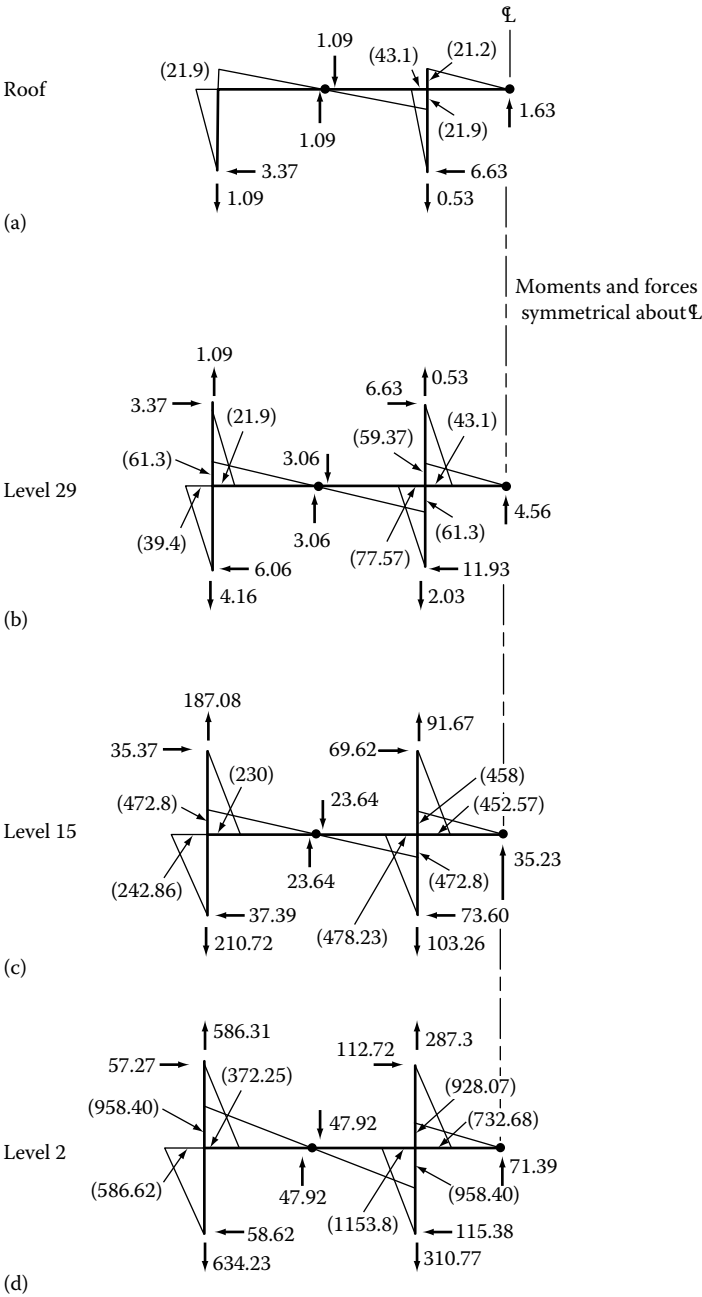


**FIGURE 9.31** Portal method. (a) Moments and forces at roof level. (b) Moments and forces at level 15. (c) Moments and forces at level 2.



assumptions the frame is rendered statically determinate and the direct forces, shears, and moments are determined by equilibrium considerations. The application of the method for an example frame will now be considered. To get a comparison with the results of the portal method, we shall apply the cantilever method for the three-bay portal frame (Figure 9.30) analyzed in the previous section.

The first assumption locates the points of contraflexure. Shown in Figure 9.32a is a free-body diagram of the top story above the points of contraflexure in the columns. The frame axis of rotation



**FIGURE 9.32** Cantilever method: (a) moments and forces at roof level, (b) moments and forces at level 29, (c) moments and forces at level 15, and (d) moments and forces at level 2.

is located at the center of gravity of the columns, which for the example problem coincides with the line of symmetry of the frame. The column axial forces for the top story are obtained by equating the moment of the column reactions about the frame axis to the moment of the wind forces taken about a horizontal plane through the assumed hinges of the top floor. These are also shown in Figure 9.32a.

In a similar manner the axial forces in the columns of other stories are computed by passing a section through the points of contraflexure of columns of each story and considering the moment equilibrium of the frame above the section (Figure 9.32).

After the column axial forces are found, the girder shears are determined at once. For example, in Figure 9.32c the tension in the exterior windward column at the 15th level is 210.72 kip (937.28 kN). Tension in the same column at the 14th level is 187.08 kip (832.13 kN). Therefore, by the relation that the summation of the axial forces in the columns and the girder shear is equal to 0 at the joint where the 15th story girder joins the exterior windward column, the girder shear is  $210.72 - 187.08 = 23.64$  (105.15 kN). Figure 9.32c shows the method of obtaining this and the remaining shears for the 15th level girder.

With the girder shears known, the girder moments follow directly. These equal the shear in the girder times one-half of the span length. The study of the various joints will show that from the relation that  $\sum M = 0$  at any joint, the sum of column moments must equal the sum of girder moments. Using this principle, the moments in the columns at the roof are obtained from roof girder moments (Figure 9.32a), since the points of contraflexure in the columns are at midheight, the column moments above the 29th level have the same value as at the roof level (Figure 9.32b). Moments in the columns below the 29th level are obtained from the relation  $\sum M = 0$ , and in a similar manner column moments in other floors are found. The column shears are obtained by dividing column moments by half the height). Since the points of contraflexure in the columns are at midheight, the column moments above the 29th level of columns. As a check, observe that the shear in the column of any level equals the sum of the horizontal external loads above the level. The moments and forces obtained by using the above procedure for the example problem are shown in Figure 9.32.

To get a feel for the accuracy of the foregoing approximate procedures, the bent in Figure 9.30 has been analyzed by a plane-frame computer analysis and the results shown in Figure 9.33. As may be expected, the computer results vary considerably from either of the two methods. Chief among the reasons for the discrepancy are (1) points of contraflexure in the lower stories are not at the midpoints, and (2) the shears are greater in exterior girders than in the interior girders of that floor.

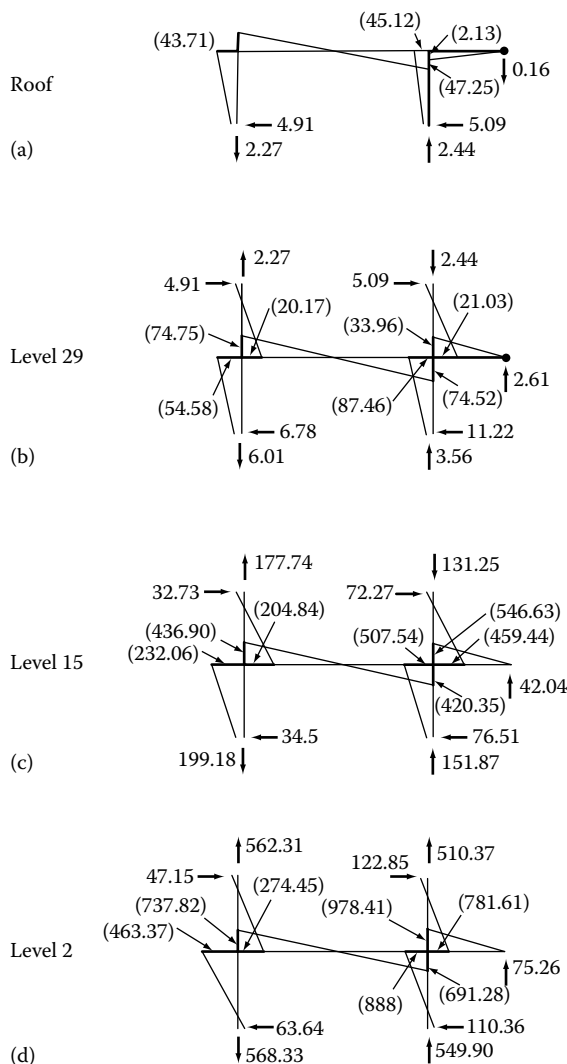
Before the advent of computers, it was common practice to use the portal or cantilever method with some modifications for the final design of structures. The modifications consisted of a number of assumptions. Chief among them are

1. Locate point of contraflexure in exterior girders at 0.55 of their length.
2. Locate the points of contraflexure in the bottom-story columns at 0.6 height from the base, in the top-story columns at 0.65 height from the top.
3. Use of rather complicated rules to divide the story shears among columns.

These approximations are no longer popular since the approximate methods are very rarely used in the final analysis of the structures.

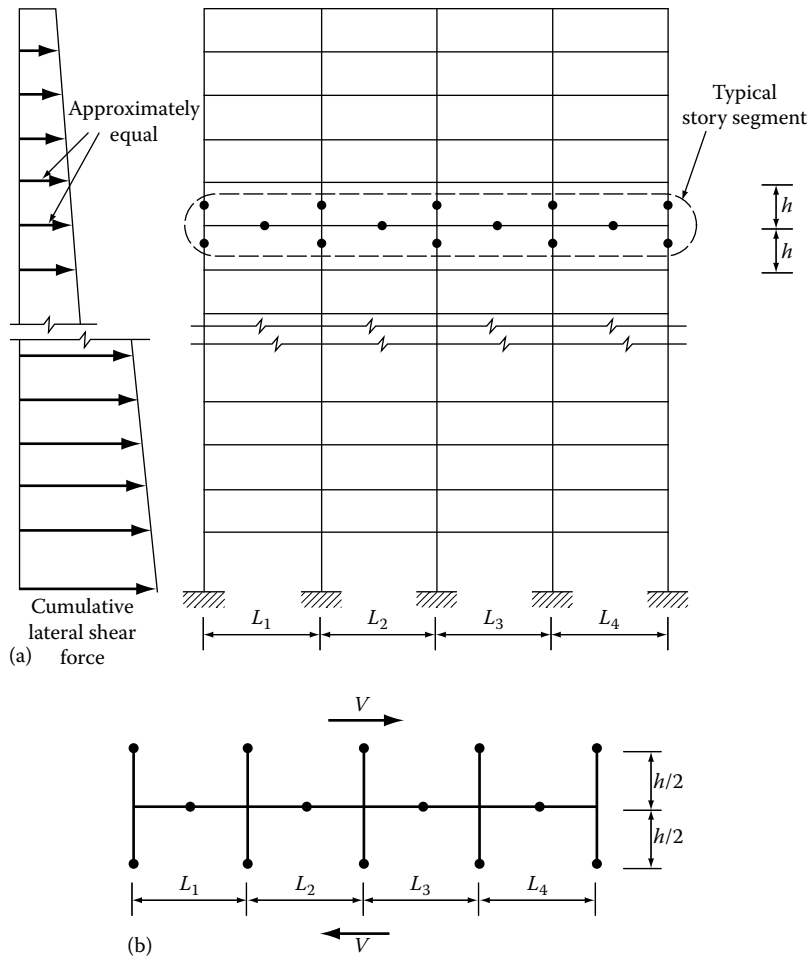
### 9.4.3 LATERAL STIFFNESS OF FRAMES

The lateral displacement of one floor relative to the floor below results from a combination of bending and shear deformation of the bent. The bending deformation of the chord drift, as it is sometimes called, is a consequence of axial deformation of the columns alone and is independent of the size, type, location, and arrangement of the web system. The shear deformation is due to the rotation of the joints in the frame, which causes bending of columns and girders of the frame. For

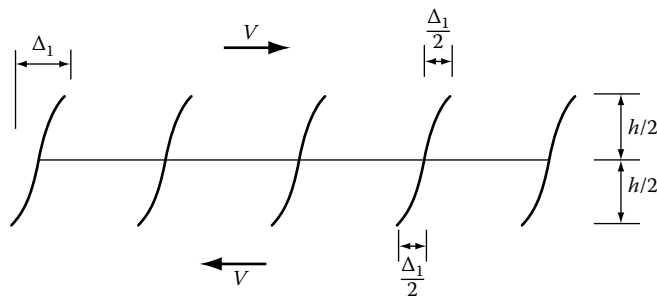


**FIGURE 9.33** Moments and forces at (a) roof level, (b) level 29, (c) level 15, and (d) level 2.

relatively short frames with height-to-width ratios less than 3, the deflection due to axial shortening of columns can be neglected and the deflection of the frame can be assumed to be entirely due to joint rotations. Its contribution to deflection can, however, be obtained by considering the frame as a cantilever with an equivalent moment of inertia  $I = 2ad^2$  where  $a$  is the area of exterior column and  $d$  is half the base of the portal frame. For taller frames, it is prudent to consider the axial deformation of the interior columns; the equivalent moment of inertia is determined by the relation  $I = \sum_1^n a_i d_i^2$ , where  $a_1, a_2, \dots, a_n$  represent the areas of the columns and  $d_1, d_2, \dots, d_n$  represent the corresponding distances from the natural axis of the frame. To derive the equations for the shear deformations, let us consider a portal frame subjected to lateral shear forces, as shown in Figure 9.34. We isolate a representative portion of the frame consisting of a typical floor and column segments between the points of contraflexure above and below the floor, as shown in the figure. We will now consider the shear deformation, which is due to bending of columns and girders of the representative segment. First, we consider the contribution of columns by assuming the girders to be infinitely rigid; then we consider the girder contribution by assuming the columns to be infinitely rigid.



**FIGURE 9.34** Portal frame shear deflections: (a) Frame subjected to lateral loads and (b) typical story segment.



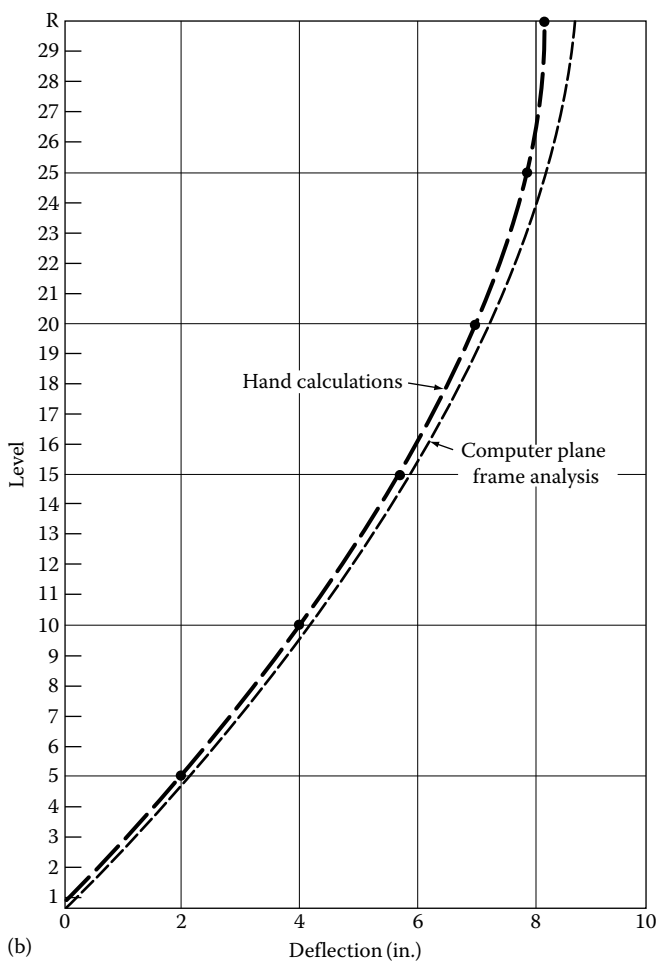
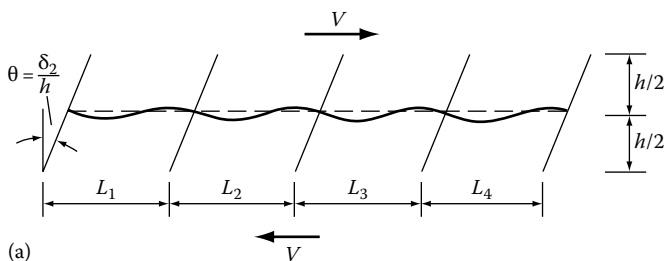
**FIGURE 9.35** Lateral deflection due to bending of columns.

**Deflection due to column rotations:** Consider the free-body diagram of a typical story bounded between the points of contraflexure in the columns above and below the  $i$ th level, as shown in Figure 9.35. When the number of stories is large, it is reasonable to assume that the shears in the columns above and below the floor do not differ appreciably. If the floor girders are rigid, the lateral deflection  $\Delta_1/2$  of each column would be equal to the sum of the deflections of the two cantilevers of length  $h/2$  under the action of wind shears  $V$  (Figure 9.35).

$$\frac{\Delta_1}{2} = \frac{V \left( \frac{h}{2} \right)^3}{3EI_c} \quad \text{or} \quad \Delta_1 = \frac{Vh^3}{12E\sum I_c}$$

For all columns  $\Delta_1 = Vh^3/12E\sum I_c$ .

**Deflection due to girder rotations:** Next consider the columns as rigid, giving rise to rotations of the girders, as shown in Figure 9.36a. Each girder undergoes a rotation equal to  $\theta$  at each end giving rise to an internal moment of  $12EI\theta/L$  for each girder. The total internal moment is given by



**FIGURE 9.36** (a) Lateral deflection due to girder rotations and (b) deflection comparison (30-story frame).

the summation of such terms for each girder. Thus the total internal moment due to girder rotation is  $12E\theta\sum(I_{bi}/L_i)$ . The external moment due to wind shears  $V$  is given by  $V \times h$ . Equating external moment to internal moment and noting that  $\theta$  produces a displacement  $\Delta_2 = \theta h$ , we get

$$\Delta_2 = \frac{Vh^2}{12E\sum(I_{bi}/L_i)}$$

The total frame shear deflection  $\Delta_s$  is given by

$$\Delta_s = \Delta_1 + \Delta_2 = \frac{Vh^2}{12} \left\{ \frac{h}{\left(\sum EI\right)_{\text{col}}} + \frac{1}{\left[\sum(EI/L)\right]_{\text{beam}}} \right\}$$

The deflection for the total number of stories is obtained by the summation of the deflections for each story.

An example of deflection calculations using the above procedure follows. To keep the presentation simple, we will consider the same example frame that was used for calculating moment and forces by the portal and cantilever methods (refer back to Figure 9.30).

#### Deflections calculations for frame shown in Figure 9.45

**Cantilever deflection:** The neutral axis for the frame lies on the line of symmetry. The moment of inertia of the frame about the neutral axis is given by  $I = 2(a_1d_1^2 + a_2d_2^2)$  where  $a_1$  and  $a_2$  are the areas of the exterior and interior columns and  $d_1$  and  $d_2$  their distance from the neutral axis. Substituting  $a_1 = 4 \text{ ft}^2$  and  $a_2 = 6 \text{ ft}^2$ ,  $d_1 = 53 \text{ ft}$  and  $d_2 = 13 \text{ ft}$ , we get  $I = 2(4 \times 53^2 + 6 \times 13^2) = 24,500 \text{ ft}^4$  (211.46 m<sup>4</sup>).

For the purpose of deflection calculation, we can assume that the frame is subjected to a uniformly distributed horizontal load  $= 12/13 = 0.9231 \text{ k/ft}$ . The cantilever deflection at the top is given by

$$\Delta_{\text{cant}} = \frac{wl^4}{8EI} = \frac{0.9231 \times 384^4}{8 \times 4,176,000 \times 24,500} = 0.0245 \text{ ft (7.47 mm)}$$

**Shear deflection due to column rotations:** This is given by

$$\Delta_1 = \frac{Vh^3}{12E\sum I_c}$$

For the example problem, the moments of inertia for the exterior and interior columns are, respectively, equal to 0.33 and 0.5 ft<sup>4</sup>, giving  $\sum I_c = 2 \times 0.33 + 2 \times 0.5 = 1.66 \text{ ft}^4$ . Using an average cumulative shear value of  $V = 210 \text{ kip}$  and  $h = 13 \text{ ft}$ ,

$$\Delta_1 = \frac{210 \times 13^3}{12 \times 4,176,000 \times 1.66} = 0.0056 \text{ ft (1.70 mm)}$$

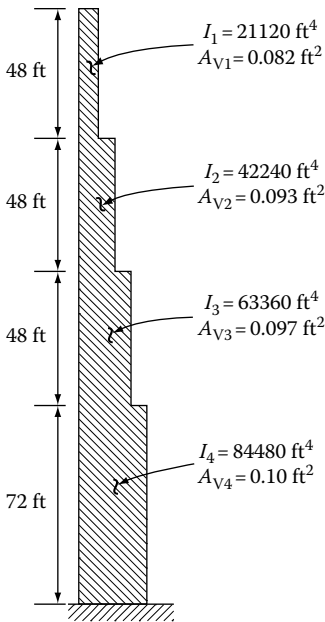
**Shear deflection due to girder rotations:** This is given by

$$\Delta_2 = \frac{Vh^2}{12E\sum(I/L)}$$

For the example problem,  $\sum I/L$  of girders  $= 0.5/40 + 0.5/26 + 0.5/40 = 0.0442 \text{ ft}$ , giving

$$\Delta_2 = \frac{210 \times 13^2}{12 \times 4,176,000 \times 0.0442} = 0.016 \text{ ft/floor (4.87 mm/floor)}$$





**FIGURE 9.38** Equivalent cantilever.

Calculate the moment of inertia of the frame about its axis of bending by the relation  $I = \sum Ax^2$ . Since the areas of the columns change at four locations, the corresponding four values of frame moment of inertia from the top work out equal to 21,120, 42,240, 63,360, and 84,480 ft<sup>4</sup>, respectively (182.3, 364.6, 546.86, and 729.15 m<sup>4</sup>).

Figure 9.38 shows the equivalent cantilever with varying moments of inertia. If the beams were infinitely rigid, the deflection calculated for the cantilever would have represented the total lateral deflection of the frame. Since in reality the beams are flexible, the deflection of the cantilever is increased by the racking component, which is equivalent to the shear deformation of the cantilever. This was shown equal to

$$\Delta_s = \frac{Vh^2}{12} \left[ \frac{h}{(EI/h)_{\text{col}}} + \frac{1}{(EI/L)_{\text{beam}}} \right]$$

Defining story stiffness as the deflection per unit of horizontal equivalent shear, the equivalent story stiffness is given by the relation

$$\frac{V}{\Delta_s} = \frac{12}{h^2 \left\{ 1/(\sum EI)_{\text{col}} + 1/\left[ \sum (EI/L) \right]_{\text{beam}} \right\}}$$

An equivalent shear area for the cantilever is worked out as follows. Consider the shear deformation of the cantilever for unit height  $h$  subjected to horizontal forces  $V$ , as shown in Figure 9.39. The shear deflection  $\Delta_s$  is given by

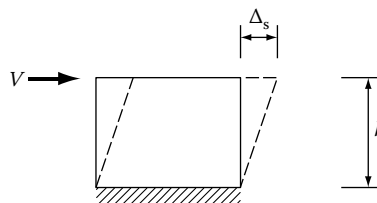
$$\Delta_s = \frac{Vh}{GA_v}$$

The story stiffness  $\frac{V}{\Delta_s}$  works out equal to  $\frac{0.4EA_v}{h}$  in which it is assumed that  $G = 0.4E$ . Equating the story stiffness relations, we get

$$\frac{0.4EA_v}{h} = \frac{12}{h^2 \left\{ 1/(\sum E_c I)_{\text{col}} + 1/\left[ \sum (E_b I/L) \right]_{\text{beam}} \right\}}$$

Assuming  $E$  is constant for beams and columns, that is,  $E_c = E_b = E$ , we get

$$A_v = \frac{30}{h \left\{ 1/(\sum I)_{\text{col}} + 1/\left[ \sum (I/L) \right]_{\text{beam}} \right\}}$$



**FIGURE 9.39** Shear deformation of a cantilever of unit height  $h$ .



Using the numerical values shown in Figure 9.37, the equivalent shear areas at four vertical locations work out, equal to 0.082, 0.093, 0.097, and 0.1 ft<sup>2</sup> (0.0076, 0.0086, 0.0090, and 0.0093 m<sup>2</sup>), respectively, from the top. These values are shown schematically in Figure 9.38.

The deflection of the equivalent cantilever of varying moment of inertia can be obtained either by long-hand methods such as virtual work or by using a relatively simple stick computer model. In keeping with the approximate nature of analysis, reasonable results can be obtained by assuming average properties for the equivalent cantilever. The average values for  $I$  and  $A$  for the example problem work out equal to 56,320 ft<sup>4</sup> and 0.093 ft<sup>2</sup> (486 m<sup>4</sup> and 0.0086 m<sup>2</sup>), respectively. Using a value of 216 kip for the average cumulative shear  $V$ , we get a total top deflection of 0.319 ft (94 mm) as compared to a value of 0.28 ft (82.3 mm) obtained from a stick computer model and a value of 0.24 ft (73 mm) as obtained from a plan frame analysis. Comparison of deflections are shown in Figure 9.40.

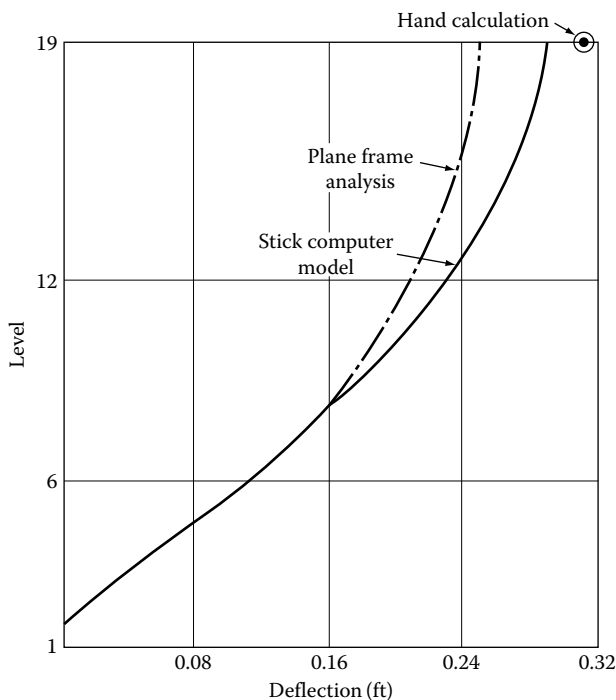
The analysis presented thus far is based on the centerline dimensions, which in general overestimate the deflection. Although all structural members have finite widths, it is unnecessary, especially in view of the approximate nature of the analysis, to be overly concerned about the effect of joint widths on the stiffness of the structure. However, in those cases in which the dimensions of the members are large in comparison to story height and girder spans, it is possible to incorporate the effect of joints by assuming that no member deformation occurs within the joint. An approximate expression for the equivalent shear area for the equivalent column can be shown to be

$$A_v = \frac{30}{h^2 \left\{ ha_1^3 / (\sum I)_{\text{col}} + a_2^3 / \left[ \sum (IL) \right]_{\text{beam}} \right\}}$$

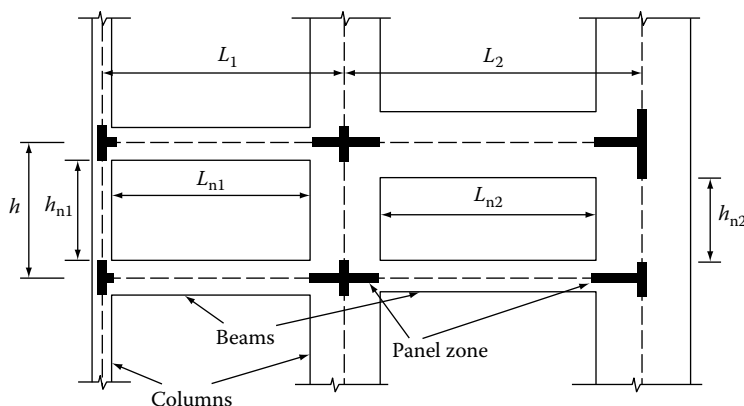
where

$a_1$  is the average ratio of clear height to center to center heights of columns (Figure 9.41)

$a_2$  is the average of the ratio of the clear span to the centerline spans of girders (Figure 9.41)



**FIGURE 9.40** Deflection comparison.



**FIGURE 9.41** Infinitely rigid panel zones.

Analytical and experimental investigations have shown that an analysis based on rigid offset lengths to the outer face of supports overestimates the stiffness of the structure. The analysis should therefore include some method of compensating the deformations that do exist in the panel zones. A rigid zone reduction factor can be used to reduce the lengths of rigid offsets—a method similar to that employed in many commercial computer programs. Arbitrary reductions are assigned to joint sizes in an effort to compensate for the joint deformation.

The underlying principle in both the portal and cantilever methods is the assumption that the point of contraflexure is located at midheight and midspan of columns and girders. Rigorous computer analyses almost invariably show that the fundamental assumption is violated in various degrees, especially at the top and bottom floors of a tall building. It is possible, however, to improve the results of the approximate analyses by assuming locations for points of contraflexure at locations representative of what is commonly found from computer analysis.

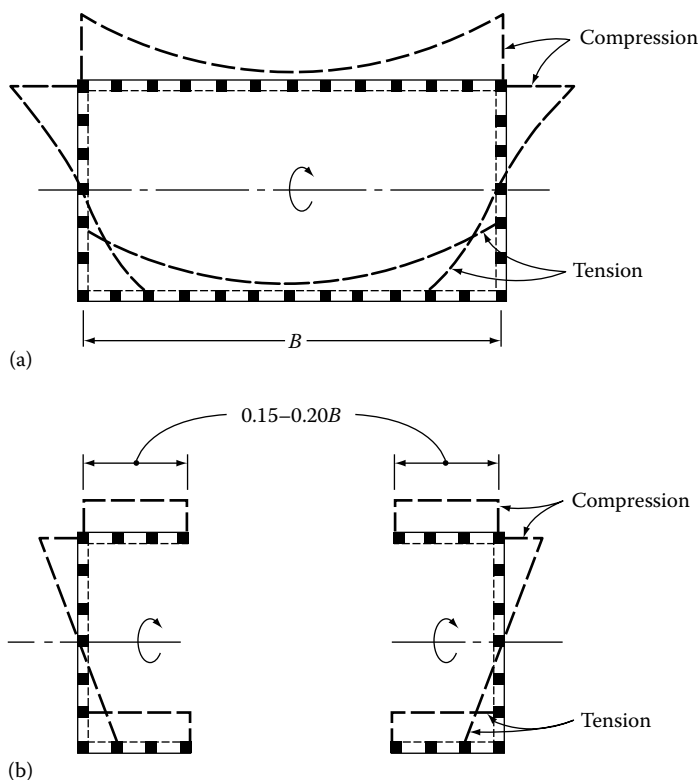
For example, it is fairly well known that the actual points of contraflexure in portal frames at the lower floors, especially at the first story, occur at a location closer to about  $h/3$  below the second floor. Expressions for equivalent shear stiffness for the first story can be shown to work out

$$A_v = \frac{20}{h^2 \left\{ 1/(\Sigma EI)_{\text{col}} + 1/5[\Sigma (EI/L)]_{\text{beam}} \right\}}$$

Further refinement of the analysis is generally considered unnecessary in view of the approximate nature of the analysis and the availability of computer techniques.

#### 9.4.4 FRAMED TUBE STRUCTURES

As mentioned earlier, the framed tube system in its simplest form consists of closely spaced exterior columns tied at each floor level by relatively deep spandrels. The behavior of the tube is in essence similar to that of a hollow perforated tube. The overturning moment under lateral load is resisted by compression and tension in the columns while the shear resisted by bending of columns and beams primarily in the two sides of the building parallel to the direction of the lateral load. The bending moments in the beams and columns of these frames, which are called web frames, can be evaluated using either of the two approximate procedures, namely, the portal or the cantilever analysis. It is perhaps more accurate to use the cantilever method because tube systems are predominately used for very tall buildings in the 40- to 80-story range in which the axial forces in the columns play a dominate role. The moments in spandrels and columns as well as the racking components of the tube deflection can be evaluated by using the cantilever method.



**FIGURE 9.42** Framed tube: (a) axial stress distribution with shear lag and (b) axial stresses distribution in equivalent channels without shear lag.

As mentioned earlier, because of the continuity of closely spaced columns and spandrels around the corners of the building, the flange frames are coaxied into resisting the overturning moment. Whether or not all the flange columns, or only a portion thereof contribute to the bending resistance is a function of shear rigidity of the tube. A device normally used in approximate analysis to reduce the tube configuration into two equivalent channels is shown in Figure 9.42. The determination of the width of channel flange is subjected to engineering judgment and is usually limited to 15%–20% of the width of the building. It is a function of the shear lag across the windward and leeward sides of the tube and the aforementioned rules of thumb give results sufficiently accurate for preliminary sizing of the tube system.

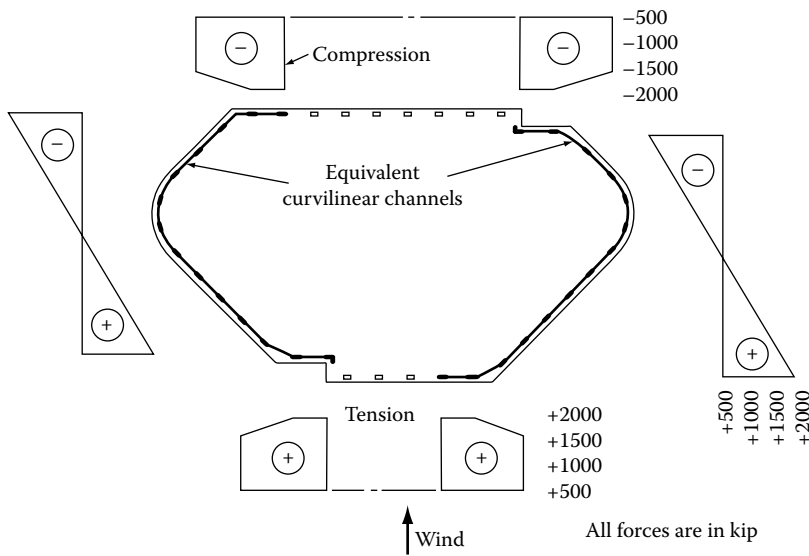
Shown in Figure 9.43 is the plan of a framed tube system delineating portions of the columns in the leeward and windward sides that were assumed to be part of the equivalent channel flanges. The axial forces were obtained on the basis of equivalent channel flanges. The axial forces were obtained on the basis of equivalent structure, as shown in Figure 9.43. Shown in Figure 9.44 are the axial forces obtained from a three-dimensional computer analysis.

An equivalent column approach, as shown in the previous section, can be used to obtain approximate deflection values. In calculating the moment of inertia of the frame it is only necessary to include the contribution of equivalent flange columns on the windward and leeward sides of the tube.

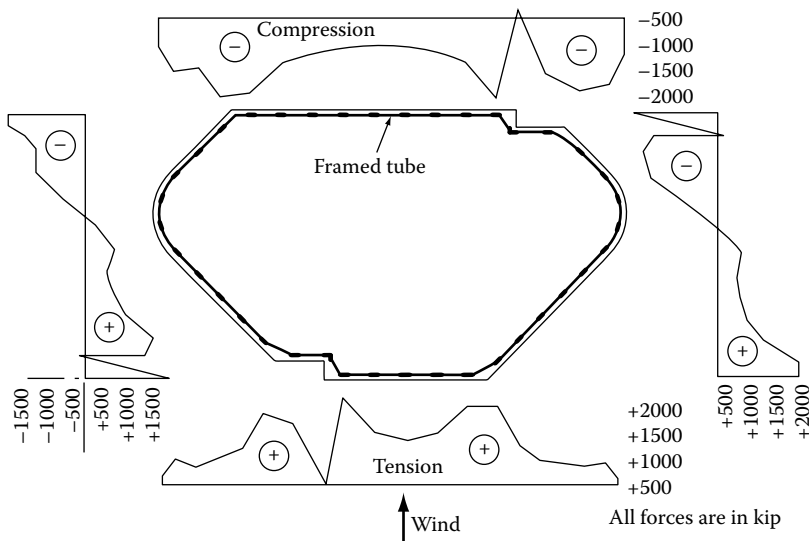
## 9.5 TORSION

### 9.5.1 PREVIEW

The stated objective of this book is to promote the ability of the engineers to sense when an answer obtained through computer is not correct. To fulfill that desire in a simple manner, we will revisit some approximate analysis techniques and yes, even dust off those classic methods



**FIGURE 9.43** Axial forces in tube columns assuming two equivalent curvilinear channels.



**FIGURE 9.44** Axial forces in tube columns from three dimensional analysis of framed tube.

that were so precious to engineers of yesteryear. One such method useful in understanding the torsional behavior of shear walls is the so-called bimoment theory also known as nonuniform or warping theory. Developed by Professor Vlasov in 1941, this elegant method paves the way for developing a feel for the structural behavior of shear walls particularly those subjected to torsional loads.

The theory is quite simple, no more complicated than the engineer's theory of bending (ETB). At first glance, the related bimoment equations may look formidable, but in practice they can be further simplified into a format well suited for preliminary back-of-the-envelope calculations.

In this section, we study in some detail the torsional response of open section shear walls. After a brief introduction to torsion, we examine the warping behavior of shear walls and then discuss warping properties that are used in calculating the warping stresses. Then we introduce the general



y-axis as just described, and the effect of the couple is to produce torsion of the wall. Thus, we observe that a lateral load acting on a wall will produce bending without twisting only if it acts through the shear center. As a consequence, locating the shear center  $S$  is an important aspect of wall design whenever the plane of bending is not a plane of symmetry.

The shear center of the singly symmetric shear wall shown in Figure 9.45a can be determined as follows. We consider the cross section to consist of three rectangular parts, namely, the two flanges and the web (Figure 9.45c). All three parts are subject to the same curvature when bending takes place, because they are integral parts of the same cross section. Therefore, the bending moment carried by each part is in proportion to its moment of inertia about the y-axis:

$$M_y = M_1/EI_1 = M_2/EI_2 = M_3/EI_3 \quad (a)$$

in which

$M_1$ ,  $M_2$ , and  $M_3$  are the moments resisted by parts 1, 2, and 3, respectively  
 $I_1$ ,  $I_2$ , and  $I_3$  are their respective moments of inertia about the y-axis  
 $M_y$  is the total applied moment

If the web is thin, as is the case in practical shear walls, its moment of inertia  $I_3$  will be very small compared to  $I_1$  and  $I_2$ . Then we may disregard the effect of the web and assume that all of the moment is resisted by the flanges:

$$M_y = M_1 + M_2$$

Also, from Equation (a) we get

$$M_1/I_1 = M_2/I_2$$

Combining the preceding two equations, we obtain

$$M_1 = M_y I_1 / (I_1 + I_2), \quad M_2 = M_y I_2 / (I_1 + I_2) \quad (b)$$

The shear forces  $V_1$  and  $V_2$  in the flanges are in the same proportions as the bending moments (because  $V = dM/dx$ ); hence

$$V_1/V_2 = M_1/M_2$$

Also, the total shear force  $V_x = V_1 + V_2$ .

By comparing this equation with Equations (b), we see that the shear forces are

$$V_1 = V_x I_1 / (I_1 + I_2), \quad V_2 = V_x I_2 / (I_1 + I_2) \quad (c)$$

The line of action of the resultant of these two shear forces determines the location of the shear center  $S$ .

To locate the shear center  $S$ , we determine the distances  $h_1$  and  $h_2$  from the centerlines of the flanges to the shear center  $S$ . Inasmuch as  $P$  is the resultant of  $V_1$  and  $V_2$ , the forces  $V_1$  and  $V_2$  must produce no moment resultant about point  $S$ ; therefore, the shear center distance is determined by

$$V_1 h_1 = V_2 h_2$$

or, using Equations (c),

$$h_1/h_2 = I_2/I_1$$

A special case occurs when the shear wall has only one flange (Figure 9.45d). For this shape, we obtain

$$h_1 = 0, \quad h_2 = h$$

This result shows that the shear center is located at the intersection of the centerlines of the flanges and web. We could have anticipated this result because in the derivation we assumed that the web was very thin so that the shear force was carried entirely by the flanges.

A similar procedure may be used to find the shear center of a group of shear walls bending about a common neutral axis (see Figure 9.45e).

The most common elements of concrete construction resisting torsion are the shear walls that enclose the elevator, stairs, and mechanical shafts. These typically are of I and C cross sections. Before developing torsion theory for these elements, it is instructive to discuss the torsional behavior of circular cross-section shafts.

Recall that the shear stresses in a circular cross section is directed tangentially. The maximum shearing stress is given by

$$V_t = \frac{T_r}{I_p} = V_t = \frac{16T}{\pi d^3}$$

where

$d$  is the diameter of the shaft

$I_p$  is the polar moment of inertia of the circular section

$T$  is the twisting moment

Also recall that the total angle of twist  $\phi$  for the length  $l$  of the shaft is determined by

$$\phi = \frac{T\ell}{GI_p}$$

In deriving these equations two assumptions are necessary: (i) plane cross sections in the untwisted state remain plane when torque is applied and (ii) the cross sections remain undistorted in their own plane.

The first assumption does not remain true for noncircular sections and particularly so for I and C sections often referred to as open sections. Without giving a proof, suffice it to state here that nature resists a given action (here a torque) always with the simplest possible stresses, and thus makes it plausible that the plane cross section in an open section does not remain plane but becomes warped vertically.

We now return to the analysis of structural systems for torsion with particular emphasis on the torsion analysis of open-section cores. At first, we take a cursory look at the classical methods of torsion of elements such as circular, noncircular, and cellular sections, and later on discuss warping torsion of structural systems consisting of open cores.

The terminology used in torsion analysis may be conveniently grouped under two headings: uniform or St. Venant's torsion and warping torsion, often times referred to as constrained torsion or torsion bending. The terms for uniform torsion are well established and given in most textbooks on structural mechanics. The purpose of recalling them here is to show how they relate to the warping theory.

The terms shown on the right-hand side of Tables 9.3 and 9.4 relating to warping torsion have, in the past, been given little attention. Consequently, designers are generally not at ease with either the concepts of warping behavior or with its methods of analysis. The aim here is to introduce the concept of importance of considering warping in practical cases.

Torsional effects on buildings as a whole are enhanced when the center of twist is eccentric from the center of gravity for inertial loading, or from the center of area for wind loading. Minimum

**TABLE 9.3**  
**Torsion Terminology**

Uniform (St. Venant) Torsion	Warping Torsion
<ul style="list-style-type: none"> <li>• Torsional shear stress</li> <li>• Twist</li> <li>• Polar moment of inertia</li> <li>• Membrane analogy</li> <li>• Shear flow</li> <li>• Cellular sections</li> </ul>	<ul style="list-style-type: none"> <li>• Shear center</li> <li>• Open section</li> <li>• Warping deformation</li> <li>• Sectorial coordinate</li> <li>• Warping moment of inertia</li> <li>• Bimoment</li> <li>• Normal stress</li> <li>• Tangential stress</li> </ul>

**TABLE 9.4**  
**Analogy between Bending and Warping Torsion**

Elementary Bending Theory	Warping Theory
Plane sections remain plane	Profile warps
$I_x = \int_A y^2 dA$	$I_\omega = \int_A \omega^2 dA$
$M_x = -EI_x \frac{d^2 x}{dz^2}$	$B = -EI_\omega \frac{d^2 \theta}{dz^2}$
$\sigma_x = \frac{MC}{I_x}$	$\sigma_\omega = \frac{B_\omega}{I_\omega}$
$\tau_x = -\frac{VQ_x}{I_x t}$	$\tau_\omega = -\frac{HQ_\omega}{I_\omega t}$

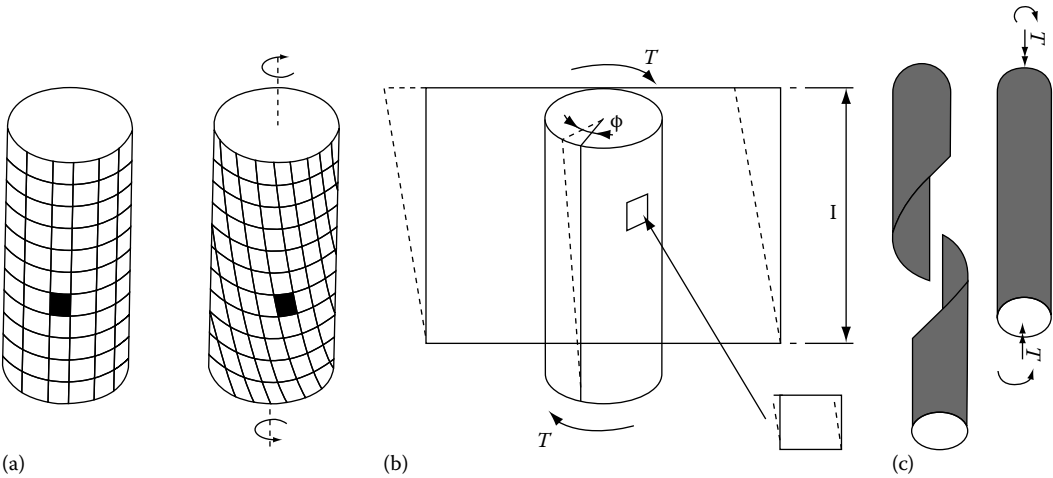
eccentricities are prescribed by building codes to account for accidental seismic torsion. And, to reflect the observed torsional behavior of buildings in turbulent wind, ASCE 7-05 in Section 6 requires that buildings be designed for partial as well as full wind loading.

Consider the twisting of a circular shaft, as shown in Figure 9.46a. The twisting of the shaft does not produce any longitudinal stress, that is, axial compression or tension, but only pure shear stresses. The shear stresses vary from zero at the center of the shaft, to maximum value at the perimeter. Because of the absence of axial deformation, a cylindrical layer peeled off of the shaft, changes its shape under the action of twist, from a rectangle to a parallelogram (Figure 9.46b). The absence of longitudinal stresses indicates that the surfaces at the ends of the shafts remain plane. In other words, no warping will take place. The work done by the twisting moment is expended in developing shear stresses, as shown in Figure 9.47.

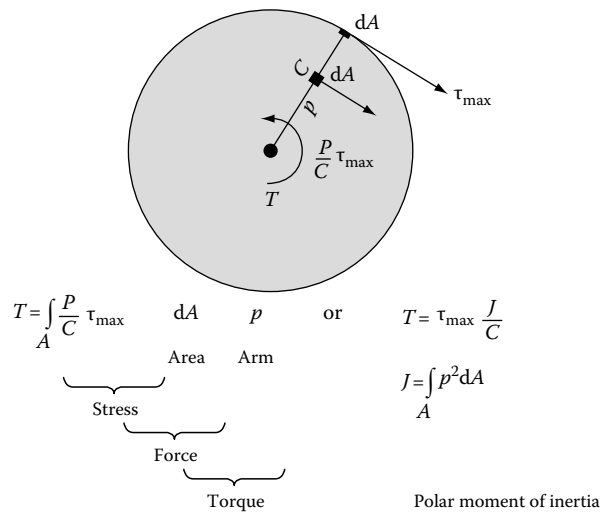
Consider a rectangular section subjected to the action of a vertical load at the center of gravity of section (Figure 9.48). To find shear stress at any horizontal section, we introduce an imaginary horizontal cut at that section and obtain the shear stresses by the relation  $VQ/It$ . By inspection, the resultant of the vertical shear stresses is at the center of gravity of the beam.

Next we take a look at the torsional behavior of a thin-walled section. The main reason why a thin-walled section must be given special consideration is, the shear stresses and strains in it are much larger than those in solid sections. An examination of distribution of shear stresses through

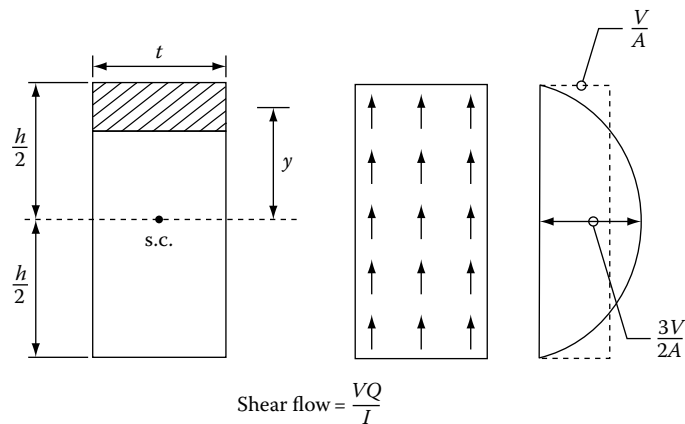




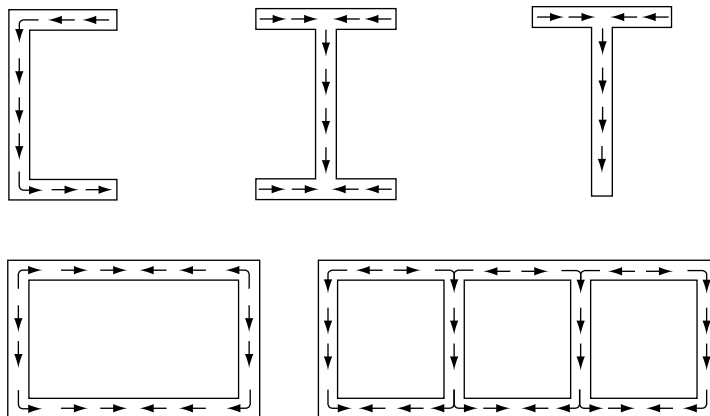
**FIGURE 9.46** (a,b) Twisting of circular shaft. (c) Torsion failure of a brittle material by tension cracking along a 45° helical surface.



**FIGURE 9.47** Variation of torsional shear stresses in circular shaft.



**FIGURE 9.48** Shear flow in a rectangular section.

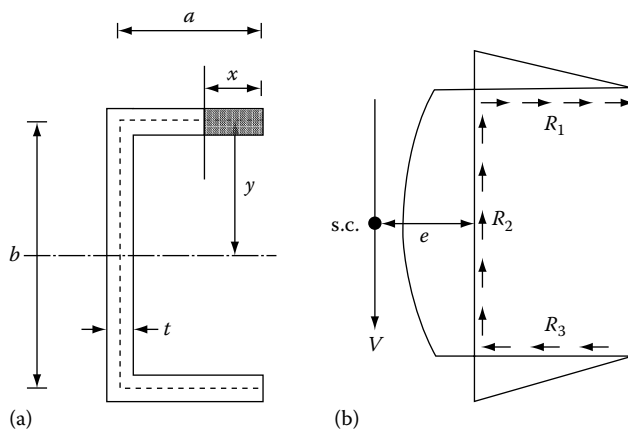


**FIGURE 9.49** Shear flow in thin-walled sections: load at shear center.

the cross section shows that the shear stresses flow through the cross section as if they were a fluid: hence the name, shear flow (Figure 9.49).

Now consider a flanged section such as a C-shaped shear wall (Figure 9.50). To find the shear flow, we abandon the idea of the horizontal cut. Instead, we consider a cut perpendicular to the profile and find the shear along the profile. The shear  $R_2$  in web is in equilibrium with the vertical load  $V$  and while the horizontal shears  $R_1$  and  $R_3$  in the webs result in no net horizontal load, the resulting moment requires offsetting of the vertical load to a location left of the web. The resultant forces from shear stresses

$$\begin{aligned}
 R_1 = R_3 &= \int_0^a \tau t dx_1 \\
 &= \frac{V b t a^2}{4 I_y} \\
 &= \frac{3 V a^2}{b^2 \left( 1 + \frac{6a}{b} \right)}
 \end{aligned}$$



**FIGURE 9.50** Shear center in C-section.

For vertical equilibrium,

$$R_2 = V$$

For zero rotational effect,

$$R_1 b = R_2 e$$

Hence

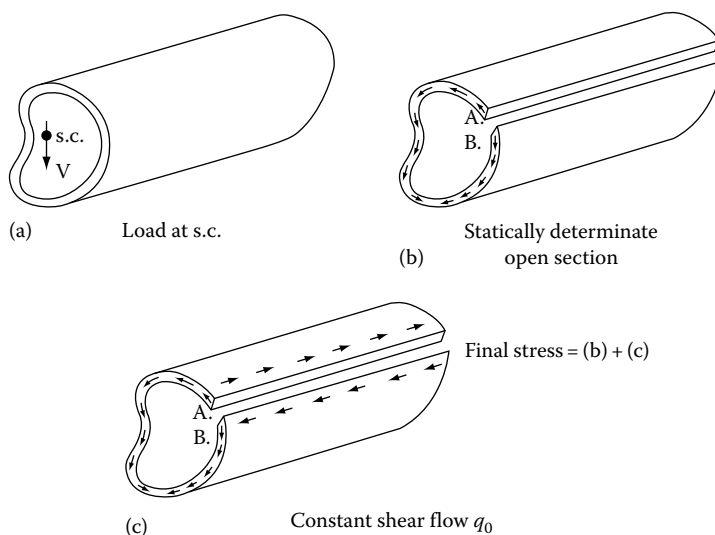
$$e = \frac{R_1 b}{R_2} = \frac{3a^2}{b \left( 1 + \frac{6a}{b} \right)}$$

To find shear stresses in a cellular section, Figure 9.51, a two-step approach is required because the problem is statically indeterminate. First, the section is rendered statically determinate by inserting a horizontal cut along the length of the section and the shear flow in the section is evaluated by the relation  $VQ/I$ . Next, the shear flow required to close the gap is evaluated. The final shear stress is evaluated by combining the two.

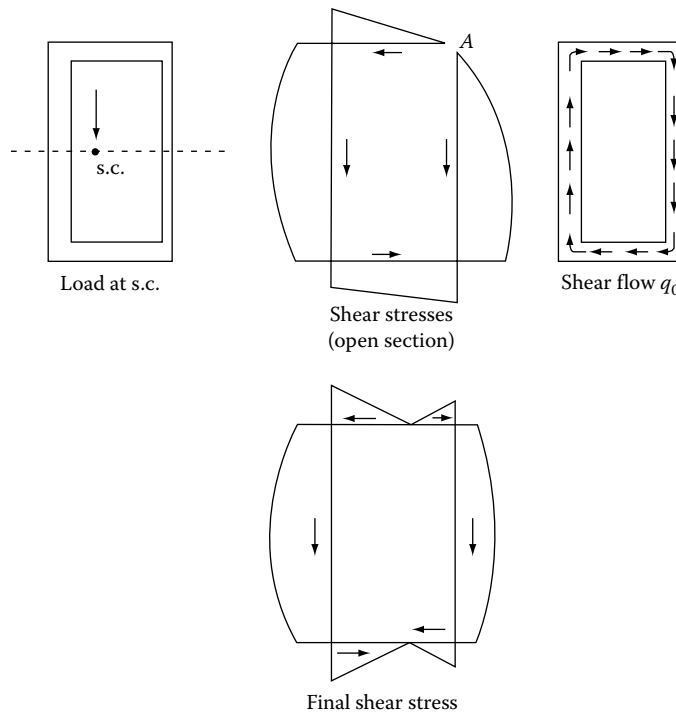
As an example, Figure 9.52 shows schematically the final shear stresses in a hollow rectangular section. The section consists of webs of unequal thickness and is subjected to a vertical load at its shear center.

If we have a multiple cellular section, the procedure is similar to that for a single-cell section. The only difference is the problem is statically indeterminate to the  $n$ th degree where  $n$  represents the number of cells. The example in Figure 9.53 has two cells, hence,  $n = 2$ . Two cuts are made at A and B to render the section open. The shear flows  $q_1$  and  $q_2$  are evaluated by solving two simultaneous equations, and the final shear stress is obtained by superposition.

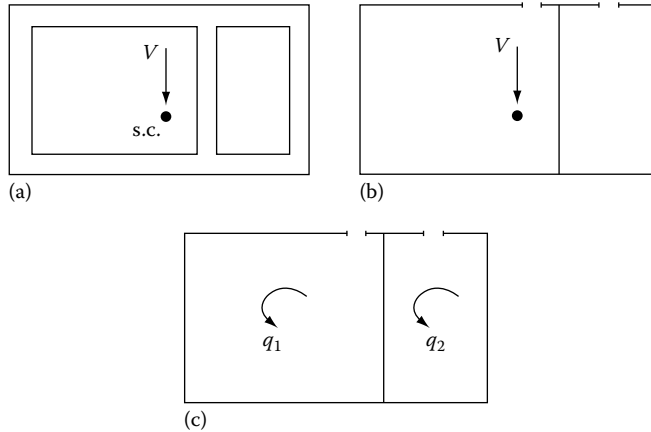
The theory of torsion and related formulas discussed above are commonly referred to as St. Venant torsion formulas, and are valid for beams of circular cross sections. His formula can be accepted for noncircular sections only when the additional stress caused by warping deformation



**FIGURE 9.51** Shear stresses in hollow section: load at shear center.



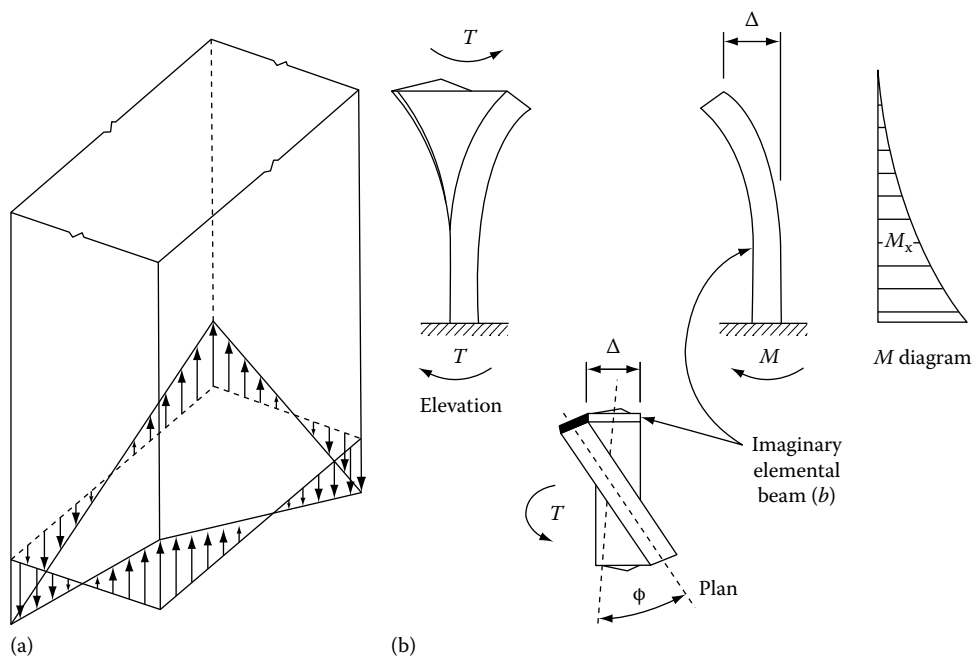
**FIGURE 9.52** Shear stresses in hollow rectangular section.



**FIGURE 9.53** Shear flow in cellular sections: (a) load at shear center, (b) section rendered open with two cuts, (c) shear flows required for compatibility, and (d) final shear flow = (b) + (c).

is ignored. Consider, for example, a rectangular section shown in Figure 9.54a. The vertical fibers of the section are moving up and down from their initial position in space due to torsion. The top and the bottom of the beam do not remain plane, but become warped. However, no additional stresses are induced because the warping deformations are not restrained either at the ends or at any section along its length.

Let us examine the case when the bottom of the beam is fixed. The warping of the bottom surface of the beam is restrained resulting in longitudinal strains and stresses. If we separate an imaginary elemental beam, as shown in Figure 9.54b, it can be seen that the deflected shape is similar to that of a laterally loaded cantilever. It is obvious that bending stresses manifest at the fixed end of the beam.



**FIGURE 9.54** (a) Warping of solid beams. (b) Thin rectangular beam: bending moment due to warping restraint.

The presence of bending stresses implies that part of the work done by the twisting moment is used up in bending the beam and only the remainder will develop shear stresses associated with the St. Venant twist. Hence the resistance to external twisting moment is offered as the sum of pure torsion plus some additional torsion which causes bending of the section. This second part is called “warping torsion, nonuniform torsion or flexural twist.”

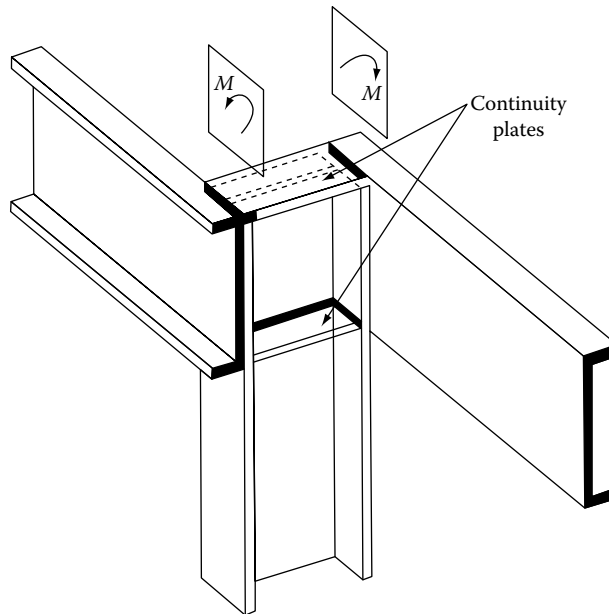
For the thin rectangular beam shown in Figure 9.54b, very little energy is expended to cause elemental bending about the weak axis. For such beams we can safely neglect the warping component of the twisting moment because the effect of constraining warping is usually restricted to the vicinity of the restraint. This phenomenon is valid, to a lesser extent for thin-walled closed sections. On the other hand, the effect of constraining warping of thin-walled open sections does not diminish rapidly and has a considerable influence on the stress distribution over a greater portion of the section.

Flexural twist causes a pair of moments. Such a pair of moments, called “bimoment” although is a mathematical function, can be visualized in most practical cases. For example, consider a two-span continuous beam supported by an interior column, as shown in Figure 9.55. Since the two channels frame into opposite flanges of the column, a bimoment is introduced at the top of the column.

Restrained warping behavior involves a set of so-called sectorial parameters each of which is counterpart in the theory of bending of beams. Since the sectorial parameters are generally unfamiliar to practicing engineers it is perhaps appropriate to review them briefly here.

The sectorial coordinate,  $\omega$ , at a point on the profile of a warping core is the parameter that expresses the axial response such as axial stress and strain at that point relative to other points around the core. The  $\omega$  diagram can be constructed with the known location of the shear center and a point of zero warping deflection as an origin. The principal sectorial coordinate in warping theory is analogous to the distance  $c$  of a point from the neutral axis of a section in bending. Just as the parameter  $c$  is used in developing the well-known bending theory, the parameter  $w$  is used in developing the warping theory.

A great advantage of the theory of bimoment is that internal strains and stresses can be found from formulas as simple as those used in the ETB. The bimoment and flexural twist can be used in



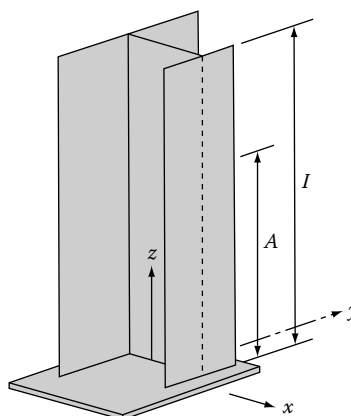
**FIGURE 9.55** Bimoment in wide flange column.

a manner similar to bending moment and shearing forces. The procedure differs in that we use the sectorial coordinate  $w$  instead of the linear coordinate  $c$ , to calculate the physical properties related to warping torsion.

To a beginner, the thin-walled beam theory with its differential equations presented later in this chapter may look too academic for use in a down-to-earth practical design. In reality, once the idea of bimoment is assimilated, its use is not much more difficult than the use of bending moments or shear forces. It provides the engineer with a means for verifying the behavior of tall shear wall buildings subjected to torsion.

### 9.5.2 CONCEPT OF WARPING BEHAVIOR

Perhaps the easiest model to describe the warping theory is an I-shaped shear wall with unequal flanges, as shown in Figures 9.56 and 9.57. In most shear wall buildings the core around elevators



**FIGURE 9.56** I-section core.

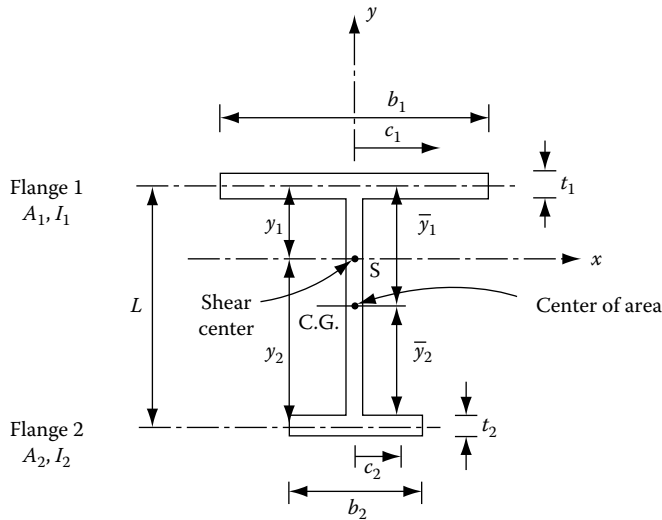


FIGURE 9.57 Core properties.

and stairs consists of a series of I- and C-shaped shear walls. Therefore, the model chosen has practical significance. Since torsion is the subject of discussion, the location of shear center of the cross section is of importance. Its location is determined in a manner similar to the location of the center of gravity of the section. The only difference is that instead of dealing with the areas of the segments, we use their moments of inertia.

If an axial force is applied to the center of area, only axial deformations and stresses will occur. If, however, the axial force is applied through a point other than the center of gravity, bending about the transverse axes, and possibly warping, can also occur. Neglecting the web, the position of the center of gravity also called the center of area is given by

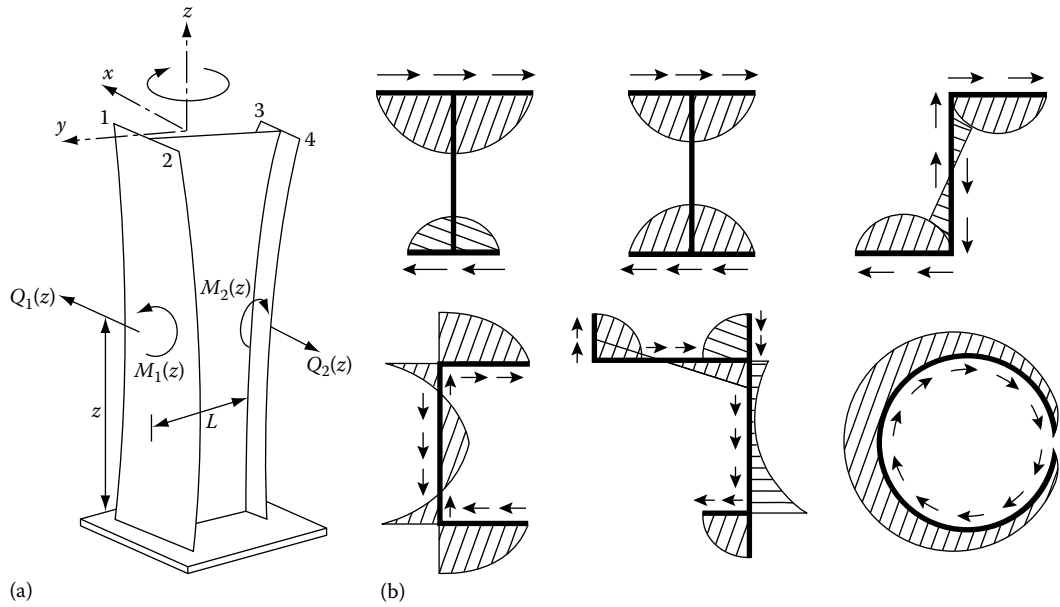
$$\bar{y}_1 = \frac{A_2 L}{A_1 + A_2} \quad \text{and} \quad \bar{y}_2 = \frac{A_1 L}{A_1 + A_2}$$

The location of center of gravity is important in relation to vertical axial forces. The shear center  $s$  on the other hand is important in relation to transverse forces. If a transverse force acts through  $s$ , the member will only bend. If, however, a transverse force acts elsewhere than through  $s$ , the member will twist and warp as well as bend. The shear center in this case is located along the  $y$ -axis by

$$y_1 = \frac{I_2}{I_1 + I_2} L \quad \text{and} \quad y_2 = \frac{I_1}{I_1 + I_2} L \quad (9.1)$$

An inspection of the equations above, indicates that the center of the area and the shear center generally will not coincide unless the section is doubly symmetric, in which case both points lie at the center of symmetry.

When a torque  $T$  is applied to the top of the member shown in Figure 9.58a, it twists about the shear center axis causing the flanges to (1) bend in opposite directions about the  $y$ -axis; and (2) twist about their vertical axes. The effect of the flange bending is to cause the flange sections to rotate in opposite direction about their  $y$ -axes so that initially plane sections through the member become nonplanar or warped. Diagonally opposite corners 1 and 4, in Figure 9.55a displace downwards while 2 and 3 displace upward. At any level  $z$  up the height of the core, the torque  $T = T_z$  is resisted internally by a couple  $T_w(z)$  resulting from the shears in the flanges and associated with their inplane



**FIGURE 9.58** (a) Bending of flanges due to torque. (b) Shear forces due to warping torsion.

bending, and a couple  $T_v(z)$  resulting from shear stresses circulating within the section and associated with the twisting of the flanges and the web. Then

$$T_w(z) + T_v(z) = T_z \quad (9.2)$$

The rotation of the member about its shear center axis at a height  $z$  from the base is  $\theta_z$ , hence the horizontal displacement of flange #1 at that level is

$$X_1(z) = y_1 \theta_z \quad (9.3)$$

and its derivatives are

$$\begin{aligned} \frac{dx_1}{dz}(z) &= y_1 \frac{d\theta}{dz}(z) \\ \frac{d^2x_1}{dz^2}(z) &= y_1 \frac{d^2\theta}{dz^2}(z) \\ \frac{d^3x_1}{dz^3}(z) &= y_1 \frac{d^3\theta}{dz^3}(z) \end{aligned} \quad (9.4)$$

Similar expressions may be written for flange #2.

The shear associated with the bending in flanges #1 and #2 can be expressed by

$$Q_1(z) = -EI_1 \frac{d^3x}{dz^3}(z) = -EI_1 y_1 \frac{d^3\theta}{dz^3}(z) \quad (9.5)$$

and

$$Q_2(z) = -EI_2 \frac{d^3x}{dz^3}(z) = -EI_2 y_2 \frac{d^3\theta}{dz^3}(z) \quad (9.6)$$



Multiplying the shear forces  $Q_1$  and  $Q_2$  by their respective distances from the shear center, we obtain the torque resisted by these factors. Therefore, the torque contributed by these shear forces is

$$\begin{aligned} T_w(z) &= Q_1 y_2 + Q_2 y_1 \\ &= -(EI_1 y_1^2 + EI_2 y_2^2) \frac{d^3 \theta}{dz^3}(z) \end{aligned} \quad (9.7)$$

or

$$T_w(z) = -EI_w \frac{d^3 \theta}{dz^3}(z) \quad (9.8)$$

where

$$I_w = I_1 y_1^2 + I_2 y_2^2 \quad (9.9)$$

$I_w$  is a geometric property of the section similar to the moments of inertia  $I_x$  and  $I_y$ , and is called the warping moment of inertia or warping constant. It expresses the capacity of the section to resist warping torsion. Neglecting the web, the torque resisted by the twisting of the section is

$$T_v(z) = GJ_1 \frac{d\theta}{dz}(z) \quad (9.10)$$

where  $J_1$  is the torsion constant of the section given by

$$J_1 = \frac{b_1 t_1^3}{3} + \frac{b_2 t_2^3}{3} \quad (9.11)$$

in which  $b_1$  and  $b_2$  are the widths, and  $t_1$  and  $t_2$  are the thickness, of flanges #1, #2, respectively.

Summing the two internal torques, Equations 9.7 and 9.11, and equating the sum to external torques as in Equation 9.1

$$-EI_w \frac{d^3 \theta}{dz^3}(z) + GJ_1 \frac{d\theta}{dz}(z) = T \quad (9.12)$$

Equation 9.12 is the fundamental equation for restrained warping torsion. It simply states that an external torque applied to an open core is resisted by a combination of internal torque due to St. Venant shear stresses and a couple due to equal and opposite shear forces in the flanges. The distribution of shear forces due to torsion in typical shear wall profiles is shown in Figure 9.58b.

Considering the stresses in the flanges due to bending, the compressive stress in flange #1 at  $c_1$  from the  $y$ -axis and  $z$  from the base is

$$\sigma_1(c_1, z) = \frac{M_1(z)c_1}{I_1} \quad (9.13)$$

The tensile stress in flange #2 at  $c_2$  from the  $y$ -axis is

$$\sigma_2(c_2, z) = \frac{M_2(z)c_2}{I_2} \quad (9.14)$$

Multiplying the right-hand side of Equation 9.5.6, by the expression

$$\frac{L}{(y_1 + y_2)} \frac{y_1}{y_1}$$

which is equal to unity, and since  $Q_1 = Q_2$  and the flange moments  $M_1 = M_2 = M$ , the equation becomes

$$\sigma_1(c_1, z) = \frac{M_{(z)} L y_1 c_1}{I_1 y_1^2 + I_1 y_1 y_2} \quad (9.15)$$

and since, from Equation 9.1

$$I_1 y_1 y_2 = I_2 y_2^2 \quad (9.16)$$

Substituting Equation 9.16 in Equation 9.15

$$\sigma_1(c_1, z) = \frac{M_{(z)} L y_1 c_1}{I_1 y_1^2 + I_2 y_2^2} \quad (9.17)$$

or

$$\sigma_1(c_1, z) = \frac{M_{(z)} \omega(c_1)}{I_\omega} \quad (9.18)$$

in which  $B(z) = M(z)L$  is an action termed a bimoment, and  $\omega_c = y_1 c_1$ , a coordinate termed the sectorial area, or principal sectorial ordinate, for that point of the section. In its simplest form, as considered here, a bimoment consists of a pair of equal and opposite couples acting in parallel planes. Its magnitude is the product of the couple and the perpendicular distance between the planes.

The above simple treatment of torsion of an I section explains the concept of warping and how the equations of torsion bending, also called restrained warping, are related to simple bending theory. The analogy is perhaps even more obvious by comparing the terms given in Table 9.4.

### 9.5.3 SECTORIAL COORDINATE $\omega'$

The sectorial coordinate, also called the warping function at a point on the profile of a warping core is the parameter that expresses the axial response (i.e., displacement, strain, and stress) at that point, relative to the response at other points around the section. Conceptually this is similar to the distance  $c$  we use in bending formula  $f = M_c/I$  to find the bending stress  $f$  at a point in the cross section located at a distance  $c$  from the neutral axis.

The warping coordinate is defined in relation to two points: a pole  $O'$  at an arbitrary position in the plane of the section, and an origin  $P_o$  at an arbitrary location on the profile of the section (Figure 9.59a and b). The value of the sectorial coordinate at any point  $P$  on the profile is then given by the area

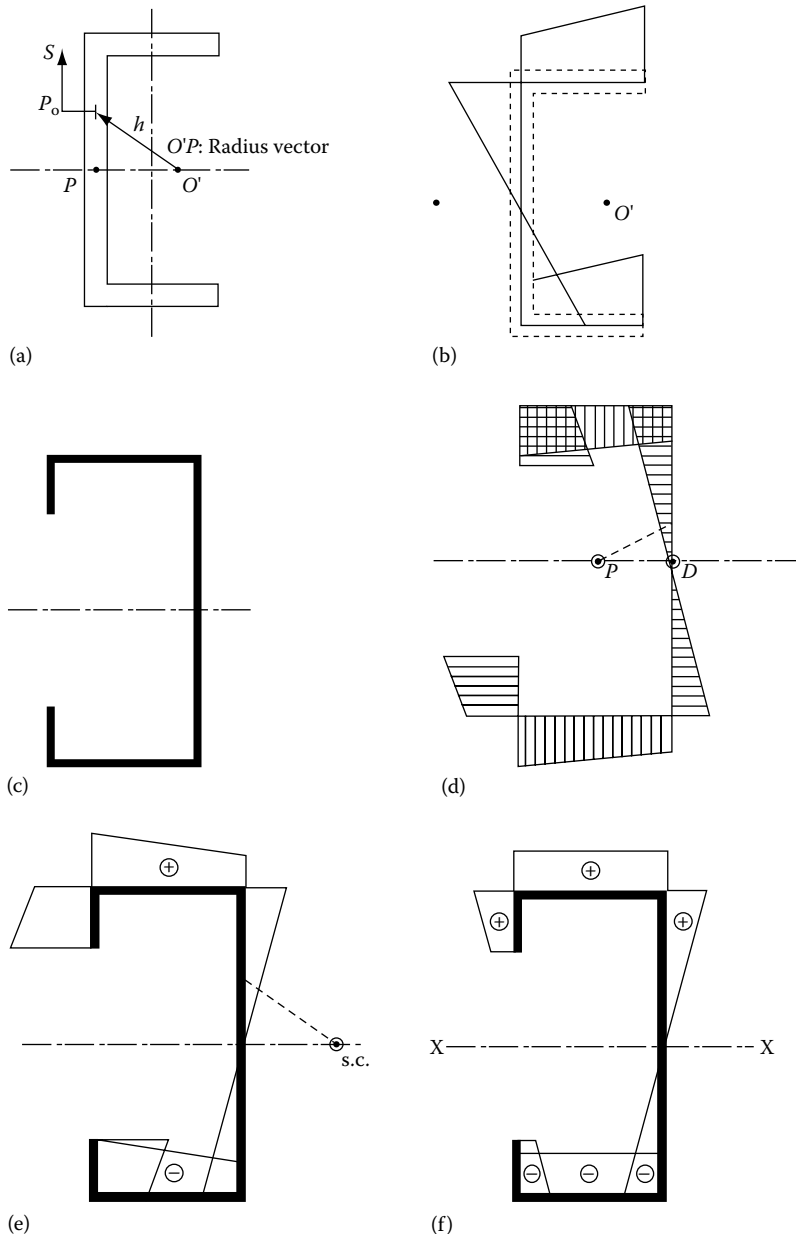
$$\omega'_{(s)} = \int_0^s h \, ds \quad (9.19)$$

where

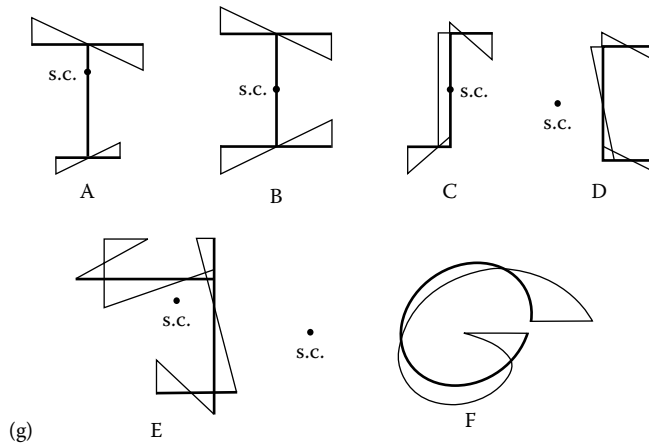
- $h$  is the perpendicular distance from the pole  $O'$  to the tangent to the profile at  $P$
- $s$  is the distance of  $P$  along the profile  $P_o$

It is evident that the warping function is an area and its magnitude depends on the location of the pole and the point in the profile from which the integration is started.

In effect, the sectorial coordinate  $\omega'$  is equal to twice the area swept out by the radius vector  $O'P$  in moving from  $P_0$  to  $P$ . The sectorial coordinate diagram (Figure 9.59b) indicates the values of  $\omega'$  around the profile. When the sectorial coordinates are related to the shear center as a pole and to the origin of known zero warping displacement, Equation 9.16 gives the principal sectorial coordinate values,  $\omega$  and their plot is the principal sectorial coordinate diagram. The principal sectorial coordinate of a section in warping theory is analogous to the distance  $c$  of a point from the neutral axis of a section in bending. The parameters  $\omega$  and  $c$  are used in



**FIGURE 9.59** (a) Section profile, (b) sectorial coordinate  $\omega_s$  diagram, (c) singly symmetric curve, (d)  $\omega_s$  diagram, (e)  $y$ -coordinate diagram, (f) principal sectorial coordinates,



**FIGURE 9.59 (continued)** and (g) sectorial coordinates for common profiles.

developing the corresponding warping and bending stiffness properties of the sections, and in determining the axial displacements and stresses. Sectorial coordinates for common profiles are shown in Figure 9.59g.

#### 9.5.4 SHEAR CENTER

The shear center of a section is a point in its plane through which a load transverse to the section must pass to avoid causing torque and twist. It is also the point in which warping properties of a section are related, in the way that bending properties of a section are related to the neutral axis.

Tall building cores are often singly or doubly symmetric in plan, which simplifies the location of the shear center. In doubly symmetric sections, the shear center lies at the center of symmetry while, in singly symmetric sections, it lies on the axis of symmetry.

The procedure for determining the location of shear for a singly symmetric section (Figure 9.59c) is as follows.

1. Construct the  $\omega_p$  diagram (Figure 9.59d) by taking an arbitrary pole  $P$  on the line of symmetry, an origin  $D$  where the line of symmetry intersects the section, and by sweeping the ray  $PD$  around the profile.
2. Using the  $\omega_p$  and the  $y$  diagrams for the section, Figure. 9.59d and e, respectively, calculate the product of inertia of the  $\omega_p$  diagram about the  $x$ -axis  $I_{\omega_p x}$  using

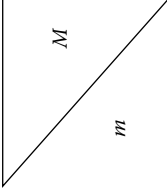
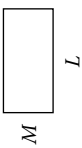
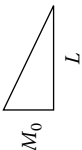
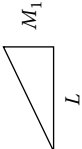

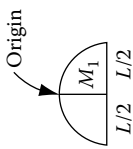
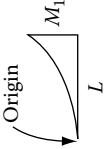
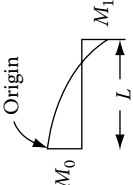
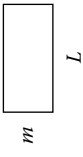



$$I_{\omega_p x} = \int_A \omega_p y dA \quad (9.20)$$

in which  $dA = t ds$ , the area of the segment of the profile of thickness  $t$  and lengths  $ds$ . The integral in Equation 9.5.6 may be evaluated simply by using the product integral table (Table 9.5).

3. Calculate  $I_{xx}$ , the second moment of area of the section about the axis of symmetry.
4. Finally, calculate the distance  $\alpha_x$  of the shear center  $O$  from  $O'$ , along the axis of symmetry, using

$$\alpha_x = \frac{I_{\omega_p x}}{I_{xx}} \quad (9.21)$$

TABLE 9.5  
Product Integral Tables

		Linear $M$ diagrams				Parabolic $M$ diagrams		
								
	$mML$	$\frac{1}{2} m_0 ML$	$\frac{1}{2} m M_1 L$	$\frac{1}{2} mL(M_0 + M_1)$	$\frac{2}{3} m M_1 L$	$\frac{1}{3} m M_1 L$	$\frac{1}{3} mL(2M_0 - M_1)$	
	$\frac{1}{2} m_0 ML$	$\frac{1}{3} m_0 M_0 L$	$\frac{1}{6} m_0 M_1 L$	$\frac{1}{6} m_0 L(2M_0 + M_1)$	$\frac{1}{3} m_0 M_1 L$	$\frac{1}{12} m_0 M_1 L$	$\frac{1}{12} m_0 L(5M_0 - M_1)$	
	$\frac{1}{2} m_1 ML$	$\frac{1}{6} m_1 M_0 L$	$\frac{1}{3} m_1 M_1 L$	$\frac{1}{6} m_1 L(2M_1 + M_0)$	$\frac{1}{3} m_1 M_1 L$	$\frac{1}{4} m_1 M_1 L$	$\frac{1}{4} m_1 L(M_0 - M_1)$	
	$\frac{1}{2} ML(m_0 + m_1)$	$\frac{1}{6} M_0 L(2m_0 + m_1)$	$\frac{1}{6} M_1 L(m_0 + 2m_1)$	$\frac{L}{6} m_0(2M_0 + 2M_1) + m_1(2M_0 + M_1)$	$\frac{1}{3} M_1 L(m_0 + m_1)$	$\frac{1}{12} M_1 L(m_0 + 3m_1)$	$\frac{L}{12} (m_0(5M_0 - M_1) + 3m_1(M_0 - M_1))$	

### 9.5.4.1 Evaluation of Product Integrals

When evaluating the integrals in Equation 9.9, we usually are dealing with members for which the material properties and cross-sectional dimensions are constant from one end of the member to the other. The integrals are in the form of a product such as

$$\int_0^{\ell} M m d_x \quad (9.22)$$

These product integrals must be evaluated over the length of each member and then added for all members. For any particular member, each quantity (such as  $m$  or  $M$ ) is a function of the distance  $x$  measured along the axis of the member; specifically, the quantity may be constant along the length, may vary linearly along the length, or may be a function of higher order, such as quadratic or cubic. To save time when performing calculations, these product integrals can be evaluated in advance and the results tabulated for ready use. A compilation of product integrals, covering the most commonly encountered functions, is given in Table 9.5. The table is presented in terms of the functions  $M$  and  $m$ , but it is apparent that these functions can be replaced by others, such as  $\omega_p$  and  $y$ . Illustrations of the use of the table are given in some of the examples.

### 9.5.5 PRINCIPAL SECTORIAL COORDINATE $\omega_s$ DIAGRAM

The  $\omega$  diagram is related to the shear center  $O$  as its pole and a point of zero warping deflection as its origin. In a symmetrical section the intersection of the axis of symmetry with the profile at  $D$  defines a point of antisymmetrical behavior, and hence of zero warping; therefore, it may be used as the origin.

Values of  $\omega$  can be found by sweeping the ray  $OD$  around the profile and taking twice the values of the swept areas.

For the section of Figure 9.59c, the principal sectorial coordinate diagram is shown in Figure 9.59f.

#### 9.5.5.1 Sectorial Moment of Inertia $I_\omega$

This geometric parameter expresses the warping torsional resistance of the core's sectional shape. It is analogous to the moment of inertia in bending.

The sectorial moment of inertia is derived from the principal sectorial coordinate distribution using the relation

$$I_\omega = \int_0^A \omega^2 dA$$

Note the similarity with the expression for the moment of inertia

$$I_{yy} = \int_0^A x^2 dA$$

### 9.5.6 TORSION CONSTANT $J$

When a beam is twisted its fibers must undergo a shear strain to accommodate the twist. Associated with the strain are the shear stresses called St. Venant shear stresses. When an open-section core is subjected to torque (Figure 9.59a), each wall twists developing St. Venant shear stresses within the thickness of the wall. The stresses are distributed linearly across the thickness of the wall, acting in opposite directions on opposite sides of the wall's middle line. As the effective lever arm of these

stresses is equal to only two-thirds of the wall thickness, the torsional resistance of these stresses is low. The torsion constant for this plate-twisting action is

$$J = \frac{1}{3} k \sum^n b t^3 \quad (9.23)$$

in which  $b$  is the width and  $t$  is the thickness of a wall. The summation includes the  $n$  walls that comprise the section. The plate-twisting rigidity of an open section core is given by  $GJ$ .

$k$  is a factor which makes allowance for small fillets within the cross section. If there are no fillets its value is equal to 1.00.

### 9.5.7 CALCULATION OF SECTORIAL PROPERTIES: WORKED EXAMPLE

Consider again the shear core with unequal flanges, as shown in Figure 9.60. To determine the core, the following is required:

1. The location of the shear center
2. The principal sectorial coordinate,  $\omega_s$  diagram
3. The sectorial moment of inertia  $I_\omega$
4. The St. Venant torsion constant  $J$

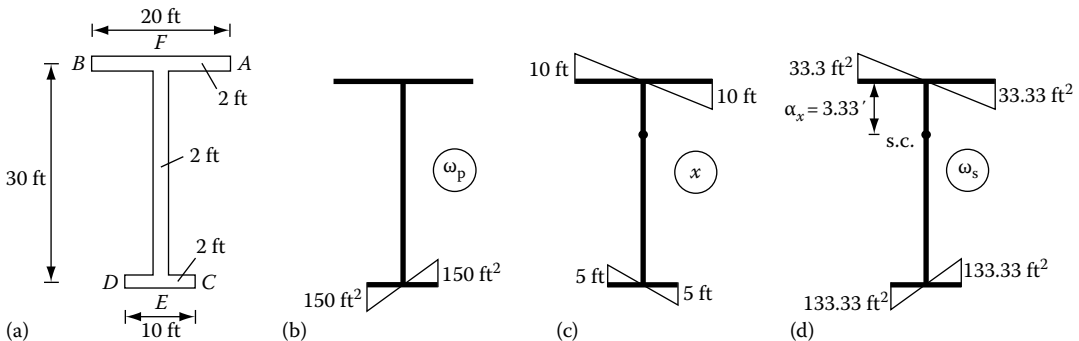
#### 1. Location of shear center

The axis of symmetry of the section is  $OY$ , therefore the shear center lies on the  $OY$  axis. We select an arbitrary pole  $P$  at the junction of the web and the upper flange of the core. The  $\omega_p$  diagram is constructed, as shown in Figure 9.60 by taking an arbitrary point on the web as the sectorial origin. The sectorial areas for the section of the upper flange and the web are equal to zero while they are distributed skew symmetrically for the lower flange.

Using the  $\omega_p$  and the  $Y$  coordinate diagrams, Figure 9.60b and c, we calculate the integral  $\omega_p dA$  by using the product integrals given in Table 9.5.

A summary of the calculations is given in Table 9.6. For the whole section,  $I_{\omega_p} = 2500 \times 2 = 5000 \text{ ft}^5$ . The moment of inertia of the section about  $y$ -axis is

$$I_{yy} = \frac{1}{12} (2 \times 10^3 + 2 \times 20^3) = 1500 \text{ ft}^4$$



**FIGURE 9.60** Calculation of sectorial properties: (a) cross section, (b)  $\omega_p$  diagram, (c)  $x$ -coordinate diagram, and (d) principal sectorial coordinate  $\omega_s$  diagram.

**TABLE 9.6**  
**Calculations for Integral  $\omega_\rho$  dA**

Segment	$\omega_\rho$	$x$	$\int_0^s \omega_\rho x \, t \, ds$
DE			$\frac{1}{3} \times 5 \times 150 \times 5 \times 2 = 2500 \text{ ft}^5$
EC			$\frac{1}{3} \times 5 \times 150 \times 5 \times 2 = 2500 \text{ ft}^5$
AF	0		0
BF	0		0

From Equation 9.5.10, the distance of the shear center from the center of web is

$$\alpha_x = \frac{I_{\omega_p x}}{I_{yy}} = \frac{5000 \text{ ft}^5}{1500 \text{ ft}^4} = 3.33 \text{ ft}$$

**2. Principal sectorial coordinate diagram**

This is constructed by using the shear center (s.c.) as the pole and sweeping the ray from the middle of the web, around the profile (Figure 9.60d).

**3. Sectorial moment of inertia  $I_\omega$**

From Equation 9.5.10

$$I_\omega = \int \omega^2 dA = \int \omega^2 t \, ds$$

Using the  $\omega$  diagram (Figure 9.60) and the product integral table (Table 9.5), the calculations for evaluating  $I_\omega$  are as shown in Table 9.7.

$I_\omega$  for the whole section  $59,260 \times 2 + 7406 \times 2 = 133,332 \text{ ft}^6$ .

**4. Torsion constant  $J$**

For the I-section core, using Equation 10.43

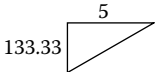
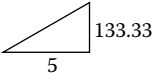
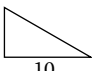
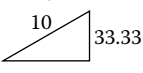
$$J = \frac{1}{3} \sum^n b t^3 = \frac{1}{3} \times 2^3 (20 + 10 + 30) = 160 \text{ ft}^4$$

**9.5.8 GENERAL THEORY OF WARPING TORSION**

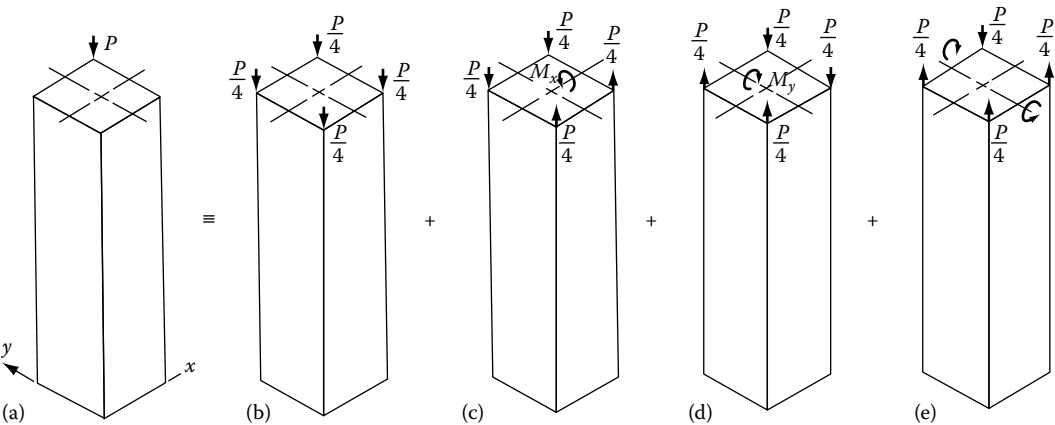
Before derivation of general warping torsion equations, it is instructive to consider qualitatively the difference between the behavior of thin-walled open sections and solid sections. A major difference lies in the manner in which the stresses attenuate along their length. Consider a square cantilever column loaded at the top corner by a vertical load  $P$ , as shown in Figure 9.61. The load



**TABLE 9.7**  
**Calculations for Sectorial Moment of Inertia**

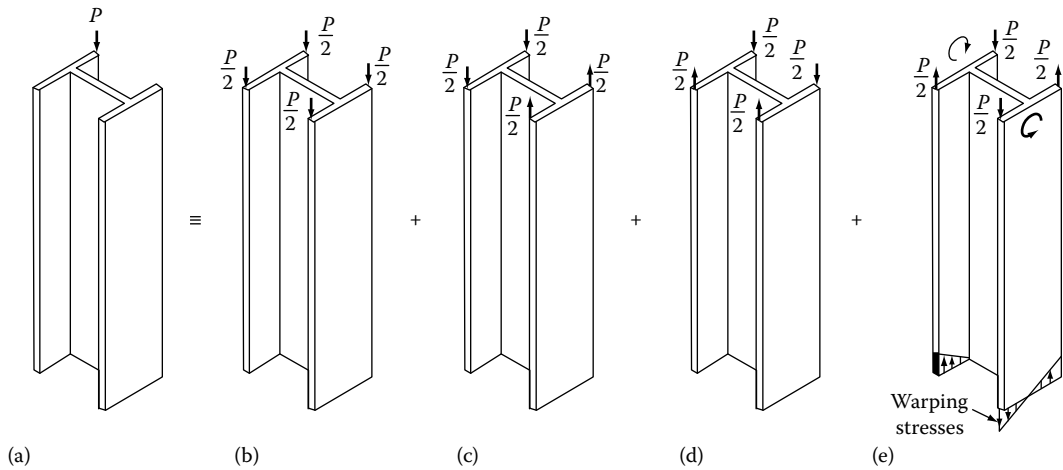
Segment	Variation of $\omega$	$\int \omega^2 t \, ds$
DE		$\frac{1}{3} \times 5 \times 133.33^2 \times 2 = 59,260 \text{ ft}^6$
EC		$\frac{1}{3} \times 5 \times 133.33^2 \times 2 = 59,260 \text{ ft}^6$
BF		$\frac{1}{3} \times 10 \times 33.33^2 \times 2 = 7,406 \text{ ft}^6$
AF		$\frac{1}{3} \times 10 \times 33.33^2 \times 2 = 7,406 \text{ ft}^6$

Note: Therefore  $I_\omega$  for the whole section  $59,260 \times 2 + 7,406 \times 2 = 133,332 \text{ ft}^6$ .



**FIGURE 9.61** Cantilever column of solid section: (a) vertical load at corner, (b) symmetrical axial loading, (c) bending about  $x$ -axis, (d) bending about  $y$ -axis, and (e) self-equilibrating loading producing bimoment.

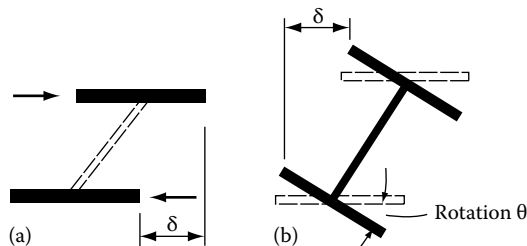
can be replaced by four sets of loads acting at each corner, which together constitute a system of loads statically equivalent to the applied force  $P$ . The first set represents axial loading, the second and third sets represent bending about the  $x$ - and  $y$ -axes. The resulting axial and bending stresses can be computed by the usual ETB, which assumes that Bernoulli's hypothesis is valid. In the last loading case, the cross sections do not remain plane because the two pairs of loads on opposite faces of the column tend to twist the cross section in opposing directions. This equal and opposite twisting results in warping of the cross section. The last set of loads is, however, statically equivalent to zero and can be ignored by invoking St. Venant's principle, which states that the perturbations imposed on a structure by a set of self-equilibrating system of forces affect the structure locally and will not appreciably affect parts of the structure simply means that the effect of self-equilibrating system of forces can be neglected in the analysis. The stresses caused by these forces equal to the characteristic dimension of the cross section. The stresses due to the self-equilibrating system of forces can be ignored throughout the whole length of the cantilever except at the very top region.



**FIGURE 9.62** I-shaped cantilever beam: (a) vertical load at a corner, (b) symmetrical axial loading, (c) bending about  $x$ -axis, (d) bending about  $y$ -axis, and (e) self-equilibrating loading producing bimoment.

Now consider an I-shaped shear wall, as shown in Figure 9.62, which has the same overall dimensions as the column with the exception that it is composed of thin plates of thickness  $t$ . The first three sets of loads result in stress distributions which can be obtained as before by using the Bernoulli hypothesis. Although the fourth loading is self-equilibrating as before, its effect is far from local. The flanges, which are bending in opposite directions, do so as though they were independent of each other. The web acts as a decoupler separating the self-equilibrating load into two subsets, one in each flange. Each subset is not self-equilibrating and causes bending in each flange. The bending action of the flanges can be thought of as being brought about by equal and opposite horizontal forces parallel to the flanges. The compatibility condition between the web and flanges results in a twisting of the cross section, as shown in Figure 9.63. Although the cross section of each of the flanges remains plane, the wall as a whole is subjected to warping deformations. The restraint at the foundation prevents free warping at this end and sets up warping stresses.

The system of skew-symmetric loads, which is equivalent to an internally balanced force system arising out of warping of cross section is termed a bimoment in thin-walled beam theory. Mathematically it can be construed as a generalized force corresponding to the warping displacement, just as moment and torsion are associated with rotation and twisting deformation, respectively. In the present example, bimoment can be visualized as a pair of equal and opposite moments acting at a distance  $e$  from each other. Its magnitude is equal to  $M$  times  $e$  and has units of force times the square of the distance ( $\text{lb} \cdot \text{in}^2$ ,  $\text{kip} \cdot \text{ft}^2$ , etc.).



**FIGURE 9.63** Plan section of I-shaped column: (a) displacement of flanges due to bimoment load and (b) rotation due to geometric compatibility between flanges and web.

Presently it will be shown that the warping stresses can be calculated by the relation

$$\sigma_{\omega} = \frac{B_{\omega} \omega_s}{I_{\omega}} \quad (9.24)$$

where

$B_{\omega}$  is the bimoment, a term that represents the action of a set of self-equilibrating forces

$\omega_s$  is the warping function

$I_{\omega}$  is the warping moment of inertia

The three terms  $B_{\omega}$ ,  $\omega_s$ , and  $I_{\omega}$  are conceptually equivalent to moment  $M$ , linear coordinate or  $x$  or  $y$ , and moment of inertia  $I$  countered in bending problems. Note the similarity between the bending stress as calculated by the familiar relation  $\sigma_b = M_y/I$  and the warping stress formula given in Equation 9.24.

### 9.5.8.1 Warping Torsion Equations for Shear Wall Structures

Two basic equations applicable to a wide variety of complex-shaped shear walls may be derived using Vlasov's general theory of warping torsion. (See reference 63 for derivation of general equations). These equations given below define  $\theta_z$  and  $B_z$ , the rotation and bimoment at height  $z$  measured from the base of shear walls, typically the foundation level. In the derivation, it is assumed the shear wall is subjected to a uniform torsional moment equal to  $m$  (kip ft/ft).

$$\begin{aligned} \theta_z &= \frac{-m}{GJ \cosh k} \left[ \frac{-l^2}{k^2} - \frac{-l^2}{k} \sinh k + z(l - \frac{z}{2}) \cosh k \right. \\ &\quad \left. + \frac{-l^2}{k^2} \cosh \frac{k}{l} z + \frac{l^2}{k} \sinh \frac{k}{l} (l - z) \right] \\ B_z &= \frac{-ml^2}{k^2 \cosh k} \left[ \cosh k - \cosh \frac{k}{l} z - \frac{k \sinh k}{l} (l - z) \right] \end{aligned}$$

Using these equations, a back-of-the-envelope calculations may be performed to determine the rotation and axial stresses throughout the height of a shear wall subject to torsion. In particular, we are mostly interested in the maximum rotation at the top of building (at  $z = l$  where  $l$  is the height of building), and the maximum axial stresses at the base (where  $z = 0$ ). Substituting these two values in the above equations we get

$$\begin{aligned} \theta_l &= \frac{-ml^2}{GJ \cosh k} \left[ \frac{1}{k^2} - \frac{1}{k} \sinh k + \frac{1}{2} \cosh k + \frac{1}{k^2} \cosh k \right] \\ B_0 &= -\frac{ml^2}{k^2 \cosh k} [\cosh k - l - k \sinh k] \end{aligned}$$

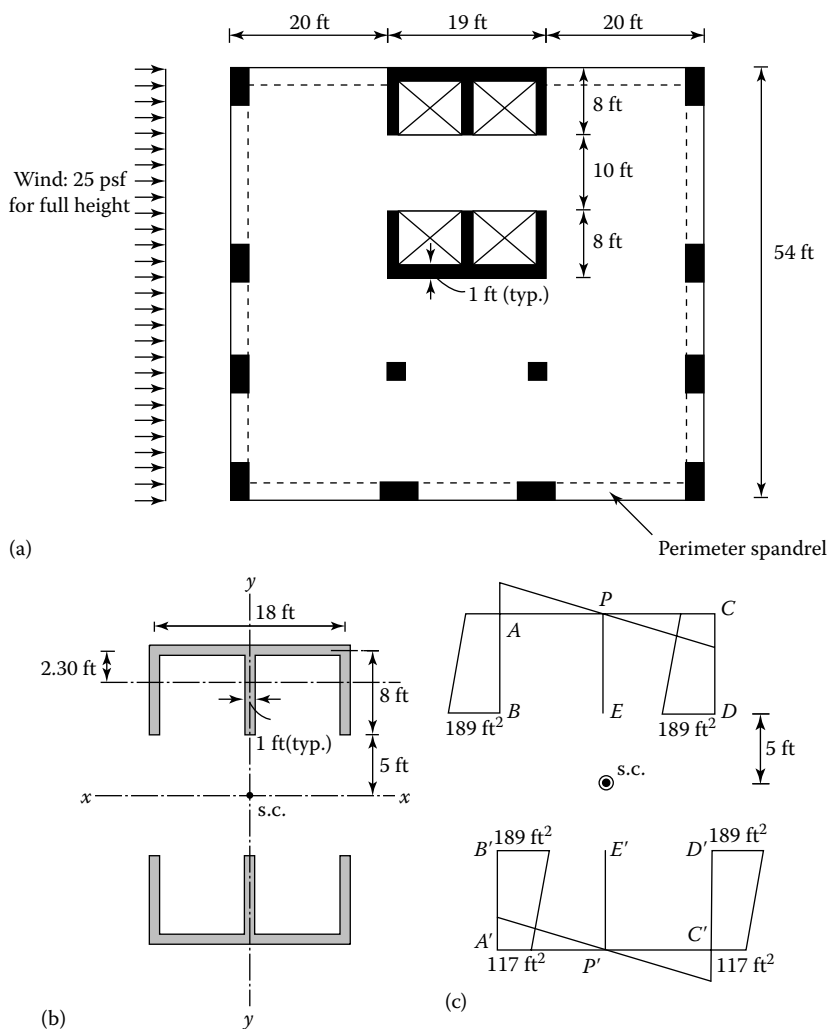
The following two examples illustrate the use of these equations in getting a tactile sense for the torsional behavior of practical shear wall structures.

### 9.5.9 TORSION ANALYSIS OF SHEAR WALL BUILDING: WORKED EXAMPLE

### Example 9.1

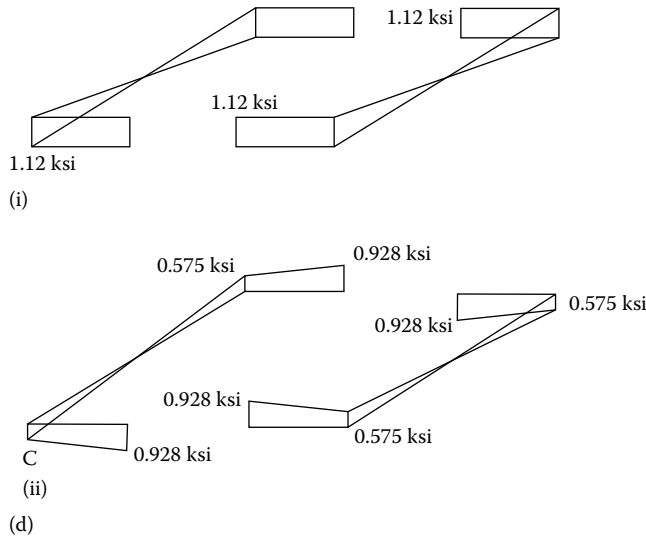
Consider a 25-story, 300 ft (91.44 m) building consisting of two cores as shown in Figure 9.64a and b. To keep the analysis simple, assume that the resistance to lateral loads and torque is provided solely by the core. The building is subjected to a uniform wind load of 25 psf (1.197 kN/m<sup>2</sup>) in the x-direction.

It is required to determine the maximum deflection and rotation at the top, and the vertical stresses at the base due to bending and twisting. An elastic modulus  $E = 3,600 \text{ ksi}$  ( $24,882 \text{ MPa}$ ) and a shear modulus  $G = 1,565 \text{ ksi}$  ( $10,791 \text{ MPa}$ ) are assumed for the concrete properties. The procedure is first described and then illustrated numerically.



**FIGURE 9.64** (a) Twin-core example. (b) Core properties. (c)  $\omega_s$  diagram (sectorial coordinates).

(continued)



**FIGURE 9.64 (continued)** (d) Comparison of stresses: (i) bending stress  $\sigma_b$  and (ii) warping stress  $\sigma_\omega$ .

The properties of the twin cores calculated from the given geometry are as follows.

$$\begin{aligned}
 \text{Area of two cores} &= 83.0 \text{ ft}^2 \\
 I_{xx} \text{ for both cores} &= 588.0 \text{ ft}^4 \\
 I_{yy} \text{ for both cores} &= 3577 \text{ ft}^4 \\
 GJ \text{ for both cores} &= 6,236,569 \text{ kft}^2 \\
 I_\omega &= 927,180 \text{ ft}^6
 \end{aligned}$$

$$k = 1 \sqrt{\frac{GJ}{EI_\omega}} = 1.08$$

$$G = \frac{E}{2(1+\mu)} = \frac{E}{2(1+0.15)} = \frac{E}{2.3}$$

(See Ref. [63] for detail calculations.)

**Step 1.** Determine the sectorial properties

For the given structure, by inspection, the location of shear center  $O$  is determined at a point midway between the two cores. The  $\omega$  diagram is related to the shear center  $O$  as its pole and a point of zero warping deflection as its origin. In a symmetrical section, as in the example problem, the intersection of the axis of symmetry with the profile at  $D$  defines a point of antisymmetrical behavior, and hence of zero warping deflection: therefore, it may be used as the origin.

Values of  $\omega$  are found from first principles, by sweeping the ray  $OD$  around the profile and taking twice the values of the swept areas. For the example problem, the principal sectorial coordinate diagram is shown in Figure 9.64c.

**Step 2.** Determine the sectorial moment of inertia  $I_\omega$  from the formula

$$I_\omega = \int_0^A \omega^2 dA = \int_0^s \omega^2 t ds$$

Using the  $\omega_s$  diagram (Figure 9.64c) and the product integral table (Table 9.5), the value for  $I_\omega$  is determined equal to 927,180 ft<sup>6</sup> (See Ref. [63] for details).

**Step 3.** Torsion constant  $J$  for the core is determined from Equation 9.23

For one core,  $J = 1/3 \sum bt^3 = 1/3 \times 1^3 (3 \times 7.5 + 1 \times 19) = 13.834 \text{ ft}^4$ , for two cores,  $J = 13.834 \times 2 = 27.671 \text{ ft}^4$ .

**Step 4.** Determine eccentricity  $e$  of the line of action of wind resultant for the shear center

The resultant wind force per unit height of the building is equal to  $25 \times 54 = 1.35 \text{ kip/ft}$  (1.83 kN/m) acting at 13.5 ft (4.12 m) to the south of shear center. Therefore the eccentricity,  $e$ , from the shear center is 13.5 ft (4.12 m). Since the external torque is the product of the horizontal loading and its eccentricity, the torsion due to wind is  $1.35 \times 13.5 = 18.225 \text{ k-ft/ft}$  (24.70 kNm) per unit height, anticlockwise.

**Step 5.** Determine the bending deflection at the top and stresses at the base of shear walls

A bending analysis is now performed to determine the maximum lateral deflection at the top and the bending stresses at the base. Deflection at the top due to bending is calculated as follows.

$$\Delta_{y(\max)} = \frac{wl^4}{8EI_{yy}} = 0.737 \text{ ft}$$

$$\begin{aligned} \text{Maximum bending stress} &= \frac{MC}{I} = \frac{60,750 \times 9.5}{13,577} \\ &= 161.34 \text{ ksf} \\ &= 1.12 \text{ ksi (16.78 MPa)} \end{aligned}$$

The bending stress diagram is shown in Figure 9.64d.

Note that the deflection and stresses calculated thus far, do not include torsion effects. These are calculated in steps 6 through 8.

**Step 6.** Determine the parameter  $k$  using the Equation

$$\begin{aligned} k &= l \sqrt{\frac{GJ}{EI_\omega}} \\ &= 300 \sqrt{\frac{1565 \times 144 \times 28}{927,180 \times 2.3}} \\ &= 1.08 \end{aligned}$$

**Step 7.** Determine the rotation and total deflection at the corner of the top floor

The rotation at any level of the building for a uniformly distributed torque “ $m$ ” may be obtained from Equation 9.25.

At the top,  $z = l$ . Substituting  $z = l$  in Equation 9.25 we get as before

$$\theta_l = \frac{-ml^2}{GJ \cosh k} \left[ -\frac{1}{k^2} - \frac{1}{k} \sinh k + \frac{1}{2} \cosh k + \frac{1}{k^2} \cosh k \right]$$

Substituting for the various parameters, we get  $\theta_H = 0.0196$  rad, anticlockwise. Therefore, the additional deflection at the southeast corner  $c$  of the top floor due to torsion is

$$\begin{aligned}\Delta_t &= \theta_H \times \text{distance of } c \text{ from shear center} \\ &= 0.196 \times 50.10 = 0.9821 \text{ ft (0.30 m)}\end{aligned}$$

The total deflection at  $c$  due to bending and torsion  $= \Delta_b + \Delta_t = 0.737 + 0.9821 = 1.72$  ft (0.52 m). This value represents 1/175 of the building height, an unacceptably large value, indicating serious deficiency in the lateral load resisting system.

**Step 8.** Determine bimoments and warping stresses

The warping stresses,  $\sigma_w$ , at the base are determined from the bimoment  $B$  at that level. The bimoment is obtained from a uniformly distributed torque from Equation 9.5.10. Then, at any point on the section where the principal sectorial coordinate is  $\omega_s$ , the vertical warping stress is obtained from Equation 9.5.9. The total axial stresses due to horizontal loading is obtained by combining the warping stresses with the bending stresses.

The vertical stresses at the base due to warping are determined from the bimoment at the base. The bimoment is given by Equation 9.26 repeated here for convenience

$$B_z = \frac{-ml^2}{k^2 \cosh k} \left[ \cosh k - \cosh \frac{k_z}{l} - k \sinh \frac{k}{l} (l - z) \right] \quad (9.25)$$

At the base

$$z = 0, \quad B_0 = -\frac{ml^2}{k^2 \cosh k} [\cosh k - 1 - k \sinh k] \quad (9.26)$$

$$k = 1.08, \quad \sinh k = 1.3025, \quad \cosh k = 1.642$$

$$\sinh 0 = 0, \quad \cosh 0 = 1$$

Substituting the above values

$$\begin{aligned}B_0 &= \frac{-ml^2}{1.08^2 \times 1.642} [1.642 - 1 - 1.08 \times 1.3025] \\ &= \frac{-ml^2}{2.504} \\ &= -\frac{18.225 \times 300^2}{2.504} \\ &= 656,100 \text{ kip/ft}^2\end{aligned}$$

Warping stresses are given by  $\omega = \frac{B_0 \times \omega_s}{I_\omega}$

At  $D$

$$\begin{aligned}\sigma_{\omega} &= \frac{656,100}{927,180} \times 189 \\ &= 133.74 \text{ ksf} \\ &= 0.928 \text{ ksi}\end{aligned}$$

At  $C$

$$\begin{aligned}\sigma_{\omega} &= \frac{656,100}{927,180} \times 117 \\ &= 82.79 \text{ ksf} \\ &= 0.575 \text{ ksi}\end{aligned}$$

Figure 9.64d shows a comparison of bending and warping stresses. The importance of warping torsion is obvious.

It was stated at the beginning of this section that warping torsion analysis is no more complicated than the Engineers Theory of Bending, ETB. Further, it was pointed out that by assuming the parameter  $k = 0$ , we can literally perform a five-minute back-of-the-envelope calculation to get a ball-park answer to torsional rotations and warping stresses of open-section shear walls. Let us put this statement to test by revisiting the twin-core problem.

The deflection at top of a cantilever subject to a uniform load of  $\omega$  is given by the well-known equation

$$\Delta_l = \frac{Wl^4}{8EI}$$

By assuming the parameter  $k = l \sqrt{\frac{GJ}{EI_{\omega}}} = 0$ , we can write a similar equation for torsional rotation at top as

$$\theta_l = \frac{ml^4}{8EI_{\omega}}$$

where

$m$  is the uniform torsional moment similar to uniform load  $\omega$

$I_{\omega}$  is the warping moment of inertia similar to moment of inertia  $I$

$$\begin{aligned}\text{For the twin-cores, the rotation } \theta_l \text{ is equal to } \frac{ml^4}{8EI_{\omega}} &= \frac{13.5 \times 300^4}{8 \times 518,400 \times 927,180} \\ &= 0.0285 \text{ rad}\end{aligned}$$

Comparing this to the more accurate value of 0.0196 radians calculated earlier, we observe that the back-of-the-envelope result is not bad after all.

We now turn our attention to the bimoment  $B_o$  which is similar to the flexural bending moment  $M_o$  for the cantilever. Again assuming  $k = 0$ , the equation for  $B_o$  simplifies to

$$B_o = \frac{ml^2}{2}$$



instead of  $B_o = \frac{ml^2}{2,504}$

calculated earlier by the more rigorous method.

This comparison clearly demonstrates the importance of the boment theory as a practical tool for verifying computer analysis of open-section shear walls.

### Example 9.2:

The warping theory described for the twin-core example can also be used to determine the bending stresses in, and torsional rotations of buildings consisting of, randomly distributed shear walls. To demonstrate the method, a 15-story building is analyzed for torsional rotation using the warping theory, and then compared with computer results. The example also illustrates the method for calculating bending stresses in shear walls.

Consider the building shown in Figure 9.65a, consisting of three walls,  $W_1$ ,  $W_2$ , and  $W_3$  in the transverse direction, and two walls  $W_4$  and  $W_5$  in the longitudinal direction. A uniform wind load of 25 psf (1.197 kN/m<sup>2</sup>) assumed for the full height results in a horizontal load equal to  $25 \times 70 = 1.75$  kip/ft (2.37 kN/m) acting at the center of gravity of the plan.

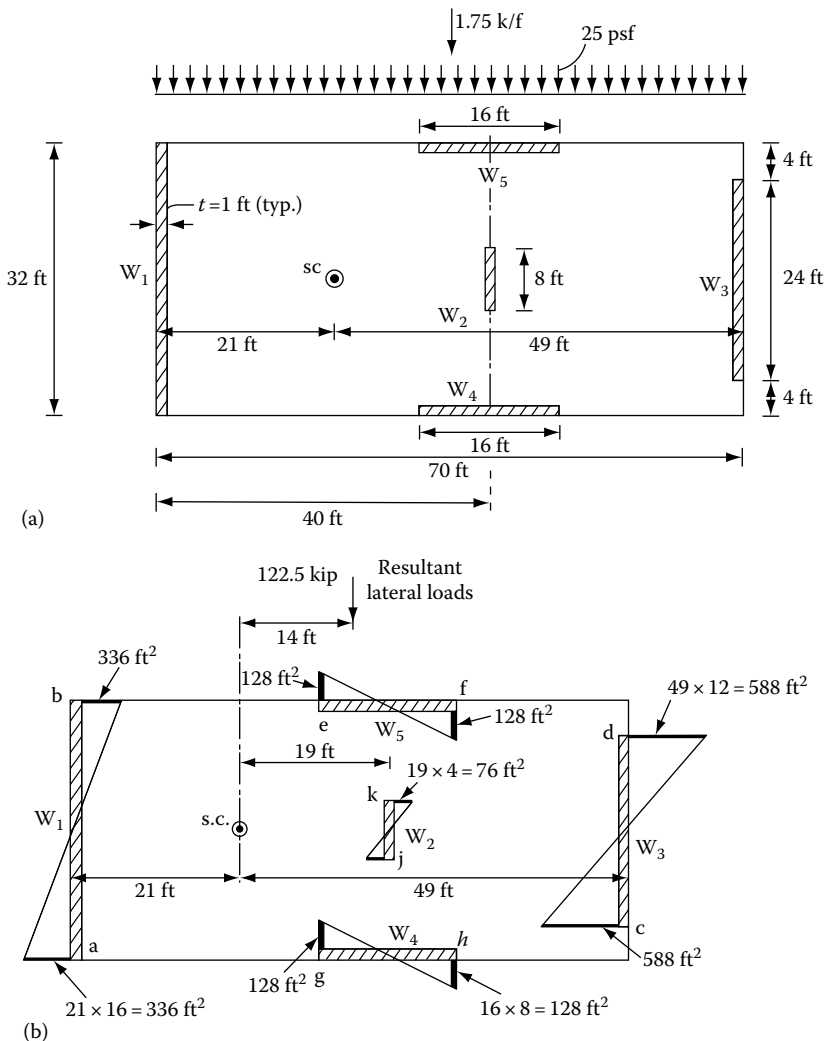


FIGURE 9.65 Torsion example; randomly distributed shear walls. (a) Plan. (b) Warping coordinates.

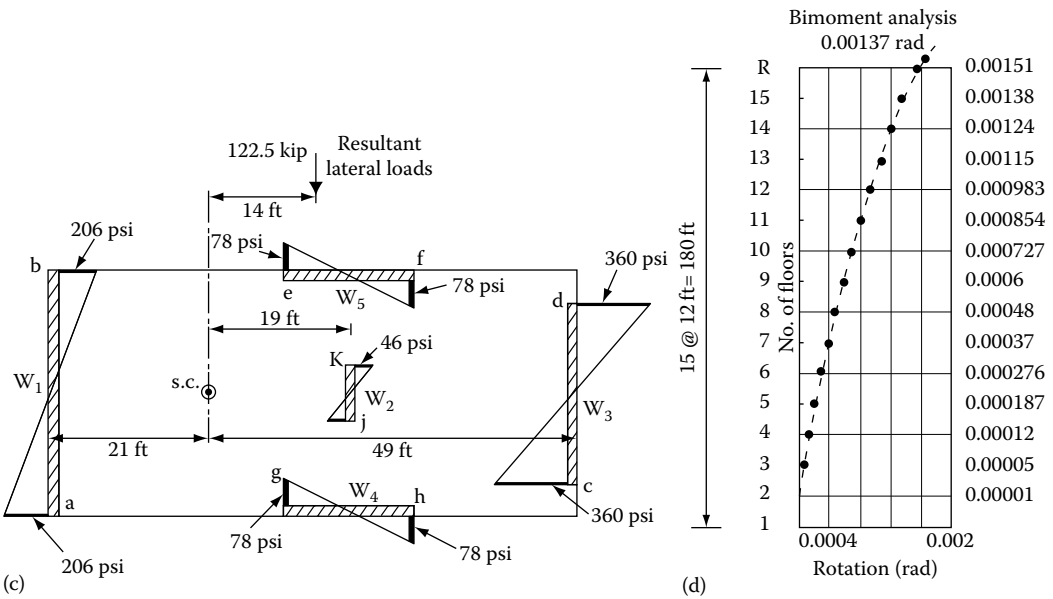


FIGURE 9.65 (continued) (c) Axial stresses due to torsion, and (d) Rotation comparison.

**Analysis outline:** By inspection, the location of the shear center (s.c.) of the building is judged to be midway between walls W<sub>4</sub> and W<sub>5</sub>. The distance  $\bar{x}$  of the shear center in the east–west direction from wall W<sub>1</sub>, is obtained from the relation

$$\bar{x} = \frac{\sum I_{xx} x}{\sum I_{xx}}$$

Next the eccentricity  $e$ , which is the distance from the line of action of the wind resultant to the shear center of the building, is determined to be 14 ft (4.27 m), as shown in the detail calculations. The resulting torque which is equal to the product of the wind load and eccentricity is calculated as  $1.75 \times 14 = 24.5$  kip/ft (10.12 kNm/m).

To keep the mathematics simple, we limit our analyses to the determination of bending stresses in the walls due to torsion only. We begin the analysis by considering the center of gravity of each wall as a point of zero warping deflection. These points are used as the origins for determining the values of the sectorial coordinate  $\omega$ . Next, we calculate the warping moment of inertia,  $I_{\omega}$ , of the shear wall assemblage and the bimoment,  $B_{\omega}$ , at the base. These are used to determine the bending stresses in each of the shear walls, as shown in the following calculations.

**Location of shear center:** By inspection, the location of s.c. is determined to be on the common neutral axis  $x$ – $x$ . Its distance from the centerline of wall W<sub>1</sub> in the  $x$ -direction is given by

$$\bar{x} = \frac{\sum I_x x}{\sum I_x}$$

Observe the similarity between this and the following equation

$$\bar{x} = \frac{\sum Ay}{\sum A}$$

which is well known for determining the location of neutral axis of built-up sections. Just as we use the areas of individual parts of a built-up section to find the neutral axis, we use the moments of inertia of individual walls to determine the location of the shear center of the building. The procedure is the same; select a reference axis ( $y$ - $y$ ), determine  $I_x$  for each shear wall (about its own neutral axis) and its distance  $x$  from the reference axis ( $y$ - $y$ ). The distance  $\bar{x}$  of the shear center of the entire group of shear walls from the reference axis is given by

$$\bar{x} = \frac{I_{x1}x_1 + I_{x2}x_2 + I_{x3}x_3 + I_{x4}x_4}{I_{x1} + I_{x2} + I_{x3} + I_{x4}}$$

or

$$\bar{x} = \frac{\sum I_x x}{\sum I_x}$$

The summation of the moment of inertia,  $\sum I_x$ , of the walls  $W_1$ ,  $W_2$ , and  $W_3$  is given by

$$\begin{aligned}\sum I_x &= 1 \times \frac{32^3}{12} = 1 \times \frac{8^3}{12} + 1 \times \frac{24^3}{12} \\ &= 2730.67 + 42.67 + 1152 \\ &= 3925.34 \text{ ft}^4\end{aligned}$$

$$\begin{aligned}x_1 &= \frac{\sum I_x x}{\sum I_x} \\ &= (2736.67 \times 0 + 42.67 \times 40 + 1152 \times 70) / 3925.24 \\ &= \frac{82,346.8}{3925.24} = 20.979 \text{ ft} \quad (\text{use } 21 \text{ ft})\end{aligned}$$

Verify location of s.c. from the center line of east wall  $W_3$ .

$$\begin{aligned}\bar{x}_2 &= (1152 \times 0 + 42.67 \times 30 + 2730.67 \times 70) / 3925.24 \\ &= \frac{192,427}{3925.24} = 49 \text{ ft} \quad \bar{x} + x_2 = 21 + 49 = 70 \text{ ft}\end{aligned}$$

The eccentricity  $e$  of the line of action of wind resultant from the shear center

$$e = 35 - 21 = 14 \text{ ft}$$

Torsional moment  $m$  per foot height of the building

$$m = 1.75 \times 14 = 24.5 \text{ kip-ft/f}$$

**Torsion properties:** As a first step, we calculate the warping moment of inertia for the entire building assuming the floor slabs are rigid. Using the centers of each wall as the principal poles, the sectorial coordinate diagram for the composite building is drawn by sweeping the radius vector passing through the shear center of the building and the principal poles of each wall. The resulting  $\omega_s$  diagram is shown in Figure 9.65b.

The warping moment of inertia is calculated as before by using the product integral table (see Table 9.5).

$$\begin{aligned} I_{\omega} &= \frac{2}{3} \times 16 \times 336^2 + \frac{2}{3} \times 4 \times 76^2 + \frac{2}{3} \times 12 \times 588^2 + \frac{2}{3} \times 8 \times 128^2 + \frac{2}{3} \times 8 \times 128^2 \\ &= 4,160,341 \text{ ft}^6 \end{aligned}$$

The St. Venant's torsion  $J$  is calculated from the relation

$$\begin{aligned} J &= \sum_{n=1}^n b t^3 \\ &= 1^3(32 + 8 + 24 + 16 + 16) \\ &= 96 \text{ ft}^4 \\ GJ &= 225,360 \times 96 \\ &= 216,345,600 \text{ kip/ft}^2 \\ k &= l \sqrt{\frac{GJ}{EI_{\omega}}}, \quad \frac{G}{E} = \frac{1}{2.3} \\ &= 180 \sqrt{\frac{96}{4,160,341 \times 2.3}} = 0.57 \end{aligned}$$

**Torsional rotation:** The rotation  $\theta_l$  at the top due to a uniformly distributed torque of  $m$  units per unit height is given by

$$\theta_l = \frac{-ml^2}{GJ \cosh k} \left[ \frac{\cosh k - 1}{k^2} + \frac{\cosh k}{2} - \frac{\sinh k}{k} \right]$$

Substituting

$$k = 0.57, \quad \sinh k = \sinh 0.57 = 0.601$$

$$\cosh k = \cosh 0.57 = 1.167, \quad GJ = 216,345,600 \text{ kip/ft}^2$$

and

$$m = 1.75 \times 14 = 24.5 \text{ k-f/f}$$

$$\theta_l = 0.00137 \text{ rad}$$

**Bending stresses due to torsion:** The bimoment  $B_o$  at the base is given by

$$B_o = -\frac{ml^2}{k^2 \cosh k} [\cosh k - 1 - k \sinh k]$$

Substituting

$$k = 0.57, \quad \sinh k = \sinh 0.57 = 0.601$$

$$\cosh k = \cosh 0.57 = 1.167, \quad m = 1.75(35 - 21) = 24.5 \text{ kip-ft/ft}$$

$$l = 15 \text{ stories @ } 12 \text{ ft} = 180 \text{ ft}$$

$$\begin{aligned} B_o &= -\frac{24.5 \times 180^2}{0.57^2 \times 1.167} [1.167 - 1 - 0.57 + 0.601] \\ &= 367,529 \text{ kip/ft}^2 \end{aligned}$$

The bending stresses,  $\sigma_\omega$ , in the walls due to torsion are calculated by the equation  $\sigma_\omega = \frac{B_o \omega_s}{I_\omega}$ , as shown below.

$$\begin{aligned} \text{Wall 1} \quad \sigma_\omega \text{ at } a, b &= \frac{367,529 \times 336}{4,160,341} \\ &= 29.68 \text{ kip/ft}^2 \\ &= 0.206 \text{ ksi} \end{aligned}$$

$$\begin{aligned} \text{Wall 3} \quad \sigma_\omega \text{ at } a, b &= \frac{367,529 \times 588}{4,160,341} \\ &= 51.941 \text{ kip/ft}^2 \\ &= 0.360 \text{ ksi} \end{aligned}$$

$$\begin{aligned} \text{Wall 5} \quad \sigma_\omega \text{ at } a, b &= \frac{367,529 \times 128}{4,160,341} \\ &= 11.30 \text{ kip/ft}^2 \\ &= 0.078 \text{ ksi} \end{aligned}$$

$$\text{Wall 4} \quad \sigma_\omega \text{ at } g, h \text{—similar to wall 5 at } e, f.$$

$$\begin{aligned} \text{Wall 2} \quad \sigma_\omega \text{ at } a, b &= \frac{367,529 \times 76}{4,160,341} \\ &= 6.71 \text{ kip/ft}^2 \\ &= 0.046 \text{ ksi} \end{aligned}$$

The calculated stresses and a comparison of torsional rotations are shown in Figure 9.61.

### 9.5.10 WARPING TORSION CONSTANTS FOR OPEN SECTIONS

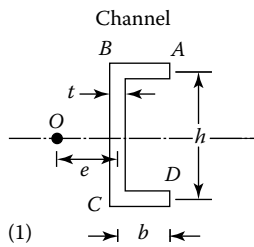
It is perhaps evident by now that although the concept of warping torsion is easy to assimilate, the calculation of sectorial properties are rather tedious. To alleviate this problem, formulas for the sectorial properties of open sections commonly used in shear wall structures are given in Table 9.8.

Let us verify the value of  $I_\omega$  derived previously for the unsymmetrical I-section (Figure 9.60) by using the formula given in the table (cross-section reference no. 7 in Table 9.8).

**TABLE 9.8**  
**Torsion Constants for Open Sections**

**Cross-Section Reference Number**

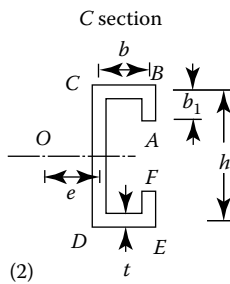
**Constants**



$$e = \frac{3b^2}{h + 6b}$$

$$J = \frac{t^3}{3}(h + 2b)$$

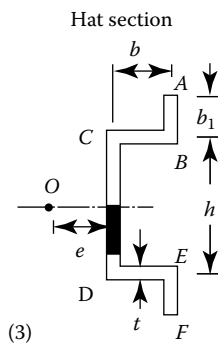
$$I_\omega = \frac{h^2 b^2 t}{12} \frac{2h + 3b}{h + 6b}$$



$$e = b \frac{3h^2 b + 6h^2 b_1 - 8b_1^2}{h^2 + 6h^2 b + 6h^2 b_1 + 8b_1^3 - 12hb_1^2}$$

$$J = \frac{t^3}{3}(h + 2b + 2b_1)$$

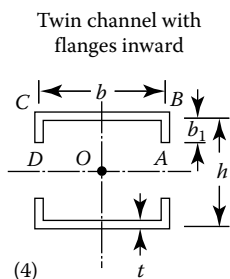
$$I_\omega = I \left[ \frac{h^2 b^2}{2} \left( b_1 + \frac{b}{3} - e - \frac{2eb_1}{b} - \frac{2b_1^2}{h} \right) + \frac{h^2 c^2}{2} \left( b + b_1 + \frac{h}{6} + \frac{2b_1^2}{h} \right) + \frac{2b_1^2}{3} (b + e)^2 \right]$$



$$e = b \frac{3h^2 b + 6h^2 b_1 - 8b_1^2}{h^2 + 6h^2 b + 6h^2 b_1 + 8b_1^3 + 12hb_1^2}$$

$$J = \frac{t^2}{3}(h + 2b + 2b_1)$$

$$I_\omega = I \left[ \frac{h^2 b^2}{2} \left( b_1 + \frac{b}{3} - e - \frac{2eb_1}{b} - \frac{2b_1^2}{h} \right) + \frac{h^2 c^2}{2} \left( b + b_1 + \frac{h}{6} + \frac{2b_1^2}{h} \right) + \frac{2b_1^2}{3} (b + e)^2 \right]$$



$$J = \frac{t^2}{3}(2b + 4b_1)$$

$$I_\omega = \frac{tb^2}{24}(8b_1^2 + 6h^2 b_1 + h^2 b + 12b_1^2 h)$$

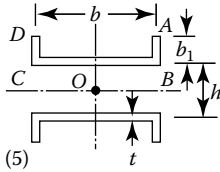
(continued)

**TABLE 9.8 (continued)**  
**Torsion Constants for Open Sections**

**Cross-Section Reference Number**

**Constants**

Twin channel with  
flanges outward

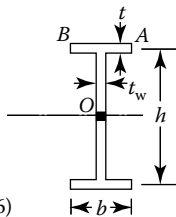


(5)

$$J = \frac{t^2}{3}(2h + 4b_1)$$

$$I_{\omega} = \frac{tb^2}{24}(8b_1^3 + 6h^2b_1 + h^2b - 12b_1^2h)$$

Wide flanged beam  
with equal flanges

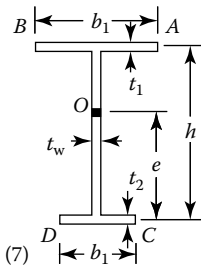


(6)

$$J = \frac{1}{3}(2t^3b + t_{\omega}^3h)$$

$$I_{\omega} = \frac{h^2tb^3}{24}$$

Wide flanged beam  
with unequal flanges



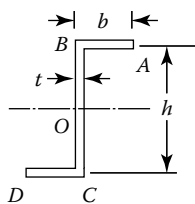
(7)

$$e = \frac{t_1b_1^2h}{t_1b_1^3 + t_2b_2^3}$$

$$J = \frac{1}{3}(t_1^3b_1 + t_2^3b_2 + t_w^3h)$$

$$I_{\omega} = \frac{h^2t_1t_2b_1^3b_2^3}{12(t_1b_1^3 + t_2b_2^3)}$$

Z section

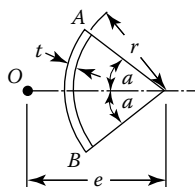


(8)

$$J = \frac{t^3}{3}(2b + h)$$

$$I_{\omega} = \frac{th^2b^3}{12} \left( \frac{b+h}{2b+h} \right)$$

Segment of a  
circular tube



(9)

$$e = 2r \frac{\sin \alpha - \alpha \cos \alpha}{\alpha - \sin \alpha \cos \alpha}$$

$$J = \frac{2}{3}t^3r\alpha$$

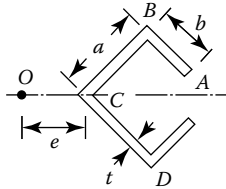
$$I_{\omega} = \frac{2tr^5}{3} \left[ \alpha^3 - 6 \frac{(\sin \alpha - \alpha \cos \alpha)^2}{\alpha - \sin \alpha \cos \alpha} \right]$$

**TABLE 9.8 (continued)**  
**Torsion Constants for Open Sections**

Cross-Section Reference Number

Constants

For  $\alpha = 45^\circ$   $e = 1.06r$   
 $= 90^\circ$   $e = 1.27r$   
 $= 180^\circ$   $e = 2r$



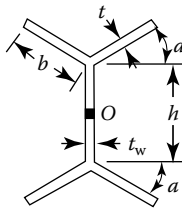
$$e = 0.707ab^2 \frac{3a - 2b}{2a^3 - (a - b)^3}$$

$$J = \frac{2}{3}t^3(a + b)$$

$$I_w = \frac{ta^4b^3}{6} \frac{3a + 2b}{2a^3 - (a - b)^2}$$

$$J = \frac{1}{3}(4t^3b + t_w^3a)$$

$$I_w = \frac{a^2b^2t}{3} \cos^2 \alpha$$



(10)

$$I_w = \frac{h^2 t_1 t_2 b_1^3 b_2^3}{12 (t_1 b_1^3 + t_2 b_2^3)}$$

$$h = 30 \text{ ft}, \quad t_1 = t_2 = 2 \text{ ft}, \quad b_1 = 20 \text{ ft}, \quad b_2 = 10 \text{ ft}$$

$$I_w = \frac{30^2 \times 2 \times 2 \times 10^3 \times 20^3}{12 (2 \times 10^3 + 2 \times 20^3)} = 133,226 \text{ ft}^6$$

This confirms the accuracy of our previous calculations.

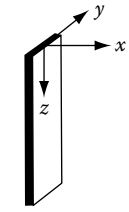
### 9.5.11 STIFFNESS METHOD USING WARPING-COLUMN MODEL

Building structures are generally analyzed as three-dimensional frames, with the members oriented in any direction and subjected to axial force, shear and moment in two orthogonal plans, and torsion about their linear axes. Therefore, a general beam or column element in the analysis of three-dimensional frames must include forces in three directions and moments about three axes. Such a beam element with six displacements at each end is shown in Figure 9.66. The stiffness matrix, which is the relationship between the end forces and displacements is a  $12 \times 12$  matrix, corresponding to six degrees of freedom at each end. The stiffness coefficients depicting the force-displacement relation for the three-dimensional beam element is found by combining the stiffness terms for axial deformation, bending about two axes, and torsion. The resulting  $12 \times 12$  stiffness matrix is given in Figure 9.66.

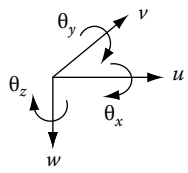
A nonplanar shear wall such as I- or C-shaped wall is modeled in a three-dimensional analysis as an assemblage of floor-to-floor panel elements connected along their edges. The continuous



		$u$	$v$	$w$	$\theta_x$	$\theta_y$	$\theta_z$						
		1	2	3	4	5	6	7	8	9	10	11	12
$u$	1	$\frac{12EI_y}{L^3}$	S										
	$v$	2	0	$\frac{12EI_x}{L^3}$	Y								
	$w$	3	0	0	$\frac{EA}{L}$	M							
	$\theta_x$	4	0	$\frac{6EI_x}{L^2}$	0	$\frac{4EI_x}{L}$	M						
	$\theta_y$	5	$\frac{-6EI_y}{L^2}$	0	0	0	$\frac{4EI_y}{L}$	E					
$\theta_z$	6	0	0	0	0	0	0	$\frac{GJ}{L}$	T				
$u$	7	$\frac{-12EI_y}{L^3}$	0	0	0	$\frac{6EI_y}{L^2}$	0	0	$\frac{12EI_y}{L^3}$	R			
$v$	8	0	$\frac{-12EI_x}{L^3}$	0	$\frac{-6EI_x}{L^2}$	0	0	0	0	$\frac{12EI_x}{L^3}$	I		
$w$	9	0	0	$\frac{-EA}{L}$	0	0	0	0	0	0	$\frac{EA}{L}$	C	
$\theta_x$	10	0	$\frac{-6EI_x}{L^2}$	0	$\frac{2EI_x}{L}$	0	0	0	$\frac{-6EI_x}{L^2}$	0	$\frac{4EI_x}{L}$	A	
$\theta_y$	11	$\frac{-6EI_y}{L^2}$	0	0	0	$\frac{2EI_y}{L}$	0	$\frac{6EI_y}{L^2}$	0	0	0	$\frac{4EI_y}{L}$	L
$\theta_z$	12	0	0	0	0	0	$\frac{-GJ}{L}$	0	0	0	0	0	$\frac{GJ}{L}$



(b)



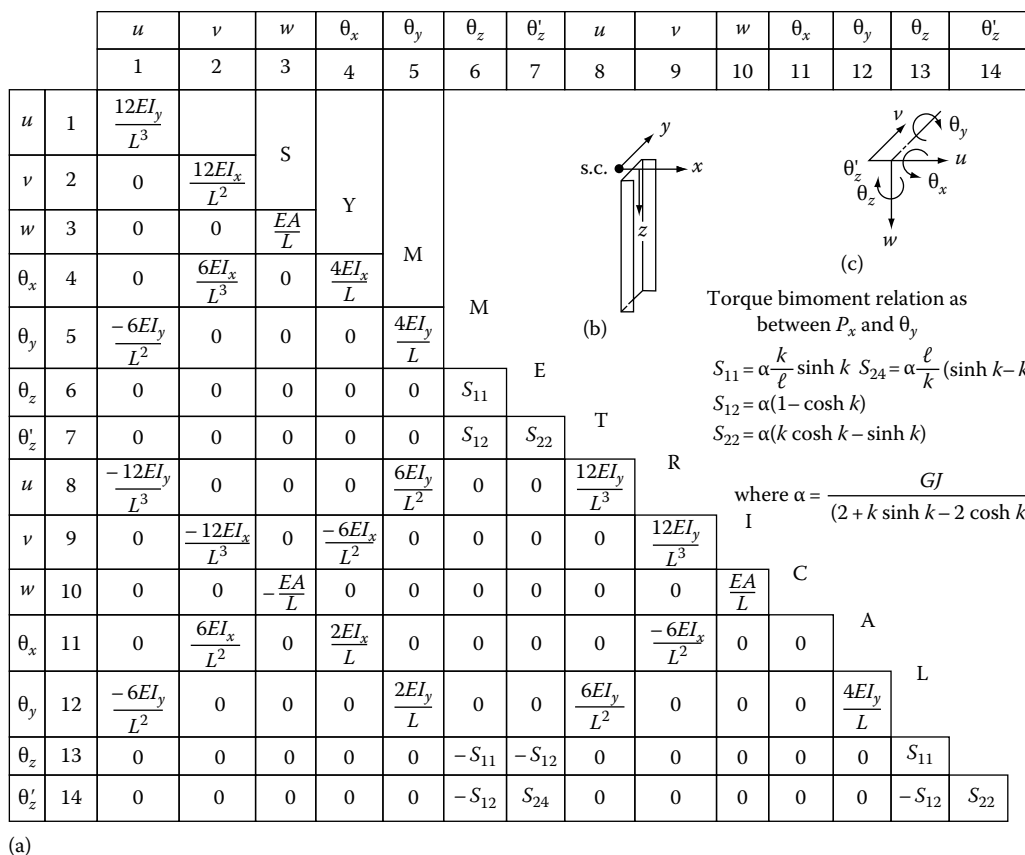
(c)

(a)

**FIGURE 9.66** (a)  $12 \times 12$  stiffness matrix for prismatic three-dimensional element, (b) coordinate axes, and (c) positive sign convention.

connection between the panels provides for the principal interaction and the vertical shear along their connecting edges.

As an alternative technique, a three-dimensional wall may be represented in all its aspects of behavior including warping, by a warping column element, with seven degrees of freedom at each floor level. Its assigned properties would include the warping moment of inertia  $I_\omega$ , in addition to the familiar area  $A$ , to represent its resistance to axial load, inertias  $I_x$  and  $I_y$  to represent its St. Venant's resistance to torsion. Such a single-column model, with an extra seventh degree of freedom, is particularly suitable for open-section walls that are uniform over the height. The seventh, warping, degree of freedom is the parameter  $d\theta/dz$ , which expresses the magnitude of warping. It is used as the warping degree of freedom, while  $B$ , the bimoment, becomes the corresponding generalized force. Thus, with seven degrees of freedom per node, the column element (Figure 9.67) has a  $14 \times 14$  stiffness matrix. A number of such story-height elements may be stacked vertically to represent a complete core. The interaction of slabs and beams at the floor levels may also be included in the stiffness matrix of the total structure by an appropriate combination of floor stiffness matrix with the stiffness matrix of the core. More information may be found in a paper "Analysis of Interconnected Open Section Shear Wall Structures" published by the author in the AISC Structural Engineering Journal. Engineers engaged in developing special-purpose computer programs may find the reference useful for including the additional warping degree of freedom for open-section shear wall buildings.



**FIGURE 9.67** (a)  $14 \times 14$  stiffness matrix for thin walled open section, (b) coordinate axes, and (c) positive sign convention.

## 9.6 PERFORMANCE-BASED DESIGN

Until recently, engineers thought that performance-based design (PBD) was not for engineers with faint hearts. Now that has changed particularly for those practicing seismic design on the West Coast. It is a new game in town that can be learnt sooner or later, if not for its intriguing suppositions but for sheer survival as a practicing engineer. What was once considered as the domain of the seismic research community, and irrelevant in the practice of design and construction, is now popular as a high-end design tool.

In its purest form, it involves a large number of probabilistic considerations, relating among other things to variability of (1) seismic input, (2) material properties, (3) dimensions, (4) gravity loads, (5) financial consequence associated with damage, and (6) collapse or loss of usage following a seismic attack.

### 9.6.1 DESIGN IDEOLOGY

Since its first publication as FEMA-273/274, performance-based seismic design procedures have received considerable acceptance. They are routinely used, nationwide, for seismic evaluation and upgrade and more recently, have been used as the basis for seismic design of a number of new, tall buildings. Following the September 11 attacks in New York and Washington, the federal

government adapted these guidelines and applied them to design progressive collapse resistance. Substantial research at the three national earthquake engineering research centers as well as improvement in the ability of structural engineering software to simulate earthquake behavior of buildings has given new impetus to these procedures. Currently in 2009, the ATC-58 project is developing next-generation criteria, applicable to both new and existing buildings that will substantially alter the present procedures.

The ideology of PBD has been around for some time, yet is just recently being applied to the design of high-rises. One of the main reasons for this sudden romance with PBD is a highly seismic region, in the west coast of the United States, that is experiencing an upsurge in the construction of high-rise buildings many of which feature framing systems that fall outside the height limits of current building codes. Rather than forcing these buildings to conform, many jurisdictions are permitting these new designs to proceed using a performance-based approach in which a rational analysis demonstrates serviceability and safety equivalent to that intended by the code prescriptive provisions. This high-end design is typically achieved by performing nonlinear dynamic analysis.

### 9.6.2 PERFORMANCE-BASED ENGINEERING

Four performance levels are commonly described as meaningful for the seismic design of structures. These may respectively be termed the operational, immediate occupancy, life safety, and collapse prevention levels. Of these, the operational level represents that least level of damage to the structure. Structures meeting this level when responding to an earthquake are expected to experience only negligible damage to their structural systems and minor damage to nonstructural systems. The structures will retain nearly all of its pre-earthquake strength and stiffness and all mechanical, electrical, plumbing, and other systems necessary for the normal operation of the structure are expected to be functional. If repairs are required, these can be conducted at the convenience of the occupants. The risk of life safety during an earthquake in a structure meeting this performance level is negligible. However, in order for a structure to meet this level, all utilities required for normal operation must be available, either through standard public service or emergency sources maintained for that purpose.

The immediate occupancy level is similar to the operational level although somewhat more damage to nonstructural systems is anticipated. Damage to the structural systems is very slight and the structure remains with all of its pre-earthquake strength and nearly all of its stiffness. Nonstructural elements, including ceilings, cladding, and mechanical and electrical components, remain secured and do not represent hazards. Exterior nonstructural wall elements and roof elements continue to provide a weather barrier. The structure remains safe to occupy; however, some repair and cleanup is probably required before the structure can be restored to normal service. In particular, it is expected that utilities necessary for normal function of all systems will not be available, although those would be expected to operate if the necessary utility service was available. Similar to the operational level, the risk of life safety during an earthquake in a structure meeting this performance level is negligible. Structural repair may be completed at the occupants' convenience, however, significant nonstructural repair and cleanup is probably required before normal function of the structure can be restored.

At the life safety level, significant structural and nonstructural damage has occurred. The structure may have lost a substantial amount of its original lateral stiffness and strength but still retains a significant margin against collapse. The structure may have permanent lateral offset and some elements of the seismic-force-resisting system may exhibit substantial cracking, spalling, and yielding. Nonstructural elements while secure and not presenting falling hazards are severely damaged and cannot function. The structure is not safe for continued occupancy until the repairs are instituted as strong ground motion from aftershocks could result in life-threatening damage. Repair of the structure is expected to be feasible; however it may not be economically feasible to do so. The risk to life during an earthquake, in a structure meeting this performance level is low.

At the collapse prevention level a structure has sustained nearly complete damage. The seismic-force-resisting system has lost most of its original stiffness and strength and little margin remains against collapse. Substantial degradation of the structural elements has occurred including extensive cracking and spalling of masonry and concrete elements and buckling and fracture of steel elements. The structure may have significant permanent lateral offset. Nonstructural elements have experienced substantial damage and may have become dislodged creating falling hazards. The structure is unsafe for occupancy as even relatively moderate ground motion from aftershocks could induce collapse. Repair of the structure and restoration to service is probably not practically achievable.

### 9.6.3 LINEAR RESPONSE HISTORY PROCEDURE

Linear response history analysis, also commonly known as time history analysis, is a numerically involved technique in which the response of a structural model to a specific earthquake ground motion accelerogram is determined through a process of numerical integration of the equations of motion. The ground shaking accelerogram, or record, is digitized into a series of small time steps, typically on the order of 1/100th of a second or smaller. Starting at the initial time step, a finite difference solution, or other numerical integration algorithm is followed to allow the calculation of the displacement of each node in the model and the forces in each element of model for each time step of the record. For even small structural models, this requires thousands of calculations and produces tens of thousands of data points. Interpretation of the voluminous data that results from such analysis is tedious.

The principal advantages of response history analysis, as opposed to response spectrum analysis, is that response history analysis provides a time dependent history of the response of the structure to a specific ground motion, allowing calculation of path-dependent effects such as damping. It also provides information on the stress and deformation state of the structure throughout the period of response. A response spectrum analysis on the other hand, indicates only the maximum response quantities and does not indicate when during the period of response these occur, or how response of different portions of the structures is phased relative to that of other portions. Although considered as one of the most comprehensive tools, it should be kept in mind that response history analyses are highly dependent on the characteristics of the individual ground shaking records. Subtle changes in these records can lead to significant differences with regard to the predicted response of the structure. This is why, when response history analyses are used in designs, it is necessary to run the analysis using a suite of ground motion records. The use of multiple records in the analyses allows observation of the difference in response, resulting from differences in record characteristics.

### 9.6.4 NONLINEAR RESPONSE HISTORY PROCEDURE

This method of analysis is very similar to linear response history analysis, except that the mathematical model is formulated in such a way that the stiffness and even connectivity of the elements can be directly modified based on the deformation state of the structure. This permits the effects of element yielding, buckling, and other nonlinear behavior on structural response to be directly accounted for in the analysis. It also permits the evaluation of such nonlinear behaviors as foundation rocking, opening and closing of gaps, and nonlinear viscous and hysteric damping. Potentially, this ability to directly account for these various nonlinearities can permit nonlinear response history analysis to provide very accurate evaluations of the response of the structure to strong ground motion. However, this accuracy can seldom be achieved in practice. This is partially because currently available nonlinear models for different elements can only approximate the behavior of real structural elements. Another limit on the accuracy of this approach is the fact that minor deviations in ground motion or even in element hysteretic behavior can result in significant differences in predicted response. For these reasons, when nonlinear response history analysis

is used in the design process, suites of ground motion time histories must be considered. It may also be appropriate to perform sensitivity studies, in which the assumed hysteretic properties of elements are allowed to vary, within expected bounds, to allow evaluation of the effects of such uncertainties on predicted response.

Applications of nonlinear response history analysis to even the simplest structures have largely been viewed as experimental. As a result of this, nonlinear response history analysis has mostly been used as a research (rather than design) tool until very recently. With the increasing adoption of base isolation and energy dissipation technologies in the structural design process, however, the need to apply this analysis technique in the design office has increased.

### 9.6.5 MEMBER STRENGTH

Nonlinear response history analysis is primarily a deformation-based procedure, in which the amount of nonlinear deformation imposed on elements by response to earthquake ground shaking is predicted. As a result, when this analysis method is employed, there is no general need to evaluate the strength demand, that is, the forces, imposed on individual elements of the structure. Instead, the adequacy of the individual elements to withstand the imposed deformation demands is directly evaluated. The exception to this is the requirement to evaluate brittle elements, the failure of which could result in structural collapse, for the forces predicted by the analysis. Since nonlinear response history analysis does not use a response modification factor, as do elastic analysis approaches, and directly accounts for inelastic structural behavior, there is no need to further increase the forces by the  $\Omega_0$  factor. Instead the forces predicted by the analysis are used directly in the evaluation of the elements for adequacy.

### 9.6.6 DESIGN REVIEW

The provisions for design using linear methods of analysis such as the equivalent lateral force technique and the modal response spectrum analysis technique are highly prescriptive. They limit the modeling assumptions that can be employed as well as the minimum strength and stiffness and the structure must possess. Further, the methods used in linear analysis have become standardized in practice such that it is unlikely that different designers using the same technique to analyze the same structure will produce substantially different results. This is not the case when nonlinear analytical methods are employed to predict the structure's strength and its deformation. Therefore, the designer using such methods must use a significant amount of independent judgment in developing appropriate analytical models, performing the analysis, and interpreting the results to confirm the adequacy of a design. Since relatively minor changes in the assumptions used in performing a nonlinear structural analysis can significantly affect the results obtained from such an analysis, it is imperative that the assumptions used be appropriate. Therefore, the designs employing nonlinear analysis methods are typically subjected to a mandatory independent design review in order to provide a level of assurance that the independent judgment applied by the designer when using these methods is appropriate and compatible with that made by other competent practitioners.

Peer review can be defined in general terms as the process of subjecting an engineer's work to the scrutiny of others who are believed to be experts in the same field. The goal of any designer is typically to develop a design that is both cost effective and safe and meets any required performance criteria. If the peer reviewer's scope includes working with the design engineering firm in a collaborative as well as review role, maximum project benefits can result.

It is important that the peer reviewer be a team player with a respectful and professional attitude toward the engineer's work being peer reviewed. This makes far less likely that there will be prolonged engineering disagreements, confrontations, and project delays. At the same time, the peer

reviewer must have integrity to speak his or her mind clearly on controversial engineering issues where there is a disagreement even when the view of the engineer being reviewed is preferred. This is particularly important where judgment plays a major role in arriving at the appropriate engineering solutions. The participation of an appropriately experienced peer reviewer will help insure that there are no major engineering mistakes or issues overlooked and the appropriate effort has been made to develop both a safe and cost effective design.

Because structural design is often based on a mix of art and science, reasonable differences of opinion among engineers based on their different experiences and training can be expected. Such potential differences can result in widely different costs and performance. Appropriate peer reviews thus offer the potential to reduce both costs and risks of poor performance.

Critics of peer review have concerns, and rightfully so, that competitive jealousies could obstruct objectivity and lead to efforts aimed primarily at enhancing one's own image and prestige rather than enhancing the project goals. Currently this is a concern of the entire design profession.

### 9.6.7 NEW BUILDING FORMS

For buildings in regions of high seismicity, that is, for buildings assigned to Seismic Design Category D and higher, the prescriptive language of the ASCE 7-05 identifies only two structural systems allowed for buildings taller than 240 ft: moment frames and dual systems. Moment frames, typically at a building's perimeter, result in large beams and columns, which can significantly encumber views, limit balconies, and create obstacles for the layout of residential unit planning. For tall buildings, with a height-to-width ratio in excess of 5–6, relatively flexible moment frames are not an efficient way to provide the required stiffness and strength.

Dual systems offer a more effective means to provide the stiffness required for a tall building by including a stiff, central core particularly if it is of concrete construction. However, the encumbrances of large perimeter columns at relatively close spacing are still present.

Consequently code-sanctioned traditional structural systems appear to be at odds with the primary goals of residential developments particularly in regions of high seismicity.

As an analytical response, a relatively new approach, commonly referred to as PBD with the principal objective of eliminating or at least minimizing the perimeter encumbrances has been making its debut within the last few years. It should be noted that the PBD methodology is not entirely new: Its application in seismic vulnerability study and retrofit design (FEMA 356, ASCE/SEI 41-06) has been in use for quite some time.

PBD provides a framework where specific performance objectives are established for various levels of demand. Typically, three levels of seismic ground motion are considered, along with three levels of building performance. Frequently occurring earthquakes (approximately once every 50 years) will result in little, if any, damage to the building. Rare earthquakes (occurring approximately once in 500 years) will result in some structural damage that will likely require repair. Very rare earthquakes postulated to occur approximately once every 1000 years, will result in significant structural damage, but the building will remain safe from collapse.

Considering each of these events, quantifiable structural performance criteria are established against which the structural design is tested through computer simulation. For the minor and moderate seismic events, traditional analysis tools allow a relatively simple assessment of the design. For very rare earthquakes, a series of different computer simulations, usually for seven distinctly different earthquakes, are performed considering different earthquake ground motions.

Sophisticated nonlinear timehistory analysis is required for each of the seven earthquake ground motions, and the results of the simulations are compared against the performance criteria to ensure the design meets the desired level of safety. The analysis tools used to conduct these simulations have become commercially viable only in the last several years. It is believed that result of this sophisticated and rigorous approach yields a safe and reliable design.

Several professional organizations, including the Structural Engineers Association of Northern California, the Los Angeles Tall Buildings Structural Design Council (LATBSCE), the San Francisco Department of Building Inspection (SFDBI), the Los Angeles Building Department, and the Pacific Earthquake Engineering Research Center, have formulated a structural frame work for PBD. SFDBI and LATBSDC have both recently published guidelines outlining the requirements for the nonprescriptive design of tall buildings.

## 9.7 WIND DEFLECTIONS

The horizontal displacement of a floor relative to the floor below is generally referred to as a “drift.” This deflection in a moment frame is the result of column shortening, and joint translation and rotation. The column shortening component is a function of the axial stress in columns and is independent of the type, size, and arrangement of the web system. However, the component due to joint translation and rotation involves deformations of all elements of the system.

Buildings particularly those that are tall and slender must be stiff enough to limit drift. If a tower is too limber, partitions and finishes will crack, and groaning noises and swaying during windstorms will produce uncomfortable psychological sensations. The drift, which is a measure of the deflection characteristics of a building, is the ratio of the deflection per story to the story height,  $\Delta/h$ , where  $\Delta$  = deflection and  $h$  = height. Oftentimes, drift is also noted as drift index.

The selection of a proper drift index for a tall building is as important as the selection of the proper wind force. Although building codes establish the minimum wind force that must be used in the design, seldom is a deflection index specified, since safety is not involved. If too low a deflection index is selected, the wind system may become unrealistically large and costly. Two factors that should be considered in establishing a deflection index are (1) the type of building and occupancy and (2) the stiffening effects of interior and exterior walls and floors.

Engineering judgment must recognize economic values involved in a building constructed as a speculative or purely commercial venture. Often such buildings in the 20-story range are designed primarily for strength and stability. A single-occupancy corporate or prestige building, however, can and must afford the luxury of added stiffness to minimize unnerving movement, unsightly plaster cracks, and eerie noises. Hotels, residences, and hospitals require special consideration also, since movement and noise are apt to be more disturbing.

The stiffening effects of floors and interior and exterior walls are highly indeterminate and are typically neglected in deflection calculations. Masonry exterior walls although not in vogue in the present day architecture, when present, add considerable stiffness by shear wall action; glass and metal curtain walls do not.

Buildings located at the center of major cities, and buildings of moderate height, are less likely to be subjected to the full design wind pressures required by the building codes. Therefore, unrealistic calculated deflections should be tempered by experience and judgment.

It is of interest to note that in New York City, many high-rise office buildings have been designed in the 1960s with a deflection index of 0.0020–0.0030 for masonry buildings and 0.0015–0.0025 for curtain wall buildings, calculated on the basis of 20 psf above the 100 ft level. Of equal interest is the fact that gross properties were used in drift calculations.

It should be noted that the total story drift is made up of shear drift and flexural rotation drift. Shear drift is the displacement within the story under consideration. Flexural rotation drift is due to the cantilever bending of the structure that causes the plane of a story level to rotate from the horizontal. The flexural rotation drift of a given story is equal to the rotation of the bottom level of the story times the story height. This rigid body rotation does not cause additional shear distortion in the story under consideration. Therefore, the trend today in verifying drift is to disregard the flexural component of the drift.

The main purpose for adopting a drift deflection limit is to limit the damage on the building façade, partitions, and interior finishes (nonstructural components) and to limit the secondary

loading effects due to  $P-\Delta$  effects. The two major contributions as stated earlier to story drift are racking (shear) and chord (bending) drifts where the sum of these gives the overall story drift. The racking drift is the component that is of greater significance in evaluating the performance of nonstructural components. Tall buildings due to their high slenderness ratio are likely to experience high chord drifts. Therefore, the nonstructural components can be designed and detailed to accommodate the racking drifts rather than the total drifts. However, the lateral system must satisfy the industry standard of a maximum story drift of 3/8 in. Also the lateral system must be designed and detailed to resist the additional  $P-\Delta$  load effects where  $\Delta$  is the total deflection that includes both the racking and bending components. The current opinion is that the drift limit of  $H/400$  to  $H/600$  for the total drift that includes both shear and rotational contributions is overly conservative.

ACI 318-08 permits the use of any set of reasonable assumptions for computing relative flexural stiffnesses of columns, walls, floors, and roof systems. The assumptions adopted should, however, be consistent throughout analysis. Ideally, the member stiffnesses  $E_c I$  should reflect the degree of cracking and inelastic action that has occurred along each member before yielding. However, simpler assumptions are required to make frame analysis efficient in design offices.

The selection of appropriate effective stiffness values depends on the intended performance of the structure. For wind loading, we invariably maintain elastic behavior in members at service load conditions. Hence, it seems reasonable to use gross section properties. When analyzing a structure subjected to earthquakes some yielding without significant damage to the members is generally considered a tolerable performance objective. Therefore, it is prudent to determine a more accurate level of stiffness based on the expected element performance.

Varying degrees of confidence can be obtained from a simple linear analysis. One option would be to start off with gross properties for elements of lateral load system, and then modify the properties based on the degree of cracking, as predicted by the results of the analysis. The results would be compared to direct tensile strength, as calculated by the ACI 318 equation,  $f_d = 6.7\sqrt{f'_c}$ , and to the modulus of rupture equation,  $f_r = 7.5\sqrt{f'_c}$ .

As stated earlier, wind drift limits in common usage for building design are on the order of 1/600 to 1/400 of the building or story height. These limits generally are sufficient to minimize damage to cladding and nonstructural walls and partitions. Smaller drift limits may be appropriate if the cladding is brittle. An absolute limit on interstory drift may also need to be imposed in light of evidence that damage to nonstructural partitions, cladding and glazing may occur if the interstory drift exceeds about 10 mm (3/8 in.) unless special detailing practices are made to tolerate movement. An interstory drift of 3/8 in. translates to  $h/400$  for a 12.5 ft floor to floor, and  $h/320$  for a 10 ft floor to floor. It should be noted that many cladding components accept deformations that are significantly larger. However, it is prudent to verify this with the curtain wall provider for the specific project before finalizing the design.

Use of the factored wind load in checking serviceability is ultraconservative. Therefore, a load combination with an annual probability of 0.05 of being exceeded, is generally used for checking wind drift. The related equation given in ASCE 7-05 Appendix C is

$$D + 0.5L + 0.7W$$

where

$D$  is the dead load

$L$  is the live load

$W$  is the wind load as defined in Chapter 6 of ASCE 7-05

Deformation limits should apply to the structural assembly as a whole. The stiffening effect of nonstructural walls and partitions may be taken into account in the analysis of drift if substantiating information regarding their effect is available.



## 9.8 2009 INTERNATIONAL BUILDING CODE (2009 IBC) UPDATES\*

### 9.8.1 AN OVERVIEW OF STRUCTURAL REVISIONS

The International Code Council (ICC) uses an 18 month code development cycle and a 3 year code publication cycle. This means a new IBC is published every 3 years with one supplement published between code editions. Thus the new 2009 IBC incorporates the successful code changes proposed during the 2007/2008 cycle along with the changes in the 2007 supplement.

There were more than 350 proposed code changes to the structural provisions in Chapters 16 through 23 of the 2006 IBC. Of these, approximately 200 have been incorporated into the 2009 IBC. The code changes vary in significance from minor editorial clarifications to substantive technical revisions or additions. The following section presents an overview of the more significant structural changes in the 2009 IBC related to reinforced concrete construction.

#### 9.8.1.1 Earthquake Loads

In the 2009 IBC, ASCE 7-05 remains the primary reference for determining earthquake, snow, and wind loads. The referenced standard now includes Supplement No. 2 which revises the earthquake base shear equation for buildings and nonbuilding structures designed using the equivalent lateral force procedure. The net effect is to reinstate a minimum threshold that had been dropped from the 2005 edition of the ASCE 7.

The requirement that concrete and masonry walls be anchored to floors and roofs that provide lateral support for the wall for a minimum strength level horizontal seismic force of 280 per linear foot (plf) has been deleted. The new requirement corresponds to the minimum design strength stated in the ASCE 7-05, Section 11.7.3. Furthermore, the provision now requires all walls, not just concrete and masonry walls, to be anchored to floors and roofs and other structural elements that provide lateral support for the wall. The minimum design strength shall not be less than 5% of the wall weight tributary to the anchor, as stated in the ASCE 7-05 Section 11.7.3.

The 2009 IBC references the 2007 edition of NFPA 13 for the installation of automatic sprinkler systems. Section 1613.6.3 of 2009 IBC clarifies that systems installed in accordance with the NFPA 13 standard are now deemed to comply with the ASCE 7-05 seismic bracing provisions. The exemptions from seismic bracing requirements of Section 13.6.7 of ASCE 7-05 is extended through a modification in the 2009 IBC to include small ducts having a component factor,  $I_p = 1.5$ .

A minimum seismic separation requirement between adjacent structures contained in prior editions of the IBC has been restored in Section 1613.6.7 of the 2009 IBC. Further explanation of this revision is given later in the section.

#### 9.8.1.2 Wind Loads

The new ICC-600, Standard for Residential Construction in High Wind Regions applies to residential buildings located where the basic wind speed is 100–150 mile/h. It provides prescriptive designs for exterior walls constructed of wall assemblies, fenestration, and roof assemblies.

The recommendations pertaining to lower limits on pressures determined by wind tunnel testing contained in the ASCE 7 commentary have been incorporated directly into the code, so they are now enforceable. This is because recent comparisons between wind tunnel studies for the same building have demonstrated differences of up to 40% in results from different wind laboratories.

A new section in Chapter 17 of 2009 IBC mandates special inspection for wind resistance that applies to buildings sited in high wind areas based on wind speed and exposure category.

---

\* The author would like to acknowledge his gratitude to Mr. John R. Henry, Principal staff engineer, International Code Council (ICC), Knights Landing, California, for providing information on 2009 IBC revisions.

#### 9.8.1.2.1 *Alternate All-Heights Method*

The intention of this section is to reduce the effort required in determining wind forces. The primary simplification is accomplished by generating a table of net pressure coefficients ( $C_{net}$ ), combining a number of parameters in a simple manner. A value of 0.85 permitted for rigid structures is used for the gust factor,  $G$ . Further discussion of this method follows later in this section.

#### 9.8.1.3 Structural Integrity

Another significant change to Chapter 16 is the addition of structural integrity requirements for high-rise buildings that are classified as Occupancy Category III or IV. This is given in the new Section 1614 of the 2009 IBC. The reason for limiting these requirements to Occupancy Category III and IV high-rise buildings is because past experience has shown that typical low-rise buildings with proven structural systems have demonstrated adequate structural integrity.

#### 9.8.1.4 Other Updates in Chapter 16

Decks and balconies will now use the same uniform live load as the occupancy they serve. This eliminates the previous distinction between deck and balcony loading. The 2009 IBC now addresses the condition where the load on a cantilevered portion of a deck-span produces uplift at the back-span support. It also explicitly adds snow load since it is conceivable that snow load could control the design of the deck.

The point of application of passenger vehicle loads for vehicle barrier systems in parking garages has been modified and a second loading condition that more closely reflects actual bumper heights of current models of passenger vehicles has been added.

To clarify live load reductions, a factor  $K_{LL}$  that applies to one-way slabs has been added to Table 1607.9.1 of the 2009 IBC.

#### 9.8.1.5 Chapter 18: Soils and Foundations

Most of the changes in this chapter are editorial. The chapter is reorganized, reformatted, and updated to reflect current foundation design and construction practice. Foundations are referred to as either deep or shallow foundations. The term “geotechnical” is used consistently throughout the chapter to refer geotechnical investigations and geotechnical reports. The general requirements related to the design of all foundations and the specific requirements related to design of shallow foundations (e.g., footings) have been reorganized. Foundation walls, retaining walls, and embedded posts and poles are consolidated into a single section. The deep foundation (piles and piers) requirements have been reorganized in order to eliminate redundancy, resolve conflicting definitions, and simplify the provisions. Deep foundations are further divided into two general categories: driven deep foundations and cast-in-place deep foundations.

#### 9.8.1.6 Chapter 19: Concrete

The majority of changes are due to coordination of 2009 IBC with the 2008 edition of the ACI 318 standard. New section references in the code correspond to the final published version of ACI 318-08.

### 9.8.2 DETAIL DISCUSSION OF STRUCTURAL REVISIONS

#### 9.8.2.1 Section 1604.8.2: Walls

The requirement that concrete and masonry walls be anchored to floors and roofs that provide lateral support for the wall for a minimum strength level horizontal seismic force of 280 plf has been replaced with a reference to the minimum design strength required by ASCE 7-05 Section 11.7.3.

However, it should be noted that the actual anchorage force may exceed the minimum force depending upon the wind design speed and seismic design category of the building. The code language now requires all walls, not just concrete and masonry walls, to be anchored to floors, roofs, and other structural elements that provide lateral support for the wall.

### 9.8.2.2 Section 1604.8.3: Decks

In this section, the code now addresses the condition where the load on a cantilevered portion of a deck-span could produce uplift at the back-span support. Design for snow load has been added since it is conceivable that snow load could control the design of the deck.

### 9.8.2.3 Section 1605.1.1: Stability

The code now permits soil resistance and strength reduction factors to be considered where strength design factored loads are used in foundation design. Strength reduction factors must be determined by a registered geotechnical engineer because they are not provided by the building codes.

### 9.8.2.4 Sections 1607.3 and 1607.4: Uniformly Distributed Live Loads and Concentrated Live Loads

Decks and balconies now use the same live load as the occupancy they serve, and the previous distinction between decks and balconies has been removed by deleting their definitions. Typical balcony/deck live loads are as follows:

One-family dwelling	40psf
Office	50psf
Assembly area	100psf

### 9.8.2.5 Section 1607.7.3: Vehicle Barrier Systems

The point of application of passenger vehicles loading (bumper height) for barrier design in parking garages has been modified and a second loading condition added based on actual bumper height data of modern passenger vehicles. It should be noted that some large pickup trucks may have loaded weight of up to 10,000 lbs. Vehicle impact restraint design involves absorption and dissipation of kinetic energy of the moving vehicle impacting the barrier. This absorbed kinetic energy is a relatively complex dynamics problem involving a combination of factors, including the weight of the resisting element such as a concrete bumper wall, the instantaneous elastic or plastic deflection of the wall, the crushing or movement of the vehicle components such as the bumper energy absorption system, the crushing of vehicle fenders, etc.

### 9.8.2.6 Section 1607.9.1.1: One-Way Slabs

A  $K_{LL}$  factor has been added to Table 1607.9.1 for one-way slabs to be consistent with Table 4-2 of ASCE 7-05. The live load reduction requirements for one-way slabs has been changed from a general prohibition on live load reduction (except for heavy live loads) to a limit on the tributary area,  $A_T$ . This revision aligns section 1607.9.1.1 with Section 4.8.5 of ASCE 7-05.

### 9.8.2.7 Section 1609.1.1.2: Wind Tunnel Test Limitations

The recommendations pertaining to lower limits on pressures determined by wind tunnel testing from ASCE 7-05 commentary have been incorporated directly into the code. Therefore, the provisions are now enforceable.

Because recent comparisons between wind tunnel studies for the same building have demonstrated differences of up to 40% in results from different wind laboratories, the new provisions provide a limit on reductions such that a baseline threshold value is established. The provisions are included in the 2009 IBC rather than the standard, because ASCE 7 may not be revised and republished again until 2010.

The relevant sections in the 2009 IBC are as follows.

#### *9.8.2.7.1 Section 1609.1.1: Determination of Wind Loads*

Wind loads on every building or structure shall be determined in accordance with Chapter 6 of ASCE 7-05. The type of opening protection required, the basic wind speed, and the exposure category for a site is permitted to be determined in accordance with Section 1609 or ASCE 7-05. Wind shall be assumed to come from any horizontal direction and wind pressures shall be assumed to act normal to the surface considered.

#### **Exceptions:**

1 through 5. No change to text.

6. Wind tunnel test in accordance with Sections 6.6 of ASCE 7-05, subject to the limitations in 2009 IBC Section 1609.1.1.2.

#### *9.8.2.7.2 Section 1609.1.1.2: Wind Tunnel Test Limitations*

The lower limit on pressures for main wind-force resisting systems and components and cladding shall be in accordance with 2009 IBC Sections 1609.1.1.2.1 and 1609.1.1.2.2.

#### *9.8.2.7.3 Section 1609.1.1.2.1: Lower Limits on Main Wind-Force-Resisting System*

Base overturning moments determined from wind tunnel testing shall be limited to not less than 80% of the design base overturning moment determined in accordance with Section 6.5 of ASCE 7-05, unless specific testing is performed that demonstrates it is the aerodynamic coefficient of the building, rather than shielding from other structures, that is responsible for the lower values. The 80% limit may be adjusted by the ratio of the frame load at critical wind directions as determined from wind tunnel testing without specific adjacent buildings, but including appropriate upwind roughness, to that determined in Section 6.5 of ASCE 7-05.

#### *9.8.2.7.4 Section 1609.1.1.2.2: Lower Limits on Components and Cladding*

The design pressures for components and cladding on walls or roofs shall be selected as the greater of the wind tunnel test results or 80% of the pressure obtained for Zone 4 for walls and Zone 1 for roofs, as determined in Section 6.5 of ASCE 7-05, unless specific testing is performed that demonstrates it is the aerodynamic coefficient of the building, rather than shielding from nearby structures, that is responsible for the lower values. Alternatively, limited tests at a few wind directions without specific adjacent buildings, but in the presence of an appropriate upwind roughness, shall be permitted to be used to demonstrate that the lower pressures are due to the shape of the building and not to the shielding.

#### *9.8.2.7.5 Section 1609.6: Alternate All-Heights Method for Determining Wind Loads*

A new simplified wind design method identified as alternate all-heights method has been added to the 2009 IBC. The alternate provisions are simplifications of ASCE 7-05 Method 2, Analytical Procedure. The title of this new method implies that it applies to buildings of all heights. However, it is not so. The method applies only to structures with height not exceeding 75 ft and the ratio height-to-least width not exceeding four. The method is permitted to be used to determine the wind effects on regularly shaped buildings, which meet all of the following conditions:

1. The building is less than or equal to 75 ft in height, with a height-to-least-width ratio of 4 or less, or the building has a fundamental frequency greater than or equal to 1 Hz.
2. The building is not sensitive to dynamic effects.
3. The building is not located on a site for which channeling effects or buffeting in the wake of upwind obstructions warrant special consideration.
4. The building shall meet the requirements of a simple diaphragm building as defined in ASCE 7-05, Section 6.2, where wind loads are only transmitted to the main-wind-force-resisting system (MWFRS) at the diaphragms.
5. For open buildings, multispans gable roofs, stepped roofs, sawtooth roofs, domed roofs, roof with slopes greater than 45°, solid-free standing walls and solid signs, and rooftop equipment apply ASCE 7-05 provisions.

The main reason for introducing the alternate all-height method is because it was perceived by engineers that Method 2 of ASCE 7-05 for buildings of any height was complex and time consuming. More importantly, it often resulted in engineers making errors when applying the method. The alternate method is expected to alleviate some of these problems.

The alternate wind design procedure is accomplished by combining certain terms in the design pressure equation of Method 2, to derive a pressure coefficient  $C_{net}$ . The derivation is as follows:

$$p = 0.00256K_zK_{zt}K_dV^2I[GC_p - (GC_{pi})]$$

Let  $q_s = 0.00256V^2$

Let  $C_{net} = K_d[GC_p - GC_{pi}]$

Then

$$p_{net} = q_sK_zC_{net}(IK_{zt}) \quad (16-34)$$

where

$q_s$  depends on the wind speed at the building site

$K_z$  depends on the exposure category of the building (B, C, or D) from ASCE 7-05 Table 6-3

$I$  is the importance factor for the building from ASCE 7-05 Table 6-1, which depends on the occupancy category from IBC Table 1604.5

$K_{zt}$  is the topographic factor from ASCE 7-05 Figure 6-4

Because  $K_d = 0.85$  for buildings (ASCE 7-05, Table 6-4) and  $G = 0.85$  (ASCE 7-05, Section 6.5.8.1) for rigid structures ( $f \geq 1$  Hz),

$$C_{net} = 0.85[0.85C_p - (GC_{pi})]$$

where  $C_p$  is the external pressure coefficient from ASCE 7 Method 2, Figure 6-5, and equals  $\pm 0.18$  for enclosed buildings and  $\pm 0.55$  for partially enclosed buildings. The above equation for  $C_{net}$  was used to develop the values given in IBC Table 1609.6.2(2).

Some example calculations of  $C_{net}$  values for MWFRS of an enclosed building are shown below:

Windward wall with positive internal pressure ( $C_p = 0.8$ )

$$C_{net} = 0.85(0.85 \times 0.8 - 0.18) = 0.43$$

Windward wall with negative internal pressure ( $C_p = 0.8$ )

$$C_{\text{net}} = 0.85(0.85 \times 0.8 + 0.18) = 0.73$$

Leeward wall with positive internal pressure ( $C_p = -0.5$ )

$$C_{\text{net}} = 0.85(0.85 \times -0.5 - 0.18) = -0.51$$

Leeward wall with negative internal pressure ( $C_p = -0.5$ )

$$C_{\text{net}} = 0.85(0.85 \times -0.5 + 0.18) = -0.21$$

Side wall with positive internal pressure ( $C_p = -0.7$ )

$$C_{\text{net}} = 0.85(0.85 \times -0.7 - 0.18) = -0.66$$

Side wall with negative internal pressure ( $C_p = -0.7$ )

$$C_{\text{net}} = 0.85(0.85 \times -0.7 + 0.18) = -0.35$$

It should be noted that design wind forces for the MWFRS shall not be less than 10 psf (0.48 kN/m<sup>2</sup>) multiplied by the area of the structure projected on a plane normal to the assumed wind direction. Design net wind pressure for components and cladding shall not be less than 10 psf (0.48 kN/m<sup>2</sup>) acting in either direction normal to the surface.

Symbols and notations for the coefficients and variables used in the alternate all-heights method equations are as follows:

$C_{\text{net}}$  is the Net pressure coefficient based on  $K_d [(G)(C_p) - (GC_{pi})]$ , in accordance with Table 1609.6.2(2)

$G$  is the Gust effect factor for rigid structures in accordance with ASCE 7 Section 6.5.8.1

$K_d$  is the Wind directionality factor in accordance with ASCE 7 Table 6-4

$P_{\text{net}}$  is the Design wind pressure to be used in determination of wind loads on buildings or other structures or their components and cladding, in psf

$q_s$  is the Wind stagnation pressure in psf in accordance with Table 1609.6.2(1)

### 9.8.2.8 Section 1613.7: ASCE 7-05, Section 11.7.5: Anchorage of Walls

Section 11.7.5 of ASCE 7-05 has been amended to replace the minimum prescribed strength level horizontal seismic force of 280 plf with the minimum design strength required by Section 11.7.3 of ASCE 7-05 (a minimum horizontal force equal to 5% of the weight of wall tributary to the anchor).

### 9.8.2.9 Section 1607.11.2.2: Special Purpose Roofs

The code now specifically prohibits live load reduction for live loads of 100 psf or more at areas of roofs classified as Group A occupancies.

### 9.8.2.10 Section 1613: Earthquake Loads

ASCE 7-05 is referenced in the 2009 IBC for structural loads, including Supplement No. 2, which revises the minimum base shear equation for both buildings and nonbuilding structures where the equivalent lateral force procedure is used.

The need for this change comes from studies that indicate that tall buildings may fail at an unacceptably low seismic level. Therefore, the minimum base shear equation is being restored to that which appeared in the 2002 edition of ASCE 7. The minimum base shear equation is given by

$$C_S = 0.044s_{DS}I_E \geq 0.01$$

For convenience, the relevant section from ASCE 7-05 Supplement No. 2 is repeated here.

*9.8.2.10.1 ASCE 7-05 Supplement No. 2 Section 12.8.1.1: Calculation of Seismic Response*

The seismic response coefficient,  $C_S$ , shall be determined in accordance with Equation 12.8-2.

$$C_S = \frac{S_{DS}}{\left(\frac{R}{I}\right)} \quad (12.8-2)$$

where

$S_{DS}$  is the design spectral response acceleration parameter in the short period range as determined from Section 11.4.4

$R$  is the response modification factor in Table 12.2-1

$I$  is the occupancy importance factor determined in accordance with Section 11.5.1

The value of  $C_S$  computed in accordance with Equations 12.8-2 need not exceed the following:

$$C_S = \frac{S_{D1}}{T\left(\frac{R}{I}\right)} \quad \text{for } T \leq T_L \quad (12.8-3)$$

$$C_S = \frac{S_{D1}T_L}{T^2\left(\frac{R}{I}\right)} \quad \text{for } T > T_L \quad (12.8-4)$$

$C_S$  should not be less than

$$\begin{aligned} C_S &= 0.044S_{DS}I \\ &\geq 0.01 \end{aligned} \quad (12.8-5)$$

In addition, for structures located where  $S_1$  is equal to or greater than  $0.6g$ ,  $C_S$  shall not be less than

$$C_S = \frac{0.5S_1}{\left(\frac{R}{I}\right)} \quad (12.8-6)$$

### 9.8.2.11 Minimum Distance for Building Separation

The seismic separation requirements in prior editions of the IBC were not included in ASCE 7-05. The provisions establishing minimum separation distance between adjoining buildings that are not structurally connected have been restored in the 2009 IBC. This clarification has been added because Section 12.12.3 of ASCE 7-05 does not provide requirements for separation distances between adjacent buildings although they were included in the 2000 and 2003 editions of the IBC.

These requirements were omitted in the 2006 IBC because ASCE 7-05 was adopted by reference for seismic provisions. In addition, ASCE 7-05 defines ( $\delta_x$ ) in Section 12.8.6 as the deflection of level  $x$  at the center of mass. The actual displacement that should be used for building separation is the displacement at critical locations with consideration of both the translational and torsional displacements. These values can be significantly different. The purpose of seismic separation is to permit adjoining buildings, or parts thereof, to respond to earthquake ground motions independently and thus preclude possible structural and nonstructural damage caused by pounding between buildings or other structures. The building separation requirements in prior editions of IBC have been restored. The details of this section are as follows.

#### 9.8.2.12 Section 1613.6.7: Minimum Distance for Building Separation

All buildings and structures shall be separated from adjoining structures. Separations shall allow for the maximum inelastic response displacement ( $\delta_M$ ).  $\delta_M$  shall be determined at critical locations with consideration for both translational and torsional displacements of the structure using Equation 16-44.

$$\delta_M = \frac{C_d \delta_{\max}}{I} \quad (16-44)$$

where

$C_d$  is the deflection amplification factor in Table 12.2-1 of ASCE 7-05

$\delta_{\max}$  is the maximum displacement defined in Section 12.8.4.3 of ASCE 7-05

$I$  is the importance factor in accordance with Section 11.5.1 of ASCE 7-05

Adjacent buildings on the same property shall be separated by a distance not less than  $\delta_{MT}$ , determined by Equation 16-45.

$$\delta_{MT} = \sqrt{(\delta_{M1})^2 + (\delta_{M2})^2} \quad (16-45)$$

where  $\delta_{M1}$ ,  $\delta_{M2}$  are the maximum inelastic response displacements of the adjacent buildings in accordance with Equation 16-44.

Where a structure adjoins a property line not common to a public way, the structure shall also be set back from the property line by not less than the maximum inelastic response displacement,  $\delta_M$ , of that structure.

#### Exceptions:

1. Smaller separations or property line setbacks shall be permitted when justified by rational analyses.
2. Buildings and structures assigned to seismic design category A, B, or C.

#### 9.8.2.13 Section 1614: Structural Integrity

This section is new for the 2009 IBC. It spells out minimum integrity requirements for high-rise buildings assigned to occupancy categories III and IV. Bearing wall structures, that is, structures in which vertical loads are primarily supported by walls, all structures shall comply with requirements of Section 1614.4. Frame structures, that is, structures in which vertical loads are primarily supported by columns, shall comply with the requirements of Section 1614.3.

Only high-rise buildings in occupancy categories III and IV are required to meet minimum structural integrity requirements. This is because requirements already embodied in the building code and standards together with current structural design and construction practices provide



the majority of structures with adequate levels of reliability and safety. The new provisions contained in Section 1614 are intended to enhance the general structural integrity and resistance of structures by establishing minimum requirements for tying the primary structural elements together.

### **9.8.3 CHAPTER 17: STRUCTURAL TESTS AND SPECIAL INSPECTIONS**

#### **9.8.3.1 Section 1704.1: General**

A significant change to Chapter 17 is the exemption for special inspection of Group R-3 occupancies and clarification of the requirements pertaining to special inspector qualifications. In high seismic areas, Group R-3 occupancies often have structural elements and systems that require special inspection.

#### **9.8.3.2 Section 1704.4: Concrete Construction**

Continuous special inspection is required for cast-in-place bolts in concrete where allowable loads have been increased for allowable stress design or where strength design is used, and periodic special inspection is required for post-installed anchors in hardened concrete.

#### **9.8.3.3 Section 1704.10: Helical Pile Foundations**

Special inspection requirements have been added for helical pile foundations that are now included in Chapter 18.

#### **9.8.3.4 Section 1706: Special Inspections for Wind Requirements**

A new section is added that requires special inspection for wind-resisting elements that applies to buildings sited in high wind areas based on wind speed and exposure category.

### **9.8.4 CHAPTER 18: SOILS AND FOUNDATIONS**

Substantial portions of Chapter 18 have been recognized, reformatted, and updated to reflect current foundation design, and construction practices. The general requirements related to design of all foundations and the specific requirements related to the design of shallow foundations (footings) have been reorganized. The deep foundation (piles and piers) requirements have been reorganized to eliminate redundancy, resolve conflicting definitions, and simplify the provisions wherever possible. Deep foundations are now classified into two categories: driven deep foundations and cast-in-place deep foundations. Requirements for foundation walls, retaining walls, and embedded posts and poles have been consolidated into one section. Although most of the changes to Chapter 18 are editorial, some technical changes have been made to update the code requirements.

#### **9.8.4.1 Section 1803: Geotechnical Investigations**

The term “geotechnical” is now consistently used throughout the chapter as it relates to geotechnical investigations and geotechnical reports.

#### **9.8.4.2 Section 1807.2.3: Safety Factor**

The determination of the safety factor against sliding for retaining walls has been clarified. A clarification in language ensures that lateral soil pressures on both sides of a keyway are considered in the sliding analysis. Where retaining walls are designed for a safety factor against sliding and overturning of 1.5, the code now states that the load combinations of Section 1605 do not apply. An exception was added that permits the factor of safety of 1.1 for overturning and sliding of retaining walls subjected to earthquake loading.

### **9.8.4.3 Section 1808.3.1: Seismic Overturning**

The code is now consistent with Section 12.13.4 of ASCE 7-05 regarding reduction of seismic overturning for foundation design where either strength design or allowable stress design load combinations are used.

### **9.8.4.4 Sections 1810.3.1.5 and 1810.3.5.3.3: Helical Piles**

New provisions have been added to the deep foundation provisions for the design and installation of helical pile foundations systems.

## **9.8.5 CHAPTER 19: CONCRETE**

The majority of changes to the concrete provisions of Chapter 19 was done to coordinate requirements with the 2008 edition of the American Concrete Institute's Building Code Requirements for Structural Concrete (ACI 318-08) Standard. New section references in the code correspond to the final published version of ACI 318-08.

### **9.8.5.1 Section 1908.1: General**

Many of the amendments to ACI 318-08 in Section 1908 have been deleted in the 2009 IBC because these provisions were subsequently incorporated in the 2008 edition of the ACI 318 standard. Changes to the deflections related to structural walls have been made to coordinate the terminology used in ACI 318-08 with ASCE 7-05.

### **9.8.5.2 Section 1908.1.9: ACI 318, Section D.3.3**

Certain exceptions have been added related to the anchorage ductility requirements of ACI 318-08 Appendix D. These apply to anchors designed to resist wall out-of-plane forces with design strengths equal to or greater than the force determined in accordance with ASCE 7-05 Equations 12.11-1 or 12.14-10.

### **9.8.5.3 Sections 1909.6.1 and 1909.6.3: Basement Walls and Openings in Walls**

The structural plain concrete provisions in the code have been updated to be consistent with the provisions of ACI 318-08.

## **9.8.6 ANTICIPATED REVISIONS IN 2012 IBC**

As a final note, it is interesting to learn that one of the scheduled enhancements to the ASCE 7-10, expected to be included in the 2012 IBC, is the new seismic maps which are based on a uniform risk of collapse rather than uniform risk of ground motion exceedence. This design approach is something the eastern-half of the United States is requesting since the IBC was first published.

Another enhancement, also scheduled for inclusion in the 2012 IBC, is the new wind maps that are based on LRFD rather than the current (2010) service level design.



---

# References

1. Building Code Requirements for Structural Concrete (ACI 318-08) and Commentary, An ACI Standard 2008.
2. *Uniform Building Code*, International Code Council, Washington, DC, 1991, 1994, and 1997.
3. American National Standards Institute (ANSI), ANSI A58.1, ANSI, Washington, DC, 1982.
4. Structuring tall buildings, *Progressive Architecture*, 61(12), December 1980.
5. J. E. Cermak, Applications of fluid mechanics to wind engineering, *Journal of Fluids Engineering*, 97, 9, March 1975.
6. Wind effects on high rise buildings, *Symposium Proceedings*, Northwestern University, Evanston, IL, March 1970.
7. T. Tschanz, Measurement of total dynamic loads using elastic models with high natural frequencies, in T. J. Reinhold (ed.), *Wind Tunnel Modeling for Civil Engineering Applications*. Cambridge, U.K.: Cambridge University Press, 1982.
8. Tall buildings, *Conference Proceedings*, Singapore, 1984.
9. R. A. Coleman, *Structural System Designs*. Englewood Cliffs, NJ: Prentice-Hall, 1983.
10. *Post-Tension Manual*, 4th ed. Phoenix, AZ: Post-Tensioning Institute, 1986.
11. T. Y. Lin and S. D. Stotesbury, *Structural Concepts and Systems for Architects and Engineers*. New York: Wiley, 1981.
12. J. R. Libby, *Modern Pre-Stressed Concrete*. New York: Van Nostrand Reinhold, 1984.
13. T. Y. Lin, *Design of Prestressed Concrete Structure*, 3rd ed. New York: Wiley, 1981.
14. G. Winter and A. H. Nilson, *Design of Concrete Structures*. New York: McGraw-Hill, 1979.
15. F. S. Merritt, *Building Design and Construction Handbook*, 4th ed. New York: McGraw-Hill, 1982.
16. E. H. Gaylord, Jr., and C. N. Gaylord, *Design of Steel Structures*, 2nd ed. New York: McGraw-Hill, 1972.
17. N. M. Newmark and E. Rosenblueth, *Fundamentals of Earthquake Engineering*. Englewood Cliffs, NJ: Prentice-Hall, 1971.
18. A. Coull and B. Stafford Smith, *Tall Buildings with Particular Reference to Shear Wall Structures*. New York: Pergamon Press, 1967.
19. M. Wakabayashi, *Design of Earthquake Resistant Buildings*. New York: McGraw-Hill, 1986.
20. Bungle S. Taranath, *Structural Analysis and Design of Tall Buildings*. New York: McGraw-Hill, 1988.
21. K. Leet, *Reinforced Concrete Design*. New York: McGraw-Hill, 1991.
22. J. M. Biggs, *Introduction to Structural Dynamics*. New York: McGraw-Hill, 1964.
23. E. H. Gaylord, Jr., and C. N. Gaylord, *Structural Engineering Handbook*, 3rd ed. New York: McGraw-Hill, 1990.
24. S. E. Cooper and A. C. Chen, *Designing Steel Structures—Methods and Cases*. Englewood Cliffs, NJ: Prentice-Hall, 1985.
25. J. Karlberg, *Preliminary Design for Post-Tensioned Structures, Structural Engineering Practice*, vol. 2. New York: Marcel Dekker, Inc., 1983.
26. W. Schueller, *High-Rise Building Structures*. New York: John Wiley & Sons, 1977.
27. W. Zbirohowski-Koscia, *Thin-Walled Beams*. London, U.K.: Crosby Lockwood, 1967.
28. M. S. Ketchum (ed.), *Structural Engineering Practice*, vol. 1 & 2, 1982; vol. 4, 1982–1983; vol. 1, 2, & 3, 1983; vol. 4, 1983–1984. New York: Marcel Dekker.
29. *National Building Code of Canada and NBCC Supplement for the 1977 Code*. National Research Council Canada, Ottawa, ON, 1995.
30. N. W. Murray, *Introduction to the Theory of Thin-Walled Structures*. New York: Oxford University Press, 1984.
31. T. J. Reinhold (ed.), *Wind Tunnel Modeling for Civil Engineering Applications*. Cambridge, U.K.: Cambridge University Press, 1982.
32. M. B. Kanchi, *Matrix Methods of Structural Analysis*. New York: Wiley Eastern Limited, 1994.
33. M. Paz, *Structural Dynamics*. New York: Van Nostrand Reinhold, 1985.
34. J. R. Choudhury, Analysis of plain and spatial systems of interconnected shear walls, PhD thesis, University of Southampton, Southampton, U.K., 1968.
35. V. Z. Vlasov, *Thin-Walled Elastic Beams*. Washington, DC: National Science Foundation, 1961.

36. Bungale S. Taranath, Torsional behavior of open-section shear wall structures, PhD thesis, University of Southampton, Southampton, U.K., 1968.
37. A. Qadeer, Interaction of floor slabs and shear walls, PhD thesis, University of Southampton, Southampton, U.K., 1968.
38. Bungale S. Taranath, A new look at composite high-rise construction, *Our World in Concrete and Structures*, Singapore, 1983.
39. Bungale S. Taranath et al., A practical computer method of analysis for complex shear wall structure, *8th ASCE Conference on Electronic Computation*, New York, 1983.
40. Bungale S. Taranath, Composite design of First City Tower, *The Structural Engineer*, 60, 9, 271–281, 1982.
41. Bungale S. Taranath, Differential shortening of columns in high-rise buildings, *Journal of Torsteel*, 1981.
42. Bungale S. Taranath, Analysis of interconnected open section wall structures, *ASCE Journal*, 1986.
43. Bungale S. Taranath, The effect of warping on interconnected shear wall flat plate structures, *Proceedings of the Institution of Civil Engineers*, 1976.
44. Bungale S. Taranath, Torsion analysis of braced multi-storey buildings, *The Structural Engineer*, 53(8), 345–347, 1975.
45. Bungale S. Taranath, Optimum belt truss locations for high-rise buildings, *AISC Engineering Journal*, 11(1), 18–21, 1974.
46. K. H. Lenzen, Vibrations of steel joist–concrete slab floors, *AISC Engineering Journal*, 3(3), 133–136, July 1966.
47. J. F. Wiss and R. H. Parmalee, Human perception of transient vibrations, *Journal of Structural Division ASCE*, 100, 773–783, April 1974.
48. T. M. Murray, Design to prevent floor vibrations, *Engineering Journal American Institute of Steel Construction*, 12(3), 82, 1975.
49. R. Halvorson and N. Isyumov, Comparison of predicted and measured dynamic behavior of Allied Bank Plaza, in N. Isyumov and T. Tschanz (eds.), *Building Motion in Wind*. New York: ASCE, 1982.
50. B. Stafford Smith and A. Coull, *Tall Building Structures, Analysis and Design*. New York: John Wiley & Sons, 1991.
51. FEMA-222 and 223, *NEHRP Recommended Provisions for the Development of Seismic Regulations for New Buildings, Part 1, Provisions, Part 2, Commentary*, Federal Emergency Management Agency, Washington, DC, 1991.
52. FEMA-140, *Guide to Application of the NEHRP Recommended Provisions in Earthquake-Resistant Building Design*, Federal Emergency Management Agency, Washington, DC, 1990.
53. FEMA-178, *NEHRP Handbook for the Seismic Evaluation of Existing Buildings*, Federal Emergency Management Agency, Washington, DC, 1992.
54. FEMA-172, *NEHRP Handbook for Seismic Rehabilitation of Existing Buildings*, Federal Emergency Management Agency, Washington, DC, 1992.
55. R. O. Hamburger, A. B. Court, and J. R. Soulages, Vision 2000: A framework for performance-based engineering of buildings, in *Proceedings of 6th SEAOC Convention*, pp. 127–146, 1995.
56. A. Coull and J. R. Choudhury, Analysis of coupled shear walls, *ACI Journal*, 64(9), 587–593, September 1967.
57. ETABS Version 6, Steeler, *Stress Check of Steel Frames*; Conker, *Design of Concrete Frames*, Computers and Structures, Inc., Berkeley, CA, January 1995.
58. M. Russell Nester and A. R. Porush, A rational system for earthquake risk management, in *SEAOC Conference Proceedings*, 1991.
59. *Seismic Design Guidelines for Upgrading Existing Buildings*, PB 89-220453. Departments of the Army, the Navy, and the Air Force, Washington, DC, 1988.
60. American Concrete Institute, *Building Code Requirements for Structural Concrete (ACI 318-95) and Commentary (ACI 318R-95)*. Farmington Hills, MI: American Concrete Institute, 1996.
61. American Institute of Steel Construction, *Manual of Steel Construction: Allowable Stress Design*, 9th ed. Chicago, IL: American Institute of Steel Construction, 1989.
62. Seismology Committee, Structural Engineers Association of California, *Recommended Lateral Force Requirements and Commentary (Blue Book)*, 7th ed. Sacramento, CA: Seismology Committee, Structural Engineers Association of California, 1999.
63. Bungale S. Taranath, *Steel, Concrete, and Composite Design of Tall Buildings*. New York: McGraw-Hill, 1997.
64. Portland Cement Association, *Notes on ACI 318-02 Building Code Requirements for Structural Concrete*, 8th ed. Skokie, IL: Portland Cement Association, 2002.

65. *2003 International Building Code*. ICC Publications.
66. *2003 International Building Code Commentary*, vol. 2. ICC Publications.
67. *2000 IBC Structural/Seismic Design Manual*, vols. 1, 2, and 3. Structural Engineers Association of California, Sacramento, CA. ICC Publications.
68. S. K. Ghosh, Seismic design using structural dynamics, in *2000 International Building Code*. ICC Publications.
69. N. Taly, *Loads and Load Paths in Buildings: Principles of Structural Design*. ICC Publications.
70. S. K. Ghosh, Seismic and wind design of concrete buildings, in *2000 International Building Code*. ICC Publications.
71. A. Williams, *Seismic and Wind Forces: Structural Design Examples*. ICC Publications.
72. W.-F. Chen and C. Scawthorn (eds.), *Earthquake Engineering Handbook*. ICC Publications.
73. Y. Bozorgnia and V. V. Bertero (eds.), *Earthquake Engineering: From Engineering Seismology to Performance-Based Engineering*. ICC Publications, 2004.
74. F. Maem (ed.), *The Seismic Design Handbook*, 2nd ed. Boston, MA: Kluwer Academic Publishers, 2001.
75. *CRSI Design Handbook*, 9th ed. Schaumburg, IL: Concrete Reinforcing Steel Institute, 2002.
76. FEMA-178, *NEHRP Handbook for the Seismic Evaluation of Existing Buildings*, developed by the Building Seismic Safety Council for the Federal Emergency Management Agency, Washington, DC, 1992.
77. FEMA-267, *Interim Guidelines, Inspection, Evaluation, Repair, Upgrade and Design of Welded Moment-Resisting Steel Structures*, prepared by the SAC Joint Venture for the Federal Emergency Management Agency, Washington, DC, 1995.
78. FEMA-267A, *Interim Guidelines Advisory No. 1*, prepared by the SAC Joint Venture for the Federal Emergency Management Agency, Washington, DC, 1996.
79. FEMA-267B, *Interim Guidelines Advisory No. 2*, prepared by the SAC Joint Venture for the Federal Emergency Management Agency, Washington, DC, 1999.
80. FEMA-273, *NEHRP Guidelines for the Seismic Rehabilitation of Buildings*, prepared by the Applied Technology Council for the Building Seismic Safety Council, published by the Federal Emergency Management Agency, Washington, DC, 1997.
81. FEMA-274, *NEHRP Commentary on the Guidelines for the Seismic Rehabilitation of Buildings*, prepared by the Applied Technology Council for the Building Seismic Safety Council, published by the Federal Emergency Management Agency, Washington, DC, 1997.
82. FEMA-302, *NEHRP Recommended Provisions for Seismic Regulations for New Buildings and Other Structures, Part 1—Provisions*, prepared by the Building Seismic Safety Council for the Federal Emergency Management Agency, Washington, DC, 1997.
83. FEMA-303, *NEHRP Recommended Provisions for Seismic Regulations for New Buildings and Other Structures, Part 2—Commentary*, prepared by the Building Seismic Safety Council for the Federal Emergency Management Agency, Washington, DC, 1997.
84. FEMA-310, *Handbook for the Seismic Evaluation of Buildings—A Prestandard*, prepared by the American Society of Civil Engineers for the Federal Emergency Management Agency, Washington, DC, 1998.
85. FEMA-350, *Recommended Seismic Design Criteria for New Steel Moment-Frame Buildings*, prepared by the SAC Joint Venture for the Federal Emergency Management Agency, Washington, DC, 2000.
86. FEMA-351, *Recommended Seismic Evaluation and Upgrade Criteria for Existing Welded Steel Moment-Frame Buildings*, prepared by the SAC Joint Venture for the Federal Emergency Management Agency, Washington, DC, 2000.
87. FEMA-352, *Recommended Postearthquake Evaluation and Repair Criteria for Welded Steel Moment-Frame Buildings* prepared by the SAC Joint Venture for the Federal Emergency Management Agency, Washington, DC, 2000.
88. FEMA-353, *Recommended Specifications and Quality Assurance Guidelines for Steel Moment-Frame Construction for Seismic Applications*, prepared by the SAC Joint Venture for the Federal Emergency Management Agency, Washington, DC, 2000.
89. FEMA-354, *A Policy Guide to Steel Moment-Frame Construction*, prepared by the SAC Joint Venture for the Federal Emergency Management Agency, Washington, DC, 2000.
90. FEMA-355A, *State-of-the-Art Report on Base Metals and Fracture*, prepared by the SAC Joint Venture for the Federal Emergency Management Agency, Washington, DC.
91. FEMA-355B, *State-of-the-Art Report on Welding and Inspection*, prepared by the SAC Joint Venture for the Federal Emergency Management Agency, Washington, DC, 2000.

92. FEMA-355C, *State-of-the-Art Report on Systems Performance of Steel Moment-Frames Subject to Earthquake Ground Shaking*, prepared by the SAC Joint Venture for the Federal Emergency Management Agency, Washington, DC, 2000.
93. FEMA-355D, *State-of-the-Art Report on Connection Performance*, prepared by the SAC Joint Venture for the Federal Emergency Management Agency, Washington, DC, 2000.
94. FEMA-355E, *State-of-the-Art Report on Past Performance of Steel Moment-Frame Buildings in Earthquakes*, prepared by the SAC Joint Venture for the Federal Emergency Management Agency, Washington, DC, 2000.
95. FEMA-355F, *State of the Art Report on Performance Prediction and Evaluation of Steel Moment-Frame Buildings*, prepared by the SAC Joint Venture for the Federal Emergency Management Agency, Washington, DC, 2000.
96. FEMA-356, *Prestandard and Commentary for the Seismic Rehabilitation of Buildings*, prepared by the SAC Joint Venture for the Federal Emergency Management Agency, Washington, DC, 2000.
97. FEMA-403, *World Trade Center Building Performance Study: Data Collection, Preliminary Observations, and Recommendations*. Federal Insurance Mitigation Association, Washington, DC, and the Federal Emergency Management Agency, Region II, New York, 2000.
98. Ghosh, S. K., Design of Reinforced Concrete Buildings under the 1997 UBC, *Building Standards*, International Conference of Building Officials, Whittier, CA, May–June 1998, pp. 20–24.
99. Ghosh, S. K., Needed adjustments in 1997 UBC, *Proceedings, 1998 Convention of the Structural Engineers Association of California*, Reno/Sparks, NV, October 1985, pp. 9.1–9.15.
100. Ghosh, S. K., Major changes in concrete-related provisions—1997 UBC and beyond, *Earthquake Spectra*. Oakland, CA: Earthquake Engineering Research Institute, 1999.
101. Notes on ACI 318-05 Building Code Requirements for Structural Concrete, PCA Publications.
102. R. Park, and T. Paulay, *Reinforced Concrete Structures*. New York: Wiley-Interscience, 1975.
103. *Post-Tensioning Manual*, 6th ed. Phoenix, AZ: Post-Tensioning Institute, 2006.
104. A. K. Chopra, *Dynamic of Structures, Theory and Applications to Earthquake Engineering*, 2nd ed. Upper Saddle River, NJ: Pearson Education, Inc., 2001.
105. Mike Mota and Bungale S. Taranath. PCA publication SP-240-3.
106. E. G. Navy, *Reinforced Concrete, A Fundamental Approach*, 5th ed. Upper Saddle River, NJ: Pearson, Prentice Hall, 2003.
107. J. G. MacGregor and J. K. Wight, *Reinforced Concrete, Mechanics and Design*, 4th ed. Upper Saddle River, NJ: Pearson, Prentice Hall, 2005.
108. Bungale S. Taranath, *Wind and Earthquake Resistant Buildings, Structural Analysis and Design*. Boca Raton, FL: CRC Press, Taylor & Francis Group, 2005.
109. B. O. Aalami and A. Bommer, *Design Fundamentals of Post-Tensioned Concrete Floors*. Phoenix, AZ: Post-Tensioning Institute, 1999.
110. B. O. Aalami, *ADAPT-PT for Analysis and Design of Post-Tensioned Buildings Beams, Slabs, and Single Story Frames*. Adapt Corporation, 2002.
111. B. O. Aalami, *ADAPT-PT User Manual*, Supplemental Volume 2000.
112. R. W. Clough and J. Penzien, *Dynamics of Structures*, 2nd ed. New York: McGraw-Hill, Inc. 1993.
113. N.W. Murray, *Introduction to the Theory of Thin-Walled Structures*. Oxford University Press, United Kingdom, 1984.
114. Seismic Evaluation of Existing Buildings, ASCE/SEI 31-03, American Society of Civil Engineers, 2003.
115. Seismic Rehabilitation of Existing Buildings, ASCE/SEI 41-06, American Society of Civil Engineers, 2006.
116. NEHRP Recommended Provisions for Seismic Regulations for New Buildings and Other Structures, Part 1, Provisions, Part 2, Commentary, FEMA 450 Parts 1 and 2, 2003.
117. M. J. N. Priestly, G. M. Calvi, and M. J. Kowalsky, *Displacement-Based Seismic Design of Structures*. Pavia, Italy: IUSS Press, 2007.
118. T. Paulay and M.J.N. Priestly, *Seismic Design of Reinforced Concrete and Masonry Buildings*. New York: John Wiley & Sons, Inc., 1992.
119. *PCI Design Handbook, Precast and Prestressed Concrete*, 6th ed. Chicago, IL: Precast/Prestressed Concrete Institute, 2004.

---

# Index

2006 International Building Code (2006 IBC)  
live-load reduction, 384  
occupancy category, 381–383  
overturning, uplifting, and sliding, 383  
partition loads, 384  
seismic-detailing, 383  
torsional forces, 384  
2009 International Building Code (2009 IBC)  
concrete, 901  
soils and foundations  
geotechnical investigations, 900  
helical piles, 901  
safety factor, 900  
seismic overturning, 901  
structural revisions  
building separation, 899  
concrete, 894  
decks, 894  
earthquake loads, 892, 898  
live loads, 894  
one-way slabs, 895  
reinforced concrete construction, 892  
soils and foundations, 893  
stability, 894  
structural integrity, 893, 899–900  
vehicle barrier systems, 894  
walls, 894  
walls anchorage, 897  
wind loads, 893  
wind tunnel test limitations, 895–897  
structural tests and special inspections, 900

## A

ACI design method, torsion, 23–25  
ACI 318-05/moment frames, 525  
ACI 318-05/shear walls, 526  
Adjacent buildings, 354–355  
Aeroelastic wind model  
cutaway view, 326  
decision factors, 329–330  
multidegree-of-freedom, 330–331  
rotation simulators, 327  
schematic representation, 327, 329  
simulating torsion, 326  
stick model  
advantages and disadvantages, 326  
schematic representation, 328  
Al Bateen Towers, UAE, 774–776  
dead and lateral loads, 777  
seismic loads, 778  
structural framing system, 773  
wind loads, 777  
All-heights method, 896–897  
Along wind displacement and acceleration  
vs. gust effect factor, 299–301

gust effect factor calculations, 293–296  
worksheet calculation, 296–299  
American Concrete Institute (ACI) 318–08  
analysis and proportioning, 605  
coupling beams, diagonal reinforcement  
full-depth confinement, 614, 616  
individual diagonals, 614, 615  
earthquake-resistant structures, 605  
flexural members, 607–608, 610  
intermediate moment frames (IMFs), 606–607  
ordinary moment frames, 606  
outline of, 600, 604–605  
shear strength requirements, 609, 611, 612  
shear wall design, 612  
special moment frames  
bending and axial loads, 609–611  
joints, 611  
mechanical splices, 606  
reinforcement, 605–606  
welded splices, 606  
special structural walls  
boundary elements, 613  
coupling beams, 611–612  
mechanical splices, 606  
reinforcement, 605–606  
welded splices, 606  
transverse reinforcement, 608–609  
two-way slabs, 607–609  
Ancient monuments, 700  
Ancient tall buildings, 688  
Architecture  
American skyscraper, 692  
development  
ancient monuments, 700  
architect–engineer collaboration, 704  
Citicorp Building, 701–703  
erection techniques, 701  
international style, 699, 701  
John Hancock Tower, Chicago, 702  
sky scraper, 704–705  
structural size, 705  
Transamerica Tower, California, 701–702  
tubular system, 701  
International Style, 692–693  
John Hancock Center, Chicago, 693–694  
revolutionary methods, 692  
Rockefeller Center, New York City, 692–693  
ASCE 7–05  
anchorage of walls, 897  
seismic design criteria  
analysis procedures, 432, 452–464  
base shear, preliminary design, 405–414  
basic requirements, 427  
building irregularities, 443–448  
catalog requirements, 473–478  
connection supports, 427



- continuous load path and interconnection, 427
- design response spectrum, USA, 414–426
- detailing requirements, 442–443
- diaphragms, 429–430, 433–434, 464–473
- drift and deformation, 435–436
- equivalent lateral force procedure, 390–398
- foundation design, 427, 436–438
- geologic hazards and geotechnical investigation, 404–405
- importance factor, 398–399
- load direction, 431–432, 451–452
- member design, connection design and deformation limit, 427
- model analysis, 433
- modeling criteria, 432–433
- occupancy categories, 399–400
- redundancy, 448–449
- SDC A buildings, 401–404
- seismic ground-motion values, 386–390
- seismic load combinations, 430–431, 449–451
- seismic resistance, 439–440
- special reinforced concrete shear wall, 442
- structural system selection, 427–429
- structural walls and anchorage, 434–435, 440–442
- seismic isolation systems
  - building characteristics, 818
  - drift limits, 817
  - effective damping, 821
  - effective stiffness, 820–821
  - equivalent lateral force (ELF) procedure, 813
  - friction pendulum system (FPS), 827–828
  - isolator displacement terminology, 814
  - lateral displacements, 814–816
  - lateral forces, 816–817
  - lower-bound limits, 817, 818
  - structural elements above isolation system, 823
  - structural elements at or below isolation interface, 822–823
  - total design displacement, 822
  - triple pendulum bearing, 828–829
  - vertical distribution, 823–827
- seismic provisions, 384–386
- wind load provisions
  - analytical procedure, 272–274
  - fastest mile speed, reasons, 272
  - simplified procedure, 268–269
  - wind-tunnel procedure, 274–304
- ASCE/SEI 41-06 design
  - deformation-controlled action, 664–665
  - earthquake hazard levels, 666
  - moment frames and shear walls, 661
  - preliminary seismic evaluation components, 662
- Axial stress, 225, 226
- B**
- Base shear
  - approximate values
    - site class C, 410–413
    - site class D, 405–409
  - interrelated factors, 405
  - USA cities, 405, 414
- Basket weave system, 109–110
- Beam–column joint
  - analysis of, 574, 576
  - column panel shear forces, 574, 575
  - panel zone shear force, 574
  - special moment frame, 577
  - strength, 42
- Beam deflection formula, 124
- Bearing wall system, 440–441
- Bending
  - crack development, 8, 12
  - flexural reinforcement comparison, 13
  - and shear rigidity index
    - building plan forms, 720–721
    - Citicorp Tower, New York City, 720
    - column layout, 720, 722
    - effective shear-resisting system, 721
    - Sears Tower, Chicago, 720
    - shear systems, 721, 723
    - wind and seismic design, 721
    - World Trade Center (WTC), New York City, 720
  - thumb rules, 8, 12–14
  - two-way slab systems, 14
  - and warping, 850, 851
- Bilinear force–displacement hysteresis loop, 352
- Blast protection, 50
- Boundary-layer wind tunnels (BLWT), 319–320
- Braced structural steel buttresses, 681
- Buckling
  - circular building characteristics, 51–52
  - rectangular building characteristics, 53
  - stability analysis, 53
- Building behavior
  - damping, 350–352
  - drift and separation, 352–353
  - motions and deflections, 352
  - soil, 349–350
- Building deformations
  - elemental deformations, 622–623
  - global deformations, 622
  - interstructural deformations, 623
  - seismic retrofit design, 622
- Building frame system, 441
- Building irregularities
  - plan/horizontal irregularities
    - force–resisting system, 447
    - redundant structure, 447–448
    - remedial measures, 444–445
    - torsional effects, 446–447
    - types, 444
    - vertical-resisting components, 447
  - seismic codes, 443–444
  - vertical irregularities
    - remedial measures, 446
    - types, 445–446
    - unsymmetrical geometry, 448
- Bundled tube, 232–234
- Burj Dubai, 687, 786–787
  - advantages, 787
  - buttressed core system, 786–789
  - structural steel buildings, 789
  - tower foundation, 789–790
  - wind tunnel models, 786–790

**C**

Cantilever column systems, 429  
 Cantilever deflection, 841  
 Cantilever method  
   free-body diagram, 836, 837  
   moments and forces, 837, 838  
 Capacity reduction factors, 534–535  
 Cap wall system, 235, 237  
 Carnegie Hall Tower, New York City, 752–753  
 Central Plaza, Hong Kong, 736–737  
   fundamental advantages, 738  
   top-down method, 737–738  
   triangular core design, 736–738  
 Cent Trust Tower, Florida, 749–751  
 Chicago skyline, 695  
 Chrysler Building, New York City, 689–690  
 Citicorp Building, New York City, 702–703, 720, 796–798  
 Citicorp Tower, *see* Citicorp Building, New York City  
 Cities Service building, 689  
 City Bank Plaza, Hong Kong, 746  
 City Spire, New York City, 740, 742  
 Cobalt condominiums, Minnesota, 754–757  
 Collapse patterns  
   blast protection, 50  
   earthquake  
     beam–column joint strength, 42  
     heavy floor collapse, 44  
     local column failure, 43–44  
     midstory collapse, 45  
     P- $\Delta$  effect, 45–47  
     pounding, 45  
     soft first-story collapse, 45  
     tension/compression failures, 42–43  
     torsion effects, 44–45  
     unintended stiffness addition, 41–42  
     wall-to-roof interconnection failure, 43  
   explosion effects  
     exterior explosion, 48  
     interior explosion, 49  
   progressive collapse  
     preventive measurements, 49  
     structural integrity guidelines, 49–50  
   wind storms, 47  
 Columns reinforcement  
   beam and slab system, 189  
   flat plates, 195  
   flat slabs, 196  
   one-way joist system, 189–191  
   one-way pan joists, 194  
   one-way solid slabs, 193  
   posttensioned system, 192  
   two-way slabs, 194  
   Waffle slab system, 191–192, 195  
 Compression, 7–8  
 Concrete floor-framing systems  
   columns and mat foundations reinforcement, 197  
   preliminary design and material quantities, 198  
 Confined concrete  
   spiral column, 3, 4  
   transverse reinforcement, 1, 2  
 Continuous load path, 361

Continuous spans  
   end bay design, 159–161, 168–172  
   end span, 163  
   equivalent loads, 153, 154  
   interior span, 161–163, 165–168  
   one-way posttensioned slab, 153, 154  
   PT flat plate design, 164  
   simple parabolic and tendon profile, 152  
   tendon profile determination, 155–157  
   through strands design, 157–159  
   typical exterior and interior span features and tendon profile, 152–153  
 Core-supported structures, 212, 214  
 Cosmopolitan Resort & Casino, Nevada, 757–759  
 Coulomb damping, *see* Friction damping  
 Coupled shear walls, 204–205  
   coupling beams  
     diagonal reinforcement, 588–591  
     transverse reinforcement, 591–593  
   elevation and plan, 587, 588  
   wall piers  
     boundary elements, 596–599  
     longitudinal reinforcement, 595–596  
     shear design, 593–595  
     shear friction, 595  
     web reinforcement, 596  
 Coupling beams  
   coupled shear walls  
     diagonal reinforcement, 588–591  
     transverse reinforcement, 591–593  
   diagonal reinforcement  
     full-depth confinement, 614, 616  
     individual diagonals, 614, 615  
 Critical damping, *see* Damping  
 Cross-bracing systems, 706–708

**D**

Damage control features, 360–361  
 Damping devices  
   nested pendulum damper, 803–804  
   passive viscoelastic dampers  
     schematics, 793–795  
     World Trade Center Towers, 793, 794  
   simple pendulum damper  
     hydraulic dampers, 800, 802  
     Taipei Financial Center, 802–803  
   sloshing water damper, 798, 799  
   tuned liquid column damper (TLCD), 799–800  
   tuned mass damper (TMD)  
     Citicorp Tower, New York, 796–798  
     design considerations, 799  
     John Hancock Tower, Massachusetts, 798–799  
 Damping ratio, 337  
 Deformation response spectrum, 372–373  
 Design requirements  
   buckling  
     circular building characteristics, 51–52  
     rectangular building characteristics, 53  
     stability analysis, 53  
   collapse patterns  
     blast protection, 50  
     earthquake, 41–47

- explosion effects, 47
- progressive collapse, 47–50
- wind storms, 47
- ductile behavior
  - joints, shear strength, 526, 527
  - transverse reinforcement, 528–529
- external loads
  - earthquakes, 26–27
  - explosion effects, 31–32
  - floods, 32
  - vehicle impact loads, 32
  - wind loads, 27–31
- lateral load-resisting systems
  - abnormal loads, 40
  - coupled shear walls, 36–37
  - diaphragm, 38–39
  - dual systems, 38
  - moment-resistant frames, 37–38
  - self-straining forces, 40
  - shear walls, 33–35
  - strength and serviceability, 39
- reinforced concrete characteristics
  - confined concrete, 1–3
  - detailing, 6–7
  - ductility, 4–5
  - hysteresis, 5–6
  - redundancy, 6
- reinforced concrete elements behavior
  - bending, 8, 12–14
  - compression, 7–8
  - punching shear, 21–22
  - shear, 14–18
  - sliding shear, 18–21
  - tension, 7
  - torsion, 22–26
- Design response spectrum, USA, 414–426
- Design wind pressures
  - enclosed building, 301–304
  - graphical procedure, ASCE 7-05, 291
  - main wind-force-resisting systems (MWFRS), 289–291
- Diagonal reinforcement
  - full-depth confinement, 614, 616
  - individual diagonals, 614, 615
- Diaphragms, 357–358
  - boundary elements, 553
  - cast-in-place concrete
    - chord and collector elements, 625
    - deficiencies, 624–625
    - existing concrete slab, chord, 625
    - plan irregularities, 624
    - superimposed diaphragm slab, 625, 626
  - chords and collectors, 433–434, 465, 472–473
  - design forces, 434
  - drag-strut design, 472
  - eccentric collectors, 466–467
  - equivalent loads, 470–471
  - force-resisting elements, 465–466
  - irregularities, 430
  - lateral-load-resisting elements, 624
  - load-resisting system, 469
  - precast concrete diaphragms, 627
  - SDC A, 465
  - SDC C, 467–468
  - SDCs B through F, 465
  - shear forces, 470–472
  - shear strength, 552–553
  - structural analysis, 429–430
  - thickness and reinforcement, 552
- Downdraft effects, 253
- Drift and deformation, 435–436
- Dual system, 429, 441–442
- Ductility
  - frame-beam, 3, 4
  - models, 5
  - seismic design, 358–360
    - joints, shear strength, 526, 527
    - transverse reinforcement, 528–529
- Dynamic analysis
  - deformation response spectrum, 372–373
  - earthquake response spectra, 379–381
  - modal superposition method, 511
  - multi-degree-of-freedom systems
    - Cramer's rule, 510
    - damping effect, 509–510
    - displacement components, 508–509
    - dynamic equilibrium equations, 509
    - eigenvector, 510–511
    - harmonic function, 510
    - MDOF, 509
  - multi-mass system, 366
  - normal coordinates, 511–512
  - orthogonality
    - amplitude ratios, 515
    - Betti's reciprocal theorem, 512
    - DOF model, 518
    - dynamic equilibrium, 516
    - equations, 514
    - fundamental mode, 515–516
    - lumped-mass system, 512
    - multiplying equations, 516–517
    - quadratic equation, 515
    - SDOF system, 517
    - shear building, 513–514
    - SRSS method, 517–518
    - vibrating shapes, 513
  - pseudo-acceleration response spectrum, 374
  - pseudo-velocity response spectrum, 373–374
  - response spectrum method, 367–372
  - single-degree-of-freedom (SDOF) systems
    - damped oscillator, 506–507
    - differential equation, 508
    - kinetic energy, 507
    - Newton's law, 507
    - portal frame, 505
    - potential energy, 508
    - seismic design, 365
  - tripartite response spectrum, 374–379
- Dynamic response
  - cantilever column, 500–501
  - impulsive force, 500
  - load response, 499
  - seismic periods, 504
  - static and dynamic analyses
    - equivalent static force, 500–501
    - examples, 501–503
  - static problem, 497–498
  - time-load functions, 498–499
  - wind loads, 503–504

**E**

Earthquake collapse patterns  
   heavy floor collapse, 44  
   inadequate beam–column joint strength, 42  
   local column failure, 43–44  
   midstory collapse, 45  
   P- $\Delta$  effect, 45–47  
   pounding, 45  
   soft first-story collapse, 45  
   tension/compression failures, 42–43  
   torsion effects, 44–45  
   unintended stiffness addition, 41–42  
   wall-to-roof interconnection failure, 43  
 Earthquake force resistance, 551–552  
 Earthquake hazard levels, 641, 666  
 Earthquake loads, 532–534, 892, 898  
 Earthquake-resistant structures, 605  
 Earthquake response spectra, 379–381  
 Earthquakes effects, 688  
 Egyptian pyramids, 688  
 Eiffel Tower, Paris, 691  
 Elastomeric isolators  
   rubber bearing, 808, 809  
   single stage friction pendulum, 808, 810  
 El Centro earthquake, 367, 369  
 Elevation irregularities, 355, 357  
 Elysian hotel and private residences, Illinois  
   floor systems, 760–761  
   foundations, 759–760  
   gravity and lateral system, 761  
   tuned liquid damper, 761–764  
 Empire State Building, New York City, 686–687, 691, 698, 700, 724–725  
 Equivalent frame method  
   concrete floor system, 75  
   nonprismatic members, 77  
   torsional elements, 76  
 Equivalent lateral force procedure  
   base shear determination, 390–395  
   deformation compatibility, 461–463  
   design base shear, 455–456  
   drift determination, 459–461  
   horizontal shear distribution, 457  
   inherent and accidental torsion, 457–458  
   intermediate reinforced concrete moment frames, 395  
   ordinary reinforced concrete moment frames, 395  
   ordinary reinforced concrete shear walls, 395–396  
   overturning moments, 458–459  
   parameters  $S_s$  and  $S_{pe}$ , 396  
   P $\Delta$  effects, 459  
   period determination, 456–457  
   permitted building systems, 395, 397  
   site-specific ground motion analysis, 397–398  
   special reinforced concrete moment frames, 395  
   special reinforced concrete shear walls, 395–396  
   vertical distribution, 457  
 European Magnel system, 108  
 Explosion effects  
   exterior explosion, 48  
   interior explosion, 49  
 Exterior diagonal tube, 230–231

## External loads

earthquakes, 26–27  
 explosion effects, 31–32  
 floods, 32  
 vehicle impact loads, 32  
 wind loads  
   circulation of, 28, 29  
   extreme wind conditions, 29–31  
   load distribution, 29

External viscous damping, *see* Viscous damping

**F**

Fiber-reinforced polymers (FRP) systems  
   design philosophy and flexure design, 668  
   mechanical properties and behavior, 667  
 Five-component force balance model, 324–325  
 Flat slab-frame system  
   floor systems, 202  
   resisting lateral loads, 203  
   shear walls, 203–204  
 Flexural members, 607–608, 610  
 Flexure design, 97–100  
 Floor systems; *see also* Posttensioned (PT) floor systems  
   band beam, 68–70  
   beam and slab, 73  
   cast-in-place concrete construction features, 65  
   design methods  
     deep beams, 83–85  
     equivalent frame, 75–77  
     one-way and two-way slab subassemblies, 73–74  
     strut-and-tie, 85–91  
     two-way systems, 74–75  
     yield-line, 77–83  
   flat plates, 65  
   flat slabs, 65–66  
   haunch girder and joist, 70–73  
   high-rise buildings characteristics, 65  
   one-way concrete ribbed slabs, 67  
   skip joist, 67–68  
   stick method, 65  
   waffle, 67  
 Fluctuations, *see* Prevailing wind; Seasonal wind  
 Formwork design  
   concrete frame economy, 57  
   design repetition, 58  
   dimensional consistency, 59–60  
   dimensional standards, 58–59  
   horizontal design techniques, 60–63  
   site-cast concrete building, 56  
   structural design, 55  
   typical floor systems, 56  
   vertical design strategy, 63–64  
 Foundations  
   added tendon placement, 175  
   anchor device  
     banded tendons, 174  
     distributed tendons, 173  
   banded tendons flaring, 176  
   construction joint with intermediate stressing, 174  
   design  
     load-deformation characteristics, 436  
     reduction, 436–437

- SDC C, 437
- SDC D, E/F, 437–438
- seismic design basis, 427
- footings, mats, and piles, 553–554
- grade beams and slabs-on-grade, 554
- lateral components, resisted, 173
- mat foundations
  - allowable pressures, 181
  - analysis, 182–183
  - net sustained pressure, 181
  - plan and schematic section, 180
  - 25-story building, 183–185
  - 85-story building, 185–187
- modeling, 432
- overturning effects, 173
- pile foundations, 178–179
- piles, piers, and caissons, 554
- skyscraper, 172
- tendon band typical reinforcement, 175
- typical column-slab section, 176
- typical drop panel section, 178
- typical interior column and column section, 177
- Four Seasons hotel and tower, Florida, 783–785
- Framed tube system
  - behavior
    - axial stress distribution, 225, 226
    - free-form tubular configurations, 225, 227
    - shear lag effects, 225, 226
  - irregular tube, 229–230
  - shear lag
    - cantilever box beam, 228
    - effects of, 228, 229
  - structural schemes, 707–713
  - structures
    - axial forces, 846, 847
    - axial stress distribution, 846
- Frames
  - beams
    - flexural and transverse reinforcement, 535–536
    - flexural reinforcement, 540–541
    - intermediate reinforced concrete moment frame, 559–561
    - ordinary reinforced concrete moment frame, 555–557
    - requirements, 535, 539–540
    - special reinforced concrete moment frame, 565–570
    - transverse reinforcement, 541–543
  - columns
    - flexural reinforcement, 541–545
    - intermediate reinforced concrete moment frame, 561–563
    - ordinary reinforced concrete moment frame, 557–559
    - requirements, 541
    - special reinforced concrete moment frame, 570–574
    - transverse reinforcement, 544–547
  - lateral stiffness
    - cantilever deflection, 841
    - column rotations, deflection, 839–840
    - column rotations, shear deflection, 841
    - deflection comparison, 844
    - girder rotations, deflection, 840–841
    - girder rotations, shear deflection, 841–845

- lateral deflection, 839
- portal frame shear deflections, 838, 839, 842
- rigid panel zones, 844, 845
- shear deformation, 843
- Free-form tubular configurations, 225, 227
- Friction damping, 350
- Friction pendulum system (FPS), 810–812, 827–828

## G

- Geologic hazards and geotechnical investigation, 404–405
- Global and elemental deformations, 622–623
- Global coordinate system, 338
- Gravity systems
  - continuous spans
    - end bay design, 159–161, 168–172
    - end span, 163
    - equivalent loads, 153, 154
    - interior span, 161–163, 165–168
    - one-way posttensioned slab, 153, 154
    - PT flat plate design, 164
    - simple parabolic and tendon profile, 152
    - tendon profile determination, 155–157
    - through strands design, 157–159
    - typical exterior and interior span features and tendon profile, 152–153
  - design methods
    - deep beams, 83–85
    - equivalent frame, 75–77
    - one-way and two-way slab subassemblies, 73–74
    - strut-and-tie, 85–91
    - two-way systems, 74–75
    - yield-line, 77–83
  - floor systems
    - band beam, 68–70
    - beam and slab, 73
    - cast-in-place concrete construction features, 65
    - flat plates, 65
    - flat slabs, 65–66
    - haunch girder and joist, 70–73
    - high-rise buildings characteristics, 65
    - one-way concrete ribbed slabs, 67
    - skip joist, 67–68
    - stick method, 65
    - waffle, 67
  - formwork design
    - concrete frame economy, 57
    - design repetition, 58
    - dimensional consistency, 59–60
    - dimensional standards, 58–59
    - horizontal design techniques, 60–63
    - site-cast concrete building, 56
    - structural design, 55
    - typical floor systems, 56
    - vertical design strategy, 63–64
  - foundations
    - added tendon placement, 175
    - anchor device, banded tendons, 174
    - anchor device, distributed tendons, 173
    - banded tendons flaring, 176
    - construction joint with intermediate stressing, 174
    - lateral components, resisted, 173
    - mat, 179–187
    - overturning effects, 173

- pile, 178–179
  - skyscraper, 172
  - tendon band typical reinforcement, 175
  - typical column-slab section, 176
  - typical drop panel section, 178
  - typical interior column and column section, 177
- hand calculations
  - one-way slab, analysis, 92–97
  - T-beam design, 97–103
  - two-way slabs, 103–108
- harped and straight tendons, 146
- load balancing technique, 146, 148
- prestressed concrete systems
  - basket weave system, 109–110
  - button-headed tendons, 109
  - disadvantages, 111
  - European Magnel system, 108
  - flexure strength design, 133–142
  - lift-slab construction method, 108–109
  - load balancing method, 109
  - materials, 111–113
  - posttensioned floors, cracking problems, 120–121
  - posttensioned floor systems, high-rise buildings, 143–146
  - posttensioning details, 172–173, 178
  - posttensioning economics, 142–143
  - preliminary design, 146–172
  - prestressed tendons, 121–123
  - prestressing methods, 111
  - primary reasons, 110–111
  - PT design, 113–119
  - secondary moments concept, 123–133
  - shortening and tendon corrosion, 110
  - simplified structural engineering method, 109–110
  - Walnut Lane bridge, 108
- simple span beam, 149–151
- tendon profile types, 147, 148
- unit quantities
  - beam and slab system, 188
  - columns reinforcement, 188–193, 197
  - conceptual estimates, 187
  - concrete floor-framing systems, 197–198
  - flat slab with drop panels, 187
  - reinforcement and concrete, floor framing systems, 196–198
- Gust effect factor
  - calculations, 287–288
  - flexible or dynamically sensitive buildings, 285–287
  - improved method, 283–285
  - sensitivity study, 289
  - simplified method, 283
  - variations, 289
- Gusts, *see* Local wind
- H**
- Heavy floor collapse, 44
- HFBB/HFFB model, *see* High-frequency base balance and high-frequency force balance model
- Highcliff Apartment Building, Hong Kong, 800, 801
- High-frequency base balance and high-frequency force balance (HFBB/HFFB) model
  - five-component high-frequency, 324
  - force balance models, 322–323
- High-rise architecture, *see* Architecture
- High-rise buildings; *see also* Architecture
  - configurations, 694
  - definition, 695
  - factors
    - innovative design concepts, 698
    - reinforcement and concrete quantities, 699
  - future, 791–792
  - height concept, 696–697
  - lateral load design philosophy, 695–696
  - structural concepts
    - bending resistance, 720
    - shear resistance, 719
  - structural cost, 697
  - technology, 718
- Home Insurance Building, Chicago, 688
- Hopewell Center, Hong Kong, 753–754
- Horizontal design techniques
  - band and narrow beams, 61
  - beam and slab systems, 60, 62
  - beam haunches, 62
  - drop panel dimensions, 61
  - flat and joist systems, 60
  - spandrel beams, 62–63
- Horizontal irregularities, *see* Plan irregularities
- Horizontal structural irregularities, 362
- Hydraulic dampers, 800, 802
- Hysteresis, 5–6
- Hysteretic damping, 350
- I**
- Idealized earthquake force, 620
- Importance factors, 381–383, 391, 398–402
- IMRF, *see* Intermediate moment-resisting frames
- Inertia forces, definition, 353
- Integrity reinforcement
  - flat slabs, 529, 530
  - joists, 529, 530
  - perimeter beams, 530, 531
- Intermediate moment frames (IMFs), 606–607
- Intermediate moment-resisting frames (IMRFs)
  - frame beams
    - flexural and transverse reinforcement, 535–536
    - requirements, 535
  - frame columns, transverse reinforcement, 537
  - two-way slab systems
    - column strip, 538, 539
    - flat-slab beams, 538
    - middle strip, 538, 539
- Internal viscous damping, *see* Viscous damping
- Inverted pendulum-type structures, 429
- Irregular buildings, 355–356
- Irregularities, *see* Building irregularities
- J**
- Jin Mao Tower, China
  - Chinese code-defined winds, 733
  - framing plan, 732–733
  - inter-story drift, 733
- John Hancock Center, Chicago, 691, 702
- John Hancock Tower, Massachusetts, 798–799

## Joints

- shear strength, 546–548
- transverse reinforcement, 546

Jumbo column scheme, 714–716

**K**

Karman vortex street, 263

K-brace, 215–217

**L**

Lateral deflection, 839

Lateral force-resisting systems, 356–357

- diaphragm, 467
- dual system, 441–442
- horizontal irregularity, 446–448
- load combinations, 451
- redundancy, 448–449
- SDC C, 468
- structural framing elements, 461–462
- vertical irregularity, 448

Lateral load design philosophy, 695–696

Lateral load-resisting systems

- abnormal loads, 40
- bundled tube, 232–234
- core-supported structures, 212, 214
- coupled shear walls, 204–205
  - coupling beam resistance, 37
- structural systems, 36

diaphragm, 38–39

dual systems, 38

exterior diagonal tube, 230–231

flat slab-frame system

- floor systems, 202
- resisting lateral loads, 203
- shear walls, 203–204

frame tube system

- behavior, 225
- irregular tube, 229–230
- shear lag, 225–229

moment-resistant frames, 37–38

outrigger and belt wall system

- cap wall system, 235, 237
- deflection calculations, 238–242
- deflection index, 245, 247
- haunch girders, 235, 236
- optimum locations, 242–251
- structures, 234, 235
- viereendeel frames, 235, 236

principles, 201

rigid frame

- bending deformation, 206, 207
- deflection characteristics, 207–210
- forces and deformations, 205, 206
- haunch girders, 210–211
- shear wall-frame interaction, 206
- structure, 205–207

self-straining forces, 40

shear wall-frame interaction, 38

behavior, 217–218

K-brace, 215–217

structural systems, 218–224

shear walls

- diaphragm concept, 34
- shear deformations, 33
- torsional resistance, 35
- spinal wall systems, 234
- strength and serviceability, 39
- tube system, 210

Lateral stiffness, frames

- cantilever deflection, 841
- column rotations, deflection, 839–840
- column rotations, shear deflection, 841
- deflection comparison, 844
- girder rotations, deflection, 840–841
- girder rotations, shear deflection, 841–845
- lateral deflection, 839
- portal frame shear deflections, 838, 839, 842
- rigid panel zones, 844, 845
- shear deformation, 843

Lift-slab construction method, 108–109

Linear and nonlinear analysis procedures, 666

Linear viscous damper, 351

Live-load reduction, 384

Load balancing method, 109

Load combinations, strength design, 532

Load path, 353–354, 361

Local column failure, 43–44

Local wind, 256

**M**

Main wind-force-resisting systems (MWFRS), 289–291

Marilyn Monroe effect, 332

Mary Poppins effect, 332

Mass moment of inertia (MMI), 337

Mat foundations

- allowable pressures, 181
- analysis
  - complexities, 182
  - complex soil-structure interaction, 183
  - key factors, 182–183
  - Winkler spring concept, 182
- net sustained pressure, 181
- plan and schematic sections, 180
- 25-story building
  - bending moment variation, 185
  - finite element idealization, 183–184
  - hunch girders, 183
  - vertical deflection, 185
- 85-story building
  - finite element idealization and cross section, 186
  - pressure contours, 185–187

Mayan temples, Mexico, 688

Mechanical splices, 606

Metropolitan Tower, New York City, 751–752

Midstory collapse, 45

Miglin-Beitler Tower, Illinois, 726–727

Millennium Tower, California, 768–773

MMI, *see* Mass moment of inertia

Moment frame system, 441

Moment of inertia, 865

Monadnock Building, Chicago, 688–689

Multidegree-of-freedom aeroelastic model, 330–331

Multi-mass system, 366

Museum Tower, California, 743–744  
 MWFRS, *see* Main wind-force-resisting systems

## N

National building code of Canada (NBCC 2005)  
   dynamic procedure  
     along-wind vs. across-wind accelerations, 314–315  
     gust effect factor  $C_g$ , 307–311  
     wind-induced building motion, 311–312  
   static procedure  
     exposure factor,  $C_e$ , 305  
     gust factors  $C_g$  and  $C_{gi}$ , 305  
     pressure coefficient  $C_p$ , 306  
     specified wind load, 304–305  
   wind load comparison, 315  
 NBCC 2005, *see* National building code of Canada  
 NCNB Tower, North California, 740, 742–743  
 Nested pendulum damper, 803–804  
 Nontubular structural schemes, 713–716  
 Nonuniform ductility, 360–361

## O

Occupancy category, 381–383, 391, 398–400, 435, 452  
 One-way slabs, 895  
   ACI coefficients, positive and negative moments, 93–94  
   ACI 318 method, 93  
   flexural reinforcement design, 94–95  
   minimum slab thickness determination, 95–97  
   torsional stiffness, 92–93  
 Ordinary moment frames (OMF), 606  
 Orthogonality  
   amplitude ratios, 515  
   Betti's reciprocal theorem, 512  
   DOF model, 518  
   dynamic equilibrium, 516  
   equations, 514  
   fundamental mode, 515–516  
   lumped-mass system, 512  
   multiplying equations, 516–517  
   quadratic equation, 515  
   SDOF system, 517  
   shear building, 513–514  
   SRSS method, 517–518  
   vibrating shapes, 513  
 Outrigger and belt truss system, 714  
 Outrigger and belt wall system  
   cap wall system, 235, 237  
   deflection calculations  
     at midheight, 241  
     quarter-height from the bottom, 241–242  
     quarter height from the top, 239–241  
     at the top, 238–239  
   deflection index, 245, 247  
   haunch girders, 235, 236  
   optimum locations  
     recommendations, 250–251  
     single outrigger wall, 242–247  
     two outrigger walls, 247–250

structures, 234, 235  
 vierendeel frames, 235, 236  
 Overturning, 383

## P

Panel zone shear force, 574  
 Partition loads, 384  
 Passive energy dissipation, 829–830  
 Passive viscoelastic dampers  
   schematics, 793–795  
   World Trade Center Towers, 793, 794  
 P- $\Delta$  effect, 45–47  
 Pedestrian wind studies, 332–334  
 Performance-based design  
   design ideology, 885–886  
   design review, 888–889  
   linear response history procedure, 887  
   member strength, 888  
   new building forms, 889–890  
   nonlinear response history procedure, 887–888  
   performance-based engineering, 886, 887  
 Petronas Towers, Malaysia, 687, 734–736  
 Pile foundations, 178–179  
 Pile–soil interaction, 438  
 Plan irregularities, 355–356  
 Pole-type structures, 437  
 Portal frame shear deflections, 838, 839, 842  
 Posttensioned (PT) floor systems  
   bonded and unbonded tendons, 144  
   posttensioned transfer girder, 144–146  
 Pounding, 45  
 Precast concrete diaphragms, 627  
 Prestressed concrete systems  
   advantages, 110–111  
   basket weave system, 109–110  
   button-headed tendons, 109  
   disadvantages, 111  
   European Magnel system, 108  
   flexure strength design  
     bonded tendons, 133  
     force diagram, 137  
     idealized and typical stress–strain curve, 134, 136, 138  
     prestressed T-beams, 140, 142  
     rectangular prestressed concrete beam, 134–137  
     strain diagram, 135–137  
   lift-slab construction method, 108–109  
   load balancing method, 109  
   materials  
     concrete, 112–113  
     posttensioning steel, 111–112  
   posttensioned floors, cracking problems, 120–121  
   posttensioned floor systems  
     bonded and unbonded tendons, 144  
     posttensioned transfer girder, 144–146  
   posttensioning details, 172–173, 178  
   posttensioning economics, 142–143  
   preliminary design  
     continuous spans, 152–172  
     harped and straight tendons, 146  
     load balancing technique, 146, 148  
     simple span beam, 149–151  
     tendon profile types, 147, 148



prestressed tendons, 121–123  
 prestressing methods, 111  
 PT design  
   building examples, 118–120  
   design thumb rules, 115–118  
 secondary moments concept  
   beam deflection formula, 124  
   compatibility method, 128–130  
   magnitude and nature of secondary moments, 123  
   numerical examples, 124  
   two-span continuous beam, 131–132  
   two-span prestressed beam, 124  
   two-span prestressed concrete beam, 125–126  
   upward and downward deflection, 128–129  
 shortening and tendon corrosion, 110  
 simplified structural engineering method, 109–110  
 Walnut Lane bridge, 108  
 Prevailing wind, 256  
 Probabilistic seismic hazard analysis (PSHA), 397  
 Progressive collapse  
   preventive measurements, 49  
   structural integrity guidelines, 49–50  
 Pseudo-acceleration response spectrum, 374  
 Pseudo-velocity response spectrum, 373–374  
 Punching shear, 21–22

## R

Reinforced concrete  
   bending  
     crack development, 8, 12  
     flexural reinforcement comparison, 13  
     thumb rules, 8, 12–14  
     two-way slab systems, 14  
   compression, 7–8  
   confined concrete  
     spiral column, 3, 4  
     transverse reinforcement, 1, 2  
   detailing, 6–7  
   ductility  
     frame-beam, 3, 4  
     models, 5  
   hysteresis, 5–6  
   punching shear, 21–22  
   redundancy, 6  
   shear  
     resisting forces, 16–18  
     stress, 14–16  
     tension, 16, 17  
   sliding shear  
     flexural cracks, 20, 21  
     friction coefficient, 18, 19  
   tension, transfer girder  
     concrete column, 7, 9  
     encased composite column, 7, 10  
     filled steel column, 7, 11  
   torsion  
     elemental torsion, 22–25  
     overall building torsion, 25–26  
 Reinforced concrete moment frame  
   frame beams  
     intermediate, 559–561  
     ordinary, 555–557  
     special, 565–570

    frame columns  
       intermediate, 561–563  
       ordinary, 557–559  
       special, 570–574  
 Response spectrum method, 367–371  
 Rigid frames  
   bending deformation, 206, 207  
   deflection characteristics  
     cantilever bending component, 207  
     shear racking component, 207–210  
   forces and deformations, 205, 206  
   haunch girders  
     elevation and reinforcement, 211  
     floor framing plans, 210, 211  
   shear wall–frame interaction, 206  
   structure, 205–207  
 Rigid panel zones, 844, 845  
 Rigid pressure model (PM)  
   building loads, 322  
   cladding pressures, 321–322

## S

Saint-Venant's principle, 85–86  
 SDC A buildings, 401–404  
 Seagram Building, New York City, 693  
 Sears Tower, Chicago, 691, 720  
 Seasonal wind, 256  
 Sectorial coordinate, torsion, 861–863  
 Seismic design  
   adjacent buildings, 354–355  
   American Concrete Institute (ACI) 318–08  
     analysis and proportioning, 605  
     coupling beams, 613–616  
     earthquake-resistant structures, 605  
     flexural members, 607–608, 610  
     intermediate moment frames (IMFs), 606–607  
     ordinary moment frames, 606  
     shear strength requirements, 609, 611  
     shear wall design, 612  
     special moment frames, 605–606, 609–611  
     special structural walls, 605–606, 611–613  
     transverse reinforcement, 608–609  
     two-way slabs, 607–609  
   ASCE 7–05  
     analysis procedures, 432, 452–464  
     base shear, preliminary design, 405–414  
     basic requirements, 427  
     building irregularities, 443–448  
     catalog requirements, 473–478  
     connection supports, 427  
     continuous load path and interconnection, 427  
     design response spectrum, USA, 414–426  
     detailing requirements, 442–443  
     diaphragms, 429–430, 433–434, 464–473  
     drift and deformation, 435–436  
     equivalent lateral force procedure, 390–398  
     foundation design, 427, 436–438  
     geologic hazards and geotechnical investigation, 404–405  
     importance factor, 398–399  
     load direction, 431–432, 451–452  
     member design, connection design and deformation limit, 427

- model analysis, 433
- modeling criteria, 432–433
- occupancy categories, 399–400
- redundancy, 448–449
- SDC A buildings, 401–404
- seismic ground-motion values, 386–390
- seismic load combinations, 430–431, 449–451
- seismic provisions, 384–386
- seismic resistance, 439–440
- special reinforced concrete shear wall, 442
- structural system selection, 427–429
- structural walls and anchorage, 434–435, 440–442
- beam bar placement, 599, 601
- building behavior
  - damping, 350–352
  - drift and separation, 352–353
  - motions and deflections, 352
  - soil, 349–350
- configuration, 362–364
- continuous load path, 361
- damage control features, 360–361
- design criteria
  - ACI 318-05/moment frames, 525
  - ACI 318-05/shear walls, 526
- design techniques
  - joints, shear strength, 526, 527
  - transverse reinforcement, 528–529
- diaphragms, 357–358
  - boundary elements, 553
  - shear strength, 552–553
  - thickness and reinforcement, 552
- ductility, 358–360
- dynamic analysis
  - deformation response spectrum, 372–373
  - earthquake response spectra, 379–381
  - procedure, 478–487
  - pseudo-acceleration response spectrum, 374
  - pseudo-velocity response spectrum, 373–374
  - response spectrum method, 367–372
  - tripartite response spectrum, 374–379
- dynamic analysis theory
  - modal superposition method, 511
  - multi-degree-of-freedom systems, 508–511
  - normal coordinates, 511–512
  - orthogonality, 512–518
  - single-degree-of-freedom systems, 505–508
- dynamic response
  - cantilever column, 500–501
  - impulsive force, 500
  - load response, 499
  - seismic periods, 504
  - static and dynamic analyses, 500–503
  - static problem, 497–498
  - time-load functions, 498–499
  - wind loads, 503–504
- earthquake force resistance, 551–552
- earthquake-resistant structures, 418–521
- elements attached to buildings, 354
- exterior and interior joints, 599, 600
- foundations
  - footings, mats, and piles, 553–554
  - grade beams and slabs-on-grade, 554
  - piles, piers, and caissons, 554
- frame columns, SDC, 599, 602
- gravity columns, SDC, 599, 602
- integrity reinforcement
  - flat slabs, 529, 530
  - joists, 529, 530
  - perimeter beams, 530, 531
- intermediate moment-resisting frames (IMRFs)
  - frame beams, 535–536
  - frame columns, transverse reinforcement, 537
  - two-way slab systems, 538–539
- irregular buildings, 355–356
- lateral force-resisting systems, 356–357
- load path, 353–354
- redundancy, 361
- response spectrum method, 367–371
- seismic design category (SDC), 523, 524
- seismic forces, 349
- shear walls
  - boundary elements, 549–550
  - coupling beams, 550–551
  - web reinforcement, 548–549
- special moment-resisting frames (SMRFs)
  - frame beams, 539–541
  - frame columns, 541–546
  - joints, 546
  - tension, bars development, 548
- spectrum analyses methods, 487–497
  - base shear, 487–488
  - seven-story building, 490, 492–498
  - story modal participation, 488
  - three-story building, 488–491
- strength design
  - capacity reduction factors, 534–535
  - earthquake loads, 532–534
  - load combinations, 532
- structural response, 353
- typical caisson, 599, 603
- Seismic design category (SDC), 523, 524, 563–565
- $S_{DI}$  and  $S_I$ , 401
- SDC A
  - design requirements, 401–404
  - diaphragms, 465
  - ductility and toughness, 442
  - seismic design requirements, 473–474
  - structures, 400
- SDC B
  - design requirements, 474–475
  - diaphragms, 465
  - ductility and toughness, 442
  - structures, 400
- SDC C
  - design requirements, 475–476
  - force-resisting system, 442–443
  - frames, 443
  - geologic hazards, 400
  - structures, 400
- SDC D
  - design requirements, 476–478
  - geologic hazards, 405
  - structures, 400
- SDC E
  - design requirements, 478
  - geologic hazards, 404
  - structures, 401

- SDC F
  - design requirements, 478
  - geologic hazards, 404
- $S_{DS}$  and  $S_1$ , 401–402
- short-period response acceleration parameter, 399
- 1 s-period response acceleration parameter, 399
- Seismic-detailing, 383
- Seismic forces, 349
- Seismic ground-motion values
  - design response spectrum, 389–390
  - MCE ground motion, 386–387
  - site class, 389
  - site coefficients, 388–389
- Seismic hazard maps, 643
- Seismic isolation systems
  - ASCE 7–05
    - building characteristics, 818
    - drift limits, 817
    - effective damping, 821
    - effective stiffness, 820–821
    - equivalent lateral force (ELF) procedure, 813
    - friction pendulum system (FPS), 827–828
    - isolator displacement terminology, 814
    - lateral displacements, 814–816
    - lateral forces, 816–817
    - lower-bound limits, 817, 818
    - structural elements, above isolation
      - system, 823
    - structural elements, at or below isolation interface, 822–823
    - total design displacement, 822
    - triple pendulum bearing, 828–829
    - vertical distribution, 823–827
  - design concept, 804, 805
  - elastomeric isolators
    - rubber bearing, 808, 809
    - single stage friction pendulum, 808, 810
  - flexibility, 806
  - mechanical properties, 808
  - salient features, 806–808
  - sliding isolators
    - base isolation, 810, 813
    - friction pendulum system (FPS), 810–812
    - installation, 810, 812
- Seismic load combinations
  - earthquake effects, 430–431
  - force-resisting systems, 449–450
  - frames, 451
  - load effect, 450
  - load effect with over strength, 451
- Seismic provisions, 384–386
- Seismic rehabilitation
  - alternate design philosophy
    - earthquake levels, 620–621
    - idealized earthquake force, 620
  - ASCE/SEI 41-06 design
    - deformation-controlled action, 664–665
    - earthquake hazard levels, 666
    - moment frames and shear walls, 661
    - preliminary seismic evaluation components, 662
  - ASCE/SEI 41-06 summary, 666
  - basic safety and enhanced rehabilitation
    - objectives, 637
  - building deformations
    - elemental deformations, 622–623
    - global deformations, 622
    - interstructural deformations, 623
    - seismic retrofit design, 622
  - code provisions, seismic upgrade
    - characteristics, 622
    - lateral-load-resisting capacity, 621
  - code-sponsored design, 619
  - common deficiencies and upgrade methods
    - clerestory, 631–632
    - deep foundations, 632–633
    - diaphragms, 624–627
    - infilling of moment frames, 629–630
    - lateral-load-resisting structure, 623
    - nonstructural elements, 633–634
    - open storefront, 631
    - provisions and commentary, 634
    - reinforced concrete moment frames, 630
    - shallow foundations, 632
    - shear walls, 627–629
  - concepts and terminology, 636
  - earthquake hazard, 617–618
  - fiber-reinforced polymers (FRP) systems
    - design philosophy and flexure design, 668
    - mechanical properties and behavior, 667
  - goals, 617
  - hazards, 636
  - intended building performances, 638
  - limited rehabilitation objectives, 637–638
  - linear static procedure (LSP), 635
  - new building codes, 634
  - nonlinear dynamic procedure (NDP), 635
  - performance levels, overview
    - earthquake hazard levels, 641
    - key maps, 642
  - permitted design methods, 642–643
  - provisions and commentary, 634
  - seismic design procedures, 635
  - strengthening details
    - braced structural steel buttresses, 681
    - common strategies, 669
    - existing building upgrade, 683–684
    - existing concrete frame building, 678
    - external concrete moment frame, 672
    - moment and longitudinal frame, 672–674
    - new concrete shear wall, 679
    - pile caps, 677
    - reinforced concrete walls, 676, 679
    - shear walls, 668–669
    - shotcrete column jacket, 680
    - steel prop, building plan and elevation, 682
    - transfer girder, 675
    - vertical and plan irregularities, 668
    - wall evaluation, 670–672
  - structural performance levels and damage
    - horizontal elements, 640
    - vertical elements, 639–640
  - systematic rehabilitation
    - as-built conditions determination, 644–645
    - capacity vs. demand, 649–651
    - combined gravity and seismic demand, 647–648
    - component capacity calculations, 648–649

- design forces determination, 645–647
  - effective stiffness values, 644
  - primary and secondary components, 643, 645
  - seismic ground motions determination, 644
  - seismic hazard maps, 643
  - seismic strengthening strategies, development, 651–661
- Seismic strengthening details
  - braced structural steel buttresses, 681
  - common strategies, 669
  - existing building upgrade, 683–684
  - existing concrete frame building, 678
  - external concrete moment frame, 672
  - moment and longitudinal frame, 672–674
  - new concrete shear wall, 679
  - pile caps, 677
  - reinforced concrete walls, 676, 679
  - shear walls, 668–669
  - shotcrete column jacket, 680
  - steel prop, building plan and elevation, 682
  - transfer girder, 675
  - vertical and plan irregularities, 668
  - wall evaluation, 670–672
- Seismic weight, 432
- Shangri-La New York hotel project, New York, 762, 765–768
- Shear
  - resisting forces, 16–18
  - stress, 14–16
  - tension, 16, 17
- Shear center
  - C-section, 853
  - product integrals evaluation, 864, 865
  - singly symmetric curve, 862, 863
  - T-section shear wall, 848
- Shear deflection
  - column rotations, 841
  - girder rotations, 841–845
- Shear design, 100–103
- Shear flow
  - cellular sections, 854, 855
  - rectangular section, 851, 852
  - thin-walled sections, 853
- Shear friction, 580–581
- Shear-friction theory, *see* Sliding shear
- Shear lag
  - cantilever box beam, 228
  - effects of, 228, 229
- Shear racking component, 207–210
- Shear strength
  - columns, 611, 612
  - joints, 526, 527, 546–548
  - requirements, 552–553, 609
- Shear stress
  - circular shaft, 851, 852
  - hollow rectangular section, 854, 855
  - hollow section, 854
- Shear wall building, torsion analysis
  - axial stress, 877
  - bending deflection determination, 873
  - bending stresses, 880
  - bimoments and warping stresses determination, 874–876
  - eccentricity determination, 873
  - moment of inertia determination, 872–873
  - parameter  $k$  determination, 873
  - properties, 879
  - rotation and total deflection determination, 873–874
  - sectorial properties determination, 872
  - shear center, 877–878
  - shear walls, 876, 879
  - torsional rotation, 879
  - torsion constant determination, 873
- Shear wall–frame interaction
  - behavior, 217–218
  - K-brace, 215–217
  - structural systems
    - analytical model, 219
    - framing plans, 218, 220–223
    - lateral load resistance, 219
    - shear forces distribution, 219, 220, 224
- Shear walls, 627–629
  - boundary elements, 549–550
  - displacement-based procedure, 583–585
  - reinforcement details, 585–587
  - stress index procedure, 583
  - coupling beams, 550–551
  - design, 612
  - diaphragm concept, 34
  - elevation and plan, 578
  - longitudinal reinforcement, 581
  - seismic design category, 563–565
  - shear deformations, 33
  - shear design, 579–580
  - shear friction, 580–581
  - size determination, 579
  - torsional resistance, 35
  - web reinforcement, 548–549, 581–583
- Shotcrete column jacket, 680
- Simple bending theory, 85
- Simple pendulum damper
  - hydraulic dampers, 800, 802
  - Taipei Financial Center, 802–803
- Singapore Treasury Building, Singapore, 739–740
- Single-degree-of-freedom (SDOF) system
  - analytical models, 506
  - damped free vibrations, 365
  - deformation response, 372
  - elevated water tank, 367, 369
  - equations of motion, 517
  - equivalent system, 519
  - ground acceleration, 372
  - independent type, 371
  - linear type, 371, 375
  - oscillators, 463
  - pseudo-acceleration response, 374–375
  - seismic design, 365
  - structures, 367
  - undamped free vibrations, 365
- Single outrigger wall, 242–247
- Sliding, 383
- Sliding isolators
  - base isolation, 810, 813
  - friction pendulum system (FPS), 810–812
  - installation, 810, 812
- Sliding shear
  - flexural cracks, 20, 21
  - friction coefficient, 18, 19

- Sloshing water dampers, 798, 799
  - SMRF, *see* Special moment-resisting frames
  - Soft first-story collapse, 45
  - Soils and foundations
    - geotechnical investigations, 900
    - helical piles, 901
    - safety factor, 900
    - seismic overturning, 901
  - South Walker Tower, Chicago, 724–725
  - Special moment frames
    - bending and axial loads, 609–611
    - joints, 611
    - mechanical splices, 606
    - reinforcement, 605–606
    - welded splices, 606
  - Special moment-resisting frames (SMRFs)
    - frame beams
      - flexural reinforcement, 540–541
      - requirements, 539–540
      - transverse reinforcement, 541–543
    - frame columns
      - flexural reinforcement, 541–545
      - requirements, 541
      - transverse reinforcement, 544–547
    - joints
      - shear strength, 546–548
      - transverse reinforcement, 546
    - tension, bars development, 548
  - Spectrum analyses methods
    - base shear, 487–488
    - seven-story building, 490, 492–498
    - story modal participation, 488
    - three-story building, 488–491
  - Spinal wall systems, 234
  - SRZ Tower, UAE, 779–781
  - Stick aeroelastic model
    - advantages and disadvantages, 326
    - schematic representation, 328
  - Stiffness method, warping-column model, 883, 884
  - Strength design
    - capacity reduction factors, 534–535
    - earthquake loads, 532–534
    - load combinations, 532
  - Structural analysis
    - cantilever method, 834, 836–837
    - framed tube structures, 845–846
    - lateral stiffness, frames, 837–845
    - portal method, 833–835
  - Structural and nonstructural building components, 662
  - Structural Engineering Institute (SEI) standard, 50
  - Structural irregularities, *see* Horizontal structural irregularities; Vertical structural irregularities
  - Structural modeling, 432–433
  - Structural revisions
    - building separation, 899
    - concrete and decks, 894
    - earthquake loads, 892, 898
    - live loads, 894
    - one-way slabs, 895
    - reinforced concrete construction, 892
    - soils and foundations, 893
    - stability, 894
    - structural integrity, 893, 899–900
    - vehicle barrier systems and walls, 894
    - walls anchorage, 897
    - wind loads, 893
    - wind tunnel test limitations
      - all-heights method, 896–897
      - wind loads determination, 895
  - Structural schemes
    - categories
      - cross-bracing systems, 706–708
      - frame tube systems, 707–713
      - nontubular schemes, 713–716
    - composite tube system, 705
    - exterior braced tube, 706
    - space efficiency, 716–717
    - 62-story building, 705, 706
    - structural cost and plan density comparison, 717–718
  - Structural systems, 200
    - analytical model, 219
    - framing plans, 218, 220–223
    - lateral load resistance, 219
    - shear forces distribution, 219, 220, 224
  - Structural tests and special inspections, 900
  - Structural walls
    - boundary elements, 613
    - coupling beams, 611–612
    - mechanical splices, 606
    - reinforcement, 605–606
    - welded splices, 606
  - Strut-and-tie method
    - C-C-C and C-C-T node, 88
    - design methodology, 86
    - reinforced concrete design, 90
    - Saint-Venant's principle, 85–86
    - simple bending theory, 85
    - transfer girder-schematic reinforcement, 91
    - trial-and-error method, 87
    - truss model, 85
  - Strut-and-tie model, 12, 21, 22
  - Superimposed diaphragm slab, 625, 626
- ## T
- Taipei Financial Center, 802–803
  - T-beam design
    - flexure, 97–100
    - shear, 100–103
  - Tendon profile, 147, 148, 152, 155–157
  - Tension
    - bars development, 548
    - transfer girder
      - concrete column, 7, 9
      - encased composite column, 7, 10
      - filled steel column, 7, 11
  - Tension/compression failures, 42–43
  - Thumb rules, bending, 8, 12–14
  - TMD, *see* Tuned mass damper
  - Torsion
    - bending and warping torsion, 850, 851
    - elemental torsion
      - ACI design method, 23–25
      - categories, 22–23
    - moment of inertia, 865
    - overall building torsion
      - center of mass (CM), 25
      - center of rigidity (CR), 25–26

- sectorial coordinate, 861–863
  - sectorial properties calculations, 866–868
  - shear center
    - C-section, 853
    - product integrals evaluation, 864, 865
    - singly symmetric curve, 862, 863
    - T-section shear wall, 848
  - shear flow
    - cellular sections, 854, 855
    - rectangular section, 851, 852
    - thin-walled sections, 853
  - shear stress
    - circular shaft, 851, 852
    - hollow rectangular section, 854, 855
    - hollow section, 854
  - shear wall building
    - axial stress, 877
    - bending deflection determination, 873
    - bending stresses, 880
    - bimoments and warping stresses determination, 874–876
    - eccentricity determination, 873
    - moment of inertia determination, 872–873
    - parameter  $k$  determination, 873
    - properties, 879
    - rotation and total deflection determination, 873–874
    - sectorial properties determination, 872
    - shear center, 877–878
    - shear walls, 876, 879
    - torsional rotation, 879
    - torsion constant determination, 873
  - stiffness method, warping-column model, 883, 884
  - torsion constant, 865–866
  - torsion terminology, 850, 851
  - twisting, 851, 852
  - warping behavior concept
    - analogy, 851, 861
    - bending, 858, 859
    - core properties, 857, 858
    - I-section core, 857
    - shear forces, 858–860
  - warping torsion constants, 881–883
  - warping torsion theory
    - cantilever beam, I-shaped, 869
    - cantilever column, 867, 868
    - I-shaped column, 869
    - shear wall structures, 870
  - wide flange column, bimoment, 856, 857
  - Torsional forces, 384
  - Torsion constant, 865–866
  - Torsion effects, 44–45
  - Torsion terminology, 850, 851
  - Tower of Dubai, *see* Burj Dubai
  - Transamerica Tower, California, 701–702
  - Transverse reinforcement, 541–547, 608–609
  - Transverse wind, 262
  - Tripartite response spectrum, 374–379
  - Triple pendulum bearing, 828–829
  - Trump Tower, Chicago, 728–731
  - Trump Tower, New York, 746–748
  - Truss model, 85
  - Tuned liquid column damper (TLCD), 799–800
  - Tuned mass damper (TMD)
    - Citicorp Tower, New York, 796–798
    - design considerations, 799
    - John Hancock Tower, Massachusetts, 798–799
  - Twin Towers, *see* World Trade Center (WTC) Towers
  - Twin-tube system, 711–712
  - Twisting, torsion, 851, 852
  - Two outrigger walls, 247–250
  - Two-phase design and analysis, 620
  - Two Prudential Plaza, Chicago, 747, 749
  - Two-way slab systems
    - column strip, 538, 539
    - direct design method, 106–108
    - flat-slab beams, 538
    - interior and exterior span moments, 104–105
    - middle strip, 538, 539
    - simple beam moment, 104
    - without beams, 607–609
- ## U
- Unintended stiffness addition, 41–42
  - Unit quantities
    - beam and slab system, 188
    - columns reinforcement
      - beam and slab system, 189
      - flat plates, 195
      - flat slabs, 196
      - one-way joist, constant depth girders, 190
      - one-way joist, haunch girders, 191
      - one-way joist system, 189–190
      - one-way pan joists, 194
      - one-way solid slabs, 193
      - posttensioned system, 192
      - two-way slabs, 194
      - Waffle slab system, 191–192, 195
    - conceptual estimates, 187
    - concrete floor-framing systems
      - columns and mat foundations reinforcement, 197
      - preliminary design and material quantities, 196, 198
    - flat slab with drop panels, 187
    - reinforcement and concrete, floor framing systems, 196–198
  - Uplifting, 383
- ## V
- Vdara tower, Nevada, 744–745
  - Vehicle barrier systems, 894
  - Vertical structural irregularities, 363
  - Vierendeel frames, 235, 236
  - Viscous damping, 350
- ## W
- Waffle slab system, 191–192, 195
  - Wall Center, British Columbia, 800, 801
  - Wall piers
    - boundary elements, 596–599
    - longitudinal reinforcement, 595–596
    - shear design, 593–595
    - shear friction, 595
    - web reinforcement, 596
  - Wall-to-roof interconnection failure, 43

- Wall Tower building, 689
- Warping behavior concept
  - analogy, 851, 861
  - bending, 858, 859
  - core properties, 857, 858
  - I-section core, 857
  - shear forces, 858–860
- Warping-column model, 883–884
- Warping torsion constants, 881–883
- Warping torsion theory
  - cantilever beam, I-shaped, 869
  - cantilever column, 867, 868
  - I-shaped column, 869
  - shear wall structures, 870
- Web reinforcement, 548–549, 596
- Welded splices, 606
- Wet layup and precured systems, 667
- Whitney Museum, New York City, 693
- Wind deflections, 890–892
- Wind-force-resisting system, 331
- Wind loads
  - ASCE 7–05
    - analytical procedure, 272–274
    - simplified procedure, 268–269
    - wind-tunnel procedure, 274–304
  - circulation of, 28, 29
  - design considerations
    - structural innovations, 255
    - sway, 253
  - downdraft effects, 253
  - dynamic nature, 264
  - effects, 254
  - extreme wind conditions
    - hurricanes, 30
    - thunderstorms, 30
    - tornadoes, 30–31
  - gradient wind speed, 255
  - gustiness, 255
  - load distribution, 29
  - local winds, 256
  - National Building Code of Canada (NBCC 2005)
    - dynamic procedure, 306–315
    - experimental procedure, 315
    - static procedure, 304–306
  - pressures and suctions
    - design loads, 266–267
    - distribution, 265–266
    - internal and external pressures, 265
    - scaling, 264–265
  - prevailing winds, 256
  - probabilistic approach, 260–261
  - seasonal winds, 256
  - tunnels
    - acceleration and human comfort, 331–332
    - aerodynamic characteristics, 319
    - aeroelastic model, 324–330
    - boundary-layer wind tunnels (BLWT), 319–320
    - components, 320
    - DIFC model, Dubai, 316
    - HFBB/HFFB model
      - five-component high-frequency, 324
      - force balance models, 322–323
    - load combination factors, 332
    - lower limit, 331
    - method
      - along-wind response, 292–296
      - characteristics, 269
      - comparison, 292–296
      - design wind pressures, 289–291
      - gust effect factor, 281–289
      - wind speedup over hills and escarpments, 280–281
      - worksheet calculation, 296–299
    - motion perception, 335
    - pedestrian studies
      - Mary Poppins effect, 332
      - types, 334
    - Pentominium model, Dubai, 317
    - period determination and damping values, 341–345
    - rigid model, 316
    - rigid pressure model (PM)
      - building loads, 322
      - cladding pressures, 321–322
    - service benefits, 317–319
- turbulence
  - anemometer measurement, 258
  - reliability, 259–260
  - structural engineering, 259
- velocity profiles
  - atmospheric boundary layer, 257–258
  - schematic representation, 257
- vertical and horizontal motions, 255
- vortex shedding
  - aeronautical engineering, 261
  - along wind and transverse wind, 262
  - frequency, 263
  - periodic shedding, 262
  - transverse pulsating force, 263
- wind-tunnel testing, 256
- Wind tunnel
  - acceleration and human comfort, prediction, 331–332
  - aerodynamic characteristics, 319
  - aeroelastic model
    - cutaway view, 326
    - decision factors, 329–330
    - multidegree-of-freedom, 330–331
    - rotation simulators, 327
    - schematic representation, 327, 329
    - simulating torsion, 326
    - stick model, 326, 328
  - boundary-layer wind tunnels (BLWT), 319–320
  - components, 320
  - DIFC model, Dubai, 316
  - HFBB/HFFB model
    - five-component high-frequency, 324
    - force balance models, 322–323
  - load combination factors, 332
  - lower limit, 331
  - method
    - along-wind response, 292–296
    - characteristics, 269
    - comparison, 292–296
    - design wind pressures, 289–291
    - gust effect factor, 281–289
    - wind speedup over hills and escarpments, 280–281
    - worksheet calculation, 296–299
  - motion perception, 335
  - pedestrian studies
    - Mary Poppins effect, 332
    - types, 334
  - Pentominium model, Dubai, 317
  - period determination and damping values, 341–345
  - rigid model, 316
  - rigid pressure model (PM)
    - building loads, 322
    - cladding pressures, 321–322
  - service benefits, 317–319

- Shams model, Dubai, 318
  - structural properties
    - base elevation, 338
    - building properties, 339–340
    - damping ratio, 337
    - dynamic properties, 343–345
    - floor heights, 338
    - Global coordinate system, 338
    - mass distribution, 337
    - mode shapes, 336–337
    - natural frequencies, 336
  - testing conditions, 319
  - test limitations
    - all-heights method, 896–897
    - wind loads determination, 895
  - types, 292–296, 315–316
  - Wind turbulence, 258–260
    - anemometer measurement, 258
    - reliability, 259–260
    - structural engineering, 259
  - Winkler spring concept, 182
  - Woolworth building, New York City,
    - 689, 690
  - World Trade Center (WTC) Towers, 686, 691, 693, 720,
    - 793, 794
  - WTC, *see* World Trade Center (WTC) Towers
- ## Y
- Yield-line method
    - equilibrium and virtual work method, 78
    - hinging moment, 77
    - limitations, 83
    - one-way simply supported slab
      - advantages, 80–81
      - upper bound characteristics, 80
      - virtual work method, 78–79
    - simply supported square slab, 81–82
    - skewed yield lines, 82–83
    - two-way slabs design, 77





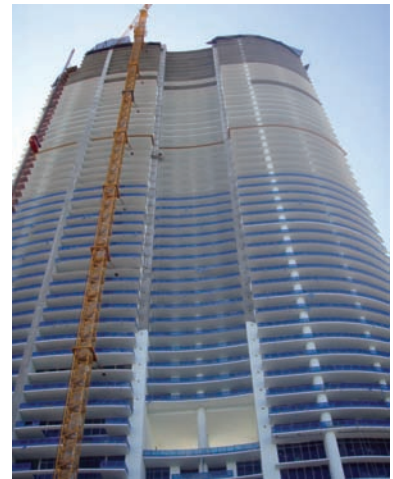
Building engineers continue the age-old human endeavor to provide society with structures which protect, serve, and inspire mankind. From pioneering new systems for better buildings with economy, to ensuring the safety of human life from nature's wrath, to stabilizing implausible forms that defy gravity, building engineers venture to create livable space from humanity's dreams and ideas. Building engineering requires a comprehensive understanding of building assembly and an appreciation of how forces are resisted within the structure and eventually by the earth.

Herein, contained in the following pages, are projects showcasing the diversity of modern challenges faced by structural engineers. Represented are projects that include gaming, hospitality, residential high-rises, commercial, academic, health care and cultural facilities. A few conceptualized designs are also included for the reader's interests. Structural engineering for the illustrated projects is by DeSimone Consulting Engineers.



### **150 Amsterdam Avenue, New York**

This project consists of a 44-story residential tower constructed over an opera house. A full floor height steel truss transfer floor is located on the top floor of the opera house, providing the base of the residential tower above, supporting the majority of the tower columns. The tower structure consists of concrete floors, columns, and walls.



**900 Biscayne Boulevard, Miami, Florida**

A 750 ft tall high rise housing residential and commercial space, the building utilized prestressed slabs and reinforced concrete shear walls.





### **1450 Brickell Ave, Miami, Florida**

A LEED silver certified office tower in Miami's financial district, 1450 Brickell's designs were heavily influenced by hurricane considerations. Structurally, link beams required embedded structural built up steel plates and a number of shear wall piers required full-story steel shear plates added to increase horizontal shear resistance.



### **The Mosaic, New York**

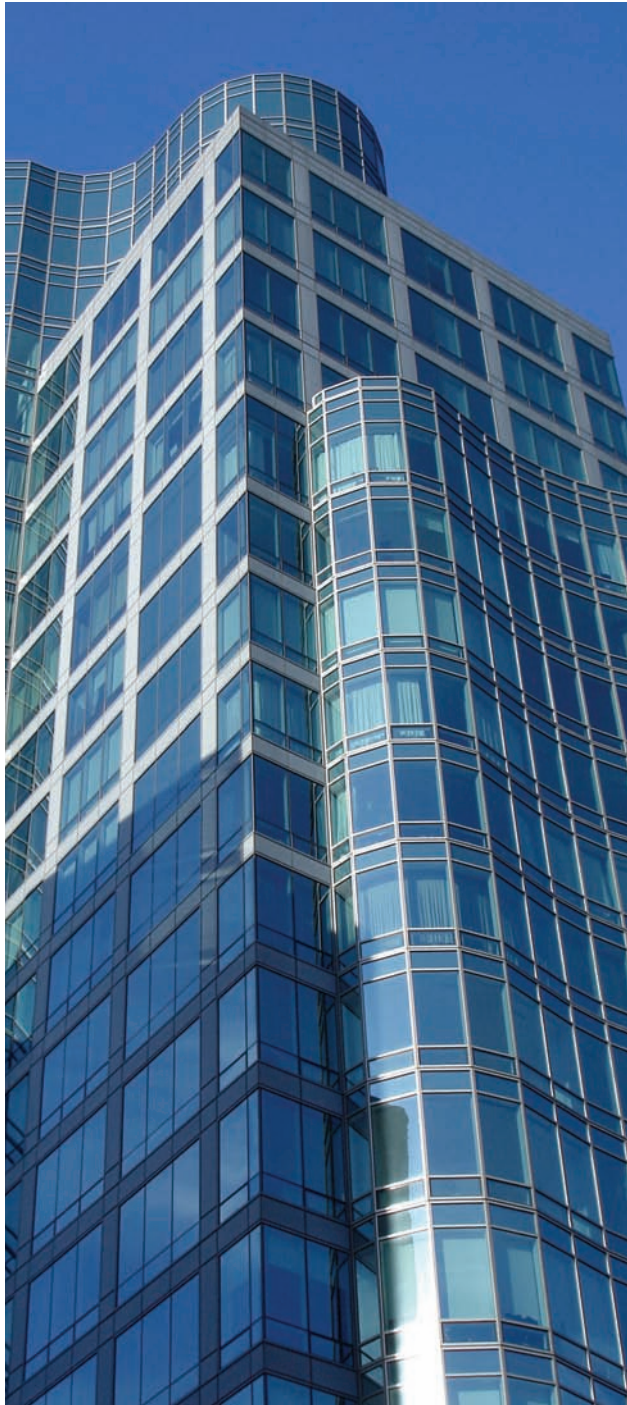
The project consists of new concrete construction built on top of a concrete and steel platform spanning over two existing Amtrak rail lines, approximately 25 ft below the existing grade. This project received basic LEED certification. Points were received for using recycled materials, some of which was in the concrete mix design. A high percentage of fly ash or slag was specified for the mixes. To ensure conformance with the required percentages while maintaining the construction schedule, a higher percentage of fly ash or slag was specified for the foundation so that the use of cement substitutes may be reduced in the superstructure to decrease set time as required.





### **Art Gallery of Alberta, Edmonton, Alberta, Canada**

The Art Gallery of Alberta was an existing facility that was partially demolished to provide room for new construction that infills and expands upward to house gallery spaces, administrative function, and rooftop gardens. The project contains a wide array of green features and the construction utilizes intelligent design and engineering strategies.



### **Astor Place, New York**

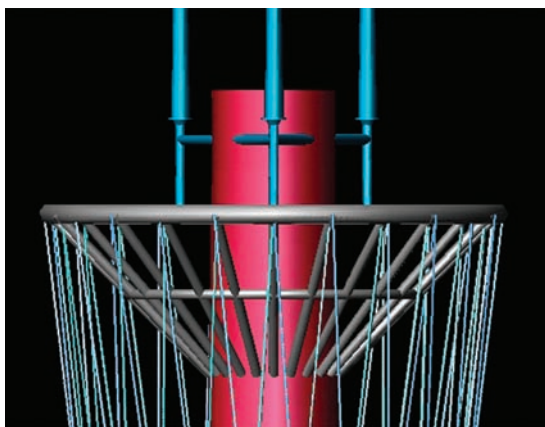
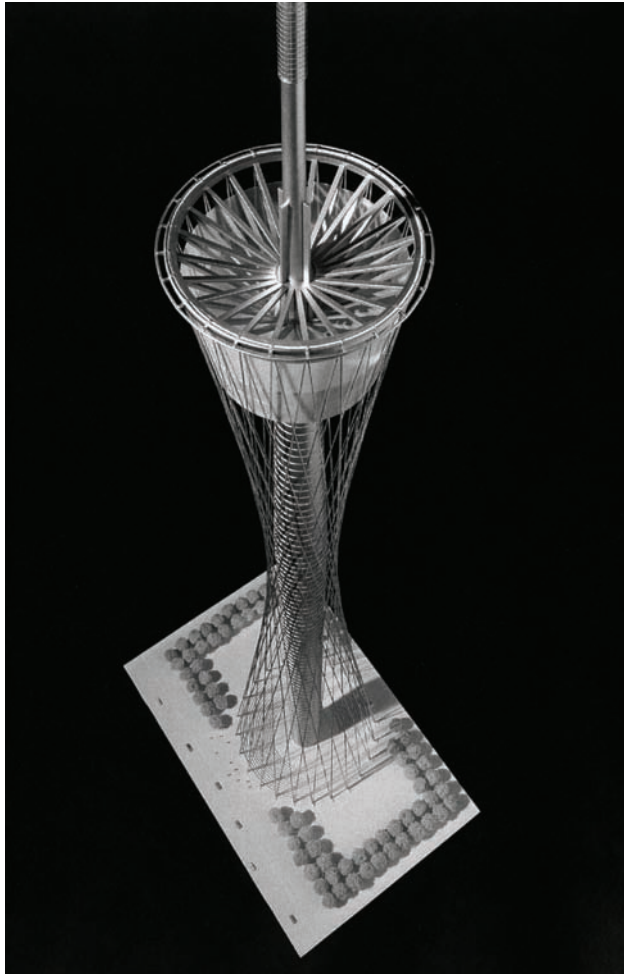
Astor Place is a 21-story mixed-use tower that features a gray-green glass facade that spirals around a zinc grid-like core. The structure utilizes a reinforced concrete flat plate design.





**Atlantis Phase II, Paradise Island, Bahamas**

The tallest structure in the Caribbean, the Atlantis hotel, comprises of two 24-story towers that are linked at the upper levels. The lower levels of the facility are submerged below sea level.



### **Bayonne Transmission Tower Concept, Bayonne, New Jersey**

Intended to replace the antenna lost with the collapse of the World Trade Center, the Bayonne Transmission Tower's design provides broadcast television to the New York metropolitan area. The primary challenge was to minimize the amount of area and material needed. The 2000 ft tall tower borrowed its design theory from sail mast technology and utilizes a composite system: a structural core with cable stays.





### **The Cosmopolitan, Las Vegas, Nevada**

Two 50-story high rises located on the Las Vegas strip. An ultra compact casino resort, this project requires a large open space below the hotel and condo towers for convention centers, retail space, meeting rooms, and casino. A sky mat foundation located 100 ft above grade was utilized to transfer the vertical and lateral forces to box columns and shear walls surrounding the podium. Drilled piers placed below the mat foundation mitigated differential settlement issues caused by large load concentrations due to force transfers.



### **Feil Hall, Brooklyn, New York**

This is a 22-story concrete, flat-plate construction building that serves as the Brooklyn Law School residence hall. The 22-story building features a two-level, below-grade parking garage.





### **Fisher Center, Annandale-on-Hudson, New York**

This performance center's auditorium and rigging towers are made of tall, slender, cast-in-place concrete walls. Special attention was given to the analysis of the first and second balcony seating sections that cantilever from these slender walls to ensure that the loads are balanced with the hallway floors outside the auditorium. The complex exterior skin of the building, geometrically formed from compound, and sinuous curves, are supported by custom built steel members spaced at 10 ft increments.



**Four Seasons Hotel & Tower,  
Miami, Florida**

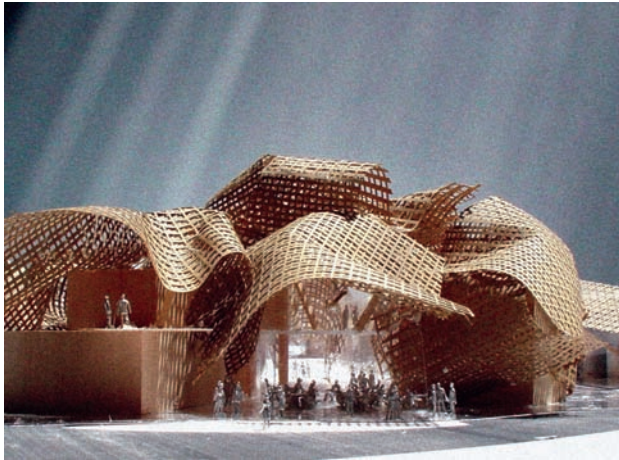
An 800 ft tall, mixed used concrete structure that consists of a 65-story tower containing offices, hotel, and condominium space. The design incorporates concrete shear walls, post-tensioned slabs and perimeter frames. Spans between columns reach 40 ft.





### **Four Seasons Tower, San Francisco, California**

A mixed-use, 40-story tower and low-rise podium located near major fault lines, in a high seismic zone area. This tower utilizes nonlinear viscous dampers to reduce wind-induced building accelerations.



### **Hall Winery, St. Helena, California**

This winery is located in Napa Valley, California. A distinctive curved wood trellis hovers over several buildings serving as a roof canopy. The construction involved new concrete construction of a hospitality center and retrofit of the original Bergfield granite stone winery built in 1885.





### **IAC/ Interactivecorp, New York**

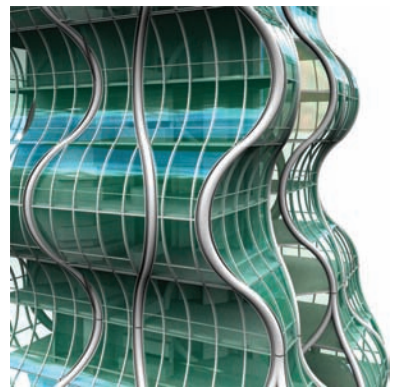
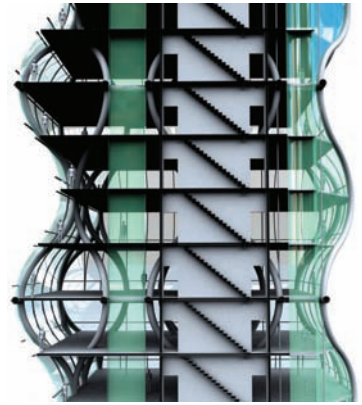
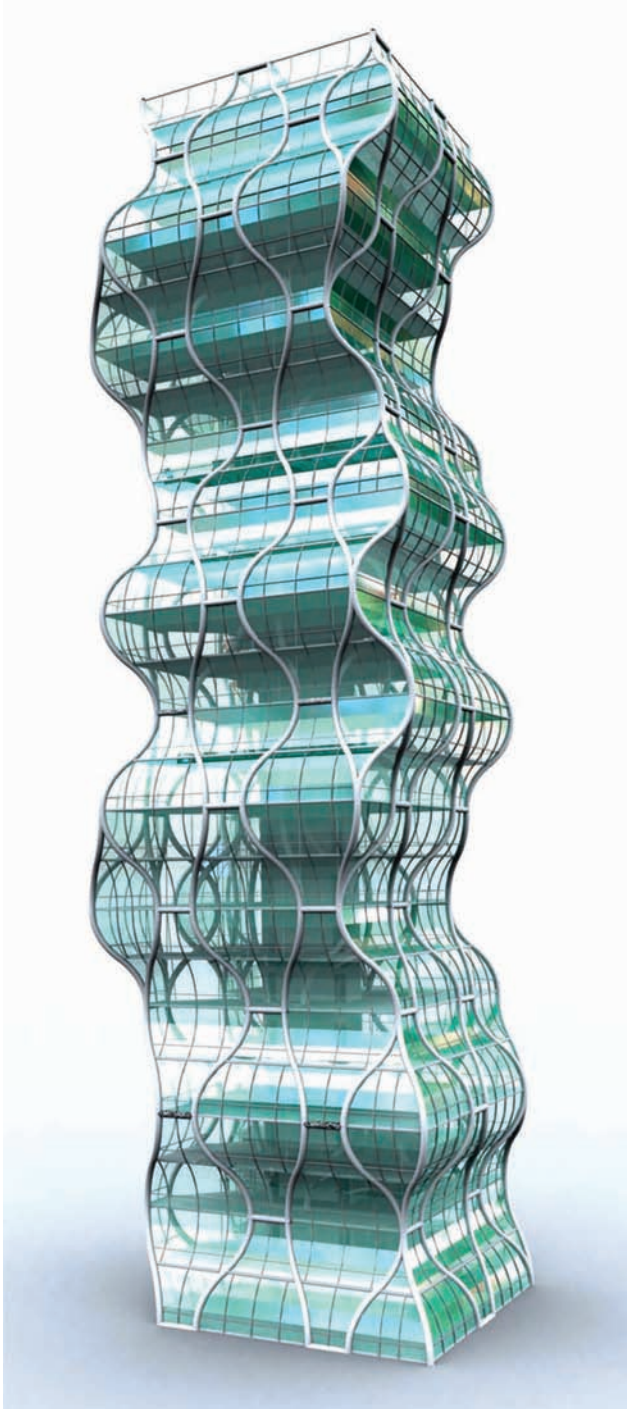
This is a 10-story concrete office building reminiscent of boat sails. The billowing exterior design is created using sculpted reinforced concrete structure clad with an all-glass curtain wall system. Concrete provided the ideal structural solution and an innovative way to achieve the complex geometric and construction requirements.



### **Koʻolani Tower, Honolulu, Hawaii**

This project consists of a 48-story condominium tower and a six-story contiguous podium/garage structure. The structural system for the tower is reinforced concrete columns with flat plate, post-tensioned slabs. Reinforced concrete shear walls provide the lateral system. The shear walls are designed as coupled shear walls with structural steel beams serving as the coupling links between two otherwise tall and slender wall piers.





### **Lalvani Concept Analysis**

This theoretical structure was analyzed to determine the most economical and practical solution. Concrete was used to maximize the floor to floor height and facilitate construction. The columns would be poured using thin-walled curved stainless steel pipe as form-work. The concrete provides strength and stiffness to withstand extreme events. The steel provides confinement and serves to act compositely to improve the serviceability requirements in a wind storm.



### **Mandarin Oriental, Miami, Florida**

A hotel tower, this building's roofline is gradually terraced to abstractly resemble the company's Mandarin sampan logo. The complex's concrete structure utilizes both conventional and post-tensioned slabs and shear walls for lateral support. A pile foundation was required for support as the building is located on reclaimed land.





### **Marquis, Tampa Bay, Florida**

The Marquis is a residential tower standing 700 ft tall in a hurricane prone area. Wind tunnel analysis was performed and the structure was designed to withstand wind speeds up to 146 mph. The structural system consists of concrete shear walls and post-tensioned flat plate slabs with columns. The foundation utilized grade 75 steel to reduce rebar congestion where localized shear reinforcing was required.



### **Millennium Place, Boston, Massachusetts**

This project is a steel framed tower with a low-rise podium and a concrete-framed below-grade parking garage. The top-down construction method allowed construction to proceed downward while the steel superstructure framing proceeded upward simultaneously. Transfer level for the towers consisted of 56 intersecting trusses and 30 transfer girders. Forty fluid viscous dampers controls the building acceleration.





### **301 Mission Street, San Francisco, California**

A 59-story residential tower, 301 Mission is one of the tallest reinforced concrete structures in the Western United States. Outrigger trusses at three intermediate levels help in controlling lateral deflection. A dynamic time-history analysis and a nonlinear push-over analysis were performed to better quantify the building performance and to validate the designed procedure.



**Mohegan Sun Phase II, Uncasville, Connecticut**

A large private gaming and hospitality development that includes a 35-story tower and a 2-story low rise housing entertainment, retail, meeting, and convention space.





### **One Bayfront Plaza, Miami, Florida**

The project comprises of two towers sitting atop a 22-story podium building. Tower one is 61 stories tall and tower two is 70 stories tall.



### **Our Lucaya Beach & Golf Resort, Grand Bahama Island**

An extensive renovation and upgrade of this resort complex included the renovation of an existing hotel into a convention center. Extensive concrete repairs and strengthening were performed on the existing structure. Several one-story concrete and masonry buildings were constructed, including four new restaurants.





**Peter B. Lewis Building, Cleveland, Ohio**

The building is a composite structure of concrete and steel. Cast-in-place concrete flat-slab construction with a 36 in. concrete transfer slab and 8 ft deep, curved concrete beams were utilized to transfer gravity forces to the columns. The building features a steel clad roof framed using 4 in. standard pipe steel.



**Residential Tower Conceptual Design,  
Las Vegas, Nevada**

The architect shows a superstructure that requires bridging to transfer the gravity and lateral loads to the foundation. Steel trusses are used to act as a support spanning from concrete core to concrete core.



### **Ritz-Carlton Downtown, New York**

This 40-story mixed-use tower comprises of reinforced concrete walls and columns supporting flat-plate construction. Shear walls are coupled to improve resistance to high wind loading.





## **Flushing Metro Center, Flushing, New York**

A mixed-use facility situated above a manufacturing/warehouse facility located on a 14 acre site in Queens.



### **The Standard, New York**

A 22-story boutique hotel erected over the Highline, a historic elevated railroad landmark in the heart of Manhattan's Meat Packing district. The building's structure consists of cast-in-place concrete. A transfer system spanning 80 ft allocated at the fifth floor enables the upper levels of the building to span over the existing Highline. Poor soil conditions and a high ground water line required a deep foundation system with the implementation of a heavily reinforced bathtub-type foundation.





**Vdara Tower, City Center, Las Vegas, Nevada**

A 57-story concrete condominium and hotel tower located at City Center, Block B. The floor system is posttensioned flat plate and the lateral system consists of reinforced concrete shear walls.





### **Westin Diplomat Resort & Spa, Hollywood, Florida**

A 41-story conventional reinforced concrete structure sits on top of two discrete structures. A 15 ft deep composite truss connects the two legs at the 10th floor, supporting the single tower above. Where the building is dramatically sloped back from the perimeter, sloped columns are used to pick up long cantilevers created by the step backs.



***"This book is the key to understanding not only the technology of concrete structures but also the organic nature of this basic material, which is used in every corner of the world."***

—From the Foreword by Vincent J. DeSimone, Chairman, DeSimone Consulting Engineers, New York, Miami, San Francisco, New Haven, Las Vegas, Hong Kong, Abu Dhabi

An exploration of the world of concrete as it applies to the construction of buildings, **Reinforced Concrete Design of Tall Buildings** provides a practical perspective on all aspects of reinforced concrete used in the design of structures, with particular focus on tall and ultra-tall buildings. Written by Dr. Bungale S. Taranath, this work explains the fundamental principles and state-of-the-art technologies required to build vertical structures as sound as they are eloquent. Dozens of cases studies of tall buildings throughout the world, many designed by Dr. Taranath, provide in-depth insight on why and how specific structural system choices are made.

The book bridges the gap between two approaches: one based on intuitive skills and experience and the other based on computer skills and analytical techniques. Examining the results when experiential intuition marries unfathomable precision, this book discusses:

- The latest building codes, including ASCE/SEI 7-05, IBC-06/09, ACI 318-05/08, and ASCE/SEI 41-06
- Recent developments in studies of seismic vulnerability and retrofit design
- Earthquake hazard mitigation technology, including seismic base isolation, passive energy dissipation, and damping systems
- Lateral bracing concepts and gravity-resisting systems
- Performance-based design trends
- Dynamic response spectrum and equivalent lateral load procedures

Using realistic examples throughout, Dr. Taranath shows how to create sound, cost-efficient high rise structures. His lucid and thorough explanations provide the tools required to derive systems that gracefully resist the battering forces of nature while addressing the specific needs of building owners, developers, and architects. The book is packed with broad-ranging material from fundamental principles to the state-of-the-art technologies and includes techniques thoroughly developed to be highly adaptable. Offering complete guidance, instructive examples, and color illustrations, the author develops several approaches for designing tall buildings. He demonstrates the benefits of blending imaginative problem solving and rational analysis for creating better structural systems.



Dr. Bungale S. Taranath

K10266

 **CRC Press**  
Taylor & Francis Group  
an informa business  
[www.crcpress.com](http://www.crcpress.com)

6000 Broken Sound Parkway, NW  
Suite 300, Boca Raton, FL 33487  
270 Madison Avenue  
New York, NY 10016  
2 Park Square, Milton Park  
Abingdon, Oxon OX14 4RN, UK

ISBN: 978-1-4398-0480-3

